


*Carnegie
Institution*

OF WASHINGTON

Year Book 62

1962-1963

-A.D. STUBER-
copy for Director's
Office



Digitized by the Internet Archive
in 2012 with funding from
LYRASIL Members and Sloan Foundation

*Carnegie
Institution*

OF WASHINGTON

Copy for Director's etc

Year Book 62

1962-1963

Library of Congress Catalog Card Number 3-16716
Garamond/Pridemark Press, Baltimore, Maryland

Contents

	<i>page</i>
Officers and Staff	v
Report of the President	1
Reports of Departments and Special Studies	1
Mount Wilson and Palomar Observatories	3
Geophysical Laboratory	51
Department of Terrestrial Magnetism	259
Committee on Image Tubes for Telescopes	331
Department of Plant Biology	341
Department of Embryology	401
Genetics Research Unit	479
Cytogenetics Laboratory	501
Bibliography	511
Administrative Reports	513
Report of the Executive Committee	515
Report of Auditors	517
Abstract of Minutes of the Sixty-Fifth Meeting of the Board of Trustees	531
Articles of Incorporation	533
By-Laws of the Institution	537
Index	541

President and Trustees

PRESIDENT

Caryl P. Haskins

BOARD OF TRUSTEES

Barklie McKee Henry
Chairman

Henry S. Morgan
Vice-Chairman

Garrison Norton
Secretary

Amory H. Bradford
Omar N. Bradley
Vannevar Bush
Walter S. Gifford
Carl J. Gilbert
Crawford H. Greenewalt
Caryl P. Haskins
Barklie McKee Henry
Alfred L. Loomis
Robert A. Lovett
Keith S. McHugh
Margaret Carnegie Miller
Henry S. Morgan
Seeley G. Mudd
William I. Myers
Garrison Norton
Richard S. Perkins
Elihu Root, Jr.
William W. Rubey
Henry R. Shepley¹
Frank Stanton
Charles P. Taft
Juan T. Trippe
James N. White
Robert E. Wilson

¹ Died November 24, 1962.

Trustees continued

AUDITING COMMITTEE

Keith S. McHugh, *Chairman*
Alfred L. Loomis
Juan T. Trippe

EXECUTIVE COMMITTEE

Henry S. Morgan, *Chairman*
Amory H. Bradford
Walter S. Gifford
Carl J. Gilbert
Crawford H. Greenewalt
Caryl P. Haskins
Barklie McKee Henry
Robert A. Lovett
Garrison Norton
James N. White
Robert E. Wilson

RETIREMENT COMMITTEE

Omar N. Bradley, *Chairman*
Henry S. Morgan
Garrison Norton
James N. White

COMMITTEE ON ASTRONOMY

Seeley G. Mudd, *Chairman*
Amory H. Bradford
Crawford H. Greenewalt
Elihu Root, Jr.

FINANCE COMMITTEE

James N. White, *Chairman*
Walter S. Gifford
Alfred L. Loomis
Henry S. Morgan
Richard S. Perkins
Elihu Root, Jr.

COMMITTEE ON BIOLOGICAL SCIENCES

Alfred L. Loomis, *Chairman*
Margaret Carnegie Miller
William I. Myers
Charles P. Taft

NOMINATING COMMITTEE

Amory H. Bradford, *Chairman*
Barklie McKee Henry
Keith S. McHugh
Charles P. Taft

COMMITTEE ON TERRESTRIAL SCIENCES

Juan T. Trippe, *Chairman*
Barklie McKee Henry
Richard S. Perkins
Robert E. Wilson

Former Presidents and Trustees

PRESIDENTS

Daniel Coit Gilman, 1902–1904

Robert Simpson Woodward, 1904–1920

John Campbell Merriam, *President* 1921–1938; *President Emeritus* 1939–1945

Vannevar Bush, 1939–1955

TRUSTEES

Alexander Agassiz	1904–05	Seth Low	1902–16
George J. Baldwin	1925–27	Wayne MacVeagh	1902–07
Thomas Barbour	1934–46	Andrew W. Mellon	1924–37
James F. Bell	1935–61	Roswell Miller	1933–55
John S. Billings	1902–13	Darius O. Mills	1902–09
Robert Woods Bliss	1936–62	S. Weir Mitchell	1902–14
Lindsay Bradford	1940–58	Andrew J. Montague	1907–35
Robert S. Brookings	1910–29	William W. Morrow	1902–29
John L. Cadwalader	1903–14	William Church Osborn	1927–34
William W. Campbell	1929–38	James Parmelee	1917–31
John J. Carty	1916–32	Wm. Barclay Parsons	1907–32
Whitefoord R. Cole	1925–34	Stewart Paton	1916–42
Frederic A. Delano	1927–49	George W. Pepper	1914–19
Cleveland H. Dodge	1903–23	John J. Pershing	1930–43
William E. Dodge	1902–03	Henning W. Prentis, Jr.	1942–59
Charles P. Fenner	1914–24	Henry S. Pritchett	1906–36
Homer L. Ferguson	1927–52	Gordon S. Rentschler	1946–48
Simon Flexner	1910–14	David Rockefeller	1952–56
W. Cameron Forbes	1920–55	Elihu Root	1902–37
James Forrestal	1948–49	Julius Rosenwald	1929–31
William N. Frew	1902–15	Martin A. Ryerson	1908–28
Lyman J. Gage	1902–12	Henry R. Shepley	1937–62
Cass Gilbert	1924–34	Theobald Smith	1914–34
Frederick H. Gillett	1924–35	John C. Spooner	1902–07
Daniel C. Gilman	1902–08	William Benson Storey	1924–39
John Hay	1902–05	Richard P. Strong	1934–48
Myron T. Herrick	1915–29	William H. Taft	1906–15
Abram S. Hewitt	1902–03	William S. Thayer	1929–32
Henry L. Higginson	1902–19	James W. Wadsworth	1932–52
Ethan A. Hitchcock	1902–09	Charles D. Walcott	1902–27
Henry Hitchcock	1902–02	Frederic C. Walcott	1931–48
Herbert Hoover	1920–49	Henry P. Walcott	1910–24
William Wirt Howe	1903–09	Lewis H. Weed	1935–52
Charles L. Hutchinson	1902–04	William H. Welch	1906–34
Walter A. Jessup	1938–44	Andrew D. White	1902–03
Frank B. Jewett	1933–49	Edward D. White	1902–03
Samuel P. Langley	1904–06	Henry White	1913–27
Ernest O. Lawrence	1944–58	George W. Wickersham	1909–36
Charles A. Lindbergh	1934–39	Robert S. Woodward	1905–24
William Lindsay	1902–09	Carroll D. Wright	1902–08
Henry Cabot Lodge	1914–24		

Under the original charter, from the date of organization until April 28, 1904, the following were ex officio members of the Board of Trustees: the President of the United States, the President of the Senate, the Speaker of the House of Representatives, the Secretary of the Smithsonian Institution, and the President of the National Academy of Sciences.

Staff

MOUNT WILSON AND PALOMAR OBSERVATORIES

*813 Santa Barbara Street
Pasadena, California 91106*

Ira S. Bowen, *Director*
Horace W. Babcock,
Associate Director

Halton C. Arp
William A. Baum
Armin J. Deutsch
Olin J. Eggen
Jesse L. Greenstein
Robert F. Howard
Robert P. Kraft
Guido Münch
J. Beverley Oke
Allan R. Sandage
Maarten Schmidt
Otto Struve¹
Olin C. Wilson
Fritz Zwicky

GEOPHYSICAL LABORATORY

*2801 Upton Street, N. W.
Washington, D. C. 20008*

Philip H. Abelson, *Director*
Francis R. Boyd, Jr.
Felix Chayes
Gordon L. Davis
Gabrielle Donnay
Joseph L. England
Hugh J. Greenwood
Thomas C. Hoering
Gunnar Kullerud
Donald H. Lindsley²
Patrick L. Parker³
J. Frank Schairer
George R. Tilton
Hatten S. Yoder, Jr.

DEPARTMENT OF TERRESTRIAL MAGNETISM

*5241 Broad Branch Road, N. W.
Washington, D. C. 20015*

Merle A. Tuve, *Director*
L. Thomas Aldrich
Ellis T. Bolton
Roy J. Britten
Bernard F. Burke
Dean B. Cowie
Scott E. Forbush
W. Kent Ford, Jr.
Stanley R. Hart
Norman P. Heydenburg⁴
Brian J. McCarthy
Richard B. Roberts
T. Jefferson Smith
John S. Steinhart
Georges M. Temmer⁴
Harry W. Wells⁵

¹ Died April 6, 1963.

² Appointed July 1, 1962.

³ Resigned June 15, 1963.

⁴ Through January 1, 1963.

⁵ Resigned July 15, 1962.

Staff continued

DEPARTMENT OF PLANT BIOLOGY

Stanford, California 94305

C. Stacy French, *Director*

Jeanette S. Brown

David C. Fork

William M. Hiesey

Harold W. Milner

Malcolm A. Nobs

DEPARTMENT OF EMBRYOLOGY

115 West University Parkway

Baltimore, Maryland 21210

James D. Ebert, *Director*

David W. Bishop

Bent G. Böving

Donald D. Brown

Robert L. DeHaan

Irwin R. Konigsberg

Elizabeth M. Ramsey

Mary E. Rawles

GENETICS RESEARCH UNIT

Cold Spring Harbor

Long Island, New York 11724

Alfred D. Hershey, *Director*

Elizabeth Burgi

Barbara McClintock

Margaret R. McDonald

Staff continued

OFFICE OF ADMINISTRATION

1530 P Street, N.W., Washington, D. C. 20005

Caryl P. Haskins	<i>President</i>
Edward A. Ackerman	<i>Executive Officer</i>
Marjorie H. Walburn	<i>Assistant to the President</i>
Ailene J. Bauer	<i>Director of Publications</i>
Lucile B. Stryker	<i>Editor</i>
James W. Boise	<i>Bursar; Secretary-Treasurer Retirement Trust</i>
Kenneth R. Henard	<i>Assistant Bursar; Assistant Treasurer Retirement Trust</i>
Donald J. Patton	<i>Administrative Associate</i>
James F. Sullivan	<i>Assistant to the Bursar¹</i>
Richard F. F. Nichols	<i>Executive Secretary to the Finance Committee</i>
Marshall Hornblower	<i>Counsel</i>

Staff Members in Special Subject Areas

Tatiana Proskouriakoff
Anna O. Shepard

¹ Retired June 30, 1963.

Staff continued

RESEARCH ASSOCIATES

Carnegie Research Associates

Paul W. Gast
University of Minnesota

J. D. McGee
Imperial College of Science and Technology, University of London

Ulrich Schmucker
Scripps Institution of Oceanography, La Jolla, California

Lyman Spitzer, Jr.
Princeton University Observatory

C. E. Tilley
Cambridge University

Research Associates of the Carnegie Institution

Louis B. Flexner
University of Pennsylvania

Harry E. D. Pollock
Carnegie Institution

Report OF
THE *President*

Excellence and a respect for it—these and these alone redeem a civilization from triviality. They are plants which thrive on the precipitous heights of Alpine landscapes, but wither in the suffocating air of equable mediocrity. Whatever its sins, a society prizing liberty and revering excellence may hope to add some imperishable mite to the sum of man's achievements.

R. H. TAWNEY
Equality and Liberty

This means, on the one hand, that for every person there should be enough room, enough freedom, to plan the use of one's time, the opportunity to reach ever higher levels of attention, some solitude, some silence.

SIMONE WEIL
"À propos de la question coloniale, dans
ses rapports avec le peuple français,"
Selected Essays, 1934–1943

TO OUR COMMON ENTERPRISE. *To the insatiate taskmaster who is ever exacting the best, last ounce of effort or the longest hour of drudgery, yet whose wage is of the highest, though he pays neither in riches nor contentment, only a craving that can never be satisfied, an unrest that will not be stilled. . . . To the goal of our endeavor, though the mists obscure it, though we know not even if that we follow be the call of truth itself or but the yearning of our own restless quest. . . . To the god of things hidden, of questionings unanswered, of mysteries unrevealed.*

JOHN MAURICE CLARK
The Amherst Monthly, December 1915

GREATNESS IN A NATION, LIKE PERSONAL GREATNESS, IS A MEASURE not only of character, not only of excellence, but also of enduring significance both in ideals and in the shape and goals of effort. In any society, but perhaps especially in our own, such greatness must necessarily be valued in coin of our own design and minting, whose very significance, moreover, we must ourselves determine. In such terms, our first historical claim to greatness was plainly a political one, springing from the very structure and texture of our society and our tradition and enduring through shifts of circumstances, through changes of scale and of kind, far greater than some that historically brought violent upheaval to other lands. A second genuine claim to American greatness in these terms is rooted in our capacities and our achievements in technology, born of a native Yankee inventiveness on the one hand and a keen intuitive appreciation of the requirements of mass production on the other, which are prime movers for us still, though their modern consequences would surely be totally incomprehensible to a resurrected, hopelessly overawed Eli Whitney. This strong technological cast, with its flavor of direct pragmatism, has reflected one important facet of our national mood since our very earliest history, and on it much of our fortune has been, and will continue to be, built. Our third, and in a sense our most recent, claim to authentic greatness has

been made possible by the first and is linked to the second, at some times in mutual aspirations and ends, at others in the tensions arising from related but often sharply differing requirements. It lies in the realm of science as the search for new knowledge—a realm to which a new generation of Americans may fairly be said to be giving wider and more vigorous address than has ever been given before, and which may ultimately provide one of our most enduring signatures.

The claims for modern science, the extolling of its virtues, the exculpating of its shortcomings, the analyses of its character, the concerns for its future, dominate our conversations today as never before. Perhaps that very fact is an indication that this claim to greatness in our society, though it was being made three generations ago by a handful of American scientific scholars ranging from Josiah Willard Gibbs to Albert Michelson, and though it has swelled to such commanding volume in our own day, is not only newer but, in its essence, still far less familiar to us as a whole people than the claims of either political or technical cast. Moreover, the dynamic growth that has so conspicuously dominated the evolution of American science in recent years has posed new and grave questions which are not yet firmly answered. Indeed, it must be said that after a century and more of experience we are still unsure about the kinds of demands that greatness in contemporary scientific scholarship imposes, about the real nature of standards and their maintenance there, even about the real nature of the effort itself.

In this facet of our national concern, in fact, we are still widely uncertain about the denominations of our own measuring coinage. And since a society can achieve and maintain greatness only if its people as a whole demand and recognize and judge greatness with an accurate and critical and uncompromising eye, it is worth a good deal of trouble to us as a nation to strive deeply to comprehend the nature of scientific scholarship in its truest sense. It is worth a good deal of trouble to understand the depth and range of its roots in our society, to visualize the requirements for its growth. It is worth much effort to try to comprehend the impact upon it and the consequences for it of the other immense social changes with which we live—changes that in part result from scientific development itself and at the same time must profoundly affect the future course of science. It is worth much inquiry to visualize, if possible, the range of challenges being presented to it that must be reasonably met if its strength and its integrity are to remain inviolate and unimpaired. Predominant among these factors is its intimate relation with technology and its deep involvement in the expansions of a technological as well as a more general social world. Around the areas where its own evolution and our conceptions of its nature and function are deeply affected by the great con-

temporary currents of our technical and social worlds, around the areas where factors for its growth and health coincide with those of its environment, and, most important perhaps, around areas where there are very real tensions that must be reconciled as far as they can be, revolve some of the most acute problems for both science and our society, today and for the future.

First of all, and at the very root of all our concerns with science, stands the link between the political and the scientific aspects of social greatness—a link so fundamental that even its nature is not always explicitly recognized. For, as Bronowski has cogently pointed out, ours is a society which sets an overriding value upon the search for truth. And that truth we define, not only in the context of satisfying and viable and self-consistent intellectual propositions, but, in the last analysis, as the kind of a view of the world which reliably describes the facts of our natural and our swift-changing social environments as we can best perceive and define them. At a very deep level we are wedded to the proposition that the search for truth, so defined, is an end, and an extremely important end, of all our inquiry. In a solemn sense, perhaps the most important commitment of our society is to this duty to seek the truth.

The assumption of that duty, of course, is far older than our own nation. It is, indeed, as old as the society of western Europe in recent times. It may be no accident that the emergence of science in its modern form occurred contemporaneously with the Renaissance revolution in political thought and action. It may be no accident that the Italian Accademia dei Lincei, the British Royal Society, and the French Académie des Sciences were established within an interval of little more than a half-century, beginning about 1611. From this acceptance of truth as an overriding value many consequences flow for an entire civilization. Indeed, it seems clear that so long as a society considers truth in this light, so long as it regards the pursuit of truth in that definition as one of its highest goals, it harbors deep and powerful incentives to remain both dynamic and flexible. A society committed to the search for truth must for that very reason give protection to, and set a high value upon, the independent and original mind, however angular, however rasping, however socially unpleasant it may be. For it is upon such minds, in large measure, that the effective search for truth depends. This is the safeguard of originality and of individuality in our society—perhaps the most powerful protection they have. In contrast, these are the precise values which suffer in a society committed to the view that truth is ordained and fixed, that all knowledge, in a literal sense, is revealed knowledge. Such a society is by that fact inherently cut off from the greatest potential any society can have, the power to evolve. This deep-rooted sequence of circumstances, so powerful in its implications, may

indeed present one of the most formidable difficulties both philosophically and practically for many traditional societies as they seek to enter the modern age.

If indeed those characteristic qualities of the rapidly and flexibly evolving society—freedom, independence, the high worth of the individual—are closely linked to the search for truth as an overriding goal, they must claim greatness in scientific scholarship as one of their major bastions as well as one of their notable products. It is that heritage, indeed, of which the philosophy and the methods—not primarily the practical results—of American science must be an important guardian in our nation today. The social gravity of this circumstance alone gives to the task of understanding the roots and the nature and the basic requirements of scientific scholarship an importance which its practical consequences, massive and conspicuous and impressive as they are, nonetheless can never equal.

Such understanding, however, poses no easy challenge. The task is made more difficult by the fact that reliable analogies with other areas of greatness in our national life are not easily achieved. For science has certain qualities that distinguish it significantly from other realms of intellectual activity, including many more traditional areas of scholarship. Important among these is its predominantly cumulative nature, involving not only the summation of information from one generation and one age to another, but also the constant reintegration of that knowledge to make of each of its branches a more or less coherent, but also a dynamically evolving, organic conceptual structure. Indeed, a striking characteristic of the body of scientific knowledge is the degree to which, in organization and growth, it recalls a developing organism, or, on a larger scale, an evolving population of organisms. Like the society that supports it and of whose basic values it is in turn an overwhelmingly important guardian, the body of science is, in something more than a purely allegorical sense, a living thing. If the differences as well as the likenesses in such a comparison be firmly remembered, if the limits of the analogy be carefully observed, it is on occasion instructive to consider some facets of the nature and the quality and the requirements of science from the vantage of that view.

It is a commonplace among students of natural evolution that the major innovations which, in the long perspective, provide the great critical advances in the history of plants and animals have occurred with comparative rarity. Once perfected they are adhered to tenaciously, and a plethora of detail is built upon them. One principal set of photosynthetic mechanisms powers all the higher green plants, from moss to sequoia, reflecting the universality of that great single invention around which the whole vast realm of vegetation most familiar to us has evolved. The chemical structure and the basic mechanisms, as well as the basic function, of oxygen trans-

port in the hemoglobin of the blood differ only in minor detail among all the vertebrates from fishes to men, and all vertebrates depend upon that constancy for sheer survival. There is little to distinguish the basic structural plan in feathers of the lowest birds from those of the highest, while the universal feathering of birds and the richness of its detailed differences among species at once emphasize the importance of the fundamental invention and underline how much minor variation is made possible by it. It seems increasingly clear that one general scheme of coding stores the genetic information of all higher living things, yet the actual information so stored must be as vast and as rich as the variety of the living world.

It is a further commonplace that the rare but successful major evolutionary innovations truly worthy to be called advances in grade constitute evolutionary "bottlenecks" in more than one sense. In any group of living things immense periods of time had to pass, immense numbers of essentially random and largely minor innovations had to be entered in the record, immense numbers of individuals generating those changes had to live and die, before adequate storehouses of variation were accumulated from which genuinely major advance could follow. Those accumulated storehouses of variation, indeed, may be reckoned as one of the most powerful sources of potential wealth, alike for organisms and for science. In the second context, they may without too much stretch of the imagination be translated as the reservoirs of accumulated scientific knowledge. Or, in a possibly more significant allegory, they may be rendered in terms of a plurality of training and capacity and potential among those who make up the contemporary scientific order. Particularly in that sense are they especially precious, and their guardianship and their enhancement are immensely important.

An especially striking consequence of this general profile of evolutionary advance is that major innovation is virtually impossible in the absence of an extensive reservoir of variation accumulated earlier. Yet, however rich that store may be, only a small sector of the vast moving front is fated at any given time to achieve truly significant advances of grade.

One of the characteristic qualities both of evolving organisms and of a growing body of scientific insights is that, viewed historically, their dynamic can in some respects be likened to the profile of beads on a chain. From a broad spectrum of multitudinous detailed variations on a common essential theme preoccupying their evolutionary history over long periods, there erupts at intervals the slender flame of really significant innovation. In turn, this dynamic phase is followed once more by a stage of elaboration on a new major theme.

It is further characteristic that such a narrow and tenuous channel of fresh advance is traversed swiftly. "Missing links" are typically ephemeral both in evolutionary sequences and in major transitions between levels of

scientific understanding—rare or obscure among the living, scarce in the fossil or the historical record. We have few contemporary examples of the early stages through which the photosynthetic process evolved to its present stature and efficiency. Animals exhibiting the transition from notochord to vertebral column are not common. We have no direct evidence, living or fossil, of exactly how feathers came to be. Nor, on the other hand, do we find much conspicuous evidence, a century after the event, of the transitional steps by which notions of preformism were replaced by current evolutionary concepts, or of those that marked the transition from a theory of pangenesis to the ideas of modern genetics, even though, as with organisms, rare vestiges of such major transitions can still be found, though well concealed, embedded within modern thinking.

This “beadlike” structure of the growth of scientific insight about the world, with characteristic bursts of conceptual advance typically initiated by one or a very few individuals when major points of view change radically and swiftly, followed by the longer periods of broader, steadier, more detailed elaboration of new patterns at the hands of a multitude of workers when the earlier gains are consolidated, implies much that relates to the nature and the requirements of science itself.

On one hand, such a picture puts in relevant setting the essential part played in the advance of science by the long accumulation of background knowledge, the long periods of “in-grade” exploration going forward sometimes almost unnoticed, the undramatic efforts that accumulate new stores of facts, new assents from nature, from which major gains may finally be rendered. It emphasizes that one proper and necessary task of science is indeed this gathering and storing of facts experimentally determined, and that on the widest possible scale. In such an aspect, it offers a real, and indeed a powerful, rationale for the tremendous range and diversity of the scientific quest in our day and for the numbers of workers involved in it, now so enormous and proliferating so rapidly.

But it also carries a warning—and a poignant one. It cautions against regarding this process alone, with its affirmation of massive and sometimes overplanned research, as synonymous with the true growth of scientific scholarship. As Americans we readily understand this side of the scientific coin. For we are firmly wedded to massiveness, and our long and triumphant experience in developing vast technology leads us easily to equate success in research too with sheer magnitude of effort. And so we may be in particular danger of forgetting that the accumulation of facts, however important, is only a secondary business of science. It still represents at base the “in-grade” phase in the evolution of our insights about the world. The real greatness of scientific scholarship inheres in the thin, tenuous, ephemeral thread of reason and vision and insight and crucial experiment,

in the acts of true understanding that from time to time and from place to place over the scientific front lead from one conceptual level to another. In the last analysis, it is by the consistency and the effectiveness of this second, germinal process, through the years and over the whole broad span of the effort, that our scientific progress and our scientific stature must be measured. In publicly misreading the principal business of science, in imagining its basic task to be primarily the accumulating of facts about the natural and the social worlds rather than the winning of significant new insights into their essence, there is a real danger that we could misunderstand its deepest requirements and so compromise its greatness, and indeed its long-term vitality, at exactly the times and places where a superficial view might suggest that we were most actively promoting it.

Now the achievement of those major insights must inevitably rest, in the future as they have in the past, in the hands of a comparatively few highly original and gifted men and women—a minuscule proportion of the entire scientific population. And so we had better ask ourselves some hard questions about that thin battle line upon which inevitably so much of scientific greatness will continue to depend. What are the characteristics of those who make it up? How are they to be discovered, comparatively rare as they are, and how given the special training required to bring their high capacities to fruition? How can the conditions of their work best be tailored to enhance their contributions? Do the circumstances and the atmosphere of contemporary American science make their creative effort, in our time, easier or harder than it was for their predecessors? How does the nature of their task itself change with the growth of the structure of science?

A glimmer of an answer is possible to some of these questions, though many of them are still wholly obscure. What these critical individuals are we can in good part divine from the record of their predecessors, whose qualities have been demonstrated and whose whole lives we have seen. From them we can gain some appreciation of the intellectual power, the capacity for novel conceptual organization, the native originality, and the deep preparedness of mind that the challenge of genuine and significant scientific innovation requires. For in a very real sense this critical line must be manned by the Newtons, the Pasteurs, the Kekules, the Rutherfords, of our day and of the future. Clearly the discovery and the appropriate training of individuals of this rarer quality, who are so critical for the further growth of science, must take a priority with us at least as high as the proper training of capable but more limited talent on a far vaster scale.

The prerequisites for success in the two enterprises may be very nearly opposite. The keen discrimination it demands, the searching and sophisticated evaluation of the individual which it requires, the self-selection of

the best by the best which is such a powerful tool for it, all define the first process as one that can be carried forward with particular effectiveness in scholarly enclaves maintaining extremely high standards both of work and of training. This is a proper concern of the universities. In its research aspects, it is a predominant concern of the Carnegie Institution.

But the work of great innovating individuals in our day, and even more in the future, will be undertaken against a background sharply different in many respects from that of their predecessors. We may well inquire whether both the circumstances of modern massive science and our own philosophy have not actually become less well attuned to this vital aspect in the last half-century, precisely as concerns necessarily preoccupied with size and organization have been magnified. Do the circumstances of science in our own day continue to provide fertile environments for such intellects? Do the widely accepted patterns of a massive American science leave adequate opportunity for the quietude—even, at times, for the relatively severe sensory deprivation—that may be a positive requirement for great creative achievement? Are the exceptional individual and his intimate working group, indeed, still truly significant factors in a picture of scientific growth characterized so much by the work of teams?

Even in the last dozen years the background, both intellectual and physical, has indeed altered strikingly in many ways. On the score of intellectual scope and content, there have been significant changes which are clearly latter-day consequences of the cumulative nature of the scientific discipline. We are vividly aware, for instance, that scientific data have been accumulating at exponentially increasing rates for three hundred years now, doubling two or three times in every generation, and the ultimate magnitudes of such curves are always of awe-inspiring dimensions. The population of scientific workers has been expanding at similar rates, so that there may well be more investigators active today than the total of all those who lived and worked in the two and a half centuries after Newton. The vast accumulation of scientific facts with which we live is a commonplace of our time. So is the intense specialization of scientific knowledge accompanying it. The incomprehensibility of one branch of science to a specialist in another is an integral part of our folklore. Is this very weight of accumulated information likely to prove fatal to the integrating mind? If the answer to this particular question is affirmative, we can well be alarmed.

Fortunately it is almost certainly negative. Many powerful scientific intellects of our day find little threat in this vast warehouse of information, or in the huge tasks of integration inevitably imposed. Many scientists,

and they are likely to be precisely those of innovating talent, instead regard it as a challenge to personal versatility and range as well as to personal depth of scientific understanding—as a challenge, indeed, unmatched in any earlier era. In its very wealth may lie the raw materials for extraordinary insights.

Another feature of substantive content in which the contemporary scientific milieu differs strikingly from that of an earlier day emphasizes once again how much the body of scientific knowledge resembles an organism in certain aspects of its growth. No course of evolution in organic nature is ever precisely reversible. Nor can an evolved organism be simply an expanded version of its predecessors. It is not only in the vastness of its information that current science differs from the science of another day. It profoundly differs also in the ever-accreting wealth of integrations of knowledge, the ever-growing store of basic insights already achieved, which in the past, characteristically, have radically altered the courses of thought in its older branches and today constantly generate new directions. The rate at which such insights occur, though far lower than the rate of accumulation of facts, has likewise accelerated with the years. And it is clear that at any given time the body of scientific knowledge, again like an organism, is deeply affected in the future courses of development available to it by integrations already made. There are phases in the development of every branch of scientific knowledge when some directions of growth, some reaches of concept that would earlier have been open, now, for better or worse, are closed. At the same time other new syntheses are almost dictated by the older ones and virtually lie ready to be made. Indeed, they might almost be said to be unavoidable—a conclusion vividly emphasized by the many occasions in the history of science when nearly identical insights occurred almost simultaneously to two or three or even more investigators who had not been directly in communication. Today this particular kind of shaping of scientific evolution goes forward more dynamically than ever.

Such changes as these, and many others that distinguish the earlier intellectual climate of science from the one in which the innovating minds of our own time and of the future must work, spring readily to mind. Their individual effects, though fascinating to conjecture, will probably remain permanently moot, precisely because the whole background against which they are projected is itself still changing with such wind-swift speed.

But when we think of the modern scientific environment less in terms of content and more in terms of physical organization, we reach firmer ground. In this context we return once more to those questions raised earlier, which relate so pointedly to the role in current scientific progress of that thin line of innovation and of innovating individuals emphasized in the drama of evolution. In this day of massive science, do we still find

highly significant advances on the furthest frontiers coming from those small and modest research environments where traditionally the freedom and the opportunities of the individual investigator have been thought to be at their highest? And if the answer to this question is affirmative, what of its converse? Do we find any notable lack of such major and penetrating contributions of scientific insight proceeding from the massive and populous research environments of our time?

Examples spring to mind at once to give a striking and unequivocal answer to the first question. In 1953, for instance, J. D. Watson and F. H. C. Crick announced their brilliant hypothesis that the unit of heredity, the "molecule" of deoxyribonucleic acid, at the structural level consists of a pair of "ribbons" wound in the form of a double helical spiral around a common axis and linked by the four bases, two purine and two pyrimidine, paired in a highly specific fashion and forming by their arrangement a true code recording all the information governing the development and the final characteristics of every plant and animal. That fundamental insight led to what has become universally recognized as one of the most significant developments in all biological history, and indeed one of the most outstanding in the record of science.

Less widely known but potentially quite as pertinent to understanding the nature of life has been another development proceeding from the same laboratory. It began several years earlier. Before the end of the second World War, indeed, J. C. Kendrew, M. Perutz, and their colleagues at the Laboratory of Molecular Biology of the British Medical Research Council at Cambridge were planning a group of inquiries of extreme difficulty, both theoretically and experimentally, into the structure of proteins at the molecular level. The methods used were those of X-ray crystallography, the proteins selected were hemoglobin and the related and in many ways similar, but somewhat simpler, myoglobin. The road led first through adaptation of the method of isomorphous replacement, hitherto only occasionally applied to crystallography in general and never to organic molecules of the size of myoglobin, to the method of successive refinement, involving the computing of Fourier syntheses from data on the diffraction patterns of the crystal to yield resolutions successively of 6, 2, and 1.4 angstroms—a stupendous task. From it there has emerged, almost twenty years later, a complete and detailed molecular model of myoglobin, the first ever deduced for a protein. It is a model that must be of profound significance, not only in the similar study of other proteins in the years to come but as basic information in approaching the crucial question of how the information coded in the hereditary material determines the structure of proteins built under its influence.

The sweeping import of both these pioneering inquiries at the Medical

Research Council's Laboratory of Molecular Biology at Cambridge has been signalized in recent years by Nobel awards. Thus from a single research group have recently come two outstanding advances in our understanding of the nature of life, which, taken in complement, may well form one of the very great contributions of all time to biological science. Now that research group began with two crystallographers. A decade later it numbered possibly a dozen workers and was housed in a temporary building near the Cavendish Laboratory and in rooms of the University—a very minimum of space. It was superbly instrumented for its task; yet that instrumentation was of extraordinarily limited cost and dimension compared with those of many other fields of science. But this almost incredibly modest material environment was fortified by two indispensable nonmaterial circumstances. It provided a free and unfettered atmosphere of inquiry, and it addressed itself to questions of unrivaled intellectual challenge. The few gifted individuals who had conceived it and those who later joined it on invitation were of course able to span the world in their choice and their use of gifted colleagues in related fields.

This is an especially striking example of the vigorous role of world scientific leadership that can be achieved by the small but unfettered group in the science of today no less than that of yesterday. But there are many other such groups, in this country and abroad and in a wide variety of fields. In the Department of Terrestrial Magnetism of the Carnegie Institution work is currently going forward involving the highly ingenious use of strands of denatured DNA, entrapped in agar gel, as an adsorption column for "messenger" ribonucleic acid of its own and of other species of organisms. The method offers the dramatic possibility of defining the relationships between animal species in terms of the proportions of their total genetic code shared in common and in the part of their coded endowment of inheritance wherein they differ. Such work promises to achieve a description of evolutionary patterns at the molecular level which not only is new but which also could provide perspectives comparable in their advancement of our understanding to those revealed by the elucidation of the structure of DNA itself. Yet the research group involved in this exploration includes but a few scientists, and the volume of the total program, like that of the Cambridge Medical Research Council's molecular biology group, is extraordinarily modest by the standards of much contemporary research.

At the California Institute of Technology, again, a single laboratory of neurobiology and neurophysiology, through work combining the delicate brain operations involved in severing the connectives of the corpus callosum uniting the hemispheres of the brains of cats and monkeys with most ingenious experiments in behavior, has for several years been gathering new information about cerebral processes in higher vertebrates that may

well lead to an enlarged understanding of some elements in the structuring of human personality.

These few striking examples, chosen almost at random among hundreds available from contemporary research, may suffice to confirm that, in this day of massive science, some of the most significant advances still come from small groups, where traditionally we have always considered the freedom and opportunities of the gifted individual to be at a maximum. There can be no reasonable doubt that research structures of this kind still offer one of the most powerful environments for the nurturing of innovation. It seems probable that they will continue to do so into the indefinite future. Indeed, in terms of the ratio of expenditure both of talent and of money to the gains made, there is every likelihood that they will continue indefinitely to be by far the most economical form of research organization that we know.

What, now, of the converse question? Do we find similarly striking contributions to the advance of scientific scholarship stemming from massive and populous research environments of our time? Once again a multitude of examples comes to mind in affirmation. The major contributions to scientific advance and to the new technical kingdoms they opened which have been made in the great industrial laboratories over many decades past as vigorously as they are being made today of course require no emphasis. The fundamental advances in the understanding of matter achieved in the laboratories of the General Electric Company, the basic progress in the science and the art of X rays coming from the same laboratories over a long period of years, the discovery and development of nylon in the du Pont laboratories, to name but a few specific examples from a possible multitude, have all formed classic chapters in the history of our science and technology. Equally classic are more immediately contemporary chapters: the development of semiconductor theory and practice in the Bell Telephone Laboratories, the creation of the Telstar satellites, with their brilliant performances over this past year, and a host of others.

Nor are such contributions limited to the environment of industrial research. In many of the great laboratories within the structure of the government itself, as well as in those predominantly under contract to government, examples again come readily to mind. Such, to cite a very few representative cases, is the fundamental work on the process of photosynthesis in green plants undertaken at the Oak Ridge National Laboratory a few years ago, which has opened important new avenues of inquiry in that difficult subject. Such is the wide-ranging and fundamental work on genetic coding conducted at the National Institutes of Health, which occupies an important place in the contemporary enlargement of the concepts stimulated by Watson and by Crick. Such is the brilliant dem-

onstration at the Argonne laboratories, following Bartlett's pioneering notion, that the gas xenon, so long thought to be inert, is in fact highly reactive chemically and that xenon fluoride can be made. And nothing, perhaps, can illustrate more vividly the closely woven and continuous nature of the framework of investigation that binds work in small and large organizations, in organizations that are private and in those that are public, in a common structure of inquiry at the frontier of research on life processes than the fact that some of the most pertinent discoveries about the way in which the hereditary material determines the amino acid sequence of a protein are also currently being made in laboratories of the National Institutes of Health.

And so it would appear that neither the total size of a research organization, nor its situation in or out of government, nor its situation in industry or foundation or university, is per se of decisive significance in determining how original, how distinguished, how relevant to modern frontiers its scientific output shall be, or how prolific it is in making such contributions. What, then, are the significant parameters?

To distinguish them requires a closer look at the detailed circumstances of the particularly creative groups within each environment who have made such distinguished contributions under such generally diverse conditions. When such a scrutiny is made, a feature found common to them all lends fresh emphasis to the vital role of the innovating individual and the small and mobile group in the advance of science. For, with few exceptions, regardless of how large the total research organization in which these original and productive elements carried on their work, within each element itself a high degree of freedom and flexibility prevailed just as surely as though such groups were physically isolated. Like the groups creating amid more limited environs, these functional units tended to be and to remain small. Like them, each included innovators of high talent associated with gifted colleagues commonly of their own selection, or self-selected by the group. Each working unit, for the duration of its life as an innovating entity, retained a high degree of autonomy in the direction and the character of its research. To each, also, was ensured in some degree and frequently by design that protection from the random noise of the world, that refuge for quiet concentration over extensive periods, that opportunity for the discipline of parsimony of the senses, without which great innovation may be quite impossible, and which the innovating group in more limited surroundings can sometimes take for granted.

It thus seems clear that the essential requirements for great scientific innovation in our own day are precisely what they have always been, and their flavor of high individuality, however achieved, remains a constant. If that basic fact is forgotten—if it ever comes to be widely believed that

the process of innovation itself is a massive thing, that itself it is subject to massive organization—then its very course can be genuinely imperiled.

Such a confusion between the requirements of the immediate environment in which scientific innovation takes place and which is so vital to it on the one hand and that larger environment in which it is formally structured on the other is undoubtedly one of the serious dangers of our time. For if it is true that the requirements for great innovation are what they have always been, it is also true that in the modern environment of massive groups devoted to research this cardinal need is much harder to remember. And even when it is kept constantly in mind, infinitely more vigilance is required to ensure that the special demands of innovation continue to be met in the face of formidable contrary pressures. Moreover, the retribution for failure to do this is not immediate, nor is the result of neglect at once visible. The effect is relatively slow to come. But when it is finally felt it can be potentially disastrous.

Any large research organization, indeed, is inherently exposed to a number of insidious hazards requiring sensitive perception and great vigilance to avoid. One is that the role of the administrator may become both blurred and exaggerated. The very weight of the administrative process in such a structure, which—as a general principle of organization—tends to increase with the size of the whole relatively more rapidly than the corresponding output of productive research, makes a proliferation of administrators in the larger environment necessary, or at least defensible. This is especially true of the laboratory operated within the structure of the federal government, where fiscal and accounting traditions designed originally for enterprises in which final objectives can be generally visualized at the outset exert strong pressures on the administrator to account in detail, not only for the amounts of his expenditures, but for the precise findings that have flowed from them.

Several unfortunate consequences may follow. One of the most likely is that, in such an environment, the scientific imagination of the administrator ultimately comes to limit the scope of the research itself. This potential danger is underlined by a circumstance that also bears heavily on the general problem of the selection of scientific administrators in our day. The volume of science continues to double, even as it has doubled since the time of Newton, at a rate ranging between seven and fifteen years, with the pace in our own country near the upper end of the scale. Thus if a man of scientific maturity and ripened experience is chosen as administrator, say an individual in his middle fifties, the volume of science will have doubled on average three times since he completed his own graduate work and possibly since he last undertook an intensive program of personal research. In such circumstances only the exceptional individual can achieve a wisdom and a

stature such that, when the limits of his own comprehension and insights may affect those of his organization, creativity will not suffer.

Other difficulties follow from a failure to distinguish the proper limits of application of the traditional pattern of accounting so essential elsewhere within government—a pattern that can be inimical in the immediate research environment and yet, paradoxically, in some form may well be essential in regulating the general course of a government science grown to massive proportions. Prominent among them is the fact that an uncritical invasion of concerns proper to the general environment into the immediate arena of research inherently leads to a drift of the criteria of judgment and recognition away from the substantive merits of the work of the individual into less relevant domains. There is strong pressure to transmute a liberal administrative trust in the researcher's own best capability to determine what he will do and how he will do it, freely given once his own qualifications are adequately established, into a sense of direct and immanent administrative responsibility for these things. Once established, such a sense of responsibility inevitably leads to frequent estimates of the substantive merits of research plans by individuals whose personal experience may lie quite outside such fields: individuals who, however sensitive and skilled and sympathetic they may be, are in the nature of things likely to miss those special and subtle features that can return from the work of the gifted investigator untrammelled by such intervention the thousandfold values which have typically attended his work in the past. Equally insidious is the philosophy, following naturally from such a view, that results in research should as a matter of logic be proportionate to money spent, and that multiplication of money therefore *ought* to lead to corresponding multiplication in significant results. In fact, of course, as sorry case after sorry case makes ever more obvious, the reverse is more nearly true.

But the application of this oversimplified sample of conventional reasoning to an area where it is inappropriate can have a number of results more damaging than the immediate and obvious one of establishing a type of accountability which, carelessly applied, may promote the superficial at the expense of the profound and difficult and may encourage the belief, currently all too dangerous to the stature of our scientific scholarship, that money and expensive equipment may of themselves substitute for penetrating thought. It also carries the implication that in original research, as in the more advanced stages of technology, the specific goals of the work are already known, and that what is required is concentration on the means of arriving at those ends. This damaging illusion is not only patently false. Not only does it imply that in areas where the qualities and requirements of science and those of advanced technology may actually be quite opposite they are the same and are amenable to identical treatment. What is perhaps

its most far-reaching effect is more subtle. For the nature to whom the lure of scientific research is keenest, one of the most important features about the work and one making it most satisfying is that the ends, far from being known, may be virtually unimaginable at the outset of the investigation. This traditional feature of scientific research, perhaps more than any other, has given it overriding verve and sparkle for its practitioners since the days of the scientific revolution. To remove that element, or to assume its absence, can be extraordinarily devastating to morale, and can only, in the long run, most seriously lower quality.

These are some of the unresolved dilemmas which confront us today between the conflicting claims of features that have given American science its greatness in the individuality of its past and more mechanical elements imposed by the mere maintenance of a massive scientific effort in our own day. These dilemmas will not be resolved easily, nor are they transient. Indeed, they may well be central issues with us for decades to come. They are most acute in federally supported research, and in that environment they will become more rather than less acute with the years. For inevitably the very massiveness of science will demand, in the coming decades, that a proportion of it even larger than at present be supported by the federal government.

And the present proportion is striking enough. Testimony given earlier this year by the Director of the Office of Science and Technology before the House Committee on Government Appropriations indicated that the government plans to allocate for the coming fiscal year the amount of 12.3 billion dollars in support of research and development in the nation. This sum represents the expenditure within a single year of more money than the federal government allocated to research and development through the entire interval from the American Revolution to and through the second World War. It involves some 15 per cent of the total federal budget. But, more significantly, it comprises well over one-third of the part of that budget subject, as it were, to voluntary control—the part that is not already irrevocably committed. The federal government today spends twice as much for research and development as the total spent by all universities, industries, and private foundations combined.

In 1950 the federal budget for research and development amounted to approximately 1.2 billion dollars—a striking contrast to the current figure. There is no indication that this pressure of increase will slacken. But it is interesting that, in contrast, our gross national product doubles about every twenty years. If the present rate of expansion continued unchecked, we should be spending our entire gross national product for research and development in seventy years or less. To be sure, such a calculation, though dramatic, may have little precise meaning. A large fraction of the sums

identified for research and development actually support development. Again, much that we label research and development today has by tomorrow become an accepted part of our way of life, thereafter to be identified in a different category, and supported accordingly. But the startling fact remains that, however steep or shallow the increase in coming years, the very volume of current federal expenditure on research and development is such that not only has it become a major item in our budget but, far more important, it imposes a significant tax on our total supply of scientific talent. Inevitably, it must exert a major influence on the availability of that talent in the future and on the very shape and quality it will assume.

Considerations such as these lead from the serious problems involved in so organizing massive federally supported research that its creativity is not destroyed to a matter even more serious, and one that will surely confront us with yet graver and more baffling dilemmas in the years ahead—the planning for science as a whole. It is clear that currents of such magnitude and import as those now sweeping science on its course, if allowed to flow undirected, if left to the whim of the winds, can bring incalculable damage, because their power to determine the shape and character of our future scientific scholarship is so great. They can, for instance, almost unnoticed produce massive imbalances among delicately related elements of our research structure. A vivid example is implicit in the call recently made for an increase in the number of doctoral degrees granted in the physical, mathematical, and engineering sciences from about 2900 in 1960 to about 7500 in 1970, an increase of more than two and one-half in ten years. An expansion of this order would clearly be highly desirable on general principles. Yet it runs the grave risk, by exceeding the available population of highly gifted scientific workers within the decade, of seriously diluting quality of scholarship. Moreover, it has been estimated that to train this number of workers adequately would require the services of some forty per cent of all those currently active in the sciences involved. Forty per cent, however, is not a likely figure for available teachers in view of the drain into federal research that a single enterprise, such as Apollo, can produce, and is in fact bringing about. So the competing claims of the federal government alone, left unchecked, are inherently capable both of seriously impeding one another and of most gravely unbalancing our whole pattern of scientific scholarship in a rather immediate future.

A further consideration underlines this issue yet more boldly. In an era when technology, and the science associated with it, have become so massive, the making of a single decision like that to achieve manned space flight can exert a decisive influence on the entire research resource of the

nation in terms even more fundamental than those of numbers or of balance. Most serious of all may be its potential impact upon diversity of training and commitment, upon plurality—in terms of the earlier biological analogy, upon the store of variability—in the scientific body politic which must constitute in the future, as it has constituted in the past, a precious and irreplaceable resource. Once a single such sweeping decision is made for reasons good or bad, relevant or irrelevant, what part of that priceless resource may then be swept irrevocably into a maw of activities structured about sharply committed goals? What part of that priceless store of variability may thus be permanently destroyed? What part may be annually consigned, during its formative years, to an environment that, even though it may mold effective operators in the areas of science and technology, may also irreversibly extinguish the full reach of their potential and make our society so much the poorer?

All the aspects of massive scientific effort—the order of expenditure in money but, far more important, the expenditure and allocation of talent in a situation where we may be close to scraping the bottom of the barrel—unite to emphasize that some order of long-range policy planning in the future, some general allocation of resources and of goals, whether we relish it or not, is likely to be an absolute necessity. We cannot, in the nature of things, simultaneously do all things well. And there is the very real danger that, without a careful and continuing general review of our over-all scientific activities in relation to their probable bearing on human welfare, we could find ourselves irrevocably overconcentrated in certain spectacular areas of science where past performance and present magnitude lend a luster that promise for the future does not match. Students of social development have pointed repeatedly to the historical tendency in some societies, as they became prosperous, to concentrate an increasing and undue share of wealth and energy upon goals which to be sure were conspicuous and remarkable and which ultimately became striking symbols of their age, yet which, from the standpoint of sheer investment of energy and talent, were but marginally pointed to their fundamental needs. Without continuing and careful thought about the problem there is a real danger that we too may be tempted to commit ourselves unduly to activities that run the risk of becoming more notable for display than for high and contemporary relevance.

Numerous and perceptive observers, in and out of government, have sensed another aspect of this clear demand for conscious foresight. When, as is increasingly the case, technological impacts are at once so pervasive and of such long-range effect that the moves of one generation radically affect the very environment of the following one and may to a considerable degree restrict the choices open to it, decisions respecting such moves

cannot be left wholly to chance or to spontaneous contemporary inspiration. The vital and frighteningly difficult questions of where and how and by whom such broad planning can and should be done within the area of technology will surely pose central issues of discussion and of thought through the coming decades. The close linking of science with technology, as well as the sheer vastness of modern science, makes it inevitable that for this same reason some measure of scientific planning too will be a necessity of our time.

There is a keen contemporary appreciation of this demand for scientific planning, witnessed by the inauguration of much thinking with respect to it in, among other places, the President's Science Advisory Committee and the Federal Council of Science and Technology, and within the National Academy of Sciences. But scientific planning, even more than planning for technology, is beset with imponderables, with contradictions, and with inherent dangers, many of them reminiscent of those surrounding questions of administration for a massive, predominantly federally supported science. To be sure, the broad issues of policy, though difficult to meet, are often readily identifiable. Questions of total size, for instance, questions of the shape of the effort in the future, questions of priorities, surely cannot be left strictly to ad hoc insights. But once again we face most serious and baffling questions. How shall we judge the relative merits of one field with respect to another? Shall our guess as to its bearing on human welfare, on social contribution, be the criterion? Shall we say that the biological sciences, currently showing such brilliant promise and achievement, should have a high priority in the share of material and especially of professional support, now and for the future? Shall we say, as has imaginatively been suggested, that a field which seems to have close underlying ties with several others should be given priority over more isolated areas of inquiry? How, indeed, shall we or can we determine degrees of relative importance?

As though such difficulties were not enough, there are more subtle ones inherent in dealing thus with science as scholarship. For here the way not only is laced with imponderables and fraught with the hazards of uninformed and sometimes uninformable judgments. It involves contradictions at a deeper level. Planning by its very definition assumes some known ends and deals with some specific consequences. It is hard enough to visualize the shape of such consequences for advanced technology. With science, not only is this feat utterly impossible but, as in matters involving accountability, the very assumption that the ends are known may damage one of the most powerful attractions of the whole activity and vitiate one of its great motivating forces. Again, the proposition that priorities can be assigned to one scientific field over another neglects the fluidity of such fields themselves and negates the tendency of the most fertile research minds con-

stantly to migrate from one field to another, or to create wholly new fields, as fresh growing points are sensed at the leading edges of the scientific effort. Today we speak of molecular biology as a field, now that it has brilliant achievements to its credit. But its very contemporary existence depends in large part on the fact that a rather small number of physicists and chemists, casting about after the second World War in search of an area of inquiry adequately challenging to creative abilities now released from the demands of conflict, drew bead on fundamental biology as their target. This, as it turned out, was major planning. But it was planning in a traditional scientific sense, a planning not only highly individual in character but conducted at the level of the work. It did indeed create a new and extraordinarily important area of inquiry. But possibly once the work in that arena has progressed so far that the discipline itself is firmly and publicly identified as a noteworthy formal scientific field, able to compete strongly with other fields in claiming its share of the available resources, the creative minority who opened it and those who have maintained its most lively work will have come to feel that its intellectual resources have been largely exhausted and will be ready to abandon it. Perhaps by the time conventional planning for it is well under way it will already, to all intents and purposes, be dead as scientific scholarship, while the real planners, assembled in enclaves which few beyond their immediate professional view are even aware of, will be creating the next great area of attention.

Perhaps no more vivid illustration than this could be adduced of the violently conflicting requirements of scientific planning at a general social level on the one hand and at the level of substantive creation on the other. It emphasizes anew at what peril to our fortunes do we confuse the two. And such confusion, unfortunately, is already much with us. It is well illustrated in various recent statements confidently asserting that our generation has invented the art of systematic innovation. How convenient it would be if this were true—if innovation in its profoundest sense were not, by its very nature, beyond all system!

Such considerations emphasize again and again how formidable are the problems that surround all planning in the arena of scientific scholarship, and underline the dangerous contradictions inherent in it. Yet none of them can negate the importance of scientific planning in its social context, with respect to its social impact, and, most emphatically of all, in respect of its own health. Undoubtedly we have a long and difficult road of exploration and of learning ahead. At this primitive stage of our knowledge and understanding perhaps the very most essential things that scientific planning can deal with, and the most significant for the future quality of scientific scholarship, will be those elements most protective of the scientific milieu:

planning to protect and increase our scientific diversity, to enrich rather than to impoverish our precious stores of variability; planning to protect and keep open the natural channels through which the substance of scientific scholarship must spontaneously evolve; planning to try to assure that the general areas to which we direct our keenest scientific effort be in broad terms of significant relevance to human and to social welfare, that, socially speaking, our investments of time and money and talents be of a solid kind.

Through all the coming years we must constantly remind ourselves that the requirements of science as scholarship, like those of living organisms, are manifold and delicate and subtle, and that it is indispensable to vitality that they be continually and adequately fulfilled. It will be essential to remember that, however much we may do for the environment of an organism, however much we may aid the expression of its qualities, it is at our peril that we tamper with its internal modes and regulations and controls, adaptively developed over the whole of its growth. For creative genius cannot be confined, else creation can be extinguished, or at the very least badly impaired, with incalculable losses. The future will clearly require from us imagination and sensitivity and wisdom, unremitting effort and also restraint, of an order greater, perhaps, than ever required before in the whole long history of our scientific scholarship.

The Year in Review

For at least two decades a familiar complaint about the progress of science describes the dangers accompanying the increasing and inevitable specialization. As Kenneth Boulding once expressed it, there is an opinion that "the Republic of Learning is breaking up into isolated sub-cultures with only tenuous lines of communication between them."¹ An intellectual anarchy is forecast, or, as Boulding expressed it further, "One wonders sometimes if science will not grind to a stop in an assemblage of walled-in hermits, each mumbling to himself words in a private language that only he can understand."² This is, of course, a refinement of the "two worlds" controversy outlining the constriction of capacities for communication between the sciences and the humanities. There is no doubt that the narrowing of channels of communication by specialization can be a source of friction for intellectual progress, and perhaps retard it significantly.

At the same time we should recognize that very few of the dangers described in the past have caused critical constrictions within science, and the vigor of interdisciplinary communication seems greater now than at any time since the days when one man could contribute to several major subjects of learning during his lifetime. One reason that interdisciplinary communication among the sciences is pursued so vigorously today is that every scientist who stands on a research frontier has either a reasoned understanding or an intuitive sense of a great overriding problem to which his research is directly related. Since science is essentially problem solving, this sense of overriding problem can be an exceedingly important stimulus to communication and common outlook. This deep-lying and compelling pressure for an ultimately unified outlook is usually forgotten in the popular expression of fears about specialization.

The sense of overriding problem has a unifying effect because these problems are remarkably few, when expressed in the most generalized manner. There are many ways in which they might be described or viewed. Each philosopher of science might have a slightly different interpretation. One

¹ Kenneth E. Boulding, General systems theory—the skeleton of science, *Management Sci.*, 2, 198, 1956.

² *Ibid.*

view of the overriding problems might divide them as follows: (1) the analysis of the structure and content of the cosmos treated by astronomy, astrophysics, and geophysics; (2) analysis of the particulate composition and structure of energy and matter treated by physics; (3) the origin, evolution, and comparative physiology of life forms; and (4) understanding the functioning of systems that include multiple numbers of often interdependent variables, especially life systems and subsystems and social systems.

One of these problems, or something akin to it, is likely to lie in the mind of nearly every research worker actively engaged on the frontiers of science, or at what has been termed a "growing point."

It is interesting to see how well the research of the Institution fits this sense of grand overriding problems. In some degree the Institution's research treats all four of the problems described in the view given above, and it is extensively concerned with three of them.

The Structure and Content of the Cosmos

The problem of the structure and content of the cosmos is, of course, one of the most ancient to excite man's intellectual curiosity, and the strides taken in recent years toward understanding it have been truly enormous. Each year adds many fascinating new pieces to our growing fund of knowledge about the cosmos, and each year the tantalizing problems opened by the new knowledge are an ever greater stimulus to research.

Through its several programs in astronomy and geophysics, the Institution has had a continuing interest in the great problems of the structure and content of the cosmos since its earliest years. Work in these programs includes every scale of distance from which observations can be made and every important type of instrumentation for such observation. Included are studies of other galaxies, stars, and interstellar matter within our own galaxy; of the sun; of planets other than the earth; of interplanetary phenomena; and of the earth itself. Among the billions of objects in the sky and the many phenomena that can be studied more closely at hand, observations are made on literally tens of thousands during a typical year like 1962-1963. Many of these observations, or experiments, are parts of continuing programs that produced no spectacular results or definite conclusions during the year. Nonetheless, they are all related to the overriding problem of describing the cosmos, and some of them may have laid the groundwork for results to be reported in future years.

Among all the results of science perhaps the most evocative to our imaginations are the observations that touch the edges of the known universe. The Mount Wilson and Palomar Observatories again produced data of

startling import on the nature of some galaxies. Like the discovery of the most remote objects yet observed (the cluster of galaxies 1410 + 5224 first reported in *Year Book 59*) the new discoveries depended upon the combined employment of radio telescopes and optical telescopes. It is thought that by far the most powerful radiator of energy thus far discovered in the universe has been found in the course of these observations. During the past three years a number of radio sources have been correlated with objects that appear to be stars on photographic plates. Yet the spectra of these objects are very unusual and for many months resisted interpretation. Using spectra he obtained this year and J. B. Oke's infrared observations, M. Schmidt has determined that one of these objects, designated 3C273, is a galaxy rather than a star, and that it is probably 100 times more luminous than galaxies like the relatively near-by Andromeda galaxy. Its radiation of energy is thought to be at the rate of 2.4×10^{38} calories per second—the equivalent of about 2640 billion suns of the same energy as our own. An abnormally strong absolute energy distribution in the infrared was shown for 3C273 by Oke. From this it is inferred that the continuous radiation is largely synchrotron radiation.³

By a similar type of analysis J. Greenstein has determined that another of these objects, the radio source 3C48, is likewise a galaxy with extremely powerful radiation. Its radiation also is abnormally large. Its luminosity is thought to be 30 times greater than that of any other previously known galaxy. This would make it about 100 times more luminous than our own galaxy. With a redshift of 0.367, the second highest determined for any galaxy, 3C48 may be the second most distant object yet observed optically. The observed phenomena are thought to indicate a superexplosion in the distant past, of which astronomers are now seeing the record. The release of energy occurring in these galaxies, unprecedented in all previous observation, is a subject challenging to astrophysical analysis and further observation.

At the same time Allan Sandage of the Observatories and C. R. Lynds of the Kitt Peak National Observatory have obtained interesting evidence that gigantic explosions have occurred in galaxies like 3C273 and 3C48, which have strong radio emissions. Photographs of the galaxy M 82 taken in hydrogen alpha light with the 200-inch Palomar reflector show a massive "filamentary" structure extending at least 10,000 light years above and below the major plane of the galaxy. Spectrograms taken along the axis of the filamentary structure show that the southeast part of the filaments is approaching the earth at the rate of 150 kilometers per second, but that the opposite, northwest part is receding from the earth at the same speed. This motion is not due to rotation, because it is along the minor axis of the

³ Radiation produced by the acceleration of electrons within a magnetic field.

galaxy. Their data suggest a linear relation between the velocity and distance, indicating further that all the matter in the expanding gas was in or near the fundamental plane of M 82 about 1,500,000 years before the stage of the galaxy recently observed.

Since the galaxy M 82 is not excessively distant (about 10 million light years) these observations are important to astronomy because they permit an inference about the general properties of radio galaxies. A review of photographic evidence from other galaxies indicates that such violent events are quite common. Thus a radio galaxy is thought to arise from an explosion of unknown origin in the galactic nucleus. "Relativistic" electrons⁴ are produced in these explosions. They give rise to radio emission through their interaction with the magnetic fields present. If the explosion is strong enough the gas may escape in directions perpendicular to the fundamental plane of the galaxy. After a time two regions of relativistic gas exist well away from the parent galaxy. They are the double radio sources which are common among the identified radio galaxies.

Interesting analyses bearing upon determination of the age and mass of our galaxy also were made during the year. Sandage and C. T. Kowal completed the photometry of 1700 selected stars to study high-velocity subdwarf stars in the vicinity of the solar system.⁵ These stars are the same type as globular cluster stars⁶ that have been used in many of the age determinations hitherto made for our galaxy. The subdwarf stars, however, are much nearer to the earth and are much brighter than the globular cluster stars. They are therefore subject to more precise measurement. Photoelectric measurements of the subdwarfs suggested that the critical color used in fixing the ages of the globular clusters might lie more toward the blue (i.e., denoting higher temperature) than hitherto determined. New photoelectric measurements of several clusters by Sandage did indeed show that they do. These data now indicate that the age of the oldest stars in the disk of the galaxy and the ages of the globular clusters that form a sort of "exoskeleton" for the galaxy are approximately the same. This newly determined age is about 12 billion years, about half of the earlier age determinations.

Another analysis of the globular cluster system of our galaxy by H. C. Arp yields a new and more definitive estimate of the position of the galactic centroid.⁷ It is now calculated to be 9.9 ± 0.5 kiloparsecs (about 32,000 light years) from the sun. After a study of the values of the constants of

⁴ Electrons whose velocities approach the velocity of light.

⁵ Subdwarf stars are smaller and denser than the "main sequence" stars, which are most common. See Carnegie Institution of Washington, *Report of the President 1961-1962*, page 59, for a diagram showing the general relation of the major groups of stars.

⁶ Globular clusters contain hundreds of thousands or even millions of stars in a very symmetrical and compact grouping.

⁷ The exact center of the entire system of stars comprising our galaxy.

galactic rotation and of the distance to the galactic center, Schmidt has constructed a model of the distribution of mass in our galaxy. The value assigned in this model is 180 billion solar masses, or the equivalent of that of 60 million billion earths.

The Institution's study of our own galaxy for some years has extended to interstellar matter as well as to stars. Such work has been carried on particularly by the radio astronomy group at the Department of Terrestrial Magnetism in their study of interstellar hydrogen. Because of the availability of a new instrument, some of the most fascinating observations of the entire program were made in 1962-1963. The Institution's mobile 90-channel hydrogen-line spectrometer was coupled with the new 300-foot transit telescope of the National Radio Astronomy Observatory at Green Bank, West Virginia, to study the hydrogen lines of the nearest external galaxies in a degree of detail never before possible. Particular attention was given to the great Andromeda nebula (M 31) and the spiral nebula in Triangulum (M 33). The opportunity to study the Andromeda nebula was considered particularly attractive because of its similarity in size and structure to that of our own galaxy. The perspective obtained from viewing the hydrogen distribution in an external galaxy avoids many of the ambiguities encountered in studying our own galaxy.

Even in the relatively short observing period (about two months) B. F. Burke, K. C. Turner, and M. A. Tuve collected data from which they made several significant observations. They note in their report that the hydrogen-line breadth in the Andromeda nebula is comparable in some regions to that observed in profiles taken of our own galaxy, although there appears to be a substantial difference between hydrogen distributions in the two halves of the nebula. They note also that interstellar hydrogen appears to be almost absent in the central section of the galaxy, a condition consistent with the presence of older stars there. On the other hand there is an interesting general agreement between hydrogen I density and the rate of bright star formation, mainly on the outer arms. They also observe a distinct lack of symmetry in the velocity of the hydrogen lines in comparing two halves of the galaxy. This is of special interest, because existing hypotheses assume symmetry for hydrogen-line velocities in our own galaxy. In addition, the type of radial outflow of hydrogen postulated for our own galaxy was not observed in the Andromeda nebula. Both these observations require a re-examination of the motion of interstellar hydrogen within our own galaxy.

Although studies of the sun and the solar system have been mainstays in the program of the Observatories since their inception, some of the more interesting results in recent years are reported, particularly for study of the planets. One intriguing observation began with a bit of Soviet-American cooperation. R. F. Howard, during a visit to the Crimean Astrophysical

Observatory, commenced a study of magnetic observations on sunspots associated with flares. Occasionally flares appear to be associated with cosmic-ray showers of unusual intensity arriving at the earth. Examination of the Crimean magnetic maps for a 1959 flare indicated a decrease in sunspot fields during the day of the flare. Howard's further investigation of flares responsible for ground-level cosmic-ray events in the last 20 years indicated that in all cases for which sunspot-area data are available the sunspots decreased in area from the day before to the day after the flare. We thus may have an indicator that distinguishes flares responsible for cosmic-ray showers from flares that are not. Howard computed that the energy lost in the magnetic field of the sun at the time of the flare of July 16, 1959, was substantially the same as the energy ejected from the flare in the form of cosmic rays.

During the year Olin Wilson of the Observatories completed a spectrographic investigation of more than 100 stars which has led to an interesting conclusion about the past output of ionizing radiation from the sun. From a study of main-sequence stars in the four clusters Hyades, Praesepe, Pleiades, and Coma he has concluded tentatively that the activity of the chromosphere in these stars decreases with time.⁸ The observed chromospheric activity among the stars studied decreases in the order: Pleiades, Hyades and Praesepe, and the sun. This is also the order of increasing age. The Pleiades are estimated to be approximately 50 million years old; the Hyades and Praesepe stars, 500 million years old; and the sun, approximately 5 billion years old. These observations suggest that the sun must once have had a much more powerfully emitting chromosphere than today. Therefore, in earlier epochs the earth and other planets were probably subjected to a greater incidence of ionizing radiation than today. This finding is of more than passing interest for hypotheses about the evolution of the earth's atmosphere, its hydrosphere, and other earth features that ultimately affected the origin of life on this planet.

Observations of other planets at the Observatories yielded an unusual amount of significant information during 1962-1963. There has, of course, for many years been great popular interest in the planets and their satellites because they are relatively near, and are the only observable objects whose environmental conditions even roughly approach those of the earth. Interest in studying them has increased greatly, however, as national plans for the exploration of the planets have been made. Information about the chemical compositions, temperatures, and atmospheric pressures of the planets has become of practical importance. By fortunate coincidence this increased need for information and increased interest in the planets has been paralleled

⁸ The chromosphere of a star is the next to the outermost layer of its "atmosphere." The chromosphere of the sun extends for several thousands of kilometers outward from the photosphere, or visible part.

by recent technical advances in observing instruments, most particularly the development of new infrared detectors of very high sensitivity.

The two most striking results obtained during the year were from observations of Venus and Mars. The observations of Venus were of special scientific interest because they were made during the period when the Mariner satellite probe passed close to Venus. B. Murray, R. Wildey, and J. Westphal of the California Institute of Technology at this time mapped the surface of Venus in the far infrared spectral region with instruments attached to the 200-inch Palomar reflector. They obtained a temperature map of the upper atmosphere of Venus for each of five successive nights. A substantial amount of hitherto unavailable information about the circulation of the atmosphere around Venus is given in these maps, as well as data indicating the presence of a violent atmospheric storm near one limb of the planet on one of the five nights. The continued utility of ground-based observations of the planets was thus brilliantly confirmed.

Mars is the planet whose temperature and other surface conditions are thought to duplicate those of the earth most closely. The atmosphere of Mars, therefore, has been a subject of special interest for a long time, as investigators have attempted to determine its content of water vapor and oxygen. G. Münch of the Observatories, and L. D. Kaplan and H. Spinrad of the Jet Propulsion Laboratory, made a new series of high-dispersion spectrograms of Mars with the 100-inch reflector at Mount Wilson. One of them, taken on a night when the atmospheric humidity over Mount Wilson was unusually low, shows for the first time four spectral lines of water that can positively be associated with Mars. These lines were detectable because Mars was moving away from the earth at the time the spectrogram was taken in April 1963. Consequently, the Martian spectral lines for water were "Doppler-shifted" (i.e., offset) away from the spectral lines due to water vapor in the earth's atmosphere. The strength of the lines indicated between 0.01 and 0.02 millimeter of condensible water in the atmosphere over Mars. This is indeed a minute amount in comparison with that in our own atmosphere, being probably not more than 1/200 of the minimum found over dry areas like the Sahara or the Arabian deserts.⁹ Such a low quantity of water vapor would be unfavorable to the existence of life in any form resembling terrestrial types. It is of further interest that the same spectrogram clearly shows lines that are assignable to carbon dioxide.

The Earth as Part of the Cosmic Problem

From our point of view the earth itself, of course, is a highly important part of the cosmos. It has importance going beyond the satisfaction of our

⁹ The antarctic atmosphere is the driest on earth, containing about 0.07 millimeter of water vapor, according to the United States Weather Bureau.

natural curiosity about the planet that is our home. It is of enormous value to us in studying the universe because it is the most accessible object. All the known chemical elements are to be found on the earth; it is incomparably the richest source of information on the molecular combinations into which these elements enter naturally, and it is an abundant source of data on naturally occurring electromagnetic phenomena. From the scholar's point of view there is still a very rich field for discovery through geophysical investigation of the earth and its environments, in spite of the fact that it is the only planet about which we can yet lay any claim to detailed knowledge.

Approaching the earth from outer space, as we are in this review of our research relating to the overriding cosmological problem, one encounters first the electromagnetic phenomena and the low-density matter diffused for 25,000 miles or more into space from the earth's surface. From the very beginning of its operational programs, the Institution has shown an interest in these phenomena, first in its pioneering study of geomagnetism, and later in its ionosphere and cosmic-ray programs.

During the past year S. E. Forbush completed a study of the amplitudes and phases of cosmic-ray ionization, cosmic-ray activity, and sunspot numbers for 1937 through 1961. During these 25 years the period of the sunspot cycle, that is, the time from one year of maximum sunspot numbers to the next maximum, was exactly ten years. Thus, data were available for roughly two and one-half cycles. Since the existence of connections between solar activity, cosmic-ray activity, and geomagnetic activity is now well established, the construction of a theoretical model to explain solar-cycle variation of cosmic rays is now desirable. Dr. Forbush's correlations of geomagnetic and cosmic-ray phenomena with sunspot numbers have given important information for the development of such a model. His data show that the maximum for geomagnetic activity (day-to-day fluctuations in field intensity) and the maximum for cosmic-ray activity (day-to-day fluctuations in cosmic-ray ionization) occur about three months after the maximum for sunspot numbers. The minimum for cosmic-ray ionization occurs three months after this, or six months after the maximum for sunspot numbers. In other words, the maxima for cosmic-ray ionization occur six months after the time of sunspot minima. Other analyses by Dr. Forbush indicate that the rate of cosmic-ray ionization is related not only to magnetic "storms" over the earth but also to some other condition or conditions in interplanetary space. His data are significant to refinement of the gradually emerging concepts of the extremely complicated mechanism of energy transfer between the sun and the earth.

Thus we come in our voyage inward from the cosmos to the surface of the earth itself, with its own fascinating component of the cosmological problem. The geophysicist of today must, in a sense, have something of a kindred feeling for the anatomist of the Middle Ages. The latter had to infer

structure and function of the interior of the human body from its surface appearance, for in some places dissecting a corpse carried a death penalty. The geophysicist is in a somewhat more fortunate position, for there appear to be no penalties attached to his dissecting and probing. His detailed observation still can reach through only the merest epidermis of the planet's surface. Yet there are many fundamental questions about the structure and behavior of a planet to which he must try to find an answer in his epidermal observations. What is the composition of the materials composing the interior of the earth, from its surface down to the center of its core? What is the structural relation of those materials by level? What goes on within the earth that causes the earth's magnetic field? How did the planet evolve, and what was its earliest form?

The probes with which the geophysicist seeks answers to these questions (for Nature permits him very little dissection) are fascinating in themselves. Within the Institution in recent years they have included a search for indicators of the temperature gradient within the earth, the use of seismic waves (either earthquake or explosion induced), the study of isotopic differentiation among rock minerals, the laboratory synthesis of minerals thought to be found within the mantle of the earth, statistical analysis of mineralogical relations, and still other approaches.

One of the deepest probes now possible into the earth's interior consists in the interpretation of seismic waves. For the last three years specially set explosions have again supplied waves for interpretation. During the past year such experiments were performed in North Carolina, using for the first time the technique of long receiver arrays (several kilometers) to measure the apparent velocity of wave arrivals, that is, the actual velocity of waves at the greatest depth of their travel. These experiments showed that the velocity of seismic waves increases continuously and evenly in that area from a depth of 20 kilometers to a depth of 36 kilometers, which appears to be the base of the earth's crust there. The results indicate that the rocks in the lower part of the earth's crust are a continuously changing mixture that becomes more basic in chemical composition with increasing depth. Other observations on local earthquakes, made particularly in the Peruvian Andes, have shown a rather high energy absorption for seismic waves at about 400 kilometers within the earth. The geophysical meaning of the absorption is not known, but, since any change in seismic wave properties must be correlated with some change in property within the crust or mantle of the earth, further inquiry seems attractive.

The geographical differentiation of the major masses of rock, both by composition and by age, has presented geological and geophysical problems of long standing. Gradually the most recalcitrant of these problems are receiving partial answers as modern research techniques are brought to bear on individual questions. Two such problems are the reasons for the dif-

ferences between the rocks of the continents and those underlying the ocean basins, and the ages of the non-fossil-bearing rocks of the earth's crust.

F. Chayes, of the Geophysical Laboratory, has adopted an unusual approach involving modern data reduction techniques and chemical sorting criteria to provide a highly interesting generalization on the first of these two questions. Petrologists have long suspected a fundamental chemical difference between the Cenozoic volcanic rocks of the ocean basins and those dominant on the continents; particularly on the continental margins. The Cenozoic period, which includes our own time, has been marked by violent and prolonged volcanic activity of global extent. The complexity of Cenozoic volcanism on the continents and the very large amount of chemical data to be analyzed, however, have discouraged generalizations based on geography. The apparent overlap in the composition of the mafic¹⁰ lavas between the oceans and the continents made it impossible to design a key to any acceptable general distinction. Chayes now presents striking evidence that he has such a key for the separation of the lavas of the ocean basins from lavas on the shoreward side of the deep trenches that separate much of the Pacific Ocean from the marginal continents and are also found in some peripheral areas of the Atlantic and Indian oceans. From a machine analysis of relevant chemical data taken from more than 7000 analyses of Cenozoic rock samples, Chayes has shown a nearly 92 per cent correspondence between geographical class and chemical composition. Chayes's analysis adds to earlier criteria a distinction in titanium dioxide (TiO_2) content. Chayes says that the relation shown by his results "seems one of the firmest generalizations yet to emerge from the study of Cenozoic volcanism." Yet, as so often happens in science, his answer raises another and yet more difficult question. The same petrographic associations he has distinguished so clearly on the continental margins and in the ocean basins are also found in shallow seas and on the continents themselves, closely adjacent to each other. Why should they be so geographically distinct as between the ocean basin and its margin, and yet show no regional separation on the continents?

Within the last decade increasing progress has been possible in obtaining a picture of the ages of Precambrian rocks and crustal movements. Isotope geology, to which the Institution has been a major contributor, is now a firmly established basic tool for unraveling the threads of ancient regional geological history. These techniques, which depend on the identification of the isotopic products of radioactive decay, are improved yearly. The puzzle of the once discordant ages of decay products (lead, strontium, argon, etc.) is now becoming a path to real understanding of the processes involved in fundamental geologic events. Not only original ages but also events in the rocks' subsequent geologic history can be determined by isotopic study.

The activities of the geochronology and isotope geology group in the De-

¹⁰ Mafic is a mnemonic term for rocks in which ferromagnesian and related minerals predominate.

partment of Terrestrial Magnetism and the Geophysical Laboratory¹¹ continued a pattern set in preceding years. Members of this group select their research with a view toward exploring its full potentialities and arriving at a generalized understanding of each facet of the results. To this end, regional dating of geologically significant ancient rock complexes and metamorphic events in Ontario, Alberta, and Finland, was undertaken. The work on the Maryland Piedmont, reported in previous years, also was continued. All these areas contain very ancient rocks, whose ages are to be measured in hundred of millions, and even billions, of years. In addition, an interesting study to test the effectiveness of these techniques in dating the complex geologic events that formed the Swiss Alps about 25 million years ago was undertaken on the igneous and metamorphic rocks of the St. Gothard massif. A further extension of the technique was started, the study of the origin and source of oceanic serpentinites. This is of particular interest because it may be capable eventually of testing models of the evolution of ocean basins.

Another major geophysical problem is the distribution of heat within the earth, particularly the thermal gradient along a radius from the surface of the globe to its core. Rough estimates of the gradient can be made by measuring the earth's electrical properties and the heat flow from the interior. Also, information about the temperature at depth is contained in mineral assemblages known to have been formed at given depths. Here the important place of the laboratory experiment in modern geophysics is clearly revealed. For example, the diamond-bearing kimberlites in the mines exploited in South Africa characteristically contain two pyroxene minerals: one like diopside ($\text{CaMgSi}_2\text{O}_6$) and the other like enstatite (MgSiO_3). The amount of enstatite present in a mutual solid solution with diopside, as in mutual solutions of other pyroxenes, is known to be a function of temperature. During the year B. T. C. Davis of the Geophysical Laboratory showed experimentally that the solubility of enstatite in diopside is, however, independent of pressure up to 30,000 atmospheres.

This discovery is described by the Director of the Geophysical Laboratory as highly interesting because it provides a method of estimating temperatures of formation of pyroxene minerals not dependent on knowledge of the pressures of their formation. For the diopsidic pyroxenes from the kimberlites the temperature of formation indicated is about 1000° . These pyroxenes have crystallized with diamond, and the minimum pressure at which diamond can form at 1000° is 40,000 atmospheres. This pressure would correspond to a depth within the earth of about 125 kilometers. Such a temperature at 125 kilometers is consistent with the lower limits of the

¹¹ In 1962-1963, S. R. Hart, L. T. Aldrich, G. L. Davis, G. R. Tilton, H. Baadsgaard, O. Kouvo, and R. H. Steiger.

temperature range estimated from heat-flow measurements in the ocean basins and the electrical properties of the earth's interior. Such a temperature also implies that lavas that have come to the surface with temperatures of 1150–1200° have formed at depths as great as 200 kilometers within the earth.

Like isotopic analysis, temperature-pressure experiments on geologic processes can be fitted to either end of the geologic time scale. Continuing an interest of several years, T. C. Hoering and P. H. Abelson of the Geophysical Laboratory obtained strong new evidence about the method of formation of petroleum. Hoering and Abelson found that mild thermal degradation of kerogen yielded a series of saturated straight-chain hydrocarbons that are especially abundant in natural petroleum. These hydrocarbons range from methane (C_1) through *n*-dodecane (C_{12}). The hydrocarbons produced in the laboratory were found to have an increasing content of C^{13} with increasing molecular weight. This distribution of stable carbon isotope ratios bears a striking similarity to that previously observed in natural petroleum. The reactions studied in the Laboratory therefore seem very similar to those occurring in Nature.

Hoering and Abelson were attracted to the study of kerogen, an insoluble substance found in sedimentary rocks, because it is the largest store of fossil organic matter on earth. There are estimated to be at least 7,300,000 billion short tons of it in the earth's crust. Its mass alone makes kerogen an important geochemical component. Knowledge of what happens to it over extended periods adds significantly to an understanding of processes taking place in the upper crust of the earth.

The Origin, Evolution, and Comparative Physiology of Life Forms

The kerogen studies have also given an interesting lead related to another of the overriding scientific problems set forth at the beginning of this discussion, namely, the origin, evolution, and comparative physiology of life forms. Hoering and Abelson have found that the yields of the simplest hydrocarbon, methane, are much greater from organic materials from older rocks than from the kerogen of recent formations. Hydrocarbons obtained from the Green River shale,¹² 40 million years old, yielded a proportion of methane to pentane that was only about 1/15 that of a "carbon leader" from South Africa that is 2.2 billion years old. Although these differences may reflect the effects of time and temperature, there is a strong possibility that the original composition of organic matter in the South African rock

¹² An extensive formation in Colorado, Utah, and Wyoming, thought to be the world's largest reserve of fossil organic matter.

was much different from the composition of organic matter in the Green River shale.

Two other research efforts related to paleogeochemistry deserve mention because of their connection with the overriding problem of the origin and comparative physiology of life forms. P. L. Parker of the Geophysical Laboratory analyzed the isotopic composition of all life forms and deposited sediments within a "closed" inshore marine community in a Texas estuary. He found that the carbon¹³–carbon¹² ratios were stable for individuals of the same species, though showing an interesting range among different species. Moreover, he found that the isotopic composition of the sediment underlying the community of algae, grass, fish, and shellfish could be accounted for by a process of simple deposition from the decaying remains of the organisms. This finding is considered of interest because a detailed knowledge of the relation between the C¹³ of plant and animal communities and the C¹³ of their sediments might permit the construction of useful inferences about fossil communities of which only deposited sediments now remain.

G. Allen, also of the Geophysical Laboratory, turned his attention to a much more difficult question, namely, tracing the process of chemical evolution that preceded and led to the first life forms. Allen has attempted to demonstrate experimentally the suggestion of several previous students that the direction of chemical evolution of the first macromolecule predecessors of nucleic acids and proteins might have been controlled not by simple chance but by a process resembling natural selection. In a steady-state ocean having a high chemical potential, some catalysts might be more effective than others, preferentially promoting the synthesis of some compounds over others. The self-synthesizing systems that were most compatible with the effective catalysts would be increased differentially, as would the multiplication of molecules structurally related to these catalysts. Allen's research was designed to test these hypotheses. His results during the year were negative, but this obviously has a very high risk.

Perhaps more than any other single subject the science of genetics has had to keep constantly in mind the overriding problem of the origin, evolution, and comparative physiology of life forms. The discovery of the chromosome, the evolution of the gene theory, the discovery of the mutability of genes, the discovery of the chemical structure of the basic building block of heredity—the DNA molecule—and the discovery of the interspecific homologies of DNA have all been gigantic steps in shaping our thought on these matters. Biochemical genetics, indeed, remains a research frontier, probing ever deeper into the materials that have been responsible for the remarkable diversity and volume of life on earth.

The Genetics Research Unit, successor to the Department of Genetics,

has continued the Institution's long tradition of sustained contribution in this field. A. D. Hershey and his associates¹³ went farther on the fascinating path they have opened in examining the biochemical structure of the single chromosome possessed by each bacteriophage particle. They are seeking to chart the structure of that single chromosome, and to discover what aspects of that structure can account for synapsis, heterozygosis, genetic deletions, and other genetically familiar and chemically obscure phenomena.

Hershey reported last year that three phages used in his experiments (T2, T5, and lambda) contain a single molecule of typical double-helical deoxyribonucleic acid (DNA) per particle. The length of the molecule was found to be characteristic of the species of phage. Through a series of ingenious and delicately precise techniques of measurement and study, Hershey and his associates have added further intriguing results to their study of this simplest of all chromosomes.

During the report year E. Burgi was able to measure the length of the chromosome of mutant strains of lambda phage. She found them to be 20 per cent shorter than the normal lambda phage molecules, and she discovered that the deleted sections had a lower guanine-cytosine content than the molecule as a whole. Hershey and Burgi found that each molecule of phage DNA carries two cohesive sites, one situated near each end of the molecule. These sites will adhere to each other, forming rings, linear dimers, and linear trimers. Although the cohesive sites adhere to each other, they will not adhere to other parts of the molecule on which they are found or to other DNA.

Gisela Mosig, working from a previous discovery, separated T4 phage DNA into particles of three classes. Two of them were individually infective, but a third, shorter class was infective only if two or more particles attached to a single bacterium. Genetic analysis showed that different individual particles of the third class lack differing parts of the gene complement for phage reproduction. In multiples of two or more, however, the entire genome might be found. These molecules, which are remarkably consistent in length, seem to be nonetheless segments cut at random with respect to the position of the genes.

Hershey also reintroduces the interesting subject of similarity and differences among species in the base composition of their DNA. He refers to work done some years ago in which it was discovered that the nucleotide composition of DNA's in bacteria were specific to each species. Bacterial DNA's were shown to vary in combined guanine-cytosine content from about 25 to 75 per cent. The content from any one species strain is relatively uniform. It is thought that DNA base composition is an indicator of

¹³ E. Burgi, F. R. Frankel, E. Goldberg, L. Ingraham, and G. Mosig.

phylogenetic origin and that the internal homogeneity in DNA composition within any chromosome is a measure of its age, that is, the time it has maintained its structural integrity. The lambda phage chromosome with which Hershey and Burgi recently have experimented has a base composition similar to that of its bacterial host (*Escherichia coli*), but its DNA is internally heterogeneous. The internal heterogeneity within lambda may mean that it contains a "young" chromosome of diverse origins. It also may very well reflect an effective functional differentiation among the segments of the lambda DNA molecule.

The Biophysics Group¹⁴ of the Department of Terrestrial Magnetism also experimented with the properties of phage lambda DNA. Using their newly invented DNA agar gel technique, they found that about one-third of the DNA of phage lambda would combine with *E. coli* DNA. Thus it may be concluded that one-third of the phage lambda DNA is homologous with *E. coli* DNA. Hershey suggests in his comment on the Biophysics Group's experiments that these homologous DNA segments must have a common origin and related functions and that they are most attractive material for further study. By the same technique it was found that lambda DNA would also combine in significant percentages with the DNA's of other bacteria (*Salmonella*, *Shigella*, and *Aerobacter*) and would not combine with some other DNA's tested.

The DNA-agar technique developed by the Biophysics Group deserves a word in itself, because it has opened so many exciting paths in the study of relations among basic genetic materials. The Group has found that single-stranded DNA, previously prepared by heating, can be fixed by mixing with a hot solution of agar. A suspension of DNA-agar particles is then prepared by passing the cooled mass through a sieve. The particles of the suspension form a very open structure which will allow large molecules to diffuse freely through the suspension. Thus the complementarity of other DNA's than the one contained in the suspension, or of messenger ribonucleic acid (RNA), can be tested, for the complementary nucleic acids will be combined with the agar DNA. Radioactive labeling offers a convenient means of measuring the degree of combination. Experiments have shown that more than 80 per cent of the agar-entrapped DNA of a species retains its capacity to form double-stranded structures with other DNA of the same species. The complementarity of RNA, which will adhere to about half the available DNA sites, is also revealed by the method.

These techniques have opened an exciting new prospect for research which is related to the overriding problem mentioned above: the origin, evolution, and comparative physiology of different life forms. As the Biophysics Group

¹⁴ In 1962-1963, E. T. Bolton, R. J. Britten, T. J. Byers, D. B. Cowie, B. Hoyer, B. J. McCarthy, K. McQuillen, and R. B. Roberts.

comments in its report this year, "the presence of genes in common may be taken as a guide, not only to taxonomic relationships among organisms, but also to probably evolutionary relationships." Because reproduction is commonly very species-specific, the usual breeding methods of genetics are of limited use in determining gene similarities. The design of a method that may permit reliable chemical determination of relations therefore becomes of extraordinary interest. The objective is to detect nucleotide sequences held in common between or among the different DNA's, following the hypothesis that sequences held in common represent similar genes. Moreover, homologies of phenotype¹⁵ could be distinguished from homologies of total genotype. The former would be revealed by the degree of complementarity of messenger RNA-DNA, and the latter by the degree of complementarity of DNA-DNA. Such possibilities have already been suggested in the mention of the phage lambda-*E. coli* comparison made above.

The Biophysics Group carried on another series of experiments comparing the interaction of the RNA's and the DNA's of different organisms. Experiments investigating the compatibility of radioactively labeled messenger RNA and DNA of *E. coli* with the DNA of a variety of other bacteria revealed significant homologies of both the *E. coli* DNA and RNA with the DNA's of other bacteria. No significant interaction of *E. coli* DNA or RNA with vertebrate DNA's was discovered. Interestingly, the ratios of *E. coli* DNA to *E. coli* RNA bound by the DNA of a given bacterium differed from species to species, suggesting that the interactions do indeed reveal phenotypic as well as genotypic relations.

Experiments with nucleic acids of animal origin show that these techniques may be applied also to the study of evolutionary relations among higher organisms, including mammals. Experiments with the interaction of mouse, rat, hamster, and guinea pig showed 75 per cent of the mouse DNA to be homologous to agar-trapped DNA from a rat. The percentage of homologous material in the mouse-hamster relation was 60. Still other preliminary experiments indicated that there is a significant homology between DNA from human tissue culture cells and those of animals. A 25 per cent cross reaction was found when human DNA was exposed to mouse DNA or calf DNA. There was even some interaction with an agar-trapped salmon DNA (5 per cent). The Group observes that these results imply "the existence of common genetic material which has been conserved during the course of vertebrate evolution." They say that there may be "some genetic homology extending from man to fishes." The Group further states, "It is conceivable that the sensitivity of the method may be increased sufficiently to provide new evidence concerning the most probable line of evolution of

¹⁵ Phenotype—a grouping based on homology of visible characters; genotype—a grouping based on the same hereditary characters.

the vertebrates from the invertebrates . . . the interaction between human and fish DNA gives hope that even . . . distant homologies can be found and measured."

Using more traditional genetic methods of experiment, W. M. Hiesey, M. A. Nobs, and H. W. Milner at the Department of Plant Biology produced some interesting evidence that the genome has integrity also for races within a single species. Data accumulated from the crossing of different altitudinal races of yarrow (*Achillea*) and crossing different races of monkey flower (*Mimulus*) were subjected to detailed statistical analysis. The analyses gave clear support to the principle of genetic coherence, the tendency for biological characters to be inherited together as a unit rather than in purely random recombinations; that is, the progeny of a racial cross tend to separate themselves into lines that resemble one parent or the other rather than being randomly hybrid. For the monkey flower, 94 per cent of the possible scored parental combinations of characteristics were significantly correlated in progeny with one or another of the parental races. Hiesey, Nobs, and Milner suggest that distinguishing features of contrasting ecological races are transmitted by systems of multiple genes whose components are carried in more than one chromosome. They suggest that the combinations of dissimilar characters distinguishing a race are transmitted together because they are "loosely tied together through genetic linkage of the multiple-gene systems. Thus combinations of characters that have attained equilibrium by natural selection tend to be preserved."

J. Clausen offers further evidence for genetic coherence from a different point of view. From his study of tree lines in the Sierras, southeast Brazil, and elsewhere, he states that "the limits of tree growth are determined not only by altitude and latitude and other factors of the environment, but to an even greater extent by the nature of the germ plasms of the tree species themselves." Clausen found a zone in the high Sierras where the erect tree or bush forms, characteristic of lower and intermediate elevations, and the elfinwood and "lawn" races, characteristic of the tree-line area, freely intermingle. Even though intermediate forms are to be found in these zones, rigid natural genetic selection appears to sort the tree and bush races suited to the lower elevations from the dwarfer forms suited to the higher elevations in the same manner as has been observed experimentally for the yarrow and monkey flower plants.

The Functioning of Systems with Multiple Variables

Another of the overriding problems mentioned in the introductory paragraphs was understanding the nature of systems. By a system is meant any entity of interacting, interdependent parts. The study of systems is at least

as old as medicine, but it is only within relatively recent years that the pervasiveness of systems in the physical and biological worlds has been realized. Even more recently it has been recognized that systems are classifiable and that there are useful generalizations to be derived about systems per se. If we include gravitational fields, as we must, the pervasiveness of systems may extend to as yet unobserved limits of the universe. To think in terms of systems or subsystems, therefore, is to recognize an overriding problem that is truly omnipresent in the structure of the universe.

Very little of the Institution's activity during the year would be considered systems analysis in the formal sense. All the examples given below might qualify as related to another overriding problem. Yet, in the minds of those undertaking the research, a particular system relation was the dominant motif to be examined. The results are expressed either in describing a system or in a hypothesis that recognizes the existence of a system. The description of the behavior of a system is an important part of the approach. Our examples are chosen from both the physical and the biological sciences.

The Geophysical Laboratory has been interested in systems longer than any other group within the Institution. The word "systems" appeared in a report of the Laboratory more than fifty years ago.¹⁶ The study of mineral systems not only has helped to clarify the relations among minerals themselves but also has opened new horizons in field geology. It now forms a large share of the total activity of the Geophysical Laboratory. Among several examples of equal merit one is chosen for illustration, the work of the Laboratory on ore minerals.

In a classification of different types of systems, mineral systems are among the less complex, having generally less dynamic informational feedback than life systems. In Boulding's description, they are "clockworks" systems.¹⁷ Yet these systems are exceedingly important in nature, particularly in the physical world, and they especially reflect the composition of matter and its many forms on the earth's surface or within its crust, or within other parts of its interior. More and more the study of mineral systems is revealing new and significant, even economically important, information about the manner of formation and structure of the earth's surface and interior.

G. Kullerud and H. S. Yoder, Jr., discovered during the year that sulfur, known as an easily reactive element, may have hitherto unsuspected influence in mineral formation. Their experiments demonstrated that sulfur readily reacts over wide temperature-pressure ranges with many of the rock-forming silicates that are so widely distributed in the earth's crust.

¹⁶ E.g., "The binary systems of alumina with silica, lime, and magnesia . . ." *Year Book* 8, 104, 1909.

¹⁷ Boulding, *op. cit.*, page 202.

Metallic elements like iron, manganese, nickel, cobalt, and copper, originally present in these silicates, react in the presence of the sulfur to produce sulfides and oxides, which are the minerals of common ores. The experiments showed that, where original silicates contain even moderate amounts of iron or related elements, the addition of only a few per cent of sulfur profoundly changes the mineralogy of the rock. For example, if sulfur is added to an iron silicate like fayalite (Fe_2SiO_4) and the mixture is subjected to the appropriate heat and pressure,¹⁸ pyrrhotite (Fe_{1-x}S), magnetite (Fe_3O_4), and quartz (SiO_2) will be formed. If larger amounts of sulfur are used, hematite (Fe_2O_3) will be formed instead of the magnetite; and if still larger amounts of sulfur are present, sulfur dioxide will be formed along with the pyrrhotite and quartz.

These relations appear diagrammatically in figure 1, taken from the report of the Geophysical Laboratory. The tetrahedral diagram shows the

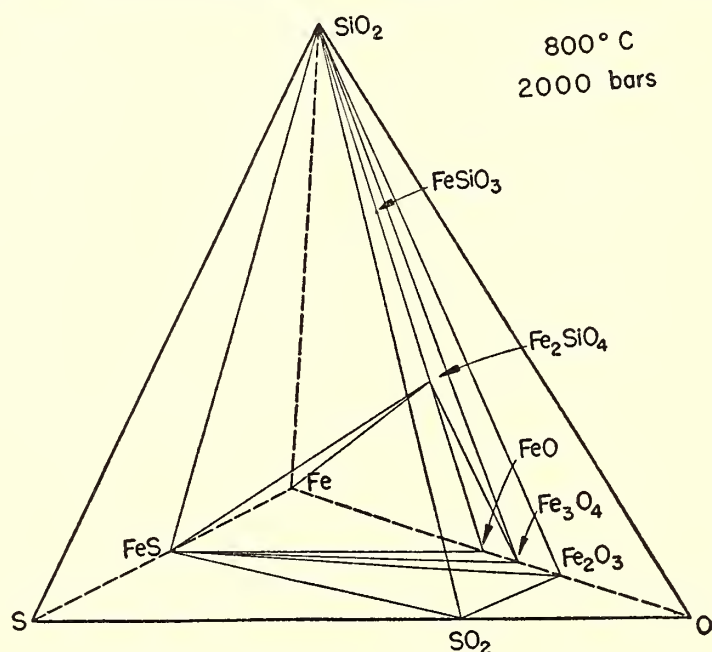


Fig. 1. A phase relations diagram of the quaternary mineral system including sulfur, iron, oxygen, and silica at 800°C and 2000 bars. The relations among the four components of the system are shown in the form of a tetrahedron with each of the four components at a corner. The minerals resulting from a given quantitative relation of the four components of the system are shown by connecting lines. Thus, at a temperature of 800°C and pressure of 2000 bars with 75 mole per cent sulfur, pyrrhotite, quartz, and sulfur dioxide are the products that result from heating iron silicate and sulfur together. For other temperatures and pressures, or other metals, somewhat different diagrams would reflect the somewhat different phase relations. There are many subsystems for the known materials, but few as yet are completely explored.

Meaning of symbols:

Fe	iron	Fe_2SiO_4	fayalite
FeO	ferrous oxide	O	oxygen
Fe_3O_4	magnetite	S	sulfur
Fe_2O_3	hematite	SiO_2	silica; quartz
FeS or Fe_{1-x}S	pyrrhotite	SO_2	sulfur dioxide
FeSiO_3	ferrosilite		

¹⁸ In this instance 800°C and 2000 bars. A bar is 1.013 average atmospheres.

mineral assemblages resulting from the presence of differing quantities of sulfur. Other experiments with more complex silicates gave results similar to those for the fayalite. Not only did the sulfur combine with the metallic components, but any metal not combined with the sulfur reacted with oxygen to form an oxide. The state of oxidation of these metals thus increases when sulfur is present. Oxidation in a silicate rock, therefore, may be accomplished by the addition of sulfur; no addition of oxygen to the system is necessary. Kullerud and Yoder conclude that these reactions indicate "the very significant role played by sulfur in determining the stable assemblage of silicate minerals in both igneous and metamorphic rocks." In a full understanding of the mineral systems that include silicates, sulfur, and metals there are likely to be important clues for the discovery of ore bodies.

Hundreds of other experiments on at least a dozen other mineral systems were run during the year. That the charting of relations within these systems can be extremely complex is illustrated in figure 2, which shows the predicted liquidus relations¹⁹ for an important mineral group, the pyroxenes.

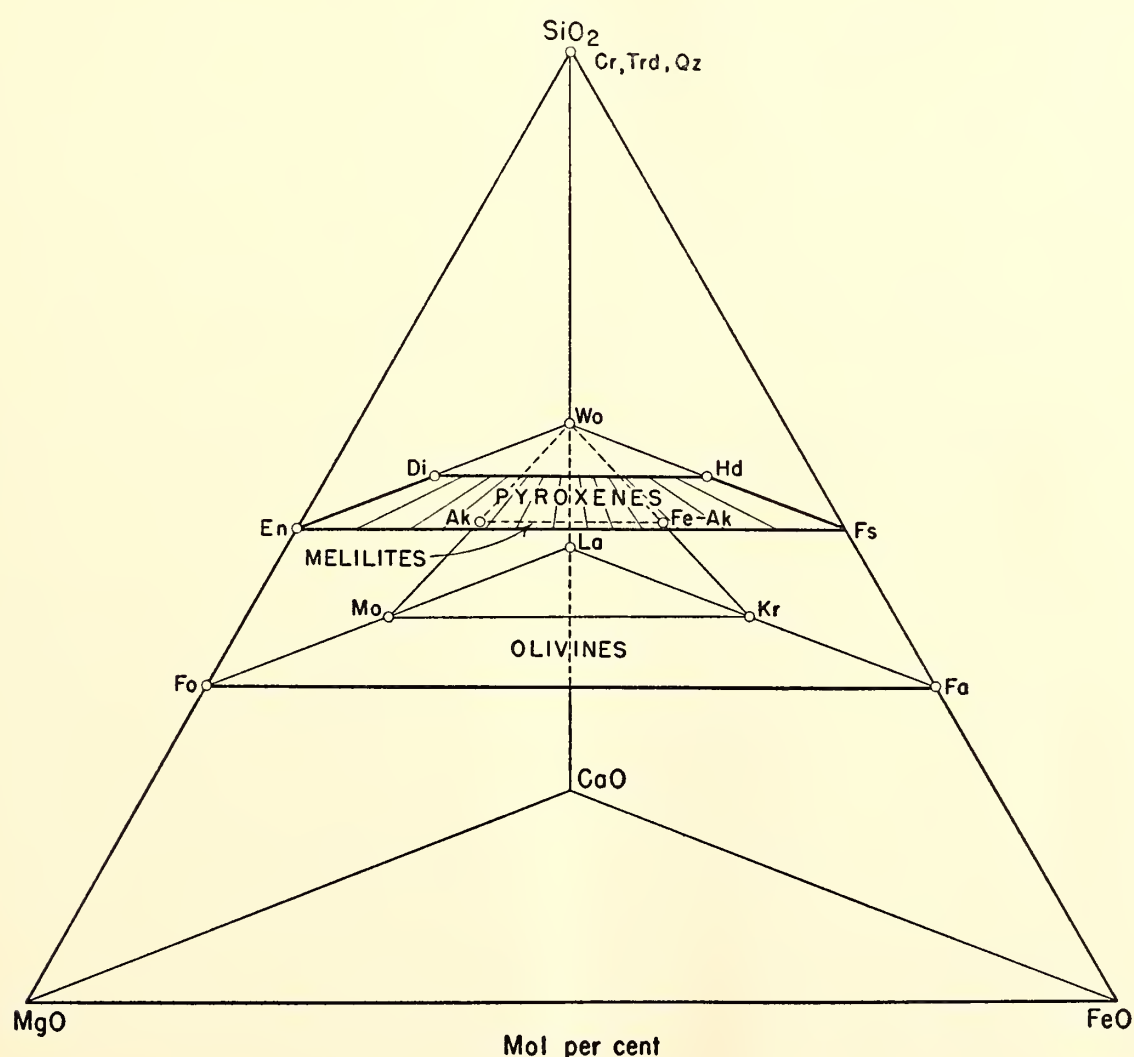


Fig. 2a. Diagrammatic tetrahedron illustrating in general the position of the pyroxenes as related to the basic components and the oxides of silicon, magnesium, calcium, and iron.

The symbols are explained in the legend of figure 2b on page 44.

¹⁹ In general, a "contour map" indicating the first mineral phases to form in various "regions" of element composition as temperatures of the molten rock are lowered.

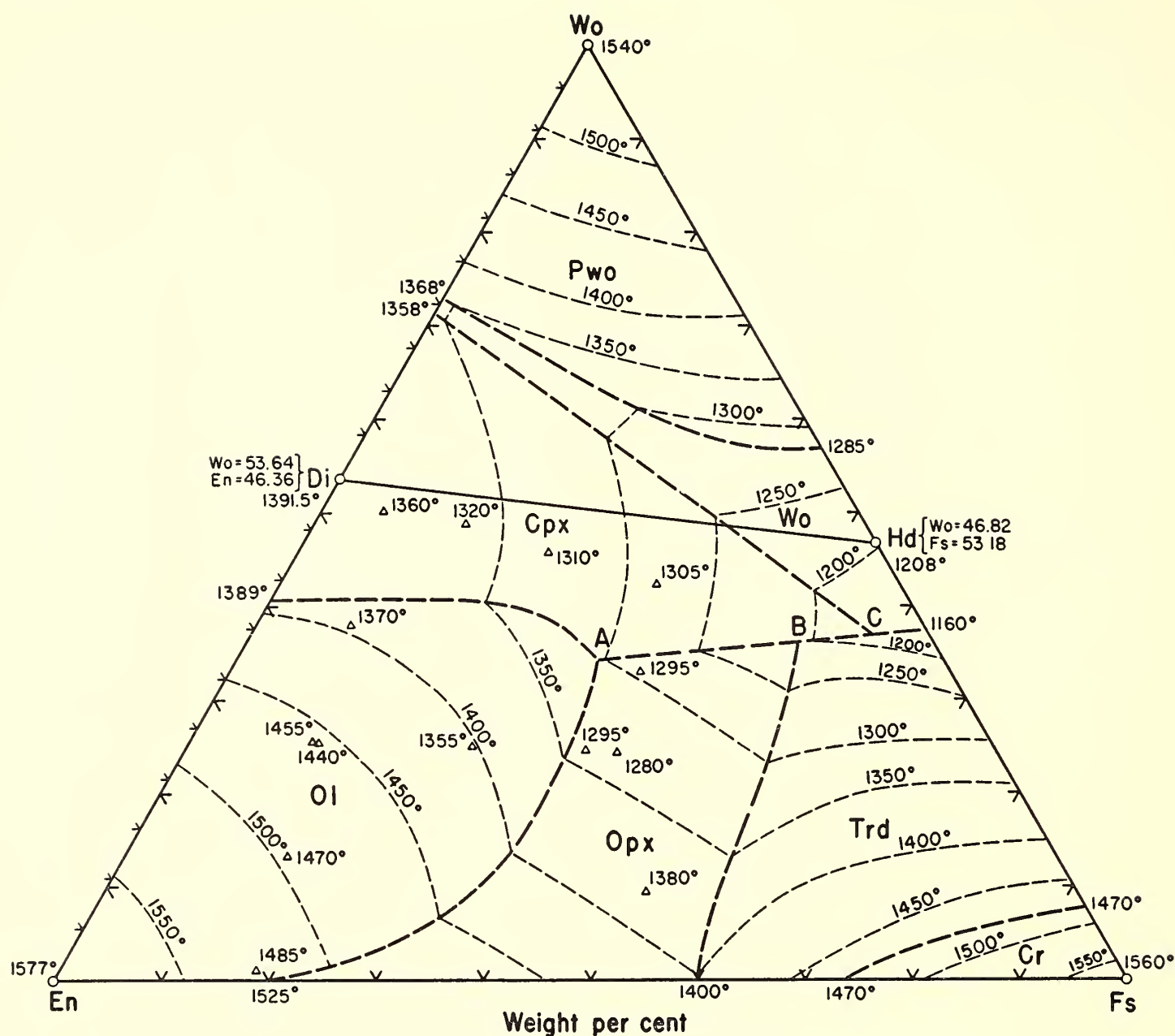


Fig. 2b. The predicted liquidus relations of minerals composing the pyroxene group. The isotherms show the temperature of melting for the minerals forming the system.

Symbols on diagrams 2a and 2b refer to the following:

Ak	akermanite	$\text{Ca}_2\text{MgSi}_2\text{O}_7$	Hd	hedenbergite	$\text{CaFeSi}_2\text{O}_6$
Cpx	clinopyroxenes	XYSi_2O_6 (generalized)	Kr	kirschsteinite	CaFeSiO_4
Cr	cristobalite	SiO_2	La	larnite	Ca_2SiO_4
Di	diopside	$\text{CaMgSi}_2\text{O}_6$	Mo	monticellite	CaMgSiO_4
En	enstatite	MgSiO_3	Ol	olivine	$(\text{MgFe})_2\text{SiO}_4$
Fa	fayalite	Fe_2SiO_4	Opx	orthopyroxenes	XYSi_2O_6 (generalized)
Fe-Ak	iron-akermanite	$\text{Ca}_2\text{FeSi}_2\text{O}_7$	Pwo	pseudowollastonite	CaSiO_3
Fo	forsterite	Mg_2SiO_4	Trd	tridymite	SiO_2
Fs	ferrosilite	FeSiO_3	Wo	wollastonite	CaSiO_3

This investigation by Yoder, C. E. Tilley, and J. F. Schairer was the beginning of a study of a system known as the pyroxene quadrilateral. These investigators consider that an understanding of this particular system has great potential for obtaining knowledge of the pressure and temperature formation of the many pyroxene-containing rocks within the earth's crust. This knowledge, in turn, of course, can lead to further information on the earth's structural history. Thus, although these systems are simple in a

classification of systems, they are by no means amenable to easy description or quick interpretation. And they are important systems if we seek full knowledge of all that lies beneath us on this planet.

A more complex type of system is found wherever a living organism or a life process is to be studied. The simpler of such systems may be illustrated by the living cell. Although we may call a cell simple in comparison with higher animals, or even with plants, it is still a vastly more complex entity than a mineral system, because it has the property of self-maintenance and the closely connected property of self-reproduction. There are within it fundamental subsystems.

For some years C. S. French and his colleagues of the Department of Plant Biology have been studying one of the most important of all cell subsystems, the photosynthetic system of higher plants, algae, and photosynthetic bacteria. It is now generally accepted that the carbohydrate and other products of photosynthesis result from two separate photochemical reactions rather than one. The photosynthetic system itself thus has at least two distinct subsystems. One of them is centered on a form of the pigment chlorophyll, and the other on an "accessory" pigment such as phycoerythrin.²⁰ Although the chemistry of the reactions that are triggered by light in the green leaves of higher plants or the tissues of algae or photosynthetic bacteria is still largely a matter of hypothesis, the existence of these two pigment systems was well established by the discovery of the Emerson enhancement effect. This is the phenomenon wherein light of two different specified wavelengths produces photosynthetic activity, as measured by oxygen evolution, greater than the sum of the single effects of either wavelength. Dr. French notes in his report that a large part of research on the mechanism of photosynthesis is now concentrated on attempts to understand this enhancement effect.

Described in the simplest terms, photosynthesis is an oxidation-reduction process wherein hydrogen is taken from water to form, with carbon dioxide, carbohydrates. The residual oxygen from the water typically is evolved. Light is thought to initiate the process of electron and ion transfer whereby the reactions occur. A prevailing hypothesis at the present time suggests that the oxygen-evolving reaction is more closely connected with the activation of the accessory pigment system by light than with the activation of the chlorophyll system. It also suggests that activation of the accessory pigment system starts off the entire series of reactions that lead ultimately to the products of photosynthesis.

The results of skillful experiments conducted by Dr. French during the year indicate that this prevailing hypothesis may have to be revised. Experimenting with the red alga *Porphyridium*, he administered light flashes of red

²⁰ The red pigment in the cells of Rhodophyceae algae. It is closely related chemically to bile pigments.

and green of wavelengths chosen to activate the two specific pigment systems of the alga. He found that the green flashes, which activate primarily the accessory pigment system, gave immediate increases in oxygen evolution when in the presence of red background light; after the flash the rate declined rapidly. A different sort of effect was found when red flashes were administered against a continuous background of green light: the initial enhancement was not as great, but the evolution of oxygen continued longer after the flash.

Dr. French suggests one interpretation of these findings: the material made by the chlorophyll system is consumed by the accessory pigment system as oxygen is produced. This conclusion may suggest that the time sequence of the two photochemical reactions should be reversed from that of the accepted model of the reactions. He also suggests that there is another interpretation. The observed differences in the kinetics of the two subsystems may reflect the necessary readjustment of pool sizes of intermediate components in the photosynthetic cycle. A set of equilibrium values maintained in the dark may be readjusted upon exposure to light to the different values required during steady-state operation in the presence of light. In either interpretation a revision of the accepted model of the system seems likely. Dr. French's experiments are continuing with the aim of developing better models of the system.

Another type of system, yet more complex and still more difficult to analyze, is that formed by a society of cells having well differentiated functions. One example is offered by higher green plants, in which the pigment-carrying chloroplasts are found; innumerable others are presented by animals, of whatever level or capacity. In these systems problems of differentiation, growth, and morphogenesis²¹ predominate. A great variety of subsystems determines these processes. Remarkably little is known about them with the exception of the subsystem of genetic control, which exists in all organisms. Yet, intensively as genetics has been studied, very little is known about the exact relation of the genetic control subsystem to the development of an organism.

One of the important steps taken toward understanding genetic control has been the discovery and description of the activator and suppressor-mutator elements controlling the action of the genes in maize, reported in a number of previous years in the Institution *Year Books* by Barbara McClintock of the Department of Genetics (now the Genetics Research Unit). She continued to extend her knowledge of these gene-regulator systems during the 1962-1963 year. Gradually she has developed from her research on the *Ac* and *Spm* controls a model of such a control system. She reports, elsewhere in *Year Book 62*, "Such a system can activate or inactivate

²¹ The origin and process of developing specific forms and structuring within an organism, including the microscopic.

particular genes in some cells early in development, and activate or inactivate other genes later in development. It can turn on the action of some genes at the same time that it turns off the action of others. It can adjust the level of activity of a particular gene in different parts of an organism.”

More and more it is the interest of J. D. Ebert and his colleagues at the Department of Embryology to examine the molecular systems within an animal organism that are associated with its differentiation, growth, and morphogenesis. They are thus particularly interested in the systems leading from the fertilized egg to the mature organism. Dr. Ebert notes in his report that one traditional question in this field of study is whether differentiation is a separable process from growth. It is possible that the experience of his colleague, I. R. Konigsberg, in analyzing developing muscle through tissue culture may throw some light on this interesting and basic question.

Last year a report was made on Konigsberg's unexpected discovery that muscle tissue cultured on “conditioned” medium exhibited a high degree of differentiation as compared with that cultured on nonconditioned culture media.²² Konigsberg found that flourishing cultures could be obtained on the nonconditioned media, but that luxuriance of growth in colonies of tissue cells had no correlation with the degree of differentiation. A properly conditioned medium, on the other hand, did lead to high degrees of differentiation, even though colony growth was not as luxuriant.

During the current year Konigsberg has extended these experiments and has demonstrated unequivocally that muscle colonies can arise from *single* cells. He did this by the delicate technique of isolating a single muscle cell within a small glass cylinder filled with the conditioned culture medium. Single cells so isolated gave rise to colonies of differentiated muscle after about two weeks of culture. Thus it was demonstrated that the capacity to differentiate was not lost during many successive cell divisions from the original specialized cell isolate.

One of the interesting by-products of Konigsberg's experiments was the discovery that cells with the power to differentiate can be recognized by their appearance. The “myoblast” cells that gave rise to muscle cell colonies have a distinctive bipolar shape which proved a reliable criterion of their character. The bipolar shape is obviously a differentiated characteristic. From the evidence provided by this marker it may be concluded that differentiation and growth (cell proliferation) are not mutually antagonistic processes, as had been thought by some students in the field.

For several years Ebert and his colleagues have been interested in the movement of cells in embryos, beginning in their earliest stages, as the cells migrate to form tissue of differentiated function. In a study closely related to Konigsberg's, Ebert, M. C. Reporter, and C. R. Green continued an analysis of the metabolism of heart-forming areas in the chick embryo.

²² Conditioned medium is a medium on which cultures have previously been grown.

Ebert and his colleagues had found earlier that the formation of the heart could be inhibited by administering antimycin A, an antibiotic. Other tissues of the same embryos, however, continued to differentiate and grow even though heart tissue did not form. This fact led Ebert to the hypothesis that there are two oxidative pathways to tissue formation in the early embryo, one of which could be labeled antimycin A-sensitive (heart and other tissues), and another antimycin A-insensitive. During the year experiments showed that an early embryo grown in a highly oxygenated atmosphere followed predominantly the first of these pathways of tissue formation, that is, the antimycin A-sensitive pathway. In addition, Reporter and his associates demonstrated that the effects of antimycin A can be counteracted by a factor isolated from frozen and thawed cell mitochondria.²³ The chemical nature of this factor and the changes in the enzyme pathways caused by disturbing the embryonic environment with antimycin A or excessive oxygen remain intriguing questions about the nature of muscle tissue differentiation.

Probing for knowledge of another aspect of differentiation at the molecular level, Y. Croisille obtained significant data about a second enzyme system: hypoxanthine dehydrogenase (HXDH). In the chick embryo, as in other organisms, this is a key enzyme in the synthesis of uric acid, the primary end product of nitrogen metabolism. Its appearance in the embryo had already been very carefully traced by Kato and others. As early as the fifth day of embryonic development it appears in the mesonephros, a kidney precursor. It reaches maximum activity there on the fifteenth day, then decreases. On the fourteenth day it starts to increase in the metanephros, another kidney precursor, where it continues to increase until the eighteenth day, and then decreases. The third stage is a dramatic increase in hypoxanthine dehydrogenase activity in the liver, just at the time of hatching. The question naturally arose whether the three HXDH's had the same protein carrier for the hypoxanthine or whether there is a "family" of related HXDH's. Croisille established during the year that the successive enzymes observed in the chick embryo are identical: the same enzyme protein is synthesized in three different locations in the embryo at three different times.

How this synthesis is regulated with such precision and specificity at the different stages of development in the embryo is both an intriguing and an important question, for it may offer a clue to understanding the regulation of other such systems in differentiation and growth. It also illustrates why developmental biology, as Dr. Ebert observes, is emerging as one of the focal fields of research for the coming decade, engaging the attention of chemists, geneticists, immunologists, microbiologists, neurobiologists, and

²³ Minute bodies present in the cytoplasm of most cells.

physicists, among others. It is a fascinating world of systems and subsystems, and their charting is likely to provide some of the most exciting intellectual adventures during the remainder of this century.

The Particulate Character of Energy and Matter

Of the four major overriding problems chosen to illustrate a generalized scientific view at the outset, three thus are well represented in the research undertaken by the staff of the Institution during the year past. They are the overriding problems of the structure and content of the cosmos, the origin and evolution of life, and the characteristics of natural systems. A fourth overriding problem, the particulate character of energy and matter, was well represented in the past, for the Institution had one of the pioneering nuclear physics programs in the nation before World War II. It thus shared in developing the enormous amount of attention devoted to this field elsewhere in the nation after the beginning of the Manhattan Project. Since the 1940's the Institution has restricted its efforts in nuclear physics to modest but highly specialized research not "popular" elsewhere. In recent years it has been represented especially in the development of a polarized ion source for studying experimentally the interaction of fast polarized deuterons and protons with atomic nuclei. Studies on the effects of tensor polarized deuterons²⁴ are now in progress at the Department of Terrestrial Magnetism in collaboration with the University of Basel, Switzerland.

As the pages of the Institution's *Year Book 62* amply reveal, the research used as illustrations in this report is only a part, even if a typical part, of the work undertaken by our staff during the year. Other studies and investigations, chosen at random, could almost as well illustrate that consciousness of overriding problem which characterizes some of the best of fundamental science. They are not the thoughts or plans or activities of narrowly specialized investigation. Rather, they represent the views and purposes of investigators who are deeply impressed by the immensity and complexity of the world around them, intrigued by its beauty and order, and impelled to know it better. Viewed in the context of their efforts and the overriding problems they recognize, the Republic of Learning does not appear in danger

²⁴ Protons, neutrons, deuterons, and many other atomic nuclei have discrete quantities of angular momentum, or "spin." If a statistically significant number of some group of these particles, e.g., a beam, has a preferred orientation in space, the particles are said to be polarized. These particles may be described in terms of their angular momentum. Those of the lowest angular momentum (protons or neutrons) may be described by vector analysis, which treats directed magnitudes in three-dimensional space. Those of the next larger angular momentum (deuterons) require a vector and a tensor for their description. A tensor is roughly a generalized vector, applicable in any system of coordinates, with any number of components.

of breaking into petty principalities. On the contrary, its structure appears stronger, its activity more vital, than ever before.

Losses . . .

It is with great sadness that I record the death of Henry Richardson Shepley, Trustee of the Carnegie Institution; of Alfred Vincent Kidder, retired Director of the Institution's Division of Historical Research; of Otto Struve, recently appointed Staff Member of the Mount Wilson and Palomar Observatories; of Edison Pettit and Seth B. Nicholson, retired Staff Members of the Observatories; of Herbert E. Merwin, retired Staff Member of the Geophysical Laboratory; and of William Wallis, retired Staff Member of the Department of Terrestrial Magnetism.

Henry Richardson Shepley died at his home in Essex, Massachusetts, on November 24, 1962. Mr. Shepley's association with the Institution dated from December 10, 1937, when he was elected a Trustee to succeed the late Andrew W. Mellon. For the next twenty-five years he served as Chairman of the Committee on Historical Research (later the Committee on Archaeology), and in 1941 he was elected a member of the Executive Committee of the Institution.

Henry Shepley was born in Brookline, Massachusetts, on May 1, 1887. He was graduated from Harvard College in 1910 with the degree of Bachelor of Science in Architecture. In 1914 he received a diploma from the École des Beaux-Arts in Paris.

A leading figure in the field of architecture and senior member of the famous firm of Shepley, Bulfinch, Richardson and Abbott in Boston, he designed for his Alma Mater the Fogg Art Museum, Hemenway Gymnasium, and so many other buildings that it was said of him, "His monument is the good red brick and mortar of his college." He was also responsible for the Rhode Island Hospital and for many buildings at Massachusetts General Hospital. One of his most notable designs was for the New York Hospital and Cornell Medical Center, inspired by the Palace of the Popes at Avignon. For this work he received in 1936 the coveted Gold Medal of the Architectural League of New York with a citation "for the orderly arrangement . . . and originality of design."

A pioneer supporter of aviation, Mr. Shepley served as Captain in the Air Force of the Army with the American Expeditionary Forces in World War I. During World War II he was a civilian consultant staff executive in the New England regional office of the Army Construction Quartermaster.

Mr. Shepley's achievements and services were recognized with many honors. In 1936 he was awarded the honor of Fellowship in the American Institute of Architects. Three years later he was elected to the National Academy of Design and was made an honorary member of Phi Beta Kappa. In 1953 the French Government conferred on him the Cross of Chevalier of

the Legion of Honor for distinguished architectural design; and Harvard University in 1957 awarded him the honorary degree of doctor of arts.

He was, indeed, in the very fullest sense, "an architect by tradition, an artist by inheritance, a designer by training, and an executive by experience and ability."

Alfred Vincent Kidder, archaeologist and from 1930 to 1950 Director of the Division of Historical Research of the Carnegie Institution (later the Department of Archaeology), died on June 11, 1963, at the age of 76. Born in Marquette, Michigan, he was graduated from Harvard University in 1908 and received a doctor of philosophy degree there six years later. From 1915 to 1929 he was director of excavations at Pecos, New Mexico, for the Phillips Academy of Andover, Massachusetts.

As Director of the Historical Division, Dr. Kidder developed a broad anthropological program of research in the Maya area, emphasizing especially the use of stratigraphic methods. He personally contributed numerous monographs and papers of importance in the field of Middle American archaeology. In 1947 the first Viking Fund Prize and Medal were presented to him for his outstanding work in the field of archaeology and for his influence in personally developing programs of research and in stimulating other investigators. The day after his retirement in 1950, the American Anthropological Association announced the creation in his honor of the Alfred Vincent Kidder Award, to be presented every three years for outstanding achievement in American archaeology. Dr. Kidder continued his productive career of research and writing after his retirement.

Otto Struve died in Berkeley, California, on April 6, 1963. Born in Kharkov, Russia, on August 12, 1897, and educated at the University there, he came to the United States in 1921 as a graduate student and assistant in stellar spectroscopy at the Yerkes Observatory. He served as director of that Observatory and of the McDonald Observatory of the University of Texas from 1932 to 1947, and during the same period was managing editor of the *Astrophysical Journal*. From 1947 to 1950 he was president of the American Astronomical Society, and from 1952 to 1955 of the International Astronomical Union. From 1950 to 1959 he served as professor of astronomy at the University of California and as director of the Leuschner Observatory, leaving those posts to become the first director of the National Radio Astronomy Observatory at Green Bank, West Virginia, in 1959. Upon his retirement from Green Bank in 1962 he was appointed Addison White Greenway visiting professor of astronomy at the California Institute of Technology and a Staff Member of the Mount Wilson and Palomar Observatories. Many awards and honors were bestowed on Dr. Struve during his long and fruitful career. His studies of close double stars and of the β Canis Majori type were especially notable.

Edison Pettit died on May 6, 1962, in Tucson, Arizona, at the age of 73.

He joined the Mount Wilson staff in 1920 after a period of teaching at the University of Chicago and two years of work at the Yerkes Observatory. During the thirty-five years of his affiliation with the Mount Wilson and Palomar Observatories, Dr. Pettit distinguished himself especially by his work in solar observation, radiation measurements on celestial objects, and photoelectric photometry. He designed and used a special monochromator and was one of the first to study the ultraviolet spectral energy of the sun to the limits permitted by the earth's atmosphere. He also developed the sensitive vacuum thermocouples that he and Dr. Seth B. Nicholson used for several years in measuring the heat radiations of stars, planets, and the moon. Between 1947 and 1955 he carried out an extensive photometric study of some 563 extragalactic nebulae. Dr. Pettit was a member of the Society of the Sigma Xi, the International Astronomical Union, the American Astronomical Society, the Astronomical Society of the Pacific, and the Optical Society of America.

Seth B. Nicholson, who joined the staff of the Mount Wilson Observatory in 1915, died on July 2, 1963, at the age of 72. During much of the period of his association of forty-two years with the Mount Wilson and Palomar Observatories he studied sunspots and their meteorological effects on the atmosphere. He developed an extraordinarily detailed knowledge of the complex phenomena of the sun's visible surface and supervised the systematic collection of data on sunspots, including the polarity and strength of their magnetic fields. The discoverer of four of Jupiter's twelve moons (the ninth, tenth, eleventh, and twelfth), Dr. Nicholson was elected to the National Academy of Sciences in 1937, and he was a member of the American Astronomical Society and the Astronomical Society of the Pacific. After his retirement in 1957 he continued to collaborate with the United States Weather Bureau, investigating for it the bearing of solar activity on the magnetic field of the earth's ionosphere.

Herbert E. Merwin died in Washington, D. C., on January 28, 1963, at the age of 86. He came to the Geophysical Laboratory of the Institution as a petrologist from Harvard University in September 1909, two years after the Laboratory had moved to its new building on Upton Street. At that time an important part of the work being done was the determination of equilibrium relations among phases in systems of the rock-forming oxides; some similar work was being done on sulfides. As petrologist, Dr. Merwin cooperated with the physical chemists and physicists in these programs, making the microscopic examinations and doing the crystallographic work. He developed exceptional skill in the use of the polarizing microscope and other tools of his art, devising new methods to meet each problem as it arose. After retirement in 1945, he continued his work as a Research Associate of the Institution for two years and as a Retired Associate until 1959. Dr. Merwin's kindly nature and willingness always to assist brought his talents into demand for many other lines of investigation. In presenting him with

the Roebling Medal of the Geological Society of America in 1949, Dr. Norman L. Bowen noted that Merwin had been a participant in almost every aspect of the investigations of the Geophysical Laboratory through four decades.

William Fisher Wallis, former member of the staff of the Department of Terrestrial Magnetism, died on June 23, 1963, at the age of 89. Educated at the Johns Hopkins University and Massachusetts Institute of Technology, he worked for ten years (1900–1910) for the United States Coast and Geodetic Survey. He joined the staff of the Department of Terrestrial Magnetism in 1913, and in 1916 he went to Watheroo, Australia, to take charge of the erection of a magnetic observatory building for the Department and the installation and operation of appropriate instruments. From 1921 to 1923 he supervised the construction of an observatory at Huancayo, Peru. Until his retirement in 1946 he worked on variations and corrections for international magnetic standards, gaining a reputation among his colleagues for his precision.

Only one retirement has occurred during the year. Mr. James F. Sullivan, long a valued member of the administrative staff, retired on June 30, 1963. Mr. Sullivan, who came to the Institution in 1926, served as secretary to the Executive Officer and for the last fifteen years as Assistant to the Bursar with special responsibility for preparing agenda and minutes and otherwise assisting in the conduct of the meetings of the Executive Committee and the Board of Trustees. A naval veteran of World War I, he took leave of absence from the Institution to serve again with the Navy as a Chief Yeoman from 1942 to 1945. He will be sadly missed in the administrative offices for his cheerful and cooperative spirit and the painstaking care he brought to all his work.

. . . and Gains

One new member was elected to the Board of Trustees of the Institution on May 10, 1963: Frank Stanton.

Mr. Stanton, a professional psychologist and former member of the faculty of Ohio State University, joined the staff of the Columbia Broadcasting System in 1935. In 1946 he was elected President of that system—the world's largest broadcasting network organization. He has been an energetic and outstanding leader in the broadcasting world. Among many other achievements in the public service, his perseverance and initiative led to a revision of regulations for the broadcasting industry that permitted the historic debate on television between Mr. Kennedy and Mr. Nixon in 1960, and that will undoubtedly revolutionize future presidential campaigns.

Born in Muskegon, Michigan, in 1908, Dr. Stanton attended Ohio Wesleyan University and Ohio State University, receiving the degree of doctor of philosophy from the latter in 1935.

Among his multifarious duties he currently serves as chairman of the board of the Rand Corporation, as a trustee of the Center for Advanced Study in the Behavioral Sciences, as a director of the Lincoln Center for the Performing Arts, Inc., and as a trustee and member of the executive committee of the Rockefeller Foundation.

It gives me great pleasure to record several outstanding honors that have come to staff members of the Institution over the past year.

At the Mount Wilson and Palomar Observatories, Allan Sandage, Staff Member, was elected a member of the National Academy of Sciences on April 23, 1963, and on January 11, 1963, he and Martin Schwarzschild of Princeton University were jointly awarded the Eddington medal of the Royal Astronomical Society for their combined theoretical and observational investigations of stellar evolution.

Shortly before his death, Seth B. Nicholson, retired staff member of the Observatories, was awarded the Bruce gold medal of the Astronomical Society of the Pacific on June 13, 1963, in recognition of his notable contributions to astronomy.

At the Geophysical Laboratory, Philip H. Abelson, the Director, was the recipient on March 14, 1963, of the Hillebrand prize for 1962, awarded by the Chemical Society of Washington, "in recognition of contributions to the paleobiochemistry and geochemistry of plant and animal remains, including the discovery of residual amino acids in fossils many millions of years old." On November 13, 1962, Hatten S. Yoder, Jr., Staff Member, was awarded the Geological Society of America's Arthur L. Day gold medal for outstanding distinction in contributing to geologic knowledge through the application of physics and chemistry to the solution of geologic problems.

Merle A. Tuve, Director of the Department of Terrestrial Magnetism, was decorated with the order of Condor de los Andes by the Honorable Victor Andrade, ambassador from Bolivia, on February 19, 1963. And on April 18, 1963, the American Geophysical Union awarded him the William Bowie medal "for unselfish cooperation in research."

Bernard F. Burke, Staff Member of the Department of Terrestrial Magnetism, was nominated for the Helen B. Warner prize by the American Astronomical Association for "a noteworthy paper, representing an outstanding contribution in science."

At the Department of Plant Biology, C. Stacy French, the Director, was elected to the National Academy of Sciences on April 23, 1963, and to the American Academy of Arts and Sciences on May 8, 1963.

Tatiana Proskouriakoff, Archaeologist, was awarded the Alfred Vincent Kidder medal of the American Anthropological Association in November 1962. The award is given every three years for archaeological work on Middle America and southwestern United States.

Reports of Departments and Special Studies

Mount Wilson and Palomar Observatories

Geophysical Laboratory

Department of Terrestrial Magnetism

Committee on Image Tubes for Telescopes

Department of Plant Biology

Department of Embryology

Genetics Research Unit

Cytogenetics Laboratory

Mount Wilson and Palomar Observatories

Operated by the Carnegie Institution
and the California Institute of Technology

Pasadena, California

Ira S. Bowen
Director

Horace W. Babcock
Associate Director

OBSERVATORY COMMITTEE

Ira S. Bowen
Chairman

Carl D. Anderson

Horace W. Babcock

Jesse L. Greenstein

Robert B. Leighton

Allan R. Sandage

Contents

Introduction	5	Gaseous Nebulae and Interstellar Gas	23
Observing Conditions	6	The presence of $\lambda 3889$ of He I in absorption	23
Solar Observations	6	Interstellar lines of CN and C ₂	24
Magnetic field changes during solar flares	6	Velocities of gas clouds from interstellar lines	24
Spectroheliograms in $\lambda 10830$ of He I	7	Internal motions in IC 4997	25
Spicules	7	Line intensities in the Orion nebula	25
Magnetic fields in active regions	7	Line intensities in planetary nebulae	26
Differential solar rotation	7	Densities from line-intensity ratios	26
Doppler fields	8	Characteristics of exciting stars	27
Magnetic fields	8	Galaxies	27
Eclipse observations	9	Rotation and dimensions of the Galaxy	27
Planets, Comets, and Satellites	9	Internal motion and structure	27
Spectra of the major planets	9	Polarization	28
Water vapor and carbon dioxide in the Martian atmosphere	10	Stellar populations	29
Spectra of comets	10	Spectra	29
Westford	10	Variable stars in galaxies	30
Stellar Spectroscopy and Photometry	11	Redshift-diameter relation	30
Chemical composition of stellar atmospheres	11	Atlas of peculiar galaxies	31
Color-magnitude and chemical- composition relationships	13	Catalogue of galaxies and of clusters of galaxies	31
Photometry of stellar clusters and related stellar types	14	Structures of clusters of galaxies	31
High-velocity stars	16	Radio Sources	32
Double stars	16	Spectra	32
Subdwarfs and white dwarfs	17	M 82	34
Faint blue stars	17	Polarization	36
Spectrophotometry	18	Theoretical Studies	36
Supernovae	20	Instrumentation	37
Novae	20	Solar magnetograph	37
U Geminorum stars	21	Photoelectric scanner	37
G and K supergiant survey	21	Microphotometer	38
Stellar rotation in the Coma cluster	21	Astronomical "seeing"	38
Spectrum of Algol	22	Image-tube installation	39
Stellar chromospheres	22	Ruling of plane gratings	39
Stellar polarization	23	Guest Investigators	39
		Staff and Organization	45
		Bibliography	46

INTRODUCTION

THE original equipment of the Owens Valley Radioastronomy Observatory of the California Institute of Technology was completed in 1959. *Year Book 59* reported the close cooperation that was developing between the staffs of the Radio Observatory and the Mount Wilson and Palomar group as well as the early results of the collaboration. During the current year this cooperation has again led to results of great importance to astronomy.

With the increased resolution and positional accuracy attainable when the radio dishes at Owens Valley are combined as an interferometer, it has become possible to make unambiguous identifications of more and more of the radio sources with objects observed optically. Thus in *Year Book 60* it was reported that Bolton and Matthews of the radio group and Greenstein, Münch, and Sandage of the Observatories had collaborated in the identification of one of these sources (3C48) with a starlike object. In the following year two sources (3C196 and 3C286) were identified with stellar objects by Matthews and Sandage, who made a study of the distribution of energy throughout the optical spectrum. Spectra of these objects obtained by Schmidt show that the objects are "peculiar and uniquely new."

During the current year, still another source (3C273) was identified with a stellar object, which was found by Schmidt to have a peculiar spectrum with broad emission lines. Oke, observing the object with the spectrum scanner in the infrared, found a strong emission line at 7590 Å. Schmidt discovered subsequently that this line and others he observed at shorter wavelengths are lines of H, O III, and Mg II with a redshift of $\Delta\lambda/\lambda = 0.16$. Greenstein and Matthews then noted that the lines in the spectra of 3C48 could be identified as O II, Ne III, Ne V, and Mg II with a redshift of $\Delta\lambda/\lambda = 0.367$.

Greenstein and Schmidt examined various possible interpretations of these large redshifts, such as an Einstein shift in the neighborhood of an exceedingly dense and massive star and the cosmological shift shown by all objects at very great distances. They reached the conclusion that the cosmological shift was the only acceptable interpretation, even though it led to the conclusion that these radio sources are at such a distance that their optical luminosity must be nearly 100 times as great as that of any normal galaxy. Evidently something has occurred in these galaxies that has caused them to temporarily emit energy at many times the normal rate.

That such explosive events may occur in a galaxy was confirmed from a study of M 82 by Sandage and Dr. C. R. Lynds of the Kitt Peak National Observatory. This galaxy, which is a weak radio source, was photographed through a narrow-band H α filter. The photographs show a remarkable system of filaments extending for at least 10,000 light-years in both directions perpendicular to the plane of the galaxy. Spectroscopic observations indicate that the gas in the filaments is moving away from the galactic plane with a velocity roughly proportional to the distance from the nucleus. This suggests that the material was blown out of the nuclear region by an enormous explosion at a time observable on earth about $1\frac{1}{2}$ million years ago.

The radio observations also point to the presence of great masses of emitting material that has been blown out to distances of some hundreds of thousands of light-years on opposite sides of a number of radio galaxies.

Spectra of 32 radio galaxies have now been assembled by Schmidt. Of these, 26 show emission lines, thus pointing to the presence of an unusual amount of gas. Although most of these radio galaxies correspond in magnitude more nearly to

normal galaxies, they may, like M 82, represent later stages of the explosive events suggested by the radio stars.

It is still too early for a complete interpretation of these results, but obviously the observations of radio galaxies have

brought to light a very important stage in the life of a galaxy in which unprecedented amounts of energy are released in its nucleus. The observations should be of fundamental importance for the understanding of galaxies and their evolution.

OBSERVING CONDITIONS

The rainfall for the year dropped to 18.90 inches, or only slightly more than half of normal. Observations were made with the 200-inch on 305 nights, with the

100-inch on 304 nights, and with the 60-inch on 286 nights; the sun was observed on 322 days during the report year.

SOLAR OBSERVATIONS

Solar observations were made by Cragg, Utter, and Howard. The number of photographs of the various kinds taken between July 1, 1962, and June 30, 1963, were as follows:

Direct photographs	203
H α spectroheliograms, 18-foot focus	384
H α spectroheliograms, 30-foot focus	754
K2 spectroheliograms, 18-foot focus	388
K2 spectroheliograms, 30-foot focus	754
Magnetograms (number of days)	153

During the course of the year, the focus used for routine spectroheliograms was changed from 18 to 30 feet. Sunspot magnetic classification data were sent monthly to interested investigators, but it is likely that these observations will cease in the near future. Magnetic classifications of groups were made on 141 days during the year.

Magnetic Field Changes during Solar Flares

Howard spent the month of November in the Soviet Union, visiting the Crimean Astrophysical Observatory and the Kislovodsk station of the Pulkovo Observatory under terms of the Inter-Academy Exchange Agreement. While in the Crimea he cooperated with the Director, Dr. A. B. Severny, on an examination of the Crimean magnetic observations of the active region that produced the flare of July 16, 1959. This flare was observed at

the Mount Wilson Observatory by Howard and Babcock (*Astrophys. J.*, 132, 218); during its course the fine-scan magnetic traces indicated no change in the weaker magnetic fields. The highest level recorded was 40 gauss—the magnetic fields observed being almost exclusively photospheric. Crimean magnetic observations were available for the day before and the day after the flare. They measured only the larger fields, and almost all the measured fields were in sunspots. An examination of these magnetic maps indicated that the sunspot fields decreased appreciably sometime during the day of the flare. Direct photographs show that the spot groups decreased in size during the day of the flare. A further investigation, by Howard, of the flares responsible for ground-level cosmic-ray events in the last twenty years indicated that, in all six cases for which spot area data are available, the spots decreased in area from the day before to the day after the flare. Since it is well known that, in general, flares occur at times when spot groups are growing, this may be a characteristic distinguishing flares that are responsible for geophysical effects from those that are not. The effect of a large 3⁺ flare on the spot group seems equivalent to a rapid aging of the spot. The energy lost in the magnetic field at the time of the flare of July 16, 1959, was

about 5×10^{32} ergs, which is comparable to that lost from the flare in the form of cosmic rays.

Spectroheliograms in $\lambda 10830$ of He I

Drs. Harold Zirin and John W. Firor of the High Altitude Observatory and Howard have taken a number of spectroheliograms in the $\lambda 10830$ line of He I and have also obtained spectra in this region. The spectroheliograph of the 60-foot solar tower was used with an infrared imaging photomultiplier tube (courtesy of the Image Tube Committee of Carnegie Institution of Washington). They plan to analyze their observations in order to learn more about the structure of the solar chromosphere.

Spicules

Cragg, Howard, and Zirin have studied an excellent $H\alpha$ spectroheliogram taken on September 17, 1962, at the 60-foot tower at Mount Wilson. A number of dark vertical structures, identified as spicules, are evident. They are always found in groups of a half-dozen or more. Near the poles they occur around small emission regions (polar faculae). Nearer the equator the clumps of spicules can still be seen, but the emission patches are not present. At distances greater than 30° from the limb it becomes very difficult to make out the spicules. There are estimated to be 2400 "bushes," with about 10 spicules per bush, on the solar surface, occupying about 1 per cent of it. Their general appearance and number leave no doubt that they are spicules. Each of the bright solar flecks could be identified (using the blink comparator) with similar features on a calcium K2 spectroheliogram and a direct photograph, both taken at nearly the same time as the $H\alpha$ spectroheliogram.

Magnetic Fields in Active Regions

Howard and Mr. John W. Harvey of the Lockheed Solar Observatory cooperated on a study of an active region on

the solar disk on September 6, 1962. A number of fine-scan magnetograms were taken of the region, while a high-resolution $H\alpha$ patrol of the region was carried out at Lockheed, both on- and off-band. It was found that the $H\alpha$ plage occurred where the magnetic field exceeded about 60 gauss. Filaments and large $H\alpha$ fibrils tended to be located along lines where the magnetic field changed polarity (neutral lines). Smaller fibrils were found aligned perpendicular to isogauss lines. The net magnetic flux from the region was zero. At approximately $\frac{1}{2}$ angstrom to the red of the line center, the regions where there were magnetic fields (and calcium plages) showed a characteristic appearance. Instead of a filamentary background there was a granular emission pattern. The brightness of these fine mottles was greater for higher fields. The mottles seemed to have longer lifetimes than the fibrils outside the magnetic-field region. The fibrils outside the magnetic fields seemed to be constantly moving, like a field of wheat in a wind; the structures within the field region showed little or no motion. Ellerman bombs occurred where the magnetic fields were about 60 gauss, and they showed a preference for regions where the magnetic gradient was steep. A class 1 flare occurred during the observations near a large spot; some changes in the spot umbra took place at the same time. Material ejected from the flare moved away from the strong fields near the spot in a direction normal to isogauss contours. The flare seemed unable to expand toward the spot. No changes in the 15-, 40-, or 60-gauss contour lines were evident before, during, or after the flare.

Differential Solar Rotation

Lately some interest has arisen in the problem of the differential solar rotation and possible changes of the latitude dependence with the solar cycle. Howard has observed the solar rotation with the magnetograph at the 150-foot tower

telescope. A rotating periscope, first suggested by Leighton, brings light from around the disk near the limb into the spectrograph. As the periscope turns, light from different solar latitudes near the limb enters the spectrograph. The servo-line-centering device keeps the spectrum line ($\lambda 5250.216$, Fe I) centered on the exit slit, and a recording of the line centering gives the line position as a function of solar latitude. It is necessary to observe for several days in order to average out the effects of active regions near the limb and the omnipresent horizontal velocity fields. The signal is punched on paper tape during the observations, and a 7090 computer gives the results. Observations made early in December, when the earth was in the plane of the sun's equator, were not as complete as had been hoped. It was necessary to stop them after two days because of instrumental malfunction. Nevertheless, they give a determination of the differential solar rotation in the form $\omega/\omega_0 = A + B \sin^2 \varphi + C \sin^4 \varphi$, where ω is the angular velocity and ω_0 is the angular velocity at the equator, $B = -0.112$, and $C = -0.173$. More observations are planned, and it is hoped to continue a study of the latitude dependence of solar rotation for several years.

Doppler Fields

Howard has continued a study of Doppler fields on the sun, using the solar magnetograph. Some of the observations have been made by Cragg, Harvey, and Utter. The position of the spectrum line is punched at intervals on paper tape while the image is held fixed, and autocorrelation functions and Fourier spectra are calculated on the 7090 computer. The well known 5-minute oscillation is easily visible on the tracings and shows up on the autocorrelation function and power spectra. In addition, a short-period oscillation well above the noise level is apparent. The short-period oscillations seem to come in bursts of a minute or two

and have wavelengths of 1 or 2 seconds. There is no simple relation between their appearance and the phase of the 5-minute oscillations, but recently punches have been made at more frequent intervals, and the relationships should be settled soon by the additional calculations. That the short-period oscillations are real and do not reflect some peculiarities of telescope or spectrograph seeing is indicated by their disappearance near the limb. The 5-minute oscillations are not always present at a given point in the sun. Over a long period of time they will start and then, after several oscillations, damp out, the cycle being repeated many times. The resulting autocorrelation function has a damped-sinusoidal form. But the results from the most recent, and longest, observations indicate that the sinusoidal oscillations of the autocorrelation function increase in amplitude after about 45 minutes. Further observations are planned to attempt to clear these matters up.

Magnetic Fields

The reduction of the daily solar magnetograms from August 1959 to December 1962 continues under the direction of Howard. This work is made possible by a contract between the Office of Naval Research and the Lockheed Solar Observatory. Isogauss drawings are being made from the original magnetograms, and magnetic regions are identified and classified. Further work will include comparison with Mount Wilson sunspot data and calcium plage data. Also, a study of the types of magnetic regions that produce solar flares will be made, as well as a study of the correlation of solar magnetic fields with coronal and geophysical data.

Dr. John M. Wilcox, of the Lawrence Radiation Laboratory, and Howard obtained some magnetic observations near the solar equator in an attempt to find some basis in the solar atmosphere for short-period fluctuations in the interplanetary magnetic field as recorded by

the Mariner II space probe. Bad weather and instrumental difficulties precluded their getting definitive results.

Eclipse Observations

With the collaboration of Dr. G. Righini of the Astrophysical Observatory of Arcetri, Deutsch has adapted a stellar spectrograph for observations of the coronal continuum at the total eclipse of

July 20, 1963. The plan is to observe from an airplane at 42,000 feet. The objective is a new determination of the ratio (electron corona brightness)/(dust corona brightness) over the range from 1 to 3 solar radii, with due regard for the polarizing properties of the spectrograph. This ratio can yield an improved model for the electron density out to about 3 solar radii.

PLANETS, COMETS, AND SATELLITES

Spectra of the Major Planets

Observation of the planets with the photoelectric scanner at the 60-inch has been continued by Münch in collaboration with Mr. R. Younkin of the Jet Propulsion Laboratory. Energy curves out to 1.1 microns of the dark belts and bright bands of Jupiter have been obtained at various latitudes. They show that the contrast between the belts and bands decreases steadily from the blue to the red in a continuous spectrum, but the dark belts are brighter in the spectral bands of the near infrared containing strong CH_4 absorption. This observation indicates that the effective level for the diffuse reflection of the solar light is higher in the dark belts than in the bands. To obtain additional information about the scattering properties of the solid particles suspended at various Jovian latitudes, the monochromatic limb-darkening curves of the planet are being measured on direct photographs taken by Münch at the coudé focus of the 200-inch telescope, in three wavelength ranges free of CH_4 absorption and another in a strong CH_4 band, all isolated by broad-band filters and plate combinations. The differences between the darkening curves of the bands and belts, as well as the phase-angle effects, have been found to be well marked. To interpret these curves, theoretical calculations are being made for the diffuse reflection of radiation in nonhomogeneous media, consisting of a

finite Rayleigh layer overlying an infinitely deep atmosphere with nonconservative and asymmetric scattering laws.

New high-dispersion spectra of Jupiter were obtained and studied last year for the purpose of searching for new Jovian absorption lines, especially any that might be attributed to NH_2 . A plate of excellent quality obtained at Mount Wilson in the red at 1.8 Å/mm, as well as other spectra with smaller dispersion, failed to show any trace of NH_2 . Two lines of unknown origin, at $\lambda\lambda 6361.1$ and 6368.4 , were found on one plate, but only near the morning limb. The line at $\lambda 6364.4$ had been detected by Dr. H. Spinrad of the Jet Propulsion Laboratory on a plate taken in 1961, but no other plates show it. The anomalous inclination of the NH_3 lines found also by Dr. Spinrad on the same 1961 Palomar plate was definitely not present on any plate taken in 1962. These observations suggest, therefore, intrinsic variability in the constitution and dynamics of Jupiter's atmosphere, possibly related to the radically different appearance of the dark equatorial bands in 1961 and 1962. Further observations are contemplated for the coming season.

A theoretical study of the pressure-induced dipole spectrum of H_2 and its effect on the thermal balance of the major planets has been undertaken by Trafton as a thesis project. On the observational side, Trafton is obtaining photometric data related to the (4, 0) and (3, 0) dipole bands in Uranus and Neptune.

*Water Vapor and Carbon Dioxide
in the Martian Atmosphere*

Münch and Drs. L. D. Kaplan and H. Spinrad of the Jet Propulsion Laboratory obtained a new series of high-dispersion plates of Mars with the 100-inch coude in April in order to set a value or an upper limit to the water-vapor content of its atmosphere. The highest-quality spectrogram, obtained on a IV-N emulsion at 5.6 Å/mm dispersion on a night when the humidity at Mount Wilson was unusually low, shows that the strongest unblended lines in the R and P branches of the $\lambda 8260$ band of telluric H_2O have faint components displaced to the red by the amount expected if they originated in the Martian atmosphere. From their equivalent widths, unavoidably quite uncertain because of their low value, it has been estimated that the amount of precipitable water vapor in the Martian atmosphere is in the range 10–20 microns. The same plate clearly shows a number of rotational lines in the $5\nu_3$ band of CO_2 at $\lambda 8600$. The observation of this band in the Venus spectrum led to the identification of CO_2 in this planet by Adams and Dunham, but earlier attempts to detect it on Mars had been unsuccessful. The presence of CO_2 in Mars had been proved by the integrated absorption of the much stronger bands at 1.575 and 1.60 microns. Comparison of the essentially unsaturated band at $\lambda 8600$ with the strongly saturated infrared bands will provide a firm determination of the value of the pressure at the base of the atmosphere of Mars when laboratory data regarding f values and collisional damping widths become available from measurements being carried out at various laboratories.

Spectra of Comets

High-resolution spectra of Comet Ikeya, which proved to have an exceptionally rich, dust-free spectrum, have been obtained by Greenstein. Wavelengths of more than a thousand features

have been measured; the interpretation on the basis of resonance fluorescence has proved to be extremely good. Arpigny found very detailed confirmation of this mechanism when electronic computing-machine techniques were used to compute the population of the ground levels during a fluorescence excitation process.

The extraordinarily bright comet Humason 1961e had an essentially tail spectrum even in the inner nucleus. Bands of CO^+ , N_2^+ , and CO_2^+ were exceptionally strong, and a complete identification of several high-vibrational sequences was possible. In addition, on one underexposed plate of high resolution, rotational structure of the CO^+ bands was observed for the first time. Arpigny again confirms that the resonance-fluorescence mechanism is responsible for the details of this ionic rotational structure.

Arpigny, who has completed a very elaborate study of all of Greenstein's material on high-resolution cometary spectra of the last few years, found that in every detail the Swings' resonance-fluorescence mechanism is successful in accounting for the various mutilations of the band structure. He predicts that some infrared transitions of the vibration-rotation bands of CO^+ will be quite strong.

West Ford

The scattered light from the sun from the small metal dipoles of the West Ford communications satellite experiment was detected on five occasions by Kowal under the supervision of Sandage, using the 20-inch reflector with its photoelectric equipment at Palomar. Predictions of the position angles for the Palomar site were made by prearrangement by the Lincoln Laboratories and were communicated to Palomar by W. Liller. The observations were made by setting the telescope on the predicted position well before the passage of the belt was to occur, opening the photometer diaphragm to its widest blocking diaphragm, letting the telescope

drive, and observing any increase in signal above the sky at the time of predicted belt passage. Five positive observations were obtained. On May 14 at 07^h 11^m 0 UT the belt was observed to be 4.5 per cent as bright as the night sky, or an equivalent surface brightness of 25.8 mag per square sec-of-arc sky area. The other results were 2.4 per cent of sky brightness on May 16; 3.5 per cent on May 17; 2.2 per cent on May 18 at 05^h 29^m UT; and 2.6 per cent on May 18, 08^h 17^m UT; and, finally, 1.6 per cent on May 30 with a doubtful record.

The first five records were very clear, with a signal-to-noise ratio of about 10 to 1. The observations were all made in one color, whose effective wavelength was $\lambda \simeq 4400 \text{ \AA}$, and when converted to absolute units gave the scattered light surface brightness to be $3.3 \times 10^{-19} \text{ erg sec}^{-1}$

$\text{cm}^{-2} \text{ \AA}^{-1} (\text{arc sec})^{-2}$ for the May 14 observation, with corresponding numbers for the other nights.

The observed surface brightnesses are probably *minimum* values, because the area of the belt was not searched during passage for the point of maximum brightness. Because the belt was wider than the 6.4-diameter diaphragm used, the observations may have been made on the fringes for some of the time. Therefore, it is fair to state that the belt was at least 3 per cent of the night sky brightness, and the densest part of the belt may have been even brighter.

Although this brightness does not interfere with normal ground-based photometric programs, a West Ford belt of 50 times the strength of the May 1963 experiment would begin to constitute undesirable interference.

STELLAR SPECTROSCOPY AND PHOTOMETRY

During the report year, 1093 spectrograms were taken with the 200-inch telescope, 860 with the 100-inch, and 580 with the 60-inch.

Chemical Composition of Stellar Atmospheres

In collaboration with Dr. George Wallerstein of the University of California, Greenstein has carried out analyses of two CH stars, HD 26 and HD 201626. These unusual objects are of a spectral type near that of the K star ϵ Virginis but have lower than normal metal abundances, their metal deficiencies being by a factor of 5 and 30, respectively. The remarkable feature of these stars is the high abundance ratio of carbon to iron, with an increase of approximately 6 in carbon abundance; C^{13} is not visible, however. In addition, the relative overabundance of the heavier elements with respect to iron (formed by the s-process neutron capture chain on iron) is by approximately a factor of 20 for barium

to neodymium, and by a factor of about 3 for yttrium and zirconium. It is thus apparent that the stars being observed are very old, presumably of solar mass, and in a highly evolved state, some material in which carbon has been synthesized having been brought to the surface. This material has also been subject to neutron bombardment, forming within the star the heavier elements from iron. It is likely that all these processes have occurred in the stars themselves. Because of their high space motion they must be old and could not have been formed at a late enough date in galactic evolution for the full development of these complex nuclear processes in other stars to have produced abundance anomalies in the surrounding interstellar material far from the galactic plane.

Greenstein finds that a substantial number of the so-called high-velocity subdwarfs are spectroscopically abnormal, in the sense of indicating higher luminosity through the strength of the ionized lines. A separate investigation of this

spectral material has been carried out by Gunn, using hydrogen-line profiles computed from model atmospheres. At the present time, the preliminary result is that an appreciable number of these objects indicate low effective surface gravities, $\log g = +2$. This is far lower than would be expected for main-sequence stars and a little higher than for the so-called horizontal-branch stars. Apparently an appreciable number of the very weak-line stars are highly evolved and lie near the RR Lyrae or horizontal-branch stars in their physical properties. The low masses that would be derived may indicate a very advanced evolutionary stage.

Greenstein has started a program of observation of a group of subgiant K stars having a large $U - B$ excess. These stars are marked by enhanced CH and have moderately high velocities. The program includes HD 5916, 44007, 74462, and 81192. Baschek will attempt a detailed spectroscopic analysis of the last of these stars.

Baschek has observed the entire accessible wavelength region, from ultraviolet to infrared, of three metallic-line A stars: 63 Tauri, 68 Tauri, and 60 Leonis. Spectral scans, colors, and blanketing corrections, in addition to refined model atmospheres, will be used to improve the knowledge of the detailed spectroscopic peculiarities of the metallic-line stars. An intermediate object which has some of the peculiarities of the magnetic and of the metallic-line stars, β Coronae Borealis, has also been observed by Baschek.

In conjunction with other programs, Baschek, Oke, and Searle have obtained scans and blanketing corrections for the normal A stars to calibrate the effective temperature scale.

Searle is working with Lungershausen on the composition and atmospheric physical conditions of peculiar A stars. The strength of a number of lines in the iron peak elements has been measured for approximately 20 stars, and relative abundances are being obtained to see

whether peculiar physical conditions alone are capable of producing the observed anomalous line intensities or whether actual abundance differences are required. Many of the groups of peculiar A stars were originally classified by such abundance anomalies as that of manganese. The question now to be solved is whether detailed changes from star to star exist in other elements.

The abundances of silicon, magnesium, carbon, and helium in 31 peculiar A stars of all subtypes have been studied by Searle. Silicon is overabundant by factors between 10 and 50 in a special group of hot peculiar A's; these stars have the temperatures and surface gravities of main-sequence B5-B8 stars. In the majority of peculiar A stars, silicon is in normal abundance; in the silicon-rich stars, however, large deficiencies of helium and carbon are also found. A new class of peculiar A's, characterized by normal C II but weak neutral helium, has been found, including α Sculptoris, 36 Lyncis, and Maia.

As a result of the general survey of these peculiar A's, data have been accumulated on the behavior of lines in late B and early A stars, as a function of $B - V$ color. Applying these empirical results, Searle has shown that the results of Wallerstein on the abundances in the high-velocity A star 7 Sextantis are incorrect, and that this star has, in fact, a normal composition.

The behavior of the iron-group metals in 20 stars has shown certain regularities. The silicon-rich stars have normal relative abundances of these elements. The so-called manganese stars have Mn/Cr increased. Both Mn/Fe and Cr/Fe are increased in all peculiar A's except the silicon-rich ones. The one metallic-line star studied showed normal relative abundances of these elements. Searle and Baschek have collaborated on a study of spectral scans and spectra of the four known stars of the λ Bootis type, i.e., λ Boo, π^1 Orionis, 29 Cygni, and θ Hydrae. In these stars the oxygen lines do not

exhibit the weakening shown by other spectral lines. In RR Lyrae this fact is also noted, and it thus appears that some of the apparently metal-poor stars may at least have normal oxygen abundances.

Coudé spectrograms have been obtained by Deutsch for curve-of-growth studies of the two very sharp-lined magnetic stars 10 Aquilae and HD 188041. The dispersions range from 3.4 to 6.7 Å/mm over the wavelength interval $\lambda\lambda 3400$ –6700. An analysis of 10 Aql by Lawrence Auer at Haverford College, under the supervision of Louis C. Green, has yielded underabundances relative to the sun of about 10 times for aluminum and barium, overabundances of about 10 times for magnesium and cobalt, and an overabundance of about 200 times for europium. Green is proceeding with an analysis of the abundances in HD 188041 near the extremes of its 226-day cycle of magnetic and spectrum variation.

Merrill, Keenan, and Deutsch have found a large systematic metal deficiency in the Mira variables that belong to a high-velocity population. The Miras of lower velocity sometimes show other spectroscopic peculiarities that simulate a large metal deficiency. To understand these effects, Deutsch is observing the blue and violet spectra of selected Mira variables at 20 Å/mm during the pre-minimum phases when interference by emission lines is at a minimum. Keenan is collaborating in the work with nearly simultaneous spectroscopic observations in the visual at lower dispersion.

Dr. Helmut Abt, of the Kitt Peak National Observatory, and Kraft are studying the chemical composition of TV Camelopardalis, a “classical” cepheid about 5000 parsecs distant in the northern Milky Way. The object has all the classical characteristics, but the amplitude of light variation is too large—somewhat like the cepheids of the Small Magellanic Cloud. The critical ionization temperatures have been obtained from $H\gamma$ intensities based on Oke’s model atmospheres for F-type stars and a

calibration of $H\gamma$ intensity versus T_e in the Hyades. The composition of TV Cam will be obtained on the basis of the assumption that the compositions of α Persei (F5Ib) and δ Cephei are like those of the sun or the Hyades.

Color-Magnitude and Chemical-Composition Relationships

Eggen has discussed the colors, luminosities, and motions of the A-type (B8 to F0) and G-type ($B - V = +0^m3$ to $+0^m8$) stars brighter than visual magnitude 5.5. Because most of the A-type objects belong to a half-dozen groups, including the Hyades, Sirius, Pleiades, and Coma Berenices groups, the usual determination of the solar motion from these stars is, statistically, not as secure as it would be if the velocities were random. The so-called “basic” solar motion of $(U', V') = (+9, -9)$ is probably too small, and a value near $(U', V') = (+10, -15)$, which is similar to what is often called the “standard” solar motion, may more correctly represent the deviation of the sun’s motion from the circular velocity at the sun’s distance from the galactic center. The color-luminosity arrays of the Hyades, Pleiades, and Sirius groups indicate that the A-type main-sequence stars (mass = 2–3 solar masses) first evolve into Ap or Am stars with little change of luminosity, next decrease in luminosity by approximately one magnitude before entering the Hertzsprung gap ($B - V = +0^m3$) and δ Scuti variables, and then exhibit a slow rise in luminosity as late-type giants. The brightest early-type objects in all the groups are mainly Ap stars with Mn and $\lambda 4200$ stars predominating in the youngest (Pleiades) and Sr stars in the oldest (Coma Berenices). A half-dozen of the brightest stars in the Pleiades cluster and a few of the group members near the sun (including β Tauri, α Columbae, and α Crucis) may be considerably younger than most of the other group members.

The colors of the brightest B8 and B9

stars outline an absorption-free region near the sun that extends about 100 parsecs in the anticenter direction but only some 20 parsecs in the direction of galactic rotation.

The three-color observations of the 400 bright G-type stars provide material for sampling the frequency with which stars of various metal abundances occur. Because of pressure effects, stars above the main sequence and in the range of $B - V = +0^m3$ to $+0^m6$ show an ultraviolet deficiency when compared with the $U - B, B - V$ relation for main-sequence stars. Therefore, the $U - B, B - V$ relation for Hyades main-sequence stars, which is generally used for ultraviolet excess determinations, has been supplemented with similar relations for stars above the main sequence; these relations were obtained from wide visual binaries with one component, a main-sequence star, showing no ultraviolet excess. When the colors of the nearest G-type stars are compared with the appropriate $U - B, B - V$ relation, the resulting ultraviolet excesses are distributed as shown in table 1.

TABLE 1

Per Cent (bright)	$\delta(U - B)$	Per Cent ($+25^\circ$ to $+30^\circ$)
1	$> -0^m04$	1
3	-0.04 to -0.02	3
21	-0.01 to $+0.01$	22
27	$+0.02$ to $+0.04$	27
25	$+0.05$ to $+0.07$	24
12	$+0.08$ to $+0.10$	13
8	$+0.11$ to $+0.13$	6
2	$+0.14$ to $+0.16$	3
1	$+0.17$ to $+0.19$	1

Luminosity classifications for all the AGK stars brighter than photographic magnitude 9 and between declination $+25^\circ$ and $+30^\circ$ are available from slit spectra, mainly as a result of observations made at the David Dunlap Observatory. The 230 main-sequence objects in this sample have been observed with the 20-

inch reflector; they were used as a control sample, and the resulting distribution of ultraviolet excesses is shown in the table.

The translation of ultraviolet excesses, which are referred to the Hyades stars, into metal abundances can be obtained from the correlation of the excesses with the spectroscopically determined abundances. However, the spectroscopic determinations are usually referred to the sun, and both the ultraviolet excesses of the sun, referred to the Hyades, and the metal abundance of the Hyades, referred to the sun, are subject to some uncertainties.

Eggen has obtained new observations of stars in and near the cluster NGC 752 with the 60-inch and 200-inch reflectors. The resulting color-magnitude diagram, based on stars having a high probability of membership in the cluster, shows a small gap between the evolved and unevolved main-sequence stars. The ultraviolet excesses of the evolved F-type stars are correlated with the values of $B - V$. The reddest F-type giants show an ultraviolet deficiency in comparison with main-sequence stars of 0^m1 . A search for faint members of $V_E = 17^m$ in a small area near the center of the cluster was largely successful. The region of the cluster contains several stars more distant than the cluster, with ultraviolet excesses similar to those found for the cluster stars (0^m1); these distant objects lie about 250 parsecs above the galactic plane. The color-luminosity array for the cluster is similar in many respects to that for the rich cluster NGC 2477. A corrected distance modulus of 7^m75 and a reddening of $E(B - V) = +0^m08$ was derived for NGC 752.

Photometry of Stellar Clusters and Related Stellar Types

The color-magnitude diagram of NGC 1866, one of the so-called "blue globular clusters" in the Large Magellanic Cloud, has been obtained by Arp. The diagram resembles very much that of NGC 458 in

the Small Magellanic Cloud. Both the break in the upper main sequence and the placement of giants close to the Hertzsprung gap show the peculiar characteristics of these Magellanic Cloud clusters rather than those of clusters observable in our own Galaxy. Two-color light curves for a half-dozen 3-day-period cepheid members of NGC 1866 have been measured. The behavior of these cepheids will be studied relative to the color-magnitude diagram of their cluster.

Work on long-period variable stars in globular clusters has been continued by Arp. Variables in the two southern globular clusters 47 Tucanae and ω Centauri have been analyzed in cooperation with J. v. B. Lourens of the Royal Observatory at Capetown and Frank Brueckel. Results on 47 Tuc have recently been published, and results on ω Cen are now being prepared for publication.

In both clusters a very definite result is emerging; namely, stars just off the end of the giant branch break into small-amplitude, semiperiodic oscillations of around a 50-day period. As they evolve more deeply into the instability zone they abruptly undergo larger-amplitude vibrations with a 150-day period, and finally a 4–5 magnitude variation sets in at a discrete period, a little longer than 200 days. In other globular clusters a 100-day period mode seems to be most frequent.

In conjunction with Dr. Landi Dessy at the Argentine National Observatory at Córdoba, plans are being made by Arp to obtain light curves of long-period variables in the galactic nucleus. The analysis of the nonvariable stars in this region (centered on NGC 6522) by Arp is almost complete.

Eggen and Sandage completed a photoelectric reinvestigation of the old galactic cluster M 67 in an attempt to improve the first photometry of Johnson and Sandage in 1955. The point was to observe all stars in the central region of the cluster brighter than $V = 14$ by photoelectric methods rather than by photographic interpolation, which uses plates

and a more limited photoelectric sequence of standard stars. The problems to be solved were (1) to separate the ultraviolet excess from the reddening parameter by observing stars both redder and bluer than $B - V = 0.80$, and (2) to check whether the break in the color-magnitude diagram at $V = 12.75$, $B - V = 0.52$ on the rising evolved main sequence at a point 0^m.2 fainter than the break point was real.

The reddening was found to be $E(B - V) = 0^m06$ by using cluster members bluer than $B - V = 0.25$ and redder than $B - V = 0.80$, limits beyond which the blanketing effect of the weak Fraunhofer lines due to low metal abundance is small or zero. After applying this reddening value to the $U - B$, $B - V$ diagram, the residual deviation of the cluster stars within the range $0.25 < B - V < 0.80$ is about 0^m.03, which is taken to be the ultraviolet excess of M 67 stars relative to the Hyades. Once again it seems that the oldest disk stars in the galaxy have experienced little or no enrichment in the past 7×10^9 years—observational results that are in some contradiction with theories of gradual enrichment of the interstellar medium with time.

The new data show that the gap, first fainter than the main-sequence termination point suggested by the earlier data of Johnson and Sandage, is indeed real and is $\Delta V = 0^m50$ wide. The theoretical evolving models must drastically speed up in their evolutionary time scales at this point, and then slow down again. This feature does exist in many computed models in the 5-solar-mass range but has not yet been found to occur in the available published models in the 1-solar-mass range.

Sandage and Kowal have completed the photometry of 1700 selected stars from the Lowell Observatory proper-motion catalogues to obtain data for the high-velocity subdwarfs in the solar neighborhood. They found a total of 175 new F and G subdwarfs with ultraviolet

excess values exceeding 0.16 mag. These are the near-by stars which presumably are identical with the globular-cluster main-sequence stars. This data sample, together with the 75 subdwarfs found by Sandage in his pilot program of several years ago, provides a sample large enough to determine the bluest color index reached by these stars, and thereby to determine at the bright magnitudes (where photometry is easy and therefore more accurate) at what color the main-sequence termination point of globular clusters should be found. The data provide a well determined turnoff color of $B - V = 0^m35$, which is about 0^m07 bluer than has heretofore been obtained for the halo globular clusters. Direct photometry on the globular clusters at the main-sequence termination point has been difficult because the levels are $V = 18.0$ to $V = 19.5$. New measures by Sandage in M 3, M 13, M 15, and M 92, where long integration times have been used to obtain a photoelectric accuracy of $\pm 0^m01$ in all three colors at $V = 19.0$, show that the turnoff colors in these clusters will be near $B - V = 0.35$ when proper reddening corrections are applied. To this end, Sandage is completing photometry of about 70 field stars near each cluster to obtain the reddening by the U, B, V method. If the present results are verified by additional photometry, the globular-cluster main sequences will all terminate near M 67 instead of NGC 188.

The theoretical models of Hoyle then predict that the age of the globular clusters will be the same as that of NGC 188 (even though the turnoff point is 0^m7 brighter) if the chemical composition of the subdwarfs is hydrogen = 100 per cent, helium = 0 per cent, heavy elements very low (see last year's report for independent evidence on this point), and if the composition of the M 67 and NGC 188 stars is hydrogen = 63 per cent, helium = 35 per cent, heavy elements = 2 per cent. If these numbers apply, the age of the oldest disk stars (NGC 188) and of the halo globular clusters is the same to

within the errors of the determination; it is about 12×10^9 years. The older ages reported in earlier reviews were due to a misassessment of the effect of the chemical composition on the ages and to the less accurate photometry then available for the globular clusters. This work is still in progress, but there is every expectation that the final photometry will be available next year.

High-Velocity Stars

Eggen has prepared for publication a catalogue of 659 stars which probably have space motions exceeding 100 km/sec with respect to the sun. In addition to the apparent motions, many of which are new determinations, the catalogue contains the space velocity vectors U, V, W ; the change in these vectors per 100-parsec increase in the assumed distance; the direction cosines $U(\alpha, \delta, \rho), V(\alpha, \delta, \rho)$, and $W(\alpha, \delta, \rho)$; and remarks about duplicity, peculiar spectra, etc.

Double Stars

Eggen has obtained some 1500 three-color observations of 600 stars in 250 wide double and multiple systems with the 200-inch, 100-inch, and 60-inch reflectors. Special emphasis has been placed on systems containing close pairs for which masses are available, variable stars, and objects of high luminosity for which luminosity calibrations are needed. The material now available indicates the following:

1. Very few of the binaries are younger than the Pleiades, but several are probably older than NGC 188.
2. The faint companions to extremely metal-poor stars do not show the break in the main sequence at $B - V$ near $+1^m4$, which is probably caused by the presence of TiO bands.
3. The pairs showing ultraviolet excesses less than $+0^m04$ are almost exclusively confined to the small region of the U, V plane (Bottlinger diagram) populated by the Hyades and Pleiades groups.

4. When reliable masses are available for the stars in paragraph 3, they populate the Hyades-Pleiades mass-luminosity relation, whereas the stars with appreciable ultraviolet excess populate the sun-Sirius mass-luminosity relation. Interpreting the differences in mass-luminosity relations as an effect of different H/He ratios suggests that the helium-rich objects (like the Pleiades and Hyades stars) are kinematically related.

5. The luminosities of the β -Cephei variables, σ Scorpii (ADS 10009), β Cep (ADS 15032), and 16 Lacertae (ADS 16381), agree well in the mean with a period-luminosity relation for these variables derived by Petrie from H γ measurements.

6. The metallic-line and peculiar A-type stars fall in the same limited region of the M_V , $B - V$ diagram that is occupied by these objects in galactic clusters.

7. The subgiant components of the eclipsing systems U Cephei and WW Draconis lie on the mass-luminosity relation for main-sequence stars.

Eggen has also prepared an extensive discussion of the empirical mass-luminosity relation. Masses have been derived from group and photometric parallaxes for a number of binaries in the Hyades, Pleiades, and Sirius groups, and in the general field. It is concluded from these selected observational data that (1) the Hyades stars and field binaries showing no ultraviolet excess with respect to the Hyades populate a mass-luminosity relation compared with which the sun is overmassive for its luminosity by a factor of 5/3, or underluminous for its mass by 1^m65; (2) the sun, members of the Sirius and 61 Cygni groups, and 3 binaries with parallaxes greater than 0".2 populate the same mass-luminosity relation, within the accuracy of the available data; (3) the separation between the mass-luminosity relations can be understood as a result of the ratio of $X_{\text{sun}}/X_{\text{Hyades}} = 1.5$. The available data for the extreme subdwarf binary ADS 16644 indicates a hydrogen abundance near 100 per cent.

Castor, working with Eggen, has programmed the 7090 for double-star orbit computation. The program will be used for systems in which the available observations cover the node of the orbit but do not define the period; the values of the mass (that is, a^3/P^2) can be obtained for many of these pairs.

The photometry of red dwarf-white dwarf systems, mentioned in *Year Book 61*, has continued. All but one or two of the suspected white dwarfs in such pairs, published by Giclas and his colleagues at Lowell Observatory, have shown the colors of white dwarfs.

Subdwarfs and White Dwarfs

Analysis of the subdwarf radial velocities of F to K stars by Greenstein has confirmed the general features of subdwarf space motions already known. The solar motion with respect to these stars is very large, and in extreme cases—for stars of exceptional line weakness and large velocity dispersion—systematic motions of more than 200 km/sec are found. The correlation between space motion and line weakening is excellent for the weakest-line stars.

Approximately 25 new white dwarfs have been found by Greenstein, largely from the *Lowell Proper Motion Survey* lists. In collaboration with Eggen, preparation of the color-magnitude diagram for the white dwarfs is being carried through by observation of proper-motion pairs that can be observed both photoelectrically and spectroscopically. The main-sequence components can be put on the standard Hyades main sequence by means of the U , B , V colors, providing accurate luminosity calibration for stars of both population types.

Faint Blue Stars

Spectrograms at 81 Å/mm have been obtained by Jacques Berger for about 60 faint blue stars, mostly in elevated

galactic latitudes; for many stars two or three spectrograms were secured. The photovisual apparent magnitudes of these stars lie in the range 7.4 to 12.0, and all of them are of spectral types earlier than A0. Attention has been concentrated in particular on measuring the radial velocities of these stars. Radial velocities have also been measured for a number of stars in the magnitude range $10 < m_p < 12$, whose spectra were obtained at 38 Å/mm and 16 Å/mm by Greenstein with the 200-inch.

The extensive data on faint blue stars on the south galactic cap, which are given in the *Catalogue* by Haro and Luyten, were subjected to a statistical analysis by Zwicky and Mrs. Jeanne Berger, using in particular Zwicky's method of dispersion subdivision curves. The distribution of the faint stars over the regions mentioned proved to be quite random. No swarm or cluster formations are in evidence. Twelve additional fields have been covered with the Haro-Luyten tricolor-image method. Around the north galactic pole, eight continuous fields have been likewise photographed separately on 103a-O and 103a-D plates with blue and yellow filter combinations. Both sets of plates are now systematically being searched for faint blue stars. Tri-image plates covering the north polar galactic regions are also being secured.

Zwicky has suggested several mechanisms that may cause a gradual mass loss from stars, which, he believes, may result in blue stars with unusually low luminosity. In a search for stars of this type, plates were taken with the 48-inch schmidt and turned over to Drs. W. J. Luyten and Jacques Berger, who have blinked some of them for very faint ($m_p > 16.0$) blue stars with large proper motions. Spectra of two of them, LP 414-106 ($m_p = 17.7$) and LP 357-186 ($m_p = 18.4$), were obtained by Zwicky with the prime-focus spectrograph of the 200-inch telescope, being characterized by blue, featureless continua. From these facts, and the proper motions of 0''.55/year and

0''.42/year, it is concluded that the absolute luminosity of these stars is about 100 times smaller than the absolute luminosities of ordinary white dwarfs, and their average densities are of the order of 10^8 grams/cm³. The search for such stars, which appear to be numerous, is being continued.

Spectrophotometry

Photoelectric spectrum scans and spectroscopic observations of SW Andromedae, an RR Lyrae star with a period of 0.44 day, have been completed and analyzed by Oke. An accurate radial-velocity curve has been obtained; it is very similar to those of other RR Lyrae stars. The velocity curve for H γ deviates very little from that for the metals, in contrast to the results for SU Draconis. This may be a consequence of the great strength of the metal lines compared with their weakness in SU Dra. The H γ profiles give an effective-temperature curve in good agreement with the continuum measures obtained with the scanner, provided that a reddening in $B - V$ of about 0.1 mag is assumed. A detailed analysis that will yield a mean radius and absolute magnitude is almost complete.

Oke is making photoelectric-scanner observations of a selection of Hyades stars and subdwarfs in order to determine accurate effective temperatures for both kinds of stars. The blanketing theory recently developed to correct U , B , V colors for the effects of variable metal-line strengths is designed, in effect, to do this. For the cooler stars, however, it is necessary to assume in the blanketing theory that the real continuum is, in fact, observed in the blue and ultraviolet. This is almost certainly not true. The scans are being made in the region from $\lambda 3400$ to $\lambda 10800$. The absolute-energy distribution in the red and infrared, where lines are very weak, is compared with fluxes computed from model atmospheres to determine the effective temperature. The

model atmosphere for the appropriate effective temperature can now be used to determine where the true blue and ultra-violet continuum lies relative to the observed one. In the extreme subdwarfs, the model atmosphere flux is found to be in excellent agreement with the observed continuum, and an effective temperature is easily obtained. In the cool Hyades stars only the red and infrared measures can be used. Certain selected hotter Hyades stars and the giant stars have also been observed in order to obtain effective temperatures over the whole range of spectral types observed in the Hyades except the very faint dwarfs.

At the request of Commission 29 on Spectroscopy of the International Astronomical Union, Dr. Kron of Lick Observatory and Oke were asked to select standard stars for photometric and spectrophotometric studies with a view to applications in spectroscopic problems. These stars were to be confined between declinations $\pm 15^\circ$ so that they would be accessible in both hemispheres. Of the fairly large list of photometric standards, 24 early-type stars have been chosen as spectrophotometric standards. They include some of the stars previously measured for standards by Oke. Smith and Oke have been observing the 24 stars with the photoelectric scanner both in the blue and in the infrared. Preliminary absolute-energy distributions, relative to the primary standard, α Lyrae, are now available for many of the stars. The range covered is from $\lambda 3390$ to $\lambda 10800$.

By means of the photoelectric Cassegrain scanner, observations are being obtained by Whiteoak of about 50 main-sequence stars with spectral types distributed between G8 and K7, which were picked from a catalogue published recently by Wilson. The purpose of the research is to obtain more information about the energy distribution of late-type stars, in addition to investigating Wilson's conclusion that late-type dwarfs of a particular spectral type have a wide variation in their colors. Observations were carried

out in the red region of the spectrum with an RCA 7102 photomultiplier. Instead of scanning a star's spectrum at a linear rate, measurements were obtained with a bandwidth of 50 Å, and with the band centered at 18 discrete wavelengths between $\lambda 5000$ and $\lambda 11000$, where the stellar spectrum is relatively free of absorption lines. The final results were achieved by means of a reduction program of Oke on the IBM 7090.

Jones has observed stars later than K5 in the spectral region $\lambda 5000$ to $\lambda 11000$ with the Cassegrain scanner and a resolution of 20 Å. A star was observed at high and low altitudes on every night; the results were combined to form a mean monochromatic extinction curve, which was then used to reduce the scans to "no atmosphere." Every night Vega was observed with the program stars; the intrinsic energy distribution of this star, carefully evaluated by Code, was used to convert the scans into true energy distributions. Selected giants and dwarfs with both high and low space velocities were observed. They have a system of (predominantly) TiO bands extending from $\lambda 5000$ to $\lambda 8500$ and a relatively undisturbed spectrum to $\lambda 11000$. The observations were planned to investigate an effect found by Kron, namely that, when absolute magnitude is plotted against $R-I$ color, the high-velocity stars tend to define a main sequence slightly below that defined by low-velocity stars. Blanketing by the TiO bands could cause this effect if the bands are weaker in high-velocity stars. Whether the bands are, in fact, weaker awaits a full discussion of the reductions, as do the effects of luminosity.

In last year's report a three-dimensional classification scheme applicable to subdwarfs was outlined. Selected stars so classified were scanned by the technique described above and compared with the model atmospheres of Swihart and Fischel. The temperatures so derived were used to calibrate the classification scheme.

Supernovae

Between July 1, 1962, and May 31, 1963, 10 supernovae were discovered on plates taken with the 48-inch schmidt telescope at Palomar (7 by Zwicky and 1 each by Mrs. Mendez, Berger, and Rudnicki). Zwicky followed most of the discoveries by additional observations, obtaining the spectra of the supernovae as well as the spectra of their parent galaxies with the prime-focus spectrograph of the 200-inch telescope. Furthermore, the spectra of those discovered by other members of the I.A.U. Committee on Supernovae were observed directly or spectroscopically. The most important among these are the supernova of type I in NGC 1073 (independent discovery by L. Rosino, G. Haro, and E. Chavira), NGC 4146 (Rosino), NGC 4178 (Saytseva), IC 3112 (Kurokin), and a supernova in an anonymous galaxy at R. A. $11^{\text{h}}48^{\text{m}}0$, decl. $+55^{\circ}38'$ (Ch. Bertaud). For the first time a supernova was found in the Corona Borealis cluster. The study by Zwicky of the luminosities of the 20 known supernovae in distant clusters, such as those in Cancer, Coma, Shane Cloud, and Corona Borealis, and especially their indicative distances from the centers of their parent galaxies, seem to confirm the finding by methods previously reported that the most probable value for the constant of the universal redshift lies close to 175 km/sec per million parsecs.

A special study was made of the supernova of type V in NGC 1058. Plates from Harvard, Lick, Mount Wilson, and Palomar covering the period from 1937 to the present show that the apparent photographic luminosity increased slowly over 20 years (from $m_p = 18.2$) and then rose abruptly in 1961–1962 to reach $m_p = 12.2$ on December 5, 1961. In March 1963, observations gave $m_p = 19.0$. The spectrum shows mainly emission lines of H, He I, and Fe II displaced toward the red by 950 km/sec and indicating an expansion velocity of the

ejected gaseous clouds of about 2000 km/sec. Even the last spectrum obtained on October 23, 1962, does not show any forbidden lines such as N1 or N2, indicating that the clouds ejected have a mass far greater than those ejected by common novae.

The symbolic velocity of recession of NGC 1058, redetermined by Zwicky, was found to be 439 km/sec rather than 80 km/sec, as given in the catalogue of Humason, Mayall, and Sandage. The supernova in NGC 1058 is thought to be of the type of η Carinae, but was perhaps 2 mag brighter at maximum, and thus 3 or 4 mag fainter than a supernova of type I at maximum.

Novae

A systematic search for binaries among old novae is being continued by Kraft, using the 200-inch nebular and coudé spectrographs. The duplicity of T Coronae Borealis ($P = 227^{\text{d}}6$), T Aurigae ($P = 4^{\text{h}}54^{\text{m}}$), DQ Herculis ($P = 4^{\text{h}}39^{\text{m}}$), and WZ Sagittae ($P = 1^{\text{h}}22^{\text{m}}$) has already been recognized through the work of Sanford, Walker, and Kraft. To these may now be added V 603 Aquilae (1918) and GK Persei (1901), which have periods of $3^{\text{h}}20^{\text{m}}$ and $1^{\text{d}}904$, respectively. V 603 Aql is a single-line binary; measurements of radial velocity are based on H δ , H γ , and He II in emission. GK Per is composite, sdBe + K2 IVp, and leads to minimum masses of 1.3 and 0.6 solar mass for the blue and red components, respectively.

More than one-third of all the old novae that can be studied spectroscopically from Palomar with sufficient time resolution are now known to be binaries; the presumption is strong that all are, and that membership in a close binary system of a certain type is a necessary condition for a star to become a nova.

If the red component of such systems overflows its lobe of the inner zero-velocity surface, it is likely that material will flow from the red star and circulate

about the blue, thus giving rise to the observed emission lines. If so, narrow emission lines should be associated with a small velocity amplitude for the blue star, depending on the viewing aspect. This appears to be confirmed in general. Nova Lacertae (1910) and Nova V 841 Ophiuchi (1848) have little or no velocity variation, but the emission lines are very narrow. It is possible they are viewed nearly pole-on, and we are unable to detect the velocity variation at the dispersion employed (~ 180 Å/mm).

Kraft finds that M_V for the red star is related to the period by the relation $M_V(\text{red}) = -10/3 \log P + \text{constant}$, if it fills the inner zero-velocity surface. This seems to be confirmed by applying the life-luminosity relation based on Arp's work on the novae of M 31 and Miss Swope's latest modulus.

There is strong evidence that "recurrence" among novae is associated with high minimal luminosity, with the presence of a late-type absorption spectrum, and with fairly long orbital periods. Kraft also suggests that old novae will be found in stellar systems in proportion to the total number of binary stars per unit mass within the system; thus, the frequency of novae per unit mass is a kind of measure of total angular momentum in the system.

Baschek has followed Nova Herculis 1963 in the infrared at 40 Å/mm during its postmaximum decline, since few data on novae are available for the infrared region.

After receipt of a telegram from the USSR announcing Nova Ursa Minoris 1956, it was picked up with the 48-inch schmidt. Its spectrum, photographed by Zwicky with the 200-inch telescope, was found to consist of a very blue continuum and emission lines showing a displacement of -20 km/sec and indicating an expansion velocity of the gaseous shells of 1200 km/sec. From the spectrum and the light curve, the nova is judged to have been of magnitude $M_p \sim -9$ at maximum, and thus located in the halo of the Galaxy,

several thousand parsecs away from the galactic plane.

U Geminorum Stars

As a part of the continuing program of detecting binaries among U Gem variables, an orbit for Z Camelopardalis, the prototype of the Z Cam subgroup, has been obtained by Kraft. The period is 0^d2880 (6^h55^m); the object is a double-line spectroscopic binary, sdBe + dK, with exceedingly evanescent absorption lines associated with the red component. According to Krzeminski and Mumford, the object also has grazing eclipses. If the red star fills its lobe of the inner zero-velocity surface, we can take $i \sim 70^\circ$, in which case the masses of the blue and red components are 0.7 and 0.8 solar mass, respectively. This is the first reliable determination of masses for a U Gem binary system. With a statistical parallax leading to $M_V \sim +9$ at minimum light for the members of this group, we have direct evidence that the red components are distinctly underluminous for their masses.

G and K Supergiant Survey

From objective-prism plates obtained by Kraft at Tonantzintla Observatory in December 1962, a search for G- and K-type supergiants is being conducted. Preliminary results indicate that about one of these per 5 square degrees will be found down to apparent magnitude 10, in harmony with predictions that 5 times as many of these supergiants as cepheids should be found per unit volume of space. Once the stars are identified, they should be useful for studies of spiral structure if their $H\alpha$ -based absolute magnitudes can be determined.

Stellar Rotation in the Coma Cluster

Coudé 9 and 10 Å/mm plates of all F-type stars in the Coma cluster have been obtained by Kraft. The lines are unusually sharp; the average rotation is about half that of the field or of the

Hyades in the same spectral-type range. The large number of Ap stars, the presence of several metallic-line stars with little or no orbital motion (12 Comae is an exception), the presence of two probably spectroscopic, but not photometric, W Ursae Majoris stars, and the slow rotation of the F-type stars in Coma all suggest that the cluster stars have a preferential orientation of rotational axes with i near 30° . Additional radial velocities will be secured.

Spectrum of Algol

During a 2-month stay as Research Associate, Spitzer used the 100-inch telescope to obtain a number of coudé spectrograms of Algol at various phases during eclipse. These plates, together with photoelectric spectrophotometric data obtained at Princeton, have been analyzed by E. Fletcher, who finds that Algol C is apparently a metallic-line A star. Spitzer has also revised his review paper, "Dynamics of Interstellar Matter and the Formation of Stars," for inclusion in volume VII of *Stars and Stellar Systems*, taking into account some of the extensive material recently published on the subject.

Stellar Chromospheres

There can be little, if any, doubt that the bright reversals observed in the centers of the H and K absorption lines in the spectra of many late-type stars are of chromospheric origin. Moreover, it is highly probable that the intensities of the reversals are a measure of the general chromospheric activities of the stars. In any limited region of the H-R plane, among stars of otherwise very similar characteristics, it is found that the H and K reversals exhibit a range of intensities that may be quite large. It may be asked, then, why it is that the chromospheres of similar stars show such a wide range in activity. An investigation completed during the past year by Wilson, and reported on partially in *Year Book 61*,

gives promise of shedding some light on the problem. The inquiry was restricted to main-sequence stars of spectral types G0 to K2, inclusive, and the results are summarized below.

1. Spectrograms of the members of 28 pairs or triples show that in such systems the chromospheric activity of the members tends to be much the same. The only exceptions are two stars which are themselves short-period spectroscopic binaries. Hence it may be concluded that the degree of chromospheric activity must depend upon the circumstances of the formation of the stars, or upon their ages, since these are the factors common to the members of multiple systems.

2. Spectrograms of more than 100 field stars provide rough statistics on the distribution of H- and K-emission intensities for these objects. For the field stars it is found that there is a strong preponderance of weak emissions, that is, of chromospheres of relatively low activity.

3. Spectrograms of well over 100 stars in the four clusters Hyades, Praesepe, Pleiades, and Coma reveal a distribution of H- and K-emission strength in striking contrast to that for the field stars. In the clusters, strong emissions, i.e., active chromospheres, are the rule rather than the exception. More detailed examination shows that the emissions are strongest in the Pleiades and somewhat weaker in Hyades, Praesepe, and Coma.

4. Tentatively, it is concluded that probably chromospheric activity in these main-sequence stars decreases with time. Approximate ages are: Pleiades 5×10^7 years, Hyades-Praesepe 5×10^8 years, the sun (which is typical of the weak-emission field stars) 5×10^9 years; and this is the observed order of decreasing chromospheric activity. If this conclusion is correct, the sun must once have had a much more potent chromosphere than it has today, and, therefore, in earlier epochs the earth and other planets may well have been subjected to an enhanced flux of ionizing radiation.

Among G- and K-type stars of every

luminosity it is observed that $H\alpha$ in absorption consists largely of a Doppler core with unexpectedly feeble wings. The width of the Doppler core is found by Kraft to increase with increasing luminosity, and it correlates very well with the width of the K2 emission in the same stars, which is already known as a reliable measure of absolute magnitude through the work of Wilson and Bappu. It is hoped that, because $H\alpha$ is seen in absorption projected on the stellar continuum, it may be possible to work with it in fainter stars than can be worked in with the K-line method. The possibility of using the equivalent width of $H\alpha$ rather than the core width is also being explored with the hope of pushing to faint apparent magnitudes.

Deutsch is continuing his coudé observations of circumstellar lines in supergiants and binary giants of late spectral type.

Stellar Polarization

The stellar polarimeter described last year has been further improved by H. W. Babcock by the addition of a commercial lock-in amplifier; stability and versatility were considerably increased thereby. At the prime focus of the 200-inch telescope,

the polarimeter was used to obtain measurements of the plane polarization in the light of some 53 stars, mostly magnetic stars and A-type stars brighter than the ninth magnitude. A number of standard stars were included. The single-phototube a-c polarimeter, with a slowly rotating ADP plate for an analyzer, gave satisfactory performance. As anticipated, it overcame the effects of atmospheric scintillation. Residual systematic errors resulting from alignment difficulties or internal reflections were generally at a level less than $P = 0.03$ per cent. It is hoped that with care they can be further reduced.

The purpose of this investigation is to discover and isolate the effects of intrinsic plane polarization in the star (due to saturation of Zeeman patterns or to synchrotron radiation), as distinguished from interstellar polarization. The intrinsic polarization should be distinguishable, owing to variations resulting from rotation of the star or from fluctuations of its magnetic field. The limited observations so far obtained have been inconclusive in establishing the existence of intrinsic or variable plane polarization, but the data constitute a set of "first epoch" results on which a further search for changes can be based.

GASEOUS NEBULAE AND INTERSTELLAR GAS

The Presence of $\lambda 3889$ of He I in Absorption

The problem of explaining the presence or absence of He I $\lambda 3889$ absorption in the spectrum of stars embedded in emission nebulae in relation to the nebular surface brightness has been the object of continued study by Münch, from both the theoretical and the observational points of view. In extension of the work of Wilson and Münch reported last year, a search has been made for the He I line on coudé spectrograms at 10 Å/mm of the fainter B stars in the Orion nebula. The line was detected in only one

additional star, HD 36982 = LP Orionis, and this star happens to have a small condensation of nebular material in its immediate neighborhood. On the evidence provided by the stars of the Orion nebula, therefore, it appears that the lack of one-to-one correlation between nebular absorption and nebular emission can be explained by the existence of density fluctuations in the nebula. However, the consideration of other emission nebulae and the stars embedded in them has raised the question whether there is not a physical agent in addition to electron collision, 2-photon emission, and ionization by direct starlight, producing the

deactivation of the 2^3S metastable level of He I. The observation of exciting stars of emission nebulae has revealed strong absorption of He I in the stars BD+66° 1675 in NGC 6822, BD+60°2522 in NGC 7635, and HD 64315 in NGC 2467. In many more similar stars, however, the line has not been detected, although the apparent surface brightness of the surrounding nebulae would appear to be sufficient to produce the line. The same remark applies to the exciting stars of some planetary nebulae of high surface brightness, such as IC 418.

A reconsideration of the theoretical problem involved has led to an important factor overlooked by K. Wurm and Wilson and Münch in their discussions of the Orion nebula, namely, the energy density of the Lyman- α radiation. In a dust-free nebula, ionization bound, the optical depth in Lyman α is so large that the trapped resonance radiation may be the most important factor determining the population of the metastable helium level. Extended emission regions where $\lambda 3889$ radiation is absorbed must have small energy density in Lyman α , probably because of the extinction produced by solid particles. To test this theory critically, observations with the Cassegrain photoelectric scanner have been started by Münch to measure the surface brightness of emission nebulae and to determine their dust content through the reddening of the nebular light. The energy density of Lyman α within a planetary nebula depends on the existence of differential motions in the layers optically thick to that radiation. It appears to be significant that the two planetaries with central stars known to have He I $\lambda 3889$ absorption, namely, HD 184738 and NGC 2392, have large expansion velocities, 53 and 107 km/sec, respectively, whereas IC 418 does not show the line—notwithstanding its high surface brightness—but has an expansion velocity of only 22 km/sec, according to Wilson.

The observation of $\lambda 3889$ in absorption,

unfortunately, needs large dispersion, which cannot be used on many interesting objects. The possibility exists, however, that the population of the 2^3S level of helium, and hence the energy density in Lyman α , can be studied also by the emission in $\lambda 10830$. Departures of the intensity in $\lambda 10830$ over the recombination value may be due to excitation of 2^3P by electron collision. Observations of the planetaries by O'Dell and of the Orion nebula by Mendez suggest that actually there are departures of the intensity in $\lambda 10830$ from the recombination value. Further observations of He I $\lambda 3889$ in absorption and He I $\lambda 10830$ in emission are being carried out.

Interstellar Lines of CN and C₂

Interstellar absorption lines due to CN have been observed before only in a few bright stars at the highest spectral resolving powers available. The detection by Münch of the CN lines at $\lambda\lambda 3874.6$ and 3874.0 in a 9.2 Å/mm spectrogram of BD+60°2522, a reddened O7 star at about 1 kpc distance, of much greater strength than had ever been found in any star before, is thus of interest. It points out in a striking fashion the nonuniform distribution of the interstellar molecules first suggested by Merrill from CH⁺ in the Pleiades.

On the basis of the recent identification of the ground state of the C₂ molecule by Ballik and Ramsay (*Astrophys. J.*, 137, 64, 1963), the (4, 0) (3, 0), and (2, 0) lines arising from the ground level of C₂ have been searched for in coudé plates of ζ Ophiuchi taken at Palomar, but have not been found. A further attempt, on the highest dispersion available, will be carried out at Mount Wilson in various other stars.

Velocities of Gas Clouds from Interstellar Lines

With the 100-inch coudé spectrograph, Van Woerden observed interstellar lines in the spectra of many early-type stars,

chiefly in Orion, with the highest available dispersions. In previous years he made an extensive study of neutral hydrogen in that region with the 25-meter radio telescope (beam width $0^{\circ}56'$) at Dwingeloo, the Netherlands, and a velocity resolution of 2 km/sec. From that study a detailed picture of the structure and motions of the hydrogen clouds is developing. Comparable velocity resolution (2 to 4 km/sec) should now be obtained for ionized calcium from the H and K lines. Twenty years ago Adams observed 27 stars in Orion with a 2.9 Å/mm dispersion. In the fall and winter, helped by good seeing, Van Woerden obtained 1.1 Å/mm spectra for 17 stars and 1.9 Å/mm spectra for 20 stars in Orion; almost all O-B5 stars brighter than sixth magnitude have been taken at least once. The gain in resolved component structure is considerable for many of Adams' stars. It is hoped to extend these observations next season and to supplement them with 4.4 Å/mm spectra of a number of fainter stars close to the trapezium which were not observed by Adams. Preliminary analysis indicates that part of the calcium components correlate well with those found in the 21-cm hydrogen line at the same position in the sky; but other calcium components are not represented in the hydrogen spectra, and they seem to be more variable with position.

A similar study is being carried out in the II Scorpius association. Van Woerden has also obtained a number of 1.9 and 4.4 Å/mm spectra of B stars in Lacerta. Further, he observed several of the brightest A-type stars at 1.1 Å/mm with a view to determining the amount of interstellar matter in the immediate neighborhood of the sun.

In early March, spectra of Nova Herculis 1963 were taken by Van Woerden and Baschek at 4.4 Å/mm in the violet and at 6.7 Å/mm in the yellow for a study of interstellar H, K, and D. At least three components are seen at K. For comparison, spectra have been taken of

the B5 star HR 6845, which is only $0^{\circ}4'$ from Nova.

Van Woerden spent part of his time on the continuation of his previous 21-cm studies in Orion and its surroundings and in Scorpius, done at the Kapteyn Astronomical Laboratory, Groningen, the Netherlands. Together with Blaauw and Mrs. Hack of Merate, Italy, he interprets two neutral hydrogen complexes with velocities of -26 and -48 km/sec, observed from 10° south of η and χ Persei, as possibly genetically related to the double cluster. The momentum required to remove the gas from the galactic plane might have been supplied by supernovae, and it seems that the number of supernovae of type II required may have been furnished by the formation and subsequent evolution of many heavy stars, in keeping with the observed luminosity function of the association surrounding the double cluster.

Internal Motions in IC 4997

Wilson and O'Dell investigated the internal velocities in the planetary nebula IC 4997. Exposures of 3, 6, and 60 minutes were obtained on two nights of very good seeing with the 32-inch camera at the coudé focus of the 100-inch telescope. Emission lines of several ions were measured for expansion widths. A velocity of expansion of 15 km/sec was derived with no systematic differences between the various ions. No line shapes were observed that were inconsistent with the interpretation of their being due to a smoothly expanding gas, in contradiction to the report of Andrillat and Andrillat. The appearance of the nebula is elliptical with a ratio of axes of about 0.7 and a major axis of about 1.5 sec.

Line Intensities in the Orion Nebula

A study of the line-intensity ratios in the Orion nebula has been completed by Mendez as a thesis project. The purpose of the investigation was to determine the range of variation, if any, of the electron

temperature in areas of the nebula with differing surface brightness and dust content. The reddening of the nebular radiations was determined from the intensity ratios between Balmer and Paschen hydrogen lines, measured photoelectrically with the Cassegrain scanner at the 60-inch. A consistent increase of the electron temperature with decreasing density was found, amounting to 10 per cent between areas close to the trapezium and the outlying Huguénian region. The study of the recombination helium spectrum has provided a good value for the hydrogen to helium abundance ratio, now fixed at 10 to 1.

Line Intensities in Planetary Nebulae

The 20-inch telescope at Palomar Mountain was used by O'Dell to extend the study of the bright planetary nebulae. Fluxes in the emission lines $H\beta$ and $N1 + N2$ were determined by means of narrow-band interference filters for 34 nebulae not included in previous surveys. The survey is now complete for 88 nebulae. This brings to 90 per cent completeness the survey in $H\beta$ of the northern ($\delta \geq -35^\circ$) bright ($m_{pg} < 14.0$) planetary nebulae. Primary importance was applied to objects not readily observed in the more northern sites used for the earlier similar studies, which include the region of the center of the Galaxy where there is a large concentration of planetary nebulae.

O'Dell has measured the relative line intensities in 11 planetary nebulae with the Cassegrain photoelectric scanner in the interval $\lambda\lambda 3426-10938$. Corrections for interstellar extinction were applied from measures of Paschen/Balmer lines arising from the same upper principal energy level. It was found that obviously some nebulae are optically thick to low Balmer-line radiation. However, a distinct deviation from recombination theory was noted for nebulae in which Balmer self-absorption should not be important. In addition, large deviations in the ratios

of the low He I triplets were observed, being correlated with nebular density. The group of four strong lines around $\lambda 10320$ has been identified as the auroral transitions ($^2P - ^2D$) of [S II]. In addition, several recombination lines in the 1-micron region were observed for the first time in nebulae. The corrected line ratios are being applied to a detailed discussion of the density, temperature, and transfer conditions within the planetary nebulae.

Densities from Line-Intensity Ratios

Spectra in the red, around $\lambda 6700$, have been obtained by O'Dell for 10 planetary nebulae for measurement of the doublet ratio of [S II] $\lambda 6717/\lambda 6731$ which arises from two close upper levels of collisionally excited S II. The relative population of the levels is dependent on the temperature and density conditions in the nebula, and hence the observed line ratios will reflect the conditions in the emitting regions. In a similar manner, the [Ar IV] doublet $\lambda 4711/\lambda 4740$ was observed in 3 planetary nebulae. These results, along with the results from older studies, were compared with the theoretical calculations of Czyzak and Krueger. It was shown that the interlevel collisions must be considered in order to put the predictions on an accurate basis. This is a result of a comparison between the predictions, obtained with the new transition probabilities but not taking into account interlevel collisions, and the densities derived for the nebula by other means. Therefore, it is shown that a detailed discussion of the collisional processes similar to that of Seaton and Osterbrock for [O II] $\lambda 3729/\lambda 3726$ is needed. Unfortunately these doublets are relatively weak in most planetary nebulae and are more difficult to measure than $\lambda 3729/\lambda 3726$; however, the new theoretical calculations and observations indicate the validity of using these lines for studying nebulae of densities up to 5×10^5 electrons/cm³.

Characteristics of Exciting Stars

The general characteristics of the planetary nebulae and their central stars have been discussed by O'Dell. Absolute photographic magnitudes for the central stars were calculated from the distances derived from measures of the nebular flux in $H\beta$ combined with the older photographic magnitudes for the central stars. The photon-counting method of Zanstra was applied to the new nebular measures to derive a temperature scale using the difference in luminosities of the star in the photographic region and the nebula in $H\beta$. This method produces lower limits to the stellar temperature for objects optically thin to the stellar Lyman continuum radiation. Using the derived temperatures and the continued assumption of black-body radiation, bolometric corrections were calculated and applied. Definite evidence was found for rapid changes in the characteristics of the central stars, with a time scale approximately equal to the dissipation time of

the gaseous shell (about 25,000 years). The stars are very hot and luminous ($M_{pg} \simeq -3.0$, $M_{bol} \simeq -5.5$, $T_s \simeq 30,000^\circ\text{K}$) soon after the shells are given off and they are first detected. As the shell expands the star contracts rapidly with an increasing temperature. In nebulae having the largest shells and presumably the longest elapsed time since the shell was lost, the central stars are extremely hot ($T_s \simeq 150,000^\circ\text{K}$) and have dropped greatly in luminosity ($M_{pg} \simeq +8.0$, $M_{bol} \simeq 0.0$). During this observed contraction phase, the radius of the stars must have changed from about 2 to 0.01 solar radius. The spatial distribution of the near-by planetary nebulae was compared with that derived by Schmidt for main-sequence stars of various masses. It was concluded that the stars giving rise to the phenomena called planetary nebulae are the advanced evolutionary products of stars originally in the range 1.4–1.8 solar masses. The central stars of the planetary nebulae are probably progenitors of some of the white dwarf stars.

GALAXIES

Rotation and Dimensions of the Galaxy

In the past year Schmidt completed a discussion of the values of the constants of galactic rotation and of the distance to the galactic center. The values finally adopted were $A = 15$ km/sec/kpc, $B = -10$ km/sec/kpc, and $R_0 = 10$ kpc. A simple model of the distribution of mass in the Galaxy, in which these values and other data are represented, was constructed. The total mass of the model is 1.8×10^{11} solar masses. The local escape velocity from the Galaxy is found to be 380 km/sec; it exceeds the local circular velocity by 130 km/sec. The observed high-velocity cutoff of 63 km/sec in the direction of galactic rotation cannot correspond to the escape velocity from the Galaxy.

The chapter on globular clusters in the *Kuiper Compendium of Astronomy* (volume entitled *Structure of Galaxy*) has been completed by Arp and awaits publication. The most important result is that a reanalysis of the globular cluster system in our own Galaxy yields a centroid which is $R_0 = 9.9 \text{ kpc} \pm 0.5$ from the sun. This value for the scale of our Galaxy appears to be supported by the radio measures of $AR_1 = 150$ km/sec and an Oort constant of $A = 15$ km/sec/kpc.

Internal Motion and Structure

A selected spiral arm of M 101 has been examined photoelectrically by Baum. M 101 (NGC 5457) is an Sc spiral galaxy oriented so that we see the spiral structure nearly face-on. The observations were

made by means of an attachment for driving the Palomar prime-focus photometer at a uniform rate back and forth across segments of the spiral arm being investigated. The focal-plane diaphragm was a slot 1 by 4 mm, and the observations were made in five of the colors of the eight-color system.

The purpose of the observations was to determine the color profile of the spiral arm and to interpret the result in terms of the distribution of stellar population within the arm. As can easily be seen on a photograph, the inner and outer edges of spiral arms are not symmetric. The asymmetry, when interpreted as a population difference, provides a clue to the degree to which the spiral arms of a galaxy do or do not share in the rotation of the disk. As found by Baum last year in M 74, the present results again suggest that the arms are lagging behind the moving material of the disk. The line of reasoning is outlined in *Year Book 61*.

From the point of view of photometric detection, the asymmetry of the arms in M 74 was not large, and the asymmetry in M 101 seems to be even smaller. In both, however, the effect is evidently real.

The determination of radial velocities of emission nebulae in the Sc system NGC 2403 was undertaken by Humason some years ago (*Year Book 51*). Because the points he obtained before his retirement scattered around a mean rotation curve considerably more than would be expected from the quality of the plates, his results were never published. To investigate the origin of the scatter around a smoothly varying curve, new observations are being made by Münch with somewhat higher dispersion and in the $H\alpha$ region instead of the blue. The plates obtained so far essentially confirm Humason's measures and suggest that the radial velocities of H II regions in NGC 2403, as in M 33, do not define a rotational curve as well as those in Sb systems do. The new material, together with Humason's, is now being prepared for publication.

Work by Baade on the position of emission nebulae in M 31 is being readied for publication by Arp. In the process of interpreting the spiral structure in M 31, the spiral structure has been photographically rectified to give views of the Andromeda nebula as it would appear flat onto the line-of-sight. A good fit for the spiral pattern in M 31 is given by the log spiral

$$r = 31' e \exp 0.13\theta$$

The spiral deviates in the sense of having an increasingly steeper pitch in the very central regions and a slightly flatter pitch in the outermost regions. These data again bear on the problem of spiral formation and maintenance and indicate that an investigation of spiral structure might profitably be made in M 31, where radio velocities of gas could be compared with optical velocities (the optical velocities should be compared and extended). Arp has emphasized that the above results show that although M 31 is a rather tightly wound spiral its arms are still separated by the order of 4 kpc. In our own Milky Way the separation of the Morgan-Sharpless-Osterbrock spiral arms is only of the order of 2 kpc. Either our own Galaxy is exceedingly tightly wound or it is multiple-armed. In either case, our own Galaxy does not seem to be a typical spiral, and any attempt to solve the problem of spiral galaxies in general by using data primarily from our own system should be regarded with misgivings.

Polarization

A survey program of photographic polarization in galaxies using the 48-inch schmidt has been initiated by Arp. About 30 galaxies (many of them peculiar, interacting, and connected) have been investigated. The emphasis at this stage has been on picking up galaxies that show large (photographically detectable) polarization.

A half dozen or so galaxies that gave indications of small amounts of polariza-

tion will now be followed up with more extensive photographic observations and quantitative photoelectric measures with the Babcock polarimeter. The radio source 3C40 consists of a group of elliptical galaxies. Preliminary indications that there are polarized "knots" in their halos will be followed up in the coming season. Favorably situated prototype spiral galaxies are also being studied, and both methods will be used to investigate their polarization properties.

Stellar Populations

Photoelectric observations in eight colors, ranging from $\lambda 3730$ in the ultraviolet to $\lambda 9875$ in the infrared, were used in 1958 by Baum to compute a stellar population model for large elliptical galaxies. The eight-color data showed that elliptical galaxies have infrared outputs too large to be accounted for by any stellar population we have known close at hand. The existence of very cool "flatiron" stars ($\sim 2000^\circ\text{K}$) was accordingly predicted. Flatiron stars, if they indeed exist, have to account for half of the total bolometric outputs of large elliptical galaxies. The eight-color data show that a similar, though not identical, situation may exist in the nuclei of spirals.

During the report year Baum endeavored to check the matter by obtaining infrared photographs at Palomar in the Sagittarius Cloud to see whether any flatiron giants could be thus identified near the nucleus of our own Galaxy. The field chosen for the study surrounds the globular cluster NGC 6522, which lies about 4° from the obscured galactic center. Blue and yellow plates were also obtained, and the infrared plates were compared with them by a positive-negative method. This photographic material shows a very large number of exceedingly red stars within about 3 mag of the infrared plate limit.

Color measurement of these stars is very difficult, both because of extreme crowding and because of the unfavorable

declination (-30°) of the field. Baum did measure one red star with the pulse-counting photometer; he found it to have a color index of about 2.5 mag. It is not yet possible to say how many stars in the Sagittarius field exceed that index. Allowance must also be made for interstellar reddening.

Further work has been done by Oke on the absolute energy distributions in the spectra of the central regions of galaxies with the photoelectric scanner. In addition to the previous blue data for about 20 galaxies, infrared measures out to $\lambda 10800$ have been obtained for NGC 4486 and NGC 4472. Enough data are now available to compute K corrections and to investigate the stellar content of some galaxies.

Spectra

Spinrad has recently estimated the intensities of the absorption lines at D in the spectra of nine galaxies in the Virgo cluster (*Astrophys. J.*, 135, 715, 1962). Deutsch finds that these intensities show a significant positive correlation with redshift. The airglow emission lines at D are undoubtedly responsible for this effect. At the scale of Spinrad's apparatus, they are able to obliterate absorption lines with equivalent widths as large as 10 Å in the brighter Virgo galaxies, when the galaxy redshifts are small, and they will appreciably weaken the galaxian D lines for redshifts of 1000 km/sec or more. Observations by Deutsch at a more favorable scale and with due allowance for the effects of airglow emission indicate that the D lines are intrinsically very strong absorption features in all the galaxies so far examined in the Virgo cluster.

Although the airglow emission lines have systematically affected the observations of D-line strengths in the fainter galaxies with small redshifts, Spinrad's proposal may nevertheless prove to be correct—that the lines are systematically weak in galaxies of low luminosity. Thus a recent spectrogram of NGC 205 shows

D lines much weaker than those of M 31, and the difference can probably not be wholly attributed to airglow emission. On the other hand, from measurements of one spectrogram in the visual region of the Great Sagittarius Star Cloud, Deutsch concludes that the D lines are probably much weaker there than in M 31 and most other galaxies of high luminosity. The count-brightness ratio is also under study in this region of the Milky Way, for confirmation of the hypothesis that late-type dwarf stars contribute little to the total brightness.

Variable Stars in Galaxies

Before his retirement Baade obtained a very extensive series of plates of four fields in the Andromeda galaxy for the study of variable stars, especially the cepheids. Miss Swope has completed the study of field IV, 96' south preceding the nucleus, and has sent the results to the *Astronomical Journal*. She has been preparing for publication the results of studies of fields I and III. The results are summarized in table 2.

By comparison, field IV had 54 variables, of which 37 per cent were cepheids and 13 per cent were population II cepheids.

In period and amplitude, the cepheids of M 31 resemble those in our Galaxy more than those in the Magellanic Clouds.

Tammann has begun the final analysis for variable stars in NGC 2403, using the extensive observational material consisting of 107 long-exposure plates taken since 1950 with the 200-inch by Hubble and Sandage. Eleven cepheids have been isolated so far, and periods have been

found for each, ranging from 58.3 to 20.2 days. A period-luminosity relation exists but has not yet been calibrated relative to a photoelectric sequence which extends to $V = 22^m8$, $B = 22^m7$. Many variables other than cepheids have been located. Among the most interesting are four very bright irregular blue stars which appear similar to the high-luminosity stars found earlier by Hubble and Sandage in M 33 and M 31. The brightest of the four reaches $V \simeq 17.5$ at maximum, which corresponds to $M_V \simeq -10$ if the modulus is $m - M = 27.5$. When photometry is completed next year, this modulus should be well determined. Two bright red irregular variables are known, and 11 variables of intermediate color for which no period could be found; there are 40 additional probable, possible, or doubtful candidates for variability for which investigation is not completed.

The sequences have been established photoelectrically by Sandage with 70 standards, many of which are bright, so as to determine the reddening of our own Galaxy in the direction of NGC 2403. The value of $E(B - V) = 0^m08$ was obtained by the normal three-color photometric method.

Redshift-Diameter Relation

All the observational tests for distinguishing between various world models are difficult. To date the most effective test has been the redshift-magnitude relation, but it is not completely free of side effects. As a supplement to the redshift-magnitude program he has been continuing during the past few years, Baum is now exploring a method of using

TABLE 2

Field	South Preceding Nucleus	No. Variable Stars	No. Novae	No. Cepheids	No. Population II Cepheids	% Cepheids	% Population II Cepheids
I	15'	109	7	31	8	28	7
III	50'	334	2	231	7	69	2

the redshift-diameter relation. In an earlier attempt involving photoelectric photometry with concentric diaphragms he found that the corrections for "seeing" became hard to handle for galaxies with redshifts beyond about 40,000 km/sec.

The present attempt is relatively immune to "seeing" and has been tested on a cluster of galaxies (Cl 1448) with a redshift of $c \Delta\lambda/\lambda = 108,000$ km/sec. It involves moving a photographic plate during exposure in such a way that field star images produce synthetic "galaxy" images of graded diameters for comparison with the images of actual galaxies photographed simultaneously. The method looks promising enough to pursue further.

Atlas of Peculiar Galaxies

An extensive program of preparing a photographic atlas of peculiar and interacting galaxies (many of them Vorontsov-Velyaminov objects) with the 200-inch telescope has been about half completed by Arp. More than 100 limiting exposures have been taken, and about 80 objects are suitable for inclusion in the atlas. It is hoped to complete the program by the end of next year by obtaining half again that many objects and publishing the atlas.

In Arp's opinion this group of interacting objects is already furnishing observational examples of the role of magnetic fields and plasmas in galaxies. Some theoretical arguments were advanced by Arp in Symposium 20 in Australia on the formation of galaxies. They were later expanded on May 22 at a seminar at Princeton, where Arp discussed the mathematical forms taken up by magnetic tubes and indicated their probable basic role in the formation of spiral galaxies.

Catalogue of Galaxies and of Clusters of Galaxies

The manuscript of volume II of the *Catalogue* has been completed by Zwicky

and Herzog and sent to the printers. This volume contains the galaxies brighter than about photographic magnitude $m_p = 15.7$, as well as the rich clusters of galaxies identifiable on limiting exposures with the 48-inch schmidt telescope which are contained in the area from R. A. 6^h30^m to 18^h30^m (1950) and decl. from $+15^\circ$ to $+33^\circ$. Considerable work has already been done on volumes III and V of the *Catalogue*.

In connection with the work on all the volumes of the *Catalogue*, positions and magnitudes of galaxies are being furnished to Drs. C. D. Shane and G. E. Kron of Lick Observatory, who are checking the magnitudes photoelectrically. Definitive information on possible systematic differences between the results obtained with the "Schraffier" method and the photoelectric measurements is now being awaited.

Theoretical analyses of the data contained in volume I of the *Catalogue* were carried out by Rudnicki and Zwicky. Among the most important conclusions are those confirming the existence of intergalactic dust and the fact that the largest clusters at all distances are of the same size, population, and structural nature. No evidence of any kind has so far been found that the distribution of galaxies and clusters of galaxies within the range of distances characterized by symbolic velocities of recession from 0 to 100,000 km/sec shows any dependence upon distance.

Structures of Clusters of Galaxies

Structural and spectral characteristics have been studied for the following medium-rich and rich clusters of galaxies: cluster around NGC 541, Cancer cluster, Hydra I cluster, clusters at R. A. $11^h8^m12^s$, decl. $+28^\circ57'$, and R. A. $11^h13^m48^s$, decl. $+29^\circ32'$, and the Coma cluster. From statistical studies the Coma cluster was found to be at least 14° in diameter; from spectral studies of the galaxies in the field it follows that it may

be as large as 20° in diameter. Analogous results are indicated for the other clusters mentioned.

Rudnicki has carried out a statistical investigation of the Perseus cluster, one of the main results of which is the finding that bright and medium-bright galaxies are partly segregated, the medium-bright being relatively more numerous on the outskirts of the cluster.

Attention has in particular been concentrated by Zwicky and Humason on the near medium-compact and medium-rich cluster of galaxies around NGC 541. Spectra of about 65 member galaxies are now available, from whose analysis it follows that the distribution in radial symbolic velocities is Maxwellian around an average value of 5321 km/sec. The distribution in apparent magnitudes follows the exponential law previously established from a study of the populations of 704 clusters of galaxies. The study of the dependence of surface brightness of 85 member galaxies on their apparent brightness led to the construction of a new type of characteristic diagram. This type of diagram strikingly reveals that many of the fainter galaxies in a cluster have much greater surface brightness than the brightest elliptical and spherical galaxies in a cluster.

The indicative relative mass-luminosity ratio for the cluster around NGC 541 is about $(m/L)/(m/L)_{\text{sun}} = 200$; that is, it lies between those of individual galaxies and those of much richer clusters of galaxies, such as the Coma cluster. Zwicky thinks that the unidentified matter within the clusters consists of intergalactic stars, very compact galaxies, pygmy galaxies, and perhaps H_2 molecules and free protons and electrons, the intergalactic stars probably contributing the major share by adding up to a photographic surface brightness of the intergalactic formations equivalent to about the 25th magnitude per square second of arc.

As a consequence of the above finding, a systematic search on 48-inch schmidt plates was undertaken for exceedingly compact galaxies whose images are actually difficult to distinguish from those of stars. Spectra of such compact galaxies obtained by Zwicky show that they run the whole range from ordinary G and K types to systems showing only emission lines and no continuum. It is conjectured that radio sources such as 3C48 and 3C273 lie at the end of this sequence, and an attempt will be made to test whether intermediate systems are weak radio sources.

RADIO SOURCES

Spectra

Schmidt has continued spectroscopic studies of galaxies associated with radio sources. The program is planned in close cooperation with Dr. T. A. Matthews of the Owens Valley Radioastronomy Observatory, who made most of the identifications. Spectra of 32 radio galaxies have been assembled now (including those mentioned in *Year Book 61*), of which 26 show emission lines. All galaxies involved have absolute magnitudes of around -20 or -21 . The largest redshift found in this

program was 0.26 for the source 3C79, which shows 10 emission lines in the range of rest wavelengths 3300 to 5100 Å.

Spectra were taken by Schmidt of the stellar objects that had been identified with the radio sources 3C196 and 3C286 by Matthews and Sandage. The spectrum of 3C196 appears continuous at 400 Å/mm; that of 3C286 shows an emission line of 50 Å width at $\lambda 5170$. The radio source 3C147 turned out to be another source identifiable with an object of stellar appearance. The identification rests on the abnormal nature of the optical spectrum, which shows no absorp-

tion features and at least two emission lines in the yellow.

An accurate position of the source 3C273 derived by Hazard of Sydney University and Mackey and Shimmins of CSIRO from occultations of the moon in 1962 coincided with that of a stellar object of the 13th magnitude and a narrow nebular streak pointing to the stellar object. From spectra of the object obtained by Schmidt in December 1962, and from Oke's observations of the infrared line noted below, Schmidt discovered that the stellar object exhibits the Balmer spectrum in emission at a redshift of 0.16. This finding was quite unexpected, because the object does look stellar and not at all like a galaxy. Furthermore, the redshift is about 10 times larger than the redshift normally found for a galaxy of this magnitude. If the redshift of the object is a cosmological one, the object is about 100 times more luminous than galaxies such as the Andromeda galaxy and, at a rate of 10^{46} ergs per second, is the most powerful radiator of energy known in the universe thus far.

The photoelectric scanner was used by Oke to measure the absolute energy distribution in the spectrum of 3C273 from $\lambda 3300$ to $\lambda 10800$. In the infrared a strong emission line several hundred angstroms broad was observed at $\lambda 7600$. Several other emission lines appeared in the infrared, of which only one has been identified. The absolute energy distribution, F_ν , is almost flat in the blue but becomes abnormally strong in the infrared. Analyses are now being made to determine what fraction of the continuum in the blue can be accounted for by bound-free, free-free, and 2-photon emission. The infrared radiation cannot be accounted for by these mechanisms, and it is reasonable to consider it synchrotron radiation.

After the identification of the emission lines in 3C273, Greenstein was able to identify successfully the spectral features he had observed in the radio source 3C48,

interpreted as an emission-line source of large redshift. The strong lines are those of [Ne V], [Ne III], and [O II], and the strongest line is apparently the resonance permitted doublet of ionized magnesium (unshifted $\lambda\lambda 2796, 2803$). The redshift of 0.367 is the second largest known. The background continuum is probably largely synchrotron radiation. The spectra are being interpreted in collaboration with Schmidt. Apparently a wide range of electron density, approximately 10^2 to $10^7/\text{cm}^3$, is acceptable; for each electron density the mass and radius are determined by the strength of the emission lines. The mass lies in the range 10^{10} to 10^5 solar masses, and the radius of a few hundred to a few parsecs. The electron temperature is high, but not abnormally so in comparison with most planetary nebulae. The apparent internal velocity indicated by line width may be the velocity of expansion of more than 1000 km/sec. It can be the driving force that supplies the total energy both for the forbidden and permitted line radiations and for the acceleration of the high-energy electrons. A superexplosion in a distant galaxy seems to be the most probable interpretation. The large size of the objects, for any reasonable electron density, makes the interpretation of light variations quite difficult. If the object is interpreted as a gas cloud in a very distant galaxy, its total bolometric luminosity is approximately 100 times greater than that of our own Galaxy and 30 times brighter than that of any other known galaxy except the other radio source, 3C273, mentioned above. The large redshift permits the detection of the ultraviolet auroral transition of [Ne V] (unshifted $\lambda 2975$) for the first time. Theoretical analysis shows that the permitted resonance doublet of ionized magnesium is, in fact, one of the strongest lines in any large cloud of ionized gas, and suggests that it will be an important distance indicator at large redshifts. Objects like 3C48 and 3C273 can be detected by radio techniques, photo-

graphically, and spectroscopically out to redshifts of $d\lambda/\lambda_0$ near unity.

The alternative interpretation of the large observed redshift, namely, a gravitational effect near the surface of a star of very large gravitational potential, has been investigated by Greenstein and Schmidt. Since the Einstein shift is essentially measured by the gravitational potential, the thickness of the emitting layer, in units of the shift, is a measure of the fractional change of the gravitational potential across the emitting region. This sets very stringent limits on the thickness of the layer. Let us imagine that the gravitational redshift is caused by the proximity of the gases to a superdense star having a mean density like that of nuclear matter, i.e., 10^{14} or 10^{15} grams/cm³. The theory of such stars indicates that they would have a radius of about 10 km and a mass near that of the sun. Under those circumstances, the thickness of the emitting layer would be less than 0.5 km. So small an emitting volume cannot produce recombination lines of sufficient intensity unless the density is very high. If the density is very high, the forbidden lines should not appear. The continuum would have to be explained, if it were thermal emission, by a surface temperature of approximately 10^9 °K for an object of 10-km radius located not too far from the sun. The intermediate possibility—that the object being observed is a star of very large mass, say 10^8 solar masses, with very large gravitational redshift—is less difficult to dismiss, but it is improbable that such stars would be found just before the onset of their gravitational collapse, which occurs very rapidly on all current theories. The full gravitational redshift observed is much too large to be explained in terms of the quasi-stable stars of large mass studied by Fowler and Hoyle.

M 82

Sandage and Dr. C. R. Lynds of the Kitt Peak National Observatory completed an investigation of the irregular

galaxy M 82. Long known to be peculiar in optical wavelengths because of the large amount of dust spread over its entire face, M 82 came under study during the report year because of Lynds' discovery that the galaxy was a radio source with an abnormally flat radio spectrum. The radiated flux varies as $\nu^{-0.23}$. Direct plates taken with the 200-inch telescope in H α light, using an interference filter of 80 Å total width to half intensity, show a remarkable system of filaments extending above and below the fundamental plane of the galaxy along the minor axis. Although filamentary structure was suspected on plates taken with broad-band red filters, nothing as extensive or massive as the observed system was expected. The H α structures extend at least 3000 parsecs above and below the plane and radiate in the H α line with a flux of 1.7×10^{-11} erg cm⁻² sec⁻¹ at the earth's surface, or 2×10^{40} erg/sec if the distance modulus of M 82 is $m - M = 27.5$ ($d = 9.8 \times 10^{24}$ cm). This flux requires that the total mass in the filamentary structure be of the order of 10^6 to 10^7 solar masses, computed on the usual assumptions of radiative recombination theory.

Spectrograms taken by Lynds at the Lick Observatory show the lines of [N II] 6548, 6583, [S II] 6717, 6731 in emission, and Na I 5893 in absorption, in addition to intense H α emission. The spectrograph slit was placed along the minor axis of the galaxy. The H α and [N II] lines extend over the entire filamentary system. The southeast portion of the filaments at 2 minutes of arc from the fundamental plane is approaching the earth at 150 km/sec; the filaments at the corresponding position on the northwest part of the minor axis are receding at 150 km/sec. This motion cannot be due to rotation, since it is along the minor axis of the body figure.

Lynds and Sandage interpret the velocity field as an expansion of the gas away from the center of M 82. The data suggest a linear velocity-distance relation,

which is a type of motion requiring that all the matter in the $H\alpha$ structures was in or near the fundamental plane at a unique time in the past, namely, one observable on earth about 1.5×10^6 years ago. The observed velocities, together with the calculated mass in the $H\alpha$ expanding structures, show that the kinetic energy in the visible filaments is about 2×10^{55} ergs. If the interpretation is correct, this would be the first direct evidence of an explosion in the center of a radio galaxy.

Further observations have shown that the filaments form fragments of loops that appear to outline lines of magnetic force. Plates taken in a spectral region devoid of emission lines show that part of the filaments radiate weakly in the continuum as well as in the emission lines. This suggests that optical synchrotron emission may be present in addition to the radio synchrotron emission at lower frequencies that gives rise to the radio spectrum. Polarization measurements of part of the expanding structure by Elvius and Hall seem consistent with this possibility. The radio flux data combined with the optical measurements show that the high-frequency cutoff in the synchrotron emission occurs near $\nu_c = 10^{15}$ cycles per second. Integrating the observed spectrum from $\nu = 10^7$ to 10^{15} and adopting a distance of 9.8×10^{24} cm gives a rate of synchrotron emission of 2×10^{42} ergs/sec, which amounts to 9×10^{55} ergs over the lifetime of 1.5×10^6 years if the power level has been constant.

Estimates of the magnetic field have been made with the usual assumption of equipartition of energy between the field and the relativistic electron gas, with the result that $H \simeq 2 \times 10^{-5}$ gauss; but various arguments suggest that this is too high. For example, if the high-frequency cutoff is 10^{15} cycles per second, the lifetime of the highest-energy electrons producing radiation at this frequency is only 2×10^4 years, which is short compared with the lifetime of the source. This result would require continuous reaccele-

ration or reinjection of relativistic electrons into the system to maintain the radio source for 1.5×10^6 years. Sandage and Lynds adopted $H = 2 \times 10^{-6}$ gauss, which gives a lifetime of the highest-energy electrons in excess of 1.5×10^6 years. Also, at this strength the energy in the magnetic field is smaller than the kinetic energy of the expanding gas, which shows that the explosion was energetic enough for the material to pull the field out of the plane of the galaxy to form the observed loops along the minor axis.

M 82 apparently represents an important example of radio galaxies because it is close enough and has been observed at an important phase after the explosion so that general properties of radio galaxies can be inferred. The Burbidges, of the University of California at La Jolla, and Sandage, having reviewed the entire evidence for the occurrence of violent events in the nuclei of galaxies, have concluded that they are quite common. Examples almost as obvious as M 82 are M 87, with its optical jet originating in the nucleus, and NGC 1275, which has an extensive system of filaments surrounding the main body of the galaxy.

The sequence of events that leads to a radio galaxy seems to start with an explosion of unknown origin at the center of a given galaxy. The total energy released ranges all the way from $\sim 10^{55}$ ergs in weak radio galaxies and Seyfert galaxies (objects like M 82 and NGC 1068) to $\sim 10^{61}$ ergs for the strongest radio galaxies (Cygnus A and 3C295). In the explosion relativistic electrons are produced, which give rise to the radio emission through interaction with the magnetic fields present. If the explosion is energetic enough, the relativistic gas is not bound by the magnetic fields but escapes freely along the direction of least constraint, which is usually perpendicular to the fundamental planes of the galaxies involved, owing to the presence of gas in the plane itself. After a time, two regions of gas, well away from the main body of

the parent galaxy, will exist, and they manifest themselves as the double radio sources so common among the identified radio galaxies. The initial explosion must appear very bright indeed, and these events are identified with such radio stars as 3C48, 3C147, 3C196, 3C273, and 3C286. Analyses of these results have been prepared for publication in the *Reviews of Modern Physics*, where many of the details are given.

Polarization

A program has been initiated by Whiteoak to study the polarization of extragalactic objects, in particular the optical counterparts of the radio sources that have been found to be linearly polarized. Observations are being obtained at $\lambda\lambda 5500, 7800, 9100$, and 9600 , with an HN22 Polaroid filter for the

visual wavelength and an HR Polaroid filter for the remainder. The polarization was measured by a series of observations where the filter is rotated in steps of 30° . Since the incident light undergoes a 90° reflection in both the 100-inch and 60-inch telescopes, the observed polarization of incident light that is unpolarized is about $3\frac{1}{2}$ per cent. This amount has been reduced by the correct orientation of photomultipliers having sensitivities that vary with the plane of polarization of the incident light. With an RCA 1P21, the over-all instrumental polarization is 2.8 per cent; with an RCA 7102, it is about 1 per cent. To convert the observed measures to absolute values, stars of known polarization, observed by A. Behr, T. Gehrels, and W. A. Hiltner, were used. The reduction of results was effected with the IBM 7090.

THEORETICAL STUDIES

Capriotti has attempted to compute idealized models of planetary nebulae in a steady state. By considering the mixture of elements and the various heating and cooling processes, the electron temperature and the electron density are computed as functions of distance from the center of the nebula. The calculation of the energy in the diffuse radiation field and the degree of ionization of each element is carried through also as a function of distance. Furthermore, the effect on the ionization of hydrogen of Lyman- α lines of neutral and ionized helium is discussed.

Another program by Capriotti is the study of self-absorption on the Balmer decrement of gaseous nebulae, assuming that most of the population of the second energy level of hydrogen is in the $2s$ -level. The previous conclusion was that, owing to high scattering of Lyman α , the $2p$ state is populated to a much higher degree than the $2s$ state. In view of the results of Osterbrock, however, it appears possible

that the $2s$ population may be much larger than that of the $2p$ state. All computations here have been carried out on the IBM 7090 electronic computer.

In connection with his thesis project, Trafton is investigating the role of molecular hydrogen in the energy balance of the major planets. The pressure-induced rotation branch at 300 to 1000 cm^{-1} and the translational branch at 100 to 300 cm^{-1} lie in the thermal region of planetary spectra. The absorption from these branches affects the energy balance. Trafton is currently trying to determine the frequency dependence of the translational band that arises when photons give up part of their energy to the kinetic energy of the absorbing molecules. The form of the rotational branch is already known experimentally. Model atmospheres will be constructed based on the calculations of the absorption coefficient. Medium-dispersion spectra of the higher vibrational transition of molecular hydrogen in the major planets will help to

determine the parameters of the atmospheric models.

A theoretical study of the detailed evolution of the helium stars is being carried out by Lungershausen. Present work, using the IBM 7090 and an iterative technique, is to create sequential models satisfying the equations of the stellar interior. Effects included are the energy release by contraction, detailed consideration of the helium-burning, relativistic partial degeneracy of the core electrons, and electron conduction. The goal is to obtain evolutionary models of the stars of masses between 0.5 and 10 solar masses. Such stars may represent the link between the hydrogen-burning stage and the heavy-element-rich white-dwarf stage, and examples may be found

in the nuclei of planetary nebulae and other unusual stars.

A computer program to calculate nongray stellar atmospheres has been written for an IBM 7090 by Mihalas. It uses a variation of Krook's technique to obtain a high degree of flux constancy in the models (usually ± 1 per cent), and it determines the source function by solving the Milne-Eddington equation, which allows for scattering in the continuum. Models have been constructed for a large range of temperatures and gravities; they are being used to compute hydrogen- and helium-line strengths on the basis of the latest broadening theories by Griem and others, with the goal of estimating the helium abundance in early-type stars.

INSTRUMENTATION

Solar Magnetograph

A new method of recording solar magnetograms has been developed by Howard. Instead of a photograph of an oscilloscope screen, a magnetogram is made on an X-Y plotter. Two pens with colored ink reproduce the motion of the image across the spectrograph slit and record at various magnetic levels a coded series of marks.

To keep the spectrum line centered for magnetic measures and to study the motions in the solar atmosphere, a servo-line-centering device was constructed and installed at the 150-foot tower. The servo system balances the d-c outputs of the two photomultiplier tubes by tilting a parallel glass plate in front of the exit slits. The position of the glass plate can be accurately recorded. Doppler shifts of 20 meters per second can easily be observed with this system.

For long observations with small apertures at one position on the solar disk, the rotation of the sun becomes a serious problem. It amounts to about 10 seconds of arc per hour at the center of the disk. To make longer observations possible, a

rotation compensator was constructed, consisting of a Porro prism that can be driven very slowly. With this instrument it is also possible to make slow traces across the solar disk to observe Doppler or magnetic fields.

During the year, water from a storm damaged the focal-plane shutter that had been used for many years to obtain direct photographs of the sun every day. Roberts constructed a new focal-plane shutter having a rotating circular disk and a shutter that is opened by a push-button and then closes after traversing the photographic plate.

Photoelectric Scanner

A new photoelectric spectrum scanner planned by Oke has almost been completed; it will go into operation at the prime focus of the 200-inch telescope in September 1963. It is intended for use in slitless form and has a resolution of about 2 Å. Bandwidths from 0 to 170 Å in the blue or 0 to 340 Å in the red and infrared are possible. The instrument has a double-beam system: one beam looks at the star plus sky; the other, at the sky alone. When the system is combined with

a light-chopping shutter and a lock-in amplifier, the sky signal can be automatically and continuously removed. Emission-line intensities can also be measured with the background continuum and sky automatically subtracted. The scanner will be provided with photomultipliers that will allow observations to be made from $\lambda 3200$ to $\lambda 12000$ and down to very faint limiting magnitudes.

During the last two years infrared photomultiplier tubes have been used extensively with the photoelectric spectrum scanner. The tubes now being employed (RCA 7102) with the scanner permit measurements to about 15th magnitude for a bandwidth of 50 Å. With a more efficient refrigeration system it should be possible to extend this limiting magnitude to substantially fainter objects.

Microphotometer

Gunn and Oke have rebuilt the microphotometer at the California Institute of Technology. The electromechanical curve-follower by means of which photographic density was converted to intensity has been replaced by a completely transistorized converter system that can operate at high speed. The calibration curve is entered into the converter by setting 16 dials, all of which are independent of each other. Two complete sets of dials are available so that one calibration curve can be set up while a second is in operation. Employing a strip-chart recorder with a balance time of 0.1 second, it is possible to trace accurately a sharp-lined spectrum at a rate of 10 mm per minute. This rate is limited only by the recorder speed and the rate at which the microphotometer screw can safely be driven. A new, very stable transistorized d-c voltage source for the lamp has also been built.

Astronomical "Seeing"

Considerable effort has been given to the problem of analyzing, measuring, and

recording astronomical "seeing," or image tremor, by instrumental means using telescopes of 4- to 8-inch aperture. Two different methods have been tested by Babcock. The first, relatively simple, depends on a fine grid or lattice-reticle placed at the focus of the telescope; this is followed by a Fabry lens and a multiplier phototube. The lattice spacing is so chosen that the light of a star focused on it is always partially, but never completely, obscured. The tremor of the image due to atmospheric turbulence results in the generation of a Fourier spectrum of frequencies in the light transmitted through the lattice. This signal is amplified, rectified, and recorded. Tests have shown that the method does permit discriminating among various grades of seeing, including excellent seeing that was rated 5 and 6 on the Mount Wilson scale. The effects of scintillation can be isolated by defocusing the image.

The second design for a seeing monitor is based on a suggestion by Dr. C. R. Lynds. Ahead of the focus of a telescope is placed an asymmetric beam-splitter that forms two images of a bright star, one twice as bright as the other; the two beams then enter separate multiplier phototubes. A transducer-driven knife-edge in the focal plane of the brighter image obscures half its light and is made to track the tremor motion of the star in response to the difference signal of the two phototubes, which is amplified and used to drive the transducer. The transducer is a piezoelectric device capable of following a signal from direct current to several hundred cycles per second. By forcing the knife-edge to track the image, the system maintains equality of the light beams reaching the phototubes. The mean amplitude of the knife-edge motion is recorded. The advantage of this system is that it provides an absolute measure of image tremor, and means for calibrating it can readily be built in. A measure of scintillation is also obtained as a by-product.

A complete portable seeing monitor

with an 8-inch Cassegrain telescope, recorder, and power supply has been designed and built especially for site-testing operations.

Image-Tube Installation

To provide for the use of photoelectric image tubes in spectroscopy, some substantial changes and additions have been made inside the coudé spectrograph of the 100-inch telescope. The new coudé installation was made as versatile as practicable so as to accommodate tubes of the several different types that continue to be of interest. It is operated in combination with the 114-inch-focal-length coudé camera, but the final recorded dispersion is not always the same as the unaided photographic dispersion of that camera.

The preparation of the equipment, undertaken mainly by Baum, included experiments with permanent magnet arrays for focusing the photoelectronic images. A magnet design was evolved for producing a very uniform magnetic field throughout a relatively large volume. The shielding of the field against external

disturbances, such as the magnetic influence of dome rotation, was found to be important. The need for these refinements in operating technique arose as the result of the improved resolution of which some tubes are now potentially capable.

Owing to the large mass and bulk of the shielded magnetic focusing system, it was necessary to install hoists, rails, dollies, and counterweights for attaching and detaching it. Auxiliary units include flat mirrors for bringing the coudé spectrum image to the photocathode of the image tube, and a schmidt-type camera for photographing the phosphor screens of tubes whose outputs are of that kind. Experimental observations with this new installation are described in the annual report of the Committee on Image Tubes for Telescopes later in this volume.

Ruling of Plane Gratings

Eleven plane gratings were ruled by Roberts under the direction of Babcock during the year. All were interferometrically controlled, and several were large (up to 6 by 10 inches).

GUEST INVESTIGATORS

The following programs have been carried out by guest investigators from other institutions during the report year.

Dr. George O. Abell of the Department of Astronomy, University of California, Los Angeles, has continued his investigation of the luminosity functions and structures of rich clusters of galaxies. An important problem concerning the structure of a cluster is the determination of the fractions of faint galaxies that are actually cluster members and that belong to the background "field." Different estimates of the numerical surface density of field galaxies in the region of the Coma cluster, for example, have led to widely differing conclusions regarding its structure.

Consequently, in connection with his investigation of that cluster, Dr. Abell has determined the luminosity function of 2773 galaxies in a 6.2 by 6.2 region surrounding the main part of the cluster itself. The data suggest that the cluster is contained in an oval region of dimensions 5.4 by 4.3 . The surface density of galaxies brighter than $m_{pv} = 18.0$ outside this region is approximately uniform and has the value 77 galaxies per square degree. The luminosity function of these galaxies agrees with that expected for a uniform distribution of galaxies in space and is very different from that of the galaxies in the cluster itself. The data suggest, therefore, that the number of cluster members more distant than 2.5

from the cluster center is relatively small. Under these circumstances, although the mass distribution of the cluster resembles that of the isothermal polytrope, there is no clear-cut difference between the radial distributions of galaxies of different luminosities.

Dr. Lawrence H. Aller of the University of California at Los Angeles has continued the reductions of the planetaries IC 4997, NGC 6572, NGC 7662, and NGC 7009, secured in 1959 and 1961. In collaboration with Dr. S. J. Czyzak of Wright-Patterson Air Force Base, Dr. Aller observed the planetaries NGC 3242 and NGC 6543 with the 8-inch camera of the X spectrograph on the 60-inch telescope.

Twenty-four spectrograms of Arcturus have been obtained at the coudé focus of the 100-inch reflector by Dr. R. F. Griffith of the Observatories of the University of Cambridge, England. All but three of them were secured with the 114-inch camera-133B grating combination, which yields the highest available dispersion; all are of good quality and suitable for the production of intensity tracings. These spectrograms complete the observational material required for the project, begun in 1961, to provide a photometric atlas of the spectrum of Arcturus from the ultraviolet to $\lambda 8800$. Since a considerable, and perhaps the major, source of photometric error in spectrograms of great width and very high dispersion appears to be uncertainty in the calibrations, very careful attention has been paid to this aspect of the problem; the spectrograms are accompanied by more than 50 plates bearing calibration data. Intensity tracings from the spectrograms have been prepared using the Sinclair-Smith microdensitometer in conjunction with the Moseley electro-mechanical curve-follower.

After preliminary experimentation, first in the darkroom and then at the 60-inch reflector, a 20 Å/mm calibrated spectrogram of the deep infrared spectrum of Arcturus was obtained with the 100-inch using the I-Z emulsion hyper-

sensitized with ammonia. This observation will permit a preliminary list of line strengths and identifications to be prepared for the region beyond that covered by the photometric atlas, out to a wavelength of more than 11000 Å.

The 60-inch reflector was used by Dr. Paul W. Hodge of the University of California, Berkeley, to obtain photoelectric measurements of the surface luminosity, density, and color of two near-by irregular galaxies. Twenty-five measurements were made across the face of the Wolff-Lundmark-Melotte galaxy in *B* and *V* of the Johnson *UBV* system. Similarly, 74 measurements in *B* and *V* were made of the system IC 1613, a dwarf irregular member of the local group of galaxies. From these measurements isophotes and isochromes of the two galaxies have been constructed.

Dr. Philip C. Keenan of the Perkins Observatory has obtained coudé spectrograms of several Mira variables in the summer sky, including S Aquilae, RY Ophiuchi, and RT Cygni, bringing to more than a dozen the number in which interstellar lines could be observed because of the Doppler shift of the stellar components. Among those lying close to the galactic equator, X Monocerotis (previously measured), V Mon, Z Ophiuchi, RY Oph, and possibly RT Cyg have early-type comparison stars that make it practicable to derive individual (though uncertain) distances for the variables. Spectrograms are being obtained for these comparison stars, and Mr. Kowal kindly measured photoelectric colors at the 60-inch for two in the field of Z Oph and four in the field of RY Oph. For Z Oph the two comparison stars suggest a distance of about 160 parsecs, corresponding to the surprisingly low luminosity of $M_v = +1.5$, but the expected scatter due to the known patchiness of interstellar matter is illustrated by the rather weak interstellar lines observed in the B5 spectrum of the well known eclipsing binary U Oph, which also lies in the field of Z Oph. The

strengths of the D lines in U Oph imply a considerably greater distance for Z Oph.

Drs. Keenan and Greenstein have prepared for publication the wavelengths and identifications of 1200 lines between $\lambda 3700$ and $\lambda 8600$ in the spectrum of R Coronae Borealis. Many of the previously unidentified lines can be assigned to C I, and improved term values for 17 energy levels of neutral carbon have been derived. The $\lambda 5876$ line of He I is present, and also the $\lambda 6708$ line of Li I, its strength indicating that lithium is about 150 times as abundant in R CrB as in the sun.

Dr. Ivan R. King of the University of Illinois undertook a study of the structure and dynamics of elliptical galaxies. On the theoretical side, an IBM 7090 program was written to calculate self-gravitating spherical models that correspond to the steady-state solution of the Fokker-Planck equation in a square-well potential. A model can include a mixture of as many as ten different stellar types. For globular clusters, where the stellar mixture is reasonably well known, the models agree well with the observed star densities. In elliptical galaxies, however, many different stellar mixtures can give rise to the observed density distribution, and the correct model cannot be chosen without further observations.

On the observational side, Dr. King has begun measuring brightness distributions in a number of E0 to E5 and S0 galaxies. The program aims particularly at determining the detailed light distribution near the center, without which the results would be of little value for dynamical studies. For this purpose, lightly exposed photographs have been taken at the Cassegrain focus of the 60-inch reflector, and the faint outer parts are being studied on 48-inch schmidt photographs. The program includes most of the galaxies whose internal velocity dispersions are known; it should be possible to derive a mass-luminosity ratio in each.

Dr. King also continued his star-count program in globular clusters, using the

48-inch schmidt to photograph the remaining clusters that appear to be good subjects for counts.

Dr. Robert Koch of Amherst College Observatory, Dr. Edward C. Olson of Smith College, and Dr. Kenneth M. Yoss of Mount Holyoke College cooperated on a program for the investigation of bright eclipsing binary systems. During the summer of 1962, three spectra of each of 17 eclipsing systems and spectra of 40 standard stars were obtained with the 16-inch camera on the X spectrograph.

Spectral classifications (of both components where visible) were obtained by tracing the spectra on a Jarrell-Ash direct-intensity microphotometer. A dispersion of 20 Å/mm was necessary to separate the components sufficiently. Equivalent widths of sensitive lines were obtained by planimetry.

Rotational velocities, corrected for $\sin i$, have been obtained from line profiles by a method similar to that of Slettebak. The presence or absence of synchronism between orbital and rotational periods has been determined using the best available orbital elements. In five systems synchronism is apparently lacking. A brief theoretical investigation to determine the order of magnitude of the time scale for transfer of angular momentum between the orbital and rotational modes will be attempted to see whether this mechanism could play a role.

Investigations of gas motions in the solar atmosphere were continued by Dr. R. B. Leighton of the Physics Division of the California Institute of Technology with the assistance of Drs. R. W. Noyes and G. W. Simon. Special attention was given to the oscillatory velocity field and the large-scale convective field. The oscillatory field was studied as a function of height by observing it in various lines; the period of the oscillation was found to diminish slowly with increasing height. Oscillations in the intensity field were also observed in several lines, including the K line of ionized calcium.

The large-scale motions were studied in relation to the emission pattern of Ca II, the magnetic field, and the chromospheric velocity field as observed in the H α -line wing. A very close correspondence was observed among these several patterns, and their close physical relationship has been convincingly established.

Dr. W. J. Luyten of the University of Minnesota has obtained acceptable plates of 250 fields on 37 nights with the 48-inch schmidt telescope. These plates repeat fields of the National Geographic Society-Palomar Observatory Sky Survey. Red-sensitive 14 by 14 inch plates and the same filters as the survey were used. All the plates have intervals of from 11 to 13 years against the original plates, and they are to be used for the discovery of faint stars with large proper motion. On the seven pairs of plates blinked thus far, more than 3000 moving objects were found, including more than 50 new white dwarfs and some very red stars, fainter than 21 pg and with motions larger than 0".3 annually. Fourteen parallax plates were taken of the star LP 658-2, one of the faintest known yellow degenerate stars, and a parallax of $0".148 \pm 0".023$ (m.e.) was determined for it.

Dr. D. H. McNamara of Brigham Young University observed with the 100-inch telescope at Mount Wilson for a 5-day period in August 1962. All the observations were made with the photoelectric photometer utilizing narrow-band interference filters. Stars in the galactic star cluster NGC 752 and the globular star cluster M 22 were observed in Stromgren's c-1 photometric system. A large number of the bright A- and F-type eclipsing binaries were also observed in the same photometric system. The photometric data should yield luminosities and intrinsic $B - V$ colors for all the stars observed.

The double-pass optical system of the McMath-Hulbert spectrometer on the Snow solar telescope was reinstalled in a more stable arrangement by Dr. Walter E. Mitchell, Jr., of the Perkins Observa-

tory. It was also improved by the addition of a new variable-speed grating drive with a tachometer-controlled motor. The system permits the grating table to be rotated at speeds from 15° to 0°15 per hour. Further tests of ratio recording were carried out with the aid of a Philbrick MU/DV and operational manifold in the signal and monitoring channels.

The double pass removed scattered light arising from Rowland ghosts up to about 5 per cent of the continuum. With a sodium vapor tube operated at a number of temperatures, the residual scattered light in the double pass was estimated at 0.4 per cent. In the water vapor band at 1.13 microns, it was estimated at 0.3 per cent. The superposition of the Rowland ghosts and the presence of the "ghosts of ghosts" were demonstrated for double-pass spectra. Most of the observations were carried out with the Babcock grating 171 BIC used in the fourth and higher orders.

The double pass was employed to obtain a high-resolution map of the spectrum at the center of the solar disk in the wavelength regions $\lambda\lambda 5900-4687$, $4351-4097$, and $3988-3918$.

Mr. Kent Volkmer participated in the instrumentation and observing programs.

The 200-inch telescope was used by Dr. B. C. Murray, Dr. R. L. Wildey, and Mr. J. A. Westphal of the Division of Geological Sciences of the California Institute of Technology to map the 8- to 14-micron emission from Venus and Jupiter, using a mercury-doped germanium photoconductor cooled with liquid hydrogen. Considerable limb darkening was found on both planets, and a bilateral symmetry about the ecliptic was observed in the case of Venus. A transient emission "storm" showing closure on one day was found on Venus. No Jovian emission variation from dark to light bands or from on to off of the Great Red Spot was found. The shadows of Io and Europa were brighter than the general disk by 55° and 40°, respectively.

Also, Calisto appears hotter than is explainable without internal heat sources or a 20 to 30 per cent error in its diameter. Twenty-five stars were also observed ranging in types from B8 to M7. Using model atmospheres (Mihalas) and the assumption that the 8- to 14-micron radiation is described by a black body at the boundary temperature of the model, discrepancies were found to exist in the predicted infrared to visual (corrected for line blanketing) flux ratio which are sensitive to $B - V$ and amount to as much as a factor of 3 from B8 to K0.

Dr. Wildey and Mr. H. A. Pohn have continued their photoelectric study of the brightness versus phase of the moon, using the 60-inch telescope. Maximum brightness appears to occur always at minimum phase, and a subsidiary angle of dependence, in addition to phase angle, appears to be the elevation angle of the sun.

Dr. Wildey has used the coudé scanner on the 100-inch telescope in a study of Mars and Venus and a search for lunar luminescence. Preliminary results of the lunar search are negative, but a 1 to possible 2 per cent luminescence cannot yet be ruled out by the data. In addition, Dr. Wildey continues his study of h and χ Persei, with emphasis on stellar evolution.

An important systematic effect has been found in the measurement of the separation of the component lines in the spectra of double-lined spectroscopic binaries by Dr. Daniel M. Popper of the University of California at Los Angeles. When the lines of the components are comparable in intensity, observers using lower dispersion tend to measure the separation systematically too large. Plates with the highest available dispersion (20 Å/mm) of the solar-type eclipsing binaries WL Ophiuchi, VL Hydrae, and UV Leonis show that these stars fall close to the mass-luminosity relation established by Eggen for visual binaries with appreciable ultraviolet excesses. The other results with lower dispersion showed marked departures from the

relation. These eclipsing binaries also have appreciable ultraviolet excesses.

RL Ophiuchi is the second eclipsing binary (after KU Cygni, reported two years ago) found to have strong ultraviolet radiation at primary eclipse, when a K5 giant totally eclipses a hotter star. These two systems are similar in types of stars, and it is not established to what extent such ultraviolet radiation, not a result of Balmer emission, is found in binaries of different characteristics.

Another feature that has emerged in the study of KU Cyg is that the F star, with an absolute magnitude near -1 , has a mass of 20 or more solar masses (excessively large for the luminosity) or the radial velocity variation through primary minimum does not result from orbital motion.

Dr. William M. Sinton of Lowell Observatory used the twilight periods of each night in the latter part of February 1963 to make observations with his infrared interferometer attached to the 200-inch Hale reflector. With this new instrument the infrared spectrum of an object can be obtained with considerably better sensitivity than was heretofore possible with a scanning infrared spectrometer. The recorded interferogram is subsequently processed by a large digital computer to yield the spectrum.

The observations were chiefly of Mars to determine the intensity of the 3.5-micron "vegetation" band in different regions of the planet. For these observations the region measured was restricted to 6 seconds-of-arc diameter. In addition to the studies of Mars, spectra of late-type stars were obtained between 2 and 4 microns. The stars observed were α Herculis, g Her, χ Her, R Serpentis, R Lyrae, T Lyr, SS Virginis, and S Cephei. This last star, of type N8e and visual magnitude 9.5, gave interferograms of fairly good signal-to-noise ratio. The spectra of these stars, when computed from the interferometric data, are expected to indicate the presence of molecular constituents that may not be

found in visible and ultraviolet spectra.

Dr. George Wallerstein of the University of California has used both the 100- and 60-inch telescopes in a search for the presence of the lithium doublet at $\lambda 6708$ in F stars. The line was not present in 5 stars taken at 6 A/mm or in 11 stars observed at 30 A/mm. Three plates at 6 A/mm were taken for the measurement of the ratio of Li^6/Li^7 in λ Tauri, a star in whose spectrum Wallerstein had found lithium at the Lick Observatory.

In 1956 Wilson and M. K. Aly reported that λ Andromedae, a K0 IV star with exceptionally strong Ca II emission, probably showed the helium line at $\lambda 5876$ in absorption. This has been confirmed by Wallerstein on spectrograms of higher dispersion (6 A/mm). Wilson and Wallerstein have examined 6 A/mm spectrograms of 48 stars of types G8–K2 for evidence of $\lambda 5876$ in absorption. It is possibly present in 3 stars: β Ceti, π Cephei, and HR 6791. Spectra of the first two of these in the violet show that the Ca II emission is not strong.

Recently the investigations of Wilson have disclosed some extremely interesting correlations involving the H and K Ca II emission in late-type stars. So far, however, a quantitative interpretation of both the width and intensity of the emission in terms of a series of model stellar chromospheres has not been made. To do this, reliable profiles of the emission peaks must be obtained.

Dr. Ray Weymann of the University of California at Los Angeles has obtained spectrograms of suitable quality for reliable microphotometry at 4.5 A/mm of a number of stars, mostly luminosity class III giants in the K0–K3 range. Striking differences in the intensity and character of the central self-reversal are apparent among stars of nearly identical spectral class.

These spectrograms have been supplemented by some at 8 A/mm covering $\text{H}\alpha$ and the Ca II infrared triplet. It is hoped that additional plates of stars showing

much more intense emission can be obtained; in particular, manifestations of chromospheric activity in the Ca II infrared triplet are being sought.

Dr. Albert G. Wilson and Dr. George Abell, cooperating with the Jet Propulsion Laboratory and the Air Force, undertook to test the feasibility of “deep space” tracking by optical methods. The Palomar 48-inch schmidt was successfully used on August 28 and 29, 1962, to photograph at distances out to 600,000 km the Agena carrier rocket which injected the Mariner II Venus probe. (These photographs were made five weeks before the Soviet announcement of their “first” photograph of a space craft on an interplanetary mission.)

Dr. D. G. Edelen of the Rand Corporation, applying the Einstein field equations to galaxies considered as aggregates of granulated matter, has found that under certain very general conditions their ellipticities must be functions of the semimajor axes. The functional relationships are multibranched, predicting that the distribution functions of the major axes of galaxies should have discrete peaks distributed proportionally to the eigen sequence, $[n(n+1)]^{1/2}$, where n is a positive integer. To test this prediction, Dr. A. G. Wilson of the Rand Corporation has resumed his earlier studies of galactic diameters (*Carnegie Year Books 49 and 50*), reexamining previous observational suggestions of discretization in the diameters of cluster galaxies. Using plates of clusters taken by Baade, Humason, and Sandage with the 200-inch, Wilson has constructed distribution functions of relative diameters of early ellipticals in the Coma and Corona Borealis clusters. The diameter distributions show asymmetric density maxima occurring at values whose ratios are consistent with the theoretical prediction to within the observational errors. The preliminary results indicate that larger samples must be studied before there can be definitive confirmation of the Edelen hypothesis.

STAFF AND ORGANIZATION

The death of Dr. Otto Struve on April 6, 1963, was a great loss to the Observatories. During the 1950's, while Dr. Struve was Professor of Astronomy and Director of the Leuschner Observatory of the University of California, Berkeley, he came regularly to the Observatories as guest investigator and made extensive spectroscopic observations, chiefly with the 100-inch on Mount Wilson. On the basis of these spectrograms he made many analyses of stellar atmospheres. His studies of close double stars of the β Canis Majoris type were especially notable. After his retire-

ment as Director of the National Radio Astronomy Observatory at Green Bank in 1962, Dr. Struve was appointed Addison White Greenway Visiting Professor of Astronomy at the California Institute of Technology and Staff Member of the Mount Wilson and Palomar Observatories. He spent the spring term of 1962 at the Institute and the Observatories, and it was anticipated that he would continue to spend one term a year for the following three years.

Dr. Horace W. Babcock was appointed Associate Director of the Observatories effective in May.

*Research Division**Staff Members*

Halton C. Arp
 Horace W. Babcock, *Associate Director*
 William A. Baum
 Ira S. Bowen, *Director*
 Armin J. Deutsch
 Olin J. Eggen
 Jesse L. Greenstein
 Robert F. Howard
 Robert P. Kraft
 Guido Münch
 J. Beverley Oke
 Allan R. Sandage
 Maarten Schmidt
 Otto Struve¹
 Olin C. Wilson
 Fritz Zwicky

Research Associate

Lyman Spitzer, Jr.

Staff Members Engaged in Post-Retirement Studies

Harold D. Babcock
 Alfred H. Joy
 Seth B. Nicholson²

Senior Research Fellows

Rudolph Kippenhahn
 Minoru Nishida
 Leonard T. Searle
 Volker Weidemann

¹ Died April 6, 1963.

² Died July 2, 1963.

Carnegie Research Fellows

Charles R. O'Dell
 Hugo van Woerden
 John B. Whiteoak

Research Fellows

Bodo Baschek
 Jacques Berger
 Eugene Capriotti
 D. H. P. Jones
 Jun Jugaku
 Konrad Rudnicki
 Wallace L. W. Sargent
 Henrietta H. Swope

Research Assistants

Christine Arpigny
 Jeanne Berger
 Frank J. Brueckel
 Sylvia Burd
 Jai H. Choy
 Mary F. Coffeen, Librarian
 Thomas A. Cragg
 Emil Herzog
 Basil N. Katem
 Charles T. Kowal
 A. Louise Lowen
 Joyce E. Sheeley
 Gustav A. Tammann
 Merwyn G. Utter
 Mary B. Whiteoak
 Gordon Worrell

Student Observers

Subhash Chandra
James E. Gunn
W. T. Lundershausen, Jr.
Manuel E. Mendez
Dimitri M. Mihalas
Laurence M. Trafton

Photographer

William C. Miller

Instrument Design and Construction

Lawrence E. Blakeé, Senior Electronic Technician
Eileen I. Challacombe, Draftsman
Floyd E. Day, Optician
Kenneth E. DeHuff, Machinist
Robert D. Georgen, Machinist
Melvin W. Johnson, Optician
Rudolf E. Ribbens, Designer and Superintendent of Instrument Shop
Stuart L. Roberts, Instrument Maker
Bruce Rule, Project Engineer
Marlin N. Schuetz, Electronic Technician³
Russell R. VanDevender, Jr., Designer and Superintendent of Instrument Shop⁴

*Maintenance and Operation**Mount Wilson Observatory and Offices*

Paul F. Barnhart, Truck Driver
Wilma J. Berkebile, Secretary
Hugh T. Couch, Superintendent of Buildings and Grounds
Helen S. Czaplicki, Typist Editor
Fannie G. Gabrielsen, Stewardess

³ Resigned April 12, 1963.

⁴ Resigned February 28, 1963.

Eugene L. Hancock, Night Assistant
Mark D. Henderson, Gardener
Margaret Higgins, Stewardess⁵
Anne McConnell, Administrative Assistant
Leah M. Mutschler, Stenographer and Telephone Operator
Bula H. Nation, Head Stewardess
Alfred H. Olmstead, Night Assistant
Arnold T. Ratzlaff, Night Assistant
Glen Sanger, Custodian
John E. Shirey, Laborer
William D. St. John, Custodian and Relief Engineer
Benjamin B. Traxler, Superintendent

Palomar Observatory and Robinson Laboratory

Audrey A. Acrea, Stewardess⁶
Fred Anderson, Machinist
Jan A. Bruinsma, Custodian
Maria J. Bruinsma, Stewardess
Eleanor G. Ellison, Secretary and Librarian
Leslie S. Grant, Relief Night Assistant and Mechanic
Byron Hill, Superintendent
Helen D. Holloway, Secretary
Charles E. Kearns, Night Assistant
J. Luz Lara, Ground Mechanic
Harley C. Marshall, Office Manager
Dwight M. Miller, Mechanic
Robert E. Sears, Night Assistant⁷
Gary M. Tutton, Night Assistant
John E. van Buuren, Custodian
Hendrika E. van Buuren, Stewardess
William C. Van Hook, Electrician and Assistant Superintendent
Gus Weber, Assistant Mechanic

⁵ Resigned September 30, 1962.

⁶ Resigned March 29, 1963.

⁷ Died January 30, 1963.

BIBLIOGRAPHY

- Aller, Lawrence, *see* Wallerstein, George.
Arp, Halton C., Intermediate-age cluster, *Astrophys. J.*, 136, 66-74, 1962.
Arp, Halton C., Polarization of a filament which connects two galaxies, *Astrophys. J.*, 136, 1148-1149, 1962.
Arp, Halton C., Strange galaxies, *Eng. and Sci.*, 26, 11-14, 1963.
Arp, Halton C., Stellar content of galaxies, *Problems of Extra-Galactic Research, Intern. Astron. Union Symp. 15*, 42-48, edited by G. C. McVittie, The Macmillan Co., New York, 1962.
Arp, Halton C., The evolution of galaxies, *Sci. Am.*, 208, 70-84, 1963.
Arp, Halton C., and James B. Cuffey, The star cluster NGC 2158, *Astrophys. J.*, 136, 51-65, 1962.
Arp, Halton C., Frank Brueckel, and J. v. B. Lourens, Long-period and red variables in 47 Tucanae, *Astrophys. J.*, 137, 228-248, 1963.
Baade, Walter, *Evolution of Stars and Galaxies*, 321 pp., edited by Cecilia Payne-Gaposchkin, Harvard University Press, Cambridge, Massachusetts, 1962.

- Babcock, Horace W., Control of a ruling engine by a modulated interferometer, *Appl. Opt.*, 1, 415-420, 1962.
- Babcock, Horace W., Photoelectric recording of astronomical seeing (abstract), *Astron. J.*, 68, 272, 1963.
- Babcock, Horace W., Concentration of elements over the surface of a magnetic star, *Astrophys. J.*, 137, 690-692, 1963.
- Babcock, Horace W., Review of *Polarized Light* by W. A. Shurcliff (Harvard University Press, Cambridge, Massachusetts, 1962), *Publ. Astron. Soc. Pacific*, 74, 540, 1962.
- Babcock, Horace W., Instrumental recording of astronomical seeing, *Publ. Astron. Soc. Pacific*, 75, 1-8, 1963.
- Babcock, Horace W., Magnetic and light variations of 53 Camelopardalis, *Publ. Astron. Soc. Pacific*, 75, 74-75, 1963.
- Babcock, Horace W., Measurement of stellar magnetic fields, *Stars and Stellar Systems*, vol. II, *Astronomical Techniques*, chapter 5, pp. 107-125, edited by W. A. Hiltner, University of Chicago Press, 1962.
- Babcock, Horace W., The solar magnetic cycle, *Trans. Intern. Astron. Union*, 11B, 419-425, edited by D. H. Sadler, Academic Press, London, 1962.
- Baum, William A., Laboratory evaluation of image tubes for astronomical purposes, *Adv. Electron. Electron Phys.*, 16, *Symposium on Photo-Electronic Image Devices*, pp. 391-401, edited by J. D. McGee, W. L. Wilcock, and L. Mandel, Academic Press, London, 1962.
- Baum, William A., Photoelectric magnitudes and red-shifts, *Problems of Extra-Galactic Research*, *Intern. Astron. Union Symp.* 15, 390-440, edited by G. C. McVittie, The Macmillan Co., New York, 1962.
- Baum, William A., The detection and measurement of faint astronomical sources, *Stars and Stellar Systems*, vol. II, *Astronomical Techniques*, chapter 1, pp. 1-33, edited by W. A. Hiltner, University of Chicago Press, 1962.
- Baum, William A., Laboratory evaluation of image tubes, *Trans. Intern. Astron. Union*, 11B, 187, edited by D. H. Sadler, Academic Press, London, 1962.
- Baum, William A., *see also* Fredrick, L. W.; Wilcock, W. L.
- Bowen, Ira S., Review of *Astronomical Dictionary* by Josip Klezcek (Academic Press, New York and London, and Publishing House of the Czechoslovak Academy of Sciences, 1962), *Icarus*, 1, 174, 1962.
- Bowen, Ira S., Spectrographs, *Stars and Stellar Systems*, vol. II, *Astronomical Techniques*, chapter 2, pp. 34-62, edited by W. A. Hiltner, University of Chicago Press, 1962.
- Bowen, Ira S., Robert Raynolds McMath (1891-1962), *Year Book Am. Phil. Soc.* 1962, pp. 149-153.
- Brueckel, Frank, *see* Arp, Halton C.
- Cayrel, Giusa, and Roger Cayrel, A detailed analysis of the spectrum of Epsilon Virginis, *Astrophys. J.*, 137, 431-469, 1963.
- Cayrel, Roger, *see* Cayrel, Giusa.
- Cuffey, James B., *see* Arp, Halton C.
- Deutsch, Armin J., Metal deficiencies in late-type giants, *Observatory*, 83, 28-30, 1963.
- Deutsch, Armin J., The aging stars of the Milky Way, *Stars and Galaxies*, chapter 3, pp. 43-63, edited by Thornton L. Page, Prentice-Hall, Englewood Cliffs, New Jersey, 1962.
- Deutsch, Armin J., and others, Astronomy, chapter 2 of *A Review of Space Research*, *Publ.* 1079, pp. 2-1 to 2-39, National Academy of Sciences-National Research Council, Washington, D. C., 1962.
- Deutsch, Armin J., *see also* Merrill, Paul W.
- Eggen, Olin J., The empirical mass-luminosity relation, *Astrophys. J.*, suppl. 76, 125-176, 1963.
- Eggen, Olin J., The astrophysics of visual binaries, *Quart. J. Roy. Astron. Soc.*, 3, 259-287, 1962.
- Eggen, Olin J., and A. R. Sandage, On the existence of the subdwarfs in the (M_{bol} , $\log T_e$)-plane, II, *Astrophys. J.*, 136, 735-747, 1962.
- Eggen, Olin J., D. Lynden-Bell, and A. R. Sandage, Evidence from the motions of old stars that the galaxy collapsed, *Astrophys. J.*, 136, 748-766, 1962.
- Eggen, Olin J., *see also* Woolley, R. v. d. R.
- Ford, W. K., Jr., *see* Fredrick, L. W.
- Fredrick, L. W., J. S. Hall, W. A. Baum, and W. K. Ford, Jr., Some astronomical uses of image intensifying tubes, *Adv. Electron. Electron Phys.*, 16, 403-408, *Second Symposium on Photo-Electronic Image Devices*, edited by J. D. McGee, W. L. Wilcock, and L. Mandel, Academic Press, London, 1962.
- Giver, L. P., *see* Oke, J. B.
- Greenstein, Jesse L., The spectrum of Comet Humason (1961e), *Astrophys. J.*, 136, 688-690, 1962.
- Greenstein, Jesse L., Radio "stars"—explosions in space, *Eng. and Sci.*, 26, 9-12, 1963.
- Greenstein, Jesse L., The role of spectroscopy in astrophysics, *Proc. Xth Colloquium Spectroscopicum Intern.*, pp. 1-36, edited by Ellis R. Lippincott and Marvin Margoshes, Spartan Press, Washington, D. C., 1963.
- Greenstein, Jesse L., Radio stars with large redshift (abstract), *Science*, 140, 382, 1963.

- Greenstein, Jesse L., Stellar evolution and the origin of the chemical elements, *Science in Progress*, 13th series, section 7, pp. 173–208, edited by Wallace R. Brode, Yale University Press, New Haven and London, 1963.
- Greenstein, Jesse L., High energy phenomena in stellar astronomy, *Space Age Astronomy*, section II, chapter 9.2, pp. 214–218, edited by Armin J. Deutsch and Wolfgang B. Klemperer, Academic Press, New York and London, 1962.
- Greenstein, Jesse L., Stellar evolution and high energy phenomena in astrophysics, *Space Science*, chapter 2, pp. 58–87, edited by Donald P. LeGalley, John Wiley & Sons, New York and London, 1963.
- Greenstein, Jesse L., and Thomas A. Matthews, Redshift of the radio source 3C48 (abstract), *Astron. J.*, 68, 279, 1963.
- Greenstein, Jesse L., and Thomas A. Matthews, Red-shift of the unusual radio source: 3C48, *Nature*, 197, 1041–1042, 1963.
- Greenstein, Jesse L., *see also* Kraft, Robert K.; Wallerstein, George.
- Gunn, James E., and Robert P. Kraft, An abundance analysis of two F-type stars in the galactic cluster NGC 752, *Astrophys. J.*, 137, 301–315, 1963.
- Hall, J. S., *see* Fredrick, L. W.
- Harwit, Martin, *see* Hoyle, Fred.
- Helfer, H. L., *see* Wallerstein, George.
- Howard, Robert, Preliminary solar magnetograph observations with small apertures, *Astrophys. J.*, 136, 211–222, 1962.
- Howard, Robert, and A. Severny, Solar magnetic fields and the great flare of July 16, 1959, *Astrophys. J.*, 137, 1242–1250, 1963.
- Hoyle, Fred, and Martin Harwit, On the fate of intergalactic bridges, *Publ. Astron. Soc. Pacific*, 74, 202–209, 1962.
- Jugaku, Jun, *see* Sargent, Wallace L. W.; Searle, Leonard.
- Kaplan, Lewis D., *see* Spinrad, Hyron.
- Keenan, Philip C., *see* Merrill, Paul W.
- Kraft, Robert P., and Maarten Schmidt, Galactic structure and galactic rotation from cepheids, *Astrophys. J.*, 137, 249–257, 1963.
- Kraft, Robert P., Jon Mathews, and Jesse L. Greenstein, Binary stars among cataclysmic variables, II, Nova WZ Sagittae: A possible radiator of gravitational waves, *Astrophys. J.*, 136, 312–315, 1962.
- Kraft, Robert P., *see also* Gunn, James E.
- Lourens, J. v. B., *see* Arp, Halton C.
- Lynden-Bell, D., *see* Eggen, O. J.; Smith, Lewis L.
- Lynds, C. R., and A. R. Sandage, Evidence for an explosion in the center of the galaxy M 82, *Astrophys. J.*, 137, 1005–1021, 1963.
- McVittie, G. C., *see* Sandage, Allan.
- Mathews, Jon, *see* Kraft, Robert P.
- Matthews, Thomas A., and Allan Sandage, 3C196 as a second radio star (abstract), *Publ. Astron. Soc. Pacific*, 74, 406–407, 1962.
- Matthews, Thomas A., *see also* Greenstein, Jesse L.
- Merrill, Paul W., *Space Chemistry*, 166 pp., Ann Arbor Science Library, University of Michigan Press, Ann Arbor, 1963.
- Merrill, Paul W., Armin J. Deutsch, and Philip C. Keenan, Absorption spectra of M-type Mira variables, *Astrophys. J.*, 136, 21–34, 1962.
- Miller, William C., Color photography in astronomy, *Publ. Astron. Soc. Pacific*, 74, 457–473, 1962.
- Minkowski, R., Internal dispersion of velocities in other galaxies, *Problems of Extra-Galactic Research, Intern. Astron. Union Symp. 15*, 112–117, edited by G. C. McVittie, The Macmillan Co., New York, 1962.
- Minkowski, R., Identification with optical objects, *Problems of Extra-Galactic Research, Intern. Astron. Union Symp. 15*, 201–209, edited by G. C. McVittie, The Macmillan Co., New York, 1962.
- Minkowski, R., Problems of observation and interpretation, *Problems of Extra-Galactic Research, Intern. Astron. Union Symp. 15*, 379–389, edited by G. C. McVittie, The Macmillan Co., New York, 1962.
- Münch, Guido, The intensity of forbidden emission lines, *Astrophys. J.*, 136, 823–831, 1962.
- Münch, Guido, Motions of the interstellar gas in the central regions of galaxies, *Problems of Extra-Galactic Research, Intern. Astron. Union Symp. 15*, 119–125, edited by G. C. McVittie, The Macmillan Co., New York, 1962.
- Münch, Guido, Structural problems of galaxies in the light of Lyman- α , *Space Age Astronomy*, section II, chapter 10, pp. 219–227, edited by Armin J. Deutsch and Wolfgang B. Klemperer, Academic Press, New York and London, 1962.
- Münch, Guido, and Olin C. Wilson, Nebular absorption of He I λ 3889 (abstract), *Astron. J.*, 68, 287, 1963.
- Münch, Guido, and Olin C. Wilson, On the structure of the Orion nebula, *Z. Astrophys.*, 56, 127–137, 1962.
- Münch, Guido, *see also* Spinrad, Hyron.
- Nicholson, Seth B., Jupiter, *Astron. Soc. Pacific Leaflet 408*, 8 pp., June 1963.
- Nicholson, Seth B., Edison Pettit, 1889–1962, *Publ. Astron. Soc. Pacific*, 74, 495–498, 1962.

- Nicholson, Seth B., and Oliver R. Wulf, The diurnal variation of K indices of geomagnetic activity on disturbed days in 1949–1957, *J. Geophys. Res.*, **67**, 4593–4599, 1962.
- Norton, R. H., *see* Smith, Lewis L.
- O'Dell, C. R., *see* Wilson, Olin C.
- Oke, J. B., Photoelectric spectrophotometry of RR Lyrae variables (abstract), *Astron. J.*, **67**, 278, 1962.
- Oke, J. B., Absolute energy distribution in the optical spectrum of 3C273, *Nature*, **197**, 1040–1041, 1963.
- Oke, J. B., Absolute energy distribution in the spectra of galaxies, *Problems of Extra-Galactic Research, Intern. Astron. Union Symp. 15*, 34–41, edited by G. C. McVittie, The Macmillan Co., New York, 1962.
- Oke, J. B., and M. Schmidt, Optical observations of the radio source 3C273 (abstract), *Astron. J.*, **68**, 288–289, 1963.
- Oke, J. B., L. P. Giver, and Leonard Searle, An analysis of the absolute energy distribution in the spectrum of SU Draconis, *Astrophys. J.*, **136**, 393–407, 1962.
- Parker, Robert, *see* Wallerstein, George.
- Rudnicki, Konrad, *see* Zwicky, Fritz.
- Sandage, Allan, Observational tests of world models, *J. Soc. Ind. Appl. Math.*, **10**, 781–794, 1962.
- Sandage, Allan, The distance scale, *Problems of Extra-Galactic Research, Intern. Astron. Union Symp. 15*, 359–378, edited by G. C. McVittie, The Macmillan Co., New York, 1962.
- Sandage, Allan (with an appendix by G. C. McVittie), The change of redshift and apparent luminosity of galaxies due to the deceleration of selected expanding universes, *Astrophys. J.*, **136**, 319–338, 1962.
- Sandage, Allan, and Lewis Smith, A four-color photometric system applied to line blanketing of subdwarfs, *Astrophys. J.*, **137**, 1057–1070, 1963.
- Sandage, Allan, *see also* Eggen, Olin J.; Lynds, C. R.; Matthews, Thomas A.; Smith, Lewis L.; Woolley, R. v. d. R.
- Sargent, Wallace L. W., and Leonard Searle, Studies of the peculiar A stars, I, The oxygen abundance anomaly, *Astrophys. J.*, **136**, 408–421, 1962.
- Sargent, Wallace L. W., and Leonard Searle, The infrared O I and Mg II lines in the spectra of the metallic-line stars, *Astrophys. J.*, **136**, 671–673, 1962.
- Sargent, Wallace L. W., Leonard Searle, and Jun Jugaku, Recent work on abundances in peculiar A stars (abstract), *Publ. Astron. Soc. Pacific*, **74**, 408–409, 1962.
- Sargent, Wallace L. W., *see also* Searle, Leonard.
- Schmidt, Maarten, Spectrum of a stellar object identified with the radio source 3C286, *Astrophys. J.*, **136**, 684, 1962.
- Schmidt, Maarten, The rate of star formation, II, The rate of formation of stars of different mass, *Astrophys. J.*, **137**, 758–769, 1963.
- Schmidt, Maarten, 3C273: a star-like object with large red-shift, *Nature*, **197**, 1040, 1963.
- Schmidt, Maarten, Evolution of stellar content of galaxies, *Problems of Extra-Galactic Research, Intern. Astron. Union Symp. 15*, 170–176, edited by G. C. McVittie, The Macmillan Co., New York, 1962.
- Schmidt, Maarten, *see also* Kraft, Robert P.; Oke, J. B.
- Searle, Leonard, Wallace L. W. Sargent, and Jun Jugaku, The luminosities and compositions of the high-galactic-latitude supergiants 89 Herculis and HD 161796, *Astrophys. J.*, **137**, 268–279, 1963.
- Searle, Leonard, *see also* Oke, J. B.; Sargent, Wallace L. W.
- Severny, A., *see* Howard, Robert.
- Smith, Lewis L., A. R. Sandage, D. Lynden-Bell, and R. H. Norton, An investigation of the variable stars in the globular cluster NGC 6712 (abstract), *Astron. J.*, **68**, 293, 1963.
- Smith, Lewis L., *see also* Sandage, Allan.
- Spinrad, Hyron, Guido Münch, and Lewis D. Kaplan, The detection of water vapor on Mars, *Astrophys. J.*, **137**, 1319–1321, 1963.
- Straka, W. C., *see* Struve, Otto.
- Struve, Otto, and W. C. Straka, Notes on diffuse galactic nebulae, *Publ. Astron. Soc. Pacific*, **74**, 473–487, 1962.
- Thorne, Kip S., The theory of synchrotron radiation from stars with dipole magnetic fields, *Astrophys. J., suppl.* **73**, 1–30, 1963.
- Tift, William Grant, Multicolor photoelectric photometry of bright galaxies, II, *Astron. J.*, **68**, 302–318, 1963.
- Utter, Merwyn G., The heavens in 1963, *Astron. Soc. Pacific, annual series*, 8 pp., January 1963.
- Wallerstein, George, Jesse L. Greenstein, Robert Parker, H. L. Helfer, and Lawrence Aller, Red giants with extreme metal deficiencies, *Astrophys. J.*, **137**, 280–300, 1963.
- Weidemann, Volker, Effektive Temperatur und Schwerebeschleunigung der weissen Zwerge, *Z. Astrophys.*, **57**, 87–116, 1963.
- Weymann, Ray, Comments on mass ejection mechanisms in red giants, *Astrophys. J.*, **136**, 476–486, 1962.
- Weymann, Ray, Physical conditions in the circumstellar envelope of α Orionis, *Astrophys. J.*, **136**, 844–865, 1962.

- Wilcock, W. L., and W. A. Baum, Astronomical tests of an imaging photomultiplier, *Adv. Electron. Electron Phys.*, 16, 383-390, *Second Symposium on Photo-Electronic Image Devices*, edited by J. D. McGee, W. L. Wilcock, and L. Mandel, Academic Press, London, 1962.
- Wilkey, Robert L., The optimum use of interstellar reddening data to obtain intrinsic stellar luminosities and colors, *Astron. J.*, 68, 190-194, 1963.
- Wilson, Olin C., Relationship between colors and spectra of late main-sequence stars, *Astrophys. J.*, 136, 793-808, 1962.
- Wilson, Olin C., Paul Willard Merrill, *Biographical Memoirs* 37, published for National Academy of Sciences of the United States by Columbia University Press, New York, 1963, in press.
- Wilson, Olin C., Lithium in a main-sequence star, *Publ. Astron. Soc. Pacific*, 75, 62-64, 1963.
- Wilson, Olin C., Do stellar chromospheres evolve? (abstract), *Science*, 140, 386, 1963.
- Wilson, Olin C., and C. R. O'Dell, Internal motions in the planetary nebula IC 4997, *Publ. Astron. Soc. Pacific*, 74, 511-514, 1962.
- Wilson, Olin C., *see also* Münch, Guido.
- Woolley, R. v. d. R., A. R. Sandage, O. J. Eggen, *et al.*, Studies in the Magellanic Clouds, IV, Photometry of cepheids in Variable Field I, LMC, *Roy. Obs. Bull.* 58, E31-E87, 1962.
- Wulf, Oliver R., *see* Nicholson, Seth B.
- Zwicky, Fritz, New types of objects (abstract), *Astron. J.*, 68, 301, 1963.
- Zwicky, Fritz, Intergalactic bridges, *Astron. Soc. Pacific Leaflet* 403, 8 pp., January 1963.
- Zwicky, Fritz, New observations of importance to cosmology, *Problems of Extra-Galactic Research, Intern. Astron. Union Symp.* 15, 347-358, edited by G. C. McVittie, The Macmillan Co., New York, 1962.
- Zwicky, Fritz, and Konrad Rudnicki, Area of the sky covered by clusters of galaxies, *Astrophys. J.*, 137, 707-719, 1963.

Geophysical Laboratory

Washington, District of Columbia

Philip H. Abelson
Director

Contents

Introduction	55	The quaternary invariant point anorthite + forsterite + melilite + diopside + spinel + liquid.	114
Experimental Petrology	60	Quartz norites and contaminated gabbros	115
Fe-Ti oxides in rocks as thermometers and oxygen barometers	60	The join diopside-pyrope at 30 kilobars	116
Equilibrium relations of coexisting pairs of Fe-Ti oxides	60	Effect of pressure on the melting of enstatite	118
Origin of igneous rocks	66	Melting of forsterite, Mg_2SiO_4 , at pressures up to 47 kilobars	119
Partial melting of the mantle	66	Some effects of pressure on phase relations in the system $MgO-Al_2O_3-SiO_2$	121
Eclogite occurrences	67	Alkaline rocks and their minerals	124
CIPW norms of eclogites	67	Crystallization of the rock-forming silicates in the system $Na_2O-Al_2O_3-Fe_2O_3-SiO_2$ at 1 atmosphere	124
Eclogite as the partial fusion product of garnet peridotite	69	Pure acmite	124
Previous hypotheses	70	Nepheline-acmite	124
Melting of garnet peridotite at 30 kilobars	71	Solid solutions in nepheline and albite	125
Melting of bimineralec eclogite at 30 kilobars	76	Nepheline solid solutions	126
Melting relations of basalts	77	Albite solid solutions	126
Pyroxenes and associated minerals in the crust and mantle	84	Crystallization in the four- component system	128
Pyroxene quadrilateral	84	The stability relations of acmite	131
Liquidus	87	Liquidus data on the system acmite- nepheline-diopside at 1 atmosphere	133
Two-pyroxene boundary curve	88	Melting of iron at high pressure	134
Inversions in CaO-poor pyroxenes	88	Hydrous systems and metamorphic rocks.	137
Inversion in CaO-rich pyroxenes.	91	Gas mixtures	137
Ferrosilite	91	The alumina content of talc	139
Solvus	92	The upper stability limit of magnesian chlorites to 10 kilobars P_{H_2O}	140
Pyroxene quadrilateral at 10 kilobars	94	The liquidus region at 10 kilobars P_{H_2O}	143
Optics	94	Probable instability of analcite + hypersthene	145
New data on the system diopside- forsterite-silica	95	The muscovite-kaolinite reaction	147
Nonbinary character of the system diopside-forsterite	95	Petrography	149
Very careful measurements on the diopside-rich portion of the system diopside-enstatite.	97	On the geographic distribution of Cenozoic volcanism	149
Résumé of new data on the system diopside-forsterite-silica	99	Available data	149
The system enstatite-diopside at 30 kilobars pressure	103	A distinction between intra- and circumoeanic Cenozoic volcanics	150
The join diopside-pyrope at atmospheric pressure	107	Some relations between salic molecules in the CIPW norm and the Niggli katanorm	152
Stable and metastable pyroxene solid solutions	107	A replacement for reference sample G-1	155
Two-pyroxene assemblages in the presence of Al_2O_3	110	Varieties of lamprophyre	156
Orthopyroxene	111		
Position of the thermal maxima on the divariant equilibria anorthite + forsterite + diopside + liquid and anorthite + forsterite + protoenstatite + liquid.	111		

Crystallography	158	Pyrrhotite phase relations at low temperatures	213
The crystal structure of mullite	158	Low-temperature sulfide synthesis	214
Experimental studies	158	Covellite	214
Structure analysis and refinement	160	Tin sulfides	215
Crystal chemistry	163	Pyrrhotite	215
Structures of micas	165	Nickel sulfides	215
Tourmaline	166	Bravoite	215
Crystal structure of synthetic iron mica	169		
Structural hints from crystal morphology	170	Sulfide-Silicate Relations	215
On the number of n -translational ($n + 1$)-dimensional groups	171	The Ages of Rocks and Minerals	218
Crystal data	171	Evaluation of zircon ages	219
The interpretation of the powder pattern of a crystalline mixture	172	Ages from the early Precambrian near Rainy Lake, Ontario	225
The crystal structure of jadeite, $\text{NaAlSi}_2\text{O}_6$	173	K-Ar ages of hornblendes from the southern Gothard massif, Switzerland	227
Ore Minerals	174	Organic Geochemistry	229
The Fe-Ni-S system	175	Hydrocarbons from kerogen	229
Discussion of phase relations	175	The isotopic composition of the carbon of Redfish Bay	234
Interpretation of natural occurrences in terms of phase diagrams	186	The organic chemicals in Precambrian rocks	236
The Cu-Ni-S system	189	An experimental approach to the study of chemical evolution	236
The Cu-Fe-S system	193		
The join $\text{Cu}_{9.2}\text{S}_5\text{-Cu}_5\text{FeS}_4$	193	The Physical Chemistry of Isotopic Substances	238
The join $\text{Cu}_5\text{FeS}_4\text{-Cu}_2\text{S}$	194	Sulfur isotope analysis with sulfur hexafluoride	238
The join $\text{Cu}_5\text{FeS}_4\text{-CuFeS}_{2-x}$	195		
The Fe-Pb-S system	196	Miscellaneous Administration	239
Sulfide systems containing Sn	197	<i>Journal of Geophysical Research</i>	239
The Sn-S system	197	<i>Journal of Petrology</i>	239
The Fe-Sn-S system	198	Lectures	239
The Cu-Sn-S system	199	Petrologists' Club	241
The Fe-Ni-As system at 800°C	200		
The MAs_3 phase	201	Summary of Published Work	242
The MAs_2 phases	201		
The MAs phases	203	Bibliography	250
Liquid fields	204	References Cited	251
The M_{11}As_8 phase	206	Personnel	258
The M_2As phases	206		
Oregonite	206		
Fe_2As solid solution	207		
The M_5As_2 phase	207		
The θ and ϕ phases	207		
The Fe-Ni phases	209		
Heating experiments on monoclinic pyrrhotites	210		

INTRODUCTION

THIS year our regular staff has been supplemented by a particularly large and productive group of fellows, associates, and visiting investigators, totaling twenty-nine. Included in the group were fourteen from abroad, representing nine countries. The principal areas of research activities were in the fields of experimental petrology, statistical petrology, high pressures, ore minerals, the ages of rocks and minerals, and organic geochemistry.

Among the most interesting developments of the year are recent experiments by Kullerud and Yoder, who have demonstrated that sulfur readily reacts with many of the common rock-forming silicates over wide temperature-pressure ranges. Elements (like iron, manganese, nickel, cobalt, and copper) originally present in the silicates react to produce sulfides and oxides. Other reaction products are quartz or nonferrous silicates when elements such as magnesium and calcium are present in the original silicates. When the original silicates contain even only moderate amounts of iron and related elements, the action of sulfur changes the mineralogy of the rock profoundly. The addition of a few per cent of sulfur to common rocks can bring about formation of typical sulfide-oxide ore assemblages.

Another investigation, by Lindsley, has developed a new means of evaluating the partial pressure of oxygen present during crystallization of magmas. The oxidation state of elements of variable valence can greatly influence magmatic crystallization paths and hence differentiation trends. For most rocks, however, no quantitative oxygen barometer has been available. Lindsley has found that the equilibrium compositions of ilmenite and titaniferous magnetite are effectively univariant functions of temperature and partial pressure (fugacity) of oxygen. Over a composition range covering the Fe-Ti oxides in many

rocks the compositions of coexisting titaniferous magnetite and ilmenite give unique values for oxygen fugacity and temperature. As these oxide minerals are of widespread occurrence, they can provide a useful thermometer and oxygen barometer for many igneous and metamorphic rocks.

Chayes has been studying the relations between lavas of the open ocean and those on the shoreward side of the deep trenches that separate much of the Pacific from marginal continental or shallow-sea areas, and are found also in certain peripheral areas of the Atlantic and Indian oceans. Using modern data reduction techniques and chemical sorting criteria, Chayes has been able to show an extraordinarily strong association between petrography and geography in the two environments. In previous work of this sort the sialic lavas had proved readily distinguishable, but the overlap in composition between the mafic magmas of both environments had proved an insurmountable obstacle; the great bulk of oceanic lava being mafic, it could hardly be said that the classification schemes were either successful or useful. In fact, the whole notion of a qualitative distinction of fundamental importance between oceanic and non-oceanic basalt, revived in 1938 by W. Q. Kennedy, has gradually been losing ground. Chayes now presents striking evidence that its demise was premature; the relation between geography and petrography in the intra- and circum-oceanic environments is so strong that well over 90 per cent of decisions about the geographic class to which particular lavas belong, based solely on their chemical compositions, will be correct.

During the past year our research at the Laboratory has yielded strong new evidence that mild thermal degradation of kerogen is the principal mechanism by which hydrocarbons in natural gas and

petroleum are produced. Under conditions similar to those common in nature, Hoering and Abelson have observed the liberation of a series of saturated straight-chain hydrocarbons, which are especially abundant in natural products, ranging from methane (C_1) through *n*-dodecane (C_{12}). Isotopic measurements on methane and on other hydrocarbons produced in the laboratory agree with those observed by others on natural gas.

Diamond-bearing kimberlites characteristically contain two pyroxenes, one which approaches diopside ($CaMgSi_2O_6$) in composition and another with a composition near that of enstatite ($MgSiO_3$). The mutual solid solution shown by pairs of such pyroxenes has been known as a function of temperature for a number of years. Work carried out this year by Brian T. C. Davis, however, has shown that the solubility of $MgSiO_3$ in $CaMgSi_2O_6$ is independent of pressure up to 30 kilobars. This is a most interesting discovery, because it provides a method of estimating temperature of formation of pyroxenes that is not subject to uncertainty due to lack of knowledge of the pressure of formation.

The temperature of formation indicated by the composition of diopsidic pyroxenes from kimberlites is about $1000^\circ C$. The minimum pressure at which diamond can form at 1000° is 40 kilobars, corresponding to a depth in the earth of about 125 kilometers. On the assumption that diamond and diopsidic pyroxene crystallized together we may thus estimate a temperature of 1000° at 125 kilometers. This is not inconsistent with geophysical estimates, but it is on the low side.

O'Hara and Yoder, seeking information bearing on the formation of basaltic magma in the upper mantle, have been using mixtures of separated, analyzed minerals from eclogite and garnet peridotite, natural eclogites, and synthetic preparations on the join diopside-pyroxene. In addition, theoretical deductions based on physicochemical principles were evolved in an effort to define the nature of liquids

derived from the partial fusion of garnet peridotite, the most likely parental material in the mantle.

Yoder, Tilley, and Schairer continued their highly successful cooperative research on the crystallization behavior of natural basalts at or near the surface of the earth. Their new results yielded a surprisingly simple relationship between liquid iron-enrichment and liquidus temperature for the nonaccumulative tholeiitic rocks of the Hawaiian volcanic province. Other results place narrow restrictions on the temperatures of beginning of crystallization and final crystallization of the famous Skaergaard intrusion of East Greenland.

Studies in the system $MgO-Al_2O_3-SiO_2-H_2O$ have been continued and extended by Fawcett and Yoder to include bulk compositions and physical conditions that may be related to a wide range of metamorphic rocks. Hydrothermal experiments carried out at 2, 5, and 10 kb P_{H_2O} show that the maximum Al_2O_3 content of talc is about 4.0 weight per cent with no significant increase as a result of higher pressures of formation.

The upper stability limit of the magnesian chlorites has been determined at water pressures between 3 and 10 kb. At high water pressures the chlorite breakdown products are enstatite, spinel, and forsterite, but at low water pressures cordierite, forsterite, and spinel. The invariant point is close to 3 kb at $735^\circ C$.

Liquidus studies of the system $MgO-Al_2O_3-SiO_2-H_2O$ at 10 kb P_{H_2O} show that several mineral assemblages stable at lower pressures are no longer compatible at this pressure. Enstatite may contain 16 weight per cent Al_2O_3 in solid solution; this expanded compositional range gives rise to a very large liquidus field for this mineral and results in the presence of enstatite in mineral assemblages obtained from widely varying bulk compositions. At 10 kb P_{H_2O} the beginning of melting in the system is more than $450^\circ C$ lower than that determined at 1 atmosphere.

Work on the system $CaO-MgO-Al_2O_3-$

SiO_2 has been continued by O'Hara and Schairer with a study of the phase relationships on the diopside-pyroxene join at atmospheric pressure. Information on stable and metastable clinopyroxene solid solutions is presented. The thermal "barrier" forsterite + anorthite + diopside solid solution has considerable petrogenetic importance as the division between liquids taking a trend toward silica enrichment or silica depletion during differentiation. The natural counterparts of these liquids are the tholeiitic and alkali basalts, respectively. This barrier has been found to lie on the silica-poor side of the plane forsterite-anorthite- $\text{CaMgSi}_2\text{O}_6$, implying that some liquids that contain Ca_2SiO_4 in their CIPW norm may yield residual liquids containing enstatite in the CIPW norm. The natural counterpart of this behavior would be the derivation of a hypersthene-normative basalt as a residual liquid from the fractional crystallization of certain alkali basalts. Two ways in which the thermal barrier in the synthetic system may be crossed by residual liquids during perfect fractionation involve either the removal of spinel or the removal of early-formed subcalcic clinopyroxene.

Considerable progress has been made by Kushiro and Schairer on the system diopside-forsterite-silica, one of the crucial systems in petrology. The work of Schairer and Yoder reported last year has been expanded to cover many additional compositions, and the quenching experiments were made with much greater precision in order to delineate precisely the complex crystallization processes that may take place over a small range of temperature. A new phase diagram is given for the system diopside-forsterite. It is not binary, because of the presence of some calcium in the olivine and because of solid solution in the diopsidic pyroxene. The intersection of the liquidus curves of olivine and pyroxene, at $1389^\circ \pm 1^\circ\text{C}$, is not a eutectic but a piercing point. The studies of Boyd and Schairer on the system enstatite-diopside reported last

year have been expanded, and the phase relations have been determined very precisely. A detailed phase diagram for the diopside-rich portion of the system enstatite-diopside is given. A surprising feature is a temperature maximum on the liquidus curve of diopsidic pyroxene at the composition 90 per cent diopside at $1393^\circ \pm 1^\circ\text{C}$.

Liquids in the system $\text{Na}_2\text{O}-\text{Al}_2\text{O}_3-\text{Fe}_2\text{O}_3-\text{SiO}_2$ are analogous to the strongly alkaline magmas that constitute a striking part of the nonorogenic magmatism of the continents. The study of this system at 1 atmosphere, by Bailey and Schairer, is nearly complete; it has been found that mineral assemblages similar to both oversaturated and undersaturated rocks crystallize in equilibrium only with strongly peralkaline liquids, because of the incongruent melting of acmite. Preliminary studies of the *PT* stability of acmite in the presence of water, by Bailey, indicate that this mineral continues to melt incongruently at pressures up to 10 kb and may be expected to exert a similar controlling influence on alkaline magma generation at appropriate depths in the crust. The low melting temperatures encountered in all these investigations suggest serious consideration of the possibility of developing peralkaline magmas by partial melting of crystalline materials above the eclogite-basalt transition zone.

In continuation of the studies of the joins acmite-diopside, nepheline-diopside, and nepheline-acmite, Yagi has obtained preliminary liquidus data on the system nepheline-diopside-acmite and has discovered that in a small composition range melilite appears as a primary phase at the liquidus.

Velde has found that the rate of conversion of kaolinite + KOH to muscovite is dependent on the structural state of the kaolinite. This suggests that the muscovite inherits at least part of the kaolinite structure, a conclusion that has an important bearing on the origin of illite (essentially potassium-poor, water-

rich muscovite) in sedimentary rocks.

B. T. C. Davis and England determined the melting curve of forsterite to 47 kb pressure using tungsten-rhenium alloy thermocouples at temperatures between 1900° and 2150°C. The melting curve dT/dP is flatter and more nearly linear than that of any other silicate yet measured. Davis also examined relations in the system enstatite-diopside at 30 kb. The melting points of all compositions are greatly increased by pressure. There is almost complete solid solution at the solidus, but an inversion loop intersects both solidus and solvus. The position of the solvus is almost unaffected by pressure.

The melting curve of iron is of great geophysical interest because it is probable that the earth's outer core is predominantly liquid iron whereas the inner core is solid iron. Boyd and England have determined the melting curve of iron to 50 kb and shown that the initial slope is complicated by the phase change δ - γ Fe. This complication makes it impossible to extrapolate the results to the pressure range present in the core within a really useful uncertainty, and further work on the precise location of the triple point δ - γ -liquid Fe is needed.

Additional results obtained by Boyd and England for the melting of the pyroxene enstatite show that, as in other silicates, the melting curve has a pronounced curvature. A Simon equation has been fitted to the enstatite data, and extrapolation of the curve to the pressure of the core-mantle boundary indicates a minimum melting temperature of rocks at that depth of about 4000°C. This estimate is in good agreement with the estimate obtained with the diopside melting curve. Only a minimum limit can be set, because the effect of phase transitions on the melting curves above the experimental pressure range is not yet adequately known.

Recent analyses of pyroxenes from kimberlites that have formed at high pressures in the mantle have revealed the

puzzling fact that they are very low in alumina. Laboratory results on synthetic systems show a very high solubility of alumina in pyroxenes at high pressures. Boyd and England's work on the join pyrope-enstatite indicates that the alumina content of enstatite drops markedly when the pressure reaches a high enough value to stabilize garnet. This fact helps to explain the discrepancy but does not eliminate it.

In Greenwood's continuing study of metamorphic processes in the presence of two-component vapors some particularly interesting observations have been made on the thermodynamics of mixing of supercritical H₂O and CO₂. These two gases, which individually depart widely from perfect gas behavior, mix together almost ideally, as deduced both from the displacement of the wollastonite-quartz-calcite equilibrium in the mixtures and from new detailed P - V - T - x data on mixtures up to a pressure of 500 bars. If this close approach to ideal mixing is general throughout the system H₂O-CO₂, calculations on mineral equilibria of wet impure limestones will be much simplified.

In the statistical aspects of petrography, Chayes and Métais have spent most of the year experimenting with various forms of machine data compilation and reduction. As raw material for this work they have prepared a card file of analyses of Cenozoic lavas. Empirical frequency distributions of a wide variety of constituents and normative parameters are now readily obtainable, and preliminary summaries have already yielded a number of interesting results. One of these—a study of the well known oceanic basalt-trachyte association—has been completed and published. A similar study of intra- and circumoceanic Cenozoic volcanics is nearing completion. A detailed study of the relation between suites of CIPW norms and Niggli katanorms is in progress. A review of the chemical and normative variation of lamprophyres has been undertaken.

Chayes and Zies have continued their work on feldspar-groundmass relations in salic alkaline extrusives, and Zies has begun separation and analysis of cossyrite from material he collected on Pantelleria during the report year.

The study of the crystal structures of the aluminum-silicate minerals was continued by Burnham this year with an investigation of the crystal structure of synthetic mullite ($1.92\text{Al}_2\text{O}_3 \cdot \text{SiO}_2$). Knowledge of the details of this structure, which is very similar to that of sillimanite, should provide a physical basis for evaluating the mullite composition limits and understanding the sillimanite-mullite stability relations. At the present time three structure models, differing in the distribution of oxygen atoms in defect sites, have been refined by least-squares techniques to essentially identical levels of precision. Work is now continuing, to determine the correct model and the details of atomic distribution in defect and disordered sites in that model.

A natural specimen of three-layer trigonal paragonite has yielded good single crystals, allowing the systematic and structural absences to be determined unambiguously; accurate unit-cell data have been obtained. Excellent single crystals have been found of 2M_1 paragonite (high in potassium) and 2M_1 muscovite (high in sodium) coexisting in a natural paragonite from a kyanite schist. Both structures are to be refined (by Radoslovich and Burnham) using three-dimensional data obtained by a counter diffractometer.

G. Donnay has studied an unusual iron tourmaline from Mexico whose properties do not fit either of the two known solid solution series. She has also shown that the crystal structure of synthetic iron mica is very close to idealized biotite, with random substitution of ferric iron for silicon. Further studies on the law of Bravais have led the Donnays to propose a general method of morphological analysis (which they have applied to hodgkinsonite) for

deriving information on the bond assemblage from (1) the cell and space group obtained by X rays, and (2) the relative frequencies of occurrence of observed crystal forms.

Studies of phase equilibria among ore minerals have led to many new results. Kullerud has made further progress in elucidating the Fe-Ni-S system. This report contains phase diagrams demonstrating the relations in the system over a temperature range from 400° to 1100°C . These diagrams illustrate the formation and stabilities of pyrrhotite-pentlandite assemblages in ores and of troilite-pentlandite, pentlandite-taenite, and pentlandite-troilite-taenite assemblages in meteorites. The strong effect of pressure on the temperature of pentlandite breakdown is a potential tool for measuring the pressures under which these assemblages formed on earth and in space.

Important quantities of tin occur in sulfide ores in the form of relatively pure tin sulfides or incorporated in more complex sulfides. Moh has made laboratory studies of systems pertinent to the understanding of such ores and has discovered two new minerals, Sn_2S_3 and SnS_2 . Buseck has found that the phase relations at 800°C in the Fe-Ni-As system are characterized by extensive solid solutions. Brett has investigated the three joins $\text{Cu}_{9.2}\text{S}_5$ - Cu_5FeS_4 , Cu_5FeS_4 - Cu_2S , and Cu_5FeS_4 - CuFeS_{2-x} of the ternary Cu-Fe-S system. Stability relations among the various low-temperature forms of pyrrhotite have been studied by von Gehlen.

The major effort in geochronology (Tilton, Davis, Steiger) continues to be evaluation of the reliability of mineral ages. Studies of ages from zones of contact metamorphism provide a dramatic illustration of the relative abilities of various minerals to preserve their age record during episodes of heating. Zircon, biotite, feldspar, and hornblende age values from such a zone in the Colorado Front Range yield data similar to some of the discordant age patterns

observed in regionally metamorphosed rocks. Metamorphism from the intrusive is sufficiently intense to lower the age values of all these minerals, although the distance from the contact, equated to temperature, at which the effect begins varies from one mineral to another. The activation energy for diffusion of lead in zircon is low at low temperature and high at high temperature. Comparison of the Colorado results with related studies in Finland shows that the change in activation energy probably occurs at different temperatures for different zircons. An investigation of potassium-argon ages from hornblende from metamorphic rocks in the Alps has provided further demonstration of the ability of hornblende to preserve its age record better than biotite during episodes of metamorphism.

The group in organic geochemistry was active on a number of projects in addition to studies of thermal degradation of kerogen. Abelson presented a paper at the International Petroleum Congress at Frankfurt, which developed some new ideas on the geochemical events leading to petroleum. Hoering looked for extractable organic matter in Precambrian rocks. Hoering and Sabels developed a good method for performing sulfur isotope studies on sedimentary rocks. Parker studied the stable carbon isotope geochemistry of a marine bay. Allen has engaged on an imaginative but chancy gamble; he has been studying model systems involving chemicals possibly present at the early stages of earth history in a search for self-catalyzing systems. These and other researches are described in the pages that follow.

EXPERIMENTAL PETROLOGY

Fe-Ti OXIDES IN ROCKS AS THERMOMETERS AND OXYGEN BAROMETERS

Equilibrium Relations of Coexisting Pairs of Fe-Ti Oxides

D. H. Lindsley

An important factor in geological processes is the variable valence of some elements. For example, Kennedy (1948) and Osborn (1959) have shown that the oxidation state of iron has a profound effect on the crystallization history and therefore the differentiation trend in basalt magmas. At relatively high oxygen pressures iron-rich spinels like magnetite crystallize early and deplete the magma in iron, thus enriching the residuum in silica—the “Bowen trend.” At lower oxygen pressures iron-rich spinels cannot crystallize, and the residuum is enriched in iron—the “Fenner trend.” Partial pressure (fugacity) of oxygen is also important in the stability of iron-rich pyroxenes and olivines. The

Fe-Ti oxides, essentially magnetite-ulvöspinel ($\text{Fe}_3\text{O}_4\text{-Fe}_2\text{TiO}_4$) and hematite-ilmenite ($\text{Fe}_2\text{O}_3\text{-FeTiO}_3$) solid solutions, provide a useful oxygen barometer for the rocks in which they occur. In favorable cases the compositions of coexisting pairs of these Fe-Ti oxides give unique values for the oxygen fugacity (f_{O_2}) and temperature (T) of their formation: The magnetite-ulvöspinel_{ss} + hematite-ilmenite_{ss} + water-rich fluid can be considered three phases in the four-component system Fe-Ti-O-H, giving a variance of 3. Experimentally the effect of total pressure on the equilibrium compositions of the solids is found to be negligible, reducing the effective variance to 2. The compositions of magnetite-ulvöspinel_{ss} and those of the coexisting hematite-ilmenite_{ss} are found to be univariant functions of f_{O_2} and T . Thus for a given oxide pair there are two simultaneous equations in f_{O_2} and T ; in part of the region studied these curves intersect, giving a unique solution. Data on the f_{O_2} - T dependence of magnetite-

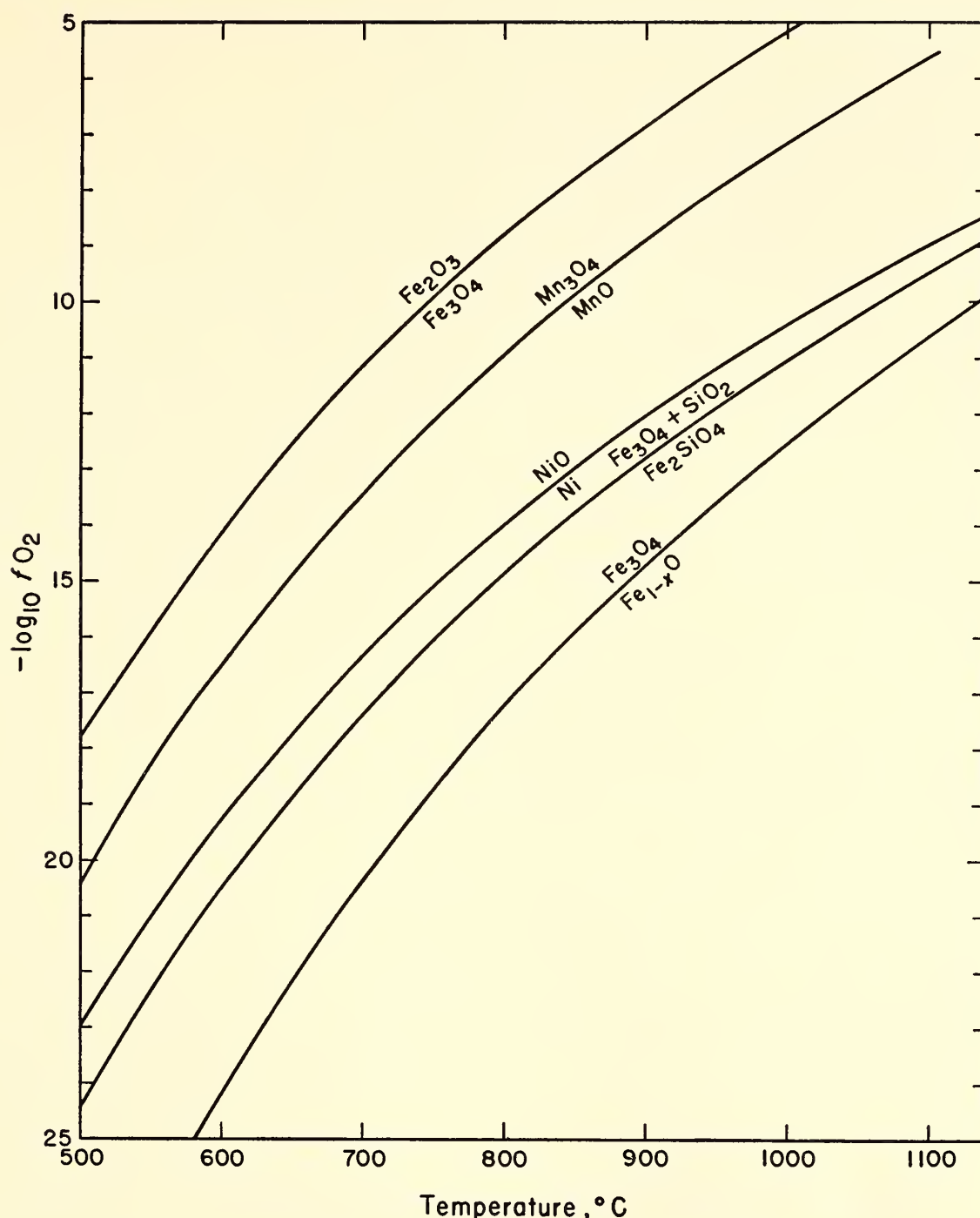


Fig. 1. Plot of oxygen fugacity versus temperature for the buffer assemblages used in the system $\text{FeO-Fe}_2\text{O}_3\text{-TiO}_2$. The magnetite-hematite (MH), nickel-nickel oxide (NNO), fayalite-magnetite-quartz (FMQ), and wüstite-magnetite (WM) curves are plotted from data given by Eugster and Wones (1962, p. 90) and are corrected to a total pressure of 2000 bars. The $\text{MnO-Mn}_3\text{O}_4$ curve, extrapolated from the data of Hahn and Muan (1960), is uncorrected for pressure.

ulvöspinel_{ss} were given last year (*Year Book 61*, p. 105); similar data for hematite-ilmenite_{ss} (henceforth called α phases by analogy with hematite, $\alpha\text{Fe}_2\text{O}_3$) are presented here. It is emphasized that the data apply only when members of the two solid solution series are in mutual equilibrium.

The compositions of α phases in equilibrium with magnetite-ulvöspinel_{ss} were determined by hydrothermal experiments in which the fugacity of oxygen

was controlled by oxygen buffers (fig. 1): nickel-nickel oxide (NNO), fayalite-magnetite-quartz (FMQ), wüstite-magnetite (WM), and $\text{MnO-Mn}_3\text{O}_4$.¹ Total pressures used were: 800°C and below, 2000 bars; 800°–900°C, 1000 bars;

¹ An oxygen fugacity-temperature ($f_{\text{O}_2}\text{-}T$) curve for this assemblage (fig. 1) is extrapolated from the data of Hahn and Muan (1960). The assemblage serves as an f_{O_2} buffer, although somewhat sluggish reaction rates require increased run lengths to ensure equilibrium.

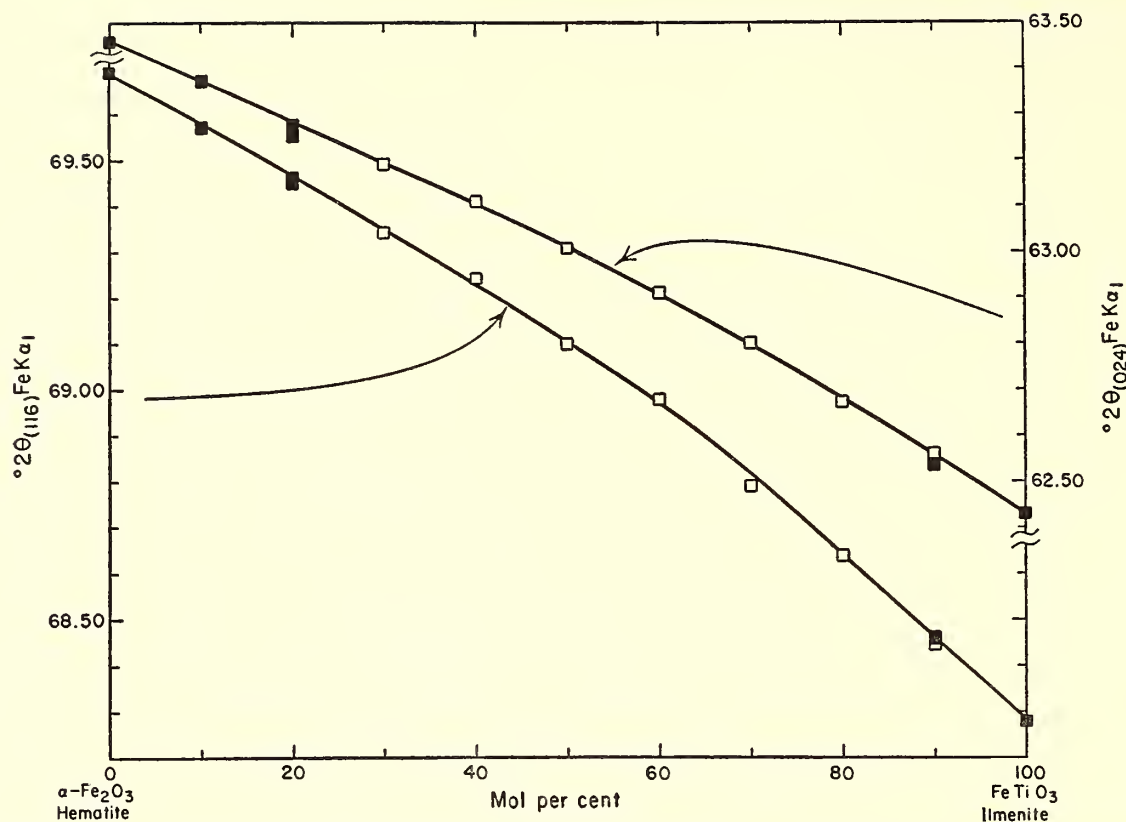


Fig. 2. Determinative curve for hematite-ilmenite solid solutions. Solid squares are for hydrothermal runs at 800°C; open squares, for runs in evacuated silica-glass tubes. CaF_2 was used as an internal standard.

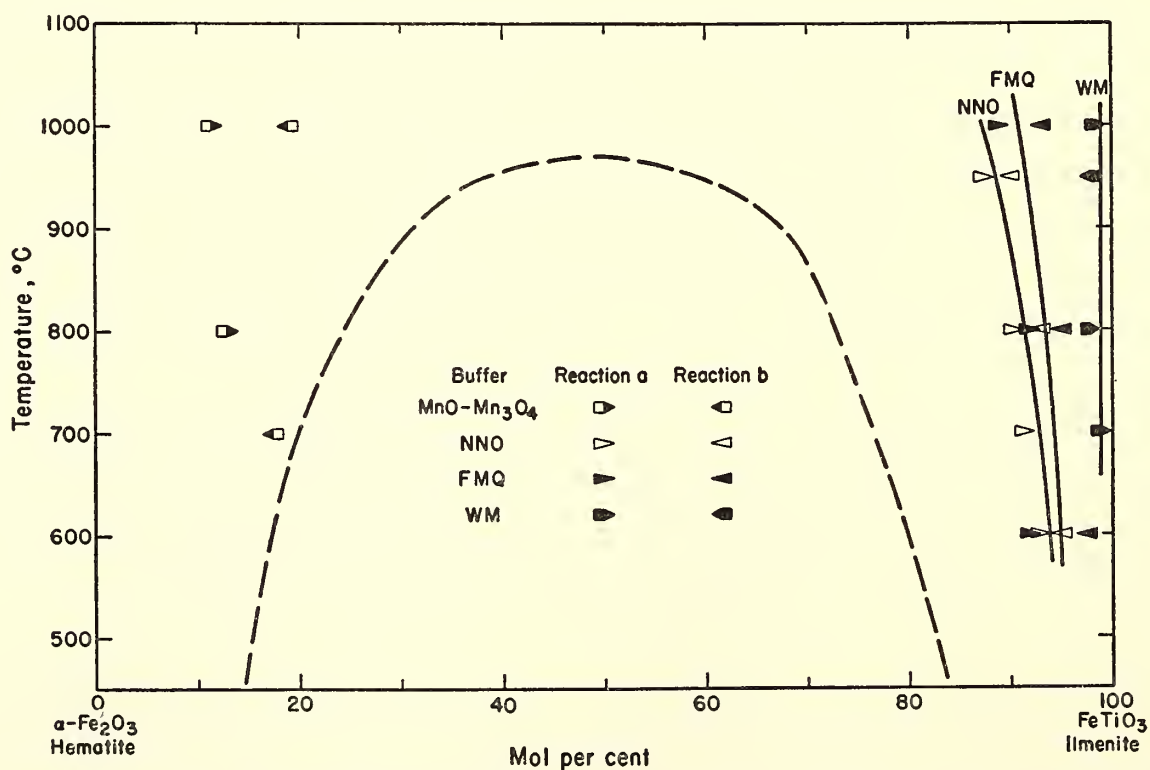


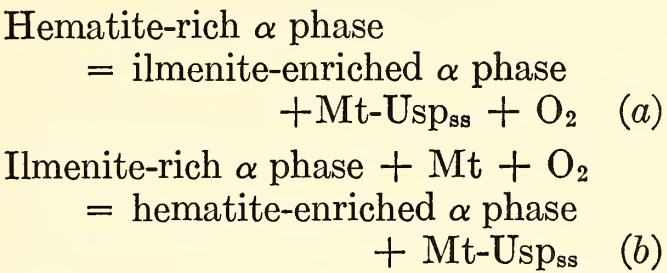
Fig. 3. Compositions of hematite-ilmenite solid solutions in equilibrium with Mt-Usp_{ss}. The solvus is from Carmichael (1961).

1000°C, 670 bars. A few duplicate runs at 800° and 900°C at 1000 and 2000 bars show no detectable effect of total pressure. A rough approximation of the effect of total pressure can be made by comparison with the calculations of Eugster and

Wones (1962, pp. 90–92) on the total pressure effect on f_{O_2} for the oxygen buffers. At 727°C the changes in $\log f_{\text{O}_2}$ range from 0.02 to 0.09 per 1000 bars.

Starting materials for f_{O_2} -buffered hydrothermal runs were either α phases or α

phases + magnetite. The following reactions took place:



These reactions were used to bracket the composition of that α phase in equilibrium with Mt-Usp_{ss} for a given buffer at a given temperature. Compositions were read from the X-ray determinative curve (fig. 2). The resulting data are

plotted in figure 3. The horizontal extent of the data points—2 mole per cent—reflects the uncertainty in the compositions as determined from figure 2.

Tie lines determined for coexisting magnetite-ulvöspinel_{ss} and α phases are shown on FeO-Fe₂O₃-FeTiO₃ plots for several isotherms in figure 4. The NNO points for 1000°C are extrapolated, as the gold-nickel eutectic at ~960°C precludes runs in gold containers above that temperature. The most noteworthy feature of figure 4 is the strong temperature dependence of magnetite-ulvöspinel_{ss} compositions in equilibrium with il-

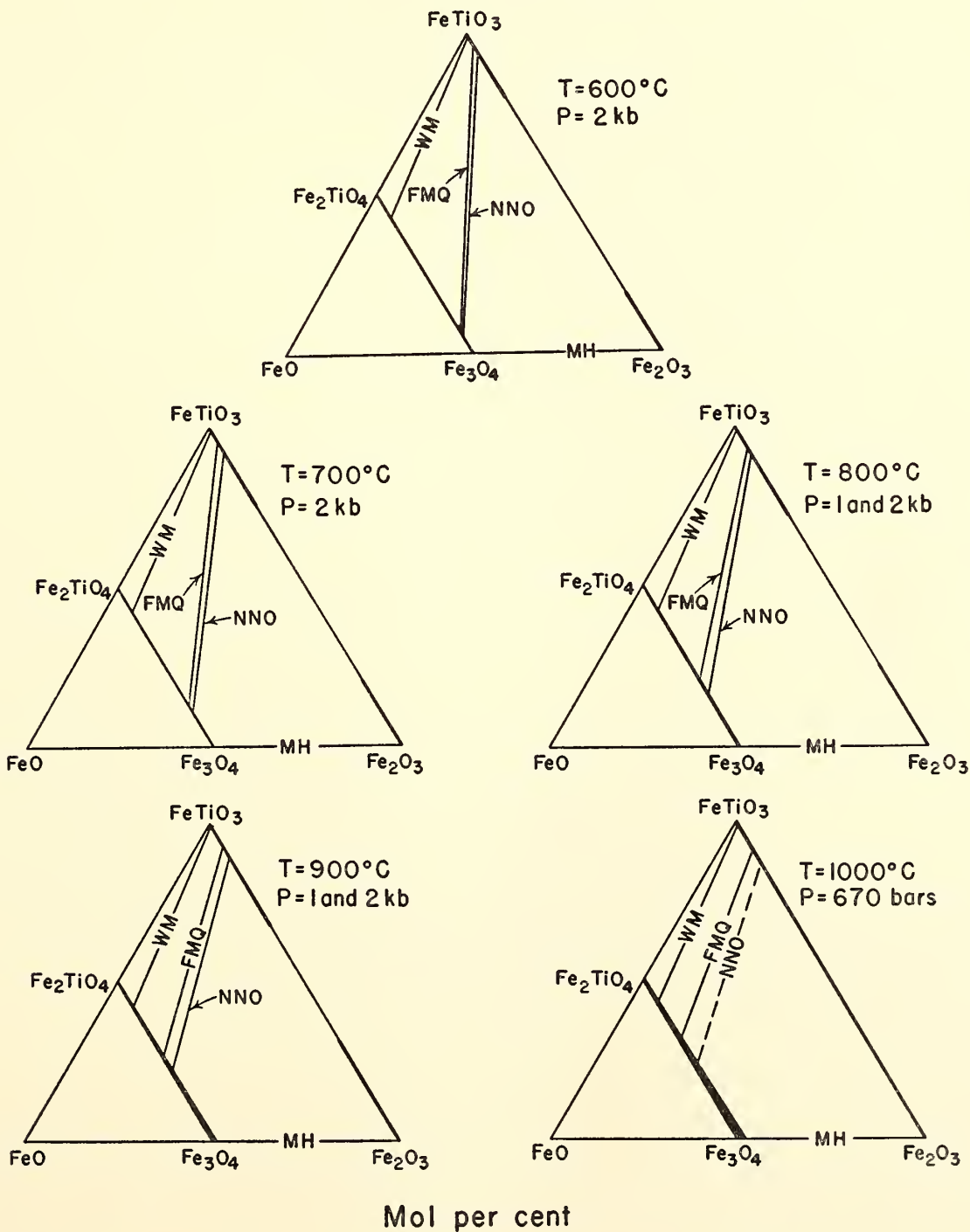


Fig. 4. Isothermal sections showing tie lines between coexisting Mt-Usp_{ss} and hematite-ilmenite_{ss} for several buffers.

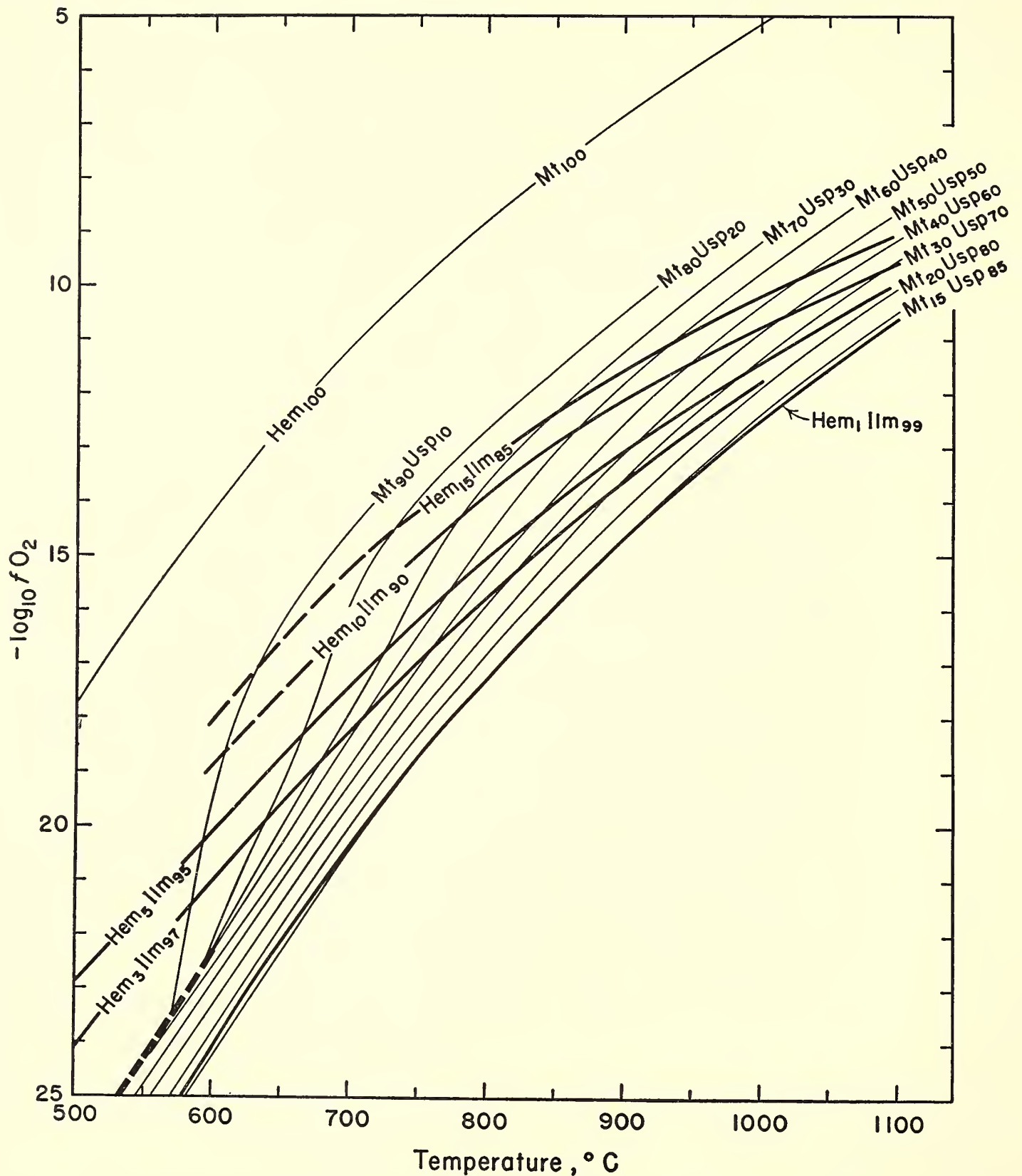


Fig. 5. Projection onto f_{O_2} - T plane of conjugate surfaces in f_{O_2} - T - X space. Projection is parallel to two composition axes, Mt-Usp_{ss} and the coexisting hematite-ilmenite_{ss}, so that intersecting contours are the projection of tie lines connecting conjugate pairs. The T - X relations of the Mt-Usp solvus are from Vincent, Wright, Chevallier, and Mathieu (1957). Available data show that the solvus must lie between the WM and FMQ buffer curves, but its exact f_{O_2} relations are unknown.

menite-rich α phases for the NNO and FMQ buffers.

The experimental data summarized in figure 4 describe a surface in f_{O_2} - T - X space for the magnetite-ulvöspinel_{ss} and another such surface for the coexisting α

phases. These two surfaces, expressed by appropriate contours, are projected onto the f_{O_2} - T plane in figure 5. The contours are effectively univariant curves, and the intersection of any two shows the temperature and f_{O_2} at which Fe-Ti oxide

pairs of the indicated compositions can coexist. For example, the coexisting pair $Mt_{70}Usp_{30}$ and $Hem_{10}Ilm_{90}$ must have formed at approximately 780°C and $10^{-14.3}$ atm f_{O_2} . The contours are based on relatively few fixed points, and they intersect at small angles; hence there is a large uncertainty in the position of any given intersection of contours. However, in the vicinity of the NNO and FMQ buffer curves (fig. 1) an intersection is accurate to $\pm 30^{\circ}\text{C}$ and within one order of magnitude f_{O_2} . For the WM and $\text{MnO-Mn}_3\text{O}_4$ buffers, and of course for the magnetite-hematite pair, the f_{O_2} - T contours are so nearly parallel that the situation is effectively univariant. Additional information, such as that provided by coexisting annite (Eugster and Wones, 1962), is therefore required to fix the f_{O_2} and T .

Application of data obtained for pure synthetic phases in the system $\text{FeO-Fe}_2\text{O}_3\text{-TiO}_2$ to natural minerals involves several assumptions. First is the assumption that the Fe-Ti oxide pairs formed in equilibrium and did so during the crystallization of the rock containing them. Textural evidence may help validate this assumption. For example, Fe-Ti oxides occur as phenocrysts in some lavas and thus may reflect pre-eruption equilibrium conditions. An additional problem is the possible escape of TiO_2 as ilmenite from titaniferous magnetite at sub-crystallization temperatures. For example, Vincent and Phillips (1954) and Wright (1961) suggested that granular aggregates of magnetite and ilmenite in the Skaergaard intrusion formed from a primary titaniferous magnetite. This so-called "granule exsolution" produces a distinctive texture and thus is recognizable microscopically.

A second assumption involves the effects of impurities in natural Fe-Ti oxides, some of which contain appreciable amounts of magnesium, manganese, calcium, chromium, aluminum, and vanadium. The quantitative effects of these impurities on the equilibria reported here

are unknown, but rough estimates can be made on the basis of data from other systems. MgO , MnO ,² and CaO replace FeO chemically if not structurally and, by diluting FeO , almost certainly extend the f_{O_2} - T stability range of the Fe-Ti oxides containing them. The sesquioxides Cr_2O_3 , Al_2O_3 , and V_2O_3 occur in solid solution with magnetite as the spinels FeCr_2O_4 , FeAl_2O_4 , and FeV_2O_4 . The effect of dissolved FeAl_2O_4 and FeCr_2O_4 on the f_{O_2} stability of magnetite is grossly similar to that of ulvöspinel (Turnock and Eugster, 1962; Richards and White, 1954); a similar effect is probable for FeV_2O_4 . Thus the presence of these spinels in the analyzed titaniferous magnetite can be compensated for by recalculation with Fe_2TiO_4 as "ulvöspinel." Cr_2O_3 , Al_2O_3 , and V_2O_3 are generally minor in ilmenite and very likely can be ignored. The main effect of dissolved impurities in the Fe-Ti oxides is probably an increase in the uncertainties of the f_{O_2} and T determined for each analyzed pair.

To apply the experimental data to analyzed Fe-Ti oxides, we must express the analyses in terms of essentially binary magnetite-ulvöspinel and hematite-ilmenite solid solutions. However, many analyses do not recalculate in these terms if conventional rules are followed. For example, many titaniferous magnetites carry appreciable normative and modal ilmenite. The experimental data presented in *Year Book 61* (p. 104) show that this ilmenite probably formed by subsolidus oxidation, thus justifying the recalculation of all TiO_2 as Fe_2TiO_4 . Similarly, all TiO_2 in the α phase is recalculated as FeTiO_3 ; normative TiO_2 can form in solid solution with an α phase only, if at all, from a bulk composition lying between the α phase and TiO_2 , and only α phases formed in equilibrium with

² Although manganese can exist in several valences, MnO has a much wider f_{O_2} - T stability range than FeO and is the stable manganese oxide over the f_{O_2} - T range considered here (Hahn and Muan, 1960).

magnetite-ulvöspinel_{ss} are under consideration. Any excess TiO_2 is therefore considered to be due to oxidation of FeTiO_3 . (Such an oxidation is readily performed in the laboratory; a $\text{Hem}_{50}\text{Ilm}_{50}$ charge held at 600°C and the f_{O_2} of the MH buffer oxidizes to about $\text{Hem}_{70}\text{Ilm}_{30}$ + "exsolved" rutile.) The recalculation procedures proposed here are solely for the purpose of applying the experimental data to natural Fe-Ti oxides. For other purposes, such as interpreting magnetic properties, conventional norms may be more useful.

ORIGIN OF IGNEOUS ROCKS

Partial Melting of the Mantle

M. J. O'Hara and H. S. Yoder, Jr.

Volcanic activity, accompanied by the extrusion of tholeiitic and alkaline basaltic liquids, is associated with deep-focus earthquakes. If these earthquakes, having foci at depths of 60 km or greater, are the scene of magma generation, the process of melting involves relationships between liquid and rocks having eclogite facies mineralogy. Yoder and Tilley (1962) have studied the melting of eclogite at high pressures; they concluded that eclogite is itself a derivative of some other rock type, such as garnet peridotite. Furthermore, they outlined three hypotheses involving equilibria between omphacite, garnet, and liquid, any one of which could lead to a variation in the liquid composition such that these closely related liquids might be committed to one or another of the divergent differentiation trends characteristic of the tholeiitic and alkaline basalts at low pressure.

In a study of garnet peridotites O'Hara and Mercy (1963) concluded that those occurring as nodules in kimberlite pipes may be samples of the upper mantle. They rejected garnet peridotites such as are found in Norway and Switzerland, the olivine nodules that occur in alkali basalts, and some other types of

peridotite (e.g., alpine-type peridotites) as samples of the undifferentiated and unaltered upper mantle. They also concluded that the eclogite nodules that occur in kimberlite could be the partial fusion product of the accompanying garnet peridotite, melted and crystallized at great depth.

Olivine and orthopyroxene are the most abundant constituents of the garnet peridotite nodules in kimberlite, yet neither of these minerals is present in the majority of the eclogites from kimberlite pipes. How can two of the crystalline phases (which must be in equilibrium with the liquid that is formed by partial fusion of garnet peridotite) be disposed of so that they do not subsequently precipitate from the isolated liquid when it cools? Another important question is how silica-saturated tholeiitic liquids can be generated by the partial melting of a garnet peridotite.

A knowledge of the temperatures at which bimineralec eclogite and garnet peridotite melt at high pressures and of the crystal-liquid relationships that exist at high pressures is desirable for further consideration of the origin of basaltic liquids. It is equally important to understand how a liquid may differentiate at high pressures if it crystallizes out of effective contact with the minerals of the garnet peridotite.

The solutions to the problems outlined above have been sought in four ways: (1) theoretical study of natural eclogites aimed at choosing eclogites that might represent the partial fusion product of garnet peridotite at high pressures and at defining the crystal-liquid relationships that would have to exist if such rocks are to be derived from garnet peridotite; (2) phase-equilibria studies of mixtures of the separated, analyzed minerals from eclogite and garnet peridotite; (3) phase-equilibria studies of natural eclogites (e.g., Yoder and Tilley, 1962); (4) phase-equilibria studies of a synthetic system, the join diopside-pyroxene, which closely approaches the chemical and mineralog-

ical composition of bimineralec eclogite (see p. 116).

Eclogite occurrences. Not all eclogites are representative of possible partial fusion products formed at great depth. Five types of eclogite, distinguished by their environment, bulk compositions, mineral compositions, or mineral assemblages, can be recognized: (1) eclogite layers and lenses in dunite or peridotite bodies of orogenic zones, e.g. Norway, Switzerland; (2) eclogite nodules in alkali basalt tuff, e.g. Salt Lake Crater, Oahu, Hawaii; (3) eclogite nodules in kimberlite pipes, e.g. South Africa, Siberia; (4) eclogite bodies among gneisses and schists of orogenic zones, e.g. Scotland, Norway, and Swiss and Austrian Alps; (5) eclogite bodies associated with low-grade metasediments and glaucophane schists, e.g. California.

Eclogites from the Norwegian dunites (garnet-websterites and garnet-clinopyroxene rocks of O'Hara and Mercy, 1963) have chemical compositions that do not correspond to any extrusive basaltic *liquid* but that might be matched by some accumulative rocks formed in *layered* gabbro intrusions. The same is true of an analyzed representative of the eclogite nodules in alkali-basalt tuff (Yoder and Tilley, 1962), which has a very low $\text{Fe}/(\text{Fe} + \text{Mg})$ ratio in the normative silicates. Nevertheless, the material from Salt Lake Crater is of great interest because it may have been quenched from high pressure and high temperature and because it may be genetically related to the alkali basalts among which it occurs.

Eclogites of the three remaining types (nodules in kimberlite, bodies in gneiss, bodies in glaucophane schists) have bulk compositions that can be matched among extrusive basalts (although eclogites in glaucophane schists appear to be relatively rich in iron oxides and soda, and eclogite nodules in kimberlite *as a group* are relatively rich in MgO and poor in SiO_2).

The environment of eclogite bodies in

gneiss or glaucophane schist (types 4 and 5), when viewed in the light of experimental data (Yoder and Tilley, 1962, fig. 43), is such that, even when allowance is made for considerable tectonic transport, these eclogites have probably formed by the metamorphic recrystallization of deep-seated gabbros, or crustal basic igneous rocks carried down in orogenic movements. Eclogites of these two groups have not been considered as possible representatives of the partial fusion product at great depth because of the probability that the liquids from which they are derived have undergone differentiation under conditions in which eclogite facies minerals are *not* stable in the presence of liquid.

The type of eclogite occurring as nodules in kimberlite may be representative of the partial fusion product formed at great depth for reasons discussed by O'Hara and Mercy (1963). It is unlikely that these rocks have formed from liquids that had undergone differentiation at low pressures where eclogite was not stable at the beginning of melting. In the following discussion the eclogites from kimberlite pipes will be considered as representative of the partial fusion product at great depth. Unfortunately, specimens of this type of eclogite tend to be extensively altered and metasomatized, and they are frequently rather small samples of very coarse-grained rocks. Before describing the origin and variation of the bulk compositions of eclogite nodules in kimberlite, two points having a bearing on the interpretation of the data will be discussed.

CIPW norms of eclogites. Because of the dominant role played by garnet-clinopyroxene assemblages in the eclogite facies it is important to investigate the range of chemical compositions that can be accommodated in this mineral pair. This may be achieved by consideration of the CIPW norms of coexisting garnet-clinopyroxene pairs. The CIPW norms of mixtures at intervals of 10 per cent by

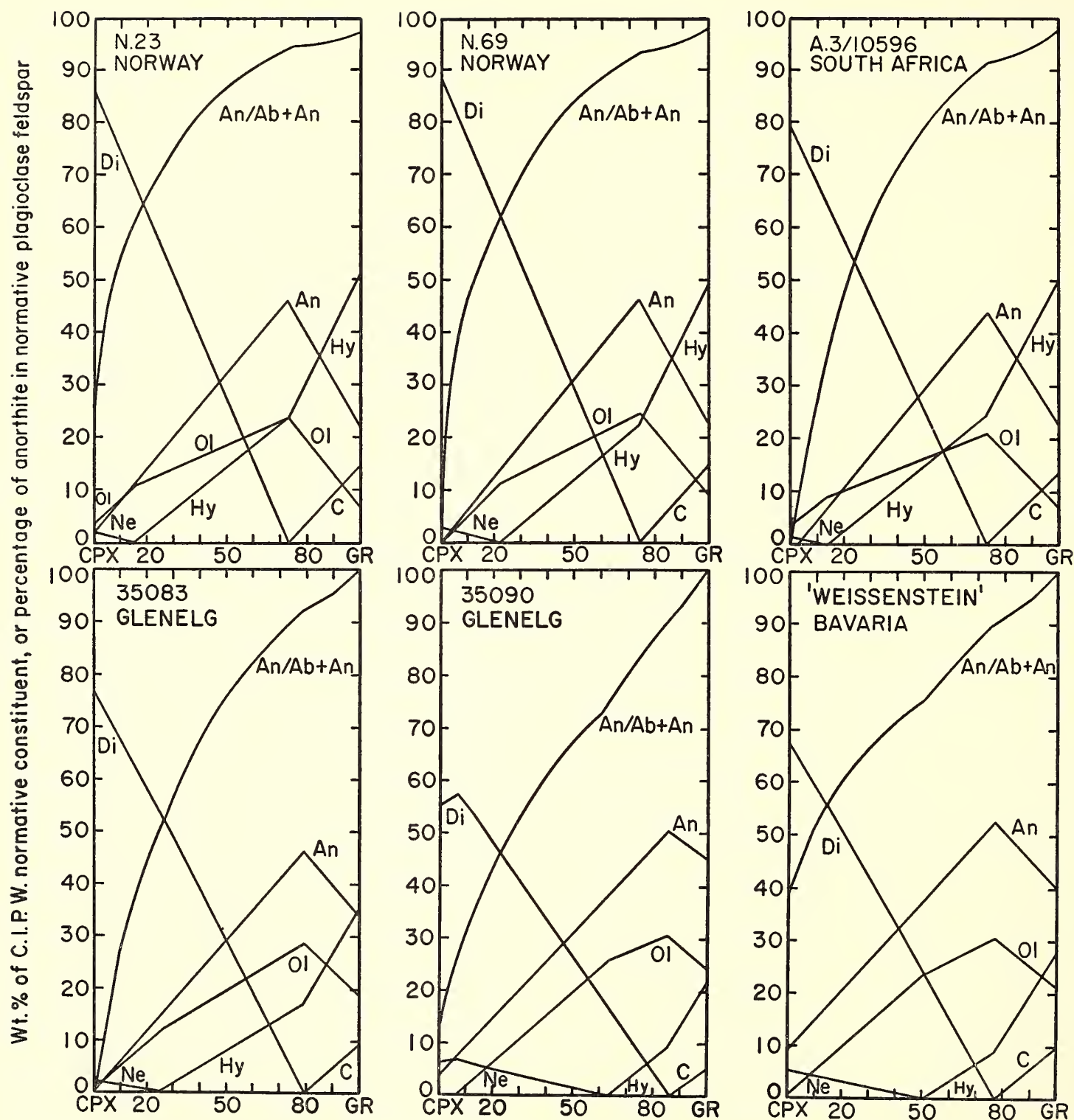


Fig. 6. Graphical representation of the variation in weight per cent of CIPW normative constituents with composition (weight per cent) in some garnet-clinopyroxene pairs from eclogite facies rocks. Normative albite is not plotted directly. The ratio of anorthite to anorthite + albite has in the normative feldspar been expressed as a percentage and plotted on the same scale as the normative amounts of the other constituents. The CIPW norm convention is followed in labeling constituents. Samples N.23, N.69, and A.3/10596 are from orthopyroxene-bearing assemblages (last two also contain olivine); data from O'Hara and Mercy (1963). 35083, 35090, and "Weissenstein" samples are quartz-bearing eclogites; "Weissenstein" also contains kyanite; data from Yoder and Tilley (1962).

weight have been calculated for six analyzed coexisting pairs; the results are shown in figure 6. The data represent material from Norwegian dunite, from kimberlite, and from gneiss, all of which are thought to be "low" or intermediate-

temperature eclogite facies assemblages. Three of the pairs are from olivine- and orthopyroxene-bearing assemblages, and one is from a kyanite-bearing assemblage. All show similar features; tholeiitic characteristics are associated with garnet-

rich compositions, whereas alkaline characteristics are associated with clinopyroxene-rich compositions, as was emphasized by Yoder and Tilley (1962). However, normative olivine culminates in the intermediate mixtures, which have compositions resembling olivine-rich basalt and picrite, yet which contain a very calcic normative feldspar. If composed of garnet-pyroxene pairs like those that coexist also with olivine and orthopyroxene, biminerally eclogites should contain olivine and hypersthene in the CIPW norm when more than 30 per cent by weight of garnet is present, or 60 per cent garnet in garnet-pyroxene pairs like those from kyanite-eclogite, or the Glenelg sample 35090.

The addition of as little as 6 per cent modal quartz to any of the biminerally eclogite compositions of figure 6 is sufficient to suppress the appearance of nepheline in the norm. The presence of kyanite, hypersthene, or rutile in the mode of natural eclogites likewise tends to suppress nepheline in the norm.

The results expressed in figure 6 indicate the difficulty likely to be encountered in sampling natural eclogites (which are often mineralogically heterogeneous) if the investigator is interested in determining whether the bulk composition is nepheline- or hypersthene-normative.

Eclogite as the partial fusion product of garnet peridotite. If the biminerally eclogites and less common kyanite-eclogites that occur in kimberlites are derived from the partial fusion product of garnet peridotite, they may be crystal accumulates from that liquid. Their bulk compositions would not, then, give direct information about the composition of the liquid from which they form. Unless that liquid has a very special relationship to the composition of garnet-clinopyroxene assemblages, the removal of eclogite accumulates will cause the residual liquid to trend toward compositions in which garnet and clinopyroxene are joined either by silica-rich or by silica-poor

phases. Quartz and coesite are not reported from eclogite inclusions in kimberlite, but spinel and corundum are known from a few eclogite inclusions (Williams, 1932, pls. 118 and 131). The liquid formed by partial fusion of garnet peridotite should, therefore, be slightly silica poor with respect to the garnet-clinopyroxene assemblages; i.e., it is picritic in composition.

If the liquid that forms by the partial fusion of garnet peridotite is to differentiate by separation of garnet and clinopyroxene *only* when it is isolated from the four-phase peridotite assemblage, both orthopyroxene and olivine must have a reaction relationship to this liquid. At the beginning of melting the relationship would then be clinopyroxene + garnet + spinel \rightleftharpoons olivine + orthopyroxene + liquid, i.e. if the liquid that forms has a composition lying within or beyond the subsolidus plane spinel + clinopyroxene_{ss} + garnet_{ss} (see fig. 7).

If these requirements are not met by the natural circumstances, the differences in geochemistry and numerical abundance between garnetiferous peridotite and eclogite nodules in kimberlite cannot at present be accounted for without postulating a separate creation of each rock type (cf. O'Hara and Mercy, 1963).

It is apparent from figure 6 that the liquid postulated to form by partial fusion of garnet peridotite may contain *either* hypersthene or nepheline in the CIPW norm. If it contains hypersthene in the norm, subsequent fractionation of olivine at low pressure could yield residual liquids that are silica-saturated and tholeiitic. Any fractionation at high pressure, such as the removal of garnet or both garnet and clinopyroxene, would cause the original hypersthene-normative liquid to become nepheline-normative and markedly undersaturated in silica.

The K₂O/Na₂O ratio of biminerally eclogite and kyanite-eclogite is very low. K₂O does not seem to enter the clinopyroxene structure, and it enters neither kyanite nor garnet. Quite large amounts

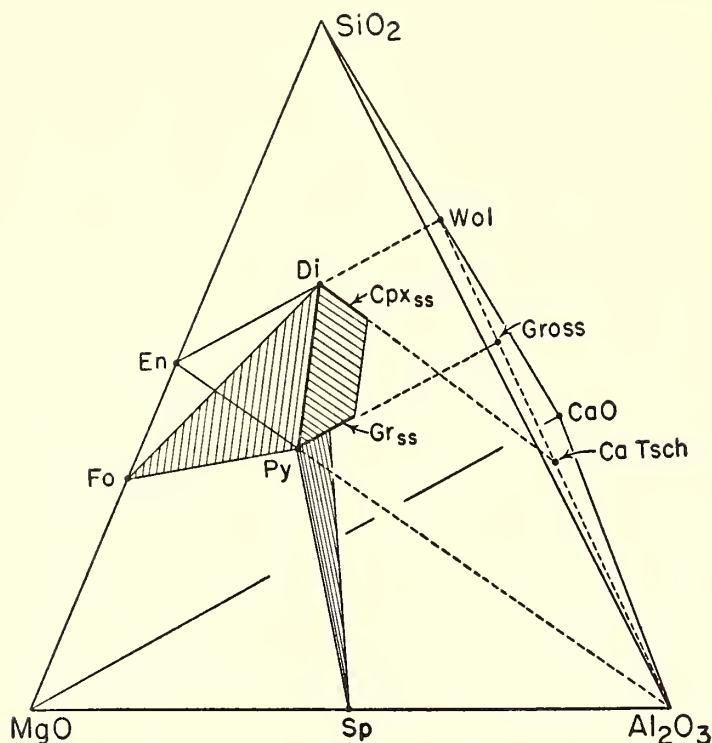


Fig. 7. Perspective view of the tetrahedron $\text{CaO-MgO-Al}_2\text{O}_3\text{-SiO}_2$, showing the composition plane MgSiO_3 (enstatite, En)- CaSiO_3 (wollastonite, Wol)- Al_2O_3 . The diopside (Di)-pyrope (Py) join lies in this composition plane, as do the joins diopside-Ca Tschermak's molecule (CaTsch) and pyrope-grossularite (Gross). The range of clinopyroxene solid solutions (Cpx_{ss}) that coexist with garnet solid solutions (Gr_{ss}) at high pressures is shown diagrammatically. The plane of compositions crystallizing to $\text{Cpx}_{ss} + \text{Gr}_{ss}$ is shaded.

The composition planes forsterite (Fo)-diopside-pyrope and diopside-pyrope-spinel (Sp) are also shown (shaded).

The liquid that coexists with forsterite, enstatite, pyrope, and diopside at high pressures is believed to lie to the *MgO-poor* side of a particular plane "diopside"-pyrope-spinel and to the SiO_2 -poor side of the plane of $\text{Cpx}_{ss} + \text{Gr}_{ss}$.

Note: For simplicity, it has been assumed that the pure phases pyrope, diopside, enstatite, and forsterite coexist at the beginning of melting. For "diopside," read, "the composition of clinopyroxene solid solution that coexists at the beginning of melting with olivine solid solution, orthopyroxene solid solution, and garnet solid solution"; the term "pyrope" should be similarly qualified.

of Na_2O may enter the clinopyroxene, however. Unless the $\text{K}_2\text{O}/\text{Na}_2\text{O}$ ratio in the original liquid is exceptionally low, the fractionation of eclogite from that liquid will cause an increase of $\text{K}_2\text{O}/\text{Na}_2\text{O}$ ratio in the residual liquids. This may be the mechanism whereby highly potassic,

silica-poor mafic lavas are generated (cf. Holmes and Harwood, 1932). The association of such rock types with kimberlite occurrences in Africa, and the highly potassic, silica-poor mafic character of the groundmass of kimberlite itself, may be indicative of fractionation of eclogite at high pressures. The close association of garnet peridotite (a possible upper-mantle material) and eclogite (a possible crystal accumulate from the partial melting product of garnet peridotite) with kimberlite (a possible residual fluid) can be regarded as evidence supporting the hypothesis presented above.

Previous hypotheses. In previous considerations of the partial melting of the mantle to yield basaltic magma, it was noted that, in the quaternary system $\text{CaO-MgO-Al}_2\text{O}_3\text{-SiO}_2$, forsterite, enstatite, diopside, and pyrope all melt congruently at pressures greater than 36 kb (Boyd and England, *Year Books* 60, pp. 113-125, and 61, pp. 107-112). If the initial liquid that coexists with all four of these crystalline phases lies within the composition tetrahedron that they define at equilibrium, the subsystem is quaternary. At the pressure of its formation the initial liquid at this isobaric invariant point can only precipitate the four crystalline phases named above. It would have no potential course of fractionation and differentiation inside or outside the subsystem so defined. Not only would the liquid be silica-under-saturated in the CIPW norm (diopside and enstatite appear as silica-saturated phases, but forsterite and pyrope-diopside mixtures both yield olivine in the norm), but it would be impossible to obtain bimineralic eclogite as a product of the crystallization of the liquid at high pressure.

Impressed by the evidence, which suggests that silica-saturated tholeiitic magma is a primary magma, and desiring some method by which it might be obtained directly by the partial fusion of natural garnet peridotites, Boyd and

England (*Year Book 61*, p. 109) postulate the existence of the melting relationship $\text{garnet} \rightleftharpoons \text{spinel} + \text{liquid}$ in the melting of natural garnet peridotite. This concept is based on their observation of an incongruent melting relationship, $\text{pyrope} \rightleftharpoons \text{spinel} + \text{liquid}$, at pressures less than 36 kb in synthetic mixtures having the pyrope composition.

A similar relationship was suggested for petrological reasons connected with the origin of peridotite nodules in basalts (O'Hara and Mercy, 1963), although spinel was not expected to appear as a crystalline phase but to remain occult in olivine and garnet.

If the relationships suggested by these authors are to be geologically significant, and yield a liquid that is silica-saturated in the CIPW norm, it must be possible to express the change at the beginning of melting as $\text{orthopyroxene} + \text{clinopyroxene} + \text{garnet} \rightleftharpoons \text{olivine} + \text{spinel} + \text{liquid}$, where the liquid is silica-saturated (in the CIPW norm), olivine and spinel crystallizing in excess amounts.

In the synthetic four-component system $\text{CaO-MgO-Al}_2\text{O}_3\text{-SiO}_2$ this relationship defines a unique point (quaternary invariant point). (The relationship is permissible over a range of pressure in the natural system because of the several additional components, e.g., FeO , Fe_2O_3 , Na_2O , and Cr_2O_3 .) Both olivine and spinel must have a reaction relationship to the liquid formed at the beginning of melting, because the composition "plane" of garnet and the two pyroxenes separates the supposed liquid composition from both forsterite and spinel. However, the existence of such relationships does not by itself satisfy all the requirements of the hypotheses of Boyd and England and O'Hara and Mercy. Not only must the liquid composition be silica rich with respect to the garnet-clinopyroxene-orthopyroxene assemblage; it must also be silica rich with respect to the hypersthene-diopside-plagioclase assemblage calculated in the CIPW norm.

Although the presence of a reaction

relationship between olivine and the liquid at the beginning of melting is essential in the hypotheses just discussed, the presence of spinel in the phase assemblage at the beginning of melting is not. The liquid, therefore, at the quaternary isobaric invariant point $\text{forsterite} + \text{enstatite} + \text{diopside} + \text{garnet} + \text{liquid}$ in the system $\text{CaO-MgO-Al}_2\text{O}_3\text{-SiO}_2$ might, on these grounds, be silica-saturated with respect to the enstatite-diopside-anorthite plane. The hypothetical relationships just discussed provide a means of obtaining silica-saturated tholeiitic liquids by the partial melting of garnet peridotite; they do *not* provide a method of obtaining biminerally eclogite, and it remains to be shown that the required relationships actually exist at some geologically reasonable pressure.

Melting of Garnet Peridotite at 30 Kilobars

M. J. O'Hara

The upper mantle of the earth may be composed of a peridotite similar in bulk composition and mineralogy to the garnet-lherzolite nodules that occur as inclusions in kimberlite pipes. The melting behavior of such a peridotite has direct application to the problems of basalt formation and to the study of various eclogite and peridotite assemblages.

In this study the samples used were reconstituted from the separated and analyzed olivine, orthopyroxene, clinopyroxene, and garnet of a garnet-lherzolite nodule from the Wesselton Mine, South Africa (specimen A.3/10596, O'Hara and Mercy, 1963; Wesselton no. 3, Holmes, 1936). This method has the advantage that alteration products present along grain boundaries in the original specimen are excluded from the samples investigated in the experiments, and it enables data to be obtained for a wide range of related bulk compositions. Samples made up from the separated minerals have modal compositions corresponding to the mineral assemblages of

a range of rock types that occur as nodules in kimberlite. The minerals used to make up these samples are closely comparable to the olivines, pyroxenes, and garnets of other peridotite nodules in kimberlite; hence the results obtained on the mixture of minerals from the specimen A.3 should be applicable to other specimens from kimberlite having the appropriate mineral assemblages.

Samples were prepared by mixing the weighed minerals and grinding them under acetone in an agate mortar. The appropriate petrographic names to express the mineral assemblages in the samples so produced are garnet-lherzolite, garnet-harzburgite, garnet-wehrlite, garnet-websterite, websterite, lherzolite, and a range of eclogites (which it must be noted are composed of garnet and chrome diopside belonging to the limiting pair that coexist with olivine and orthopyroxene). None of the samples has a bulk composition corresponding to that of the original specimen, A.3, and the proportion of garnet in many of the assemblages is

much higher than is found in nodules from kimberlite that have similar petrographic names. This was arranged deliberately for ease in observation and to ensure that garnet remained as a separate phase in the assemblage until melting began. Because of the high solubility of garnet molecule in the pyroxenes at high temperature and pressure (see below) the petrographic names given to the samples do not necessarily apply at temperatures near the beginning of melting.

The experiments were performed at 30 kb in the dry system, using a solid media high-pressure apparatus similar to that described by Boyd and England (1963). The charge was always contained in an open platinum capsule. There are uncertainties about the absolute pressure and temperature of the runs (Boyd and England, 1963). Oxidation or reduction of the iron oxides, or loss of iron to the platinum, is not likely to have a large effect on the bulk composition, because of the low iron content of the samples and the short runs. In spite of these limita-

TABLE 1. Selected Run Results on Garnet Peridotite and Synthetic Materials

Cpx, clinopyroxene; Opx, orthopyroxene; Ol, olivine; Gr, garnet; Sp, spinel; Fo, forsterite; En, enstatite; q, quenching products.

Composition	T, °C	Time	Products
10596, Cpx ₂₅ Opx ₂₅ Gr ₅₀	1550	½ hr	Cpx,* Opx,* Gr
	1575	½ hr	Opx,*† Gr, Sp, ?‡Cpx, q
10596, Cpx ₂₀ Opx ₂₀ Ol ₂₀ Gr ₄₀	1450	1 hr	Cpx,* Opx,* Ol, Gr
	1475	1 hr	Opx,*† Ol, Gr, Sp, ?‡Cpx, q
	1550	½ hr	Opx,† Ol, Gr, Sp, ?‡Cpx, q
	1575	½ hr	Opx,† Ol, Sp, trace Gr, ?‡Cpx, q
10596, Cpx ₂₅ Ol ₂₅ Gr ₅₀	1400	1 hr	Cpx,* Ol, Gr
	1425	1 hr	Opx,† Ol, Gr, Sp, ?‡Cpx, q
	1550	½ hr	Opx,† Ol, Gr, Sp, ?‡Cpx, q
	1575	½ hr	Opx,† Ol, trace Gr, Sp, ?‡Cpx, q
Synthetic diopside ₂₅ forsterite ₂₅ pyrope ₅₀	1500	1 hr	Fo, Gr, Cpx, trace En
	1600	20 min	Fo, En,† ?‡Cpx, q, glass
	1650	20 min	Fo, (En), q, glass
	1700	10 min	Fo, q, glass

* Pyroxene known to have recrystallized from peak shifts in X-ray pattern.

† Orthopyroxene appears as large rectangular prisms with rims of spiky or fine granular clinopyroxene.

‡ Owing to the granular texture of the quench product (chiefly clinopyroxene) the presence or absence of primary clinopyroxene cannot be positively established.

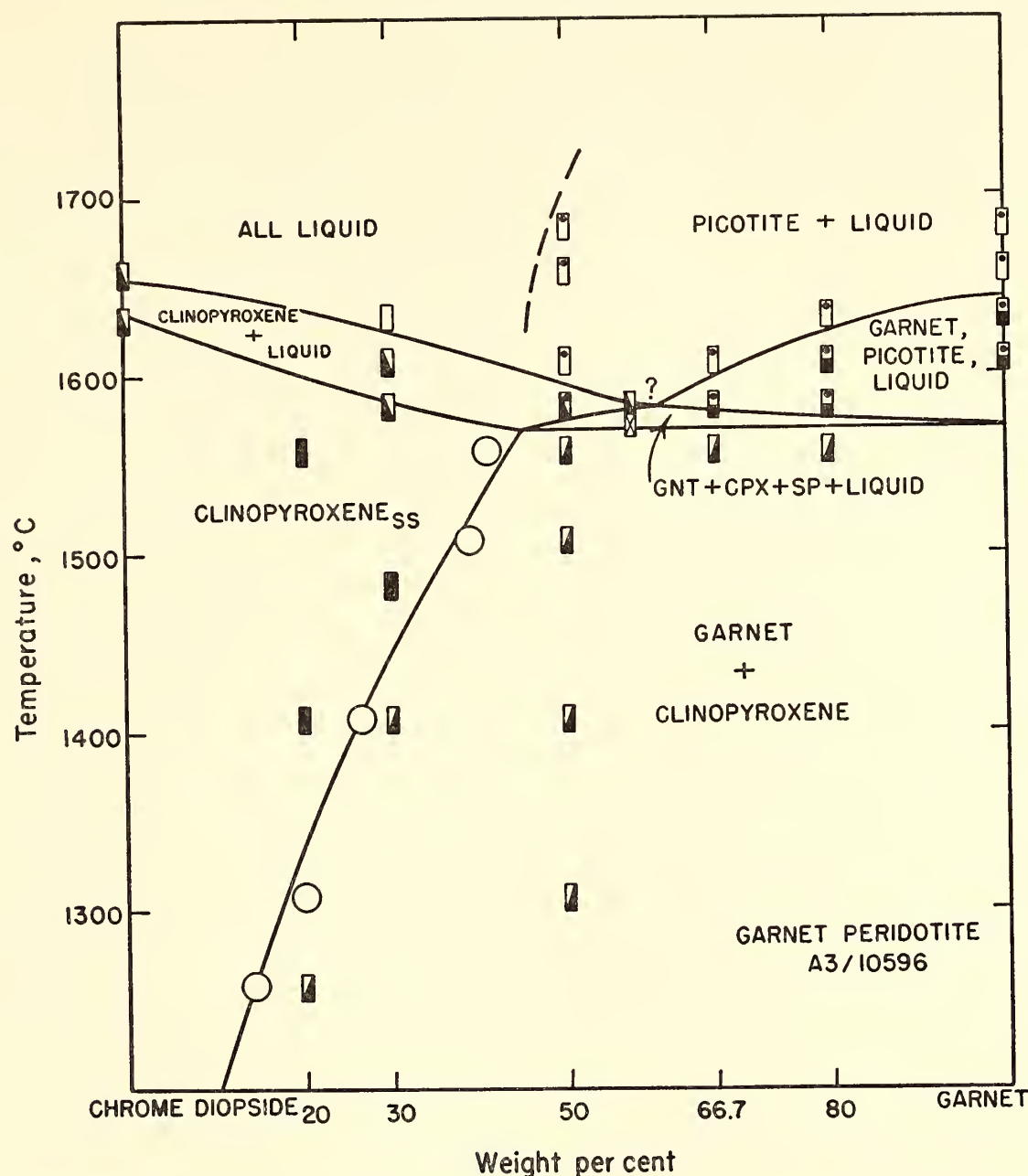


Fig. 8. Interpretation of results of runs at 30 kb on mixtures of garnet and chrome diopside from the specimen A.3/10596. Open circles give points on solvus boundary determined by X-ray measurements assuming binary behavior. The existence of three small fields of Opx + Sp + liquid, Opx + Cpx + Sp + liquid, and Opx + Gr + Sp + liquid in this join is possible in view of the observation that the mixture of chrome diopside₂₅ enstatite₂₅ garnet₅₀ begins to melt at or near the same temperature as the clinopyroxene-garnet mixtures (table 1). The extensive solid solution of garnet molecule in the clinopyroxene at temperatures of 1250° to 1600°C indicates that the minerals separated from the natural rock would be in equilibrium at lower temperatures than 1200°C at this pressure. A similar argument may be applied to figures 9 and 11.

tions some significant results have been obtained, and the conclusions based on them are unlikely to be greatly changed by experiments under controlled conditions. The results are expressed in figures 8 and 9 and in table 1.

Mixtures of chrome diopside, garnet, and olivine melt to yield orthopyroxene plus liquid. This is one of the essential relationships if eclogite is to be the precipitate from this liquid as discussed above. The analogous composition in the

synthetic system $\text{CaO-MgO-Al}_2\text{O}_3\text{-SiO}_2$ containing diopside 25, pyrope 50, and forsterite 25 per cent, which crystallizes at 30 kb and 1500°C to forsterite, garnet, and clinopyroxene with a trace of orthopyroxene, melts to forsterite, abundant enstatite, and liquid at 1600°C. This relationship, therefore, is not due solely to the presence of spinel in the liquid or to oxidation of FeO in the charge.

X-ray measurements of the ortho-

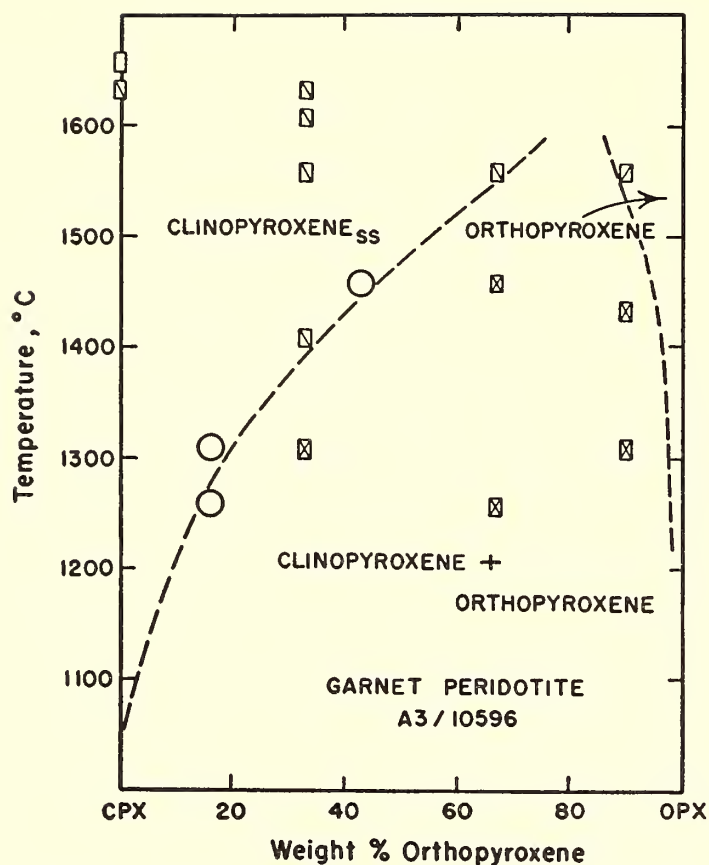


Fig. 9. Results of subsolidus experiments at 30 kb on mixtures of chrome diopside and enstatite from the specimen A.3/10596. Open circles represent points on the solvus boundary obtained from X-ray measurements, assuming true binary behavior.

pyroxene produced in the melting of the synthetic mixture diopside 25, forsterite 25, pyrope 50 per cent indicate that it contains about 10 per cent Al_2O_3 (Boyd and England, *Year Book* 59, pp. 49–52).

Liquid forms by the partial fusion of the olivine-bearing assemblages at temperatures 100° to 150°C lower than the beginning of melting of mixtures in the garnet-two pyroxenes composition plane. This composition “plane” (analogous to part of the plane $\text{CaSiO}_3\text{--MgSiO}_3\text{--Al}_2\text{O}_3$) is a thermal barrier separating quartz-bearing and olivine-bearing eclogites at 30 kb. The liquid that forms by the partial fusion of the olivine-two pyroxenes-garnet assemblage must be silica poor with respect to the garnet-pyroxene assemblages. Bearing in mind the probable ratio of “garnet” to “chrome diopside” in the liquid composition (cf. fig. 6 above), and the presence of a small amount of spinel, the

CIPW norm of this liquid is likely to contain both hypersthene and olivine.

The assemblage olivine-two pyroxenes-garnet is stable up to the beginning of melting in suitable bulk compositions. Garnet molecule dissolves very readily in the clinopyroxene and orthopyroxene at high temperatures, and it is likely that many natural garnet peridotites (which contain only a small amount of garnet relative to pyroxene) would be represented at the beginning of melting by olivine-spinel-two pyroxene assemblages, these pyroxenes being rich in Al_2O_3 , Fe_2O_3 , and Cr_2O_3 ; i.e., the garnet will dissolve in the pyroxenes. The minerals of the original garnet-peridotite sample clearly represent an assemblage stable at temperatures about 400°C below the beginning of melting (see figs. 8 and 9). The coexisting pyroxenes reported from the eclogite nodules in alkali basalt tuff in Hawaii (Yoder and Tilley, 1962), rich in Al_2O_3 and Fe_2O_3 , represent an eclogite facies assemblage stable at high temperatures. Oriented intergrowths such as that of enstatite and garnet figured by Williams (1932, pl. 102) or that of orthopyroxene and chrome diopside described by O'Hara and Mercy (1963, table 2, no. 10598) in nodules from kimberlite indicate that, although some of these rocks have been at high temperatures and high pressures, the high-temperature minerals subsequently recrystallized within the eclogite mineral facies.

The very extensive solid solution of enstatite molecule in the clinopyroxene that is observed between the alumina-poor pyroxenes of the peridotite (fig. 9) does not persist in the presence of excess garnet. The mixture containing 25 per cent each of chrome diopside and orthopyroxene plus 50 per cent of garnet retains two pyroxene phases until the beginning of melting. The coexisting pyroxenes in this mixture appear from their X-ray patterns to have taken up substantial amounts of Al_2O_3 . There is also a moderate amount of “diopside”

molecule in solid solution in the orthopyroxene at high temperature, but it is not clear whether this feature persists in the presence of garnet.

The small temperature interval through which garnet and clinopyroxene coexist with liquid in mixtures on the chrome diopside-garnet join, coupled with the uniform temperature of beginning of melting of the two-phase assemblage, suggests not only that relationships in the subsolidus are similar to those in a binary system but also that the limiting garnet-clinopyroxene tie line at high temperatures is very nearly coincident with that at low temperatures, although the clinopyroxene contains substantial amounts of garnet molecule in solid solution at the higher temperature (see fig. 10).

Melting of Bimineralic Eclogite at 30 Kilobars
M. J. O'Hara

Eclogites from kimberlite are likely to contain garnets richer in almandine and grossular molecules, and clinopyroxenes richer in jadeite and Ca-Tschermak's molecules, than the corresponding phases from the garnet peridotite A.3/10596. Analyses of the coexisting garnet and clinopyroxene from a bimineralic eclogite nodule (37079) in kimberlite, provided by Dr. E. L. P. Mercy, are given in table 2. This mineral pair belongs to an eclogite that is apparently rich in FeO relative to MgO in comparison with the majority of eclogites from kimberlite. The tie line for the coexisting pair, when plotted in an A-C-Fm diagram, lies beyond the position of the limiting tie line from a kyanite-bearing assemblage (from an eclogite in gneiss, and not from kimberlite) (fig. 10). The experimental results for this mineral pair, and those for the similar minerals from the garnet peridotite described above, therefore, exhibit two extremes of bimineralic eclogite composition and behavior.

The analyzed minerals from the

bimineralic eclogite in kimberlite represent a paragenesis appreciably lower in FeO/MgO ratio than the Glenelg eclogites studied previously at 30 kb (Yoder and Tilley, 1962). Both the Glenelg eclogites contain quartz and sundry other phases; thus it is to be expected that the temperatures of beginning of melting and disappearance of the last crystalline phases observed in the Glenelg eclogites will be lower than those observed in the mineral pair from kimberlite.

Experimental samples were made up from the analyzed minerals in the manner described above, and runs followed the same techniques. The results of runs at 30-kb pressure in the dry system are presented in figure 11.

The results obtained may be considered in relation to the data for the garnet-clinopyroxene pair from the peridotite

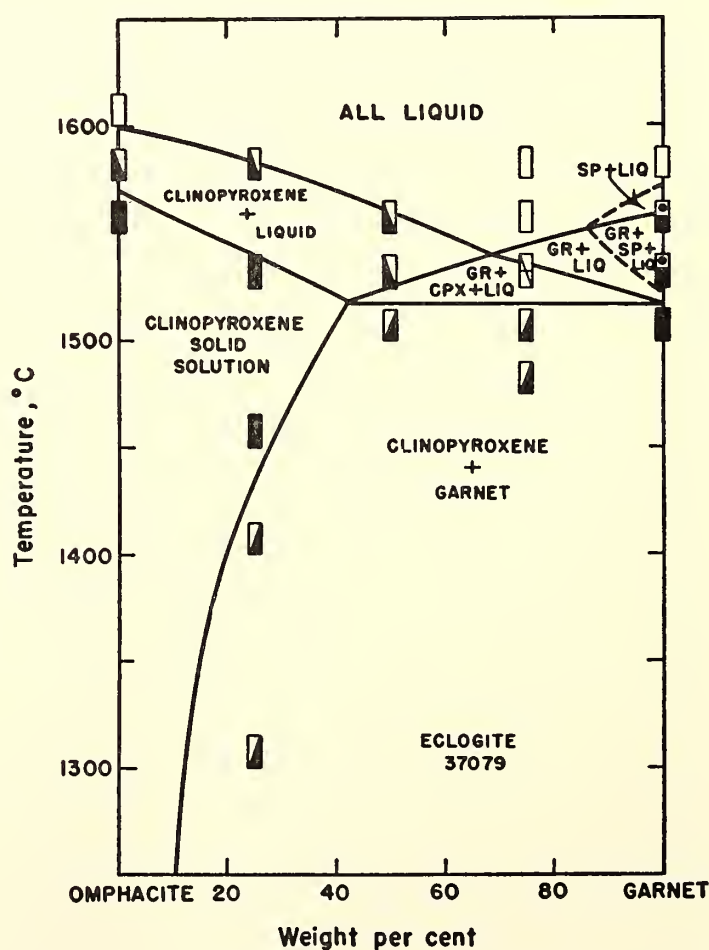


Fig. 11. Interpretation of results of runs at 30 kb on mixtures of garnet and omphacite from the eclogite 37079. Relationships in the subsolidus are not binary, and the boundary of the clinopyroxene solid solution field is based partly on estimates of the amount of garnet present in the runs.

assemblage A.3/10596. The increased Fe/Mg ratio and increased CaO, Al_2O_3 , and Na_2O content of the bimineralic eclogite pair produce only a 50°C decrease in the temperature of the beginning of melting of the garnet-clinopyroxene assemblage; consistent with this, only a small temperature interval is observed where both garnet and clinopyroxene coexist with liquid.

The very extensive solid solution of potential garnet molecule in the clinopyroxene at high temperatures already noted in garnet peridotite is also present in the garnet-pyroxene pair from eclogite. The minerals of the eclogite nodule appear to be in equilibrium at some temperature more than 200°C below the beginning of melting at 30-kb pressure (see figs. 8 and 11). The existence of oriented intergrowths of garnet and clinopyroxene in certain eclogite nodules from kimberlite (Williams, 1932, pls. 82 and 83) suggests that some of the eclogites may have recrystallized from a high-temperature assemblage. There is evidence, therefore, that some of the peridotites and some eclogites that occur in kimberlite have been at temperatures high enough for partial fusion of the peridotite and precipitation of the eclogite to have occurred in the dry system. The possibility of kyanite exsolution from clinopyroxenes formed at high temperature (Williams, 1932, pl. 126) should not be overlooked.

The temperature required to obtain a liquid by the partial melting of bimineralic eclogite at 30 kb ($1515^\circ\text{--}1565^\circ\text{C}$) is appreciably higher than that required to obtain liquid by the partial melting of garnet peridotite ($1425^\circ\text{--}1450^\circ\text{C}$). The refusion of bimineralic eclogite during a second cycle of heating therefore does not provide an easy way of obtaining basic magmas. Partial melting of garnet peridotite will be the dominant source of liquid where both rock types are present at this pressure.

If liquid is formed by the partial fusion of the eclogite mineral pair, the

proportion of garnet that enters the liquid phase at the beginning of melting is high enough to make that liquid hypersthene-normative (compare figs. 6 and 11). The normative composition of the liquid from which this eclogite may have *precipitated* is a quite different matter, and cannot be predicted from these experiments alone.

The presence of quartz and other phases in the Glenelg eclogites investigated by Yoder and Tilley (1962) together with the higher FeO/MgO ratio of these rocks has lowered the temperature of the beginning of melting by 150°C .

Because the temperatures of beginning of melting of garnet-clinopyroxene and garnet-clinopyroxene-orthopyroxene assemblages ($1515^\circ\text{--}1565^\circ\text{C}$) are higher than the temperatures at which these same assemblages begin to melt when olivine or quartz is added to the assemblage ($1425^\circ\text{--}1450^\circ\text{C}$ and $1350^\circ\text{--}1375^\circ\text{C}$, respectively), the whole range of garnet-pyroxene assemblages must be considered a thermal barrier at 30-kb pressure; i.e., a quartz-bearing eclogite, or a liquid of this composition, cannot be derived from a garnet peridotite at this pressure.

A green transparent spinel (hercynite) forms during the melting of the garnet of this eclogite, 37079, but the range of compositions in which spinel is present in the liquid is much reduced in comparison with the garnet-clinopyroxene pair from the peridotite A.3/10596. This reduction may be due in part to the smaller Cr_2O_3 content of the eclogite minerals.

At lower pressures the range of compositions from which spinel crystallizes may be more extensive, and the amount of spinel may be significant in rendering liquids silica-saturated in the CIPW norm.

Melting Relations of Basalts

*C. E. Tilley, H. S. Yoder, Jr., and
J. F. Schairer*

Experimental studies on the melting relations of a group of basalts under

anhydrous conditions at 1 atm, briefly described in earlier annual reports (Yoder and Tilley, *Year Book 55*, pp. 169–171; *Year Book 56*, pp. 156–161) and discussed more fully in Yoder and Tilley (1962, pp. 371–394), have been continued during the report year to cover a more extended range of composition among basic igneous rocks. The behavior of twelve additional rocks ranging from accumulative tholeiitic rocks of the Hawaiian volcanic province to extreme iron-enriched assemblages, including an accumulative fayalite-ferrogabbro of the layered series of the Skaergaard intrusion of East Greenland, has been investigated. Analytical data are available on all these assemblages, six already reported in the literature and six hitherto unpublished. The new analytical data are given in table 3, which includes an analysis of the chilled marginal gabbro of high-alumina type of the Skaergaard intrusion already reported³ (Wager, 1960, p. 375).

The experimental procedure adopted in the thermal study of the new assemblages has already been detailed in previous studies (Yoder and Tilley, 1962), but the examination of the Skaergaard fayalite-ferrogabbro and the Kilauean and Ōshima iron-rich schlieren required a special technique to avoid significant oxidation. The rock reduced to –76 mesh was ground for 2 hours under water-free acetone. The fine powder dried at 110°C for 24 hours was sealed in a platinum tube and surrounded with iron filings in an evacuated silica tube. The silica tube was suspended by platinum wire in a quenching furnace. At the termination

of the run the tube was dropped into mercury. It was necessary to seal the sample in a platinum tube because of the creep properties of the iron-rich liquids under vacuum; open capsules were completely emptied by creep in an hour's run. The results of these studies showing the liquidus temperatures and the succession of silicate phases encountered at various temperatures below the liquidus are given in figure 12. The assembled data include some corrections to results previously reported, especially relating to the temperature of the first appearance of clinopyroxene. Magnetite or a translucent spinellid appears frequently at a higher temperature than the first silicate phase in runs carried out in platinum tubes, but owing to variability of oxidation and iron content of the charge the stage of its appearance may be modified.

In the more basic assemblages olivine appears on the liquidus, whereas in the more iron-enriched members it gives way to plagioclase, clinopyroxene, or hypersthene (quartz dolerite, Honolulu). In the Kauai basalt the range of temperature for the appearance of the four phases olivine, orthopyroxene, plagioclase, and clinopyroxene extends over 225°C, and in the Kilauea picrite basalt of 1840 the range is extended to 270°C (Ol, 1435°C; Cpx, Pl, 1165°C). These are accumulative rocks. At the other end of the series, in the iron-enriched schlier of a Kilauea basalt, the liquidus is at 1080°C (Cpx, Pl), and for the extreme iron-enriched Skaergaard ferrogabbro (EG 4472), at 2350 meters in the layered series, plagioclase is on the liquidus at 1035°C, fayalite, iron-wollastonite solid solution, and clinopyroxene appearing at 1010°C. In this same rock the ferroaugite, recognized in equivalent assemblages by Wager and Deer (1939) as an inverted iron-wollastonite solid solution, undergoes partial inversion with heating to the iron-wollastonite phase above 970°C, as does the ferroaugite in an associated ferrogabbro (EG 4143) at 2400 meters in the layered succession.

Though these are accumulative rocks,

³ Of the nineteen rocks listed in figure 12, analyses of seven are reported in Yoder and Tilley (1962, table 2, analyses 3, 5, 7, 7a, 14, 16; table 11, analysis 3); the Koolau basalt (Ko) in Wentworth and Winchell (1947, table 4, analysis 4); the two 1955 Kilauea lavas in Tilley (1960, table 4, analyses 77 and 82); the iron-rich schlier of Kilauea (K) in Kuno et al. (1957, table 5, analysis 6); the chilled margin of the Stillwater intrusion (St) in Hess (1960, table 12, analysis 1). The remaining seven analyses are given in table 3.

TABLE 3. Chemical Analyses and Norms of Investigated Rocks

	1	2	3	4	5	6	7
Analyses							
SiO ₂	46.94	50.56	51.15	48.69	48.08	45.01	51.35
Al ₂ O ₃	9.03	12.85	14.22	10.23*	17.22	8.32*	11.08
Fe ₂ O ₃	1.74	1.52	2.55	1.63	1.32	3.67	5.32
FeO	10.25	10.32	9.56	10.13	8.44	24.48	14.09
MnO	0.17	0.17	0.18	0.17	0.16	0.64	0.30
MgO	20.10	8.30	5.65	17.72	8.62	0.19	4.22
CaO	7.76	9.06	9.96	7.51	11.38	10.99	9.57
Na ₂ O	1.59	2.63	2.58	1.68	2.37	2.34	1.46
K ₂ O	0.35	0.72	0.57	0.29	0.25	0.27	0.36
H ₂ O ⁺	0.13	0.13	0.22	0.17	1.01	0.55	0.35
H ₂ O ⁻	Nil	Nil	Nil	0.00	0.05	0.08	0.45
TiO ₂	1.80	3.47	3.35	1.61	1.17	2.49	1.65
P ₂ O ₅	0.17	0.36	0.23	0.21	0.10	0.95	0.10
Cr ₂ O ₃	0.18	n.d.	n.d.	n.d.*	n.d.	n.d.*	n.d.
S	n.d.	n.d.	n.d.	0.00	n.d.	0.02	n.d.
F	n.d.	n.d.	n.d.	0.01	n.d.	0.09	n.d.
	<hr/>	<hr/>	<hr/>	<hr/>	<hr/>	<hr/>	<hr/>
O = F, S	100.21	100.09	100.22	100.05	100.17	100.09	100.30
	<hr/>	<hr/>	<hr/>	<hr/>	<hr/>	<hr/>	<hr/>
Total	100.21	100.09	100.22	100.04	100.17	100.04	100.30
Norms							
Qz	---	0.78	4.92	---	---	---	11.40
Or	2.22	3.89	3.34	1.67	1.11	1.67	2.22
Ab	13.62	22.53	22.01	14.15	19.91	19.91	12.31
An	16.12	21.13	25.31	19.46	35.86	11.12	22.66
Di	17.08	17.73	18.64	13.12	16.25	33.28	20.30
Hy	13.74	24.29	15.14	26.50	8.57	18.99	19.57
Ol	30.58	---	---	18.99	12.94	2.13	---
Il	3.50	6.61	6.38	3.04	2.28	4.71	3.12
Mt	2.78	2.09	3.71	2.32	1.86	5.34	7.66
Ap	0.34	0.85	0.51	0.51	0.34	2.18	0.34
Rest	0.13	0.13	0.22	0.17	1.06	0.74	0.80
	<hr/>	<hr/>	<hr/>	<hr/>	<hr/>	<hr/>	<hr/>
	100.11	100.03	100.18	99.93	100.18	100.07	100.38

1. Picrite basalt (66070), lava of the lower vents of the 1840 eruption of Kilauea, Nanawale Bay, Hawaii.

2. Basalt (66102c), olivine-bearing, 1840 Kilauea lava of the upper vents, northwest of Makaopuhi Crater.

3. Basalt (68227), 1840 Kilauea lava of the upper vents, northwest of Makaopuhi Crater.

4. Hypersthene olivine basalt (Ka), east wall of Olokele Canyon, Kauai, Hawaiian Islands (cf. Cross, 1915, pp. 10-12).

5. Olivine gabbro (EG 4507) chilled margin, 1 meter from southern contact with basalts, Skaergaard intrusion, East Greenland (Wager, 1960, p. 375).

6. Fayalite ferrogabbro (EG 4472), 2350 meters in layered series, small nunatak, foot of Base Glacier, Skaergaard intrusion, East Greenland. Specimen kindly supplied by Professor L. R. Wager.

7. Iron-rich segregation vein (K₁₀) in hypersthene olivine basalt, Okata, Ō-shima Island, Izu, Japan. Specimen and analysis kindly supplied by Professor H. Kuno.

Analyses 1, 2, and 3 by J. H. Scoon; 4 and 6 by C. O. Ingamells.

* Includes ZrO₂, Cr₂O₃, V₂O₅, and other undetermined oxides.

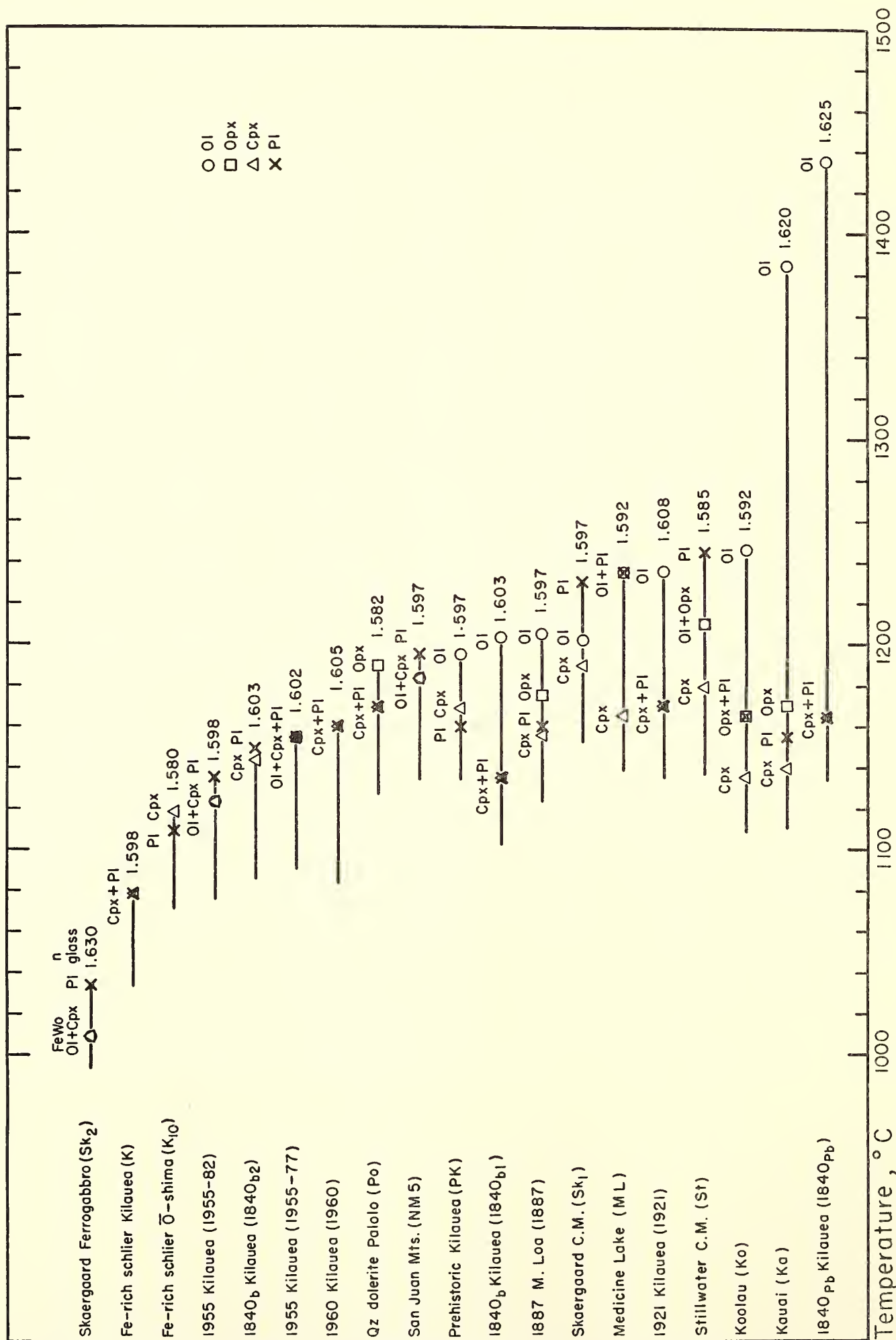


Fig. 12. Results of thermal treatment of selected basalts, principally of tholeiitic suites. Ol is olivine; Opx, orthopyroxene; Cpx, clinopyroxene; and Pl, plagioclase. The temperatures are those at which a particular phase disappears on heating long enough to reach equilibrium at approximately 1 atm.

the liquids from which they crystallized must have had temperatures below the liquidus of these assemblages (1035°C). Magmatic temperatures must therefore have been above 970°, the inversion temperature, and below 1035°, the temperature of the liquidus of the accumulate. The final consolidation temperature of the layered series must, however, have been below 970°C.

If the Skaergaard chilled margin (liquidus 1230°C) is taken as representative of the composition of the

original Skaergaard magma, the temperature difference between the start of crystallization and its virtual completion is at least 260°C. Hess (1941, p. 583) estimated the maximum temperature difference for the observed Skaergaard rocks as 185°C, utilizing the inversion data on synthetic magnesium-iron pyroxenes and the synthetic hedenbergite-ferrosilite solid solutions.

The liquidus of the Stillwater chilled margin (St) determined at 1245°C may be compared with the value 1125°C

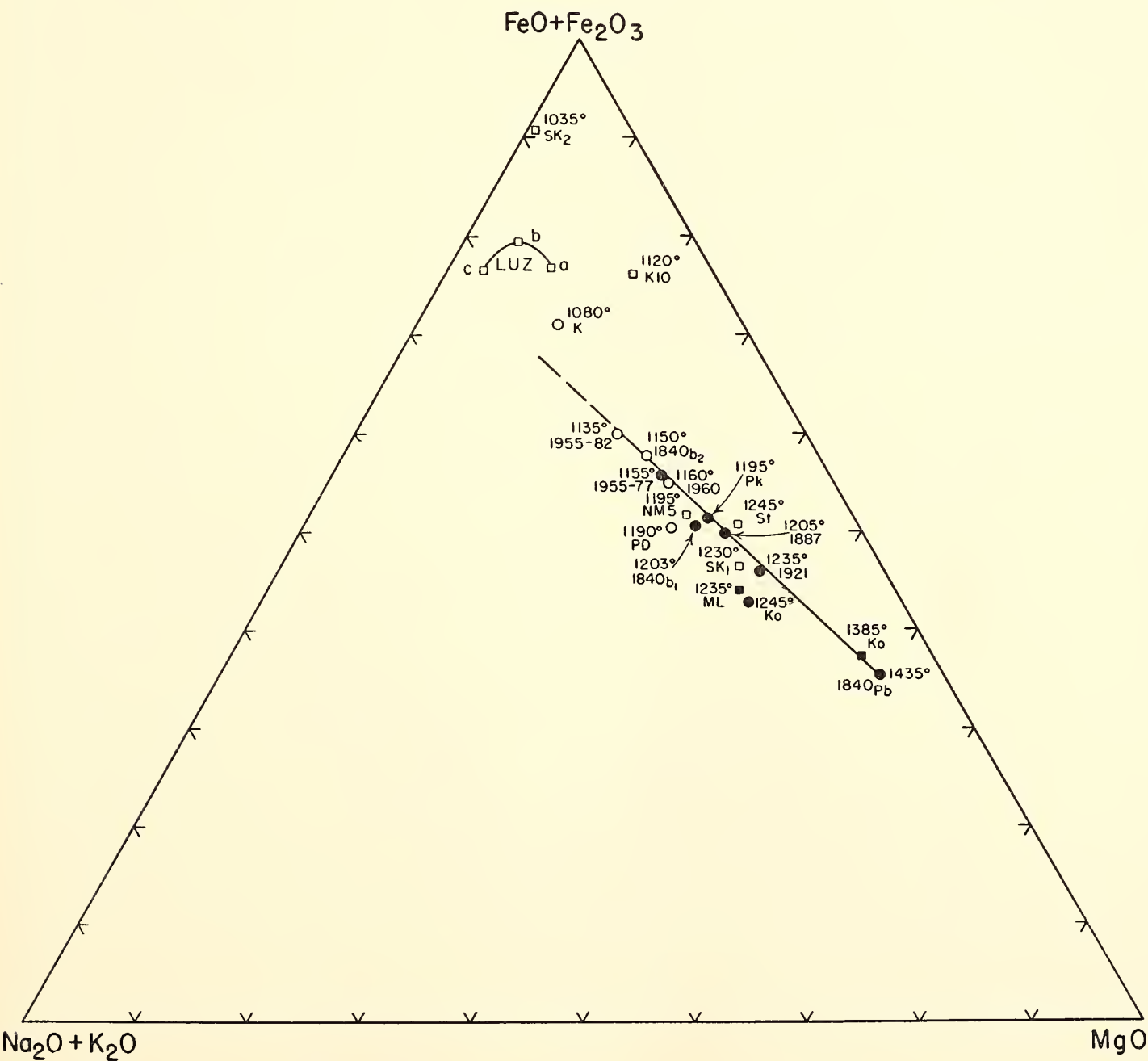


Fig. 13. Plot of the analyzed basalts in the system FMA: F (FeO + Fe₂O₃), M (MgO), A (Na₂O + K₂O). Liquidus temperatures are attached to each point: circles, Hawaiian rocks; squares, other rocks. Filled circles or squares are for assemblages having olivine on the liquidus. Lettered points as in figure 12. Additional points marked are LUZa-c, the estimated compositions of successive residual liquids of the Skaergaard layered series (Wager, 1960).

estimated by Hess for the Stillwater magma temperature at the beginning of crystallization (Hess, 1960, p. 85).

In both the Skaergaard and Stillwater chilled margins the hypersthene is described as inverted pigeonite (Brown, 1957, p. 513; Hess, 1960, p. 40), from which it must be concluded that no safe estimate of the temperature of beginning of crystallization can be given on the basis of the inversion.

Wager (1960) has calculated the approximate compositions of the successive residual magmas (L.UZa-c) of the Skaergaard upper layered series corresponding to 95.7 to 99.3 per cent solidification. Of these the composition L.UZc is designated as the liquid from which an accumulative ferrogabbro of the type of EG 4472 (Sk_2) has been precipitated. The iron enrichment of this estimated liquid (0.96) with the temperature limits of its liquidus as indicated by the behavior of the ferrogabbro (Sk_2) and of the temperature of inversion of its ferroaugite is indicated in figure 14 along with the plot of the

position of the accumulate Sk_2 in relation to the extension of the liquidus line of the Hawaiian assemblages to be described next. It will be observed that the accumulate has a higher iron enrichment than the estimated liquid, L.UZc, from which the accumulate is supposed to be derived.

In the FMA plot (F, FeO + Fe₂O₃; M, MgO; A, Na₂O + K₂O) of figure 13 the positions of the nineteen rocks experimentally treated are set out. The trend of iron enrichment is indicated in the join 1840_{Pb}-1840_{b2} of the Kilauea picrite basalt-basalt suite, beyond which lie the points for the Kilauean iron-enriched schlier and the Skaergaard ferrogabbro. The temperature attached to each point indicates the liquidus temperature, the rocks with olivine on the liquidus being marked by a filled circle or filled square. The dependence of the liquidus temperature in a tholeiitic series, as the majority of the rocks studied represent, on iron enrichment can be more effectively illustrated by figure 14, which

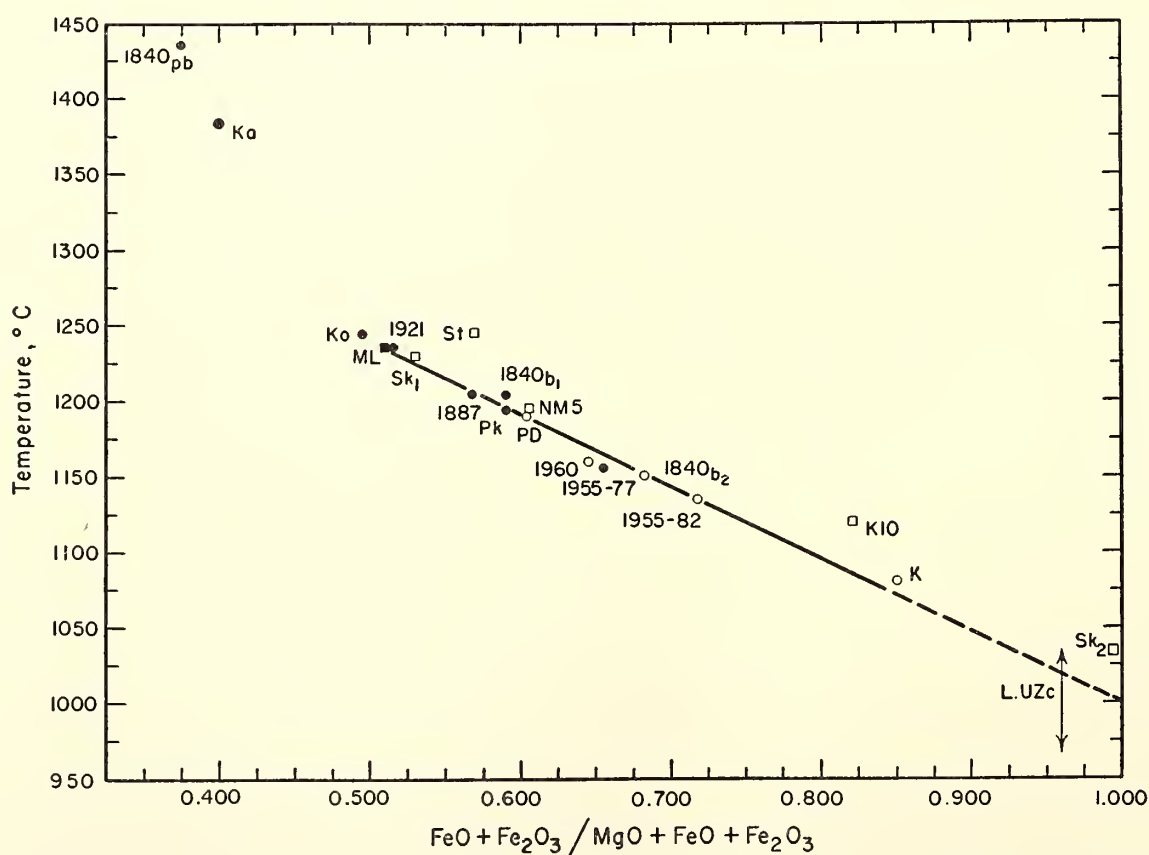


Fig. 14. Plot correlating liquidus temperatures with iron enrichment. Numbered and lettered points as in figure 13.

plots liquidus temperature and iron enrichment $(\text{FeO} + \text{Fe}_2\text{O}_3)/(\text{MgO} + \text{FeO} + \text{Fe}_2\text{O}_3)$.

Examination of the plot shows that it can be divided into two parts: a region in which there is effectively a linear relation of liquidus temperature to iron enrichment (Kilauea, 1921, iron-enriched schlier, K), and a region extending from the strongly accumulative picrite basalt (1840_{pb}) to the mildly accumulative 1921 Kilauea basalt characterized by a curve of steeper gradient which includes the plot of the liquidus of the mafic Kauai hypersthene olivine basalt (Ka). The reason for the marked change of slope of the temperature/composition trend can be traced to the nature and number of the crystallizing phases. In the upper temperature region the major crystallizing phase is olivine, whereas over much of the lower temperature region the prime phases separating are clinopyroxene and plagioclase.

Thus for the olivine-rich basalts (1840_{pb}, Ka) over a range of temperature of 270° and 215°C, respectively, olivine only crystallizes, whereas for the majority of the basalts of the lower liquidus region two to three phases separate over a narrow range not exceeding 10° to 25°C.

The course of crystallization of these Kilauean liquids thus shows significant resemblance to that portrayed in the simple critically undersaturated iron-free basalt system (diopside-forsterite-albite-anorthite, Yoder and Tilley, 1962, p. 395, fig. 10), the liquid passing from the olivine volume to a shared surface (Ol-Pl, Ol-Cpx), and ultimately to a four-phase curve (Ol, Pl, Cpx, liquid), a gas phase being neglected.

The removal of 25 per cent olivine (Fo₈₀ weight per cent) from the 1840 Kilauea picrite basalt produces an assemblage chemically comparable to the 1921 Kilauea lava. For a more quantitative match, removal of some clinopyroxene and plagioclase is essential, and in table 4 are given the compositions of possible extracts for the Kilauean rocks

TABLE 4. Calculated Compositions of Possible Extracts in Derivation of the Grouped Kilauean Lavas Indicated

Series	Extract, %	Composition		
		Ol	Cpx	Pl
1840 _{pb} -1921 (K)	40	60	23	10
1840 _{pb} -1840 _{b1} (K)	50	61.5	19	16.5
1921-1955 ₈₂ (K)	50	28	28	42
1840 _{b1} -1840 _{b2} (K)	40	15	33.5	43
1955 ₇₇ -1955 ₈₂ (K)	25	---	41.5	48.5

indicated, through a range of compositions to the most siliceous Kilauean lava (1955₈₂) experimentally treated.

Through the series olivine gives way to clinopyroxene and plagioclase until, in the 1955 Kilauea series, apart from iron ores, clinopyroxene and plagioclase are the essential phases removed. Two rocks, the Stillwater chilled margin (St) and the iron-enriched segregation vein or schlier of Ō-shima (K₁₀), fall significantly above the Hawaiian trend. The reason for this departure is revealed when consideration is given to the model composition of the Stillwater rock carrying 53½ per cent plagioclase, 37¼ per cent hypersthene, and 8 per cent clinopyroxene, and thus the composition of the rock is seen to be removed from a four-phase curve analogous to that of the simple basalt system referred to above.

The anomalous position of the Ō-shima iron-rich schlier (K₁₀) can be traced in part at least to the low value of its alkalies (1.82 per cent) and normative feldspar content (37 per cent, Or_{6.0}Ab_{33.1}An_{60.9}) as compared, for example, with the Kilauean schlier (K) of comparable iron enrichment with alkalies, 3.79 per cent, and normative feldspar content of 48 per cent (Or_{10.4}Ab_{52.5}An_{37.1}) (cf. fig. 13).

It is clear that for the nonaccumulative Hawaiian tholeiite series in the linear region the liquidus temperature can be estimated from a chemical analysis yielding the iron enrichment. The most

basic liquid recognized at the Kilauea volcanic center is given by the analysis of a Pele's hair from Kilauea Iki (1959 eruption) presented by Macdonald and Katsura (1961, table 1, analysis 1). Unlike previously analyzed Pele's hair, this glass, freed from olivine phenocrysts, contains normative olivine (6.8 per cent). The iron-enrichment value (0.56₃) corresponds in figure 14 to a liquidus temperature of $\sim 1200^{\circ}\text{C}$. The observed temperature of the erupting lava at Kilauea Iki in 1959 ranged from 1120° to 1190°C (Richter and Eaton, 1960, p. 906). A slightly higher temperature of 1200°C was reported by Jagger (1947) for the 1921 Kilauean eruption.

PYROXENES AND ASSOCIATED MINERALS IN THE CRUST AND MANTLE

Pyroxene Quadrilateral

*H. S. Yoder, Jr., C. E. Tilley, and
J. F. Schairer*

The pyroxenes constitute one of the most important mineral groups—second only to the feldspars—in recording the history of rocks. Their wide range of stability, composition, and structural variations provides a great potential for storing information on the pressure and temperature of formation of the pyroxenes as well as the rocks containing them. Direct correlation of the physical and chemical properties of the pyroxenes

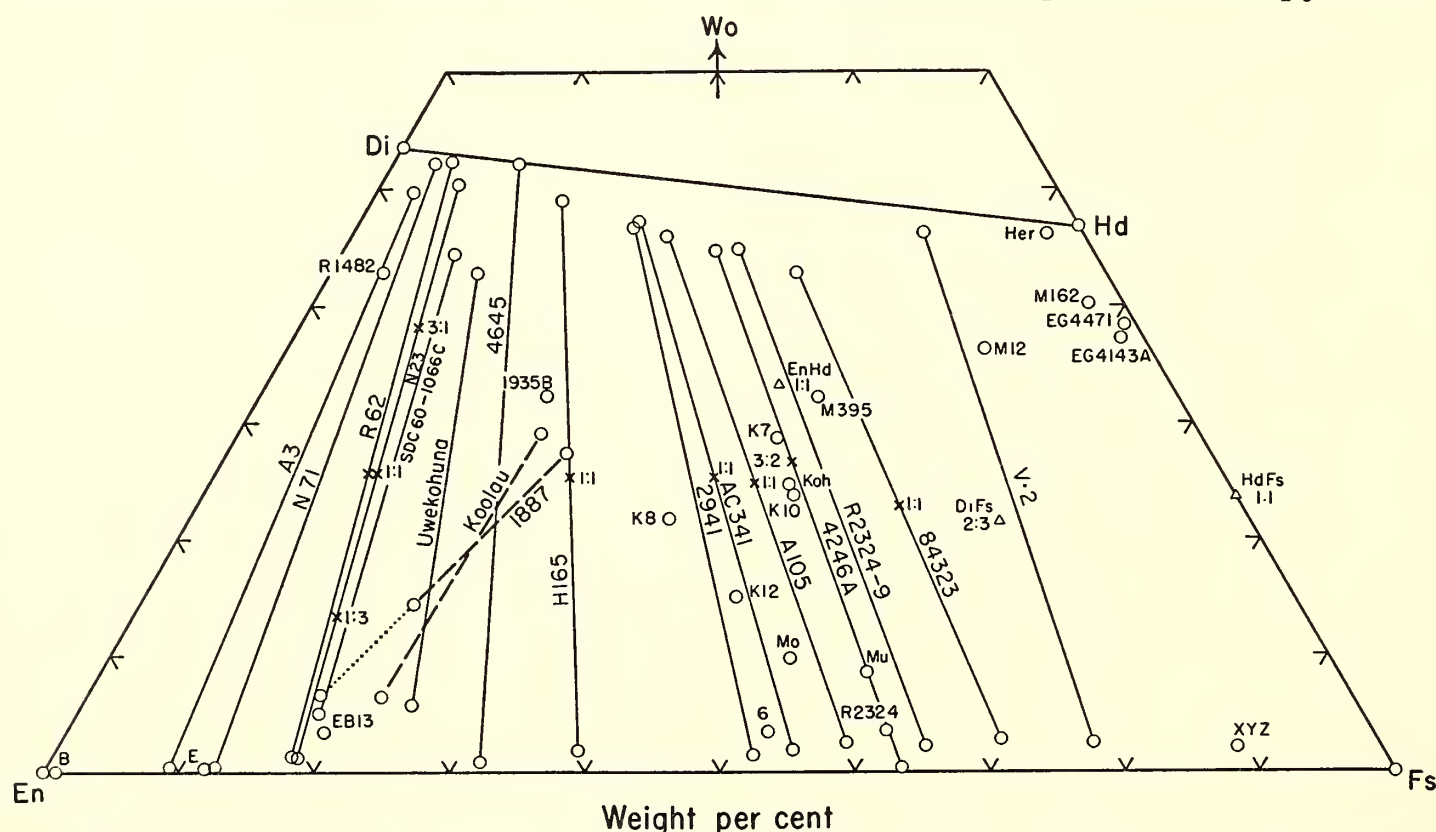


Fig. 15. Plot of analyzed natural pyroxenes (indicated by open circles); mixtures of analyzed natural coexisting pyroxenes (crosses); mixtures of natural or synthetic pyroxenes or equivalent materials (triangles) used or to be used in the present study. Full lines are tie lines. Dashed lines connect phenocrysts and groundmass pyroxenes and are not tie lines. Dotted line indicates assumed correction due to admixture of associated pyroxene. The writers are greatly indebted to the donors of the analyzed pyroxenes; additional analyzed specimens are desired. Projections of points are weight percentage of CaO, MgO, and FeO converted to metasilicate and recalculated to 100 per cent, except specimen Her, where MnO was included with FeO.

References. A3, N71, N23: O'Hara and Mercy, unpublished data, 1963. Koolau, 1887, 1935B: Muir and Tilley, 1963. Uwekahuna: Muir, Tilley, and Scoon, 1957. V2: Howie and Subramaniam, 1957. R62: Howie, unpublished data, 1963. 4645, 2941, 4642A: Howie, 1955. H165: Hargraves, 1962. R1482: University of Minnesota Rock Analysis Laboratory. EB13: Hess, 1960. 6: Buddington, 1950. R2324, R2325-9: Hess, unpublished data, 1957. A105, AC341: Engel and Engel, unpublished data, 1963. 84323: Binns, 1962. Mo: Hess and Henderson, 1949. Mu: Hallimond, 1914. M395, M12, M162: McDougall, 1961. EG4471: Wager, unpublished data, 1962. EG4143A: Muir, 1951. Her: Wyckoff, Merwin, and Washington, 1925. XYZ: Ramberg and De Vore, 1951. K7, K8, K10, K12: Kuno, 1955. SDC60-1066C: Irvine, unpublished data, 1963. Koh: Fenner, 1929.

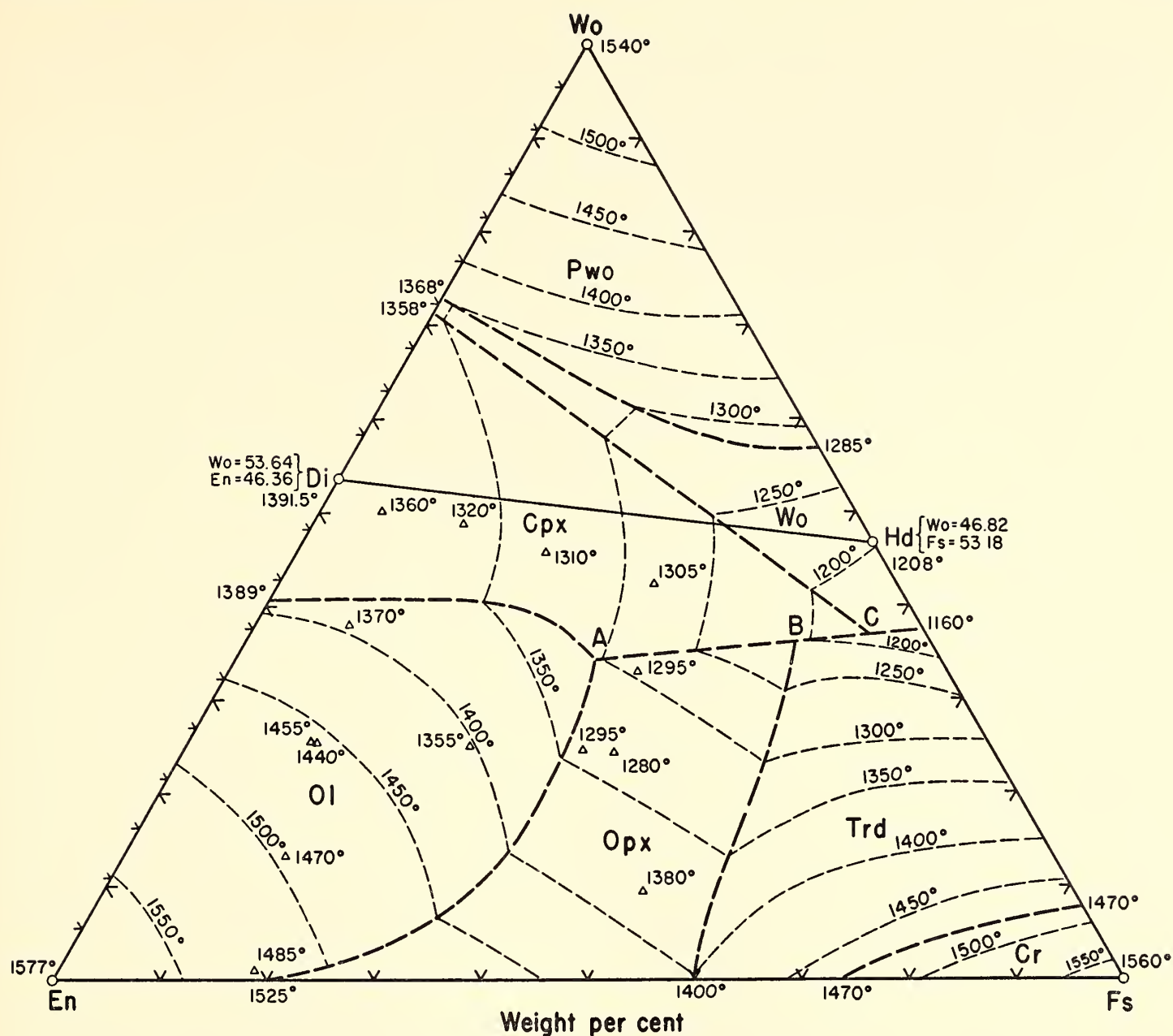


Fig. 16. Working liquidus diagram for the synthetic CaSiO_3 - MgSiO_3 - FeSiO_3 system based on results of peripheral systems by Boyd and Schairer (*Year Book 61*); Bowen, Schairer, and Posnjak (1933); Bowen and Schairer (1935a); Turnock (*Year Book 61*); Schairer and Bowen (1942); Schairer and Yoder (*Year Book 61*). All boundary curves and isotherms are estimated. All phases are in equilibrium with native iron; P_{O_2} is variable, and the Fe_2O_3 content of liquids is not defined. Triangles are compositions of natural pyroxenes for which liquidus has been determined. Ol, olivine; Cpx, clinopyroxene; Opx, orthopyroxene; Wo, wollastonite; Pwo, pseudowollastonite; Trd, tridymite; Cr, cristobalite.

with pressure and temperature does, of course, require experimental determination.

The composition of the pyroxenes can be represented for the most part in the system diopside (Di , $\text{CaMgSi}_2\text{O}_6$)-hedenbergite (Hd , $\text{CaFeSi}_2\text{O}_6$)-enstatite (En , MgSiO_3)-ferrosilite (Fs , FeSiO_3) shown in figure 15. The thermal relations at 1 atmosphere for the peripheral binary systems have been or are under investigation, and one preliminary attempt (Roedder, 1956, personal communica-

tion) has been made to study the liquidus surface of the entire quadrilateral. These data have been used to construct a working liquidus diagram (fig. 16). It is clear from the phases appearing on the predicted liquidus (e.g., olivine, tridymite, wollastonites) that the thermal relations must be considered from the more general aspect of the CaO - MgO - FeO - SiO_2 tetrahedron (fig. 17) and, in fact, because of the way in which some of the experiments were performed, the Ca - Mg - Fe - Si - O_2 system. The major deter-

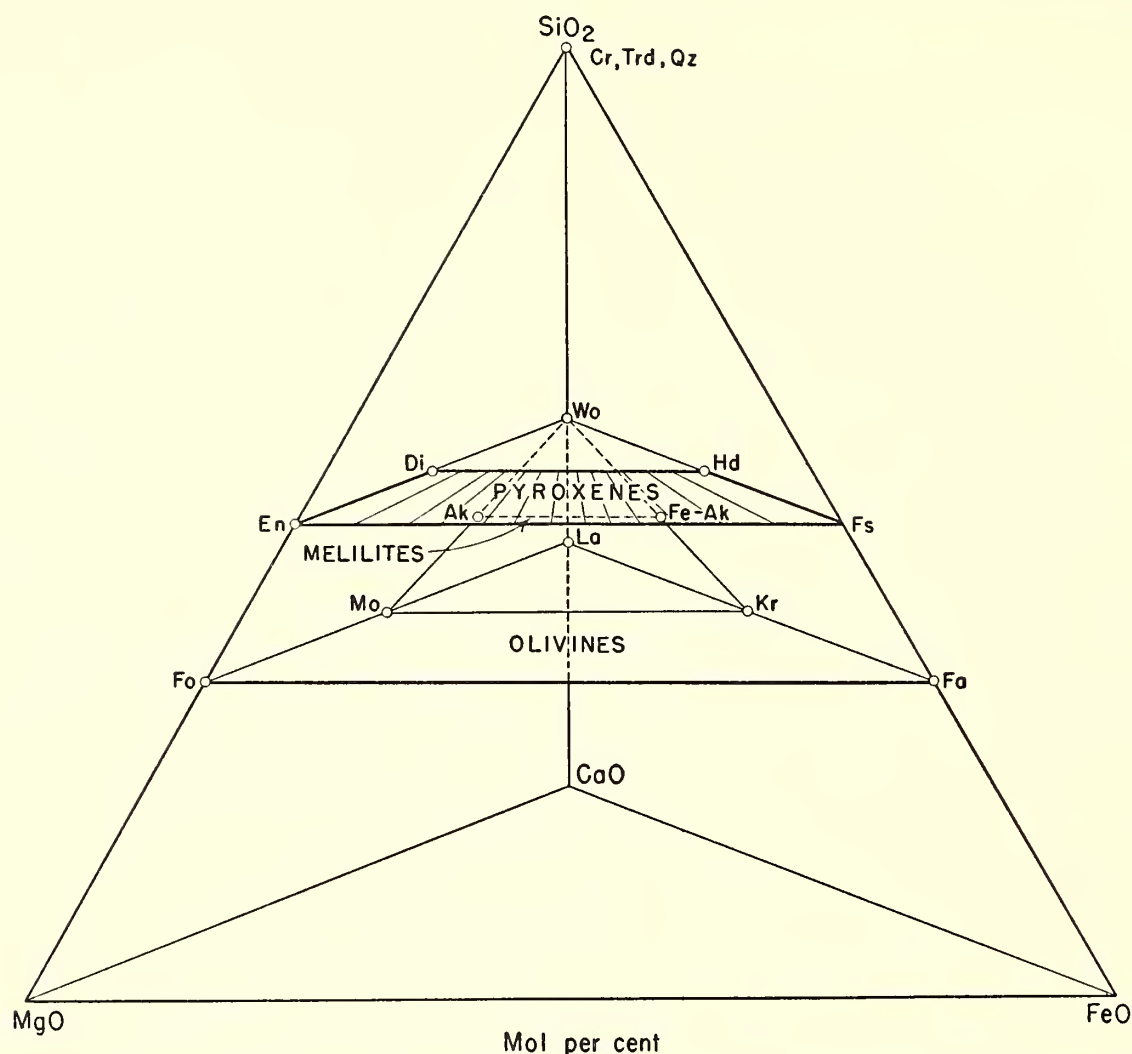


Fig. 17. The CaO-MgO-FeO-SiO₂ system, showing the relationships of the pyroxene quadrilateral to the olivines, melilites, and SiO₂ minerals. The melilites lie in the Wo-Mo-Kr plane; they were studied by Schairer and Osborn (1950). Ak, akermanite; Fa, fayalite; Fo, forsterite; Kr, kirschsteinite; La, larnite; Mo, monticellite.

rent in studying any of these systems successfully is in fixing the oxygen and iron content of the initial starting material and keeping these constituents constant during the run. In view of the lack of suitable containers and technique for maintaining the Fe and O₂ content of a charge constant, the writers, impatient for the results, believed that a less rigorous attempt should be made to outline the general thermal relations of the pyroxene quadrilateral. It was hoped that these studies would be a useful guide in more accurate and detailed studies at a later date in the more important regions of the system.

Three principal approaches to the study of the pyroxene quadrilateral are now being pursued with the following materials and technique:

1. Heating mixtures of analyzed, coexisting, natural pyroxenes from

various environments in fixed proportions at various pressures. Each pair of pyroxenes is treated as an independent pseudobinary system. The various pseudobinary systems can then be used to construct the general phase relations in the quadrilateral if allowance is made for the variance of minor constituents (e.g., Na₂O, Fe₂O₃, Al₂O₃, and MnO) in the natural minerals.

2. Heating mixtures of the purest natural or synthetic end member pyroxenes obtainable so that all possible compositions in the quadrilateral could be investigated with the same contaminants. In lieu of ferrosilite, which occurs very rarely and in minute quantity, a mixture of fayalite and cristobalite in the requisite proportions may be substituted for compositions more iron rich than the join enstatite-hedenbergite.

3. Heating the rocks from which the

pyroxenes used in the first approach have been separated and analyzed. The purpose is to evaluate the thermal behavior of pyroxenes in their normal environmental compositions and to compare such behavior with the thermal behavior of the same pyroxenes when isolated.

Preliminary data, obtained on many aspects of the pyroxene relations, are undergoing constant revision as more pyroxenes become available and technique is improved. Some of the more significant problems are outlined here.

Liquidus. The temperature of complete melting has been determined for the natural pyroxenes or mixtures of natural pyroxenes as indicated in figure 16. The primary phase on the liquidus is consistent with the primary phase field predicted for the synthetic system; because of the various contaminants, however, the temperatures are usually lower than those predicted. Several

significant observations can be made. Most of the magnesium-rich pyroxene compositions (or pyroxene assemblages) melt with olivine on the liquidus, a finding in disagreement with Barth's (1960, p. 26) conclusion that no reaction relation with olivine exists in the pyroxene diagram for pyroxene compositions to be expected in basalt magma. On the other hand, most of the iron-rich pyroxene compositions (or pyroxene assemblages) melt with tridymite or cristobalite on the liquidus. The liquids are enriched in silica relative to the pyroxenes where olivine is on the liquidus and are deficient in silica where tridymite or cristobalite is on the liquidus. Because of the possible solid solution of the augites toward olivine and melilite compositions, it is likely that the liquid will lie in the plane of the pyroxene quadrilateral only when the bulk compositions are all liquid. A field of protohypersthene appears to dominate the central part of the quadrilat-

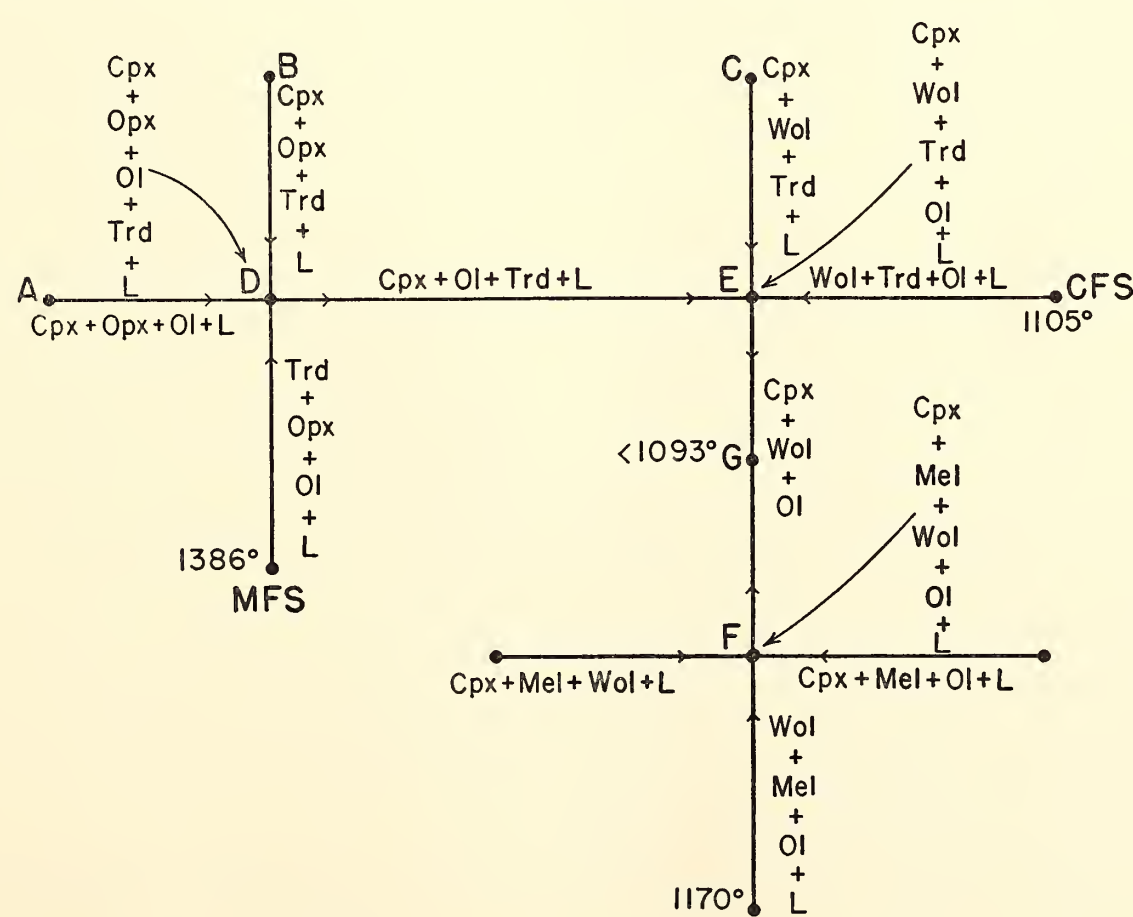


Fig. 18. Predicted "flow sheet" for a portion of the CaO-MgO-FeO-SiO₂ system pertinent to the crystallization of compositions on or near the pyroxene quadrilateral. The indicated temperatures are from Bowen and Schairer (1935a); Bowen, Schairer, and Posnjak (1933); Schairer and Osborn (1950); and Kushiro and Schairer (this report). Points A, B, and C are the piercing points of figure 16. Points D, E, and F are quaternary reaction points, and point G is a quaternary minimum.

eral liquidus, and the augites extend along most of the upper part. Iron wollastonite solid solutions occur on the liquidus about the hedenbergite composition.

Points *A*, *B*, and *C* of figure 16 mark the piercing points of the univariant curves $Ol + Cpx + Opx + L$, $Cpx + Opx + Trd + L$, and $Cpx + Wol + Trd + L$, respectively. The predicted "flow sheet" pertinent to the final consolidation of liquids in the pyroxene quadrilateral is given in figure 18. The proposed ternary piercing points *A* and *B* have significant bearing on the consolidation of the large layered intrusions such as Skaergaard, Stillwater, Bushveld, Muskox, and Red Hill. Piercing point *A* indicates that in the course of fractionation the relatively magnesian olivines may terminate in the crystallization of *some* bulk compositions. In addition, piercing point *B* suggests that pigeonite (presumably an inversion product of Opx) may also terminate its crystallization in the cooling of *some* bulk compositions. There appears to be no limit to the iron content of natural pigeonites. An analyzed pigeonite phenocryst from a dacite at Asio, Japan, has the composition $Wo_9En_{12}Fs_{79}$, according to Kuno (1950, p. 997). Bown and Gay (1960, p. 386) found "pigeonite" exsolving from augite EG 4143 (see fig. 15). They presumed that the "pigeonite" was probably close to clinoferrosilite but noted that the required ($h + k$) odd diffraction spots were missing. It would be of great importance to fix the composition of augite and protohypersthene or pigeonite in equilibrium with liquids *B* and *D*. The termination of pigeonite crystallization may also bring about the crystallization of an iron-rich olivine (e.g., a fayalite solid solution) as indicated at the quaternary reaction point, *D*. The reaction relation of pigeonite with liquid to form a fayalitic olivine was first outlined as a possible explanation of observed relations in a series of rocks by Poldervaart and Hess (1951, p. 479). The

inversion of iron wollastonite solid solution to another clinopyroxene (see below) will presumably take place with further lowering of the temperature below the final invariant minimum point, *G*. It seems that in the full course of fractionation and inversion for *some* bulk compositions an olivine as well as a clinopyroxene will disappear and reappear.

Caution must be exercised in comparing the schematic liquidus diagram to similar diagrams purporting to show the trends of pyroxenes in crystallizing magmas. These diagrams represent the projection of complex relations usually between feldspar and pyroxene, and the relations, therefore, do not lie in or near the plane of figure 16.

*Two-pyroxene boundary curve.*⁴ Several suggestions have been made in regard to the location of the "two-pyroxene boundary curve" (fig. 19). It may be presumed that what has been described by some is in part the trace of the $Cpx + Opx + Ol + L$ curve. There is a second curve involving two pyroxenes, $Cpx + Opx + Trd + L$, which is of equal significance and has been described by others. Still others (e.g., Kuno, 1955, p. 91) believe that under equilibrium conditions there is a continuous two-pyroxene + liquid surface in basalts carrying olivine to dacites carrying quartz. The traces of the two four-phase curves predicted from this study are shown in figure 19. The normative pyroxene of rocks that contain phenocrysts of a single pyroxene and are olivine normative supports the new position of the $Cpx + Opx + Ol + L$ curve.

Inversions in CaO-poor pyroxenes. Many important conclusions have been drawn from the Opx - Cpx inversion curve

⁴ Not to be confused with the "two-pyroxene field" boundary of Kuno (1936, p. 143; see also Hess, 1941, p. 586, fig. 12), which appears to represent his estimate of the limit of bulk compositions that can produce two pyroxenes. Kuno's curve does not represent a field boundary in the usual thermodynamic sense, as noted by Brown (1957, p. 254, footnote).

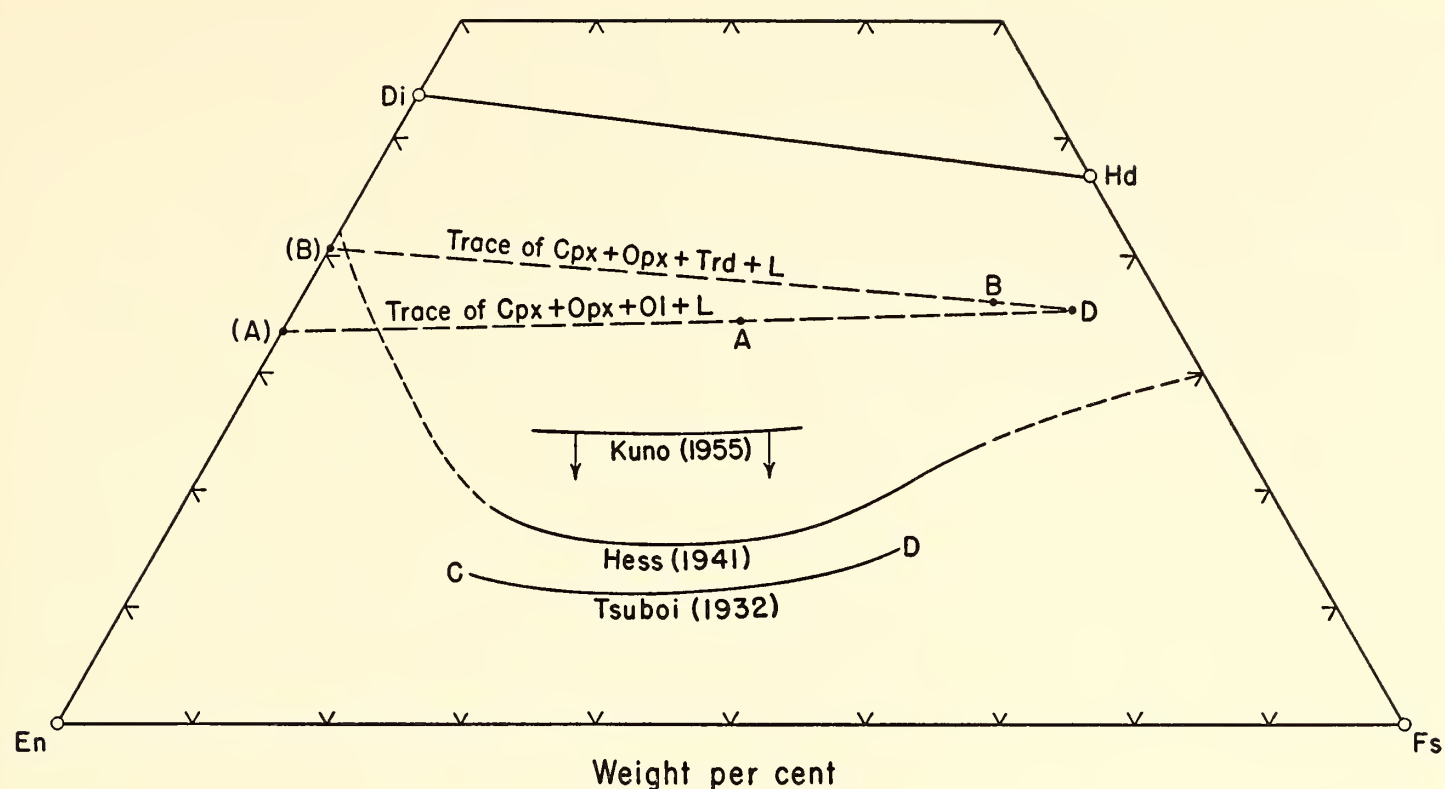


Fig. 19. Plots of two-pyroxene + L boundary curve as given by Tsuboi (1932) mainly for andesitic rocks and by Hess (1941) and Kuno (1955) based mainly on basaltic rocks. Kuno indicated schematically that the two-pyroxene + L line moves toward the En-Fs join with increasing SiO_2 content of the rock. The traces of the $\text{Cpx} + \text{Opx} + \text{Trd} + L$ and $\text{Cpx} + \text{Opx} + \text{Ol} + L$ lines predicted from this study are shown; it is to be emphasized that they are for a synthetic system *not* involving plagioclase, whereas curves based mainly on natural rocks are for liquids also carrying plagioclase. For this reason the two types of curves may not be comparable. Points A and B are the piercing points of figure 16, and point D is the quaternary reaction point shown in figure 18. Points (A) and (B) are projections of those of Schairer and Yoder (*Year Book 61*, p. 76) for the system Di-Fo- SiO_2 .

of Bowen and Schairer (1935a, p. 164) for the MgSiO_3 - FeSiO_3 series. The inversion was then believed to take place at 1140°C at the MgSiO_3 end, gradually decreasing in temperature to 955° at $\text{En}_{12}\text{Fs}_{88}$ (weight per cent). It should be noted that they also obtained the monoclinic form below the inversion curve, considering such growth to be metastable on the grounds that a high-temperature polymorph commonly forms rapidly at low temperatures in the field of stability of the low-temperature polymorph. Subsequent studies have indicated that the inversion in pure MgSiO_3 is probably nearer 1125°C and may be as low as 985° . Moreover, the inversion is believed to be from orthoenstatite to protoenstatite, clinoenstatite being a metastable low-temperature inversion from protoenstatite. Yoder and Tilley

(1962, p. 390) found that an orthorhombic pyroxene crystallized from two natural basalts held at 1175°C , a temperature well above the Bowen and Schairer inversion curve. Since there was no decisive evidence that the orthorhombic form observed by them was either an enstatite-like or a protoenstatite-like structure, the general term Opx was used.

Because the Bowen and Schairer curve had been fixed mainly by heating natural hypersthene with and without a NaF flux, similar experiments were made on other natural hypersthene. Whereas a monoclinic form was produced, the flux reacted with the pyroxene as well to yield fluorokupfferite + forsterite or a fluorogrünerite + olivine. Some of the sodium of the flux may have entered the amphibole too. Bowen and Schairer (1935b) recorded in a separate paper the

production of fluoroamphiboles by heating pyroxenes with NaF flux, but they did not comment on the influence of the flux on the pyroxene inversion. In the absence of a flux, some of the pyroxenes maintained orthorhombic symmetry up to the beginning of melting. Although some grains were multiply twinned, indicating transformation to monoclinic symmetry,⁵ others had wavy extinction. Some others had the characteristic curved crack structure perpendicular to the length of the crystal indicating that a volume change had taken place; and still others had parallel extinction with no signs of inversion. The relationships are not clear; it appears, however, that the inversion to be considered is from hypersthene to protohypersthene and not to clinohypersthene.

In the light of this conclusion, we must inquire about the significance of pigeonite and its supposed constant CaSiO_3 content of about 9 per cent. Is pigeonite an inversion product of a protohypersthene of the same composition, or is it a quenched stable product? Are the so-called "inverted pigeonites" that exsolve augite in fact inversion products of a protohypersthene? Three natural pigeonites (pigeonite no. 12, Kuno, 1955; Mull "uniaxial augite," Hallimond, 1914; Moore County, North Carolina, meteorite pigeonite, Hess and Henderson, 1949) were heated and their inversion characteristics studied. In the presence of liquid the Moore County, North Carolina, pigeonite produced protohypersthene; the Mull pigeonite recrystallized as pigeonite at 1150°C, the only temperature at which the material was held; and Kuno no. 12 recrystallized in part to pigeonite and another pyroxene as yet not fully determined (either hypersthene or protohypersthene).

⁵ Polysynthetic twinning alone is not sufficient evidence for clinohypersthene or pigeonite in mixtures of pyroxenes. Synthetic diopside often shows polysynthetic twinning when formed at high pressures (e.g. 30 kb), and natural diopside where crushed in marbles also exhibits this feature.

The Bowen and Schairer (1935a) inversion curve for the $\text{MgSiO}_3\text{-FeSiO}_3$ system has been related to a curve presumably indicating the first appearance of the low-CaO pyroxenes in natural magma (Tsuboi, 1938, 1949; Hess, 1941; Brown, 1957). In general, hypersthene is the first to appear in magma where the pyroxene composition is more magnesian than $\text{En}_{64}\text{Fs}_{36}$ (weight per cent); clinohypersthene (or pigeonite), where the composition of the pyroxene is less magnesian than that value. Unfortunately, the experimental inversion curve would not be applicable to natural magmas, even if it were not suspect, because of the considerable influence of the CaSiO_3 component. In other words, the presence of augite (or plagioclase) and the accompanying partition of calcium will bring about a lowering or raising of the inversion. Both Atlas (1952, p. 146, fig. 4) and Boyd and Schairer (*Year Book 61*, p. 70, fig. 8) indicate that the inversion from enstatite to protoenstatite may be raised in the presence of diopside. The difference in composition of pigeonite relative to hypersthene suggests that the inversion should be lowered in the presence of augite (see Barth, 1951, p. 220, fig. 1). However, these two observations may be quite unrelated if pigeonite is not the metastable inversion product of protohypersthene. It is necessary, therefore, to redetermine the hypersthene inversion to clinohypersthene, protohypersthene, or pigeonite with and without augite present.

Of interest to the petrographer is the common observation of an orthorhombic pyroxene rimmed by a clinopyroxene (e.g., 1887 lava of Mauna Loa, Hawaii). Such a relationship was observed frequently in runs of the 1:3 (Cpx:Opx) mixture of the analyzed coexisting pyroxenes N23 (fig. 15), where the principal products were $\text{Opx} + L$. The usual interpretation is that the rim formed as the temperature dropped and the iron enrichment increased beyond the $\text{En}_{64}\text{Fs}_{36}$

(weight per cent) point, where pigeonite⁶ becomes the stable phase. In the experiments described, the temperature was constant and no iron enrichment was possible. The present tentative interpretation is that the rims are formed during the quenching process and the clinopyroxene is a metastable product not related to the orthopyroxene-clinopyroxene inversion curve of Bowen and Schairer. If the orthorhombic pyroxene is indeed a protohypersthene, the rim may represent the initiation of inversion to clinohypersthene. In that event such rims in natural rocks may be a clue to the presence of protohypersthene.

Other modifications of the CaO-poor pyroxenes have been listed, β hypersthene (Lacroix, 1904, p. 533; 1910, p. 765) and pseudohypersthene (Tomita, 1931, p. 214). The β hypersthene, on reexamination, seems to be an alteration product in fractures or rimming hypersthene. Pseudohypersthene, which consists of granular clinopyroxene and olivine surrounding hypersthene, appears, on study in thin section, to be a contamination reaction product, as suggested by Tomita (1933, p. 3). Neither β hypersthene nor pseudohypersthene can be considered a polymorph of hypersthene.

Inversion in CaO-rich pyroxenes. The inversion of hedenbergite to a ferrowollastonite solid solution at 965°C was first recognized by Bowen, Schairer, and Posnjak (1933, p. 271), and inverted ferrowollastonites were first observed in nature at the Skaergaard intrusion by Wager and Deer (1939, p. 111). Because of the important bearing this inversion has on fixing the final consolidation temperature of the Skaergaard intrusion three hedenbergites from the uppermost part of the Upper Layered Series (UZc) were studied (EG 4471, 4472, and 4143, which are at 2350, 2350, and 2400 meters,

respectively, in the intrusion). All three hedenbergites inverted to a ferrowollastonite at $970^\circ \pm 5^\circ\text{C}$ on the basis of 7-day runs; reversal has not yet been attempted. It may be concluded that the final consolidation of the layered series of the Skaergaard intrusion must have taken place below 970°C.

Some inversion of synthetic ferrowollastonite of the requisite composition to hedenbergite has been achieved at 950°C after 4 weeks, in accord with the value for the inversion point, 965°C, given by Bowen, Schairer, and Posnjak (1933). It appears that magnesium raises the inversion, but the amount and extent have not been determined.

Ferrosilite. The early work of Bowen and Schairer (1932, p. 202) indicated the nonexistence of FeSiO_3 as a crystalline compound. At temperatures as low as 660°C the products were fayalite and "amorphous material" corresponding to the common natural assemblage of fayalite and quartz. Later, Bowen (1935, p. 487) indicated that the data were inconclusive because of the possible metastable formation of fayalite, a compound whose rate of growth is known to be very great. The discovery of natural pyroxenes with optical properties approaching those predicted for FeSiO_3 in the lithophysae of obsidians was not considered sufficient evidence for the existence of the compound FeSiO_3 because of the possible influence of MnO , for example, on the stability of the compound. It is of significance that the natural pyroxenes closely approaching clinoferrosilite occur with fayalite and magnetite, and hence the P_{O_2} required for formation is not unusual. One-month runs on suitable mixtures in the presence of iron have not produced a pyroxene at temperatures as low as 800°C. One of the most iron-rich natural hypersthene known (Ramberg and De Vore, 1951, p. 207, specimen XYZ), having $\text{Wo}_2\text{En}_{11}\text{Fs}_{87}$ (weight per cent) and an exceptionally low MnO content, begins to break down to olivine + cristobalite at a temperature as low as

⁶ The rims surrounding orthopyroxenes in natural rocks have been identified as pigeonite on the basis of optical properties, but they may be clinohypersthene. Careful study with the electron probe should resolve this question.

850°C after 7 days, in accord with the Bowen, Schairer, and Posnjak (1933) phase diagram. Runs at lower temperatures and for longer times are required. At present it may be assumed that the compound FeSiO_3 does exist. The possible polymorphism of FeSiO_3 introduces further complications into the meaning of the inversion curve of Bowen and Schairer.

Solvus. Sosman (1911) and Asklund (1925), who plotted compositions of analyzed natural pyroxenes, concluded that the magnesium-rich pyroxenes had limited solid solution whereas the iron-rich pyroxenes were completely miscible. Barth (1931, 1936), taking exception to these views (cf. fig. 20), presented new trend lines which he believed indicated complete miscibility of all pyroxenes in the quadrilateral, citing in support the early experimental results on the diopside-clinoenstatite series (Bowen, 1914), which have since been shown to have limited solid solution (Boyd and Schairer, *Year Book 61*, pp. 68-75).

Tsuboi (1932) thought the two views were not necessarily incompatible if the pyroxenes were completely miscible at the extrusive stage and limited in solubility at the intrusive stage. He did not define

the conditions required to produce the two results. Bowen and Schairer (1935a) interpreted the conclusions of Tsuboi to mean that the clinopyroxenes (Barth's "pigeonites," now called subcalcic augites) formed rapidly at the extrusive stage are metastable whereas slow crystallization *at the same temperature* would produce a CaO-poor orthorhombic pyroxene (hypersthene) and a CaO-rich clinopyroxene. Although it is not specifically stated by Bowen and Schairer (1935a, p. 203), it seems that they believed all natural pigeonites in the quadrilateral (except the Mull "uniaxial augite") form *below* the temperatures indicated by their MgSiO_3 - FeSiO_3 inversion curve.

Kuno (1936, p. 148) supported the Bowen and Schairer interpretation of the observations of Tsuboi for the most part, but he believed that compositions more iron rich than a line drawn from Wo to $\text{En}_{52}\text{Fs}_{48}$ (weight per cent) would crystallize *both* rapidly and slowly as a single monoclinic pyroxene. The line given by Kuno cannot be presumed to be a tie line connecting augite and hypersthene (or pigeonite) in equilibrium with liquid; rather, it is the locus of possible critical points where augite and pigeonite become identical in composition. It is not known

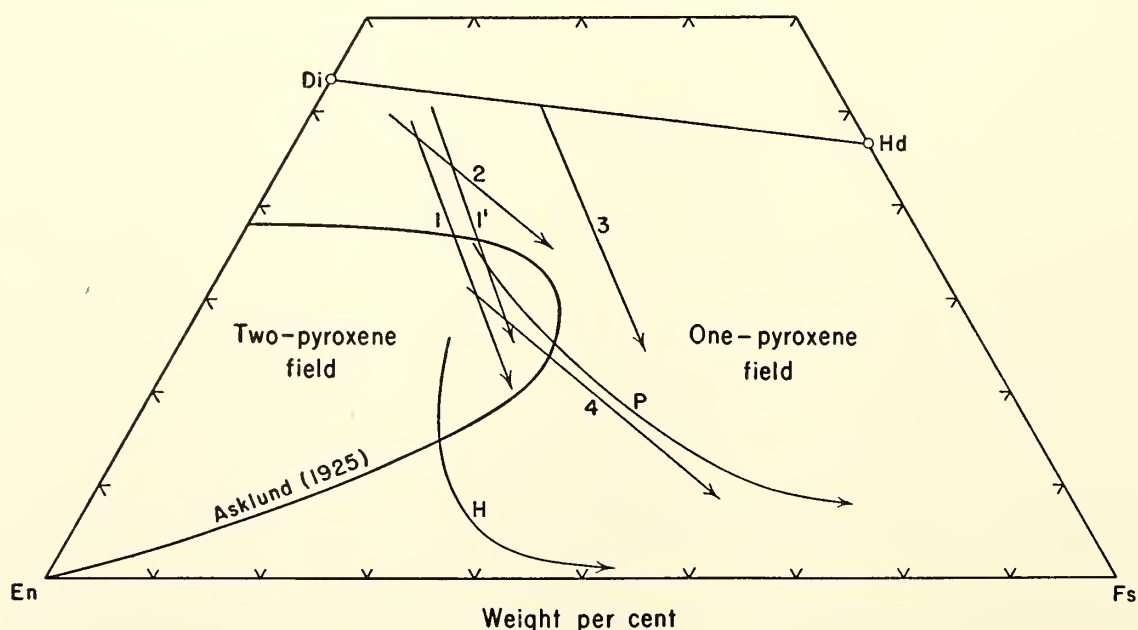


Fig. 20. Limit of two-pyroxene field as outlined by Asklund (1925) for intrusive rocks and trend lines of pyroxenes from extrusive rocks given by Barth (1936, nos. 1, 1', 2, 3, and 4) and by Kuno (1950, *H* and *P*).

whether such a change in composition of both augite, $C2/c$, and pigeonite, $P2_1/c$, is possible on crystal structural grounds. If "pigeonite" is indeed a family of intermediate structural states between protohypersthene, $Pbcn$, and augite, a complete series may be possible.

Hess (1941, p. 586) produced a similar line with the orientation of a possible tie line and with the implication that pigeonite was lost by reaction (1941, p. 591) without the formation of olivine and not because a critical point had been reached. Some question must be raised about the present writers' interpretation of the Hess line, because the presumed tie line extends beyond the compositions of the pyroxenes indicated by Hess as crystallizing from liquid at that stage of fractionation.

Further studies on extrusive rocks by Kuno (1950, 1955) appear to support the trend lines of Barth (1936), and Kuno proposed two series based on the groundmass pyroxenes, hypersthene, or pigeonite. There is, however, a unique difference between the trend lines of Kuno (1955) and Barth (1936). Those of Kuno are based on a series of chemically analyzed pyroxenes from several rocks, whereas those of Barth are constructed mainly from estimated compositions of phenocryst and groundmass pyroxene using optical data or calculations involving the rock analysis and mode. Kuno believed the hypersthene series to be essentially the result of "assimilation of granitic and related rocks" (1950, p. 995), and therefore it is not relevant to the present discussion. The pigeonitic series, he thought, in 1950 (p. 994), was "chiefly controlled by fractional crystallization"; in 1955 (p. 89), however, he stated that pyroxenes with less than Wo_{25} were the products of rapid cooling. Barth reiterated his views in 1951 and 1962, considering the subcalcic augites as stable phases at high temperatures. He visualized the subsolidus of the pyroxene quadrilateral with complete miscibility at high temperatures and with the

miscibility gap between augite and the pigeonites or hypersthene expanding with decreasing temperature and increasing iron content below a critical curve extending from the magnesium-rich side to the iron-rich side.

These complex arguments and opinions lead to the following questions:

1. Are the subcalcic augites and pigeonites of Barth (1931) and Kuno (1955) metastable phases formed during the quenching of extrusive rocks, or are they stable phases produced in the normal course of fractionation of both quenched intrusive and extrusive magmas?

2. Are two pyroxenes (augite + pigeonite or hypersthene) restricted to the intrusive rocks, or can they coexist with liquid in the extrusive lavas as well?

3. Does the solvus terminate with increasing iron content at a critical curve, or is the pigeonite limb terminated by reaction?

4. Is the hypersthene limb of the solvus terminated with iron enrichment by the breakdown of a ferrosilite-rich pyroxene to an olivine and tridymite, or is there a solvus on the hedenbergite-ferrosilite join as indicated by Barth (1951)?

Questions 3 and 4 revolve around the interpretation of pigeonite and the existence of ferrosilite. The experiments bearing on these subjects have been presented above in other connections. Question 2 can be answered by noting the presence of hypersthene and zoned subcalcic augite in the 1887 lava of Mauna Loa, Hawaii (Muir and Tilley, 1963, table 2). Question 1 has been attacked in the following ways.

The subcalcic augites in figure 15 labeled 1935B, 1887, and Koolau, when heated, were found to break up into an orthorhombic pyroxene and a clinopyroxene below the solidus and into two pyroxenes + olivine + liquid immediately above the solidus. Mixtures of equal portions of analyzed coexisting pyroxenes (N23, R62, and H165a) yielded two pyroxenes below the solidus and two pyroxenes + olivine + liquid imme-

diately above the solidus. It may be concluded that the subcalcic augites within these ranges of compositions are not stable at 1 atmosphere. It is believed that they should be considered metastable products formed during the slow natural quenching⁷ process.

The subcalcic augites labeled Koh, K7, and K10 gave conflicting results. The Koh specimen yielded one zoned clinopyroxene, whereas both K7 and K10 yielded two clinopyroxenes. The 1:1 mixtures of the analyzed coexisting pyroxenes of AC341 and A105 and a 3:2 mixture of the 4642A pyroxenes also gave conflicting results. The AC341 pair yielded multiply twinned clinopyroxenes, and the A105 pair formed two pyroxenes. The 4642A pyroxenes homogenized into a single clinopyroxene. Mixtures of natural end member pyroxenes or equivalents, Hd + En in the ratio of 1:1 (mole), yielded two clinopyroxenes. Clearly, this region of composition must be given more detailed study before the nature of the solvus can be outlined.

It should also be stated that there is no obvious reason why the trend of the metastable subcalcic augites outlined by Barth (1931), Kuno (1936), and Yoder and Tilley (1962, p. 366, fig. 4) for extrusive rocks is from the augites toward the pigeonites with iron enrichment. Such courses may be the fractionation curves of augites trending to the Cpx + Opx + Ol + L curves; however, it would appear from Kuno's pigeonitic series that the four-phase curves as now traced are crossed. The subcalcic augites of Koolau and 1887, both occurring with hypersthene, would appear to be examples of the limit of such fractionation curves. The

present data as well as the new work on $\text{CaMgSi}_2\text{O}_6$ - MgSiO_3 rule out the possibility of a complete series of solid solutions in the magnesium-rich part of the pyroxene quadrilateral under equilibrium conditions.

Pyroxene quadrilateral at 10 kilobars.

Recent studies have indicated that pressure has a significant effect on the polymorphism, extent of solid solution, and melting relations of the pyroxenes (Boyd and England, *Year Book* 60, p. 115; Yoder and Tilley, 1962, pp. 492, 501). For this reason some of the magnesium-rich natural pyroxenes plotted in figure 15 have been studied at various temperatures at 10 kb.

Although there are too few data to present the exact phase relations, some general observations may be made. The magnesium-rich olivine field of figure 16 appears to be absent at the elevated pressure. The melting range of pyroxene solid solutions is greatly reduced. The solid solution in the CaO-rich clinopyroxene is extended, the solvus being shifted toward the En-Fs join. One of the most important effects is the shift of the Opx + Cpx + L line toward the En-Fs join relative to the Ol + Opx + Cpx + L line position at 1 atmosphere.

There is little doubt that great care will have to be exercised in interpreting the pyroxenes observed in lavas. The phenocrystic pyroxenes may be inherited from depth. They are not in equilibrium with the groundmass pyroxene formed at the surface. The reaction relation of $\text{Ol} + \text{L} \rightarrow \text{Opx}$ which is absent at depth may produce complex relationships when it becomes effective in the magma reaching shallow depths. The narrow melting range of the pyroxenes at depth will bring about rapid compositional changes with small changes in temperature, and complex zoning may result.

Optics. The $2V$ curves of clinopyroxenes used for determinative purposes are in general based heavily on the results of synthetic studies. Of particular concern is the curve for $2V = 0^\circ$, one end of which

⁷ The word *quenching* is used in a specific sense here. A *quenched* product is a stable or a metastable phase formed at the run temperature brought quickly to room temperature, where it may be metastable. A *quenching* product is a phase that formed during the quick cooling process and may be metastable at all temperatures. The term *quench* product is used as a general term when the time of formation of a phase cannot be or has not been ascertained.

originates on the diopside-clinoenstatite join. The original point fixed by Bowen (1914, p. 249) was $\text{Di}_{33}\text{ClEn}_{67}$ (weight per cent). This composition has since been shown to lie within the solvus (Boyd and Schairer, *Year Book 61*, fig. 8). Apparently Bowen's runs at 1300° – 1350°C for several days were too short to reach equilibrium, and a single metastable phase was produced which only slowly exsolved. Crystals believed to be equilibrium products have been made, and measurements of $2V$ are now under way.

In the early work the $2V$ for pure clinoenstatite was given as $53\frac{1}{2}^{\circ}$ (Allen, White, Wright, and Larsen, 1909, p. 30), and this value was accepted by Bowen in 1914. In 1935 Bowen and Schairer indicated that all the synthetic clinopyroxenes along the join MgSiO_3 – FeSiO_3 have "a small optic axial angle of about 20 – 25° positive and the plane of the optic axes is $\perp 010$." The reasons for the drastic change were not given. The discrepancy was noted by Henry (1938, p. 28). Some determinative diagrams have not taken the change into account.

A cautionary note should again be recorded that TiO_2 may greatly affect $2V$. For example, Mawson (1950) reported two pyroxenes with $2V = 35^{\circ}$ and 40° which he interpreted as subcalcic augites approaching pigeonites. The pyroxenes are from rocks having 13.63 and 10.79 per cent, respectively, normative nepheline! It will be recalled that a uniaxial titaniferous (5.7 per cent TiO_2), high- CaO augite has been recorded by Dixon and Kennedy (1933, p. 112).

New Data on the System Diopside-Forsterite-Silica

I. Kushiro and J. F. Schairer

During the past year significant progress has been made in the study of the system diopside-forsterite-silica, which is important for an understanding of the crystallization of basic igneous rocks, particularly the basalts. Last year Schairer and Yoder (*Year Book 61*, pp. 75–82)

reported on preliminary studies of a portion of this system. Since then these studies have been expanded by Kushiro and Schairer to cover many additional compositions, and the quenching experiments were made with much greater precision in order to delineate accurately the complex crystallization processes that may take place over a small range of temperatures.

It was found necessary to employ small charges with calibration of the thermoelement before and after each run, and to conduct the experiments for considerably longer periods of time, to ensure attainment of equilibrium between the several crystalline phases and liquid. Rapid quenching of small charges in mercury was necessary to prevent any devitrification of the liquid phase during the quench.

Only a brief summary of some of the results obtained so far is presented here. A discussion of geological application must await completion of the studies of this complex system.

Nonbinary character of the system diopside-forsterite. Bowen (1914) suggested that the system diopside ($\text{CaMgSi}_2\text{O}_6$)–forsterite (Mg_2SiO_4) was binary with a eutectic at 88 weight per cent diopside, 12 per cent forsterite, at 1387°C . Present results, however, show that this system is not binary, because the diopside and forsterite crystallizing from it are not pure crystals of $\text{CaMgSi}_2\text{O}_6$ and Mg_2SiO_4 , respectively, but solid solutions with compositions off this join. The revised phase diagram is shown in figure 21, and the following new results are noteworthy.

1. The minimum liquidus corresponding to the eutectic of Bowen is not an invariant point but a piercing point at 89 per cent diopside, 11 per cent forsterite, at $1389^{\circ} \pm 1^{\circ}\text{C}$.

2. The liquidus of diopside solid solution has a maximum at about 95 weight per cent diopside. The temperature of the maximum is about 2° higher than the melting point of diopside, which is 1391.5°C by definition.

3. That diopside can contain about 5

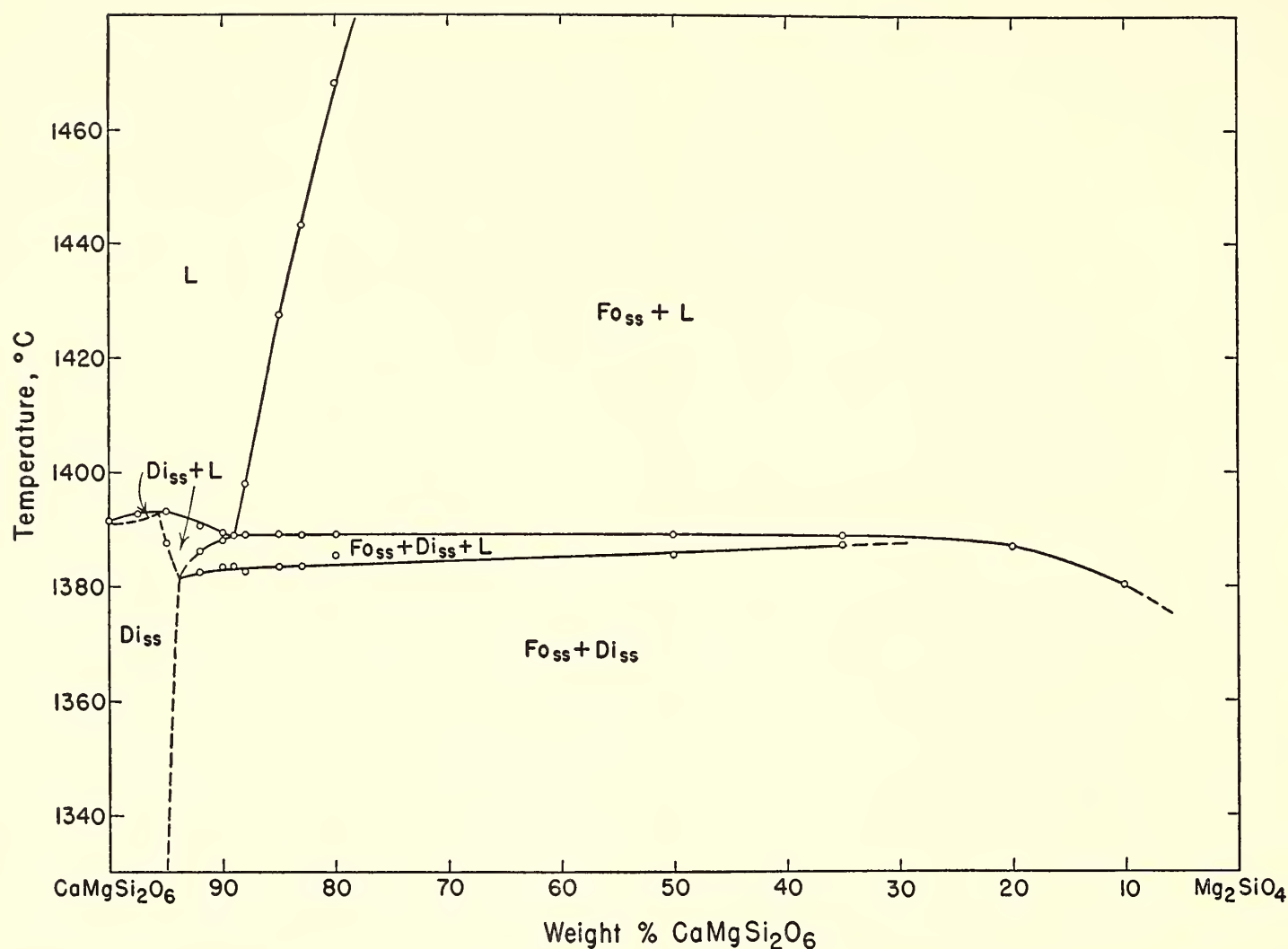


Fig. 21. Revised equilibrium diagram of the system diopside ($\text{CaMgSi}_2\text{O}_6$)-forsterite (Mg_2SiO_4). Fo_{ss} , forsterite solid solution; Di_{ss} , diopside solid solution; L , liquid.

weight per cent forsterite in solid solution, at least at temperatures above 1300°C , was ascertained by the following experiments. A mechanical mixture consisting of 95 weight per cent pure diopside, 5 per cent pure forsterite, was prepared. The X-ray powder pattern of the mixture shows distinct reflections of forsterite. After the mechanical mixture was heated at 1355°C for 7 days and at 1360° and 1370°C for 4 days the forsterite reflections disappeared. Glass of the same composition was also crystallized as diopside solid solution without forsterite at 1340° and 1370°C . This evidence indicates that about 5 per cent forsterite dissolved in diopside in solid solution. A glass of the composition 92 per cent diopside, 8 per cent forsterite, crystallized at 1350° and 1355°C contains forsterite. Therefore the maximum limit of diopside solid solution is less than 8 per cent forsterite and

probably about 5 per cent at temperatures above 1300°C , although it could be less than 5 per cent because of the limitation of X-ray resolution. The limit of solid solution would decrease with decreasing temperature. The presence of a maximum on the diopside liquidus may be explained by solid solution.

4. The temperature at which forsterite solid solution is joined by diopside solid solution progressively decreases as the forsterite content of the mixture increases for the compositions rich in forsterite. For the compositions between 11 and 65 per cent forsterite, forsterite solid solution is joined by diopside solid solution at 1389°C , whereas for the compositions 80 and 90 per cent forsterite, forsterite solid solution is joined by diopside solid solution at 1386° and 1380°C , respectively. These results indicate that there must be a small amount of solid solution in

TABLE 5. *d* Values of (130) Reflections of Forsterite Solid Solutions Crystallized at 1350°C from Mixtures of Different Compositions

Composition of Mixture, wt. %		Duration of Run, hr	<i>d</i> Value of (130) Reflection, Å
Di	Fo		
89	11	46	2.775 ± 0.003
88	12	46	2.776 ± 0.003
85	15	46	2.778 ± 0.003
83	17	46	2.775 ± 0.003
50	50	6	2.769 ± 0.002
35	65	96	2.770 ± 0.002
20	80	6	2.770 ± 0.002
10	90	6	2.768 ± 0.002
0	100		2.766*

* Yoder and Sahama (1957).

forsterite. The X-ray powder pattern of the crystals of forsterite solid solution shows slight but distinct differences from that of pure forsterite. Table 5 gives *d* values of the (130) reflection of forsterite solid solution crystallized at 1350°C from the mixtures of different compositions. As shown in the table, all the forsterite solid solutions have larger *d* values of the (130) reflection than pure forsterite. The *d* values of other reflections, (021) and (112), are also larger than those of pure forsterite. This evidence suggests that the Ca ion enters into forsterite, forming CaMgSiO₄ (monticellite) molecule.

5. The temperature at which diopside solid solution is joined by forsterite solid solution progressively decreases as the diopside content of the mixture increases for the compositions rich in diopside. This fact indicates that there must be a small amount of solid solution in diopside. It is probably a diopside containing MgSiO₃, Mg₂SiO₄, or both. The X-ray powder pattern of the crystals is appreciably different from that of the crystals of pure diopside. The values of Δ2θ[2θ(311) – 2θ(310)] of diopside solid solution crystallized at 1350°C from the mixtures of different compositions are shown in table 6.

6. The field of the three-phase assemblage Di_{ss} + Fo_{ss} + *L* exists between the fields of Fo_{ss} + Di_{ss} and Fo_{ss} + *L* or Di_{ss} + *L*. This evidence also indicates that the system is not binary.

Very careful measurements on the diopside-rich portion of the system diopside-enstatite. The system diopside-enstatite (MgSiO₃) has been studied experimentally by several investigators. Allen et al. (1909) and Bowen (1914) determined the liquid-solid relationships; Atlas (1952) studied the subsolidus equilibria. Recently Boyd and Schairer (*Year Books* 56, pp. 223–225, and 61, pp. 68–75) determined the solvus, finding that it intersects the solidus over a compositional interval of about 35 weight per cent.

The present experiments are concerned mostly with the liquid-solid relationships along the diopside-rich part of this join, which was investigated in connection with the determination of the liquid-solid equilibria in the system diopside-forsterite-silica. Figure 22 shows the revised phase equilibria for a diopside-rich part of the system diopside-enstatite. The point of projection of the ternary reaction point lies at 62.5 per cent diopside and 1386° ± 1°C (point *A*). Mixtures with

TABLE 6. Values of Δ2θ[2θ(311) – 2θ(310)] of Diopside Solid Solutions Crystallized from Mixtures of Different Compositions at 1350°C (Measured by CuKα^{III} radiation)

Composition of Mixture, wt. %		Duration of Run, hr	Δ2θ[2θ(311) – 2θ(310)], degrees
Di	Fo		
100	0		0.620 ± 0.005
89	11	46	0.594 ± 0.005
88	12	46	0.596 ± 0.005
85	15	46	0.592 ± 0.010
83	17	46	0.589 ± 0.010
50	50	6	0.583 ± 0.008
35	65	96	0.563 ± 0.015
20	80	6	0.386 ± 0.008
10	90	6	0.377 ± 0.020

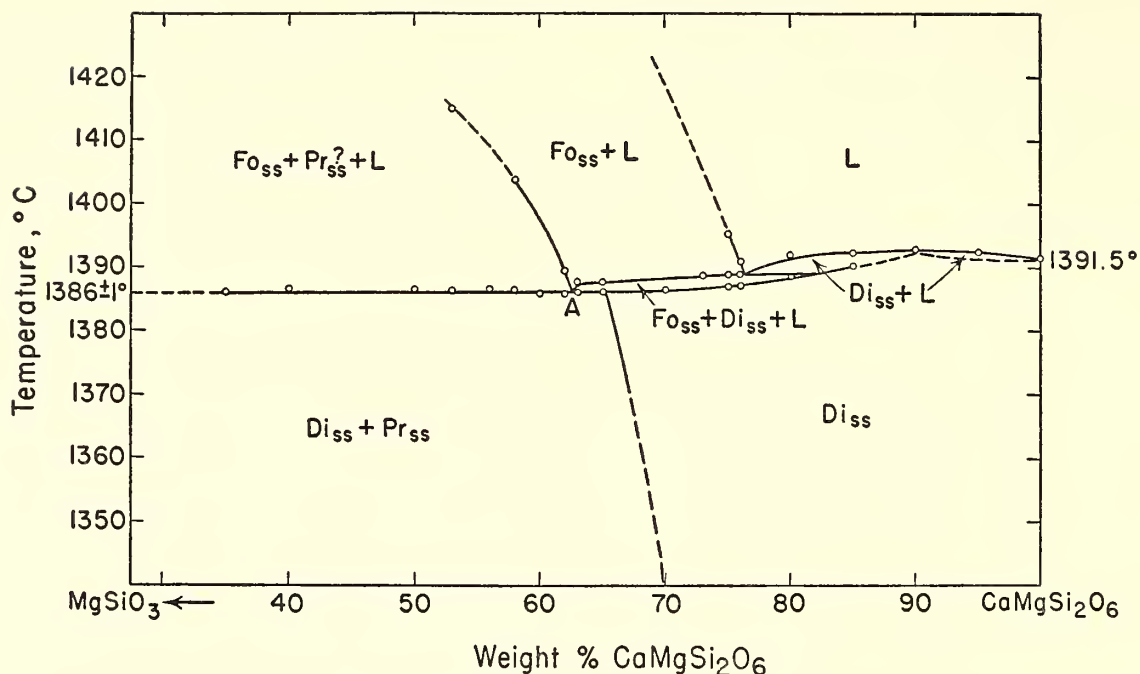


Fig. 22. Revised equilibrium diagram of the diopside-rich portion of the system diopside ($\text{CaMgSi}_2\text{O}_6$)-enstatite (MgSiO_3). Abbreviations as in figure 21; Pr_{ss} , protoenstatite solid solution.

compositions less than 62 per cent diopside contain clinoenstatite and forsterite solid solutions and a considerable amount of liquid with or without diopside solid solution at 1387° and 1388°C . However, at 1387°C , mixtures containing 63 and 65 per cent diopside do not contain clinoenstatite solid solution but consist of diopside and forsterite solid solutions and liquid. At temperatures below 1385°C all mixtures are completely crystalline, consisting of either two pyroxenes or a single pyroxene. These results indicate that protoenstatite and diopside solid solutions should crystallize simultaneously and forsterite solid solution should disappear at the point 62.5 per cent diopside at about 1386°C . In the experiments clinoenstatite solid solution was usually observed instead of protoenstatite solid solution. Assuming that protoenstatite solid solution is the stable Ca-poor pyroxene at high temperatures, as suggested by Foster (1951), clinoenstatite solid solution evidently formed from protoenstatite solid solution by inversion in the quench as discussed by Boyd and Schairer (*Year Book 61*, p. 69). The forsterite solid solution described here probably contains a small amount of Ca replacing Mg.

Boyd and Schairer (*Year Book 61*, pp. 70–71, figs. 8 and 9) indicated that diopside solid solution is stable below 1405°C for the compositions less than about 60 per cent diopside. In some runs of the present experiments, diopside solid solution was also observed at temperatures higher than 1387°C for the compositions less than 62 per cent diopside. We believe, however, that diopside solid solution is metastable under this condition. By comparing runs of long duration with short ones, we found that the amount of diopside solid solution relative to other phases was much reduced in the long runs above 1387°C in compositions with less than 62 per cent diopside. The quantitative change of diopside solid solution was observed by X-ray powder patterns. Figure 23 shows the X-ray powder patterns of (220) peaks of clinoenstatite and diopside solid solutions at 1390°C for the composition 53 per cent diopside. The extent of diopside solid solution is less for the run of 71 hours than for that of 22 hours. The same results were obtained for the mixtures 50 and 35 per cent diopside at 1390°C and a mixture 56 per cent diopside at 1388°C . Evidently, diopside solid solution, which is the principal constituent of the starting

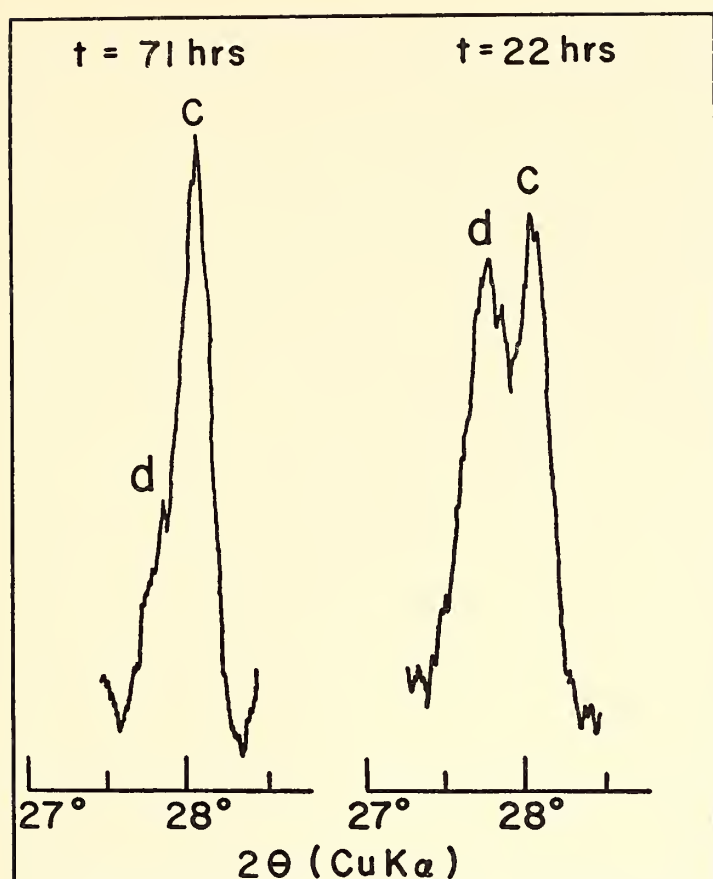


Fig. 23. Change of relative intensities of (220) reflections of diopside and clinoenstatite solid solutions with time of run (t). Temperature, 1390°C; composition of the mixture, 53 weight per cent diopside. The condition of the X-ray diffractometer is the same for both patterns (CuK α radiation). c, clinoenstatite solid solution; d, diopside solid solution.

material, persists above 1387°C in short runs, but its amount decreases with time.

There is a maximum on the liquidus of diopside solid solution at about 90 per cent diopside and 1393°C, which is inconsistent with the results obtained by Bowen (1914), although the temperature of the maximum is included within the error of his experiments (i.e., 1390° \pm 4°C).

The composition and temperature of the point where the liquidus of forsterite solid solution intersects the liquidus of diopside solid solution were determined as 76 per cent diopside and 1389°C, respectively, nearly identical with those determined by Bowen (1914) and Boyd and Schairer (*Year Book 61*, p. 69).

The liquidus of forsterite solid solution was determined for the compositions near 76 per cent diopside in the present experiments. It is the same as that determined by Bowen (1914).

The intersection of solvus and solidus of diopside solid solution lies at or beyond about 65 per cent diopside. A charge of composition 65 per cent diopside consists of two pyroxenes at 1375° and at 1380°C.

In these experiments we found a systematic change of 2θ difference between (311) and (310) reflections in the X-ray powder pattern of the diopside solid solution from pure diopside to Di₇₀En₃₀. Figure 24 shows the relation between the 2θ difference ($\Delta 2\theta$), measured by CuK α radiation, and composition of the diopside solid solution. Each $\Delta 2\theta$ value is an average of the values obtained by about ten successive oscillations. The $\Delta 2\theta$ changes from 0.620° for pure diopside to 0.340° for Di₇₀En₃₀. The (311) and (310) reflections are the strongest of the diopside solid solutions, and $\Delta 2\theta$ can be measured accurately. Therefore this method is useful for the accurate determination of the composition of the diopside solid solution in the pure CaMgSi₂O₆-MgSiO₃ series.

Résumé of new data on the system diopside-forsterite-silica. The new data on

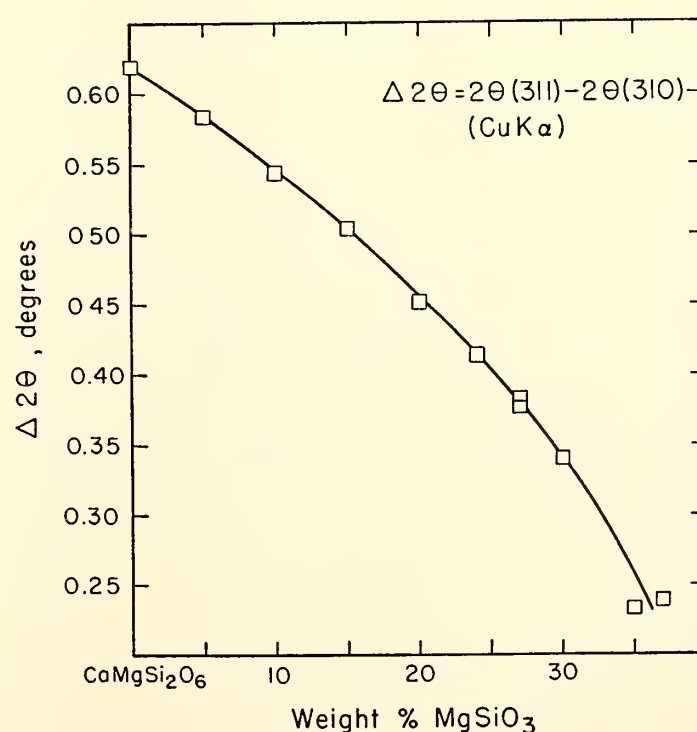


Fig. 24. Relation between composition and $\Delta 2\theta [2\theta(311) - 2\theta(310)]$ of diopside solid solution in the system diopside-enstatite (CuK α radiation).

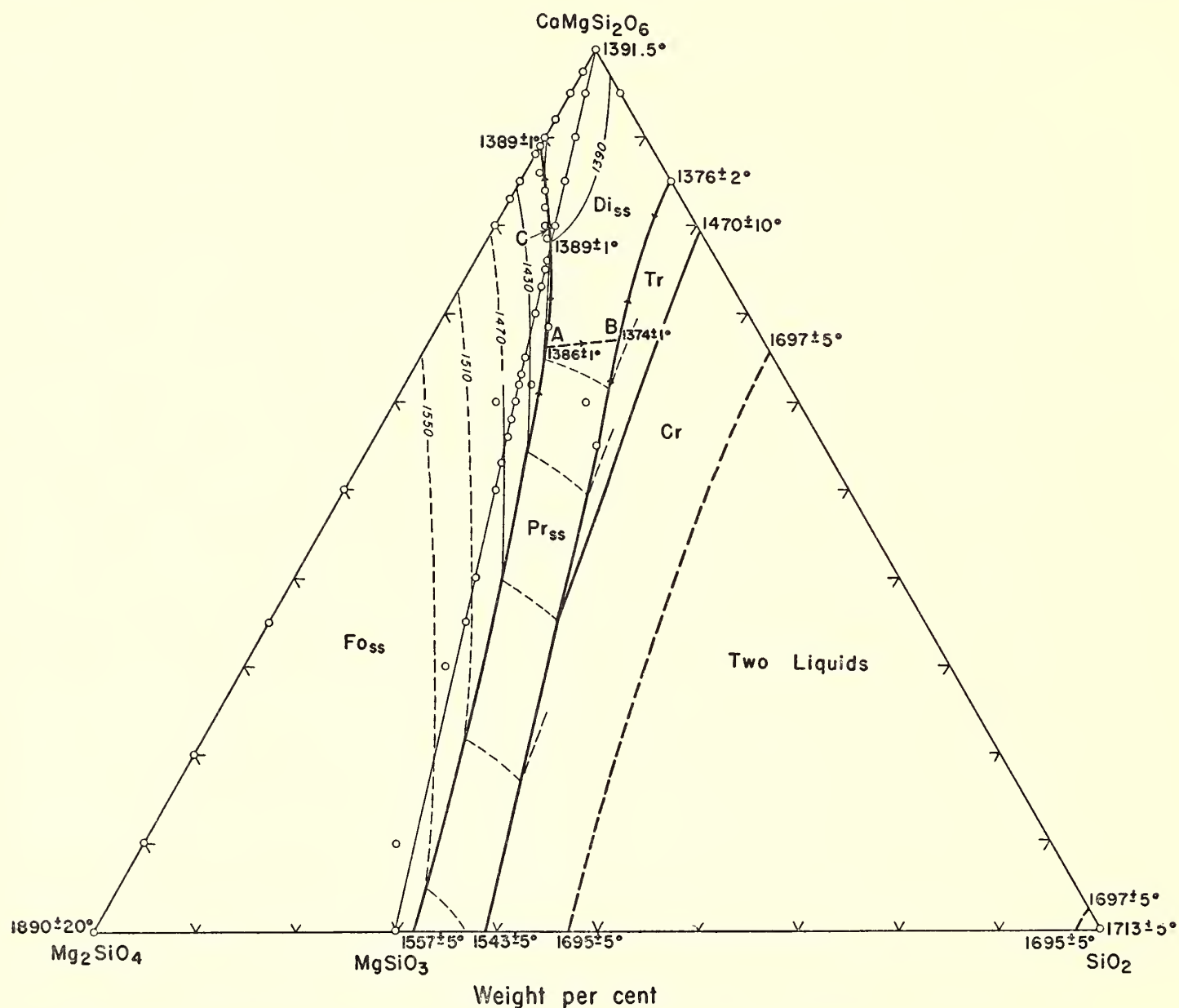


Fig. 25. Liquidus diagram of the system diopside ($\text{CaMgSi}_2\text{O}_6$)-forsterite (Mg_2SiO_4)-silica (SiO_2). Abbreviations as in figures 21 and 22. Cr, cristobalite; Tr, tridymite.

the joins diopside-forsterite and diopside-enstatite indicate that the liquid-crystal equilibria in the system diopside-forsterite-silica proposed by previous investigators require modification. New data on the ternary system are consistent with the new results on both joins. The principal results found in the present experiments follow.

1. A reaction point (A of fig. 25) exists on the Fo_{ss} -pyroxene boundary curve in the silica-oversaturated area.

2. A maximum on the Fo_{ss} - Di_{ss} boundary curve exists close to but slightly to the left of the point of intersection of the boundary curve and the Di-En join. It is indicated by C of figure 25.

3. The join Di-Fo is not binary, and consequently is not an equilibrium thermal barrier dividing liquids of enstatite-bearing composition from those of akermanite-bearing composition. However, the plane including forsterite solid solution, the maximum on the Fo_{ss} - Di_{ss} boundary curve, and diopside solid solution is a new thermal barrier dividing liquids that trend toward silica from those that trend toward akermanite.

4. There is a small *field* of diopside solid solution between the joins Di-En and Di-Fo.

The revised diagram of the system diopside-forsterite-silica is shown in figure 25. Except for the Di_{ss} - Pr_{ss} curve, loca-

tions of the boundary curves of the solid phases are very like those determined by Bowen (1914) and by Schairer and Yoder (*Year Book 61*, pp. 75–82).

Instead of a distribution point, there is a reaction point (*A*) at about $\text{Di}_{66}\text{Fo}_{22}\text{silica}_{12}$ and 1386°C . The temperature of this point was not determined directly but should be the same as the temperature of the point *A* in figure 22. The composition of the reaction point should be represented by the point of intersection of the Fo_{ss} -pyroxene boundary curve and the extension of the tie line between Fo_{ss} and *A* of figure 22. The point of the intersection could not be determined exactly, however, because of uncertainty of the exact composition of Fo_{ss} . At this point forsterite solid solution reacts with liquid to produce both diopside and protoenstatite solid solutions whose compositions are about $\text{Di}_{65}\text{En}_{35}$ and $\text{Di}_{25}\text{En}_{75}$, respectively.

The $\text{Di}_{\text{ss}}\text{-Pr}_{\text{ss}}$ boundary curve begins at the reaction point, but its exact location was not determined. Experiments are now in progress to find the exact position of point *B* of figure 25.

The maximum on the $\text{Fo}_{\text{ss}}\text{-Di}_{\text{ss}}$ boundary curve lies close to the point of intersection of the boundary curve and the join Di-En . It is represented by the point *C* in figure 25. The temperature of the maximum is $1390.5^\circ \pm 1^\circ\text{C}$, which is about 5° higher than the temperature of the reaction point and about 2° higher than that of the minimum on the liquidus of the join Di-Fo .

The presence of the maximum on the $\text{Fo}_{\text{ss}}\text{-Di}_{\text{ss}}$ boundary curve indicates that a silica-oversaturated liquid cannot change its composition to a silica-undersaturated composition. In other words, the maximum is an equilibrium thermal barrier. This conclusion significantly affects the expected course of fractional crystallization of basaltic magma; tholeiitic magma which is oversaturated with silica cannot produce olivine tholeiite magma or the silica-undersaturated differentiates by fractional crystallization. Other compo-

nents in the magma may change this conclusion.

Present data also throw light on the reaction relation between olivine and pyroxene. Bowen (1914) indicated that the resorption of forsterite could take place even in the silica-undersaturated area, but, according to the present data and those of Schairer and Yoder (*Year Book 61*, pp. 75–82), the resorption of forsteritic olivine cannot take place in the silica-undersaturated area, simultaneous crystallization of forsteritic olivine and diopsidic pyroxene taking place even in the silica-oversaturated area, although the area of simultaneous crystallization is small. The presence of the reaction point indicates that forsteritic olivine reacts with liquid to produce both Ca-poor and Ca-rich pyroxenes at the same time. The temperature interval in which forsteritic olivine reacts with liquid to produce diopsidic pyroxene is so small (less than 5°), however, that the temperature of the reaction point is easily attained. Accordingly, forsteritic olivine with a reaction rim of augite alone is not to be expected in natural tholeiitic rocks and is seldom found.

As shown in the previous section, the join Di-Fo is not binary, forsterite and diopside containing, most probably, monticellite and enstatite molecules, respectively. The probable tie lines between the coexisting forsterite and diopside solid solutions at 1350°C are shown in figure 26, and the three-phase triangles $\text{Di}_{\text{ss}}\text{-Fo}_{\text{ss}}\text{-L}$ at 1388° , 1385° , and 1380°C are shown in figure 27. The field of diopside solid solution is also shown. Compositions of forsterite solid solution have been estimated by assuming that the *d* value of the (130) reflection changes linearly from pure forsterite toward monticellite at compositions rich in forsterite. The maximum content of monticellite is about 8 per cent (about 2.9 weight per cent CaO) between 1350° and 1388°C . The compositions of the diopside rich in MgSiO_3 are estimated from the $\Delta 2\theta[2\theta(311) - 2\theta(310)]$. The maximum content of MgSiO_3 is about 27

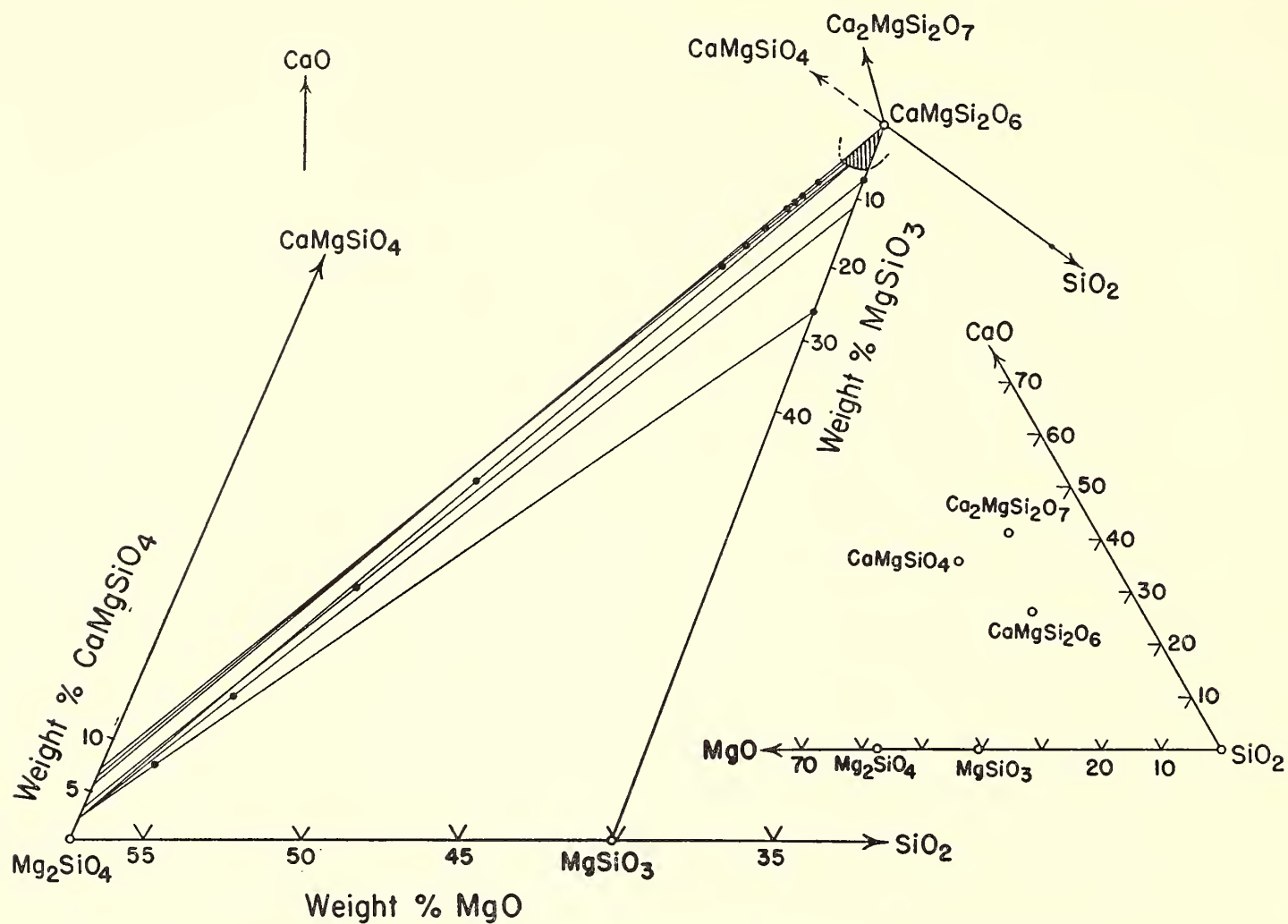


Fig. 26. The tie lines of coexisting forsterite and diopside solid solutions at 1350°C.

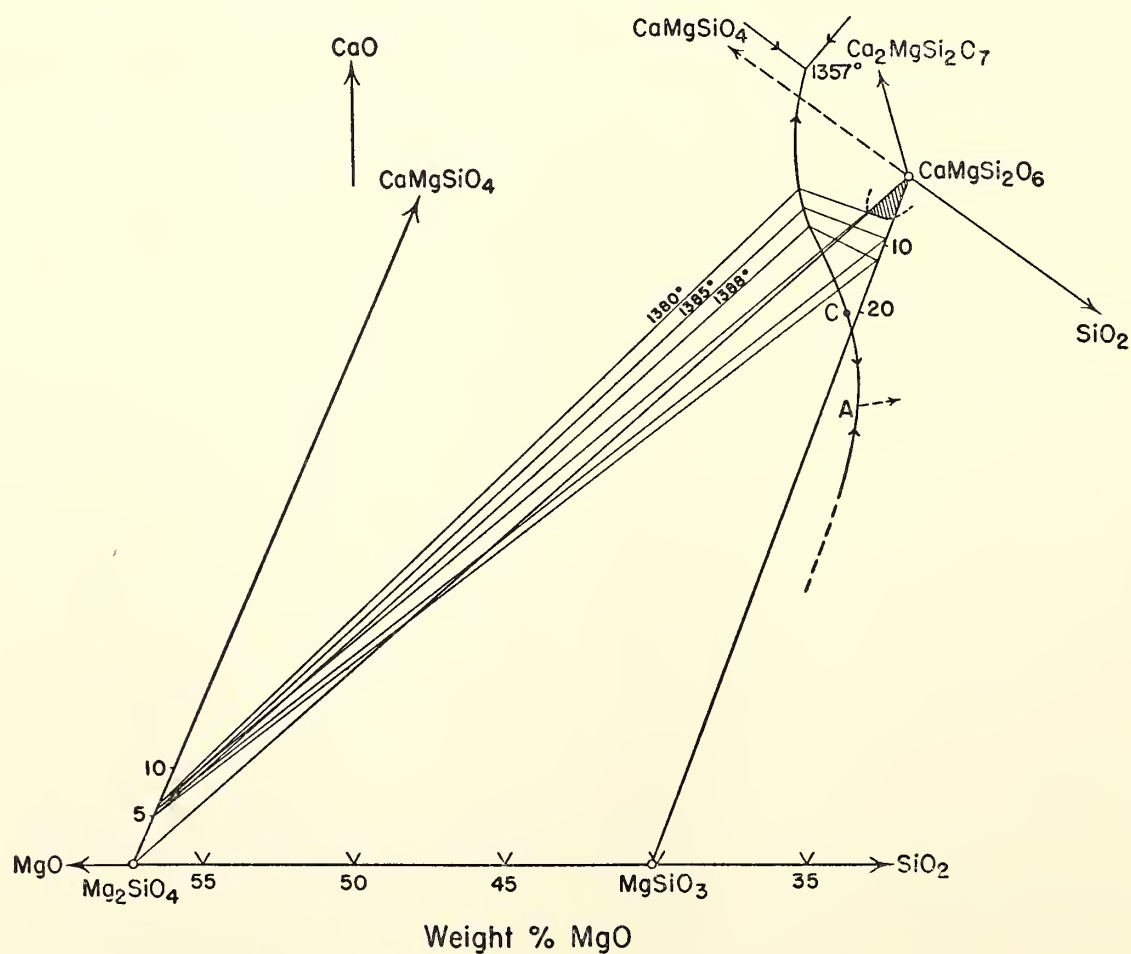


Fig. 27. Three-phase triangles at 1388°, 1385°, and 1380°C.

per cent in the same temperature range.

The three-phase triangle moves toward the ternary eutectic of diopside, forsterite, and akermanite with decreasing temperature, and at 1380°C the three-phase boundary leaves the join Di-Fo. Below 1380°C, therefore, no liquid is present in the system diopside-forsterite-enstatite. It is indicated from these considerations that the join Di-Fo is not a thermal barrier and that the liquid can change its composition from the enstatite-bearing composition to the akermanite-bearing composition across the join Di-Fo. Such behavior is expected for a liquid whose composition lies in a field Di-Fo-C in figures 25 and 27. (In this case Fo is not pure forsterite but solid solution containing the monticellite molecule. The content of monticellite molecule would be small, however, and Fo is approximately represented by pure forsterite.)

Therefore it is suggested that olivine basalt magma containing a small amount of hypersthene molecule could produce nepheline normative differentiates by fractional crystallization. (Akermanite molecule in the magma would change a part of albite to nepheline.) Thus the plane including diopside solid solution, the maximum (C) on the Fo_{ss}-Di_{ss} boundary curve, and Fo_{ss} is a new thermal barrier separating the olivine tholeiite magma from the alkali basalt magma, and the join Di-Fo is no longer a thermal barrier dividing these two types of basalt magma.

The existence of diopside solid solution on the join Di-Fo indicates that diopside has an area of solid solution between the joins Di-En and Di-Fo in the system diopside-forsterite-silica. Examination of the join Di-SiO₂ does not show a measurable amount of solid solution between diopside and SiO₂. A glass of the composition 95 weight per cent diopside, 5 per cent SiO₂, crystallized as diopside and cristobalite at 1320°C. This evidence suggests that the area of diopside solid solution is smaller in the silica-over-saturated area of this system.

The System Enstatite-Diopside at 30 Kilobars Pressure

B. T. C. Davis

The earth's upper mantle is of particular interest as the source of basaltic lavas. Several ultrabasic rock types—kimberlite, eclogite, and peridotite—have been suggested as representative of the composition of the upper mantle. Reasoning based on heat-flow and seismologic data supports the hypothesis that this region has an ultrabasic composition, but such reasoning cannot unambiguously ascertain the minerals present at depth or their relative abundances. All hypotheses yet proposed include pyroxenes rich in the end members enstatite, MgSiO₃, and diopside, CaMgSi₂O₆, among the minerals present. It is therefore of interest to examine phase relations in the system enstatite-diopside at a pressure equivalent to a depth of 100 km, representative of upper mantle conditions.

A considerable amount of information on phase relations in the system enstatite-diopside at low pressure is available from both experimental studies and the examination of natural assemblages. In addition, the effect of pressure on the melting of CaMgSi₂O₆ and MgSiO₃ has recently been determined (Boyd and England, 1963, and this report, respectively).

As is shown in figure 28, at 30 kb pressure the system enstatite-diopside is characterized by nearly complete solid solution at the solidus, with a narrow melting interval, and with peritectic relations in the enstatite-rich part of the system. All melting temperatures are substantially raised by the application of 30 kb pressure, diopside by roughly 325°C and enstatite by about 280°C. An inversion loop intersects both the solvus and the solidus, but the extent of solid solution at the solidus is much greater than in the same system at atmospheric pressure (Kushiro and Schairer, this report, fig. 22).

The present study was conducted using the single-stage apparatus (Boyd and

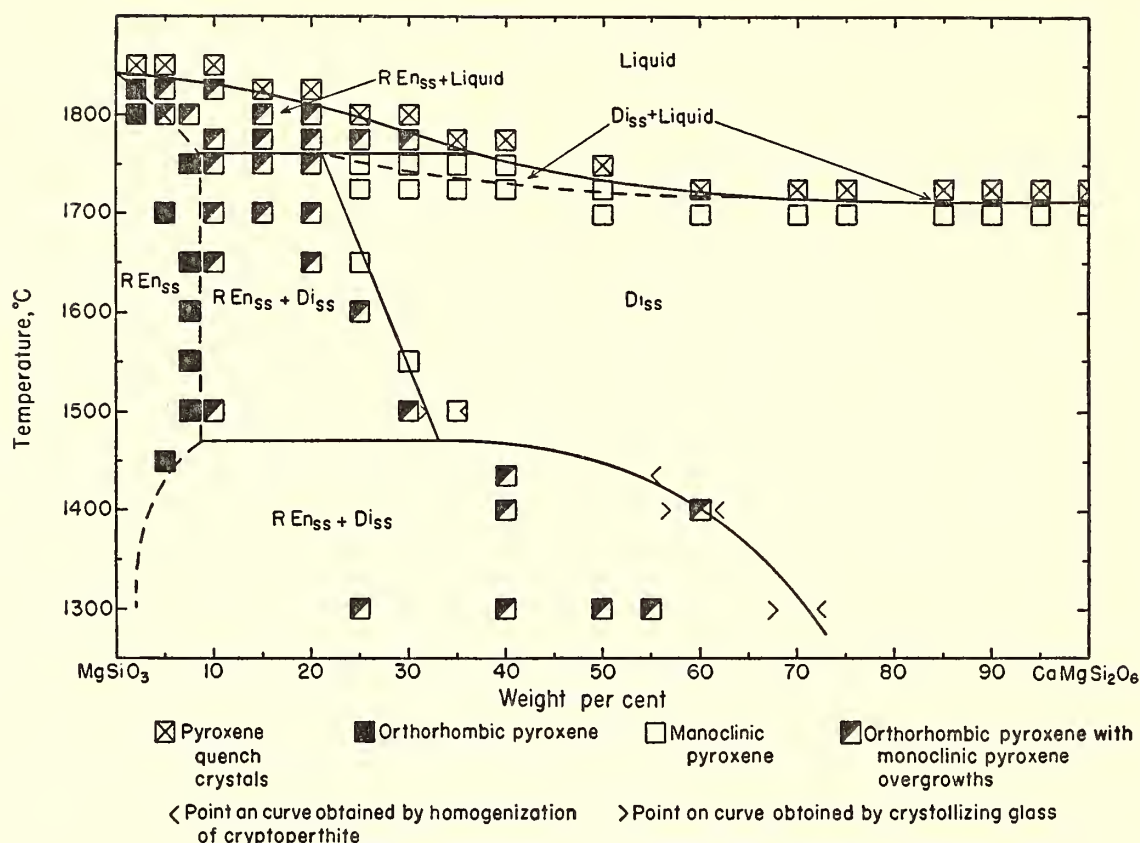


Fig. 28. The system $\text{MgSiO}_3\text{-CaMgSi}_2\text{O}_6$. P , 30 kb.

England, *Year Book 60*) and glasses prepared by Schairer. Reactants were heated to temperature at constant pressure. Products were quenched isobarically and examined by optical and X-ray methods.

Reactions fixing boundaries of phase fields were reversed wherever possible, but some uncertainties of interpretation remain. As has previously been noted by Boyd and England (*Year Book 60*), enstatite does not always quench to glass at high pressure; instead, it commonly forms distinctive, fibrous quench crystals. The same effect was noted above the liquidus in the present study for compositions containing more than about 25 per cent enstatite. Since quench crystals persist at solidus temperatures for times exceeding the stability of the thermocouple, so that it was not possible to reverse the liquidus, another method was used to confirm its location. Reactants were intimately mixed with 15 to 20 per cent platinum black. Above the liquidus the platinum settled out because of its high density. Below the solidus, silicate grains were uniformly sieved with fine platinum globules. The

liquidus determined in this fashion agreed within $\pm 10^\circ$ with that determined from silicate textures.

In the melting interval near enstatite composition a mixture of quench crystals and coarse, subhedral, primary orthopyroxenes is found below the liquidus. At lower temperatures within this interval, quench crystals do not form: most grains consist of subhedral orthopyroxene cores rimmed by thin, irregular overgrowths with inclined extinction. The presence of clinopyroxene in runs conducted at such temperatures was confirmed by X-ray powder patterns. Similar overgrowth textures characterize runs performed within the solvus and inversion loop, so that the solidus cannot be located by an obvious change in the texture of the runs. However, an isothermal lower boundary to the melting interval is required from phase-rule considerations by the presence of the peritectic. The peritectic relation orthopyroxene + liquid \rightleftharpoons clinopyroxene + liquid (inferred) has been reversed for four compositions between 21 and 38 weight per cent diopside.

A determination chart for clinopyroxene

was prepared using silicon (111) as internal standard, measuring the shift of the clinopyroxene (220) as a function of composition (fig. 29). This function is linear between 21 and 70 weight per cent diopside, with a slope of $0.007^\circ/\text{weight per cent diopside}$ and a reproducibility of ± 2 weight per cent. An unexplained break in slope occurs at 70 per cent diopside. The remainder of the function to pure diopside is also roughly linear, but with a slope of only $0.0035^\circ/\text{weight per cent}$, corresponding to ± 4 per cent.

It was not possible to establish a determinative curve for orthopyroxenes. The only orthopyroxene peak not subject to interference from clinopyroxene peaks and having pronounced compositional shift, (420), suffers interference from another orthopyroxene peak, (221).

The limit of solubility of enstatite in diopside was determined with excellent agreement between optical and X-ray methods. This boundary has been reversed at 1500° , 1435° , 1400° , and 1300°C by homogenization of cryptoperthites prepared at 1 atm by Boyd and Schairer. The position of this curve at 1300°C determined from cryptoperthite starting materials in a 24-hour run agrees within 3 per cent with that determined in a 12-hour run using glass as reactant.

Such good agreement is not found for

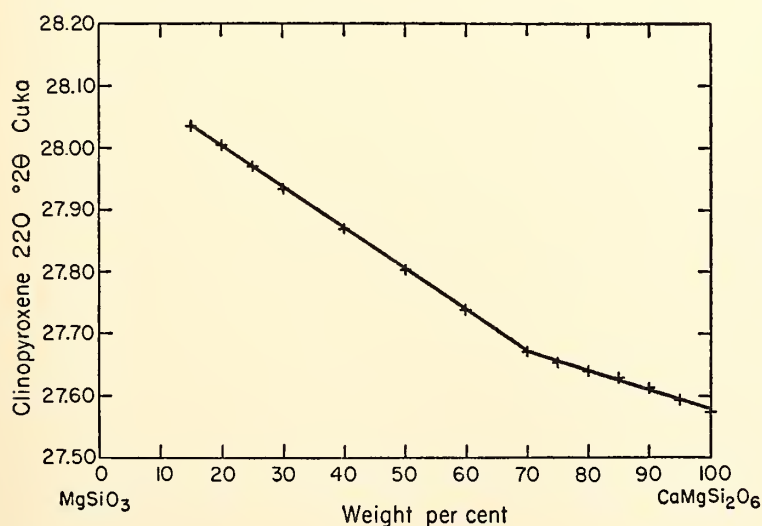


Fig. 29. X-ray determinative curve for clinopyroxenes on the join $\text{MgSiO}_3\text{-CaMgSi}_2\text{O}_6$. P , 30 kb.

the solvus boundary on the enstatite side. The clinopyroxene (221) peak in two-phase runs decreases greatly in intensity from 15 to 10 per cent diopside and is absent in $7\frac{1}{2}$ per cent diopside runs at all temperatures between 1500° and 1765°C , although a few overgrowths were found in some runs with 5 and $7\frac{1}{2}$ per cent diopside. Accordingly, the enstatite-rich side of the inversion loop is dashed in figure 28. Below 1500°C the solubility of diopside in enstatite should decrease, as is also shown by a dashed line in figure 28. Attempts to reverse this boundary are currently in progress.

Some noteworthy effects are produced in the system diopside-enstatite by the application of 30 kb pressure. First, the incongruent melting of enstatite-rich pyroxenes to forsterite + liquid disappears below 5 kb and does not recur in the range 5 to 40 kb (Boyd and England, this report). Second, the polymorphism of enstatite in the low-pressure diagram is eliminated, orthoenstatite being the stable polymorph at all temperatures investigated at 30 kb. Third, a much greater extent of solubility of enstatite in diopside is found on the solidus at high pressure. The flat liquidus and narrow melting interval on the diopside-rich side of the join are common to both low- and high-pressure diagrams. Finally, not only are the melting points of the end members increased by 30 kb pressure (diopside, 325° ; enstatite, 280°), but the temperature of the entire liquidus is raised proportionally.

In simple eutectic systems without solid solution the temperature of the eutectic will not be as greatly affected by pressure as the melting points of the end members, because of the effect of an entropy-of-mixing term on the free energy of the liquid (Newton, Jayaraman, and Kennedy, 1962). In continuous solid solution, however, no such great increase in the melting interval should be observed, for entropy-of-mixing terms occur in the equations describing both solid and liquid phase, and their effect should tend to

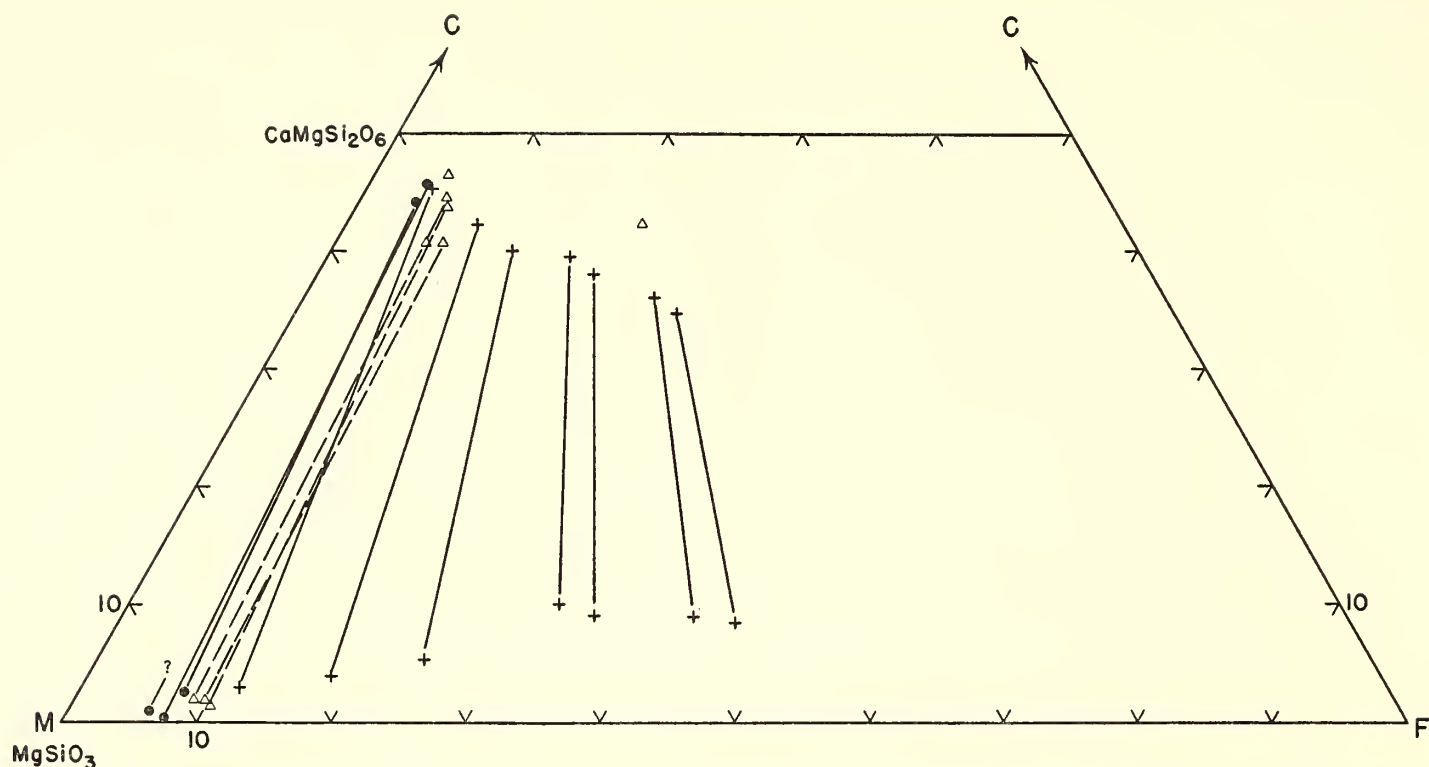


Fig. 30. C-M-F projection of some igneous pyroxene pairs (after Ross, Foster, and Myers, 1954; Brown, 1957; Wilshire and Binns, 1961; O'Hara and Mercy, 1963; and Banno, Kushiro, and Matsui, 1963). Triangles, pyroxenes from inclusions in alkali basalt; solid circles, pyroxenes from inclusions in kimberlite; crosses, pyroxenes from gabbroic rocks.

cancel. This is apparently the situation in the system diopside-enstatite.

Two ultramafic rock types that have particularly attracted the attention of petrologists as possible samples of the upper mantle are the inclusions in diamond-bearing kimberlites and the peridotite inclusions commonly found in alkali basalts. Both these rock types usually contain two coarse-grained pyroxenes, one with a composition approaching enstatite and the other with a composition near diopside. Data on the compositions of pyroxene pairs from such rocks are shown in figure 30, a standard C-M-F projection. These pyroxenes are poor in iron, and they rather closely approach the pure system MgSiO_3 - $\text{CaMgSi}_2\text{O}_6$; $\text{Mg}/(\text{Mg} + \text{Fe})$ ratios fall in the range 0.90 to 0.95. The influence of extraneous components like Al_2O_3 on the solid solution relations between such pyroxenes is not yet known quantitatively, but in the kimberlites this should not be a problem inasmuch as the Al_2O_3 contents of kimberlite pyroxenes are only 1 to 2.5 per cent. Al_2O_3 contents of

pyroxenes from mafic and ultramafic inclusions in basalts range up to 8 per cent, and the mutual solubility of these pyroxenes may accordingly depart significantly from the relations determined for the join MgSiO_3 - $\text{CaMgSi}_2\text{O}_6$.

Comparison of the phase relations shown in figure 28 with those determined at atmospheric pressure (Boyd and Schairer, *Year Book 61*, p. 70) shows that, although the melting relations are greatly changed, the position of the solvus on the diopside-rich side is not measurably affected by the application of 30 kb pressure. Thus the composition of a clinopyroxene in equilibrium with an orthopyroxene is predominantly a function of temperature. The temperature indicated by the MgSiO_3 contents of diopsidic pyroxenes from kimberlites is of the order of 1000°C . These rocks also contain diamond, and at a temperature of 1000°C the pressure required to stabilize diamond is about 40 kb (Bundy, Bovenkerk, Strong, and Wentorf, 1961), corresponding to a depth of about 125 km.

A temperature of 1000°C at a depth of

125 km is near the lower limit of the temperature range established by heat-flow measurements in the ocean basins (Verhoogen, 1960) and the electrical properties of the earth's interior (Tozer, 1959). Unless convection currents have locally raised the temperature at shallow levels in the mantle, the evidence from kimberlitic pyroxenes suggests that basaltic lavas with temperatures of the order of 1200°C have formed at depths in excess of 125 km.

The Join Diopside-Pyroxene at Atmospheric Pressure

M. J. O'Hara and J. F. Schairer

The join diopside-pyroxene, lying in the plane $\text{CaSiO}_3\text{-MgSiO}_3\text{-Al}_2\text{O}_3$ of the system $\text{CaO-MgO-Al}_2\text{O}_3\text{-SiO}_2$, intersects the sub-

solidus assemblage forsterite + anorthite + diopside + protoenstatite in a range of compositions that are analogous to natural tholeiitic olivine basalts. The study of compositions on this join and in neighboring parts of the plane $\text{CaSiO}_3\text{-MgSiO}_3\text{-Al}_2\text{O}_3$ continues the general study of the quaternary system and provides one of the most generalized models of natural basalts that has been studied to date. Results of quenching experiments on twenty-four mixtures on the join are presented in a pseudobinary diagram (fig. 31).

Stable and metastable pyroxene solid solutions. The inferred limits of stable pyroxene solid solutions at immediately subsolidus temperatures, and the assemblages stable under these conditions in

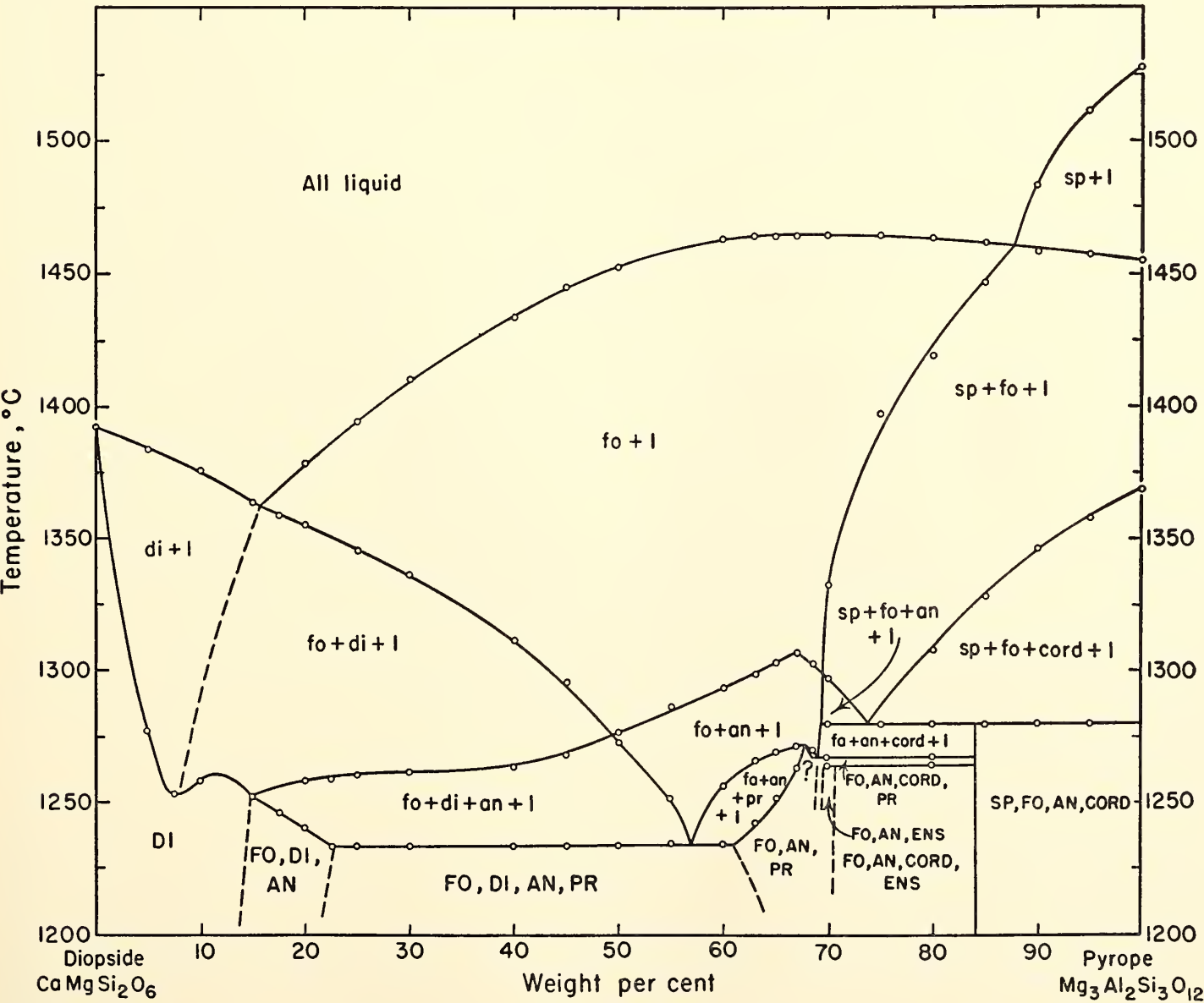


Fig. 31. Temperature-composition plot of data obtained on the join diopside-pyroxene at 1 atm. For abbreviations, see figure 32. Capital letters are used for entirely crystalline assemblages. Di and Pr signify diopside solid solutions and protoenstatite solid solutions irrespective of their composition.

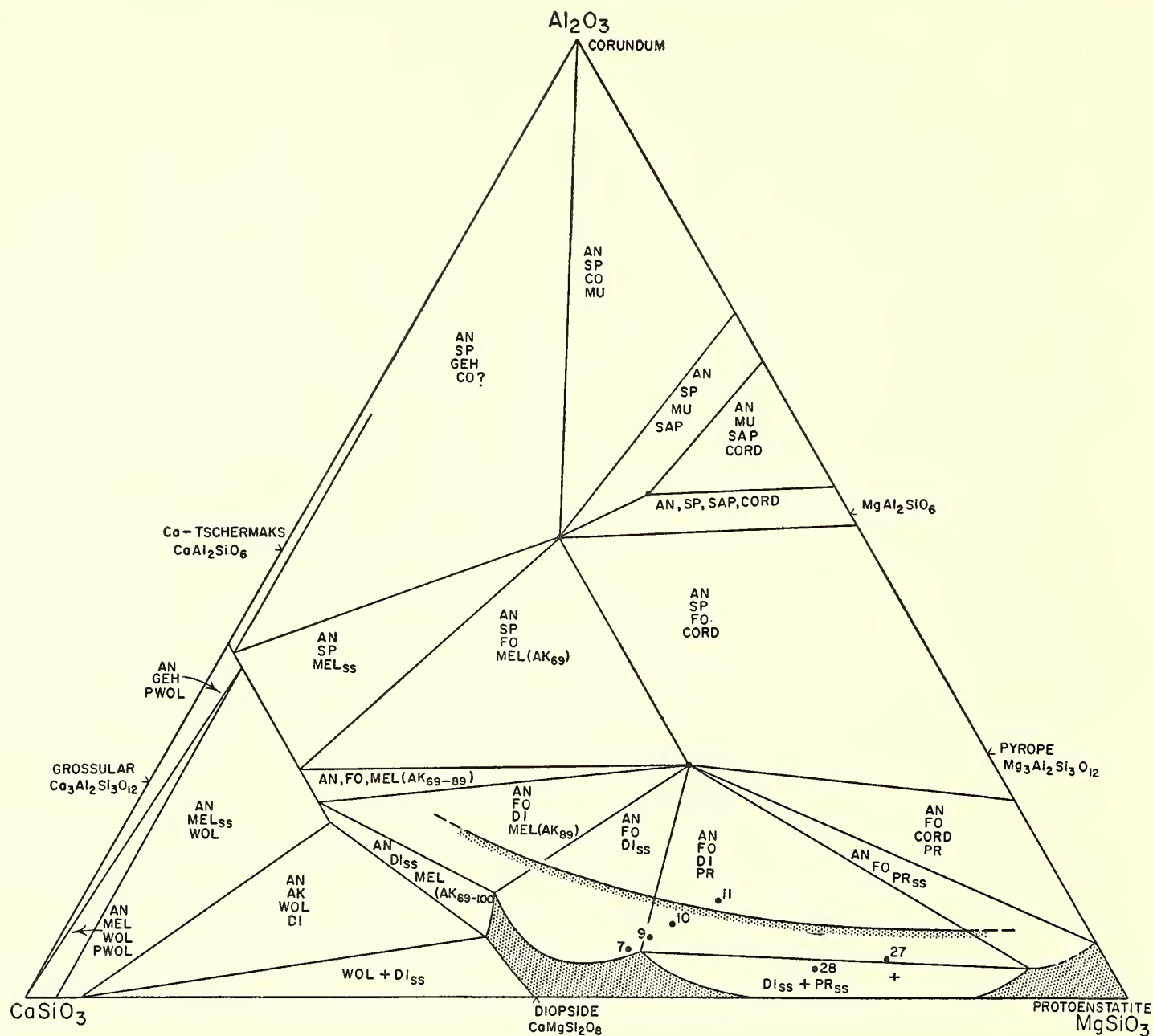


Fig 32. Plan of the mineral assemblages stable in various parts of the plane $\text{CaSiO}_3\text{-MgSiO}_3\text{-Al}_2\text{O}_3$ at the beginning of melting in each volume. The diagram is *not* an isothermal section. Based on limited data; solid solution effects in cordierite, spinel, sapphirine, and forsterite are neglected. N.B.: The join diopside-anorthite-spinel may exist between 1220° and 1240°C , replacing anorthite-forsterite-melilite.

AK, akermanite; AN, anorthite; CO, corundum; CORD, cordierite; DI, diopside solid solutions of fixed compositions; DI_{ss} , diopside solid solutions of variable compositions; ENS, enstatite solid solutions; FO, forsterite (olivine solid solutions); GEH, gehlenite; MEL_{ss} , melilite solid solutions; MU, mullite; PR, protoenstatite; PWOL, pseudowollastonite; SAP, sapphirine; SP, spinel; WOL, wollastonite.

The piercing points for the tie lines AN-SP, AN-FO, AN-SAP, and AN- MEL_{ss} are shown in the area of the triangle; those for MU-SP, MU-SAP, SAP-CORD, CORD-SP, and CORD-FO occur in this order on the join $\text{Al}_2\text{O}_3\text{-MgSiO}_3$.

Note that the four-phase volumes intersect the plane in quadrilateral areas *unless* three of the phases lie in or to the same side of the plane.

The shaded boundary shows an approximate limit to metastable clinopyroxene solid solutions at 1 atm, estimated from Hytönen and Schairer (*Year Book* 60, pp. 134-139), Sakata (1957), Segnit (1953), and new data. The inferred stable limits to diopside and protoenstatite solid solutions are shown, based on data by the above authors and some new data. N.B.: The compositions on the diopside-Ca Tschermak's molecule join containing 20, 25, 30, and 40 per cent Ca Tschermak's molecule, respectively, have been reexamined, crystallizing them from glass at 1220°C for 21 days. Forsterite is present in small amounts in the compositions with 30 and 40 per cent Ca Tschermak's molecule (contrast with subsolidus assemblages reported by de Neufville and Schairer in *Year Book* 61, fig. 1, where metastable diopside solid solutions are suspected to have formed on devitrification and to have persisted during their experiments).

various parts of the plane $\text{CaSiO}_3\text{-MgSiO}_3\text{-Al}_2\text{O}_3$, are shown in figure 32. The pyroxene solid solution field boundaries are *not* isothermal.

Metastable clinopyroxene solid solutions form readily during devitrification of mixtures lying outside the limits of stable solid solutions. An approximate limit to the range of compositions that can yield a homogeneous clinopyroxene under these conditions is shown in figure 32. [Schreyer and Schairer (1961) and Chinner and Schairer (1962) have commented on the formation of metastable *orthopyroxene* by devitrification of mixtures in the system $\text{MgO-Al}_2\text{O}_3\text{-SiO}_2$.] Glasses of the six compositions indicated by numbered points in figure 32 were devitrified at 1050°C , the conditions used in a previous study of alumina-bearing pyroxenes by Hytönen and Schairer (*Year Book 60*, pp. 134-139). Five of the compositions yielded a single clinopyroxene after 1 hour, and the sixth (no. 11) yielded clinopyroxene plus a small amount of forsterite and anorthite. The stable assemblages corresponding to these compositions may be read from figure 32. Practically no change occurred in any of the charges after 40 hours at 1050°C . After 50 days at 1050°C , compositions 7, 9, 10, and 11 apparently still consisted of a single clinopyroxene phase, accompanied by a trace of anorthite and forsterite in composition 11. Compositions 27 and 28 show the presence of a small amount of a second pyroxene, but the X-ray patterns do not resemble those obtained from the stable assemblages. The appearance of X-ray patterns from composition 11 shows that, even at 1180°C , 8 days of crystallization is not enough to yield a stable mineral assemblage, but that a further 7 days of crystallization at 1230°C is sufficient to yield the stable pyroxene compositions (fig. 33). Measurements of an X-ray parameter for the clinopyroxene solid solutions obtained from mixtures on the diopside-pyroxene join under various crystallization conditions are plotted against

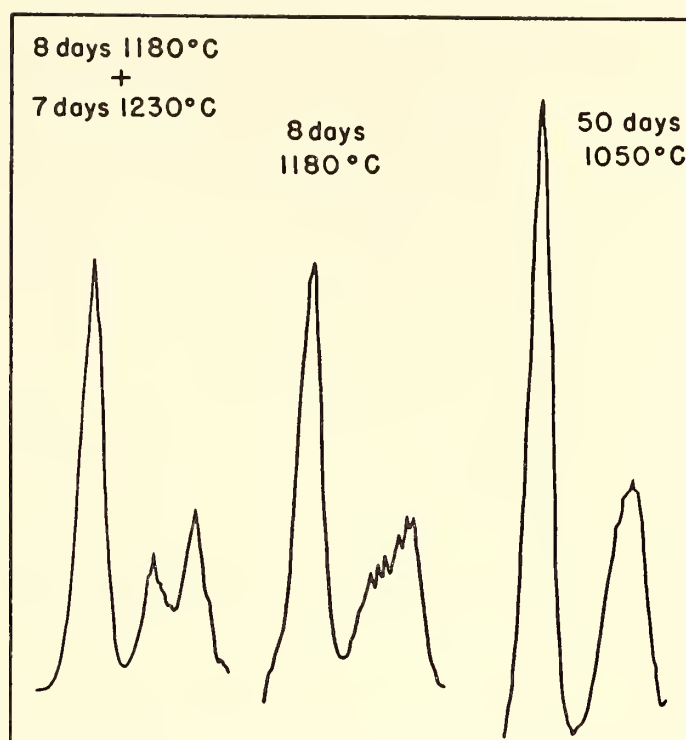


Fig. 33. Appearance of reflections from stable and metastable diopside solutions in X-ray diffractometer charts. Three samples of pyroxene obtained by different heat treatments of glasses having the composition diopside 60, pyroxene 40 are shown, each depicting the strong reflection at 29.7° $\text{CuK}\alpha$ radiation, and the neighboring peaks at 30° to 31° 2θ .

the bulk composition of the mixtures in figure 34. Two breaks in the curve for the stable pyroxene compositions indicate transition from the composition range represented by clinopyroxene only, to clinopyroxene + anorthite + forsterite, and from this assemblage to the two-pyroxene + anorthite + forsterite assemblage. In the last assemblage the pyroxene composition and the X-ray parameter do not vary with variation in the bulk composition of the charge.

These results indicate the need to devitrify the glasses at temperatures as near to the temperature of the beginning of melting as possible if stable products are desired. The ease of formation and subsequent persistence of the metastable pyroxene solid solutions, which have compositions analogous to those of subcalcic augites and pigeonites, may have important petrological applications among the extrusive igneous rocks (see Yoder, Tilley, and Schairer, this report).

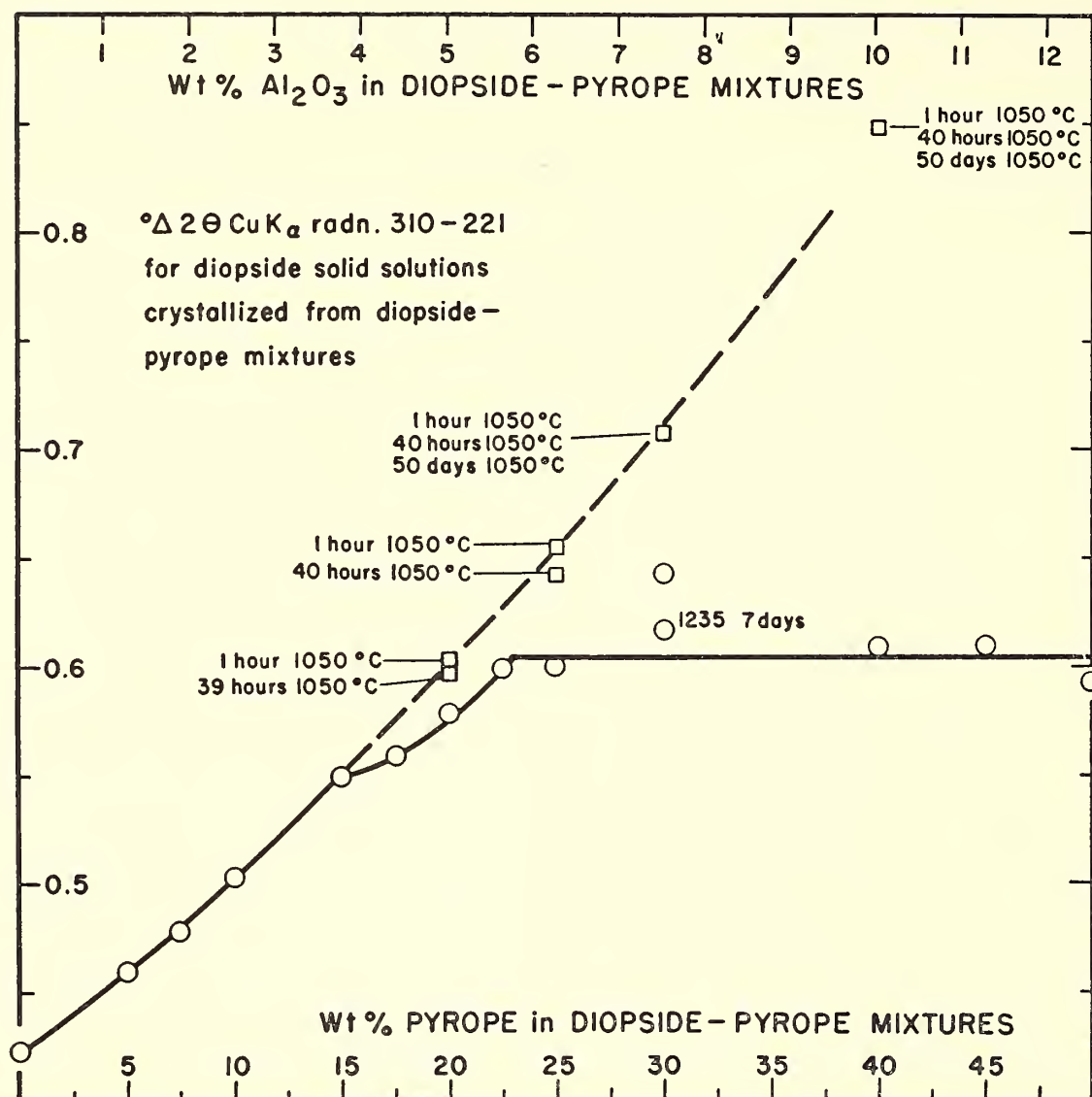


Fig. 34. Variation of an X-ray parameter of diopside solid solutions obtained from mixtures on the diopside-pyrope join. Unless otherwise stated, all mixtures were crystallized from glass for 7 to 9 days at 1180°C followed by 7 to 9 days at 1235°C . The solid curve expresses the variation in mixtures believed to contain stable pyroxene solid solutions.

The alumina content of the stable diopsidic pyroxene coexisting with melilite, anorthite, and forsterite appears to be greater than that from melilite-free assemblages, whereas the $\text{Ca}/(\text{Ca} + \text{Mg})$ ratio in these pyroxenes is greater than that of pyroxenes from melilite-free or protoenstatite-bearing assemblages (fig. 32). Provided that this behavior persists into the more general system containing FeO , Fe_2O_3 , Na_2O , etc., the results furnish an explanation of the relationship between alumina content and $\text{Ca}/(\text{Ca} + \text{Mg} + \text{Fe})$ ratio of the clinopyroxene and the magma type (tholeiitic or alkaline) commented on by Kushiro (1960) and Le Bas (1962).

Two-pyroxene assemblages in the pres-

ence of Al_2O_3 . Three glasses lying in the subsolidus composition field of diopside + protoenstatite, nos. 27 and 28 of figure 32, and one with the composition marked by a cross in the same figure, which contain respectively 4, 3, and 2 per cent Al_2O_3 , have been studied. The temperatures at which forsterite and then protoenstatite appear in the liquids on cooling are little different from those observed for mixtures of comparable Ca/Mg ratio on the diopside- MgSiO_3 join. The temperature at which the last liquid disappears on cooling is reduced to 1275°C in the mixture containing 2 per cent Al_2O_3 and to 1238°C in the mixture containing 4 per cent Al_2O_3 , a very large reduction from the 1386°C at which the alumina-free pyrox-

ene pair begins to melt. Alumina saturation of the coexisting pyroxenes is observed only in equilibrium with anorthite.

The $\text{CaSiO}_3/\text{MgSiO}_3$ ratios (weight per cent) of the diopsidic pyroxene that coexists with protoenstatite, forsterite, anorthite, and liquid is approximately 45:55; that of the diopside coexisting with protoenstatite at this temperature (1238°C) on the diopside-enstatite join is 40:60 (Boyd and Schairer, *Year Book 61*, pp. 68–75). Therefore the $\text{Ca}/(\text{Ca} + \text{Mg} + \text{Fe})$ ratios of natural coexisting pyroxenes precipitated from complex liquids in the presence of other crystalline phases cannot be used directly to obtain an estimate of the temperature of crystallization, because of this effect, even assuming that pressure effects on the solvus are small.

The ratio of normative diopside to total normative pyroxene in the *liquids* that coexist with forsterite and two pyroxenes falls from 65 per cent in the diopside-enstatite join (Kushiro and Schairer, this report) to ~ 50 per cent in the liquid that precipitates anorthite as well at 1238°C (estimated from Hytönen and Schairer, *Year Book 60*, fig. 22, and other, unpublished data).

Orthopyroxene. Orthopyroxene obtained from mixtures on the diopside-pyroxene join containing 70 to 84 per cent pyroxene (fig. 31) contains up to 6 per cent Al_2O_3 . It forms readily in glasses devitrified for 7 to 9 days at 1180°C , and persists unchanged for at least 7 days at temperatures as high as 1260°C . It has been observed only in mixtures lying within the composition volume anorthite-forsterite-enstatite-cordierite, and persists under conditions where the metastable orthopyroxenes recorded by Schreyer and Schairer (1961) and Chinner and Schairer (1962) break down quickly. The orthopyroxenes observed in the subsolidus of the diopside-pyroxene join are taken to be stable. The influence of alumina in stabilizing the enstatite structure relative to protoenstatite is particularly striking.

Note that the orthopyroxene inverts to protoenstatite solid solution shortly before the beginning of melting.

Position of the thermal maxima on the divariant⁸ equilibria anorthite + forsterite + diopside + liquid and anorthite + forsterite + protoenstatite + liquid. The thermal maximum on the divariant line anorthite + forsterite + protoenstatite + liquid is at $1273^\circ \pm 3^\circ\text{C}$, at a composition lying a little inside the tetrahedron anorthite-forsterite- MgSiO_3 -cordierite, and involves an alumina-bearing protoenstatite solid solution. In consequence, a mixture of anorthite, forsterite, and pure MgSiO_3 consists at 1265°C of a liquid whose CIPW norm contains a small amount of diopside, and a crystalline aggregate of anorthite, forsterite, and pyroxene whose norm contains a small amount of corundum.

The thermal maximum on the divariant “line” anorthite + forsterite + diopside + liquid lies at $1278^\circ \pm 3^\circ\text{C}$ and to the silica-poor side of the “plane” anorthite-forsterite- $\text{CaMgSi}_2\text{O}_6$. In consequence some bulk compositions whose CIPW norms contain dicalcium silicate may yield residual liquids during crystallization that contain normative enstatite. The interpretations of run data that lead to this conclusion are shown in figures 35 and 36.

Data supplied by Hytönen and Schairer (*Year Book 60*, pp. 139–141) and the conclusions of Chinner and Schairer (1962, fig. 8, p. 631) apparently suggest that the thermal maximum on this divariant “line” lies at some point inside the tetrahedron anorthite-forsterite- $\text{CaMgSi}_2\text{O}_6$ - MgSiO_3 , but the composition of the diopsidic pyroxene indicated as being present at the thermal maximum would have to lie in the two-pyroxene

⁸ Pressure has been retained as a variable property of the system, conferring an extra degree of freedom. The reason will be apparent below. The terms “point,” “line,” “surface,” etc., refer to the range of compositions within the quaternary system that describe the equilibria under *isobaric* conditions.

field, because of geometrical considerations.

Certain compositions lying near the anorthite-forsterite join but within the anorthite-forsterite-melilite-diopside tetrahedron (fig. 32) crystallize spinel at an early stage. Provided that the spinel is retained and reacts with the liquid, these

liquids finish their crystallization at the point *D* of Chinner and Schairer (1962, fig. 4). If spinel is fractionated from such a liquid at an early stage, the residual liquids may finish their crystallization at any point on the divariant "line" anorthite + forsterite + diopside + liquid between *D* and *X* (Chinner and Schairer,

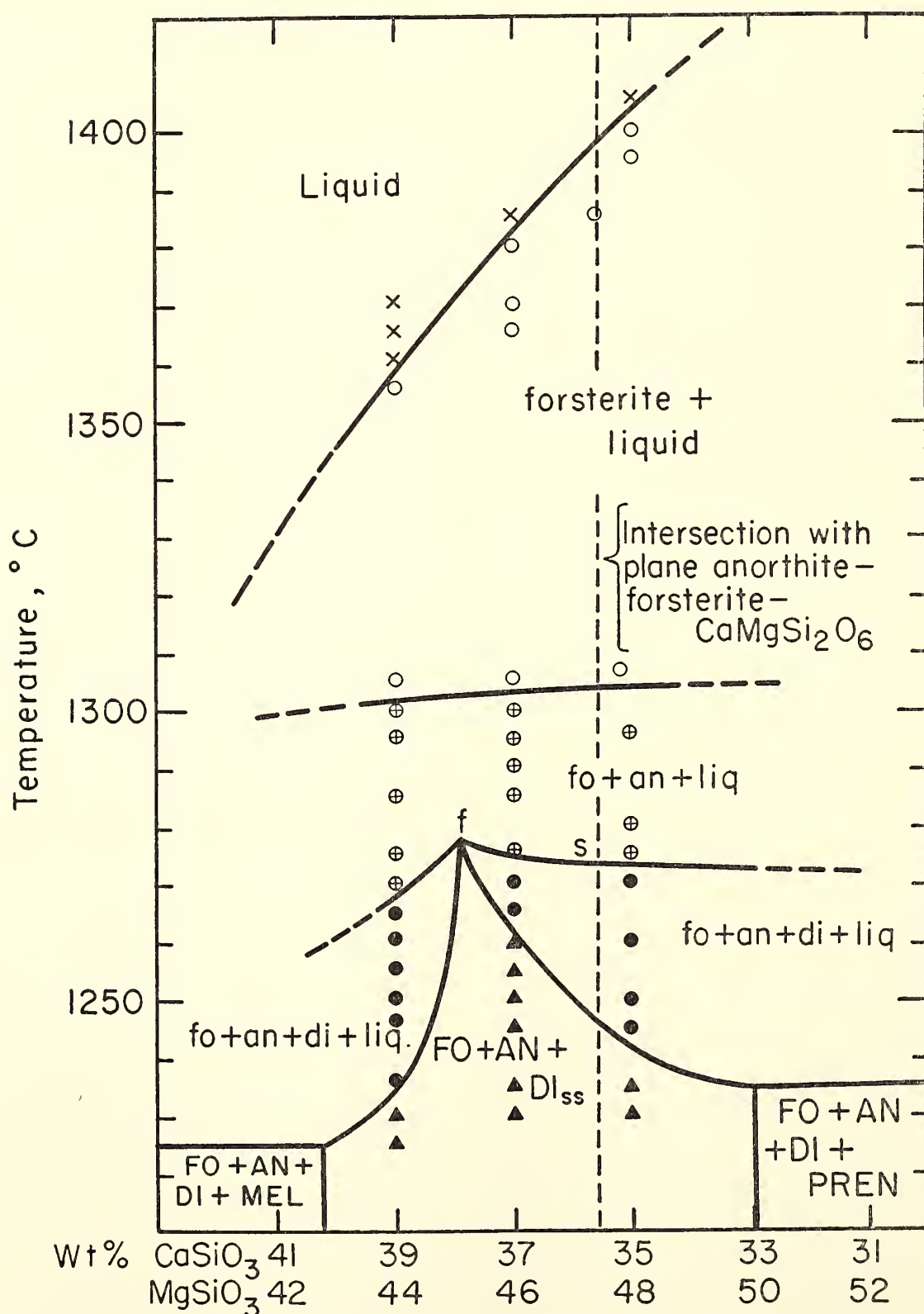


Fig. 35. Interpretation of data from three compositions on the pseudobinary join $(83\text{CaSiO}_3 + 17\text{Al}_2\text{O}_3) - (83\text{MgSiO}_3 + 17\text{Al}_2\text{O}_3)$ in weight per cent, bearing on the position of the thermal maximum, *f*, on the divariant line an + fo + di + liq, relative to the plane anorthite-forsterite- $\text{CaMgSi}_2\text{O}_6$. The plane forsterite-anorthite-diopside₉₁ + alumina₉ intersects this join at *f* (wollastonite₃₃ enstatite₄₅ alumina₁₇). Compare with figure 36.

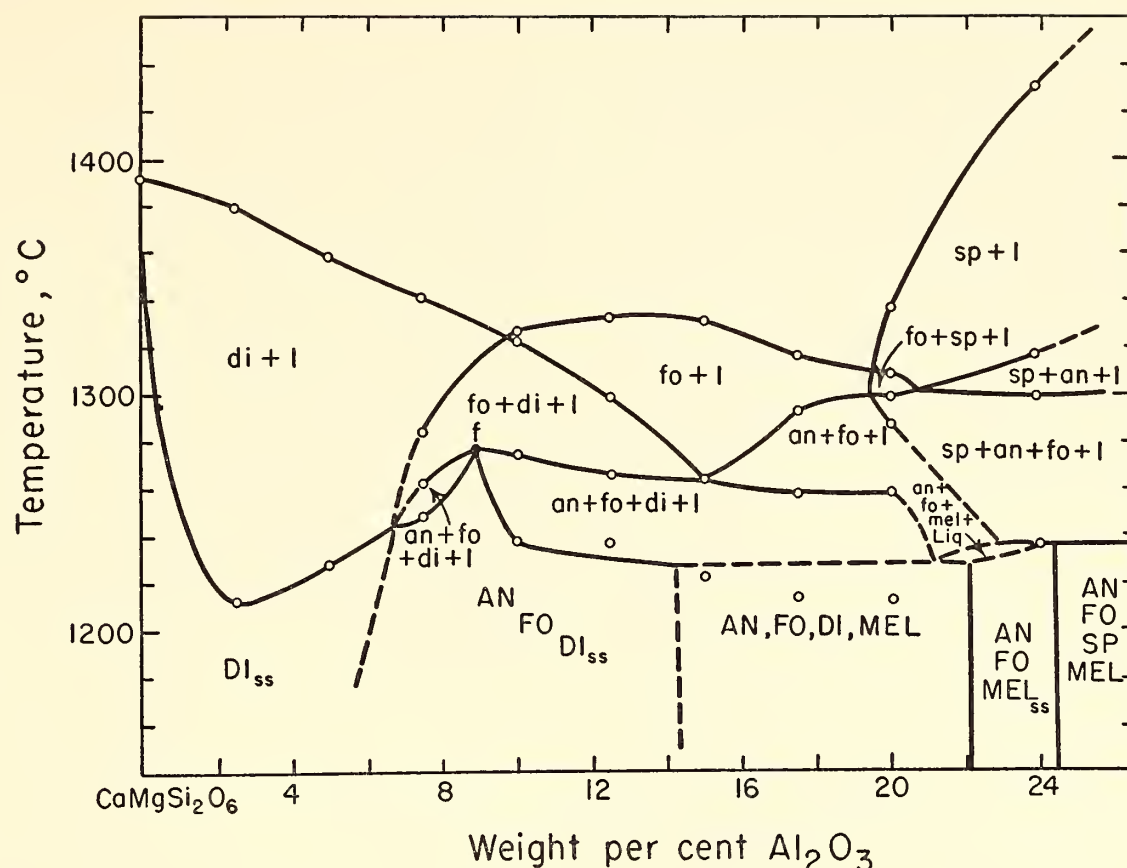


Fig. 36. Pseudobinary diagram of phase relations in the join $\text{CaMgSi}_2\text{O}_6$ - Al_2O_3 at atmospheric pressure. This is an interpretation based on the data of Hytönen and Schairer (unpublished) and Chinner and Schairer (1962) (this join intersects the garnet join at 23.9 per cent Al_2O_3). Note the inferred thermal maximum, f , on $\text{an} + \text{fo} + \text{di} + \text{liq}$. Note also that some of the beginning of melting data are assumed to be erroneous because of recrystallization of metastable devitrification products, that the invariant point anorthite + forsterite + diopside + melilite + liquid is drawn as a quaternary eutectic, and that the divariant line anorthite + forsterite + melilite + liquid is drawn with neither maximum nor minimum (the last two assumptions are discussed in the text).

1962, fig. 4) at temperatures between 1225° and 1278°C , the final crystalline products ranging from melilite-bearing assemblages to protoenstatite-bearing assemblages according to the proportion of spinel removed.

Our results, which will not be described in detail here, indicate that some compositions that lie to the enstatite-rich side of the plane anorthite-forsterite- $\text{CaMgSi}_2\text{O}_6$, and that crystallize diopsidic pyroxene as first or second phase, precipitate pyroxene crystals having a higher $\text{MgSiO}_3/\text{CaSiO}_3$ ratio than the liquid; i.e., the clinopyroxene contains an excess amount of enstatite molecule. Consequently some of the residual liquids pass into the larnite-normative volume during crystallization. If reaction between the early-formed diopside, rich in enstatite molecule, and the residual liquid is pre-

vented by removal of the pyroxene crystals, the residual liquid may finish its crystallization with the appearance of melilite.

Geological analogues of the compositions and trends discussed above are easily envisaged. If the behavior described persists into the more complex system represented by natural basaltic magmas it appears that there are several ways, deriving from several starting compositions, in which a liquid may yield alternative residual liquids, following an "alkaline" or a "tholeiitic" trend dependent upon the extent of fractionation, without change in pressure. If it is also true that pressure may move the position of the thermal maximum on the divariant line anorthite-forsterite-diopside-liquid, we may conclude that the "thermal barrier" that apparently separates liquids

following an "alkaline" trend from those following a "tholeiitic" trend may not be very efficient *under natural circumstances* at preventing the derivation of both main trends of natural basalts from a single parent liquid.

The quaternary invariant point anorthite + forsterite + melilite + diopside + spinel + liquid. The results of previous workers in the system $\text{CaO-MgO-Al}_2\text{O}_3\text{-SiO}_2$ (Osborn et al., 1954; Prince, 1954; De Vries and Osborn, 1957; Chinner and Schairer, 1962; de Neufville and Schairer, *Year Book 61*, pp. 56-69; and Hytönen and Schairer, unpublished data) suggest that the quaternary invariant point anorthite + forsterite + melilite + diopside + spinel + liquid must be at a pressure close to atmospheric, and at a temperature near 1230°C . Chinner and Schairer (1962, fig. 4) have presented a flow sheet for the system $\text{CaO-MgO-Al}_2\text{O}_3\text{-SiO}_2$ in which the isobaric invariant points (strictly, univariant equilibria) *C*, anorthite + diopside + melilite + forsterite + liquid, and *D*, anorthite + melilite + forsterite + spinel + liquid, are represented connected by the divariant equilibrium anorthite + forsterite + melilite + liquid, which as shown contains a minimum. The subsolidus phase volumes shown in figure 32 are drawn in accordance with this interpretation, as are those shown by de Neufville and Schairer (*Year Book 61*, fig. 1, p. 57). But this is not the only interpretation permitted by the data now available. The appearance of diopside at equilibrium in mixtures on the grossular-pyrope join (Chinner and Schairer, 1962) requires that the assemblage diopside + spinel + liquid be stable at atmospheric pressure, and that the stable assemblages at *immediately* subsolidus temperatures are not those drawn in figure 32. The assemblages anorthite + forsterite + diopside + melilite and anorthite + forsterite + melilite + spinel must be replaced at the beginning of melting by the assemblages anorthite + forsterite + diopside + spinel, anorthite + melilite + diopside

+ spinel, and melilite + forsterite + diopside + spinel.

The melting of these subsolidus assemblages gives rise to three quaternary univariant equilibria replacing the two labeled *C* and *D* by Chinner and Schairer (1962, fig. 4). A partial flow sheet showing the three new quaternary univariant equilibria and their connecting divariant equilibria is given in figure 37. This figure represents an alternative to the part of Chinner and Schairer's (1962, fig. 4) flow sheet near the univariant equilibria (isobaric invariant points) *C* and *D*.

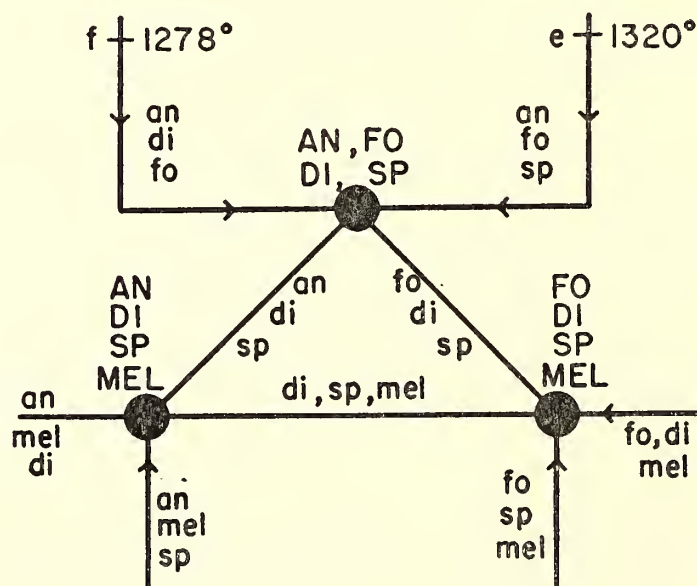


Fig. 37. Partial flow sheet for the system $\text{CaO-MgO-Al}_2\text{O}_3\text{-SiO}_2$ designed to replace the part of Chinner and Schairer's flow sheet (1962, fig. 4) near the points *C* and *D*. See text for explanation. Note that there is insufficient evidence to justify the placing of arrows on some of the divariant lines, and it is impossible to predict whether the univariant points are eutectics or reaction points.

We have not been able to prove or disprove the existence of a *stable* relationship diopside + spinel + liquid at atmospheric pressure. Difficulties arise from a possible phase transition in the subsolidus within a few degrees of the beginning of melting and from the small amounts of liquid present in the composi-

tions studied at the temperatures of interest. Diopside and spinel have been observed together in the composition diopside 50, Ca Tschermak's molecule 50, held for 3 weeks at 1240° and 1235°C, but they are accompanied by anorthite, forsterite, and melilite. One of these phases must be metastable.

Alternatively, the diopside encountered by Chinner and Schairer (1962) in compositions on the grossular-pyroxene join may be metastable. Results presented in this report on the ease of formation and persistence of metastable clinopyroxenes support such an interpretation. The flow sheet presented by Chinner and Schairer (1962, fig. 4) may then be the correct interpretation of the system at atmospheric pressure.

The reasoning that led Chinner and Schairer (1962, p. 627) to deduce that the relationship anorthite + forsterite + melilite + diopside + liquid is a reaction point where diopside is resorbed must be viewed in the light of the results of de Neufville and Schairer (*Year Book* 61, pp. 56–59). These results show that, for diopside to be resorbed at this isobaric invariant point, the isobaric univariant lines involving diopside must penetrate not only the plane anorthite-forsterite-akermanite but the plane anorthite-forsterite-melilite (Ak_{89}) as well. A derivation of the liquidus surface in this composition plane from the data of Osborn et al. (1954) and Prince (1954) gives no indication of the existence of a diopside + liquid field. Other data (de Neufville and Schairer, unpublished) do not prove or disprove the existence of a field of diopside + liquid in the plane anorthite-forsterite-melilite (Ak_{89}). Hence we must also retain the possibility that the equilibrium anorthite + forsterite + melilite + diopside + liquid is a quaternary isobaric eutectic. The flow sheet of Chinner and Schairer (1962, fig. 4) would then have to be modified either by allowing the isobaric univariant line anorthite + forsterite + melilite to flow down-temperature from point *D* to point *C* (eliminating the

minimum) or by placing a temperature maximum on this line between the point *C* and the minimum shown by Chinner and Schairer (1962, fig. 4). Note that the former of these two possibilities has been assumed in drawing the phase relationships of figures 35 and 36. The substitution of any of the alternatives would not affect the important feature of these two diagrams, which is the position of the thermal maximum, *f*, on the divariant equilibrium anorthite + forsterite + diopside + liquid.

Quartz norites and contaminated gabbros. The liquid that coexists with forsterite, spinel, cordierite, and $MgSiO_3$ pyroxene at 1265°C lies within the tetrahedron SiO_2 - $MgSiO_3$ -anorthite-cordierite (Chinner and Schairer, 1962, p. 628) and is one of the liquids that may be generated by the partial fusion of mixtures of quartz, enstatite, anorthite, and cordierite when mixed in proportions similar to those observed in natural pelitic rocks. This liquid will crystallize to quartz-anorthite-enstatite if separated from the crystalline phases at 1265°C (fig. 31), i.e., to a mixture analogous to quartz norite containing a small amount of normative corundum.

If the effect of pressure, or the presence of other components in the system, is such that the field of spinel crystallization is extended, the reaction points forsterite + anorthite + spinel + cordierite + liquid and forsterite + anorthite + enstatite + cordierite + liquid may become reaction points within the tetrahedron SiO_2 -diopside-enstatite-anorthite. Most of the liquid formed by the partial fusion process would then crystallize as quartz norite, or differentiate from quartz norite toward quartz gabbro. These considerations suggest that not only the cordierite norites (Chinner and Schairer, 1962, pp. 632–633) but some of the quartz norites and quartz gabbros observed in the border zones of contaminated olivine gabbros may also be essentially partial fusion products and not differentiated or contaminated gabbro.

The Join Diopside-Pyropite at 30 Kilobars

M. J. O'Hara

At 30 kb the pure phases diopside and pyrope (which represent the two essential minerals of natural eclogite) are stable. Phase relationships in the join diopside-pyrope may therefore yield information about the mineral paragenesis of eclogites. Because of the way in which the join lies athwart the tie lines between garnet solid solutions and clinopyroxene solid solutions and between garnet solid solutions and orthopyroxene solid solutions (see fig. 10), the subsolidus phase assemblages encountered along the join are clinopyroxene solid solution, clinopyroxene solid solution + garnet solid solution, clinopyroxene + orthopyroxene + garnet, and orthopyroxene solid solution + garnet solid solution.

Large amounts of Al_2O_3 enter both the orthopyroxene and the clinopyroxene (up to 11 per cent in the pyroxenes of the garnet-clinopyroxene-orthopyroxene assemblage at the beginning of melting). The clinopyroxene that coexists with garnet and orthopyroxene at 1600°C contains much less enstatite molecule than the clinopyroxene that coexists with orthopyroxene at the same temperature

and pressure in the system diopside-enstatite (see B. T. C. Davis, this report). This result is in agreement with that obtained from experiments on the natural mineral pairs of the garnet peridotite, 10596, described above. The garnet that coexists with two pyroxenes contains about 13 per cent by weight of grossularite, in good agreement with the composition of garnet from natural garnet-two pyroxene assemblages. Garnets containing less grossularite than 13 per cent are obtained from garnet-orthopyroxene assemblages. The orthopyroxene of the CaO-free assemblage pyrope-orthopyroxene has been determined to contain 16 per cent Al_2O_3 at 1675°C and 30 kb. These results are in qualitative agreement with the explanation of the scarcity of Al_2O_3 -rich pyroxenes in natural garnet-bearing assemblages suggested by O'Hara and Mercy (1963). It is obvious, however, that relatively low temperatures of equilibration of most natural orthopyroxene- and garnet-bearing granulites and eclogites are also very important factors in limiting the extent of Al_2O_3 substitution in the orthopyroxene.

The melting of mixtures in the diopside-pyrope join can yield important information about the nature of the equilibrium

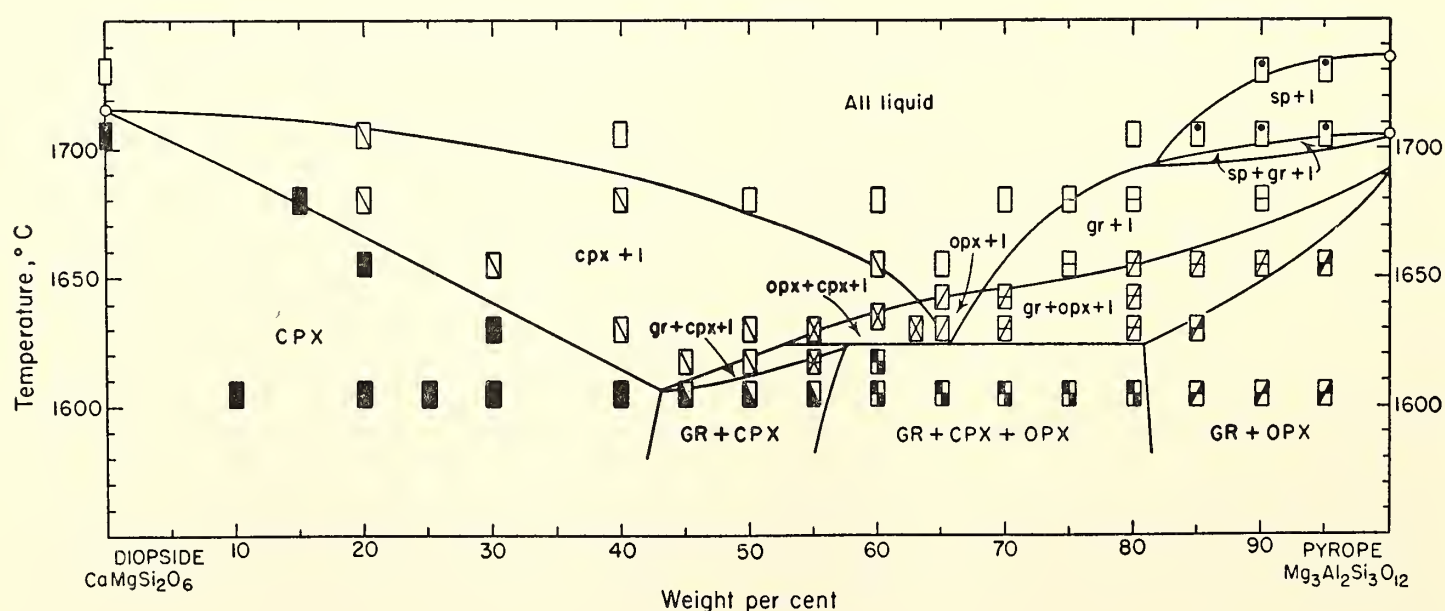


Fig 38. Preliminary diagram of phase relationships on the diopside-pyrope join at 30 kb pressure. Melting points of diopside and pyrope are taken from Boyd and England (1963, and *Year Book 61*, fig. 37). CPX, clinopyroxene; GR, garnet; OPX, orthopyroxene; *l*, liquid; *sp*, spinel. Capital letters used for wholly crystalline assemblages.

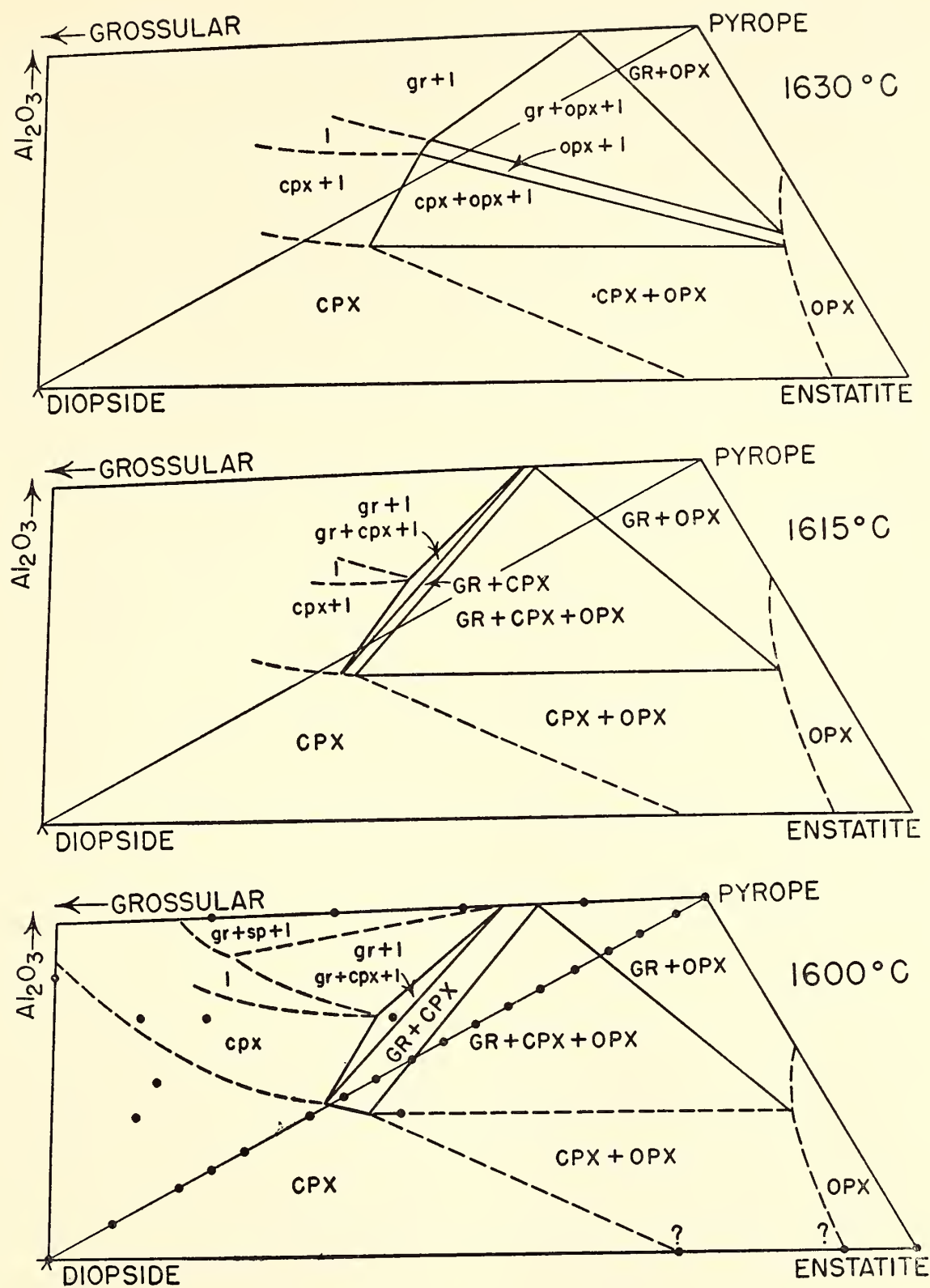


Fig. 39. Isothermal sections for part of the plane $\text{CaSiO}_3\text{-MgSiO}_3\text{-Al}_2\text{O}_3$ at 30 kb pressure. Data points are shown in the 1600°C section. Relationships in the 1615° and 1630°C sections are deduced from the relationships on the diopside-pyrope join. Abbreviations as in figure 38.

clinopyroxene + orthopyroxene + garnet + liquid. Unfortunately, the temperature intervals between solidus and liquidus are so small in the critically important region that it is difficult to determine the relationships by means of the present apparatus, which is subject to relatively large temperature uncertainties ($\pm 15^\circ\text{C}$). These difficulties are compounded by the

fact that two of the primary crystalline phases encountered in the presence of liquid (orthopyroxene and clinopyroxene) also appear as quenching products of these same liquids. In the presence of a large proportion of primary crystals the quenching products do not develop the characteristic spray texture but form overgrowths, often in optical continuity

with the primary crystals, in which the feathery texture and glass inclusions are discernible only with difficulty.

However, if the phase relationships in the join diopside-pyrope are ternary except for the appearance of spinel, as they appear to be within the present limits of observational error, there are several different ways to construct the phase diagram bearing in mind the subsolidus assemblages. In making one particular choice among these (fig. 38), great reliance has been placed on the observation that at 1600°C and 30 kb pressure the mixture diopside₄₅-pyrope₅₅ crystallizes to clinopyroxene + garnet with no orthopyroxene detectable by optical examination or X-ray study. At 1612.5° and 1625°C this same mixture yields orthopyroxene, clinopyroxene, and liquid, the orthopyroxene being readily detectable by optical examination and X-ray study. Thus, the assemblage garnet + clinopyroxene + orthopyroxene encountered in the subsolidus on the join diopside-pyrope begins to melt at a "ternary" reaction point at 1625° ± 15°C. Fractionation of liquids having compositions in the diopside-pyrope join with between 55 and 100 per cent pyrope leads to a unique residual liquid composition at 1625° ± 15°C. Further fractionation of this liquid (which can also be obtained directly as the first liquid appearing in the partial melting of the garnet + two pyroxenes assemblage) leads to a series of accumulates consisting of garnet solid solution + clinopyroxene solid solution, the residual liquid becoming depleted in MgSiO₃ and enriched in CaSiO₃ and Al₂O₃ during the process. These relationships are illustrated by the isothermal sections deduced for a part of the plane CaSiO₃-MgSiO₃-Al₂O₃ (fig. 39) at 1630°, 1615°, and 1600°C.

*Effect of Pressure on the
Melting of Enstatite*

F. R. Boyd and J. L. England

Evidence gained from petrographic study of rocks of mantle origin, such as

kimberlites, indicates that pyroxenes make up a substantial fraction of the upper mantle. Knowledge of the effects of pressure on pyroxene melting curves and on phase relations in more complex pyroxene systems is thus necessary for an understanding of the chemistry of the mantle. Preliminary data on the melting of enstatite to 30 kb were reported in *Year Book 60* (pp. 115-117). They have been revised and extended to 50 kb by techniques developed in determining the diopside melting curve (Boyd and England, 1963).

Our new results, shown in figure 40, confirm the disappearance of the incongruent melting interval of MgSiO₃ and the presence of a protoenstatite ⇌ rhombic enstatite inversion curve. Determination of the precise location of the triple point protoenstatite-rhombic enstatite-liquid proved impossible because of the sluggish nature of the inversion. Attempts to flux the reaction with small amounts of H₂O directly below the melting curve caused complete melting and obscured the inversion.

These new data over a more extended pressure range reveal a curvature that was not apparent in the preliminary diagram. A Simon equation has been fitted to the melting curve by a computer technique; the constants are given in table 7. Values for *A* and *c* are very similar to those found for diopside and albite. At 30 to 40 kb the slopes of these melting curves are about half their initial slopes.

Extrapolation of the enstatite curve to the pressure of 1400 kb present at the core-mantle boundary indicates a melting point of 3750°C. The same value is obtained by extrapolating the melting

TABLE 7. Simon Constants for Silicate Melting Curves

	<i>T</i> ₀ , °K	<i>A</i> , kb	<i>c</i>
Enstatite	1830	28.5	5.01
Diopside	1665	23.3	4.64
Albite	1391	19.5	5.1

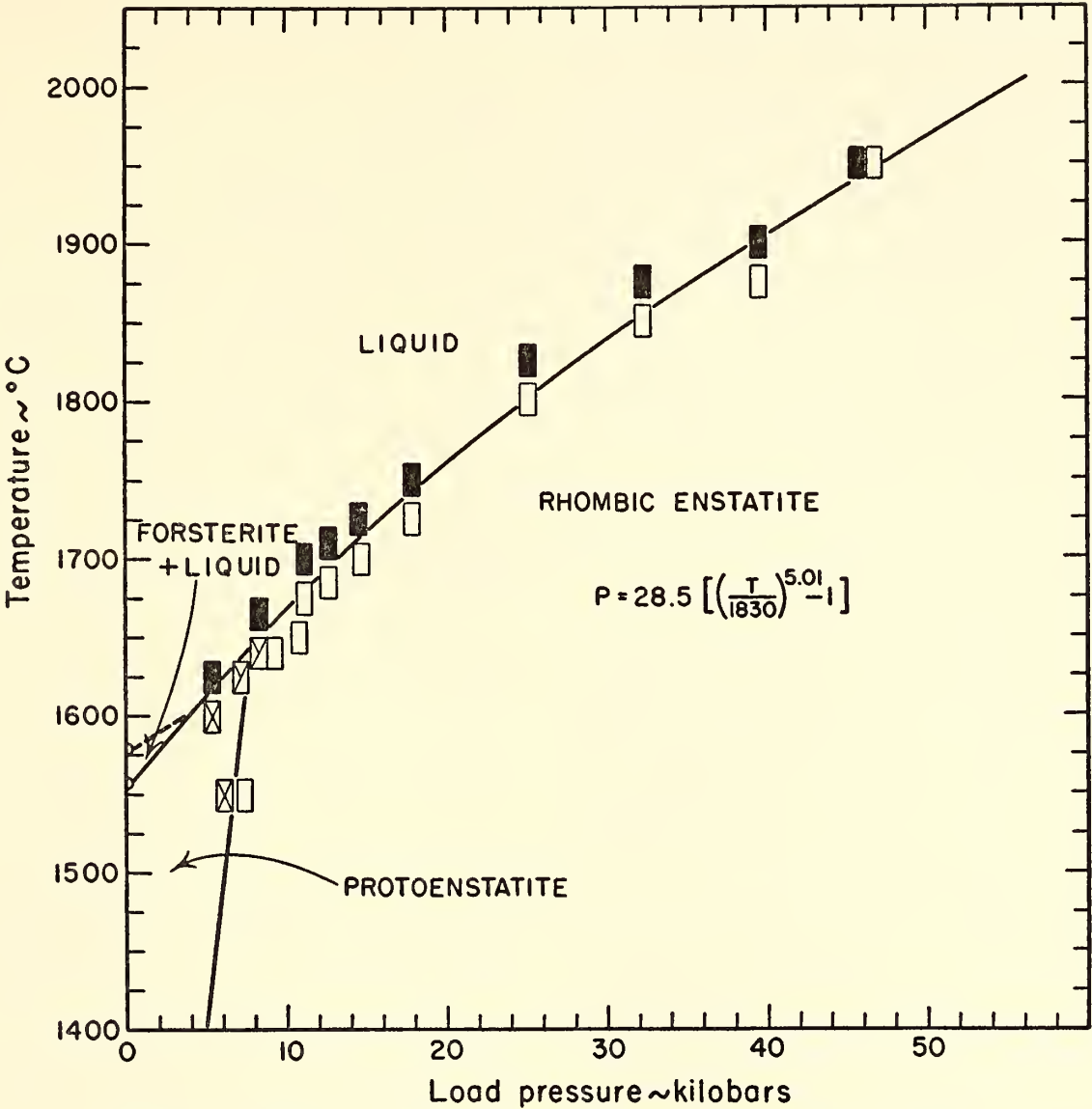


Fig. 40. Effect of pressure on the melting of enstatite, MgSiO_3 .

curve of diopside. For reasons previously discussed (Boyd and England, 1963), these estimates should not be taken literally. However, they are much lower than estimates based on silicate melting data obtained in a lower pressure range, and it is interesting that they are more in line with the expected melting point of iron at 1400 kb. As is shown elsewhere in this report, the melting point of iron at 1400 kb is estimated to be equal to or less than 5000°C.

*Melting of Forsterite, Mg_2SiO_4 ,
at Pressures up to 47 Kilobars*

B. T. C. Davis and J. L. England

Forsterite, Mg_2SiO_4 , is a major constituent in most proposed models for the earth's mantle. Knowledge of its melting behavior as a function of pressure combined with similar information for other

minerals permits rough calculation of the effect of pressure on the eutectic of any simple binary system in which Mg_2SiO_4 is a component and thus is useful in predicting compositional shifts in low-melting regions of silicate systems with pressure.

As is shown later, the change in melting temperature of forsterite with pressure is remarkably small, 5°/kb, and is linear, within the precision of measurement, to 47 kb. Because the melting curves of all other silicates so far investigated have steeper initial slopes, the application of pressure up to 30 kb should shift the eutectic of any simple binary system involving forsterite toward forsterite. Flattening of silicate melting curves to values approaching $dT/dP = 6^\circ/\text{kb}$ at higher pressure should confine the emphasis of this effect to pressures between 1 bar and 30 kb. Qualitatively, in more

complex systems, melting at higher pressure should yield more basic magmas, an effect already predicted from thermochemical data at atmospheric pressure (Kushiro and Kuno, 1963).

The equipment for this study is the single-stage apparatus of Boyd and England (1963). At temperatures exceeding 1800°C and pressures less than 12 kb considerable trouble was experienced from the melting of ceramic inserts in the furnace assembly and the diffusion of contaminants through the graphite reaction capsule. The difficulty was overcome by substituting molybdenum for graphite in the reaction capsule. Olivines grown in molybdenum capsules were X-rayed and found not to differ in cell size from pure Mg_2SiO_4 . Furthermore, because of the high temperature involved, instead of platinum thermocouples W/75 W-25 Re thermocouples were used; they were found satisfactory to temperatures as high as 2200°C. They were calibrated by comparing a tungsten-alloy thermocouple with a Pt/Pt-10 Rh thermocouple at various pressures and at temperatures up to the melting of the platinum thermocouple. The curve obtained, extrapolated to 2200°C, is shown in figure 41.

The EMF/temperature curve obtained for the tungsten-alloy thermocouple in this study (fig. 41) is of the same form as one determined at atmospheric pressure (Nadler and Kempter, 1961, fig. 3) but lies at consistently higher EMF values for a given temperature. The reason for this difference is not certain; it may be due to a variability in composition of different batches of the tungsten alloy. To further establish the validity of the present curve, the melting points of two silicates previously determined with Pt/Pt-10 Rh thermocouples were redetermined with the tungsten-alloy thermocouple. At 30 kb the melting of diopside (1715°C) was found to lie between 1700° and 1730°C; at 40 kb the melting of enstatite (1905°C) was found to lie between 1895° and 1925°C.

At constant temperature the ΔEMF of

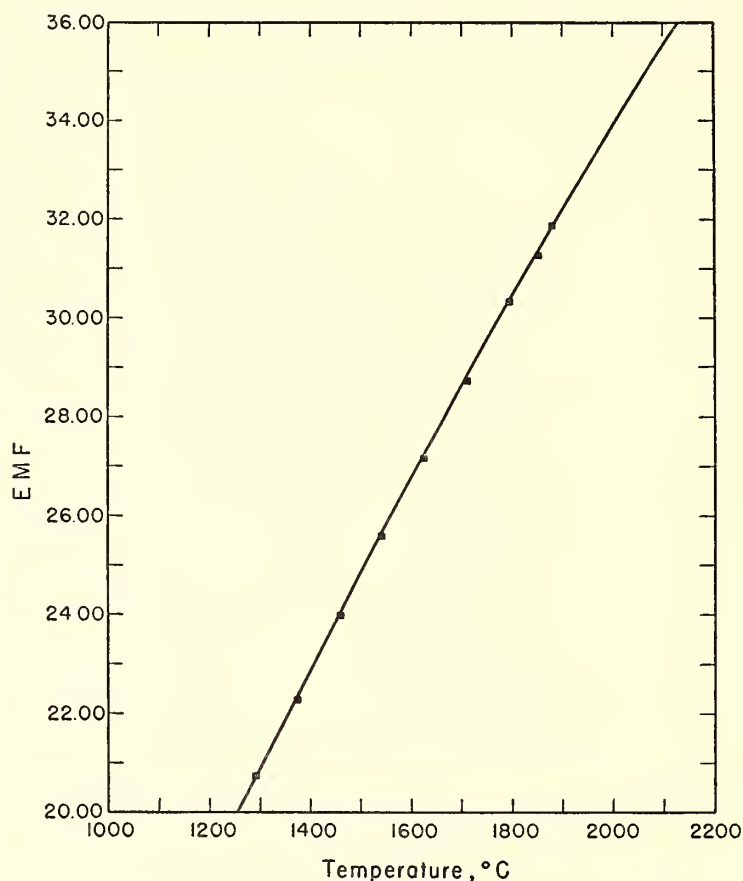


Fig. 41. EMF of W/75W-25 Re thermocouple at elevated temperatures and pressures, in millivolts.

platinum-alloy and tungsten-alloy thermocouples was found to be independent of pressure in the range 10 to 40 kb. Either the effect of pressure on the EMF of both thermocouples is of the same sign and magnitude, or, more likely, it is negligible.

The forsterite used was microcrystalline Mg_2SiO_4 prepared by Schairer. Runs were brought to temperature at constant pressure, held for 1 minute, and quenched isobarically. Products were subsequently examined optically and X-rayed to ensure the absence of contamination. No phases other than forsterite were encountered. Melting was established by the presence of distinctive, lamellar, pale brown quench crystals of forsterite; melting was confirmed by mixing platinum black with the starting material, as described elsewhere in this report (p. 104).

The melting curve of forsterite to 47 kb is shown in figure 42. The best linear equation for this curve, determined by a least-squares fit, is $T = 4.77P + 1898$, with T expressed in degrees Centigrade,

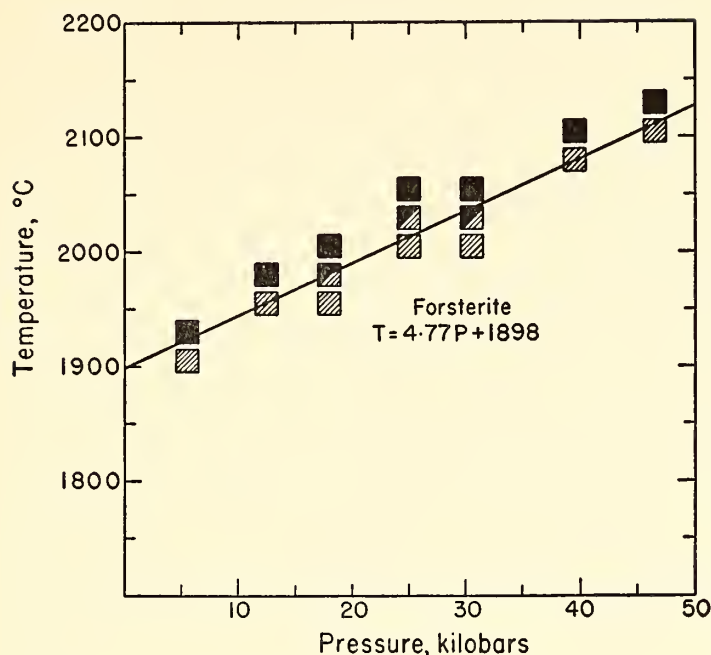


Fig. 42. The melting of forsterite, Mg_2SiO_4 , at pressures up to 47 kb.

P in kilobars. Inspection indicates that no better fit of the data could be expected from substitution of a Simon equation for the linear equation chosen. The linearity of the melting curve is unusual in comparison with the melting equations of other silicates thus far determined.

Bowen and Schairer (1935a), using the Clausius-Clapeyron equation, predicted a slope for the melting curve of forsterite of $4.7^\circ/\text{kb}$. As Ringwood (1960) and Kushiro and Kuno (1963) have already noted, the molar volume of forsterite "glass" was determined by extrapolation of refractive index on a weight per cent scale. A redetermination by Kushiro on a mole per cent scale yielded a value of $5^\circ/\text{kb}$. Recalculation by the present authors gave $3.1^\circ/\text{kb}$. The cause of the disagreement between different calculated results is that the ΔV is critically dependent on the extrapolated value of the index of forsterite "glass." This extrapolation is poorly controlled, for there is little control on the slope of the isofracts on the original diagram (Bowen and Schairer, 1935a, fig. 27).

In terms of the Geophysical Laboratory temperature scale, the melting point of forsterite at atmospheric pressure is given by Bowen and Andersen (1914) as 1890°

$\pm 20^\circ\text{C}$. Conversion of this value to the International Scale of 1948, in terms of which the present results are given, yields a figure of 1895°C . The melting point of forsterite at atmospheric pressure, by extrapolation from the present linear least-squares fit, is $1898^\circ \pm 10^\circ\text{C}$.

Some Effects of Pressure on Phase Relations in the System $\text{MgO-Al}_2\text{O}_3\text{-SiO}_2$

F. R. Boyd and J. L. England

Continuing study of phase relations in the system $\text{MgO-Al}_2\text{O}_3\text{-SiO}_2$ now makes it possible to construct equilibrium diagrams of this system for a variety of pressures. Four such diagrams are shown in figure 43. Some aspects of the phase relations illustrated are known in considerable detail; others are conjectured and subject to modification by future work. For example, the stability relations of pyrope and kyanite and the solubility of Al_2O_3 in enstatite (described below) are known, but probable compositional variation in such phases as sapphirine and spinel is not yet determined.

The major changes produced by high pressures in the phase relations in this system are closely related to the variable coordination of aluminum. In silicates stable at low pressures, an aluminum ion is usually surrounded by either four or six oxygen ions. Sometimes aluminum is partitioned between both the four and six coordination positions in a single structure, as in the minerals sillimanite and aluminous enstatite. Pressure favors structures with the aluminum in six coordination, because a higher coordination leads to denser, more closely packed arrangements of ions.

The sequence of phase changes shown in figure 43 illustrates this principle. The only aluminosilicate in this system that persists through the pressure range thus far investigated is sapphirine. Sapphirine is a very dense mineral ($\rho = 3.5$), but its crystal structure is not yet known. In cordierite, however, the aluminum is all

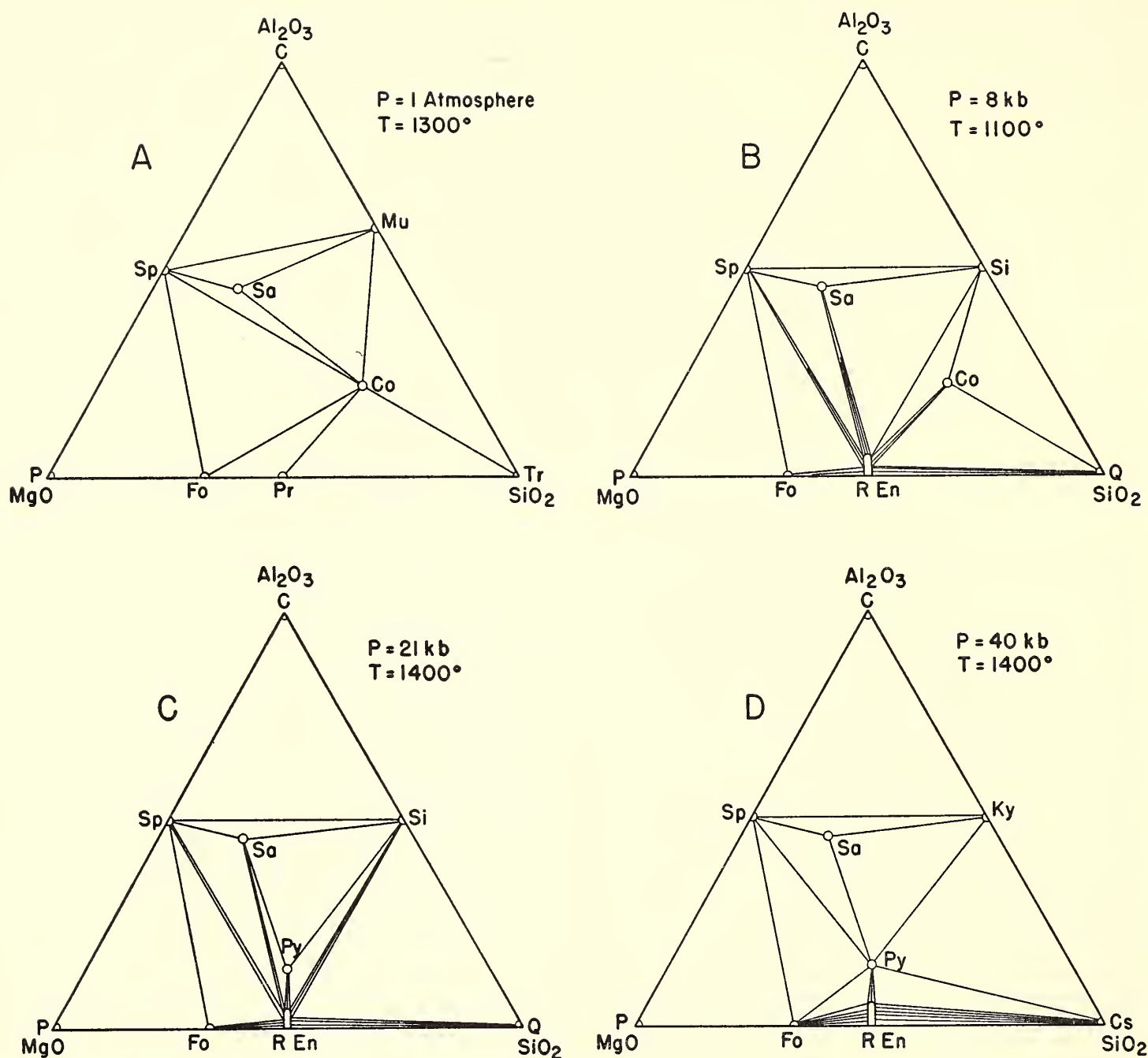


Fig. 43. Equilibrium diagrams for the system $\text{MgO}-\text{Al}_2\text{O}_3-\text{SiO}_2$ at a series of pressures. The joins are based predominantly on experimental data, but petrologic evidence has been used for a few. References to the experimental details are: Boyd and England, *Year Books* 58, pp. 83-87; 59, pp. 49-52; and 61, pp. 109-112; Schreyer and Yoder, *Year Book* 59, pp. 90-91; Clark, 1961. C, corundum; Co, cordierite; Cs, coesite; Fo, forsterite; Ky, kyanite; Mu, mullite; P, periclase; Pr, protoenstatite; Py, pyrope; Q, quartz; REn, rhombic enstatite; Sa, sapphirine; Si, sillimanite; Sp, spinel; Tr, tridymite.

in tetrahedral coordination, and at a pressure of the order of 10 kb cordierite breaks down to sillimanite + aluminous enstatite + quartz. The coordination of aluminum in sillimanite is partly fourfold and partly sixfold. At a little over 20 kb sillimanite inverts to kyanite in which the aluminum is entirely in sixfold coordination. The high-pressure garnet pyrope becomes stable at about the same pressure as that at which kyanite makes its appearance. In pyrope as in kyanite the alumi-

num is entirely in octahedral coordination.

At atmospheric pressure (fig. 43, A) the low-pressure phase cordierite can coexist with a wide variety of other phases in the system. With increasing pressure, join shifts progressively restrict the number of other phases with which cordierite can coexist. At a pressure just less than that required to break down cordierite (fig. 43, B) it can crystallize in equilibrium only with the three phases aluminous enstatite, sillimanite, and quartz.

The behavior of the high-pressure phase pyrope is precisely the opposite. At a pressure just high enough to stabilize pyrope (fig. 43, *C'*) it can coexist only with aluminous enstatite, sapphirine, and sillimanite. As the pressure is increased (fig. 43, *D*), however, join shifts permit pyrope to crystallize in equilibrium with a much wider variety of phases.

One aspect of the phase relations in the system $\text{MgO-Al}_2\text{O}_3\text{-SiO}_2$ that is of particular petrologic interest is the effect of pressure on the solubility of alumina in enstatite. In the course of a study of the stability field of pyrope we found that 14 to 19 per cent Al_2O_3 would dissolve in MgSiO_3 at 20 kb and 1400°C (Boyd and England, *Year Book 59*, pp. 49–52). The precise amount of Al_2O_3 in a saturated enstatite under these conditions proved indeterminate by the X-ray method used because enstatites containing more than 14 per cent Al_2O_3 were not binary; i.e., there proved to be a variation in the Mg/Si ratio as well as in Al_2O_3 content. Since only a few per cent of Al_2O_3 will dissolve in MgSiO_3 at atmospheric pressure, the high solubility found at 20 kb was interpreted as an effect of pressure.

The maximum Al_2O_3 content found in natural orthopyroxenes is of the order of 9 per cent. These natural high-alumina pyroxenes are from granulites, which are metamorphic rocks of crustal origin. It was suggested that still higher alumina contents might be found in orthopyroxenes from kimberlites believed to have formed at depths of 100 km or more in the mantle.

Recently a number of orthopyroxenes from kimberlites have been analyzed (Banno, Kushiro, and Matsui, 1963; O'Hara and Mercy, 1963). Most surprisingly they show Al_2O_3 contents in the range 0.75 to 1.50 per cent. Not only are these kimberlitic pyroxenes less aluminous than synthetic pyroxenes crystallized at comparable pressures, but they are less aluminous than natural pyroxenes from most other geologic environments.

Most of the kimberlitic orthopyroxenes

TABLE 8. Al_2O_3 Contents of Saturated, Mg-Rich Pyroxenes

Pressure, kb	T , $^\circ\text{C}$	Weight Per Cent Al_2O_3	Saturated Assemblage
Atmospheric	1300	$<2\frac{1}{2}$	$\text{Pr}_{ss} + \text{Fo} + \text{Co}$
19.7	1400	14–19*	$\text{REn}_{ss} + \text{Sa} + \text{Si}$
28.7	1400	9 ± 1	$\text{REn}_{ss} + \text{Py}$
40.0	1400	11 ± 1	$\text{REn}_{ss} + \text{Py}$

* Pyroxene not binary with Al_2O_3 contents >14 per cent; see Boyd and England, *Year Book 59*, pp. 49–52.

REn_{ss} , rhombic enstatite; Pr_{ss} , protoenstatite; Fo, forsterite; Co, cordierite; Sa, sapphirine; Si, sillimanite; Py, pyrope.

come from assemblages including pyrope-rich garnet. The determination of Al_2O_3 solubility in MgSiO_3 at 20 kb and 1400°C is at a pressure just less than that required to stabilize pyrope. It was thought that at higher pressures, where pyrope is a stable phase, the solubility of Al_2O_3 in enstatite might drop because of the reaction aluminous enstatite \rightarrow pyrope + less aluminous enstatite.

More runs were made on the join $\text{MgSiO}_3\text{-Al}_2\text{O}_3$ at a variety of pressures to test this possibility; the results are given in table 8. New data at atmospheric pressure show that the solubility of alumina in protoenstatite is very slight. It is less than $2\frac{1}{2}$ per cent, in contrast with the high solubility found in rhombic enstatite at higher pressures. Comparison of the results obtained at 29 and 40 kb with those at 20 kb shows that the saturation limit of Al_2O_3 in enstatite does in fact drop markedly when pyrope appears as a stable phase. Nevertheless, the solubilities obtained at 29 and 40 kb are still very much higher than those found in natural kimberlitic pyroxenes. Moreover, continued increase of pressure within the pyrope stability field produces a slight but significant increase in the solubility of Al_2O_3 in enstatite. Precisely the opposite result was expected. These data suggest that the low Al_2O_3 contents of kimberlitic enstatites cannot be explained by suppos-

ing that the kimberlites crystallized at pressures much higher than 40 kb.

The low alumina contents of these orthopyroxenes are thus an enigma. Perhaps the explanation of the anomaly will prove to lie in the effect of temperature, and possibly also the effect of iron, on the solubility of Al_2O_3 in enstatite. Reactions in this system are sluggish, and experiments have thus far been confined to the rather high-temperature range 1300° to 1400°C . If experiments at lower temperatures prove practicable they may well show that the solubility of Al_2O_3 in enstatite drops off markedly with decreasing temperature.

ALKALINE ROCKS AND THEIR MINERALS

Crystallization of the Rock-Forming Silicates in the System $\text{Na}_2\text{O}-\text{Al}_2\text{O}_3-\text{Fe}_2\text{O}_3-\text{SiO}_2$ at 1 Atmosphere

D. K. Bailey and J. F. Schairer

The crystallization of alkaline rocks, expressed in the simplest possible terms, involves equilibria between a liquid and crystals of alkali feldspars and pyroxenes, plus either nepheline or quartz, depending on the degree of silica saturation in the bulk composition. Such conditions are found in the system $\text{Na}_2\text{O}-\text{Al}_2\text{O}_3-\text{Fe}_2\text{O}_3-\text{SiO}_2$, in which the crystallization paths of the four rock-forming minerals nepheline, albite, acmite, and quartz have been worked out at 1 atm by studies on six triangular joins within the tetrahedral system.

As was reported in *Year Book 61*, pages 91–94, thirty-three compositions in the sixth join, nepheline-acmite- $(\text{Na}_2\text{O} \cdot 4\text{SiO}_2)$, were made, and work on their crystallization sequences is now nearly complete. Two new compositions in this join, close to the piercing points nepheline + albite + acmite + liquid and quartz + albite + acmite + liquid, have also been studied to provide additional data on the two important quaternary points at which the respective univariant lines are

joined by sodium disilicate. Some subsidiary studies that have been started within the four-component system will be reported before the main results are outlined.

Pure acmite. A homogeneous glass of “acmite” composition, prepared by repeated fusion of the correct proportions of $\text{Na}_2\text{O} \cdot 2\text{SiO}_2$, Fe_2O_3 , and SiO_2 at 1350°C , was crystallized for 2 days at 700°C , 1 day at 800° , and 143 days at 930° , yielding a pale yellow powder of acmite. This material was prepared for the study of acmite stability, reported elsewhere in this report, but it was also used to determine the crystallization data at 1 atm required for parts of the present investigation. It appears to be the first preparation of pure acmite at 1 atm, the fusion relations of acmite having been previously determined by Bowen and Schairer (1929) from compositions in the join $\text{Fe}_2\text{O}_3-\text{Na}_2\text{O} \cdot 4\text{SiO}_2$. The present material, in agreement with the earlier results, begins to melt at $975^\circ \pm 5^\circ\text{C}$, yielding hematite plus liquid; acmite completely disappears only at $988^\circ \pm 5^\circ$, and over this melting interval it recrystallizes as coarse prisms in equilibrium with hematite and liquid. The hematite liquidus of this composition, which at these temperatures is quaternary owing to reduction of $\text{Fe}_2\text{O}_3 \rightarrow \text{FeO}$, is at $1310^\circ \pm 10^\circ\text{C}$.

Nepheline-acmite. Yagi, in *Year Book 61*, page 99, figure 31, published his results on the join nepheline-acmite, which forms a side line of four of the triangular joins studied by us in the four-component system. By interpolation of data on compositions $\text{Ac}_{40}\text{Ne}_{60}$ and $\text{Ac}_{30}\text{Ne}_{70}$, Yagi obtained the value of $\text{Ac}_{37.5}\text{Ne}_{62.5}$ for what is sometimes loosely called the minimum on the liquidus (labeled A in fig. 44) but could more accurately be described as the intercept of the line joining acmite and nepheline with the divariant surface hematite + carnegieite + liquid within the quaternary system (neglecting the FeO component). One of our compositions, $\text{Ac}_{35}\text{Ne}_{65}$, appears, however, to be very close to

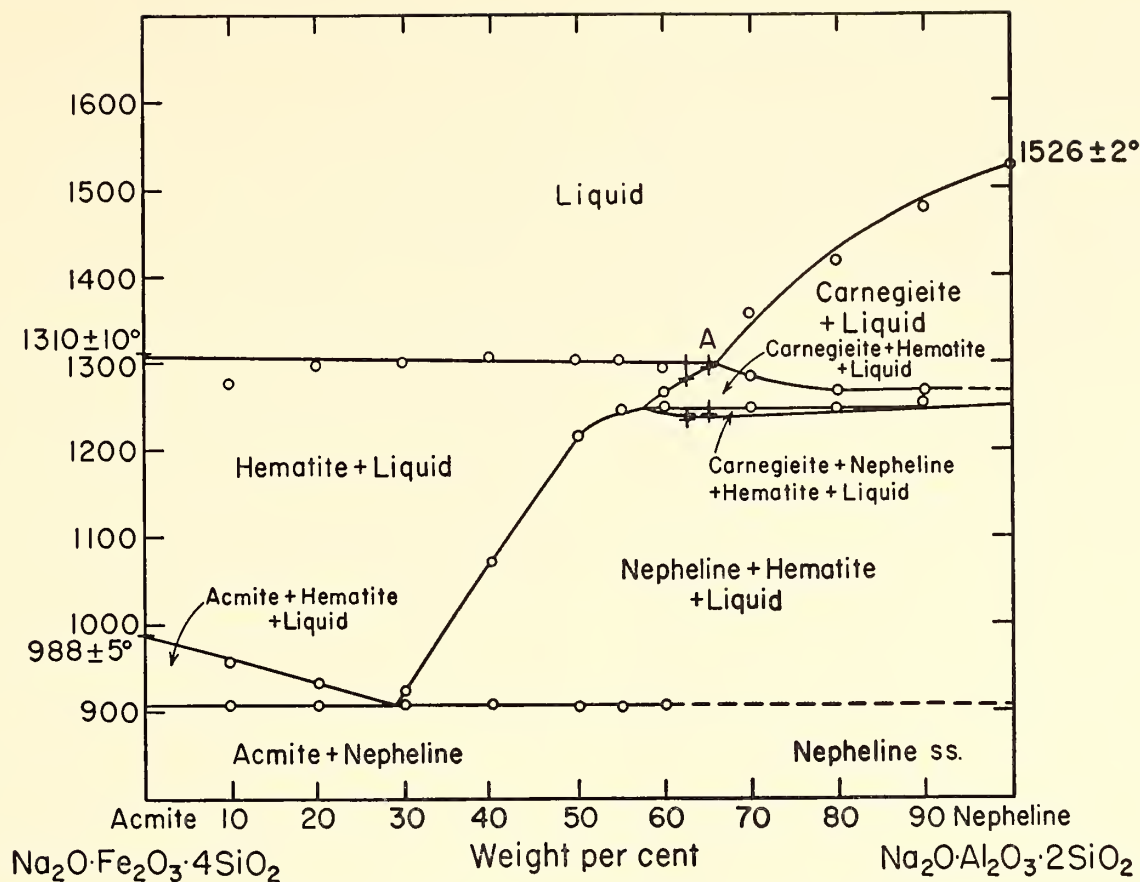


Fig. 44. Pseudobinary diagram of the join nepheline-acmite. After Yagi. Data of Yagi shown by circles; new data, by crosses.

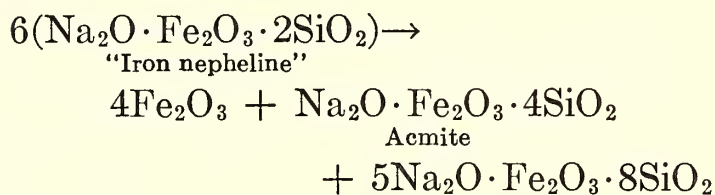
point A, and confirmation has been obtained in check runs with a new composition, $Ac_{37.5}Ne_{62.5}$, having a hematite liquidus approximately 20°C above the first appearance of carnegieite. The system is, of course, complicated by the reduction $Fe_2O_3 \rightleftharpoons FeO$ at these liquidus temperatures, making it quinary, and the present modifications to Yagi's data are given only to eliminate a discrepancy in a side line common to four of our triangular joins. A revised diagram is presented in figure 44, on which are also included the newly obtained data on the pure acmite composition. Some other changes from Yagi's diagram may be noted here: the four lines meeting at point A are not parts of two continuous curves, since each of the fields so defined represents a different aspect of the larger system projected into the pseudobinary; the steplike extension of the carnegieite + nepheline + hematite + liquid field into the hematite + liquid field has been eliminated, because it requires that crystallization of hematite from a range

of liquid compositions moves them directly to a univariant curve, whereas this would be expected only for one, unique composition. The hematite liquidus for compositions in this system cannot be defined better than within $\pm 10^\circ C$, crystallization of hematite being affected by loss of iron to the platinum container, possibly by loss of sodium by volatilization, by the initial condition of the charge, and particularly by the availability of oxygen in contact with the charge. In contrast the first appearance of carnegieite is easily observed and reproducible within the usual limits of $\pm 5^\circ C$.

Solid solutions in nepheline and albite. In the current study of the join nepheline-acmite- $(Na_2O \cdot 4SiO_2)$ it has been noticed that both the nepheline and the albite crystallizing from the more iron-rich compositions have anomalously high refractive indices. Detailed comparative X-ray examinations have yet to be made, but there are only minor changes in the high-albite powder diffraction pattern,

whereas the nepheline patterns show distinct changes in peak positions, especially noticeable for the (203) and (311) reflections. The problem of these solid solutions has been probed by several experiments, but much more remains to be done, so that the following notes are merely a preliminary report.

Nepheline solid solutions. Fine-grained nepheline crystallizing from the more iron-rich compositions in the nepheline-acmite-($\text{Na}_2\text{O} \cdot 4\text{SiO}_2$) join has mean refractive indices as high as 1.59, which prompted a new examination of two compositions in the join nepheline-($\text{Na}_2\text{O} \cdot \text{Fe}_2\text{O}_3 \cdot 2\text{SiO}_2$) "iron nepheline," namely, $\text{Ne}_{60}\text{Fe}-\text{Ne}_{40}$ and $\text{Ne}_{40}\text{Fe}-\text{Ne}_{60}$, prepared by Schairer in 1951. The pure iron end member plots in the plane $\text{Na}_2\text{O}-\text{Fe}_2\text{O}_3-\text{SiO}_2$ (Bowen, Schairer, and Willems, 1930) and would be expected to crystallize at the ternary eutectic acmite + hematite + $5\text{Na}_2\text{O} \cdot \text{Fe}_2\text{O}_3 \cdot 8\text{SiO}_2$ + liquid, expressed thus:



The compositions $\text{Ne}_{60}\text{Fe}-\text{Ne}_{40}$ and $\text{Ne}_{40}\text{Fe}-\text{Ne}_{60}$ crystallize to gray powders composed predominantly of nepheline, having mean refractive indices of 1.59, with small amounts of hematite and acmite, giving modified nepheline X-ray powder diffraction patterns with weak hematite peaks and no peaks of acmite or the 5:1:8 compound. Both powders begin to melt at $763^\circ \pm 5^\circ\text{C}$, this temperature probably representing that of the quaternary eutectic nepheline_{ss} + acmite + hematite + 5:1:8 + liquid (point *E* on fig. 46).

Compositions used in the nepheline-acmite study, $\text{Ne}_{65}\text{Ac}_{35}$ and $\text{Ne}_{62.5}\text{Ac}_{37.5}$, also crystallize to nepheline solid solutions with only traces of acmite or hematite, which are insufficient to give reflections in X-ray powder diffraction examination. For this reason a field of nepheline solid solutions has been broadly

designated in the nepheline-acmite diagram (fig. 44). All these results indicate that significant and variable solid solution of soda-iron silicates is possible in nepheline formed under atmospheric conditions, and it would seem that, as in other nepheline-bearing systems, the nepheline compositions that result will generally be related to the bulk compositions of the starting materials. By analogy with the variation in nepheline compositions in other systems (e.g., $\text{Na}_2\text{O} \cdot \text{Al}_2\text{O}_3 \cdot 2\text{SiO}_2$ - $\text{K}_2\text{O} \cdot \text{Al}_2\text{O}_3 \cdot 2\text{SiO}_2$) under different physical conditions, and also in igneous rocks with different histories, it would be expected that there would be a convergence field, similar to the Morozewicz-Buerger field described by Tilley (1954), for iron-bearing nepheline formed under pressure in the presence of volatiles.

Albite solid solutions. Albite with mean refractive indices higher than 1.54 crystallizes from the more iron-rich compositions in the join nepheline-acmite-($\text{Na}_2\text{O} \cdot 4\text{SiO}_2$), and the possibility of solid solution in the albite has been approached by an examination of the compositions $\text{Ab}_{90}\text{Fe}-\text{Ab}_{10}$ and $\text{Ab}_{70}\text{Fe}-\text{Ab}_{30}$ (prepared by Schairer in 1951). These compositions plot in the join nepheline-acmite- SiO_2 , the first having an albite liquidus ($1103^\circ \pm 5^\circ\text{C}$) and the second a hematite liquidus ($1185^\circ \pm 5^\circ\text{C}$). Both compositions should crystallize completely at the quaternary reaction point albite + acmite + hematite + tridymite + liquid (point *C* in fig. 46), but experimentally it has not been possible to eliminate all the hematite formed in these compositions during crystallization at 1 atm. An unusual feature of the fully crystallized compositions is that $\text{Ab}_{90}\text{Fe}-\text{Ab}_{10}$ contains more hematite and acmite than $\text{Ab}_{70}\text{Fe}-\text{Ab}_{30}$, giving some measure of the extent of solid solution in the albite of the latter composition. Albite formed from $\text{Ab}_{90}\text{Fe}-\text{Ab}_{10}$ has a mean refractive index close to that of pure albite and has sufficient associated acmite to suggest that there is little if any solid solution. Albite from

the $\text{Ab}_{70}\text{Fe}-\text{Ab}_{30}$ composition is associated with less acmite and hematite, and a small amount of quartz, and has a mean refractive index of 1.55. Neither this composition nor the first has sufficient acmite or quartz to appear on the X-ray powder diffraction patterns. Compositions close to pure Fe-Ab prepared for the study of the system $\text{Na}_2\text{O}-\text{Fe}_2\text{O}_3-\text{SiO}_2$ (Bowen, Schairer, and Willems, 1930) have also been crystallized, yielding only acmite and quartz, and it would appear probable from present observations that soda-iron silicate does not enter the albite structure simply in the form of an isomorphous iron albite molecule, for which acmite + quartz is the stable assemblage.

$\text{Ab}_{90}\text{Fe}-\text{Ab}_{10}$ glass, $\text{Ab}_{70}\text{Fe}-\text{Ab}_{30}$ glass, and a glass of composition close to Fe-Ab

have also been crystallized at 700°C , at 2 kb total pressure, with different results from those at 1 atm. The first two glasses yielded optically similar albite; the $\text{Ab}_{90}\text{Fe}-\text{Ab}_{10}$ had no significant amounts of minerals other than albite solid solution, but the $\text{Ab}_{70}\text{Fe}-\text{Ab}_{30}$ contained abundant acmite in addition. The composition close to Fe-Ab crystallized to acmite + quartz. From these preliminary results it seems that a more limited solid solution is possible in albite crystallized under pressure than at 1 atm but that this is probably nearer to being an equilibrium product than the solid solutions formed at 1 atm from the same starting materials. The albite in the iron-rich compositions in the join nepheline-acmite- $(\text{Na}_2\text{O} \cdot 4\text{SiO}_2)$ that initiated these experiments also crystallized under con-

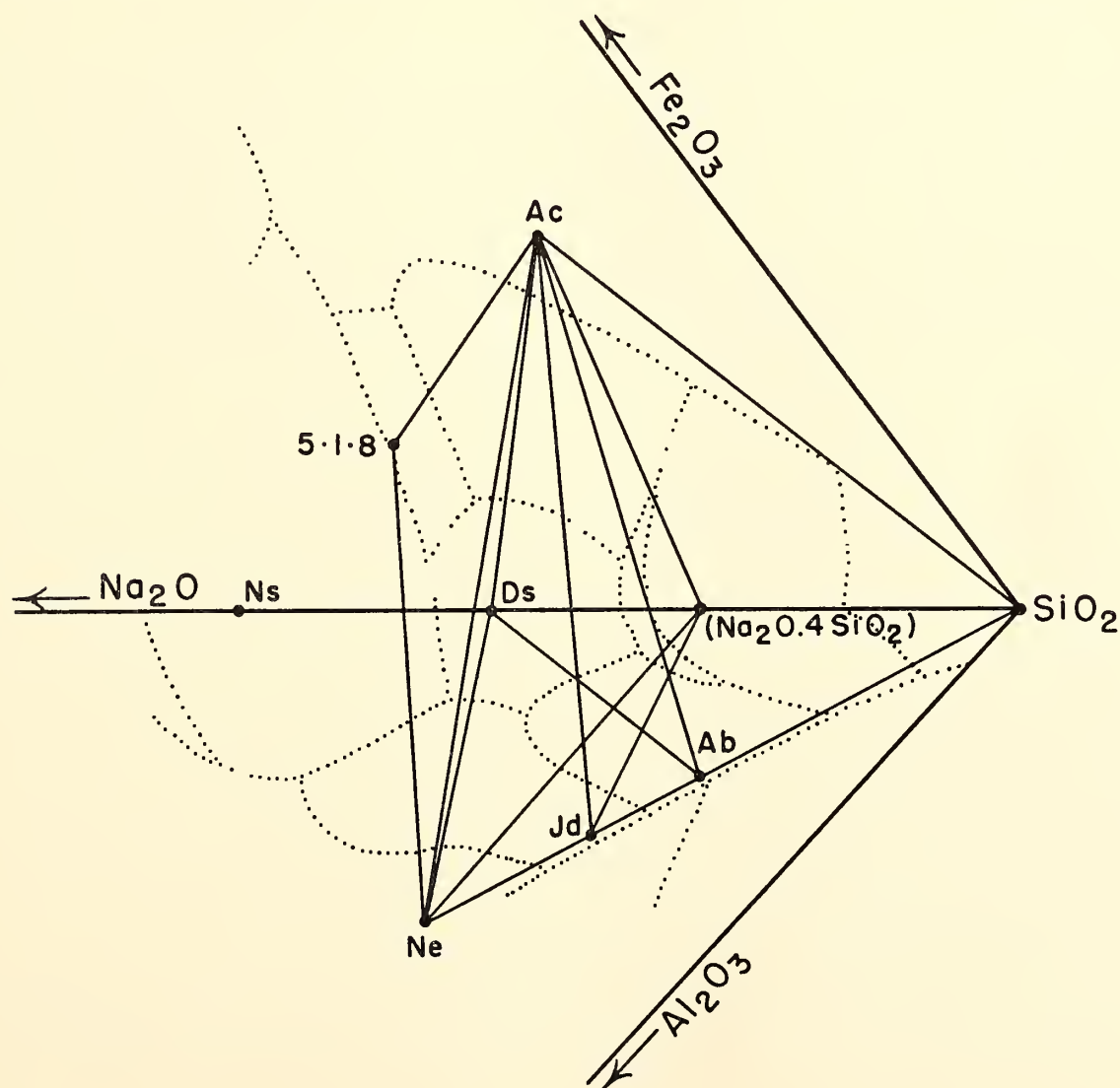


Fig. 45. Perspective diagram to show the position of the six joins studied in the composition tetrahedron $\text{Na}_2\text{O}-\text{Al}_2\text{O}_3-\text{Fe}_2\text{O}_3-\text{SiO}_2$, as viewed through the $\text{Al}_2\text{O}_3-\text{Fe}_2\text{O}_3-\text{SiO}_2$ face, looking into the volume between the faces $\text{Na}_2\text{O}-\text{Fe}_2\text{O}_3-\text{SiO}_2$ and $\text{Na}_2\text{O}-\text{Al}_2\text{O}_3-\text{SiO}_2$, on which the ternary liquidus fields are shown by dashed lines. All six joins have acmite as a common apex.

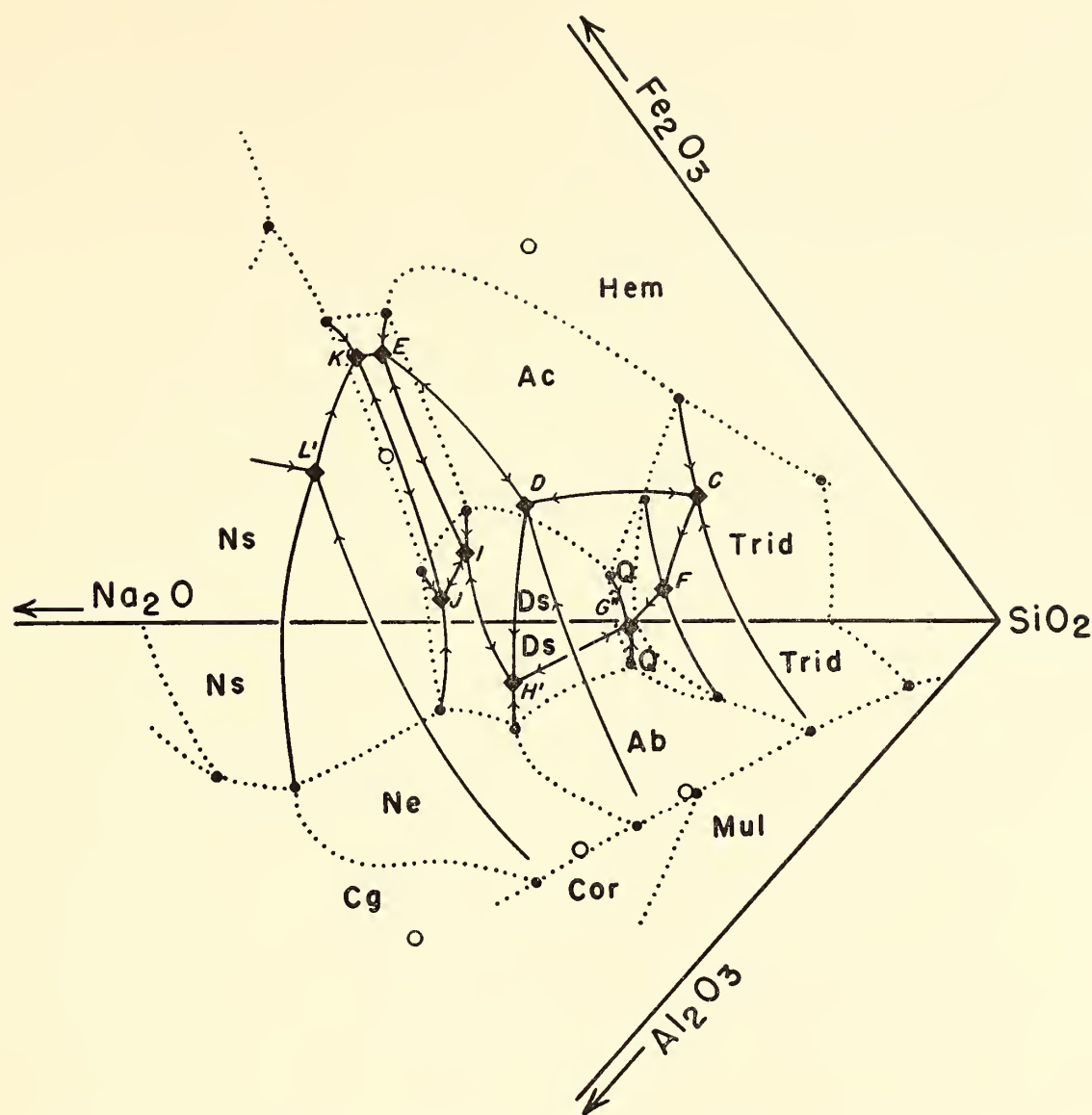


Fig. 47. Perspective view, similar to figure 45, of part of the crystallization flow diagram. This has the form of a framework of univariant lines and quaternary points spanning the volume between the ternary faces $\text{Na}_2\text{O}-\text{Fe}_2\text{O}_3-\text{SiO}_2$ and $\text{Na}_2\text{O}-\text{Al}_2\text{O}_3-\text{SiO}_2$. Broken lines mark field boundaries on the ternary faces; univariant lines are solid; quaternary points are shown as squares and labeled as in figure 46.

with strongly peralkaline liquids within the volume acmite-sodium metasilicate-nepheline-silica. Liquids with initial compositions within this volume move, with crystallization, toward either of two quaternary eutectics, nepheline + albite + acmite + sodium disilicate + liquid (H') or quartz + albite + acmite + sodium disilicate + liquid (G''), which are comparatively close in composition and separated by a low thermal divide. Fractionation of, or failure to react by, any early-formed hematite would greatly enhance the alkalinity of liquids in the system. For instance, liquids having initial compositions in the plane Ne-Ab-Ac would move during equilibrium crystallization toward the quaternary reaction point D , and here the liquid

would be used up simultaneously with the reacting out of the last trace of hematite; failure of any of the hematite to react would leave a liquid that would become progressively more alkaline and would crystallize completely only at the quaternary eutectic H' . Similar considerations apply to liquids with initial compositions in the acmite-albite- SiO_2 field, which with perfect equilibrium would completely crystallize at C but by failure of the hematite reaction could completely crystallize only at G'' . The probability of reaction failure in circumstances comparable to the experimental conditions is high for a wide range of compositions, owing to the ready formation of hematite in large plates that cannot be consumed by the small amounts of liquid available

in the closing stages of crystallization.

Reaction failure of hematite could result in the generation of oversaturated from initially undersaturated liquids, over a limited range of compositions. This can best be illustrated by consideration of the plane of "silica saturation," acmite-albite-sodium disilicate, which has a hematite liquidus field around the acmite composition. Crystallization of hematite will move the initially saturated liquid compositions through the plane acmite-albite-sodium disilicate to more silica-rich or oversaturated compositions, and the same will be true for undersaturated compositions within the "cone" formed by this liquidus field as a base and the hematite apex of the tetrahedral system. In this way a limited range of liquids of acmite + albite + nepheline composition could, by early fractionation of iron oxide, become saturated or slightly oversaturated.

No simple method of moving an oversaturated liquid to an undersaturated composition would seem to be available, either by equilibrium crystallization or by fractionation, in this system. Reaction of residual liquids similar to that at the quaternary eutectic G'' , albite + acmite + quartz + sodium disilicate + liquid, with aluminous wall rocks could, under favorable circumstances, give nepheline-bearing assemblages, as indicated in *Year Book 61*, pages 94-96.

Probably the most important single observation on this system is that the assemblages nepheline + albite + acmite and quartz + albite + acmite crystallize in equilibrium only with liquids in which the molecular ratio alkali/ R_2O_3 is greater than unity. Such a condition offers great scope for the differentiation of late peralkaline liquids and alkali metasomatism of wall rocks by residual fluids. Furthermore, the initial melting of these compositions yields peralkaline liquid + hematite, which in many compositions is melted only at much higher temperatures—partial melting could thus have an important role in the production of rocks in which alkalies are in excess of R_2O_3

group oxides, because the large temperature interval between initial melting and the iron oxide liquidus offers abundant opportunity for separation of the early melt phase.

The liquid composition at the undersaturated quaternary reaction point D may have a special bearing on the problem of the generation of ijolites (nephelinites), rocks of this group being composed largely of nepheline and pyroxene in various proportions, ranging from the nepheline-rich urtites to the mafic melteigites. They are difficult to derive by any of the customary schemes of fractional crystallization from a basaltic parent because increase in alkalies is normally concomitant with increase in silica content. Evidence from the present system indicates one way in which liquids of ijolitic composition may be derived from a slightly undersaturated parent. Liquids with compositions that can be expressed as $Ne + Ab + Ac$, or $Ne + Ab + Ac + Hem$, will crystallize completely only at the quaternary point D , under equilibrium conditions. To reach this point a syenitic composition, i.e. largely composed of albite + acmite, will follow a path along the univariant reaction curve $C-D$ (acmite + albite + hematite + liquid) from a point below the temperature maximum, in the "silica saturation" plane, acmite-albite-sodium-disilicate, toward D . Our investigations show that D lies in the small volume nepheline-jadeite-acmite- $(Na_2O \cdot 4SiO_2)$, and from temperature considerations must lie close to the ternary reaction point nepheline + acmite + hematite + liquid in the plane nepheline-acmite- $(Na_2O \cdot 4SiO_2)$ as shown in figure 48; the liquid at this ternary point has a composition $Ac_{48}Ne_{31}(Na_2O \cdot 4SiO_2)_{21}$, and it must be closely similar to the liquid at point D . It would be possible, therefore, to generate liquids of this type by fractionation or partial melting of syenitic material (albite + acmite) containing only small amounts of nepheline.

The deficiencies of theories that postulate the production of alkaline rocks

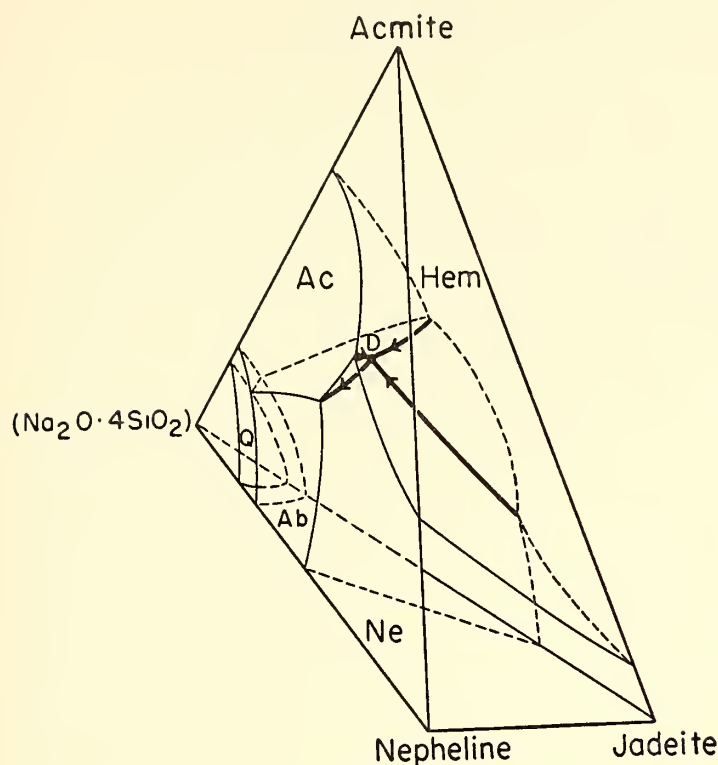


Fig. 48. Illustration of the phase relations in the volume nepheline-jadeite-acmite-($\text{Na}_2\text{O} \cdot 4\text{SiO}_2$) showing the proximity of the quaternary reaction point *D*, albite + nepheline + acmite + hematite + liquid, to the ternary reaction point nepheline + acmite + hematite + liquid. Phase boundaries on the faces of the volume are shown by thin lines (broken on the two concealed faces). Univariant curves, bridging the faces, are shown by heavy lines.

by simple processes of differentiation from a parent magma, like alkali basalt, are several. Rocks of the ijolite series pose a special compositional problem, and although rocks such as phonolites, trachytes, and soda rhyolites do not share this difficulty they present the usual problem that fractional crystallization can produce only small volumes of residual liquids from vast quantities of parent magma. The difficulty may be overcome by invoking partial melting of crystalline parent materials, which must be a distinct possibility for basaltic starting materials above the eclogite-basalt transition zone in the mantle, because before these can yield basalt liquid they must presumably be subjected, for prolonged periods, to temperatures suitable to partial melting. The above arguments, in conjunction with the experimental evidence, require that serious consideration be given to the role of

partial melting in the generation of alkaline rocks, and it has already been suggested elsewhere (Bailey, 1963) that such melting may be facilitated by relief of lithostatic load consequent on warping of the rigid continental crust.

The Stability Relations of Acmite

D. K. Bailey

As a first stage in the study of the system $\text{Na}_2\text{O}-\text{Al}_2\text{O}_3-\text{Fe}_2\text{O}_3-\text{SiO}_2-\text{H}_2\text{O}$, the melting relations of acmite have been investigated at 2 and 5 kb, using cold-seal bombs with the charges unbuffered and with Ni/NiO and $\text{Fe}_3\text{O}_4/\text{Fe}_2\text{O}_3$ buffers. In addition a few exploratory unbuffered runs have been made at 10 kb in an argon-atmosphere, internally heated apparatus (Yoder, 1950). Starting materials were a glass prepared from pure chemicals in the correct proportions to form acmite and crystalline acmite prepared from this glass in a furnace open to the atmosphere at 930°C . The crystalline material is pale yellow and free of other phases, and it melts over the interval from 975° to 988°C , at 1 atm, to hematite + liquid.

Unbuffered runs at 2 and 5 kb were made in sealed platinum capsules in bombs composed principally of nickel with lesser amounts of chromium, cobalt, and molybdenum (Haynes alloy, R41), yielding results closely similar to those obtained with a Ni/NiO buffer (see fig. 49). At first, however, it was found that the 2- and 5-kb results, which required different bombs, were not mutually consistent, but by using the same bomb for both pressure ranges consistency was attained, indicating differences in the natural "bomb buffers" and presumably reflecting different degrees of corrosion of the bomb walls. In the initial runs with the Ni/NiO buffer the charges were sealed in $\text{Ag}_{70}\text{Pd}_{30}$ capsules inside gold buffer capsules. It was found that the nickel alloyed with the $\text{Ag}_{70}\text{Pd}_{30}$ and rapidly rendered the container granular and brittle, causing breakdown of the membrane and creating an open system between charge and buffer. This effect

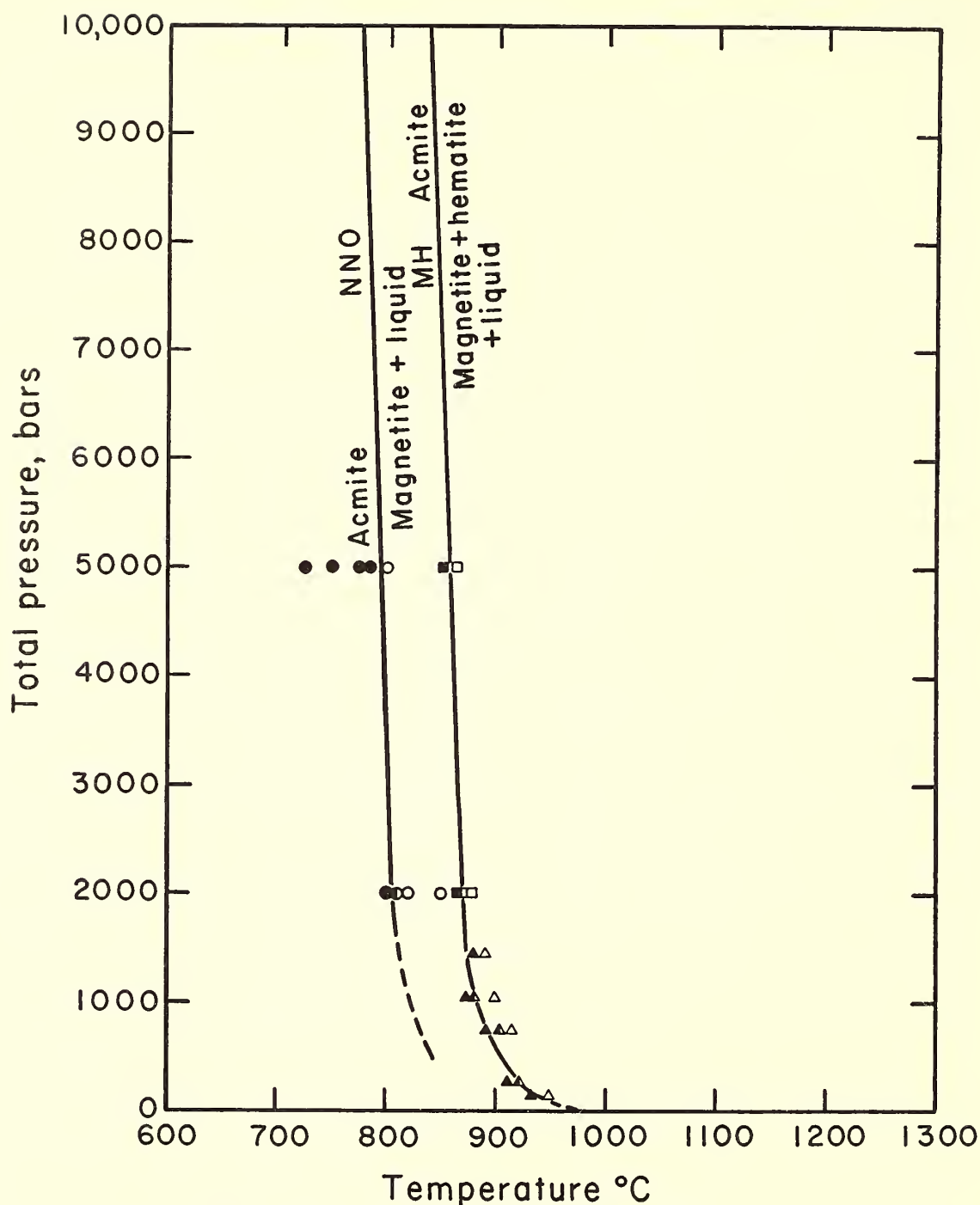


Fig. 49. Preliminary diagram showing the PT stability curves for acmite with P_{O_2} controlled by nickel/nickel oxide (circles) and magnetite/hematite (squares) buffers. Triangles indicate data obtained by W. G. Ernst (personal communication) with the magnetite/hematite buffer.

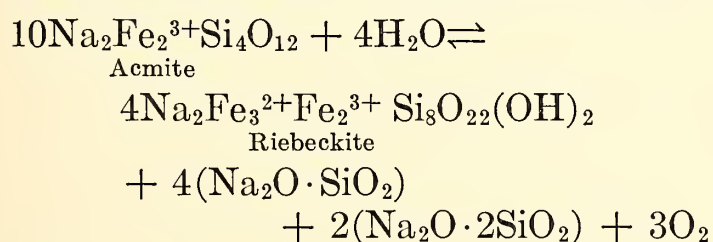
was much less noticeable on the platinum capsules employed in subsequent runs with this buffer.

In experiments using the Fe_3O_4/Fe_2O_3 buffer the $Ag_{70}Pd_{30}$ tubes were satisfactory, and, as shown in figure 49, the higher P_{O_2} provided by this buffer results in a rise of about $60^\circ C$ in the melting curve. The temperatures of acmite fusion at P_{O_2} defined by the Fe_3O_4/Fe_2O_3 buffer at 2 and 5 kb are within the range of failure for R41 bombs over extended periods, the bombs eventually failing after several short-run periods (5 to 24 hours) at these temperatures. Runs of less

than 5 hours have generally been found too short to allow attainment of equilibrium between charge and buffer, or even complete recrystallization of the charge at temperatures below the melting curves.

At temperatures below the melting curves shown in figure 49 the charges recrystallize to relatively coarse (0.1 mm), very pale green acmite prisms, which are colorless in transmitted light, and have optical properties similar to those given by Washington and Merwin (1927, p. 239). So far no readily observable differences have been detected optically or by X-ray

examination in the acmite formed under these different conditions and that formed at 1 atm. From these observations, and from the lack of sodium silicate glass formed in runs below the melting curves, it is assumed that no significant amount of ferrosilite molecule (FeSiO_3) has entered the acmite structure. At temperatures above the melting curves the acmite melts incongruently to give magnetite, or magnetite and hematite, + liquid, which on quenching yields varying amounts of quench amphibole, characteristically in clusters of radiating prisms around ore mineral centers. This amphibole has properties similar to those described by Ernst (1962) for synthetic riebeckite-arfvedsonite solid solutions, with occasional anomalous optic orientation (X nearly parallel to c) as in natural riebeckite (Peacock, 1928). The existence and nature of the possibly stable amphibole field below the range of acmite stability is currently being investigated. It raises the possibility that acmite may break down at lower temperatures to give amphibole + sodium silicates, expressed in simplified form as



The production of arfvedsonite would increase the amount of sodium disilicate at the expense of the metasilicate, which could be achieved in several ways, including tetrahedral coordination of part of the iron as suggested by Ernst's data (1962).

In addition to showing incongruent melting above the melting curves, the charges obtained show evidence of partition of material between the melt and gas phases. Some runs contain glass globules and quench amphiboles precipitated from the gas in equilibrium with the melt phase, and almost invariably the capsule contains a clear liquid, which congeals rapidly, on opening of the tube, to a glass with low refractive index (~ 1.55) as-

sumed at present to be of sodium silicate composition. In some cases, too, there has been precipitation from the gas of coarse euhedral magnetite. This aspect of the study is receiving more detailed investigation, but it would appear that separation and transport of materials in a dense gas phase could have a crucial role in the development of alkaline rocks.

The incongruent melting of acmite appears to persist to pressures up to 10 kb in the few unbuffered runs made so far. These runs were made in platinum capsules, and it might be expected that loss of hydrogen to the external argon atmosphere would maintain the high oxidation state in the capsule; but, in fact, the iron oxide formed on melting is magnetite, indicating sufficient P_{H_2} in the external atmosphere to provide a buffer for the charge within the magnetite stability field. This P_{H_2} might be provided by breakdown of hydrocarbon impurities in the external atmosphere.

Persistence of the incongruent melting relations of acmite to pressures of 5 and 10 kb indicates that this property may still be expected to influence the generation and development of alkaline and peralkaline liquids at appropriate depths in the crust, in similar fashion to that described for the system $\text{Na}_2\text{O}-\text{Al}_2\text{O}_3-\text{Fe}_2\text{O}_3-\text{SiO}_2$ at 1 atm, and it also places useful upper temperature limits on the formation of rocks containing acmite phenocrysts. There is in addition the exciting prospect that the flexibility of the differentiation processes will be enhanced, perhaps even controlled, by partition of components between melt and gas phases in alkali- and iron-rich compositions.

Liquidus Data on the System Acmite-Nepheline-Diopside at 1 Atmosphere⁹

Kenzo Yagi¹⁰

Results for the three side lines of the system acmite - nepheline - diopside, namely, nepheline-diopside, acmite-

⁹ The work reported here was carried out partly at this Laboratory and partly at Tohoku and Hokkaido Universities, Japan.

¹⁰ Hokkaido University, Sapporo, Japan.

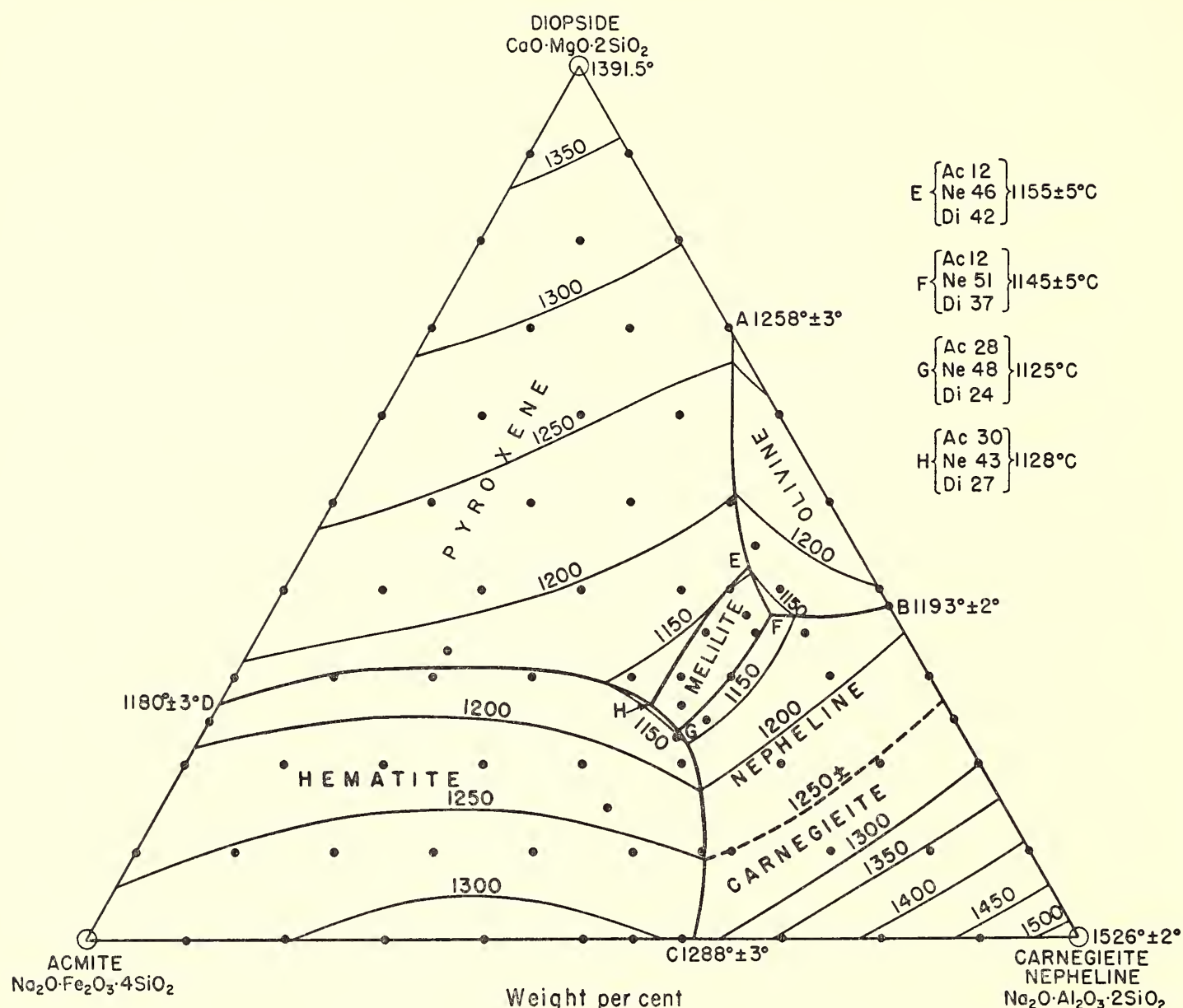


Fig. 50. Preliminary liquidus diagram for the join acmite-nepheline-diopside at 1 atm. Filled circles indicate compositions studied.

diopside, and acmite-nepheline, were presented in *Year Book 61*, pages 96–99, and liquidus results on compositions within the system are presented now in figure 50. Only the liquidus data may be read from the diagram. The solid phases separating from liquids in this join are all complex solid solutions, the compositions of which have yet to be determined precisely. Nepheline and carnegieite form solid solutions that cause changes in the inversion temperature, which is shown only approximately in figure 50 as 1250°C.

In the join nepheline-diopside it was found that melilite crystallized from all compositions as either the second or the third solid phase, reaffirming Bowen's

earlier observations (1922), and that this mineral persisted throughout the sub-solidus. Attention is drawn in particular, therefore, to the crystallization of melilite as the primary phase from a narrow range of liquids that have acmite in addition to nepheline and diopside in their compositions. It is hoped to discuss the implications of this finding, and other aspects of the join, when more data are available on the behavior of these compositions at lower temperatures.

MELTING OF IRON AT HIGH PRESSURE

F. R. Boyd and J. L. England

Knowledge of the effect of pressure on the melting of earth materials enables us to limit the present temperature gradient

in the earth and provides controls on estimates of the earth's thermal history. Considerable progress has been made in the past several years in obtaining data on the melting of pure silicates and on melting relations in multicomponent silicate systems in the pressure range up to 50 kb. Nevertheless, for a number of reasons, extrapolations of these data to the far higher pressures present in the lower mantle are uncertain. One of the principal uncertainties is that we do not adequately know the effect on silicate melting curves of phase transitions at pressures above the present experimental range. Such phase changes are now rather generally believed to be responsible for the transition zone between the upper and lower mantle.

The earth's core is believed to be largely metallic iron, and the seismic transition between the inner and outer core is probably a change from a liquid outer to a crystalline inner core. If the melting curve of iron were known sufficiently well at these pressures it would be possible to fix the temperature at the inner core boundary and to put a minimum limit on the temperature of the core-mantle boundary.

Many of the uncertainties in extrapolating silicate melting curves appear also in the extrapolation of the melting curve of iron. But in one regard the extrapolation may be simpler. The form of iron stable at the melting point at atmospheric pressure is the body-centered cubic δ phase. Clark (1963) has calculated that δ Fe inverts to the denser, face-centered cubic form at a pressure of 10 to 12 kb along the melting curve. Since this is the densest possible structure for iron there should be no further inversions with increasing pressure until the electron shells collapse. However, this expectation is not certain, inasmuch as shock-wave data have indicated that the behavior of iron at high pressures may be more complex than this (Johnson, Stein, and Davis, 1962).

Strong (1959), determining the melting

curve of iron to a pressure that he believed to be 90 kb, found a slight curvature of the sort usually present in melting curves. Subsequent work has shown that the calibration points used by Strong above 25 kb were about 30 per cent too high (Kennedy and LaMori, 1962). Strong's (1962) correction of his data to the revised pressure scale indicates that the melting curve of iron is linear with a slope of $2.6^\circ/\text{kb}$.

By analogy with other materials it is unlikely that the melting curve of iron is actually linear, and the present study was undertaken to see whether a method of determining the melting curve different from that used by Strong might not reveal detectable curvature. As will be shown, the results approximately confirm Strong's measurements, but the matter of curvature is still an open question.

The method of determining the melting curve was similar to our procedure in determining pyroxene melting curves (Boyd and England, 1963). For each run a 1-mm length of 10-mil iron wire was embedded in a silicate mixture with the composition 95 per cent SiO_2 , 5 per cent Na_2O . The silicate mixture was packed into a capsule machined from a platinum-rhodium alloy. At atmospheric pressure this mixture begins to melt at the eutectic $\text{Na}_2\text{Si}_2\text{O}_5\text{-SiO}_2$ at 790°C , but the liquidus is not reached until 1600° . The iron wire was thus suspended in a liquid-crystal mush which was too viscous to permit the iron to sink and touch the platinum capsule. In runs below the melting curve, the iron wire was recovered in the same shape as when it was introduced. If the iron melted, however, the surface tension of the liquid iron caused it to form a globule. Slight discoloration of the silicate mixture around the iron after a run suggested that the silicate liquid may have dissolved a little of the iron. Silicates are not soluble in metals, however, and potential diffusion of carbon from the graphite furnace sleeve to the iron was blocked by the thick-walled platinum capsule.

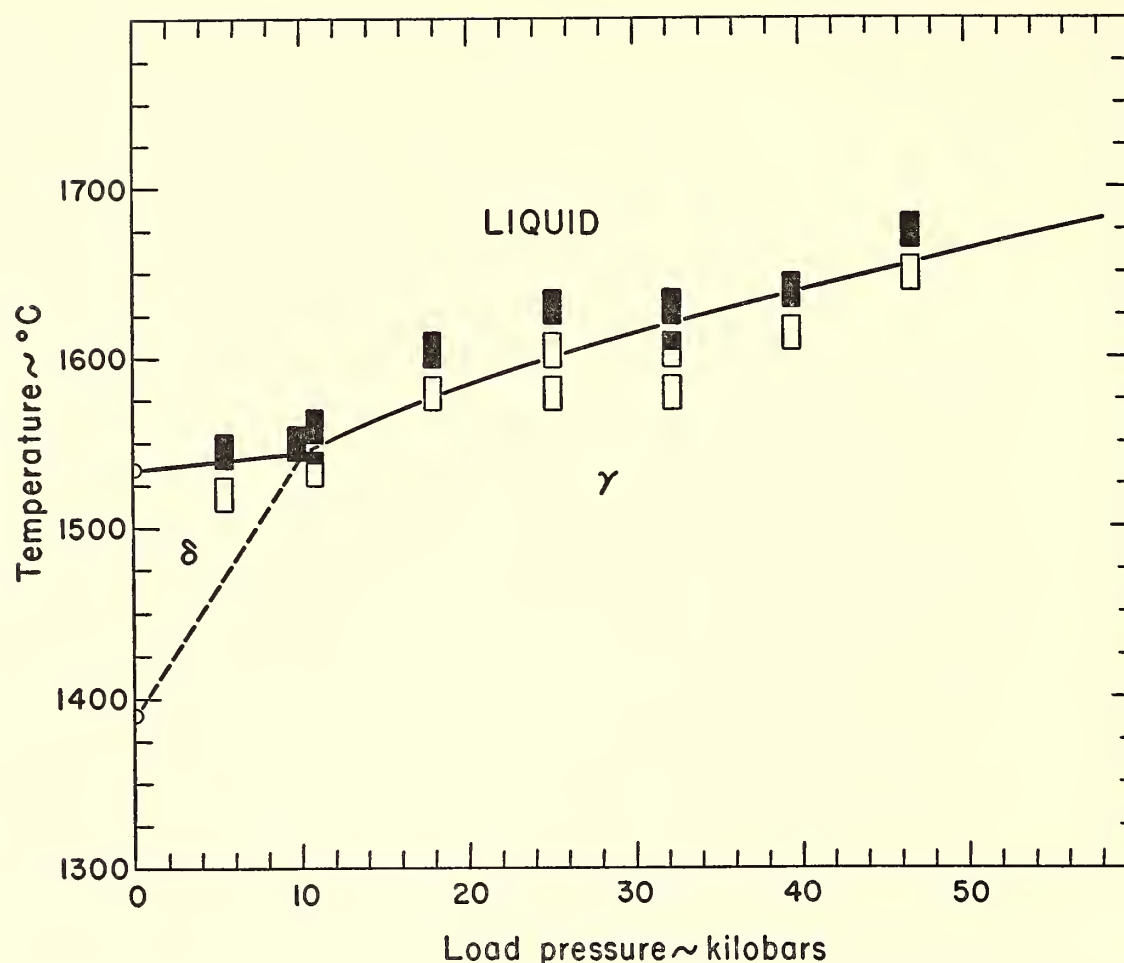


Fig. 51. Effect of pressure on the melting of iron. The δ - γ transition is not determined by these runs but is taken from the calculation of Clark (1963).

Results of these quenching experiments are shown in figure 51. The criterion for detecting melting proved to be sharp, although at several points duplicate or triplicate runs gave divergent results. For reasons not well understood, the precision is not so good as we have obtained with pyroxene melting curves.

It is possible to fit these data within reasonable limits of error by a straight line with a slope of $2.5^\circ \pm 0.1^\circ/\text{kb}$. Such a curve would be in good agreement with Strong's (1962) value of $2.6^\circ/\text{kb}$. Nevertheless, an improved fit can be obtained by taking the slope of the melting curve of δFe to be about $1^\circ/\text{kb}$ with a triple point, δ - γ liquid, at 1545° and 10 kb. The melting curve of γFe would then show appreciable curvature. This construction is used in figure 51.

The difference between these alternatives is a maximum of about 10° . Inasmuch as the precision obtainable with single-stage apparatus in this temperature

range is only about $\pm 5^\circ$ – 10° , it is not possible to be sure that the δ - γ inversion does inflect the melting curve in the manner shown. Confirming evidence might be obtained by other techniques. As Birch (1963) has suggested, points on melting curves in the megabar range might be obtainable by shock-wave experiments. The triple point δ - γ -liquid is within the pressure range of gas apparatus, and the precision of temperature measurement in such apparatus is at least potentially good enough to fix the position of the triple point with the required accuracy.

Linear extrapolation of these data to 1400 kb, the pressure at the core-mantle boundary, indicates a melting point for iron at that pressure of about 5000°C . This should be a reliable maximum limit, inasmuch as curvature of the γFe melting curve like that shown in figure 51 would reduce the melting temperature at depth. Calculation of Simon constants for the

γ_{Fe} melting curve is critically dependent on the location of the triple point and is not warranted with data available at present.

HYDROUS SYSTEMS AND METAMORPHIC ROCKS

Gas Mixtures

H. J. Greenwood

The system $\text{H}_2\text{O}-\text{CO}_2$ is of great interest to the metamorphic petrologist because of the large number of important chemical reactions involving these two components. It is consequently desirable to know something of the thermodynamics of mixing of H_2O and CO_2 . During the last year two independent methods were employed to examine the question. The first method was the effect on the calcite-quartz-wollastonite reaction, described in *Year Book 61* (p. 85). New data have been added and the results compared with various assumptions on the ideality of mixing of H_2O and CO_2 . The equilibrium curve is essentially the same as reported last year, although the brackets are somewhat narrower. Its position in a T - x plot of $\text{H}_2\text{O}-\text{CO}_2$ is indistinguishable from a curve calculated by assuming ideal mixing. This method of detecting nonideality is not very sensitive, but with the data used, in which the curves are known to $\pm 7^\circ\text{C}$, it is possible to say that the activity coefficient of CO_2 in these CO_2 - H_2O mixtures at 600° - 700°C and 2000 bars is 1.0 ± 0.2 .

The fugacity coefficient must be calculated in a way that is internally consistent with the data on crystal-vapor equilibrium in the gas mixture and so that it depends to a minimal extent on data from other laboratories. Data on the wollastonite equilibrium in the presence of pure CO_2 were taken from Harker and Tuttle (1956). The ΔH of reaction was found by plotting their data in terms of log fugacity versus reciprocal temperature and taking into account the separate effects of total pressure and CO_2 pressure. With the value of ΔH thus

obtained the change in the equilibrium temperature with concentration of CO_2 was calculated by means of the relation

$$\Delta \frac{1}{T} = - \frac{\Delta H}{2.303R} \log_{10} x_{\text{CO}_2}$$

This procedure avoids comparing pressures calculated from the data of one laboratory with those measured in another, a risky operation because of the large difference in pressure occasioned by a small interlaboratory difference in temperature calibration. It does, however, retain the essential information, the rate of change of the equilibrium pressure of CO_2 with temperature at constant total pressure. Recent calculations of the same sort have been reported by Walter (1963) on the system CO_2 - H_2O . Walter used the magnesite-periclase equilibrium as the means of estimating the fugacity of CO_2 in the mixtures. He reported that the activity coefficients for CO_2 are significantly more than 1.00 (~ 2.0). The difference in Walter's conclusions and those presented here may be due to the fact that he transferred pressures from one set of data (Harker and Tuttle, 1955) to another (Walter, Wyllie, and Tuttle, 1962) rather than proceeding from the ΔH of reaction.

The second method, studying gas mixtures by means of their P - V - T - x properties, is more direct and more precise but does not yield some of the information of the first method. The crystal-vapor phase-equilibrium method gives a measure of the activities of individual species in the mixture, whereas the P - V - T - x properties give the gross behavior of the system and the activities of the idealized end members. A P - V - T - x apparatus has been set up and calibrated during the past year, and measurements on the CO_2 - H_2O system have been completed for the 410° , 450° , 500° , 550° , and 600°C isotherms. The working volume of the apparatus was calibrated with pure argon, pure CO_2 , and pure H_2O under

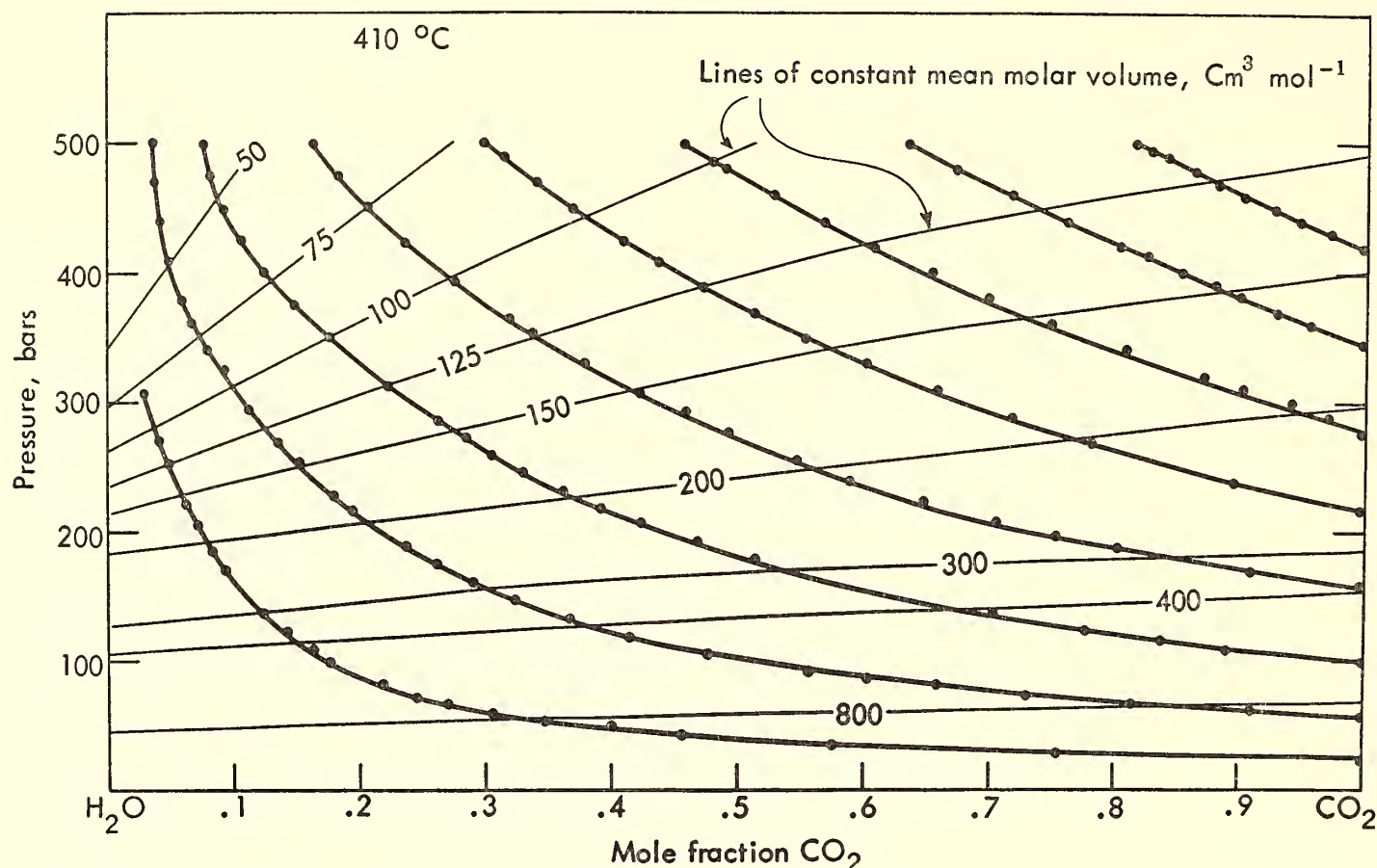


Fig. 52. 410°C isotherm for the system $\text{CO}_2\text{-H}_2\text{O}$ up to a pressure of 500 bars. Small dots are data points; the curves passing through them indicate the path followed during each run, from low pressure and pure CO_2 to 500 bars and a mixture of CO_2 and H_2O .

conditions of pressure and temperature where the P - V - T properties of these compounds are known very precisely. The data of Michels et al. (1935, 1949) for argon and CO_2 were used in the range where their properties are known to five significant figures. The data of Keenan and Keyes (1936), Kennedy, Knight, and Holser (1958), and Holser and Kennedy (1958) were used for H_2O . The mixture data are internally consistent and agree with the data on the pure end members to better than 1 per cent. Figure 52 shows a P - x plot of the typical isotherm. The method of obtaining the data may be understood by reference to the diagram. The bomb is brought to the operating temperature of the isotherm and evacuated. Carbon dioxide is introduced at an accurately known pressure, measured with a calibrated Bourdon gauge. Next, a known amount of water is injected with a calibrated volumeter or screw press, and the new pressure is recorded. The injection of water continues until the total

pressure reaches 500 bars. The contents of the bomb are then extracted quantitatively and analyzed for H_2O and CO_2 . The amounts of CO_2 and H_2O recovered are checked against the amounts injected into the bomb. The permanent gas fraction of the fluid from the bomb is analyzed with the mass spectrometer for traces of CO and H_2 to make sure that the mixture was truly binary during the measurements. The data obtained so far show that the bomb has contained less than 1 part in 10^6 of gases other than H_2O and CO_2 .

After the P - x isotherm has been traversed a number of times with different initial pressures of CO_2 , the P - x diagram is contoured in terms of the mean molar volume, $\text{cm}^3 \text{ mole}^{-1}$. Curvature of the lines of constant molar volume indicates the degree of ideality of mixing of the two components. Isometrics convex toward higher pressures indicate a net repulsion between the components and fugacities in the mixtures that are larger than would be calculated on the assumption of ideal

mixing. Isometrics concave toward higher pressures indicate a net attraction between the components and fugacities in the mixtures that are less than would be calculated on the assumption of ideal mixing. In figure 52 the mixing is seen to be essentially ideal for a mean molar volume of more than $400 \text{ cm}^3 \text{ mole}^{-1}$. Mixtures of lower molar volume, found at higher pressures, are convex toward high pressure (activity coefficients of more than 1.00). These data, together with the data from the wollastonite-calcite-quartz equilibrium, indicate that the approach to ideal mixing of the system $\text{CO}_2\text{-H}_2\text{O}$ is remarkably close, at least in the parts of the system so far studied. If this nearly ideal behavior is general throughout the system, calculation of the T - x curves for metamorphic reactions in wet calcareous rocks will be much simplified.

The Alumina Content of Talc

J. J. Fawcett

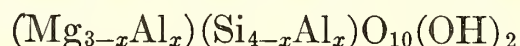
The chemical compositions of more than twenty rock-forming minerals may be plotted in the system $\text{MgO-Al}_2\text{O}_3\text{-SiO}_2\text{-H}_2\text{O}$. Many of these minerals, such as cordierite, the chlorites, anthophyllite, and the SiO_2 group, have each been the subject of detailed research in recent years, but the interrelationships among the various minerals and mineral groups, particularly at water pressures above 2 kb, are as yet not well understood. In *Year Book 61* (p. 88) the importance of these studies to the interpretation of physical conditions prevailing during low-grade regional metamorphism was emphasized, and preliminary data were presented on quartz-chlorite assemblages in the system. This work has been continued and also extended to include physical conditions and bulk compositions applicable to a greater variety of metamorphic rocks.

One of the main problems encountered during the determination of the stability limits of the quartz-chlorite assemblage at

2 and 5 kb $P_{\text{H}_2\text{O}}$ was the rapid but often metastable growth of talc ($3\text{MgO} \cdot 4\text{SiO}_2 \cdot 2\text{H}_2\text{O}$) from a wide range of compositions extending from pure talc to mixtures containing 30 weight per cent Al_2O_3 . Aluminous anthophyllite glasses containing up to 10 weight per cent Al_2O_3 produced mixtures of talc + chlorite between 500° and 700°C at 2 and 5 kb $P_{\text{H}_2\text{O}}$. Under the same conditions, however, more aluminous compositions produced quartz + chlorite. To avoid the intersection of tie lines in the isothermal sections it is necessary to assume that talc may take considerable amounts of Al_2O_3 into solid solution. Yoder (1952) and Stemple and Brindley (1960) have reported on the effect of Al_2O_3 on the X-ray powder diffraction pattern of talc, but few data are available on talc synthesized above 1 kb in the presence of Al_2O_3 . Yoder noted that talc synthesized in the presence of Al_2O_3 showed a measurable reduction in its c dimension. Stemple and Brindley, on the basis of an X-ray study of synthetic talcs, suggested that the maximum Al_2O_3 content of the mineral is about 3.7 weight per cent. To maintain electrical neutrality in the talc structure Al ions must be introduced by one of the coupled substitutions $\text{MgSi} \rightleftharpoons 2\text{Al}$ or $2\text{Al} \rightleftharpoons 3\text{Mg}$. In accordance with the first of these two substitutions four compositions were made up as oxide mixes, containing 0.00, 3.53, 7.05, and 8.81 weight per cent Al_2O_3 . Liquidus temperatures of the above compositions are very high, and glasses have not been prepared. Mix 14 (3.53 weight per cent Al_2O_3) has been completely converted to talc at 2, 5, and 10 kb $P_{\text{H}_2\text{O}}$, confirming the existence of the first substitution noted above. Reaction products from this mixture, held at 5 kb $P_{\text{H}_2\text{O}}$ and 725°C in runs of 1 hour, 65 hours, and 768 hours, were talc + chlorite + quartz, talc + quartz, and talc, respectively. At 2 kb $P_{\text{H}_2\text{O}}$ and 750°C talc alone was produced after 1104 hours, but shorter runs under the same conditions produced mixtures of talc, chlorite, and quartz. At 525°C and 2 kb

P_{H_2O} the 3.53 per cent Al_2O_3 composition was not completely converted to talc after a run of 2760 hours (115 days).

Yoder (1952) reported that the effect of Al_2O_3 on the talc lattice was reflected as a reduction in its c dimension. Stemple and Brindley confirmed this observation and discussed the results of experiments in which aluminous talc was synthesized from a series of compositions of the type



where x varied from 0.0 to 1.0. To judge by crystallographic spacings determined in the present work, the measurements of $2\theta(006)$ of Stemple and Brindley indicate that their talc contains more than the equilibrium portion of Al_2O_3 .

X-ray powder diffraction patterns confirm previous work that indicated the reduction of the c lattice spacing of talc with increased Al_2O_3 content. Talc produced from mix 14 (3.53 per cent Al_2O_3) between 750° and $775^\circ C$ has $2\theta(006)$ of $28.72^\circ \pm 0.01^\circ$, $28.74^\circ \pm 0.01^\circ$, and $28.76^\circ \pm 0.01^\circ$ at 2, 5, and 10 kb P_{H_2O} , respectively (CuK α radiation). The effect of pressure on the cell size of talc is thus seen to be small. Basal spacings of talc produced in the limiting assemblage of chlorite + quartz + talc, from more aluminous compositions, show only very small increases in $2\theta(006)$ at all three pressures, suggesting that the maximum alumina content of talc is about 4.0 per cent with no significant increase due to increased pressure of synthesis. Natural talcs, from different environments, are now being examined by X-ray powder diffraction in order to determine the variation in their basal spacings. The highest Al_2O_3 content of talc, reported in a recent analysis, is 3.95 per cent in a talc yoderite quartz kyanite schist (McKie, 1959).

The Upper Stability Limit of Magnesian Chlorites to 10 Kilobars P_{H_2O}

J. J. Fawcett

Investigations of phase relations in the system $MgO-Al_2O_3-SiO_2-H_2O$ at 5 and 10

kb P_{H_2O} are complicated by the extent of solid solution in some of the minerals encountered (e.g. talc, chlorite, enstatite, and anthophyllite). Study of the clinocllore composition has been undertaken as part of a more extensive investigation of the magnesian chlorites at 5 and 10 kb P_{H_2O} with a view to establishing X-ray determinative curves for chlorites synthesized at high pressures. Such curves are necessary for the determination of chlorite compositions in two- and three-phase assemblages in the system as a whole.

The stability and phase relationships of the magnesian chlorites have been studied by several workers (Yoder, 1952; Roy and Roy, 1955; Nelson and Roy, 1958), but each of these investigations has been confined to water pressures up to 2 kb. Crowley and Roy (1960) have shown that basal spacings of some synthetic sheet minerals, including the chlorites, vary according to the pressure of synthesis. X-ray determinative curves based on materials synthesized at 2 kb P_{H_2O} cannot be used, therefore, on minerals produced at higher pressures.

The range and number of experiments carried out during this study have been greatly increased by the use of cold-seal hydrothermal pressure vessels manufactured from the alloy R41 (Haynes Stellite Company) in addition to internally heated pressure vessels. Temperatures up to $860^\circ C$ at 5 kb P_{H_2O} have been imposed on cold-seal pressure vessels of $1\frac{1}{4}$ -inch diameter. These are the most severe conditions imposed on such a vessel, but they have been maintained for 6 hours without failure. It should be emphasized, however, that each vessel has its own characteristics on approaching the limiting P and T conditions. Similar vessels have been employed repeatedly between 775° and $825^\circ C$ at 5 kb, but two have failed during long runs (3 weeks) in the same temperature range but at lower pressures after successful runs under extreme conditions. Fortunately, failure of the R41 bombs is similar to that of the more common Haynes alloy 25, i.e. by flow rather than

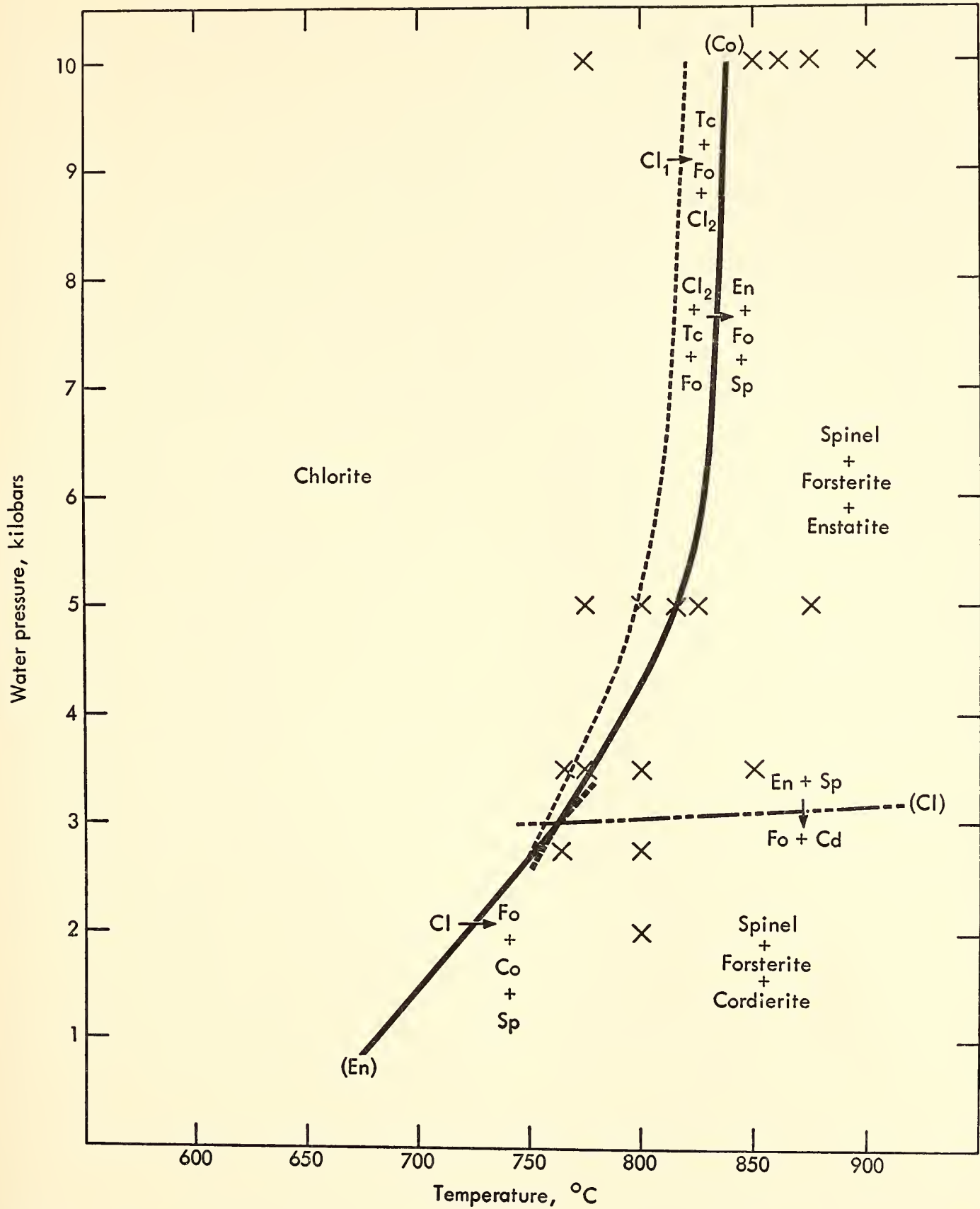


Fig. 53. Upper stability limit of magnesian chlorites to 10 kb P_{H_2O} . The dashed curve represents the upper stability limit of clinochlore, and the solid curve the upper stability limit of magnesian chlorite of variable composition (see text). Symbols in parentheses—(En), (Cl), and (Co)—refer to the absent phases on the respective curves.

by fracture. The two failures in these vessels have been uneventful.

Starting materials for this investigation were oxide mixes of the appropriate composition ($5MgO \cdot Al_2O_3 \cdot 3SiO_2$), synthetic clinochlore produced from the oxide mix,

and a natural analyzed leuchtenbergite (Kerr and Callaghan, 1935). The upper stability limit of clinochlore is shown in figure 53, in which the data up to 2 kb are taken from Yoder (1952). Reactions have not yet been reversed at all pressures of

investigation, but additional data from other compositions within the quaternary system are in agreement with the position of the curve as shown. The first point to note is that clinochlore is in fact stable at water pressures up to 10 kb. Indeed, the maximum stability of the mineral, in terms of both temperature and pressure, is surprising in view of its restriction, in regionally metamorphosed rocks, to lower-grade assemblages. It is evident, therefore, that the absence of chlorite from metamorphic rocks of higher grades is due to its reaction with other minerals rather than to breakdown under high pressure. However, the possible effects of iron, the most common additional constituent of the natural minerals, in reducing the chlorite stability field must not be overlooked.

The effect of pressure on the crystal structure of clinochlore is reflected in the basal spacings measured on the minerals synthesized at 2, 5, and 10 kb P_{H_2O} . Yoder (1952) synthesized clinochlore with a basal spacing of 14.42 Å at 2 kb P_{H_2O} ; in the present investigation clinochlore synthesized at 5 kb has a basal spacing of 14.278 ± 0.004 Å, and at 10 kb 14.265 ± 0.004 Å. This feature may represent a genuine contraction of the chlorite lattice in response to pressure of formation but has also been interpreted by Crowley and Roy (1960) as a possible indication of Al-Si ordering in the tetrahedral layer of the chlorite structure.

Data presented by Nelson and Roy (1958) showed that, at 1000 atmospheres water pressure, magnesium chlorites close to the clinochlore composition are more stable than amesite or penninite members of the series. The present experiments suggest that the composition of maximum stability varies with pressure and that the most stable magnesium chlorite at 5 and 10 kb P_{H_2O} lies between the clinochlore and amesite compositions. In figure 53 the upper stability curve is shown for the magnesium chlorites, but it may be noted that the actual composition of the chlorite on this curve varies with pressure. The

dashed curve shown about 15°C below the maximum chlorite stability represents the upper stability of clinochlore, which above 3 kb P_{H_2O} breaks down to a more aluminous chlorite + talc + forsterite. A family of analogous curves may be constructed to show the upper stability limits of specific chlorite compositions. It should be emphasized that the dashed curve applies only to the clinochlore composition, and the pressure above which clinochlore is no longer the most stable of the magnesian chlorites is not necessarily coincident with the invariant point.

The stable breakdown products of the Mg chlorites vary according to the pressure of decomposition. At high pressures, between 5 and 10 kb P_{H_2O} , the stable assemblage is forsterite + enstatite + spinel, whereas below 3 kb P_{H_2O} forsterite + cordierite + spinel is the stable assemblage. Early work in this system established that the forsterite-cordierite tie line is stable between 1 atmosphere and 2 kb P_{H_2O} . Chinner and Yoder (*Year Book 59*, p. 80), however, found that this tie line is broken at 10 kb P_{H_2O} and the two tie lines enstatite-spinel and enstatite-sapphirine are stable. Chinner (personal communication) has confirmed the early data at 2 kb P_{H_2O} .

An attempt has been made, therefore, to establish the invariant point along the chlorite breakdown curve at which clinochlore, forsterite, cordierite, enstatite, and spinel coexist. The determination of this point has been greatly hindered by the very slow rates of reaction. Clinochlore, enstatite, and cordierite each persist metastably for long periods, and progress toward equilibrium is slow. Although the invariant point has not been accurately located it probably lies between $2\frac{1}{2}$ and $3\frac{1}{2}$ kb at $735^\circ \pm 15^\circ\text{C}$.

The precise nature of the distribution of univariant curves around the invariant point in figure 53 was deduced by a graphic analysis of the relationships of the five solid phases in equilibrium at that point (Morey, 1957). This analysis shows

that two univariant reactions, in addition to those shown, converge at the invariant point: the forsterite-absent curve (chlorite + cordierite = enstatite + spinel), and the spinel-absent curve (chlorite + enstatite = forsterite + cordierite). As these curves cannot be realized experimentally from the clinocllore composition they are not shown in figure 53. The forsterite-absent curve would lie between the stable extension of the cordierite-absent and the metastable extension of the chlorite-absent curves, and the spinel-absent curve would lie between the stable extension of the enstatite-absent and the metastable extension of the chlorite-absent curves.

The enstatite-spinel assemblage is now known to be stable, in synthetic systems, over a wide range of temperature and pressure, as suggested by natural assemblages. Enstatite-spinel is a common mineral assemblage, but forsterite-cordierite, the assemblage found to be stable at low pressures, is certainly rare, if indeed it exists.

Locating precisely the invariant point described above is further complicated by the fact that, above 2 kb P_{H_2O} , clinocllore does not break down directly to the appropriate stable assemblage. Both talc and anthophyllite are produced during the breakdown of magnesian chlorite between $3\frac{1}{2}$ and 10 kb P_{H_2O} . This reaction is probably analogous to that described by Greenwood (*Year Book 61*, p. 86) for the production of metastable anthophyllite from talc. The chlorite structure consists of interlayered "talc" and "brucite" sheets, and breakdown of chlorite probably results in the separation of the sheets followed by disintegration of the "talc" sheets to anthophyllite + enstatite. Greenwood reported quartz as a breakdown product of talc, but it was not detected in the chlorite breakdown. Silica released during the disintegration of "talc" layers in the chlorite structure must react immediately with the "brucite" layer, the reaction products depending on the temperature and pressure.

This reaction should provide interesting starting material for an attempt to synthesize aluminous anthophyllite.

The Liquidus Region at 10 Kilobars P_{H_2O}

J. J. Fawcett and H. S. Yoder, Jr.

Most metamorphic reactions take place in the absence of a liquid phase, and therefore the investigation of relevant synthetic systems as an aid to the interpretation of these rocks may be expected to yield the most useful results when conducted in the solid state. Investigation of the stability and phase relations of aluminous anthophyllite in the system $MgO-Al_2O_3-SiO_2-H_2O$ was begun below solidus temperatures at 5 and 10 kb P_{H_2O} but proved to be highly complex owing to problems of metastability and of solid solutions in enstatite, anthophyllite, chlorite, talc, and probably sapphirine. It was decided, therefore, to investigate the liquidus region of the system at 10 kb P_{H_2O} with a view to clarifying the relationships in the subsolidus.

A preliminary 900°C isothermal section is shown in figure 54, using a projection of the phase relationships from the H_2O apex of the quaternary system. It is apparent that many aspects of the section are in direct contrast to the relationships determined both at 1 atm (dry) and between 1 and 2 kb P_{H_2O} (Keith and Schairer, 1952; Yoder, 1952; Roy and Roy, 1955). Although the diagram has not yet been completed either in the low-MgO or sapphirine areas, all phase relations shown have been confirmed by experiments at temperatures above and below the temperature of the section.

The beginning of melting in this system, at 10 kb P_{H_2O} , is more than 450°C lower than that determined at 1 atm, and the composition of the first liquid formed is considerably more siliceous than that at 1 atm. Perhaps the most striking contrast to the phase diagrams determined at lower pressures is the extent of aluminum solid solution in enstatite. Boyd and England (*Year Book 59*, p. 49) determined

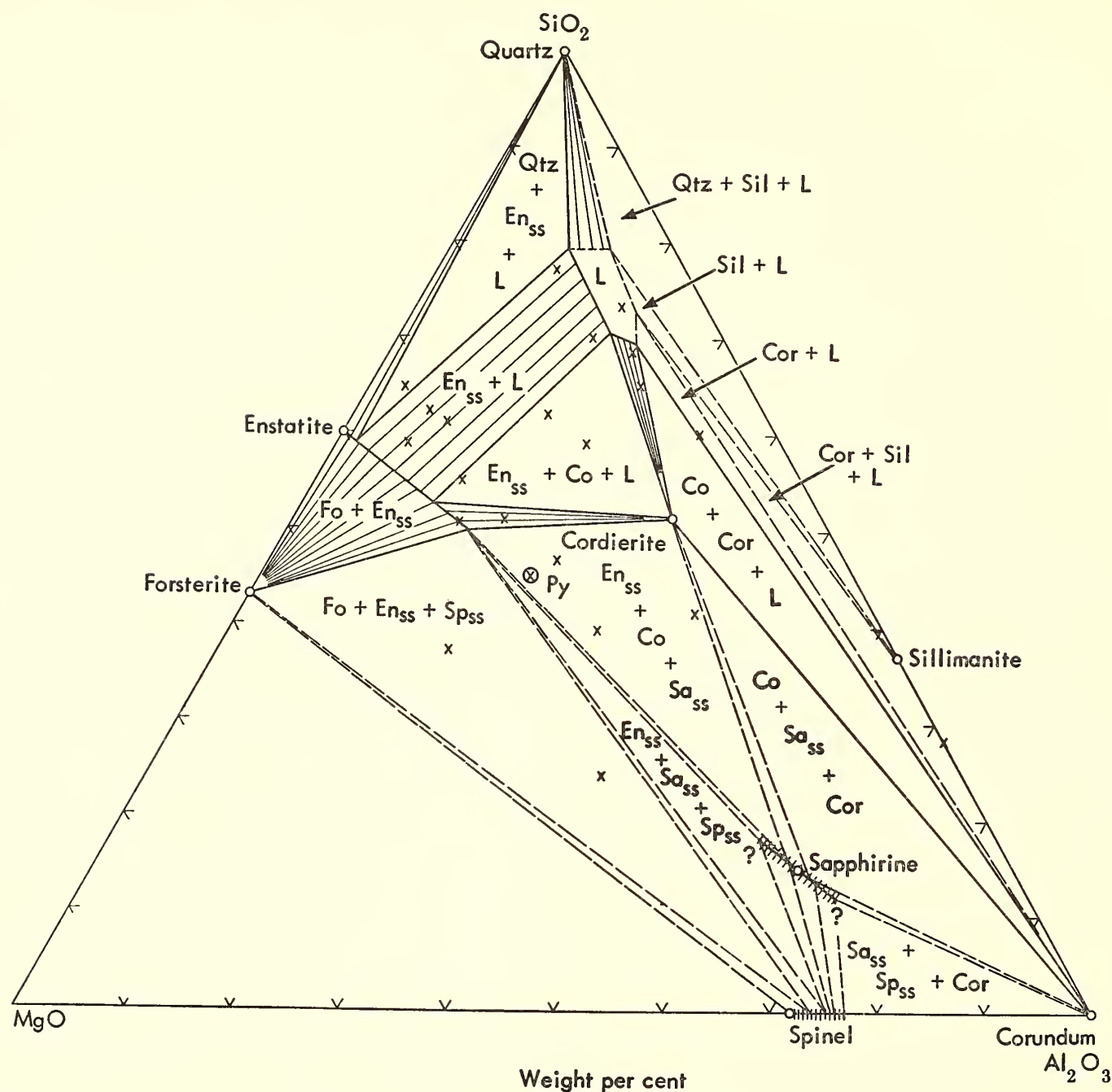


Fig. 54. Isothermal section at 900°C and 10 kb P_{H_2O} through the system $MgO-Al_2O_3-SiO_2-H_2O$ projected from the H_2O apex of the quaternary system.

the limits of aluminum solid solution in enstatite at 18.2 kb and 1400°C. The determinative curves they constructed for this solid solution series have been used in the present study; they indicate a maximum of 16 per cent Al_2O_3 in enstatite at 900°C and 10 kb P_{H_2O} . The distribution of tie lines determined from several compositions is in accord with the high but unexpected alumina content in enstatite at that pressure. Boyd and England commented on the possibility of ternary solid solutions in enstatite. An indication of this phenomenon has been detected in our investigation during experiments on the pyrope composition (Py in fig. 54).

This composition produced only enstatite solid solution and sapphirine at 900°C and 10 kb P_{H_2O} after a run of 46 hours. The phenomenon has not been investigated further, but the relationship may also be complicated by the solid solution of aluminum in sapphirine.

A notable absence in figure 54 is a stability field for mullite. This is based on unpublished data of Yoder and Schreyer, who found sillimanite + corundum to be stable at 10 kb P_{H_2O} . The corundum + liquid field cuts any possible aluminosilicate + either spinel or sapphirine joins that are stable at lower pressures and necessarily defines the cordierite +

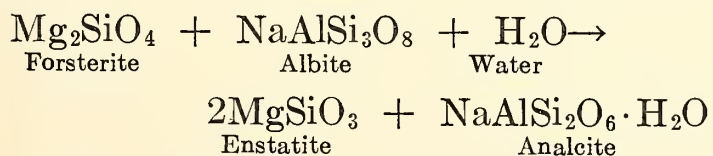
corundum + liquid and cordierite + sapphirine + corundum fields.

An interesting possibility contemplated at the beginning of our study was the occurrence of a hydrous phase on the liquidus surface. A careful search has been made for such minerals (e.g., aluminous anthophyllite) at the liquidus, but evidence collected to date indicates that all liquidus phases, with the possible exception of cordierite, are anhydrous. The liquidus data so far determined at 10 kb P_{H_2O} have already assisted in the interpretation of the subsolidus equilibria. A more complete solution of the liquidus relationships at that pressure will enable us to pursue our studies of the more applicable subsolidus region.

*Probable Instability of Analcite
+ Hypersthene*

H. S. Yoder, Jr., and J. J. Fawcett

An occurrence has been reported of an intrusive sheet in Japan with veins and schlieren of analcite dolerite containing, among other minerals, analcite + hypersthene or pigeonite (Kushiro, 1959). In one zone of the sheet the assemblage analcite + hypersthene + plagioclase + altered¹¹ olivine was observed. The relationships of the reactants are shown in the compositional diagram forsterite-nepheline-silica (fig. 55), using a one-point projection from H_2O . The implication is that analcite + hypersthene is more stable in some regions of pressure and temperature than the common assemblage olivine + plagioclase in the presence of an excess of water. Expressed in terms of the pure end members, the probable reaction is



The coexistence of analcite and hypersthene appears to be reasonable until the stability curves of the minerals involved

¹¹ The alteration is presumed to be montmorillonite or chlorite (Kushiro, 1963, personal communication).

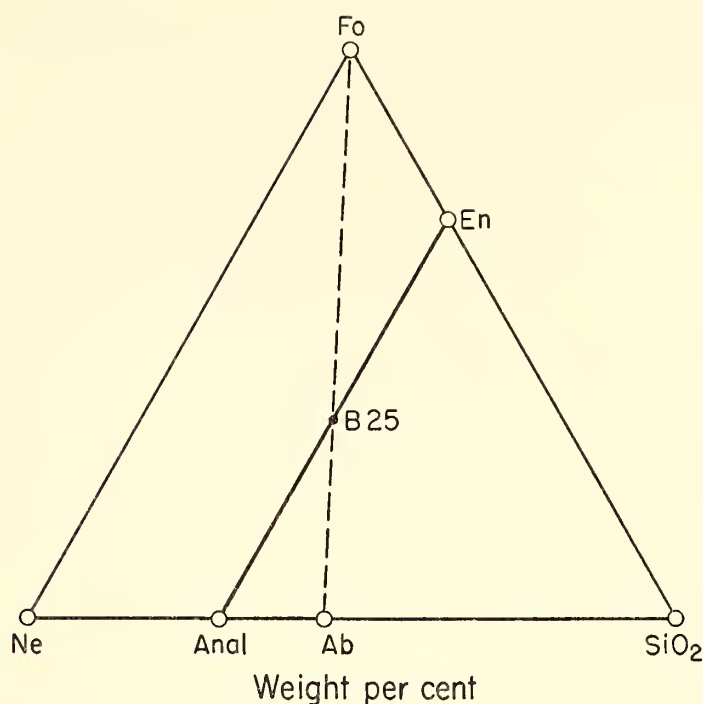


Fig. 55. Illustration of the implied reaction between forsterite (Fo) and albite (Ab) in the presence of an excess of water to yield analcite (Anal) and enstatite (En) in the system forsterite (Fo)-nepheline (Ne)-silica (SiO_2).

are compared. In figure 56 are given the upper stability curve for analcite (Yoder, *Year Book 53*, pp. 121-122) and the lower stability curve for enstatite (Greenwood, *Year Book 61*, pp. 85-88). It is clear that at none of the pressures and temperatures studied is the association of analcite and enstatite possible in the presence of an excess of water. Where the water pressure is less than the total pressure the two minerals would still be incompatible, but they may become compatible if the water content is reduced so that no free water exists. Under these water-deficient conditions an amphibole (e.g., anthophyllite) would be expected as a phase. No amphibole was observed by Kushiro. In figure 56 are also given the lower stability curves of albite (Saha, 1961) and of forsterite (Bowen and Tuttle, 1949) in the presence of an excess of water. The ruled area in figure 56 is the only region of pressure and temperature where forsterite, albite, and analcite are all stable in the presence of an excess of water. The presence of iron in the orthopyroxene may lower the lower stability limit of the orthopyroxene below that of enstatite; however, the presence of

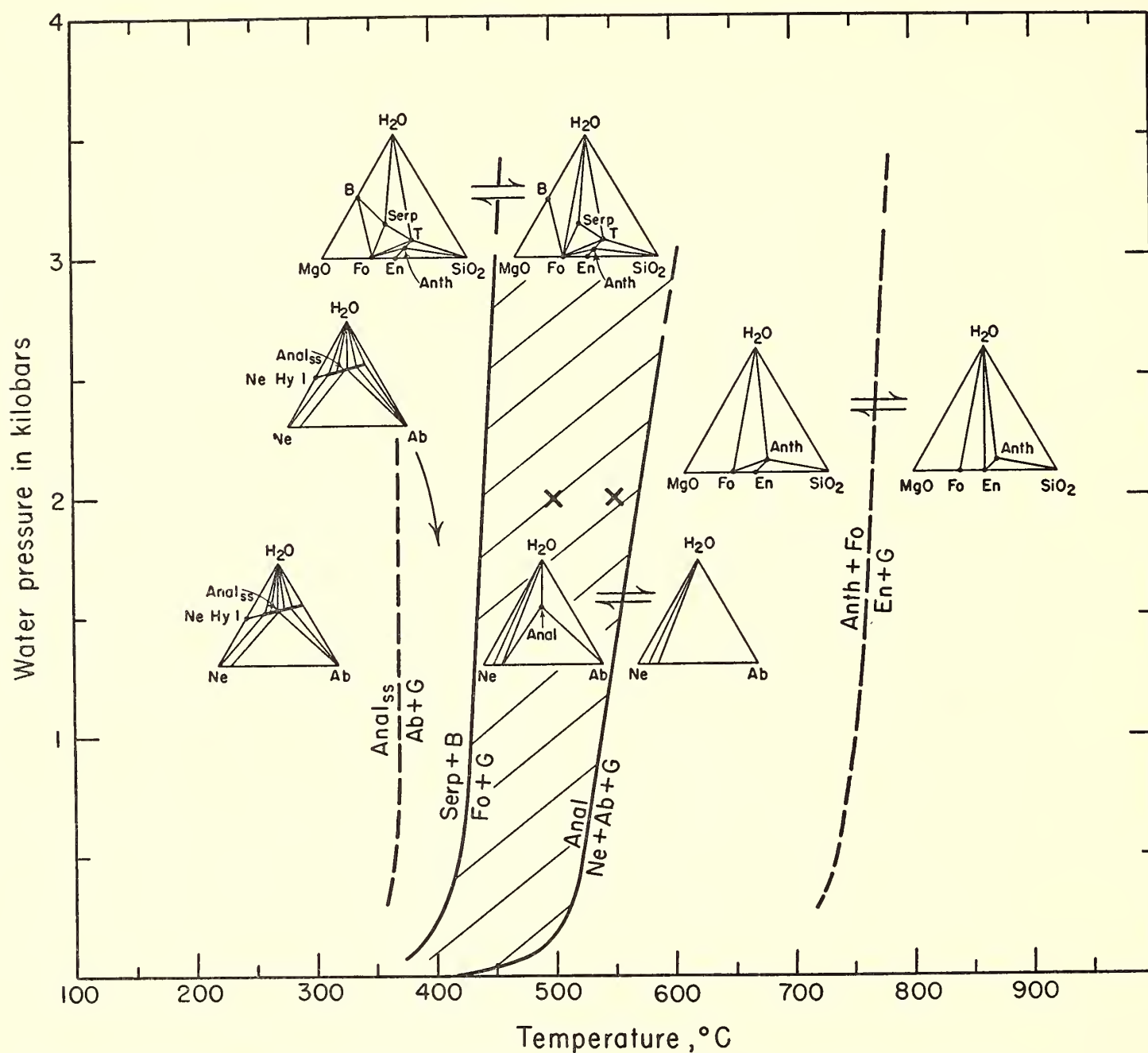


Fig. 56. Comparison of the upper stability curve of analcite (Yoder, *Year Book 53*, p. 121) with the lower stability curve of enstatite (Greenwood, *Year Book 61*, p. 87). Ab, albite; Anal, analcite; Anth, anthophyllite; B, brucite; En, enstatite; Fo, forsterite; G, gas; Ne, nepheline; Ne Hy I, nepheline hydrate I; Serp, serpentine; Tc, talc. The lower stability curves for Ab suggested by Saha (1961) and for Fo (Bowen and Tuttle, 1949) are given to indicate further restrictions to the proposed reaction.

calcium in the analcite (the wairakite molecule) may lower the upper stability limit of the zeolite slightly below that of pure analcite (Ames and Sand, 1958a). It is unlikely that these effects would lead to an overlap of the fields of stability of analcite and hypersthene.

Several exploratory experiments were conducted, using a glass of the composition $\text{Fo}_{3.5}\text{Ab}_{6.5}$ (B25 noted in fig. 55) and the same glass crystallized at 1050°C for 58 days, containing forsterite, albite, and some glass. A third starting material

consisted of a mixture of an analyzed natural analcite and MgSiO_3 glass in 1:2 molecular proportions. The pressure was 2 kb and the temperatures 500° and 550°C , conditions within the area of possible reaction (see ruled area in fig. 56). The products were montmorillonite (probably a soda-bearing stevensite or a saponite) + albite in all experiments, indicating that $\text{En} + \text{Anal}$ is not the more stable assemblage in the presence of an excess of water at relatively low temperatures.

Montmorillonite readily grows metastably from the composition $\text{Na}_2\text{O} \cdot 3\text{MgO} \cdot \text{Al}_2\text{O}_3 \cdot 8\text{SiO}_2$ according to Ernst (1961, p. 743); however, montmorillonite formed at the expense of forsterite (and presumably some albite or analcite) in the present experiments from the composition $\text{Na}_2\text{O} \cdot 4\text{MgO} \cdot \text{Al}_2\text{O}_3 \cdot 8\text{SiO}_2$ seems to be stable. Some soda-bearing montmorillonites (e.g., saponite) are known to be stable at temperatures as high as 750°C at 1 kb (Ames and Sand, 1958b).

It is concluded that the igneous rocks containing the common assemblage olivine + plagioclase were formed either in the absence of water or, more probably, at a temperature above the stability of the hydrous minerals. It is also suggested that the coexistence of analcite and hypersthene (or pigeonite) is the result of nonequilibrium conditions. Support for this suggestion comes from Kushiro, who considers the magma to have been contaminated by assimilation.

It has been suggested that hypersthene may result from the oxidation of the olivine (Muir, Tilley, and Scoon, 1957) and that the formation of analcite could be contemporaneous with the oxidation process or a product of a later hydrothermal alteration. In the present occurrence, however, this explanation is not satisfactory because the hypersthene found in the rocks is iron-rich (Fs_{42-45}); in fact, the hypersthene is more iron-rich than that which would normally coexist with the observed clinopyroxene. The pyroxenes themselves are probably not in equilibrium with each other.

Wilshire (1961) describes sedimentary xenoliths with orthopyroxene reaction rims produced by the action of an enclosing alkali basalt. The water content of the xenoliths apparently contributed to the formation of zeolites, mainly natrolite and also analcite. It is noteworthy that, surrounding large amygdules in the basalt, the olivine and plagioclase are altered to montmorillonite, analcite, and natrolite. The alkali dolerite of Kushiro also penetrates shale, although xenoliths were not

reported. It is likely, therefore, that the assemblage analcite + hypersthene reported by Kushiro is the result of a nonequilibrium process or two separate unrelated processes.

The Muscovite-Kaolinite Reaction

B. Velde

Kaolinite is abundant in many recent sediments, whereas illite is the dominant clay mineral in most shales (Pettijohn, 1957). Although chemically the conversion of kaolinite to illite requires only the exchange of K^+ for H^+ and the loss of water (Hemley, 1959), some workers have contended on structural grounds that kaolinite can be converted to illite only by complete breakdown of the kaolinite structure and subsequent formation of a dioctahedral mica (muscovite) structure. Rate studies of the formation of muscovite from kaolinite and KOH suggest that the kaolinite structure is partially inherited. This reaction can also give insight into the structural controls that dictate the muscovite polymorph.

As kaolinite and muscovite have the same Al/Si ratios, a purified kaolinite and KOH could be starting materials for rate studies. A natural kaolinite (0.15 per cent Na_2O , 0.06 per cent K_2O impurities by weight) and KOH (0.02 per cent Na by weight) were weighed and then mixed in a water solution. The mixture was dried and ground, and the individual runs were finally made by adding water to the dried solids. The starting materials had an excess of water present for both kaolinite and muscovite phases. The experiments were run from 150° to 700°C at 1 and 2 kb pressure.

Two initial products that resulted from the conversion were 1Md muscovite and 1M muscovite. Subsequent polymorph inversions that occurred are dealt with later. In figure 57 solid lines represent conversions at 2 kb; the dashed line, conversions at 1 kb. Initial mica phases were distinguished by a low hump in the diffraction pattern at about $8^\circ 2\theta$ ($\text{CuK}\alpha$). This hump was accompanied by a sharp-

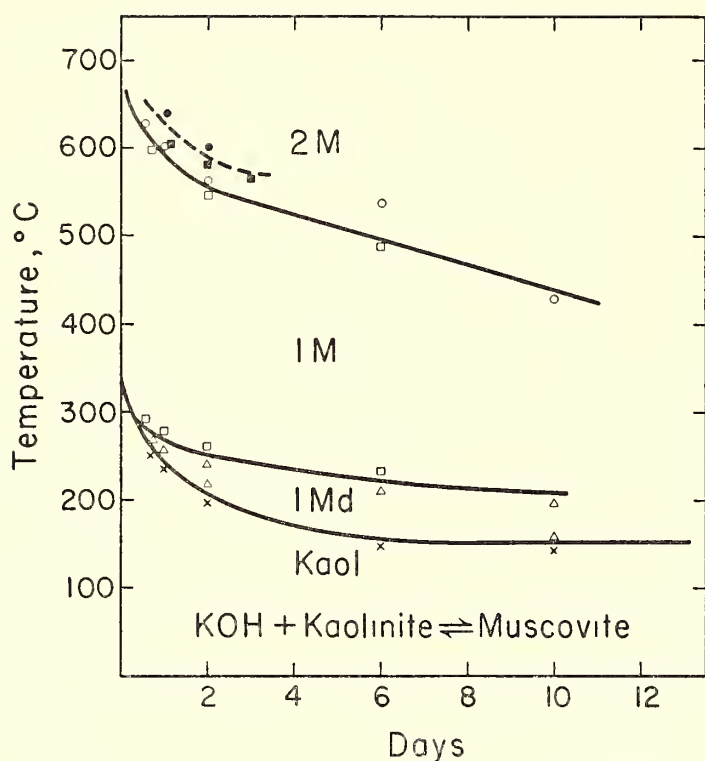


Fig. 57. Products in the reaction kaolinite + KOH \rightarrow muscovite. Crosses indicate only kaolinite present; triangles, 1Md muscovite present; squares, 1M muscovite present; circles, 2M muscovite present. Solid symbols indicate a pressure of 1 kb; open symbols, a pressure of 2 kb.

ening and increase in intensity of the kaolinite reflections at $19.8^\circ 2\theta$ and $34.5^\circ 2\theta$. 1M and 2M₁ polymorphs were distinguished by the presence of reflections between 18° and $35^\circ 2\theta$ as described by Yoder and Eugster (1955).

In similar experiments Yoder and Eugster (1955) reported the conversion of kaolinite to a disordered¹² (1Md) mica polymorph after 144 hours at 400°C and 1 kb pressure. In the present study, under the same pressure and temperature conditions, 1M muscovite resulted in less than 6 hours. Kaolinite was a starting material in both studies, but potassium was added in different forms. Yoder and Eugster used a KAlSiO_4 glass; in the present study the necessary potassium was added in the form of KOH in aqueous solution. The KOH in solution was immediately available for reaction, whereas the potassium

in a glass would be much slower in entering the fluid of the charge. The availability of potassium was thus quite different in the two series of experiments and apparently affects the rate at which kaolinite is converted to ordered (1M) muscovite.

The kaolinite structure is partly destroyed by heating to 550°C at 1 atm (Brown, 1961), the resulting phase being known as metakaolinite. Metakaolinite was also formed in the present study at temperatures as low as 200°C at 2 kb water pressure. It therefore seems probable that in experiments where the potassium ions were not readily available for reaction (e.g., when K^+ is in a silicate glass) metakaolinite was formed before conversion to muscovite. The reaction might then have proceeded more slowly because the 1M muscovite could not inherit essential parts of its structure from metakaolinite. Rate studies were made for several starting materials to assess the importance of the structural state of kaolinite in the conversion to muscovite: (1) KOH + unaltered kaolinite, (2) KOH + metakaolinite, and (3) KOH + kaolinite only partly converted to metakaolinite. For a given pressure and temperature, runs made with starting material 1 produced 1M muscovite plus little or no 1Md (disordered) muscovite, whereas those made with starting materials 2 and 3 formed mostly 1Md muscovite, which only slowly inverted to 1M muscovite. It is clear that the structure of the starting material exerts a control in the formation of an ordered (1M) muscovite structure and that the structure of kaolinite is somehow inherited by the muscovite.

The structures of muscovite and kaolinite are quite different within the variation possible in layer silicates. Basically, muscovite has three layers of aluminum-silicon cations per unit cell, and kaolinite has two layers. The conversion involves the loss of a hydrogen ion from the Al-OH coordinations, the charge deficiency being balanced by a potassium interlayer ion in

¹² Order is used here in the sense of continuity in stacking of the 10 Å layers in the mica structure (see Yoder and Eugster, 1955).

the muscovite structure. For the structure to be inherited, however, the cation-anion relations must change in half of the kaolinite layers. (This problem has in the past prompted the conclusion that the kaolinite structure must be destroyed and a completely new structure formed in order to convert kaolinite to muscovite.) It is significant that the first or most intense X-ray reflections of the newly formed muscovite are the (020) and (130) (200). The d values of these planes are closely similar to those of the (020) (110) and (130) ($\bar{1}30$) planes in kaolinite. This similarity of ($h\bar{k}0$) reflections suggests that the a - b plane network of the kaolinite structure is inherited by muscovite.

The importance of the structural continuity during the kaolinite muscovite conversion is better understood when considered with respect to the $2M_1$ muscovite structural analysis by Radoslovich (1960). He suggested that the ordered dioctahedral array of aluminum ions in octahedral coordination is the factor that controls the accommodations made by the remainder of the structure. These accommodations result in a distortion of the hexagonal oxygen net with which interlayer potassium ions coordinate, and the extent of this distortion determines which mica polymorph forms. The preservation of a regular octahedral arrangement

of aluminum ions appears to be the initial condition that permits the rapid formation of a 1M muscovite. This condition is no longer met when the kaolinite passes through a metakaolinite stage, and it appears that the direct conversion of kaolinite to 1M muscovite is dependent on the availability of K^+ in the starting materials, which compensates for the expelled H^+ .

Yoder and Eugster (1955) proposed that 1M muscovite is stable below $200^\circ C$ and that the $2M_1$ polymorph is stable above that temperature. However, they did not observe the reaction $2M_1$ to 1M in the proposed stability field of the 1M polymorph. They also found that the 1M polymorph has a slightly larger unit cell than the $2M_1$, which suggests that the 1M might be a low-pressure polymorph relative to $2M_1$. The suggestion is supported by rate studies showing that the time required to invert 1M to $2M_1$ muscovite at a given temperature is reduced by increased water pressure (fig. 57). Thus it is possible that 1M muscovite formed from the metastable 1Md polymorph is itself metastable. Further experiments are in progress to test this tentative hypothesis, and the possibility that the 1M polymorph has a high-temperature, low-pressure stability field is being investigated.

PETROGRAPHY

ON THE GEOGRAPHIC DISTRIBUTION OF CENOZOIC VOLCANISM

Available Data

F. Chayes and D. Métais

The Cenozoic period has been characterized by enormous volcanic activity, and although knowledge of the geochemistry of most individual Cenozoic volcanic complexes is still fragmentary we are already faced with an accumulation of analytical data so vast that most of us simply ignore all but the minute fraction of it immediately relevant to our current research.

Probably many petrologists will be surprised, as we were, by the amount of analytical information the well informed student of Cenozoic volcanism ought to have at his command. Our file, for instance, already contains nearly 6000 published analyses of Cenozoic volcanic rocks. Considering that our coverage of Slavic and other eastern literature is inadequate and that we have so far made no attempt to obtain full coverage of any of the major continental areas, we think that there are probably 7000 and perhaps over 9000 reasonably modern analyses of Cenozoic volcanic rocks sufficiently com-

plete to permit useful normative calculations.

In this vast number of analyses, petrographers must be concerned with frequency distributions not only of various of the oxides considered individually but also of combinations of oxides by weight per cent, or mole per cent, as well as of normative parameters taken individually and in sets. It is not at all surprising that large-scale generalizations about areal geochemistry or the relations between geography and petrography are usually regarded as matters of conviction rather than discussion. How can we evaluate conclusions based on data we are unable to examine effectively or summarize efficiently?

The sorting and computational procedures involved in efficient examination of such a mass of data are ideally suited for machine operation. If one can state numerically what it is he wants to examine and record in a set of analyses, and devise a set of numerical criteria upon which to base acceptance or rejection, he can accomplish in seconds or minutes an amount of inspection and tabulation that might otherwise require weeks or months of labor, if indeed it were to be attempted at all. During the past year we have been accumulating a card file of analyses of Cenozoic volcanics and experimenting with methods of storing and retrieving these data, as well as of manipulating them in ways of interest to the petrographer. Although the catalogue, as mentioned above, is still incomplete, we have been able to prepare data summaries of considerable petrographic interest. One of these has already been published (Chayes, 1963).

Another is briefly described immediately below, and a third in a later section of this report. Although no great modification of major conclusions is anticipated, we should like to remind readers that neither study is complete and that numerical estimates in tables and text are to be regarded as provisional. Even if one is prepared to rely on secondary sources,

literature search of this type generates an enormous overburden of bibliography; for practical reasons we defer the listing of source references until the finished work is ready for publication.

A Distinction between Intra- and Circum-oceanic Cenozoic Volcanics

F. Chayes

The Cenozoic volcanism of the continents proper and of the shallow-sea areas of the globe is petrographically so complex as to have obscured a simple and marked distinction between the Cenozoic volcanics in and around the open oceans.

For the sake of brevity we shall here define "around" the ocean as being immediately on the shoreward side of one of the great deeps or troughs that often separate oceans from continents or from shallow-sea areas. Our "circum-oceanic" volcanics thus include those of the Aleutians, the Kuriles, Kamchatka, Hokkaido, Eastern Honshu, the Izu Islands, the Bonin group, the Marianas and Saipan, Wallis Island and—for lack of data closer to the Tonga deep—the New Hebrides, as well as the lavas of the western Andes, southwestern Central America and Mexico, Java, Sumatra, and the Lesser Antilles. The oceanic islands include all those lying in deep water isolated from or on the ocean side of these great deeps. With the exception of São Tomé, which is probably an outlier of the Cameroun chain, and Jan Mayen, which is probably a remnant of plateau lava of continental affinity, the oceanic islands of our present definition are those listed in table 1 of Chayes (1963), as well as all of the Hawaiian group, Réunion, and other open ocean basaltic islands omitted from the earlier tabulation because they contain no known salic lavas.

It is well known that what are here termed circumoceanic lavas are ordinarily *calcalkaline* whereas the salic lavas of the open oceans are nearly always *alkaline*, the terms being taken as redefined by Holmes (1921, p. 303–306). Partial chemical equivalents of these initially miner-

alogical definitions are readily formulated in terms of the CIPW norm. A lava in whose norm $(ne + ac) > 0$ is clearly alkaline in the sense of the Holmes definition; a salic lava in whose norm $(ne + ac) = 0$ will almost certainly be calcalkaline, but a femic or intermediate one may not be. Ambiguity arises for a variety of reasons in rocks relatively rich in iron and magnesium. Oxidation of iron may free enough silica to convert normative nepheline to albite, for instance, or the rare modal assemblage acmite + plagioclase + quartz may take the normative form wollastonite + albite + hematite. The CIPW conventions regarding TiO_2 , a constituent usually abundant in oceanic basalts, may also be responsible; FeO combined with TiO_2 to form ilmenite frees silica, which automatically generates (normative) albite in place of nepheline. Since oceanic lavas are dominantly basaltic, the normative quantity $(ne + ac)$ may unambiguously discriminate only a small proportion of oceanic lavas from circumoceanic ones.

Oceanic basalts are often both more femic and less siliceous than circumoceanic ones, but the normative expression of these and other chemical properties generates no marked qualitative distinction, and much current research seems to suggest that there is none. We believe there is, and that it has been overlooked for reasons discussed in the preceding section, viz., a plethora of data and a lack of adequate methods of data reduction.

As a bookkeeping device we constructed a simple code that prints out what is in essence a geographically classified gazette of our card file. Examination of large groups of analyses listed in identical format soon suggested the use of TiO_2 as a discriminant, and machine-generated frequency distributions of all available data provided strong confirmation. Geographically circumoceanic lavas ordinarily contain less than 1.5 per cent and almost never more than 2.0 per cent of TiO_2 ; geographically intraoceanic basic lavas ordinarily contain more than 2.0 per cent

and almost never less than 1.5 per cent of TiO_2 . There is in fact surprisingly little overlap, and we are now using a value of 1.75 as a dividing point.

For purpose of machine sorting, accordingly, we define the quantities $A = (ne + ac)_{CIPW}$ and $B = TiO_2 - 1.75$ weight per cent. An analysis in which $A > 0$ or $B > 0$ is classified as petrographically intraoceanic; an analysis in which $A = 0$ and $B \leq 0$ is classified as petrographically circumoceanic. The relation between petrographic and geographic criteria obtained in this fashion is shown in table 9,

TABLE 9. Two-Way Classification of Geographically Circum- and Intraoceanic Cenozoic Volcanics

	C_p	I_p	Σ
C_g	1013	61	1074
I_g	94	678	772
Σ	1107	739	1846

C , circumoceanic; I , intraoceanic; p , petrographic; g , geographic.

in which C and I denote circum- and intraoceanic, and subscripts g and p denote geographic and petrographic, respectively. If the agreement were complete, the upper right and lower left cells of the table would be empty; the sum of the entries in the other two cells divided by the grand sum is thus a crude measure of the efficiency of the cross classification. It is obviously quite high, specifically, $(1013 + 678)/1846$, or 91.6 per cent. Entries in class $I_g C_p$ are mostly genuinely rhyolitic lavas like those of Easter Island and salic lavas whose lack of normative ne is occasioned by extensive hydrothermal silicification or oxidation. Entries in class $C_g I_p$ are nearly all analyses of basaltic lavas containing more than 1.75 per cent TiO_2 and usually very rich in H_2O .

It is evident that the apparent efficiency of the classification—that is to say, the apparent strength of the association

between petrography and geography—will depend somewhat on the geographic definitions of “in” and “around” the ocean. It is also evident that this definition cannot be exact. Cenozoic lavas of circumoceanic petrography abound, for instance, in California, Oregon, New Britain, New Guinea, and eastern New Zealand, along none of which is the ocean bounded by a deep trough. All, however, are in other senses marginal to the Pacific; in some, titaniferous basalts occur, and others, notably New Zealand, contain feldspathoidal lavas as well. It is therefore of considerable interest that the apparent strength of the association between petrography and geography is not weakened by their inclusion; using all data now available in our file, the effect of including these areas is to increase the number of analyses by more than 230 and reduce the efficiency of the cross classification by less than 0.4 per cent.

Although not the all-or-none type of relation that naturalists overinfluenced by the exact sciences tend to prefer, this association is clearly far too strong to be dismissed as a sampling accident. On the contrary, it seems one of the firmest generalizations yet to emerge from the study of Cenozoic volcanism. The petrographic associations here called circum- and intraoceanic are the principal elements of Cenozoic volcanism in the shallow-seas areas and on the continents proper, in both of which environments they may and often do occur in close juxtaposition. Why should their isolation from each other be so marked in the oceanic environment?

SOME RELATIONS BETWEEN SALIC MOLECULES IN THE CIPW NORM AND THE NIGGLI KATANORM

F. Chayes and D. Métais

The systematic calculation procedures of chemical petrography are of two rather distinct types. In one, the calculated parameters bear no immediate (chemical) resemblance to minerals and are not

assigned mineral names or abbreviations of mineral names; the systems of Osann, von Wolff, Hommel, Eskola, Savaritsky, and the original “Niggli-numbers” other than *q* are all members of this group. In the second category the parameters of interest are purposely assigned compositions very like those of simplified or “end-member” natural minerals and are denoted either by the names of these minerals or by abbreviations of them. There are two major systems of this type, the CIPW norm, still exceedingly popular in North America and widely used in Britain and France, and the Niggli katanorm, favored to the virtual exclusion of the CIPW norm elsewhere on the continent.

By means of type face and case some attempt is often made to indicate whether a particular abbreviation denotes a calculation based on CIPW or the Niggli katanorm. No standard system of reference has been adopted, however, and in any event it would be useful largely for the silent appreciation of diagrams and tables. In any discussion in which the full names are used the confusion of systems is complete. If the numerical values assumed by the parameters in the two systems were either identical or perfectly linearly correlated over a series of analyses, this confusion in terminology would be of little moment. In fact, however, relations between parameters having the same name may be exceedingly complex, varying greatly both between different pairs of parameters in the same set of analyses and between the same pair of parameters in different sets of analyses. Though an attentive reading of the computation rules for the two systems would certainly lead one to anticipate complications of this sort, it is nevertheless true that in certain mineral assemblages—specifically, in oversaturated calcalkaline rocks of low color index—agreement between analogous parameters of the two systems is usually good. To our knowledge no detailed examination of the relation between suites of CIPW norms

and Niggli katanorms has been undertaken by earlier workers; we describe below some of the results of such a study, begun last fall.

Our initial intention was to compare the standard CIPW procedure with the standard Niggli katanorm, but we soon found that the treatment of TiO_2 , usually a minor constituent, was different enough in the two systems to generate puzzling and complex differences between results. CIPW first combines TiO_2 with FeO to form ilmenite and then with CaO (and SiO_2) to form perovskite (and sphene). In the Niggli standard katanorm, on the other hand, no ilmenite is formed; ferrous iron consumed in this way by CIPW is thus available for the formation of silicates, the amount of quartz will be less, the amount and fayalite content of olivine will be larger, and even the relation between nepheline and albite may be appreciably shifted. Accordingly, all comparisons summarized here are of the CIPW norm with what Burri calls the "ilmenite-variant" of the Niggli katanorm. This, incidentally, is the variant he himself uses in similar comparisons (Burri, 1959, p. 175).

All our comparisons are based on a simple regression analysis now widely used in discussions of this type. Denoting any Niggli parameter by X , for instance, and the analogous CIPW parameter by Y , we may calculate for any group of analyses the quantities r_{xy}^2 , b , and c , where r^2 is the proportion of the total sum of squares of Y linearly correlated with variation in X , and $\hat{Y} = bX + c$ is the least mean squares estimate of Y as a linear function of X . It may be shown that $0 \leq r^2 \leq 1$, the lower limit describing a situation in which knowledge of X is ordinarily of no use in predicting Y , and the upper limit indicating that the estimate of Y from x is exact. If $b = 1$ and $c = 0$, the parent quantities x and y are the same, whereas if $b \neq 1$ or $c \neq 0$ the relation between them is not one of identity. In either case, a good estimate of one may be made from the other if $r^2 \sim 1$, and rather indifferent predictions may be expected unless $r^2 \sim 0.80$. Some of our results are summarized in table 10.

In oversaturated rocks of low color index the estimates of quartz by the two procedures are usually in excellent agreement. The only exceptions of any conse-

TABLE 10. Percentage of Correlated Variation ($100r^2$) of Analogous Salic Parameters of Niggli Katanorms and CIPW Norms in Some Studies of Analyses

	No. Analyses	Q	<i>or</i>	<i>ab</i>	<i>ne</i>	<i>an</i>
Plutonics						
Rapakivi granites, Fennoscandia	40	99.0	99.7	99.6		99.9
California batholith	44	99.7	99.9	99.8		99.9
Adirondacks	99	99.8	99.9	98.0		99.9
Cenozoic volcanics						
East Africa	33	99.6	99.9	91.8		99.9
Hakone	22	99.9	99.9	99.8		99.8
Slovakia	70	99.4	99.7	99.5		99.8
Phlegrean Fields	27		66.8	91.7	74.5	99.6
Vesuvius	30		64.7	44.1	66.1	99.9
Limagne	85		93.0	69.2	77.0	99.1
Velay	33		99.8	90.2	52.9	99.9
Kaiserstuhl	39		83.3	61.1	79.8	99.8
Nyiragongo	35			40.3	92.4	99.8
Honolulu Series	9			87.6	94.9	99.9
West Maui	6		99.3	91.6	99.2	99.8
Victoria	99		99.9	90.0	89.1	99.9

quence occur in hyperaluminous rocks, in which CIPW simply reports the excess Al_2O_3 as corundum, a procedure that has been criticized on the ground that modal quartz and corundum are incompatible. The Niggli katanorm avoids this unrealistic association by forming cordierite or sillimanite from excess alumina, the results being, in most igneous rocks, hardly less unrealistic. Both Niggli compounds consume silica, so that less will be available for quartz in the Niggli katanorm than in the CIPW norm of a particular analysis.

In the examples so far studied the agreement of Niggli anorthite with CIPW anorthite is excellent, values for the same analysis rarely differing by as much as 1 per cent. Similarly, in oversaturated rocks

Niggli orthoclase and CIPW orthoclase are in close agreement, and the same holds for albite, though ab_{Niggli} is larger than ab_{CIPW} . The situation is much less satisfactory for individual analyses or groups of analyses in which silica is not present in excess. In such rocks the correlation between nepheline in the two systems is generally quite poor and that for albite is rarely good.

For other major normative minerals, chiefly femic ones but also leucite, the calculation conventions differ so much that good agreement between results would hardly be expected. The appearance of leucite in the CIPW norm signals the end of useful direct comparisons, for leucite is not defined or used in the

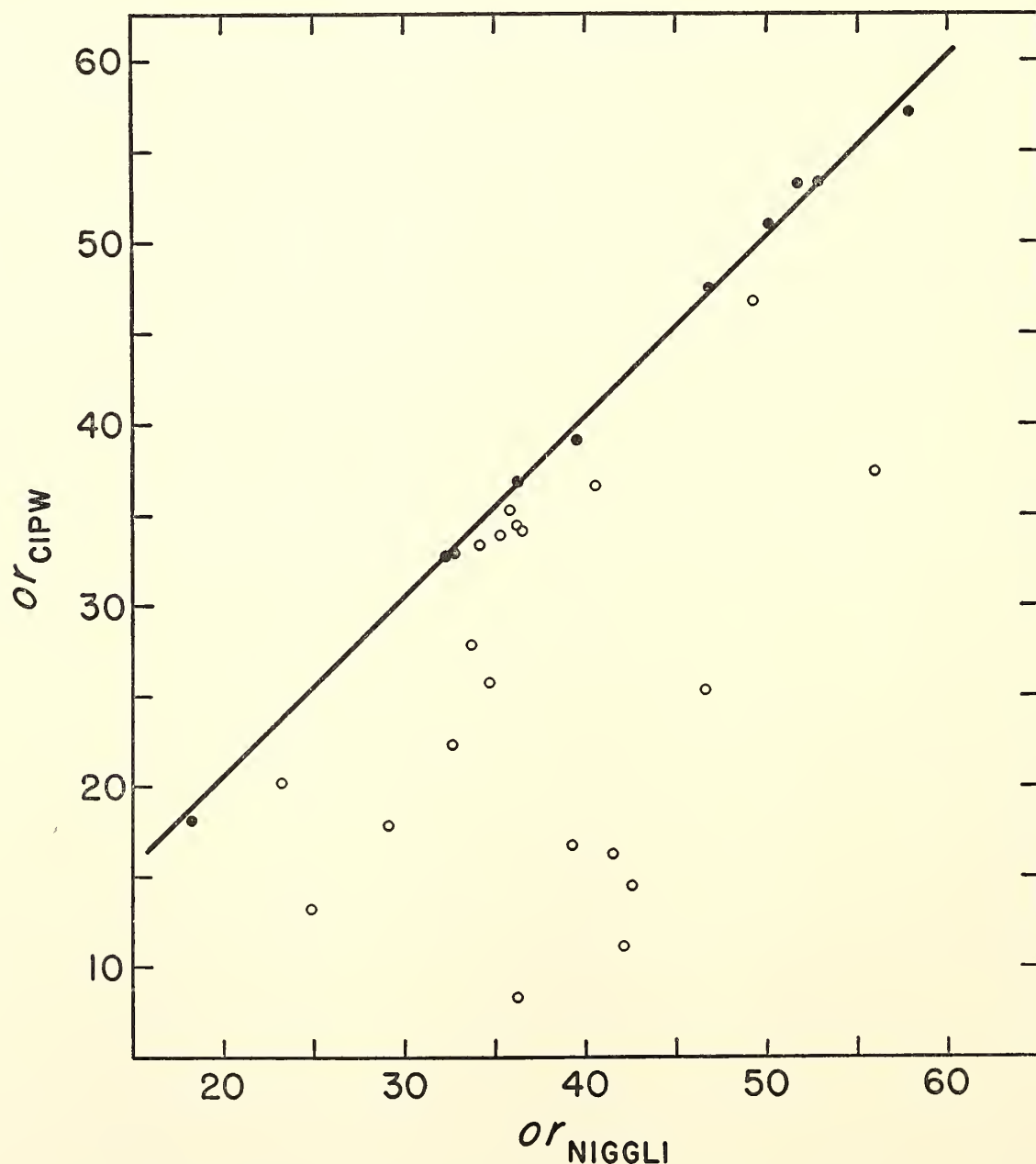


Fig. 58. Niggli and CIPW *or* in lavas of Vesuvius. Open circles, CIPW norm contains *lc*; solid circles, no *lc* in CIPW norm.

standard katanorm. A striking example is shown in figure 58; Niggli and CIPW orthoclase are in excellent agreement in Vesuvius lavas whose norms are free of CIPW leucite, but where this normative mineral is present the orthoclase agreement is very poor indeed.

In general, the more nearly the combining rules agree, the better the agreement between Niggli katanorm and CIPW norm. This is hardly surprising, and the final step toward bringing the systems together seems to have been taken by Barth (1962, pp. 65–70), who now uses the normative minerals of CIPW and the calculating technique of Niggli. Under these circumstances excellent agreement is to be expected in suites of analyses characterized by either very low or very high color index; in such suites we may anticipate that $r^2 \sim 1$, $b \sim 1$, and $c \sim 0$. In suites characterized by great range of color index, however, differences between the weight percentages of the CIPW norm and the “ion equivalents” or molar percentages of the Niggli calculation may well lead to either or both $b \neq 1$ and $c \neq 0$ and also to some significant departure from linearity. It seems likely, nevertheless, that r^2 will usually remain large enough so that the parameters of the two systems, though not identical, will be interconvertible with fair precision. With so many variables interacting, however, predictions of this sort are often belied by practice. Work on this project is continuing; the final report will include a bibliography of source references.

A REPLACEMENT FOR REFERENCE SAMPLE G-1

F. Chayes and Y. Suzuki

The “standard” granite sample G-1, widely used in interlaboratory calibration since 1949, was obtained by Chayes in the form of a 6-foot strip from the Smith quarry at Westerly, Rhode Island. After control sampling and crushing, about 96 pounds of this material was available for distribution. The Geological Survey re-

ported in 1959 that the supply would be exhausted in a few years, and the Standards Committee of the Geochemical Society accepted responsibility for selecting and obtaining a replacement.

After extended discussion the committee finally decided that for purposes immediately in view it would be best to procure as fine grained a granite as possible. Material of suitable freshness could be conveniently obtained only from quarries, and in the eastern United States the finest-grained commercially exploited granites are those of the Westerly-Bradford area. The original test strip was exceedingly fine grained, finer than most of the Westerly-Bradford quarry products, and it was agreed that a duplicate of G-1, in an amount calculated to yield 300 pounds of crushed sample instead of less than 100, would be suitable. Unfortunately, the quarry from which G-1 was obtained and others that might have yielded similar material are now part of a suburban housing development in the outskirts of the town of Westerly. At the time of our visit, spring of 1961, only the Sullivan quarry in Bradford, Rhode Island, operated by the Westerly Granite Corporation, could provide a suitable block.

Like most of the rock of the Bradford sill, our specimen is somewhat coarser than the fine blue granite once quarried in Westerly. The difference is not great, however, the Bradford material being much finer than any obtainable from available sites in, for instance, the Barre, Vermont, or Mount Desert, Maine, districts.

The essential minerals of the Bradford specimen are indistinguishable from those of G-1 (for which see Chayes in Fairbairn et al., 1951); the Bradford material, however, is appreciably poorer in quartz and microcline and richer in plagioclase and biotite.

In the spring of 1963 the Standards Committee of the Geochemical Society released the Bradford block to the Geological Survey. A dozen small hand

specimens, trimmed from the block in a regular pattern, have been retained at the Geophysical Laboratory.

VARIETIES OF LAMPROPHYRE

D. Métais and F. Chayes

The lamprophyres were included by Rosenbusch in his class of "diabase-rocks," and the nomenclature he adapted and developed for them was "genetic" in the most extreme sense of the word, the name to be applied to any specific member being determined primarily by the nature of the plutonic rocks with or in which it occurred and from which it was presumed to have "differentiated." The resulting chaos has been admirably described by Knopf (1936), who points out that a particularly well known example he himself describes as vogesite had been described previously by Pirsson as minette, by Rosenbusch as camptonite, and by Beger as monchiquite. Each of these names is used by Rosenbusch to denote a major subgroup of lamprophyres; it is hardly surprising that nonspecialists, even including authors of text and reference works, try to avoid detailed explication of the nomenclature and classification of this group.

Most petrologists will nevertheless agree that the rocks called lamprophyre, though exceedingly variable in composition, do form some kind of natural group. Commonly, for instance, the term is applied only to porphyritic dike rocks of high color index in which feldspar is confined to the groundmass. Although these rocks are usually very rich in H_2O and CO_2 , they are ordinarily lustrous and "fresh" in appearance; although olivine is usually completely transformed to talc, and pyroxene may be extensively replaced by carbonate and chlorite, biotite and amphibole rarely show such effects and feldspar is nearly always free of earthy alteration indicative of weathering or low-grade hydrothermal attack. The minerals of phenocrysts and groundmass alike tend to be markedly euhedral, and the phenocrysts are often very large. The

persistently euhedral habit makes for inefficient packing and a miarolitic texture.

The literature of the lamprophyres is badly scattered. The last major summary of the geochemistry of the group, based on 382 analyses, is due to Beger (1923). In the 40 years since Beger's study appeared many new analyses have been published, and this note presents preliminary results of a new compilation of available data. The collection now contains 633 analyses in 33 groups. No inclusions have been retained, and rocks recorded under names other than those denoting varieties of lamprophyre (analcime-basalt, theralite-diabase, etc.) have also been excluded. Where an author applies a particular name to a rock and his petrographic description is not incompatible with that name, the author's choice classifies the rock. Where the rock name is incompatible with the description the analysis is designated simply as lamprophyre, and the same designation is applied if no specific name is proposed or the petrographic description is insufficient to check the specific name. Only complete analyses have been used, and, because of the discontinuities they impose on normative parameters, analyses quoted to only one decimal have been rejected.

As might be expected, most of the 33 groups contain few analyses. Thirty or more analyses are available for each of the six major varieties, however, and table 11 presents new average compositions for each of them. The new averages differ considerably from earlier values given by Johanssen (1931) and Daly (1933), chiefly in the direction of reducing differences between groups. Present data will suffice to distinguish monchiquites and camptonites from other lamprophyres and possibly also from each other, but in terms of average chemical composition minettes, vogesites, kersantites, and spessartites seem virtually indistinguishable. Except for potash, the observed averages for all major oxides in these four groups are so similar that significant differences

TABLE 11. Average Compositions of Six Varieties of Lamprophyre

No. Analyses	64	30	95	45	78	61
	Minette	Vogesite	Kersantite	Spessartite	Camptonite	Monchiquite
SiO ₂	51.17	51.13	51.80	52.37	44.67	40.68
Al ₂ O ₃	13.87	14.35	14.84	15.44	14.35	13.20
Fe ₂ O ₃	3.27	3.63	3.03	3.27	4.50	4.87
FeO	4.16	4.74	5.32	5.35	7.19	6.47
MgO	6.91	6.84	6.29	6.27	7.02	9.17
CaO	6.58	7.05	6.24	7.36	9.45	11.02
Na ₂ O	2.12	3.00	2.98	3.30	2.99	3.06
K ₂ O	5.49	3.81	3.68	2.54	1.91	2.16
TiO ₂	1.36	1.44	1.32	1.31	2.46	2.34
CO ₂ *	1.30	0.74	1.14	0.41	1.58	1.38
H ₂ O (total)	2.42	2.62	2.56	2.36	3.12	3.52

* Minimum estimates only; a zero has been used whenever the analysis does not include a value for CO₂.

would be difficult to establish even if within-group variation were very small. In fact, however, for each of the individual oxides it is very large, as may be inferred from table 12, which shows the incidence of (normative) silica saturation and undersaturation in each of the groups. The within-group variation of other normative parameters is also very large; in no group is the range of *hy* less than 25, for instance, or the range of *or* less than 20. Though still mentioned in text discussions as a matter of historic interest, Rosenbusch's "genetic" subdivision of the group has long been abandoned in practice. Despite this, and the close similarity

of the first four groups in bulk composition with respect to all but one of the major oxides, the names of these groups, properly applied, do denote mineralogical differences of considerable interest; the minettes contain essential amounts of biotite and alkali feldspar, the kersantites only of the former, the vogesites only of the latter, and the spessartites of neither. These distinctions are so far unexplained in terms of geological environment or history, and the relation between the group as a whole and the highly potassic but otherwise somewhat similar extrusives, such as those of Uganda for example, is still an unsolved problem.

TABLE 12. Incidence of Norms with Quartz or Nepheline in Analyses of Six Varieties of Lamprophyre

	Minette	Vogesite	Kersantite	Spessartite	Camptonite	Monchiquite
Quartz	35	13	63	24	17	3
No quartz, no nepheline	13	7	23	10	21	3
Nepheline-bearing	19	10	32	9	39	55
	—	—	—	—	—	—
Total	67	30	118	43	77	61

CRYSTALLOGRAPHY

The Crystal Structure of Mullite

Charles W. Burnham

Since 1926 it has been recognized that mullite, an aluminum-silicate mineral whose composition ranges from approximately $3\text{Al}_2\text{O}_3 \cdot 2\text{SiO}_2$ to $2\text{Al}_2\text{O}_3 \cdot \text{SiO}_2$, is, on the basis of X-ray diffraction patterns, almost indistinguishable from sillimanite, Al_2SiO_5 ($\text{Al}_2\text{O}_3 \cdot \text{SiO}_2$). After solving the sillimanite crystal structure, Taylor (1928), realizing that the two minerals must have very similar structures but that mullite is less dense than sillimanite, suggested that the mullite structure could be derived from that of sillimanite by substituting aluminum for silicon in some tetrahedral sites and removing sufficient oxygen atoms to compensate for the change of positive charge.

Two structural studies of mullite, both of which confirm Taylor's basic hypothesis, have been reported recently. Sadanaga, Tokonami, and Takeuchi (1962), in a two-dimensional film study of synthetic mullite of composition $2\text{Al}_2\text{O}_3 \cdot \text{SiO}_2$ (2:1) described by Roy and Aramaki (1962), determined that its unit cell is almost identical with the sillimanite substructure unit cell, with a c axis half the length of the true sillimanite unit cell. They derived the mullite structure by replacing 0.8 silicon atom per sillimanite substructure cell with 0.8 aluminum atom at random and removing 0.4 two-coordinated oxygen atom (O_c , *Year Book 61*, p. 138) to adjust the alumina:silica ratio from 1:1 to 2:1. The loss of oxygen atoms makes 20 per cent of the tetrahedral cation positions untenable, but Sadanaga, Tokonami, and Takeuchi found electron-density peaks corresponding to new tetrahedral positions unfilled in sillimanite, in which they placed the 0.8 aluminum atom per unit cell that had been forced out of the normal tetrahedral position. This configuration increases the coordination of some of the remaining oxygen

atoms, O_c , and according to Sadanaga, Tokonami, and Takeuchi the additional cations force these atoms into new positions slightly different from those of the two-coordinated atoms.

Durovic (1962) reported a similar structure based on three-dimensional analysis of film data from a synthetic mullite of 1.71:1 composition. His model proposes that all the oxygen atoms, O_c , whether in two or higher coordination, are statistically distributed on either side of the symmetry center at $\frac{1}{2}$, 0, $\frac{1}{2}$, and that the new cation site contains both aluminum and silicon in a disordered arrangement.

Although these two studies point out the basic differences between the mullite and sillimanite structures, they disagree on two critical points, namely, the nature of the silicon-aluminum distribution and the spatial distribution and positions of atoms in the incompletely filled O_c site. A structural model adequate for detailed crystal-chemical description must necessarily include a determination of these distributions. Such detail is critical to an understanding of the sillimanite-mullite stability relations and mechanisms of transformation. Furthermore, it is important that such crystal-chemical information be brought to bear on the problem of the solid-solution limits of mullite. No theoretical limits with a sound physical basis have yet been proposed, and the accepted limits cannot be supported by structural evidence. In view of this situation, the investigation of the structures of the aluminum-silicate minerals has been extended to mullite this year, with particular emphasis on a detailed study of defect oxygen distribution, silicon-aluminum disordering, and their effects on atomic thermal motion.

Experimental studies. Single crystals of mullite were obtained from Dr. J. V. Smith, University of Chicago. These synthetic crystals, labeled R β ec by Agrell

TABLE 13. Rβec Mullite Unit-Cell Dimensions

	Weissenberg Single-Crystal Photographs	Powder Diffraction, Agrell and Smith (1960)
<i>a</i> , Å	7.584 ± 0.003	7.579 ± 0.001
<i>b</i> , Å	7.693 ± 0.003	7.693 ± 0.001
<i>c</i> , Å	2.890 ± 0.001	2.8884 ± 0.0002
Unit-cell volume, Å ³	168.61 ± 0.20	168.41

and Smith (1960), were found coexisting with corundum in electrically fused glass-tank block and were first described by Rooksby and Partridge (1939).

An electron-microprobe analysis of this material, kindly made by Dr. J. V. Smith, shows that it contains 11.0 + 0.2 weight per cent silicon, 0.71 + 0.05 weight per cent titanium, no iron, and no manganese.¹³ Neglecting titanium content and assuming that the remaining cations are aluminum and that mullite is oxygen deficient compared with sillimanite but contains the same total number of cations (Taylor, 1928; Sadanaga, Tokonami, and Takeuchi, 1962), the formula for Rβec mullite is 1.92Al₂O₃·SiO₂. The titanium content is equivalent to 0.05 atom per unit cell, or 0.8 per cent of the cations per unit cell. Location of this small amount of titanium would require very careful analysis of relationships between occupancy factors and temperature factors of cation sites in a very precisely refined model; such an attempt is not justified at the present level of refinement.

Preliminary *c*-axis rotation and precession photographs demonstrate that the *a* and *b* axes of Rβec mullite are essentially the same as those of sillimanite but that the mullite *c* axis is half the length of the sillimanite *c* axis. The characteristic mullite superstructure reflections (Agrell and Smith, 1960) are visible only on *c*-axis oscillation photographs. With nickel-filtered CuKα radiation, extremely

diffuse reflections corresponding to an approximate quadrupling of the *c*-axis appear after 7 hours of exposure. These reflections cannot be obtained on *c*-axis precession cone-axis photographs and cannot be indexed, but they do indicate that the Rβec mullite is a diffuse mullite (D-mullite) in the terminology of Agrell and Smith (1960).

Unit-cell dimensions were determined by least-squares refinement of 50 measurements from *b*- and *c*-axis zero-level Weissenberg photographs. The computations, carried out on the IBM 7090 computer, included corrections for systematic absorption and camera eccentricity errors (*Year Book 61*, pp. 132–135). The results are listed in table 13 along with those obtained from powder diffraction data by Agrell and Smith (1960).

The density of this sample was measured by suspending small single crystals in a mixture of bromoform and methyl iodide and varying the proportions of the two constituents until the crystals remained suspended for at least 1 hour. The average of four independent measurements is 3.118 g/cm³; the standard error (of the mean) is 0.006 g/cm³. The expected density based on the measured unit-cell volume and the 1.92:1 formula is 3.123 g/cm.³ From these results the number of formula units (*Z*) per unit cell is 1.24.

Systematic extinctions on precession and Weissenberg photographs correspond to diffraction symbol *mmmPba*–; space groups compatible with this symbol are *Pba*2 (noncentric) and *Pbam* (centric). The standard *N*(*z*) test (Howells, Phillips, and Rogers, 1950) was applied to corrected intensity data, and comparison with

¹³ Precise analysis for aluminum could not be obtained, owing to wavelength shifts with coordination changes and interference from the third-order titanium spectrum (J. V. Smith, personal communication).

theoretical intensity distribution curves for centric and noncentric structures demonstrated that in all probability the symmetry center is present and $Pbam$ is the correct space group.

A small triangular prism having a maximum length of 0.16 mm was selected for intensity measurement with a single-crystal counter diffractometer based on equi-inclination Weissenberg geometry. The intensities of 792 independent reflections were measured using $\text{MoK}\alpha$ radiation and a thorium-activated NaI scintillation detector associated with a pulse-height analyzer set to pass 90 per cent of the characteristic radiation. Digital intensity data for each reflection were measured and automatically reduced to observed structure-factor data by

methods described in detail by Burnham (1963). To maintain a close check on the functioning of the electronic equipment, one reflection (420) was measured 70 times throughout the period of data collection. The standard deviations computed from this repeated measurement are ± 4 per cent for the integrated intensity and ± 2.5 per cent for the observed structure factor.

Structure analysis and refinement. To determine the essential differences between $R\beta\text{ec}$ mullite and the refined sillimanite structure, a three-dimensional Fourier difference synthesis was computed using the calculated structure factors of sillimanite and the properly scaled observed structure factors of mullite with l indices doubled. A section through the

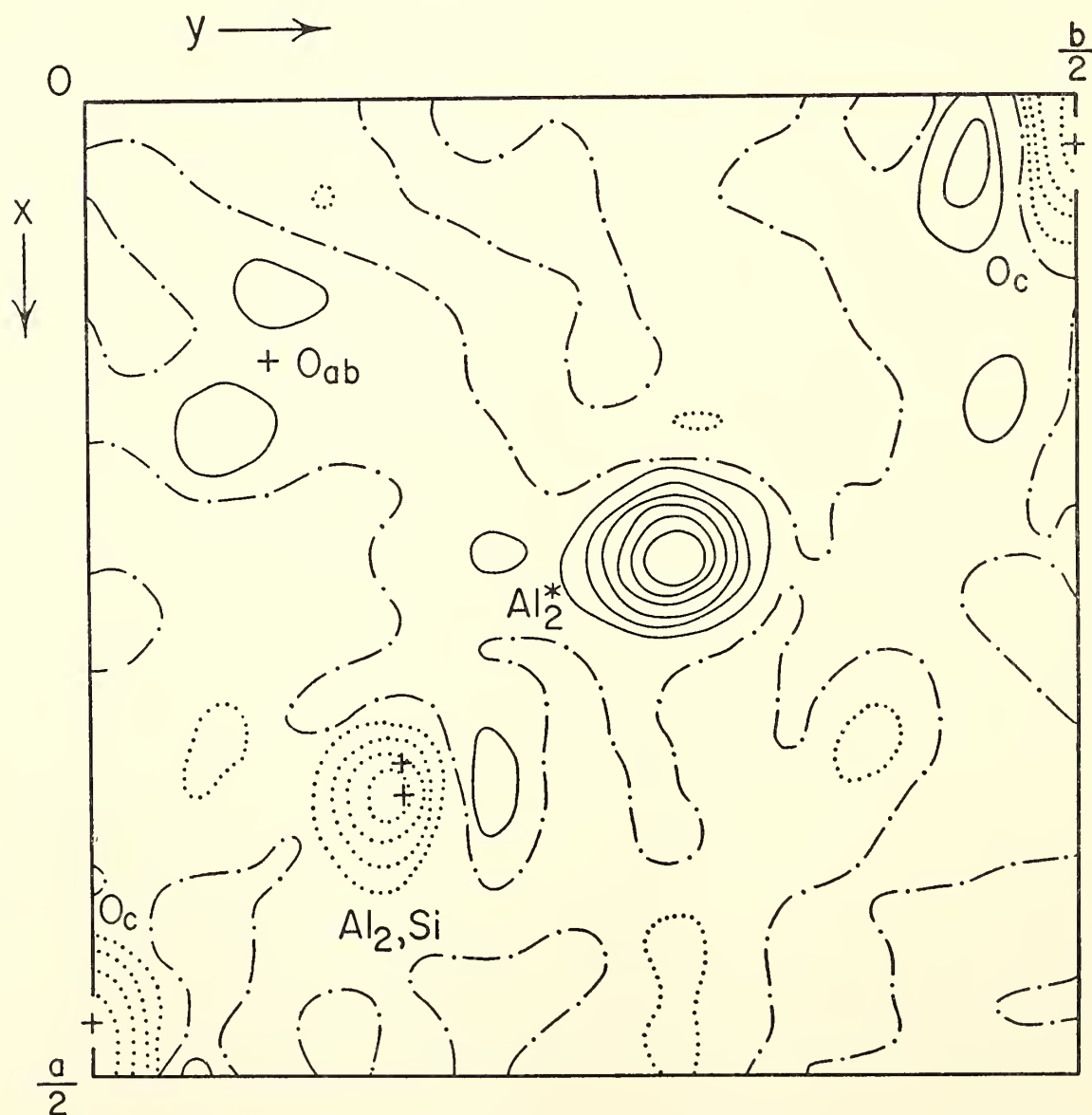


Fig. 59. Section at $z = \frac{1}{2}$ (mullite) through three-dimensional Fourier difference synthesis computed using mullite F_{obs} and sillimanite substructure F_{calc} . Crosses indicate atom positions in sillimanite. The origin is equivalent to the point $\frac{1}{2}, \frac{1}{2}, 0$ in figure 60. Positive contours are solid; zero contours are alternating dot-dash; negative contours are dotted. Contour interval = $2.5 e/\text{\AA}^3$.

synthesis normal to c at $z = \frac{1}{4}$ ($z = \frac{1}{2}$ in the true mullite unit cell) contains the centers of atoms in special positions on mirror planes and exhibits the critical differences between the two structures (fig. 59). The large positive peak represents a tetrahedral site, unoccupied in sillimanite, which is incompletely filled with aluminum (Sadanaga, Tokonami, and Takeuchi, 1962) or aluminum + silicon (Durovic, 1962) in mullite. Corresponding to this is a negative peak at the (Al_2, Si) position (the Al_2 and Si positions of sillimanite are indistinguishable in mullite), indicating that the position is left partly vacant by cations that have taken up the new tetrahedral position. The absence of some of the two-coordinated oxygen atoms (O_c) is evidenced by the negative peak at the sillimanite O_c position. Smaller positive peaks adjacent to this negative peak indicate that the remaining oxygen atoms, O_c , may be statistically distributed on either side of the symmetry center at $\frac{1}{2}$, 0, $\frac{1}{2}$, as Durovic (1962) has suggested. Small positive peaks on either side of the O_{ab} position (superposition of the O_a and O_b positions of sillimanite) suggest either relatively large anisotropic thermal motion or positional disordering of this atom in mullite.

Least-squares refinement was initiated using the atomic distribution for ideal 2:1 mullite listed for model 1 in table 14.¹⁴ In this model 20 per cent of the oxygen atoms, O_c , are assumed to be missing, and the remaining ones are distributed equally on either side of the symmetry center at $\frac{1}{2}$, 0, $\frac{1}{2}$ (position O_c^*) as was suggested by Durovic (1962). The (Al_2, Si) position is assigned a random distribution of unequal amounts of aluminum and silicon, whereas the new tetrahedral position, Al_2^* , is assumed to contain only aluminum, as Sadanaga, Tokonami, and Takeuchi (1962) have suggested. This model has been refined through five cycles of least

TABLE 14. Atom Distribution in $2\text{Al}_2\text{O}_3 \cdot \text{SiO}_2$ Mullite, Space Group $Pb\bar{a}m$

Atom	Equipoint	Site Occupancy (Ideal = 1.0)		
		Model 1	Model 2	Model 3
O_{ab}	$4h$	1.0	1.0	1.0
O_c	$2c$	---	0.4	0.8
O_c^*	$4h$	0.4	0.2	---
O_d^*	$4g$	1.0	1.0	1.0
Al_1	$2a$	1.0	1.0	1.0
Al_2	$4h$	{ 0.5	0.5	0.5
Si				
Al_2^*	$4h$	0.2	0.2	0.2

squares during which atomic coordinates were varied and four more cycles during which atomic coordinates, anisotropic temperature factors, and site occupancy factors for both tetrahedral cation positions and the O_c^* position were varied.

Two additional models, differing only in the spatial distribution of atoms in the partially occupied O_c position, have each been refined through four cycles of least squares. Model 2, equivalent to that suggested by Sadanaga, Tokonami, and Takeuchi (1962), assigns O_c to the O_c^* positions 20 per cent of the time and to the symmetry center 40 per cent of the time (table 14). The physical interpretation of this model is that the oxygen atom moves to the O_c^* position wherever an aluminum atom occupies the Al_2^* position (hence increasing the oxygen coordination to three) but remains on the symmetry center when it is coordinated to only two cations. In model 3 all O_c atoms are placed on the symmetry center, which suggests that the positive peaks on the difference Fourier adjacent to the O_c negative peak (fig. 59) are due solely to large anisotropic thermal motion of these atoms.

All least-squares computations were carried out on the IBM 7090 computer using the Busing-Levy (1959) full matrix program as modified by Fischer (1963) for refinement of scattering factor curves and site occupancies. Atomic scattering

¹⁴ The electron microprobe analysis was not completed until refinement had been carried to its present status.

TABLE 15. Mullite Atomic Coordinates

Atom, coordinate		Initial	Model 1	Model 2	Model 3
O_{ab} :	x	0.36	0.3591 ± 0.0002	0.3595 ± 0.0003	0.3591 ± 0.0002
	y	0.42	0.4221 ± 0.0002	0.4219 ± 0.0002	0.4222 ± 0.0002
	z	$\frac{1}{2}$	$\frac{1}{2}$	$\frac{1}{2}$	$\frac{1}{2}$
	B	0.4	0.99	0.96	0.99
O_c :	x	$\frac{1}{2}$		$\frac{1}{2}$	$\frac{1}{2}$
	y	0		0	0
	z	$\frac{1}{2}$		$\frac{1}{2}$	$\frac{1}{2}$
	B	0.4		2.83	6.14
O_c^* :	x	0.47	0.4757 ± 0.0036	0.4424 ± 0.0042	
	y	0.05	0.0293 ± 0.0015	0.0569 ± 0.0046	
	z	$\frac{1}{2}$	$\frac{1}{2}$	$\frac{1}{2}$	
	B	0.4	3.53	0.51	
O_d :	x	0.12	0.1269 ± 0.0002	0.1269 ± 0.0002	0.1268 ± 0.0002
	y	0.22	0.2193 ± 0.0002	0.2194 ± 0.0002	0.2193 ± 0.0002
	z	0	0	0	0
	B	0.4	1.02	0.94	1.00
(Al_2, Si) :	x	0.15	0.1488 ± 0.0001	0.1486 ± 0.0001	0.1487 ± 0.0001
	y	0.34	0.3401 ± 0.0001	0.3401 ± 0.0001	0.3401 ± 0.0001
	z	$\frac{1}{2}$	$\frac{1}{2}$	$\frac{1}{2}$	$\frac{1}{2}$
	B	0.3	0.53	0.46	0.49
Al_2^* :	x	0.27	0.2596 ± 0.0005	0.2601 ± 0.0006	0.2594 ± 0.0006
	y	0.21	0.2062 ± 0.0005	0.2062 ± 0.0005	0.2062 ± 0.0005
	z	$\frac{1}{2}$	$\frac{1}{2}$	$\frac{1}{2}$	$\frac{1}{2}$
	B	0.3	0.50	0.75	0.49
Al_1 :	x	0	0	0	0
	y	0	0	0	0
	z	0	0	0	0
	B	0.3	0.44	0.40	0.44

factors were computed according to (Fischer, 1963)

$$f(x) = \exp \sum_{n=0}^6 a_n x^n \tag{1}$$

where $x = (\sin \theta)/\lambda$, and the a_n are constants obtained by least-squares adjustment of equation 1 to curves for fully ionized atoms given in the *International Tables for X-Ray Crystallography*, volume 3. During all computations, data from 228 reflections having intensities less than the minimum observable were rejected from the least-squares normal equations.

Atomic coordinates and equivalent isotropic temperature factors (B) are listed for each model in table 15. Refined values of occupancy factors for the partly

filled sites in models 1 and 3 are listed in table 16. Occupancy factors for model 2 have not been refined as yet.

R factors for the three models are listed in table 17. Comparisons of these figures, and the coordinates in table 15, indicate that the gross features of the structure are

TABLE 16. Refined Occupancy Factors

Atom	Occupancy Factor	
	Model 1	Model 3
O_c		0.85 ± 0.01
O_c^*	0.425 ± 0.005	
(Al_2, Si) :		
Al_2	0.16 ± 0.09	0.23 ± 0.10
Si	0.61 ± 0.08	0.54 ± 0.09
Al_2^*	0.185 ± 0.003	0.185 ± 0.003

TABLE 17. *R* Factors

	Model 1	Model 2	Model 3
Unweighted <i>R</i> , all reflections, %	8.8	9.1	9.0
Unweighted <i>R</i> , 564 observable reflections, %	5.7	5.9	5.8
Weighted <i>R</i> , all observations, %	3.3	3.6	3.4
Standard error of observation of unit weight, $[\sum w(F_o - F_c)^2/(m - n)]^{1/2}$	1.51	1.72	1.65

certainly correct but that the distribution of the tetrahedron-linking oxygen atoms, O_c , is, at this level of refinement, indeterminate. Since the statistical reliability of the data is approximately 2–3 per cent (at the 67 per cent confidence level), further analysis and modification of the structure model followed by additional least-squares refinement should allow a more positive determination of correct structural detail.

Crystal chemistry. A schematic diagram illustrating the relationships between coordination polyhedra in model 2 is shown in figure 60. The extreme similarity between mullite and sillimanite may be seen by comparing figure 60 with the analogous diagram for sillimanite (*Year*

Book 61, p. 138, fig. 43). Interatomic distances computed from the atomic coordinates in table 15 are listed in table 18.

Cation-anion distances in the (Al_2Si) tetrahedron are indicative of substitutional disorder. The average $(Al,Si)-O$ distance varies, depending on the model, from 1.705 to 1.744 Å. Since the average oxygen positions are affected by the absence of the central cation in approximately 20 per cent of these tetrahedra, it is impossible at this time to select the most probable model on the basis of average cation-anion bond distance or, conversely, to confirm the percentage of silicon or aluminum in the cation site. The $(Al_2Si)-O_c$ distance of 1.669 Å (for

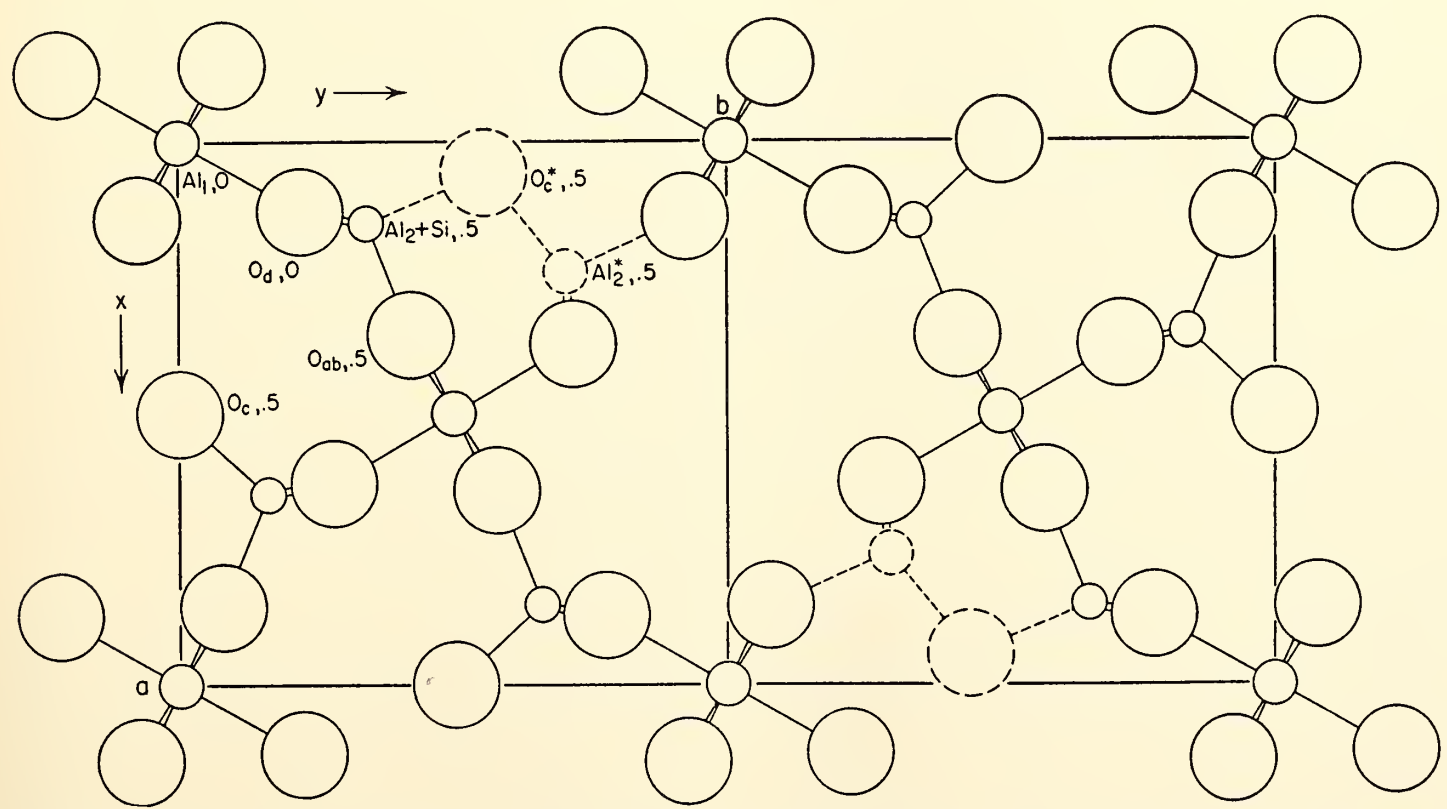


Fig. 60 Projection on (001) of model 2 for the mullite structure. Two unit cells show the effect of removing one O_c atom but do not exhibit the true symmetry resulting from statistical absence of O_c and rearrangement of cations.

TABLE 18. Mullite Interatomic Distances*

Atom Pair	Multi- plicity	Distance, Å	Standard Error
Al octahedron:			
Al ₁ -O _{ab}	4	1.895	0.001
Al ₁ -O _d	2	1.942	0.002
O _{ab} -O _{ab} '	2	2.450	0.004
O _{ab} -O _{ab}	2	2.890	0.001
O _{ab} -O _d ''	4	2.708	0.002
O _{ab} '-O _d ''	4	2.719	0.002
(Al ₂ ,Si) tetrahedron:			
Cation-O _{ab}	1	1.717	0.002
Cation-O _d	2	1.726	0.001
Cation-O _c ''	1	1.669	0.001
O _{ab} -O _c ''	1	2.788	0.002
O _{ab} -O _d	2	2.761	0.002
O _c ''-O _d	2	2.771	0.002
O _d -O _d	1	2.890	0.001
Cation-O _c '''*	1†	1.735	
Cation-O _c ''''*	1†	1.652	
Cation-O _c ''''*	1‡	1.805	
Cation-O _c ''''*	1‡	1.753	
Al ₂ * tetrahedron:			
Al ₂ *-O _{ab}	1	1.825	0.004
Al ₂ *-O _d	2	1.764	0.003
Al ₂ *-O _c	1	2.418	0.004
O _{ab} -O _c	1	3.419	0.002
O _{ab} -O _d	2	2.761	0.002
O _c -O _d	2	3.598	0.002
O _d -O _d	1	2.890	0.001
Al ₂ *-O _c *	1†	2.130	
Al ₂ *-O _c *	1‡	1.797	

* Distances are computed for model 3 except where specifically stated. Where standard errors are missing they were not computed. Atoms designated with a single prime represent transformation of the coordinates listed in table 15 according to $x' = -x$, $y' = -y$, $z' = z$. Double primes represent transformation according to $x'' = \frac{1}{2} - x$, $y'' = \frac{1}{2} + y$, $z'' = z$. Triple primes represent transformation according to $x''' = \frac{1}{2} + x$, $y''' = \frac{1}{2} - y$, $z''' = z$.

† Model 1.

‡ Model 2.

O_c on the symmetry center) appears reasonable for disordered tetrahedra when compared with the bond distances to O_c in sillimanite (Si-O_c = 1.564 Å, Al₂-O_c = 1.721 Å). If any O_c atoms do, in fact, lie on the symmetry center, it is most likely on chemical grounds that their coordination is only two (as in model

2) rather than three (as it would have to be for approximately 20 per cent of the O_c in model 3), since the (Al₂,Si)-O_c-(Al₂,Si) angle is fixed at 180°. The (Al₂,Si)-O_c* distances for model 2 appear to be abnormally long, but, since the O_c* position is assumed only 20 per cent of the time (when the atom is three-coordinated), the distances may be reduced by a slight shift of the (Al₂,Si) cations, which will increase their apparent thermal motion.

Whenever an oxygen atom, O_c, is missing, the tetrahedral cations on each side of the missing atom must move to the Al₂* tetrahedral sites to complete their coordination, and the double tetrahedral chains of the original sillimanite structure become discontinuous (fig. 60). The Al₂*-O_{ab} and Al₂*-O_d distances (table 18) are normal for a tetrahedral site occupied only by aluminum, but the Al₂*-O_c distance of 2.418 Å is unreasonably long. It is thus highly unlikely that O_c remains on the symmetry center when it must coordinate to a third cation. In this respect the distance for model 2, 1.797 Å, appears to be the most reasonable. The average Al₂*-O distance for model 2 is 1.788 Å, compared with 1.770 Å for the Al₂ tetrahedra in sillimanite.

The isotropic temperature factors (*B*) in table 15 are all higher than expected. Comparison of those for O_c in the three models shows that model 3 is highly unlikely on this basis alone. One obvious point, however, is that analysis of apparent thermal motion in a defect and disordered structure of this type is essential and may well lead to rejection of a structure model, even when the agreement between observed and calculated data is acceptable (see table 17).

Refinement of occupancy factors for the incompletely filled positions has been only partly successful. The expected occupancies, based on the electron microprobe analysis and neglecting titanium content, are 0.81 for O_c (model 3), 0.19 for Al₂*, and 0.81 for the (Al₂,Si) tetra-

hedral site (0.31 for Si, 0.50 for Al₂). The refined value of 0.85 for O_c is probably too high because of errors in the distribution of this atom. The occupancies of Al₂ and Si in the disordered tetrahedral site, although totaling to approximately the correct value (0.77 in models 1 and 3), have no individual meaning, as their least-squares correlation coefficient, ρ_{ij} , is -0.999 . The refined occupancy of the Al₂* site is 0.185 for both models, a value reasonably close to the predicted value of 0.19 for the 1.92:1 composition. Such close agreement is further indication that this position is occupied solely by aluminum and not aluminum + silicon.

Further analysis and refinement of this structure is now being carried out to determine the details of the O_c distribution. A correct model should permit a meaningful analysis of the silicon and aluminum distribution either directly, by occupancy refinement, or indirectly by analysis of the apparent anisotropic thermal motion of the coordinating oxygen atoms.

Structures of Micas

E. W. Radoslovich

The structures of the layer silicates have been understood in broad terms for the last thirty years. "Ideal" structures are described even in very recent monographs in terms of geometrically regular polyhedral groups; and of course this description is adequate to account for many of their physical and chemical properties, e.g., the ready cleavage of micas. On the other hand, many properties of the clay minerals and other layer silicates now being studied intensively in various laboratories simply cannot be understood on the basis of these geometrical models. There is, for example, no obvious explanation of the limited solid solution between muscovite and paragonite, or between muscovite and biotite, in terms of their "ideal" structures. Likewise any discussion of the stability

fields and the relative frequency of occurrence of the different polymorphs of micas will require a more sophisticated understanding of their detailed bond lengths and angles.

Fewer than five layer-silicate structures have been published in which the bond lengths and angles have been obtained with reasonable accuracy. For this reason alone it is worth while refining a mica structure using three-dimensional data obtained by counter diffractometer techniques. The observed bond lengths and angles can then be compared with precise bonds and angles in other silicates (such as the framework structures) to look for effects due to the type of polyhedral linkage involved. The nature of any structural control over the regular stacking arrangements in the different mica polymorphs should also become more obvious once several closely related structures are known precisely.

General rules have recently been proposed (e.g., Radoslovich, 1963) by which the departure of a layer-silicate structure (of given composition) from its geometrically ideal structure may be predicted in considerable detail. As a further objective, then, the refinement of certain mica structures should provide accurate data to test these general hypotheses critically.

The only published refinement of a mica structure is that for 2M₁ muscovite (Radoslovich, 1960), and for this reason single crystals suitable for detailed analysis were sought among 1M and 3T muscovites, and 1M, 2M₁, and 3T paragonites. Considerable care was taken to find small crystals with a minimum of physical distortion in order to take full advantage of the precision available in measuring intensities on the single-crystal diffractometer. This search was further protracted because a paragonite originally reported as 2M₁ is in fact 3T (three-layer trigonal, with $c = 30$ Å approximately). There is no optic axial plane to assist in choosing an a or b axis, because $2V = 0$, and the structural extinctions only permit

$h00$ reflections with $h = 6$, whereas the reciprocal lattice planes are very close together in the c^* direction. This makes the orientation of these crystals quite difficult, but eventually the trigonal symmetry was clearly shown by precession and Weissenberg photographs of several crystals giving sharp patterns. The diffraction symbol is $\bar{3}mP3_1- -$, and the possible space groups are therefore $P3_121$, $P3_221$, $P3_112$, $P3_212$. It would seem more convenient to describe this structure in terms of a nonprimitive orthohexagonal cell with $a = 5 \text{ \AA}$ and $b = 9 \text{ \AA}$ approximately, as for many other layer silicates. Certain kinds of hkl reflections (in the orthohexagonal notation, those for which $k = 3n$ and $h + l \neq 3n$) are either absent or very weak for structural reasons rather than as a space-group requirement. The cell dimensions were determined using a calibrated 19-cm-diameter camera and quartz internal standard, from which $a = 5.143 \pm 0.002$, $b = 8.908 \pm 0.004$, $c = 29.061 \pm 0.02 \text{ \AA}$. The observed powder pattern agrees closely with the pattern calculated using these values.

Very good single crystals have also been obtained from a $2M_1$ paragonite in kyanite schist from Alpe Sponda, Switzerland. Although a full chemical analysis of the paragonite phase is not yet available, this specimen must be quite high in potassium. The cell dimensions have been determined by least-squares refinement of powder diffractometer data obtained with silicon as an internal standard; the monoclinic angle was confirmed by precession techniques. The values are $a = 5.142 \pm 0.005$, $b = 8.878 \pm 0.005$, $c = 19.39 \pm 0.02 \text{ \AA}$, and $\beta = 95^\circ 18' \pm 7'$. The space group appears to be $C2/c$, as for $2M_1$ muscovite.

Three-dimensional data are now being collected (using the counter diffractometer) for a refinement of the $2M_1$ paragonite structure. The $3T$ paragonite structure may present difficulties because long X-ray wavelengths are needed to resolve successive reflections sufficiently for counter techniques.

Tourmaline

Gabrielle Donnay

Tourmaline is famous for its wide range of composition. Structural information enables us to simplify its formula as follows: $\text{NaM}_3\text{Al}_6\text{B}_3\text{Si}_6\text{O}_{27}(\text{OH})_4$. Idealized end members are: *elbaite* (e), for $M = (\text{Li}, \text{Al})$; *schorl* (s), for $M = \text{Fe}$; *dravite* (d), for $M = \text{Mg}$. Elbaite and schorl, on the one hand, schorl and dravite, on the other, form complete series of solid solutions. There is a miscibility gap between elbaite and dravite. *Uvite* is usually given the formula $\text{CaMg}_3(\text{Al}_5\text{Mg})\text{B}_3\text{Si}_6\text{O}_{27}(\text{OH})_4$ (Deer, Howie, and Zussman, 1962; Strunz, 1957; Epprecht, 1953); note, however, that Ca substitutes for Na in all tourmaline compositions.

Epprecht (1953) obtained cell dimensions for 31 tourmalines, shown in figure 61 in Arabic numerals. The Roman numerals refer to literature data, quoted by Epprecht. Where the composition is known it is indicated by the position of the dot in a composition triangle of arbitrary size, with lower left corner (e), lower right corner (s), and upper corner (d).

From elbaite to schorl both a and c increase, linearly to a first approximation; from schorl to dravite a decreases as c increases. There is thus a discontinuity in the way the structure changes with composition. Buerger, Burnham, and Peacor (1962) refined the structure of a dravite tourmaline (fig. 61, II). It is planned to determine and refine a schorl and an elbaite structure.

Dr. Brian Mason of the American Museum of Natural History found a new variety of black tourmaline in San Luis Potosí, Wadley District, Mexico. The cell dimensions that he determined by single-crystal work ($a = 15.88$, $c = 7.19 \text{ \AA}$, $c/a = 0.453$) were refined from powder data by two different programs of least squares (C. W. Burnham and D. Appleman): $a = 15.873 \pm 0.002$, $c = 7.187 \pm 0.002 \text{ \AA}$, with an axial ratio $c/a = 0.4528$ that compares well with our goniometric

ratio $(c/a)_{\text{gon.}} = 0.4521$. These cell dimensions form an unusual combination of c and a (see fig. 61). The most striking anomaly of this Mexican tourmaline, however, is found in its refractive indices. Hardie's optical data are: $\omega = 1.735$, yellow-brown; $\epsilon = 1.670$, very pale yellow; $\delta = 0.065$. The normal range of indices is as follows: $\omega = 1.635\text{--}1.675$, $\epsilon = 1.610\text{--}1.650$, $\delta = 0.017\text{--}0.034$ (Deer, Howie, and Zussman, 1962, p. 300). The observed values are plotted (fig. 62) on a graph taken from Deer, Howie, and Zussman (1962, p. 311), on which the predicted values are also shown. The predicted and observed refractive indices are so far apart that a new name for this Mexican tourmaline would seem to be justified.

Dr. H. B. Wiik, research associate of

the American Museum of Natural History, performed a chemical analysis on the Mexican tourmaline with the following results: SiO_2 , 33.19; TiO_2 , 0.46; Al_2O_3 , 30.87; FeO , 18.6; MnO , 0.20; MgO , 0.17; CaO , 0.36; Na_2O , 3.40; K_2O , 0.08; H_2O^+ , 0.42; H_2O^- , 0.02; B_2O_3 , 11.5; F^- , 1.77; total, 101.04. The oxidation state of iron is uncertain, according to the analyst. Assuming all the iron to be ferrous, the formula, reduced to 150 atomic sites per cell, is: $(\text{Na}_{3.43}\text{K}_{0.05}\text{Ca}_{0.20})(\text{Fe}^{++}_{8.10}\text{Ti}_{0.18}\text{Mg}_{0.13}\text{Mn}_{0.09})\text{Al}_{18.94}\text{B}_{10.33}\text{Si}_{17.28}\text{O}_{86.90}\text{F}_{2.91}(\text{OH})_{1.46}$.

We are dealing with an iron tourmaline, very low in hydroxyl ions and high in fluorine, a composition which should lower rather than raise the refractive indices. But perhaps the presence of

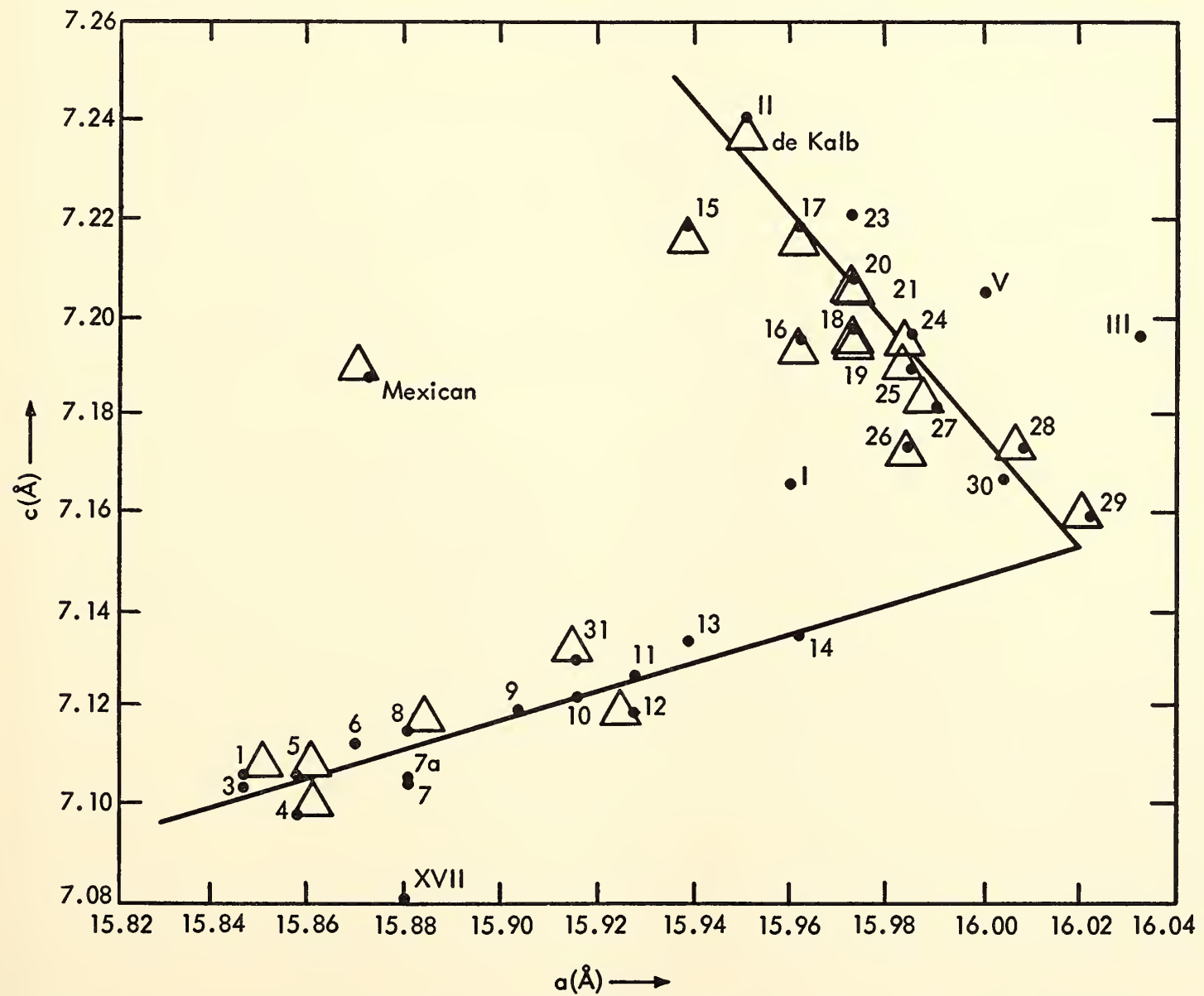


Fig. 61. Cell dimensions (c versus a) of tourmalines. Each composition, when known, is shown in a composition triangle. Data from Epprecht (1953).

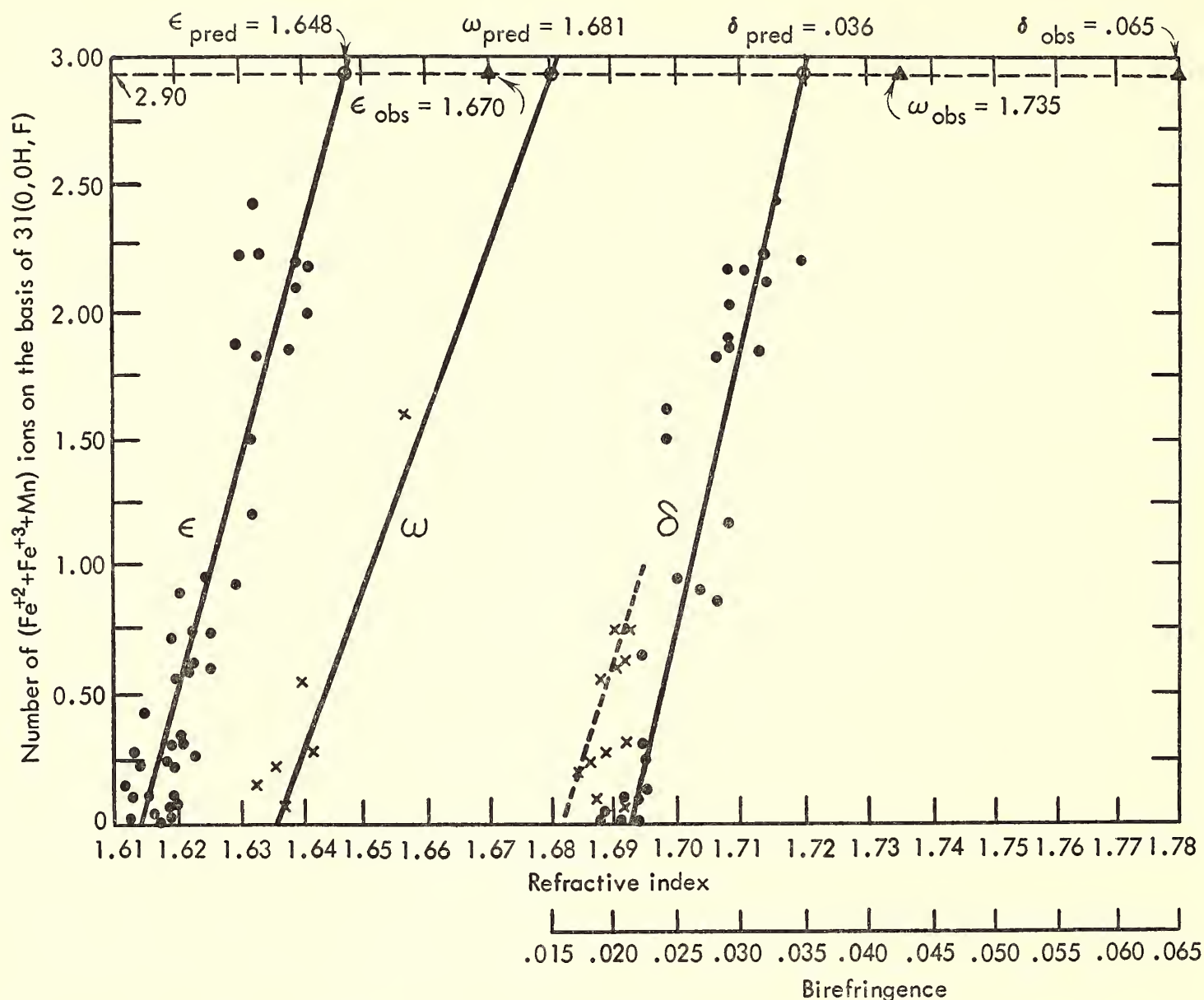


Fig. 62. Optical properties of tourmalines in relation to the number of $(\text{Fe}^{+2} + \text{Fe}^{+3} + \text{Mn})$ ions on the basis of 31 $(\text{O}, \text{OH}, \text{F})$. After Deer, Howie, and Zussman (1962, p. 311).

titanium, combined with the high iron content, is responsible for the unusual optics. There is otherwise nothing striking about this composition. Similar ones can be found in the literature: for example, Epprecht's no. 25 (fig. 61) from Brissago, Switzerland, analyzed by Jakob (1937), or no. 27 from Andreasberg, Germany, analyzed by M. Dittrich and F. Noll (in Doelter, 1917).

Mason's measured density of 3.31 g/cm^3 compares well with the calculated value of 3.32 g/cm^3 . It was expected that the analysis would be high in ferric iron and that the latter not only would fill the octahedral sites but also would substitute for silicon. This substitution would

account for the cell dimensions which fall outside the ranges of the two known solid-solution series (fig. 61) and for the high density, which is a direct consequence of the relatively small cell volume. The normal range of densities is $3.03\text{--}3.25 \text{ g/cm}^3$, as reported by Deer, Howie, and Zussman (1962, vol. 1, p. 300).

Since it is difficult by analytical means to determine the $\text{Fe}^{+2}/\text{Fe}^{+3}$ ratio of tourmaline, we have tried electron-spin resonance (ESR) and shall also try nuclear magnetic resonance (NMR). Mrs. M. L. Brown and Mr. J. Leone under Professor W. Koski and Dr. Ruth Weiner of the Johns Hopkins University carried out the experimental work, obtaining a

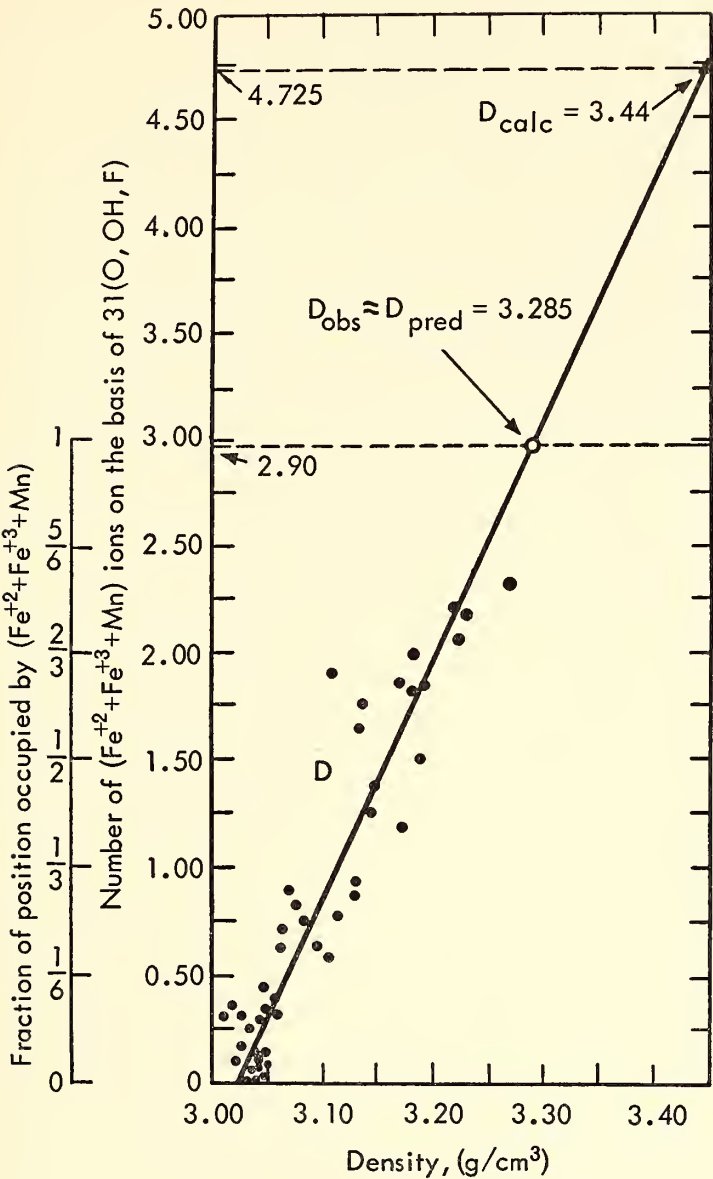


Fig. 63. Densities of tourmalines in relation to the number of (Fe²⁺ + Fe³⁺ + Mn) ions on the basis of 31 (O,OH,F). After Deer, Howie, and Zussman (1962, p. 312).

spectrum that shows a broad peak at room temperature, indicating Fe³⁺ or Mn²⁺, or both. NMR work, which is sensitive to

the coordination number of Fe⁵⁷, should give more information. In a broad-band spectrum we may expect to find evidence of tetrahedrally—as well as octahedrally—coordinated iron. For reasons of ionic size we can be certain that only ferric iron can be tetrahedrally surrounded by oxygens.

Regardless of the results of the NMR study and of the repeated analysis, a refined structure determination of the Mexican tourmaline is needed and has been begun.

Crystal Structure of Synthetic Iron Mica

Gabrielle Donnay, N. Morimoto, H. Takeda,¹⁵
and J. D. H. Donnay¹⁵

The structure determination of “ferriannite,” KFe₃²⁺(Fe³⁺Si₃)O₁₀(OH)₂, the synthetic iron mica prepared by Wones (*Year Book* 57 and 1963), was begun by Donnay and Kingman (*Year Book* 57). It has finally been completed and will be submitted for publication in an appropriate journal.

The atomic coordinates (table 19) refer to a monoclinic cell with the following dimensions: *a* = 5.43, *b* = 9.40, *c* = 10.32 Å, all ±0.2 per cent; β = 100°0' ± 10'. With 2 molecules per cell the calculated density is 3.46 g/cm³. The space group is *C*2/*m*. The slight departure from hexagonal symmetry of the tetrahedra (fig.

¹⁵ The Johns Hopkins University.

TABLE 19. Atomic Coordinates in Synthetic Iron Mica

Position	Atom	<i>x/a</i>	σ(<i>x</i>)	<i>y/b</i>	σ(<i>y</i>)	<i>z/c</i>	σ(<i>z</i>)	<i>B</i>
2 <i>b</i>	K	0	---	1/2	---	0	---	2.20
2 <i>c</i>	Fe _I ⁺⁺	0	---	0	---	1/2	---	0.80
4 <i>h</i>	Fe _{II} ⁺⁺	0	---	0.333	0.0004	1/2	---	0.88
4 <i>i</i>	OH	0.634	0.002	0	---	0.401	0.001	0.95
4 <i>i</i>	O _I	0.015	0.003	0	---	0.166	0.001	1.93
8 <i>j</i>	O _{II}	0.820	0.002	0.264	0.002	0.167	0.001	2.61
8 <i>j</i>	O _{III}	0.633	0.002	0.334	0.001	0.391	0.001	1.22
8 <i>j</i>	(Si,Fe ⁺⁺⁺)	0.575	0.001	0.333	0.0004	0.224	0.0003	0.87

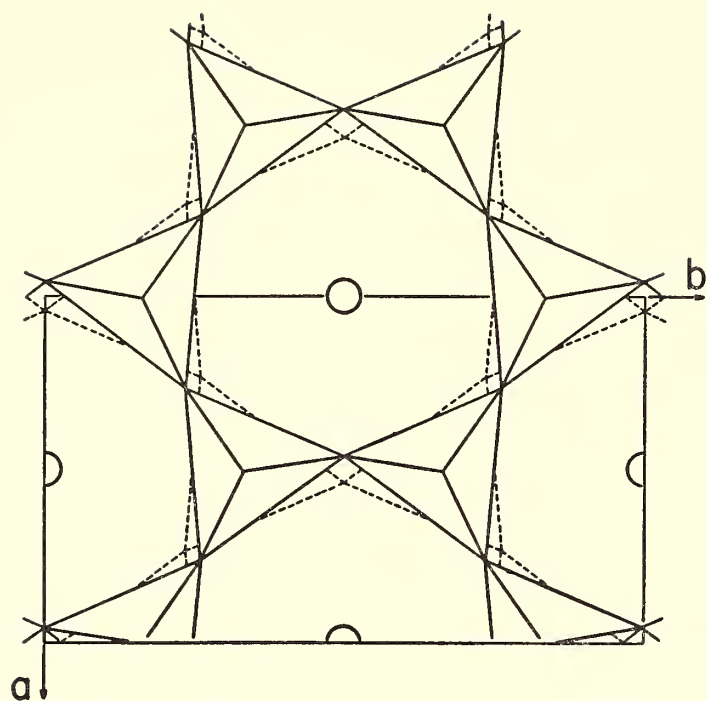


Fig. 64. Orthogonal projection of tetrahedral sheets onto (001). Open circles are potassium ions; dashed lines represent the top tetrahedral sheet in the cell below. Note ditrigonal symmetry of six-membered tetrahedral ring.

64) is sufficient to reduce the potassium coordination number from 12 to 6.

Structural Hints from Crystal Morphology

J. D. H. Donnay¹⁶ and Gabrielle Donnay

By suitable statistical survey the *crystal forms* of the substance studied are listed according to their observed frequencies of occurrence, taken in decreasing order. This *observed list* epitomizes the relevant morphological data. The structural cell dimensions **a**, **b**, **c** and space group having been determined by X rays, the net planes are listed according to their calculated *effective* interplanar distances $d(nh \cdot nk \cdot nl)$, taken in decreasing order, where nh , nk , nl are the smallest multiple indices that obey the space-group criteria and, if any, non-space-group (structural) criteria as well. Accordingly, n is the lowest permitted order of reflection; evidently $d(nh \cdot nk \cdot nl) = (1/n) d(hkl)$. From the second generalization of the law of Bravais, if this *theoretical list* duplicates the observed list, the

¹⁶ The Johns Hopkins University

symmetry of the *crystal structure* is also that of the *bond assemblage*. If the two lists disagree, bond assemblage and crystal structure have different symmetries (and possibly different cell dimensions).

If the *general form* that would be chosen morphologically as *unit form* is not structural (111) but, say, structural (pqr), the cell dimensions **a'**, **b'**, **c'** of the bond assemblage are $\mathbf{a}' = \mathbf{a}/p$, $\mathbf{b}' = \mathbf{b}/q$, $\mathbf{c}' = \mathbf{c}/r$. If the general forms, referred to cell **a'b'c'**, must have their indices multiplied by some factor (to obey a lattice-mode criterion) before their calculated *d*'s will express their relative frequencies, additional lattice nodes of the bond assemblage can be found. Example: let ($h'k'l'$) be the morphological symbol of the structural (hkl); if $(h' + k' + l')$ must be even for every general form, cell **a'b'c'** is body-centered.

Tautozonal faces give information on the two-dimensional bond assemblage of a planar projection of the structure (projected parallel to the zone axis). If the zone axis is normal to a symmetry plane, the faces belong to *special forms*, e.g., the ($hk0$)'s in point group *mmm*. If the theoretical listing of these forms conflicts with the observed list, even when multiple indices are used to comply with lattice-mode and glide-plane requirements, an additional condition must be imposed on the indices. Example: let $\mathbf{a}' = \mathbf{a}$, $\mathbf{b}' = \mathbf{b}$, $\mathbf{c}' = \mathbf{c}$; suppose that the ($hk0$)'s must have h even because of a structural a glide plane; if, in addition, they must have k even to express the morphological facts, we infer that, in the ab projection, **a** is halved for both structure and bond assemblage, and, in addition, **b** is halved for the bond assemblage only.

Information on the one-dimensional bond assemblages of linear projections can likewise be obtained.

The above method has been applied to haidingerite (with W. Kleber), narsarsukite, and hodgkinsonite (with L. A. Hardie and J. L. Munoz).

On the Number of n -Translational $(n + 1)$ -Dimensional Groups

J. D. H. Donnay¹⁶ and Gabrielle Donnay

Let G_d^t be the number of symmetry groups \mathbf{G}_d^t with t independent translations in d -dimensional Euclidean space. Let $(G_d^t)'$ be the number of antisymmetry groups ("black-white" groups, excluding both "colorless" and "gray" groups), also t -translational in d -space. We state and prove the following relation

$$G_{n+1}^n = 2G_n^n + (G_n^n)'$$

This relation obviously holds for $n = 0$ to 2, since

$$\begin{aligned} G_0^0 &= 1, & (G_0^0)' &= 0, & G_0^0 &= 2 \\ G_1^1 &= 2, & (G_1^1)' &= 3, & G_1^1 &= 7 \\ G_2^2 &= 17, & (G_2^2)' &= 46, & G_2^2 &= 80 \end{aligned}$$

It is known that, in the 80 groups \mathbf{G}_3^2 , the plane parallel with the net of translations may be: (a) no symmetry plane at all, containing no 2-axis and no center; (b) a mirror; or (c) a glide plane or a plane containing 2-axes or centers. The groups that can be enumerated under (a) are isomorphic with the 17 colorless groups \mathbf{G}_2^2 ; under (b) they are isomorphic with the 17 gray groups; under (c), with the 46 black-white groups.

Likewise, in 4-space ($xyzu$, there exists a three-dimensional mirror (xyz) in which reflection

$$\begin{pmatrix} 1 & \cdot & \cdot & \cdot \\ \cdot & 1 & \cdot & \cdot \\ \cdot & \cdot & 1 & \cdot \\ \cdot & \cdot & \cdot & -1 \end{pmatrix}$$

can be performed. Thus 3-space is the one that is spanned by the lattice of translations. Again, there are three possibilities: (a) this 3-space is *not* used as an element of symmetry at all; 230 groups can be enumerated in this case because they must be isomorphic with the 230 groups \mathbf{G}_3^3 ; (b) the 3-space is used as a three-dimensional mirror, and 230 groups result that correspond to the 230 gray groups \mathbf{G}_3^3 ; (c) the 3-space is used as a three-dimensional glide plane, and the resulting groups must be isomorphic with

the 1191 black-white $(\mathbf{G}_3^3)'$ groups. Hence $G_4^3 = 460 + 1191 = 1651$.

The proof holds for any value of n .

Crystal Data

J. D. H. Donnay¹⁶ and Gabrielle Donnay

The continuing work of critical evaluation and collection of crystallographic data has culminated, on April 1, 1963, in the publication of the second edition of part II (Determinative Tables) of *Crystal Data* (Donnay, Donnay, Cox, Kennard, and King, 1963).

The first edition of the book (Donnay, Nowacki, and Donnay, 1954) was published as *Memoir 60 of the Geological Society of America*. The second edition of the determinative tables appears as *Monograph 5 of the American Crystallographic Association*. Dr. E. G. Cox, professor of chemistry at the University of Leeds, England (now with the Agricultural Research Council in London), served as coeditor for inorganic substances until 1959. Mrs. Olga Kennard, crystallographer for the Medical Research Council, London, and secretary of the Crystal Data Commission of the International Union of Crystallography, is the coeditor for organic compounds. Dr. Murray Vernon King, research fellow, Orthopedic Research Laboratory, Massachusetts General Hospital, Boston, compiled and edited the protein data, which are collected in an appendix. The *Donnay-Harker Tables of Extinctions* have again been reprinted in the appendix.

The book comprises 1028 pages of data, 240 pages for name and formula indexes. The total number of entries is estimated at 13,000, more than double that of the first edition. Many pre-1951 errors and omissions have been made good. The data that appeared during the decade 1951-1960 have been added; although some of the 1960 data reached us too late to be included, the coverage should be fairly wide, at least as complete as that of the *Bulletin Signalétique* of the French Docu-

mentation Center, which provided a start for the literature search.

The entries are arranged by crystal systems. Within each system they are listed in the order of increasing values of a determinative number, which is either an axial ratio (a/b in the trimetric systems, c/a in the dimetric systems), or the cubic cell edge (a , in Å) in the isometric system. The determinative method rests on a conventional choice of the cell, dictated by metric considerations. A large proportion of the trimetric entries (which make up almost half of the total) had to be recast in the desired setting. The triclinic and monoclinic transformations of coordinates were performed on Pegasus computers at the University of Leeds and at Northampton Polytechnic, in London, using programs written by Miss D. Pilling. In the second edition the Bravais-reduced cell (shortest three translations) for triclinic substances replaces the Delaunay-reduced cell (shortest three translations that permit all three interaxial angles to be nonacute). The transformation matrix is now given in full in the entry itself, along with the original data.

Many crystallographers and organizations in several countries have contributed to this project, particularly the American Crystallographic Association, the (British) Institute of Physics and Physical Society, the International Union of Crystallography, the National Science Foundation, and the Office of Critical Tables, National Academy of Sciences—National Research Council.

The third edition is tentatively scheduled to appear in 1966. Two new coeditors have been chosen: Dr. Helen Ondik, National Bureau of Standards, for inorganic substances; and Miss Mary Mrose, U. S. Geological Survey, for minerals. The book will be published by the National Bureau of Standards. Plans are being made for transcribing the data on a 15-channel paper tape on the Mergenthaler keyboard, then on magnetic tape for computer processing, and back on

paper tape for final book production by the Linofilm photocomposition machine at the Government Printing Office.

The Interpretation of the Powder Pattern of a Crystalline Mixture

J. D. H. Donnay¹⁶ and Gabrielle Donnay

X-ray diffraction patterns of crystalline mixtures may be quite difficult to interpret. With current methods of identification there is no straightforward solution. Recommended practice consists in circumventing the problem as far as possible (1) by fractionating the sample (by physical or chemical means) and irradiating each fraction separately; or (2) by using differences in grain size of the components, which may lead to fine, broad, or gritty diffraction lines, so that the lines of one compound may be sorted out of the complex pattern. If the components have the same grain size, the second scheme fails.

The problem can be stated in the following way: What are all the compounds whose powder patterns have their strongest n lines in common with the pattern of the mixture (n being given successively decreasing values, say 7, 6, . . . , 1)? No mechanized solution has been found to this problem, except that it could, of course, be programmed on an electronic computer. The Census multi-column sorter was considered, but it does not seem to be applicable.

The method we propose rests on the following remark: What the various components of a mixture have in common is the absence of strong lines at a large number of θ values. The problem can now be restated as follows: What are all the compounds whose powder patterns have *no* strong line where the pattern of the mixture shows no line?

This is a retrieval problem easily solved by means of a system of grids, such as the one published by J. D. H. Donnay (1937) for the determination of minerals. In this system the absence as well as the presence

TABLE 20. Jadeite Unit-Cell Dimensions

Specimen	<i>a</i> , Å	<i>b</i> , Å	<i>c</i> , Å	β
Santa Rita Peak, Calif.	9.409	8.564	5.220	107°30'
White jadeite, Clear Creek, Calif., sample 54-RGC-58 (Coleman, 1961). Composition: 96.5% Jd, 2.4% Ac, 1.1% Di*	9.402	8.580	5.244	107°27.1'
Green jadeite, Clear Creek, Calif., sample J28-7 (Coleman, 1961). Composition: 74.3% Jd, 15.1% Ac, 7.6% Di, 3.2% He*	9.461	8.680	5.251	107°13.6'

* Cell dimensions from D. E. Appleman and R. G. Coleman, personal communication, 1963. Jd, jadeite; Ac, acmite; Di, diopside; He, hedenbergite.

of a certain property could be used as a determinative criterion. (Example: on the grid labeled “silver” the punched holes correspond to minerals that contain silver, whereas on the complementary grid, labeled “no silver,” the holes designate the minerals that do not contain silver.) Dr. F. W. Mathews has used this chemical scheme in his Coordinate Index for the determination of inorganic compounds. It can be extended to the present problem by punching “negative” grids for all the possible values of the glancing angle, say at every tenth of a degree, in θ or 2θ , the holes in a grid corresponding to all the compounds whose patterns do not show any strong line at that θ value.

The question arises which quantity to use— $d(hkl)$, $Q(hkl) = 1/d^2(hkl)$, or $\theta(hkl)$ —for a specified wavelength. The angular value (θ or 2θ) would appear to be the most advantageous, since (for the chosen wavelength) it is obtained directly from the measurement. A compact reference library of powder patterns could, for instance, be constructed as follows. Each pattern is represented by a number of 90 digits (each of which corresponds to a 1° range in θ) in the undecimal system of numeration. The letter *a*—the eleventh numeral—stands for *absence of line* in the 1° range to which it refers. Numerals 0 to 9 indicate at which tenth of degree a strong line occurs in $\text{CuK}\alpha_1$ radiation. (Only strong lines are considered, because weak lines might not show at all in a

mixture.) This scheme of describing a powder pattern lends itself well to punched-card methods.

The Crystal Structure of Jadeite,
NaAlSi₂O₆

Charles T. Prewitt¹⁷ and Charles W. Burnham

The crystal structures of phases formed at high pressures are currently of considerable interest, particularly with regard to investigating the effect of pressure on stability and structure. Although it is difficult to obtain reliable diffraction data at high pressures and temperatures, such work is now being done. It is found, however, that in many of the systems of interest insufficient reference data are available under standard conditions where most of these materials are actually observed and where they are presumably in a metastable state. Jadeite, for example, is a high-pressure phase which occurs naturally and which has also been synthesized in the laboratory by a number of workers. The crystal structure of jadeite has not been determined, although its diffraction pattern is similar to that of diopside, $\text{CaMgSi}_2\text{O}_6$. The diopside structure is known (Warren and Bragg, 1928) but has not been refined by modern techniques.

A detailed investigation of the jadeite

¹⁷ Central Research Department, E. I. du Pont de Nemours and Co., Wilmington, Delaware.

structure has been undertaken to provide precise information on cation coordinations, interatomic distances and angles, and atomic thermal vibrations. Since the available artificial material is extremely fine grained, a natural crystal from Santa Rita Peak, California, provided by Yoder, has been selected for X-ray analysis. Unit-cell dimensions of this specimen, listed in table 20, when compared with

those of analyzed jadeites indicate that in all probability this is close to a pure jadeite. The material is now being analyzed chemically.

Diffraction photographs were checked carefully for possible deviations from space group $C2/c$, but none was noted. Three-dimensional counter-diffractometer data have been obtained, and they are now being evaluated.

ORE MINERALS

During this past year laboratory investigations of several sulfide-type systems have been completed, and the results are now being applied to ores. A systematic study of the deposits of the Sudbury district has been initiated; it will benefit from nearly all the knowledge obtained through our previous studies of sulfide-type systems. The recently gained information on the iron-nickel-sulfur system, discussed in this report, and even more the knowledge currently being obtained of the copper-iron-nickel-sulfur system, will be of prime importance for the interpretation of the conditions existing during ore formation in this and similar districts.

In this report phase diagrams of the iron-nickel-sulfur system are presented at ten different temperatures from 400° to 1100°C. They are directly applicable to the appropriate mineral assemblages in ores and meteorites, although most of the phase relations have not yet been determined in detail. The breakdown of pentlandite, which occurs at 610°C in the presence of vapor, is affected strongly by pressure; it may take place at about 1000°C at 10,000 bars. The pressure-temperature curve of the pentlandite breakdown is a potential tool for estimation of the pressures existing during formation of pentlandite-pyrrhotite assemblages in ores as well as of troilite-pentlandite or of pentlandite-taenite assemblages in meteorites.

The copper-nickel-sulfur system was

studied in detail at 600°, 500°, 400°, and 300°C, and phase diagrams are given for these temperatures. In addition, melting relations were determined by differential thermal analyses. A new phase of composition CuNi_2S_6 was found to exist at 500°C and lower temperatures. This phase, which is isostructural with bravoite, $(\text{Fe,Ni})\text{S}_2$, forms limited solid solution toward both the Cu-S and Ni-S boundaries of the ternary system Cu-Ni-S but remains essentially stoichiometric.

Further studies have been completed of the copper-iron-sulfur system at low temperatures. The joins $\text{Cu}_{9.2}\text{S}_5$ - Cu_5FeS_4 , Cu_5FeS_4 - CuFeS_{2-x} , and Cu_5FeS_4 - Cu_2S were investigated between 50° and 300°C.

The ternary systems Fe-Ni-S, Cu-Ni-S, and Cu-Fe-S, all of which have now been studied, form three of the four boundaries of the complicated quaternary system Cu-Fe-Ni-S. The work now in progress on this system is focused on the chalcopyrite (CuFeS_{2-x}), pyrrhotite (Fe_{1-x}), and pentlandite ($[\text{Fe,Ni}]_9\text{S}_8$) relations. This assemblage is very common in ores of the Sudbury type, and knowledge of these phase relations will contribute greatly toward an understanding of the conditions obtaining during formation and cooling of the numerous deposits of this kind.

The common coexistence of lead-zinc type deposits of galena (PbS) with either or both of the iron sulfides pyrrhotite (Fe_{1-x}S) and pyrite (FeS_2) prompted an investigation of the phase assemblages in

the Fe-Pb-S system. The galena-pyrite pair was found to be stable below 717°C in the presence of vapor. This, therefore, is the highest temperature at which the pyrite-galena assemblage can coexist in ores when vapor is present.

The mineral cassiterite (SnO_2) has in the past served as the almost exclusive source of tin. Deposits of this mineral are dwindling, however, and other types of ores must in the future be counted on to satisfy the demands for this metal. The mineralogy of tin-containing minerals, which frequently occur in sulfide-type ores, is largely unknown. Studies of the phase relations among the minerals of such ores have now been initiated. Investigations of the Sn-S system with subsequent applications to ores led to the discovery of two new minerals, Sn_2S_3 and SnS_2 . The phase relations in the ternary Fe-Sn-S and Cu-Sn-S systems have been studied at 600°C.

The Fe-Ni-As system was studied at 800°C by quenching and DTA experiments. Reaction rates are very slow even at this high temperature, requiring from 1 to 3 months for attainment of equilibrium. This ternary system is characterized by extensive solid-solution fields running parallel to the Fe-Ni boundary.

Monoclinic pyrrhotites from ores were separated and heated at various temperatures over time periods up to 1 year. Hexagonal pyrrhotite was obtained at as low as 265°C. Synthetic monoclinic pyrrhotite, however, appears to be stable even at 300°C. The approximate compositions of three of the low-temperature pyrrhotite-type phases have also been determined by experiments on synthetic materials.

Additional work has been performed to synthesize numerous sulfides at low temperatures in the presence of various types of solutions. These experiments demonstrated that "blaubleibender" covellite is a mineral species that contains 2 to 3 weight per cent S less than ordinary covellite and that is stable below about 157°C.

THE Fe-Ni-S SYSTEM

G. Kullerud

Continued progress in the investigations of this system was achieved through quenching experiments performed in silica and gold tubes, differential thermal analyses, and high-temperature X-ray powder diffraction studies. It is now possible to indicate the phase relations in the entire system at a number of temperatures, although many relations still remain to be explored in detail.

Iron-nickel sulfide ores such as those of the Sudbury area in Canada are believed to have formed as a result of magmatic segregation. In this process the sulfides separated from the silicate magma by gravity settling.

The studies reported on last year indicated that the metal-rich sulfide drops not only separate by gravity settling from a silicate magmatic solution but actually formed before this event through liquid immiscibility among the sulfide phases.

In principle, the extensive field of liquid immiscibility existing in the Fe-Ni-S system (see *Year Book 61*) could provide a mechanism of separating metal-rich from extremely sulfur-rich liquids. In ore bodies, however, there is little evidence of excess sulfur. Moreover, sulfur-rich liquids readily react with the silicates to form additional metal sulfides (see another section of this report), which in turn are segregated by gravity settling of the liquids. This process would continue until the available sulfur had been exhausted. The kinds of mineral assemblages formed on cooling of iron-nickel sulfides from this metal-rich liquid can be explained with the aid of diagrams picturing the phase relations in the Fe-Ni-S system at successively lower temperatures. In order to apply the knowledge obtained through laboratory investigations to ores and meteorites, it is necessary to discuss the Fe-Ni-S system first.

Discussion of Phase Relations

The first diagram (fig. 65) shows the phase relations in the system at 1100°C.

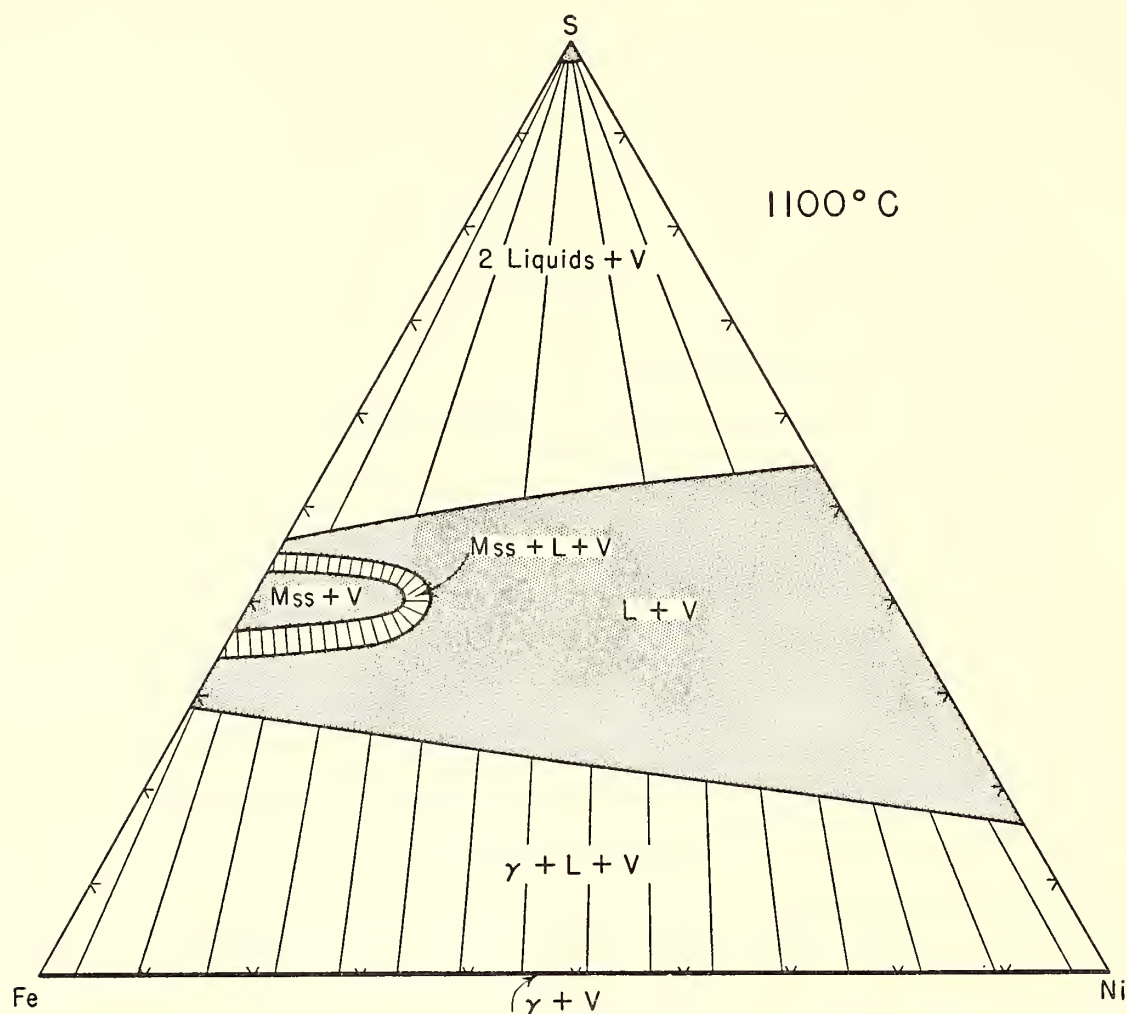


Fig. 65. Phase relations in the Fe-Ni-S system at 1100°C are characterized by a large field of liquid immiscibility and an extensive central liquid field. The Mss phase is the only stable sulfide at this temperature.

The critical point of sulfur is at about 1030°C and 118 bars. The courses of the critical curves connecting the critical point of sulfur to those of iron and nickel are not known. However, since the critical point of iron as well as that of nickel lies well above 3000°C, the critical curve must rise rather steeply toward higher temperatures when metal is added to sulfur. For this reason it is believed that only compositions very close to the sulfur corner are supercritical at 1100°C. The remaining part of the sulfur field of figure 65 contains liquid and vapor. Immiscibility exists in a large divariant field, marked with tie lines, between the sulfur-rich liquid containing about 98 weight per cent S and a metal-rich liquid that, depending on the iron-to-nickel ratio, contains from about 46.5 to 54.5 weight per cent S. Below the field of liquid immiscibility a large central field containing homogeneous liquid and vapor extends from about 45.5 to 84

weight per cent Ni along the Ni-S side of the ternary system. Aside from the region between 55 and 66 weight per cent, it extends from about 53.5 to 71 weight per cent Fe along the Fe-S boundary. The disruption of the homogeneous liquid field is caused by the pyrrhotite solid solution series, which at 1100°C extends from 36.5 to 43.3 weight per cent S in the pure Fe-S system. The pyrrhotite solid solution protrudes into the ternary system, and the maximum solid solution of nickel is about 14 weight per cent at 1100°C. This solid solution which at lower temperatures forms a complete series between Fe_{1-x}S and Ni_{1-x}S is usually referred to as the monosulfide solid solution (Mss) of the Fe-Ni-S system. As demonstrated in the diagram of figure 65 a divariant field containing Mss and liquid separates Mss from the homogeneous central liquid field.

At this temperature Fe and Ni are isostructural and form a complete γ -type

solid solution. This is indicated by a heavy solid line extending from the Fe to the Ni corner of the diagram. This γ solid solution coexists with homogeneous liquid in a divariant region that extends across the entire ternary system and that along the Fe-S boundary extends from almost pure Fe to about 29 weight per cent S and along the Ni-S boundary from almost pure Ni to about 16 weight per cent S. Tie lines indicating the compositions of coexisting γ FeNi solid solution (ss) and liquid are shown in figure 65.

On cooling, various changes take place in the phase relations. The liquid immiscibility field extends completely across the system from the Ni-S to the Fe-S boundaries only above 1083°C. Below this temperature pyrrhotite becomes stable with liquid S on the Fe-S join, and the divariant field containing Mss, liquid, and vapor widens gradually with decreasing temperature. At the same time the Mss

field extends increasingly further into the ternary system. At 1007°C the NiS_2 phase becomes stable.

The phase relations at 1000°C are shown in figure 66. Monosulfide solid solution over a wide composition range is noted to coexist with sulfur-rich liquid in the divariant field marked $\text{Mss} + L + V$. At this temperature the region of liquid immiscibility, marked 2 liquids + V, is rather narrow, and a univariant field containing Mss, sulfur-rich liquid, metal-rich liquid, and vapor now exists between the two divariant regions $\text{Mss} + L + V$ and 2 liquids + V. The maximum Fe content of the NiS_2 phase at 1000°C is about 1 per cent as determined by L. A. Clark and Kullerud (*Year Book 58*, pp. 142-145). The NiS_2 phase is surrounded by a divariant field containing NiS_2 , liquid, and vapor. The tie lines between NiS_2 and this liquid are indicated in figure 66. The monosulfide solid solution is

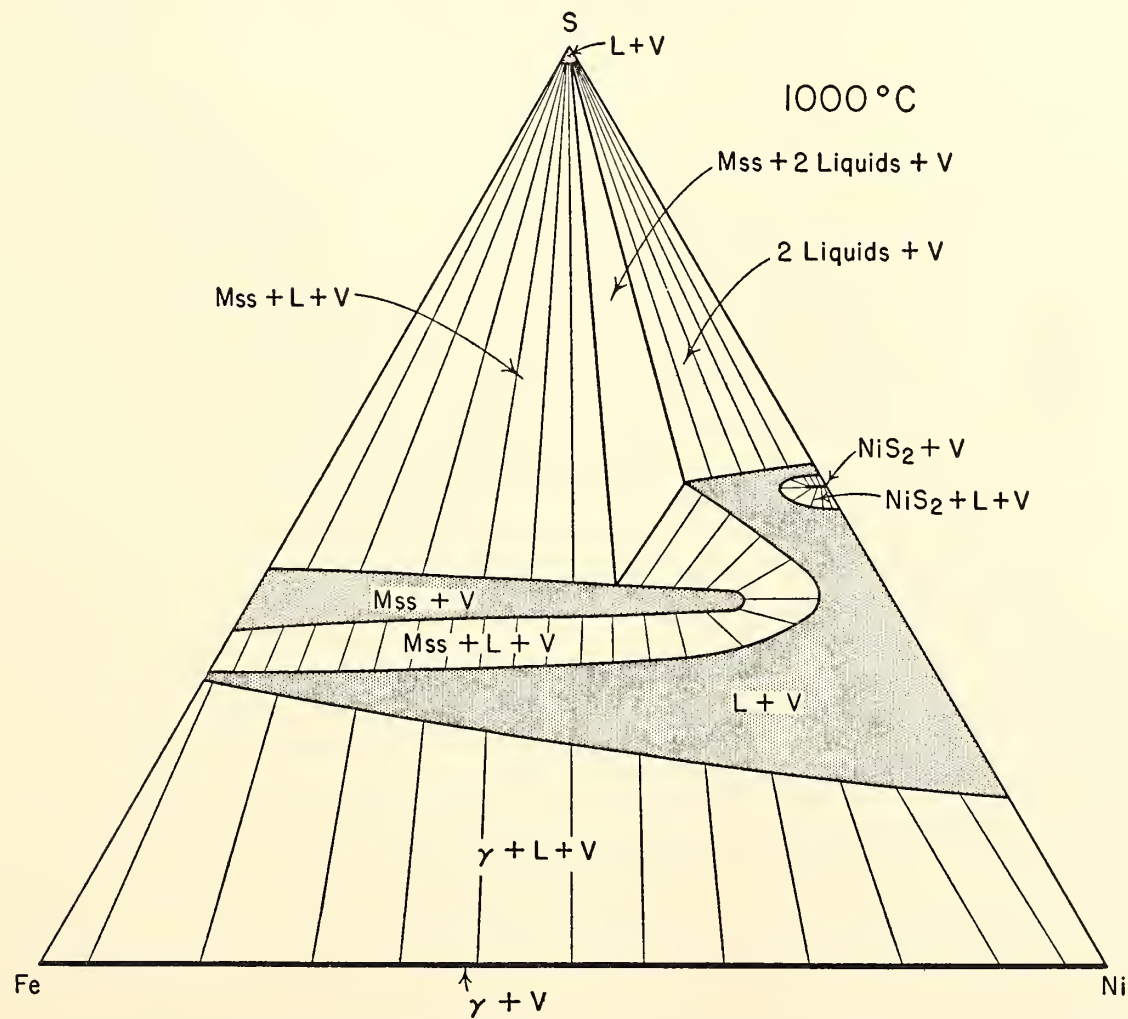


Fig. 66. At 1000°C the liquid immiscibility and the central liquid fields are much smaller but the monosulfide solid solution is considerably more extensive than at 1100°C. The NiS_2 phase is stable at 1000°C.

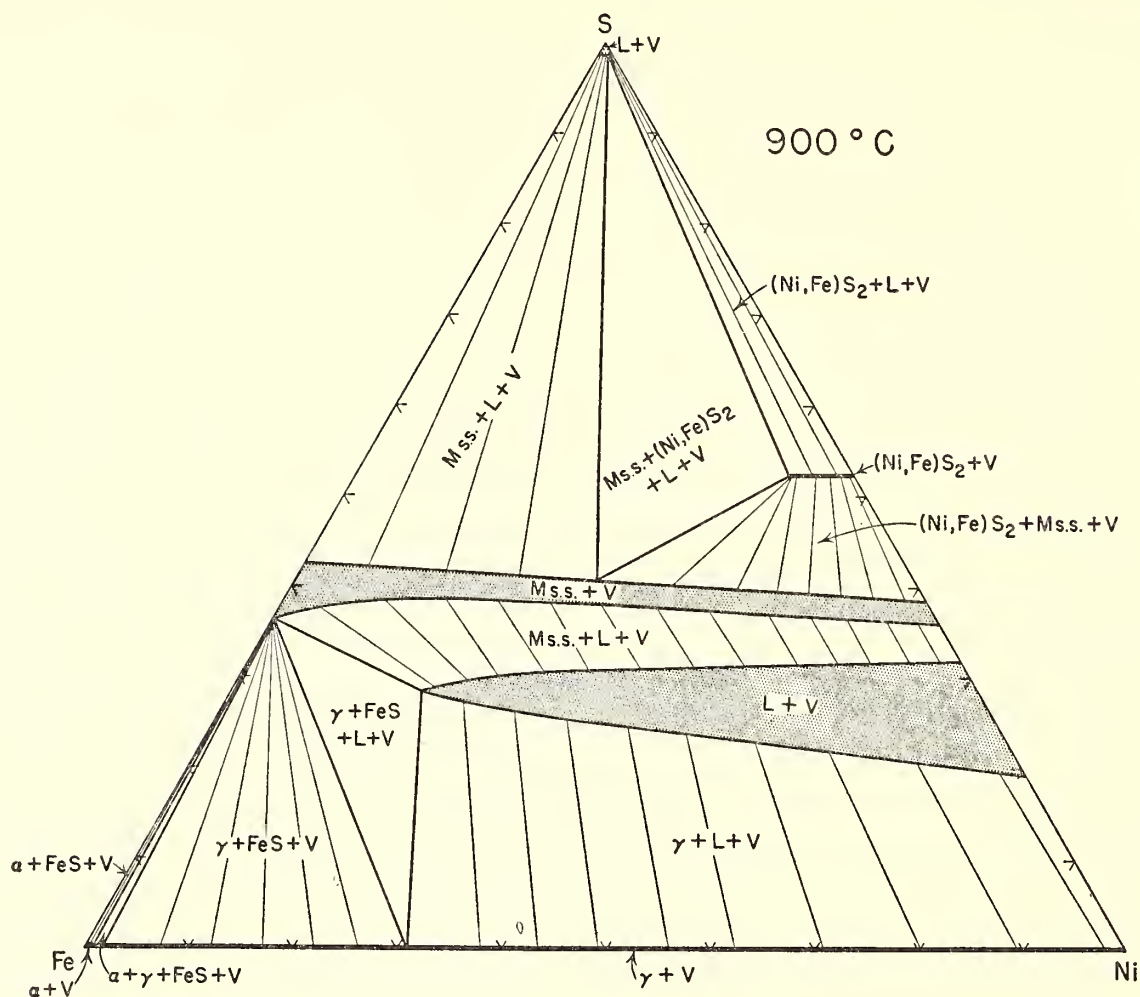


Fig. 67. The monosulfide solid solution is complete between Fe_{1-x}S and Ni_{1-x}S at 900°C . The central liquid field no longer spans across the ternary system.

separated from the liquid by a divariant field containing $\text{Mss} + \text{L} + \text{V}$. The trend of the liquid boundary curve was determined by S. P. Clark and Kullerud (*Year Book 58*, pp. 168–170). The tie lines in the divariant $\text{Mss} + \text{L} + \text{V}$ field are indicated in figure 66. The central liquid field is much smaller at 1000° than at 1100°C ; compare figures 65 and 66. It extends to about 69 weight per cent Fe along the Fe-S boundary and to about 81.5 weight per cent Ni along the Ni-S boundary. It is separated from the γFeNi solid solution, which at 1000°C is still complete, by a divariant field containing $\gamma + \text{L} + \text{V}$. The tie lines relating the compositions of coexisting liquid and γ solid solution are indicated in the diagram of figure 66.

On cooling below 1000°C , the monosulfide solid solution becomes complete between Fe_{1-x}S and Ni_{1-x}S at 992°C . The liquid immiscibility field disappears at 991°C (Kullerud and Yund, 1962), and

below this temperature NiS_2 coexists with liquid sulfur. The eutectic between NiS_2 and Ni_{1-x}S (Kullerud and Yund, 1962) appears at 985° , and below this temperature nickel mono- and disulfide coexist. Along the Fe-S boundary the Fe-FeS eutectic appears at 988°C , which is the lowest temperature at which the central liquid field spans the ternary system from the Ni-S to the Fe-S boundaries. The central liquid field on further cooling gradually shrinks away from the Fe-S boundary, resulting in the development of a univariant field containing γFeNi solid solution, FeS, liquid, and vapor. Pure Fe inverts at 913°C from the high-temperature γ to the low-temperature α form. In the Fe-Ni system the temperature of this inversion depends strongly on composition.

The phase relations at 900°C are shown in figure 67. The solubility of Fe in NiS_2 at this temperature was determined by L. A. Clark and Kullerud (*Year Book 58*).

This phase now coexists stably with sulfur-rich liquid as shown by the divariant $(\text{Ni,Fe})\text{S}_2 + L + V$ field of figure 67. This field is separated from the divariant $\text{Mss} + L + V$ region, which also existed at 1000°C , by the univariant $\text{Mss} + (\text{Ni,Fe})\text{S}_2 + L + V$ field. The $(\text{Ni,Fe})\text{S}_2$ or vaesite phase at 900°C coexists stably with Mss . This field is outlined in figure 67, and tie lines relate the compositions of coexisting phases. The Mss field at this temperature extends from pure Fe_{1-x}S to pure Ni_{1-x}S . It is separated from the central liquid field by a divariant $\text{Mss} + L + V$ region. The boundaries of the central liquid field at 900°C were determined by S. P. Clark and Kullerud (*Year Book 58*). The central liquid still coexists with γFeNi solid solution, but the divariant field in which both phases occur is much smaller at 900°C (fig. 67) than at 1000°C (fig. 66). The compositions of the phases occurring in the FeS , γFeNi , L , and V univariant field were determined at 900°C by S. P. Clark and Kullerud (*Year Book 58*). The monosulfide phase of this assemblage contains less than 0.5 weight

per cent Ni, its metal-to-sulfur ratio is stoichiometric or nearly stoichiometric, and the γFeNi phase of this assemblage contains 31 weight per cent Ni. The αFeNi phase is stable over a very narrow composition range, of less than 0.5 weight per cent Ni, at 900°C because the γ - α inversion temperature is lowered rapidly with increasing Ni content in the alloy. The α solid solution range and the width of the $\alpha\text{FeNi} + \text{FeS} + V$ divariant region are exaggerated in figure 67 for the sake of illustration. In the binary Fe-Ni system the univariant field containing $\alpha\text{FeNi} + \gamma\text{FeNi} + V$ is very narrow; both α and γFeNi contain less than 0.5 weight per cent Ni. In figure 67 the compositional differences between these two phases have been exaggerated to demonstrate the presence of the $\alpha\text{FeNi} + \gamma\text{FeNi} + \text{FeS} + V$ univariant field. The $\gamma\text{FeNi} + \text{FeS} + V$ divariant field is wide in its metal-rich portion. Stoichiometric FeS can at 900°C coexist with γFeNi alloys containing from about 0.5 to 31 weight per cent Ni.

Cooling below 900°C results in a gradual narrowing of the $\text{Mss} + L + V$

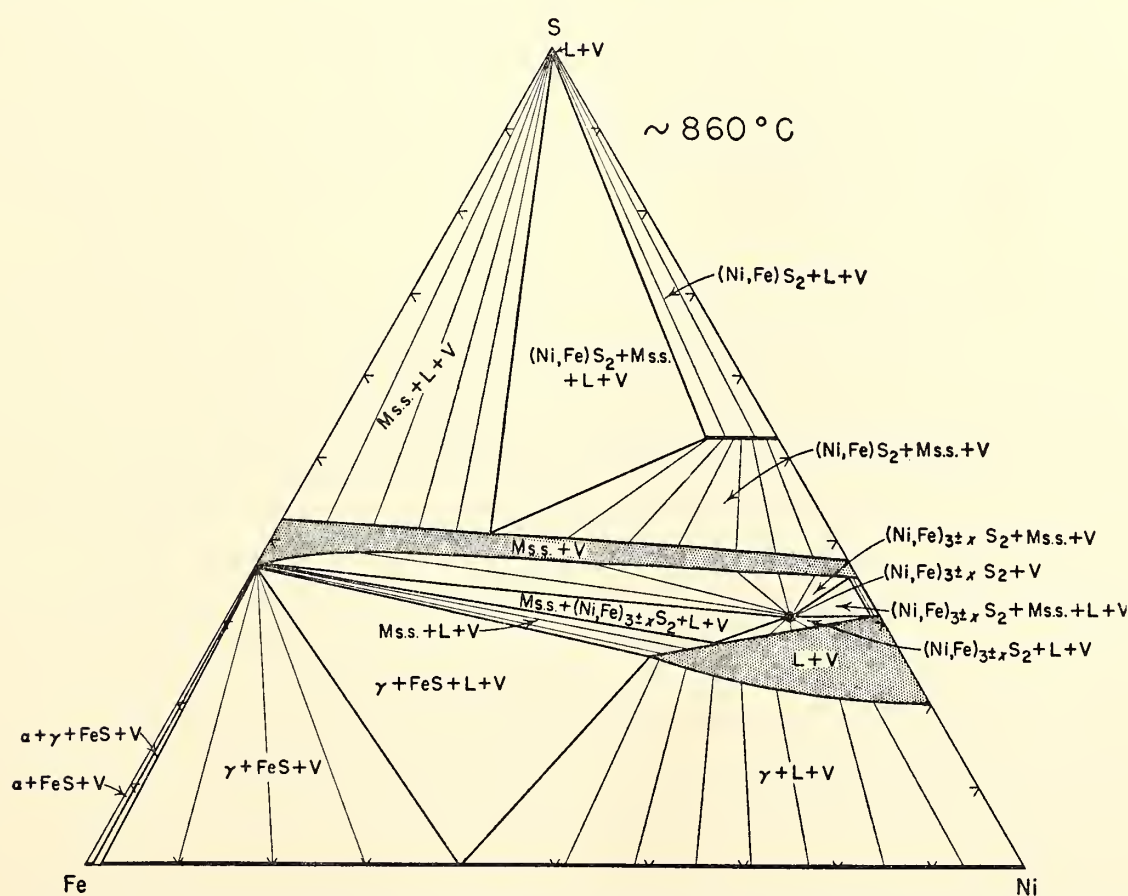


Fig. 68. The $(\text{Ni,Fe})_{3\pm x}\text{S}_2$ phase becomes stable slightly above 860°C . Its appearance leads to the establishment of two new univariant and two new divariant fields.

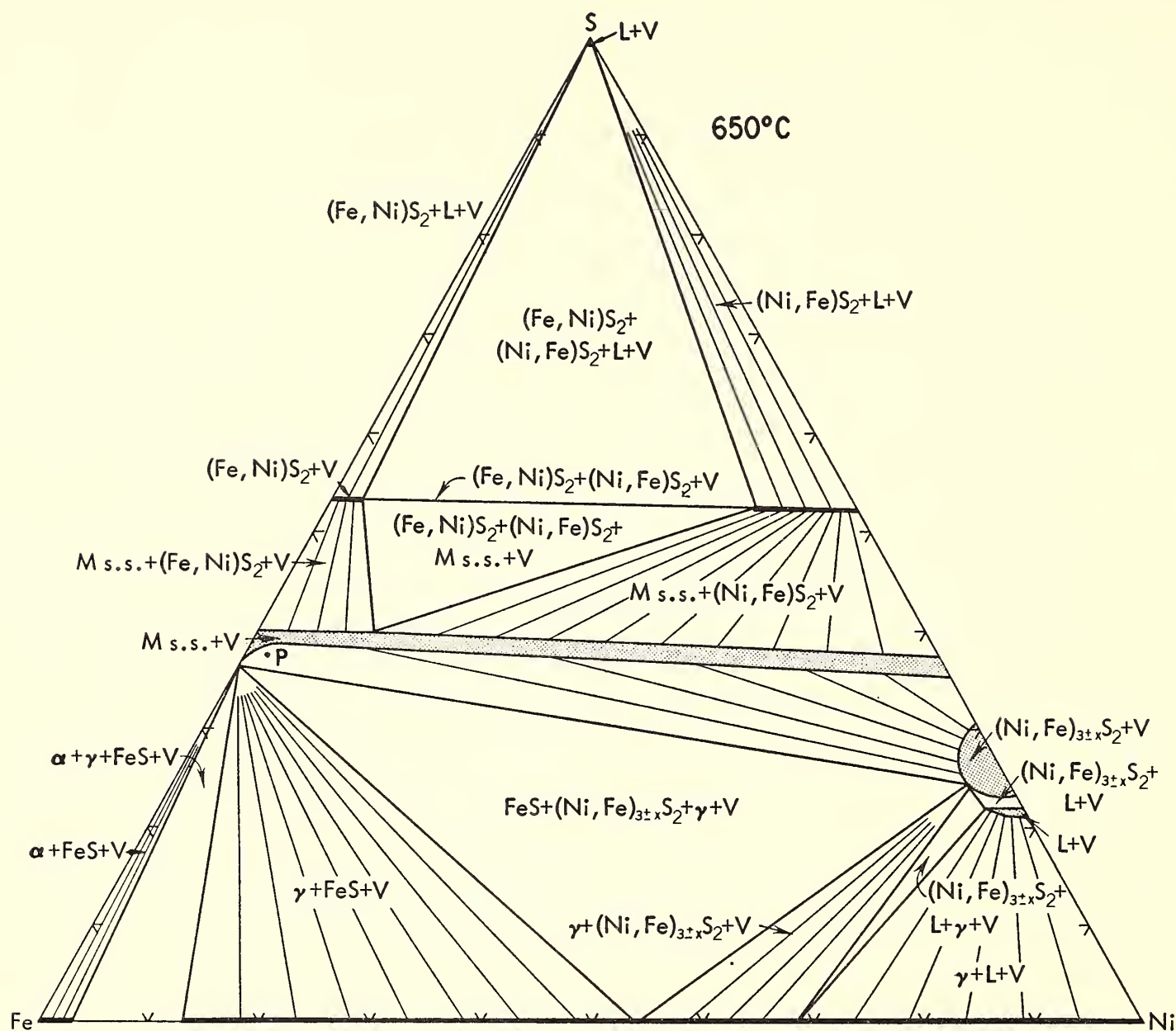


Fig. 69. The Fe-Ni-S system at 650°C. Pyrite, which became stable at 743°C, contains appreciable Ni in solid solution. The central liquid field at 650°C is very small and disappears at 635°C. The composition indicated by P, which at 860°C was situated in the Mss field, at 650°C lies in the Mss + (Ni,Fe)_{3±x}S₂ + V divariant region.

divariant field, a widening of the Mss + (Ni,Fe)S₂ + L + V field, and an increase in the solubility of Fe in NiS₂. The monosulfide solid solution remains complete between Fe_{1-x}S and Ni_{1-x}S. The central liquid field is gradually becoming smaller, whereas the γ FeNi + FeS + L + V univariant field becomes larger. The γ FeNi + FeS + V, the α FeNi + γ FeNi + FeS + V, and the α FeNi + FeS + V fields are all becoming wider along the Fe-Ni boundary. The FeS in all these assemblages remains essentially stoichiometric and contains less than 0.5 weight per cent Ni. The Ni_{3±x}S₂ phase in the pure Ni-S system melts incongruently to Ni_{1-x}S and liquid, which correspond in the ternary

system to Mss and central liquid, respectively. This Ni_{3±x}S₂ can take considerable Fe into solid solution. How much is not yet accurately known, but DTA experiments have indicated that the Fe-saturated (Ni,Fe)_{3±x}S₂ phase melts incongruently at 862° ± 3°C.

Figure 68 shows the phase relations a few degrees below 862°C. The major changes in phase relations are caused by the appearance of the (Ni,Fe)_{3±x}S₂ phase. The divariant region in which Mss + L (central) + V coexist is narrow at 860°C. The (Ni,Fe)_{3±x}S₂ phase, which has a metal-to-sulfur ratio somewhat less than 3:2, should at this temperature technically be formulated as (Ni,Fe)_{3-x}S₂. This phase

now coexists with Mss over a wide divariant region labeled $(\text{Ni,Fe})_{3\pm x}\text{S}_2 + \text{Mss} + \text{V}$ in figure 68. The $\text{Mss} + \text{L} + \text{V}$ and $(\text{Ni,Fe})_{3\pm x}\text{S}_2 + \text{Mss} + \text{V}$ divariant regions are separated by the univariant field $(\text{Ni,Fe})_{3\pm x}\text{S}_2 + \text{Mss} + \text{L} + \text{V}$. The latter divariant region and the divariant region in which $(\text{Ni,Fe})_{3\pm x}\text{S}_2 + \text{L} + \text{V}$ coexist are separated by the $(\text{Ni,Fe})_{3\pm x}\text{S}_2 + \text{Mss} + \text{L} + \text{V}$ univariant field.

At temperatures below 860°C the $(\text{Ni,Fe})_{3\pm x}\text{S}_2$ ss field widens rapidly in the direction of increasing metal-to-sulfur ratio. At the same time it also approaches the Ni-S boundary and its ability to take Fe in solid solution decreases. The central liquid field diminishes gradually and disappears entirely at 635°C , which is the temperature of the Ni-Ni $_{3\pm x}\text{S}_2$ eutectic in

the Ni-S system. At about 700°C the tie lines between Mss and central liquid are broken and are replaced by tie lines between $(\text{Ni,Fe})_{3\pm x}\text{S}_2$ and γFeNi solid solution. This tie-line change leads to the development of a very large univariant field in which $\text{FeS} + (\text{Ni,Fe})_{3\pm x}\text{S}_2 + \gamma\text{FeNi} + \text{V}$ coexist and of a small univariant field containing $(\text{Fe,Ni})_{3\pm x}\text{S}_2 + \gamma\text{FeNi} + \text{L} + \text{V}$. In the sulfur-rich portion of the system FeS_2 becomes stable at 743°C , and at 729° tie lines between FeS_2 and NiS_2 are established. The latter phase relations were determined by L. A. Clark and Kullerud (*Year Book 58*). The phase relations at 650°C are shown in figure 69. It is noted that the monosulfide solid solution remains complete between Fe_{1-x}S and Ni_{1-x}S . Because of the FeS_2 - NiS_2 tie

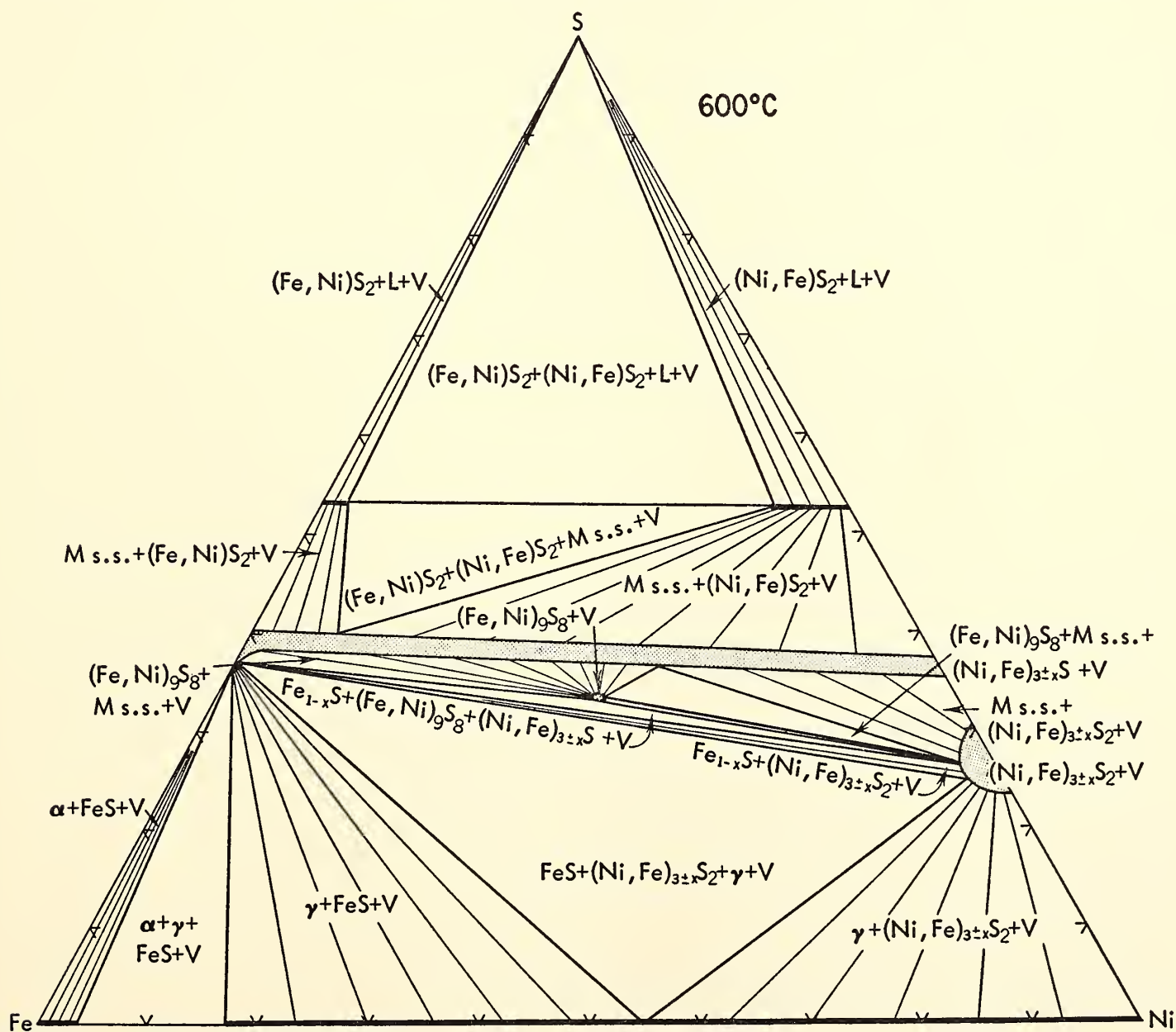


Fig. 70. At 600°C pentlandite is stable, and the former $\text{Mss} + (\text{Ni,Fe})_{3\pm x}\text{S}_2 + \text{V}$ divariant field, which at 650°C was extensive, is now divided into four divariant and two invariant fields.

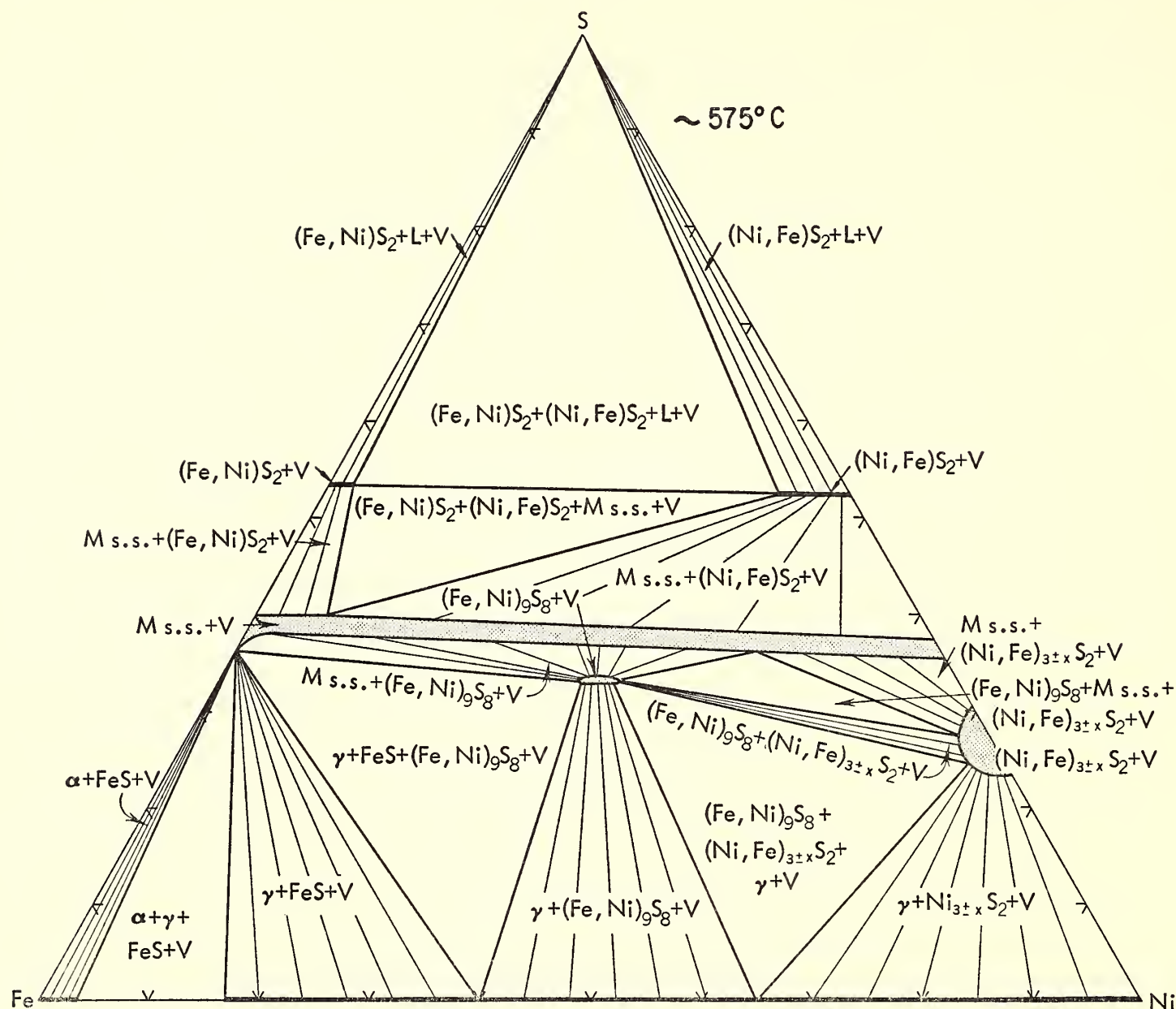


Fig. 71. At 575°C the FeS-(Ni,Fe)_{3±x}S₂ tie lines which existed at 600°C have been replaced by tie lines between (Fe,Ni)₉S₈ and γFeNi ss.

lines now in existence, two new univariant fields occur. The stable assemblages in these fields are: (Fe,Ni)S₂ + (Ni,Fe)S₂ + L + V and Mss + (Fe,Ni)S₂ + (Ni,Fe)S₂ + V. The Mss + (Ni,Fe)_{3±x}S₂ + V divariant field is now very wide, and the (Ni,Fe)_{3±x}S₂ solid solution extends into the ternary system from the Ni-S boundary. The central liquid field has all but disappeared at 650°C. The αFeNi phase at this temperature contains a maximum of about 3 weight per cent Ni, and the α + γFeNi region extends from 3 to about 13 weight per cent Ni. Stoichiometric FeS containing less than 0.2 weight per cent Ni coexists with these phases as shown by the divariant αFeNi + FeS + V, the

univariant αFeNi + γFeNi + FeS + V, and the divariant γFeNi + FeS + V regions. The Ni content in γFeNi of the last region varies from about 13 to about 50 to 55 weight per cent Ni. FeS of stoichiometric composition also occurs in the large γFeNi + FeS + (Ni,Fe)_{3±x}S₂ + V univariant field.

Further lowering of the temperature leads to very important development in the Mss + (Ni,Fe)_{3±x}S₂ + V divariant field. At 610°C the (Fe,Ni)₉S₈ compound (pentlandite) appears. The phase relations at 600°C are indicated in figure 70. Tie lines still exist between Mss and (Ni,Fe)_{3±x}S₂, but the divariant region of coexistence of the two phases is very nar-

row and the Mss phase has nearly FeS composition. A very narrow univariant region still permits coexistence of Mss (near FeS in composition) + (Fe,Ni)₉S₈ + (Ni,Fe)_{3±x}S₂ + V. The (Fe,Ni)₉S₈ phase coexists with Mss in which the Ni content may vary from less than 0.5 to about 40 weight per cent. This region apparently becomes wider at lower temperatures. The (Ni,Fe)_{3±x}S₂ phase still coexists with Mss, which, however, at 600°C and lower temperatures contains at least 40 weight per cent Ni. A second univariant region, produced by the appearance of (Fe,Ni)₉S₈, contains (Fe,Ni)₉S₈ + Mss + (Ni,Fe)_{3±x}S₂ + V.

On cooling below 600°C the (Fe,Ni)₉S₈ phase forms solid solution on both sides

of the 1:1 ratio of the metals. This solid solution on the Fe side intersects the $\text{FeS} + (\text{Ni,Fe})_{3\pm x}\text{S}_2 + V$ divariant region, and a tie-line change occurs at about 580°C . Figure 71 shows the phase relations at 575°C . Tie lines now exist between $(\text{Fe,Ni})_9\text{S}_8$ and γFeNi solid solution, and two new univariant fields occur— $\gamma\text{FeNi} + \text{FeS} + (\text{Fe,Ni})_9\text{S}_8 + V$ and $\gamma\text{FeNi} + (\text{Fe,Ni})_9\text{S}_8 + (\text{Ni,Fe})_{3\pm x}\text{S}_2 + V$.

At lower temperatures the Ni_7S_6 phase appears at 573°C , and at 556° the stoichiometric Ni_3S_2 inverts from a high-temperature possibly tetragonal to a low-temperature hexagonal (heazlewoodite) form (Kullerud and Yund, 1962). The high-temperature phase forms solid solution on both the Ni and S sides of Ni_3S_2

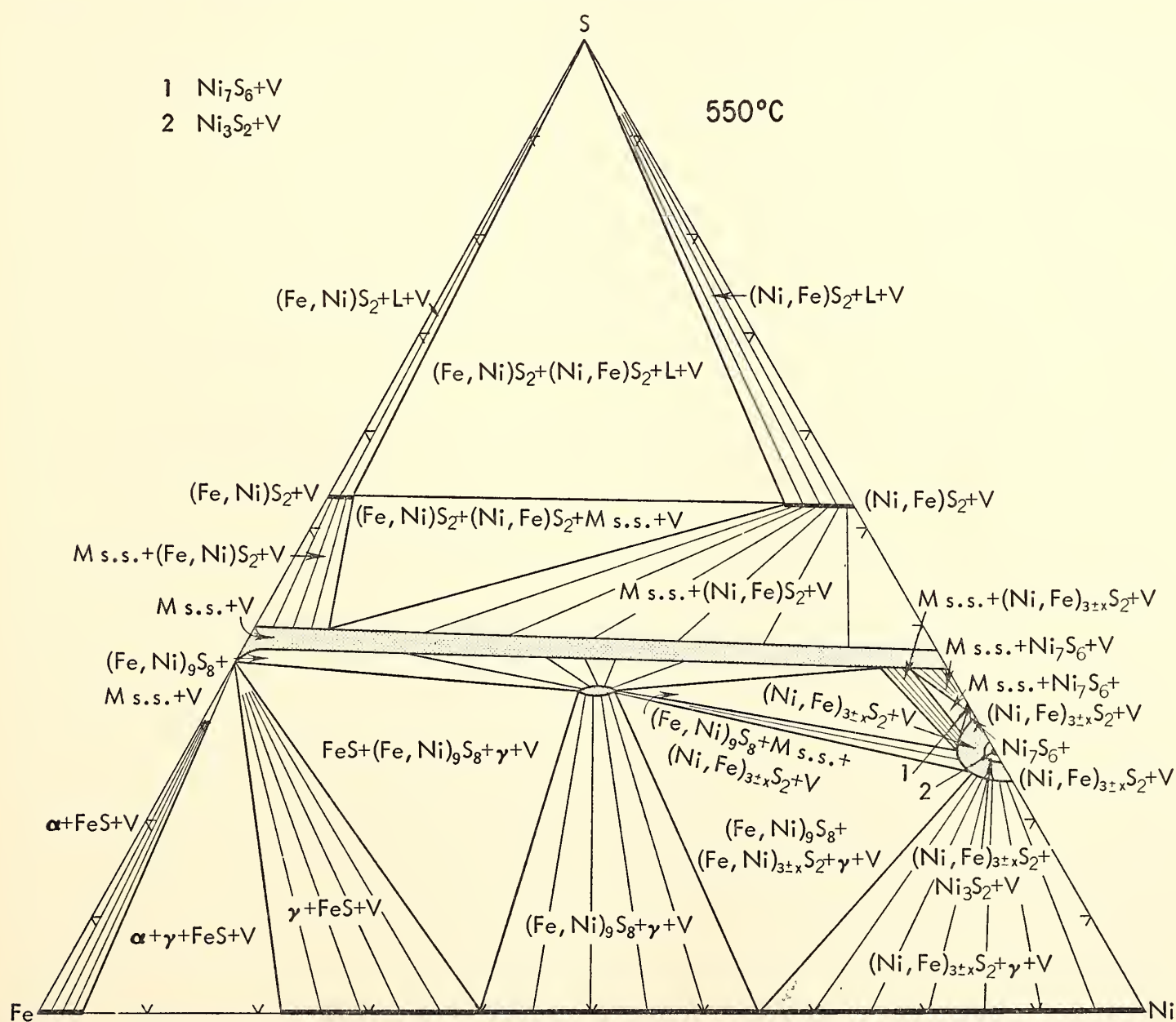


Fig. 72. At 550°C the low-temperature form of Ni_3S_2 (heazlewoodite) and the $(\text{Ni,Fe})_{3\pm x}\text{S}_2$ phase coexist because the high-low inversion in stoichiometric Ni_3S_2 takes place at 556°C. The Ni_7S_6 phase becomes stable at 573°C.

tion extending from the Ni-S boundary. These solid solutions at 500°C are separated by a divariant field containing $(\text{Fe,Ni})_{1-x}\text{S} + (\text{Ni,Fe})_{1-x}\text{S} + V$ as shown in figure 73. Further developments, also shown in figure 73, directly referable to the breakdown of the high-temperature homogeneous Mss phase, are the $(\text{Fe,Ni})_{1-x}\text{S} + (\text{Ni,Fe})\text{S}_2 + V$ and $(\text{Fe,Ni})_9\text{S}_8 + (\text{Ni,Fe})_{1-x}\text{S} + V$ divariant fields, and the $(\text{Fe,Ni})_{1-x}\text{S} + (\text{Ni,Fe})_{1-x}\text{S} + (\text{Ni,Fe})\text{S}_2 + V$ and $(\text{Fe,Ni})_{1-x}\text{S} + (\text{Ni,Fe})_{1-x}\text{S} + (\text{Fe,Ni})_9\text{S}_8 + V$ univariant fields. In the metal-rich portion of the system the new FeNi_3 phase is stable with γFeNi and Ni_3S_2 as shown in figure 73 by the $\gamma\text{FeNi} + \text{FeNi}_3 + V$ assemblage

along the Fe-Ni boundary, the $\text{FeNi}_3 + \text{Ni}_3\text{S}_2 + V$ divariant, and the $\gamma\text{FeNi} + \text{FeNi}_3 + \text{Ni}_3\text{S}_2 + V$ univariant assemblages. The solid solutions of Fe and Ni in FeNi_3 are very limited at 500°C; the compositional limits of the phase are at about 74 and 75 weight per cent Ni.

At lower temperatures the solubilities of both Fe and Ni increase considerably. It appears that at some as yet undetermined temperature between 500° and 400°C the tie lines between γFeNi (containing ~60 to 72 weight per cent Ni) and Ni_3S_2 are broken and replaced by tie lines connecting FeNi_3 and $(\text{Fe,Ni})_9\text{S}_8$. Figure 74 shows the phase relations at 400°C. The FeNi_3 phase now forms solid solution

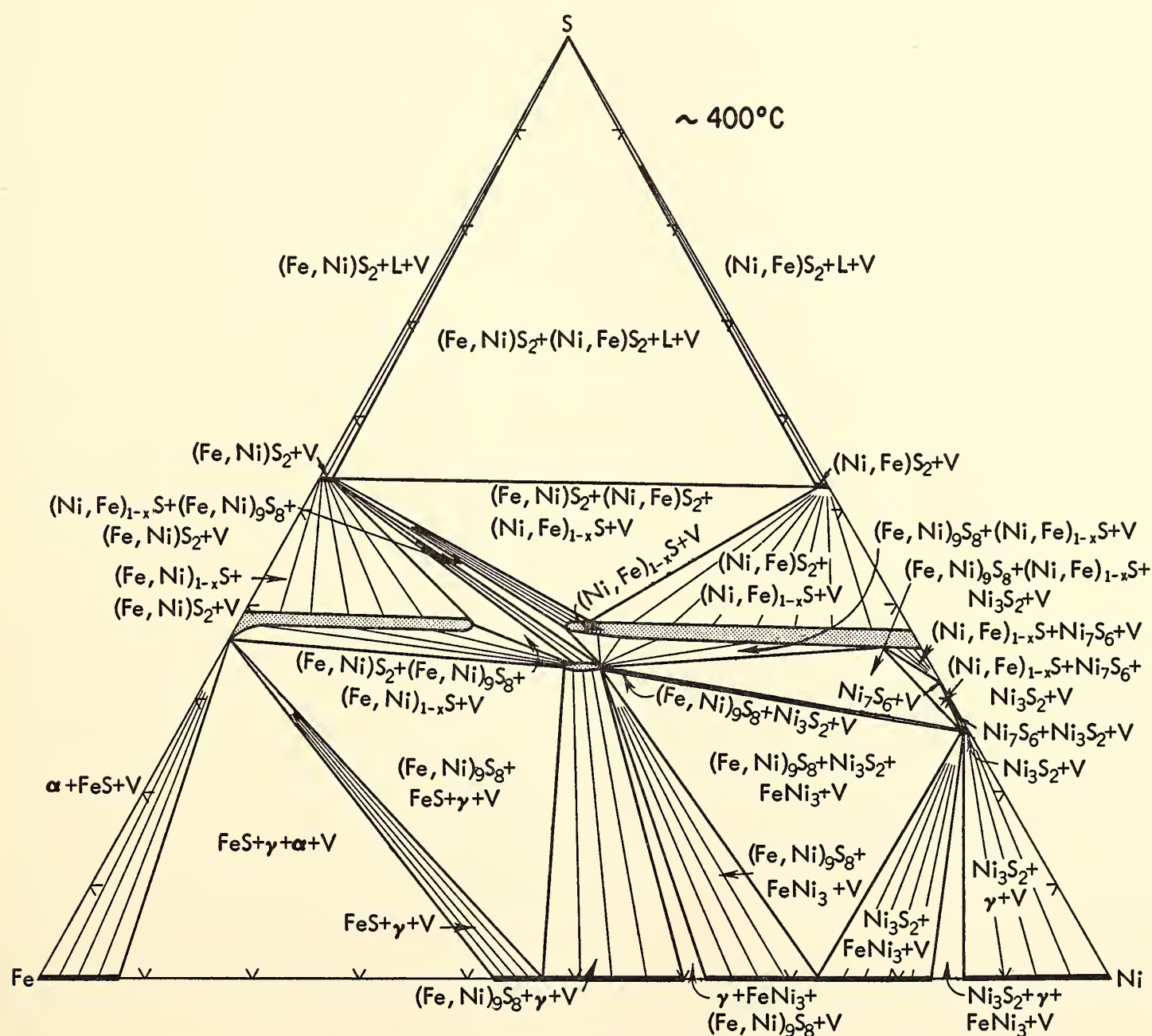


Fig. 74. Below 500°C the miscibility gap between the $(\text{Fe,Ni})_{1-x}\text{S}$ and $(\text{Ni,Fe})_{1-x}\text{S}$ solid solutions gradually increases. Below about 400°C tie lines may exist between $(\text{Fe,Ni})\text{S}_2$ and $(\text{Fe,Ni})_9\text{S}_8$.

extending from about 62 to 83 weight per cent Ni. As a result of the tie-line change mentioned above, a univariant field containing γFeNi (~ 60 weight per cent Ni) + FeNi_3 (~ 62 weight per cent Ni) + $(\text{Fe,Ni})_9\text{S}_8$ + V separates the γFeNi + $(\text{Fe,Ni})_9\text{S}_8$ + V and FeNi_3 (Ni varies from 62 to ~ 73 weight per cent) + $(\text{Fe,Ni})_9\text{S}_8$ + V divariant fields. The phases $(\text{Fe,Ni})_9\text{S}_8$ + Ni_3S_2 + FeNi_3 + V coexist in a large univariant field, and the divariant fields FeNi_3 (Ni varies from ~ 73 to 83 weight per cent) + Ni_3S_2 + V and γFeNi + Ni_3S_2 + V are separated by the narrow FeNi_3 (~ 83 weight per cent Ni) + γFeNi (~ 86 weight per cent Ni) + Ni_3S_2 + V univariant region.

The solid solutions of Ni and Fe in the $(\text{Fe,Ni})_{1-x}\text{S}$ and $(\text{Ni,Fe})_{1-x}\text{S}$ phases, respectively, decrease markedly in the 500° to 400°C temperature range. As noted in figure 74 the solubility gap has widened considerably, and the coexistence of FeS_2 and $(\text{Fe,Ni})_9\text{S}_8$ is now possible below 450°C . Coexistence of these phases is indicated by the $(\text{Fe,Ni})_9\text{S}_8$ + FeS_2 + V divariant field of figure 74. Two new univariant fields, $(\text{Fe,Ni})_9\text{S}_8$ + $(\text{Fe,Ni})_{1-x}\text{S}$ + FeS_2 + V and $(\text{Fe,Ni})_9\text{S}_8$ + $(\text{Ni,Fe})_{1-x}\text{S}$ + FeS_2 + V , and one new divariant field, $(\text{Ni,Fe})_{1-x}\text{S}$ + FeS_2 + V , exist at this temperature.

Interpretation of Natural Occurrences in Terms of Phase Diagrams

The phase relations illustrated in figures 65 through 74 are of fundamental importance to the interpretation and understanding of the occurrence of minerals and mineral assemblages of the iron-nickel-sulfur system whether these are disseminated in basic rocks, enriched in ore deposits, or distributed with the iron-nickel phases in various types of meteorites.

Disseminated iron-nickel sulfides in basic rocks may have crystallized from a magma, with the exception of pentlandite, which must have formed through reactions in the solid state between primary sul-

fides. Such sulfides may also have originated through reactions between certain silicates and sulfur introduced at a post- or late-magmatic stage. Reactions of this kind are discussed in a separate section.

The iron-nickel sulfide ore deposits of the Sudbury, Canada, type are generally considered magmatic in origin. The enrichment of such ores has been envisioned as a result of extensive liquid immiscibility between sulfides and silicates; because of the higher density of the sulfide liquid it segregated from the silicate magma through gravity settling.

The ore-bearing irruptive in typical areas such as Sudbury is thought of as having been intruded as a single body (Hawley, 1962). If the irruptive material originated in a magma chamber, and if sulfide-silicate immiscibility existed under the *PTX* conditions in the chamber, gravity settling of the sulfide liquid would already have taken place during magma generation. The irruptive would then be depleted in sulfides at the time of intrusion. For this reason, before intrusion and final emplacement of the irruptive, sulfide-silicate immiscibility cannot be called upon as a factor in the enrichment of such ores.

In general, liquid miscibility existing under the *PT* conditions in the magma chamber, followed by liquid immiscibility under the changed *PT* conditions existing after intrusion without accompanying change in magma composition, is not physically impossible but highly improbable.

It is known that, in the absence of sulfur, elements like iron, nickel, cobalt, and copper are present in rocks as silicates.

If one pictures a homogeneous magma initially containing these elements as silicates and then adds sulfur only after intrusion and emplacement, the silicate-sulfide immiscibility scheme may well prove valid. Sulfur may have been available during the later stages of volcanic activity. In such a scheme the introduction

of sulfur at a time when possibly only the core of the irruptive was still liquid must have been structurally controlled. Faults, fissures, breccia zones, etc., would serve as chutes for the sulfur gas. This sulfur would readily react with the solid silicates and extract iron, nickel, and copper to produce pyrrhotite, pentlandite, and chalcopyrite as described in a separate section of this report. The melting points of certain silicates are considerably lowered by sulfur and its reaction products. The introduction of sulfur at sufficiently high temperatures may then lead to the formation of immiscible silicate-sulfide liquids at temperatures well below those of melting of the pure silicates or sulfides.

The addition of large amounts of sulfur gas at very high temperatures to a source of iron and nickel such as a basic rock, some minerals of which can accommodate significant amounts of nickel in addition to iron, would produce a sulfide liquid in coexistence with excess sulfur. Because of the high iron-to-nickel ratio of such rocks, this liquid would in composition lie comparatively close to the Fe-S boundary of the ternary Fe-Ni-S system. At 1100°C it would contain about 47 weight per cent S for an Fe:Ni ratio of 17 and about 49 weight per cent S for a ratio equal to 4 (see fig. 65). Liquid immiscibility exists on cooling down to only about 1065°C even when the Fe:Ni ratio is as low as 4. Below this temperature but above 743°C the bulk composition in question is accounted for by the two condensed phases, monosulfide solid solution and liquid sulfur. In the 743° to 729°C temperature range, depending on the Fe:Ni ratio, pyrite appears, and, with excess sulfur, pyrite, vaesite $(\text{Ni,Fe})\text{S}_2$, and sulfur are the stable phases down to 137°C, where bravoite comes in on the FeS_2 - NiS_2 join. The final equilibrium assemblage after cooling to room temperature would be pyrite, bravoite, and sulfur, which is not a typical assemblage in basic rocks.

The introduction of limited amounts of sulfur gas may first lead to the formation

of two immiscible sulfide liquids, one containing slightly more than 50 weight per cent Fe + Ni (51 to 53 weight per cent) and the other containing at least 98 weight per cent S. The second liquid will continue to react with the silicates and produce additional metal-rich liquid until it is depleted. The metal-rich liquid may react with the silicates, and thus more of the metals of the latter phase may be converted into sulfides, or a liquid immiscibility region may exist between the silicates and the metal-rich sulfide phase. The metal-rich liquid exists only above 1065°C (see above). Below this temperature monosulfide solid solution and sulfur-rich liquid appear instead. This liquid, until its depletion, reacts with the silicates to form monosulfide solid solution containing the maximum amount (~ 43 weight per cent) of sulfur. During continued cooling the solubility of sulfur in the monosulfide phase decreases; this sulfur reacts with the silicates. Although the details are not known, present evidence indicates that metal-deficient (or sulfur-rich) monosulfide solid solution reacts with certain silicates such as olivine. The result of the reaction is a monosulfide containing about 37 weight per cent S and probably 2 to 5 per cent Ni.

On further cooling, the monosulfide solid solution narrows, and two phases, $(\text{Fe,Ni})_{1-x}\text{S}$ (containing gradually diminishing amounts of Ni) and $(\text{Ni,Fe})_{3\pm x}\text{S}_2$, occur together to account for the bulk composition *P*, which at higher temperatures was situated inside the monosulfide solid solution field. This situation is shown in figure 69. The tie lines running through bulk composition *P* at 650°C show coexisting $(\text{Fe,Ni})_{1-x}\text{S}$, with about 1.0 to 1.5 weight per cent Ni and about 38 weight per cent S, and $(\text{Fe,Ni})_{3\pm x}\text{S}_2$ with about 25.5 weight per cent S.

At 610°C the $(\text{Fe,Ni})_{1-x}\text{S}$ (pyrrhotite) phase reacts with the high-temperature nonquenchable $(\text{Fe,Ni})_{3\pm x}\text{S}_2$ phase to form $(\text{Fe,Ni})_9\text{S}_8$ (pentlandite) under the experimental conditions existing in rigid silica tubes. Because the bulk composition

P lies between pentlandite and the Fe-S boundary, the stable phases are now pyrrhotite and pentlandite, as demonstrated in figure 70. The pyrrhotite still contains about 1.0 to 1.5 weight per cent Ni and appears to have the formula $(\text{Fe,Ni})_{0.94 \pm 0.01}\text{S}$.

Pentlandite formed at 610°C evidently has stoichiometric, or nearly stoichiometric, composition (Fe 32.55, Ni 34.22, S 33.23, all in weight per cent); at lower temperatures it forms limited solid solution toward both the Fe-S and Ni-S boundaries. Its metal-to-sulfur ratio shows very little variation. Its maximum metal-to-sulfur ratio appears to be reached at about 580°C, where pentlandite on cooling becomes stable with γFeNi alloy as shown in figure 71.

On further cooling of the pyrrhotite-pentlandite assemblage, the pyrrhotite solid solution decreases in width somewhat, resulting in exsolution of pentlandite from pyrrhotite. The remaining pyrrhotite due to exsolution of pentlandite contains less nickel and more sulfur than the original pyrrhotite. The temperature of maximum solubility of pyrrhotite in pentlandite has not been accurately determined but is believed to lie at about 580°C. Below this temperature some pyrrhotite will exsolve from pentlandite during continued cooling. Such exsolution textures are frequently observed in pentlandite-pyrrhotite ores.

Pyrite and pentlandite have often been observed as a mineral pair in certain parts of such ores. At temperatures below 500°C, where the solid solution between Fe_{1-x}S and Ni_{1-x}S is incomplete, pyrite and pentlandite may become a stable assemblage as seen from figure 74. Experiments with mixtures of synthetic pyrite and pentlandite produce $(\text{Fe,Ni})_{1-x}\text{S}$ solid solution at 450°C. The coexistence of pyrite and pentlandite in ores, therefore, probably represents equilibrium conditions that are possible only below 450°C and that are attained through equilibration of phases deposited at higher temperatures.

The Ni_7S_6 phase, which is stable below 573°C (Kullerud and Yund, 1962) in the presence of vapor, has not been observed in nature. As noted from figure 72 the tie lines between $(\text{Ni,Fe})_{1-x}\text{S}$ and Ni_3S_2 prohibit coexistence of Ni_7S_6 with ternary compounds. Most natural occurrences contain significantly more Fe than Ni, and therefore Ni_7S_6 in such localities cannot exist under equilibrium conditions. The mineral equivalent of Ni_7S_6 should be sought in localities virtually free of iron and other elements that can exert the same effect as iron and on which the Ni:S ratio lies between 3:2 and 1:1.

The FeNi_3 phase, awaruite, which on cooling becomes stable at 503°C in the presence of vapor, is a rather rare mineral. It occurs usually with heazlewoodite, Ni_3S_2 . Figures 73 and 74 show the two minerals in coexistence. In some localities awaruite occurs with pentlandite, and figure 74 demonstrates the coexistence of pentlandite and awaruite at 400°C. Presumably they are also stable together at lower temperatures, and so is the awaruite, pentlandite, heazlewoodite assemblage.

Recently pentlandite has been reported as a phase in stony meteorites (Sztrokay, 1960; Ramdohr and Kullerud, *Year Book 60*), and it is usually associated with troilite. It occurs in meteorites that have a relatively high sulfur-to-metal ratio, in other words where the FeNi phase is either absent or present in very small amounts. Sztrokay (1960) observed thick exsolution lamellae of troilite from pentlandite in the Kaba meteorite. This particular type of texture has not been observed in terrestrial materials. Exsolution of small grains of pentlandite from troilite is common in many meteorites.

The phase diagrams presented above indicate that troilite and pentlandite in the presence of vapor form a stable mineral pair below 610°C. The troilite, pentlandite, γFeNi , and vapor assemblage is stable only below about 580°C. These diagrams also show that γFeNi , if it is to coexist with pentlandite alone or with

pentlandite as well as troilite, must contain well over 40 weight per cent Ni. Such a high nickel concentration is not common in meteorites and may explain the scarcity of the pentlandite- γ FeNi assemblage. The diagram of figure 73, for instance, shows that, through a scheme of sulfur addition to FeNi alloys situated on the iron side of the Fe-Ni boundary, the γ phase will react with sulfur to produce FeS, during which process the γ FeNi phase becomes gradually richer in nickel, until the bulk composition is situated in the γ FeNi + FeS + (Fe,Ni)₉S₈ + V univariant field.

Although the pentlandite phase in many stony meteorites is produced by weathering after arrival on earth, textures testify that pentlandite must have existed in numerous meteorites long before their fall. The temperatures existing at the time of the extraterrestrial formation of this mineral are commonly regarded as considerably higher than 610°C, the temperature of breakdown of pentlandite in the presence of vapor. Evidence is found in many meteorites of pentlandite as an exsolution product and in one polished section together with pyrite as a product of cooling of originally homogeneous nickel-rich monosulfide solid solution (see figs. 72 and 74). However, textural features observed in polished sections indicate that pentlandite is a primary phase in many meteorites. Evidence has not been found to suggest that pentlandite formed during cooling through reactions between troilite and (Ni,Fe)_{3±x}S₂.

Meteorites are believed to have been exposed to considerable pressures, which as a rule do not greatly influence mineral stabilities. Apparently pentlandite, however, represents an exception to this rule. When heated from room temperature it shows a considerable expansion in its cell dimensions, which implies that pressure may strongly affect its breakdown temperature. Preliminary experiments designed to determine the breakdown temperature at various confining pressures show that this effect may be of the order

of 35°C per 1000 bars. Thus at confining pressures of 10,000 bars pentlandite may be stable even at 1000°C.

The pressure-temperature relations of pentlandite breakdown may serve as a very useful tool when temperature of formation of associated minerals can be derived through applications of independent geothermometers. The stability curve of pentlandite will then delineate the minimum pressure required to maintain pentlandite as a phase at the indicated temperature.

THE Cu-Ni-S SYSTEM

G. Moh and G. Kullerud

The phase relations at 600°C were reported in *Year Book 61*. During this past year more detailed studies have been carried out at 600°C, and the phase relations are now well known also at 500° and 400°C. In addition, the 300°C isotherm is nearly completed, and considerable information has been obtained on the melting relations at temperatures above 600°C.

The liquid immiscibility fields, which exist above 813°C and from 25.5 to more than 95 weight per cent S (Kullerud, *Year Book 59*) in the Cu-S system, and above 991°C and from 54.5 to more than 97.6 weight per cent S in the Ni-S system (Kullerud and Yund, 1962), extend across the ternary system. Liquid immiscibility in part of the ternary system occurs at lower temperatures than in the bounding systems. Thus, in mixtures containing equal amounts of Cu and Ni, liquid immiscibility exists above 780°C and over a region extending from about 52 to more than 95 weight per cent S. The curve relating the temperature of appearance of liquid immiscibility to the Cu:Ni ratio seems to pass through a minimum at 770°C and Cu:Ni \sim 2:1.

Information on phase relations at 600°C additional to that given in last year's report is presented in figure 75. A small liquid region is noted to exist at

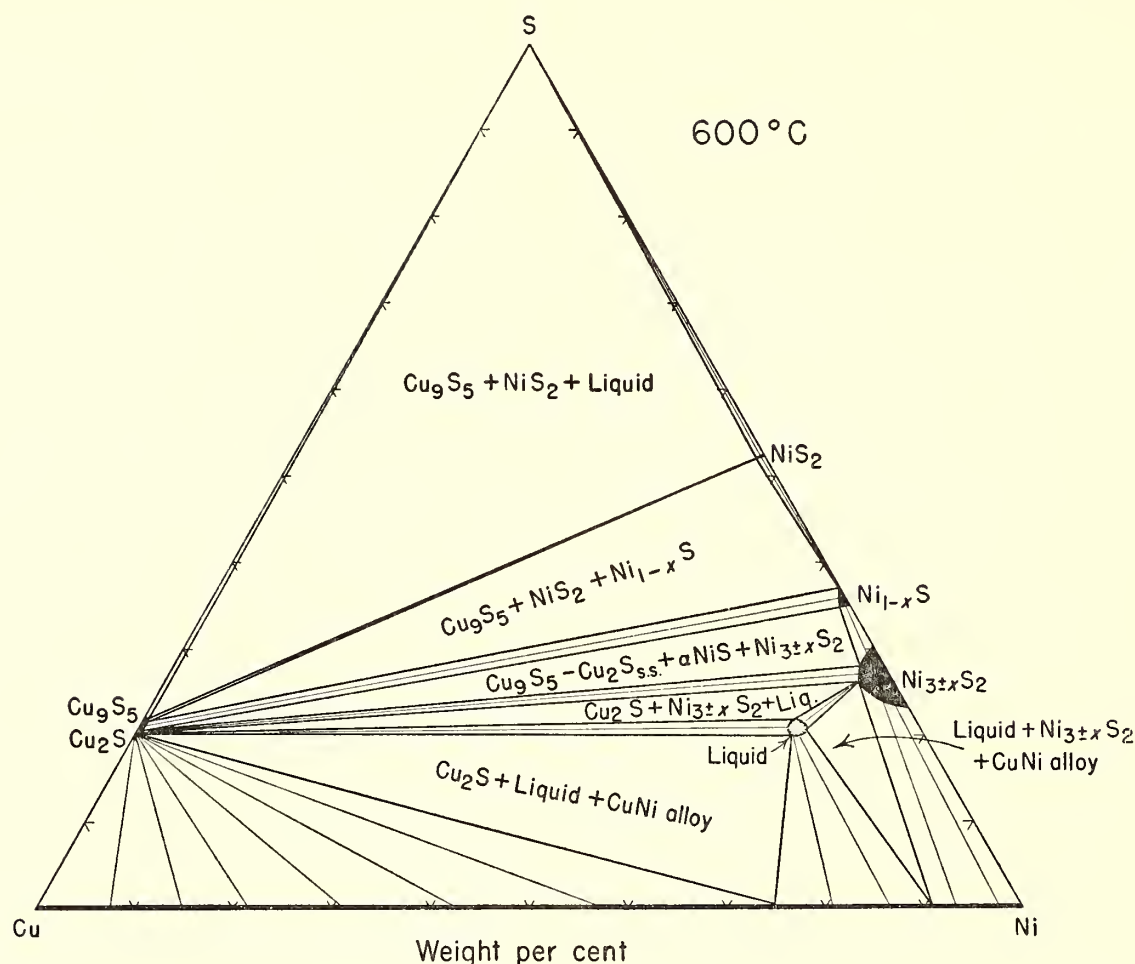


Fig. 75. Phase relations in the Cu-Ni-S system at 600°C. There are no stable ternary phases at this temperature.

600°C in the Ni-rich part of the system. Liquid of this phase can coexist in equilibrium with either of the three Cu_2S , CuNi alloy, and $\text{Ni}_{3\pm x}\text{S}_2$ phases as shown by the divariant regions $L + \text{CuNi} + V$, $L + \text{Cu}_2\text{S} + V$, $L + \text{Ni}_{3\pm x}\text{S}_2 + V$, and the univariant fields $\text{Ni}_{3\pm x}\text{S}_2 + \text{CuNi} + L + V$, $\text{CuNi} + \text{Cu}_2\text{S} + L + V$, and $\text{Cu}_2\text{S} + \text{Ni}_{3\pm x}\text{S}_2 + L + V$. CuNi alloy ranging in composition from pure Cu to 75 ± 1 per cent Ni coexists with Cu_2S . The alloy coexisting with liquid ranges in composition from 75 to 91 weight per cent Ni, and that coexisting with the $\text{Ni}_{3\pm x}\text{S}_2$ phase contains from 0 to 9 weight per cent Cu. The solubility of S in this alloy is less than can be measured by our experimental methods.

At temperatures below the isotherm of figure 75 a ternary eutectic exists at $572^\circ \pm 5^\circ\text{C}$ and at a composition of about 12 weight per cent Cu, 67 weight per cent Ni, and 21 weight per cent S.

The $\text{Ni}_{3\pm x}\text{S}_2$ phase, which at 600°C

contains 3.5 weight per cent Cu, becomes unstable at about 520°C. Below this temperature the heazlewoodite (Ni_3S_2) phase is stable.

At 573°C the Ni_7S_6 phase appears on the Ni-S boundary, and at 507°C CuS (covellite) becomes stable on the Cu-S bounding join. The phase relations existing at 500°C are shown in figure 76. At this temperature a cubic $Pa\bar{3}$ type ternary phase, which has a metal-to-sulfur ratio of 1:2, is stable. Several per cent solid solution exists from CuNi_2S_6 composition toward the vaesite (NiS_2) phase as well as toward the Cu-S join. At this temperature the vaesite phase can take into solid solution a significant amount of copper, which substitutes for nickel in the cubic NiS_2 structure. This compound remains stoichiometric, or nearly stoichiometric, and at 500°C can take a maximum of 2.7 ± 0.2 weight per cent Cu into solid solution. Tie lines connect digenite (Cu_9S_5) containing 0.3 weight per cent

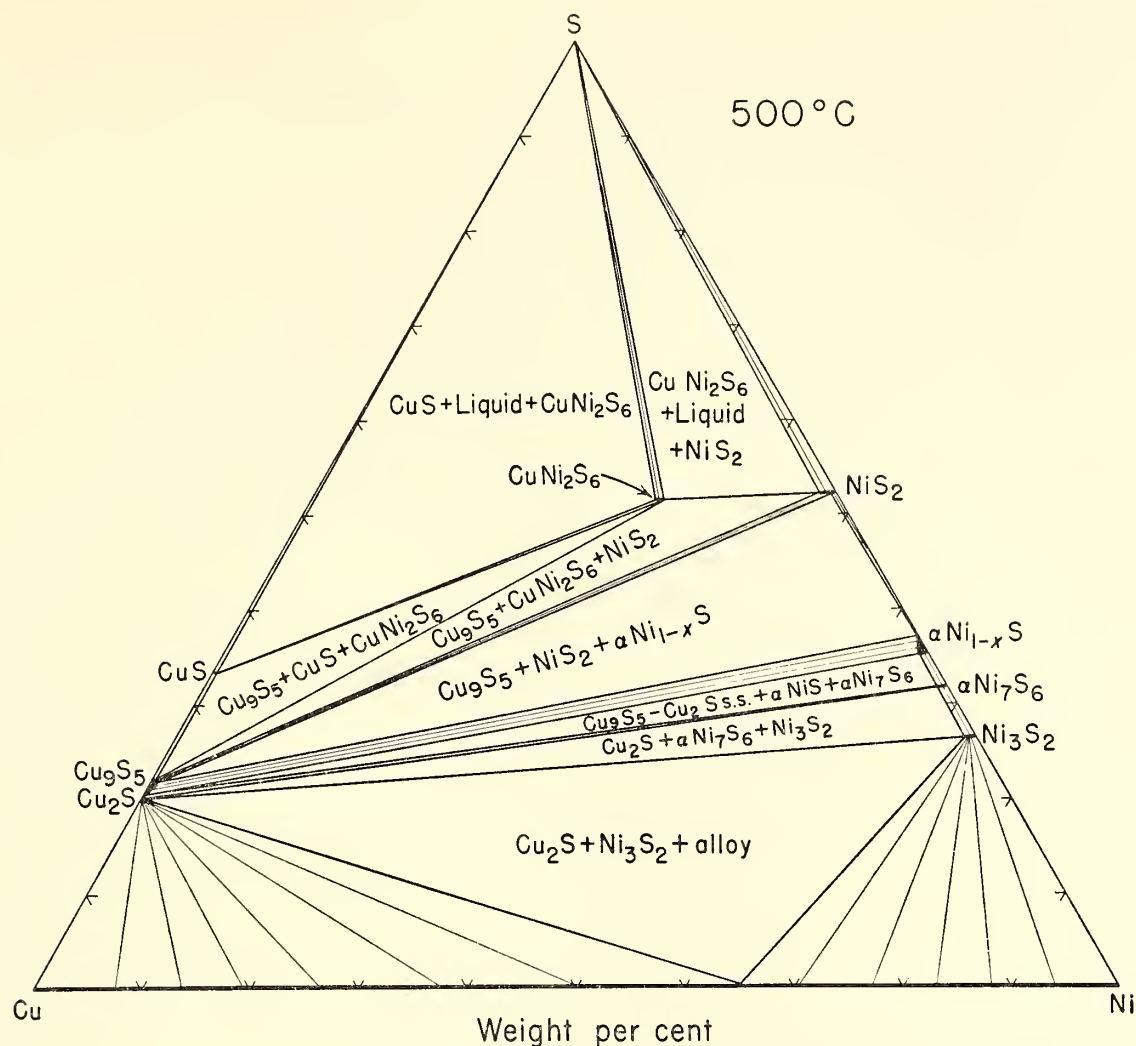


Fig. 76. At 500°C the ternary phase CuNi_2S_6 is stable. It forms limited solid solution toward both the Ni-S and Cu-S boundaries but remains essentially stoichiometric.

Ni in solid solution with vaesite containing from 0.5 to 2.7 weight per cent Cu as demonstrated in figure 76.

Stoichiometric αNiS containing about 0.8 weight per cent Cu coexists with digenite-chalcocite solid solution, which contains about 0.3 weight per cent Ni. At this temperature, 1.0 weight per cent Cu goes in solid solution in $\alpha\text{Ni}_7\text{S}_6$ and tie lines exist between this phase and the digenite-chalcocite solid solution. Ni_3S_2 in equilibrium with Cu_2S contains 0.8 weight per cent Cu, and the Cu_2S phase contains ~ 0.2 weight per cent Ni.

At temperatures below 500°C the Cu_9S_5 - Cu_2S solid solution becomes incomplete at $430^\circ \pm 10^\circ\text{C}$, and $\alpha\text{Ni}_7\text{S}_6$ inverts to $\beta\text{Ni}_7\text{S}_6$ at 400°C. As noted in figure 77, which shows the phase relations at 400°C, the solid solutions extending from the binary joins into the ternary

system are much more limited than at 500°C.

The tie-line relations have also been investigated at 300°C, although the limits of solid solution in the various phases have not been determined accurately as yet. The major changes taking place on lowering the temperature from 400° to 300°C are: stoichiometric αNiS inverts to βNiS at 379°C, but the most Ni-deficient Ni_{1-x}S is stable to 282°C, and Ni_3S_4 (polydymite) becomes stable at 356°C. It is noted from figure 78 that $\alpha\text{Ni}_{1-x}\text{S}$ at this temperature cannot coexist with any of the copper sulfides because of tie lines connecting polydymite and βNiS (millerite). The solubility of Cu in $\alpha\text{Ni}_{1-x}\text{S}$ at this temperature is less than 0.1 and probably less than 0.02 weight per cent. Millerite is stable with digenite and chalcocite.

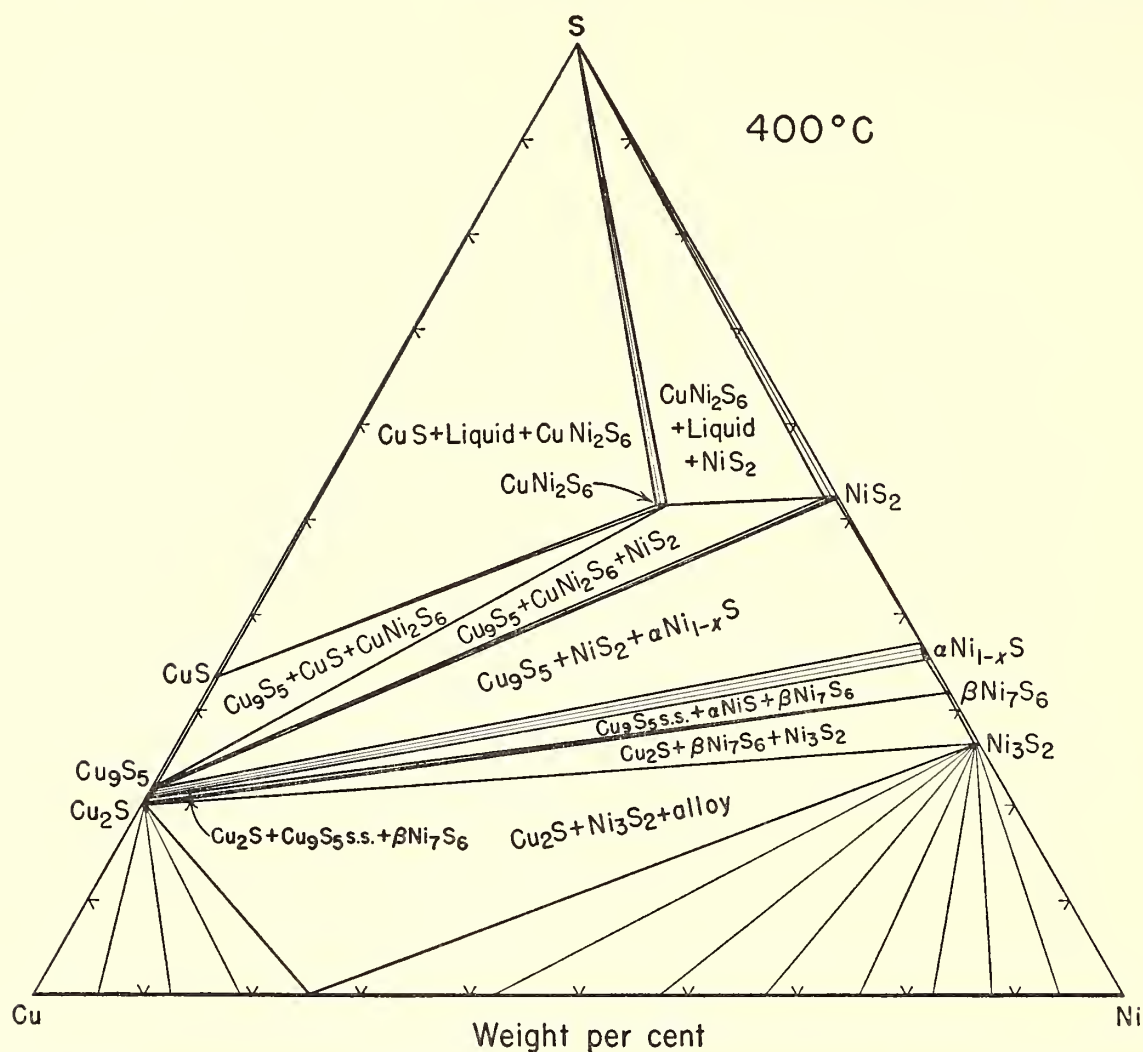


Fig. 77. The phase relations at 400°C are essentially the same as at 500°C and are characterized by a general lack of extensive solid solution fields.

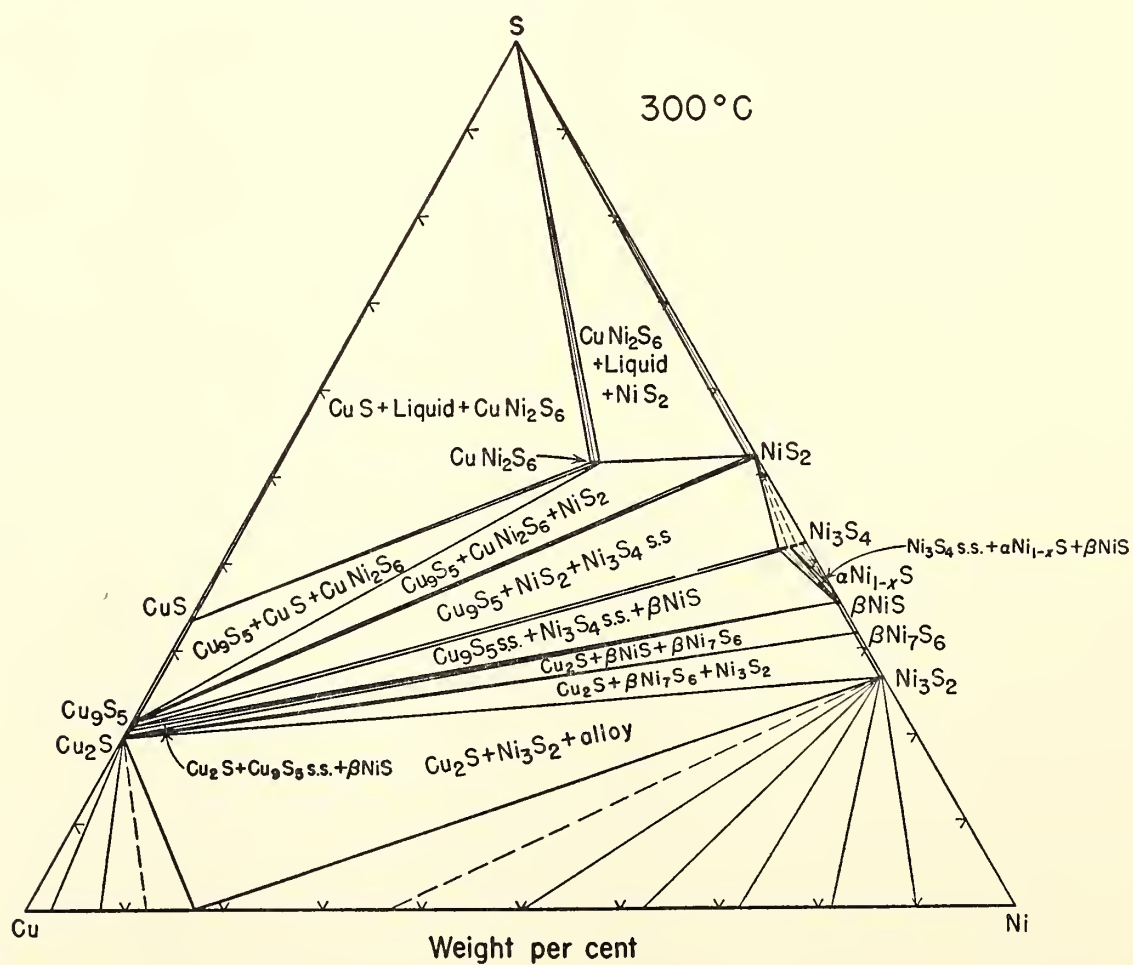


Fig. 78. At 300°C the Ni_3S_4 (polydymite) and βNiS (millerite) phases are stable. The extents of solid solution of Cu_9S_5 and Cu_2S in Ni_3S_4 have not been determined accurately.

THE Cu-Fe-S SYSTEM

P. R. Brett

The Join $\text{Cu}_{9.2}\text{S}_5\text{-Cu}_5\text{FeS}_4$

The join $\text{Cu}_9\text{S}_5\text{-Cu}_5\text{FeS}_4$ was described by Kullerud in *Year Book 59*. The present study was undertaken to observe the change in equilibrium relations resulting from a slight variation from Kullerud's compositions. Experimental methods and the identification of many of the reaction products have been described by Kullerud (*Year Book 59*).

The results of the present study are shown in figure 79. Cu_5FeS_4 on cooling inverts from cubic to tetragonal symmetry at 228°C (Morimoto and Kullerud, 1961). Stoichiometric Cu_9S_5 inverts from the cubic high-temperature form to the cubic low-temperature form at $73^\circ \pm 3^\circ\text{C}$ (Morimoto and Kullerud, 1963).

Figure 79 is similar to Kullerud's solvus curve (*Year Book 59*). The cubic-to-tetragonal inversion of bornite solid solution is lower than 205°C , determined by Kullerud. The solid solubility of

bornite in digenite in the present study may be greater by some 10 mole per cent; also the solid solubility of digenite in bornite is slightly less than that determined by Kullerud. In figure 79 the solvus crest is at least 30°C lower than that given by Kullerud, and the miscibility gap was found to be narrower on the $\text{Cu}_{9.2}\text{S}_5\text{-Cu}_5\text{FeS}_4$ join than on the $\text{Cu}_9\text{S}_5\text{-Cu}_5\text{FeS}_4$ join.

Figure 79 represents a pseudobinary projection. At 50°C , djurleite ($\text{Cu}_{1.96}\text{S}$) (Morimoto, 1962; Roseboom, 1962) was obtained in copper-rich runs. Djurleite occurs with digenite in the most copper-rich runs and with bornite and digenite in runs nearer bornite in composition.

The presence of chalcopyrite in two runs that lie close to bornite in composition may be explained by a weighing uncertainty of less than 0.01 mg, so that the compositions lie in the field cp-bn-dg.

The steepness of the solvus on the bornite side suggests that ores consisting predominantly of bornite, but with greater than 5 mole per cent exsolved digenite, were formed above 250°C .

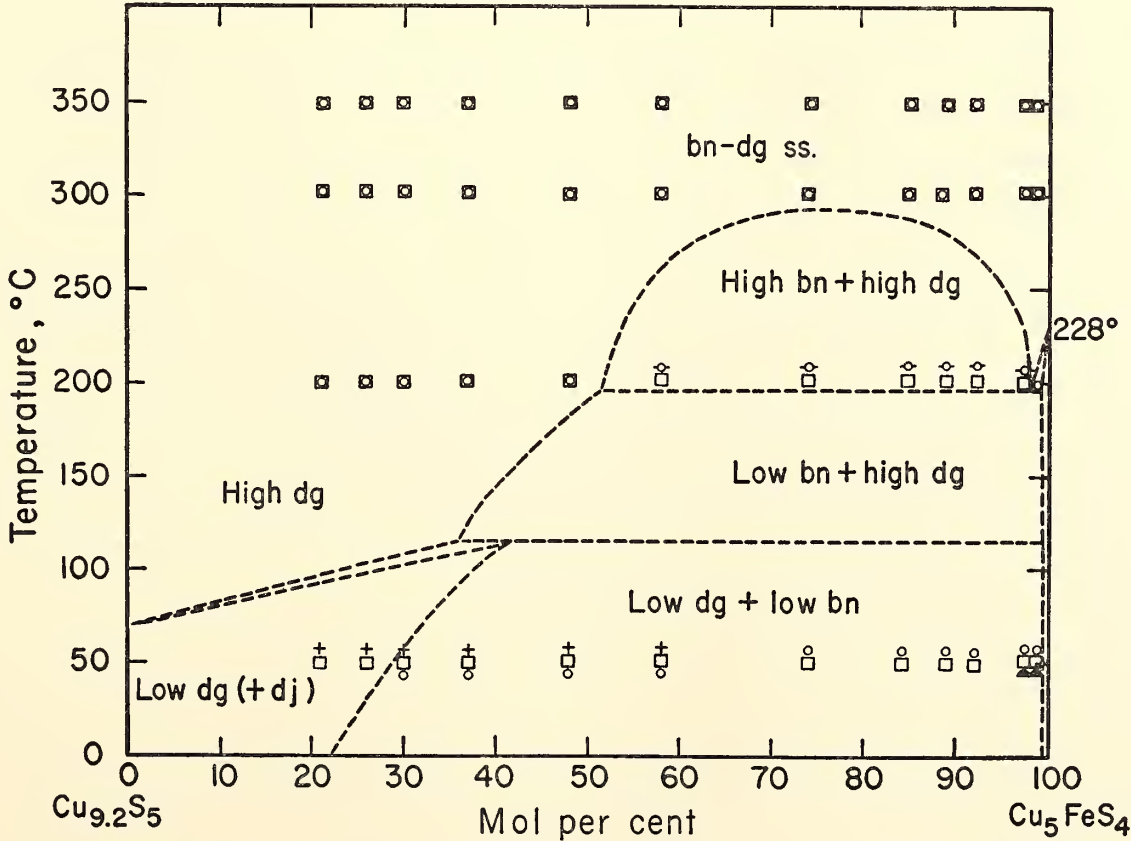


Fig. 79. Stable phases on the join $\text{Cu}_5\text{FeS}_4\text{-Cu}_{9.2}\text{S}_5$.

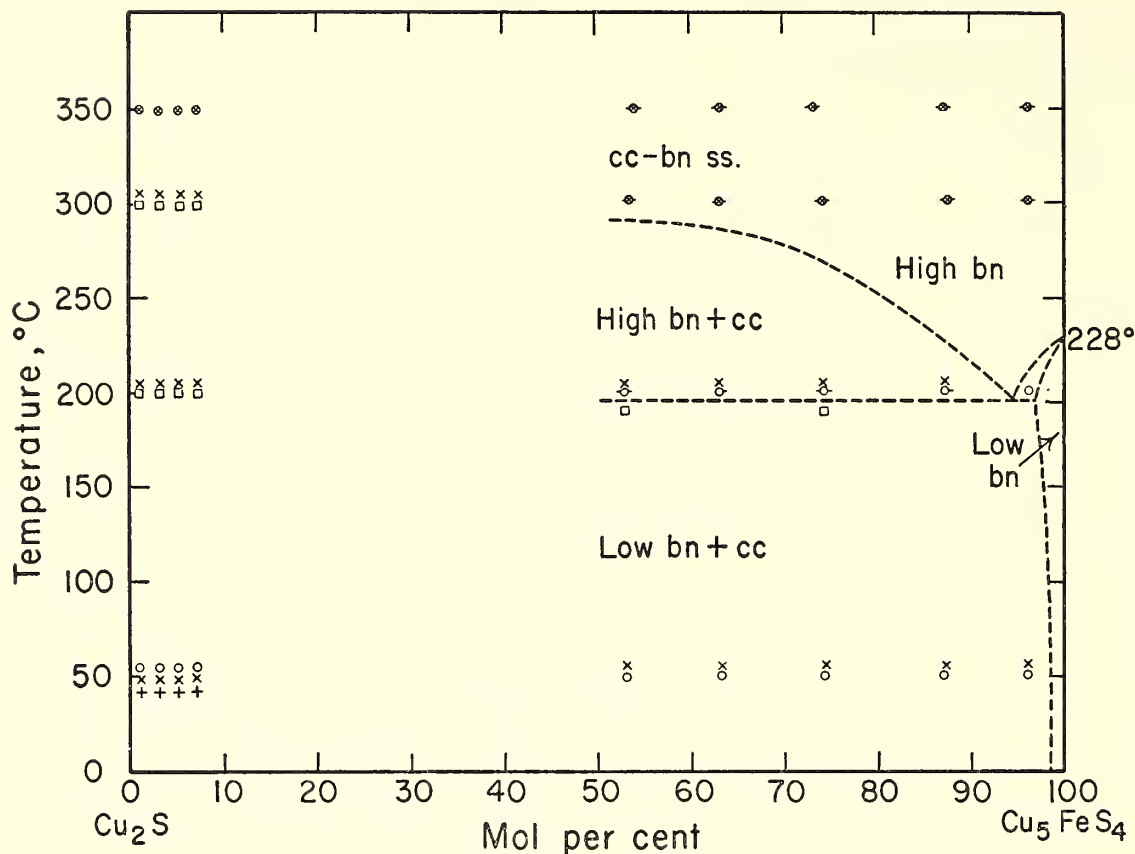


Fig. 80. Stable phases on the join $\text{Cu}_5\text{FeS}_4\text{-Cu}_2\text{S}$.

The Join $\text{Cu}_5\text{FeS}_4\text{-Cu}_2\text{S}$

The results of experiments designed to determine the phase relations on this join are compiled in figure 80, which is pseudobinary owing to the presence of digenite and djurleite in some runs.

The cubic-to-tetragonal inversion temperature of bornite when in equilibrium with chalcocite lies below 200°C . This temperature is significantly lower than the 228°C value established for the inversion of pure bornite by Morimoto and Kullerud (1961).

Djurleite was present as a stable phase in some runs annealed at 50°C but not in runs at 200°C or above.

Digenite and chalcocite were present in chalcocite-rich runs quenched from 300° and 200°C . Digenite, bornite, and chalcocite were present in two runs quenched from 200°C , and the presence of this three-phase assemblage is suspected in other runs at this temperature. The existence of $\text{cc} + \text{dg}$ and $\text{cc} + \text{dg} + \text{bn}$ as stable assemblages indicates phase relations as shown in figure 81 in this portion of the Cu-Fe-S

system at about 200°C . This figure indicates that $\text{cc ss} + \text{dg ss}$ are stable exsolution products for all compositions along the join from the cc ss boundary to the point X, the position of which is dependent on temperature. From X to the bn ss field, all compositions along the join lie in the three-phase region $\text{cc ss} + \text{dg ss} + \text{bn ss}$. At lower temperatures the solid solution fields shrink so that

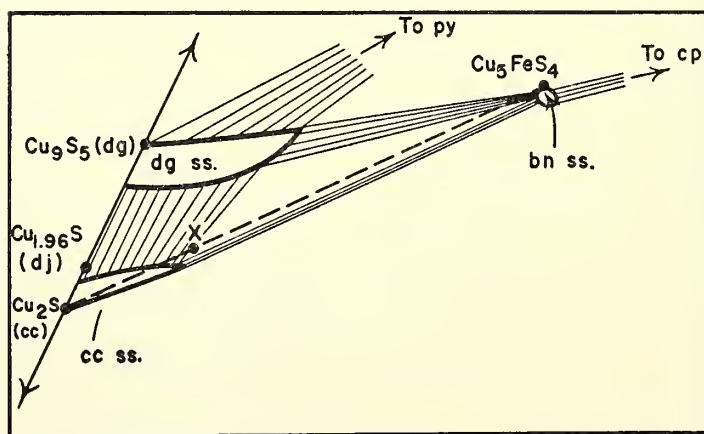


Fig. 81. Schematic diagram of the phase relations in the bornite-chalcocite-digenite region at about 200°C . The dashed line marks the $\text{Cu}_5\text{FeS}_4\text{-Cu}_2\text{S}$ join. X marks the composition under discussion. dj marks the position of djurleite, which is stable below approximately 155°C (Kullerud, in preparation).

only bn + cc exsolve from bornite-chalcocite solid solutions, except for compositions near chalcocite, from which djurleite is exsolved as an additional phase.

The ternary nature of the bornite-chalcocite join prohibits the use of cell dimensions as a means of determining composition. Also the positions and intensities of chalcocite X-ray diffraction reflections vary greatly with slight changes in composition, complicating measurements of one peak or even a series of peaks (over a range of compositions).

The steepness of the solvus on the bornite side suggests that ores consisting predominantly of bornite but with greater than 5 mole per cent exsolved chalcocite were formed above 200°C.

The Join $\text{Cu}_5\text{FeS}_4\text{-CuFeS}_{2-x}$

The results of experiments along this join are compiled in figure 82. Owing to the presence of digenite in some runs, the join is pseudobinary only.

The inversion temperature of bornite solid solution of composition lying on the

solvus was determined as $200^\circ \pm 5^\circ\text{C}$.

At 50°C a phase in addition to bornite and chalcopyrite was obtained in all runs. This third phase was observed also in two runs quenched from 200°C; under the microscope it resembles chalcocite and digenite. The amount obtained in each experiment was insufficient for identification by X-ray diffraction.

R. A. Yund (personal communication) and the writer have shown independently that bornite solid solution at 700°C can take up to 0.8 weight per cent more sulfur in solid solution than the stoichiometric Cu_5FeS_4 formula indicates. The present study was made at 700°C, and in each experiment an excess of sulfur was added. On cooling, the bornite became less sulfur rich, so that at 200°C runs lay in the three-phase field bn-cp-dg suggested by McKinstry (1959).

The writer suggested in last year's report that tie lines existed between chalcopyrite and chalcocite. It was at that time not known that bornite synthesized at 700°C can contain more sulfur than is indicated by the formula for stoichiometric Cu_5FeS_4 . The present

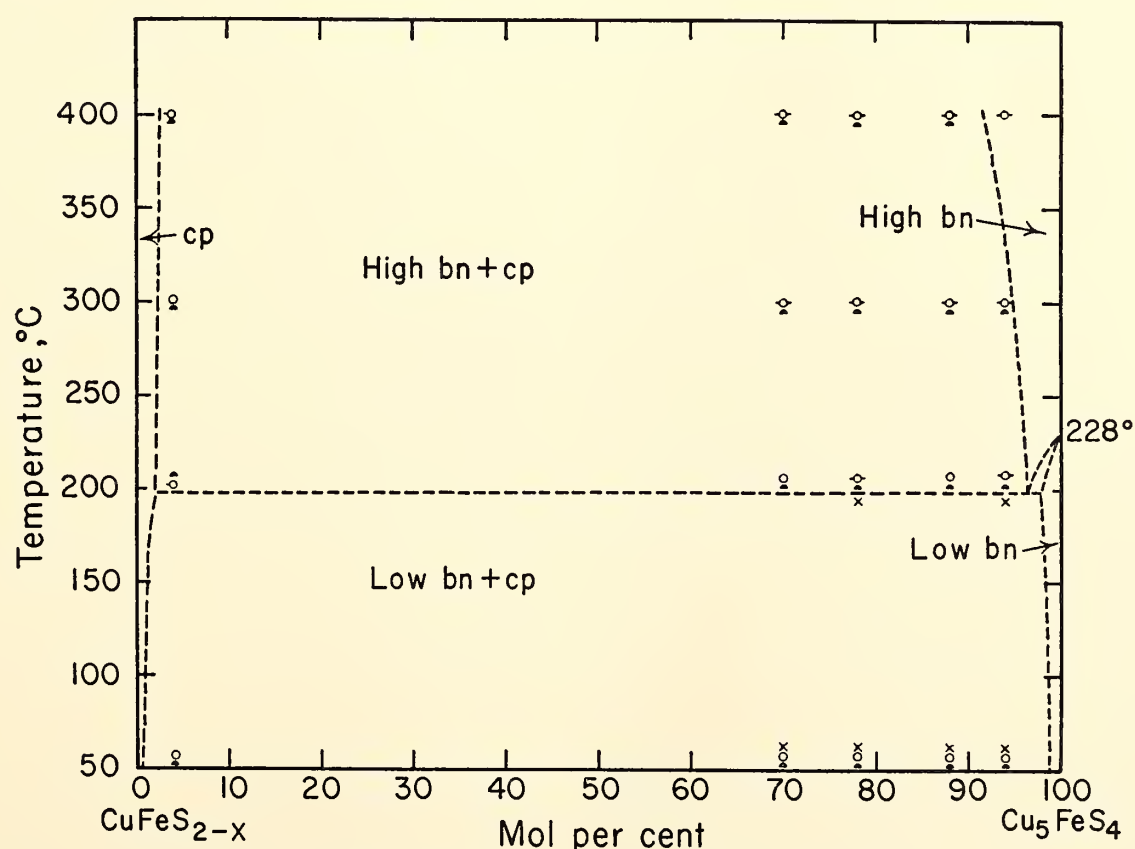


Fig. 82. Stable phases on the join $\text{Cu}_5\text{FeS}_4\text{-CuFeS}_{2-x}$.

work invalidates the existence of the cp-cc tie line.

The steepness of the solvus curves on both the chalcopyrite and bornite sides of figure 82 suggests that ores consisting predominantly of bornite but with greater than 8 mole per cent exsolved chalcopyrite, or vice versa, were deposited above 400°C.

THE Fe-Pb-S SYSTEM

P. R. Brett and G. Kullerud

The iron sulfides pyrite or marcasite and pyrrhotite occur in association with galena (PbS) at thousands of localities and under a considerable range of geological conditions. The immediate purpose of the present investigation was to delineate the stability range of the Fe_{1-x}S - FeS_2 -PbS assemblage and to determine whether the Fe_{1-x}S - FeS_2 geothermometer generally can be applied also in the presence of PbS.

The phase relations at 700°C are shown in figure 83. The univariant assemblages are PbS + FeS_2 + liquid S + V, PbS + FeS_2 + Fe_{1-x}S + V, PbS + Fe_{1-x}S + liquid Pb + V, and Fe_{1-x}S + liquid Pb

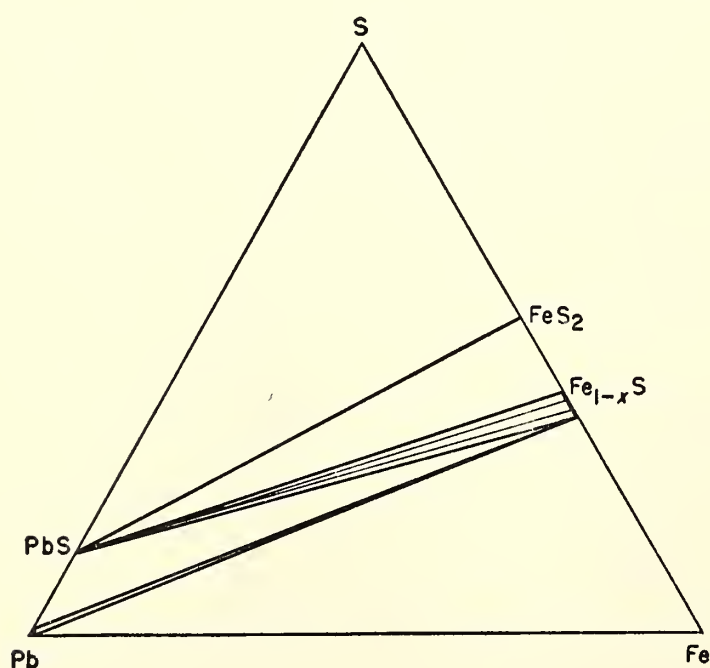


Fig. 83. Phase relations in the Fe-Pb-S system at 700°C. The diagram remains essentially unchanged down to about 300°C except for a gradual decrease in the Fe_{1-x}S (pyrrhotite) solid solution along the Fe-S boundary.

+ Fe + V. Pyrite and galena are essentially stoichiometric compounds, and the $\text{PbS} + \text{FeS}_2 + \text{V}$ divariant region, therefore, is very narrow. Determination of the cell dimensions of pyrite heated at 700°C with excess galena for 3 months shows $a = 5.419 \pm 0.003 \text{ \AA}$. This value is identical with that given by Kullerud and Yoder (1959) for pure pyrite. Measurements on galena from the same experiments give $a = 5.932 \pm 0.002 \text{ \AA}$, differing slightly from the value of 5.9362 \AA determined on pure PbS by Swanson and Fuyat (1953). Assuming that the a values would be affected measurably if significant amounts of solid solution existed between PbS and FeS_2 , it can be concluded that very little, if any, PbS is soluble in FeS_2 and that only small amounts, if any, of FeS_2 can dissolve in PbS at 700°C. The cell edges of pyrite and galena from the equilibrium assemblage pyrite + galena + pyrrhotite were found identical with those determined on pyrite and galena from assemblages containing these two phases only (see above). Pyrrhotites of various quenchable compositions were heated with galena, and measurements were made of d_{102} of pyrrhotite and of d_{220} of galena. Comparisons of the original d_{102} values measured on individual pyrrhotites with those obtained after heating with PbS showed that, within the limits of errors of measurement, the presence of galena does not alter the d_{102} of pyrrhotite. This indicates very limited solubility of PbS in pyrrhotite. Quenching experiments with mixtures of galena and pyrrhotite demonstrate that the solubility of PbS in Fe_{1-x}S is less than 0.5 weight per cent at 700°C. The PbS from all experiments in which it was heated with Fe_{1-x}S always has $a = 5.932 \pm 0.002 \text{ \AA}$, which indicates very limited solubility of pyrrhotite in galena.

Stoichiometric FeS was heated with Pb in a series of experiments. The presence of metallic lead did not change the FeS d_{102} value. These experiments indicated the presence of tie lines between

Pb and FeS. Heating at 700°C of mixtures of PbS and Fe produced the assemblages PbS + Pb + FeS, Pb + Fe + FeS, and Pb + FeS, depending on the PbS:Fe ratio of the starting materials. Thus Pb and FeS coexist stably at this temperature.

The field of liquid Pb is very small. Even at 700°C it contains less than 1 weight per cent S and less than 0.25 weight per cent Fe.

By quenching runs the PbS-FeS₂ tie line was found to break at $717^\circ \pm 4^\circ\text{C}$. Above this temperature tie lines exist between liquid and Fe_{1-x}S. In DTA experiments on mixtures of PbS and FeS₂ and an excess of sulfur a strong thermal effect was recorded at $715^\circ \pm 5^\circ\text{C}$ during both heating and cooling. Thus invariant conditions involving the five phases PbS, Fe_{1-x}S, FeS₂, *L*, and *V* exist at about 717°C. In the presence of vapor this is the highest temperature at which galena and pyrite can coexist.

Pyrite melts incongruently at 743°C in the pure Fe-S system. The appearance of tie lines in the ternary system between liquid sulfur and pyrrhotite at 717°C, therefore, implies a solubility of PbS in liquid S or in Fe_{1-x}S or both. The solubility of lead in liquid S is not known at 700°C, but from analogy with other metal-sulfur systems it is believed to be less than 1 weight per cent. The solubility of lead in Fe_{1-x}S was found to be less than 0.5 weight per cent at 700°C but may approximate this value at the invariant point.

Below 700°C the phase relations remain essentially as shown in figure 83. The Fe_{1-x}S solid solution field decreases in width with decreasing temperature as determined by Arnold (1962), and pure Pb solidifies at 327°C.

SULFIDE SYSTEMS CONTAINING Sn

G. Moh

In the past, tin has been obtained almost exclusively from cassiterite (SnO₂) deposits. Such deposits are dwindling in

many countries, however, and other sources of this metal must be sought. Tin occurs in many sulfide ores in the form of relatively pure tin sulfides or incorporated with a number of other metals in more complex sulfides. The economic importance of tin from such sources has not been adequately explored; in the USSR some deposits of this type are actually being mined.

The compositions and phase relations of the minerals in such deposits are largely unknown. The minerals are commonly referred to as "stannites" of various compositions (Moh and Ottemann, 1962; Ramdohr, 1944; Ramdohr, 1960). Stannites occur under widely differing geological conditions, which in hydrothermal deposits range from very high to very low temperatures, and are also found in pegmatitic-pneumatolitic type deposits.

To provide more information on sulfides of tin we have begun investigations in the system Cu-Fe-Sn-S. This has been supplemented by an examination of natural ore specimens, which resulted in the discovery of two new minerals of composition Sn₂S₃ and SnS₂.

The Sn-S System

The Sn-S system was studied by Albers and co-workers (Albers, Haas, Vink, and Wasscher, 1961; Albers and Schol, 1961). Their results and those obtained in the present investigation are incorporated in figure 84.

SnS, which has a natural equivalent in the mineral herzenbergite, is orthorhombic. It is a nearly stoichiometric phase that even at 740°C takes less than 1 weight per cent S into solid solution beyond the amount prescribed by the SnS formula.

Sn₂S₃, which is orthorhombic (Mosburg, Ross, Bethke, and Toulmin, 1961), melts incongruently at 758°C to liquid and αSnS₂. DTA experiments on Sn₂S₃ give a thermal effect at $732^\circ \pm 2^\circ\text{C}$ both on heating and cooling, indicating the possible existence of a high-tempera-

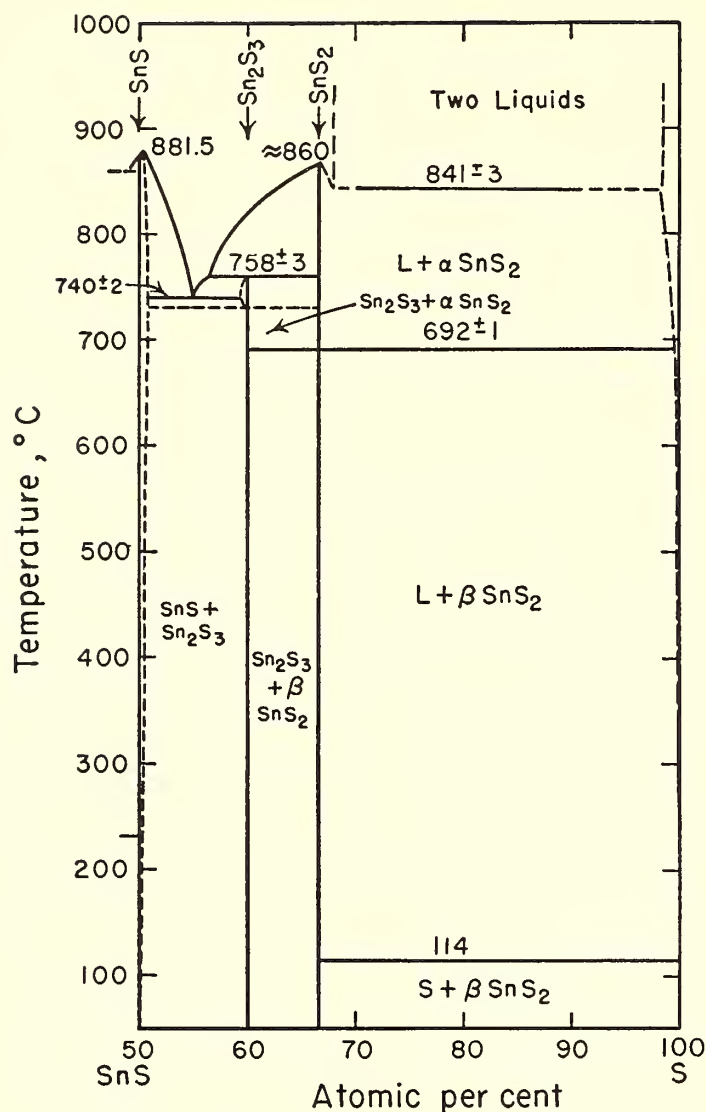


Fig. 84. Phase relations in the SnS-S portion of the system Sn-S. The compound Sn_3S_4 earlier reported to occur in this system was not encountered in the present study.

ture polymorph. It forms limited solid solution with SnS at elevated temperatures.

SnS_2 exists in two modifications; hexagonal βSnS_2 on heating inverts to cubic αSnS_2 at 692°C . The inversion is too sluggish to be observed by DTA. The inversion temperature was readily determined by quenching experiments. This phase melts congruently at about 860°C . In agreement with the observations of earlier workers, a eutectic was found to exist between SnS and SnS_2 at about 740°C and 55 atomic per cent S. A wide field of liquid immiscibility extending from about 68 to 98 weight per cent S exists between SnS_2 and S above 841°C .

A compound of Sn_3S_4 composition was reported to exist in the system by Albers

and co-workers (1961). This compound did not appear in any of the experiments of the present study.

Polished sections of ore specimens from Cerro Rico de Potosí, Bolivia, were studied as part of this investigation. Two new minerals, one identical with synthetic Sn_2S_3 and the other identical with SnS_2 , were observed in minute quantities in some of these polished sections. The mineral of Sn_2S_3 composition appears to replace stannite as a secondary weathering product. Small, almost idiomorphic Sn_2S_3 crystals also occur in a matrix of cassiterite, and in one specimen Sn_2S_3 was observed to replace pyrite. Twinning lamellae in Sn_2S_3 were frequently observed. The mineral of SnS_2 composition was invariably observed to replace pyrite.

The Fe-Sn-S System

The phase relations in this system have been investigated at 600°C by the rigid-silica-tube method. The stable phases at this temperature are pyrrhotite (Fe_{1-x}S) and pyrite (FeS_2) on the Fe-S join; herzenbergite (SnS), Sn_2S_3 , and SnS_2 on the Sn-S join; and αFe solid solution with up to 6 atomic per cent Sn, hexagonal FeSn, and liquid on the Fe-Sn join. No ternary compounds exist at 600°C .

Solid solutions between phases such as FeS_2 and SnS_2 , Sn_2S_3 and Fe_{1-x}S , are restricted to less than 1 per cent, whereas the mutual solubilities between SnS and Fe_{1-x}S exceed 1 per cent. The solubility of sulfur in either αFe or FeSn as well as that of the metals in liquid sulfur is too small to be detected by our methods.

The phase relations at 600°C are given in figure 85. The univariant assemblages are pyrite + SnS_2 + L + V, pyrite + pyrrhotite + SnS_2 + V, SnS_2 + pyrrhotite + Sn_2S_3 + V, Sn_2S_3 + pyrrhotite + herzenbergite + V, pyrrhotite + herzenbergite + L + V, pyrrhotite + L + FeSn + V, pyrrhotite + FeSn + αFe + V.

Divariant regions are pyrite + L + V, SnS_2 + L + V, pyrite + SnS_2 + V,

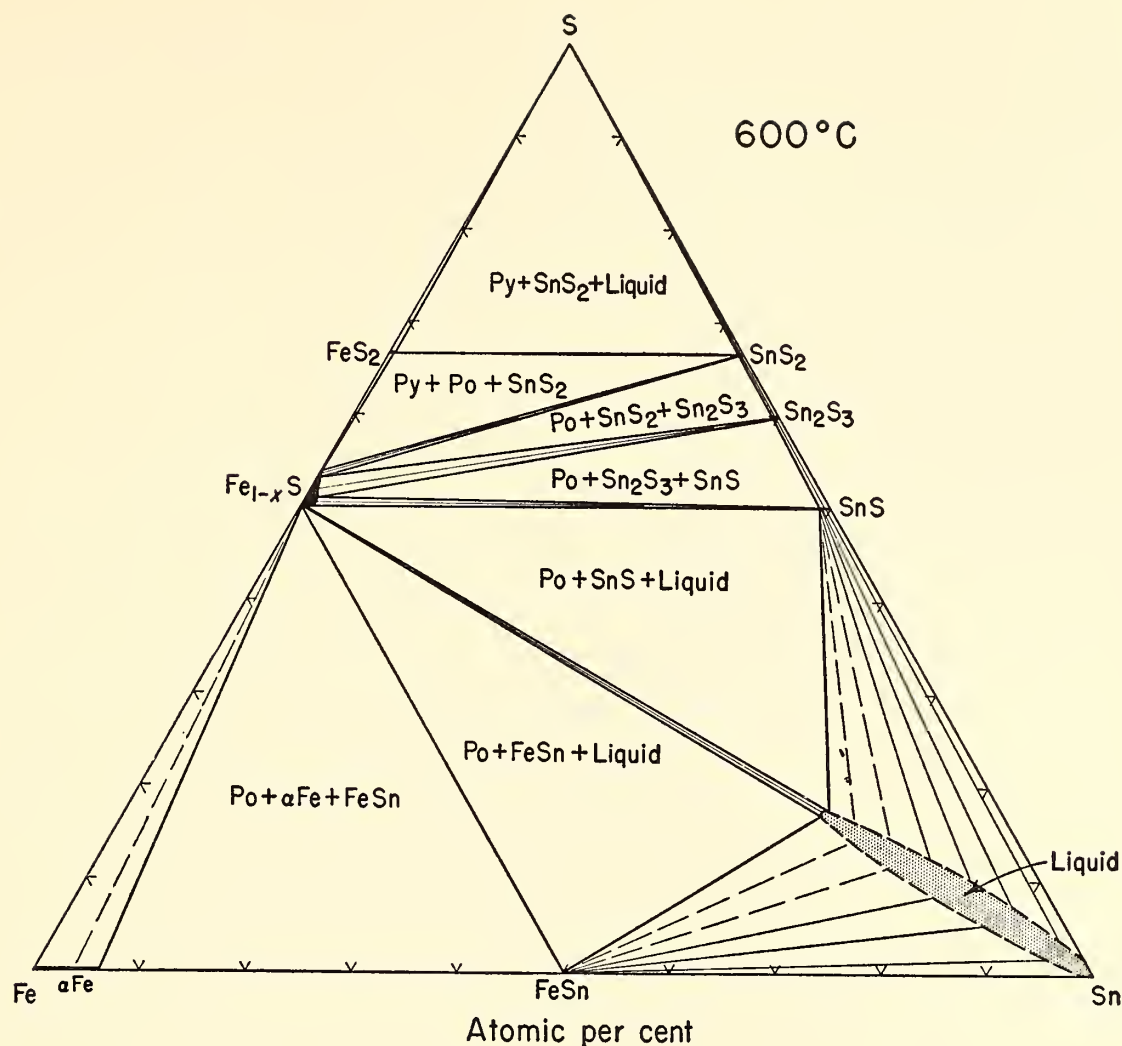


Fig. 85. At 600°C the Fe-Sn-S system does not contain any ternary phases. It is noted that SnS (herzenbergite) and FeS₂ (pyrite) do not form a stable mineral pair.

pyrite + pyrrhotite + V, pyrrhotite + SnS₂ + V, SnS₂ + Sn₂S₃ + V, pyrrhotite + Sn₂S₃ + V, Sn₂S₃ + herzenbergite + V, pyrrhotite + herzenbergite + V, pyrrhotite + L + V, herzenbergite + L + V, FeSn + L + V, pyrrhotite + FeSn + V, pyrrhotite + αFe + V. The divariant region αFe + FeSn + V is too narrow to be determined.

The Cu-Sn-S System

The phase relations in the ternary system copper-tin-sulfur were studied at 600°C in evacuated, sealed silica tubes with minimum vapor space. The binary phases at 600°C are digenite-chalcocite solid solution (Cu₉S₅-Cu₂S) on the Cu-S join; and herzenbergite (SnS), Sn₂S₃, and SnS₂ on the Sn-S join. In addition a number of phases exist on the Cu-Sn join:

αCu containing 0 to 8.9 atomic per cent Sn; a cubic β phase with 14.9 per cent Sn; a cubic γ phase with about 15.5 to 20 atomic per cent Sn; a hexagonal ε phase, Cu₂₀Sn₆; an orthorhombic ζ phase, Cu₃Sn; and liquid. This liquid field extends from Sn to 47 atomic per cent Cu along the Sn-Cu join but only 1 atomic per cent toward S along the Sn-S join. At 600°C it extends very far into the system and includes a composition of 42 atomic per cent Cu, 16 atomic per cent Sn, and 42 atomic per cent S.

At this temperature two stable ternary phases exist: (1) Cu₂SnS₃, which was reported earlier to have Cu₂(Cu,Sn)SnS₃₋₄ composition with atomic ratio Cu:Sn = 2:1 (Moh and Ottemann, 1962), has the tetragonal stannite lattice. Stoichiometric Cu₂SnS₃ at 780° ± 3°C inverts to a cubic form that melts incongruently at

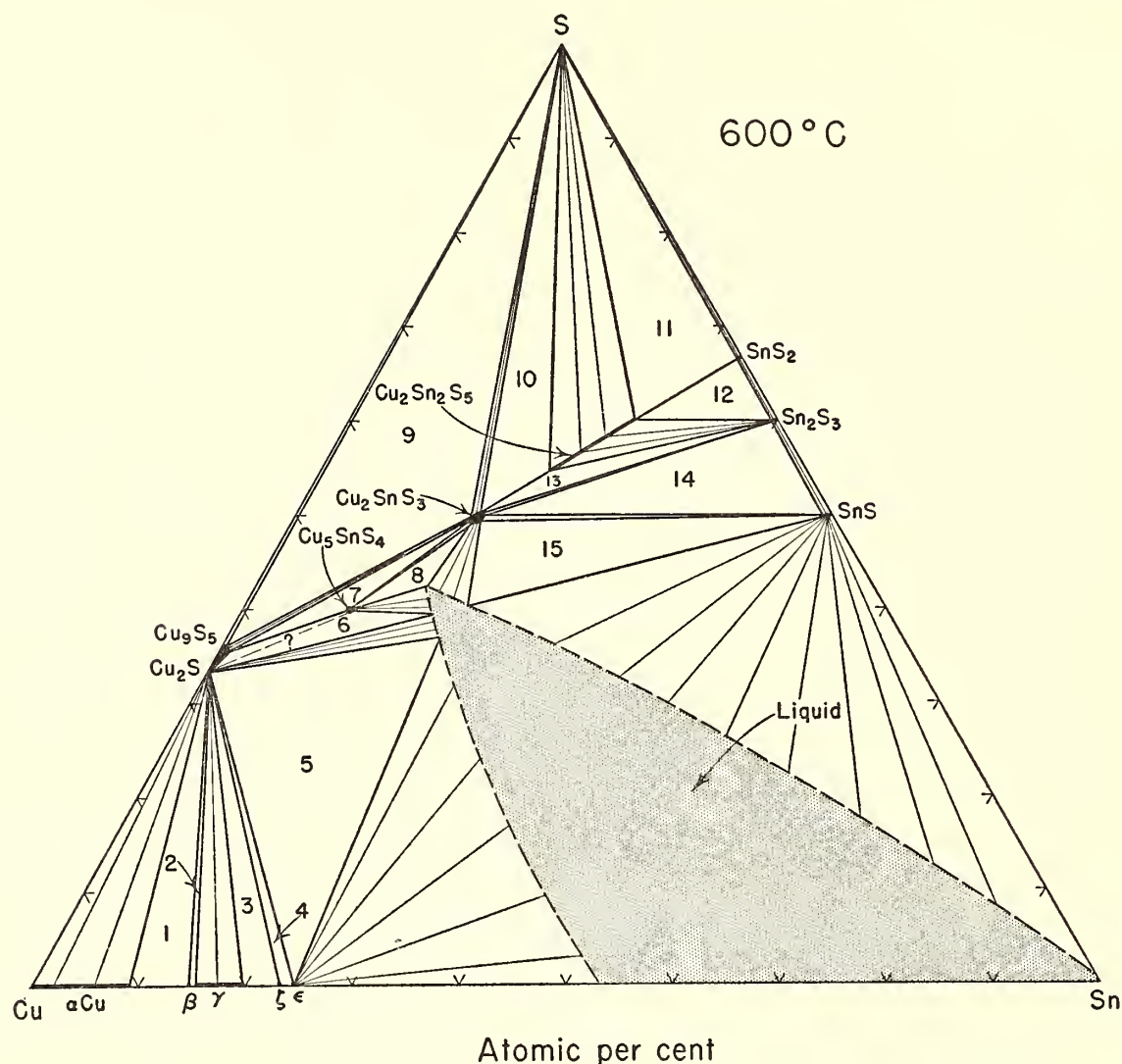


Fig. 86. At 600°C a large liquid field exists in the Cu-Sn-S system. Two ternary phases, Cu_2SnS_3 and $\text{Cu}_2\text{Sn}_2\text{S}_5$, are stable at this temperature. The univariant assemblages, all including vapor in addition to the phases listed below, are: 1, $\alpha\text{Cu} + \beta$ phase + Cu_2S . 2, β phase + γ phase + Cu_2S . 3, γ phase + ζ phase ($\text{Cu}_{20}\text{Sn}_6$) + Cu_2S . 4, ζ phase ($\text{Cu}_{20}\text{Sn}_6$) + ϵ phase (Cu_3Sn) + Cu_2S ss. 5, ϵ phase (Cu_3Sn) + Cu_2S ss + L . 6, Cu_2S ss + Cu_5SnS_4 + L (experiments indicate that the relations in this field are more complicated than indicated here). 7, Cu_9S_5 - Cu_2S ss + Cu_5SnS_4 (tin bornite) + Cu_2SnS_3 ss. 8, Cu_5SnS_4 (tin bornite) + Cu_2SnS_2 ss + L . 9, Cu_9S_5 ss + L + Cu_2SnS_3 ss. 10, Cu_2SnS_3 ss + L + $\text{Cu}_2\text{Sn}_2\text{S}_5$ ss. 11, $\text{Cu}_2\text{Sn}_2\text{S}_5$ ss + L + SnS_2 . 12, $\text{Cu}_2\text{Sn}_2\text{S}_5$ ss + SnS_2 + Sn_2S_3 . 13, Cu_2SnS_3 ss + $\text{Cu}_2\text{Sn}_2\text{S}_5$ ss + Sn_2S_3 . 14, Cu_2SnS_3 ss + Sn_2S_3 + SnS . 15, L + Cu_2SnS_3 ss + SnS .

$842^\circ \pm 3^\circ\text{C}$. (2) The $\text{Cu}_2\text{Sn}_2\text{S}_5$ phase, which is noncubic and anisotropic, forms a large field of solid solution that as yet has not been studied in detail. In addition a third anisotropic compound of Cu_5SnS_4 composition, which is analogous to bornite, occurs at lower temperature (Moh and Ottemann, 1962).

DTA experiments on Cu_5SnS_4 show thermal effects indicating inversions at about 94° and at $395^\circ \pm 8^\circ\text{C}$. Congruent melting is indicated below 600°C in quenching experiments. The phase relations are given in figure 86.

THE Fe-Ni-As SYSTEM AT 800°C

Peter R. Buseck

The Fe-Ni-As system is of considerable interest because it includes several important minerals common in nickel deposits throughout the world. The origin of many of these deposits is in dispute, and it is hoped that the phase relations will shed some light on the conditions existing during ore formation. The system also constitutes one side of the important Fe-Ni-As-S system, which contains many common minerals found

in both arsenide- and sulfide-type deposits and thus provides a link between the two.

At 800°C seven stable phases are present on the binary bounding joins: FeAs_2 , FeAs , Fe_2As , NiAs_2 , $\text{Ni}_{1\pm x}\text{As}$, $\text{Ni}_{11}\text{As}_8$, and $\text{Ni}_{5-x}\text{As}_2$; four ternary phases: $\text{Fe}_x\text{Ni}_{1-x}\text{As}_{3-y}$, $(\text{Fe}_x\text{Ni}_{1-x})_2\text{As}_{1\pm y}$, $\sim\text{Fe}_2\text{NiAs}$, and one of undetermined composition; three elemental phases; and two liquid fields. Aside from the number of phases, the single most striking feature of this system is the extensive solid solution exhibited by almost all the phases. Only slight variations in the arsenic content are noted in a given phase, but iron and nickel proxy for each other extensively. As all seven of the phases along the bounding joins can show considerable Fe-Ni substitution they have ternary composition for most assemblages in this system (fig. 87). However, at 800°C no pairs of binary phases show complete Fe-Ni solid solution; they are generally separated by solvi. In an isothermal section such solvi are expressed as joins between coexisting phases with equivalent arsenic-to-metal ratios. This results in a phase diagram subdivided into what appear as successive tiers subparallel to the Fe-Ni binary join, containing progressively greater amounts of arsenic (see fig. 87). The mono- and diarsenide tiers extend completely across the diagram; the triarsenide tier reaches neither binary join; M_{11}As_8 and M_5As_2 tiers extend from the Ni-As join toward the Fe-As join but never meet it; and an M_2As tier extends from the Fe-As join toward the Ni-As join but never reaches it. The M_2As tier is, however, extended toward the Ni-As side of the diagram by almost reaching the subparallel field of oregonite. The detailed phase relations will be discussed by considering successively more arsenic-poor tiers and the areas between them.

Vapor occurs with all the assemblages mentioned. The formulas of binary end members of solid solutions (ss) are used to designate the entire series.

The MAs_3 Phase

Only one triarsenide is stable in this system at 800°C: a ternary phase having the formula $(\text{Fe}_x\text{Ni}_{1-x})\text{As}_{3-y}$, where x varies from about 0.25 to 0.46 and y from about 0.02 to 0.09 (Pleass and Heyding, 1962). The formula should not be interpreted in a structural sense, because it is not certain that the departure from stoichiometry is actually the result of an anion deficiency. Although no cobalt-free natural material has been reported, the natural analogue of this triarsenide is skutterudite. It is cubic and has the space group $Im\bar{3}$ (Palache, Berman, and Frondel, 1944).

The triarsenide is stable in three univariant and three divariant regions as seen from figure 87. It can coexist with elemental arsenic and/or the MAs_2 phase.

The MAs_2 Phases

There are two diarsenides exhibiting almost complete solid solution between FeAs_2 (loellingite is the mineral equivalent) and NiAs_2 (rammelsbergite is the mineral equivalent) at 800°C. The solvus separating these two phases extends from 31 ± 2 to 8 ± 2 weight per cent FeAs_2 . On the basis of the analyses compiled by Holmes (1947), the limits of solubility of natural specimens are approximately 18 atomic per cent NiAs_2 in loellingite and 8 per cent FeAs_2 in rammelsbergite. Both diarsenides are orthorhombic, belong to space group $Pmnn$, and exhibit very little departure from stoichiometry in their arsenic contents (Heyding and Calvert, 1960; Roseboom, 1963).

The iron diarsenide is stable in four univariant and four divariant regions (fig. 87) and can coexist with elemental arsenic, triarsenide containing greater than 38 weight per cent " FeAs_{3-y} ," iron-rich NiAs_2 ss, or $\text{Ni}_{1-x\text{ max}}\text{As}$ ss containing as least 7 weight per cent FeAs .

The NiAs_2 ss is stable in three univariant and three divariant regions (fig. 87) and can coexist stably with

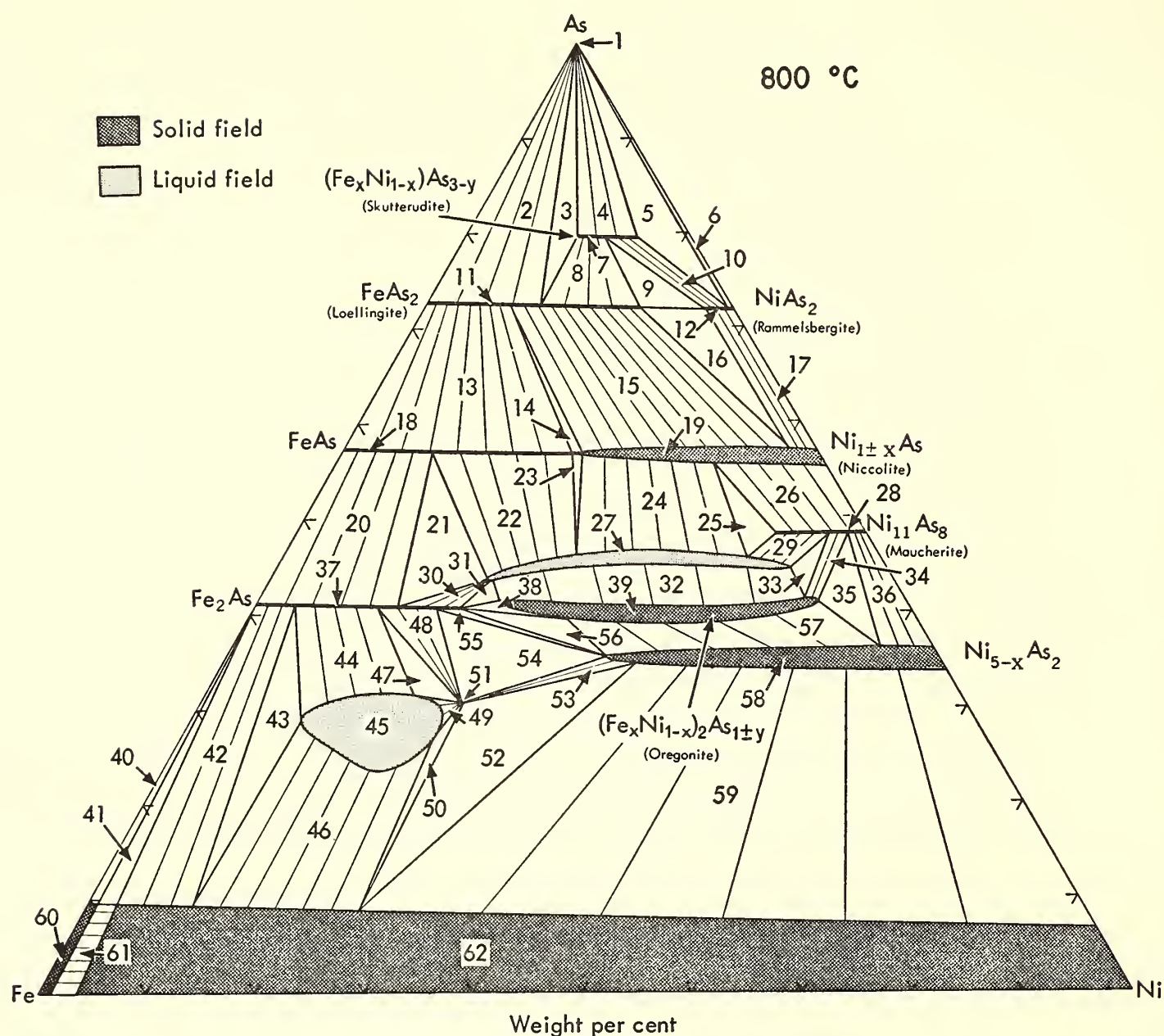


Fig. 87. Phase relations at 800°C in the Fe-Ni-As system. Tie lines involving liquids are not rigidly determined. In the vicinity of the θ phase ($\sim\text{Fe}_2\text{NiAs}$) tie lines are schematic. Mineral names rather than chemical formulas are used for simplification in the list below. The fields indicated by numbers in the figure contain the following phases in addition to vapor:

- | | |
|---|---|
| 1. As | 22. FeAs ss + L |
| 2. As + lo ss | 23. FeAs ss + nc ss + L |
| 3. As + lo ss + sk ss | 24. nc ss + L |
| 4. As + sk ss | 25. nc ss + ma ss + L |
| 5. As + sk ss + rm ss | 26. nc ss + ma ss |
| 6. As + rm ss | 27. L |
| 7. sk ss | 28. ma ss |
| 8. sk ss + lo ss | 29. ma ss + L |
| 9. sk ss + lo ss + rm ss | 30. Fe ₂ As ss + L |
| 10. sk ss + rm ss | 31. Fe ₂ As ss + og ss + L |
| 11. lo ss | 32. og ss + L |
| 12. rm ss | 33. og ss + ma ss + L |
| 13. lo ss + FeAs ss | 34. og ss + ma ss |
| 14. lo ss + FeAs ss + nc ss | 35. og ss + ma ss + $\beta\text{Ni}_{5-x}\text{As}_2$ ss |
| 15. lo ss + nc ss | 36. ma ss + $\beta\text{Ni}_{5-x}\text{As}_2$ ss |
| 16. lo ss + rm ss + nc ss | 37. Fe ₂ As ss |
| 17. rm ss + nc ss | 38. Fe ₂ As ss + og ss |
| 18. FeAs ss | 39. og ss |
| 19. nc ss | 40. αFeNi ss + Fe ₂ As ss |
| 20. FeAs ss + Fe ₂ As ss | 41. αFeNi ss + γFeNi ss + Fe ₂ As ss |
| 21. FeAs ss + Fe ₂ As ss + L | 42. γFeNi ss + Fe ₂ As ss |

elemental arsenic, triarsenide containing up to 38 weight per cent " FeAs_{3-y} ," nickel-rich FeAs_2 ss, and $\text{Ni}_{1-x} \text{max} \text{As}$ ss containing less than 7 weight per cent FeAs .

The MAs Phases

There are two stable monoarsenides, $\text{Ni}_{1\pm x}\text{As}$ (niccolite is the mineral equivalent) and FeAs (not reported to occur naturally). FeAs is orthorhombic, with space group $Pmcn$, and shows no appreciable arsenic deficiency or excess (Heyding and Calvert, 1957a; written communication, 1962). $\text{Ni}_{1\pm x}\text{As}$, on the other hand, is hexagonal with space group $P6/mmc$ and can contain between 55.4 and 57.0 weight per cent arsenic (Yund, 1961). These values may be compared to stoichiometric NiAs , which contains 56.07 weight per cent arsenic.

There is extensive but incomplete solid solution between FeAs ss and $\text{Ni}_{1\pm x}\text{As}$ ss. Because iron-rich $\text{Ni}_{1\pm x}\text{As}$ ss and nickel-rich FeAs ss have an almost identical appearance in reflected light, the limits of solid solution could not be determined optically and X-ray methods had to be used. These have their limitations, however, because the X-ray patterns are very similar and the strongest peaks of FeAs ss, (021, 111) and (112), coincide with the strongest $\text{Ni}_{1\pm x}\text{As}$ ss peaks, (101) and (102), respectively. As a result, the weaker peaks for both phases must be used for differentiation, thereby decreasing the possible resolution, the more so as all but the two strongest peaks

for each phase are depressed by the addition of the "foreign" cation.

$\text{Ni}_{1-x} \text{max} \text{As}$ ss can accept varying amounts of As and Fe into its structure. Yund (1961) used variations in the d_{103} for synthetic iron-free $\text{Ni}_{1\pm x}\text{As}$ to indicate changes in the Ni-As atomic ratio. Although occurring at a relatively high angle of 2θ , the (103) peak is comparatively weak ($I = 20$) and its intensity decreases further with increasing iron content. Therefore, it was unsuitable for this study. Instead, the (110) peak was used, this being the only reasonably strong $\text{Ni}_{1\pm x}\text{As}$ ss peak that does not coincide with the pattern of FeAs ss. A further advantage is that it does not overlap with FeAs_2 ss or NiAs_2 ss peaks.

Either arsenic or iron alone will cause changes in the lattice spacing of $\text{Ni}_{1\pm x}\text{As}$ ss, these changes being linear with composition if Vegard's law is obeyed. However, if both elements are varied concurrently a complicated pattern of change emerges. Niccolite generally occurs with other nickel-iron arsenides; if it is in equilibrium with them, then, depending on whether it coexists with higher or lower arsenides, the niccolite will have either the maximum or the minimum possible arsenic content for its particular iron content. Spacing curves would be desirable for these two situations.

To satisfy the requirement that synthetic $\text{Ni}_{1\pm x}\text{As}$ ss be saturated in regard to arsenic, it must be made together with members of the diarsenide solid solution.

43. γFeNi ss + Fe_2As ss + L

44. Fe_2As ss + L

45. L

46. γFeNi ss + L

47. Fe_2As ss + θ + L

48. Fe_2As ss + θ

49. θ + L

50. θ + γFeNi ss + L

51. θ

52. θ + γFeNi ss + $\beta\text{Ni}_{5-x}\text{As}_2$ ss

53. θ + $\beta\text{Ni}_{5-x}\text{As}_2$ ss

54. θ + $\beta\text{Ni}_{5-x}\text{As}_2$ ss + Fe_2As ss

55. $\beta\text{Ni}_{5-x}\text{As}_2$ ss + Fe_2As ss

56. $\beta\text{Ni}_{5-x}\text{As}_2$ ss + Fe_2As ss + og ss

57. $\beta\text{Ni}_{5-x}\text{As}_2$ ss + og ss

58. $\beta\text{Ni}_{5-x}\text{As}_2$ ss

59. $\beta\text{Ni}_{5-x}\text{As}_2$ ss + γFeNi ss

60. αFeNi ss

61. αFeNi ss + γFeNi ss

62. γFeNi ss

lo = loellingite = FeAs_2 ; ma = maucherite = $\text{Ni}_{11}\text{As}_8$; nc = niccolite = $\text{Ni}_{1\pm x}\text{As}$; og = oregonite = $(\text{Fe}_x, \text{Ni}_{1-x})_2\text{As}_{1\pm y}$; rm = rammeisbergite = NiAs_2 ; sk = skutterudite = $\text{Fe}_x\text{Ni}_{1-x}\text{As}_{3-y}$.

Mixtures having bulk compositions intermediate between the mono- and diarsenides lie within either a uni- or a divariant region (fig. 87): if within a univariant region, the composition of the one or two diarsenides is fixed independently of the starting bulk compositions; if within a divariant region, the intercept of the monoarsenide field with a line going through the measured diarsenide composition and the bulk composition gives the monoarsenide composition. As the univariant regions are rather small, most bulk compositions fall within a divariant region, requiring that for each run both the monoarsenide and the diarsenide composition be determined. This was done by X-ray diffraction methods, using the table of Roseboom (1963) for the d_{ss} versus 2θ plot for the diarsenides. Lake Toxaway quartz was used as an internal standard for both sets of oscillations. Numerous experiments were performed to determine the direction of tie lines in various divariant fields. In the diarsenide-monoarsenide divariant regions these experiments served to determine the compositions of monoarsenides in equilibrium with diarsenides of known compositions. Application of this indirect method involves an uncertainty of about ± 1.5 weight per cent in the niccolite d_{110} values of figure

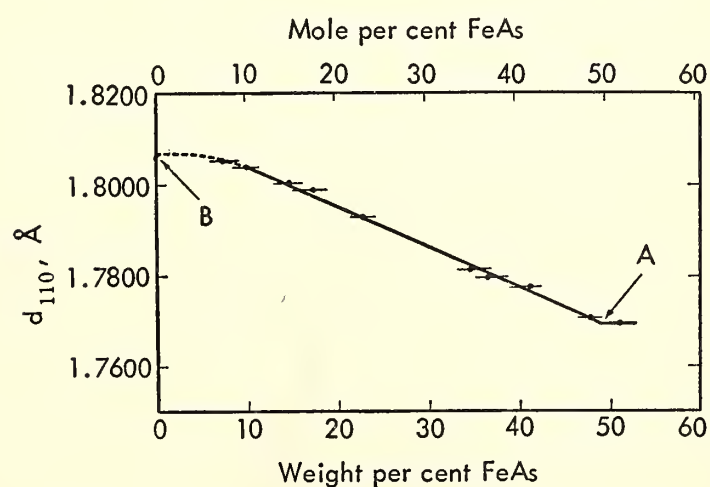


Fig. 88. Variation in the d_{110} value of arsenic saturated Ni_{1-x}As ss (niccolite) as function of FeAs content, at 800°C . Point A indicates maximum solubility at this temperature. The position of point B was calculated from data given by Yund (1961).

88. The curve in figure 88 was fitted to the plotted points by a regression analysis. The bend toward the iron-poor portion is determined by a (110) value calculated from the unit-cell dimensions of Yund (1961). As $\text{Ni}_{1\pm x}\text{As}$ has a larger (110) spacing when arsenic deficient than when arsenic rich, such a bend suggests that an increasing iron content depresses the amount of arsenic that can enter the structure.

The strongest FeAs ss peak that does coincide with any $\text{Ni}_{1\pm x}\text{As}$ ss peak is produced by the d_{121} reflection. For anything but pure FeAs ss the (121) is not strong enough for precise measurement, and so it is not suitable for use for a spacing curve. However, by noting for which bulk compositions it is present and for which it is absent, the Ni-rich limit of the FeAs ss field can be determined. This limit (48 ± 1 weight per cent NiAs) is substantiated by the fact that the measured compositions of diarsenides coexisting with FeAs ss changed concurrently with compositional variations of FeAs ss.

Iron monoarsenide can occur stably in three divariant and three univariant fields. It may coexist with FeAs_2 ss containing no more than 27 ± 1 weight per cent NiAs₂ in solid solution, with iron-rich $\text{Ni}_{1\pm x}\text{As}$ ss, with Fe_2As ss, and with liquid.

Nickel monoarsenide can exist in four univariant and four divariant regions. It can be made stably together with NiAs₂ ss, with FeAs_2 ss containing between 27 ± 1 and 69 ± 2 weight per cent NiAs₂ in solid solution, with nickel-rich FeAs ss, with $\text{Ni}_{11}\text{As}_8$ ss, and with liquid.

Liquid Fields

The phase relations for compositions less arsenic rich than the monoarsenides are greatly complicated by the presence of an extensive liquid field partly separating the M_2As tier from the monoarsenides. Another liquid field partly separates the M_2As tier from the binary metal join.

The presence of liquid can be noted in several ways for runs in this system. The charges in a few runs were completely globular upon quenching, having been wholly molten at 800°C. These runs typically contain round vesicles that enclosed vapor at or above the melting temperature. In many more runs shrinkage cracks or individual grains that are slightly globular suggest partial melting, but are not conclusive proof. Because the several phases are optically almost identical the microscope is of little use in delimiting the liquid fields. However, in some runs globular and/or myrmekitic-eutectoid textures could be seen, again suggesting melting. Some of these textures could be made more evident with the help of a 30-second etch using 50 per cent concentrated HCl and 50 per cent saturated FeCl₃. This mixture is particularly effective in preferentially attacking the fine-grained and intimate eutectoid mixture produced when liquid lying between the field of oregonite and Ni_{1±x}As ss is quenched. In a few runs, especially those near the M₁₁As₈ ss end of the liquid field, there are indications of two coexisting immiscible liquids, for there is a eutectoid quench mixture interstitial to larger globules of another, former liquid.

Although the several features mentioned above are all indicative of the former presence of a liquid, especially when taken collectively, they are generally not sufficiently clear cut to be thoroughly reliable. To outline the liquid field more definitively several differential thermal analysis runs were made, the charges being placed in evacuated, sealed silica tubes containing quartz as an internal standard.

All the material used in the DTA runs was first allowed to react for at least 4 weeks at temperatures close to the temperature of the solidus. Thus, the charges contained assemblages whose compositions were at or near equilibrium for temperatures close to those at initial melting, thereby minimizing the effects of

the sluggishness of reactions characteristic of arsenides.

Differential thermal analyses for compositions close to the more arsenic-rich liquid field indicate that initial melting occurred at temperatures no higher than $782^\circ \pm 12^\circ\text{C}$. Strong endothermal peaks produced by initial melting from several runs all show similar temperatures, suggesting that the trough forming the liquid field is relatively shallow in the direction of constant arsenic content (parallel to the Fe-Ni join). Optical examinations of etched polished sections indicate that the liquid field is narrow; thus the liquidus has a steep slope perpendicular to the long direction of the field. Changes in arsenic content apparently produce more profound variations in melting temperatures than changes in the Fe:Ni ratio.

In shape, the more arsenic-deficient liquid field appears less regular than the arsenic-rich field, but it is probably also relatively shallow. Initial melting seems to occur at similar temperatures in both fields. The arsenic-deficient field is elongated toward the binary eutectic between iron and Fe₂As.

Microscopic examination in reflected light of runs having compositions close to and within the arsenic-deficient liquid field indicate several textural features. Globules of metal, once having been molten droplets, are commonly separated by an interstitial intergrowth of metal and arsenide, presumably the result of eutectic crystallization. Also common is an extremely fine-grained and intimate intergrowth of two arsenides, locally also exhibiting lamellar or feathery textures. It is possible that this represents a decomposition of a single high-temperature phase related to the ternary θ phase (see below).

At 800°C there is probably a thermal divide running between nickel-rich Fe₂As ss and iron-rich oregonite; one run close to this hypothetical divide indicates a strong exothermal peak representing initial melting at $842^\circ \pm 7^\circ\text{C}$. It seems

likely, however, that at higher temperatures the liquid fields will expand to come together in this region and thereby to separate Fe_2As ss and oregonite.

The $M_{11}\text{As}_8$ Phase

There is one phase with composition $M_{11}\text{As}_8$ (maucherite is the mineral equivalent) occurring along the Ni-As binary join; no analogous phase is found on the Fe-As binary join. $\text{Ni}_{11}\text{As}_8$ is tetragonal, probably belongs to space group $P4_22_1$ or $P4_32_1$, and exhibits a compositional variation of less than 0.2 weight per cent As (Yund, 1961); i.e., it is essentially stoichiometric. The $M_{11}\text{As}_8$ can take up to 16 ± 1 weight per cent " $\text{Fe}_{11}\text{As}_8$ " into solid solution. Such increases in the iron content of $M_{11}\text{As}_8$ produce a limited increase in the (116) spacing. It also produces a slight splitting of the (200) peak, suggesting that there may be a small symmetry change.

Pure $\text{Ni}_{11}\text{As}_8$ melts incongruently at 830°C to liquid plus $\text{Ni}_{1+x}\text{maxAs}$. There is, additionally, a eutectic between $\text{Ni}_{11}\text{As}_8$ and $\text{Ni}_{5-x}\text{maxAs}_2$ occurring at $818^\circ \pm 5^\circ\text{C}$ (Yund, 1961). On the basis of these data it might be expected that a liquid field would occur close to $\text{Ni}_{11}\text{As}_8$ at 800°C , and both the differential thermal analyses and polished sections indicate that it does. Addition of Fe to the $\text{Ni}_{11}\text{As}_8$ structure does not, however, depress its melting point to 800°C , the temperature of the isothermal section (fig. 87).

The $M_{11}\text{As}_8$ phase is stable in three univariant and four divariant regions and can occur together with Ni_{1+x}As ss containing up to 23 ± 2 weight per cent FeAs in solid solution, with nickel-rich oregonite, with nickel-rich $\beta\text{Ni}_{5-x}\text{maxAs}_2$, and with liquid of varying composition.

The $M_2\text{As}$ Phases

Oregonite. This ternary phase exhibits both extensive nickel-iron substitution and changes in the metal-to-arsenic ratio. Because of its complicated composition and also to avoid confusion with the other $M_2\text{As}$ phase, its mineral name, oregonite, will be used, although it should

be understood that only synthetic material was employed for the experimental work. Almost 60 runs containing oregonite as the main phase were made. In determining the compositional limits of oregonite minimal reliance was placed on optical methods—in reflected light it looks so similar to most of the phases with which it can coexist that minor amounts of phases other than oregonite are extremely difficult to detect. Therefore the limits of the stability field of oregonite had to be primarily determined by means of X rays. However, with unfiltered radiation, less than 5 per cent of the coexisting quench phases, $\text{Ni}_{1+x}\text{maxAs}$ ss and $\beta\text{Ni}_{5-x}\text{maxAs}_2$ ss, can be detected in X-ray patterns. The upper and lower arsenic limits of oregonite could be determined to within 0.5 weight per cent, because numerous runs containing different Fe:Ni ratios produce concordant results regarding the upper and lower limits of arsenic solubility. The limits of Fe-Ni substitution are somewhat less precise, perhaps to within 1 weight per cent.

The oregonite field extends to neither of the binary metal-arsenic joins. The composition, in atomic percentages, of the most iron-rich and most arsenic-rich run coincides and is given below, followed by the most nickel-rich run and the most arsenic-deficient run:

Fe	40.43	11.79	26.40
Ni	24.86	53.91	40.86
As	34.71	34.30	32.73

Oregonite was the only phase detected in all these samples. The phase relations at 800°C suggest that the most nickel-rich oregonite can take an additional 2 per cent nickel into its structure, primarily at the expense of iron. Although the metal-to-arsenic ratio is roughly 2, there is a slight but appreciable range in arsenic content for any given Fe:Ni ratio. Thus, the oregonite composition can be summarized by the formula $(\text{Fe}_x, \text{Ni}_{1-x})_2\text{As}_{1\pm y}$, where x can range between 0.15 and 0.62 and y between -0.03 and 0.06 . As the structure is

unknown this formula should be taken only in a chemical sense.

Precise measurements of the (202) and (112) reflections, using Lake Toxaway quartz for an internal standard, indicate that these spacings increase with increases in the iron content.

Oregonite as a natural phase has been reported occurring together with awaruite from Josephine County, Oregon (Ramdohr and Schmitt, 1959). These authors describe it as hexagonal and indicate an X-ray pattern almost identical to that of the synthetic material, although their estimate of the composition, based on X-ray fluorescence, is Ni_2FeAs_2 . The fact that in X-ray fluorescence it is possible to fail to find an impurity would explain the compositional discrepancy.

A differential thermal analysis of an oregonite containing 22.08 and 38.06 weight per cent of iron and nickel, respectively, was made to determine the melting temperature and to see whether any polymorphic inversions could be noted (etched polished sections of oregonite appear inhomogeneous). No peaks were observed between room temperature and 800°C. The sample was heated to 1180°C, and only one peak appeared—a strong endothermic reaction at 844°C, presumably caused by total melting. Upon cooling, a strong exothermic peak appeared at 810°C, the result of crystallization. The gap between the melting and freezing temperatures is the combined result of superheating and supercooling; the true melting temperature probably lies somewhere between.

Oregonite can occur in at least four univariant and four divariant fields. It is stable together with M_{11}As_8 ss, with all but the most nickel-rich compositions of $\beta\text{Ni}_{5-x}\text{maxAs}_2$ ss, with nickel-rich Fe_2As ss, and with at least one liquid.

Fe₂As solid solution. This phase is roughly coextensive with oregonite, although it is essentially stoichiometric in regard to metal-to-arsenic ratio; it is tetragonal rather than hexagonal and

belongs to the $P4/mmm$ space group (Clark, 1960; Heyding and Calvert, 1957b). It can take up to 31 ± 3 weight per cent “ Ni_2As ” into solid solution, this producing a slight decrease in the (112) and (003) spacings. Fe_2As has not been reported to occur naturally.

Fe_2As ss is probably stable in seven univariant and eight divariant regions (fig. 87). It can coexist stably with FeAs ss, with oregonite, with αFeNi ss, with nickel-poor γFeNi ss, with two liquids, probably with the θ and/or ϕ phases, and with iron-rich $\beta\text{Ni}_{5-x}\text{As}_2$.

The M_5As_2 Phase

The binary M_5As_2 phase falls along the Ni-As join, is hexagonal, space group $P\bar{6}3$, and exhibits a range in arsenic content of 1.8 weight per cent at 800°C. This is caused by a formation of vacant nickel sites (Heyding and Calvert, 1957b), thus the accepted general formula of $\text{Ni}_{5-x}\text{As}_2$ for this phase. The stoichiometric formula expresses the maximum nickel content. To distinguish the high-temperature phase from a metastable form occurring below approximately 200°C, Heyding and Calvert labeled it β and the low-temperature form β' . $\beta\text{M}_5\text{As}_2$ can accept up to 46 ± 5 weight per cent “ Fe_5As_2 ” in solid solution. Such an increase in the iron content results in an increase in the (115) and (106) spacings. It has not been reported as occurring naturally.

The $\beta\text{M}_5\text{As}_2$ phase is probably stable in four univariant and five divariant fields (fig. 87). $\beta\text{Ni}_{5-x}\text{As}_2$ ss can coexist with nickel-rich $\text{Ni}_{11}\text{As}_8$ ss, with oregonite containing all Fe/Ni ratios, with γFeNi ss, probably with liquid, with nickel-rich Fe_2As ss, and possibly with the θ and ϕ phases.

The θ and ϕ Phases

Two ternary phases are evident in runs having compositions where $\text{M}/\text{As} > 2/1$ and $\text{Fe}/\text{Ni} > 1/1$. At 800°C, liquid is also present in this part of the phase diagram, thereby complicating the phase relation-

TABLE 21. X-Ray Powder Diffraction Data of the Cubic ϕ Phase, Quenched from 800°C
Mn filtered Fe radiation, $K\alpha = 1.9373 \text{ \AA}$;
 $a_0 = 4.305_2 \text{ \AA}$

$d_{\text{obs}}, \text{ \AA}$	$d_{\text{calc.}}, \text{ \AA}$	I_{obs}	hkl
2.487	2.486	65	111
2.152	2.153	100	200
1.522	1.522	70	220
1.299	1.298	25	311

ships and suggesting the possibility that these are metastable quench products.

The presence of the new phases was first noticed from X-ray patterns containing peaks that did not fit any of the known phases. The lattice spacings and intensities of the ϕ phase, determined from these patterns, are shown in table 21. The d values can be successfully indexed on cubic coordinates, in accord with observed crystals that appear octahedral. Both the (200) and (220) spacings were precisely measured by repetitive oscillation with Lake Toxaway quartz used as an internal standard. The value of a_0 , calculated from the weighted values of 2θ from the several peaks, is 4.305_2 \AA . The lattice spacings of the θ phase are given in table 22. The indicated values were averaged from 13 different runs. It is clearly more

TABLE 22. X-Ray Powder Diffraction Data of the θ Phase, Quenched from 800°C
Mn filtered Fe radiation, $K\alpha = 1.9373 \text{ \AA}$

$d_{\text{obs}}, \text{ \AA}$	I_{obs}
3.221	15
2.328	20
2.129	30
2.053	90
1.950	100
1.920	55
1.753	8
1.709	7
1.479	5
1.426	4
1.298	6
1.292	10

complicated than ϕ and cannot be indexed on cubic coordinates.

A macroscopic inspection of numerous quenched charges indicated a phase different from the known iron-nickel arsenides. Many runs contained a black, nonmetallic material coating portions of the surface of the charge. Others contained small vuglike holes on their surfaces, and the black material was then in fine, octahedral crystals within these holes. In these respects it resembles a quenched vapor. In view of the very low vapor pressure over some of the phases richer in arsenic, however, it would certainly be surprising to have an appreciable vapor pressure over these high-metal-content phases. An alternative explanation of its occurrence may be that it segregated itself by being the only unmolten phase. X rays indicate that this black phase is ϕ .

The presence of liquid at 800°C in the part of the diagram where θ and ϕ were observed suggested that one or both might be the result of quenching from a liquid. The lowest temperature at which liquid can exist is above 700°C, and so several runs were annealed at 700°C, thereby avoiding complications incident upon melting. Both ternary phases appeared in a number of these runs, indicating that they are not a result of melting. However, unless one was in fact vapor, one or both must be the result of metastability, presumably developed during rapid quenching. This is demonstrated by the fact that two bulk compositions each contained the Fe_2As ss, FeNi ss, and θ and ϕ phases when quenched from 700°C. As vapor is present in all the runs, the above five-phase assemblages could be stable only if each represented the phases at an invariant point, and it is assumed that one or more of the phases must be metastable.

Thirty-eight runs contained either θ or ϕ , and in almost all of them both phases were observed. This high degree of association plus the lack of systematic change in relative abundances with

changes in the bulk composition of the starting run suggests that one of the ternary phases is the breakdown product of the other. As ϕ shows a more sporadic distribution and is generally less abundant than θ it is thought that ϕ is the metastable quench phase. A differential thermal analysis failed to show any heat effects between room temperature and 700°C, and so the temperature of possible decomposition is not known.

As neither θ nor ϕ is present in runs containing only two elemental components they must be ternary phases. Possible joins, sketched on the basis of the phases present in the runs quenched from 800°C, meet at a composition represented by the hypothetical formula Fe_2NiAs . The run having a composition closest to this formula is the only one containing only θ and minor metal. Furthermore, other runs having similar compositions contain predominantly θ . It therefore seems probable that Fe_2NiAs is a close approximation of the composition of the θ phase.

As the melting temperatures of the ternary phases are not yet known, it is not certain that they are stable at 800°C, the isotherm at which figure 87 is drawn. They have therefore not been indicated on the figure. It may be noted, however, that both θ and ϕ have been observed in assemblages together with FeNi ss, Fe_2As ss, $\beta\text{Ni}_{1-x}\text{As}_2$ ss, and probably with oregonite.

The Fe-Ni Phases

At 800°C there is almost complete solid solution between cubic body-centered αFeNi (called kamacite when in meteorites) and face-centered γFeNi (called taenite when in meteorites), the solvus extending from 1.5 to 4 weight per cent nickel (Hansen and Anderko, 1958). However, although γFeNi extends from 4 to 100 per cent nickel at 800°C, a metastable body-centered quench product is produced for γ phases containing up to approximately 34 weight per cent nickel (Owen and Sully, 1939). The

X-ray patterns of α and α_2 are similar except at high angles of 2θ (the back-reflection region), where certain weak peaks of α_2 become diffuse. The mineral awaruite, Ni_3Fe , is not stable at 800°C.

Runs containing large percentages of the metal phases cannot be finely ground, and so conventional powder mounts for X-raying cannot be made. Instead, a flat surface was ground onto the metallic chunks, and these polished mounts were then placed on the X-ray diffractometer. By this method α and γ FeNi can readily be distinguished although peaks in the back-reflection region cannot be resolved.

The solubility of arsenic in metal was investigated for pure iron, pure nickel, and an alloy containing 25 weight per cent nickel, by examining a series of polished sections containing progressively increasing amounts of arsenic. To assure equilibrium these runs were first heated at temperatures up to 915°C and then annealed at 800°. All were kept at or above 800°C for at least 4 months. The results indicate that αFe can take at least 9.03 and probably less than 10.11 weight per cent arsenic into solid solution. γNi mixed with 8.73 weight per cent arsenic indicated a eutectoid mixture of metal + arsenide. Runs with 6.23 and 4.00 weight per cent arsenic contained no eutectoid intergrowths but did have trace amounts of another metallic phase, harder than the γNi but in appearance different from $\beta\text{Ni}_5\text{As}_2$. The alloy containing an Fe/Ni ratio of 3/1 can take at least 7.96 weight per cent arsenic into solid solution. The several per cent arsenic that can go into solid solution appears to produce a significant expansion in the unit cell edge of γFeNi ss. Thus, the maximum a_0 value for FeNi containing no arsenic is 3.5690 Å (Pearson, 1958), whereas measurements of the (111) spacing on two samples having compositions fairly similar to each other indicate $a_0 = 3.6105$ and 3.6117 Å.

Arsenic depresses the melting temperatures of iron and nickel. When pure they melt at 1534° and 1455°C, re-

spectively, whereas they form binary eutectics with arsenides at 835° and 895°C, respectively (Hansen and Anderko, 1958). These values are further depressed in the ternary field, so that liquid in equilibrium with metal, judged on the basis of differential thermal analyses, occurs even below 790°C.

HEATING EXPERIMENTS ON MONOCLINIC PYRRHOTITES

*G. Kullerud, B. R. Doe,¹⁸ P. R. Buseck,
and P. F. Tröften¹⁹*

Pyrrhotite occurs in at least two natural crystallographic modifications—hexagonal and monoclinic. These forms are commonly encountered, either together or singly, in studies of ores. It is not known whether they are polymorphs or whether the inversion from one modification to the other involves a compositional change. In many mines monoclinic pyrrhotite formed through inversion of hexagonal pyrrhotite. Grønvold and Haraldsen (1952) reported from their work on synthetic materials that low-temperature monoclinic pyrrhotite inverts to the hexagonal form at about 320°C.

It would be desirable to extend the pyrrhotite geothermometer to include not only the hexagonal (Arnold, 1962) but also the monoclinic form. To explore the feasibility of such extension, a number of natural monoclinic pyrrhotites were heated in evacuated, sealed silica-glass tubes.

Hexagonal pyrrhotite has a strong, well defined (102) spacing whose exact position, dependent on composition, occurs at a 2θ between 43.5° and 44.0° when $\text{CuK}\alpha$ radiation is employed. X-ray diffraction patterns of monoclinic pyrrhotite contain two reflections, the (202) and ($\bar{2}$ 02), in this 2θ region. The appearance of one, two, or three peaks on the X-ray

powder diffraction chart was taken as indication of the occurrence of monoclinic or hexagonal or both types of pyrrhotites in the samples.

Most of the samples used in this study are associated with pyrite. They were collected at the Vaddas no. 1 and 2 mines of Norway; at Balmat, New York; at Tem Piute, Nevada; and at Concepción del Oro, Mexico. The Tem Piute and Concepción del Oro deposits are contact metasomatic deposits; Balmat is a high-temperature conformable ore body; and the Vaddas deposits are hydrothermal.

Monoclinic pyrrhotites were completely converted to the hexagonal form when heated for 0.1 hour at temperatures above 320°C, as seen from figure 89. The specific annealing temperature is difficult to establish in these short runs, because the time is insufficient to allow the temperature of the sample to equilibrate with that of the furnace. It is noted from figure 89 that below 320°C monoclinic and hexagonal pyrrhotite coexist for long periods. The transition of monoclinic to hexagonal pyrrhotite takes place in a year at 260°C.

In attempting to use monoclinic pyrrhotite as a geothermometer, Arnold and Reichen (1962) heated pyrrhotite at 600°C for 18 hours. This appears to be a dangerous procedure, for in runs where the Tem Piute (Buseck, *Year Book 61*) and Balmat specimens were heated at temperatures above 455°C for 0.1 hour significant decreases in the (102) spacing occurred in two of the three specimens. For example, d_{102} of one of the Balmat specimens decreased from 2.056 Å at 346° and 455°C to 2.054 Å at 555°C and 2.051 Å at 600°C, showing that at 555° and 600°C the pyrrhotites become more iron deficient.

The other Balmat sample showed no effect from incubation at 600° but gave $d_{102} = 2.059$ Å at all temperatures. The rapid changes in the Tem Piute and one of the Balmat specimens might be due to reaction with mineral impurities or to the presence of catalyzing agents producing

¹⁸ U. S. Geological Survey.

¹⁹ Norges Geologiske Undersøkelse, Trondheim, Norway.

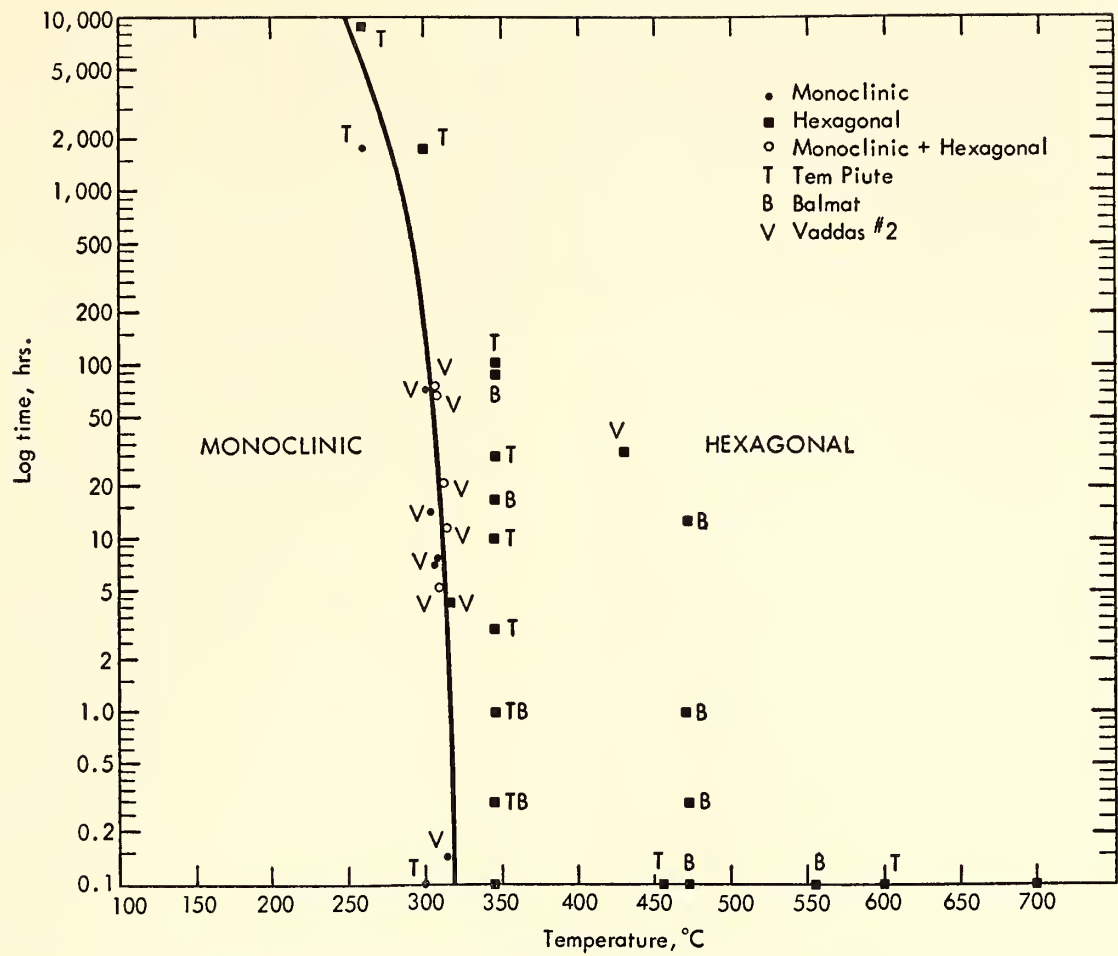


Fig. 89. Results of heating natural monoclinic pyrrhotites over periods lasting from 6 minutes to 1 year and at temperatures ranging from 265° to 470°C. Conversion to the hexagonal form occurs in 1 year at 265°C.

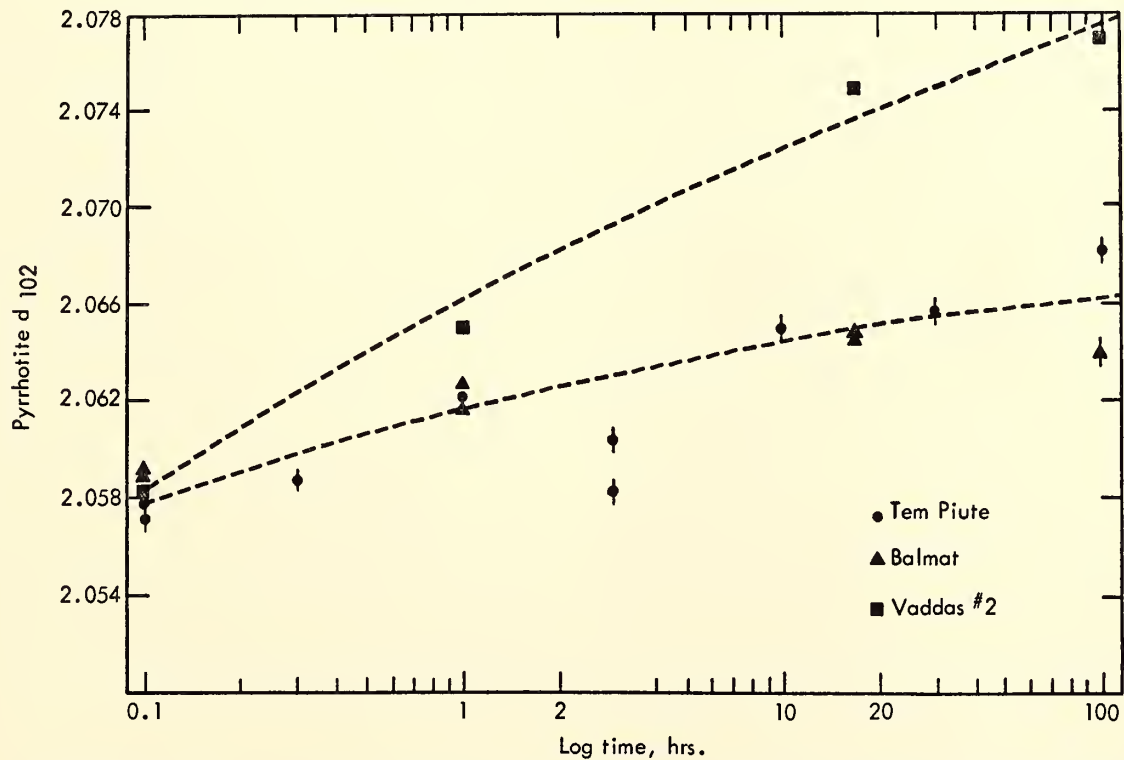


Fig. 90. Measured d_{102} values of natural pyrrhotites, which were converted from the monoclinic to the hexagonal form by heating for various periods of time.

rapid pyrrhotite-pyrite equilibration. As the conversion of monoclinic pyrrhotite to hexagonal pyrrhotite is established in 0.1 hour at 346°C, most annealing was done at this time and temperature, with some runs at longer times (fig. 90). All 0.1-hour runs annealed at temperatures between 346° and 472°C have (102)

spacings between 2.056 and 2.059 Å, indicating compositions between 46.45 and 46.70 atomic per cent Fe. On the pyrrhotite-pyrite solvus (Arnold, 1962) this would give temperatures equivalent to 465° to 516°C, a highly restricted range considering that four deposits are involved.

One of the Balmat specimens permits a comparison with the results of thermometry using the FeS-ZnS geothermometer. The annealed monoclinic pyrrhotite indicates a temperature of 465°C, whereas coexisting sphalerite gives 440°C, with no corrections made for pressure. Considering the pressure effects involved the agreement is good. Results on annealed monoclinic pyrrhotite are, therefore, encouraging. If monoclinic pyrrhotite is the primary form (i.e., not formed through the inversion of hexagonal pyrrhotite), however, the monoclinic pyrrhotite-pyrite rather than the hexagonal pyrrhotite-pyrite solvus is applicable. The d_{102} value obtained after heating monoclinic pyrrhotite that did not originally have hexagonal symmetry cannot be used to obtain a temperature of formation but serves only to indicate a composition. A temperature estimate cannot be obtained, since the appropriate solvus is not known. Until the mechanism involved in the monoclinic-hexagonal pyrrhotite phase change is understood, there is no reason to assume that the extension of the hexagonal solvus to lower temperatures would apply to the monoclinic form.

Runs annealed at 346°C for periods longer than 0.1 hour (fig. 90) exhibit increases in the lattice spacings, suggesting equilibration by pyrite exsolution. The Balmat specimen had no observed impurities, and the d value derived from the (102) reflection coincided with the temperature of heating after 17 hours. Microscopic examination of the powder showed the development of pyrite blebs in runs annealed for 1 hour or longer. No exsolution was noted in any runs annealed at 472°C. Although Arnold (1962, p. 87)

did not find any pyrite exsolved from pyrrhotite heated at 400°C for 17 days, the clearly visible exsolution in 1 hour at 346°C in a Balmat pyrrhotite indicates that heating periods should be kept short; again, 0.1 hour appears adequate.

The rapid increase in the (102) spacing of the Vaddas specimen with time was far greater than was expected from the experience gained through heating of samples from other localities (fig. 90). The spacings are indicative of a temperature much lower than the temperature of annealing. Nothing unusual was noted in the 0.1-hour run at 346°C. The explanation for this anomalous behavior of the Vaddas material is suggested in polished sections. A gray nonopaque substance was observed surrounding sparse grains of pyrite in the runs annealed for 1 hour or longer. The gray substance was in turn surrounded by a fragile network of pyrrhotite. The gray matter increased at the expense of the pyrite in the 17-hour run. In the 96-hour run pyrite was apparently consumed entirely. Although the gray phase in any experiment never exceeded a few per cent, its formation must have involved reaction with pyrrhotite, resulting in an increase in d_{102} of the pyrrhotite. The difficulties arising from such reactions were apparently of no consequence in the 0.1-hour runs.

Conclusions from the present investigation are:

1. Heating for 0.1 hour in the range 346° to 470°C is desirable for conversion of monoclinic pyrrhotite to the hexagonal form. Under these conditions the pyrrhotite retains its composition, which can be determined through d_{102} measurements after inversion.

2. Results on heated monoclinic pyrrhotite from Balmat, New York, are in agreement with temperatures obtained from the FeS-ZnS solvus (Kullerud, 1953).

3. Monoclinic pyrrhotites from four widely separated localities after being converted to the hexagonal form give

d_{102} values all of which lie within the narrow range 2.056 to 2.059 Å. This restricted range in d , which corresponds to a variation from 46.45 to 46.70 atomic per cent Fe, suggests that monoclinic pyrrhotite, at least when coexisting with pyrite, has nearly constant composition.

PYRRHOTITE PHASE RELATIONS AT LOW TEMPERATURES

*K. v. Gehlen*²⁰

At temperatures above approximately 300°C the pyrrhotite (Fe_{1-x}S) phase has hexagonal B8-type structure and forms appreciable solid solution with pyrite. At lower temperatures four different pyrrhotites have been reported to exist:

1. Stoichiometric FeS (troilite) with hexagonal B8-type superstructure (Grønvold and Haraldsen, 1952).

2. Intermediate pyrrhotite with homogeneity range between $\text{Fe}_{0.935}\text{S}$ and $\text{Fe}_{0.900}\text{S}$, corresponding to a range in Fe from 48.32 to 47.37 atomic per cent. This phase has hexagonal B8-type structure (Grønvold and Haraldsen, 1952).

3. Monoclinic pyrrhotite with composition near $\text{Fe}_{0.877}\text{S}$, corresponding to 46.72 atomic per cent Fe (Byström, 1945; Grønvold and Haraldsen, 1952).

4. Tetragonal pyrrhotite with FeS composition recently found in ores by Kouvo and Vuorelainen (1962). This type was not encountered in the present experiments.

Lamellar pyrrhotites that exhibit two different phases in polished sections and that have already been described from ores by Schneiderhöhn (1922) were studied by X-ray powder diffraction techniques. Specimens from four localities gave $d_{102} = 2.0924 \pm 0.0022$ Å (mean), which, by application of the d_{102} versus composition curve by Arnold and Reichen (1962), indicates stoichiometric hexagonal FeS. This composition was also indicated by electron microprobe analyses of this phase occurring in lamellar pyrrhotite

from Dracut, Connecticut, and is in agreement with the findings by Kouvo and Vuorelainen (1962) and with the composition postulated by Ramdohr (1955).

The second phase in the lamellar pyrrhotites is more abundant than the one discussed above; consequently, the intensity of its 102 peak is much higher than that of the first phase. Measurements of d_{102} for this strong peak gave 2.0704 ± 0.0015 Å, corresponding to a composition of 47.69 ± 0.14 atomic per cent Fe. This Fe content is 0.63 atomic per cent less than the 48.32 atomic per cent Fe given by Grønvold and Haraldsen (1952) as the limit of solubility of Fe in intermediate pyrrhotite at 290°C.

Hexagonal pyrrhotite containing 49.18 atomic per cent Fe was synthesized from the elements at 700°C. After a homogeneous product was obtained the temperature was lowered to 94°C, where it remained for 56 days. X-ray powder diffraction studies on the quenched product revealed the presence of two apparently hexagonal pyrrhotite phases with $d_{102} = 2.0922 \pm 0.0006$ Å and $d_{102} = 2.0766 \pm 0.0005$ Å, respectively. The first d_{102} value indicates stoichiometric FeS; the second, an Fe content of 48.26 ± 0.06 atomic per cent, agreeing within the limit of error of measurement with the limit of solution of Fe in intermediate pyrrhotite at 290°C given by Grønvold and Haraldsen (1952).

Heating of pyrrhotite with 49.18 atomic per cent Fe (which had previously been homogenized at 700°C) at 300°C for 51 days produced no measurable change. This indicates that hexagonal pyrrhotite containing 49.18 atomic per cent Fe might be stable at 300°C.

Efforts to find natural mixtures of intermediate and monoclinic pyrrhotites were unsuccessful. Such an assemblage if located would indicate the limits of solubilities of sulfur in intermediate pyrrhotite and of iron in monoclinic pyrrhotite. During the study of natural assemblages it was found, however, that

²⁰ University of Erlangen-Nürnberg.

a number of specimens earlier assumed to contain monoclinic pyrrhotite actually contain mixtures of stoichiometric hexagonal FeS and intermediate pyrrhotite.

Next, pyrrhotite of Fe_7S_8 composition was synthesized at 700°C , homogenized over a 265-hour period, and quenched. X-ray powder diffraction patterns showed one phase. Then this pyrrhotite was heated at 300°C for 50 days and quenched. X-ray powder diffraction patterns now showed two peaks with $d = 2.062$ and 2.054 \AA in the region where previously the hexagonal d_{102} peak existed. These two peaks are slightly closer together on the chart than those of monoclinic pyrrhotite at room temperature ($d = 2.062$ and 2.051 \AA). However, there is little doubt that they are reflections from monoclinic pyrrhotite, which apparently undergoes a change in β as a function of temperature. These results indicate that synthetic monoclinic pyrrhotite is stable to 300°C , whereas Kullerud and co-workers found that natural monoclinic pyrrhotite inverts to the hexagonal form even at 265°C .

This monoclinic pyrrhotite was reheated at 350°C for 6 minutes, during which period it completely converted to the hexagonal form with a d_{102} value practically the same as that of the original material.

LOW-TEMPERATURE SULFIDE SYNTHESIS

G. Moh

Covellite

Two kinds of covellite have been described from ores: ordinary covellite, and so-called "blaubleibender" covellite, which is distinguished from the ordinary covellite under oil immersion ($N_D = 1.515$) in polished sections. It does not display the strong reflection pleochroism ($R_0 = \text{purple red}$) so typical for ordinary covellite, but instead produces rich blue to soft pale or even violet-blue colors (Ramdohr, 1960). Frenzel (1959) synthesized blaubleibender covellite at room temperature by treating digenite and

chalcocite with inorganic acids such as HNO_3 . Analysis of the products revealed that the synthesized material contains 1.5 to 2.0 weight per cent Cu more than that of stoichiometric CuS. Frenzel concluded that blaubleibender covellite is a copper sulfide and did not consider the possibility that oxygen from the strong acids might substitute for or oxidize some of the sulfur in CuS.

In the present study synthesis was undertaken in the absence of oxygen. Synthetic digenite and chalcocite were the starting materials. They were heated separately in the presence of carbon disulfide containing only small amounts of dissolved sulfur. Reactions took place in evacuated reflux distillation vessels equipped with a reflux condenser and heated on a constant-temperature water bath.

After 2 weeks on a 50°C bath the digenite and chalcocite were found to have reacted to about 95 per cent blaubleibender and about 5 per cent ordinary covellite. Additional experiments containing considerable amounts of sulfur dissolved in carbon disulfide produced only ordinary covellite.

Experiments in silica-glass tubes with digenite and ammonium sulfide produced blaubleibender covellite in 48 hours and at temperatures ranging from 0° (ice bath) to 155°C . At 160°C ordinary covellite formed.

In further experiments also in evacuated silica-glass tubes but with copper filings and sulfur, after 4 weeks at 50°C , a disequilibrium assemblage in individual grains contained chalcocite in the center with successive rings of digenite, blaubleibender covellite, and ordinary covellite. At 125°C , digenite and chalcocite when heated with slight excess of sulfur rapidly formed blaubleibender covellite. In these experiments rims of blaubleibender covellite always appeared between digenite and ordinary covellite. This breakdown is very sluggish at low temperatures but becomes rapid at more elevated ones. After 10 hours at 400°C

about 7 per cent of blaubleibender covellite was found to have broken down.

The X-ray powder diffraction pattern obtained for blaubleibender covellite is similar to that given by Frenzel (1959). Several of the weak reflections occurring in the pattern of ordinary covellite are missing in the pattern of blaubleibender covellite. It apparently is a stable phase in the system Cu-S at temperatures below $157^{\circ} \pm 3^{\circ}\text{C}$ and has higher symmetry than ordinary covellite.

Tin Sulfides

Synthetic SnS (herzenbergite) was heated at 50°C with carbon disulfide containing appreciable amounts of dissolved sulfur. The equipment and method were the same as described in the covellite section. The reaction rates are slow at this temperature; even after 96 days only 1 per cent Sn_2S_3 had formed. It occurred in oriented intergrowths with the original herzenbergite. As the alleged compound Sn_3S_4 was not obtained, we conclude that it is not stable at 50°C .

Pyrrhotite

Stoichiometric FeS was treated at 50°C with CS_2 containing appreciable

amounts of dissolved sulfur. After 38 days the product was found to be very anisotropic hexagonal pyrrhotite. Treatment of the same FeS with ammonium disulfide at 130°C for 4 days produced monoclinic pyrrhotite.

Nickel Sulfides

Efforts were made to synthesize the alleged Ni_2S compound, which in natural occurrences contains small amounts of iron and copper. Dry experiments in which the elements nickel, sulfur, and traces of iron and copper were mixed in silica tubes produced only metal and heazlewoodite at 125°C . Ni_2S was not obtained at 125°C . Kullerud and Yund (1962) demonstrated that Ni_2S does not exist at 200°C or higher temperatures.

Bravoite

Silica-tube experiments for 96 days at 50° – 55°C containing Fe-Ni sponge and CS_2 with dissolved sulfur, as well as dry experiments for 4 months at 125°C containing (Ni,Fe)S powder and excess sulfur, all produced bravoite in agreement with the observations by Kullerud (*Year Book 61*), who used a different reaction system.

SULFIDE-SILICATE RELATIONS

G. Kullerud and H. S. Yoder, Jr.

Recent experiments have demonstrated that sulfur readily reacts with many of the common rock-forming silicates over wide temperature-pressure ranges. Elements (like iron, manganese, nickel, cobalt, and copper) originally present in the silicates react to produce sulfides and oxides. Other reaction products are quartz or non-ferrous silicates when elements like magnesium and calcium are present in the original silicates. When the original silicates contain even only moderate amounts of iron and related elements, the action of sulfur changes the mineralogy of the rock profoundly. Moreover, the

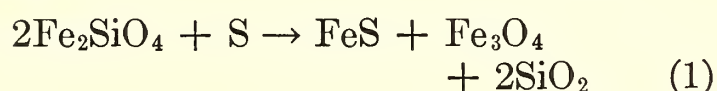
addition of a few per cent of sulfur to common rocks can bring about formation of typical sulfide-oxide ore assemblages.

Thus an understanding of the reactions leading to the formation of sulfide ores in magmatic and metamorphic rocks can be obtained through systematic studies of pertinent silicate-sulfide systems. Detailed information on the phase relations of important silicate and sulfide systems has been obtained at this laboratory through a large number of independent studies conducted over wide pressure-temperature ranges.

These known systems serve as

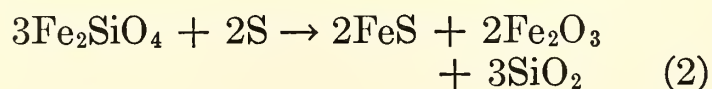
boundaries of the sulfide-silicate systems now being explored. Basic information on some of the pertinent reactions can be obtained through a study of the phase relations in a system such as Fe-S-O-SiO₂. A series of experiments was conducted by heating synthetic Fe₂SiO₄ (fayalite) with various amounts of sulfur in collapsible gold tubes at 800°C and 2000 bars. Under these conditions Fe_{1-x}S (pyrrhotite) is the only stable sulfide; FeO, Fe₃O₄, and Fe₂O₃ are the stable iron oxides; and Fe₂SiO₄ (fayalite) is the stable silicate.

Fe₂SiO₄ reacts rapidly with sulfur under the outlined conditions; sulfur combines with iron to give pyrrhotite. If the mole fraction of sulfur present is less than one-third, the univariant assemblage Fe₂SiO₄ + FeS + Fe₃O₄ + SiO₂ occurs; and if the mole fraction of sulfur in the Fe₂SiO₄ + S starting materials equals one-third, the reaction can be described as



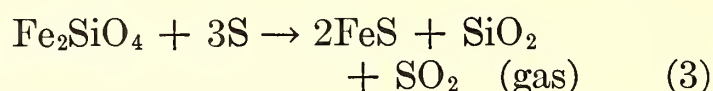
Considering the molecular weights involved, it is noted that only small amounts of sulfur are required to produce large amounts of pyrrhotite, magnetite, and quartz from fayalite.

The amount of magnetite decreases when sulfur is added beyond the 33⅓ mole per cent indicated by reaction 1. At the same time hematite (Fe₂O₃) appears as a phase and increases rapidly in amount with an increase in sulfur up to 40 mole per cent. A univariant assemblage containing pyrrhotite + magnetite + hematite + quartz, therefore, is produced when $33\frac{1}{3} < \text{S} < 40$ mole per cent. When the amount of sulfur added to fayalite equals 40 mole per cent the reaction may be expressed as

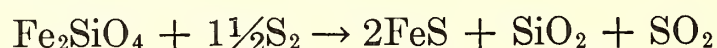


When more than 40 mole per cent sulfur is added to fayalite the amount of hematite decreases and SO₂ appears in

increasing amounts. When the amount of sulfur reaches 75 mole per cent hematite can no longer exist as a phase and the reaction can be described as



Isaacs in 1961 (as cited by Du Fresne and Anders, 1962*a,b*) synthesized FeS by heating (Fe,Mg)₂SiO₄ with sulfur at 1000°C. Du Fresne and Anders (1962*a,b*) suggested that the reaction



may be responsible for generation of SO₂ during the evolution of carbonaceous chondrites. However, quartz, which is a significant product of reaction 3, is absent, or present only in accessory amounts, in meteorites (Mason, 1962).

The phase relations in the Fe-S-O-SiO₂ system at 800°C and 2000 bars as deduced from experiments with fayalite and various amounts of sulfur are shown in the diagram of figure 91. (The univariant assemblages are Fe-FeO-FeS-Fe₂SiO₄, Fe-Fe₂SiO₄-FeS-SiO₂, FeO-Fe₃O₄-FeS-Fe₂SiO₄, Fe₃O₄-FeS-Fe₂SiO₄-SiO₂, Fe₃O₄-Fe₂O₃-FeS-SiO₂, Fe₂O₃-FeS-SO₂-SiO₂, Fe₂O₃-SiO₂-O-SO₂, and FeS-SiO₂-S-SO₂.)

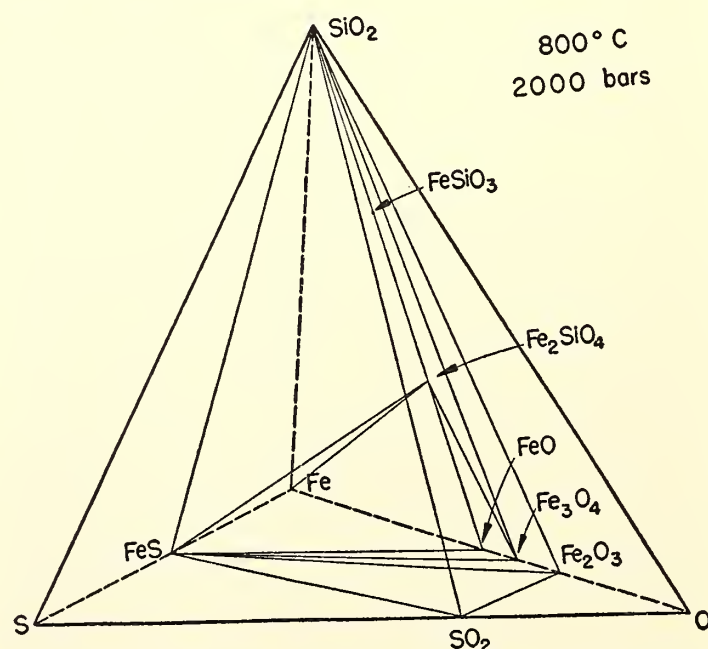
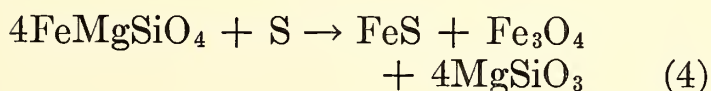


Fig. 91. Phase relations in the Fe-S-O-SiO₂ quaternary system at 800°C and 2000 bars. For simplicity in presentation, the limited solid solutions displayed among some of the phases, such as Fe_{1-x}S, are not shown in this diagram.

In one experiment fayalite containing a small amount of nickel was heated with 33⅓ mole per cent S at 800°C and 2000 bars. Polished sections of the products showed, in addition to pyrrhotite, magnetite, and quartz, very small amounts of pentlandite also. The pentlandite, as discussed in a separate section on the Fe-Ni-S system, was formed through reaction between pyrrhotite and $(\text{Ni,Fe})_{3\pm x}\text{S}_2$ during the quenching period at the termination of the experiment. It is intimately associated with pyrrhotite, and the two display textures very similar to those commonly observed in pentlandite-pyrrhotite ores.

Systematic experimentation has not as yet been performed on mixtures of Fe,Mg olivines and sulfur. However, some experiments, described below, indicate that magnesium in silicates probably does not react to form sulfides.

Olivines containing equal amounts of iron and magnesium would react with sulfur as follows:

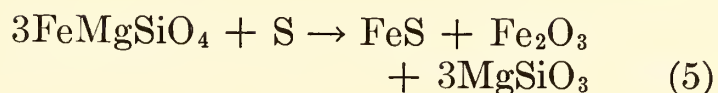


This reaction may have taken place in many meteorites. The reaction products—troilite, magnetite, and enstatite—are all common minerals in meteorites.

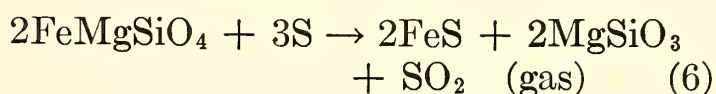
The effect of sulfur may be illustrated by considering a troctolite consisting of 50 weight per cent olivine with Fe:Mg ratio = 1 and 50 weight per cent plagioclase. Plagioclase does not react measurably with sulfur. The addition of 2.3 weight per cent sulfur is sufficient to break down all olivine in this rock. After reaction, the rock, aside from 48.88 per cent unchanged plagioclase, would contain 6.25 per cent FeS, 16.42 per cent Fe_3O_4 , and 28.45 per cent MgSiO_3 .

If more than 20 but less than 25 mole per cent sulfur is reacted with this olivine, hematite appears as a phase together with pyrrhotite, magnetite, and enstatite. The amount of magnetite decreases with increasing amounts of sulfur and is absent when S = 25 mole

per cent. The reaction may be expressed



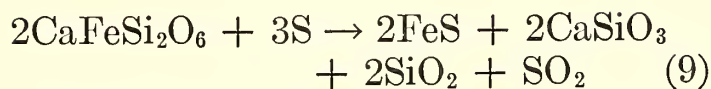
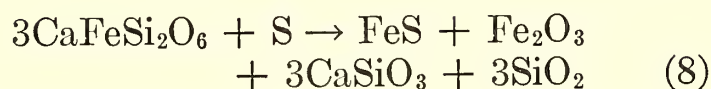
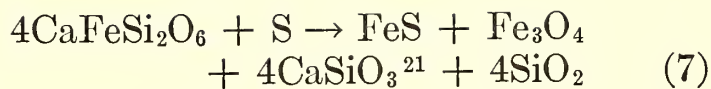
If more than 25 mole per cent sulfur reacts with FeMgSiO_4 , the amount of hematite decreases and SO_2 (gas) is produced. When the amount of sulfur reaches 60 mole per cent, hematite can no longer exist as a phase and the reaction can be expressed



The above discussion emphasizes that sulfur may play an important role in ultrabasic and basic rocks. Small amounts of it can react with certain silicates such as olivines and produce sulfide ores of the pyrrhotite-pentlandite type. Moreover, magnetite, hematite, or mixtures of the two form by reactions with oxygen made available through the breakdown of olivine as demonstrated in the above equations. Sulfur combines to form sulfides with some of the ferrous metals that previously occurred in the silicates. The remaining ferrous metals react with oxygen made available through breakdown of the silicates to form oxides. The state of oxidation of these metals increases with increase in sulfur. Thus sulfur has an oxidizing effect on the ferrous metals, which do not enter the sulfide phase, and in effect the amount of sulfur determines which oxide assemblage is stable at any given temperature. Therefore, oxidation in a rock can be accomplished by the addition of sulfur; the addition of oxygen to the system is not necessary.

The role of sulfur in certain metamorphic processes was indicated by the results of exploratory experiments with hedenbergite ($\text{CaFeSi}_2\text{O}_6$), almandite ($\text{Fe}_3\text{Al}_2(\text{SiO}_4)_3$), and Fe cordierite ($\text{Fe}_2\text{Al}_4\text{Si}_5\text{O}_{18}$).

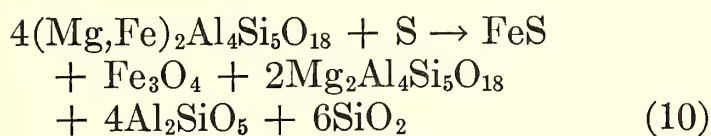
The experiments conducted at 800°C and 2000 bars indicate the following reactions between hedenbergite and sulfur:



Almandite reacts with sulfur at 750°C and 2 kb to form pyrrhotite + quartz + cordierite + pyroxene.

Cordierite containing equal amounts of magnesium and iron would probably react with small amounts of sulfur to form pyrrhotite, magnetite, Mg cordierite, Al_2SiO_5 , and quartz.

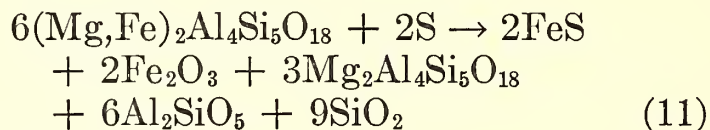
All Fe,Mg cordierite reacts when 20 mole per cent sulfur is present according to the reaction



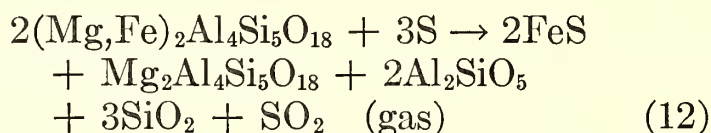
Further addition of sulfur leads to the formation of hematite in addition to the above phases. The amount of hematite increases and the amount of magnetite decreases with increasing sulfur. When

²¹This wollastonite may contain some iron in solid solution.

the amount of sulfur reaches 25 mole per cent, magnetite can no longer exist and the reaction can be described



Increase in sulfur beyond 25 mole per cent leads to the formation of SO_2 (gas) and a corresponding decrease in hematite. When 60 mole per cent sulfur or more occurs hematite is no longer stable. For 60 mole per cent sulfur the following reaction is indicated:



These reactions point up the very significant role played by sulfur in determining the stable assemblage of silicate minerals in both igneous and metamorphic rocks. It would appear that the recognition of such reactions in nature would be important clues in the discovery of ore bodies. The effect of sulfur in determining the apparent oxidation state of a rock without the addition or subtraction of oxygen is of significance. Indeed, in some rocks sulfurization may be a more important process than oxidation.

THE AGES OF ROCKS AND MINERALS

G. L. Davis, G. R. Tilton, L. T. Aldrich,²² S. R. Hart,²² R. H. Steiger, O. Kouvo²²

Our work in the field of geochronology continues to utilize five radioactive clocks to determine the time of formation of minerals. It is known that the clocks do not always keep the same time, but each year's work brings further insight into the problem, and this knowledge can be used to study diffusion processes and to delimit conditions of metamorphism. A large part of our recent effort has been a search for the conditions that alter the time record of one or more of the clocks.

Studies of the effects of contact metamorphism on uranium-lead ages from zircon are under way. It has been

found that such metamorphism may produce sudden loss of lead but that the temperature at which the loss takes place may vary considerably from one zircon to another.

New lead age measurements have been completed on rocks from the Karelian basement complex and associated gneiss domes in eastern Finland. Previous results on these rocks were used to suggest that loss of lead by continuous diffusion is an important cause of discordant lead ages. The additional observations

²² Department of Terrestrial Magnetism.

strongly support the continuous diffusion hypothesis. Zircons from Svecofennian metagraywackes in southwestern Finland have yielded an age of 2300 m.y.—the first indication found for ages between 2600 and 1900 m.y. in Finland.

The zircon age studies on Coutchiching sediments and associated igneous rocks at Rainy Lake, Ontario, reported last year, have been augmented by rubidium-strontium measurements on whole-rock samples. These sediments are known to have been deposited earlier than 2600 m.y. ago, the data indicating that their source rocks are but little older than this.

A promising start has been made on resolving the complex history of the Alps by means of potassium-argon ages from hornblende. Hornblende appears to record earlier periods of metamorphism than biotite does.

Evaluation of Zircon Ages

In *Year Book 59* we suggested a mechanism for the loss of lead from zircon by continuous diffusion, at a rate characteristic of each sample. We also inferred that the activation energy for lead diffusion is generally low, 10 kcal/mole or less, up to a temperature of perhaps 500°C. This model clarified two contrasting features of zircon ages: (1) zircons from Precambrian shield areas often have discordant ages indicating loss of lead even though no metamorphic event (episode of heating) can be recognized to explain the loss; (2) where rocks have been subjected to regional metamorphism intense

enough to remove all the radiogenic strontium and argon from biotite, the rate of diffusion of lead in zircon did not increase appreciably.

Studies based on regionally metamorphosed rocks have the disadvantage that the temperature-time history of the metamorphism is poorly known. This uncertainty in thermal history can be reduced considerably by utilizing a contact-metamorphic complex consisting of an intrusive and its surrounding formations. If the size of the body, its temperature, and the temperature of the enclosing rock at the time of intrusion can be estimated, the thermal effects at various distances from the intrusive can be calculated from heat conduction theory. Hart (*Year Books 60 and 61*) has already discussed the application of this method to biotite, hornblende, and potassium feldspar in the enclosing rock of an intrusive stock in the Front Range at Eldora Colorado. We are extending this study to include zircon. The stock is a quartz monzonite mass about 2 by 2 miles in outcrop. The stock is 55 m.y. old, and intrudes Precambrian gneisses and schists of the Idaho Springs formation. The zircon ages are given in table 23. In figure 92 the ages of the zircon samples are superimposed on the pattern of ages reported previously by Hart for biotite and hornblende. It is evident from the U^{238} - Pb^{206} ages that the zircons near the contact have lost lead just as the biotite and hornblende lost strontium and argon. As indicated by distance from the contact,

TABLE 23. Effect of Contact Heating on Zircon Ages, Colorado

Location	Distance from Contact, ft	Age, million years			
		$\frac{Pb^{206}}{U^{238}}$	$\frac{Pb^{207}}{U^{235}}$	$\frac{Pb^{207}}{Pb^{206}}$	$\frac{Pb^{208}}{Th^{232}}$
Eldora	2	220	335	1255	57
Eldora	12	290	435	1395	110
Eldora	50	1280	1405	1600	1300
Eldora	14,000	1380	1420	1480	1490
Jamestown	6	160	245	1175	180
Jamestown	56	195	300	1210	330

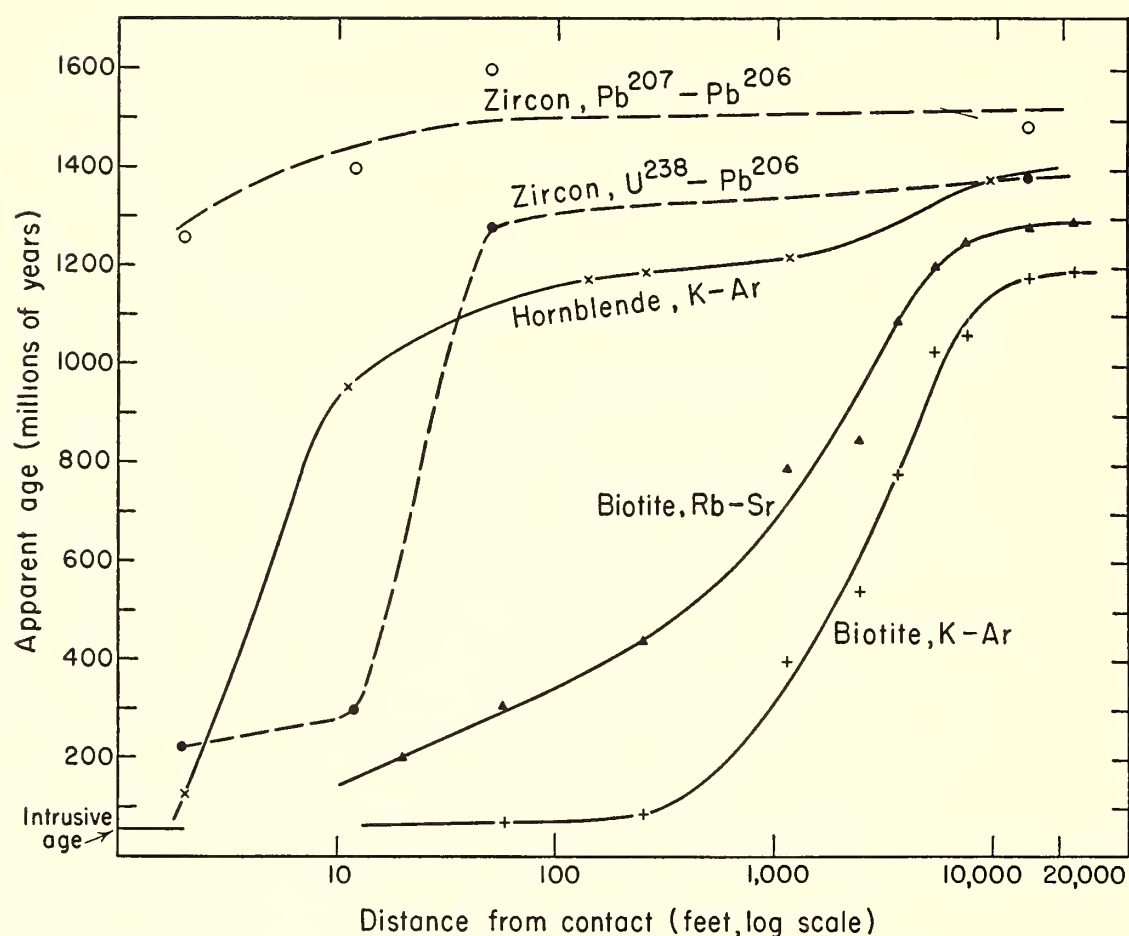


Fig. 92. Variation of measured age with distance from an intrusive contact at Eldora, Colorado, for zircon, biotite, and hornblende.

zircon is less affected by temperature than biotite. Loss of argon from the hornblende and of lead from the zircon occurred at about the same temperature.

The fact that biotite from rocks of regionally metamorphosed areas has been repeatedly shown to have lost much or all of its radiogenic strontium and argon, whereas coexisting zircon has been little affected, can be explained on the basis of the contact pattern—that conditions of regional metamorphism may be similar to those obtaining at some distance from the contact.

All biotite samples in figure 92 are from pegmatites and have a crystal size of about 5 mm. Hart (*Year Book 61*) has shown that larger crystal size favors retention of argon and strontium in biotite. Smaller biotite crystals in granites and gneisses would lose these elements at even lower temperatures than the biotite in figure 92.

Table 23 also includes two zircons from Jamestown, Colorado, 15 miles northeast

of Eldora. The Jamestown stock, a granodiorite mass about 2 by 3 miles in extent, is intrusive into the Precambrian Silver Plume granite. It was presumably emplaced at the same time as the Eldora stock, about 55 m.y. ago. The Silver Plume granite is known to be at least 1400 m.y. old on the basis of biotite age determinations.

The zircon results are plotted on a concordia diagram in figure 93. A chord has been drawn from 1600 m.y. on concordia, the oldest age shown in table 23, through the four points near the origin, intersecting concordia again at 70 m.y., a time not appreciably different from the measured age of the intrusive. The closeness of fit of the experimental points to the chord supports the interpretation that 1600-m.y.-old zircons lost lead at the time of intrusion of the stocks, those closest to the contact losing the highest proportion. Any attempt to interpret the four most discordant zircons on the basis of a continuous diffusion model leads to

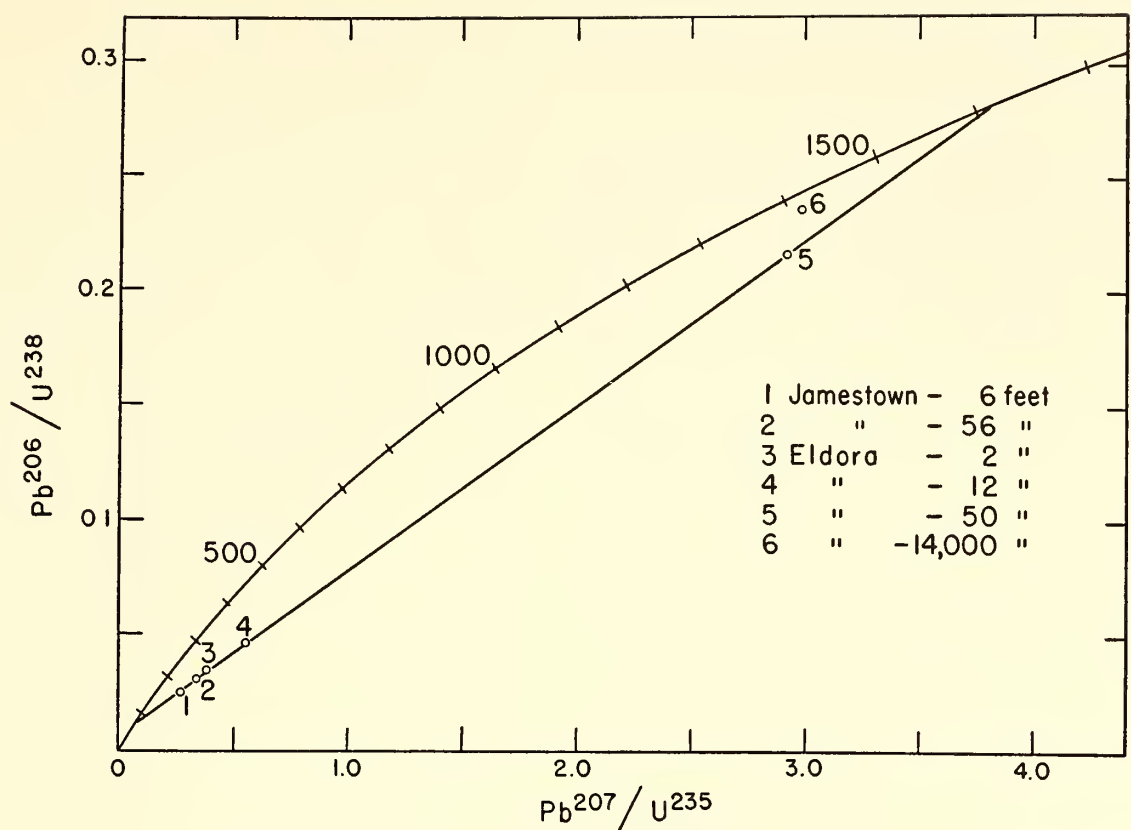


Fig. 93. Concordia diagram showing uranium-lead ratios for zircons in the vicinity of the Eldora and Jamestown, Colorado, stocks. The chord illustrates the pattern expected for samples 1610 m.y. old that lost varying proportions of lead episodically 75 m.y. ago.

an unreasonable age of many billions of years.

The failure of one sample, 14,000 feet from the contact at Eldora, to fit the chord satisfactorily is attributed to the possibility that the zircon from this granite-like rock is younger than the zircon from the remaining rocks. Since the Idaho Springs formation is a complex unit consisting of gneiss, schist, and granite-pegmatite, not all rocks will necessarily contain zircon of the same age.

Although episodic loss of lead at the time of intrusion of the stocks is indicated, it is unlikely that the zircon ages were concordant before that time, since zircons generally show loss of 10 per cent or more of their lead even when no metamorphic history is known. The pattern of figure 93 is probably the result of loss of about 10 to 20 per cent of lead by continuous diffusion earlier than 70 m.y. ago followed by additional loss at the time of intrusion of the stocks.

An interesting feature of the Eldora data is illustrated in figure 94. That the

concentrations of uranium and thorium in the zircons appear to be related to the distance from the contact suggests addition of these elements to the minerals near the contact. All samples were cleaned in hot 6 M nitric acid before analysis, so that none of the measured uranium and thorium is loosely bound. Gastil and Delisle (1962) have described a similar relationship in the α activities of zircon near intrusive contacts in Cali-

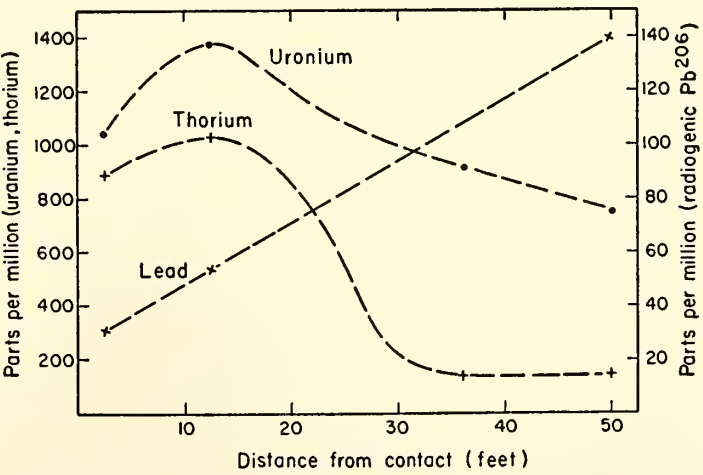


Fig. 94. Change in concentration of uranium, thorium, and lead with distance from the Eldora stock.

fornia. The same pattern obtains at Jamestown, according to our α -activity data.

Figure 92 indicates loss of considerable amounts of lead from the Eldora zircons near the contact. To estimate the temperature we assume that the stock was intruded as a magma at 780°C with latent heat of crystallization of 80 cal/g into country rock at an ambient temperature of 35°C. Under these conditions the temperature at the contact would be 510°C. The maximum temperature attained 50 feet from the contact was some 10° to 50°C lower, depending on which of several reasonable geometrical arrangements is used for the thermal calculations. These are minimum temperatures, since higher temperatures could have been produced in the vicinity of the contact by post-intrusion convection in the magma.

Most of the zircons used in this study were not typical of the zircons generally

obtained from igneous rocks, sediments and metasediments. They were sub translucent to opaque, and so magnetic that separations were difficult. Only sample El-14000 resembled the usual transparent, nonmagnetic zircons. Further study of the chemical composition of these zircons is planned.

The Jamestown results are too fragmentary to discuss at length. The granodiorite, being more mafic, was probably intruded at a higher temperature than the quartz monzonite stock at Eldora. This could account for the extensive lead loss from the zircon 56 feet from the contact at Jamestown, whereas the Eldora 50-foot sample shows little, if any, loss.

Some pertinent studies have been made on rocks from Finland. In *Year Book 59* it was shown that five zircons from the Karelian basement complex and related mantled gneiss domes have ages consistent with the continuous diffusion

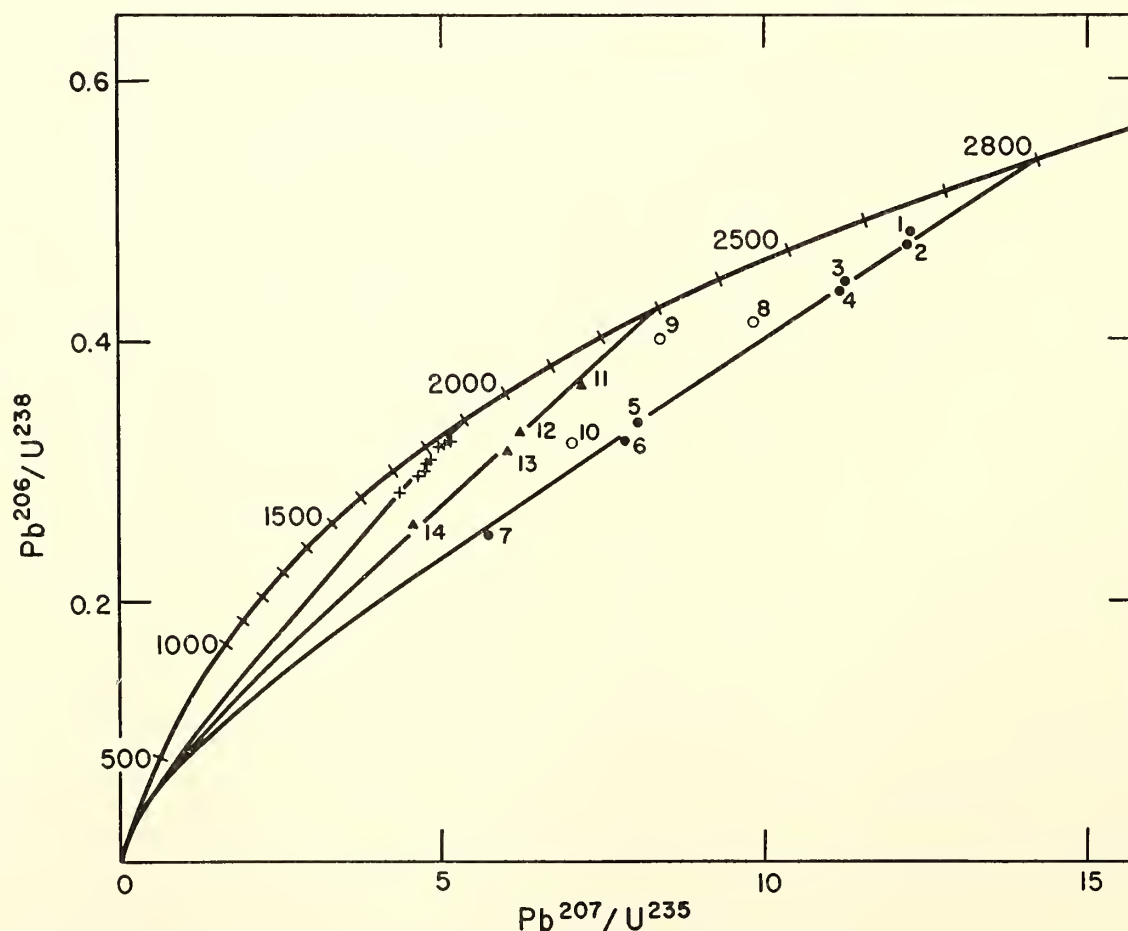


Fig. 95. Concordia diagram showing uranium-lead ratios for Finnish zircons. Points representing the zircons are compared with calculated ratios for minerals 2800, 2300, and 1900 m.y. old that lost lead by continuous diffusion. Closed circles, pre-Karelian basement complex of eastern Finland; open circles, mantled gneiss domes; triangles, Svecofennian graywackes near Tampere; crosses, intrusive rocks from the Svecofennian and Karelian belts.

TABLE 24. Mineral Ages from the Karelian Basement Complex

No. (fig. 95)	Location and Rock	Mineral*	Age, million years					
			Pb ²⁰⁶	Pb ²⁰⁷	Pb ²⁰⁷	Pb ²⁰⁸	Sr ⁸⁷ †	Ar ⁴⁰
			U ²³⁸	U ²³⁵	Pb ²⁰⁶	Th ²³²	Rb ⁸⁷	K ⁴⁰
1	Riihilahti, gneiss	z	2575	2660	2725			
2	Mätäsvaara, gneiss	z	2520	2660	2770	2750		
		b					1775	1740
		f					2410	
3	Suomussalmi, granodiorite	z	2400	2575	2725	2405		
4	Ilomantsi, granite	z	2360	2575	2750			
		b					1750	
5	Koli, gneiss	z	1890	2270	2650	1790		
6	Huhtilampi, gneiss	z	1820	2240	2640	1850		
	granite	b					2010	
		m					2630	
7	Sompujärvi, granite	z	1460	1960	2545	2215		
		f					2100	
8	Heinävaara Dome, granite-gneiss	z	2250	2440	2620	1275		
		b					1785	1740
		f					2580	
9	Kuopio Dome, granite-gneiss	z	2195	2300	2400			
		b					1715	
10	Sotkuma Dome, granite-gneiss	z	1810	2150	2470	1760		
		b					1760	1740
		f					2090	

* z, zircon; b, biotite; m, muscovite; f, potassium feldspar.
† Rb-Sr ages calculated using $1.39 \times 10^{-11} \text{ yr}^{-1}$ for the decay constant of Rb⁸⁷.

mechanism for lead loss. We now have measured ten zircons, three of them from gneiss domes. All the results are given in table 24, together with ages from micas and feldspars. The biotite ages are all about 1750 m.y., showing that this was a time of regional metamorphism. The zircon results are plotted on a concordia diagram in figure 95 (points 1–10). The curve intersecting concordia at 2800 m.y. is calculated for loss of lead by continuous diffusion from samples having an age of 2800 m.y. The value of the parameter, diffusion coefficient divided by the square of the crystal radius (D/a^2), is taken as a constant at all times for a given sample. Samples 1 through 7 fit the curve quite well and give further support to the continuous diffusion hypothesis. There is no evidence that any of these samples lost more than a small fraction of

lead at the time of metamorphism 1800 m.y. ago.

Samples 8 through 10 are from gneiss domes that lie to the west of the basement complex containing samples 1 through 7. Two of these samples plot somewhat above the 2800-m.y. diffusion curve; the third is greatly displaced. These departures would result if these samples underwent episodic loss of lead 1800 m.y. ago, the loss being greatest at the Kuopio dome, which is the westernmost of the three and may have been subjected to more intense metamorphism.

Last year we reported briefly on zircon ages from metagraywacke in the vicinity of an intrusive granodiorite near the city of Tampere in southwestern Finland. The intrusive has a diameter of about 20 km; the schists belong to the Svecofennian belt, which extends across southern Fin-

TABLE 25. Mineral Ages from a Svecofennian Intrusive and Its Surrounding Sediments, Tampere, Finland

No. (fig. 95)	Rock	Mineral	Age, million years				
			$\frac{\text{Pb}^{206}}{\text{U}^{238}}$	$\frac{\text{Pb}^{207}}{\text{U}^{235}}$	$\frac{\text{Pb}^{207}}{\text{Pb}^{206}}$	$\frac{\text{Pb}^{208}}{\text{Th}^{232}}$	$\frac{\text{Sr}^{87}}{\text{Rb}^{87}}$
11	Granodiorite A	Zircon	1710	1810	1920	1900	1760
		Biotite					
	Granodiorite B	Zircon	1800	1840	1880		1880
		Graywacke	2030	2160	2280	2130	
12	Graywacke	Microcline					1880
		Zircon	1850	2030	2220	1580	
		Biotite					
13	Graywacke	Muscovite					1770
14	Graywacke	Zircon	1790	2000	2230	1720	1850
		Zircon	1490	1800	2110	1600	

land in an east-west direction. This study has been continued; the results are summarized in table 25. The ages from the granodiorite indicate that it was emplaced about 1900 m.y. ago. The two granodiorite zircons from table 25 are included in the group of zircons lying on the 1900-m.y. diffusion loss curve in figure 95. Three of the metagraywacke samples (11, 12, 13) were collected within a few kilometers of the granodiorite. Sample 14 is from a lens of schist about 40 by 150 meters, occurring within the granodiorite body 2 km from the edge.

On the concordia plot in figure 95 the four zircons lie close to a continuous diffusion curve for 2300-m.y.-old minerals. The true age of the minerals is probably about 2300 m.y., although no igneous rocks of that age are known in Finland. Several attempts to identify igneous rocks of 2300 m.y. in southern Finland by studying possible basement samples have all yielded age values of about 1900 m.y. One great problem in Finnish geology is, in fact, the failure to locate the basement rocks in the Svecofennian belt. The most likely interpretation of these ages is that the zircons from the graywackes are about 2300 m.y. old and that intrusion of the granodiorite did not cause substantial loss of lead. This is very significant in sample 14, which attained the full tem-

perature of the intruding granodiorite mass—about 800°C or above, a temperature substantially higher than any of the other zircons mentioned above are likely to have experienced, including those from Colorado. The best estimate of the maximum temperature reached by the Colorado zircons is about 500°C. Moreover, if the entire granodiorite body at Tampere was intruded at one time, the elevated temperatures were maintained about 40 times longer than in Colorado.

The cause of the difference in behavior between the zircons from Finland and those from Colorado is unknown, although a number of possibilities can be imagined, including differences in the amount of radiation damage, the details of the heating schedule (since annealing of damaged crystal structure may occur during heating), variations in the initial crystallization process (which might influence the effective radius for diffusion), and the bulk chemical composition of the crystals (which might affect the value of the diffusion coefficient). The unusual magnetic character of the zircons from Colorado has already been mentioned.

In summary, our earlier belief that diffusion of lead in zircon takes place with a low activation energy at temperatures up to 400°–500°C is supported by the newer data. Diffusion rates at low

temperature might be controlled by vacancies in the lattice created by radiation damage, which would readily explain the low activation energy. Above 500°C, rapid increase in the diffusion rate of lead may occur, but the exact temperature at which this happens varies from one zircon to another for reasons as yet unknown.

Ages from the Early Precambrian near Rainy Lake, Ontario

The Rainy Lake area contains a classic section of early Precambrian rocks that is unique for the interest and controversy it has provoked among geologists for more than 75 years. Near the type locality of the Keewatin, Lawson in 1888 discovered a sedimentary section he believed to underlie the Keewatin. He named it the Coutchiching. Interest in the age and source of these ancient sediments stimulated the present study of Coutchiching rocks and of the overlying Keewatin greenstones and younger Laurentian granites as well.

Near Rice Bay on Rainy Lake, the Coutchiching, comprised largely of meta-graywackes, occurs as a large domal structure overlain with apparent con-

formity by the metamorphosed Keewatin volcanics. Age determinations on micas show that the sediments were deposited at least 2600 m.y. ago. In the center of the dome is a granite-gneiss originally mapped by Lawson as intrusive Laurentian granite but believed by Yardley, Goldich, Peterman, and Frye (1959) to be a different and more highly metamorphosed facies of the Coutchiching. One of the few geologically definable Laurentian granites in the area is found to the east at Bad Vermilion Lake, where it cuts the Keewatin and is in close proximity to conglomerates of the younger Seine series (Timiskaming).

In *Year Book 61* we discussed the results of age determination on nine zircons from these rocks. The work has been extended to include whole-rock Rb-Sr analyses in a further effort to determine the age and the time interval involved for this early Precambrian rock sequence. At the same time, it was thought desirable to compare the extent to which these two dating methods might record similar events in the history of such a sequence.

The location of dated samples is given in table 26. Figure 96 presents the zircon

TABLE 26. Location of Precambrian Samples, Ontario

Sample No.	Rock Unit	Rock Type	Locality
RL45	Coutchiching	Outer paragneiss, composite	Upper Rice Bay, Rainy Lake
RL71	Coutchiching	Metagraywacke	Dude Island, Rainy Lake
RL105	Coutchiching	Metagraywacke	Sand Point Island, Rainy Lake
RL109	Coutchiching	Outer paragneiss	Upper Rice Bay, Rainy Lake
CC21	Coutchiching	Central paragneiss	Upper Rice Bay, Rainy Lake
CC22	Coutchiching	Central paragneiss	Upper Rice Bay, Rainy Lake
CC26	Coutchiching	Outer paragneiss	Upper Rice Bay, Rainy Lake
CC29	Coutchiching (?)	Porphyroblastic paragneiss	Rocky Islet Inlet, Rainy Lake
CC20	Keewatin	Rhyolitic metatuff	Sand Point Island, Rainy Lake
CC23	Keewatin	Ellipsoidal greenstone	Red Pine Island, Rainy Lake
CC30	Keewatin	Amphibolite	Rice Bay Inlet, Rainy Lake
CC33	Laurentian	Tonalite	Southwest shore, Bad Vermilion Lake
CC34	Laurentian	Tonalite	Southeast shore, Bad Vermilion Lake
CC35	Laurentian	Tonalite	Southeast shore, Bad Vermilion Lake
CC36	Laurentian	Tonalite	Southeast shore, Bad Vermilion Lake
CC43	Laurentian	Granite	Saganaga Lake, Minnesota

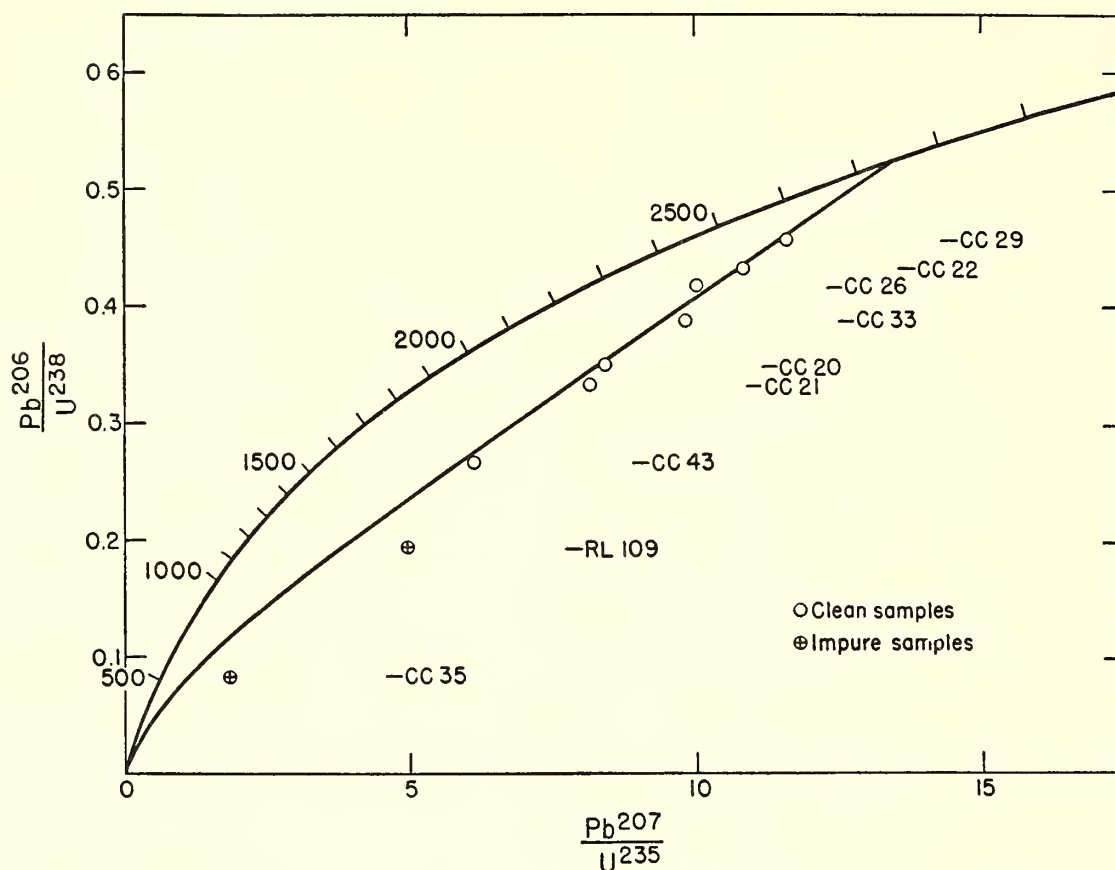


Fig. 96. Parent-daughter ratios for zircons from Rainy Lake, Ontario, compared with the curve calculated for loss of lead by continuous diffusion for 2750 m.y.

results on a concordia plot. Considering these first, it is apparent that all the samples fall within a small spread in age. When the two impure samples are omitted the continuous diffusion curve for the remaining points corresponds to an average age of 2750 m.y. Here, then, are detrital zircons, a volcanic zircon, several granite-gneiss zircons, and several Laurentian granite zircons all showing the same age within the limits of error. Two explanations for the zircon data were given in *Year Book 61*: all the zircons crystallized about 2700 m.y. ago within a short interval of time, of the order of 100 m.y.; or the zircons in older rocks had their clocks "reset" by intense metamorphism 2700 m.y. ago.

Addition of the whole-rock Rb-Sr results provides certain restraints in interpretations based on the zircon data alone. Isochron diagrams of the whole-rock data are presented in figures 97 and 98. The consistency of the isochrons is quite marked. As in the zircon work, the Coutchiching and Keewatin points are

again indistinguishable, giving an isochron age of about 2700 m.y. It is also noteworthy that the total-rock and zircon studies include samples from the granite-like central portion of the dome at Rice Bay as well as ones from the surrounding metagraywacke. Taken together, the zircon and whole-rock Rb-Sr data indicate

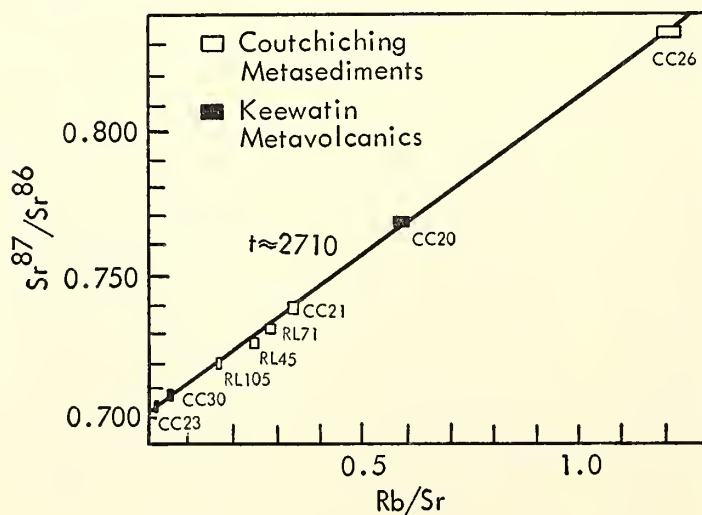


Fig. 97. Rb-Sr isochron diagram for Coutchiching and Keewatin whole-rock samples from Rainy Lake, Ontario. Mole ratio $\text{Sr}^{87}/\text{Sr}^{86}$ is plotted against weight ratio of rubidium to nonradiogenic strontium.

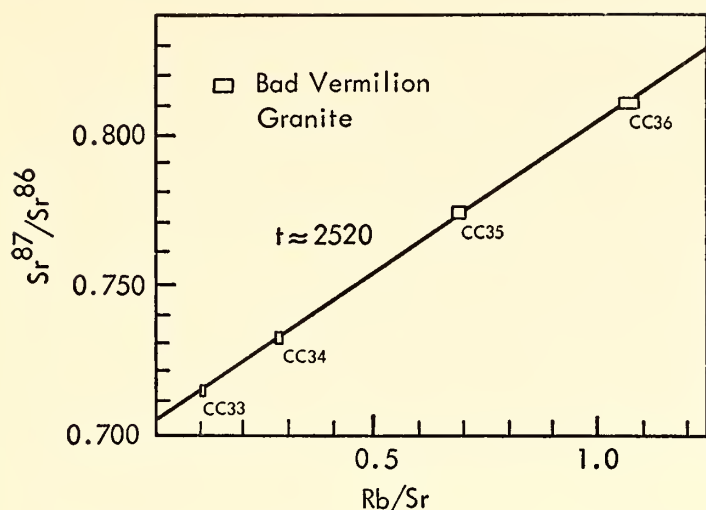


Fig. 98. Rb-Sr isochron diagram of Laurentian granite whole-rock samples, Bad Vermilion Lake, Ontario. Mole ratio $\text{Sr}^{87}/\text{Sr}^{86}$ is plotted against weight ratio of rubidium to nonradiogenic strontium.

a source for the Couthiching that is nearly equivalent in age to the Keewatin.

It is significant that the isochron in figure 97 extrapolates to an initial $\text{Sr}^{87}\text{-Sr}^{86}$ ratio of 0.701, which is the ratio found in such igneous rocks as basalt and its differentiates and is nearly independent of the age of the basalt. On the other hand, granitic rocks have sufficiently high ratios of rubidium to strontium on the average to cause measurable enrichment of Sr^{87} in relatively short intervals of time. If for example, the central part of the dome was formed by reconstitution of granitic rocks 400 m.y. older, the initial $\text{Sr}^{87}\text{-Sr}^{86}$ ratio expected would be about 0.705, suggesting that the close agreement of the zircon ages is not due to erasure of the age record in substantially older zircons by intense metamorphism. Consideration of the conformable nature of these units and the volcanic-graywacke association so typical of eugeosynclines suggests that these formations are part of an early Precambrian geosynclinal sequence. The source of materials for the Couthiching might be found within the geosyncline itself in rocks that crystallized only shortly before the time of sedimentation.

For the Rainy Lake sequence, excellent agreement exists between the zircon and whole-rock methods. The ages of the Laurentian granite as determined by the

two methods, however, are in poor agreement, and possible explanations may be considered. In view of the badly sheared nature of the Bad Vermilion granite, it is possible that the whole-rock samples have been altered during a younger period of metamorphism (Algoman?). The consistent whole-rock isochron, however, would require a complete and pervasive period of remixing of the strontium. Even though the assumption of a "closed system" for whole rocks has seldom been questioned, our understanding of it is imperfect at present. The only other explanation for the zircon and whole-rock discrepancy would require that the zircons have been inherited from older rocks.

K-Ar Ages of Hornblendes from the Southern Gothard Massif, Switzerland

The Gothard massif in central Switzerland is one of the few places in the Swiss Alps where the autochthonous basement of the Alpine orogenic belt crops out. This massif extends with a west-south-west-east-northeast trend over a length of about 80 km, its width in the center exceeding 10 km. The southern border of the massif is marked by the front of the Penninic nappes. On the northern side it is separated from the Aar massif by a narrow zone of Mesozoic sediments (root zone of the Helvetic nappes). The Gothard massif is in itself a complex body of extensive polymetamorphic zones of both sedimentary and plutonic origin. Zircon ages (Grünenfelder, 1962, and written communication) in combination with petrographic evidence suggest Precambrian sedimentation (Gurschen gneiss) and late Precambrian intrusion (Streifen gneiss) of a main part of the primary rock. Several granitic stocks intruded these older rocks, their zircons showing Hercynian age values and one of them (Rotondo granite) probably an Alpine age.

It has been known for a long time that the southern margin of the Gothard

massif was strongly metamorphosed during the Alpine orogeny, and during recent years the influence of Alpine metamorphism has been found to be more extensive in the interior of the massif. Fabric data from field observations gave strong evidence that Alpine fabric elements of the Penninic nappes, especially a consistently north-south oriented lineation (preferred orientation of micas and hornblendes) and an east-west buckling, can be observed right into the center of the Gothard massif and that older structures were obliterated along the southern border. Rb-Sr dating of oriented biotites (Jäger, 1962) confirmed the Alpine age (15–17 m.y.) of a main fabric element by absolute measurements. The southern margin of the central Gothard massif is formed of a belt of rock units, all of which are dominantly of sedimentary origin and were probably deposited in Precambrian times as clays, clayey-limy sandstones, and dolomitic marls. In particular the southernmost of these zones (Tremola series) still shows sedimentary structures. By pre-Alpine and mainly by the Alpine orogeny these sediments were altered to mica gneisses and schists, hornblende schists and gneisses, quartzites, siliceous calc-schists, and amphibolites.

Petrographic observations (Steiger, 1962) of these rocks show that up to six different generations of minerals can be established in the rock texture of the southern Gothard massif. All were formed during different phases of orogeny. A fine-grained cataclastic mosaic of quartz and feldspar (first generation) is considered to

be a relict of a pre-Alpine phase. A second generation of minerals (first Alpine generation) consists of north-south oriented micas and finely nematoblastic hornblendes as well as elongated quartz crystals. This generation was formed during a period of tectonic movement responsible for the north-south lineation. Postkinematic growth of large porphyroblasts (third generation) of garnet as well as hornblende that cuts the foliation occurred in a later phase under the influence of a heat front arising from the northern Penninic nappes. Both minerals contain oriented inclusions of minerals of the second generation. Later on, during clearly defined consecutive phases, biotite cutting the foliation was formed, and then alteration products like chlorite, biotite, and sericite. Finally veins and cracks were filled with quartz and carbonates.

A new approach to elucidate the metamorphic history of the southern Gothard massif by means of age determinations is being attempted. It is hoped that some information about the timing of metamorphic events and especially of the phases of Alpine orogeny will be obtained.

Hornblendes, biotites, and zircons have been separated from the rocks of the Tremola series and adjacent zones to the north (Guspis and Corandoni zones). To date, the K-Ar ages of four hornblendes have been determined. The potassium content of the hornblendes is 0.27 to 0.47 weight per cent. The argon extracted was 27 to 42 per cent radiogenic. The ages are given in table 27.

TABLE 27. K-Ar Ages of Hornblendes from the Southern Gothard Massif

Sample No.	Spatial Array of Hornblende Crystals in the Rock	Mineral Generation (from petrographic observations)	Zone	Age, m.y.
Hbl. 486	Oriented	2	Guspis zone	42
Hbl. 382	Oriented	2	Corandoni zone	42
Hbl. 352	Oriented	2	Tremola series	46
Hbl. r175	Random	3	Tremola series	25

All hornblendes are of Alpine age, thus confirming the result of fabric analysis; but the ages are definitely older than the Rb-Sr ages of biotites of near-by rocks reported by Jäger (1962). As shown in *Year Book 60*, K-Ar ages of hornblendes are usually less affected by subsequent metamorphism than Rb-Sr ages of biotites. The grouping of three hornblende age values at 42 to 46 m.y. suggests that the ages have not been influenced appreciably by inherited radiogenic

argon. The 42- to 46-m.y. ages occur in hornblendes from different zones and from rocks that differ greatly in origin, primary age, and temperature history. The younger age of 25 m.y. obtained on a hornblende that cuts the foliation (third generation) is in agreement with petrographic observations previously mentioned. More data will be required, however, to reach a definite conclusion about the ages of different generations of hornblendes within the Tremola series.

ORGANIC GEOCHEMISTRY

Hydrocarbons from Kerogen

T. C. Hoering and P. H. Abelson

During the past year our research has yielded strong new evidence that mild thermal degradation of kerogen is the principal mechanism by which hydrocarbons in natural gas and petroleum are produced. Under conditions similar to those common in nature we have observed the liberation of a series of saturated straight-chain hydrocarbons, which are especially abundant in natural products, ranging from methane (C₁) through *n*-dodecane (C₁₂). Isotopic measurements on methane and on other hydrocarbons produced in the laboratory agree with those observed by others on natural gas. We were attracted to kerogen as an object of study since the sheer mass of it (65×10^{20} grams) in the earth's crust makes it an important geochemical component. Determination of its fate as a function of time and temperature is a matter of considerable interest. Moreover, kerogen is a possible source of information about past life, and our studies this year have provided an interesting lead arising from a difference in the gaseous hydrocarbons emitted by some Precambrian specimens and kerogen of younger age.

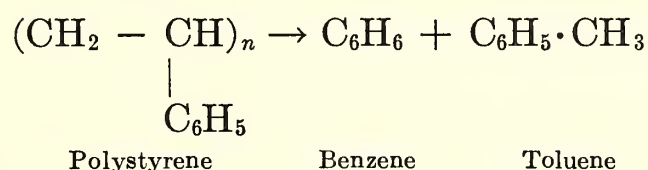
Most of the organic matter remaining from past biological activity is found in

the sedimentary rocks as kerogen, an insoluble complex material. Actually there are many kerogens, for the word represents an operational procedure and is a name for what remains after sedimentary rocks are demineralized and the organic residue is extracted by various solvents.

When organic matter is deposited in organic sediments it is attacked by microorganisms, but this action largely stops in a few years. The elemental composition of the organic matter is then quite similar to that of typical living material, although major structural changes have occurred. The composition of the organic matter of diatoms (A. P. Vinogradov, 1953, in Emery, 1960, p. 274) is 45.9 per cent C, 35.7 per cent O, 9.4 per cent H, 9.0 per cent N. With time the composition changes—carbon dioxide is evolved, nitrogen gradually disappears, and the ratio of C/H increases. After an interval such as 300 m.y., much of the oxygen and nitrogen is gone. Forsman and Hunt (1958) have reported that a kerogen from Woodford shale has the composition of 65.6 per cent C, 4.96 per cent H, 2.51 per cent N, and 3.68 per cent O. The remainder is sulfur and ash. The ultimate product of the residue is graphitic carbon, but it is reached only if the organic matter is subjected to moderately high temperatures. Enormous volumes of sedimentary rocks are found in which the kerogen has

probably not been exposed to temperatures above 100°C, and in these the changes in chemical composition are moderate. Indeed, there are other areas in which the materials have probably not experienced temperatures above 50°C. In some situations hot intrusives have provided localized hot spots, and in others the organic matter is buried deeply beneath a thick layer of sediments. Temperatures of about 180°C arising from the normal geothermal gradient have been noted in holes drilled to 20,000 feet or more.

At sufficiently high temperatures (400° to 500°C) almost all organic matter including polymers is broken down to simpler molecules in a few minutes. The reaction products give insight into the molecular structure of the chemicals originally present. For instance, when polystyrene is pyrolyzed, benzene and toluene are observed as major products. The structural formulas involved are



At these high temperatures secondary reactions can occur, and when kerogen is exposed to such temperatures a wide variety of products are formed, including olefins. Since we are interested primarily in geological processes, we investigated the products formed when kerogen was heated under moderate conditions, approaching as closely as possible those usually encountered in sedimentary rocks. Recent advances in chemical instrumentation make such an investigation feasible.

One hundred or more grams of finely ball-milled shales or kerogens was placed in an all-glass high-vacuum system. The sample was thermostated to 1°C and then connected to an automatic Toeppler pump through a tube containing sodium hydroxide pellets. After a preliminary outgassing the system was sealed off from the pump, and the evolved gases were

rapidly pumped into a gas burette. They could then be removed for analysis. Extremely low rates of gas evolution could be measured.

Gas-liquid chromatography, mass spectrometry, and infrared spectrometry were employed for qualitative and quantitative analysis of the small amounts of volatile materials collected. Microgram or smaller quantities of hydrocarbons were routinely analyzed.

A large number of shales and kerogens were examined this way. Most intensively studied has been the Green River shale of Colorado, Utah, and Wyoming. This 40-m.y.-old formation contains the world's largest reserve of fossil organic matter, which is largely in the form of kerogen. We have performed more than thirty measurements of the gases evolved by mild thermal treatment of this material. We have also worked with recent marine sediments, the Woodford shale of Mississippian age, the Alun shale of Cambrian age, and four Precambrian specimens. All together we have determined the composition of the light hydrocarbons in more than 100 samples produced from shale or kerogen.

On the Green River shale we made the following observations. Light saturated hydrocarbons can be produced at a measurable rate at temperatures as low as 185°C. Figure 99 shows a GLC trace of the hydrocarbons obtained after 17 days of incubation. In figure 100 are shown results of experiments conducted at temperatures ranging from 185° to 400°C. We have plotted the rate of evolution of methane as the ordinate on a logarithmic scale, and the reciprocal of the absolute temperature as the abscissa. Such a plot yields a straight line. Similar results were observed for other hydrocarbons containing 2 to 7 carbons. For comparison a theoretical line is also shown, indicating what would be expected if the chemical kinetics were first order, that is, if the reaction proceeded through simple breakage of carbon-carbon bonds in an ordinary hydrocarbon. A number of studies have

indicated that saturated hydrocarbons on heating break up into fragments. Activation energy for the process, which is first order, is 58 kcal. In our calculation we have assumed that the frequency factor $A = 5 \times 10^{13}$. In figure 100 it may be noted that the kinetics for degradation of kerogen with attendant production of light hydrocarbons does not follow first-order kinetics and that the degradation of kerogen is much less sensitive to temperature than a straight-chain hydrocarbon. Our observations can be fitted by the equation

$$k = 10^9 \times E^{-40,250/RT}$$

It is somewhat surprising to find such apparently simple behavior of so complex a material.

In the cracking of straight-chain hydrocarbons we would expect to obtain saturated and unsaturated fragments in equal

numbers. We have examined the gases evolved from Green River kerogen at 250°C and have found that more than 90 per cent of the hydrocarbons were saturated and less than 10 per cent unsaturated. This is further evidence that the processes involved at such low temperature are different from ordinary pyrolysis.

Many others who have written on the formation of petroleum have postulated that the mineral matrix plays an important role in catalyzing the formation of hydrocarbons from organic matter. In our investigations we studied the thermal degradation of kerogen both in a shale matrix and in a demineralized form. The gases obtained from pyrolysis of both specimens under the same temperature conditions were, within experimental error, qualitatively and quantitatively identical. Thus, at least in this one study, there was no sign of a catalytic effect.

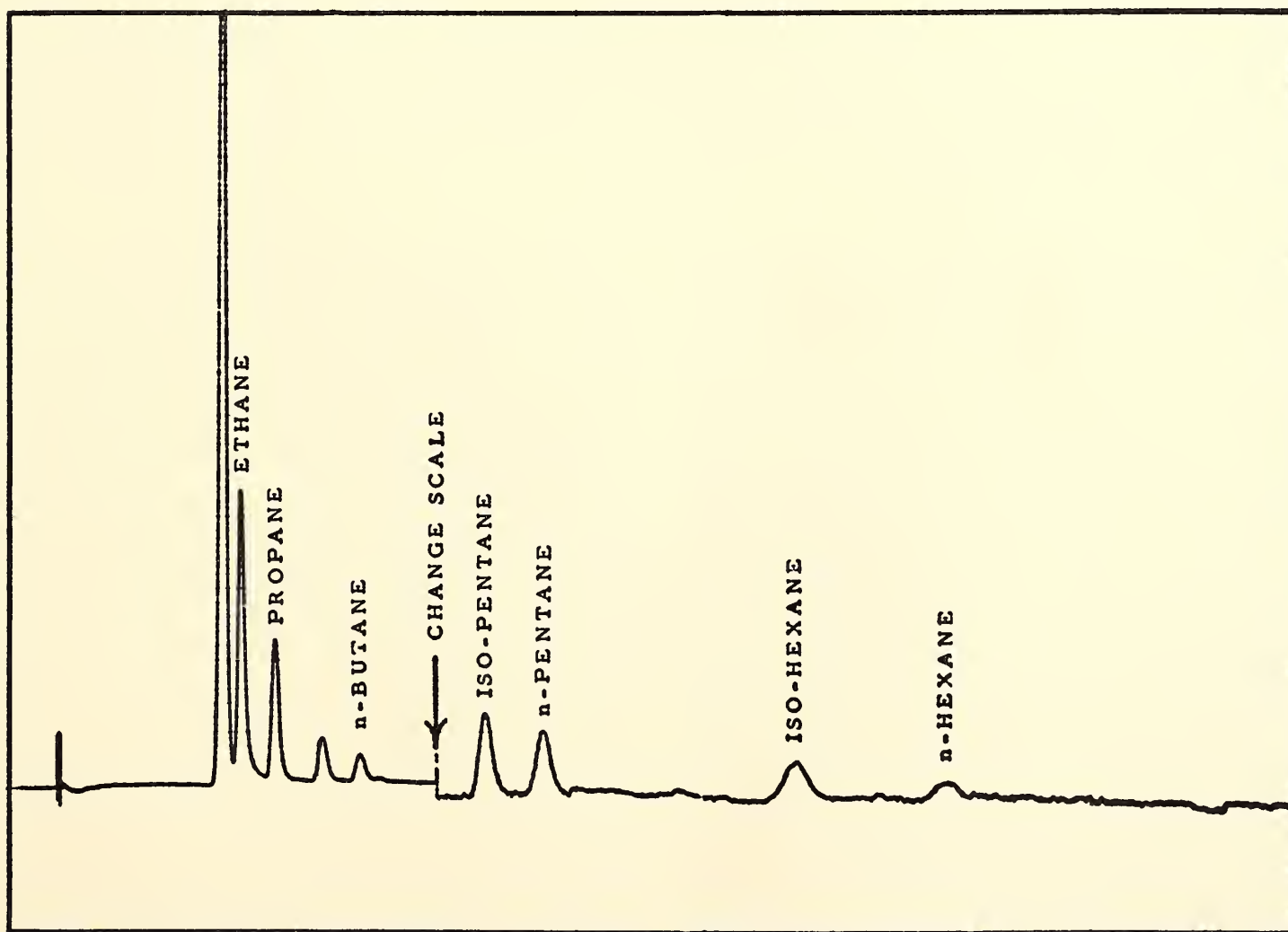


Fig. 99. Gas-liquid chromatogram of hydrocarbons formed by incubation of kerogen at 185°C. The kerogen was prepared from Green River shale. The first peak on the left (unlabeled) is methane (off scale). At the point indicated by an arrow, sensitivity was lowered by a factor of 16.

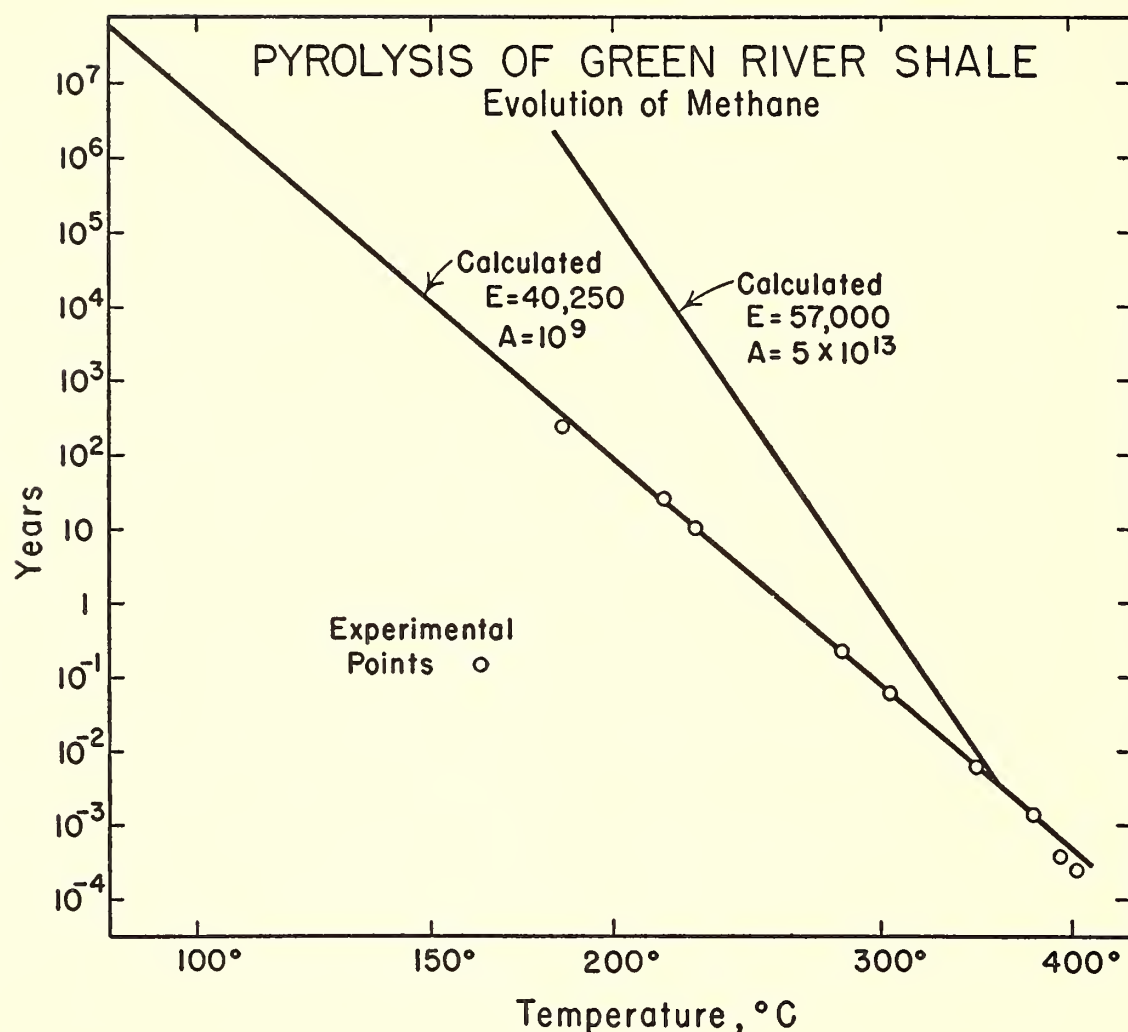


Fig. 100. Temperature dependence of evolution of methane from Green River shale. Experimental points are fitted by a straight line calculated from $k = Ae^{-E/RT}$, where $A = 10^9$ sec and $E = 40,250$ cal/mole. The upper straight line is a theoretical curve corresponding to cracking of straight-chain hydrocarbons.

The relative proportions of hydrocarbons produced by heating are influenced by the temperature at which the process occurs. At low temperatures (185° to 230°C) methane is prominent relative to heavier hydrocarbons like *n*-pentane and *n*-hexane. At higher temperatures (350° to 400°C) methane is less dominant. We have pyrolyzed Green River kerogen at 325°C for 6 days and have examined the hydrocarbons in the range from C_4 to C_{12} . About 4 per cent of the original organic matter appeared in this fraction. The major components of the liquid were saturated straight-chain hydrocarbons of both even and odd carbon numbers with appreciable amounts of simple branched hydrocarbons and cycloparaffins. The relative abundances of the various substances resembled those noted in petroleum.

The following informative experiment was performed on the Green River shale. A large sample was heated at 325°C for several days. The gases evolved were separated into three fractions. The first, containing gases volatile at the temperature of liquid nitrogen, was mainly methane. The second was not volatile at liquid nitrogen temperatures but was volatile at the temperature of dry-ice slush. After removal of carbon dioxide, the main carbon-containing gases of this fraction were ethane and propane. The third fraction was not volatile at dry-ice temperature but was volatile at room temperature. It contained compounds with boiling points in the range of butane to octane. The residual shale was treated with hydrochloric acid and dried. All samples were then quantitatively burned to carbon dioxide and analyzed for their

TABLE 28. Isotopic Composition of the Carbon in Green River Shale and Its Hydrocarbons

Sample	δC^{13}
Methane (C_1)	-41.25
Ethane and propane (C_2 - C_3)	-35.23
Butane and higher (C_4 - C_8)	-33.86
Residual shale	-27.40

C^{13} content in the mass spectrometer. The results are expressed in parts per thousand difference in the C^{13}/C^{12} ratio compared with a standard, National Bureau of Standards isotope reference sample 20, a marine limestone:

$$\delta C^{13} = \frac{(C^{13}/C^{12})_x - (C^{13}/C^{12})_{std.}}{(C^{13}/C^{12})_{std.}} \times 1000$$

The results are given in table 28. This distribution of stable carbon isotope ratios, increasing δC^{13} with increasing molecular weight, bears a striking similarity to that observed in natural petroleum (S. R. Silverman, unpublished) and gives supporting evidence that the reactions being studied in the laboratory are similar to those occurring in nature.

A number of other interesting observations were made on the Green River shale. On initial heating to 200°C large quantities of carbon dioxide were noted. The off gas also contained relatively large amounts of hydrocarbons, methane being especially dominant. When the temperature was raised to 300°C for half an hour the composition of the gas changed. At the end of that time production of carbon dioxide had practically ceased and the principal products were hydrocarbons. On cooling back to 200°C the gases observed consisted of hydrocarbons, but they were emitted at a rate much lower than the initial rate, and the composition differed both from the initial composition and from that at 300°C. These events can be interpreted as follows. The processes leading to evolution of carbon dioxide tend to occur at lower temperatures than those giving rise to hydrocarbons, and the degradation of kerogen to form carbon

dioxide is relatively complete in a short time at 300°C. The initial hydrocarbons found at 200°C were probably residual from changes that had occurred during the 40 m.y. since the Green River shale was deposited. On heating to 300°C these preformed hydrocarbons were removed and the new gas coming off was characteristic of that formed at 300°C. On cooling back to 200°C the composition of the hydrocarbons emitted changed to that characteristic of a lower temperature, indicating that we were now finding the gases being formed at 200°C.

Our study of recent mud from the San Nicolas Basin off Los Angeles was less extensive. The light hydrocarbons found were qualitatively and quantitatively similar to those obtained from Green River shale, and the temperature dependence on rate of emission of gas was also similar within a factor of 2. One obvious difference could be noted by simply using what is often a very sensitive instrument—the human olfactory system. Gases obtained from Green River shale have a strong odor (probably due to traces of mercaptans) quite similar to that noted around oil refineries. The odor of the gases from the recent sediments was reminiscent of burned meat.

The Woodford shale sample of Mississippian age was a core, furnished by Jersey Production Research Laboratories, that had been taken from the formation at 2000 meters' depth. Gas from this sample was unusual in that ethane was more abundant than methane. Another sample studied was a Swedish Alun shale of Cambrian age. The light hydrocarbons obtained from this specimen were qualitatively similar to those from Green River shale, but the yield was much lower.

The Precambrian samples that we studied included the Carbon Leader from South Africa (2200 m.y. old), the Soudan slate of Minnesota (2300 m.y. old), and the Michigamme coal of Michigan (1800 m.y. old). The gases emitted from the Precambrian samples consisted largely of methane. Butane, pentane, and hexane

were detected, but they were present at a level less than 1 per cent of that of methane. Thus, there was a striking quantitative difference in the components of the gases obtained from Precambrian and post-Cambrian specimens. Typical values of the ratio of methane to pentane in the studies of the Green River shale were 15/1, whereas corresponding values from the Carbon Leader were 230/1. These differences almost certainly indicate that at the present time the organic matter in the Precambrian Carbon Leader is quite different from anything we have seen from samples of post-Cambrian times. We are inclined to think that the composition of organic matter in the Carbon Leader has always differed considerably from that present in Green River shale. However, we cannot yet foreclose the possibility that the differences noted merely reflect effects of time and temperature.

In one interesting respect the Green River shale and Carbon Leader are similar. We have studied the rate of emission of methane from the Carbon Leader at temperatures between 217° and 325°C. In this range the rate of production and the temperature dependence of the evolution of methane were almost identical with those observed in Green River shale.

The Isotopic Composition of the Carbon of Redfish Bay

P. L. Parker

The most general observation on the geochemistry of the stable isotopes of carbon is that organic or reduced carbon is slightly depleted in C¹³ with respect to atmospheric CO₂, sea-water carbonates, and limestone. This fractionation is brought about by isotope effects (presumably kinetic) in reactions of carbon in organisms. For example, Park and Epstein (1960) and Abelson and Hoering (1961) have measured the carbon isotope fractionation in photosynthesis in laboratory systems. Park and Epstein measured the fractionation in the enzymatic fixation of CO₂ into 3-phosphoglyceric

acid in a cell-free system. Carbon in an organism undergoes many chemical reactions, each of which may have its own isotope effect, so that different types of molecules of a single organism may have a variety of isotopic compositions. These various amino acids were shown by Abelson and Hoering to have isotopic compositions different from each other and from the total carbon of the organism. Parker (*Year Book 61*, p. 187) has reported that the fatty acids of an organism have the same isotopic composition, which is different from that of the total carbon.

In May 1962 biological samples were collected from Redfish Bay, a shallow marine estuary near Port Aransas, Texas. All the samples were collected at the same time and within a few yards of one another at the edge of a highly productive bed of marine "grass," *Thalassia testudinum*. They were frozen immediately and brought back to the laboratory. Bicarbonate of sea water was the source of the carbon for all the plants. The animals were free to move, but at least at the time of collection they were a part of the semi-closed community.

Some of the samples were divided into a lipid fraction and a protein-carbohydrate fraction by Soxhlet extraction of the sample with chloroform-methanol. All the samples were combusted to carbon dioxide, which was used for the carbon isotope analyses. The results are expressed in terms of δC¹³, the parts per thousand difference in the C¹³/C¹² ratio of the sample and a standard material, NBS isotope reference sample 20.

$$\delta C^{13} = \frac{(C^{13}/C^{12})_{\text{sample}} - (C^{13}/C^{12})_{\text{std.}}}{(C^{13}/C^{12})_{\text{std.}}} \times 1000$$

Positive values of δC¹³ mean that the sample is enriched in C¹³ relative to the standard; negative values mean that it is depleted.

The results of the isotope analyses are given in table 29. All the organic materials are depleted in C¹³ relative to the

TABLE 29. Isotopic Composition of Redfish Bay Samples*

No.	Sample	δC^{13} , Total C	δC^{13} , Lipide C
2	Total inorganic carbon of water	-6.7	
15	Sediment	-13	-18
4	Grass, <i>Thalassia testudinum</i> (blades)	-9.1	-17.5
1	Grass, <i>Thalassia testudinum</i> (roots)	-6.0	-17.6
5	Shoal grass, <i>Diplanthera wrightii</i>	-9.5	-17
7	Widgeon grass, <i>Ruppia maritima</i>	-9.7	-13
10	Algae, <i>Laurencia poitei</i> (Lamouroux) Howe	-10.8	-26
22	Algae, <i>Enteromorpha salina</i> Kutzing	-17	
18	Algae, <i>Laurencia obtusa</i> (Hudson) Lamouroux	-14	-19
21	Algae, <i>Digenia simplex</i>	-17	-17.5
16	Grass shrimp, <i>Palemonetes vulgaris</i>	-14	-19
9	Brown shrimp, <i>Penaeus aztecus</i>	-11	-14
17	Pistol shrimp, <i>Crangon heterochaelis</i>	-14	
12	Fiddler crab, <i>Uca pugilator</i>	-13	-18
20	Blue crab, <i>Callinectes sapidus</i>	-17	-19
24	Clam, unidentified, flesh	-26	
	shell	+5.3	
19	Oyster, unidentified, flesh	-15	
	shell	+1.3	
3	Killifish, <i>Fundulus similis</i>	-7.7	
6	Killifish, <i>Cyprinodon variegatus</i>	-9.3	-11.5
8	Silver perch, <i>Baindiella chrysura</i>	-11	-13
11	Mullet, <i>Mugil cephalus</i>	-12	-14
13	Pinfish, <i>Lagodon rhomboides</i>	-13	-16
14	Spot, <i>Leiostomas xanthuras</i>	-13	-13
23	Needlefish, unidentified	-17	

* All values of δC^{13} are based on NBS 20 as the reference material.

sea-water carbon. Every unit value of δC^{13} between -6 and -17 is taken by some species. The plants, even two related species of algae, have significantly different values of δC^{13} . This is taken to be the result of diverse isotope effects in the chemical reactions in the plants as discussed in the preceding paragraphs. The animals show a similar range in δC^{13} . Unlike the plants the animals have access to source carbon (food) with a variety of δC^{13} values. Thus δC^{13} for the animals is determined by their food source and subsequent chemical reactions. The results in table 29 permit some generalizations about the eating habits of the animals studied.

It was found that different samples of the same species of algae had the same value of δC^{13} , which assures us that, given the same source carbon, different individuals of the same species will, on the

average, carry out chemical reactions with the same isotope effect. Different individuals of the same species of the animals were also found to have the same δC^{13} to within ± 1 per mil. Then, assuming that the same isotope effects are operative in individual animals of the same species, as was true for the algae, different individuals of the same species have, on the average, the same diet—at least with respect to the δC^{13} of the food.

Table 29, last column, shows the values of δC^{13} for the lipide fraction (chloroform-methanol/soluble) of several organisms. This material is consistently more depleted in C^{13} than the total carbon. Since it is mostly the triglyceride esters of the fatty acids the data give the approximate values of δC^{13} for the fatty acids of the community. Thus all the organisms have made (or acquired as food) the same compounds (the fatty acids) by the same

pathway but with a variety of isotopic compositions.

The total organic carbon of the sediment had $\delta C^{13} = -13$, whereas for the lipide fraction $\delta C^{13} = -18$. Table 29 indicates that the community could supply carbon of this isotopic composition to the sediment by simple deposition. Detailed knowledge of the relation between δC^{13} of a few communities and δC^{13} of their sediments might lead to useful inferences about fossil communities of which only the sediment remains.

*The Organic Chemicals
in Precambrian Rocks*

T. C. Hoering

The studies of the organic substances that can be obtained by chemical degradation of the reduced carbon of Precambrian sedimentary rocks, on which a preliminary report was made last year, have been continued. The detailed studies of the hydrocarbons obtained on pyrolysis are described in another section of this report.

One very characteristic property of the organic molecules produced by biological systems is asymmetry. This results in optical activity of solutions of these compounds. It is well known that crude oils, coals, and other sedimentary organic material of biological origin have optically active molecules. A number of Precambrian organic chemicals were examined in a Bendix-Ericson automatic polarimeter. This electro-optical device is considerably more sensitive than the conventional mechanical-optical polarimeter; it can detect a change in the rotation of the plane of polarization of light of 0.0001° . The materials examined were the mixtures of acids produced by the oxidation of Precambrian reduced carbons with alkaline potassium permanganate and the hydrocarbons produced by treatment with anhydrous hydrogen iodide. Milligram quantities of ether-soluble material obtained from 10 grams of the carbons yielded only marginal amounts of optical activity, two to three times the sensitivity of the instrument. Apparently, if any

centers of asymmetry exist in the carbons, these two chemical treatments yield molecules with molecular weight too low to preserve it. Methods are being sought that will yield soluble fragments of higher molecular weight.

Attempts to isolate organic chemicals from Precambrian rocks by extraction with organic solvents were abandoned. The amounts that could be isolated from a series of rocks are very small and close to the "blank" of the solvent. Although perhaps some rocks of this kind will yield soluble substances, it is concluded that this is not a general method.

*An Experimental Approach to the
Study of Chemical Evolution*

Gordon Allen

In the interval of earth history preceding the origin of life, any organic compounds formed were necessarily the product of relatively simple processes. Several physical agents are known to convert such compounds as CO_2 , CH_4 , and NH_3 into amino acids and similar molecules. It is commonly assumed that these organic building blocks reached sufficient concentration, at least locally, to combine into macromolecules, including, at last, nucleic acids and proteins. It is further assumed that nucleic acids or proteins or both came together by chance in a combination capable of self-reproduction and mutation. From that point on, evolution could proceed by natural selection much as it does today, constituting organic evolution. In contrast, the succession of organic chemical reactions prior to the first organism is often referred to as chemical evolution.

Several authors (see Yčas, 1955; Anker, 1961) have independently suggested that chemical evolution might have been controlled not by simple chance but by a process partly analogous to natural selection. This phenomenon, as proposed, would tend to organize and direct chemical reactions toward greater efficiency of syntheses, obviating great quantities or

high concentrations of intermediates. Such a conserving and guiding principle would operate if self-synthesis of an indirect nature were achieved by some simple organic catalysts. Although examples of this phenomenon are not known, it is apparently not improbable under conditions that might have prevailed in the period of chemical evolution. The line of reasoning can be briefly summarized as follows:

In a steady-state ocean maintained at high chemical potential by continual production of formaldehyde, amino acids, etc., diverse additions and rearrangements would be possible. Many of the products would be expected, on the basis of known mechanisms, to influence the relative rates at which certain reactions approached equilibrium. By catalysis and inhibition they would, with the passage of time, increase some products and decrease others. If there were many catalysts, some might act reflexively, that is, if not actually autocatalytic, they would increase the concentration of a precursor or catalyst for some step in their own synthesis; these would tend to increase exponentially. Competition and mutual facilitation among such self-synthesizing systems would result in the differential increase of those that were most compatible, and in the multiplication of molecules structurally related to the most effective catalysts.

The objectives of this year's research were fourfold: first, to develop necessary analytical methods; second, to establish a series of highly reactive steady-state mixtures ranging from simple to moderately complex; third, to define the base-line composition of these steady states; and, fourth, to begin a search for late changes or "mutations" that might indicate catalytic effects.

Starting compounds were chosen for high reactivity and for availability in high grades of purity. Six reagents were used in six combinations: formaldehyde and sodium cyanide in all and ammonium hydroxide in five; allyl alcohol, pyruvic

acid, and diacetyl were added separately or together in four. Each combination was duplicated at approximately *pH* 7 and *pH* 9 with buffers of phosphate and chloride. Concentration of the reagents was 0.1 *M* except for CH_2O , NaCN , and NH_4OH , which were 0.3 *M* in some of the solutions.

The reactions were maintained in a nitrogen atmosphere at 90°C under reflux. High temperature and concentrations were thought desirable in order to accelerate reactions and to exclude microorganisms. A steady state was approximated by periodic removal of part of the mixture and replacement with fresh solution. Ten per cent was renewed daily for 2 or 3 months, then 20 per cent twice weekly. As each experimental solution was started, a portion was set aside as control, not to be renewed, and thus allowed to undergo changes further in the direction of thermodynamic equilibrium. Compounds or characteristics appearing in the steady-state solutions that were not found at any time in the control solutions could thus be attributed to interaction of late products with starting materials, either catalytically or by direct reaction.

Samples for analysis were concentrated by evaporation at 40°C under a stream of nitrogen. The earliest distillate was collected by freezing and analyzed by gas chromatography on a 2-meter column of castorwax on chromosorb-W (HMDS, Wilkens). The concentrated residue was extracted twice with methyl acetate containing 10 per cent of methanol, then twice with methanol containing 20 per cent of methyl acetate, and the remainder was redissolved in water. The three extracts, referred to as the methyl acetate, methanol, and water fractions, were analyzed by two-dimensional thin-layer chromatography. The adsorbent was silica gel G, buffered for use with the methanol and water fractions. A separate solvent pair was devised for use with each of the three fractions; the six solvents were composed of methanol, methyl acetate, ammonium hydroxide, and/or

water in varying proportions. The chromatograms were sprayed with alkaline potassium permanganate and photographed through a green filter as negative prints. In seeding tests (see below) that employed C^{14} , the same chromatograms were subsequently used for autoradiography. Figure 101 illustrates one of the autoradiographs.

Crucial in detecting or ruling out catalysts and reflexive catalysts in connection with apparent mutations are the seeding tests. In a "short" seeding test fresh solution is placed in two vessels under the standard conditions, and one is seeded with an aliquot of the aged solution to be tested. Samples are withdrawn at intervals for comparison of the seeded and unseeded solutions. If any compound were to appear in the seeded flask alone, a likely explanation would be that the aged solution contained one or more catalysts. If the difference persisted in a second and third cycle without attenuation, it would appear that the catalyst had reproduced

itself in some manner. In a "long" seeding test, more sensitive but less definitive, a recently established steady-state mixture is seeded with a large aliquot of the aged solution of the same composition and maintained for a week or more. In this test a transmitted mutation would presumably increase despite daily dilution by fresh solution. The long test may also be used for comparison of seeded and unseeded solutions. In the unseeded solutions, with C^{14} -labeled compounds in the last one or two renewals before analysis and with autoradiographic recording of the chromatograms, the long seeding test appears to be a very sensitive way to search for compounds whose synthesis is catalyzed by late products.

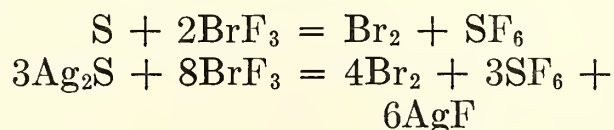
Analyses have recorded at least twenty detectable compounds in the simplest solutions, forty in the most complex. The late chromatograms present several spots not seen in early analyses, but seeding tests have failed to give evidence of catalysis in those studied.

THE PHYSICAL CHEMISTRY OF ISOTOPIC SUBSTANCES

Sulfur Isotope Analysis with Sulfur Hexafluoride

B. E. Sabels and T. C. Hoering

A new technique was developed for the analysis of small differences in the ratio of the stable isotopes of sulfur. It may have some advantages over the existing ones for the study of the geochemistry of the stable isotopes of sulfur. Elemental sulfur and metallic sulfides react rapidly and quantitatively with the halogen fluorides to give sulfur hexafluoride, e.g.:



There is a sufficiently great difference in the boiling point of bromine trifluoride and sulfur hexafluoride to permit easy separation. Sulfur hexafluoride has many

desirable properties as the gas for introduction of sulfur into the mass spectrometer for isotope analysis, for instance: (1) it is a chemically inert substance, not readily adsorbed on the walls of vacuum systems; (2) fluorine has only one stable isotope, F^{19} ; (3) the boiling and freezing points are convenient for handling small quantities of it in a vacuum system; (4) it gives a fairly simple spectrum of positive ions on electron bombardment in the mass spectrometer.

A vacuum system was constructed similar to that described by Tudge (1960) and by Clayton and Mayeda (1963). The nickel reaction vessels were filled with the sulfur compound, and evacuated; then bromine trifluoride was distilled into them. The reaction was allowed to proceed at $100^\circ C$ overnight. The reaction product was distilled out of the bomb at the

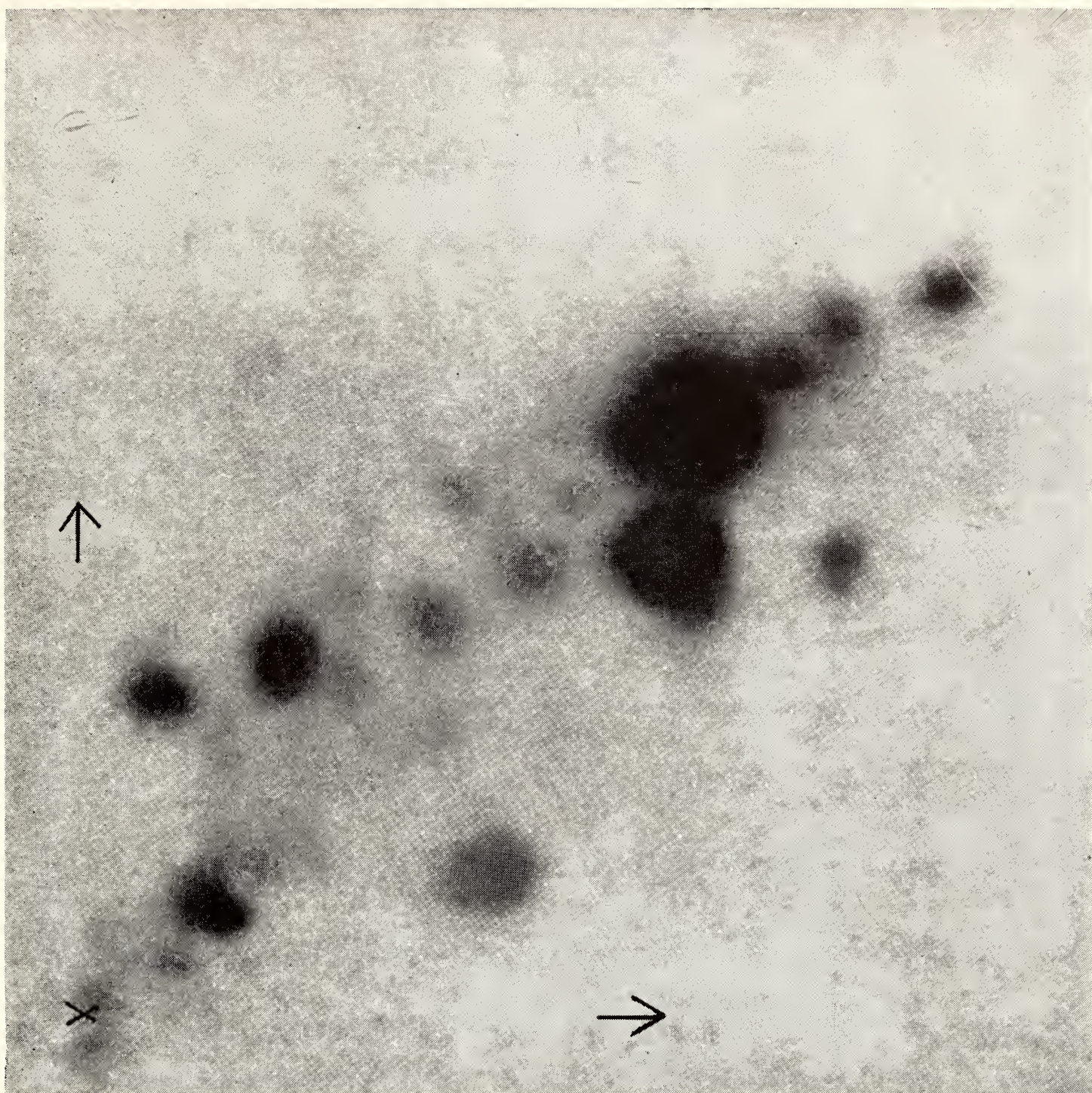


Fig. 101. Thin-layer chromatogram of methyl acetate extract of cyanide-formaldehyde mixture (0.3 *M*, pH 9) maintained for 6 days by daily renewal of 20 per cent and analyzed on the eighth day. Solution added on the fifth and sixth days contained C¹⁴-labeled formaldehyde (35 mc/mole). The film exposure time was 6 weeks.

temperature of solid carbon dioxide. As the process is somewhat slow, isotope fractionation can result at this stage because of low yields. The sulfur hexafluoride was scrubbed with moistened sodium hydroxide pellets to remove any trace of acidic substances. The gas was then purified by preparative gas-solid chromatography on a $\frac{3}{4}$ -inch-by-60-inch column of coarse Molecular Sieve 5A held at 100°C. A very pure gas, suitable for the mass spectrometer, and a quantitative record of the yield of product result. The main experimental difficulty is connected with handling the extremely reactive bromine trifluoride.

In the mass spectrometer the ratio of $S^{34}F_5^+$ to $(S^{32}F_5^+ + S^{33}F_5^+)$ was deter-

mined, and a small correction for the S^{33} was made in order to calculate the variation in S^{34} content

$$\delta S^{34} = \frac{(S^{34}/S^{32})_x - (S^{34}/S^{32})_{std.}}{(S^{34}/S^{32})_{std.}} \times 1000$$

The subscripts x and $std.$ refer to the sample being investigated and an arbitrary reference standard. The method was tested on a sample of synthetic cadmium sulfide, and the δS^{34} between it and a sample of commercially available sulfur hexafluoride was determined. The results of 19 runs gave $\delta S^{34} = +13.17$ with standard deviation of 0.24. Thus it appears that the method is satisfactory for cadmium sulfide. Satisfactory results on FeS_2 and Ag_2S were also obtained.

MISCELLANEOUS ADMINISTRATION

Journal of Geophysical Research

The *Journal of Geophysical Research* is published semimonthly by the American Geophysical Union with P. H. Abelson (Geophysical Laboratory) and James A. Peoples (University of Kansas) as co-editors. About half of the editorial work, including manuscripts on upper atmosphere and space, as well as some of the papers involving geochemistry, are handled at this Laboratory. The *Journal* is regarded by many as the world's leading geophysical publication.

Though publishing about 7400 pages a year, the *Journal* has one of the fastest publication times among scientific journals. This accomplishment is due to the effective efforts of Dr. and Mrs. Peoples at Kansas, and the cooperation of Mrs. Lucile Stryker and Miss Mary Jane Miles of Carnegie Institution, and Mr. A. D. Singer and Miss Marjorie E. Imlay of the Geophysical Laboratory.

Journal of Petrology

Two of the four editors of the *Journal of Petrology* are associated with the Geophysical Laboratory: Professor C. E.

Tilley (Cambridge University, Geophysical Laboratory), H. S. Yoder, Jr. (Geophysical Laboratory), L. R. Wager (Oxford), and T. F. W. Barth (Oslo). The aim of the editors is to provide a place for the publication of original researches in the whole range of subjects that fall within a liberal definition of petrology. Now in its fourth year of publication, the *Journal of Petrology* has established a reputation for papers of outstanding quality. The format and production by the Oxford University Press under the direction of the Managing Editors, G. M. Brown (Oxford) and S. R. Nockolds (Cambridge), are of the highest caliber. The bulk of the papers originate in North America, and many of the staff members of the Laboratory serve with their international colleagues as critical reviewers.

Lectures

During the report year staff members and fellows were invited to present lectures as follows:

While serving as Regents' Lecturer in the Institute of Geophysics, University of California at Los Angeles, during the period October 22 to November 2, 1962,

P. H. Abelson gave a series of lectures entitled "The origin of life—geochemical considerations," "Extraterrestrial life," and "Paleobiochemistry." As a representative of the United States to the Sixth World Petroleum Congress held at Frankfurt, Germany, June 19–26, 1963, Dr. Abelson participated in a panel discussion by presenting a paper entitled "Organic geochemistry and the formation of petroleum." He gave a lecture, "Chemicals from ancient life," at the annual meeting of the Board of Trustees, Carnegie Institution of Washington. As recipient of the Hillebrand Award for 1962, he addressed the Chemical Society of Washington. He acted as moderator of a panel discussion on the effect of governmental support on science and the universities at the annual meeting of the National Research Council, and was a member of a panel to discuss "Future problems of science" at the Science Talent Institute sponsored by Science Service and Westinghouse. He also participated in the Symposium on the Living State, at Western Reserve University; the Conference on the Origin and Evolution of Atmospheres and Oceans, at the National Aeronautics and Space Administration Goddard Institute for Space Studies, New York City; the Conference on Education for Creativity in the Sciences, at New York University; and he addressed the Symposium on Biomedical Information at the 47th annual meeting of the Federation of American Societies for Experimental Biology, at Atlantic City, New Jersey. Dr. Abelson also lectured to the American Philosophical Society at its annual meeting in Philadelphia; the Ohio Agricultural Experiment Station at Wooster, Ohio; the Albert Einstein Medical Center in Philadelphia; and the University of Maryland chapter of the Society of the Sigma Xi at its annual meeting.

P. R. Brett lectured at the department of geology at Princeton University and addressed a seminar at the geology department, Brown University.

Charles W. Burnham delivered lectures

at the geology department, University of California at Los Angeles, and the Lamont Geological Observatory of Columbia University.

F. Chayes gave an address, "A brief history of modal analysis," at the First Congress of the International Society for Stereology at Vienna, and a lecture entitled "Some aspects of the geochemistry of Cenozoic volcanism" at the Czechoslovakian Society for Mineralogy and Geology at Prague, the department of geology and petrology at the University of Paris, and the department of geology at the University of Manchester.

B. T. C. Davis addressed the Geological Society of Washington.

G. Donnay gave a lecture, "Solid solution series of tourmaline," at the Georgia Institute of Technology at Atlanta.

K. von Gehlen gave a lecture, "Orientation studies with the X-ray texture goniometer," at the department of geology, Lehigh University.

T. C. Hoering participated in the International Symposium on Organic Geochemistry at Milan, Italy; he addressed the Physikalische Institut of the University of Heidelberg, Germany; the department of biochemistry at Georgetown Medical School; and the Gordon Research Conference on the Physics and Chemistry of Isotopes.

G. Kullerud gave a series of three lectures a month, from September through June, at Lehigh University, on sulfide phase equilibria, and he is directing the sulfide laboratory there in which three students are working for their Ph.D. degrees.

P. L. Parker lectured at the department of zoology at Cornell University.

E. W. Radoslovich addressed the geology departments at Pennsylvania State University, Ohio State University, Indiana University, University of Illinois, University of Wisconsin, and the University of Minnesota, and the agronomy department at Purdue University.

J. F. Schairer lectured at the Mineralogical Society of the District of Columbia

and the Central Pennsylvania Section of the American Chemical Society at Pennsylvania State University.

B. Velde addressed the Geological Society of Washington.

H. S. Yoder, Jr., spoke at the Symposium on Inorganic Chemistry under Unusual Conditions sponsored by the American Chemical Society at Indiana University. As recipient of the Arthur L. Day Medal, he addressed the Geological Society of America at their annual meeting in Houston, Texas. He delivered lectures at the departments of geology of Brown University, Franklin and Marshall College, Stanford University, and Montana State University, and at the Experimental Station of the E. I. du Pont de Nemours and Company in Wilmington, Delaware. He also gave a lecture before the Pick and Hammer Club of Menlo Park, California, and at the joint departments of geology of Western Reserve University and Case Institute of Technology in Cleveland, Ohio.

Petrologists' Club

Twelve meetings of the Petrologists' Club were held at the Laboratory during the year. A field trip to examine the Baltimore gabbro was made under the guidance of Professors Aaron C. Waters and Clifford Hopson, of the Johns Hopkins University. D. H. Lindsley was elected Secretary for the coming year. The following papers were presented:

"Magma distribution in ocean basins," by Felix Chayes (Geophysical Laboratory).

"Review of new work on granitization and granites in the Black Forest, Germany," by Kurt von Gehlen (Geophysical Laboratory and University of Erlangen-Nürnberg).

"Petrology and isotopic mineral age relations of a contact zone in the front range," by Stanley R. Hart (Department of Terrestrial Magnetism).

"The Glaucophane schists of Panoche Pass, California," by W. Gary Ernst (University of California, Los Angeles).

"Metasomatism in thermal gradients," by P. M. Orville (Yale University).

"Effects of a gabbro intrusive in alkali feldspars in a granitic environment," by W. C. Phinney (University of Minnesota).

"Garnet peridotites and eclogite," by M. J. O'Hara (University of Edinburgh).

"Some tall tales about pyroxenes," by F. R. Boyd (Geophysical Laboratory).

"Carbonatite volcanoes in Central Africa," by D. K. Bailey (Geophysical Laboratory and Trinity College, Dublin).

"Characteristics of lead isotopes in granitic rocks," by Bruce R. Doe (U. S. Geological Survey).

"Petrology of West Indian volcanic rocks," by Thomas W. Donnelly (Rice University).

"A further look at the orthoclase microcline inversion," by Tom Ll. Wright (U. S. Geological Survey).

The Summary of Published Work below briefly describes the papers published in scientific journals during the report year. In addition, the following papers are now prepared for publication: P. H. Abelson, "Geochemistry of amino acids"; P. H. Abelson, T. C. Hoering, and P. L. Parker, "Fatty acids in sedimentary rocks"; Charles W. Burham, "Refinement of the crystal structure of kyanite"; F. Chayes and Y. Suzuki, "Geological contours and trend surfaces"; L. A. Clark and G. Kullerud, "The sulfur-rich portion of the Fe-Ni-S system"; S. P. Clark, Jr., "The variation of density in the earth and the melting curve in the mantle"; S. P. Clark, Jr., "Temperatures in the continental crust"; H. J. Greenwood, "The synthesis and stability of anthophyllite"; H. J. Greenwood and H. L. Barnes, "Binary mixtures of volatile components"; G. Kullerud, "Review and evaluation of recent research on geologically significant sulfide-type systems"; G. Kullerud, "Sulfide research"; G. Kullerud, "Sulfide-type systems"; G. W. Morey and J. S. Burlew, "Studies of solubility in systems containing alkali and water, IV, The field of NaOH in the system NaOH-Na₂CO₃-H₂O"; N. Morimoto, "Structures of two polymorphic forms of Cu₅FeS₄"; N. Morimoto, "On the transition of bornite"; W. Schreyer, G. Kullerud, and P. Ram-

dohr, "Metamorphic conditions of ore and country rock of the Bodenmais, Bavaria, sulfide deposit"; B. Velde and J. Hower, "Petrological significance of illite poly-

morphism in Paleozoic sedimentary rocks"; D. R. Wones, "Physical properties of synthetic biotites on the join phlogopite-annite."

SUMMARY OF PUBLISHED WORK

- (1375) Altersbestimmungen an Gesteinen des ostbayerischen Grundgebirges und ihre geologische Deutung. G. L. Davis and W. Schreyer. *Geol. Rundschau*, 52, 146-169, 1962.

Rb-Sr biotite ages of Moldanubian gneisses and granites fall in the range 330 to 345 m.y. The biotite age of a pre-Moldanubian garnet-kyanite gneiss was found to be 440 m.y., and that of a metagranodiorite of the Münchberg Mass 385 m.y. Zircon from a Moldanubian gneiss yielded nearly concordant ages of approximately 450 m.y.

These results indicate that both the Münchberg Mass and large parts of the Moldanubicum have undergone considerable heating during early Variscan (= early Hercynian) time, probably in the course of regional metamorphism. The relations of these strongly metamorphosed complexes with the neighboring less affected sediments of the Saxothuringicum (in the case of the Münchberg Mass) and the Barrandium (in the case of the Moldanubicum) are presumed to be caused by different depths of metamorphism in Variscan time. Higher ages seem to be related at least partly to Caledonian intrusions.

- (1378) Numerical correlation and petrographic variation. F. Chayes. *J. Geol.*, 70, 440-452, 1962.

Of the $\binom{M}{2}$ covariances in any M -variable array characterized by a constant sum, at least $(M - 1)$ must be negative. If the parent variance for all variables is homogeneous, the expected value of the correlation between any pair of variables is $(1 - M)^{-1}$. In general, the larger the contribution any variable makes to the total variance, the more strongly negative are its expected correlations with other variables. No standard deviation may exceed the sum of the other standard deviations. The effect of these restrictions on the Harker variation diagram is discussed. Cloture restrictions which limit interpretation of Harker

diagrams are not removed and may be strengthened by partial correlation.

- (1379) Fe-Al oxides: Phase relationships below 1000°C. A. C. Turnock and H. P. Eugster. *J. Petrol.*, 3, 533-565, 1962.

The subsolidus phase relationships of magnetite, hercynite, hematite, corundum, wüstite, and iron are described. The phases were synthesized from chemical mixtures. Reactions and solid solution between them were induced under controlled conditions of composition, temperature, total vapor pressure, and partial pressure of oxygen. Reaction rates are slow, so that the experiments lasted from 1 to 40 days, and quenching is completely successful.

A solvus was determined that limits solid solution along the magnetite-hercynite join at temperatures below $860^\circ \pm 15^\circ\text{C}$. Compositions of the spinel solid solutions were determined by measuring the shift of the (440) reflection by means of a powder X-ray diffractometer. The calibration curve, 2θ versus composition, was made from measurements of spinel solid solutions synthesized in the one-phase region. The cell edge a_0 changes from $8.391 \pm 0.002 \text{ \AA}$ (magnetite, $\text{Fe}^{+2}\text{Fe}^{+3}\text{O}_4$) to 8.150 ± 0.004 (hercynite, $\text{Fe}^{+2}\text{Al}_2\text{O}_4$) by $a_0 = 8.391 - 0.00190X - 0.5X^2 \cdot 10^{-5}$ (X is mole per cent FeAl_2O_4 in solid solution).

In the system $\text{Fe-Al}_2\text{O}_3\text{-O}$ there are five univariant assemblages: (1) hematite + corundum + magnetite + V , (2) corundum + magnetite + hercynite + V , (3) magnetite + hercynite + wüstite + V , (4) hercynite + wüstite + iron + V , (5) hercynite + iron + corundum + V . Tie lines were located by determining the composition of the magnetite, hercynite, hematite, and corundum solid solutions for each assemblage.

The diagrams provide a basis for the discussion of the paragenesis of the oxide minerals. The progressive metamorphism of laterite deposits can be represented by (1) laterites and bauxites, hematite + hydrated aluminum oxides; (2) diasporites, hematite +

diaspore + corundum, with magnetite as a rare accessory; (3) emery, corundum + magnetite, with hematite as an accessory. The path of these mineral changes on the diagrams shows the decrease in oxygen content of the solids with decrease in the partial pressure of oxygen and relates the aluminum content of the magnetite to temperature.

The occurrences of hercynite are discussed. It is a rare mineral because it requires unusual conditions to grow, i.e., relatively low oxygen pressure and an extremely Fe,Al-rich environment.

- (1380) Relationships of lead isotopes among granites, pegmatites, and sulfide ores near Balmat, New York. B. R. Doe. *J. Geophys. Res.*, 67, 2895-2906, 1962.

The isotopic composition of lead from potassium feldspars of granite and pegmatites and from galena of near-by sulfide ores near Balmat, New York, was measured. Mineral ages have been measured by the Rb-Sr and K-Ar methods on potassium feldspars and associated micas. The best Rb-Sr age is 1100 m.y., and the K-Ar age is in good agreement at 1000 m.y. There is no evidence of any metamorphism of these rocks subsequent to the billion-year event. Lead in the feldspars is slightly more radiogenic than the lead in the galena. The ores could not have been derived from the near-by igneous rocks unless lead had been added to the potassium feldspars of the igneous rocks after the formation of the ores. The potassium feldspars and ore galenas each have lead with isotopic constitutions that lie close to the normal growth curves for conformable lead ores. In addition, the model lead ages for the potassium-feldspar leads of these syntectonic granites and pegmatites are in fair agreement with the radioactive ages. The reproducibility of the lead isotope measurements is established from sixteen analyses of a shelf lead and duplicate determinations of each sample. The data are corrected for discrimination by the electron multiplier through analyses of gravimetric mixtures of enriched isotopes of Pb^{206} and Pb^{208} .

- (1381) X-ray method for rapid determination of sulfur and cobalt in loellingite. L. A. Clark. *Can. Mineralogist*, 7, 306-311, 1962.

Loellingite, $(\text{Fe},\text{Co})\text{As}_2$, which frequently also contains 1 or 2 per cent S, is one of the common constituents in arsenide-type ores.

The amounts of both Co and As can be determined rapidly by X-ray powder diffraction measurements. The interplanar spacings of this mineral vary as functions of both S and Co, and these relations are plotted in a graph for four reflections. The values obtained by measurements of either d_{210} and d_{111} or d_{120} and d_{101} by application of this graph give both the S and Co content of loellingite specimens.

- (1383) The join $\text{Ca}_3\text{Al}_2\text{Si}_3\text{O}_{12}$ - $\text{Mg}_3\text{Al}_2\text{Si}_3\text{O}_{12}$ and its bearing on the system CaO - MgO - Al_2O_3 - SiO_2 at atmospheric pressure. G. A. Chinner and J. F. Schairer. *Am. J. Sci.*, 260, 611-634, 1962.

At atmospheric pressure the "garnet" join $\text{Ca}_3\text{Al}_2\text{Si}_3\text{O}_{12}$ (grossularite composition)- $\text{Mg}_3\text{Al}_2\text{Si}_3\text{O}_{12}$ (pyrope composition) is quaternary. Data on quenching runs for eleven compositions along the join are presented; they give the temperatures of two quaternary invariant points within the system CaO - MgO - Al_2O_3 - SiO_2 , viz., anorthite-wollastonite-pseudowollastonite-melilite-liquid ($1205^\circ \pm 5^\circ\text{C}$) and anorthite-forsterite-spinel-cordierite-liquid ($1280^\circ \pm 5^\circ\text{C}$).

The garnet join cuts three subsolidus tetrahedra: anorthite-wollastonite-gehlenite-akermanite, anorthite-forsterite-gehlenite-akermanite, and anorthite-forsterite-spinel-cordierite. Subsolidus tetrahedra in the vicinity of the "garnet" join are anorthite-akermanite-diopside- CaSiO_3 , anorthite-akermanite-diopside-forsterite, anorthite-forsterite-spinel-gehlenite, anorthite-forsterite-diopside-enstatite, anorthite-forsterite-enstatite-cordierite, and anorthite-enstatite-cordierite- SiO_2 . The liquidus relations on the bounding planes of most of the subsolidus tetrahedra are known from the data of previous workers, and from these figure 4 has been constructed showing the relationship between univariant lines and invariant points where liquid is present in the silica-rich part of the system CaO - MgO - Al_2O_3 - SiO_2 .

From the viewpoint of igneous petrology, the line *efgh* of this figure represents the temperature maximum on the divariant surfaces that separates liquids taking a saturated (silica-rich) trend from those taking an undersaturated (melilite-rich) trend. It is shown that part of the line *efgh* runs within the tetrahedron anorthite-forsterite-diopside-enstatite, so that "simplified basalt" compositions within the system CaO - MgO - Al_2O_3 -

SiO₂ may take either the saturated or the undersaturated trend, depending on the relative amounts of "normative" olivine, anorthite, diopside, and hypersthene. The classic gabbro-norite sequence produced by the contamination of basic rock with argillaceous material is illustrated in terms of the synthetic system, and it is suggested that the garnet- and cordierite-bearing magmatic rocks found at igneous contacts, rather than representing the end product of the gabbro-norite contamination sequence, may sometimes have been formed by the fractional melting of country rock.

- (1384) Location of argon and water in cordierite. J. V. Smith and W. Schreyer. *Mineral. Mag.*, 33, 226-236, 1962.

Evaluation of X-ray powder diffraction data shows that argon atoms (radius 1.9 Å) lie at the centers of the large holes in the cordierite structure. The reflection intensities for hydrous cordierite differ from those for anhydrous cordierite but to a lesser degree than those for argon-bearing cordierite. Although analysis is uncertain, it appears that the smaller water molecules (radius 1.4 Å) do not occupy either the centers of the six-membered rings or the centers of the large cavities. It is possible that they may be attached to the walls of the large cavities or occur partly as hydroxyl groups in the framework. Single-crystal X-ray analysis is necessary to resolve this problem.

- (1385) Mineral ages from the Wichita and Arbuckle Mountains, Oklahoma, and the St. Francis Mountains, Missouri. G. R. Tilton, G. W. Wetherill, and G. L. Davis. *J. Geophys. Res.*, 67, 4011-4019, 1962.

Isotopic age determinations show that intrusion of rocks took place 520 to 560 m.y. ago in the Wichita Mountains. It is likely that the geographic extent of rocks of this age is limited. In the St. Francis and Arbuckle Mountains older micas and feldspars give ages of 1300 to 1450 m.y. The associated zircons have discordant uranium-lead ages. The uncertainties are such that the zircons might be of the same age as the micas, or as old as 1500 to 1550 m.y. Muscovite from a pegmatite in the Decaturville uplift in central Missouri gives age values similar to those from the St. Francis Mountains. These rocks are correlated with pegmatites and granites of the same age to the west in New Mexico and

Arizona. The pattern of distribution of ages for part of the North American continent is discussed in relation to the new results.

- (1386) The system Ni-As-S: Phase relations and mineralogical significance. R. A. Yund. *Am. J. Sci.*, 260, 761-782, 1962.

Phase relations in the ternary system Ni-As-S were determined in rigid silica-glass tubes between 700° and 450°C, with some additional data at lower temperatures.

The only ternary phase in the system, corresponding to the mineral gersdorffite, for which the accepted formula is NiAsS, has a large variation in its As/S ratio. It is homogeneous from NiAs_{1.77}S_{0.23} to NiAs_{0.77}S_{1.23} at 700°C. Gersdorffite in equilibrium with NiAs₂ (rammelsbergite or pararammelsbergite) has the composition NiAs_{1.80}S_{0.20} and NiAs_{1.72}S_{0.28} at 660° and 450°C, respectively. This is a difference of only 2 weight per cent arsenic. The unit cell edge of gersdorffite between stoichiometric NiAsS and NiAs_{1.80}S_{0.20} is given by the equation $a = 5.6939 + 0.000470X$, where a is the unit cell edge of gersdorffite (in Å) containing X weight per cent NiAs₂. Gersdorffite analyses from the literature are reviewed, and several new specimens are examined to demonstrate that natural gersdorffite also has a large variation in its As/S ratio.

Complete solid solution exists between niccolite (Ni_{1±x}As) and αNi_{1-x}S (the high-temperature modification of millerite) above 595° ± 5°C. The solvus was determined from 595° to 400°C along the join from NiAs to NiS.

Approximately 1 weight per cent sulfur substituting for arsenic lowers the polymorphic inversion of rammelsbergite to pararammelsbergite from 590° ± 10°C to 475° ± 25°C.

Stable assemblages in the synthetic system correspond closely to the associations found in nature.

- (1387) Origin of basalt magmas: An experimental study of natural and synthetic rock systems. H. S. Yoder, Jr., and C. E. Tilley. *J. Petrol.*, 3, 342-532, 1962.

Natural basalts and eclogites were investigated experimentally at a series of temperatures in the pressure range 1 atm to 40 kb and with water pressures 1 to 10 kb. Some runs were also made on related synthetic systems at 10 and 33 kb.

The two principal magma types recognized by field investigators—tholeiite and alkali basalt types—appear to be separated by equilibrium thermal divides at 1 atm. The principal divides were found by experiment at elevated pressures to give way to a new set of equilibrium thermal divides resulting from a new mineralogy. The change of the equilibrium thermal divides with pressure leads to the derivation of the two principal magma trends from the same bulk composition.

The melting behavior of basalts and eclogites indicates that both are the partial melting products of a more primitive rock (e.g., garnet peridotite). In the region of magma generation (below 60 km) the parental material, presumed to be garnet peridotite, yields an eclogitic magma, and its fractionation depends on the garnet and omphacite of the eclogite, not on plagioclase and clinopyroxene of a basaltic magma. Increase of the garnet constituents in the magma at high pressure by effective removal of omphacite or shift of the garnet-omphacite boundary “surface” will give rise to a tholeiite-type magma at low pressure. Similarly, increase of the omphacite constituents in the magma at high pressure by physical or physicochemical means will give rise to an alkali basalt-type magma at low pressure. In general, alkali basalt-type magmas are to be expected to be generated at greater depths than tholeiite-type magmas from the same primary source rock.

Establishment of the two major basalt series takes place in the region of generation; additional minor diversification of each series may come about after emplacement in or on the crust by crystal settling, oxidation or reduction, gas fluxing, contamination, and other processes. The derivative magmas are greatly restricted by the course of liquid thermal descent imposed at generation.

Pressure-temperature limits established experimentally suggest that the basalt-eclogite transformation may be responsible for the M discontinuity under the continents, but not under the oceans.

The field of stability of basalt is drastically reduced in the presence of water, and amphibolite is produced. The melting of amphibolite takes place over a much greater range of temperature than the melting of basalt. At 10 kb water pressure the beginning of melting of amphibolite closely approaches that of granite. Partial melting of amphibolite may

yield anorthositic liquids having a relatively low anorthite content at exceptionally low temperatures. Eclogite itself is not stable in the presence of water and gives place to amphibolite or pyroxene hornblendite. Magmas that crystallize to basalt, gabbro, or eclogite must have had a low water content at the time of crystallization.

Fifteen rock and twenty-three mineral analyses as well as numerous partial chemical analyses of experimental products were made by J. H. Scoon in the course of the investigation. These chemical analyses bear on many mineralogical and petrological problems.

- (1388) Temperature of crystallization of pyrrhotite and sphalerite from the Highland-Surprise Mine, Coeur d'Alene District, Idaho. R. G. Arnold, R. G. Coleman, and V. C. Fryklund. *Econ. Geol.*, 57, 1163–1174, 1962.

The ore bodies of the Highland-Surprise Mine are replacements along shear zones in quartzose slate, quartzite, and phyllite of the Prichard formation of the Belt series (Precambrian). Pyrite, arsenopyrite, pyrrhotite, sphalerite, chalcopyrite, and galena are the chief metallic minerals and were probably deposited in that order.

Temperatures of formation were estimated for pyrrhotite-pyrite and sphalerite-pyrrhotite assemblages contained in the steeply dipping vein system. Measurements on sixty-two pyrrhotites indicate a range in temperature of crystallization between 370° and 492°C (no correction required for confining pressures <2000 bars below 670°C), and measurements on fourteen sphalerites indicate crystallization temperatures between 375° and 460°C (uncorrected for confining pressure). No systematic temperature gradients were recognized.

Minor elements in twenty-three pyrrhotite, eight pyrite, thirteen sphalerite, and two galena samples were determined. Partition ratios of nickel and cobalt in pyrrhotite-pyrite and sphalerite-pyrrhotite pairs are erratic. This suggests (a) a disequilibrium distribution of these elements between the phases of each mineral pair and/or (b) crystallization of the mineral pairs under different physical conditions.

- (1389) Effect of pressure on the melting of diopside, $\text{CaMgSi}_2\text{O}_6$, and albite, $\text{NaAlSi}_3\text{O}_8$, in the range up to 50 kb. F. R. Boyd and J. L. England. *J. Geophys. Res.*, 68, 311–323, 1963.

The melting curves of albite and diopside

have been determined in the pressure range 5 to 50 kb by means of single-stage apparatus. Data are given for $\text{NaAlSi}_3\text{O}_8$ composition only at pressures below 33 kb, where albite is the phase stable at the liquidus. Simon equations have been calculated for both curves, and they fit the data well. The melting curves have a pronounced curvature, and the slopes at pressures above 25 kb are only about half the initial slopes. These results suggest that the effect of pressure on the melting of rocks in the mantle will decrease notably with depth. Extrapolation of the diopside curve to a pressure of 1400 kb, equivalent to that present at the core-mantle boundary, gives a melting temperature of 3750°C . Experience with single-stage apparatus has shown that the fraction correction of -8 per cent that we previously applied is probably too large. Results of this study are given as load pressures and are believed to be accurate within ± 5 per cent.

(1390) Annual report of the Director for 1961-1962.

(1391) The action of water on calcite, magnesite, and dolomite. G. W. Morey. *Am. Mineralogist*, 47, 1456-1460, 1962.

CO_2 -free liquid water was pumped at 200 atm pressure over calcite, magnesite, and dolomite. Calcite was dissolved without decomposition, but, in both magnesite and dolomite, brucite, $\text{Mg}(\text{OH})_2$, was formed by the decomposition of MgCO_3 .

(1392) On pyroxene molecules in the CIPW norm. F. Chayes. *Geol. Mag.*, 100, 7-10, 1963.

Barth argued that the CIPW conventions governing the calculation of normative pyroxenes and olivines are based on inadequate or incorrect mineralogical information and should be abandoned. The real occasion for the conventions appears to be petrological, not mineralogical. Qualitative agreement between norms and modes of undersaturated rocks requires the use of these or very similar conventions. Ease of calculation is no longer a major consideration, and a more realistic set of rules could now be adopted if it were available.

(1393) Alkali ion exchange between vapor and feldspar phases. P. M. Orville. *Am. J. Sci.*, 261, 201-237, 1963.

The high alkali chloride contents of fluid

inclusions and most connate waters suggest that metamorphic rocks and many igneous rocks have crystallized in the presence of rather concentrated solutions of Na and K salts. Equilibria involving alkali ions in solution in a fluid phase and alkali silicates should therefore be of interest to petrologists.

The system KAlSi_3O_8 - $\text{NaAlSi}_3\text{O}_8$ - NaCl - KCl - H_2O has been investigated at temperatures of 350° to 700°C at a pressure of 2000 atm with the fluid phase 2M in total alkali chloride. Alkali feldspars were the only crystalline phases encountered in these experiments. Phase assemblages observed were: (1) a univariant two-phase assemblage consisting of a single alkali feldspar and an alkali chloride solution; (2) an invariant three-phase assemblage consisting of two alkali feldspars and an alkali chloride solution.

The proportion of K to (K + Na) in the vapor phase that coexists with two alkali feldspars in the invariant phase assemblage decreases with falling temperature from 0.260 at 670° to less than 0.16 at 400°C . This is consistent with, and provides an explanation for, the small amount of K relative to Na found in the waters of hot springs.

The crest of the alkali feldspar solvus is near 680°C at a feldspar composition of $\text{Ab}_{70\pm 10}\text{Or}_{30\pm 10}$.

A comparison of melt-crystal equilibria and vapor-crystal equilibria suggests that fractionation of alkalis between a fluid phase and crystalline feldspars is strongly dependent on temperature but only slightly dependent on the physical condition of the fluid. Melt-crystal and vapor-crystal equilibria appear to be nearly the same for the alkali feldspars at a given temperature.

Because the alkali ratio in a vapor phase that coexists with two feldspar phases varies with temperature, the presence of a thermal gradient in a two-feldspar rock requires the presence of compositional gradients with respect to the alkalis in the vapor phase. Alkali ions will tend to diffuse through the vapor in response to these gradients, and alkali metasomatism within the rock mass will take place. In general, the cooler rock will be enriched and the warmer rock depleted in K feldspar. This mechanism of alkali transport has been demonstrated on a small scale in the laboratory.

The presence of Ca feldspar as a constituent in coexisting feldspar phases has a significant effect on the alkali ratio in a coexisting vapor

phase. At constant temperature, an increase in the Ca content of the feldspar phases will result in a higher K/Na ratio in the vapor phase. Original inhomogeneities in Ca content within a mass of sedimentary rocks will result in compositional gradients with respect to alkalis in the vapor phase that will favor alkali metasomatism during metamorphism. Rocks originally rich in Ca will tend to be depleted in K feldspar, and rocks originally poor in Ca will tend to be enriched in K feldspar.

It seems likely that alkali metasomatism will take place in the presence of an alkali-bearing vapor phase as a natural consequence of temperature, pressure, and compositional gradients in the earth's crust.

- (1394) Radioactive heat production in eclogite and some ultramafic rocks. G. R. Tilton and G. W. Reed. In *Earth Science and Meteoritics*, compiled by J. Geiss and E. D. Goldberg, North-Holland Publishing Company, Amsterdam, pp. 31-43, 1963.

The concentration of uranium in five ultramafic rocks (peridotite) is taken to average 0.006 part per million on the basis of neutron activation and isotope dilution measurements. This value may be an upper limit. Eclogite nodules of probable mantle origin from tuff at Salt Lake Crater, Hawaiian Islands, were found to contain about ten times more uranium than the peridotites, but more than ten times less uranium than Hawaiian basalt. Potassium was also determined in these rocks.

These results are discussed in terms of their bearing on the thermal history of the outer mantle of the earth. Heat production in the peridotites is too low to explain heat flow in oceanic areas if the outer mantle consisted solely of such rock. Rock of the chemical composition of peridotite might be a major constituent of the outer mantle in continental areas or of the deep mantle.

The eclogites have heat production rates too low to account for the heat flow in the ocean floor if heat transfer takes place in the mantle solely by thermal conduction. Eclogite could provide a satisfactory heat source if convective transfer accompanies thermal conduction. It is doubtful that radiation plus conduction without convection would be sufficient. Rock two to three times more radioactive than the eclogites could provide sufficient heat flow in oceanic areas by thermal conduction alone.

Reasons are given for believing that the

eclogites provide a better guide to the proportions of the radioactive elements in the mantle than chondritic meteorites do.

- (1395) Relative abundance of intermediate members of the oceanic basalt-trachyte association. F. Chayes. *J. Geophys. Res.*, 68, 1519-1534, 1963.

The relative abundance of analyses of intermediate and salic lavas of the oceanic basalt-trachyte association supports Daly's suggestion, based originally on field study, that in the oceanic islands rocks intermediate in composition between basalt and trachyte are much less common than trachyte. The sample distribution of SiO₂ shows a clearly defined central minimum, but the effect is considerably stronger in CaO. It is perhaps best shown by the Thornton-Tuttle index. A bimodal frequency distribution of any major oxide or normative parameter is difficult if not impossible to explain as a consequence of crystal fractionation alone. Partial melting, the most reasonable alternative to crystal fractionation, is also open to a variety of objections. A satisfactory explanation of the oceanic basalt-trachyte association will require both new data and new thinking.

- (1396) Polymorphism in digenite. N. Morimoto and G. Kullerud. *Am. Mineralogist*, 48, 110-123, 1963.

Single-crystal investigations of synthetic as well as natural specimens have revealed the existence of three polymorphs of digenite: a high-temperature form, a low-temperature form, and a transitional metastable form, in close analogy with the bornite polymorphs described earlier. The high-temperature form is stable above $73^{\circ} \pm 3^{\circ}\text{C}$ and has cubic symmetry with $a = 5.570 \pm 0.005 \text{ \AA}$. The unit cell contains Cu_{7.2- x} S₄. The space group is *Fm3m*. The crystal structure of this polymorph was determined. The arrangement of the sulfur atoms is that of cubic closest packing, and 9/10 of the copper atoms occupy statistically 24 equivalent sites inside the sulfur tetrahedra. The coordinates are $x = 0.310$, $y = 0.300$, $z = 0.290$ for 7.2 Cu, and $x = y = z = 0$ for 4S.

The metastable form, which is obtained by cooling from $73^{\circ} \pm 3^{\circ}\text{C}$ or higher temperatures, has cubic symmetry with $a = 27.85 \pm 0.05 \text{ \AA}$ and space group *Fd3m*. The special extinction rules observed among the X-ray reflections indicate that this cubic symmetry can be interpreted as due to twinning of fine

domains with rhombohedral symmetry. This form is the same as that described as the low-temperature form of digenite ($a_{rh} = 16.16 \text{ \AA}$, $\alpha = 13^\circ 56'$) by Donnay and others. In the present study, however, it was found to be transitional metastable. It changes gradually with time to a stable low-temperature form. This form also has cubic symmetry with $a = 27.85 \pm 0.05 \text{ \AA}$, without the special extinction rules. Its structure can be explained by twinning in the same way as that of the metastable form.

Synthetic material of exact Cu_9S_5 composition behaves somewhat differently from natural digenite, suggesting that the composition of digenite should be formulated as $\text{Cu}_{9-x}\text{S}_5$. The thermal behavior of natural digenite is readily explained through its close analogy to that of synthetic $\text{Cu}_{9-x}\text{S}_5$.

- (1397) The opaque minerals in stony meteorites. P. Ramdohr. *J. Geophys. Res.*, 68, 2011–2036, 1963.

The opaque and semiopaque minerals were examined in polished sections of 135 stony meteorites. The following minerals, all of which were previously known from meteorites, were observed: kamacite and taenite and intergrowths of these minerals (plessite), cohenite, schreibersite, graphite, native copper, native gold, troilite, pentlandite, oldhamite, daubréelite, chromite, magnetite, and ilmenite. The following minerals, which are well known from terrestrial occurrences, were observed for the first time in stony meteorites: chalcopyrrhotite, valleriite, sphalerite, chalcopyrite, pyrite, and bravoite. Entirely new minerals observed were $(\text{Ni,Fe})_x\text{Si}_y$, $(\text{Mg,Fe,Ca,Mn})\text{S}$ with NaCl structure, and a hexagonal layer-structure mineral containing Fe-C-S, as well as the following minerals identified by letters: *A*, a strongly anisotropic, dark yellow-green mineral; *B*, a mineral occurring in thin lamellae as a decomposition product of *A*; *C*, a dark olive-colored mineral; *D*, a colorless transparent mineral with high refractive index, replacing ilmenite and chromite; *E*, a dark brown, probably isotropic mineral; *F*, a white mineral, probably containing arsenic; *G*, a light blue mineral; *H*, a yellow, almost metallic mineral; *I*, a colorless spinel-like mineral, with exsolution of ilmenite; *K*, a very dark gray sulfide; and *L*, a very strongly pleochroic mineral. Structures and textures as well as effects of weathering processes are described.

- (1398) Thermal stability of pentlandite. G. Kullerud. *Can. Mineralogist*, 7, 353–366, 1963.

The thermal stability of pentlandite was studied by quenching, differential thermal analysis, and high-temperature X-ray diffraction experiments. Rigid silica tubes were employed as reaction vessels, and vapor, therefore, is an inherent phase in all three types of experiments.

Synthetic pentlandite of $\text{Fe}_{4.5}\text{Ni}_{4.5}\text{S}_8$ composition was found to decompose at $610^\circ \pm 2^\circ\text{C}$ to $(\text{Fe,Ni})_{1-x}\text{S}$ with hexagonal pyrrhotite structure and to a high-temperature non-quenchable phase, equivalent to $\text{Ni}_{3\pm x}\text{S}_2$ of the pure NiS system, but containing some iron. Of these phases $(\text{Fe,Ni})_{1-x}\text{S}$ has low Ni content and a metal-to-sulfur ratio of 9:10 or possibly slightly higher, and the $\text{Ni}_{3\pm x}\text{S}_2$ phase has a metal-to-sulfur ratio of 3:2 or slightly less.

The first appearance of liquid was recorded at 862°C in differential thermal analysis experiments on synthetic material of $\text{Fe}_{4.5}\text{Ni}_{4.5}\text{S}_8$ composition. This temperature corresponds to that given in the literature as the “melting point” for pentlandite. Experiments on pentlandite from Frood Mine, Sudbury, show breakdown of pentlandite at 613°C and melting effects in the temperature region 864° to 881°C .

These experimental results have important bearing on the geological interpretation of pentlandite-pyrrhotite assemblages in ores like those of the Sudbury area.

In the pure Fe-Ni-S system a field containing homogeneous liquid of composition pertinent to the formation of pentlandite-pyrrhotite or pentlandite-heazlewoodite assemblages exists above approximately 1000° to 1100°C . On cooling, $(\text{Fe,Ni})_{1-x}\text{S}$ first crystallizes from the liquid. This phase coexists down to 862°C with a metal-rich iron-nickel-sulfur liquid. Below 862°C but above 610°C , the $(\text{Fe,Ni})_{1-x}\text{S}$ phase coexists with $(\text{Ni,Fe})_{3\pm x}\text{S}_2$. At 610°C , pentlandite appears and the $(\text{Fe,Ni})_{1-x}\text{S}$ - $(\text{Ni,Fe})_{3\pm x}\text{S}_2$ assemblage is no longer stable. At lower temperatures, depending on bulk composition, the pyrrhotite-pentlandite or pentlandite- $(\text{Ni,Fe})_{3\pm x}\text{S}_2$ pairs are stable. The $(\text{Ni,Fe})_{3\pm x}\text{S}_2$ phase breaks down on cooling below about 550°C , and, depending on the metal-to-sulfur ratio, heazlewoodite and pentlandite, or heazlewoodite, awaruite, and pentlandite, or heazlewoodite, millerite (or

Ni_7S_6), and pentlandite will form stable assemblages.

- (1399) Refinement of the crystal structure of sillimanite. Charles W. Burnham. *Z. Krist.*, 118, 127–148, 1963.

The crystal structure of sillimanite, Al_2SiO_5 , has been refined as part of a detailed structural study of the aluminum-silicate minerals. Three-dimensional least-squares refinement reduced the disagreement factor, R , for 347 hkl reflections to 5.6 per cent.

The previously determined sillimanite structure was found to be fundamentally correct. Chains of aluminum octahedra, similar to those in andalusite, lie parallel to the c axis. They are supported by double chains of tetrahedra containing aluminum and silicon cations alternating in an ordered sequence. The three independent octahedral Al-O distances are 1.957, 1.919, and 1.861 Å, all ± 0.003 Å. The Si-O distances are 1.629 ± 0.007 , 1.633 ± 0.004 , 1.633 ± 0.004 , and 1.564 ± 0.006 Å. The tetrahedral Al-O distances are 1.758 ± 0.005 , 1.800 ± 0.004 , 1.800 ± 0.004 , and 1.721 ± 0.006 Å. The shortest Si-O and tetrahedral Al-O distances represent bonding to a common oxygen atom through a Si-O-Al angle of 171.6° . The indicated thermal motion of this oxygen atom is nearly twice as great as that of the other three oxygen atoms in the asymmetric unit and, in addition, is strongly anisotropic.

- (1401) Phase equilibria of "ferriannite," $\text{KFe}_3^{+2}\text{Fe}^{+3}\text{Si}_3\text{O}_{10}(\text{OH})_2$. David R. Wones. *Am. J. Sci.*, 261, 581–596, 1963.

Stability of "ferriannite," $\text{KFe}_3^{+2}\text{Fe}^{+3}\text{Si}_3\text{O}_{10}(\text{OH})_2$, has been determined as a function of total pressure ($P_{\text{H}_2\text{O}} + P_{\text{H}_2}$), temperature, and oxygen fugacity. Ferriannite will react with such a gas to form the following assemblages: iron feldspar + hematite, iron feldspar + magnetite, melt + magnetite, melt + magnetite + wüstite + fayalite, melt + wüstite + iron + fayalite.

X-ray powder data show that ferriannite is monoclinic with the following cell dimensions: $a = 5.430 \pm 0.002$ Å, $b = 9.404 \pm 0.003$, $c = 10.341 \pm 0.006$, $\beta = 100^\circ 4' \pm 10'$. The indices of refraction are: $\alpha = 1.698 \pm 0.003$ to 1.715 ± 0.003 ; $\beta \approx \gamma = 1.739 \pm 0.002$ to 1.755 ± 0.005 . Variations in indices of refraction correspond to variations in the hydrogen fugacity of experiments in which ferriannite is the stable phase.

- (1404) Geochronology. G. R. Tilton and S. R. Hart. *Science*, 140, 357–366, 1963.

Advances in geochronology since 1958 are emphasized, using data taken primarily from North American rocks. Age measurements from the Precambrian country rock in the vicinity of a Tertiary stock in the Front Range in Colorado illustrate the effect of contact metamorphism on the age record of biotite, potassium feldspar, and hornblende. Activation energies can be estimated for the diffusion of argon and strontium in biotite. When rocks undergo metamorphism, radiogenic Sr^{87} may be redistributed among the various mineral phases; that is, minerals containing negligible rubidium may nevertheless have radiogenic strontium picked up from other minerals such as biotite. Discordant lead ages are discussed in terms of continuous diffusion of lead; data from Precambrian shield areas seem to fit the theory well. It is also becoming apparent that episodes of metamorphism cause sudden loss of lead in some, but not all, instances.

The oldest granitic rocks found on the continents give ages of around 3300 m.y. It is possible that granites formed in negligible quantity, if at all, before that time. The geographic distribution of age values for North America shows regularities that could indicate growth of the continent during geological time. Finally, the temporal distribution of Rb-Sr ages from North America shows pronounced grouping of values, those at 350, 1000, 1800, and 2600 m.y. occurring most frequently.

- (1405) The effect of contact metamorphism on lead in potassium feldspars near the Eldora stock, Colorado. B. R. Doe and S. R. Hart. *J. Geophys. Res.*, 68, 3521–3530, 1963.

The isotopic composition and the concentration of lead have been determined for samples of potassium feldspar from the quartz monzonite of the Eldora stock and from Precambrian pegmatites in the surrounding Idaho Springs Formation near Boulder, Colorado. The isotopic data show that lead entered the potassium feldspar up to 1000 feet from the stock, which is about 10,000 feet across. The isotopic results also prove that not all the lead that entered the feldspar could have come from the quartz monzonite. The isotopic constitution of the lead in potassium feldspars was more easily affected by the contact metamorphism

than the Rb-Sr system of the feldspars or the K-Ar system of hornblende but less easily than the K-Ar and Rb-Sr systems of biotite. The transition of microcline to orthoclase in pegmatites of the Idaho Springs Formation took place without major effect on the isotopic composition or the concentration of lead. Comparison of the Rb-Sr and lead isotopes data indicates that lead can be added to the feldspars without solution and redeposition of the feldspar. Isotopic data on Precambrian

feldspars from Colorado and New York and feldspars from the Laramide quartz monzonite are not compatible with generation of all their lead from an "infinite reservoir" with fixed present-day values of U/Pb and Th/Pb. The existence of such a reservoir, however, is not precluded, for the departures could be caused by contamination at the time of intrusion. The variations found for the Precambrian rocks could also have been caused by metamorphism subsequent to intrusion.

BIBLIOGRAPHY

- Arnold, R. G., R. G. Coleman, and V. C. Fryklund, Temperature of crystallization of pyrrhotite and sphalerite from the Highland-Surprise Mine, Coeur d'Alene District, Idaho, *Econ. Geol.*, 57, 1163-1174, 1962.
- Boyd, F. R., and J. L. England, Effect of pressure on the melting of diopside, $\text{CaMgSi}_2\text{O}_6$, and albite, $\text{NaAlSi}_3\text{O}_8$, in the range up to 50 kb, *J. Geophys. Res.*, 68, 311-323, 1963.
- Burnham, Charles W., Refinement of the crystal structure of sillimanite, *Z. Krist.*, 118, 127-148, 1963.
- Chayes, F., Numerical correlation and petrographic variation, *J. Geol.*, 70, 440-452, 1962.
- Chayes, F., On pyroxene molecules in the CIPW norm, *Geol. Mag.*, 100, 7-10, 1963.
- Chayes, F., Relative abundance of intermediate members of the oceanic basalt-trachyte association, *J. Geophys. Res.*, 68, 1519-1534, 1963.
- Chinner, G. A., and J. F. Schairer, The join $\text{Ca}_3\text{Al}_2\text{Si}_3\text{O}_{12}\text{-Mg}_3\text{Al}_2\text{Si}_3\text{O}_{12}$ and its bearing on the system $\text{CaO-MgO-Al}_2\text{O}_3\text{-SiO}_2$ at atmospheric pressure, *Am. J. Sci.*, 260, 611-634, 1962.
- Clark, L. A., X-ray method for rapid determination of sulfur and cobalt in loellingite, *Can. Mineralogist*, 7, 306-311, 1962.
- Coleman, R. G., see Arnold, R. G.
- Davis, G. L., and W. Schreyer, Altersbestimmungen an Gesteinen des ostbayerischen Grundgebirges und ihre geologische Deutung, *Geol. Rundschau*, 52, 146-169, 1962.
- Davis, G. L., see also Tilton, G. R.
- Doe, B. R., Relationships of lead isotopes among granites, pegmatites, and sulfide ores near Balmat, New York, *J. Geophys. Res.*, 67, 2895-2906, 1962.
- Doe, B. R., and S. R. Hart, The effect of contact metamorphism on lead in potassium feldspars near the Eldora stock, Colorado, *J. Geophys. Res.*, 68, 3521-3530, 1963.
- England, J. L., see Boyd, F. R.
- Eugster, H. P., see Turnock, A. C.
- Fryklund, V. C., see Arnold, R. G.
- Hart, S. R., see Doe, B. R.; Tilton, G. R.
- Kullerud, G., Thermal stability of pentlandite, *Can. Mineralogist*, 7, 353-366, 1963.
- Kullerud, G., see also Morimoto, N.
- Morey, G. W., The action of water on calcite, magnesite, and dolomite, *Am. Mineralogist*, 47, 1456-1460, 1962.
- Morimoto, N., and G. Kullerud, Polymorphism in digenite, *Am. Mineralogist*, 48, 110-123, 1963.
- Orville, P. M., Alkali ion exchange between vapor and feldspar phases, *Am. J. Sci.*, 261, 201-237, 1963.
- Ramdohr, P., The opaque minerals in stony meteorites, *J. Geophys. Res.*, 68, 2011-2036, 1963.
- Reed, G. W., see Tilton, G. R.
- Schairer, J. F., see Chinner, G. A.
- Schreyer, W., see Davis, G. L.; Smith, J. V.
- Smith, J. V., and W. Schreyer, Location of argon and water in cordierite, *Mineral. Mag.*, 33, 226-236, 1962.
- Tilley, C. E., see Yoder, H. S., Jr.
- Tilton, G. R., and S. R. Hart, Geochronology, *Science*, 140, 357-366, 1963.
- Tilton, G. R., and G. W. Reed, Radioactive heat production in eclogite and some ultramafic rocks, in *Earth Science and Meteoritics*, compiled by J. Geiss and E. D. Goldberg, North-Holland Publishing Company, Amsterdam, pp. 31-43, 1963.
- Tilton, G. R., G. W. Wetherill, and G. L. Davis, Mineral ages from the Wichita and Arbuckle Mountains, Oklahoma, and the St. Francis Mountains, Missouri, *J. Geophys. Res.*, 67, 4011-4019, 1962.

Turnock, A. C., and H. P. Eugster, Fe-Al oxides: Phase relationships below 1000°C, *J. Petrol.*, **3**, 533-565, 1962.

Wetherill, G. W., *see* Tilton, G. R.

Wones, David R., Phase equilibria of "ferrianite," $\text{KFe}_3^{+2}\text{Fe}^{+3}\text{Si}_3\text{O}_{10}(\text{OH})_2$, *Am. J. Sci.*, **261**, 581-596, 1963.

Yoder, H. S., Jr., and C. E. Tilley, Origin of basaltic magmas: An experimental study of natural and synthetic rock systems, *J. Petrol.*, **3**, 342-532, 1962.

Yund, R. A., The system Ni-As-S: Phase relations and mineralogical significance, *Am. J. Sci.*, **260**, 761-782, 1962.

REFERENCES CITED

Abelson, P. H., and T. C. Hoering, Carbon-isotope fractionation in formation of amino acids by photosynthetic organisms, *Proc. Natl. Acad. Sci. U. S.*, **47**, 623-632, 1961.

Agrell, S. O., and J. V. Smith, Cell dimensions, solid solution, polymorphism, and identification of mullite and sillimanite, *J. Am. Ceram. Soc.*, **43**, 69-76, 1960.

Albers, W., C. Haas, H. J. Vink, and J. D. Wasscher, Investigation on SnS, *J. Appl. Phys.*, **32**, 2220-2225, 1961.

Albers, W., and K. Schol, The *P-T-X* phase diagram of the system Sn-S, *Philips Res. Repts.*, **16**, 329-342, 1961.

Allen, E. T., W. P. White, F. E. Wright, and E. S. Larsen, Diopside and its relation to calcium and magnesium metasilicates, *Am. J. Sci.*, **27**, 1-47, 1909.

Ames, L. L., and L. B. Sand, Hydrothermal synthesis in wairakite and calcium-modernite, *Am. Mineralogist*, **43**, 476-480, 1958a.

Ames, L. L., and L. B. Sand, Factors effecting maximum hydrothermal stability in montmorillonites, *Am. Mineralogist*, **43**, 641-648, 1958b.

Anker, H. S., On the geogenous evolution of self-reproducing systems and macromolecules, *Perspectives Biol. Med.*, **5**, 86-88, 1961.

Arnold, R. G., Equilibrium relations between pyrrhotite and pyrite from 325° to 743°C., *Econ. Geol.*, **57**, 72-90, 1962.

Arnold, R. G., and L. E. Reichen, Measurement of the metal content of naturally occurring, metal-deficient, hexagonal pyrrhotite by an X-ray spacing method, *Am. Mineralogist*, **47**, 105-111, 1962.

Asklund, B., Petrological studies in the neighborhood of Staysjö at Kolmården, *Sveriges Geol. Undersökn. Årsbok*, **17**, [6], 122 pp., 1925.

Atlas, L. The polymorphism of MgSiO_2 and solid-state equilibria in the system MgSiO_3 - $\text{CaMgSi}_2\text{O}_6$, *J. Geol.*, **60**, 125-147, 1952.

Bailey, D. K., Crustal warping and rifting—a possible tectonic control of alkaline magmatism, *Trans. Am. Geophys. Union*, **44**, 115, 1963.

Banno, S., I. Kushiro, and Y. Matsui, Enstatite in garnet-peridotite inclusion in kimberlite, *J. Geol. Soc. Japan*, **69**, 157-159, 1963.

Barth, T. F. W., Crystallization of pyroxenes from basalts, *Am. Mineralogist*, **16**, 195-208, 1931.

Barth, T. F. W., The crystallization process of basalt, *Am. J. Sci.*, **31**, 321-351, 1936.

Barth, T. F. W., Subsolidus diagram of pyroxenes from common mafic magmas, *Norsk Geol. Tidsskr.*, **29**, 218-221, 1951.

Barth, T. F. W., The Bowen reaction series and the development of different magma types, *Indian Mineralogist*, **1**, 24-28, 1960.

Barth, T. F. W., *Theoretical Petrology*, John Wiley & Sons, New York, 2nd ed., 1962.

Beger, P. J., Der Chemismus der Lamprophyre, in *Gesteins- und Mineralprovinzen*, by P. Niggli, Gebrüder Bornträger, Berlin, vol. 1, pp. 217-586, 1923.

Binns, R. A., Metamorphic pyroxenes from the Broken Hill district, New South Wales, *Mineral. Mag.*, **33**, 320-338, 1962.

Birch, F., Some geophysical applications of high-pressure research, in *Solids under Pressure*, edited by W. Paul and D. M. Warschauer, McGraw-Hill Book Company, New York, 1963.

Bowen, N. L., The ternary system diopside-forsterite-silica, *Am. J. Sci.*, **38**, 207-264, 1914.

Bowen, N. L., Genetic features of alnoitic rocks at Isle Cadieux, Quebec, *Am. J. Sci.*, **3**, 1-34, 1922.

Bowen, N. L., "Ferrosilite" as a natural mineral, *Am. J. Sci.*, **30**, 481-494, 1935.

Bowen, N. L., and O. Andersen, The binary system MgO-SiO_2 , *Am. J. Sci.*, **37**, 487-500, 1914.

Bowen, N. L., and J. F. Schairer, The fusion relations of acmite, *Am. J. Sci.*, **18**, 365-374, 1929.

Bowen, N. L., and J. F. Schairer, The system FeO-SiO_2 , *Am. J. Sci.*, **24**, 177-213, 1932.

- Bowen, N. L., and J. F. Schairer, The system MgO-FeO-SiO_2 , *Am. J. Sci.*, **29**, 151-217, 1935a.
- Bowen, N. L., and J. F. Schairer, Grunerite from Rockport, Massachusetts, and a series of synthetic fluoroamphiboles, *Am. Mineralogist*, **20**, 543-551, 1935b.
- Bowen, N. L., J. F. Schairer, and E. Posnjak, The system CaO-FeO-SiO_2 , *Am. J. Sci.*, **26**, 193-284, 1933.
- Bowen, N. L., J. F. Schairer, and H. W. V. Willems, The ternary system $\text{Na}_2\text{SiO}_3\text{-Fe}_2\text{O}_3\text{-SiO}_2$, *Am. J. Sci.*, **20**, 405-455, 1930.
- Bowen, N. L., and O. F. Tuttle, The system $\text{MgO-SiO}_2\text{-H}_2\text{O}$, *Bull. Geol. Soc. Am.*, **60**, 439-460, 1949.
- Bown, M. G., and P. Gay, An X-ray study of exsolution phenomena in the Skaergaard pyroxenes, *Mineral. Mag.*, **32**, 379-388, 1960.
- Boyd, F. R., and J. L. England, Effect of pressure on the melting of diopside, $\text{CaMgSi}_2\text{O}_6$, and albite, $\text{NaAlSi}_3\text{O}_8$, in the range up to 50 kb, *J. Geophys. Res.*, **68**, 311-323, 1963.
- Brown, G. M., Pyroxenes from the early and middle stages of fractionation of the Skaergaard intrusion, East Greenland, *Mineral. Mag.*, **31**, 511-543, 1957.
- Brown, G. M., *The X-Ray Identification and Crystal Structures of Clay Minerals*, Mineralogical Society, Clay Minerals Group, London, 1961.
- Buddington, A. F., Composition and genesis of pyroxene and garnet related to Adirondack anorthosite and anorthosite-marble contact zones, *Am. Mineralogist*, **35**, 659-670, 1950.
- Buerger, M. J., C. W. Burnham, and D. R. Peacor, Assessment of the several structures proposed for tourmaline, *Acta Cryst.*, **15**, 583-590, 1962.
- Bundy, F. P., H. P. Bovenkerk, H. M. Strong, and R. H. Wentorf, Jr., Diamond-graphite equilibrium line from growth and graphitization of diamond, *J. Chem. Phys.*, **35**, 383-391, 1961.
- Burnham, C. W., Refinement of the crystal structure of sillimanite, *Z. Krist.*, **118**, 127-148, 1963.
- Burri, C., *Petrochemische Berechnungsmethoden auf äquivalenten Grundlagen*, Birkhäuser Verlag, Basel, 1959.
- Busing, W. R., and H. A. Levy, A crystallographic least-squares refinement program for the IBM 704, Oak Ridge National Laboratory, Oak Ridge, Tenn., 1959.
- Byström, A., Monoclinic magnetic pyrites, *Arkiv Kemi, Mineral., Geol.*, **19B**, no. 8, 8 pp., 1945.
- Carmichael, C. M., The magnetic properties of ilmenite-hematite crystals, *Proc. Roy. Soc. London, A*, **263**, 508-530, 1961.
- Chayes, F., Relative abundance of intermediate members of the oceanic basalt-trachyte association, *J. Geophys. Res.*, **68**, 1519-1534, 1963.
- Chinner, G. A., and J. F. Schairer, The join $\text{Ca}_3\text{Al}_2\text{Si}_3\text{O}_{12}\text{-Mg}_3\text{Al}_2\text{Si}_3\text{O}_{12}$ and its bearing on the system $\text{CaO-MgO-Al}_2\text{O}_3\text{-SiO}_2$ at atmospheric pressure, *Am. J. Sci.*, **260**, 611-634, 1962.
- Clark, L. A., The Fe-As-S system: Phase relations and applications, *Econ. Geol.*, **55**, 1345-1381, 1631-1652, 1960.
- Clark, S. P., Jr., A redetermination of equilibrium relations between kyanite and sillimanite, *Am. J. Sci.*, **259**, 641-650, 1961.
- Clark, S. P., Jr., The variation of density in the earth and the melting curve in the mantle, in *Problems in Geology*, edited by T. W. Donnelly, University of Chicago Press, in press, 1963.
- Clayton, R. N., and T. K. Mayeda, The use of bromine pentafluoride for the extraction of oxygen from oxides and silicates for isotopic analysis, *Geochim. Cosmochim. Acta*, **27**, 43-52, 1963.
- Coleman, R. G., Jadeite deposits of the Clear Creek area, New Idria district, San Benito County, California, *J. Petrol.*, **2**, 209-247, 1961.
- Cross, W., Lavas of Hawaii and their relations, *U. S. Geol. Surv. Prof. Paper* **88**, 1-97, 1915.
- Crowley, M. S., and R. Roy, The effect of formation pressures on sheet structures—a possible case of Al-Si ordering, *Geochim. Cosmochim. Acta*, **18**, 94-100, 1960.
- Daly, R., *Igneous Rocks and the Depths of the Earth*, McGraw-Hill Book Company, New York, 1933.
- Deer, W. A., R. A. Howie, and J. Zussman, *Rock-Forming Minerals*, vol. 1, John Wiley & Sons, New York, 1962.
- De Vries, R. C., and E. F. Osborn, Phase equilibria in high alumina part of the system $\text{CaO-MgO-Al}_2\text{O}_3\text{-SiO}_2$, *J. Am. Ceram. Soc.*, **40**, 6-15, 1957.
- Dixon, B. E., and W. Q. Kennedy, Optically uniaxial titanite from Aberdeenshire, *Z. Krist.*, **A**, **86**, 112-120, 1933.
- Doelter, C., *Handbuch der Mineralchemie*, vol. 2, pt. 2, T. Steinkopff, Dresden and Leipzig, 1917.
- Donnay, J. D. H., A small set of grids for the determination of non-opaque minerals, published by the author, 1937. (2nd ed., 1963. See *Am. Mineralogist*, **23**, 91-100, 1938.)

- Donnay, J. D. H., G. Donnay, E. G. Cox, O. Kennard, and M. V. King, *Crystal Data, Determinative Tables*, 2nd ed., American Crystallographic Association Monograph 5, 1963.
- Donnay, J. D. H., W. Nowacki, and G. Donnay, Crystal data, *Geol. Soc. Am. Mem.* 60, 719 pp., 1954.
- Du Fresne, E. R., and E. Anders, On the retention of primordial noble gases in the Pesyanoe meteorite, *Geochim. Cosmochim. Acta*, 26, 251-262, 1962a.
- Du Fresne, E. R., and E. Anders, On the chemical evolution of the carbonaceous chondrites, *Geochim. Cosmochim. Acta*, 26, 1085-1114, 1962b.
- Durovic, S., A statistical model for the crystal structure of mullite, *Soviet Phys.-Cryst.*, 7, 271-278, 1962.
- Emery, K. O., *The Sea off Southern California*, John Wiley & Sons, New York, 1960.
- Epprecht, W., Die Gitterkonstanten der Turmaline, *Schweiz. Mineral. Petrog. Mitt.*, 33, 481-505, 1953.
- Ernst, W. G., Stability relations of glaucophane, *Am. J. Sci.*, 259, 735-765, 1961.
- Ernst, W. G., Synthesis, stability relations, and occurrence of riebeckite and riebeckite-arfvedsonite solid solutions, *J. Geol.*, 70, 689-736, 1962.
- Eugster, H. P., and D. R. Wones, Stability relations of the ferruginous biotite, annite, *J. Petrol.*, 3, 85-125, 1962.
- Fairbairn, H. W., et al., A cooperative investigation of precision and accuracy in chemical, spectrochemical and modal analysis of silicate rocks, *U. S. Geol. Surv. Bull.* 980, 1951.
- Fenner, C. N., The crystallization of basalts, *Am. J. Sci.*, 18, 225-253, 1929.
- Fischer, K., Least-squares refinement of atomic scattering factors: possibilities, techniques, and applications, *Abstracts Ann. Meeting Am. Cryst. Assoc.*, Cambridge, Mass., 1963.
- Forsman, J. P., and J. M. Hunt, Insoluble organic matter (kerogen) in sedimentary rocks, *Geochim. Cosmochim. Acta*, 15, 170-182, 1958.
- Foster, W. R., High-temperature X-ray diffraction study of the polymorphism of MgSiO_3 , *J. Am. Ceram. Soc.*, 34, 255-259, 1951.
- Frenzel, G., Idait und "blaubleibender Covellin," *Neues Jahrb. Mineral., Abhandl.*, 93, 87-132, 1959.
- Gastil, R. G., and M. DeLisle, Variations in the lead-alpha ratio of zircons under varying grades of contact metamorphism (abstract), *Geol. Soc. Am. Spec. Papers*, 73, 158, 1962.
- Grønvold, F., and H. Haraldsen, On the phase relations of synthetic and natural pyrrhotites (Fe_{1-x}S), *Acta Chem. Scand.*, 6, 1452-1469, 1952.
- Grünenfelder, M., Mineralater kristalliner Gesteine im Gotthardmassiv, *Schweiz. Mineral. Petrog. Mitt.*, 42, 6-7, 1962.
- Hahn, W. C., Jr., and A. Muan, Studies in the system Mn-O: The Mn_2O_3 - Mn_3O_4 - MnO equilibria, *Am. J. Sci.*, 258, 66-78, 1960.
- Hallimond, A. F., Optically uniaxial augite from Mull, *Mineral. Mag.*, 17, 97-99, 1914.
- Hansen, M., and K. Anderko, *Constitution of Binary Alloys*, McGraw-Hill Book Company, New York, 1958.
- Hargraves, R. B., Petrology of the Allard Lake anorthosite suite, Quebec, in *Petrologic Studies*, edited by A. E. J. Engel, Harold L. James, and B. F. Leonard, Geological Society of America, New York, pp. 163-189, 1962.
- Harker, R. I., and O. F. Tuttle, Studies in the system CaO-MgO-CO_2 , I, The thermal dissociation of calcite, dolomite, and magnesite, *Am. J. Sci.*, 253, 209-224, 1955.
- Harker, R. I., and O. F. Tuttle, Experimental data of the P_{CO_2} - T curve for the reaction calcite + quartz = wollastonite + carbon dioxide, *Am. J. Sci.*, 254, 239-256, 1956.
- Hawley, J. E., The Sudbury ores: Their mineralogy and origin, *Can. Mineralogist*, 7, pt. 1, 207 pp., 1962.
- Hemley, J. J., Some mineralogical equilibria in the system $\text{K}_2\text{O-Al}_2\text{O}_3\text{-SiO}_2\text{-H}_2\text{O}$, *Am. J. Sci.*, 257, 241-270, 1959.
- Henry, N. F. M., A review of the data of the Mg-Fe clinopyroxenes, *Mineral. Mag.*, 25, 23-29, 1938.
- Hess, H. H., Pyroxenes of common mafic magmas, *Am. Mineralogist*, 26, 515-535, 573-594, 1951.
- Hess, H. H., Stillwater igneous complex, Montana, *Geol. Soc. Am. Mem.* 80, 230 pp., 1960.
- Hess, H. H., and E. P. Henderson, The Moore County meteorite: A further study with comment on its primordial environment, *Am. Mineralogist*, 34, 494-507, 1949.
- Heyding, R. D., and L. D. Calvert, Arsenides of the transition metals: The arsenides of iron and cobalt, *Can. J. Chem.*, 35, 449-457, 1957a.
- Heyding, R. D., and L. D. Calvert, Arsenides of the transition metals, II, The nickel arsenides, *Can. J. Chem.*, 35, 1205-1215, 1957b.
- Heyding, R. D., and L. D. Calvert, Arsenides of the transition metals, III, A note on the higher arsenides of iron, cobalt, and nickel, *Can. J. Chem.*, 38, 313-316, 1960.
- Holmes, A., *Petrographic Methods and Calculations*, T. Murby and Company, London, 1921.

- Holmes, A., A contribution to the petrology of kimberlite and its inclusions, *Trans. Geol. Soc. S. Africa*, 39, 379-428, 1936.
- Holmes, A., and H. F. Harwood, Petrology of the volcanic fields east and southeast of Ruwenzori, Uganda, *Quart. J. Geol. Soc. London*, 88, 370-439, 442, 1932.
- Holmes, R. J., Higher mineral arsenides of cobalt, nickel, and iron, *Bull. Geol. Soc. Am.*, 58, 299-392, 1947.
- Holser, W. T., and G. C. Kennedy, Properties of water, IV, Pressure-volume-temperature relations of water in the range 100°-400°C and 100-1400 bars, *Am. J. Sci.*, 256, 744-753, 1958.
- Howells, E. R., D. C. Phillips, and D. Rogers, The probability distribution of X-ray intensities, II, Experimental investigation and the X-ray detection of centers of symmetry, *Acta Cryst.*, 3, 210-214, 1950.
- Howie, R. A., The geochemistry of the charnockite series of Madras, India, *Trans. Roy. Soc. Edinburgh*, 62, 725-768, 1955.
- Howie, R. A., and A. P. Subramaniam, The paragenesis of garnet in charnockite, enderbite, and related granulites, *Mineral. Mag.*, 31, 565-586, 1957.
- Jäger, E., Rb-Sr age determinations on micas and total rocks from the Alps, *J. Geophys. Res.*, 67, 5293-5306, 1962.
- Jagger, T. A., Origin and development of craters, *Geol. Soc. Am. Mem.* 21, 508 pp., 1947.
- Jakob, J., Analysen dreier tessiner Turmaline, *Schweiz. Mineral. Petrog. Mitt.*, 17, 146-148, 1937.
- Johanssen, A., *A Descriptive Petrography of the Igneous Rocks*, University of Chicago Press, 4 vols., 1931.
- Johnson, P. C., B. A. Stein, and R. S. Davis, Temperature dependence of shock-induced phase transformations in iron, *J. Appl. Phys.*, 33, 557-561, 1962.
- Keenan, J. J., and F. G. Keyes, *Thermodynamic Properties of Steam*, John Wiley & Sons, New York, 1936.
- Keith, M. L., and J. F. Schairer, The stability field of sapphirine in the system $MgO-Al_2O_3-SiO_2$, *J. Geol.*, 60, 181-185, 1952.
- Kennedy, G. C., Equilibrium between volatiles and iron oxides in igneous rocks, *Am. J. Sci.*, 246, 529-549, 1948.
- Kennedy, G. C., W. L. Knight, and W. T. Holser, Properties of water, III, Specific volume of liquid water to 100°C and 1400 bars, *Am. J. Sci.*, 256, 590-595, 1958.
- Kennedy, G. C., and P. N. LaMori, The pressures of some solid-solid transitions, *J. Geophys. Res.*, 67, 851-856, 1962.
- Kerr, P. F., and E. Callaghan, Scheelite-leuchtenbergite vein in Paradise Range, Nevada, *Bull. Geol. Soc. Am.*, 46, 1957-1974, 1935.
- Knopf, A., Igneous geology of the Spanish Peaks region, Colorado, *Bull. Geol. Soc. Am.*, 47, 1727-1784, 1936.
- Kouvo, O., and Y. Vuorelainen, Magneettikiisun Koostumuksesta ja rakenteesta, *Geologi (Helsinki)*, no. 6, 79-82, 1962.
- Kullerud, G., The FeS-ZnS system: A geological thermometer, *Norsk Geol. Tidsskr.*, 32, 61-147, 1953.
- Kullerud, G., and H. S. Yoder, Jr., Pyrite stability relations in the Fe-S system, *Econ. Geol.*, 54, 533-572, 1959.
- Kullerud, G., and R. A. Yund, The Ni-S system and related minerals, *J. Petrol.*, 3, 126-175, 1962.
- Kuno, H., On the crystallization of pyroxenes from rock magmas, with special reference to the formation of pigeonite, *Japan. J. Geol. Geography*, 13, 141-150, 1936.
- Kuno, H., Petrology of Hakone volcano and the adjacent areas, Japan, *Bull. Geol. Soc. Am.*, 61, 957-1020, 1950.
- Kuno, H., Ion substitution in the diopside-ferropigeonite series of clinopyroxenes, *Am. Mineralogist*, 40, 70-93, 1955.
- Kuno, H., K. Yamasaki, C. Iida, and K. Nagashima, Differentiation of Hawaiian magmas, *Japan. J. Geol. Geography*, 28, 179-218, 1957.
- Kushiro, I., Preliminary note on alkali-dolerite of Atumi District, northern Japan, *Japan. J. Geol. Geography, Trans.*, 30, 259-272, 1959.
- Kushiro, I., Si-Al relations in clinopyroxenes from igneous rocks, *Am. J. Sci.*, 258, 548-554, 1960.
- Kushiro, I., and H. Kuno, Origin of primary basalt magmas and classification of basaltic rocks, *J. Petrol.*, 4, 75-89, 1963.
- Lacroix, A., *La Montagne Pelée et ses éruptions*, Masson et Cie., Paris, 1904.
- Lacroix, A., *Minéralogie de la France*, vol. 4, p. 765, Ch. Béranger, editor, Librairie Polytechnique, Paris, 1910.
- Le Bas, M. J., The role of aluminum in igneous clinopyroxenes with relation to their parentage, *Am. J. Sci.*, 260, 267-288, 1962.
- Macdonald, G. A., and T. Katsura, Variations in the lava of the 1959 eruption of Kilauea Iki, *Pacific Sci.*, 15, 358-369, 1961.
- McDougall, I., Optical and chemical studies of pyroxenes in a differentiated Tasmanian dolerite, *Am. Mineralogist*, 46, 661-687, 1961.
- McKie, D., Yoderite, a new hydrous magnesium iron aluminosilicate from Mavtia Hill, Tanganyika, *Mineral. Mag.*, 32, 282-307, 1959.

- McKinstry, H. E., Mineral assemblages in the sulfide ores: The system Cu-Fe-S-O, *Econ. Geol.*, 54, 203-284, 1959.
- Mason, B., *Meteorites*, John Wiley & Sons, New York, 1962.
- Mawson, D., Basaltic lavas of the Balleny Islands A.N.A.R.E. Report, *Trans. Roy. Soc. S. Australia*, 73, 223-231, 1950.
- Michels, A., C. Michels, and H. H. Wouters, Isotherms of CO₂ between 70 and 3000 atmospheres, *Proc. Roy. Soc. London, A*, 153, 214-224, 1935.
- Michels, A., H. Wijker, and H. K. Wijker, Isotherms of argon between 0°C and 150°C and pressures up to 2900 atmospheres, *Physica*, 15, 627-633, 1949.
- Moh, G. H., and J. Ottemann, Neue Untersuchungen an Zinnkiesen und Zinnkiesverwandten, *Neues Jahrb. Mineral., Abhandl.*, 99, 1-28, 1962.
- Morey, G. W., The system water-nepheline-albite: A theoretical discussion, *Am. J. Sci.*, 255, 461-480, 1957.
- Morimoto, N., Djurleite, a new copper sulfide mineral, *Mineral. J. Tokyo*, 43, 338-344, 1962.
- Morimoto, N., and G. Kullerud, Polymorphism in bornite, *Am. Mineralogist*, 46, 1270-1282, 1961.
- Morimoto, N., and G. Kullerud, Polymorphism in digenite, *Am. Mineralogist*, 48, 110-123, 1963.
- Mosburg, S., D. R. Ross, P. M. Bethke, and P. Toulmin, X-ray powder data for herzenbergite, teallite, and tin trisulfide, *Short Papers in the Geological and Hydrological Sciences*, article 273, C347-C348, 1961.
- Muir, I. D., The clinopyroxenes of the Skaergaard intrusion, eastern Greenland, *Mineral. Mag.*, 29, 690-714, 1951.
- Muir, I. D., and C. E. Tilley, Contributions to the petrology of Hawaiian basalts, 2, The tholeiitic basalts of Mauna Loa and Kilauea, *Am. J. Sci.*, 261, 111-128, 1963.
- Muir, I. D., C. E. Tilley, and J. H. Scoon, Contributions to the petrology of Hawaiian basalts, 1, The picrite basalts of Kilauea, *Am. J. Sci.*, 255, 241-253, 1957.
- Nadler, M. R., and C. P. Kempter, Thermocouples for use in carbon atmospheres, *Rev. Sci. Instr.*, 32, 43-48, 1961.
- Nelson, B. W., and R. Roy, Synthesis of the chlorites and their structural and chemical constitution, *Am. Mineralogist*, 43, 707-725, 1958.
- Newton, R. C., A. Jayaraman, and G. C. Kennedy, The fusion curves of the alkali metals up to 50 kb, *J. Geophys. Res.*, 67, 2559-2566, 1962.
- O'Hara, M. J., and E. L. P. Mercy, Petrology and petrogenesis of some garnetiferous peridotites, *Trans. Roy. Soc. Edinburgh*, 65 [12], 1-64, 1963.
- Osborn, E. F., Role of oxygen pressure in the crystallization and differentiation of basaltic magma, *Am. J. Sci.*, 257, 609-647, 1959.
- Osborn, E. F., R. C. De Vries, K. G. Gee, and H. M. Kraner, Optimum composition of blast furnace slag as deduced from liquidus data for the quaternary system CaO-MgO-Al₂O₃-SiO₂, *J. Metals*, 6, 3-15, 1954.
- Owen, E. A., and A. H. Sully, The equilibrium diagram of iron-nickel alloys, *Phil. Mag.*, [7] 27, 614-636, 1939.
- Palache, C., H. Berman, and C. Frondel, *The System of Mineralogy*, vol. 1, John Wiley & Sons, New York, 1944.
- Park, R., and S. Epstein, Carbon isotope fractionation during photosynthesis, *Geochim. Cosmochim. Acta*, 21, 110-126, 1960.
- Peacock, M. A., The nature and origin of the amphibole asbestos of South Africa, *Am. Mineralogist*, 13, 241-285, 1928.
- Pearson, W. B., *A Handbook of Lattice Spacings and Structures of Metals and Alloys*, Pergamon Press, New York, 1958.
- Pettijohn, F. J., *Sedimentary Rocks*, Harper and Brothers, New York, 1957.
- Pleass, C. M., and R. D. Heyding, Arsenides of the transition metals, VI, Electrical and magnetic properties of the triarsenides, *Can. J. Chem.*, 40, 590-600, 1962.
- Poldervaart, A., and H. H. Hess, Pyroxenes in the crystallization of basaltic magma, *J. Geol.*, 59, 472-489, 1951.
- Prince, A. T., Liquidus relations on 10 per cent MgO plane of the system lime-magnesia-alumina-silica, *J. Am. Ceram. Soc.*, 37, 402-408, 1954.
- Radoslovich, E. W., The structure of muscovite, KAl₂(Si₃Al)O₁₀(OH)₂, *Acta Cryst.*, 13, 919-932, 1960.
- Radoslovich, E. W., The cell dimensions and symmetry of layer silicates, IV, Interatomic forces, *Am. Mineralogist*, 48, 76-99, 1963.
- Ramberg, H., and G. De Vore, The distribution of Fe⁺⁺ and Mg⁺⁺ in coexisting olivines and pyroxenes, *J. Geol.*, 59, 193-210, 1951.
- Ramdohr, P., Zum Zinnkiesproblem, *Abhandl. Preuss. Akad. Wiss. Math.-Naturw. Kl.*, no. 4, 1944.
- Ramdohr, P., *Die Erzminerale und ihre Verwachsungen*, Akademie-Verlag, Berlin, 2nd ed., 1955.
- Ramdohr, P., *Die Erzminerale und ihre Verwachsungen*, Akademie-Verlag, Berlin, 3d ed., 1960.

- Ramdohr, P., and M. Schmitt, Oregonit, ein neues Nickel-Eisenarsenid mit metallartigen Eigenschaften, *Neues Jahrb. Mineral., Monatsh.*, 239–247, 1959.
- Richards, R. G., and J. White, Phase relationships of iron oxide-containing spinels, II, Relationships in the systems Fe-Cr-O, Fe-Mg-O, Fe-Al-Cr-O, and Fe-Al-Cr-Mg-O, *Trans. Brit. Ceram. Soc.*, 53, 423–459, 1954.
- Richter, D. H., and J. P. Eaton, The 1959–60 eruption of Kilauea Volcano, *New Scientist*, 7, 994–997, 1960.
- Ringwood, A. E., Some aspects of the thermal evolution of the earth, *Geochim. Cosmochim. Acta*, 20, 241–249, 1960.
- Rooksby, H. P., and J. H. Partridge, An X-ray study of natural and artificial mullites, *J. Soc. Glass Technol.*, 23, 338–346, 1939.
- Roseboom, E. H., Djurleite, $\text{Cu}_{1.96}\text{S}$, a new mineral, *Am. Mineralogist*, 97, 1181–1184, 1962.
- Roseboom, E. H., Co-Ni-Fe diarsenides: Compositions and cell dimensions, *Am. Mineralogist*, 48, 271–299, 1963.
- Ross, C. S., M. D. Foster, and A. T. Myers, Origin of dunites and of olivine-rich inclusions in basaltic rocks, *Am. Mineralogist*, 39, 693–737, 1954.
- Roy, R., and S. Aramaki, Revised phase diagram for the system $\text{Al}_2\text{O}_3\text{-SiO}_2$, *J. Am. Ceram. Soc.*, 45, 229–242, 1962.
- Roy, D. M., and R. Roy, Synthesis and stability of minerals in the system $\text{MgO-Al}_2\text{O}_3\text{-SiO}_2\text{-H}_2\text{O}$, *Am. Mineralogist*, 40, 147–178, 1955.
- Sadanaga, R., M. Tokonami, and Y. Takeuchi, The structure of mullite, $2\text{Al}_2\text{O}_3\cdot\text{SiO}_2$, and relationship with the structures of sillimanite and andalusite, *Acta Cryst.*, 15, 65–68, 1962.
- Saha, P., The system NaAlSiO_4 (nepheline)- $\text{NaAlSi}_3\text{O}_8$ (albite)- H_2O , *Am. Mineralogist*, 46, 859–884, 1961.
- Sakata, Y., Unit-cell dimensions of synthetic aluminian diopsides, *Japan. J. Geol. Geography, Trans.*, 28, 161–168., 1957.
- Schairer, J. F., and N. L. Bowen, The binary system CaSiO_3 -diopside and the relations between CaSiO_3 and akermanite, *Am. J. Sci.*, 240, 725–742, 1952.
- Schairer, J. F., and E. F. Osborn, The system CaO-MgO-FeO-SiO_2 , I, Preliminary data on the join $\text{CaSiO}_3\text{-MgO-FeO}$, *J. Am. Ceram. Soc.*, 33, 160–167, 1950.
- Schneiderhöhn, H., *Anleitung zur mikroskopischen Bestimmung und Untersuchung von Erzen und Aufbereitungsprodukten besonders in auffallendem Licht*, Selbstverlag der Gesellschaft Deutscher Metallhütten- und Bergleute e.V., Berlin, 1922.
- Schreyer, W., and J. F. Schairer, Compositions and structural states of anhydrous Mg-cordierites: A reinvestigation of the central part of the system $\text{MgO-Al}_2\text{O}_3\text{-SiO}_2$, *J. Petrol.*, 2, 324–406, 1961.
- Segnit, E. R., Some data on synthetic aluminous and other pyroxenes, *Mineral. Mag.*, 30, 218–226, 1953.
- Sosman, R. B., Minerals and rocks of the composition $\text{MgSiO}_3\text{-CaSiO}_3\text{-FeSiO}_3$, *J. Wash. Acad. Sci.*, 1, 54–58, 1911.
- Steiger, R. H., Petrographie und Geologie des südlichen Gotthardmassivs zwischen St. Gotthard und Lukmanier Pass, *Schweiz. Mineral. Petrol. Mitt.*, 42, 381–577, 1962.
- Stemple, I. S., and G. W. Brindley, A structural study of talc and talc-tremolite relations, *J. Am. Ceram. Soc.*, 43, 34–42, 1960.
- Strong, H. M., The experimental fusion curve of iron to 96,000 atmospheres, *J. Geophys. Res.*, 64, 653–659, 1959.
- Strong, H. M., High-temperature methods at high pressure, in *Modern Very High Pressure Techniques*, edited by R. H. Wentorf, Jr., Butterworths, Washington, D. C., pp. 93–117, 1962.
- Strunz, H., *Mineralogische Tabellen*, Geest und Portig, Leipzig, 3rd ed., 1957.
- Swanson, H. E., and R. K. Fuyat, Standard X-ray diffraction powder patterns, *Natl. Bur. Std. (U. S.) Circ.*, 539, [2], 18–19, 1953.
- Sztrokay, K. I., Über einige Meteoritenmineralien des kohlenwasserstoffhaltigen Chondrites von Kaba, Ungarn, *Neues Jahrb. Mineral., Abhandl.*, 94, 1284–1294, 1960.
- Taylor, W. H., The structure of sillimanite and mullite, *Z. Krist.*, 68, 503–521, 1928.
- Tilley, C. E., Nepheline-alkali feldspar parageneses, *Am. J. Sci.*, 252, 65–75, 1954.
- Tilley, C. E., Differentiation of Hawaiian basalts: Some variants in lava suites of dated Kilauean eruptions, *J. Petrol.*, 1, 47–55, 1960.
- Tomita, T., Geological and petrological study of Dogo, Oki, XI, *J. Geol. Soc. Tokyo*, 38, 214–218, 1931.
- Tomita, T., Olivine-trachyandesitic basalt from Hsueh-hua-shau Hill, Ching-hsing District, North China, *J. Shanghai Sci. Inst.*, 1, 1–10, 1933.
- Tozer, D. C., The electrical properties of the earth's interior, in *Physics and Chemistry of the Earth*, edited by L. H. Ahrens, F. Press, K. Rankama, and S. K. Runcorn, Pergamon Press, New York, vol. 3, pp. 414–437, 1959.
- Tsuboi, S., On the course of crystallization of pyroxenes from rock magmas, *Japan. J. Geol. Geography*, 10, 67–82, 1932.
- Tsuboi, S., Petrological studies of pyroxenes (in Japanese), *Kwagaku (Science)*, 8, 13–20, 1938.

- Tsuboi, S., On the genetic relations of igneous pyroxenes, *Proc. Japan Acad.*, 25, 34-40, 1949.
- Tudge, A. P., A method of analysis of oxygen isotopes in orthophosphate, *Geochim. Cosmochim. Acta*, 18, 81-93, 1960.
- Turnock, A. C., and H. P. Eugster, Fe-Al oxides: Phase relationships below 1000°C, *J. Petrol.*, 3, 533-565, 1962.
- Verhoogen, J., Temperatures within the earth, *Am. Scientist*, 48, 134-159, 1960.
- Vincent, E. A., and R. Phillips, Iron-titanium oxide minerals in layered gabbros of the Skaergaard intrusion, East Greenland, I, Chemistry and ore-microscopy, *Geochim. Cosmochim. Acta*, 6, 1-26, 1954.
- Vincent, E. A., J. B. Wright, R. Chevallier, and S. Mathieu, Heating experiments on some natural titaniferous magnetites, *Mineral. Mag.*, 31, 624-655, 1957.
- Wager, L. R., The major element variation of the layered series of the Skaergaard intrusion and a reestimation of the average composition of the hidden layered series and of the successive residual magmas, *J. Petrol.*, 1, 364-398, 1960.
- Wager, L. R., and W. A. Deer, Geological investigations in East Greenland, III, Petrology of the Skaergaard intrusion, Kaugerdlugsuq, East Greenland, *Medd. Groenland*, 105, [4], 355 pp., 1939.
- Walter, L. S., Data on the fugacity of CO₂ in mixtures of CO₂ and H₂O, *Am. J. Sci.*, 261, 151-156, 1963.
- Walter, L. S., P. J. Wyllie, and O. F. Tuttle, The system MgO-CO₂-H₂O, at high pressures and temperatures, *J. Petrol.*, 3, 49-64, 1962.
- Warren, B. E., and W. L. Bragg, The structure of diopside CaMg(SiO₃)₂, *Z. Krist.*, 69, 168-193, 1928.
- Washington, H. S., and H. E. Merwin, The acmitic pyroxenes, *Am. Mineralogist*, 12, 233-252, 1927.
- Wentworth, C. K., and H. Winchell, Koolau basalt series, Oahu, *Bull. Geol. Soc. Am.*, 59, 49-78, 1947.
- Williams, A. F., *The Genesis of the Diamond*, Ernest Benn, London, 1932.
- Wilshire, H. G., Sedimentary xenoliths and dolerite patch pegmatites from an analcite basalt intrusion, *Am. J. Sci.*, 259, 260-279, 1961.
- Wilshire, H. G., and R. A. Binns, Basic and ultrabasic xenoliths from volcanic rocks of New South Wales, *J. Petrol.*, 2, 185-208, 1961.
- Wones, D. R., Phase equilibria of "ferriannite," KFe₃⁺²Fe⁺³Si₃O₁₀(OH)₂, *Am. J. Sci.*, 261, 581-596, 1963.
- Wright, J. B., Solid solution relationships in some titaniferous iron oxide ores of basic igneous rocks, *Mineral. Mag.*, 32, 778-789, 1961.
- Wyckoff, R. W. G., H. E. Merwin, and H. S. Washington, X-ray diffraction measurements upon the pyroxenes, *Am. J. Sci.*, 10, 383-397, 1925.
- Yardley, D. H., S. S. Goldich, Z. E. Peterman and J. K. Frye, Precambrian geology of the Minnesota-Ontario border region (abstract), *Geol. Soc. Am. Bull.*, 70, 1703, 1959.
- Yčas, M., A note on the origin of life, *Proc. Natl. Acad. Sci. U. S.*, 41, 714-716, 1955.
- Yoder, H. S., Jr., High-low quartz inversion up to 10,000 bars, *Trans. Am. Geophys. Union*, 31, 827-835, 1950.
- Yoder, H. S., Jr., The MgO-Al₂O₃-SiO₂-H₂O system and related metamorphic facies, *Am. J. Sci.*, *Bowen Vol.*, 569-627, 1952.
- Yoder, H. S., Jr., and H. P. Eugster, Synthetic and natural muscovites, *Geochim. Cosmochim. Acta*, 8, 225-280, 1955.
- Yoder, H. S., Jr., and Th. G. Sahama, Olivine X-ray determinative curve, *Am. Mineralogist*, 42, 475-491, 1957.
- Yoder, H. S., Jr., and C. E. Tilley, Origin of basalt magmas: An experimental study of natural and synthetic rock systems, *J. Petrol.*, 3, 342-532, 1962.
- Yund, R. A., Phase relations in the system Ni-As, *Econ. Geol.*, 56, 1273-1296, 1961.

PERSONNEL

Scientific Staff

Director: P. H. Abelson.

Retired Associate: E. G. Zies, *Chemist*.

Staff Associates: G. Allen, National Institutes of Health;¹ W. F. Schreyer, University of Kiel.

Physical Chemists: F. R. Boyd, H. J. Greenwood, T. C. Hoering, J. F. Schairer, G. R. Tilton.

Petrologists: F. Chayes, D. H. Lindsley,² H. S. Yoder, Jr.

Geochemists: G. L. Davis, G. Kullerud.

Organic Geochemist: P. L. Parker.³

Physicist: J. L. England.

Crystallographer: G. Donnay.

Fellows: D. K. Bailey, Trinity College, Dublin; P. R. Brett, Harvard University; C. W. Burnham, Massachusetts Institute of Technology; P. R. Buseck, Columbia University; B. T. C. Davis, Princeton University;⁴ J. de Neufville, Yale University;⁵ J. J. Fawcett, University of Manchester; I. Kushiro, Tokyo University;⁶ D. Métais, University of Paris;⁴ G. Moh, University of Heidelberg; N. Morimoto, Tokyo University;⁷ M. J. O'Hara, University of Edinburgh;⁶ E. W. Radoslovich, Commonwealth Scientific and Industrial Research Organization, Adelaide, South Australia;⁶ B. E. Sabels, Desert Research Institute of the University of Nevada;⁸ R. Steiger, Institut für Kristallographie und Petrographie, Zurich, Switzerland;⁹ Y. Suzuki, Hokkaido University;¹⁰ B. Velde, Montana State University.⁶

Guest Investigators: H. Baadsgaard, University of Alberta; B. R. Doe, U. S. Geological Survey; J. D. H. Donnay, Johns Hopkins University; P. W. Gast, University of Minnesota; K. von Gehlen, University of Erlangen-Nürnberg; E. C. Hansen, Yale University; R. Hart, Yale University; D. Presnall, Pennsylvania State University; C. E. Tilley, Cambridge University.

Operating and Maintenance Staff

Executive Officer: A. D. Singer.

Accountant: E. T. Orozco.

Editor and Librarian: Miss D. M. Thomas.

Stenographer: Miss M. E. Imlay.

Typist: Mrs. N. O. Doe.

Stockroom Assistant: M. L. Kirby.

Mechanic's Helper: M. Ferguson.

Janitors: E. L. Jackson,¹¹ R. L. Truesdale.¹²

Chief Mechanician: F. A. Rowe.

Instrument Makers: C. A. Batten, L. C. Garver, J. F. Kocmanek, W. H. Lyons,¹³ O. R. McClunin, G. E. Speicher.

Mechanic and Carpenter: E. J. Shipley.

Electrician: E. C. Huffaker.

Machinist: J. R. Thomas.

Building Engineer: R. L. Butler.

¹ Appointment from July 1, 1962, through June 30, 1963.

² Appointment from July 1, 1962.

³ Resigned June 15, 1963, to accept position as Research Associate and Lecturer in Chemistry with the Institute of Marine Science, University of Texas.

⁴ Appointment from November 1, 1962.

⁵ Appointment terminated September 15, 1962, to continue graduate study at Harvard University.

⁶ Appointment from September 1, 1962.

⁷ Appointment terminated July 31, 1962, to return to Tokyo University.

⁸ Appointment terminated July 31, 1963, to return to the Desert Research Institute, University of Nevada.

⁹ Appointment from October 1, 1962.

¹⁰ Appointment terminated July 31, 1962, to accept position with Geological Survey of Japan.

¹¹ Appointment terminated May 15, 1963.

¹² Appointment from October 16, 1962.

¹³ Appointment from February 18, 1963.

*Department
of Terrestrial Magnetism*

Washington, District of Columbia

Merle A. Tuve
Director

Contents

Introduction 261

Experimental Geophysics 264

 The earth's crust 264

 Geochronology and isotope geology 264

 Seismic studies 280

 Radio astronomy 289

 Radio hydrogen 289

 Angular size interferometer 298

 South American cooperation 298

Theoretical and Statistical Geophysics 299

 Conductivity anomaly program for Peru 299

 Induction effects over the night hemisphere arising from the motion of the daytime
 diurnal variation current system 300

 Solar-cycle variations of cosmic-ray intensity, cosmic-ray activity, and geomagnetic
 activity, 1937-1961 301

 Cosmic-ray program 302

Laboratory Physics 302

 Nuclear physics 302

 Polarized ion source 302

 Biophysics 303

 Introduction. 303

 The DNA-agar method 303

 Kinetics of synthesis of messenger RNA 304

 DNA-RNA hybrid formation as an indicator of genetic activity 307

 Fractionation of complementary RNA 314

 The DNA of bacteriophage λ 316

 The measurement of genetic relatedness among organisms 319

 Current status of the doublet code 323

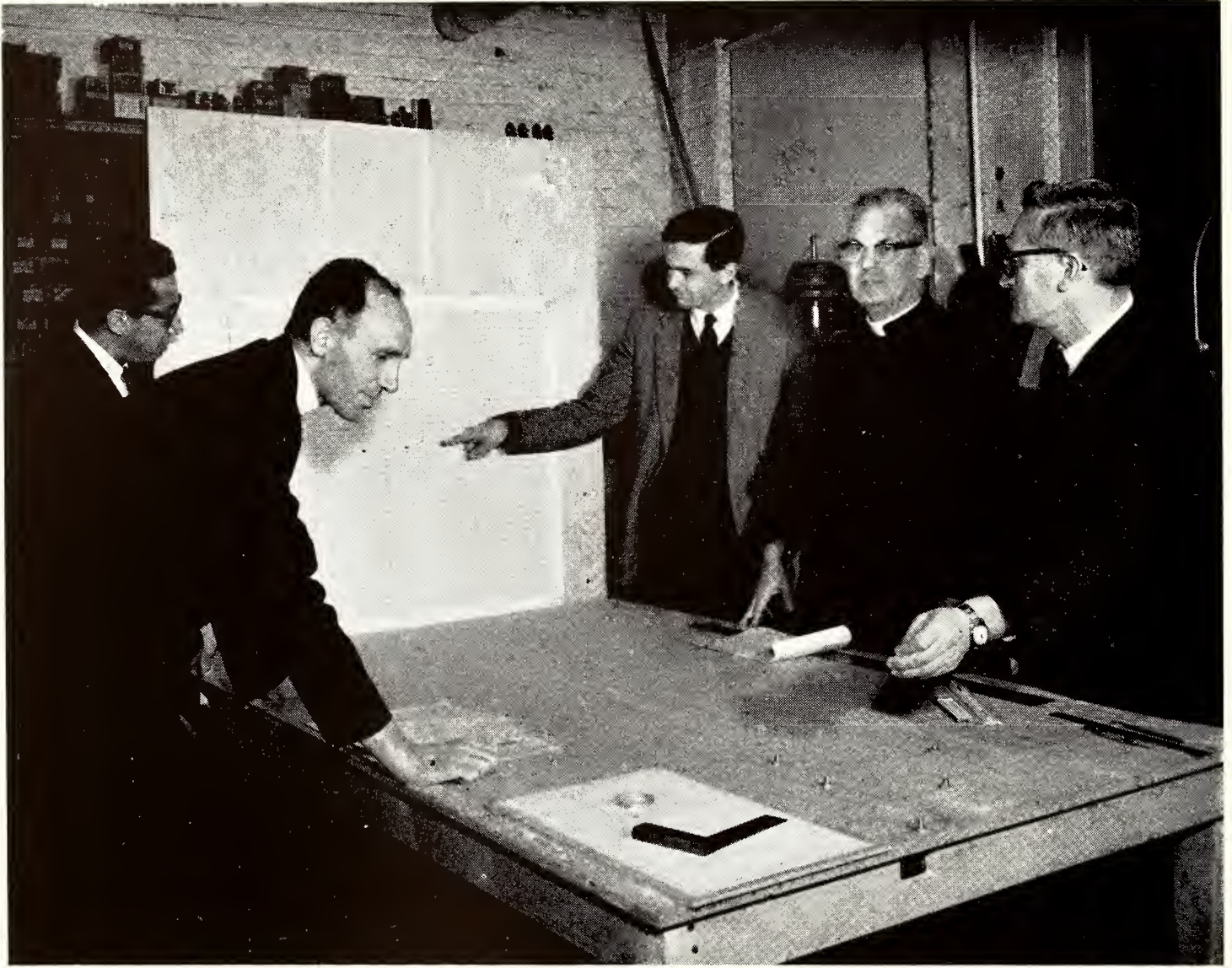
 Studies of RNA synthesis in *Euglena* 324

Image Tubes for Large Telescopes 326

Bibliography 326

 Major publication 327

Personnel 328



Geophysics of the earth's crust and mantle is a very interesting study in regions of active mountain building, as in the Andes. Sixteen Carnegie collaborators in six university groups of western South America spent two months in early 1963 at a special seminar on local and regional earthquakes at the Department of Terrestrial Magnetism. The device pictured is a simple analog computer for positions and depths of local earthquake shocks observed with our cooperative network of more than twenty-three stations.

INTRODUCTION

THE activities of our Department this year have again illustrated the vitality and effectiveness of personal research efforts carried forward by selected individuals. To examine this point one should scan the detailed reports given in the following sections, viewing them in relation to the output that might have been expected from some other group of similar size (roughly 15 investigators), all of whose efforts were focused and directed as a group toward previously defined goals. Viewed in this way, our report serves as a concrete illustration of "basic research." To a large extent, of course, even the research of a man who works individually on his own problems is planned and directed to specific goals, but the planning and direction arise within him, and the goals are valued by him in terms of personal satisfaction, instead of being valued for their importance to some aim imposed on the group by external considerations. In a sense, the activities described here are a form of artistic expression, in modern terms and using fresh means. The elaboration of various patterns and ideas in research is more coherent and less disturbed than most of the kinds of elaboration currently seen in the graphic arts or even in serious music. Perhaps it frequently is also a more satisfying personal expression.

Physics is the rootstock supporting a tremendous growth of technical and technological activities in recent years, and the ideas and techniques of physics are proving extremely useful in subject areas like geology and biology, which originally developed out of questions and descriptive procedures that were not a part of physics, except, perhaps, in the broad terms of cosmology. As a physics department, minimizing (but not eliminating) our special attention to the magnetic field of the earth, during the year just past a half dozen widely different kinds of ideas and research efforts were given particular

emphasis. Some of them were favored with successful progress as described in the reports that follow. Other efforts were less successful, but even a disappointing result is often a valuable guide in research.

It is of some interest to scan in a broad fashion a typical example of successes and disappointments of one of our programs over the past fifteen years. In the middle and late 1920's this Department gave much attention to geophysical phenomena in the upper atmosphere, including cosmic rays, airglow, and the ionosphere; but after the end of World War II huge military and civilian groups directed their energies to these fields, and it seemed rather pointless for us to contribute the efforts of two or three men to such a large and well supported activity. We therefore turned to radio astronomy and to geophysical studies of the crust and mantle of the earth. In both these fields our electronics background would be usefully joined to new kinds of questions about the world around us.

The research on the earth's crust was concentrated in two programs: one to measure the ages (time since deposition) of ancient rocks by means of isotope procedures; the other to study the outer structures of the earth by means of elastic waves from explosions and from local earthquakes.

At first (1946-1948) our modest efforts to study the earth's crust, familiarly described in terms of "granitic and basaltic layers" for two decades previously in geophysical literature, seemed quite successful. But repetition of the measurements in slightly different locations always seemed to yield different patterns of layer thicknesses and velocities. By 1952 we had demonstrated and reported the intrinsic ambiguity of interpretations of such "travel-time" curves in terms of hypothetical buried layers and had emphasized the importance to observational

data of the mathematical cusps (often hidden) on the travel-time curves that arise from changes in the elastic constants as the waves progress downward. Such changes occur, for example, at the boundaries of buried layers or irregular bodies of differing materials. Nevertheless, in 1954 we were able to deduce and report, from our reconnaissance work in Arizona and New Mexico with explosions in open-pit mines, that regional or lateral variations were indicated for the upper part of the earth's mantle below the crust. This result has been conspicuously verified and widely extended over the United States during the past two years by the data from atomic explosions.

In our report last year a clear illustration of the ambiguity of various interpretations of travel-time curves in deducing the variation of wave velocity with depth in the crust was given, using our Gulf of Maine data from the 1961 expedition. This year, we are glad to say, a constructive and complementary result is reported from the 1962 North Carolina expedition. Taking the apparent arrival velocity, from beginning to end of a long line or "spread" of seismometers, for shots fired at various distances, and hence for waves that have penetrated to different maximum depths before bending back to the surface, a proper measure of the velocity for each depth has been charted. This analytical observing procedure is possible only when the data change slowly and consistently with distance, indicating no "shadow zones" or other reversals, but for most localities this requirement appears to have been met, although our earlier observations were not designed for accurate determinations of apparent velocity at the receiving spread. Our new procedures will have a further test in the special set of explosion observations in and near Lake Superior that are being carried out by our Department during the summer of 1963 as a part of the International Upper Mantle Project of the International Union of Geodesy and Geophysics.

This quick review of just one facet of

our activities omits reference to the many ways the work itself has given rise to other vigorous relationships, such as our comprehensive geophysics program in the Andes and much of the Department's participation in the IGY and related international programs.

A quick scan of other significant happenings of the year may be of value as a guide to the contents of the detailed reports below.

Probably the most fruitful and far-reaching result has been the whole body of interrelated work in our biophysics group, which is based on the use of single-stranded DNA as an adsorption column to select matching "genetic message" units on complementary RNA or DNA. This procedure, pioneered here about two years ago, is now widely recognized as a peerless tool for analysis in biosynthesis as controlled by genetics. The comprehensive nature of our biophysics reports each year may give some indication of the importance we attach to this part of our activities and our satisfaction in the kinds of questions that are answered in the experiments.

The radio astronomy program entered a fresh phase this year when the 300-foot parabolic antenna at the National Radio Astronomy Observatory was completed, and we were invited to use it for studies of our own galaxy and external galaxies such as the Andromeda nebula M31, M33, and M81. Materials and fabricated parts were shipped to La Plata, Argentina, for the 100-foot Carnegie parabolic antenna to be installed there in cooperation with a group organized under the National Research Council of Argentina. A similar 100-foot parabola is being erected in Maryland for studies of the angular diameters of radio objects, to be operated jointly with our 60-foot Derwood parabola as an interferometer.

Initial reconnaissance observations seeking anomalies in electrical conductivity of the upper mantle were about half completed during the year in southern Peru. Instrumental difficulties with the

nine semiportable magnetometer installations defeated part of the effort, but some indication of anomalous induced currents in the earth appeared in the records at Cuzco and Pucara. Further data are needed in eastern Peru and in Bolivia.

By late 1962 our cooperative program for studies of local earthquakes in the Andes had evolved to the point where consolidation and revision of technical procedures and instrumentation would be effective. A working seminar in Washington was held by all participants, including 17 of our colleagues from the Andes, for two months in early 1963. Fruits of these discussions will be evident in the recordings and studies now being prepared at the six university centers and twenty-six Carnegie sites in the Andes.

Nuclear physics studies of detailed relationships important to theoretical analysis (matrix elements for tensor analysis) progressed, using polarized deuteron and proton beams from our high-voltage generator, in the Department's cooperative program with the University of Basel, Switzerland. Some mechanical (and vacuum) difficulties were encountered, as is commonplace at the start of such complex efforts.

The work of the Carnegie Committee on Image Tubes for Telescopes (CCITT) has been supported as before from the Department, with Dr. Ford of our staff as the full-time technical aide of the Committee in charge of the industrial development and testing of the five or six different types of image intensifiers selected by the Committee for emphasis. The previous difficulties with resolving power and uniformity of phosphor screens were surmounted by the RCA development group; uniform screens showing a resolution of 80 or 90 line pairs per millimeter have now resulted. This number

is degraded by the viewing lens, of course, but the Committee is in a position to recommend the purchase of 30 to 80 image tubes of two or three types which will give an advantage of a factor of 10 or more over the direct use of photographic emulsions. This factor, compared with direct photography, is measured in different ways for different instrumental procedures or astronomical end results, but a real gain of 10 or more is now at hand. Incidentally, a revision of the astronomers' own estimates of the sensitivity of photographic emulsions has reduced the theoretically attainable gain with photoelectric procedures from a possible 100 to 140 down to a possible 15 or 20, and our samples of image tubes appear to give performance in about this range. We hope to help bring these tubes into wide application in astronomy and astrophysics during the next several years.

Supplementary funds from the National Science Foundation are used in several of the cooperative activities of the Department, primarily to cover costs of field activities involving other groups, such as our geophysical studies in the Andes and the radio astronomy center for the southern sky which is under way in Argentina. Other examples are the large expenditures in industrial laboratories connected with our image tube program, and the cost of explosives and other logistic expenses for the international upper mantle experiment on Lake Superior. The Institution carries the salaries and operating expenses for our staff, but the fruitfulness of our efforts is greatly enlarged by these outside funds made available for cooperative activities. The U. S. Navy, through the Office of Naval Research, and the U. S. Coast Guard are also making funds, manpower, and ships available to the Lake Superior project.

EXPERIMENTAL GEOPHYSICS

THE EARTH'S CRUST

The activities of the crust group this year would be expected to be more extensive than those described in *Year Book 61* simply because the work of nearly half again as many men is being reported. But the larger group has also meant a more intensive experience for the participants in the work, and this is not always the result of increased numbers.

The research ranged from seismic studies in Peru to mineral age studies in the Precambrian Shield of Finland. The research facilities of the laboratory have been made available to scientific colleagues from Canada, Peru, Switzerland, Finland, Brazil, South Africa, and Japan. Technical assistance has been provided which will send a complete mass spectrometer to the Geological Survey of Finland in late summer or early autumn.

In addition to the fundamental research efforts, the Carnegie Intensive Seminar on Local and Regional Earthquakes was conducted in January and February to bring Carnegie staff members and their colleagues in Peru, Bolivia, Chile, and Argentina into a comparable state of preparedness to utilize, to alter, and to add to the facilities that have been created in these countries largely through the efforts of Dr. Tuve and our South American colleagues.

Even as the seminar was in progress, plans were under way for the execution of a major United States effort in the International Upper Mantle Project. The Department assumed responsibility for shooting and accurately locating a number of 1-ton and larger shots in Lake Superior during July 1963. The seismic effects of the shots will be observed by more than a dozen groups in Canada and the United States. As this is written, nearly all the Crust Section is involved in preparations for the shooting and our own observations. To add yet another facet to our work, the first heat-flow measure-

ments in the bottom of Lake Superior will also be attempted. This, in summary, is the attempt of a half dozen men to commit themselves properly to the opportunity that is almost uniquely available to Carnegie scientists.

GEOCHRONOLOGY AND ISOTOPE GEOLOGY

S. R. Hart, L. T. Aldrich, G. L. Davis,¹ G. R. Tilton,¹ H. Baadsgaard,² O. Kouvo,³ and R. H. Steiger³

Although the measurement of absolute geologic age is not becoming any easier, the direction in which the effort is best spent becomes increasingly apparent. What was once a bewildering array of discordant ages is now becoming the path to real understanding of the processes involved in fundamental geologic events. It not only leads to the original age of a rock unit but, on the way, points to many of the interesting events in the subsequent geologic history of the rock. Not infrequently the side excursions are more exciting than the destination.

A substantial sampling of this path and its detours is provided in the following pages. Definitive results have been obtained from regional dating in Ontario, Finland, and Alberta. The Ontario results suggest a close time-grouping of geologic events and lead to recognition of an early Precambrian geosynclinal sequence. The Finland and Alberta results demonstrate the existence of events widely separated in time and present evidence for previously unrecognized activity in both areas about 2300 m.y. ago. At the other end of the time scale, hornblende K-Ar dating has been applied to study the complex geologic events that were forming the Swiss Alps some 25 m.y. ago.

Continuation of work in the Maryland Piedmont affirms the severity of the

¹ Geophysical Laboratory, Carnegie Institution of Washington.

² Guest Investigator; from University of Alberta.

³ Carnegie Institution Fellow.

Appalachian metamorphism, with K-Ar ages on hornblendes, pyroxenes, and plagioclases being rather consistently younger than the true age of the Piedmont rocks.

Inquiry into the causes of discordant zircon U-Pb ages is under way in a study of the effects of contact metamorphism on these ages. Results so far show that contact metamorphism can be quite effective in producing episodic lead loss.

An investigation of the origin and source of oceanic serpentinites has been started, using strontium isotopes as natural tracers. The data are at present insufficient to allow any test of the various models of ocean basin evolution.

(Rb half-life used = 50×10^9 years; strontium ratios normalized to 86/88 = 0.1194.)

Ages from the Early Precambrian near Rainy Lake, Ontario

The Rainy Lake area contains a classic section of early Precambrian rocks that is unique for the interest and controversy it has provoked among geologists for more than 75 years. Near the type locality of the Keewatin, Lawson in 1888 discovered a sedimentary

section he believed to underlie the Keewatin, which he named the Coutchiching. Interest in the age and source of these ancient sediments stimulated the present study of Coutchiching rocks and of the overlying Keewatin greenstones and younger Laurentian granites as well.

Near Rice Bay on Rainy Lake, the Coutchiching, comprised largely of metagraywackes, occurs as a large domal structure overlain with apparent conformity by the metamorphosed Keewatin volcanics. In the center of the dome is a gneiss originally mapped by Lawson as intrusive Laurentian granite but believed by Yardley, Goldich, Peterman, and Frye⁴ to be a different and more highly metamorphosed facies of the Coutchiching. One of the few geologically definable Laurentian granites in the area is found to the east at Bad Vermilion Lake, where it cuts the Keewatin and is in close proximity to conglomerates of the younger Seine series (Timiskaming). Zircon and whole-rock Rb-Sr analyses

⁴ D. H. Yardley, S. S. Goldich, Z. E. Peterman, and J. K. Frye, Precambrian geology of the Minnesota-Ontario border region, *Bull. Geol. Soc. Am.*, 70, 1703, 1959.

TABLE 1. Location of Early Precambrian Samples

Sample No.	Rock Unit	Rock Type	Locality
Rainy Lake, Ontario			
RL45	Coutchiching	Outer paragneiss, 60 ft composite	Upper Rice Bay
RL71	Coutchiching	Metagraywacke	Dude Island
RL105	Coutchiching	Metagraywacke	Sand Point Island
RL109	Coutchiching	Outer paragneiss	Upper Rice Bay
CC21	Coutchiching	Central paragneiss	Upper Rice Bay
CC22	Coutchiching	Central paragneiss	Upper Rice Bay
CC26	Coutchiching	Outer paragneiss	Upper Rice Bay
CC29	Coutchiching (?)	Porphyroblastic paragneiss	Rocky Islet Inlet
CC20	Keewatin	Rhyolitic metatuff	Sand Point Island
CC23	Keewatin	Ellipsoidal greenstone	Red Pine Island
CC30	Keewatin	Amphibolite	Rice Bay Inlet
Bad Vermilion Lake, Ontario			
CC33	Laurentian	Tonalite	Southwest shore
CC34	Laurentian	Tonalite	Southwest shore
CC35	Laurentian	Tonalite	Southeast shore
CC36	Laurentian	Tonalite	Southeast shore
CC43	Laurentian	Granite	Saganaga Lake, Minnesota

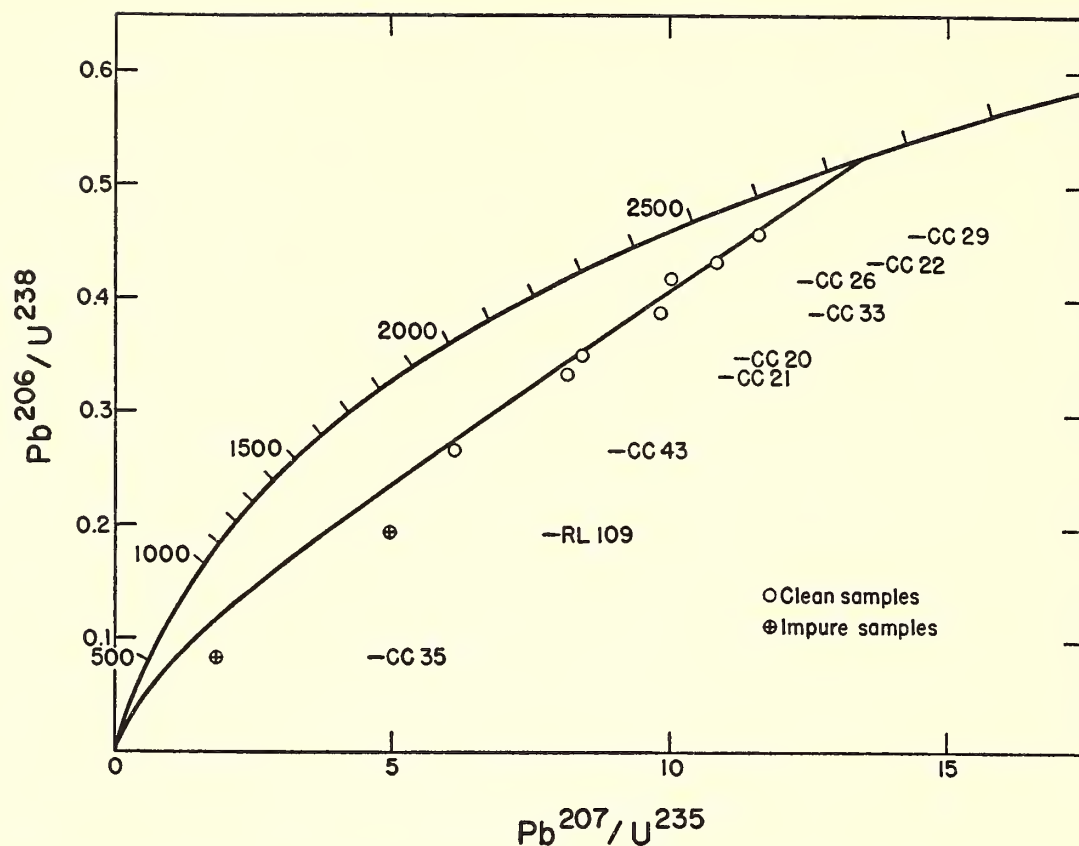


Fig. 1. U-Pb concordia diagram for Ontario zircons. Note the good fit of data to a 2750-m.y. continuous diffusion curve.

were performed on a number of samples from these units in an effort to determine their age and the time interval involved in this early Precambrian rock sequence. At the same time it was thought desirable to compare the extent to which these two dating methods can be expected to record similar events in the history of such a sequence.

The location of dated samples is given in table 1. Figure 1 presents the zircon results on a concordia plot. Considering these data first, it is apparent that all the samples fall within a small spread in age, especially if the impure samples are omitted. The continuous diffusion curve for the remaining points corresponds to an average age of 2750 m.y. Here, then, are zircons, from a diversity of rock types, all showing essentially the same age within the limits of error. Several explanations for this were discussed in *Year Book 61*, page 177.

Addition of the whole-rock Rb-Sr results provides certain restraints to interpretations based on the zircon data alone. Isochron diagrams of the whole-

rock data are presented in figures 2 and 3. The consistency of the isochrons is quite marked. The Couthiching and Keewatin points are again indistinguishable, giving an isochron age of about 2700 m.y. On the other hand, the Laurentian granite isochron is clearly resolved with an age of about 2500 m.y.

Taken together, the zircon and whole-rock Rb-Sr data indicate a source rock

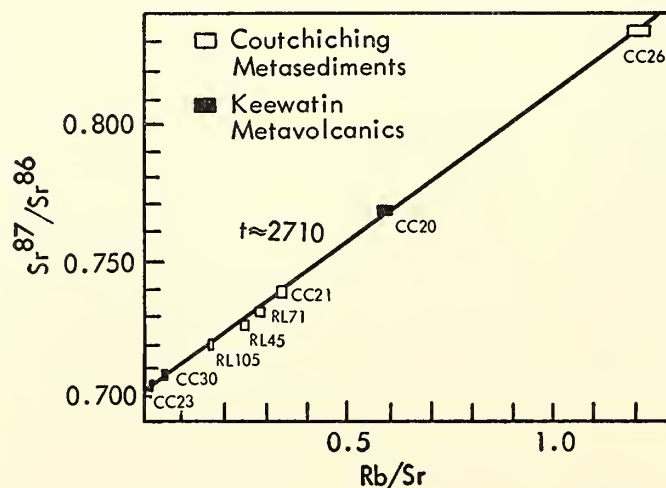


Fig. 2. Rb-Sr isochron diagram of Couthiching and Keewatin whole-rock samples from Ontario. Mole ratio $\text{Sr}^{87}/\text{Sr}^{86}$ against weight ratio of rubidium over normal strontium.

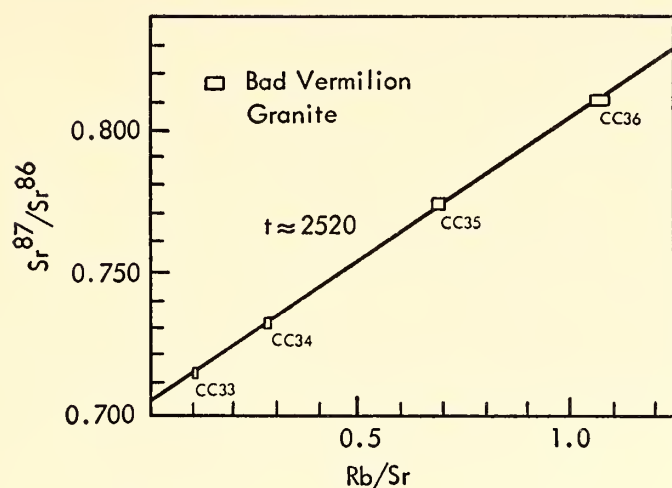


Fig. 3. Rb-Sr isochron diagram of Laurentian granite whole-rock samples, Bad Vermilion Lake, Ontario. Mole ratio $\text{Sr}^{87}/\text{Sr}^{86}$ against weight ratio of rubidium over normal strontium.

for the Couthiching nearly equivalent in age to the Keewatin. Consideration of the conformable nature of these units, and of the volcanic-graywacke association so typical of eugeosynclines, suggests these formations to be part of an early Precambrian geosynclinal sequence. The source of materials for the Couthiching might be found within the geosyncline itself, derived by a process Krynine aptly termed "cannibalistic." That little of the material in this sequence could have been provided by much older sialic basement is suggested by the low initial ratio of $\text{Sr}^{87}/\text{Sr}^{86} = 0.701$.

For the above sequence, excellent agreement exists between the zircon and whole-rock methods. But the age of the Laurentian granite as determined by these two methods is in very poor agreement, and possible explanations may be considered. In view of the badly sheared nature of the Bad Vermilion granite, it is possible that the whole-rock samples have been altered during a younger period of metamorphism (Algoman). The consistency of the whole-rock isochron, however, would require a very complete and pervasive period of remixing of the strontium. Even though the assumption of a "closed system" for whole rocks is seldom questioned, it must be pointed out that our understanding of this assumption is decidedly imperfect. The

only other explanation for the zircon-whole-rock discrepancy would require that the zircons have in some sense been "inherited" from older rocks.

Isotope Mineral Ages on the Finnish Precambrian

Over the past decade, knowledge of the orogenic events in the Finnish Precambrian has greatly increased. Instead of having two orogenic belts of quite different age, Karelian and Svecofennian, better understanding of sedimentary stratigraphy has made it possible to distinguish the Karelian foreland sediments (orthoquartzite with dolomites) from the Svecofennian eugeosynclinal associations (arkoses, graywackes, and basic and intermediate volcanics), all belonging to the same cycle. Most of the fundamental facts concerning this evaluation have been presented by T. Mikkola and Simonen. The huge discordance of deep erosion between the Karelian formations and the ancient preexisting craton (the Prekarelian basement complex) has long been one of the best-known facts in Finnish geology.

The geochronological data obtained up to the present support this stratigraphic scheme. For instance, the Prekarelian basement complex appears to be 2700–2800 m.y. old. Syntectonic intrusions in both orogenic belts show close agreement, suggesting an age of 1800–1900 m.y. for the time of revolution. The anorogenic rapakivi formation was found to be 1650–1700 m.y. old. This age distribution is distinctly revealed by analyses of zircons (concordia diagram, fig. 4; rapakivi ages excluded). Isotopic ages on micas and feldspars either confirm zircon ages or reflect the metamorphic events at 1800–1900 m.y. In summary, the radiometric isotope ages are in obvious accord with the field evidence. It has also become apparent that there are problems intimately associated with the complex matter of rock genesis. Also, the radiometric isotope ages do not exclude the

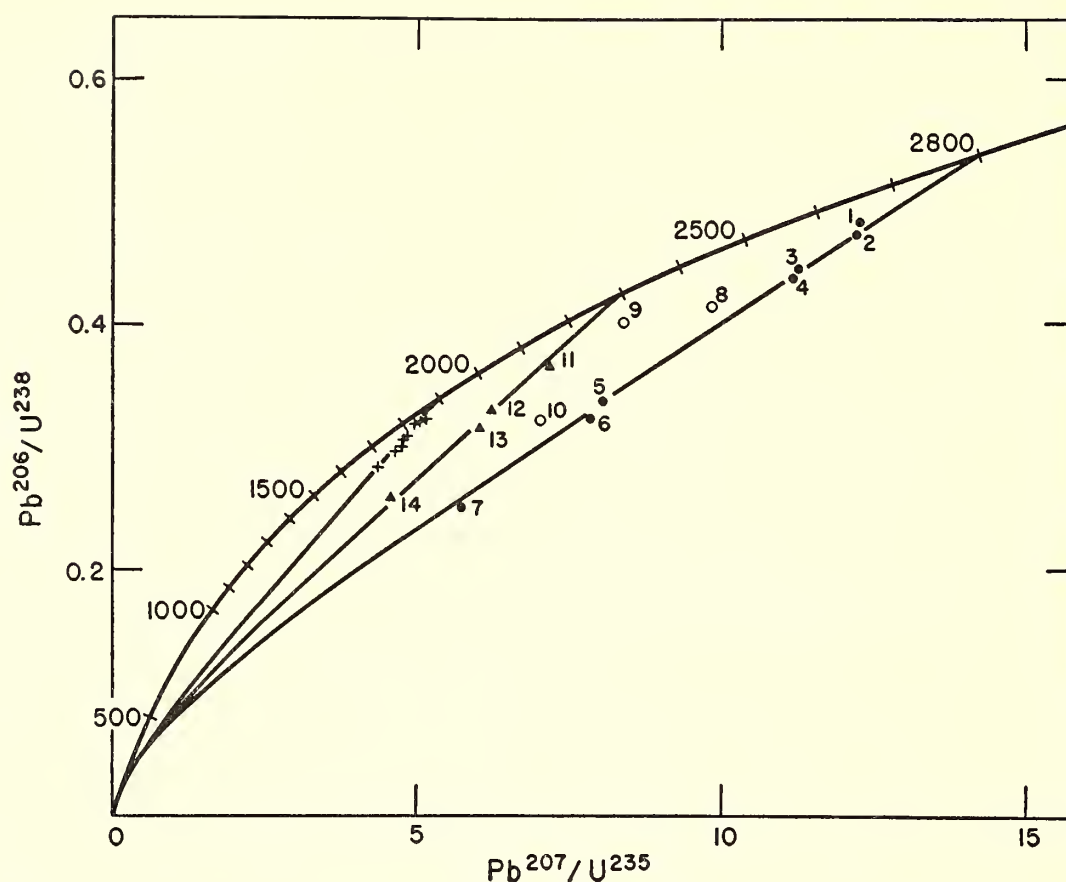


Fig 4. Parent-daughter ratios for zircons from 2800-m.y.-old Prekarelian basement complex (1-7), gneiss domes (8-10), Tampere graywackes (11-14), and 1800- to 1900-m.y.-old intrusive rocks.

existence of short time intervals between successive phases of events of the order of 100 m.y., e.g., pulses of orogeny confirmed by breaks in sedimentary records and polycyclic magmatic activity.

The material collected for dating in 1962-1963 includes some miscellaneous samples for regional problems, but the main substance of the work has been to increase the number of points on the concordia diagram mentioned above.

The Prekarelian basement complex of 2800-m.y. age. Four basement samples were collected in an attempt to increase the spread on the 2800-m.y. discordia curve of the concordia diagram. Two of them, quite far from the borderline between the younger and the older formations (A28-Suomussalmi and A50-Ilomantsi), yielded almost similar ages which lie on the 2800-m.y. discordia curve. Two additional samples were collected from the contact zone of 1800-m.y. intrusives. Zircon A52-Sompujärvi was about 50 meters from a Karelian layered basic-ultrabasic series. It showed

considerable loss of lead but still plots on the 2800-m.y. diffusion curve. Another sample (A75-Riihilahti) was collected some meters from the Maarianvaara intrusion (1800-m.y. zircon and mica ages). It also lies on the 2800-m.y. discordia curve and has lost little if any of its lead as the result of the 1800-m.y. intrusive near by.

Two attempts were made to find traces of the old basement in the deeper geosynclinal region far to the west of the eastern basement complex. Both zircons (A10-Tiirismaa and A54-Vimpeli) showed an 1800-1900-m.y. age.

It has been found that mica ages confirm zircon ages in formations of 1800-1900-m.y. age but show 1800-m.y. age in samples from 2800-m.y. basement complex. This zircon/biotite discrepancy was also found in A53-Kuopio and A50-Ilomantsi (table 2). In addition, the Suomussalmi granodiorite (A28) showed a 2800-m.y. zircon age whereas an earlier K-Ar measurement on biotite gave 1720 m.y.

TABLE 2. Ages of Minerals from the Finnish Precambrian

No. in Fig.	Sample	Rock	Mineral	Ages, millions of years				
				U ²³⁸	U ²³⁵	Pb ²⁰⁷	Th ²³²	Rb-Sr
				Pb ²⁰⁶	Pb ²⁰⁷	Pb ²⁰⁶	Pb ²⁰⁸	
...	A2-GSF 61	Nokia granodiorite	Zircon	1710	1810	1920	1900	...
			Biotite	1760
...	A4-GSF 60	Hämeenkyrö diorite	Zircon	1800	1840	1880
...	A10-GSF 62	Tiirismaa diorite	Zircon	1750	1820	1885
...	A54-GSF 60	Vimpeli gneissic granite	Zircon	1735	1810	1890
...	A7-GSF 62	Kalkku porphyry	Zircon	1690	1790	1890	1610	...
...	A8-GSF 62	Aitolahti porphyry	Zircon	1685	1785	1910	1730	...
14	A6-GSF 62	Alisenjärvi inclusion	Zircon	1490	1800	2110	1600	...
12	A1-GSF 61	Vihola graywacke	Zircon	1850	2030	2220	1580	...
			Muscovite	1850
			Biotite	1770
			Orthoclase	1880
13	E57-J Geol.	Siivikkala graywacke	Zircon	1790	2000	2230	1720	...
11	A9-GSF 62	Mutikko graywacke	Zircon	2030	2160	2280	2130	...
			Microcline	1880
3	A28-GSF 61	Suomussalmi granodiorite	Zircon	2400	2575	2725	2405	...
4	A50-GSF 61	Ilomantsi granite	Zircon	2360	2575	2750
			Biotite	1750
7	A52-GSF 61	Sompujärvi granite	Zircon	1460	1960	2545	2215	...
			Microcline	2100
9	A53-GSF 61	Kuopio dome gneiss	Zircon	2195	2300	2400
			Biotite	1715
1	A75-GSF 62	Riihilahti granodiorite gneiss	Zircon	2575	2660	2725

The mantled domes. Within the orogenic belts can be found gneiss domes or cupolas having a protective sedimentary mantle around them. Eskola has suggested that a necessary condition for their formation is that they have been subjected to two orogenic revolutions.

Earlier examination of two Karelian dome zircons has shown that the history of these rocks may differ from the history of those in the basement area proper. It was found that zircons from the Heinävaara dome and Sotkuma dome (only 6 and 32 km, respectively, from the eastern basement quartzite horizon) do not fit the 2800-m.y. chord mentioned above but lie slightly above it. A third dome zircon sample (A53-Kuopio) was collected from the well studied Kuopio area, about 90 km farther west from the Sotkuma dome. This zircon has lost more lead, and it lies farther above the 2800-m.y. chord, than

the other dome zircons. These zircons require further investigation, but it appears likely that the discordance is caused partly by episodic loss of lead by the 1800-m.y. metamorphism. Furthermore, the dome gneiss at Vuorimäki, where sample A53 was collected, represents a complicated variety of paragneiss with pink granite injections, as pointed out by Preston.

Tampere region, southwest Finland. The Tampere graywackes were selected for study because of their essential stage in the cycle of sedimentation within the ancient geosyncline preceding the 1800-m.y. revolution in this area and because they represent material of rapid sedimentation. Clues to the source areas of this material have not been obtained. At the moment we know only that the graywacke zircons have their origin in rocks predating the orthogeosyncline. However,

the idea of a "cannibalistic" process presented by Krynine is of utmost interest: some uplifted, folded, and thrust segments of the same area are eroded, and the geosyncline feeds upon itself.

Zircons were studied from different distances from the Nokia-Hämeenkyrö granodiorite body (with a diameter of 20 km), which intrudes Svecofennian schists. Sample E57-Siivikkala was collected from the sandstone part of a 200-cm-thick megavarve at Siivikkala Peninsula about 5 km from the contact. This graywacke represents the best-preserved part of the area. Another zircon (A1-Vihola) is from the sandstone part of a megavarve (reaching 3 to 4 meters) at Nokia, about 2 km from the contact of the Nokia granodiorite. The elastic structure is well preserved, and the rock is characterized by large poikilitic flakes of muscovite and monoclinic potash feldspar which shows only traces of triclinicity. To get more spread in loss of lead two other samples were collected, one from an extremely coarse-grained graywacke schist about 25 km away and about 3 km from the nearest intrusive granite (A9-Mutikko), and another (A6-Alisenjärvi) from the middle of an inclusion lens of schist (40 by 150 meters) occurring 2 km within the granodiorite mass.

The zircon results indicate that all the graywacke samples have Pb^{207} - Pb^{206} ages of about 2250 m.y. (table 2) and lie on a 2300-m.y. discordia curve (fig. 4). They serve as isolated guides only, but they do show that zircons give an old age even in materials most strongly reworked during disintegration, transport, recrystallization, and new weathering. The existence

of a group of this age is given some support by the regional distribution of Karelian common lead galena ages of 2100-2300 m.y., but this has to be considered an open question because it is based on detrital zircon for which the source rock has not been found.

As far as the thermal history of zircons is concerned, it is of some interest to find that the most concordant age pattern was produced by the coarse-grained graywacke (A9) and that the most discordant age pattern is represented by the inclusion of schist (A6) within the granodiorite (showing the most schistose appearance and abundance of tourmaline). However, not even the zircon from this inclusion shows episodic loss of lead related to the time of intrusion.

Both granodiorite zircons (A2-Nokia and A4-Hämeenkyrö) show an age of 1800-1900 m.y. and closely fit a 1900-m.y. discordia curve.

Rb-Sr ages were determined for muscovite, biotite, and potash feldspar from some of these rocks. All minerals showed ages of about 1800-1900 m.y. (table 3). The age of 1850 m.y. for muscovite is of special interest, because it indicates the time of the regional metamorphism of this area. As strontium from feldspars A1 and A9 was only 3 and 7 per cent radioactive, the error in the age is large.

To get more information about the time of sedimentation of the Tampere eugeosynclinal sediments, two samples of acid porphyries (A7-Kalkku and A8-Aitolahti) were collected. They gave identical ages of 1900 m.y. (table 2). The extrusive origin of these two rocks is not supported by sufficient geological evi-

TABLE 3. Rb-Sr Ages on Some Minerals from the Finnish Precambrian Rocks

Sample	Location	Rock	Mineral	Ages, millions of years
				Rb-Sr
A39-GSF 62	Murtomäki	Pegmatite	Muscovite	1850
A45-GSF 61	Kyyneljärvi	Granite	Microcline	1820
			Biotite + chlorite	1550
A49-GSF 62	Outokumpu	Ore contact	Phlogopite	1820

dence, however, and they may be later intrusions into the sedimentary section.

According to the nuclear dating thus far, the time of paroxysm in the Svecofennian orogeny coincided with the Karelian revolution. This does not necessarily mean contemporaneous beginning of geosynclines or sedimentation. From the data collected in this work, three problems of especially great interest are open: the history of mantled domes; the origin of detrital zircons found in the Tampere graywackes; and the age of the Svecofennian volcanic rocks as compared with those in the Karelian mountain belt.

Mineral Ages from the Andrew Lake Area, Precambrian Shield, Northeast Alberta

The detailed surface mapping and study of the Precambrian Shield in northeast Alberta by the Research Council of Alberta offers an excellent test of the usefulness of radioactive dating. In the area under consideration, about 350 square miles around Andrew Lake, are four groups of rock types: an old basement complex; relatively unmetamorphosed sediments; massive-leucocratic and -biotite granites; and foliated porphyroblastic granites. The old basement complex comprises biotite and hornblende granite gneisses, high-grade metasedimentary

rocks, foliated granites, and mylonitic zones. The relatively unmetamorphosed sedimentary rocks (mainly greenschist facies) are composed of silty graywackes, which show clastic textures and graded bedding where well preserved, as well as a lesser amount of 'intermediate' extrusive rocks showing ophitic and trachytic textures. Very likely these low-grade metasedimentary rocks represent a period of deposition later than that of the high-grade metasediments of the basement complex. The massive-leucocratic and -biotite granites intrude most other rocks, whereas the foliated porphyroblastic granites seem to be metamorphic equivalents of the low-grade metasediments. The field relations suggest two, and possibly three, orogenic events in this region.

Reconnaissance K-Ar dating of the principal rock types gave a range of mica ages from 1740 to 1830 m.y. (Godfrey and Baadsgaard, 1962).⁵ With further work, 28 mica K-Ar ages yielded a mean value of 1810 ± 20 m.y., though the geology of the area indicates a much larger possible spread in the true age of the various rock

⁵ J. D. Godfrey, and H. Baadsgaard, Structural patterns of the Precambrian Shield in northeastern Alberta and mica age dates from the Andrew Lake District, *Proc. Roy. Soc. Can., Spec. Publ.* 4, 30-39, 1962.

TABLE 4. U-Pb, Th-Pb Ages, Andrew Lake Area, Northeast Alberta Precambrian Shield

Sample No.	Rock and Mineral Used (Petrographic term)	Ages, millions of years				
		Pb ²⁰⁶	Pb ²⁰⁷	Pb ²⁰⁷	Pb ²⁰⁸	
		U ²³⁸	U ²³⁵	Pb ²⁰⁶	Th ²³²	
151-11*	Granite boss (quartz monzonite)	Zircon	1320	1600	2000	1330
128-5†	Basic plug (hybrid granite)	Zircon	1540	1680	1860	1530
729-3†	Massive granite intrusive (granodiorite)	Zircon	1390	1580	1850	1530
729-4	Older granite (quartz monzonite)	Zircon	1230	1430	1750	...
90-2	Porphyroblastic granite gneiss (composite) (quartz monzonite gneiss)	Allanite‡	1850	1840	1820	1880
		Allanite†	1990	2000	1960	1930
		Zircon	1870	2020	2190	1950
		Monazite	2290	2120	1950	1880
44-1†	Mineralized biotite schist (biotite schist, granodioritic pegmatite)	Uraninite	1410	1570	1800	1090
149-1*	Granite gneiss-basement complex (quartz monzonite gneiss)	Zircon	1540	1840	2200	1500

* Common lead correction, 204 : 206 : 207 : 208 = 1 : 15.3 : 15.5 : 35.3.
† Common lead correction, 204 : 206 : 207 : 208 = 1 : 14 : 14.6 : 34.2.
‡ Common lead correction, K-feldspar lead (90-2).

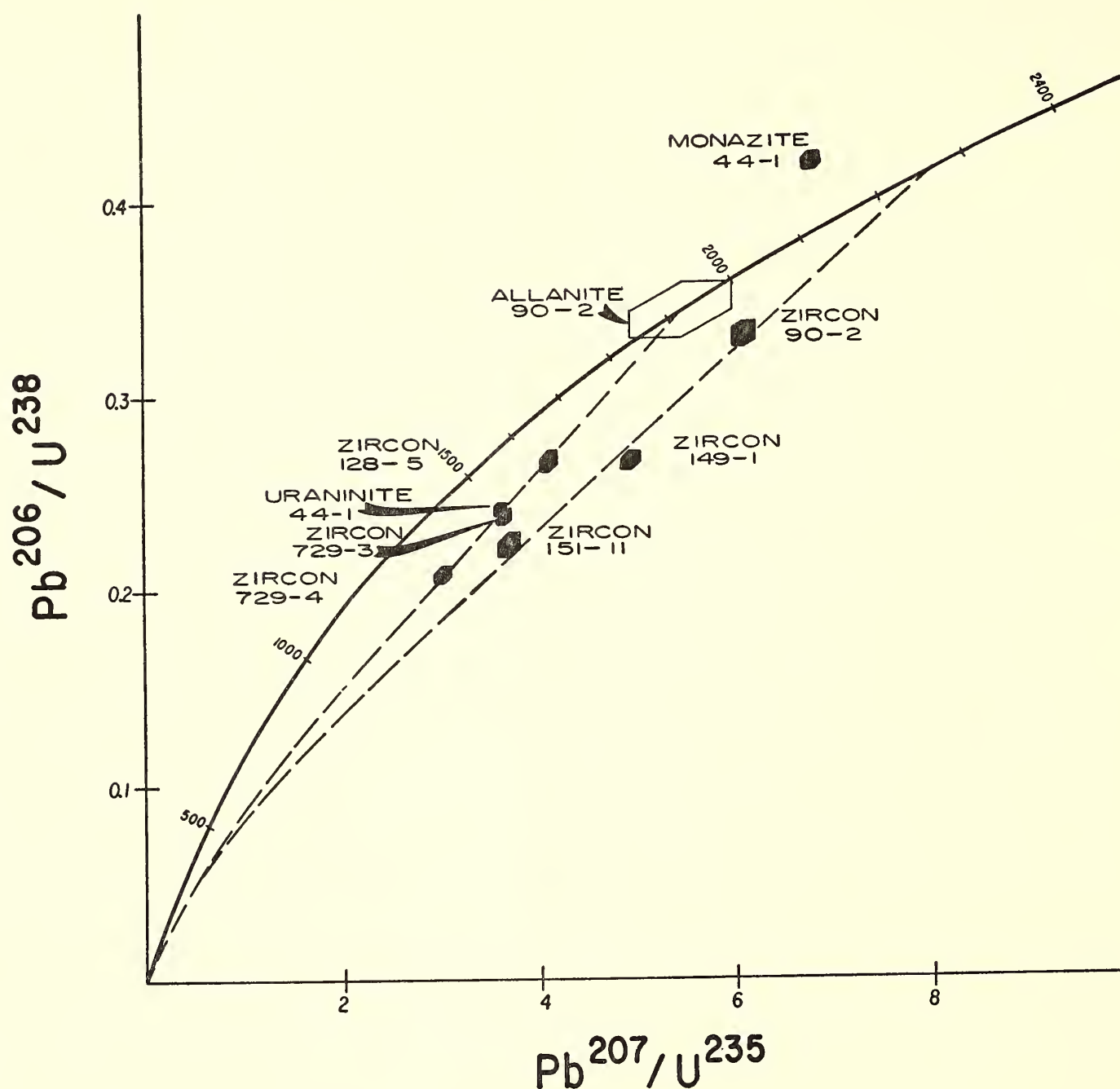


Fig. 5. Parent-daughter ratios for uranium-bearing minerals from the Andrew Lake area, north-eastern Alberta, compared with two curves calculated for loss of lead by continuous diffusion for 1920 and 2270 m.y.

units. The value of 1810 m.y. may be regarded as the time of the latest metamorphic event in the area.

The minerals listed in table 4 were separated and the U-Pb ages determined. Very little zircon was recovered from samples of the low-grade metasediments. Despite discordance, the Pb^{207} - Pb^{206} ages definitely indicate primary crystalline material older than 1800 m.y. in the area. The U-Pb data are plotted on a concordia diagram in figure 5, although the minerals are from a variety of stratigraphic positions and rock types. Since the 1810-m.y. mica dates apparently rule out an episodic

lead-loss discordance, curves are calculated and plotted for loss of lead by continuous diffusion (Tilton, 1960)⁶ for 2270 and 1920 m.y. Although not permitted by the Pb-diffusion-loss model, the 1920-m.y. curve has been extrapolated above the concordia since the uraninite and monazite are apparently cogenetic. The 1920- and 2270-m.y. diffusion ages probably delineate two events involving magmatic crystallization, provide clues to the source of the metasediments, but do

⁶ G. R. Tilton, Volume diffusion as a mechanism for discordant lead ages, *J. Geophys. Res.*, 65, 2933-2945, 1960.

TABLE 5. Mineral Ages from the Andrew Lake Area, Northeast Alberta Precambrian Shield

Sample No.	Rock and Mineral (Petrographic term)		Ages, millions of years		
			Rb-Sr	Pb Model Ages (Russell-Stanton-Farquhar)	
				208/204	207/206
151-11	Granite boss (quartz monzonite)	K feldspar	1800 ± 300		
729-4	Older granite (quartz monzonite)	K feldspar	1850 ± 150		
90-2	Porphyroblastic granite gneiss (composite) (quartz monzonite gneiss)	K feldspar	2220 ± 100	1570	2160
149-1	Granite-gneiss, basement complex (quartz monzonite gneiss)	K feldspar	2060 ± 150	-120	2020
1-3	"Younger" metasediments, mineralized (orthoquartzite)	Galena		3600	1890

not aid in specifying the time of sedimentation.

Table 5 gives Rb-Sr ages for four feldspars and model lead ages for two of the four feldspars plus a galena. These data also indicate that the geologically older rocks are more than 1800 m.y. old. In addition, four K-Ar hornblende ages for these rocks were from 1850 to 1930 m.y. The hornblendes appear to have been affected to a lesser degree than the biotites by the last metamorphic event (Hart, 1961).⁷ If an older Rb-Sr age for the feldspars has not been affected by later metamorphism, the model lead ages should be comparable. The data for 149-1 and 90-2 feldspar seem to indicate partial alteration, to judge from the 2270-m.y. zircon diffusion age. The galena is evidently a product of the later 1920-m.y. event.

Whole-rock rubidium-strontium ages for six samples of granite gneiss from the basement complex have recently been determined at the University of Alberta; figure 6 presents the data in an isochron plot. The somewhat surprising division of the samples between two isochrons indicates that the basement complex is directly or indirectly involved in both the events given by the U-Pb data. The dual division is not easily explained, despite

⁷ S. R. Hart, The use of hornblendes and pyroxenes for K-Ar dating, *J. Geophys. Res.*, 66, 2995-3001, 1961.

abundant field evidence of gneissic xenoliths in a gneissic matrix. For example, in sample 149-1, apatite has $Sr^{87}/Sr^{86} = 0.711$; feldspar gives 1850 m.y.; zircon, 2270 m.y.; and biotite, 1790 m.y. The apatite should have picked up some extra radiogenic Sr^{87} in the later metamorphic events, but it is possible that the apatite used (>200 mesh) represents unaltered detrital apatite rather than mixed apatite.

- Some preliminary conclusions are:
1. Two primary magmatic events occurred about 2000 and 2300 m.y. ago in the Andrew Lake area.
 2. Both these source materials appear in the gneissic or metasedimentary phases of the basement complex and are thus older than the massive-leucocratic granites.
 3. The massive-leucocratic and -biotite granites, young according to field relations, are very close in age to the "younger" portions of the gneissic basement complex.
 4. The latest metamorphic event (1810 m.y.), as given by the K-Ar mica dates, likely accounts for much of the obscuring of the field relations between the two earlier events.

K-Ar Ages of Hornblendes from the Southern Gothard Massif, Switzerland

The Gothard massif in central Switzerland is one of the few places in the Swiss Alps where the autochthonous basement

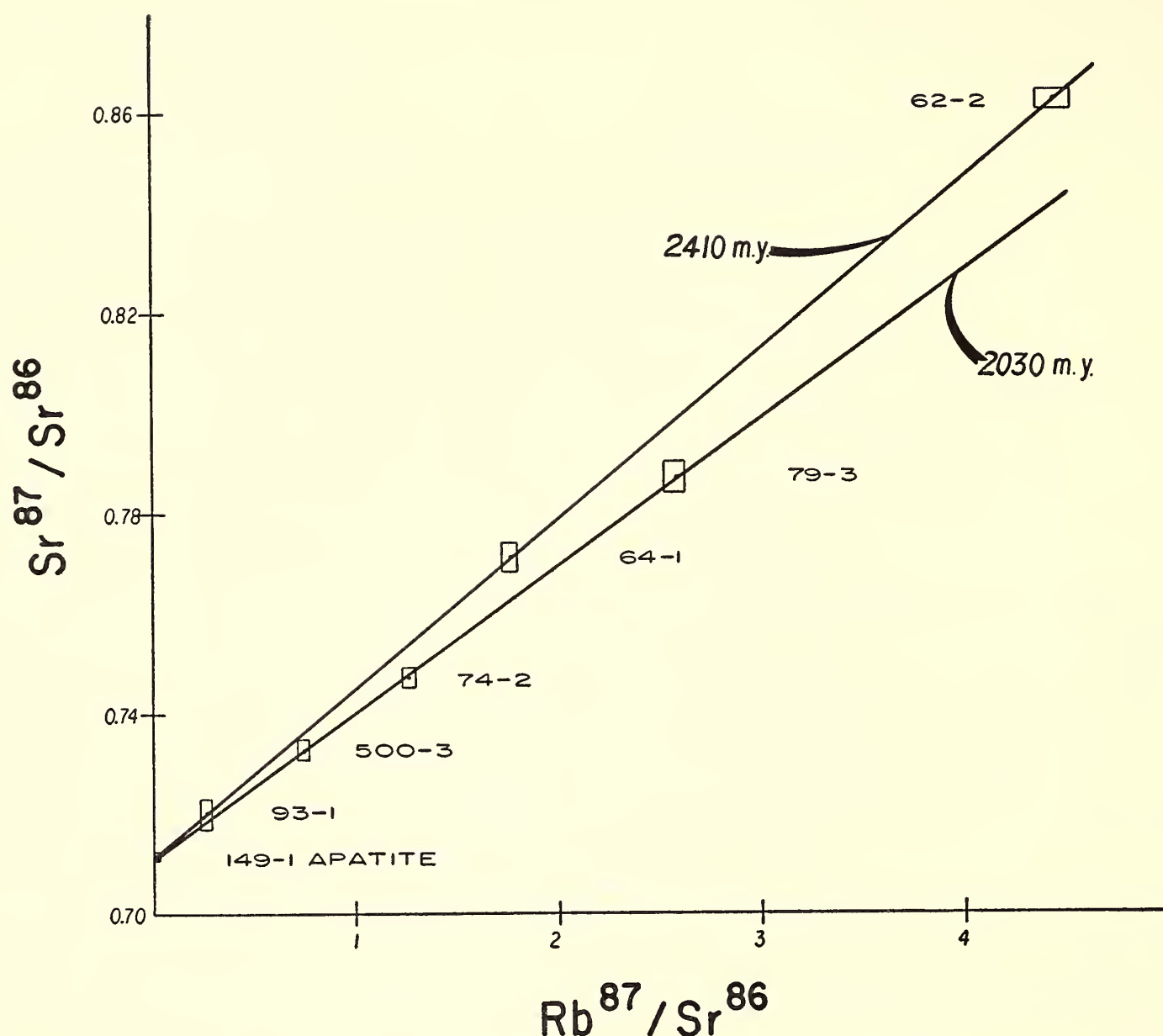


Fig. 6. Plot of Sr^{87}/Sr^{86} ratios versus Rb^{87}/Sr^{86} ratios for six whole-rock samples and one apatite from the basement gneiss complex of the Andrew Lake area in northeastern Alberta.

of the Alpine orogenic belt crops out. It extends with a west southwest-east northeast trend over a length of about 80 km, its width in the center exceeding 10 km. Its southern border is marked by the front of the Penninic nappes. On the northern side it is separated from the Aar massif by a narrow zone of Mesozoic sediments (root zone of the Helvetic nappes). The Gothard massif is in itself a complex body of extensive polymetamorphic zones of both sedimentary and plutonic origin. Zircon ages (Gruenfelder, 1962,⁸ and written communication) in combination with petrographic evi-

dence suggest Precambrian sedimentation (e.g., Gurschengneiss) and late Precambrian intrusion (Streifengneiss) of a main part of the primary rock. Several granitic stocks intruded these older rocks, their zircons showing Hercynian age values and in one of them (Rotondo granite) probably an Alpine age.

It has been known for a long time that the southern margin of the Gothard massif was strongly metamorphosed during the Alpine orogeny, but only during recent years has the influence of Alpine metamorphism been found to be more extensive in the interior of the massif. Fabric data from field observations gave strong evidence that Alpine fabric elements of the Penninic nappes, especially

⁸ M. Gruenfelder, Mineralalter kristalliner Gesteine in Gotthardmassiv, *Schweiz. Mineral. Petrog. Mitt.*, 42, 6-7, 1962.

a consistently north-south oriented lineation (preferred orientation of micas and hornblendes) and an east-west buckling, can be observed right into the center of the Gothard massif and that older structures were obliterated along the southern border. Rb-Sr dating of oriented biotites (E. Jaeger, 1962)⁹ confirmed the Alpine age (15 to 17 m.y.) of a main fabric element by absolute measurements. The southern margin of the central Gothard massif is formed of a belt of rock units, all of which are dominantly of sedimentary origin and were probably deposited in Precambrian times as clays, clayey-limy sandstones, and dolomitic marls. In particular, the southernmost of these zones (Tremola series) still shows sedimentary structures. By Prealpine and mainly by the Alpine orogeny these sediments were altered to mica gneisses and schists, hornblende schists and gneisses, quartzites, siliceous calcschists, and amphibolites.

Petrographic observations (Steiger, 1962)¹⁰ of these rocks show that as many as six different generations of minerals can be established in the rock texture of the southern Gothard massif. All were formed during different phases of orogeny. A fine-grained cataclastic mosaic of quartz and feldspar (first generation) is considered to be a relict of a Prealpine phase. A second generation of minerals (first Alpine generation) consists of north-south

oriented micas, finely nematoblastic hornblendes, and also elongated quartz crystals. This generation was formed during a period of tectonic movement responsible for the north-south lineation. Postkinematic growth of large porphyroblasts (third generation) of garnet as well as hornblende which cuts the foliation occurred in a later phase under the influence of a heat front arising from the northern Penninic nappes. Both minerals contain oriented inclusions of minerals of the second generation. Later on, during clearly defined consecutive phases, biotite was formed cutting the foliation, then alteration products like chlorite, biotite, and sericite were formed. Finally, veins and cracks were filled with quartz and carbonates. A new approach to determining the metamorphic history of the southern Gothard massif is being attempted based on age determinations. It is hoped that some information about the timing of metamorphic events and especially of the phases of Alpine orogeny will be obtained.

Hornblendes, biotites, and zircons have been separated from the rocks of the Tremola series and adjacent zones to the north (Guspis and Corandoni zones). To date, the K-Ar ages of four hornblendes have been determined. The potassium content of the hornblendes is 0.27 to 0.47 weight per cent. The argon extracted was 27 to 42 per cent radiogenic. The ages are given in table 6.

All hornblendes are of Alpine age, confirming the result of fabric analysis. However, the ages are definitely older than the Rb-Sr ages of biotites of near-by rocks reported by E. Jaeger (1962). As

⁹ E. Jaeger, Age determinations from rocks of the Alps, *J. Geophys. Res.*, 67, 5293-5306, 1962.
¹⁰ R. H. Steiger, Petrographie und Geologie des suedlichen Gotthardmassivs zwischen St. Gotthard- und Lukmanierpass, *Schweiz Mineral. Petrog. Mitt.*, 42, 381-577, 1962.

TABLE 6. K-Ar Ages of Hornblendes from the Southern Gothard Massif

Hornblende Sample No.	Spatial Array of Hornblende Crystals in Rock	Mineral Generation (from petrographic observations)	Zone	Ages, millions of years
486	Oriented	2	Guspis zone	47
382	Oriented	2	Corandoni zone	44
352	Oriented	2	Tremola series	46
r 175	Random	3	Tremola series	27

TABLE 7. K-Ar Ages on Low-Potassium Minerals from Maryland

No.	Rock Unit	Rock Type	Mineral	K, %	K-Ar Ages, millions of years
B65	Baltimore gneiss	Amphibolite	Hornblende	1.26	367
			Diopside	0.0781	328
			Plagioclase	0.951	309
B68	Baltimore gneiss	Amphibolite	Hornblende	0.512	301
B69	Baltimore gneiss	Amphibolite	Hornblende	0.483	292
B60	Baltimore gabbro	Gabbro, amphibolitized	Hornblende	0.208	372
B66	Baltimore gabbro	Gabbro, fresh	Pyroxene	0.0461	702
			Plagioclase	0.0345	580

shown in *Year Book 60*, K-Ar ages of hornblendes are usually less affected by subsequent events than Rb-Sr ages of biotites. The grouping of three hornblende age values at 44 to 47 m.y. suggests that the ages have not been influenced appreciably by inherited radiogenic argon. The 44- to 47-m.y. ages occur in hornblendes from different zones and from rocks differing greatly in origin, primary age, and temperature history. The younger age of 25 m.y. obtained on a hornblende which cuts the foliation (third generation) is in agreement with petrographic observation previously mentioned. However, more data will be required to reach a definite conclusion about the ages of different generations of hornblendes within the Tremola series.

*Ages of Low-Potassium Minerals from
the Maryland Piedmont*

Work has continued on the evaluation of low-potassium minerals for K-Ar dating, especially with reference to their ability to retain argon during metamorphism and the apparent tendency for some of them (pyroxenes) to contain excess radiogenic argon. A number of samples from mafic rocks in the Maryland Piedmont were selected for study because of the extensive work already done in this area. Table 7 shows the results of K-Ar determinations on this sample suite, which contains hornblendes as well as several pairs of coexisting pyroxene and plagioclase.

The minerals from the Baltimore gneiss show K-Ar ages between 290 and 370 m.y. Since the gneiss is known to be at least 1 billion years old, the low ages may be attributed to loss of argon during Appalachian metamorphism. The 300-m.y. age has also been found repeatedly by biotite K-Ar and Rb-Sr dating of Piedmont rocks; it apparently represents the time of last heating in the area. Some retention of argon is indicated by the B65 hornblende. It is interesting to note that the B65 pyroxene, with its rather low potassium content, shows no sign of excess argon. The B65 plagioclase age is in good agreement with the inferred time of last heating.

The Baltimore gabbro is of unknown age but is a critical unit geologically, being the oldest rock known to cut the Glenarm series. The Glenarm series is a dominant metasedimentary unit in the Piedmont whose age is known only to be between 550 m.y. and 1100 m.y. Sample B60, which has a metamorphic fabric, shows the effects of Appalachian metamorphism, the hornblende giving an age of 372 m.y. Sample B66, which has fresh igneous texture with little sign of later metamorphism, shows definitely pre-Appalachian ages on both pyroxene and plagioclase. In view of the very low potassium contents, however, it is difficult to rule out the existence of excess argon in either mineral. Until further work is completed, a pre-700 m.y. age for the Glenarm will remain an exciting possibility.

Effect of Contact Metamorphism on Zircon Ages

Although zircons have become one of the most important and useful of all minerals for age determination, there is as yet no real understanding of the conditions that produce discordant zircon U-Pb ages. For example, it has been clearly shown that some zircons are resistant to very severe regional metamorphism (Tilton, Wetherill, Davis, and Hopson, 1958),¹¹ whereas others may show episodic lead loss during much lower-grade metamorphism (Silver and Deutsch, 1961).¹² In addition, many discordant zircon ages have been shown to arise from continuous diffusion of lead under essentially ambient conditions (Tilton, 1960).¹³

A study of one of these possible mech-

¹¹ G. R. Tilton, G. W. Wetherill, G. L. Davis, and C. A. Hopson, Ages of minerals from the Baltimore gneiss near Baltimore, Maryland, *Bull. Geol. Soc. Am.*, 69, 1469-1474, 1958.

¹² L. T. Silver, and S. Deutsch, Uranium lead method on zircons, *Proc. N. Y. Acad. Sci.*, 91, 279-283, 1961.

¹³ G. R. Tilton, Volume diffusion as a mechanism for discordant lead ages, *J. Geophys. Res.*, 65, 2933-2945, 1960.

anisms has been started by determining the effect of contact metamorphism on zircon ages. The contact metamorphic zone adjacent to the Tertiary stock at Eldora, Colorado, was chosen because of the extensive work done on other mineral ages in the same zone (*Year Book 61*, p. 238). Since the country rocks are dominantly Precambrian metasediments, some variability might be expected in the zircon populations. The effect will be minor, however, in view of the large spread in age between the country rock and intrusive (1500 m.y.).

Preliminary samples have been analyzed at distances of 2, 12, 37, 50, and 14,000 feet. The variation of lead and uranium concentrations is shown in figure 7. The lead content drops very sharply near the contact, demonstrating the presence of episodic loss in these zircons. The uranium and thorium, however, increase as the contact is approached, thus magnifying the decrease in the U-Pb ages. The same effect was noted from Pb-alpha studies of zircon in a contact zone by Gastil and Delisle, 1962.¹⁴

¹⁴ R. G. Gastil, and M. Delisle, Variations in the lead-alpha ratio of zircon under varying grades of contact metamorphism (abstract), *Program, Geol. Soc. Am. Annual Meeting*, 1962.

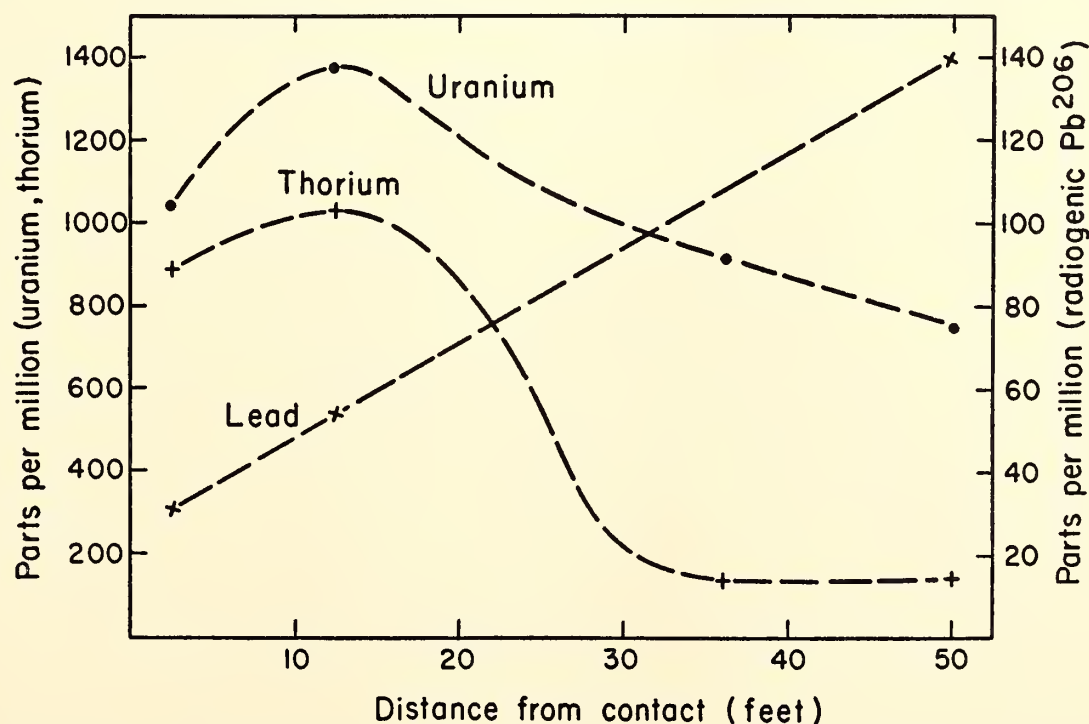


Fig. 7. Change in concentration of uranium, thorium, and lead with distance from the Eldora stock.

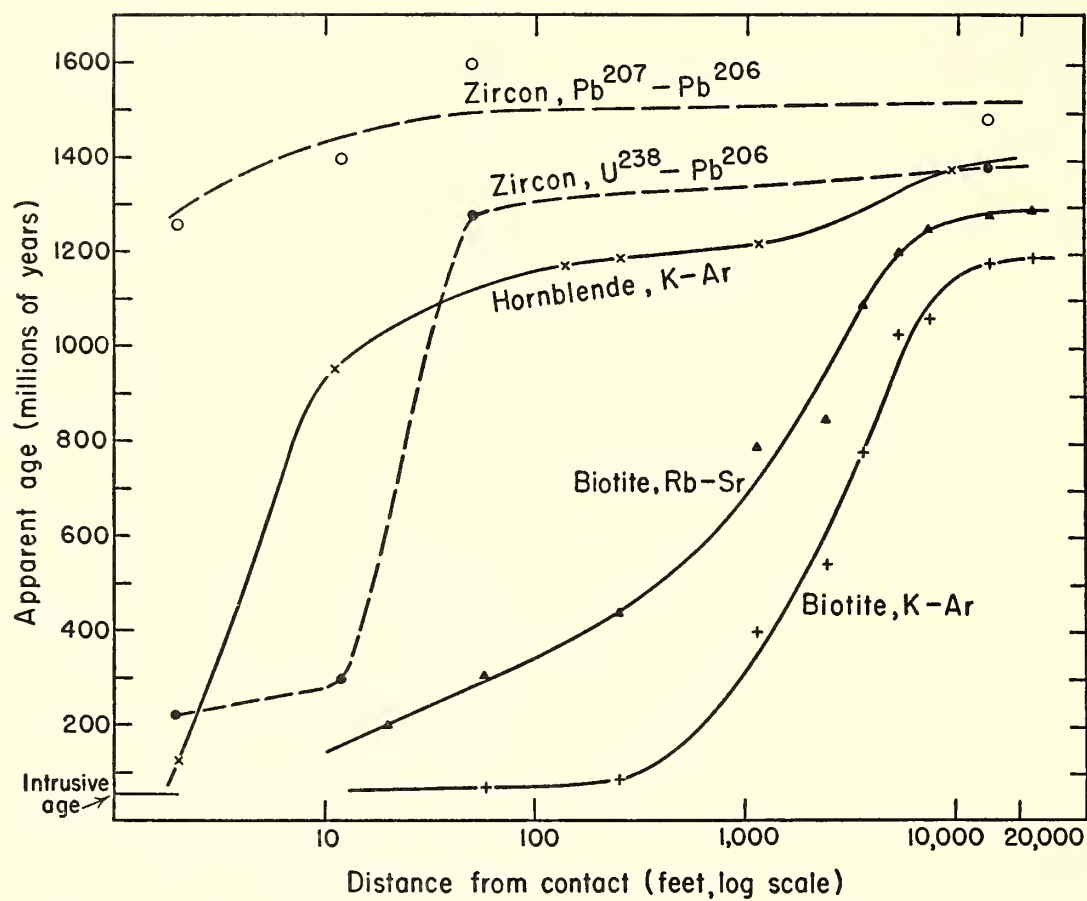


Fig. 8. Variation of measured age with distance from an intrusive contact at Eldora, Colorado, for zircon, biotite, and hornblende.

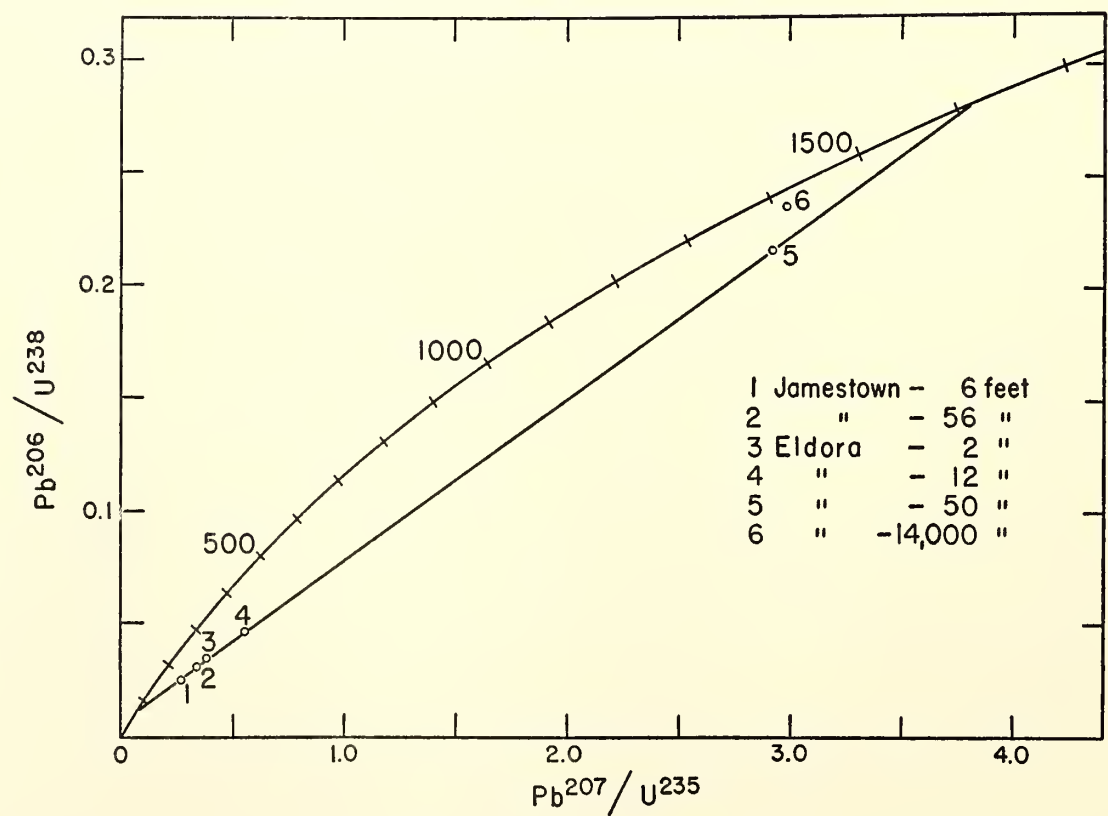


Fig. 9. Concordia diagram showing uranium-lead ratios for zircons in the vicinity of the Eldora and Jamestown, Colorado, stocks. The chord illustrates the pattern expected for samples 1610 m.y. old that lost varying proportions of lead episodically 75 m.y. ago.

It is interesting to note also that the common lead in potassium feldspars becomes increasingly radiogenic near the contact (*Year Book 60*, p. 191), perhaps representing in part a “sink” for the zircon lead.

Variations in the U-Pb ages are shown in figure 8, along with previously determined curves for hornblende K-Ar ages and biotite K-Ar and Rb-Sr ages for comparison. The sharpness of the zircon age effect is striking. Whereas calculations from heat conduction theory and diffusion theory suggest activation energies of 20 to 30 kcal/mole for argon and strontium in biotite, similar calculations for lead in zircon suggest activation energies of over 100 kcal/mole. As these calculations have the greatest uncertainty very near the contact, owing to possible convective cooling, this difference in activation energies must be considered tentative at present.

The zircon data are shown on a concordia plot in figure 9. Also included are two zircons from a similar contact zone near a Tertiary stock at Jamestown, Colorado. Since the 14,000-foot Eldora sample is from a Precambrian granite which cuts the metasediments, it should not be expected to be colinear with the other points. The chord defined by the other samples indicates an age of about 1600 m.y. for the zircons in the metasediments and an age of about 70 m.y. for the

metamorphic episode. The 70-m.y. age agrees well with the 55-m.y. age for the intrusive as determined by biotite K-Ar.

If the regular relationships between lead and uranium content, age, and distance from the contact are maintained during further work, there is real hope of understanding at least this one facet of what makes zircons tick.

Oceanic Serpentinites

A recent model for the evolution of ocean basins (Hess, 1962)¹⁵ proposes an important role for oceanic serpentinites. The model considers serpentinites to form on the rising limbs of convection cells by hydration of mantle peridotite. They are then swept away from the mid-oceanic ridges by lateral convection components with a time scale of the order of a few times 10⁸ years. With this model in mind, a study of the origin and age of oceanic serpentinites has been started using strontium isotopes as natural tracers.

The results of strontium and rubidium concentration and strontium isotope analyses of three oceanic serpentinites are given in table 8. The St. Pauls Island sample, from the mid-Atlantic ridge, is a partially serpentinitized peridotite. The Puerto Rico trench samples are completely serpentinitized peridotites dredged

¹⁵ H. H. Hess, History of ocean basins, in *Petrologic Studies*, a volume to honor A. F. Buddington, pp. 599–620, 1962.

TABLE 8. Data for Potassium, Rubidium, and Strontium in Oceanic Serpentinites

Location	Rock Type	Parts per Million			Sr ⁸⁷ /Sr ⁸⁶
		K	Rb	Sr	
St. Pauls Island	Serpentinized peridotite	500	0.90	35	0.7071,* 0.7053,* 0.7054†
Puerto Rico trench (D2-1)	Serpentinite	62	0.09	1.3	0.7078,* 0.7094*
Puerto Rico trench (D10-6)	Serpentinite	125	0.27	2.8	0.7070,* 0.7088*
Mid-Atlantic ridge	Basalt	1400	0.98	102	0.7026‡
Average oceanic region	Basalt				0.7027§
Sea water					0.7096‡

* Different aliquots, same sample dissolution.
† Separate sample dissolutions.
‡ P. W. Gast, Limitations on the composition of the upper mantle, *J. Geophys. Res.*, 65, 1287–1297, 1960.
§ C. F. Hedge and F. G. Walthall, Radiogenic Sr⁸⁷ as an index of geologic processes, in press, 1963.

from the north wall of the trench in 7 km of water (Bowin and Nalwalk, 1963).¹⁶ Basalt from the mid-Atlantic ridge is included in the table for comparison. The first point to be made is that the serpentine $\text{Sr}^{87}/\text{Sr}^{86}$ ratios are different from each other and appear to be significantly higher than oceanic basalts. This suggests either a different source region or a different age for the two rock types. Considering the data for the trench serpentinites at face value, the strontium isotopic ratios would converge with those for basalt sources some 1 to 2 billion years ago. In view of the low strontium concentrations in these samples, the possibility of contamination by sea-water strontium must be assessed.

The St. Pauls Island sample is less likely to involve contamination, and here an even greater time period is required for the isotope ratios to converge with those of basalt sources. Although a real test of the model must await further work, the data thus far do not provide any positive support to the model.

SEISMIC STUDIES

J. S. Steinhart, T. J. Smith, I. S. Sacks,¹⁷ R. Sumner,¹⁸ Z. Suzuki,¹⁹ A. Rodríguez,²⁰ C. Lomnitz,²¹ M. A. Tuve, and L. T. Aldrich

Explosion Seismology

Our dissatisfaction with the traditional methods and results of explosion studies of crustal structure (*Year Books 60 and 61*) has led us in several directions in the past year. Substantial amounts of time

and effort have gone into the development and construction of new frequency-modulation tape-recording systems, amplifiers, and procedures. The equipment will be first employed in the summer of 1963 in the joint United States-Canadian seismic experiment in Lake Superior. Magnetic tape recording should permit detailed analysis that was not feasible from photographic records.

Year Book 61 gave some results of analysis of apparent velocity variation with distance. They were scattered and not very satisfying even though statistically significant. It was then shown from information theory that, given the parameters of the observations, the scatter was to be expected. Further analysis suggested that increasing the length of the observing spread to about 8 km would provide the accuracy to considerably enhance the apparent velocity results. An opportunity to test these predictions came in a cooperative experiment organized by the University of Wisconsin under the leadership of Professor R. P. Meyer. The experimental technique was the fixed station-moving shot point method previously described (*Year Book 61*) and used in the Maine experiment.

A special double observing station was assembled, giving a linear array 8 km long with 14 vertical seismometers.

Results of the North Carolina work are displayed in figures 10 and 11. Figure 10 is the typical reduced travel-time plot. Because our station was 80 km from the shore, no data at short ranges were obtained. Assuming that nothing unusual occurred at shorter ranges, the old interpretation methods would suggest a crustal velocity of about 6 km/sec, a mantle velocity of about 8.5 km/sec, and a crustal thickness of about 32 km. Using 8 km/sec for the upper mantle would reduce this to 29 km. Figure 11 shows that this picture is far too simple. If the crust were indeed constant velocity, the apparent velocities would have to remain constant out to a range of 155 km or so. This is clearly not possible. In the region

¹⁶ C. Bowin, and A. Nalwalk, Serpentinized peridotite dredged from the north wall, Puerto Rico trench (abstract), *Program, Am. Geophys. Union Annual Meeting*, 1963.

¹⁷ Carnegie Institution Fellow; from Bernard Price Institute, Johannesburg, South Africa.

¹⁸ Carnegie Institution Fellow; from University of Wisconsin.

¹⁹ Carnegie Institution Fellow; from Tohoku University, Sendai, Japan.

²⁰ University of San Agustín, Arequipa, Peru.

²¹ Carnegie Staff Associate; University of Chile, Santiago.

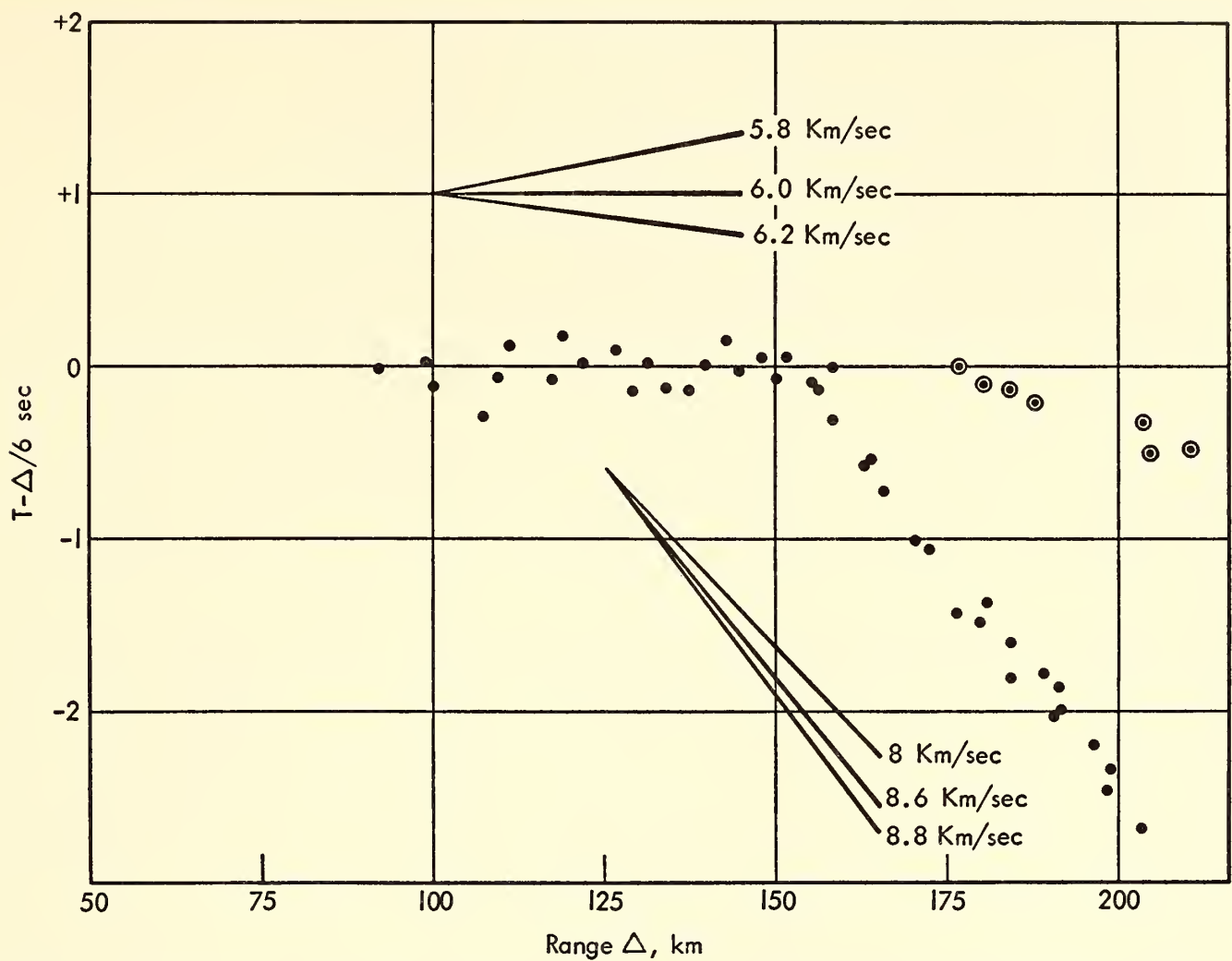


Fig. 10. Reduced travel times, North Carolina, 1962. Closed circles indicate first arrivals; circles around dots indicate very large-amplitude secondary arrivals.

95 to 155 km the apparent velocity increases continuously from about 6 to about 7.4 km/sec. The only reasonable conclusion is that the velocity increases continuously from a depth of about 20 km to the base of the crust near 36 km. The increased crustal thickness, although interesting, is not the important result. These results with a continuous change in velocity with depth suggest that the material in the lower part of the crust is a continuously changing mixture of rocks, becoming more and more basic in composition with depth. A picture of layers with sharp discontinuous changes is simply not consonant with figure 11.

Another feature of figure 11 merits special attention. Near the “crossover” distance at about 155 km two wave trains are interfering with each other. Such interference phenomena may sometimes be observed on records taken at these ranges. Under these circumstances one

would expect that the apparent velocities observed would assume wild and usually meaningless values. A glance at figure 11 shows that this is precisely what happens. It may be that this feature of an apparent velocity versus distance graph offers a very sensitive way of identifying crossover zones. If so, the wild value near 195 km would seem to indicate another such interference zone, where no crossover is seen on the travel-time curve. The data cannot be regarded as conclusive on this point. It is possible, however, to have such a crossover due to rather minor fluctuations in the velocity depth function (Green and Steinhart, 1962).²²

It is encouraging to note that the predictions about apparent velocity measurement mentioned earlier seem to have

²² R. Green, and J. S. Steinhart, On crustal structure deduced from seismic time-distance curves, *New Zealand J. Geol. Geophys.*, 5, 579-591, 1962.

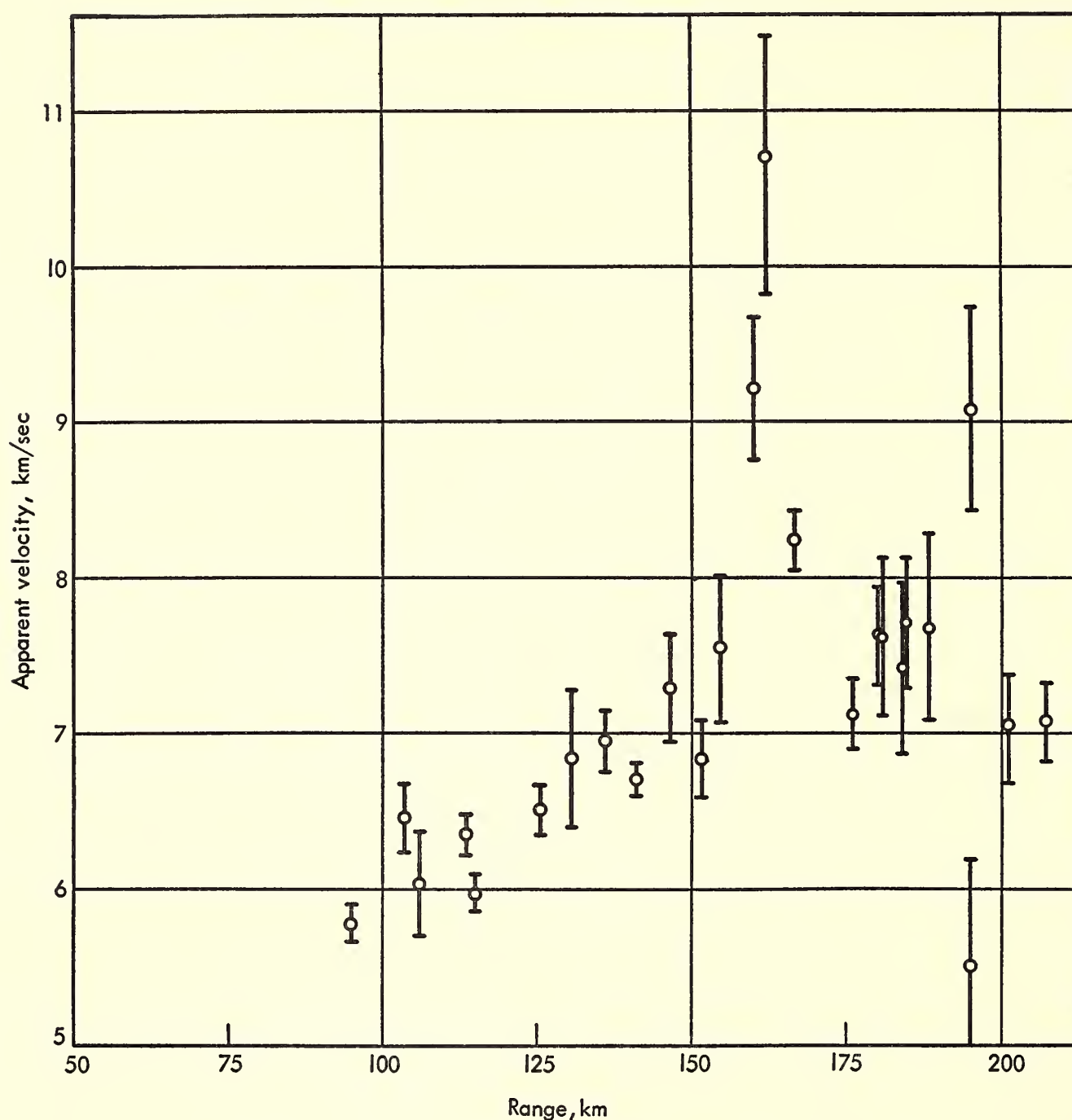


Fig. 11. Apparent velocity versus range, North Carolina, 1962; 95 per cent confidence limits are shown.

been borne out by the North Carolina experiment. A far more extensive test of the technique will be made in the summer of 1963 at the international Lake Superior experiment.

Earthquake Seismology

Pseudo dispersion in body waves. The onset of motion in a seismogram from the common station seismograph (1-second pendulum, 0.75- to 0.25-second galvanometer) often shows a small emergent one-fourth cycle just before the large energy arrival when the signal-to-noise ratio is very high. Observation of broad-

band records has shown that this effect is due to the fact that higher-frequency energy, which may lie in the center of the pass band of the seismograph, arrives later than the lower-frequency energy which is attenuated by the seismograph and, therefore, appears with small amplitude.

A number of South American earthquakes were recorded at Characato, San Gregorio, and Puno in Peru, and Antofagasta in Chile. The recording equipment consisted of an 0.8-second vertical seismometer, transistor amplifier, and frequency-modulation tape recording using a

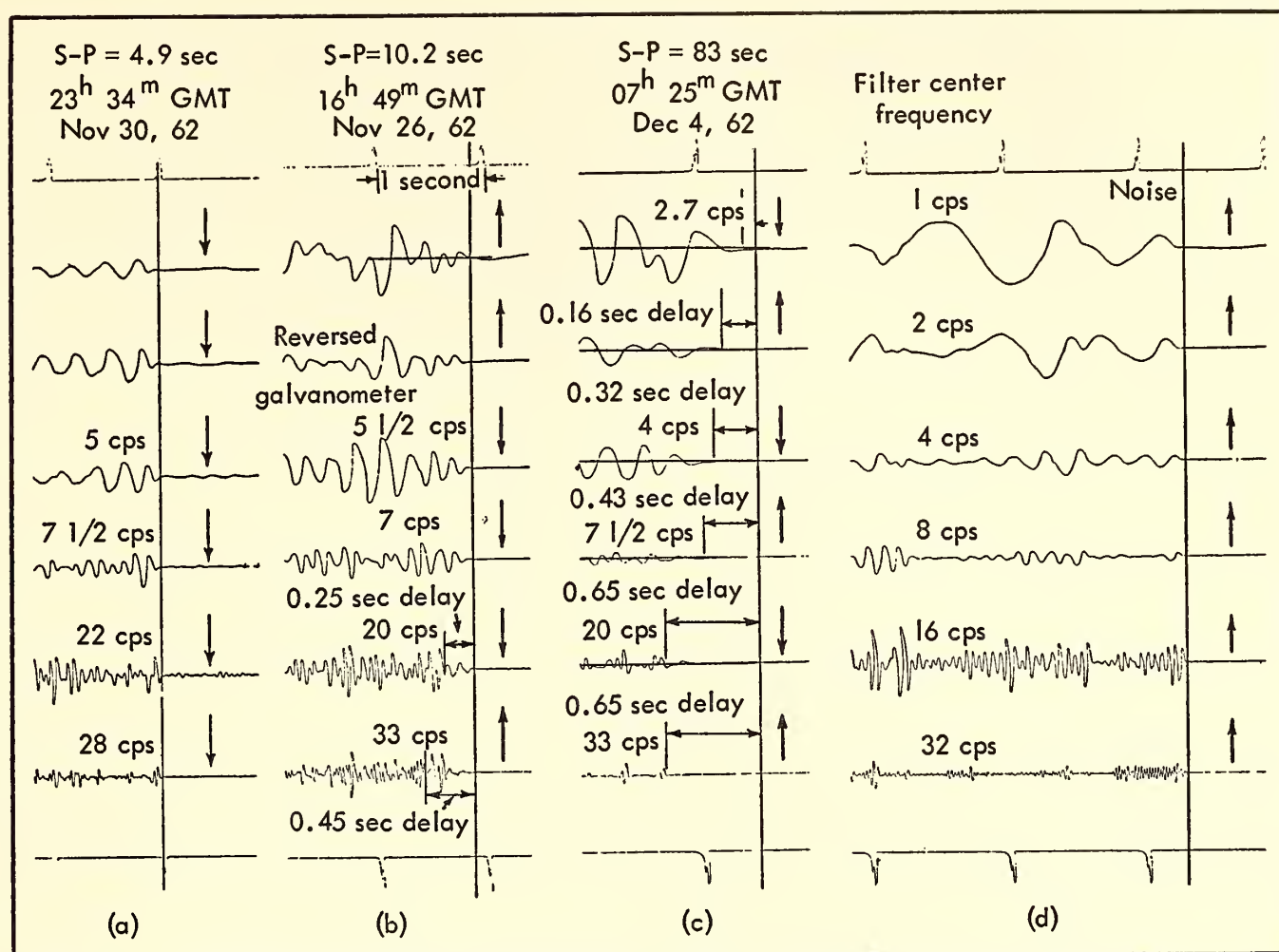


Fig. 12. Filtered seismograms from Characato, Peru. The arrows show the relative directions of first motion.

center frequency of 2 kc/s and tape speed of 15/16 in./sec. The demodulated output was replayed through a set of filters with center frequencies 1, 2, 4, 8, 16, and 32 cps. The Q of the upper four frequencies was 3.5, and that of the lower two filters was 2. The Q of the VELA short-period seismograph is about 1.5.

Figure 12 shows some records obtained at Characato for earthquakes at various distances. Figure 12a shows the relative arrival times of the various frequencies for an earthquake with an $S-P$ time of 4.9 seconds. It will be seen that the 28-cps energy is less than 0.1 second later than the lower frequencies, which all arrive at about the same time. Figure 12b shows the arrival of an earthquake more than twice as distant as 12a, having an $S-P$ time of 10.2 seconds. At this range, not only is the energy at 33 cps later by 0.45 second, but the lower frequencies are somewhat delayed as well. Figure 12c, a record of an earthquake with an $S-P$ time of 83

seconds, shows that all frequencies are delayed relative to the lowest frequency, the higher frequencies being delayed more than the lower. The delays for the same earthquake recorded at Characato and San Gregorio with similar $S-P$ times are at least twice as great at Characato as at San Gregorio. Characato is 7872 feet above sea level on the flanks of the Andes. The San Gregorio station is near the coast in a rather less disturbed geological region. Figure 13 shows some of the results obtained.

It is occasionally apparent that some small higher-frequency energy arrives on time, even though the main energy at that frequency is somewhat delayed. Signal-to-noise ratios of the order of 100:1 are required to observe this. Figure 14 shows one example.

Figure 15 shows arrivals from a more distant earthquake on the VELA uniform short-period and long-period seismographs of the Georgetown seismograph station

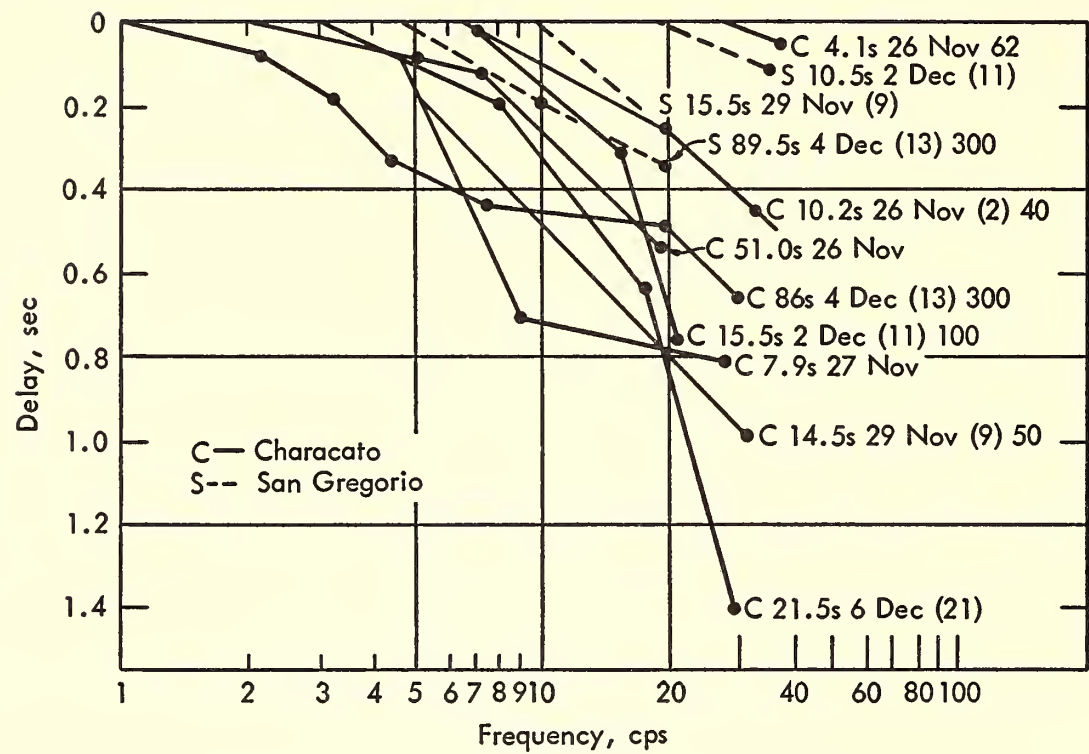


Fig. 13. Relative arrival times for various small earthquakes recorded in Characato and San Gregorio, Peru. The first letter in the curve identification is the station; the first number indicates the *S-P* time in seconds; following are the date; bracketed earthquake identification number; and, where determined, the depth in kilometers.

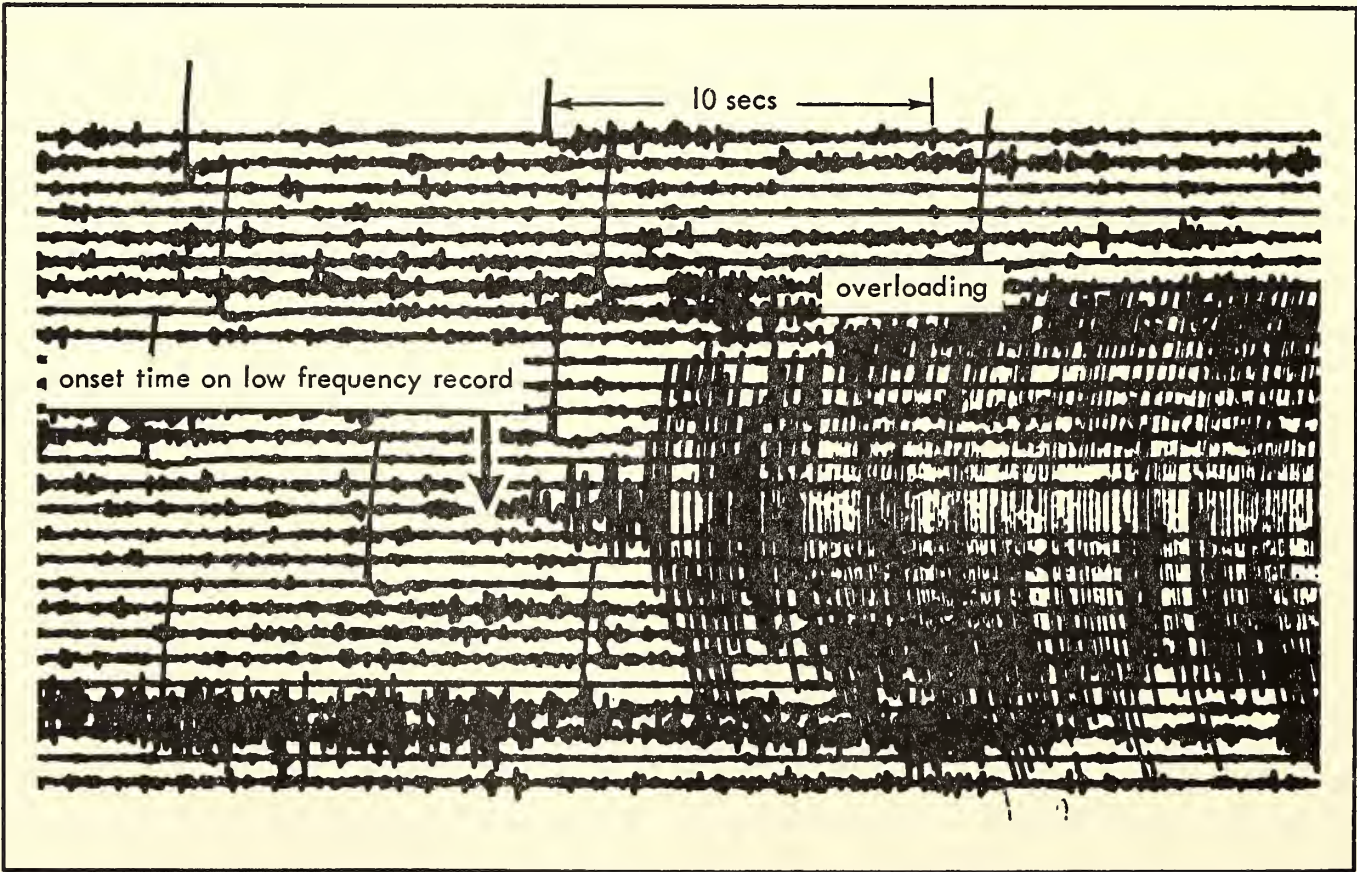


Fig. 14. *P* arrival with an *S-P* time of 128 seconds. The filter center frequency is 8 cps, and the filter *Q* is 2. The start is emergent from the noise even though the arrival overloads the amplifier after a few seconds.

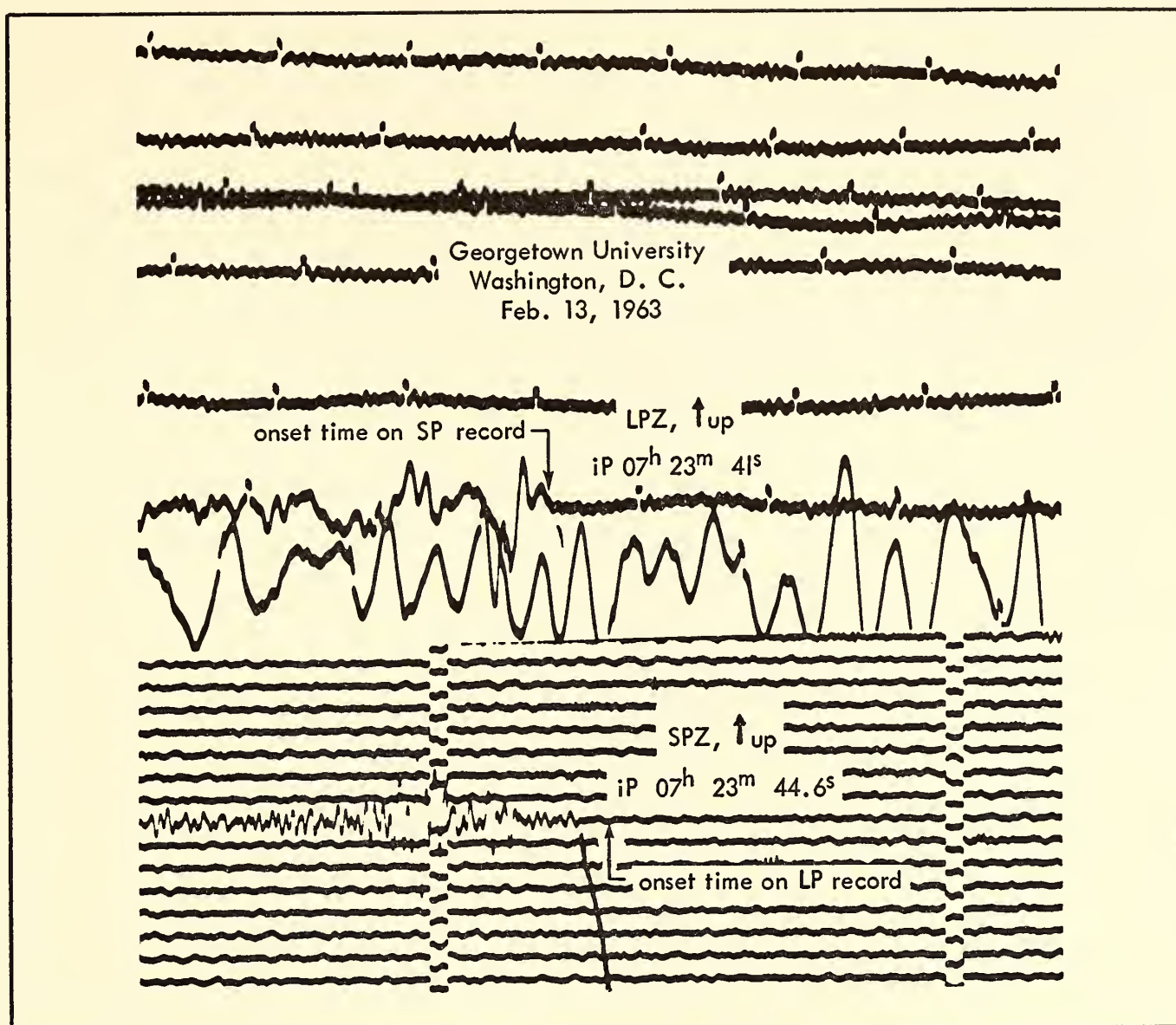


Fig. 15. Late arrival of high-frequency energy over a long path (circa 75°).

in Washington, D. C. The marker on each record indicates the time of arrival on the other record. The path length for this event is about 75° , and the time delay of the 1-cps frequency relative to the $1/7$ -cps frequency is 3.5 seconds. The characteristics of this effect suggest that it is due to inhomogeneities. The magnitude of the time delay is affected by the region through which the seismic waves have propagated and is therefore a function of the station and the direction of approach. Some of the following mechanisms may be involved: (a) scattering in a field with relatively few scatterers; (b) dispersion and path differences due to gradients in some elastic constants; and (c) distortion in a medium with viscous loss in which the phase shift at any

frequency is not proportional to frequency.

It can be seen from figure 12b that, even when delays are quite small, the direction of first motion (marked with arrows) may be determined incorrectly. Short-period seismographs with a sharp low-frequency cut, e.g., a cut proportional to f^{-3} as commonly used, may give directions of first motion different from those recorded by long-period instruments. Also the direction may be affected by the signal-to-noise ratio—a matter of importance in fault plane and earthquake mechanism studies that depend on first-motion determinations.

Further experiments are under way to increase the quantitative understanding of this phenomenon.

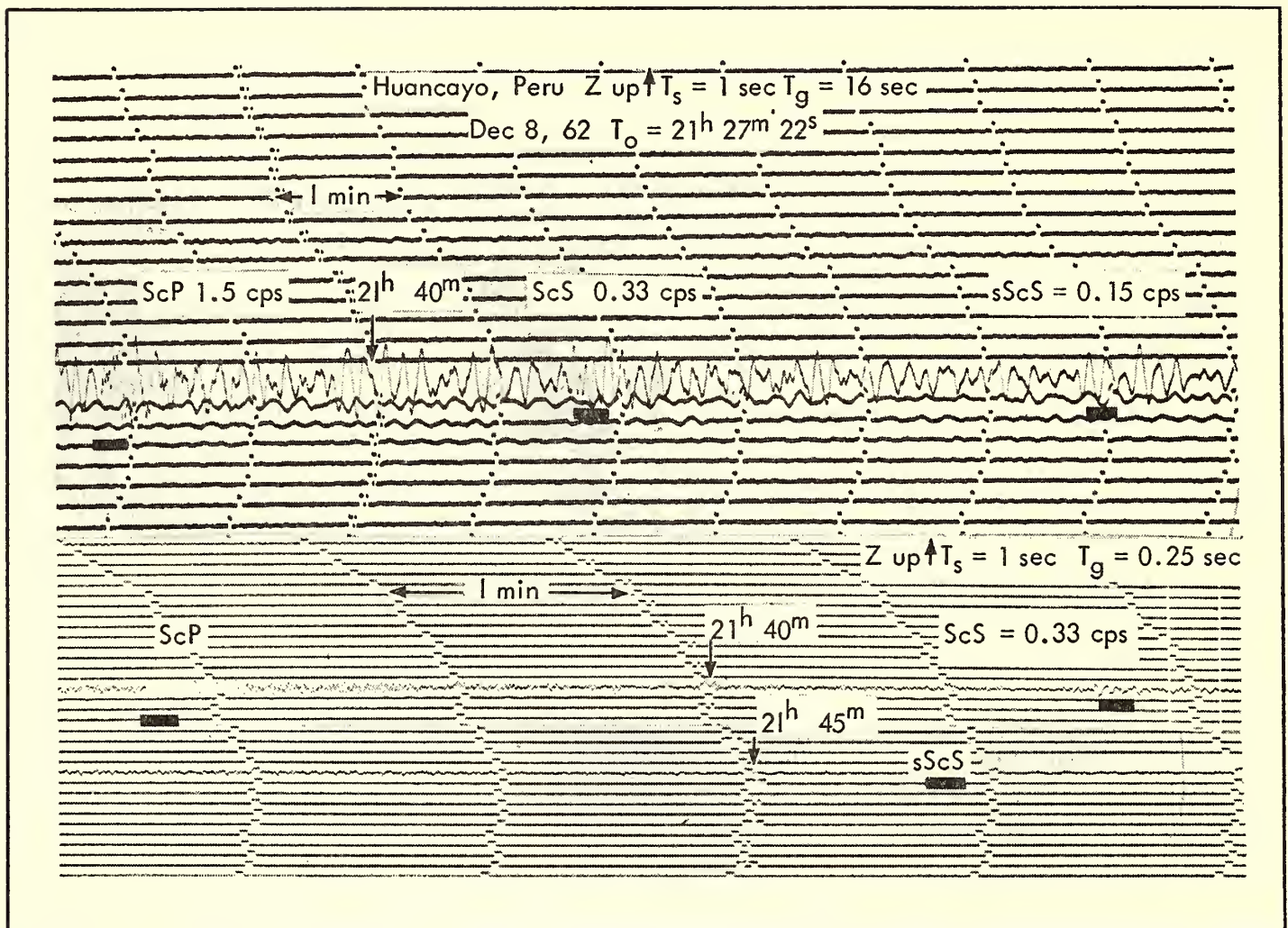


Fig. 16. Huancayo records of a 600-km-deep earthquake at $21^{\text{h}}27^{\text{m}}22^{\text{s}}$ on December 8, 1962. *ScP* travels through the upper mantle and crust as *P* and is rich in high frequencies (1.5 cps), whereas *ScS*, having traveled through a lossy zone in the upper 600 km as *S*, shows a dominant frequency of 0.33 cps. *sScS* passes through the lossy zone three times and loses its higher frequencies to such an extent that they are below noise on the short-period record and have a dominant frequency of 0.15 cps on the longer-period record.

A lossy, lower-velocity layer in the mantle. The difference in appearance of *ScS* and *sScS* for deep earthquakes (600 km) suggests the existence of a lossy (low- Q) zone for shear waves between the surface and 600 km. Short periods are evident for *ScS* but not for *sScS*, which has two additional paths through the upper mantle (fig. 16). This low- Q zone does not allow the original spectrum of *S* to be measured for deep quakes, since even direct *S* has had at least one passage through it. Q may be defined as follows: If dE is the energy loss per cycle, and E the total energy, then $1/Q = dE/(2\pi E)$.

There is, however, an efficient conversion to compressional (*P*) energy at the core. This *P* energy focuses at the surface at about 132° from the source (*SKP*). *P*

waves do not appear to be so drastically affected by their passage through the upper mantle, since *P* and *PP* phases remain rich in high frequencies to large distances. Some idea can be had of the source spectrum for *S* if *P* energy converted from *S* is considered.

A comparison of the spectrum of *ScS* and *SKP* makes it possible to estimate the Q for *S* waves of the upper mantle. The maximum value of Q is 160, which is, of course, the effective Q for the upper 600 km. Figure 17 shows the wave paths discussed.

The amplitude decay of multiple reflections of *ScS* was used to ascertain the Q for the lower mantle, i.e., the region between 600 km and the core at about 2900 km. The results are shown in figure

18. Unfortunately, since reflection loss as well as Q absorption yields an exponential law of amplitude decay, it is not possible to separate them, but minimum limits on

both can be given. They are: $Q_{\min} = 500$, and $R_{\text{amp min}} = 0.92$.

Five successive reflections of ScS and $sScS$ were compared in the above study. It will be possible to separate Q and reflection coefficient if the change in spectrum for the various reflections is accurately evaluated. Large dynamic range equipment to provide really broadband recording (50 seconds to 10 cps) is being prepared for the purpose.

The amplitude decrease with distance of earthquakes of various depths, but in the same geographical region, was studied to locate the upper limit of the low-velocity, high-loss zone (fig. 19). S arrivals from a depth of 600 km showed no shadow zone, but S amplitudes from 300-km-deep earthquakes dropped very sharply once the ray path penetrated much below 300 km. The range at which the arriving ray left the source horizontally was determined by locating the point of inflection in the travel-time curve. The result was confirmed by considering sS amplitudes

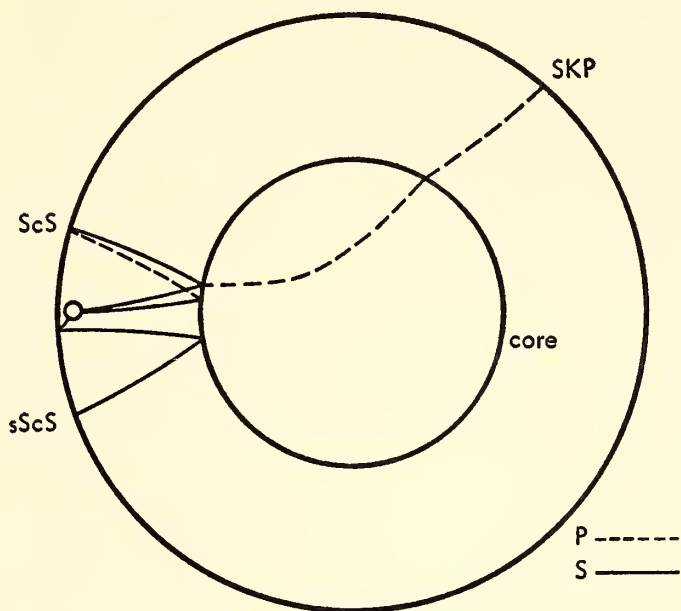


Fig. 17. Wave paths discussed in the text. It should be noted that, for epicentral distances less than about 20° , the path of S energy to the core is rather similar for ScS and ScP . It is also similar to SKP at an epicentral distance about 132° , at which point this energy focuses.

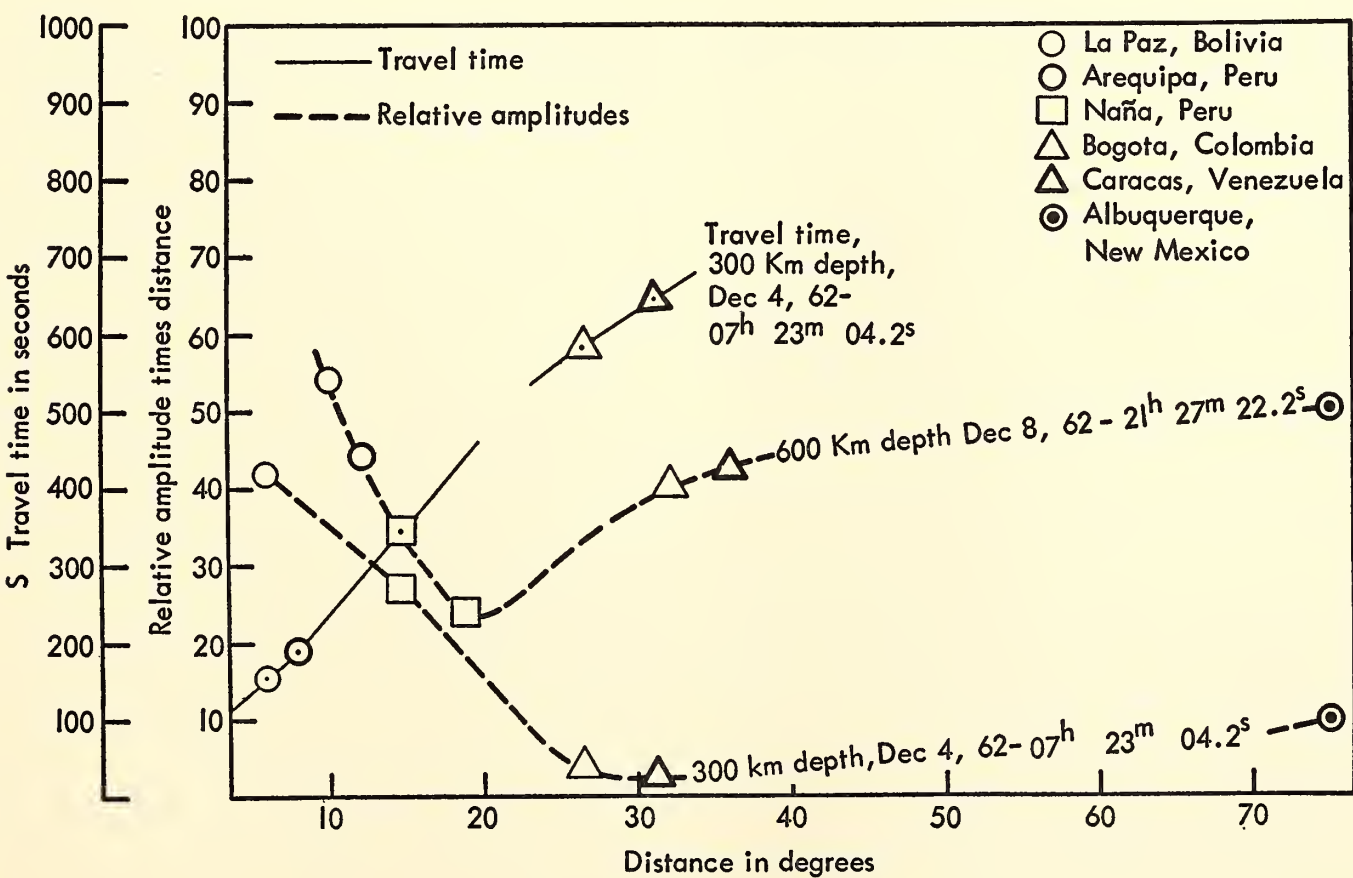


Fig. 18. Amplitudes of multiple reflections of ScS and $sScS$ from the deep earthquake (600 km) at Santiago del Estero on December 8, 1962, at $21^h 27^m 22^s$. Long-period east-west horizontal component records from Arequipa, Peru, and La Paz, Bolivia, were used. The amplitudes given are for 30-second-period waves.

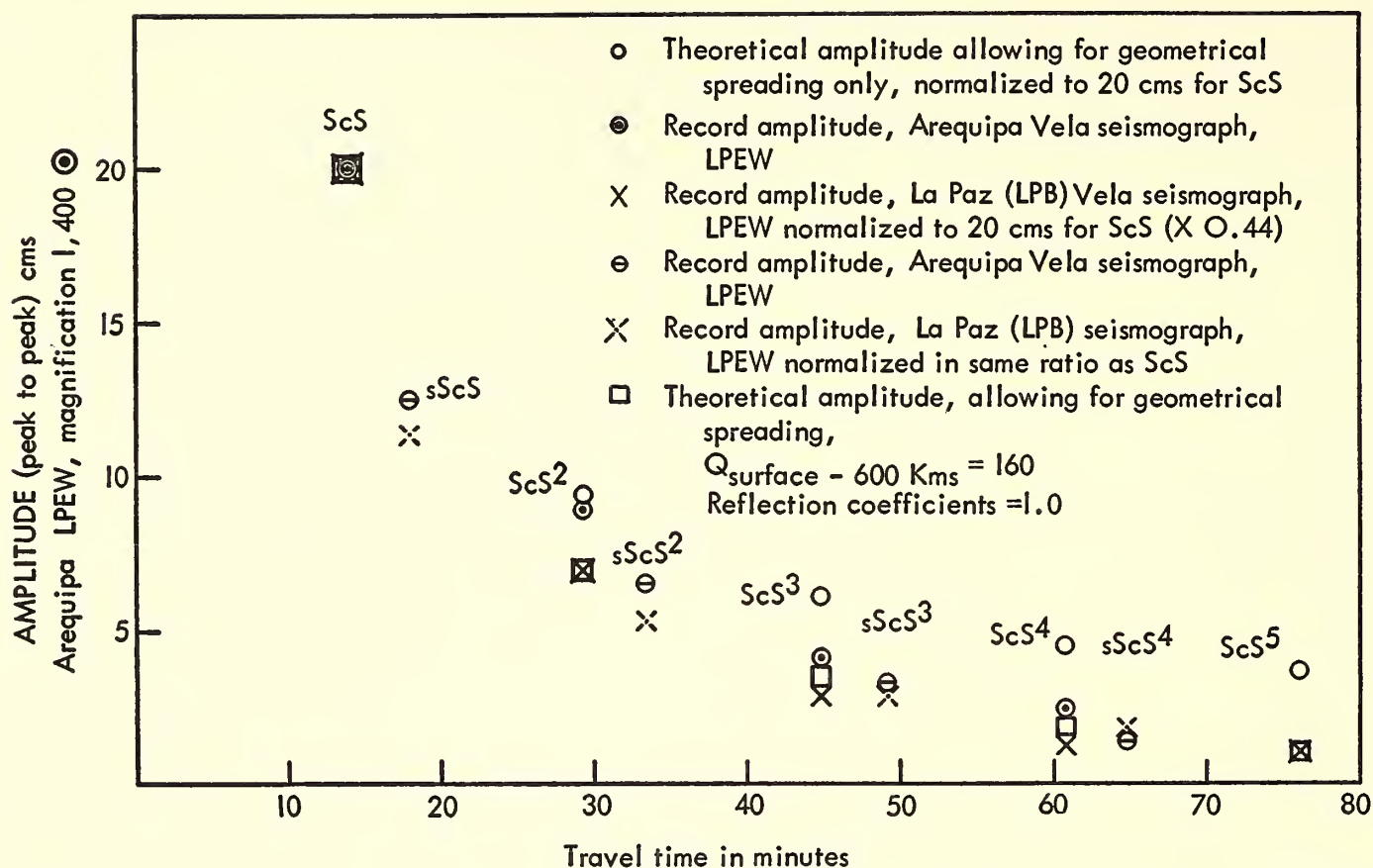


Fig. 19. The product of relative amplitude and distance versus distance of a 600-km-deep earthquake and one 300 km deep. The travel-time curve for S for the 300-km earthquake is also plotted. It can be seen that the point of inflection of the travel-time curve lies between Arequipa and Bogotá. In this range too the amplitude decreases very markedly. Waves of 16- to 25-second period have been used.

versus distance. The fact that the same attenuation pattern was found for both long and short periods is evidence that the lossy layer also has a lower S velocity than the media on either side.

It should be noted that for the region considered, South America, there appear to be very few earthquakes in the depth range 350–500 km, as is compatible with a region of low rigidity.

Seminar on Local and Regional Earthquakes

During January and February the Department's Intensive Seminar on Local and Regional Earthquakes was held. The principal investigators and their students from each of the Carnegie-Andean networks were brought to Washington to join with Carnegie staff members in a comprehensive study of seismological problems pertinent to a system of observatories of this type. The goals of the seminar were the establishment of a

common research background for United States and South American participants in the Carnegie cooperative geophysics program in the Andes and the selection of appropriate and feasible objectives for the program during the next three years.

The seminar opened with a two-week review of fundamental seismology as found in standard texts, after which there were series of invited lectures by visiting professors on surface waves, attenuation, focal mechanism, earthquake statistics, and related topics. The final third of the meeting was devoted to a study of selected papers from the recently published literature on near earthquakes, a critical examination and recalibration of the instrumental systems currently in use in the Andes, and a number of informal conferences on experiment design. As a result of these studies, changes in the suspension of the Wilson-Lamson seismometer were recommended which both minimize objectionable vibrational modes

in the seismometer spring and make it possible to vary the resonant period of the instrument from 1.2 to 4 seconds. The Carnegie TR-2 seismic amplifier was also modified to incorporate the temperature compensation long considered desirable in the extreme operating conditions of the Andes, a differential input permitting the use of longer data-transmission lines, and an adjustable band-pass filter. A preliminary analysis of data from the entire network indicated that the number of small shocks reliably recorded each month at stations on both sides of the Andes is large enough to support an examination of the attenuation problem in this area, which has attracted much interest. To this end, regular radio schedules and standard record formats were agreed upon to improve the exchange of information between the various centers, thus increasing the opportunity for these and other studies requiring regional data. Several methods of epicentral determination using both local and regional networks were evaluated, and the prototype of an easily operated analog calculator for finding depths and epicenters was constructed, which will materially reduce the amount of time formerly required by this routine but highly important task. Plans were made for gradually expanding the size of the local networks in several areas to facilitate the study of shocks and structure at increasingly greater depths, preparing the way for an intensive search for small, deep quakes.

Added assurance that our seismic studies in the Andes will have the benefit of guidance from the whole of theoretical seismology was provided by the appointment early in 1963 of Dr. Cinna Lomnitz, Director, Instituto de Geofísica y Sismología of Chile, Santiago, as a Staff Associate of the Department. Dr. Lomnitz will be on part-time assignment for research activities related to our general interests. He will continue to work in Santiago with such travel arrangements as are required by his research program.

RADIO ASTRONOMY

B. F. Burke, K. C. Turner, and M. A. Tuve

RADIO HYDROGEN

The completion last October of the 300-foot National Radio Astronomy Observatory transit telescope at Green Bank, West Virginia, had a major effect on the year's activities. The Carnegie multi-channel hydrogen-line spectrometer is uniquely suited to observations with a transit instrument, since the simultaneous measurement of radio noise intensity at many different frequencies reduces observation time of H-line profiles enormously. The resolving power of the new telescope, 10 minutes of arc at 21 cm, offered new possibilities for studying the hydrogen distribution in our own galaxy, and in the nearest external galaxies, especially the great Andromeda nebula, M31, and the prominent spiral nebula in Triangulum, M33. In collaboration with the National Radio Astronomy Observatory, two observing periods were arranged, one brief period of two weeks (November 6 to 19) to acquaint us with the problems associated with the new instrument, and a major one (December 5, 1962, to January 24, 1963) during which the telescope was devoted exclusively to H-line observations with the Carnegie spectrograph.

Moving feed. Before the observations started, it was clear from our exploratory work on M31 and M33 with the 60-foot Derwood telescope that the time available with the transit telescope would not be sufficient. At 21-cm wavelength, a point on the celestial equator traverses the 10' half-power beamwidth of the 300-foot telescope in 40 seconds of time, whereas at the declination of M31 only a negligible increase, to 50 seconds, is obtained in observing time. Since a satisfactory signal-to-noise ratio could be achieved only with an integration time of at least 150 seconds, it was decided that a moving-feed system should be built to track the

radio image in the focal plane. Mr. Ecklund designed the system and supervised its construction in our shops. It consisted of a weather-tight box, containing the dipole feed, crystal mixer, and preamplifier, moving on a set of east-west rails for a total travel of 90 cm, driven at a variable rate to match the declination being observed, with remote indicators for the observer on the ground. A heavy-duty hydraulic doorstop provided a quick-return motion to enable observations of different points to be made in rapid succession. The entire system was built in less than a month, and it operated remarkably well under extremely adverse weather conditions, including heavy snow and temperatures as low as -20°F .

Supplementary channels. The multi-channel spectrometer, as used since 1957, has consisted of 54 channels, each of about 10-kc/s half-power bandwidth, spanning approximately 1 Mc/s. To improve signal-to-noise ratio of individual channels, filters could be of wider bandwidth, if the line profiles under study vary sufficiently slowly with frequency. A supplementary set of 36 wider-band channels, primarily for the extragalactic observations, was therefore built, each 50 kc/s wide, and spaced to span a total frequency range of 2.4 Mc/s. Consequently all our observations were made with a total of 90 channels. Although the new channels functioned well, the wider bandwidth was not especially valuable, for the decreased fluctuation level did not compensate for the loss in frequency resolution. As a result of this experience, a new set of filters has been built, identical electrically to the original 10-kc/s filters, and a new set of transistorized plug-in video and audio amplifiers has been developed.

M31. The principal objective of our observations was to determine, as far as time permitted, the density distribution and motions of the hydrogen in the Andromeda nebula, M31. Among the neighboring galaxies this giant spiral most nearly typifies our own galaxy, and it is

hoped that through studying this system, where the relative positions of the hydrogen concentrations can be determined without ambiguity, we can be led to a better understanding of our own galaxy, in which a distance scale must be inferred through velocity measurements.

The tracking range available with the moving feed enabled us to observe, as a rule, two independent 150-second integrations at two different points each night on M31, and in the time available to us we were able to observe, at least once, a series of points spaced at $10'$ intervals along the major axis over a range of 5° , $2\frac{1}{2}^{\circ}$ each way from the center. In addition, a series of points was observed along the minor axis, and several off-axis points were taken to check on deviations between our adopted major axis (position angle 38°) and the symmetry axis as determined by the hydrogen motions themselves. The observing procedure consisted of making readings at a pair of standard reference points in the sky before transit (usually at $\delta = +41^{\circ}$, $\alpha = 00^{\text{h}}12^{\text{m}}$ and $\alpha = 00^{\text{h}}20^{\text{m}}$) with the local oscillator set for the velocity range used for the first point on the nebula. After observing the two points on M31, a pair of standard reference points (usually at $\delta = +41^{\circ}$, $\alpha = 00^{\text{h}}42^{\text{m}}$ and $00^{\text{h}}50^{\text{m}}$) were observed with the local oscillator setting of the second point. By taking differences between the standard points and the observations on the nebula, it was expected that the effects of base-line irregularities could be corrected. It is necessary to distinguish carefully between radiation from M31 and the background radiation from our own galaxy.

Figure 20 shows an example of a record taken on the major axis, $70'$ north following from the center, using the 10-kc/s channels. The open circles and crosses represent averages of observations at the two reference points, and the lines show the reading for each of the two 150-second integrations on M31. At the far right, close to the velocity of the local standard of rest, the background hydro-

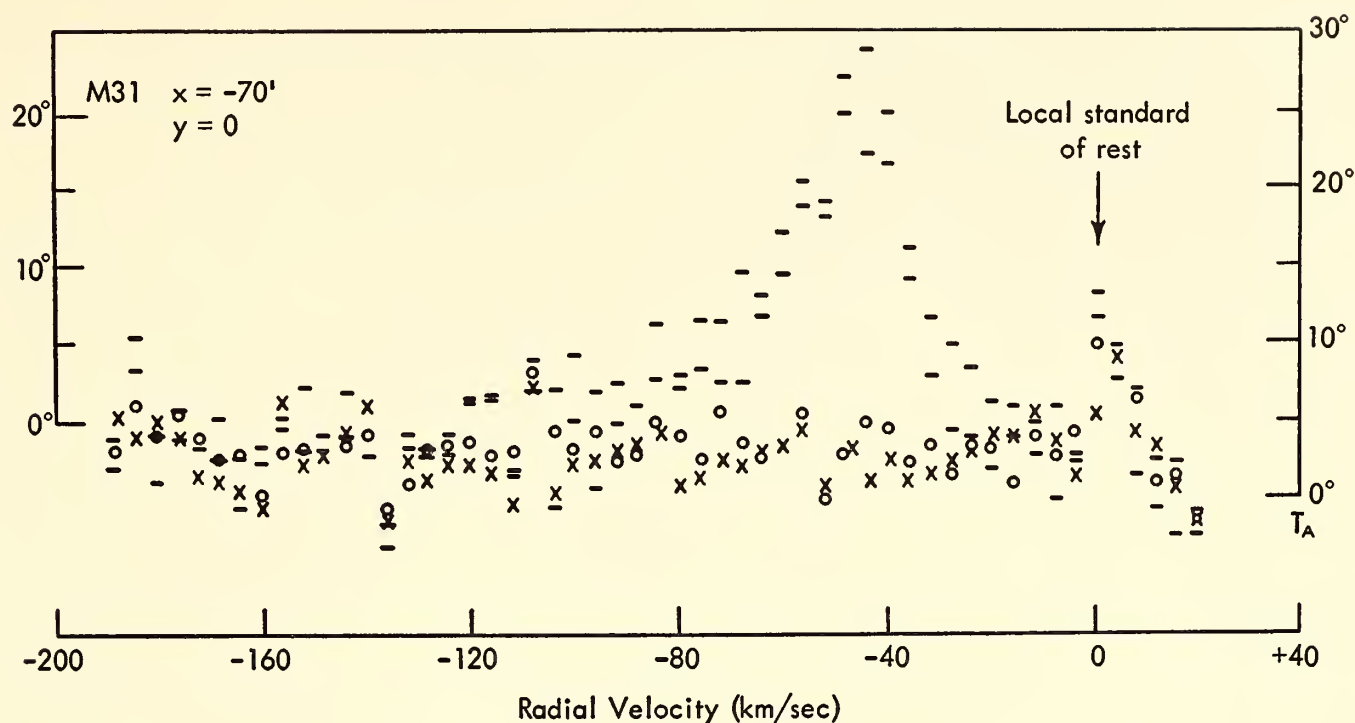


Fig. 20. Hydrogen peak observed from M31 70' from center along major axis (north following).

gen of the Milky Way can be clearly distinguished. Since both reference points and the point on M31 show similar shapes for this peak, the galactic background must be very regular in this part of the sky, and hence the subtraction procedure should not introduce artifacts. The hydrogen peak from M31, immediately to the left of the background, is well enough separated in velocity to make it possible to distinguish unequivocally between M31 and the Milky Way. As it turned out, the same is true for the entire nebula.

The peak antenna temperature observed at this point is 24°K, which corresponds to an actual surface brightness of 30°K (adopting 100°K as the peak temperature at $\ell^I = 50$, $b^I = 0$). This is the brightest point observed, and so it is probable that the optical depth is always less than 0.25 (assuming a spin temperature of 125°). Therefore, self-absorption effects, though not negligible for the brighter parts, are not serious, amounting to corrections of no more than 30 per cent.

The line is markedly asymmetrical, and the steepness of the leading edge is remarkable. Within 20 kc/s, the temperature changes by a factor of 2. For such a

curve the 50-kc/s channels are inadequate, and only the 10-kc/s channels were sufficiently narrow to give the true line profile shown in figure 20. The line breadth is comparable to that observed in profiles taken of our own galaxy, and a preliminary calculation indicates that broadening by differential rotation in this region of M31 is not great. With only small corrections the line width is given by the random motions over the volume within the 10' beamwidth of the 300-foot telescope. (Ten minutes of arc corresponds to a distance of 1800 parsecs at M31.)

A summary of all our major axis observations is given in figure 21, which shows antenna temperature as a function of radial velocity and position along the major axis. The difference between hydrogen distributions in the two halves of M31 is immediately apparent. The south preceding (SP) half exhibits lower peak temperatures and is split into two distinct concentrations having no obvious relation to the optical spiral structure. The north following (NF) half is more compact, with higher peak temperatures, but does not extend to as great a distance from the center, detectable ($T_A > 2^\circ$) hydrogen being seen no more than 100'

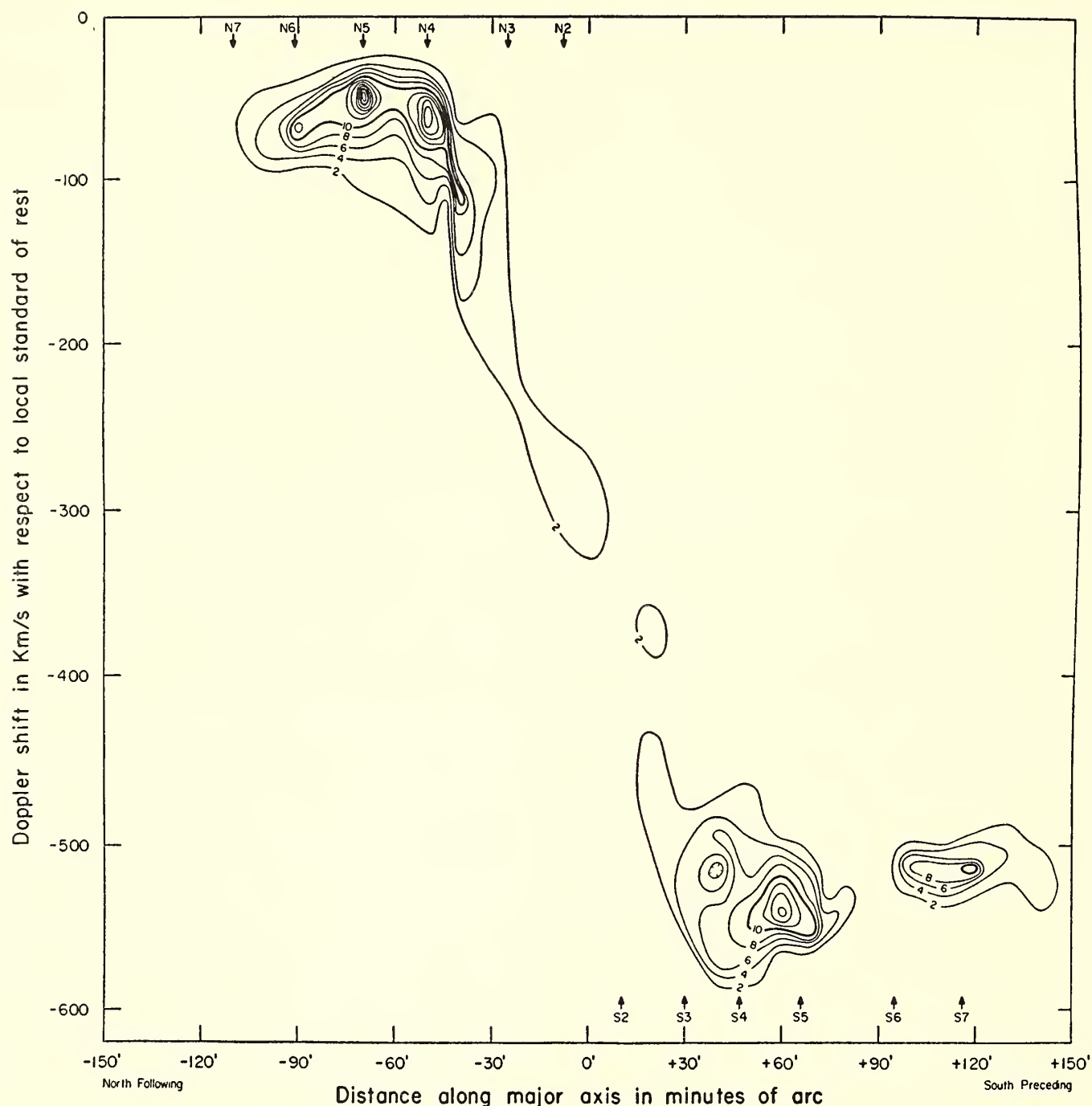


Fig. 21. Hydrogen velocities in M31 along major axis.

out, compared with 140' on the SP side.

One of the most interesting comparisons to be made is the relationship between the 21-cm H I density and the observed stellar distribution, and in particular with Baade's spiral arms, which are composed of bright OB associations. In the NF half there is almost exact agreement between the positions of the three major H I concentrations and the major axis crossings of the spiral arms designated by Baade as N4, N5, and N6. Along the SP side the agreement is not nearly so good—in fact, it is little better than might be expected by chance. Baade's arm S6 falls in a region of

markedly low concentration, S4 and S5 straddle the most intense H I concentration, and only for S7 does there seem to be good correspondence. Optically, M31 is an asymmetrical object, with the SP and NF halves differing in appearance and in spiral-arm structure, and having different major axes. The tidal effects of M32 have been invoked to explain the difference, but the quantitative details of the mechanism are not clear.

There is an interesting general agreement, setting aside the small-scale fluctuations, between the H I density and the rate of bright star formation. Baade has pointed out that the inner arms show few

blue supergiants, the frequency of occurrence increasing as one moves outward. The number of population I objects reaches a maximum in arms N4-S4 and N5-S5, and then definitely declines in N6-S6 and N7-S7. The hydrogen density follows the same distribution on the average, reaching a maximum about 60' from the center, i.e., between N4-S4 and N5-S5. There is noticeably less H I near the center, which is predominantly population II optically, with few blue supergiants visible. Thus, the common population I occurrence of H I and blue supergiants is demonstrated in particularly clear form.

The observed hydrogen distribution has been compared with the Leiden distribution, derived from a survey with a much smaller (25-meter) telescope. The Leiden model showed a strong central concentration of hydrogen and a second sharp concentration 1° from the center. The central concentration was not seen in our survey, and, though the principal hydrogen concentration does in fact occur 1° from the center, it is not as sharp as in the Leiden model. Indeed, the Leiden workers have themselves pointed out that they have exhibited only one possible solution consistent with their data. It seems probable that the central concentration was an artifact introduced in the reduction procedure. Fundamentally, of course, there is no substitute for resolving power.

Attempts are being made to construct a mass distribution model that will yield the rotation law deduced from the data of figure 21. A complication is presented by a lack of symmetry between NF and SP sides in velocity as well. Within 30' of the center, there is an asymmetry between the two halves of at least 40 km/sec. In the outer parts, the asymmetries are smaller, 10 km/sec or so, and are still easily noticeable. Until now most reductions of hydrogen-line motion have assumed azimuthal symmetry of the hydrogen velocity field. This assumption is not justified for M31, and the extent to which it is valid for our own galaxy must be evaluated.

The observations along the minor axis of M31 are summarized in figure 22, which presents the antenna temperature as a function of velocity and position along the minor axis. Five points were observed, at 0, $\pm 10'$, and $\pm 20'$. If only rotational motions exist (except for random motions), figure 22 would be expected to show symmetry in velocity about some V_0 , which would be the radial velocity of the center of mass of M31. The rotational curve in figure 21 should also be symmetrical with respect to a double reflection, about $V = V_0$, and, if X is position along the major axis, about $X = X_0$, where X_0 is the point at which the minor and major axes intersect. The vertical line, at $V_0 = -298$ km/sec, shows the V_0 derived from the symmetry

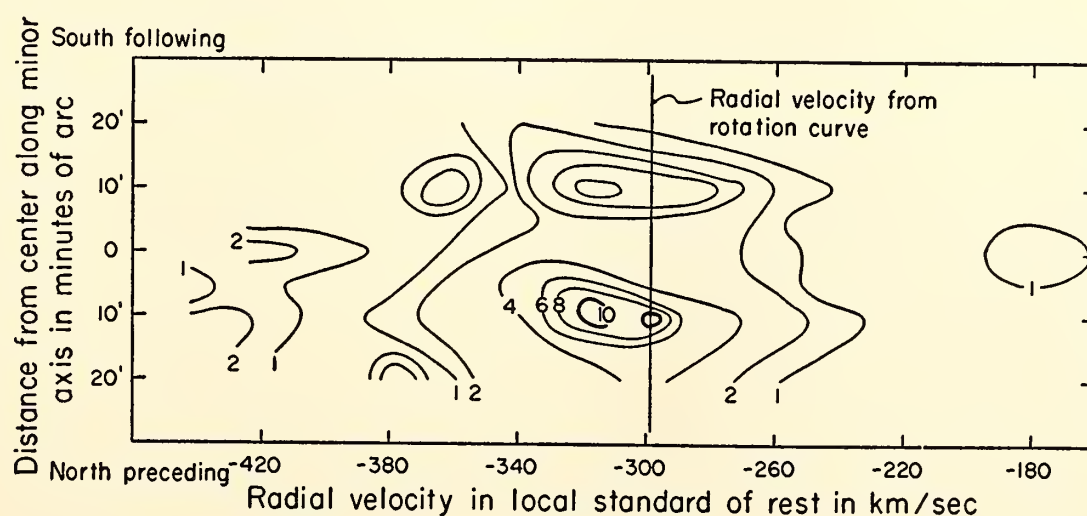


Fig. 22. Hydrogen velocities in M31 along minor axis.

of motion derived from the best-fit reflection point of figure 21. If X_0 is determined from the symmetry of figure 22, a significantly higher value, between 310 and 320 km/sec, is obtained. Furthermore, there is a high-velocity wing at -420 km/sec that has no counterpart on the low-velocity side. Since low antenna temperatures are involved (1° – 2°) confirmation of this curious dynamical effect is certainly required.

The symmetry of the contours for the minor axis in figure 22 makes it possible to check Kerr's expansion hypothesis. In order to fit the Dutch and Australian galactic surveys to one model, Kerr postulated a general radial outflow of H I, with velocity decreasing as distance from the center increases. The radial outflow, at the distance of the sun from the galactic center, would be 7 km/sec. The contours of figure 22, if such an outflow were also in progress in M31, would be skewed. There may be a slight skew, with velocities on the NP side slightly lower than on the SF side. This, however, would correspond to an infall, rather than outflow, of perhaps 2 km/sec at 8 kiloparsecs, but the effect is marginal. It is safe to say, however, that radial motions

of the magnitude postulated by Kerr for our own galaxy do not exist in M31.

M33. The large Sc spiral in Triangulum, M33, lies at about the same distance as M31, but is noticeably smaller. Observations were made at 5' intervals along the major and minor axes, and the hydrogen brightness observed as a function of position and velocity is given in figures 23 and 24. The observations along the major axis (fig. 23) show marked differences from the equivalent observations in M31. There seems to be much more hydrogen in the central regions of M33 in comparison with the central regions of M31, a difference that may be associated with the galactic type. (Since M33 is a much smaller object than M31, resolution problems arise.) In an Sc-like M33, star formation is still proceeding in the inner regions, and there is a less well developed central concentration of old population II stars. Thus, the population I nature of the H I concentrations is again emphasized. From $+10'$ to $-10'$ along the major axis, the motion appears to be like that of a rigid body, but beyond, where the highest concentration of H I exists, shear occurs. At the outermost reaches of observable hydrogen, the mass

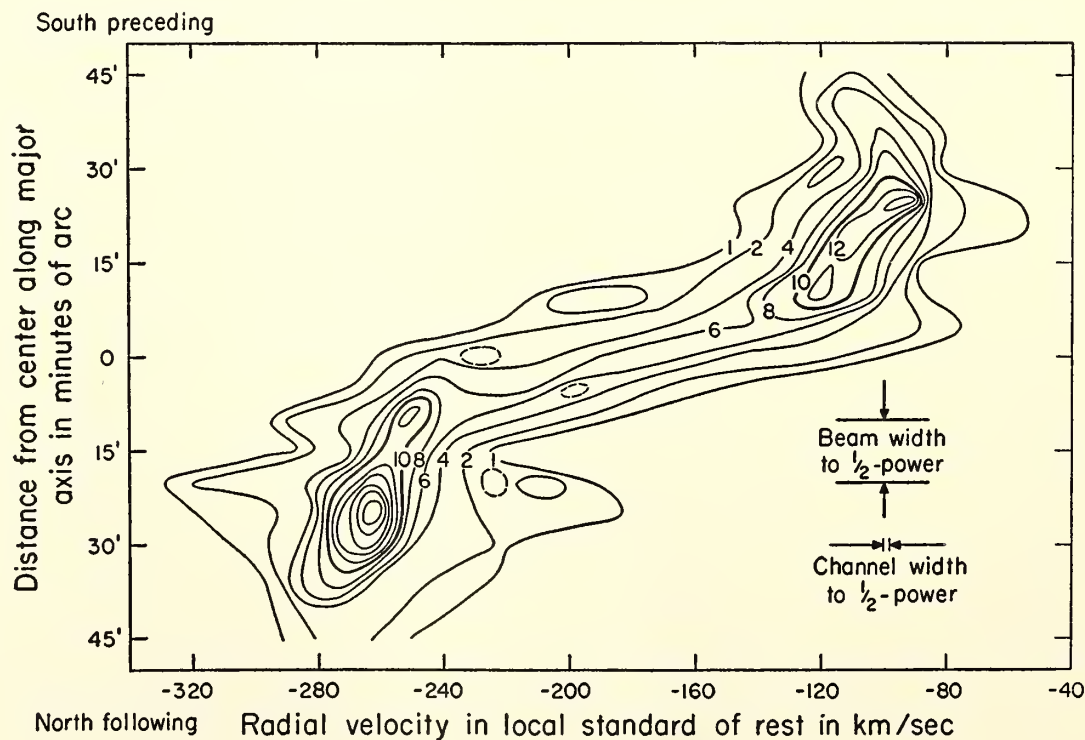


Fig. 23. Hydrogen velocities in M33 along major axis.

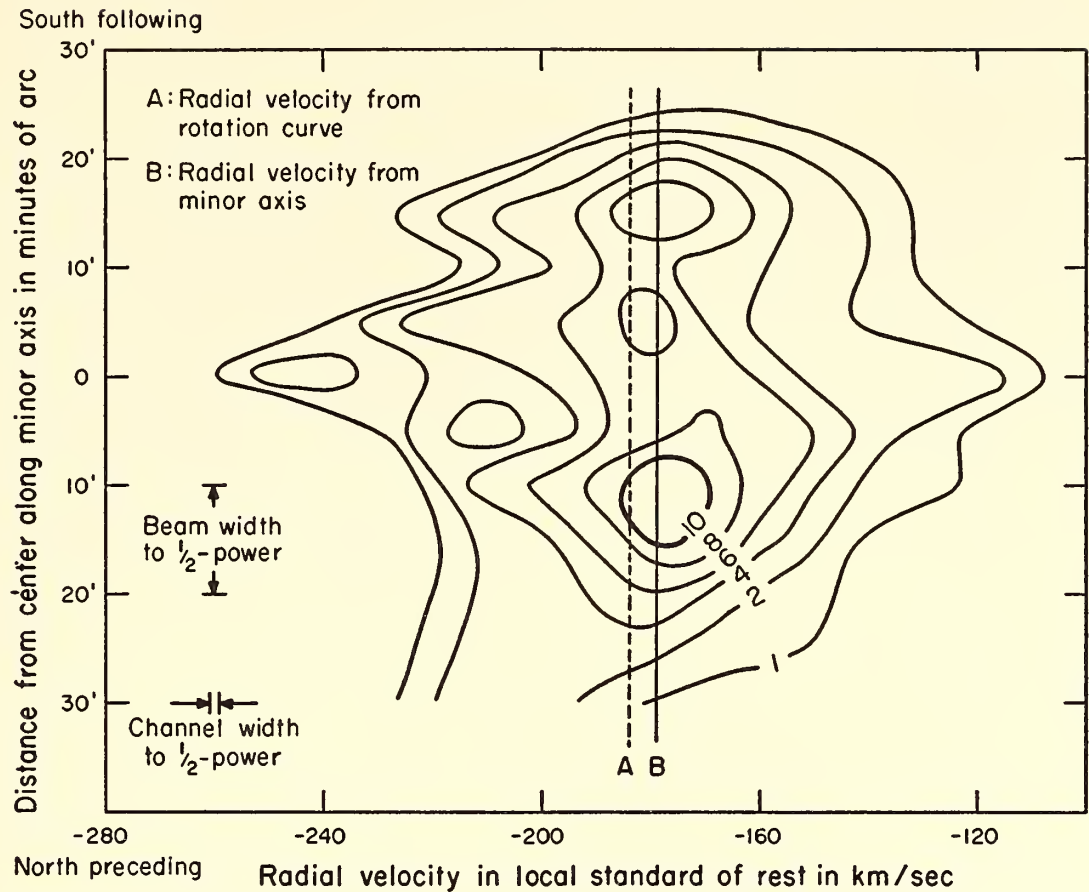


Fig. 24. Hydrogen velocities in M33 along minor axis.

density appears to remain high, since rotational velocity changes slowly with distance from the center.

The motions observed along the minor axis, in figure 24, show a similarity to the contours obtained for M31, except for the greater central density in M33. There is also, as in M31, a displacement of the center of symmetry with respect to the rotation symmetry. Line A is the center-of-mass velocity expected from the rotation curve; the center-of-mass velocity determined from the minor axis density observations is shown by line B. The difference, of 5 km/sec, is significant but is not understood.

NGC 6822. Observations were also made at Green Bank of NGC 6822, a dwarf/irregular member of the local group of galaxies. Although this object is only about 20 minutes of arc in diameter optically, associated hydrogen was found over a much larger area of at least a degree in diameter. Our preliminary explorations of the extent of this hydrogen will be used in preparing the next

observational program at the National Radio Astronomy Observatory.

Galactic studies. Line profiles were taken at 160 points from $\ell^{\text{II}} = 11^\circ$ to $\ell^{\text{II}} = 50^\circ$ to study the angular structure of the far circular arm of our galaxy. Meridional sections were made every 5°

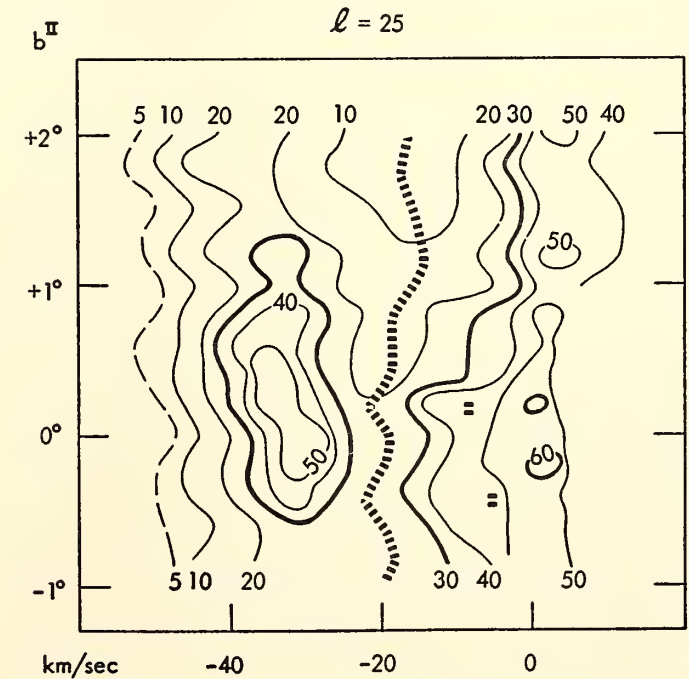


Fig. 25. Galactic hydrogen intensity along $\ell^{\text{II}} = 25$.

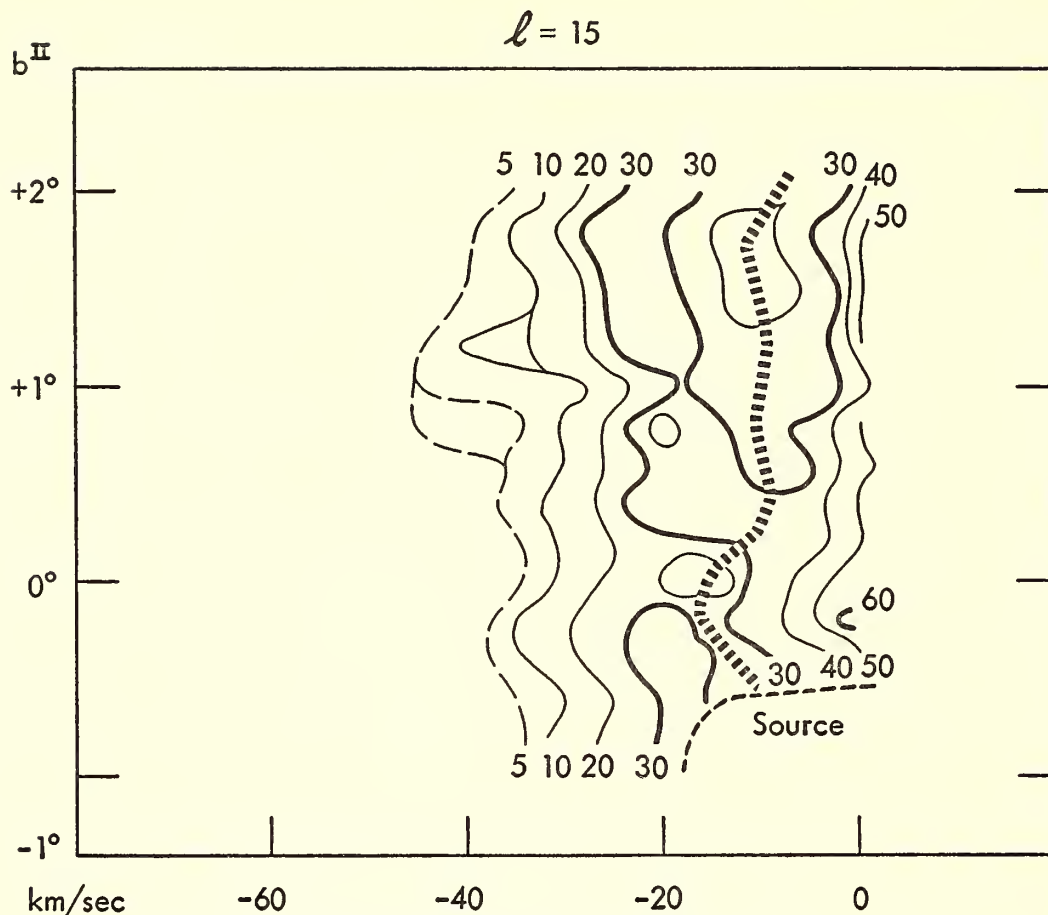


Fig. 26. Galactic hydrogen intensity along $\ell^{\text{II}} = 15$.

in ℓ , from $b = -0.8^\circ$ to $b = +2.0^\circ$ in steps of 0.2° . A single longitudinal section taken at $b = +0.4^\circ$, in steps of 1° in ℓ , was also produced. Examples of the meridional sections are shown in figures 25 and 26. The dashed lines indicate intensity minima.

The section at $\ell^{\text{II}} = 25^\circ$ (fig. 25) shows several characteristics of the far arm to good advantage. The large extension of the arm in galactic latitude is clear. (At this distance 2° corresponds to 580 parsecs, more than twice the thickness of the inner parts of the galaxy.) It will also be noted that the 10°K and 20°K contours show no sign of closing over the entire 3° range investigated. Its large size makes this interesting structure susceptible to investigation with the Carnegie 60-foot dish at Derwood, Maryland; such an investigation is being planned.

The section at 15° (fig. 26) is a somewhat more typical meridional section. The large scale is evident, but a distinct far arm is not so obvious. The source indicated in the lower right corner is M17, an H II region containing an association

of bright young stars; it was seen in absorption.

Figure 27 shows the longitudinal section studied. It will be seen that the far arm is not a single continuous structure, but rather the locus of scattered small clouds. Neither the peak intensities nor the minima change their velocities with longitude in a very smooth way. By contrast, a plot of the velocity of the 10°K contour against $\sin \ell^{\text{II}}$ (fig. 28) shows very regular behavior over the entire range of ℓ studied. Such a plot, for objects in the same circular orbit, could be a straight line going through the origin of the coordinate system. The 20-km/sec offset of the straight line observed suggests that we are seeing the high-velocity edge of a structure in circular motion with a very high-velocity dispersion, in which are embedded scattered clouds of higher density and lower-velocity dispersion.

Studies were made at $\ell^{\text{II}} = 130^\circ$ to 160° in cooperation with Professor G. Westerhout of the University of Maryland, and at $\ell^{\text{II}} = 194^\circ$ to 196° in cooperation with

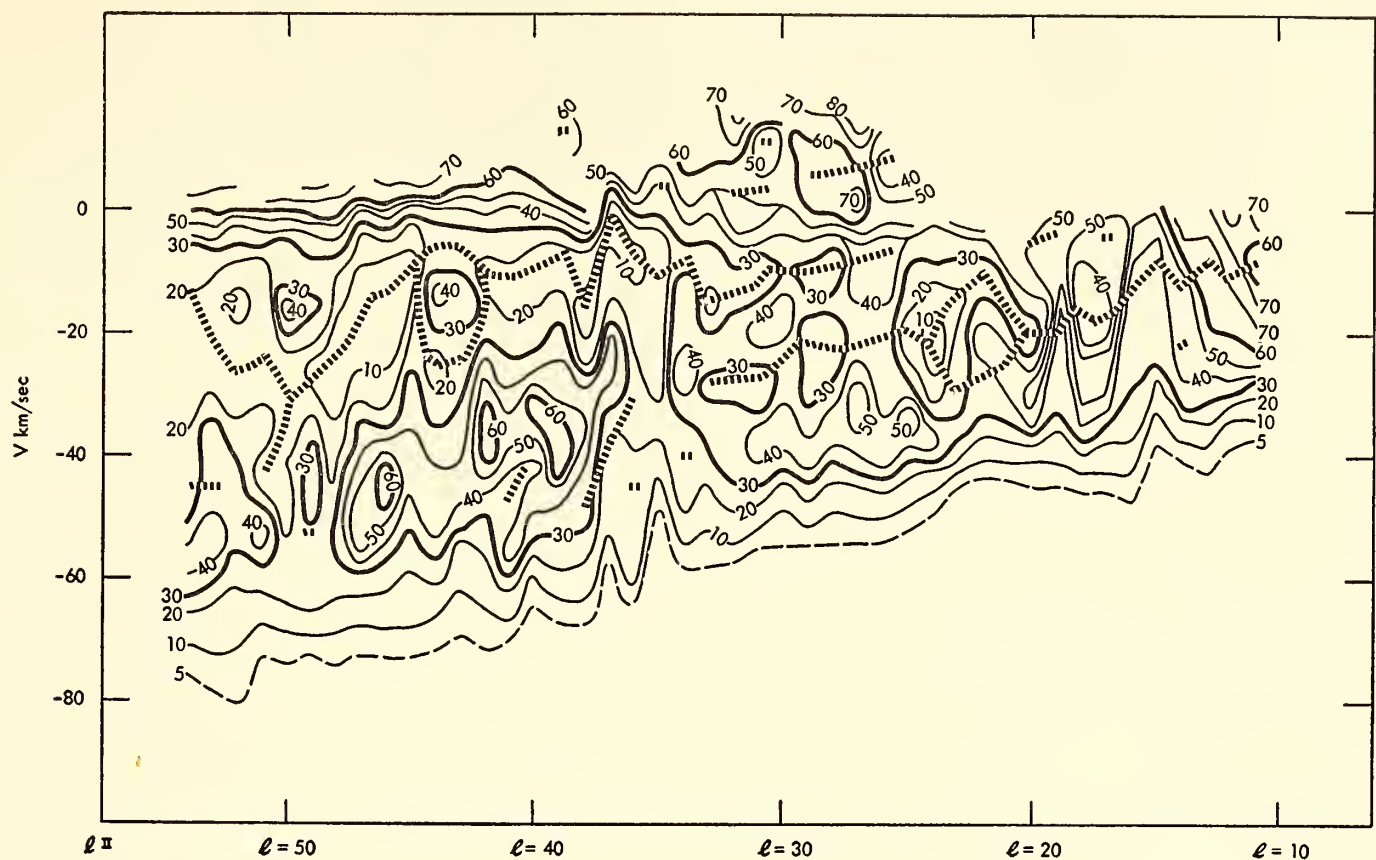


Fig. 27. Galactic hydrogen intensity along $b^{\text{II}} = +0.4^\circ$.

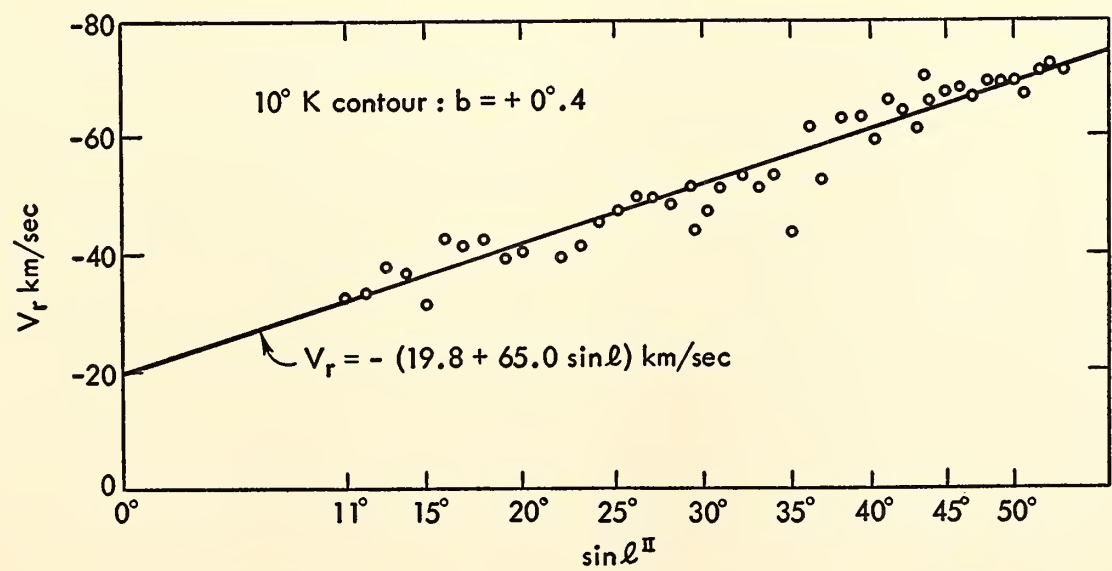
Dr. B. Hoglund of NRAO. The data are still being reduced.

In cooperation with Dr. C. Wade of NRAO, several regions were examined near stars in whose spectra interstellar calcium absorption lines have been measured. In all spectra so far examined, the low-velocity calcium lines fell in the broad peak of the hydrogen of the local spiral arm. Further studies of regions near stars exhibiting very high-velocity lines,

well separated from velocity of local hydrogen, are planned.

Also in cooperation with Dr. Wade, an unsuccessful search for H-line radiation from the galaxy M82 was made. The search will be repeated if the use of a parametric amplifier enables us to reduce the receiver noise figure sufficiently.

The spectra of the radio sources Cas A, Cyg A, Her A, Vir A, and the Orion nebula were examined for absorption due



Radial velocity of the 10°K contour at $b = + 0.4$ vs $\sin l^{\text{II}}$

Fig. 28. Radial velocity of the 10°K contour at $b = +0.4^\circ$ versus $\sin l^{\text{II}}$.

to galactic hydrogen. No absorption was observed in the spectra of Her A and Vir A, but the well known absorption lines in the spectra of the other sources will be studied in detail. An extended program of absorption studies for a large number of radio sources is planned for the next observing period at the NRAO.

ANGULAR SIZE INTERFEROMETER

Planning and construction of a long base-line interferometer, as discussed in *Year Book 61*, page 220, have proceeded. The central ring structure has been completed, and the construction of the ribs is about to begin at Derwood. The central ring is welded in four pieces, which are bolted together, to permit the transportation of the dish from one site to another. The original La Plata design has been somewhat strengthened to allow for possible snow and wind loading, more of a problem in Montgomery County than in Argentina. The construction here has also served to give experience in techniques that will prove valuable when the South American construction is begun later this year.

Negotiations are under way for a site about 2 km east of our Derwood station, where the simple transit mount will be built. Receiver design and some construction are under way, but, owing to the threatened loss of channel 37 for radio astronomical purposes, the design frequency has been changed from 610 to 1400 Mc/s. At this frequency the base line of the interferometer will be about 15,000 wavelengths long, still a good choice for initial observations.

SOUTH AMERICAN COOPERATION

The effort to establish a major center of radio astronomy in South America has progressed this year. The major weldments forming the polar mount and declination axis were shipped in March 1963, together with all the steel pipe and aluminum necessary to complete the 30-meter dish. The changes in design of the dish that were made for the angular size

interferometer were also incorporated into the telescope design. The added strength makes the dish strong enough to withstand winds of at least 90 miles per hour. A site has been selected in the Bosque Pereira near the town of Villa Lisa, midway between Buenos Aires and La Plata. After soil tests have been completed, work on the foundations can progress. Construction of the dish itself is planned for late 1963. The Instituto Nacional de Radio Astronomía, the Argentine Institute with which we shall be cooperating, has been operating as an effective partner both in obtaining the land and in obtaining a government decree passing all equipment into Argentina duty free, a feat perhaps too little appreciated from a North American vantage point. Moreover, the Instituto has now grown large enough so that effective scientific participation can certainly be expected. Dr. Carlos M. Varsavsky has been named its Director and representative from the University of Buenos Aires; Dr. Carlos O. Jaschek of La Plata University, Assistant Director; Ing. Humberto R. Ciancaglini represents the Consejo; and Dr. Jorge Sahade, the Comisión de Investigación Científica.

Visits from South American colleagues have continued, Dr. Carlos Varsavsky spending a month here working with our equipment at Derwood and at Green Bank. An exploratory survey of the Taurus region was started to examine the relationship between T associations and interstellar hydrogen. The project is expected to continue for several months, discussion and reduction of the data to be shared between the University of Buenos Aires and our Department. In June we were also joined by Mr. Hector Alvarez of the University of Chile, now studying at the University of Michigan; he will spend the summer working at DTM with our group. Brief visits were also made by Mr. Filloy and Mr. Dugatkin, associated with the Instituto. Work is progressing on the equipment trailer that will house the multichannel receiver. Construction

of the individual channel filters and the transistorized amplifiers is in progress, and it is our expectation that a complete receiver of about 40 channels will be ready

for shipment by November 1963. Components for 20 to 40 additional channels will be sent by us for assembly by Argentine technicians.

THEORETICAL AND STATISTICAL GEOPHYSICS

S. E. Forbush

Conductivity Anomaly Program for Peru

To determine whether crustal conductivity anomalies exist in Peru the Instituto Geofísico del Peru with the cooperation of the Department has begun continuous simultaneous registration of geomagnetic variations at eight locations in Peru by means of Askania variographs. The variations regularly recorded at the John A. Fleming Observatory in Huan-cayo provide data from nine more stations. When the adjustment and tests of the variometers in the observatory at Arequipa are completed an additional variograph will be available for field use.

To cooperate with the Instituto Geofísico del Peru in the conductivity anomaly program the Department provided four variographs obtained by loan from the U. S. Coast and Geodetic Survey, together with 16-mm film recording equipment and other accessories for four other variographs that had similarly been provided for the equatorial electrojet program during the International Geophysical Year (IGY) and the International Geophysical Cooperation Year (IGC).

At most of the variograph stations in Peru facilities are unavailable for adequate time control of the magnetograms. Consequently, eleven timing devices were designed, constructed, and tested at the Department and shipped to Peru. The basic control is from Bulova Accutron electric watches. The sweep second hand of the watch short-circuits, every minute, a pair of very light contacts installed in the watch, operating a transistor amplifier which in turn actuates a stepping relay that turns on the timing lamp every

10 minutes. A second circuit controlled similarly and independently by the minute hand marks the film each hour. These Bulova timers are much more convenient for field use than the large battery-wound Mercer chronometers they replaced, and they consume much less power—an important consideration at field stations, where unattended operation for several weeks is essential. In addition, devices for automatic twice-daily calibration of the equipment, operated by battery-driven Elix motors, were constructed and sent to Peru. When an attempt to replace the fiber system in a Z-variometer that broke in the field proved unsuccessful, a new instrument was ordered on an exchange basis.

Results of observations made in Arequipa with two Askania variographs for checking the operation of the variometers at the Arequipa Observatory were analyzed at the Department. They indicated serious defects in the operation of the H-variometer at Arequipa and also serious errors in the Z variations from the Askania operated in a tent 6 km from the observatory. The cause for these discrepancies is being investigated.

Carnegie Institution of Washington Publication 620, *Equatorial Electrojet in Peru*, contains a description of the results of the separation of the observed magnetic field of the electrojet into components originating from sources external and internal to the earth's surface. Ideally any local conductivity anomaly would be indicated by irregularities in the variation, with position, of the field components of internal origin. Consequently a new separation into internal and external components has been effected from the

same electrojet data but including an important correction, pointed out by Olaf Hartmann, which arises from the fact that the Kertz operator used in the earlier separation involved a certain sum that was only a first approximation to an integral.

The results of the new separation have been thoroughly examined jointly with Dr. Ulrich Schmucker, who became a staff associate at the Department on March 15, 1963. The investigation indicated that to obtain reliable information on the field of internal origin from the electrojet primary system in Peru would require simultaneous observations at some ten or twelve locations more or less uniformly spaced over a range of 20° or so in latitude and at distances of 100 km or more from the coast to eliminate effects from induction in the conducting ocean.

On May 6, 1963, Dr. Schmucker went to Peru to study results obtained from the variograph stations there for possible indications of conductivity anomalies and to consider whether or not daytime electrojet effects at the present stations may be of value to reveal any existing conductivity anomalies. Although the inducing field of the electrojet in Peru is present during every midday period, and with variations of different periods which are required to estimate variations of conductivity with depth, nevertheless the nonuniformity of the inducing field, and even variations in the nonuniformity from day to day, may mean that the daytime inducing field cannot be utilized in the search for anomalies. The variations of external field during the night are quite uniform and suitable, except that they are far less frequent especially near sunspot minimum.

*Induction Effects over the Night
Hemisphere Arising from the Motion
of the Daytime Diurnal Variation
Current System*

To study the effects of induction by the quiet-day diurnal variation, S_q , current

system from IGY data, Professor A. T. Price of Exeter College, England, follows a procedure based on numerical integration instead of spherical harmonic analysis. By this means the external and internal potentials can be separated from data obtained on the daylight hemisphere. Thus induction effects can be determined over separate areas of the earth, as for example over land and water. In Price's procedure it is important to know from what base to measure the departure, at a given hour, of the observed field components of the diurnal variation. It has generally been accepted that, near local midnight on magnetically quiet days, there are no appreciable external ionospheric currents, and consequently departures should be measured from midnight values. However, Professor Price showed that the motion, relative to the earth, of the diurnal variation current system over the daylight hemisphere could, with certain earth conductivity models, induce earth currents under the night hemisphere, the field of which would then change the base from which diurnal variation departures should be measured.

From Price's estimate of the morphology of induced currents it was seen that near midnight near the equator the horizontal magnetic component would be the one chiefly affected. Near the latitude of the foci of the diurnal variation current system, near midnight, the horizontal component would be little affected by the currents induced by the moving S_q current system. The strength of Price's calculated induced earth-current system would vary with the amplitude of the S_q variation, which varies by a factor of about 2 with the sunspot cycle. Consequently, Price's calculated induced earth-current system should give rise to a variation with sunspot cycle in the horizontal field near midnight near the equator but not near middle latitudes. However, the field of the external equatorial ring current (ERC) system also varies during the sunspot cycle, but in

such a manner that its magnitude is a simple function of latitude.

Three-hour means of H centered near local midnight were averaged for all (60) quiet days of each year from 1944 to 1959 for Tucson, Arizona, and Huancayo, Peru. The yearly averages for Tucson and for Huancayo indicated large but linear secular variations, which were removed, leaving a solar-cycle variation in H at Tucson that is due only to the solar-cycle variation in the strength of the ERC. The solar-cycle variation in H near midnight at Huancayo arising from the ERC could be reliably estimated from that in H at Tucson by multiplying the latter by $\cos \theta_1 / \cos \theta_2$, where θ_1 and θ_2 are the geomagnetic latitude, respectively, of Huancayo and of Tucson. From the solar-cycle variation observed in these values of H at Huancayo the solar-cycle variation in H for Huancayo as computed from the Tucson results was deducted. The difference was essentially constant within about ± 5 gammas and showed no appreciable variation with sunspot cycle, indicating no appreciable horizontal component near midnight that could arise from earth currents induced by the moving S_q current system. These results have an important bearing on electrical conductivity models for the earth's interior.

Solar-Cycle Variations of Cosmic-Ray Intensity, Cosmic-Ray Activity, and Geomagnetic Activity, 1937-1961

In considering models to explain the solar-cycle variation of cosmic-ray intensity it is desirable to know its phase relative to that for geomagnetic activity and cosmic-ray activity. Continuous data for cosmic-ray ionization from Huancayo were available for the interval 1937-1961. During this interval the period of the sunspot cycle was 10.0 years. Therefore, for the interval 1937-1961, the amplitude and time of maximum were determined for the 10-year waves in each of the following variates: cosmic-ray ionization (Huancayo), cosmic-ray activity (Huan-

cayo), geomagnetic activity, and sunspot numbers. For these 10-year waves the *maximum* for magnetic activity occurs about 3 months after that for sunspot numbers, the *minimum* for cosmic-ray ionization occurs about 6 months after the *maximum* for sunspot numbers or about 3 months after the *maximum* for magnetic activity, and within the statistical uncertainty the *maximum* for cosmic-ray activity occurs about the same time as the *maximum* for geomagnetic activity. The amplitudes of the 10-year waves in sunspot numbers from three 10-year intervals beginning the first day of 1937, 1947, and 1951 were, respectively, 61, 84, and 101, which were well correlated with the corresponding amplitudes for geomagnetic activity, cosmic-ray intensity, and cosmic-ray activity. Estimates of the lower limit for statistical uncertainties in differences between times of maxima were derived.

Differences ($D - Q$) from yearly means on magnetically disturbed and quiet days for cosmic-ray intensity were compared with those for the equatorial geomagnetic ring current field (ERC) relative to the magnitude, $(S - C)_q$, of their respective solar-cycle variations for quiet days. For cosmic-ray intensity, $(S - C)_q / (D - Q)$ is about 10 times that for ERC. $(S - C)_q$ in ERC probably arises entirely from the fact that yearly means of ERC for quiet days are generally not free of the effect of preceding storms. If this effect were comparable for cosmic-ray intensity, for which the recovery from observed magnetic-storm decreases occurs at a rate comparable to that for ERC, then $(S - C)_q / (D - Q)$ for cosmic-ray intensity should be comparable to that for ERC. It seems clear, then, that the $(S - C)_q$ variation in cosmic-ray intensity is not directly due to the cumulative effects of cosmic-ray-intensity decreases often observed during magnetic storms. During the solar cycle a state prevails in interplanetary space, or beyond, which results, except near solar minimum, in a persistent lowering of cosmic-ray inten-

sity, even on magnetically quiet days, that is not directly due to storm-time decreases in cosmic-ray intensity. This conclusion appears to be in accord with the apparent lag in the *minimum* of the solar-cycle variation in cosmic-ray intensity relative to the *maximum* in the solar-cycle variation in geomagnetic activity.

Cosmic-Ray Program

Observations and reductions of data. Cosmic-ray ionization chambers were operated throughout the report year at

Huancayo, Peru, and at Fredericksburg, Virginia. Scalings and reduction of records have been maintained current for Fredericksburg and Huancayo.

Cooperation in operation of cosmic-ray meters. Grateful appreciation is expressed to the U. S. Coast and Geodetic Survey and the staff of its magnetic observatory at Fredericksburg, Virginia, for efficient operation of the meters during the past report year, and to the Government of Peru and the Director and staff of the Instituto Geofísico del Peru for making cosmic-ray records from Huancayo available.

LABORATORY PHYSICS

NUCLEAR PHYSICS

L. Brown²³ and H. Rudin²⁴

Polarized Ion Source

The collaboration of the Carnegie Institution and the University of Basel for studying experimentally the interaction of fast, polarized deuterons and protons with nuclei has produced an instrument of unique capability by uniting the large Department of Terrestrial Magnetism electrostatic generator with the Basel source of polarized ions. This apparatus has been improved markedly during the past year, giving it the expected current of ions and the reliability of operation necessary for useful measurements. The effects of tensor polarization on two reactions have been studied, and further work is now in progress.

The total polarized beam of 10^{-9} ampere reported last year was less than that obtained from the source in preliminary tests in Basel. The current has been raised to 15×10^{-9} ampere by experimentation with the ionizer and replacement of the original two-cylinder ion-optical lens with a unipotential system. At the target

the beam is 6 to 8 mm in diameter, which is large, in comparison with beams of conventional machines, as a consequence of the large volume in which the ions originate. To secure reasonable target geometry the beam is collimated to 4 mm, thereby reducing the usable current to 3×10^{-9} ampere. The unpolarized background current that accompanies the beam is about 8 per cent of the polarized beam for deuterons and 100 per cent for protons. The proton polarization has not yet been verified, but the background measurement gives a good basis for planning work with polarized protons.

The Department of Terrestrial Magnetism scattering chamber was returned from Florida State University and installed. It improves the accuracy of the measurements of deuteron polarization and makes studies of other reactions possible. A larger yield from the analyzing reaction resulted from the use of a better-quality nickel foil on the entrance of the gas target, as it allowed higher pressures of He^3 . The improvements of beam and target add up to counting rates two orders of magnitude greater than those of a year ago.

The refrigeration system for cooling the diffusion pumps in the high-voltage terminal had been a major source of trouble.

²³ Carnegie Institution Fellow.

²⁴ Carnegie Institution Fellow and Fellow of the Swiss National Foundation.

Complete reconstruction proved necessary, after which no further difficulties arose.

The $\text{He}^3(d, p)\text{He}^4$ reaction is more interesting than just as a means of measuring the polarization of the beam. A compound nucleus, composed of the basic nuclear elements, an α particle and a proton, furnishes a satisfactory explanation for all observed measurements at bombarding energies in the 100-kev range. Such a picture is no longer valid at the higher energies now within the capabilities of the Department's equipment, and information about the direct interaction can be obtained. Measurements of the effect of a tensor polarized beam show a substantial change in asymmetry between 1500 kev and 700 kev. This study is being continued over the energy range of the generator. The measurements of beam polarization at constant bombarding energy give consistent values. A constant beam polarization is, of course, an essential experimental requirement. A discrepancy exists between the predicted value of $P_{zz} = -1/3$ (see *Year Book 61* for a discussion of tensor polarization) and the measured value of $P_{zz} = -0.266 \pm 0.011$ for deuteron energy $E_d = 705$ kev. The cause must be explained by the energy variation of the reaction, an instrumental effect not yet mastered, depolarization of the beam, or incorrect theory as applied either to prediction of beam polarization or to angular distribution of the protons.

J. R. Rook and L. J. B. Goldfarb of the University of Manchester have calculated the angular distribution for the $\text{D}(d, p)\text{T}$ reaction when excited with a polarized beam. Their calculations rest on a few reasonable assumptions and relate the matrix elements (complex numbers) of seven allowed transitions to coefficients of spherical harmonics; three of the coefficients have been measured in studies with unpolarized beams at other laboratories. We have made preliminary measurements of two more coefficients and should soon add another four to the list.

Until more data have been collected it will not be clear to what degree the matrix elements can be evaluated. The matrix elements are important as links connecting experimental measurements with theoretical ideas about the forces that control this simple but imperfectly understood interaction.

BIOPHYSICS

E. T. Bolton, R. J. Britten, T. J. Byers,²⁵ D. B. Cowie, B. Hoyer,²⁶ B. J. McCarthy, K. McQuillen,²⁷ and R. B. Roberts

Introduction

During the report year the work of the Biophysics Section has centered around the application of a new technique to fundamental biological problems. In general such problems exist because there are insufficient means by which to investigate them rather than because they are not recognized or because they are merely ignored. A new method suited to meet the old challenges is therefore most welcome.

In *Year Book 61* a method for studying complementary interactions of nucleic acids was reported briefly. The past year's work extends the studies and demonstrates the versatility of the new procedures; for example, the kinetics of synthesis of "messenger" RNA, the fractionation of complementary nucleic acids, the transcription of genetic information in bacteria, and the measurement of genetic relatedness among organisms have been investigated. These and related studies are reported below.

The DNA-Agar Method

A solution of high-molecular-weight DNA is heated to 100°C for several minutes, a procedure that melts the hydrogen bonds holding the two strands together and yields single-stranded DNA.

²⁵ Postdoctoral Fellow, U. S. Public Health Service.

²⁶ Visiting Investigator, NIH, Rocky Mountain Laboratory, Hamilton, Montana.

²⁷ Carnegie Institution Fellow.

This hot solution is mixed with a hot solution of agar, and the mixture is cooled. Upon cooling, the agar gels around the DNA strands and effectively immobilizes them. The semisolid mass is then passed through a sieve to provide a suspension of particles of DNA agar. These particles are very open structures and will allow even large molecules to diffuse freely. After washing, the particles are incubated for several hours with solutions of radioactive RNA or radioactive, sheared, denatured DNA. If the radioactive nucleic acid contains molecules complementary to regions in the embedded DNA, they will combine to form duplexes. The incubated preparation is then washed to remove uncombined radioactive nucleic acid. By altering the conditions, for example by raising the temperature or lowering the salt concentration, the radioactive strands

are released from the immobilized DNA and can be collected for further study.

The key element of this procedure is, of course, the immobilization of the DNA. Another method for achieving this, in which single-stranded DNA is cross-linked by the action of either ultraviolet light or dilute nitrous acid to give pure DNA gels that also can form duplexes with complementary nucleic acids, is being tested. It appears promising but has not yet been studied sufficiently to permit further comment.

Kinetics of Synthesis of Messenger RNA

Results of the interaction between the RNA produced in *E. coli* immediately after bacteriophage T2 infection and various DNA-agar preparations are shown in figure 29, where it can be seen that

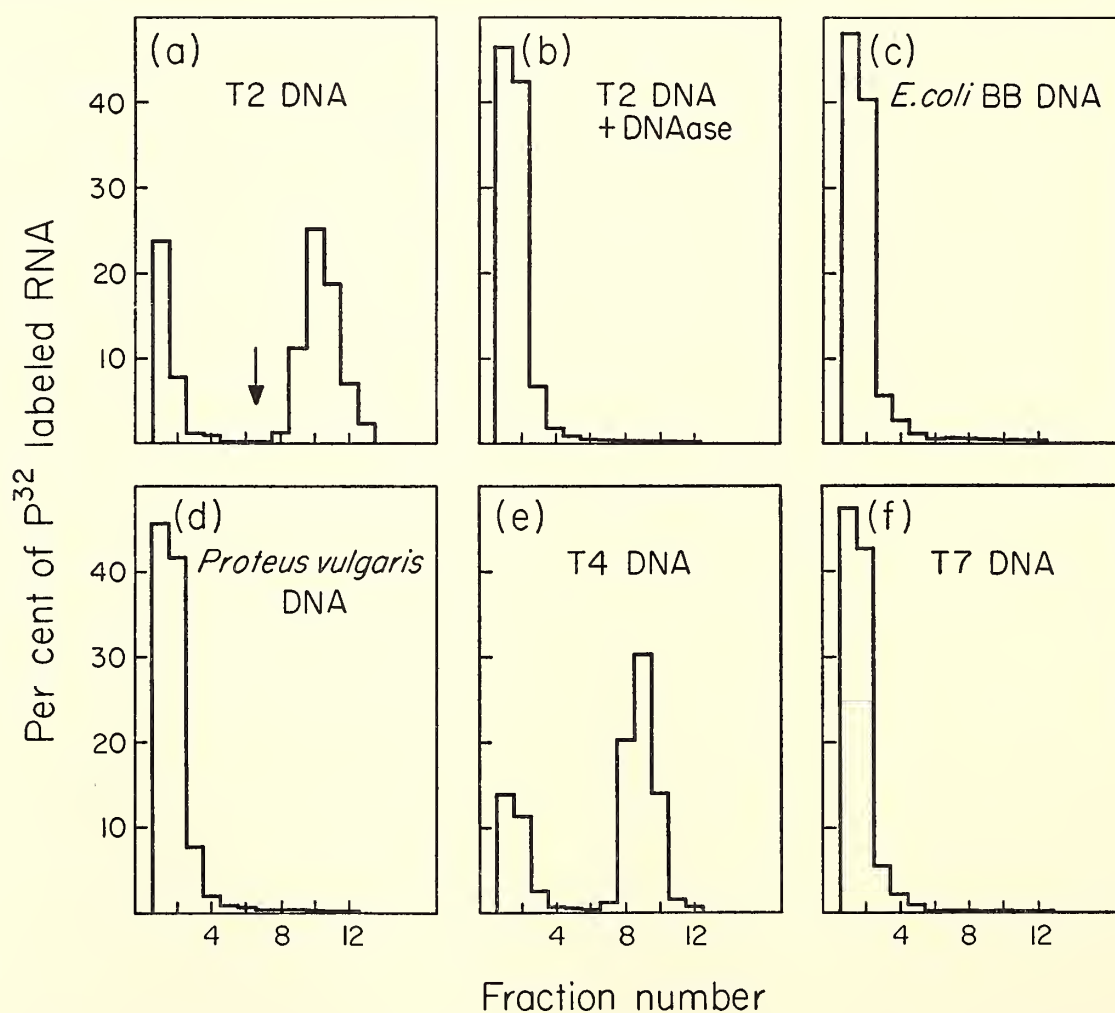


Fig. 29. The specificity of the adsorption of T2-specific RNA to columns of DNA-agar gel. Fifty micrograms of RNA prepared from T2-infected cells labeled after infection with P^{32} was incubated for 15 hours with 1 gram of agar gel containing 0.5 mg of DNA from various sources. Eluting solution was changed at fraction 7. Fractions were assayed for the percentage of the P^{32} -labeled RNA. (a) Agar containing T2 DNA. (b) T2 DNA trapped in agar and treated with DNase at 20 $\mu\text{g}/\text{ml}$ for 2 hours at 25°C. (c) *E. coli* BB DNA. (d) *P. vulgaris* DNA. (e) T4 DNA. (f) T7 DNA.

considerable interaction has taken place between the phage-specific RNA and the phage DNA (a). On the other hand, the RNA does not combine with a preparation from which the DNA has been removed by enzyme action (b), nor is there interaction with the bacterial host DNA (c) or the DNA of another bacterial species (d). Interestingly, there is a large cross reaction between T2-specific RNA and the DNA of phage T4 (e) but no interaction with the DNA of phage T7 (f). These results show that duplex formation is DNA dependent and that it is highly specific. Nevertheless, the cross reaction noted between T2 and T4 suggests the possibility of determining genetic relatedness among species—a possibility that has, in fact, been realized and is well documented by results reported below.

Interaction between the rapidly labeled RNA of bacteria and DNA agar is also highly specific, as figure 30 demonstrates. *Proteus vulgaris* was chosen for these experiments because the guanine plus cytosine content of its DNA (38 per cent GC) is very different from that of ribosomal RNA (52 per cent). This difference provided the opportunity for an unequivocal demonstration that the DNA in agar was, in fact, selecting a special class of RNA molecules whose average nucleotide composition was different from that of ribosomal RNA and reflected that in the DNA. Accordingly, hybridization was

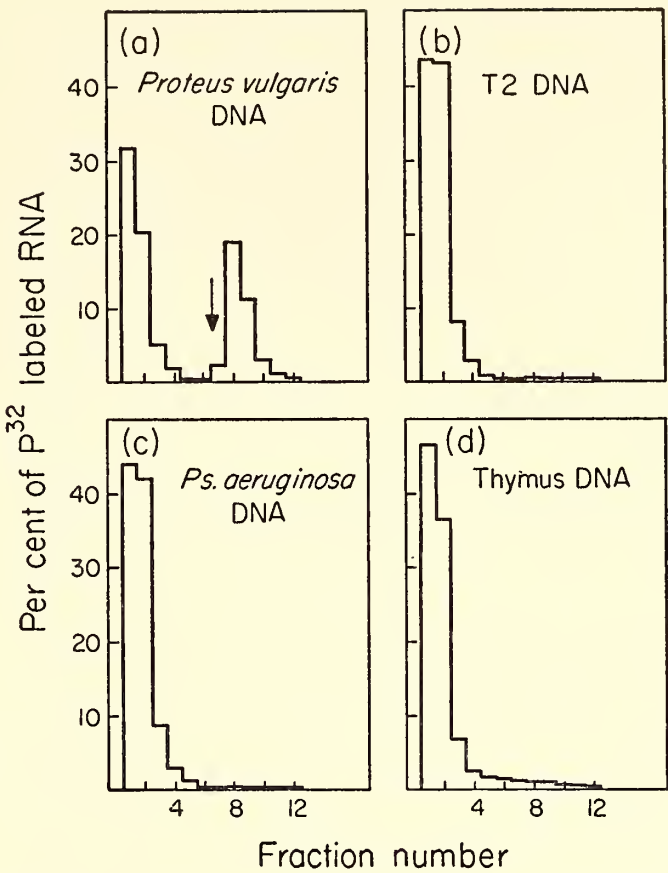


Fig. 30. The specificity of the adsorption of RNA from *P. vulgaris* labeled with P^{32} for 1 minute to columns of DNA-agar gel. Conditions as for figure 29. (a) Agar containing *P. vulgaris* DNA. (b) T2 DNA. (c) *Ps. aeruginosa* DNA. (d) Calf thymus DNA.

carried out as described in figures 29 and 30, and nucleotide analyses were made on the front and back peaks. The results are recorded in table 9, where it can be seen that the base composition of the adsorbed *P. vulgaris* RNA is unlike that of ribosomal RNA and resembles that of the bacterial DNA.

TABLE 9. Base Composition of P^{32} -Labeled RNA Separated by DNA Agar

	Mole Fraction				% GC
	C	A	G	U(T)	
T2-specific RNA					
Unadsorbed RNA 34%	18.4	28.6	24.1	28.9	43
Adsorbed RNA 66%	17.4	31.0	21.9	28.7	39
Bacteriophage DNA	18	32	18	32	36
Pulse-labeled <i>P. vulgaris</i> RNA					
Unadsorbed RNA 65%	22.5	23.3	32.1	22.1	55
Adsorbed RNA 35%	19.8	30.1	20.9	29.2	41
Purified 14S RNA fraction of <i>P. vulgaris</i> labeled for 5 minutes with P^{32}	22.7	26.7	27.6	23.0	49
<i>P. vulgaris</i> ribosomal RNA	21.7	26.2	31.4	20.7	53
<i>P. vulgaris</i> DNA	19	31	19	31	38

In contrast, the unadsorbed RNA has a composition similar to that of ribosomal RNA. Other experiments have shown that relatively few DNA sites are capable of forming hybrids with ribosomal RNA. These sites are filled by RNA of low specific radioactivity, since the newly formed (C^{14} -labeled) ribosomal RNA is diluted by the bulk of the ribosomal RNA that was formed earlier and lacks C^{14} .

The separation of pulse-labeled bacterial RNA into two components and the consequent purification of the D-RNA make it possible to study the rate of synthesis of the D-RNA. Previous studies of the kinetics of labeling of the rapidly labeled 14S fraction, often referred to as "messenger" RNA, have been concerned with a mixture of ribosomal RNA precursor (R-RNA) and D-RNA. As a result the quantity and half-life of the D-RNA molecules could only be estimated by correlation of the results of kinetic studies and the changes in base composition of the total RNA with time of labeling. The present method permits the measurements to be made directly.

Cells of *P. vulgaris* were grown for

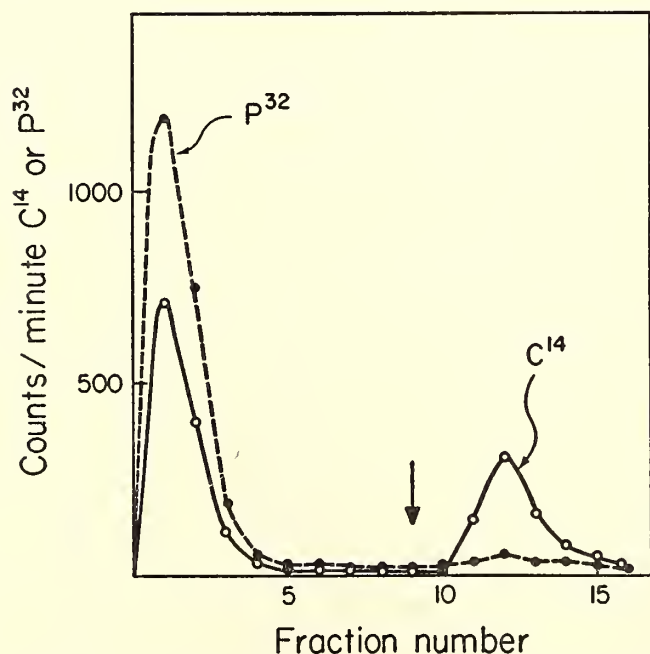


Fig. 31. The adsorption of *P. vulgaris* RNA labeled for three generations with P^{32} and for 1 minute with C^{14} -uracil to a column of DNA-agar gel. Incubation 15 hours at 60°C . Elution with eight 5-ml portions of $2 \times \text{SSC}$ followed by eight 5-ml portions of $0.01 \times \text{SSC}$.

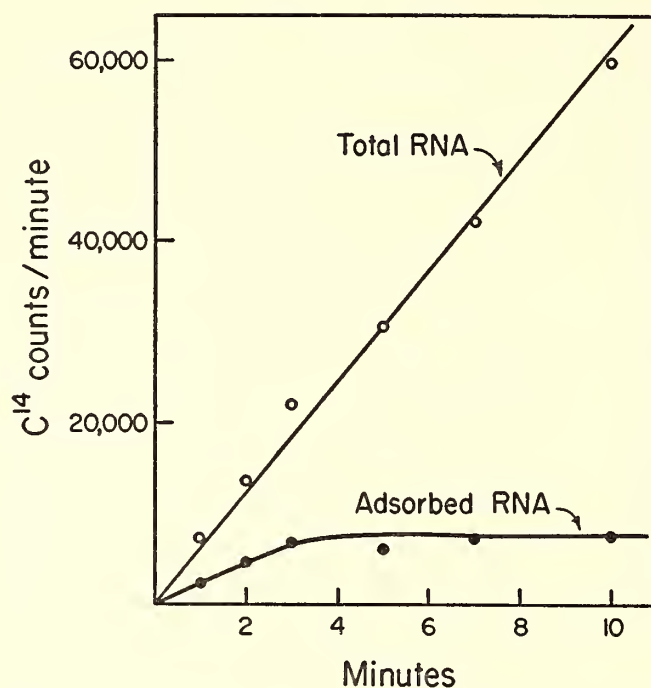


Fig. 32. The rate of synthesis of RNA adsorbable by a DNA-agar gel column. Six samples of RNA from *P. vulgaris* cells grown for three generations in P^{32} with a generation time of 72 minutes were taken after exposures of 1, 2, 3, 5, 7, and 10 minutes to C^{14} -uracil. Each was incubated with an agar gel containing *P. vulgaris* DNA, $30 \mu\text{g}$ RNA/ 0.5 mg DNA (see figure 31). The C^{14} cpm in the total RNA and the adsorbable material was normalized for the amount of RNA employed by means of the P^{32} cpm and plotted against time. Data from figure 31 and five additional analyses.

three generations in C medium containing P^{32} . The generation time was 72 minutes. C^{14} -uracil was then added, and samples were taken for the isolation of RNA after 1, 2, 3, 5, 7, and 10 minutes.

Thirty micrograms of each of the RNA samples was then incubated for 15 hours at 60°C with agar gel containing 0.5 mg of *P. vulgaris* DNA. The fractionation of the 1-minute sample is shown in figure 31. It is evident that about one-third of the C^{14} -labeled RNA is in the hybrid peak and is accompanied by only a small fraction of the total RNA as represented by the P^{32} label. The C^{14} and the P^{32} radioactivity in the front and back peaks were computed for each time point. After normalization to the same size sample of RNA by means of the total P^{32} eluted, the C^{14} radioactivity in the total RNA and in the adsorbed peak was plotted (fig. 32).

The rate of entry of C^{14} -uracil into total

RNA produces a straight line through the origin as in *E. coli*. Apparently the initial rate of entry of label into the D-RNA accounts for about one-third of this flow. The entry of C^{14} -uracil into the D-RNA soon levels off, indicating an average lifetime of about 2 minutes for these molecules. Estimation of the quantity of D-RNA from these kinetics is made somewhat inaccurate by the large correction at late times, but the curve suggests an amount corresponding to the RNA synthesized during 1 minute; i.e., approximately 1 per cent of the total RNA content. This quantity has been carefully determined in *E. coli* as 1.2 per cent of the total RNA.

This application of the method to the rapidly labeled RNA of bacteria has resulted in considerable clarification of some questions relating to messenger RNA. The labeled RNA, all of which is present in the 14S peak in extracts made after short exposures to P^{32} , can be cleanly separated into two types of molecule easily distinguishable by their base composition. The 14S RNA comprises 3 per cent of the total RNA. Hence, at least half of the RNA commonly referred to as "messenger" as judged by its sedimentation coefficient and its high rate of labeling is actually ribosomal RNA, presumably in some precursor stage before entering ribonucleoprotein particles. Moreover, the fact that such a high proportion of the P^{32} enters ribosomal RNA in 1 minute shows that the rate of synthesis of the D-RNA fraction cannot be higher than that of the bulk RNA. Rather, it seems that approximately one-third of the total cellular synthesis of RNA is in the form of D-RNA. The final level attained by the C^{14} -uracil in the D-RNA peak demonstrates that about 1 per cent of the cellular RNA of growing cells is in this form. This estimate depends upon quantitative removal of the D-RNA by the DNA-agar column. The base analysis of the separated R-RNA and D-RNA (table 9) shows that the removal was highly effective.

Measurement of the rate of labeling of the hybridizable RNA with C^{14} -uracil indicates an average lifetime of these molecules of about 2 minutes, which is similar to that of the β -galactosidase forming unit. Such a period of activity on the part of template- or messenger-RNA molecules, which should form part, at least, of the D-RNA fraction, would allow the direction of the synthesis of perhaps fifty protein molecules. The participation of template RNA in protein synthesis would therefore appear to be catalytic rather than stoichiometric.

DNA-RNA Hybrid Formation as an Indicator of Genetic Activity

The reaction of denatured DNA fragments with DNA trapped in agar. The binding of RNA to the DNA-agar material seems to be the result of hybrid DNA-RNA double strands. A similar reaction can be demonstrated in which both reacting nucleic acids are DNA. Some of the conditions necessary for fixation of DNA to the column material are shown in table 10. In these experiments 100 mg of P^{32} -labeled DNA containing either 11 or 20.5 μ g of DNA was incubated at 60°C for 15 hours with 0.2 ml of a solution of P^{32} -labeled DNA in $2 \times$ SSC. (SSC = standard saline citrate = 0.15 M NaCl, 0.15 M Na citrate solution.) The unadsorbed DNA was then removed by elution with 100 ml of $2 \times$ SSC, and the bound DNA was dissociated by raising the temperature to 75°C and reducing the salt concentration to $0.01 \times$ SSC. The number of micrograms of DNA adsorbed is recorded in table 10. The ratio of this amount to the DNA present in the agar gives a measure of the fraction of nucleotide sites participating in DNA duplex formation.

In the first series of experiments both native and sheared DNA were used, and each was tested before and after heat denaturation. It is evident that high-molecular-weight DNA will not function in the reaction even after denaturation. Reduction of the molecular weight by

TABLE 10. Effect of Heating and Shearing on the Ability of DNA to Bind to a DNA-Agar Preparation

The 100 mg of DNA agar used contained 11 μ g of DNA in the first four experiments and 20.5 μ g of DNA in the other two.

Treatment of DNA		Micrograms Incubated	Micrograms Fixed	$\frac{\text{DNA bound}}{\text{DNA in agar}} \times 100$
1	Native	57	0.16	1.4
2	Native, denatured	57	0.27	2.5
3	Sheared	64	0.85	7.7
4	Sheared, denatured	64	5.2	47
5	Sheared, denatured	24	6.1	29.6
6	Sheared, denatured, and incubated 16 hours in $2 \times \text{SSC}$ at 60°C	24	2.5	12.2

shearing did increase the binding ability of the native DNA marginally. The sheared and denatured DNA preparation showed by far the most reaction. Calculation of the amount of DNA bound showed that approximately half of the DNA in the agar preparation had reacted.

In any attempt to renature denatured DNA molecules with trapped DNA molecules there are of course two types of reaction. In addition to duplex formation between the free and the trapped DNA, the free DNA molecules in solution also have a tendency to combine. The relative extent of these two competing reactions depends on detailed experimental conditions such as the ratio of the amounts of free and trapped DNA and the ratio of the volume within the gel to that outside. The last two experiments of table 10 do, however, demonstrate this competition. In one experiment 24 μ g of sheared, denatured DNA was incubated with 100 μ g of DNA agar under standard conditions. A duplicate sample of DNA was incubated alone for 16 hours at 60°C , then added to 100 mg of DNA agar for the standard incubation. The results show that preincubation of the DNA sample reduces the amount bound to the DNA in the column by some 60 per cent. This agrees with the fraction of renatured molecules of DNA encountered under these incubation conditions. Thus the formation of double strands in the population of free DNA molecules reduces the

yield in the reaction with the bound DNA.

Saturation of a DNA-agar column with RNA or DNA. A question of practical and theoretical importance is concerned with the extent to which DNA can still function in double-strand formation after being trapped in the agar. Accordingly, experiments were carried out in which DNA agar was incubated with increasing amounts of RNA, and the amount of RNA bound was determined. Since the amounts of RNA bound were small, measurements of either ultraviolet absorption or of a random isotopic label were inappropriate. Therefore, the experiments were performed with a mixture of pulse-labeled RNA and unlabeled carrier RNA. A sample (2.5 μ g) of standard P^{32} pulse-labeled RNA was mixed with increasing amounts of a preparation of unlabeled total RNA. All incubations were carried out with 100 mg of DNA agar containing 20.5 μ g of DNA in a total volume of 0.3 ml of $2 \times \text{SSC}$ at 60°C for 15 hours.

After the usual elution program the fraction of the P^{32} -labeled RNA bound was determined. The determination showed that 23.5 per cent of the P^{32} -labeled RNA corresponded to 1.20 per cent of the total RNA. This conversion factor was used to estimate, from the amount of RNA added, the amount bound to the DNA. Although neither the fraction of P^{32} present in messenger RNA molecules nor the percentage of the total

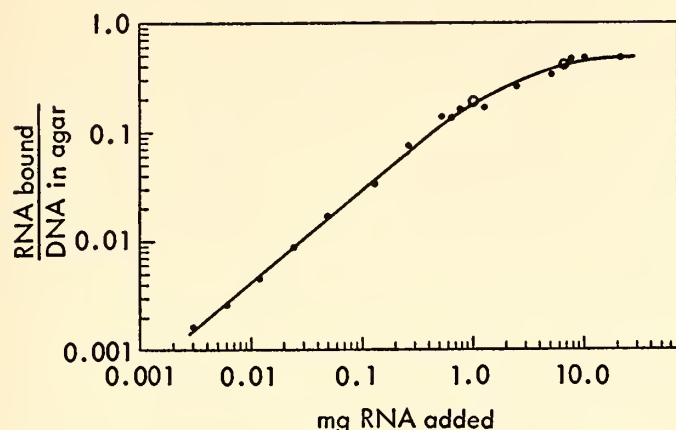


Fig. 33. Saturation of a DNA-agar column with RNA. The ratio of the amount of messenger RNA bound to the DNA agar to the DNA present in the agar is plotted as a function of the amount of total RNA present in the incubation mixture. One hundred milligrams of agar containing 20.5 μ g of DNA was used in each incubation. The open circles represent direct measurements of the amount of RNA bound from ultraviolet absorbance in incubations with 1 gram of agar containing 20.5 μ g of DNA.

RNA represented by the messenger fraction is known with any great precision, a value can confidently be assigned to their ratio. It is this ratio that is used in the calculation of the amount of bound RNA.

Since these experiments were conducted over a wide range of RNA concentrations the results were plotted on logarithmic coordinates (fig. 33). The points represent quantities of RNA bound, calculated by the method outlined above, except for the two marked with circles, which are direct ultraviolet absorption measurements of the amount of RNA bound. For these two points the whole incubation was scaled up by a factor of 10 to provide measurable quantities of bound RNA. To eliminate the trail of unadsorbed RNA very complete washing of the column with $2 \times$ SSC was carried out. These data are in agreement with the experiments in which only the P^{32} -labeled RNA was measured.

One feature of interest is the saturation level where no more RNA can be adsorbed. The fact that this value is essentially 50 per cent leads immediately to the conclusion that the messenger RNA is complementary only to one strand of the

DNA and that essentially all possible molecules are represented in the RNA from a culture of cells. This conclusion is, of course, only one of several possible, but the high figure does show that a large fraction of the DNA remains available after embedding in the agar and that there are in the population RNA molecules representing at least 50 per cent of the sequences in DNA. If an estimate were available of the fraction of the trapped DNA that can enter into duplex formation, the significance of the 50 per cent saturation by RNA would be easier to assess.

An obvious approach is to use the DNA-DNA reaction as a comparison. Since the same elements of nucleotide sequence are represented in the DNA embedded in the agar and in the pieces of sheared DNA reacting with it, the maximum amount of DNA bound should be a measure of the availability of the trapped DNA. Therefore, saturation experiments analogous to those described above were performed with sheared DNA. One-hundred-milligram aliquots of DNA agar containing 20.5 μ g of DNA were incubated with a range of concentration of DNA from 1 to 400 μ g. The results are plotted in figure 34 on a linear scale together with some of the RNA data of figure 33. These figures show that more than 80 per cent

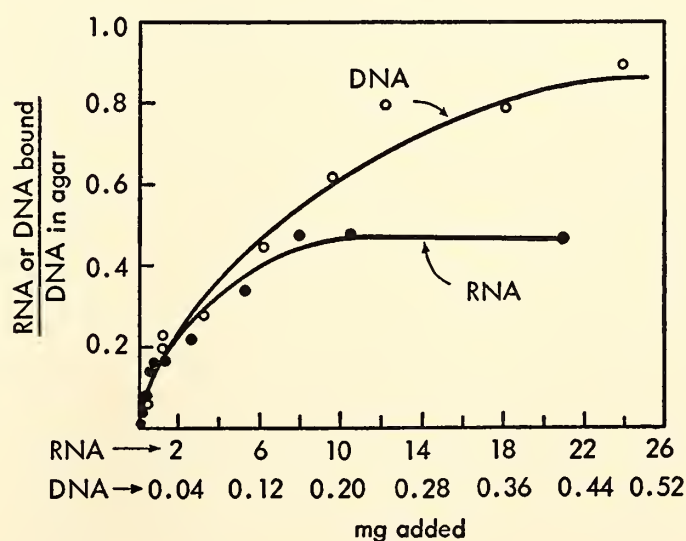


Fig. 34. Saturation of a DNA agar column with RNA and DNA fragments. The RNA curve is taken from figure 33.

TABLE 11. Effect of Preincubation with DNA and RNA on the Binding of P³²-Labeled RNA and DNA to DNA-Agar Preparations

Experiment	First-Day Incubation	Second-Day Incubation with Labeled Nucleic Acids	Micrograms Bound	Per Cent DNA Nucleotide Occupied
1. 200 mg agar containing 41 μ g DNA				
a.	440 μ g sheared DNA	300 μ g P ³² sheared DNA	2.2	5.4
b.	440 μ g sheared DNA	800 μ g P ³² pulse-labeled RNA	1.8	1.4
c.	...	330 μ g P ³² sheared DNA	34.4	84.0
2. 180 mg agar containing 37 μ g DNA				
a.	13.0 mg RNA	363 μ g P ³² sheared DNA	14.3	38.6
b.	...	363 μ g P ³² sheared DNA	28.5	77.0
c.	13.0 mg RNA	800 μ g P ³² pulse-labeled RNA	0.51	1.4
d.	...	800 μ g P ³² pulse-labeled RNA	4.0	10.8
3. 200 mg agar containing 41 μ g DNA				
a.	10.9 mg RNA	217 μ g P ³² sheared DNA	7.0	17.1
b.	16.9	41.2

of the DNA in the agar can accept the sheared DNA in contrast to the 47 per cent available to RNA. Since the DNA is sheared and probably has a molecular-weight distribution around a factor of only about 2, it would not be expected that it could fill all the sites on the high-molecular-weight DNA. Noteworthy also is the fact that for both RNA and DNA the curves do remain level even when a great excess of DNA is used in the incubation. Extension of the capacity of the column by further addition of nucleic acid to extended, unmatched portions of the bound DNA to produce strings of partially helical and overlapping structures does not therefore appear to be a serious problem.

The availability of different fractions of the embedded DNA to RNA and DNA can be demonstrated in another way. A series of experiments were performed in which the DNA-agar preparation was incubated with a large enough quantity of either DNA or RNA to achieve saturation and then reincubated with either RNA or DNA after removal of unadsorbed material. In experiment 1 of table 11 the primary incubation was carried out with DNA. Subsequent incubation with either

RNA or DNA gave very little increase in the total bound nucleic acid. The control experiment in which the DNA agar was preincubated alone showed that 84 per cent of the DNA was available for DNA in the second incubation. In the other experiments a comparison was made between the binding of DNA to DNA-agar preparations preincubated alone or with high concentrations of RNA. In experiment 2 about 40 per cent of the DNA was available to the DNA fragments after preincubation with RNA compared with somewhat less than 80 per cent when no RNA had been previously bound. Parts *c* and *d* of experiment 2 showed that the preincubation with RNA had been sufficient to fill essentially all the sites available to RNA. In experiment 3 the amounts of RNA used in the preincubation were somewhat lower and the P³² DNA concentration was also reduced, but the experiment shows again that approximately half the possible sites are filled by RNA.

Relative abundance of messenger molecules. The data of figure 33 can also be interpreted to estimate the quantities of RNA formed under the direction of different parts of the DNA. The amount

of RNA bound to the DNA increases as more RNA is added. Although at low levels of RNA some 80 per cent of the messenger fraction is adsorbed, as has been shown above, the percentage yield steadily decreases as the amount of RNA is increased. With large amounts of RNA, close to the amount necessary to achieve saturation of the DNA, less than 5 per cent of the messenger fraction is actually bound to the DNA. If the reaction can be regarded as a filling of sites on the DNA by a collection of different added RNA molecules, the above results are consistent with large differences in the relative abundance of the various RNA molecules. The shape of this saturation curve would be a function of the differential activity of the regions of DNA responsible for the various messages.

The primary assumption in the interpretation, that the saturation curve represents the sum of individual saturation functions for the various sites in the DNA, implies that the individual reactions are specific and unaffected by the presence of other polynucleotide molecules in the solution. Thus it is assumed that RNA molecules are totally adsorbed only when there is a vacant homologous site on the DNA. This assumption is justified at low RNA concentrations, since about 80 per cent of the messenger RNA is adsorbed and the 20 per cent loss can be accounted for by loss of the DNA from the column. An experiment to show that it is justified even at very high concentrations is shown in table 12. A very low level of P³² pulse-labeled *E. coli* RNA

was incubated with 0.5 gram of DNA agar. If a large quantity of unrelated RNA such as that prepared from yeast or mouse liver is included in the incubation, no reduction in the amount of P³² RNA bound is observed. That the addition of a similar quantity of homologous RNA does, however, greatly reduce the amount of P³²-labeled RNA bound demonstrates that competition for sites in the DNA is exhibited only by closely related polynucleotide molecules. It should also be noted that all the reactions of messenger RNA with DNA are carried out in the presence of 100 times the concentration of ribosomal and soluble RNA.

The other assumption made is that all the messenger RNA molecules have the same lifetime in the growing cell. The earlier measurements of the rate of labeling of *Proteus vulgaris* messenger RNA indicate that this is so, and the fact that the rate of formation or decay of the enzyme-forming system is similar for several induced enzymes is also consistent with it. Moreover, as appears likely, if the degradation of messenger RNA is a random event, the lifetimes of all molecules would be the same.

From the data of figure 33 the quantities of RNA that are formed under the direction of various portions of the DNA can be estimated. Thus (fig. 35, top) as larger quantities of RNA (*R*) are added a smaller fraction is duplexed with the DNA. The quantity *A* represents RNA molecules for which the corresponding homologous sites in the DNA are fully occupied. Alternatively, as in figure 35 (bottom), we can imagine the sites in DNA arranged in order of their activity in producing RNA replicas. The most active sites might produce many molecules of complementary RNA per generation; and the least active, one molecule or less. The total messenger RNA is represented by the area under the curve of figure 35 (bottom). Area *A* represents unbound RNA; area *B*, RNA adsorbed to DNA sites that are totally occupied; area *C*, RNA adsorbed to unsaturated DNA

TABLE 12. Effect of Addition of Heterologous RNA

P ³² <i>E. coli</i> RNA	Unlabeled RNA		Per Cent P ³² Bound
20 μg	25.5
20 μg	Yeast	10 mg	26.9
20 μg	<i>E. coli</i>	10 mg	6.7
20 μg	<i>E. coli</i>	12 mg	12.3
20 μg	Mouse	2 mg	24.6

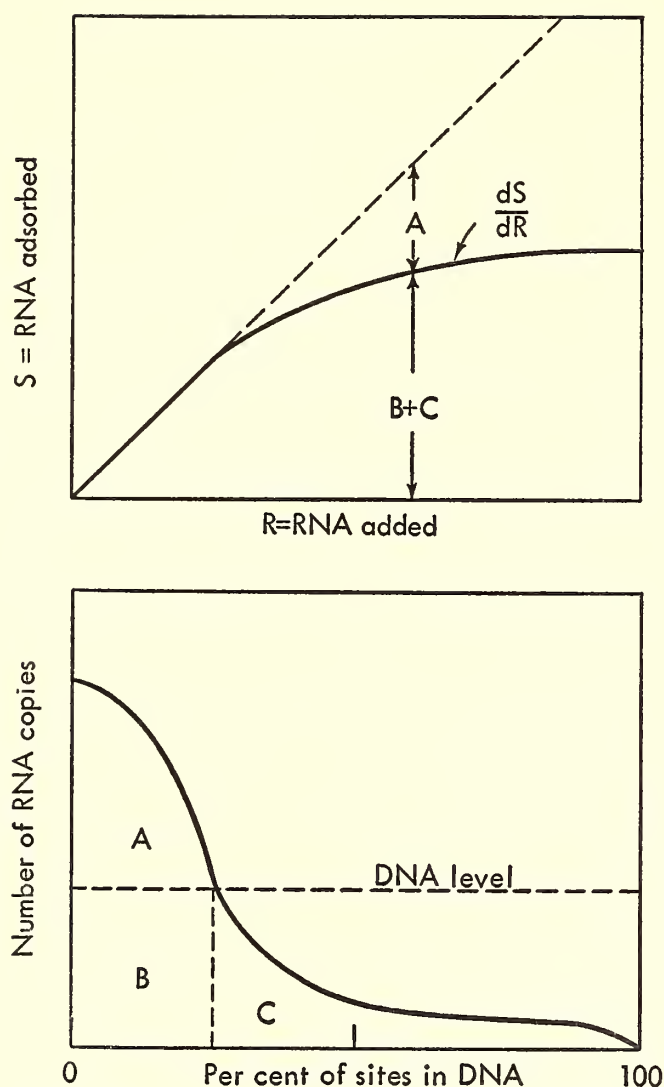


Fig. 35. Schematic diagram illustrating the interpretation of the data of figure 33. In the upper figure the RNA forming a hybrid duplex with the DNA in an agar column (S) is plotted against the amount of RNA added (R). At any given point, A represents the fraction of the RNA molecules for which there are no larger homologous sites available in the DNA, and $B + C$ represents the fraction adsorbed. In the lower diagram the genetic sites in the DNA are arranged in order of their activity in making RNA copies. The total population is represented by the area under the curve. The DNA may be represented by a horizontal line, since, by definition, there are equal numbers of each genetic site. For any experiment the position of this dotted line represents the DNA/RNA ratio employed. Then the area A represents RNA molecules homologous to saturated sites in the DNA; B , to RNA molecule adsorbed on saturated sites; and C , to RNA molecules adsorbed to DNA sites, of which more copies are available.

sites. $R = A + B + C$, and $S = B + C$.

For any RNA-DNA ratio employed in an experiment, the DNA level can be represented on figure 35 by a horizontal line (dotted), since it is assumed that

equal numbers of each genetic site are present. This line divides area A from area B .

The steps in transforming the data of figure 33 into the form required were as follows:

1. The data were replotted in the linear form of figure 34 to allow estimation of A and $B + C$ from the amount of RNA bound, S .

2. The quantity of RNA, C , may be estimated from the slope of the curve. When a small increment of RNA is added, only the fraction, C/R , for which sites remain can be adsorbed. Thus, $dS/dR = C/R$.

3. This allows calculation of B , the amount of RNA bound to DNA sites that are then fully occupied. Then, if D is the weight of DNA present, B/D represents the fraction of the genetic sites responsible for an amount, $A + B$, of RNA product. Therefore, a plot of B/D against the fraction $(A + B)/R$ will represent the activity of various fractions of the DNA in specifying complementary RNA copies. This plot is presented in figure 36.

The curve suggests that the contribu-

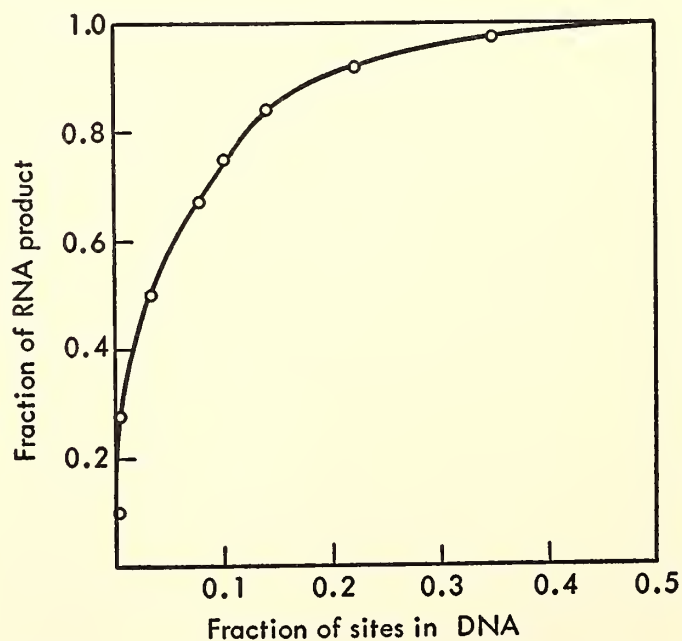


Fig. 36. The differential activity of various sites in the DNA of an *E. coli* culture growing exponentially. The sites are ordered with respect to activity in the production of RNA copies. The fraction of the total RNA product is plotted against the fraction of the corresponding sites in the DNA.

tion of different sites in the DNA in producing messenger RNA is extremely variable. A small fraction of the sites seem to be very active, so that less than 1 per cent of the sites are responsible for some 20 per cent of the product, and about 10 per cent for 75 per cent of the product.

Discussion. The basic finding in the present series of experiments is that the ability of high-molecular-weight denatured DNA to enter into complementary strand formation reactions with either RNA or DNA is not seriously affected by its being immobilized in agar. In the interaction with sheared, denatured DNA fragments an amount of polynucleotide equivalent to more than 80 per cent of the nucleotide residues in the immobilized DNA can be bound. There is as yet no certain measurement of the fraction of the bound nucleic acid that occurs in true helical regions. Nevertheless, the specificity of the reaction and the stability of the structures to increasing temperature and decreasing salt suggest that it is large. On the other hand, regions must exist in the immobilized DNA that are close to the cross-linked agar molecules where base pairing with other nucleic acids becomes impossible as a result of steric hindrance. Perhaps, in these regions the bound molecule can form looped structures or leave free ends. It should be noted, however, that in 3 per cent agar gels the effective pore radius is 800 Å (Acker and Steere, 1962). Even if the trapped DNA were extended between the closest of cross links, the steric impediments would be placed at intervals of about 250 nucleotides. Thus, even in this limiting case, only five such regions would be encountered in the reaction with a molecule of DNA or RNA of the size here employed ($\sim 3 \times 10^5$). The contacts between agar and DNA are probably not so frequent, since DNA of molecular weight less than 5×10^6 daltons is only inefficiently trapped. These considerations suggest that the high degree of functional integrity that has been observed is reasonable.

The capacity to form double-stranded structures with DNA is retained by more than 80 per cent of the entrapped DNA. It is therefore of great interest that no more than approximately half of the entrapped DNA can bind RNA. In a bacterial cell population grown exponentially a very high proportion of the total possible RNA molecules must be represented. It amounts to about half of those possible by copying both strands of the DNA, or essentially all, if RNA is representative of only one of the DNA strands. Taking 1.4×10^9 daltons as the minimum molecular weight of *E. coli*, this would mean a total of 7×10^8 daltons of RNA. Since the messenger RNA fraction of an individual cell amounts to only about 2×10^8 daltons (1.3 per cent of the total RNA), each cell cannot contain all the different messenger molecules at one time even if they are equally abundant. Since the various RNA molecules are almost certainly made at different rates, the number of different RNA molecules present in a cell at one instant is probably a small fraction of the total.

The rate of saturation of the DNA by increasing amounts of added RNA has been used to calculate the differential activity of the various sites in the DNA. It has been assumed that the decreasing fraction of the messenger molecules which are bound as more RNA is added results from filling of the more active homologous sites in the DNA. The fact that the binding is unaffected by the presence of large quantities of unrelated RNA seems to preclude a reduced reaction rate resulting from the large quantities of RNA present. An RNA molecule whose relative frequency in the messenger population is equal to that of its parent cistron in the DNA should saturate its site in the DNA when the amount of RNA added is equal to the amount of DNA present in the agar. From figure 33 it is clear that there are some molecules whose occurrence in the population is perhaps only one-fifth of this. The average rate of synthesis of nucleotides in messenger is

about $0.04 \mu\text{mole/gram}$ of cells/sec compared with about $0.015 \mu\text{mole/gram}$ of cells/sec for DNA. Thus, if RNA is representative of only half of the DNA, the average molecule of RNA would be produced 5 times per generation, and the minimum rate would be 1 copy per generation. At the other extreme there seem to be very active sites in the DNA producing RNA at about 200 times the average rate. Figure 36 shows that less than 1 per cent of the sites are responsible for about 20 per cent of the RNA.

These results may be considered in the light of the hypotheses of Jacob and Monod (1961) relating to genetic regulatory mechanisms. There is evidence that most of the genes function through the production of RNA copies. The very common messenger molecules synthesized at a rate of 200 times the average would be representative of the induced genes. The factor of 200 is consistent with estimates of the increased rate of β -galactosidase synthesis after induction. Between these sites and the most inactive ones in the DNA would be a whole spectrum of rates of genetic expression under greater or less control by regulator genes. Perhaps the rarest RNA molecules represent the regulator genes and the repressor molecules themselves.

The rate of synthesis of messenger, which differs in orders of magnitude from one site to another in the chromosome, must be reconciled with the evidence for sequential replication of the bacterial chromosome. In the experiments of Cairns it appears that only a very small proportion of the DNA is in a single-stranded form at any one time. If RNA were made on single-stranded DNA, the transcription would be possible only at infrequent intervals even though the rate of synthesis of messenger RNA were higher than that of DNA. Perhaps a more attractive mechanism would be the formation of RNA on a double-stranded DNA. Zubay has suggested a possible model in which the RNA made is identical to one strand of the DNA and

complementary to the other. This model would allow transcription of any segment of the DNA irrespective of the stage of replication of the chromosome itself.

Fractionation of Complementary RNA

It is evident from the foregoing results and discussions that many kinds of messages must be sent from DNA to the various cellular factories. It would be of special significance could such messages be separated from one another, for then their chemical constitution could be ascertained, and the information might be interpreted in detailed terms of how the messages transfer information from the gene to the protein product formed.

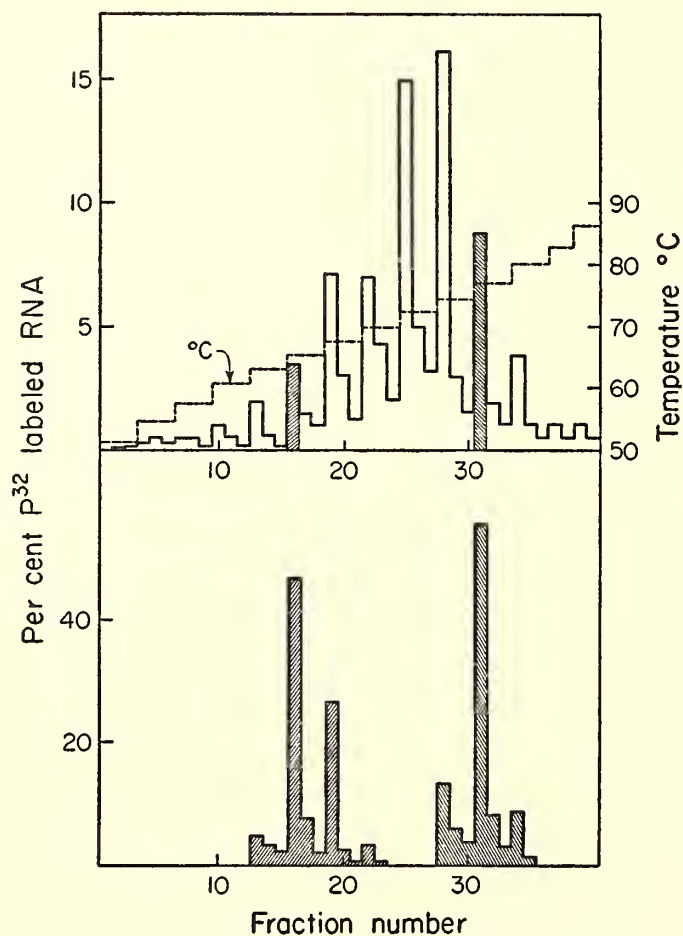


Fig. 37. Fractionation of messenger RNA. *E. coli* DNA agar was incubated with homologous P^{32} pulse-labeled RNA and incubated overnight at 60°C in $2 \times \text{SSC}$. The preparation was then transferred to a heated column and washed at 60°C with $2 \times \text{SSC}$. The eluting solution was changed to $0.1 \times \text{SSC}$, and three 10-ml fractions were collected at each temperature change (right-hand ordinate). The radioactivity eluted is shown on the left-hand ordinate. Aliquots of two fractions (shaded, upper) were separately reincubated and rerun as for the upper diagram. The result is shown on the lower diagram.

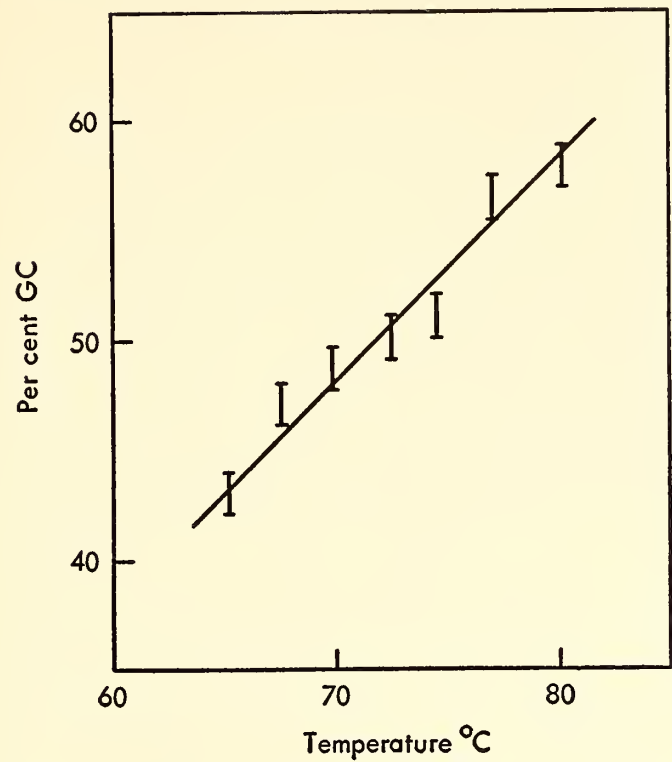


Fig. 38. Chemical composition of fractionated messenger RNA. The nucleotide composition of aliquots of the fractions eluted at each temperature change (fig. 37) was determined by isotope dilution analysis. The guanine plus cytosine content is shown on the ordinate.

A beginning has been made toward fractionating messenger RNA. Advantage has been taken of the knowledge that the strands forming the helical nucleic acid duplexes are separated from one another only after they have been exposed to appropriate temperatures or other environmental conditions.

Figure 37 demonstrates that the RNA-DNA hybrids of *E. coli* may be decomposed by a stepwise increase in elution

temperature to yield unique RNA fractions. In the upper part of figure 37 is an elution diagram for P^{32} -labeled *E. coli* complementary RNA. It is evident from this pattern that, at each change in temperature, radioactive RNA is removed from its combination with DNA in agar. The amount of RNA eluted depends on the temperature employed: a small amount is eluted at 60°C, more at 70°C, and less again at 80°C.

Aliquots of the fractions eluted at 65°C and 78°C were added to C^{14} pulse-labeled *E. coli* RNA, and each of these P^{32} - C^{14} mixtures was separately allowed to incubate with *E. coli* DNA agar. After the two incubated preparations were washed, each was eluted according to the program for figure 37 (top). The C^{14} radioactivity served as an internal standard, and its distribution followed closely upon the P^{32} pattern already observed. The P^{32} of the previously selected fractions eluted at 65°C and 72°C, as it did originally. Thus, it is evident that the selected fractions behave discretely—each repeatedly hybridizes with DNA, and each may be selectively and separately eluted. By inference all the remaining fractions shown in figure 37 would behave similarly. The inference is supported by the result of figure 38. In this illustration the GC content of the several fractions separated in figure 37 has been related to the temperature at which each was eluted. Clearly, each fraction contains RNA of

TABLE 13. Base Composition of Fractions of *E. coli* RNA Separated on DNA Agar

Fraction Number	Temperature, °C	Base Composition				
		C	A	G	U	% GC
1		22.2	25.0	32.1	20.7	54.3
26	65.2	19.7	26.6	23.4	28.9	43.1
29	67.6	23.0	26.4	24.0	26.6	47.0
32	69.7	23.5	25.9	25.2	25.4	48.7
35	72.4	23.6	25.1	26.5	24.8	50.1
38	74.4	24.9	25.1	26.2	23.8	51.1
41	77.0	26.1	23.4	30.3	20.2	56.4
44	80.2	27.3	22.1	30.4	20.2	57.7
Ribosomal RNA		22.0	25.1	32.4	20.5	54.4
DNA		26	24	26	24	52

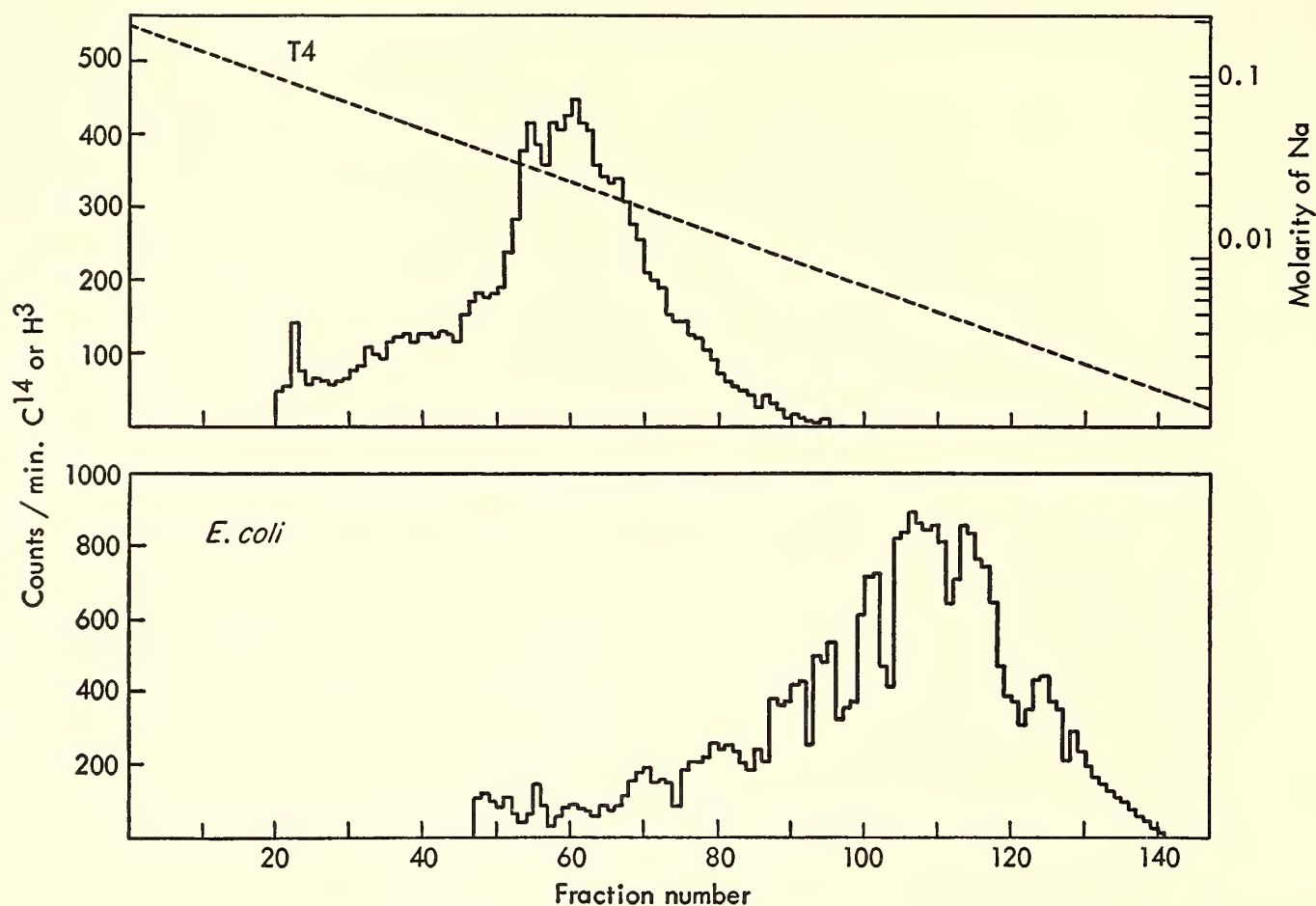


Fig. 39. Fractionation of C^{14} -labeled bacteriophage T4 DNA and H^3 -labeled *E. coli* DNA by means of an exponentially decreasing salt gradient at 65°C .

differing chemical constitution. Thus classes, at least, of RNA messenger molecules have been separated. It is noteworthy that, as seen most plainly at the extremes of the distribution (table 13), the rule of "base pairing" fails. This implies that only a limited region of all the DNA gives rise to a particular messenger molecule, as would be expected from the proposition that individual cistrons are transcribed to yield particular messages.

Another means of separating messenger molecules is illustrated in figure 39. For this separation an exponentially decreasing salt gradient was allowed to flow over an incubated preparation of either T4-specific RNA and T4 DNA agar or *E. coli* RNA and *E. coli* DNA agar. It is evident that the bacteriophage RNA is essentially completely separated from the RNA of the bacteria. It is also seen that the bacteriophage messenger RNA molecules are eluted in a band narrower than that for the bacterial RNA, an observation in

keeping with the relative complexity of the two genomes.

These results demonstrate that the DNA-agar procedure can be adapted to the fractionation of messenger RNA. Individual components have not yet been resolved. Nevertheless, the fractionation methods described show promise in providing chemically distinguishable classes of messenger molecules.

The DNA of Bacteriophage λ

Homology with E. coli BB DNA. The lysogenic bacteriophage λ , which is borne by certain strains of *E. coli*, appears to be intimately associated with a specific locale of the bacterial chromosome. Recently Hershey and his co-workers at the Genetics Research Unit have shown that the DNA of λ had unusual physical properties: centrifugation in sucrose gradients revealed two or more sedimenting forms, and heat denaturation occurred over a broader temperature range than that observed for virulent phages. These

data suggested that adversity of molecular structures, differing especially in size and conformation, might account for the differing physical properties and curious biological attributes observed.

Transduction, a relatively common feature of lysogenic phages, suggests that homology with the bacterial DNA might be a property of the phage DNA. Accordingly, investigations were carried out by the DNA-agar technique to determine whether such homologies could be demonstrated.

It is evident from the data shown in figure 40a that a part of the λ DNA can combine with the DNA of *E. coli*. In this run 26 per cent of the λ DNA was bound to the *E. coli* DNA by complementary double-strand formation. This interaction is in sharp contrast to the results obtained with virulent bacteriophage DNA, where no homology between host and phage DNA can be demonstrated. When sam-

ples of the front and back peaks (fig. 40a) were heated, cooled, and rerun (figs. 40b and c) on fresh *E. coli* DNA agar, only 8 per cent of the front peak material combined but 45 per cent of the back peak recombined. (The low yield in the rerun results from the fact that duplex formation in free solution competes with duplex formation in the immobilized DNA as discussed earlier.) Thus, in the first run an authentic selection of homologous from nonhomologous fragments of λ DNA had been achieved. The proportion of λ DNA that combined with the bacterial DNA in the two runs was 26 per cent + (8 per cent of [100 - 26 per cent]), or 32 per cent. It may be concluded, therefore, that approximately one-third of the λ DNA is homologous with *E. coli* DNA. Conversely, two-thirds of the λ DNA shows no tendency to form stable duplexes with the bacterial DNA and must therefore be quite dissimilar.

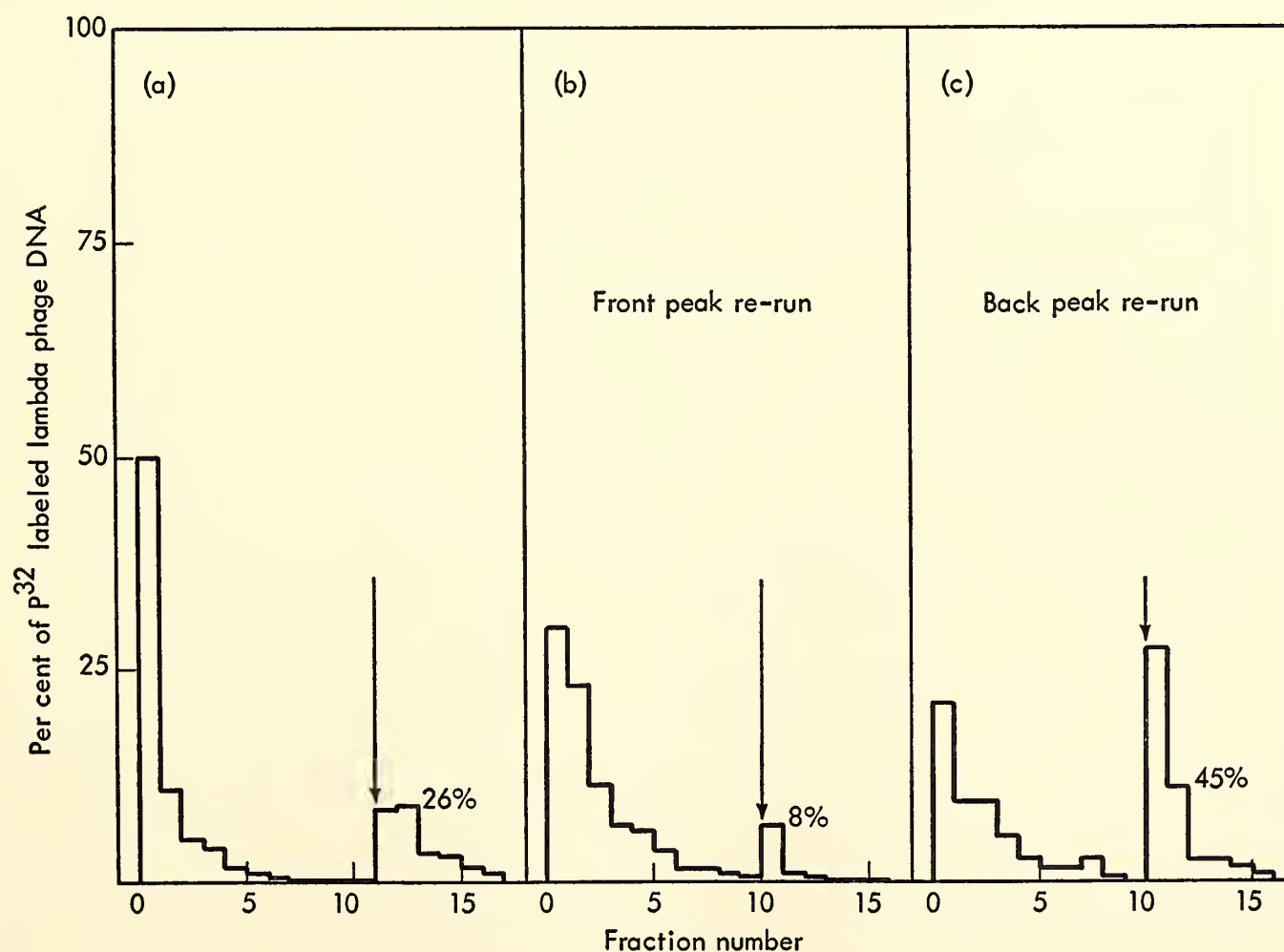


Fig. 40. Reaction of λ DNA fragments with *E. coli* DNA trapped in agar. After incubation at 60°C ten washes were given at 60°C with $2 \times$ SSC. The temperature was then raised to 75°C, and seven 10-ml fractions of $0.01 \times$ SSC were passed through. Equal aliquots of the λ DNA appearing in the two peaks were each reincubated with a similar agar preparation.

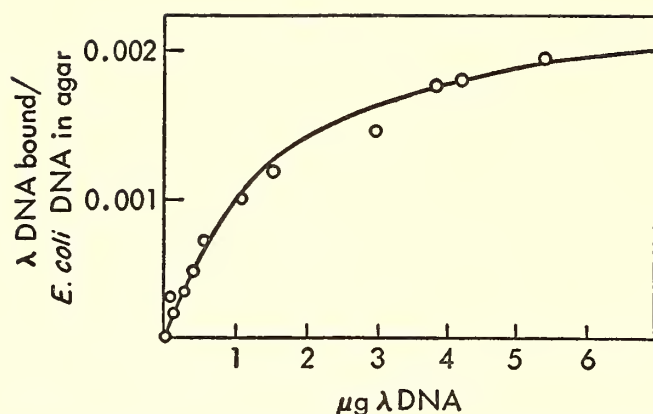


Fig. 41. Reaction of λ DNA fragments with *E. coli* B DNA. Increasing quantities of P^{32} -labeled λ DNA fragments were incubated overnight at 60°C with 0.1 gram of agar containing 30 μg *E. coli* B DNA.

The molecular weight of the DNA of *E. coli* BB. The demonstration that a part of λ DNA may interact with regions of the *E. coli* DNA raises the question of how much of the host DNA is related to the DNA of the lysogenic phage. The extent of the relationship can be determined by simply measuring the quantity of λ DNA fragments (molecular weight $\sim 10^6$) required to saturate a known amount of denatured *E. coli* DNA fixed in agar. The results of such an investigation are shown in figure 41. As the quantity of λ DNA is raised, the amount of complementary double-strand formation increases, approaching, as a limit, 0.2 per cent of the *E. coli* DNA.

This measure of the size of the homologous region provides a means of calculating the molecular weight of the *E. coli* BB DNA:

$$\frac{3.9 \times 10^7 \text{ (molecular weight } \lambda \text{ DNA)}}{\text{Molecular weight } E. coli \text{ DNA}} = \frac{\text{Per cent homologous}}{0.33}$$

$$E. coli \text{ molecular weight} = \frac{1.3 \times 10^7}{0.002} = 6.5 \times 10^9$$

where Hershey's value for the minimum size of λ DNA is used and only a third of the molecule is considered to be capable of stable duplex formation with the *E. coli* DNA.

This value, however, is 5 times greater than the minimum estimate, 1.4×10^9 , recently published by Cairns. Assuming

Cairns' value correct, some explanation is required to account for the excessive quantity of λ DNA adsorbed to the *E. coli* DNA.

One possible interpretation of the data of figure 41 is that the DNA of the λ phage is not completely homogeneous: it may vary from phage to phage. The λ DNA used for these experiments was prepared from ultraviolet-irradiated *E. coli* K12, and the lysogenic phage released from a large bacterial population may well represent a variety of prophage genomes. Thus, in addition to the essential λ parts of the phage DNA, various other parts of the DNA of the host may have been integrated into the various viral entities. Furthermore, the denaturation temperatures obtained for λ DNA by Hershey show a broad range similar to bacterial DNAs, implying large variations in nucleotide sequences.

The possibility also exists that the ultraviolet irradiation liberated other lysogenic forms in addition to λ phage. They would not be detected under normal circumstances, but the DNA from such phages could markedly alter the saturation value expected for a single genetic line of λ .

Genetic relatedness of λ DNA to several strains of enterobacteria. The strain BB of *E. coli* is not normally a host for λ ; nevertheless, homologies between their DNAs exist. It was of considerable interest, therefore, to test other bacterial

DNAs for homology with λ DNA.

The last column in table 14 ranks, in descending order, the degree of homology observed between the *E. coli* DNA and the DNA of the other organisms (from table 15). The homologous regions varied from 71 to 14 per cent of the *E. coli* DNA. The first column in table 14 indicates that

TABLE 14. Binding of λ DNA Fragments to Various DNA-Agar Preparations

Source of DNA	Percentage of Total λ DNA Bound*	Relative Percentage of <i>E. coli</i> DNA Bound
Group A		
<i>E. coli</i> B	6.8	100
<i>E. coli</i> K12 λ	9.5	101
<i>E. coli</i> K12 λ sensitive	5.8	
<i>Salmonella typhimurium</i>	8.2	71
<i>Shigella dysenteriae</i>	13.5	71
<i>Aerobacter aerogenes</i>	11.1	51
Group B		
<i>Klebsiella pneumoniae</i>	0.7	25
<i>Proteus vulgaris</i>	0.2	14
<i>Serratia marcescens</i>	0.3	2
T4 bacteriophage	0.0	1

* The quantity of fragmented λ DNA for each determination was the same, but the quantity of DNA present in the agar was not known precisely. Any value in excess of 1 per cent, however, would represent homology.

λ DNA, which is homologous to only 0.2 per cent of the *E. coli* DNA, is also capable of forming complementary strands with the DNA of some, but not all, of the organisms tested.

Organisms having the highest proportion of DNA homologous to *E. coli* also contained a region homologous to λ (group A). Other organisms (group B) showed little or no relatedness to λ despite the fact that *Klebsiella pneumoniae* and *Proteus vulgaris* contained DNA regions homologous to *E. coli*.

The data in table 14 were obtained by incubating fragmented, heat-denatured λ DNA with DNA-agar preparations of each of the strains of bacteria. The percentage bound (homologous DNA) represents the part of the total λ DNA that remained complexed after washing with 2 × SSC at 60°C. As a further control, a rerun of the fractions of λ DNA obtained from the K12 λ sensitive *E. coli* and the *Serratia marcescens* experiments gave a 37 per cent reaction with the *E. coli* DNA and only 0.7 per cent for the *Serratia marcescens* DNA.

It is probable that the region of the λ DNA that is homologous to the DNA of *E. coli* is also the segment that is complementary to the other DNAs tested.

The results shown in table 14 do not unequivocally allow this conclusion, however, since λ regions showing no affinity for the *E. coli* DNA might be those capable of double-strand formation with the other DNAs. This possibility can be tested by first selecting only λ DNA that is homologous to the *E. coli* DNA. Interaction of the selected material with the other DNAs would be a demonstration that it was only the specific “*E. coli* region” of the λ DNA that was involved. In this connection it is of considerable interest that such a procedure provides a possibility for the physical chemical mapping of the phage and bacterial chromosomes. The procedure is currently being applied in mapping studies.

The Measurement of Genetic Relatedness among Organisms

The presence of genes in common may be taken as a guide not only to taxonomic relationships among organisms but also to probable evolutionary relationships. However, reproductive isolation of distantly related forms precludes the determination of gene similarities by means of the usual methods of genetics.

According to contemporary understanding the nucleotide sequences in

deoxynucleic acids (DNA) represent the total genetic potential of organisms, and sequences held in common are indicative of similar genes.

Since this chemical basis of heredity appears firmly established the *in vitro* detection of genetic homology by physical chemical means is a clear possibility. Moreover, a distinction can be made between the *presence* and the *activity* of genes when similarities and differences among the primary gene products, messenger RNA molecules, are also compared. Thus, RNA molecules that interact with DNA indicate phenotypic similarities; cross-reacting DNA molecules reveal genotypic similarity.

Interaction of E. coli messenger RNA with the DNA of other organisms. The extent of homology between *E. coli* and a variety of other organisms was studied by means of the reaction of *E. coli* pulse-labeled RNA with DNAs from several species. In the homologous reaction some 30 per cent of the rapidly labeled RNA fraction, equivalent to only 1 per cent of the total RNA, is bound. The unbound part is mostly ribosomal RNA of low specific radioactivity. This RNA is homologous to such a small part of the DNA that it contributes little to the bound radioactivity unless the DNA-RNA ratio is extremely high. In figure 42 are shown the actual data for this experiment as well as for three similar ones in which trapped DNAs from other sources were used. With the DNA of two other organisms generally classified with *E. coli* in the Enterobacteriaceae there is appreciable, although lower, binding. An experiment (fig. 42d) in which DNA of calf thymus was used showed no significant reaction. A list of the results of these and other experiments with various DNA preparations is given in the left-hand columns of table 15. In the right-hand columns the percentage of *E. coli* pulse-labeled RNA bound is recorded as 100 and the heterologous reactions are normalized to the homologous reaction.

A number of features are immediately

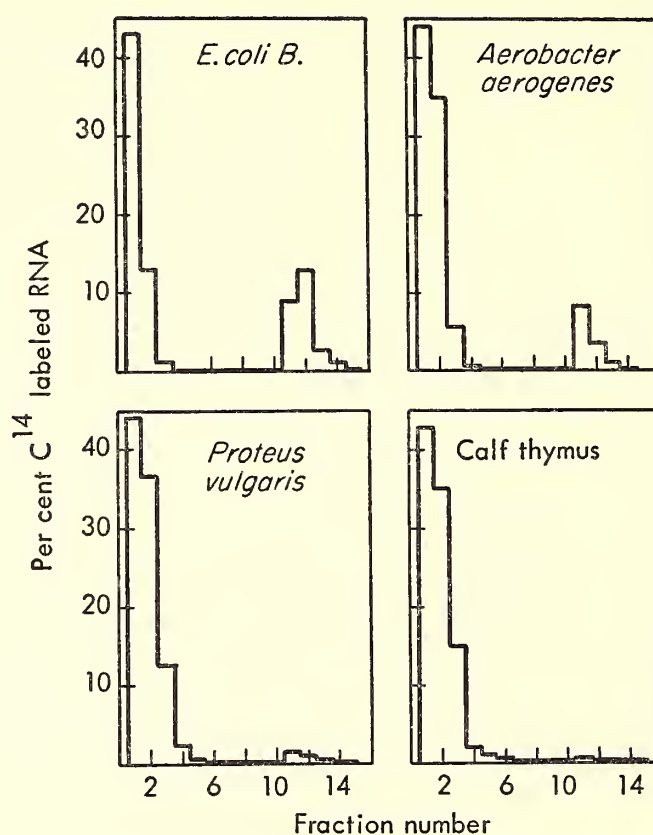


Fig. 42. Reaction of C^{14} pulse-labeled RNA from *E. coli* with agar containing DNA of various bacterial species. Fifty micrograms of RNA prepared from cells labeled for 1 minute with C^{14} -uracil was incubated with 0.5 gram of each DNA agar at 60°C for 15 hours. Ten washes were given at 60°C with $2 \times \text{SSC}$. The temperature was then raised to 75°C , and five 10-ml fractions of $0.01 \times \text{SSC}$ were passed through. The percentage of the labeled RNA appearing in each fraction was then determined.

apparent. The cross reactions are not significant with any of the DNAs of vertebrate origin. The same is also true of T4 bacteriophage DNA and two DNAs from different families of bacteria. On the other hand, two other strains of *E. coli* were not distinguishable from *E. coli B*, the source of the labeled RNA. Likewise, the DNA from two strains of *Aerobacter aerogenes* gave the same amount of cross reaction with *E. coli* RNA. Within the group of enterobacteria the degree of cross reactions ranged between 90 and 10 per cent.

Interaction of E. coli with the DNA of other organisms. Similar reactions are possible where both the interacting nucleic acids are of the deoxy type, provided that a few modifications are made. In order that the free DNA be able to

TABLE 15. Binding of *E. coli* B Pulse-Labeled RNA and DNA Fragments to Various DNA-Agar Preparations

In the left-hand columns are given the results of experiments in which 50 μ g of *E. coli* pulse-labeled RNA was incubated with 0.5 gram of the various DNA-agar preparations. Where *E. coli* sheared denatured DNA was used (right-hand columns) 15 μ g was incubated with a quantity of agar containing 150 μ g of trapped DNA (about 0.5 gram).

Source of DNA	Percentage of Labeled RNA Bound	Percentage of RNA Bound Relative to <i>E. coli</i> DNA	Percentage of Labeled DNA Bound	Percentage of DNA Bound Relative to <i>E. coli</i> DNA
<i>E. coli</i> B	27.0	100	39.8	100
<i>E. coli</i> ML 30	28.6	106		
<i>E. coli</i> K12 λ	26.4	98	40.3	101
<i>Aerobacter aerogenes</i> 211	13.1	48	20.4	51
<i>Aerobacter aerogenes</i> 13048	14.3	53	17.9	45
<i>Klebsiella pneumoniae</i>	5.7	21	10.2	25
<i>Proteus vulgaris</i>	3.0	11	5.5	14
<i>Salmonella typhimurium</i>	23.5	87	27.9	71
<i>Serratia marcescens</i> 4180	2.1	8	2.8	7
<i>Serratia marcescens</i> S.M. 11	1.6	6		
<i>Shigella dysenteriae</i>	23.8	88	27.7	71
<i>Aeromonas hydrophila</i>	1.2	4		
<i>Bacillus subtilis</i>	0.4	1		
<i>Pseudomonas aeruginosa</i>	0.5	2	0.4	1
T2 bacteriophage	0.3	1	0.4	1
Calf thymus	0.4	1	0.5	1
Mouse liver	0.4	1		

penetrate the agar gel to react with the trapped DNA, it must be sheared to reduce its molecular weight. Shearing has the added advantage that the fragments of DNA may be made to resemble the messenger RNA molecules in size and be roughly of cistron or gene length. All the available evidence suggests that messenger RNA molecules are representative of only one strand of the DNA, whereas the DNA fragments contain both complements. This difference introduces a complication because two complementary strands of DNA can form a duplex molecule in free solution as an alternative to combining with trapped DNA. From a practical point of view, then, it is important that the ratio of trapped DNA to sheared DNA be kept large and that in experiments in which comparison is made among homologous and heterologous reactions the ratio be constant.

Aliquots of the same DNA-agar preparations as in the RNA experiments were

used for incubations with *E. coli* C¹⁴-labeled DNA. The ratio of trapped DNA to sheared DNA was maintained at 10 by adjusting the quantity of DNA agar. The right-hand columns of table 15 contain the results. Again, animal DNAs show no significant binding, and the bacterial DNAs show cross reactions ranging from 90 per cent to zero. The extent of homology measured in these DNA experiments is in good agreement with that measured by the binding of RNA.

Agreement of reciprocal cross reactions. For quantitative evaluation of genetic relatedness it is important to know how well reciprocal reactions agree. The reaction of *E. coli* RNA or DNA with the DNA of *A. aerogenes* indicates a 50 per cent cross reaction. The question remains whether the same conclusion would be reached by study of the inverse reaction. A mixture of two sheared denatured DNAs, *E. coli* DNA labeled with C¹⁴ and *A. aerogenes* DNA labeled with P³², was

incubated in parallel with the DNA agar of *E. coli* and the DNA agar of *A. aerogenes*. The ratios of the amounts of each DNA bound in the two experiments indicate the extent of the agreement. As is shown in figure 43, in one experiment the ratio of C^{14} - to P^{32} -labeled DNA is 2, and in the other it is 0.5. Thus, there is good agreement between the two estimates of the fraction of overlapping sequences in the two DNAs. It is perhaps worth noting that this is not a *necessary* result since the total complement of DNA may well differ from one organism to another.

In each of the two parts of figure 43 it appears that the heterologous DNA is rather more easily displaced from the DNA agar than the homologous mole-

cules. Perhaps the fragments of heterologous DNA are not perfectly matched to the immobile DNA strand, and so the resulting structure is less stable.

The results presented demonstrate the potential usefulness of procedures which discern genetic homology at the molecular level. Among bacteria especially, where there exist only the faintest paleontological record and the simplest of all ontogenetic processes, the molecular approach seems most promising for understanding evolutionary relationships. Nevertheless, it might be argued that the mere presence of genes in common is an insufficient basis for judging relationships, since many genes might be dormant and contribute little to the structure or function of an organism. However, the DNA-agar procedure permits quantitative assessment of both potentially active and actually active nucleotide sequences in DNAs. Thus the results with bacterial nucleic acids are equivalent, whether RNA-DNA or DNA-DNA interactions are examined. This observation implies that a quantitatively similar fraction of the genes, perhaps all, in each bacterial type are expressed during exponential growth.

The above estimates of nucleotide sequences held in common among bacterial species are somewhat arbitrary, inasmuch as only the molecules of RNA or DNA that form duplexes stable to 60°C have been considered to be related. It is to be expected that corresponding sites in the DNAs of two related organisms will exhibit a spectrum of similarities, and there is evidence (fig. 43) that some of the heterologous duplexes are more easily dissociated than corresponding homologous ones. Hence, more information could be obtained by testing the stability of the duplexes under a variety of conditions. It is probable that with this modified method more distant relationships may be perceived.

Animal relationships. Experiments with nucleic acids of animal origin have shown that essentially similar techniques can be

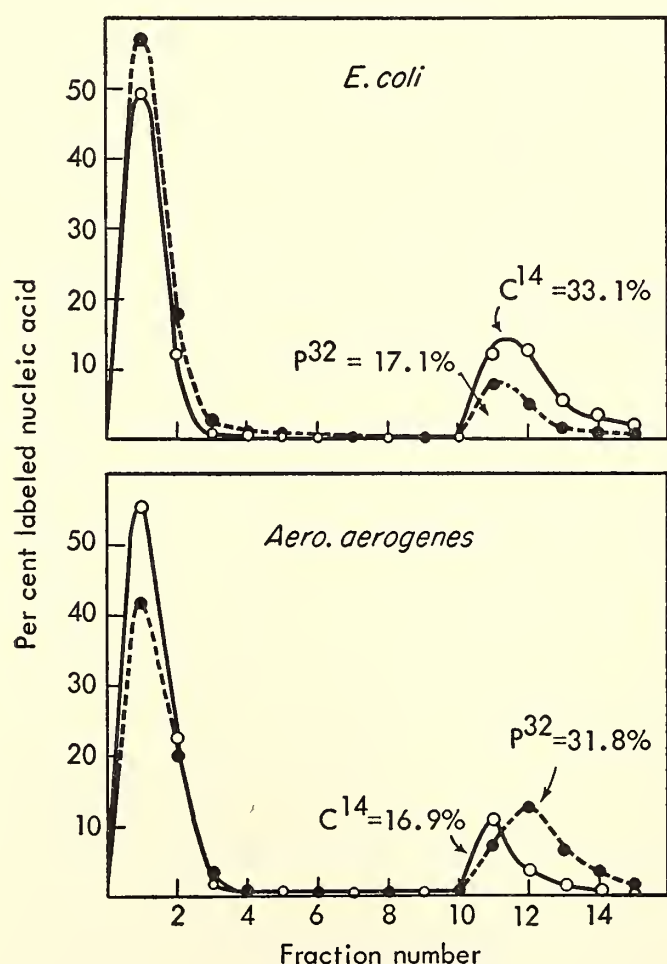


Fig. 43. Reaction of a mixture of DNA fragments of *E. coli* (C^{14} -labeled) and of *Aerobacter aerogenes* (P^{32} -labeled) with the DNA agar of each organism. Thirty-five micrograms of C^{14} -labeled DNA and 25 μ g of P^{32} -labeled DNA were incubated with 0.5 gram of each of the DNA-agar preparations at 60°C for 15 hours. Fractions were collected as in figure 42.

TABLE 16. Binding of DNA Fragments from Animals and Bacteria to Denatured DNA Embedded in Agar

Human DNA was obtained from C¹⁴-labeled Hela tissue culture cells. Mouse DNA was obtained from P³²-labeled BALB/c mouse embryos. About 10 μg of human and 20 μg of mouse DNA fragments were incubated 18 hours at 60°C with about 200 μg of denatured DNA in 0.5 gram agar gel.

DNA in Agar	Per Cent P ³² DNA Bound Relative to the Homologous DNA		
	Human	Mouse	<i>E. coli</i>
Human	100	25	...
Mouse	25	100	0
Rat	15	75	...
Hamster	15	60	...
Guinea pig	15	15	...
Rabbit	15	15	...
Calf	25	10	0
Salmon	5	10	0
<i>E. coli</i>	0	0	100

applied to the study of evolutionary relationships among higher organisms, including mammals.

Table 16 lists some representative results, from which it is clear that there is considerable cross reaction among vertebrate DNAs but none with the bacterial DNA (columns 1 and 2), nor does the radioactive bacterial DNA (column 3) react with the animal DNAs in the reciprocal tests. It is to be noted that the reciprocal tests between the human and mouse DNAs are positive and also agree. The results with the labeled mouse DNA show a progressive decrease in affinity among the rodent DNAs in the order mouse, rat, hamster, guinea pig. Such a progression is in accord with present understanding of the taxonomic relationships among these organisms. The studies with radioactive human DNA (column 1) reveal still another feature of these interactions: there appears to be a strong tendency for the results with the heterologous mammalian DNAs to cluster about a 20 per cent cross reaction. This observation implies the existence of common

genetic material that has been conserved during the course of vertebrate evolution. Other experiments, even though preliminary, have supported the idea that some genetic homology, extending from man to fishes, exists. If, indeed, it does, conceivably the sensitivity of the method may be increased sufficiently to provide new evidence about the most probable line of evolution of the vertebrates from the invertebrates. The possibility presupposes the availability in the present day of forms harboring genes so conservative that they have altered little over eons. The interaction between human and fish DNA gives hope that even such more distant homologies can be found and measured.

Current Status of the Doublet Code

In *Year Book 61* it was mentioned that many of the data on the incorporation of amino acids stimulated by synthetic polymers could be interpreted in terms of a doublet code. During recent months many more experimental data both on amino acid incorporation and on amino acid interchanges in mutants have been produced.

A surprisingly large proportion of the new material is consistent with the doublet interpretation. Many of the predictions of the doublet have been fulfilled; for example, the set of polymers containing only two kinds of nucleotides stimulates the incorporation of almost all the amino acids. There are, however, certain inconsistencies, which may be ascribed to imperfections in the specificity of the cell-free system or may be true implications of inadequacies in the doublet interpretation.

In any event, it is now clear that doublets can carry most of the information and the third member of a hypothetical triplet contributes far less. The doublet code has been of heuristic value, at least, in focusing attention on the significant part of the coding site. Moreover, the doublet interpretation has brought out some surprising relationships between the

structure of the amino acids and the composition of the coding units.

Studies of RNA Synthesis in Euglena

RNA synthesis and its intracellular localization have been studied in *Euglena gracilis*, a single-celled alga possessing chloroplasts and capable of photosynthesis. The intention was to determine whether various aspects of RNA synthesis that had been studied in this laboratory with bacteria could be generalized to an organism structurally more complex. *Euglena* has several attributes that make it a suitable subject for such a study. Its relatively large size (60 microns long) and a large, well defined nucleus (8-micron diameter) make radioautographic studies of the localization of newly synthesized RNA possible. *Euglena* can be grown axenically in a completely defined medium in either light or darkness, and cell division can be synchronized by an alternation of light and dark growth periods. Light-grown organisms become bleached in the dark but rapidly regain their chlorophyll upon exposure to light. Synthesis of protein and a specific fraction of RNA in the plastic fraction has been reported to accompany regreening.

To facilitate the kinetic studies of RNA synthesis, an attempt has been made to prepare isolated *Euglena* nuclei. It has been found possible to break the cells by sonic disintegration in a 50 per cent acetone-buffer medium with a good yield of nuclei free of attached cytoplasmic fragments. Attempts to separate the nuclei by sedimentation or flotation in solvents of high density have not met with much success, however, owing to reaggregation of the fragments and the presence of dense paramylum granules.

Of various tracer compounds tested, C^{14} -guanine and $P^{32}O_4$ have been found useful for studies of RNA synthesis. C^{14} -guanine is taken up specifically into RNA and DNA. $P^{32}O_4$ is taken up into lipides and polyphosphate as well as nucleic acids. The storage of polyphosphate by these cells makes it possible to

get sufficient incorporation of P^{32} into RNA with little delay. *Euglena* may store all the phosphate supplied—enough in fact to allow many generations of growth after exhaustion of the external phosphate. Under these conditions a small quantity of tracer is completely taken up into the pool of low-molecular-weight compounds in a few minutes and passes on into polyphosphate and RNA in a few hours. During the period of constant rate, which lasts for about 2 hours, about 25 per cent of the added P^{32} enters RNA. Uracil, cytidine, and orotic acid are not measurably incorporated by *Euglena*. Formate at low concentrations is utilized primarily for nucleic acid synthesis but at high concentrations is not specifically utilized. Label from thymine and thymidine is incorporated principally into compounds other than nucleic acid.

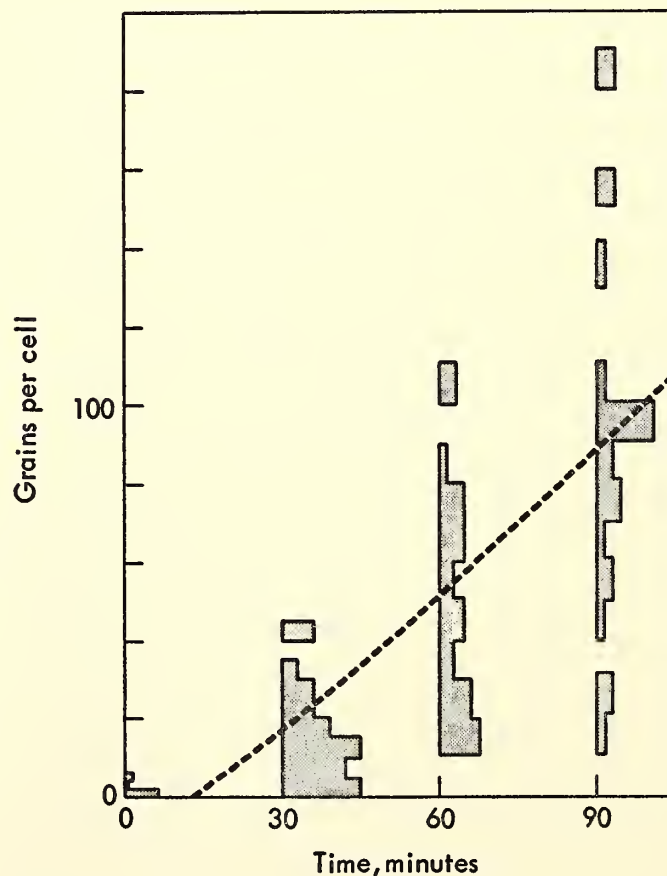


Fig. 44. Increase in total number of radioautographic grains counted over the surface of cells fixed at various intervals after the addition of C^{14} -guanine to the culture medium. Cells were grown in constant light and were in the logarithmic phase of growth. The shaded areas show the distribution observed for 25 cells at each sample time; the dotted line is drawn through the average values.

Radioautographic studies using C^{14} -guanine as a tracer indicate that the greater part of the RNA of *Euglena* is synthesized in the cytoplasm, in contrast to the general observation in other organisms that RNA synthesis appears to occur dominantly in the nucleus. Figure 44 shows the number of grains lying over the whole cell plotted as a function of time of exposure to C^{14} -guanine. Figure 45 shows the grains lying over the nucleus. The spread in number of grains per cell or nucleus is quite large, presumably owing to the variation in the rate of RNA synthesis with time in the division cycle. (The cells were grown in constant light and are randomly phased.) It is clear that on the average only about 25 per cent of the grains appear over the nucleus even at the earliest times (15 minutes corresponds to 0.8 per cent increase in cell mass).

Figure 46 shows the percentage of the radioactivity appearing in the nucleus, uncorrected and corrected for the spread-

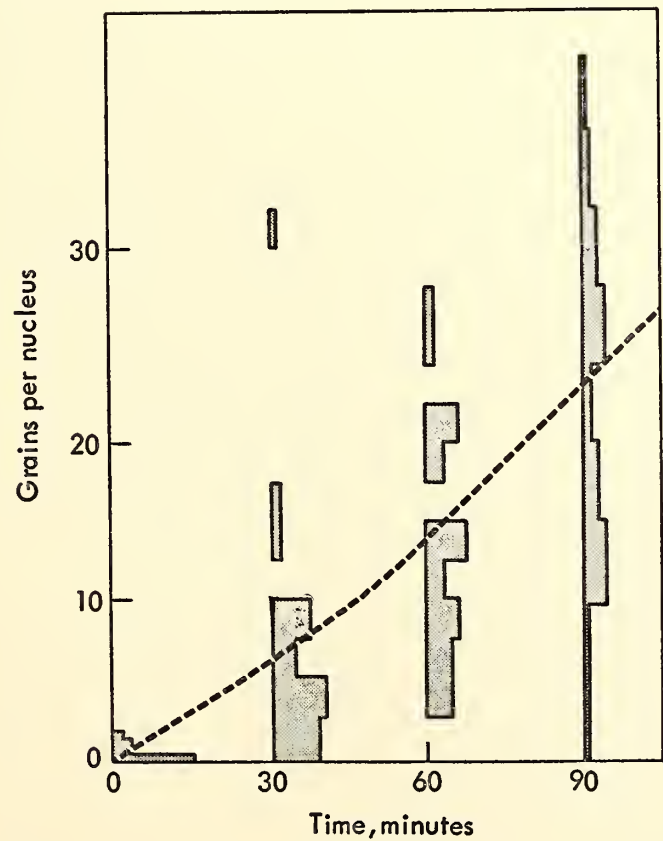


Fig. 45. Increase in total number of radioautographic grains per nucleus in cells fixed at intervals after the addition of C^{14} -guanine to the culture medium (see fig. 44 for details).

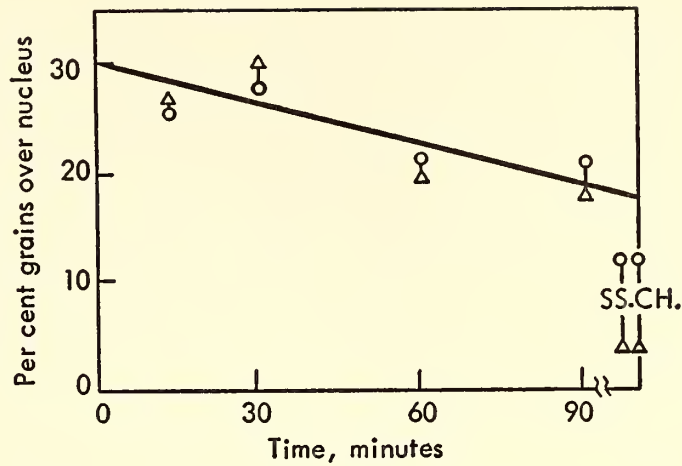


Fig. 46. Per cent of radioautographic grains over the nucleus in cells fixed at intervals after the addition of C^{14} -guanine to the medium. SS represents cells exposed to the label for 24 hours. CH represents cells exposed to C^{14} -guanine for 17 hours and then chased with C^{12} -guanine for 7 hours. The circles are values derived from counts made over the cell and nuclear surfaces and are not corrected for C^{14} scatter. The triangles are values corrected for scatter.

ing due to the range of the C^{14} β particles. On this figure are also shown the values for a 24-hour labeling period and a 17-hour labeling period followed by a 7-hour chase in the presence of C^{12} -guanine. At these late times the labeling of the nucleus is relatively small, and, because of a large correction, a precise estimate cannot be made of the steady value of RNA content and DNA labeling in the nucleus. Chemical separation indicates that the DNA labeling with C^{14} -guanine is less than 8 per cent of the total.

It is evident that about 20 per cent of the RNA of *Euglena* appears first in the nucleus or nucleolus and then passes out with a time constant somewhere between 1 and 2 hours (about 1/10 of the generation time). If the remainder of the RNA is also synthesized in the nucleus, it must pass out to the cytoplasm with a time constant of less than a minute. This seems quite unlikely, and therefore we must tentatively assume that a major fraction of the RNA synthesis occurs in the cytoplasm, perhaps in the chloroplasts. Similar studies with cells grown in the dark

indicate that a higher percentage of the RNA synthesis occurs in the nucleus, but it is still less than half the total.

Preliminary studies of the kinetics of labeling of RNA show that at the earliest times ($\frac{1}{2}$ hour) only 10 to 15 per cent can be hybridized with DNA and that the percentage falls slowly with time. It is possible that this fraction corresponds to

the fraction synthesized in the nucleus, but further experiments are required to establish this point. Autoradiographic studies utilizing actinomycin D are being pursued in an effort to determine whether the cytoplasmic RNA synthesis is DNA dependent, and the DNA-agar-column technique is being tried in an effort to detect a unique cytoplasmic DNA.

IMAGE TUBES FOR LARGE TELESCOPES

The activities of our Department include a vigorous participation in the development of image intensifiers for astronomical applications. One contribution to this project has been the design by Ford of a small spectrograph suitable for work with experimental image tubes.

This instrument was constructed in the DTM shop, and it has been tested at Lowell Observatory on the Morgan telescope. The report of the Committee on Image Tubes for Telescopes follows this report.

BIBLIOGRAPHY

- Asada, T., *see* Rodríguez B., A.
- Baum, W. A., J. S. Hall, L. L. Marton, and M. A. Tuve, Committee on Image Tubes for Telescopes, *Carnegie Inst. Wash. Year Book* 61, 296-301, 1962.
- Baum, W. A., *see also* Fredrick, L. W.
- Bolton, E. T., and B. J. McCarthy, A general method for the isolation of RNA complementary to DNA, *Proc. Natl. Acad. Sci. U. S.*, 48, 1390-1397, 1962.
- Bolton, E. T., *see also* Hoyer, B. H., and Matthews, R. E. F.
- Britten, R. J., and F. T. McClure, The amino acid pool in *Escherichia coli*, *Bacteriol. Rev.*, 26, 292-335, 1962.
- Britten, R. J., and F. T. McClure, The mechanism of amino acid pool formation in *Escherichia coli*, in *Amino Acid Pools*, pp. 595-609, edited by J. T. Holden, Elsevier Publishing Company, Amsterdam, 1962.
- Britten, R. J., *see also* Buchwald, M., and Roberts, R. B.
- Brown, L., H. Rudin, and N. P. Heydenburg, Operation of a source of polarized ions in a pressure-tank Van de Graaff generator (abstract), *Bull. Am. Phys. Soc.*, [2] 8, 377, 1963.
- Brown, L., *see also* Rudin, H.
- Buchwald, M., and R. J. Britten, Incorporation of ribonucleic acid bases into the metabolic pool and RNA of *E. coli*, *Biophys. J.*, 3, 155-166, 1963.
- Burke, B. F., K. C. Turner, and M. A. Tuve, Hydrogen motions in M31 (abstract), *Astron. J.*, 68, 274, 1963.
- Burke, B. F., E. T. Ecklund, P. A. Johnson, K. C. Turner, and M. A. Tuve, Hydrogen line observations of M31 and M33 with NRAO 300-ft telescope (abstract), *Astron. J.*, 68, 70, 1963.
- Burke, B. F., *see also* Turner, K. C.
- Cowie, D. B., Metabolic pools and the biosynthesis of protein, in *Amino Acid Pools*, pp. 633-645, edited by J. T. Holden, Elsevier Publishing Company, Amsterdam, 1962.
- De La Haba, G., *see* Flexner, J. B.
- Dodd, R. T., Jr., *see* Hart, S. R.
- Doe, B. R., and S. R. Hart, The effect of contact metamorphism on lead in potassium feldspars near the Eldora Stock, Colorado, *J. Geophys. Res.*, 68, 3521-3530, 1963.
- Ecklund, E. T., *see* Burke, B. F.
- Flexner, J. B., L. B. Flexner, E. Stellar, G. De La Haba, and R. B. Roberts, Inhibition of protein synthesis in brain and learning and memory following puromycin, *J. Neurochem.*, 9, 595-605, 1962.
- Flexner, L. B., *see* Flexner, J. B.
- Forbush, S. E., G. Pizzella, and D. Venkatesan, The morphology and temporal variations of the Van Allen radiation belt, October 1959 to December 1960, *J. Geophys. Res.*, 67, 3651-3668, 1962.

- Ford, W. K., Jr., and M. A. Tuve, Astronomical applications of image intensifiers in *ERDL-NASA Image Intensifier Symposium*, pp. 205-210, Fort Belvoir, Virginia, October 24-26, 1961.
- Ford, W. K., Jr., *see also* Fredrick, L. W.
- Fredrick, L. W., J. S. Hall, W. A. Baum, and W. K. Ford, Jr., Some astronomical uses of image intensifying tubes, *Adv. Electron. Electron Phys.*, 16, 403-408, *Second Symposium on Photo-Electronic Image Devices*, edited by J. D. McGee, W. L. Wilcock, and L. Mandel, Academic Press, London, 1962.
- Green, R., The hidden layer problem, *Geophys. Prospecting*, 10, 166-170, 1962.
- Green, R., and J. S. Steinhart, On crustal structure deduced from seismic time-distance curves, *New Zealand J. Geol. Geophys.*, 5, 579-591, 1962.
- Hall, J. S., *see* Baum, W. A., and Fredrick, L. W.
- Hart, S. R., and R. T. Dodd, Jr., Excess radiogenic argon in pyroxenes, *J. Geophys. Res.*, 67, 2998-2999, 1962.
- Hart, S. R., *see also* Doe, B. R., and Tilton, G. R.
- Heydenburg, N. P., *see* Brown, L., and Rudin, H.
- Hoyer, B. H., B. J. McCarthy, and E. T. Bolton, Complementary RNA in nucleus and cytoplasm of mouse liver cells. *Science*, 140, 1408, 1963.
- Johnson, P. A., *see* Burke, B. F.
- McCamy, K., R. P. Meyer, and T. J. Smith, Generally applicable solutions of Zoeppritz' amplitude equations, *Bull. Seismol. Soc. Am.*, 52, 923-955, 1962.
- McCarthy, B. J., Kinetic studies of ribonucleic acid synthesis, *Biochem. J.*, 84, *Proc. Biochem. Soc.*, p. 60, 1962.
- McCarthy, B. J., *see also* Bolton, E. T., Hoyer, B. H., Midgley, J. E. M., and Roberts, R. B.
- McClure, F. T., *see* Britten, R. J., and Roberts, R. B.
- Marton, L. L., *see* Baum, W. A.
- Matthews, R. E. F., E. T. Bolton, and H. R. Thompson, Kinetics of labeling of turnip yellow mosaic virus with P³² and S³⁵, *Virology*, 19, 179-180, 1963.
- Meyer, R. P., *see* McCamy, K.
- Midgley, J. E. M., The kinetics of transfer ribonucleic acid synthesis in *Escherichia coli*, *Biochim. Biophys. Acta*, 68, 354-364, 1963.
- Midgley, J. E. M., The nucleotide base composition of ribonucleic acid from several microbial species, *Biochim. Biophys. Acta*, 61, 513-525, 1962.
- Midgley, J. E. M., and B. J. McCarthy, The synthesis and kinetic behavior of deoxyribonucleic acid-like ribonucleic acid in bacteria, *Biochim. Biophys. Acta*, 61, 696-717, 1962.
- Pizzella, G., *see* Forbush, S. E.
- Roberts, R. B., Enzyme induction and ribosome synthesis, in *The Molecular Basis of Neoplasia*, pp. 519-534 (15th Annual Symposium on Fundamental Cancer Research, 1961), University of Texas Press, Austin, 1962.
- Roberts, R. B., Further implications of the doublet code, *Proc. Natl. Acad. Sci. U. S.*, 48, 1245-1250, 1962.
- Roberts, R. B., and F. T. McClure, Is there an alternative to the arms race? reprinted from *Educational Record*, pp. 255-268, American Council on Education, Washington, D. C., October 1962.
- Roberts, R. B., R. J. Britten, and B. J. McCarthy, Kinetic studies of the synthesis of RNA and ribosomes, *Molecular Genetics*, pt. 1, pp. 291-352, edited by J. H. Taylor, Academic Press, New York, 1963.
- Roberts, R. B., *see also* Flexner, J. B.
- Rodríguez B., A., J. S. Steinhart, and T. Asada, The San Agustín fault system of southern Peru, *Bull. Seismol. Soc. Am.*, 52, 793-805, 1962.
- Rudin, H., L. Brown, and N. P. Heydenburg, Excitation of the D(*d,p*)T reaction with tensor-polarized deuterons at 710 kev (abstract), *Bull. Am. Phys. Soc.*, [2] 8, 377, 1963.
- Rudin, H., *see also* Brown, L.
- Smith, T. J. *see* McCamy, K.
- Steinhart, J. S., *see* Green, R., and Rodríguez B., A.
- Stellar, E., *see* Flexner, J. B.
- Thompson, H. R., *see* Matthews, R. E. F.
- Tilton, G. R., and S. R. Hart, Geochronology, *Science*, 140, 357-366, 1963.
- Turner, K. C., M. A. Tuve, and B. F. Burke, Hydrogen line observations of M33 (abstract), *Astron. J.*, 68, 295, 1963.
- Turner, K. C., *see also* Burke, B. F.
- Tuve, M. A., International upper mantle project, proposed U. S. program, *News Report*, 12, 89-93, National Academy of Sciences-National Research Council, 1962.
- Tuve, M. A., *see also* Baum, W. A., Burke, B. F., Ford, W. K., Jr., and Turner, K. C.
- Venkatesan, D., *see* Forbush, S. E.

MAJOR PUBLICATION

Studies of Biosynthesis in Escherichia coli. By R. B. Roberts, P. H. Abelson, D. B. Cowie, E. T. Bolton, and R. J. Britten, *Carnegie Inst. Wash. Publ.* 607, third printing, with brief addenda. Octavo, xiv + 521 pp., 114 figs., 1963.

PERSONNEL

Director

M. A. Tuve

Staff Members

L. T. Aldrich
 E. T. Bolton
 R. J. Britten
 B. F. Burke
 D. B. Cowie
 S. E. Forbush
 W. K. Ford, Jr.

S. R. Hart
 N. P. Heydenburg¹
 B. J. McCarthy
 R. B. Roberts
 T. J. Smith²
 J. S. Steinhart
 G. M. Temmer¹

H. W. Wells³*Staff Associates*Cinna Lomnitz⁴Ulrich Schmucker⁵*Section Chairmen*

Biophysics: R. B. Roberts
 E. T. Bolton, Deputy Chairman
 Earth's Crust: L. T. Aldrich

Radio Astronomy: B. F. Burke
 Theoretical Geophysics: S. E. Forbush

Fellows and Associates

L. Brown, University of Basel, Basel, Switzerland.
 T. J. Byers, Fellow of U. S. Public Health Service (from September 1962).
 R. C. Hall, University of Indiana
 K. E. Kissell, Ohio State University (from October 1962).
 O. Kouvo, Geological Survey of Finland, Otaniemi, Finland (from September 1962).
 K. McQuillen, Cambridge University, Cambridge, England (August–December 1962).
 J. E. Midgley, Oxford University, England (through September 1962).
 A. Rodríguez B., Universidad de San Agustín, Arequipa, Peru.

H. Rudin, University of Basel, Basel, Switzerland.
 I. S. Sacks, University of Witwatersrand, Johannesburg, South Africa (from September 1962).
 R. Salgueiro, Instituto Tecnológico Boliviano, La Paz, Bolivia.
 H. R. Striebel, University of Basel, Basel, Switzerland (June 1962).
 R. Sumner, University of Wisconsin (from September 1962).
 Z. Suzuki, Tohoku University, Sendai, Japan (from November 1962).
 K. Turner, Princeton University.
 C. Varsavsky, University of Buenos Aires, Buenos Aires, Argentina (June 1963).

¹ Through January 31, 1963.² Professor at Kalamazoo College, September 23 to December 15, 1962.³ Resigned July 15, 1962.⁴ From January 1, 1963, at University of Chile, Santiago, Chile.⁵ From March 15, 1963, at Instituto Geofísico del Peru, Lima, Peru.

Junior Fellows

- P. Aparicio, Universidad Mayor de San Andres, La Paz, Bolivia (from September 1962).
 Daniel Ochoa, Universidad de San Agustín. Arequipa, Peru (from September 1962).
 L. Ocola, Instituto Geofísico del Peru, Lima, Peru (from February 1963).
 D. Simoni, Universidad de San Agustín, Arequipa, Peru (from April 1963).

Collaborators and Visiting Investigators

- H. Alvarez, University of Michigan (from January 1963).
 H. Baadsgaard, University of Alberta, Edmonton, Canada (through September 1962).
 R. Cabre, S.J., Observatorio San Calixto, La Paz, Bolivia.
 L. N. Edmunds, Jr., Princeton University (through July 1962).
 J. Gerken, Universidade de Minas Gerais, Belo Horizonte, Brazil (from January 1963).
 Bill Hoyer, NIH Rocky Mountain Laboratory, Hamilton, Montana (from September 1962).
 G. Saa, S.J., University of Chile, North Zone, Antofagasta, Chile.
 M. Sakko, Geological Survey of Finland, Otaniemi, Finland (from January 1963).
 F. Volponi, Universidad Nacional de Cuyo, San Juan, Argentina (from January 1963).
 J. A. Young, Dalhousie University, Halifax, Nova Scotia (September–December 1962).

Research Assistants

- J. B. Doak
 E. T. Ecklund
 P. A. Johnson
 C. A. Little
 W. E. Scott

Laboratory Assistants

- Mrs. L. Beach
 S. J. Buynitzky
 Mrs. S. Lohman (from September 5, 1962)
 G. R. Poe
 Mrs. A. Shirven
 Miss Eva Stern (through September 30, 1962)

Laboratory Helper

- Mrs. W. Griffin (from September 24, 1962)

Office

- Chief, Fiscal Section: Miss H. E. Russell
 Office Manager: W. N. Dove
 Librarian: Mrs. L. J. Prothro (part time)
 Secretary: Mrs. C. Ator (part time)
 Stenographers: Mrs. D. Burke (part time, May 16 to June 30, 1963); Mrs. D. B. Dillin; Mrs. M. Suddath (part time, September 24, 1962, to May 15, 1963)

- Typist: Mrs. M. T. Sheahan (part time)
 Accounting Assistant: Miss G. J. Johnston

Shop

Chief of Section: W. F. Steiner	Instrument Maker: M. Seemann
Senior Instrument Maker: J. G. Lorz (Chief Instrument Maker and Foreman of Instru- ment Shop from June 1, 1963)	Machinist-Instrument Maker: D. E. Mossor Machinist: F. J. Caherty

Buildings and Grounds

Carpenter, Buildings and Maintenance Fore- man: L. J. Haber	Assistant Caretakers: S. Gawrys, S. Swant- kowski
Caretaker: E. Quade	

Part-Time and Temporary Employees

John Brauer	Alan Hoover
Manuel Buchwald	John Randall
Mrs. Gertrud Frick	James Roddy
Barry Goss	John Roddy
Lin Ho	Kai Schwarz
Norbert Thonnard	

Special Project Appointee

L. W. Fredrick (Image Tubes, through January 31, 1963)

Committee on Image Tubes for Telescopes

Cooperative Project of Mount Wilson and Palomar Observatories
Department of Terrestrial Magnetism, Lowell Observatory
National Bureau of Standards, and United States Naval Observatory

W. A. Baum
Mount Wilson and Palomar Observatories

John S. Hall
*Director, Lowell Observatory
Flagstaff, Arizona*

L. L. Marton
National Bureau of Standards

M. A. Tuve (*Chairman*)
Department of Terrestrial Magnetism

INTRODUCTION

THE Carnegie Image Tube Committee is engaged in the development of photoelectric image intensifiers that will extend the range of telescopes for astronomical observations. We are endeavoring to perfect techniques, utilizing the greater quantum efficiency of photoelectric surfaces, that will supplement existing photographic processes. During the report year the Committee has been especially concerned with evaluating cascaded image intensifiers, mica-window converters, and Lenard-window tubes.

A cascaded tube consists of a photocathode, an electron multiplier, and a phosphor screen. The phosphor screen is photographed with a copy, or relay, lens. Cascaded tubes are made with multipliers consisting of a phosphor screen supported by a thin piece of mica, and a second photocathode. Photoelectrons impinging on the screen produce scintillations which are seen by the photocathode, and, therefore, secondary photoelectrons are emitted. This is an efficient process for electron multiplication compared with secondary electron emission. With a single intensifying screen, sufficient gain is achieved to allow all information contained in the primary photoelectron image to be recorded from the final phosphor with a fast relay lens. The gain in exposure time is then primarily a function of the efficiency of the first photocathode. The principal advantage of this type of device is its relative simplicity and general ruggedness as compared with other types of image intensification.

During the report year, RCA Electron Tube Division, Lancaster, Pennsylvania, has built for the Committee several developmental tubes having efficient fine-grain screens, giving about twice the resolution of the previous phosphors. The new phosphor technique is a great advance, but, unfortunately, these particular tubes had poor-quality photocathodes,

and they have been used primarily for investigation of resolution and problems associated with focusing magnets and optics rather than for actual astronomical observations.

A mica-window converter is a single-stage tube having a photocathode, electron optics, and a phosphor screen deposited on a thin exit window. Exposures are made by pressing film into contact with the thin window. In this way the necessity of internal electron multiplication is avoided, since the contact exposures provide good transfer of light from the phosphor to the emulsion without the use of relay optics. Windows of mica, 5 to 7 microns thick, can be made, which support atmospheric pressure over a slot 40 mm by 2 mm. It appears, on the basis of test exposures made thus far, that mica-window tubes have more contrast than cascaded tubes. Mica-window tubes are particularly suited for infrared work, since infrared-sensitive photocathodes can be made more easily in them than in other tubes, such as the cascaded types. For spectroscopy, however, the usefulness of the tube is limited by the dimensions of the slit. The main disadvantage of the mica-window tube is that exposures must be made on film which has less dimensional stability than photographic plates.

Lenard-window tubes, built under the supervision of Professor McGee at Imperial College, have been evaluated during the report year by Baum and McGee. They are single-stage devices designed to operate with an accelerating potential of 40–45 kv. They are equipped with thin mica exit windows (Lenard windows) which withstand atmospheric pressure. The electrons penetrate the windows and impinge upon a nuclear stripping emulsion. The tube as developed by Professor McGee and his colleagues has excellent resolution, low spurious background, and linearity of response to light of given

wavelength. Thus far, exposures have been made only on stripping emulsions, which

leave much to be desired in the way of dimensional stability.

TESTS AND EVALUATION OF SAMPLE TUBES

Cascaded tubes. The Carnegie Committee has been particularly interested in a general type of cascaded tube having moderate gains and image areas 40 mm in diameter. These have been represented in the past by the ITT 152 and by a similar type developed by RCA, the C70 056. The results of tests on the first sample of the C70 056 were reported in *Year Book 61* (p. 299).

Several two-stage cascaded intensifiers were tested by Ford at DTM and on the Morgan 24-inch reflector at Lowell Observatory. The first (C70 056-4) had a 135- μ A/lumen S20 photocathode and a P20 phosphor. Resolution was limited, primarily by phosphor graininess, to 20 line pairs per millimeter. The gain in exposure time over photography was also somewhat less than could be attained with P11 phosphors, which have higher radiant-energy efficiencies for photography. The tube was sufficiently free of spurious emission to permit exposures longer than 2 hours. Another tube, C70 056-5, also has a P20 phosphor and is similar in general characteristics to tube C70 056-4.

The second tube of this type, C70 056-11, had a 62- μ A/lumen cathode (low for S20 photosurfaces) but a rather good electron multiplication across the phosphor mica cathode sandwich. Instead of the grainy P20 phosphor of the previous tubes, this tube had an extremely fine-grain P11 type phosphor (blue) deposited by a new technique developed at RCA, Lancaster. The screens made by this new technique are remarkably free of mottling and graininess, which so limited the previous tubes (see report in *Year Book 58*). As a result of these new screens on both the sandwich and final output phosphors, the resolution is about double that obtained previously. Consequently, the

resolving power of the two-stage cascaded intensifying system is now limited primarily by the combination of relay optics and photographic emulsion. Since the electron multiplication of a two-stage tube is 30 to 50 across the sandwich, a relay lens working at $f/1.5$ (for example, a pair of $f/1.5$ lenses front to front) is required in order to utilize an appreciable fraction of the quantum efficiency of the photocathode. The resolution of magnetically focused tubes in their present state of development is nearly uniform across the 40-mm screen. The improved resolution and large field impose severe requirements on the resolving power of the relay optics. Since the resolving power displayed by the tube at the screen is comparable to that ordinarily obtained on fast astronomical emulsions, the lens system should work at unity magnification or greater. We know of no lens that fully meets these requirements, and the design of such a relay system is now of great importance to the Image Tube Committee.

Tube C70 056-11, with the new fine-grain phosphors, unfortunately had a very large component of spurious emission. In electrostatic tubes, and in some of the darker, magnetically focused tubes, the spurious emission increases with voltage on the tube, at low voltages being very small and at higher voltages, say 8 or 10 kv per stage, increasing very rapidly. This exponential increase is frequently attributed to field emission. In the present cascaded tubes, such as the C70 056, the voltage gradients are relatively small because of a series of four or more accelerating electrodes per stage, and in a well constructed tube the exponential component can be less important than a second type known as ion scintillation. This background consists of discrete scintillations visible on the screen of a

two-stage tube with moderate gain. These scintillations are bunches of electrons arriving from the first photocathode. (It is easily demonstrated that they are indeed electron bunches rather than individual ions, since they can be defocused by defocusing the first-stage optics.) It is thought that their origin is due to positive ions (perhaps thermally emitted) impinging on the cathode and sputtering off electrons.

The third tube tested (C70 056-12) also had a rather fine-grain phosphor screen. It had a poor cathode, so that the rate-of-blackening gain was limited to about 6. It was free of ion scintillations, however, and exposures of 2 hours' duration could be made without cooling. This tube has been used in some spectrographic tests in Flagstaff and is now being employed in various experiments at DTM to determine the relative importance in the resolving power of the over-all intensifier system of various parameters such as magnet uniformity, drift in voltage divider networks, relay lens characteristics, and emulsion contrast.

It is interesting to note that the three tubes mentioned above, C70 056-4, -11, and -12, all show tremendous improvements over the tubes of the electrostatically focused variety initially tested by the Carnegie Committee. None of these tubes has all the properties and characteristics required of an intensifier device to be useful in astronomical work, although each of the properties required can be found separately in two of the three tubes. It is hoped that improved control in fabrication techniques will soon permit a satisfactory number of tubes received for testing and evaluation to have adequate resolution, sufficient cathode sensitivity, and low spurious background.

One of these three tubes (tube 4) was used in July 1962 by Baum, Wilson, and Ford at the coude spectrograph of the Mount Wilson 100-inch telescope in a series of comparative exposures. The tube was set up to operate at the focus of the

114-inch camera, and the phosphor screen was photographed with a schmidt optical system having a $2\frac{1}{2}$ to 1 reduction in image size. Exposures obtained with this equipment were compared with direct plates made at the focus of the 32-inch camera. It was found that the rate-of-blackening gain of the image tube system was of the order of $7\frac{1}{2}$ times over IIa-D plates in the yellow and green regions of the spectrum. However, the resolution of the direct photographic process was estimated to be $1\frac{1}{2}$ times that of the image tube system with the particular arrangements used. This implies that the information regime of the intensifying system was actually only of the order of 3 times that of direct photography. Unfortunately, neither tube 11 nor 12 exhibiting the improved resolution with the new phosphors was available for this particular series of tests. With twice the resolution the information rate would be about 12 (with suitable relay optics) times that of direct photography. Also, the rate-of-blackening gain can be somewhat improved by operating the tube at voltages slightly higher than the 16 kv used in these tests. Exposures of 1 hour's duration were made which showed no appreciable spurious background. Gain in the region of the H and K lines (in the violet) was disappointingly low. These results emphasize the need for improved laboratory measurements of the spectral sensitivity of the individual photocathodes.

Mica-window tubes. Several mica-window tubes built by ITT Laboratories have been used on the Morgan telescope primarily by Fredrick. One type, the FW 117, is a single-lens, magnetically focused tube; another, the FW 159, is a similar tube utilizing two accelerating electrodes or lenses. These tubes have infrared-sensitive (S1) photocathodes, and are cooled with dry ice to reduce thermionic emission. Exposures are made by pressing film, such as Plus X of IIa-O, into contact with the thin window supporting the phosphor screen. Results of tests on the first series of F 117's have been reported

in previous Year Books. The FW 159 has an improved seal between the mica and the supporting flange. Wrinkles in the supporting mica in previous tubes made it extremely difficult to maintain uniform contact between the photographic emulsion and the screen.

The first sample of the FW 159 had a moderately sensitive S1 photocathode (IR index greater than $4 \mu\text{A}/\text{lumen}$ to 2870°K light through a 2540 filter). The mica in this tube was flat, and good contact could be made with the emulsion. Exposures were severely limited by strong ion scintillations in the center of the window, but considerable information could be recorded on either side of the ion spot. Fredrick succeeded in making a series of observations of the red (O, O) CN bands in late-type giants with this experimental tube.

The second tube of this type has similar spurious emission characteristics which limit exposures to 10 or 20 minutes, and the cathode is somewhat less sensitive than that of the first tube. Subsequent attempts to make tubes of this type at ITT have been beset with the old problem of slumping photocathodes. The difficulty may in part be connected with the materials used in supporting the mica in the tube structure. Another fabrication difficulty involves the low-melting glass frit used in sealing the mica to the supporting structure. Most of the satisfactory frits have rather low melting points, which prohibit the outgassing of the tube structure at sufficiently high temperatures during processing. Work on this problem is continuing at ITT; it is hoped that improved samples will soon be available for testing and evaluation.

RCA furnished two excellent mica-window tubes, with multialkali (S20) photocathodes, to the Committee for testing and evaluation last year. One of them, RCA C70 026-6, was used to obtain a series of exposures of spectra of various stars on the Morgan telescope. During the current year these spectra have been compared with exposures on the same

stars made with cascaded tubes of improved resolution as well as with direct plates. The exposures made with the S20 mica-window tubes tend to surpass the cascaded-tube exposures in contrast and in resolution. Work at RCA is currently directed toward improving the flatness of the windows and toward fabricating screens with the improved fine-grain phosphors mentioned above.

It will be interesting to compare exposures with the mica-window device made with the old phosphors (where the visual resolution was 50 line pairs per millimeter at the screen) with the exposures that can be made with the improved phosphors. What fraction of this resolving power will be lost in the contact printing process is not known, but it is clear that improvements over the test exposures of the first sample tubes are possible. In the initial test of C70 026-6, exposures of rather long duration were made on Plus-X emulsions. The rate-of-blackening gains over direct photography for long exposures have improved considerably now that satisfactory Ila-O emulsion on film base has become available for our test purposes. It appears, therefore, that the gain available with the mica-window technique is quite comparable with that attainable by other techniques.

Lenard-window tubes. The development of a practical Lenard-window tube by McGee and his co-workers has opened up astronomical possibilities that we did not foresee a few years ago. Earlier electronographic systems were so much more complicated than other types of image tubes that their routine use by many astronomers at many different observatories did not appear practicable. We now find that Lenard-window tubes of McGee's design can be operated almost as easily as any of the other types of tubes we have tested.

The astronomical tests thus far have been made with Lenard-window tubes having antimony-cesium photocathodes with sensitivities up to $30 \mu\text{A}/\text{lumen}$. At the output end they have mica windows

ranging in thickness from 4.4 to 5.4 microns. The mica is attached to a metal end plate, and it covers a slot 5 mm (3 mm useful image) wide by 30 mm long. One tube with a 10-mm slot (7 mm useful) was also successfully tested, and McGee foresees no particular difficulty in making future tubes with slots of that size. Inside the tube a series of conducting angular rings divides the accelerating voltage uniformly between the photocathode and the mica window. Total accelerating voltages have been between 40 and 45 kv. The photoelectrons are focused by means of a uniform magnetic field parallel with the axis of the tube. If an electron is to make two helical loops along its flight path, the required focusing field is about 150 gauss. Since the photoelectrons lose about 20 kv in passing through the mica window, they have an average residual energy of 20 to 25 kv when they strike a nuclear-track emulsion placed in contact with the outside of the window. According to earlier data for the Ilford G5-type emulsion, these impinging electrons should blacken an average of 4 or 5 grains each. Although there is doubtless some statistical spread in the number of blackened grains per incident electron, we believe that most of the photoelectrons are being recorded.

Two series of astronomical tests of the Lenard-window tubes were made. The first took place in September and October 1962, and the second in April and May 1963. These tests were carried out mainly by McGee and Baum, but various observers were also present during some of the nighttime exposures.

The tests of 1962 began at the Morgan telescope and laboratory at Lowell Observatory in Flagstaff, Arizona. In preparation for that work, a substantial amount of operating hardware had been prepared at Lowell and at Mount Wilson. After the tubes were put into operation and given a preliminary check-out at Flagstaff, they were brought to the Mount Wilson Observatory and installed in the coudé spectrograph of the 100-inch telescope.

Equipment had been prepared for mounting them and operating them in a preliminary way at the focus of the 114-inch-focal-length coudé camera.

Encouraging results were obtained in the laboratory at Flagstaff, but some difficulties were encountered when the same equipment was initially installed in the coudé spectrograph at Mount Wilson. These difficulties were due mainly to very serious disturbances of the magnetic focusing field, partly because of the steel structure of the spectrograph and pier and partly because of changes in the local magnetic field caused by rotation of the massive steel dome of the 100-inch telescope. It was clear from these 1962 tests that, although the Lenard-window tubes had interesting possibilities for astronomy, much more extensive preparations would be necessary to obtain satisfactory results at the telescope and to utilize their potential advantages to the full.

In the interval between October 1962 and April 1963, McGee and his co-workers in London made some improvements in the tube, keeping the basic design unchanged. They also built up a stock of reliable tubes. Meanwhile at Mount Wilson the time was devoted to a thorough redesign of the operating equipment. Baum spent several months experimenting with permanent-magnet arrays and with magnetic shields in order to arrive at an optimum design for a new coudé installation. In its final design the Mount Wilson magnet is about 10 inches in diameter and 15 inches long. It provides an adjustable field having a uniformity of about 2 per cent throughout a volume large enough to accommodate most of the magnetically focused tube designs now foreseeable. The magnet array is enclosed by a large shield, 22 inches in diameter and 30 inches long, consisting of two layers, one of Armco iron for high flux capacity and the other of mu-metal for high permeability. The shield serves two purposes: it symmetrically shunts the outer lines of force from the enclosed magnet array so that the internal field of

the array is not distorted by large asymmetric masses of iron near it; and it shields the system from changes in external magnetic fields due to dome rotation and passing motors.

The tests of April and May of 1963 were carried out entirely at Pasadena and Mount Wilson. McGee brought six Lenard-window tubes with him; all of them survived the trip and the experiments without damage. Tests of photocathode sensitivity in London, before and after the trip, showed no change at all. All together, 256 exposures were made through the Lenard-window tubes; a few unaided exposures were also made on Ila-O plates for comparison. The tube exposures included test patterns, focus plates with an iron arc, photometric calibrations, stellar spectra, and day-sky spectra. The exposures on stellar spectra ranged up to more than 5 hours at 44 kv without serious background interference and without requiring the tubes to be cooled.

A comparison was made between the Lenard-window tubes and unaided photography to determine the relative rates at which information was being recorded. The information rate involves three factors: the rate of blackening, the granularity, and the resolution. The rate of blackening can be measured in terms of the time required to produce a prescribed density above background. In other words, the rate of blackening is proportional to $1/t$. The granularity can be measured in terms of the noise in a microphotometer tracing. Since density is linearly proportional to the number of grains (or grain clumps) per unit area, the fluctuation ΔD in a microphotometer tracing is proportional to the square root of the number of grains per unit area. The resolution R can be measured in terms of line pairs per millimeter. Although the resolution can be affected by the granularity, both quantities must be measured and taken into account when an information gain is computed. Applying the definitions above, we can express the

relative information rate as

$$\text{Information rate} = R^2/t(\Delta D)^2$$

When the apparatus was adjusted in an optimum way, the resolution of the Lenard-window tubes was found to be about 70 line pairs per millimeter. With the same test pattern and optical system, the resolution of unaided Ila-O plates was found to be about 60 line pairs per millimeter. On long exposures with the Lenard-window tubes, the resolution was generally poorer than 70 line pairs per millimeter, owing to a drift of the image. There are at least three potential contributors to image drift that must be guarded against in the future, namely, emulsion creep, voltage-divider drift, and electrostatic disturbance. McGee has recently found that an electrostatic disturbance does occur as the result of the buildup of charge on glass surfaces, and he has made a design change to reduce it. He has also had success in eliminating emulsion creep by means of G5 emulsion coated on a melinex film backing.

To measure the relative rates of blackening, tube 44 was compared with baked Ila-O emulsion. The test source was the step scale contained in the 4-mm pattern produced by a microprojector. A blue filter, 2 mm of Schott BG 12, was used to limit the spectral range to a band about 1000 Å wide centered roughly at 4300 Å.

Similar exposures were obtained with tube 45 at Mount Wilson with the built-in intensity step calibrator of the coude spectrograph. The resulting calibration strips on G5 and Ila-O were then compared with a microphotometer. It was found that the speed gain of tube 44 was 1.85 times higher than the speed gain of tube 45. This figure is compatible with McGee's earlier measurement of the relative cathode sensitivity ($\mu\text{A}/\text{lumen}$) of the two tubes. The rate-of-blackening gain of tube 44 is about 3 in the optical density range 0.2–1.0 on the unaided Ila-O plate.

The factor introduced by the difference in resolution $(70/60)^2$ amounts to 1.36. The factor introduced in the denominator of the information gain by the square of the ratio of microphotometer noise is 0.52. The rate-of-blackening gains can therefore be translated into actual information gain rates by multiplying them by a factor 2.6. For tube 44 the information rate gain over IIa-O at intermediate densities was about 7 or 8. This is very promising; current efforts are directed toward revision of the stripping emulsion, protection against image drift due to charges on the glass walls, and less bulky shielding.

The measured photocathode sensitivity of tube 44 was $30 \mu\text{A}/\text{lumen}$, and we can assume that most of the photoelectrons were being recorded. This means that

unaided IIa-O plates have an effective equivalent speed of about $4 \mu\text{A}/\text{lumen}$ when exposed to intermediate densities. If the resolutions obtained on G5 and on IIa-O were the maxima that the emulsions themselves are inherently capable of, this equivalent speed of $4 \mu\text{A}/\text{lumen}$ for IIa-O would have an important general significance. We could then say that no image tube with an antimony-cesium photocathode will ever be able to excel unaided photography in the blue region by a factor greater than about one-fourth of its $\mu\text{A}/\text{lumen}$ value. Actually, that conclusion might be somewhat inaccurate. We have to explore further the dependence of speed and resolution upon emulsion thickness and grain size. We can suspect that the $4\text{-}\mu\text{A}/\text{lumen}$ figure may turn out to be a little high.

SUMMARY AND ACKNOWLEDGMENTS

The Committee is accumulating a large number of sample exposures and measurements in the evaluation of the relative merits of the cascaded intensifiers, mica-window converters, and Lenard-window tubes, as well as some other types of devices. For cascaded tubes it is not yet clear whether it is better to use a two-stage cascaded tube with higher resolution than a three-stage tube having greater gain but inherently less resolution. The Committee is not clear on the future of the mica-window device. In the past this tube has been looked upon somewhat as a stopgap measure. It has been particularly useful because it can be produced with efficient infrared photosurfaces. The exposures made with the mica-window tubes, however, compare quite favorably with those made with other devices, and because of their relative simplicity, gain, and reliability they may indeed have a future in routine astronomical observations. The Lenard-window tube is a more recent

development, and so its long-range possibilities are more difficult to predict. Its superior resolution and linearity of response to light of a given color are certainly enticing advantages. Emulsion creep and other difficulties can probably be circumvented in the near future.

Dr. Lawrence W. Fredrick has left the Lowell Observatory and DTM staff, where he was engaged in the work with infrared mica-window tubes and in photography of close double stars, to become the Director of the Leander-McCormick Observatory at the University of Virginia. It is hoped that he will be able to continue participation in the activities of the Image Tube Committee. Most of the routine tests of experimental tubes have been conducted at the Department of Terrestrial Magnetism by Dr. Ford.

The development of these image intensifiers has been supported to a large extent by a generous grant from the National Science Foundation.

Department of Plant Biology

C. Stacy French
Director

Stanford, California

Contents

Introduction 343

Personnel 348

Biochemical Investigations 349

 Experiments with colored light flashes 349

 Studies on the enhancement of some photochemical reactions carried out by whole cells and by cell-free preparations 352

 Action spectra for separated light reactions in photosynthesis 357

 Nature of the forms of chlorophyll *a* 361

 New algae for photosynthesis studies 362

 Photosynthesis in *Stichococcus* 363

 Some observations on the reversible light-induced inhibition of respiration in non-sulfur purple bacteria 365

 Is the photoconversion of protochlorophyll immediate? 371

 Fractionation of protochlorophyll holochrome by density gradient centrifugation . 373

 Oxygen exchange by *Euglena* cells undergoing chloroplast development 375

 A reversible phosphate electrode and its possible application to physiological processes 379

 Automatic control of scanning speed for the action spectrophotometer 381

 An automatic plotter for plane table surveying with a range finder 382

Experimental Taxonomy Investigations 386

 Genetic coherence in three species-complexes 387

 Transplant responses of *Mimulus* in relation to genetic coherence 389

 Physiology of climatic races 392

 Studies on tissue cultures 392

 Studies on the distribution of tree species 394

 Cytotaxonomy and distributional ecology of western North American violets . . . 398

Speeches 399

Bibliography 400

INTRODUCTION

AN understanding of how different parts of the photosynthetic mechanism of plants fit together to make up the complete process continues to be the objective of one group in the Department of Plant Biology. As in past years our main concern has been with the functional relationship and the chemical nature of the various pigments that absorb light to supply power for driving the separate reactions.

This aspect of research on photosynthesis is a rapidly developing field that is being taken up by an increasing number of other laboratories. Communication between different groups of workers through meetings, visits, publications, and interlaboratory exchange of active investigators has rapidly expanded. This situation is probably typical of many scientific fields.

Close contact between individuals and groups working on the same subject generally favors the advancement of knowledge, but it does introduce a potentially undesirable factor. A danger to the field of photosynthesis is that through frequent exchange of ideas we may all come to have far too similar concepts about the process and about the relative importance of different areas of investigation. Diversity of opinion in the search for truth is essential at the existing state of knowledge in this subject.

The increase in the pace of scientific advance results in some consequences that are of immediate concern to each individual participating in the endeavor. One of the most obvious is the ever-narrowing specialization that is essential for maintaining professional competence. Over-specialization may reduce the spirit of amateurish enthusiasm for starting work in subjects lying outside the investigator's previous experience, which has great value in a research laboratory. Fresh approaches to fundamental questions without too much detailed knowledge of

previous theories, practices, and conclusions have sometimes led to unexpected discoveries and to unconventional interpretations. As a field gets more complex the need for the fresh mind increases, yet the chance for real success by the amateur continually diminishes because of the sheer volume of relevant known facts and because the tools of the trade become harder to master.

Strangely enough the number of significant questions awaiting investigation, rather than decreasing, grows ever larger, for each successful study raises more problems at a deeper level of understanding than it solves at the previously attainable level. In the field of photosynthesis there is an abundance of new concepts to be tested, old theories to be revised, new effects to be explained, and always the certainty of new discoveries arising as the result of improved experimental methods with different and unusual plant species.

A large part of research on the mechanism of photosynthesis is now concentrated on attempts to understand the Emerson enhancement effect: the increase in photosynthetic rate achieved when two appropriate colors of light are given together as compared with the sum of the rates from the two colors given separately. The discovery of this effect was one of the main reasons for believing that two pigment systems are involved in photosynthesis. Measurements of enhancement have become the most widely used means for studying the nature and the interactions of the two systems.

Most of the experiments on enhancement have been made by measuring oxygen evolution. While visiting the Department in the summer of 1962, Professor Martin Gibbs with his collaborators, Dr. Charles A. Fewson and Mr. Marvin D. Schulman, all from Cornell University, investigated the uptake of

carbon dioxide, finding enhancement effects similar to those known from oxygen measurements. They also measured the reduction of the hydrogen-transferring material, TPN, and the formation of high-energy phosphate, ATP, from inorganic phosphate by isolated chloroplasts. Both these photochemical reactions are considered to be intermediate steps of photosynthesis. The enhancement effect was not observed for either of them. The lack of enhancement in some of the individual steps indicates that the effect may be due to changes in the steady-state concentration of intermediate products rather than to an influence on the efficiency of the photochemical reactions themselves.

During the report year measurements of the rate of photosynthesis have been made with short light flashes of colors chosen to activate specific pigment systems of algae. In the red alga *Porphyridium* we found the response to single short flashes when given with or without continuous background light to show the enhancement effect in two distinctly different ways. Green flashes with red background light gave an immediately increased initial rate of oxygen evolution over that obtained without the continuous red light. After the flash the rate declined just as rapidly with or without the red light. When red flashes were given with a continuous green background light, however, a different kind of enhancement was found. The initial rate of oxygen evolution was no greater than without the green background light, but the evolution of oxygen continued longer after the flash. Thus, either an increased initial rate or a prolongation of the time of gas evolution gives an enhancement effect, but the kinetics in the two responses are very different.

Variation of the time schedule of repetitive flashes of red or green light affects the photosynthetic rate differently. With green light, lengthening the flash time and reducing the dark time has less effect on the photosynthetic rate than

a similar change in the time distribution of red light flashes. Such experiments are being continued to study the interaction of the two pigment systems of photosynthesis.

A theory proposed some years ago by Hill and Bendall ties together in a logical way some of the known intermediate reactions of photosynthesis on the basis of their oxidation-reduction potentials. Many different investigators have elaborated on this model. Witt has used its basic framework to correlate the chemical events indicated by the small changes of light absorption measurable in various parts of the spectrum when photosynthetic cells are illuminated. Essentially the same scheme has also been used by Arnon, Duysens, and others to show how the interrelations of numerous partial reactions, observed in isolated chloroplasts and in whole cells, can be correlated into a reasonable picture of the part of photosynthesis that is closely related to the photochemical function of the two pigment systems.

Although the details of the current concepts and the language used to describe them vary in different laboratories, it is generally agreed that the oxygen-evolving reaction is more closely connected with the activation of the accessory pigment system than with the long-wavelength chlorophyll system. Furthermore, activation of the accessory pigment system is widely believed to be the initial act starting off the series of reactions. Some of our recent results at first sight appear to be in sharp contrast to this point of view.

We may look at photosynthesis as a system driven by two inputs: (1) light absorbed by or transferred to long-wavelength chlorophyll *a*, and (2) light absorbed by the accessory pigment system. We may then ask in which order these two distinct energy inputs act on the resulting chain of chemical events. Is a product of one photochemical reaction used as a substrate for the other one; and, if so, does the accessory pigment reaction or

the long-wavelength chlorophyll *a* reaction come first?

On the other hand the two light inputs may equally well be considered to act simultaneously and independently on the two systems. The model that we used previously for describing the various shapes of induction time course curves obtained in *Porphyridium* assumed that the two pigment systems acted in a parallel fashion rather than one after the other.

The obvious conclusion at present from the recent flashing light experiments in red algae is that material made by chlorophyll *a* is used up by the accessory pigment system as oxygen is produced. This conclusion, if taken at its face value, would reverse the accepted time sequence of the operation of the two photochemical reactions by placing the long-wavelength chlorophyll *a* system at the starting point.

There is, however, a consideration that prevents this obvious interpretation of the experimental results from being a necessary conclusion, namely, the fact that a cycling system having a certain dynamic equilibrium concentration of components during steady-state photosynthesis in the light may be changed during a dark period to a different set of concentration levels of the components. Thus the result of chlorophyll *a* activation may only be the necessary readjustment of the various pool sizes of intermediates from their dark equilibrium values to the different values required for the efficient operation of the system in the equilibrium condition.

One of our main objectives is to ascertain the extent to which the parallel reaction model or a series-type model can account for the effects observed in the flashing light experiments and can relate them to other known properties of the photosynthetic system.

The properties of the different forms of chlorophyll *a* such as their comparative extractability by organic solvents and their sensitivity to heat, light, and deter-

gents have been further studied by Dr. Brown in the past year. The longer-wavelength forms of chlorophyll are more susceptible to these destructive treatments than C₆₇₂ is.

A clear separation of the function of several of these forms of chlorophyll was achieved by Dr. Fork in collaboration with Professor Witt and Dr. Müller at Marburg. They found that the small increase in light absorption of spinach chloroplasts at 515 m μ is caused by the accessory pigment system composed of chlorophyll *b* and the form of chlorophyll *a* absorbing at 674 m μ . On the other hand the absorption decrease of chlorophyll *a* measured at 433 m μ was found to be caused by the two long-wavelength forms of chlorophyll *a* absorbing at 682 and 695 m μ .

The kinetics of several of the partial reactions of photosynthesis have been studied by rapid electrical recording methods. Thus Nishimura and Chance have measured phosphate uptake rapidly by following *pH* changes. Since other reactions than phosphate uptake can also give *pH* changes, the conditions under which this method is used must be carefully chosen. An attempt is being made by Dr. Smith to develop an electrode as specific as possible for phosphate ion itself. A silver electrode coated with a thin layer of a dense suspension of silver phosphate has been found to give excellently reproducible measurements of very small amounts of phosphate in buffered solutions. Unfortunately the substances present in phosphorylating suspensions of chloroplasts preclude the use of this system for its intended application. Experiments with other electrode systems are in progress with the hope of developing a general-purpose electrode for phosphate determination in biological systems.

Dr. Jerome A. Schiff of Brandeis University visited the Department to work on one aspect of his program on the development of the photosynthetic apparatus in *Euglena*. He found that when the dark-grown alga is transferred to

light the ability to produce oxygen develops in about 4 hours; up to this time light accelerates oxygen consumption by the alga. The Department profited greatly from Dr. Schiff's interest in experimental techniques. While here he improved the performance of the equipment for measuring action spectra and added an automatic device to keep the wavelength sweep speed at the optimum value.

Purple bacteria utilize light for a form of photosynthesis that produces material for their growth but without evolving oxygen like green plants. These bacteria are particularly useful in the study of photosynthesis because both their photosynthetic products and their pigment systems contrast with those of green plants. In the dark, photosynthetic bacteria, like other plants, consume oxygen when it is available. If they are exposed to light the oxygen uptake is strongly inhibited, presumably by the diversion of respiratory substrates into the photosynthetic pathway. Dr. Fork, working at Utrecht in collaboration with a former Institution Fellow, Dr. Goedheer, and Professor Thomas, investigated this effect of light on purple bacteria. They found that the action spectra of the light inhibition of respiration is a near match to those previously known for bacterial photosynthesis, for the excitation of fluorescence in bacteriochlorophyll, and for the effect of light in orienting the swimming of the bacteria. In all these effects bacteriochlorophyll is active while the carotenoids are sometimes only partly functional.

The formation of chlorophyll from protochlorophyll in plants grown in the dark requires light. Whether this reaction is a single-step photochemical reaction or whether light initiates a series of reactions leading to the final product—chlorophyll—has long been discussed. This year Mr. Axel Madsen, visiting the Department from the Royal Veterinary and Agricultural College, Copenhagen, found that the transformation of protochlorophyll to

chlorophyll was complete in leaves in the shortest time that could be measured, 4 milliseconds. With protochlorophyll holochrome solutions as prepared by Dr. Smith, which do not scatter light, a different optical system was used, in which the time resolution could be reduced to 1 msec. After this time no more transformation was seen. It is therefore certain that if any dark reactions are involved they are completed within a thousandth of a second.

A green alga, apparently a *Stichococcus*, was found growing in an unusual habitat—a 1 *M* solution of MgSO_4 on the laboratory bench. When Dr. Brown isolated this strain in pure culture she found it to contain an unusually high proportion of chlorophyll *b*, which makes it particularly useful for comparative studies of pigment functions. Enhancement effects and the action spectrum for this alga are under investigation by Dr. Govindjee.

During the past year some time was spent on a project far removed from our normal activities. It came about because we thought we saw a way to improve one of the standard methods for making large-scale topographic maps of small areas. The idea was to use an optical range finder for plane table mapping in such a way that a point observed through the range finder telescope is automatically located on the map by an index marker. At the same time the elevation of this point also appears on a dial. All calculating and plotting are done by the instrument itself. The device should make it possible for one or two men to do much more rapidly the work now requiring a survey party of three or more.

An experimental instrument incorporating these principles has been built. Although tests and modifications are still in progress, it appears that distance accuracy within 1 foot and elevation accuracy of about 0.1 foot will be attainable at a scale of 1 inch = 10 feet. Other scales are also possible.

Parts of the accumulated data from long-term genetic and transplant experi-

ments on *Achillea* and *Mimulus* have been analyzed with the help of an electronic computer to determine whether the principle of genetic coherence, an important concept that emerged from earlier work on *Potentilla*, applies to other groups of higher plants as well. The results, in conclusive agreement with those found in *Potentilla*, indicate that the principle is a general one.

Genetic coherence is the tendency for sets of characters that distinguish one recognizable biological entity from another to be inherited together as a block rather than to segregate separately in a purely random Mendelian fashion. Coherence results from the fact that the vast majority of characters distinguishing biological entities, rather than being determined by single genes located on a single chromosome, are controlled by multiple genes, the components of which may be distributed over more than one chromosome. The principle of coherence is important, because it not only provides a rational genetic basis for the differentiation of ecological races, subspecies, and species but also orients studies aimed at discovering physiological mechanisms underlying natural selection.

The existence of genetic coherence has been difficult to prove experimentally because of the wide segregation of character combinations typically observed in the second-generation progeny of crosses between contrasting climatic races. The overwhelming array of new combinations of characters tends to obscure the important effects of coherence. Measurements of specific characters of individual plants in fairly large samples of segregating hybrid populations when tested as cloned transplants at the altitudinal transplant stations provide the data essential for determining the existence of genetic coherence and its role in natural selection.

By means of controlled growth cabinets it is now possible to grow alpine forms of *M. lewisii* at Stanford so that measurements on rates of photosynthesis can be

made. Preliminary work indicates that photosynthetic rates of high-altitude races of *M. lewisii* are distinct from those of races of *M. cardinalis* that range at lower altitudes. The data are yet too incomplete to allow conclusions.

Methods for establishing and growing tissue cultures of different races of *Mimulus* are being perfected so that the comparative growth and development of parts of cloned individuals can be studied under sterile, controlled conditions. This work is being closely coordinated with the studies at the transplant stations, in the controlled cabinets, and by photosynthetic measurements.

Biochemical studies on key clones of *Mimulus cardinalis* used in the photosynthetic measurements have been started by Mr. D. McMahon, a graduate student working with Professors Olmsted and Bogorad at the University of Chicago. Mr. McMahon is making a comparative study of enzyme systems concerned with assimilation and respiration in different climatic races. His work, which is being carried on independently, can be coordinated with our investigations through the use of the same cloned plants having identical genetic composition.

Dr. Clausen has devoted considerable effort to the tree lines in the Harvey Monroe Hall Natural Area, in which the Timberline station is situated. A field study of altitudinal segments representing different slope exposures discloses characteristic differences both in the composition of genetic variants and in the over-all levels of tolerance to high altitudes of three distinct species of conifers, *Tsuga mertensiana*, *Pinus murrayana*, and *P. albicaulis*.

Miss Yvonne Aitken, senior lecturer in the School of Agriculture at the University of Melbourne, Australia, is spending part of her sabbatical year at the Department, studying growth and flowering responses of 30 varieties of important crop plants at the Stanford, Mather, and Timberline transplant stations. This is part of a larger investigation on the com-

parative development of early and late crop varieties at different latitudes and altitudes. Other plantings are located at the University of Melbourne, the University of Hawaii, Oregon State College, the University of Saskatchewan, and the Welsh Plant Breeding Station at Aberystwyth.

Dr. Theodosius Dobzhansky is continuing evolutionary studies on native *Drosophila* populations across the Sierran transect, using the Mather transplant station as headquarters for his operations during part of the summer of 1963. This is part of a long-term survey in progress for many years.

PERSONNEL

Biochemical Investigations

Staff: C. Stacy French, *Director*, Jeanette S. Brown, David C. Fork, James H. C. Smith, *Emeritus*

Visiting Investigators: Charles A. Fewson, Martin Gibbs, Govindjee, Rajni Govindjee, Axel Madsen, Jerome A. Schiff, Marvin D. Schulman

Technical Assistants: Robert A. Clair, Harriet M. Fulk, David N. Lion, D. David Perfect, Devender C. Reddy

Experimental Taxonomy

Staff: Jens C. Clausen, *Emeritus*, William M. Hiesey, Harold W. Milner, Malcolm A. Nobs

Visiting Investigator: Yvonne Aitken

Summer Research Assistant: Andrew N. Lenz

Technical Assistants: Frank Nicholson, Kathe A. Picken

Clerical Assistant: Marylee H. Eldredge

Gardeners: Joseph S. Chang, Emmett R. Clagg, Erica Duveneck, Wesley B. Justice

Administrative Assistant

Wiley Knight, Jr.

Mechanic

Richard W. Hart

Custodian

Jan Kowalik

Wesley B. Justice retired on April 30, 1963, after 16 years as gardener with the Department.

Dr. Jeanette S. Brown and Dr. David C. Fork attended the Photosynthesis Colloquium at Gif-sur-Yvette in July 1962. In August 1962 Dr. Brown attended

a colloquium on the metabolism of chlorophyllous pigments in the leaf, at Centre de Recherches de Gorse, St. Trond, Belgium. At the end of June 1963 she left for a 4-month period of work with Dr. J. Duranton of the Département de Biologie, Commissariat à l'Énergie Atomique, Saclay, on the chemical separation of chlorophyll holochrome. The remainder of the coming year she plans to spend in the Philippines collecting algae for future use in studies of pigment function.

This spring Dr. David C. Fork returned from a year in Europe, where he worked in three laboratories. After a month's visit at Laboratoire de Photosynthèse in Gif-sur-Yvette near Paris he spent 6 months in the Physical-Chemical Institute of Professor H. Kuhn at the Philips University of Marburg, where he worked with Professor H. T. Witt and Dr. A. Müller on the action spectra for the production of fast absorption changes associated with different light reactions of photosynthesis. He spent the remainder of his time in Professor J. B. Thomas's Biophysical Research Group of the State University at Utrecht. There he collaborated with Dr. Goedheer on a study of the light-induced inhibition of respiration in photosynthetic purple bacteria and also observed Dr. Goedheer's apparatus for measuring the luminescence of photosynthetic organisms.

Dr. Jens Clausen lectured at the National Science Foundation Summer Institute for College Teachers at Vanderbilt University in July 1962 on the function of populations in the evolution

of species and their adjustment to environment. In April 1963 he attended the annual meeting of the National Academy of Sciences in Washington, D. C. There, and at the University of Tennessee, Knoxville, and at Vanderbilt University, Nashville, he presented papers and seminars on the distribution and evolution of trees.

After his work as a visiting investigator at the Royal Agricultural College at Uppsala, Sweden, last year, Dr. Malcolm Nobs took part in an international botanical symposium held at Prague during July 1962.

Dr. William M. Hiesey participated in an international symposium on the en-

vironmental control of plant growth at Canberra, Australia, during August 1962, held in connection with the official opening of the Controlled Environment Research Laboratory (Ceres) built by the Division of Plant Industry of the Commonwealth Scientific and Industrial Research Organization. The symposium on environmental control was preceded and followed by meetings at the University of Sydney and the University of Melbourne dealing with various aspects of plant science, including physiology, genetics, and microclimatology, sponsored independently by the Australian and New Zealand Association for the Advancement of Science and by the CSIRO.

BIOCHEMICAL INVESTIGATIONS

EXPERIMENTS WITH COLORED LIGHT FLASHES

C. S. French

Some of the more useful information for the interpretation of the kinetics of photosynthesis over the past few decades has come from the study of rates of photosynthesis in flashing light. From such measurements, the concept of the "photosynthetic unit" has developed and the time constants for the rates of some of the enzymatic steps in photosynthesis have been determined by various workers.

Many of these investigations have been carried out with great experimental ingenuity, high precision of measurement, and extensive theoretical insight. Except for the recent work of Whittingham, these flashing light experiments were done before it was known that two separate photochemical reactions participated in the process, and so no attention was paid to the influence of wavelength on the rates of photosynthesis in flashing light. We are therefore studying the kinetics of photosynthesis in flashing light of different colors chosen to activate certain pigments preferentially.

Last year we reported that, in the red alga *Porphyridium*, green light flashes of a few seconds' duration gave more oxygen if preceded by a flash of red light lasting several seconds. The production of oxygen from long red flashes, however, was not enhanced by a previous green flash. In those experiments the time course of oxygen evolution from each flash, rather than steady-state rates, was measured. The material produced by activating chlorophyll *a* with red light disappeared in the dark with a half-life of about 18 seconds.

We reasoned by analogy that perhaps a substance might be produced by green light that could enhance oxygen evolution by a succeeding red flash but that it might have too short a survival time to be detected in those experiments.

This year we tested that hypothesis by measuring the steady-state rate of oxygen evolution from paired flashes of the two colors given repeatedly. The flashes themselves were much shorter, and the dark interval between them was greatly reduced. Experiments were made with two timing schedules: flash time 10 or 4 msec; time between flashes 50 or 10 msec; time between pairs of flashes 500 or 430 msec.

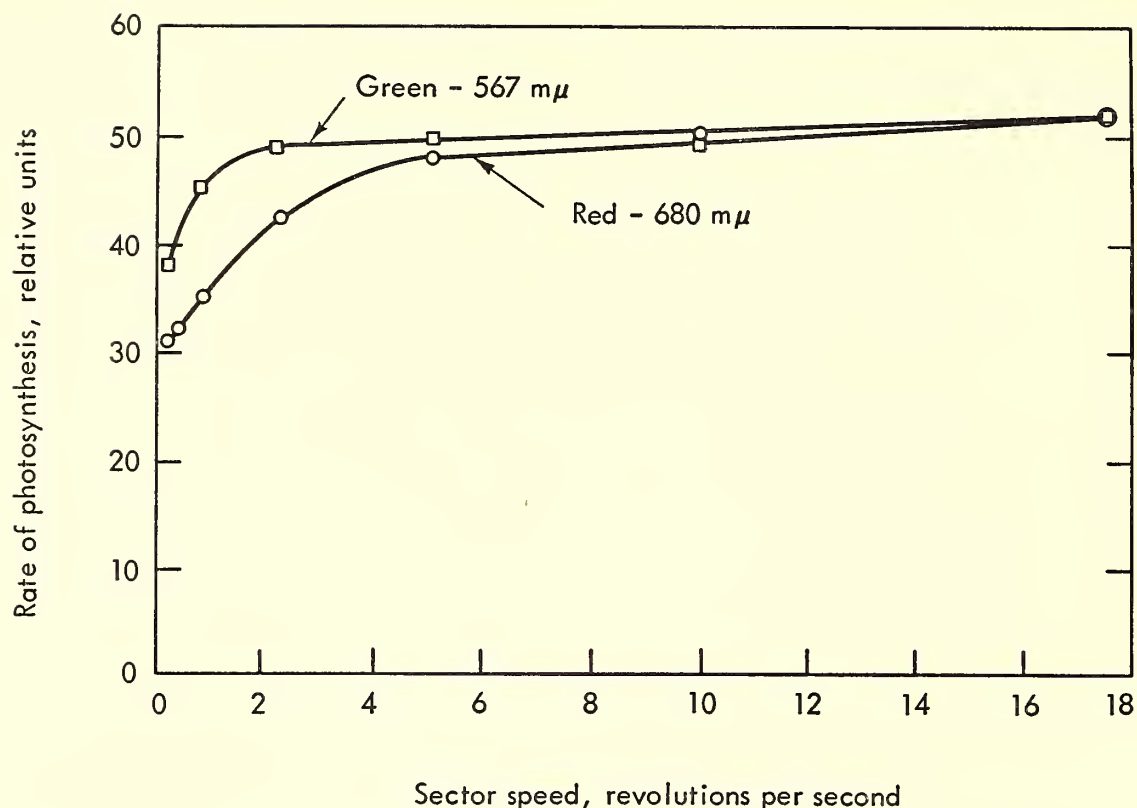


Fig. 1. The variation of photosynthetic rate of *Porphyridium* with sector speed in two colors of flashing light. Conditions: artificial sea water, 5 per cent CO_2 in air, about 23°C , sector opening about 1.2 per cent of circumference.

Dark intervals between the closely spaced pairs of flashes were long enough to allow for the decay of the hypothetical product of the green light but short in comparison with the lifetime previously found for the product of the red light. The idea was that, if an enhancing green light product with a very short lifetime existed, more oxygen would be produced per minute if the green flash came just before rather than after the red flash. No such effect was found. We therefore conclude that, in *Porphyridium*, material made by chlorophyll *a* enhances the production of oxygen by green light but that the opposite situation does not exist. No evidence was found for the presence of a substance made by green light that can enhance photosynthesis subsequently in red light.

Among other effects that have been observed with various regimes of colored light flashes in *Porphyridium* is the difference in the way the steady-state rates of photosynthesis in red and in green light depend on the flash duration or on the dark time between flashes. In

these experiments a sector with a single opening about 1.2 per cent of the circumference was used. It rotated about 10 times per second, and the intensities of red and of green light were adjusted to give the same rates of photosynthesis at this high speed. Measurements were then made with slower speeds, but with the cells always having the same amount of light per minute and the same intensity as at the faster speed. At lower speeds both the light and the dark periods were of longer duration.

The results are shown in figure 1. With green light the rate declined with decreased sector speed much less rapidly than with red light. The implications of this effect are not yet evident, beyond showing a difference in the kinetics of photosynthesis in red and in green light on a short time scale.

In other experiments the photosynthetic rate with high and low sector speed both with red and with green light was measured at several intensities. In figure 2 the ratio of the rates at low and at high speeds is plotted for the two

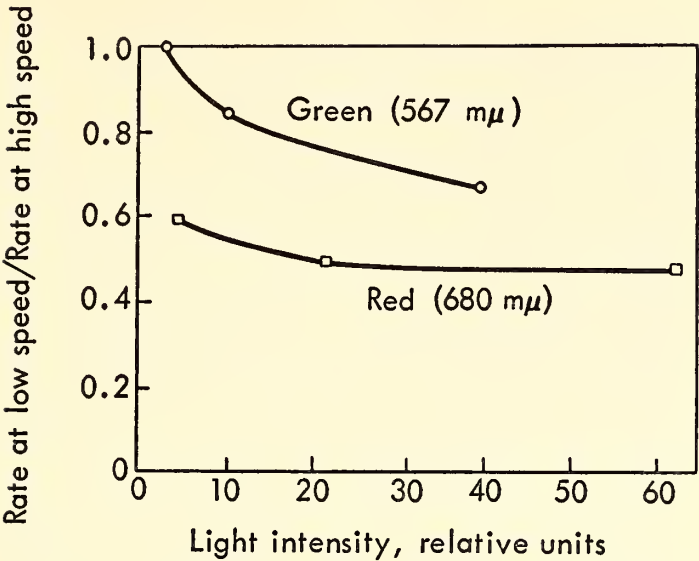


Fig. 2. The decrease in photosynthetic rate at low sector speed at different intensities of red and green lights.

colors. The high speed was 9.5 rps, which gave a light exposure time of 2.3 msec; the low speed was 0.49 rps, giving 49-msec exposures. The amount of light per minute was the same for both speeds. After measurements at two sector speeds for each color the intensity was changed

to a new value. The rate of photosynthesis with the high-speed flashes was used as a measure of effective light intensity. It is the abscissa of figure 2.

At the lowest intensity of green light flashes the slow and fast speeds were equally effective; as the intensity increased, photosynthesis at low speed became less effective than at the higher speed. With red flashes the rates at low speed were far below those at high speed. It looks as though higher intensities of green would have given results approaching the same low-speed ratio as was found for red light if sufficient intensity had been available.

In a different type of experiment unexpected effects were found when the oxygen production from single short flashes was studied. Red or green flashes lasting about 50 msec were given at 46.8-second intervals both with and without continuous background illumination, as shown in figure 3. Because of the long time between flashes the time course for

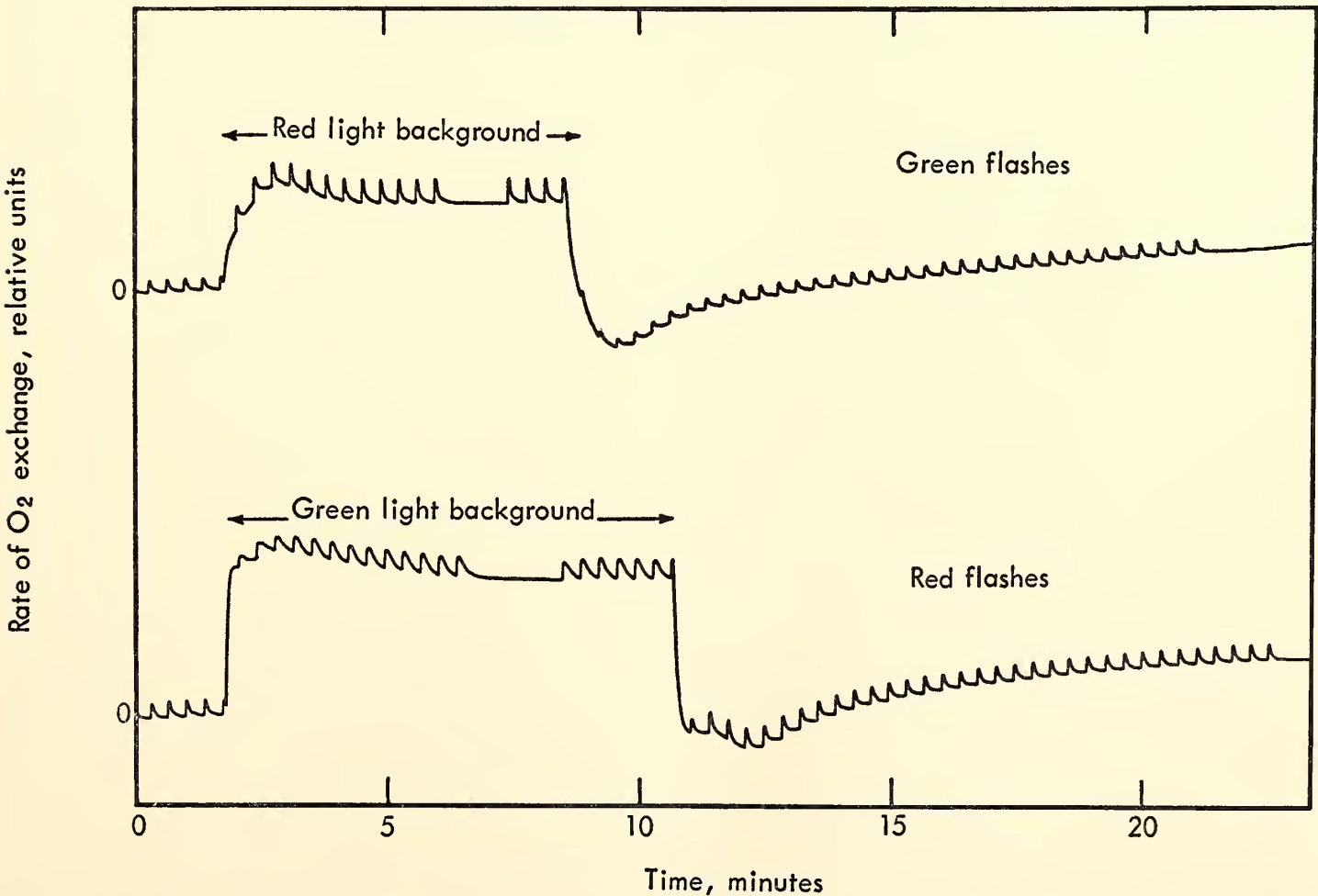


Fig. 3. The rate of oxygen exchange following 50-msec flashes given repetitively with and without complementary background light.

rate of oxygen evolution from each flash appeared on the record. The rate reached its peak value in about 2 seconds and dropped halfway back to the base line in about 6 seconds.

The lag in the apparatus response is greater for the drop than for the rise, because the drop depends on oxygen removal by diffusion through the cellophane membrane over the cells. The instrumental lag for the drop would have a half-time of about 3 seconds for a sudden stopping of oxygen evolution (*Year Book 61*, p. 346). After the flashes with no background light the observed lag was about 6 seconds for either green or red, showing an appreciable continuation of oxygen production after the flash.

When either red or green flashes were given on a background of the opposite color more oxygen evolution was found from each flash than without the background light. The shape of the time course curve for oxygen evolution following each flash with complementary background light, however, was very different.

The green flashes had about twice the peak rate when given on a continuous red background illumination, as seen in the upper right of figure 3. Here the drop back to the base line was as rapid as without the continuous red light.

By contrast the red flashes when given on the continuous green background showed no increase in the peak rate but the rate dropped back to the base line more slowly, thus also giving more total oxygen than without the background light. The half-time was about 10 seconds. The total oxygen evolution from each flash, that is, the area under the rate curve, was larger for either color of flash with complementary background light, thus showing the enhancement effect either way but with very different kinetics.

In summary, the enhancement of oxygen evolution from a single flash produced by the background light can appear in two different ways: through an increase of the initial rate, or by pro-

longing the time during which oxygen evolution continues after the flash.

In the upper part of figure 3 the peak rates of oxygen production from green flashes given during the few minutes following the red light exposure are smaller than before the continuous red light exposure. This is just opposite to the effect expected from last year's work with longer flashes of green light following flashes of red light.

Thus we see that many factors controlling the rate of photosynthesis with different regimes of light exposure to various wavelengths are still unknown. These phenomena, which appear to offer promising ways to study the two pigment reactions in photosynthesis, are being investigated further by Drs. Govindjee and Rajni Govindjee.

STUDIES ON THE ENHANCEMENT OF SOME PHOTOCHEMICAL REACTIONS CARRIED OUT BY WHOLE CELLS AND BY CELL-FREE PREPARATIONS

*Martin Gibbs, Charles A. Fewson, and
Marvin D. Schulman*

One of the first indications that two different photochemical reactions are involved in photosynthesis by algae and higher plants came from the enhancement studies of Emerson. It had been known for some years that photosynthesis is less efficient in the far-red (beyond about 695 m μ) than at shorter wavelengths. Emerson discovered that there is a synergistic effect on photosynthetic oxygen evolution if red light and light of a shorter wavelength are presented simultaneously. The enhancement of photosynthesis may be considered in two ways: either as a mutual enhancement or as an increase in the efficiency of only the long-wavelength light. The effect can therefore be described by two ratios:

$$\text{Mutual enhancement (E total)} = \frac{\text{Rate } (\lambda_{\text{short}} + \lambda_{\text{long}})}{\text{Rate } \lambda_{\text{short}} + \text{Rate } \lambda_{\text{long}}}$$

$$\text{Red enhancement (E red)} = \frac{\text{Rate } (\lambda_{\text{short}} + \lambda_{\text{long}}) - \text{Rate } \lambda_{\text{short}}}{\text{Rate } \lambda_{\text{long}}}$$

where the parentheses indicate simultaneous exposure to short and long wavelengths.

French, Brown, and Fork (*Year Books* 60, pp. 351–362, and 61, pp. 345–357) have studied the photostimulated oxygen uptake carried out by algae. It is clear that this phenomenon could interfere with determinations of photosynthetic enhancement as measured by oxygen evolution. Apparently this light-dependent oxygen uptake is not accompanied by carbon dioxide evolution and is thus quite distinct from respiration; rather, it is a side effect of the photochemical mechanism (*Year Book* 60, p. 354). We therefore wished to study the enhancement of carbon dioxide assimilation by whole algal cells, since most previous enhancement studies have been made on oxygen evolution. By measuring the assimilation of C^{14} carbon dioxide we thought that we might minimize the possibility of obtaining spurious results caused by side reactions. We also wished to see whether the various chloroplast reactions such as oxygen evolution and TPNH and ATP formation show an enhancement effect.

Algae. The blue-green alga *Anacystis nidulans*, the red alga *Porphyridium cruentum*, and the green alga *Scenedesmus obliquus* were harvested from actively growing cultures and resuspended in artificial sea water before use. No damage from sea water to the *Scenedesmus* appeared within the hour needed for the experiments.

Chloroplasts. Swiss chard and spinach were grown in the garden at Stanford, and some additional plants were purchased from local stores. Mature leaves were rinsed with distilled water and chilled in an ice-slush for 20 minutes. All further steps were carried out in a cold room in dim light. The midribs were removed, and the leaf blades were

chopped into small fragments. The fragments were then ground with sand in a solution containing 0.35 *M* NaCl and 0.02 *M* tris buffer, pH 7.6. The slurry was strained through 8 layers of cheesecloth and centrifuged at 200*g* for 2 minutes. The supernatant fluid was then centrifuged at 1000*g* for 10 minutes. The precipitated chloroplasts were resuspended in 0.35 *M* NaCl, 0.02 *M* tris, pH 7.6, and stored at about 4°C in the dark.

Particle preparations from *Anacystis* were made by freeze-drying as described elsewhere (*Nature*, 198, 88, 1963).

Measurement of oxygen evolution. The rates of oxygen output by chloroplasts or algae were measured with a platinum electrode covered with a thin layer of Teflon as described by Dr. Fork (*Year Book* 61, p. 343). The standard circulating fluid contained 0.4 *M* sucrose, 0.01 *M* NaCl, and 0.05 *M* KH_2PO_4 – K_2HPO_4 (pH 7.4). The illumination was provided either from a monochromator with supplementary stray light filters or from tungsten lights with interference and stray light filters as described in the *Year Books* of the last four years.

Measurement of carbon dioxide assimilation. The reaction mixture for measuring carbon dioxide fixation contained algal suspension (10^5 to 10^6 cells in artificial sea water, pH 6.9, without HCO_3^-); NaHCO_3 , 10 micromoles (containing approximately 10 microcuries C^{14}); total volume 1.5 ml. After various times of illumination 0.10-ml aliquots were removed and added to 0.90 ml of 0.25 *N* HCl in 95 per cent ethanol contained in planchets. The samples were evaporated to dryness, and the radioactivity was determined. The reaction mixture was contained in a Beckman 1-cm-light-path cuvette.

Illumination was provided from two opposite sides by projector lamps. The filaments of the lamps were imaged on the cuvette faces. The far-red light was obtained by passing the beam through a 12-cm water filter, a Bausch and Lomb interference filter of wavelength as indi-

cated in tables 1-4, and Corning glass filter 2030. The short-wavelength beam was obtained by passage through a 5-cm 1 per cent w/v CuSO₄ solution, an appropriate Bausch and Lomb interference filter, a Corning glass filter 2408, 2418, 3387, or 3484, and an infrared blocking filter. Beam intensities were controlled by variable voltage transformers. Shutters were interposed between the filters and the cuvette.

TPNH formation. The reduction of TPN by chloroplasts or by *Anacystis*

preparations was measured in reaction mixtures containing tris-HCl buffer, pH 7.6, 24 micromoles; MgCl₂, 4 μmoles; KH₂PO₄-K₂HPO₄, pH 7.5, 1.54 μmoles; ADP, 2 μmoles; TPN, 1.5 μmoles; photosynthetic pyridine nucleotide reductase purified from spinach, 1 unit; chloroplasts or *Anacystis* particles containing about 30 μg chlorophyll; total volume 2 ml. After illumination under the same conditions as used for measuring carbon dioxide assimilation, the reaction mixtures were centrifuged in the dark at

TABLE 1. Oxygen Evolution by Intact Algae
Results in arbitrary units of oxygen evolution per minute

<i>Anacystis nidulans</i>					
Expt.	627 mμ	694 mμ	627 mμ + 694 mμ	<i>E</i> Red	<i>E</i> Total
1	14	7	33	2.71	1.58
2	16	12	35	1.58	1.25
3	14	2	23	4.50	1.43
<i>Scenedesmus obliquus</i>					
Expt.	650 mμ	710 mμ	650 mμ + 710 mμ	<i>E</i> Red	<i>E</i> Total
1	28	9	41	1.45	1.11
2	15	6	24	1.50	1.14
3	14	3	22	2.66	1.29

TABLE 2. Carbon Dioxide Fixation by Intact Algae
Results in counts per minute fixed per 0.1 ml aliquot

<i>Prophyridium cruentum</i>					
Expt.	567 mμ	694 mμ	567 mμ + 694 mμ	<i>E</i> Red	<i>E</i> Total
1	1839	316	3283	3.66	1.52
2	3252	728	4865	2.22	1.22
3	1954	406	4485	6.24	1.90
<i>Anacystis nidulans</i>					
Expt.	613 mμ	694 mμ	613 mμ + 694 mμ	<i>E</i> Red	<i>E</i> Total
1	132	36	248	3.0	1.48
2	324	162	630	1.89	1.30
<i>Scenedesmus obliquus</i>					
Expt.	650 mμ	710 mμ	650 mμ + 710 mμ	<i>E</i> Red	<i>E</i> Total
1	1,072	186	1,547	2.55	1.23
2	10,654	166	11,768	6.95	1.09

4°C. TPNH formation was determined by absorbancy measurements at 340 m μ .

Enhancement of oxygen evolution by algae. Table 1 shows, in confirmation of the results obtained by many workers, that there was a consistent enhancement of the rate of oxygen evolution by whole cells of *Anacystis* and *Scenedesmus* when red and short-wavelength lights were presented together.

Enhancement of carbon dioxide assimilation by algae. An enhancement of the rate of carbon dioxide uptake could be observed with the green, red, and blue-green algae studied, as shown in table 2. The similarities of the degrees of enhancement shown by carbon dioxide fixation and by oxygen output suggest that previous estimates of enhancement have probably not been greatly affected by the photostimulated oxygen uptake, provided, of course, that there is definitely no carbon dioxide output associated with the light-activated oxygen uptake. Figure 4 demonstrates that the degree of enhancement is markedly affected by the

ratio of the two lights. The precise significance of this is not clear, although it is undoubtedly a reflection of the pigment complement of the organism. Myers and Graham (*Plant Physiol.*, 38, 105, 1963) have presented a similar type of curve for the effect of ratio of incident energies on the enhancement of oxygen evolution by *Chlorella*. Figure 4 also illustrates the variation in the value obtained for enhancement according to the method of calculation.

Lack of enhancement of the Hill reaction. Table 3 illustrates experiments in which we attempted to obtain enhancement of the rate of oxygen production by Swiss chard and spinach chloroplasts and by *Anacystis* particles. Under no conditions were we able to find a positive enhancement. Experiments were carried out with ferricyanide as the electron acceptor, and we also studied the endogenous chloroplast reaction described in detail by Dr. Fork (*Year Book* 61, p. 334). A wide range of wavelength combinations, relative and absolute light intensities, and different particle preparations all gave uniformly negative results.

A few experiments were also carried out on TPN reduction by spinach chloroplasts and by *Anacystis* particles. No enhancement could be observed, a finding that confirms preliminary results obtained in collaboration with Dr. C. C. Black and Dr. S. A. Gordon at the Argonne National Laboratory. In these earlier experiments we did notice one consistent and very pronounced interaction of monochromatic lights, namely an inhibitory effect of prior exposure to light of wavelength longer than 700 m μ on TPNH and ATP formation and carbon dioxide fixation by spinach chloroplasts at shorter wavelengths.

Valid enhancement studies on ATP formation by chloroplasts do not appear to be possible at the moment because of the sigmoid response of ATP formation to increasing light intensity (Turner, Black, and Gibbs, *J. Biol. Chem.*, 237, 577, 1962).

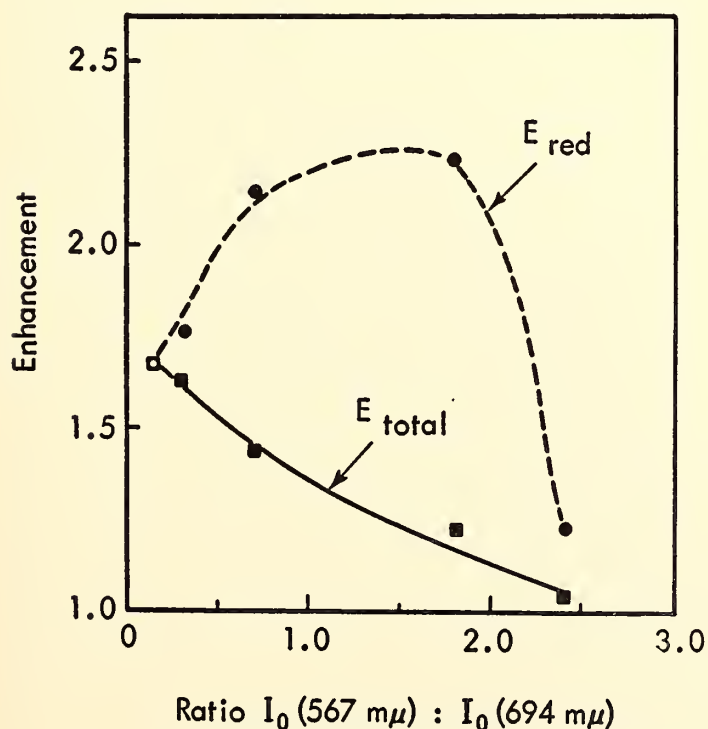


Fig. 4. Effect of ratio of incident energies on the enhancement of carbon dioxide assimilation by *Porphyridium cruentum*. The incident energy at 694 m μ was maintained at 2750 ergs cm⁻² sec⁻¹, and the incident energy at 567 m μ was varied from 400 to 6400 ergs cm⁻² sec⁻¹.

TABLE 3. Effect of Combinations of Monochromatic Light on the Hill Reaction
Results in arbitrary units of oxygen evolution per minute

Spinach chloroplasts							E Total
Expt.	Acceptor	650 m μ	694 m μ	700 m μ	650 m μ + 694 m μ	650 m μ + 700 m μ	
1	Ferricyanide	3.5	2.5	---	6	---	1.00
2	Ferricyanide	15	---	8	---	22	0.96

Swiss chard chloroplasts							E Total
Expt.	Acceptor	650 m μ	694 m μ	700 m μ	650 m μ + 694 m μ	650 m μ + 700 m μ	
1	---	7	15	---	23	---	1.05
2	---	23	10	---	29	---	0.88
3	Ferricyanide	16	8	---	24	---	1.00
4	Ferricyanide	18	---	13	---	30	0.97
5	Ferricyanide	10	---	4	---	14	1.00

Anacystis nidulans preparation					E Total
Expt.	Acceptor	627 m μ	694 m μ	627 m μ + 694 m μ	
1	Ferricyanide	2	7	9	1.00
2	Ferricyanide	7	1	7	0.88
3	Ferricyanide	9	2.5	10	0.87
4	Ferricyanide	7	6	12.5	0.96

The absence of enhancement of TPN reduction and oxygen evolution by isolated chloroplasts is difficult to explain if present ideas about the photosynthetic electron transport system are correct. Although an enhancement might possibly be observed after a more extensive search for optimal conditions it appears to be unlikely, since a wide range of conditions has been tried and, furthermore, enhancement was very readily and consistently observed with intact cells. It is noteworthy that the experiments on whole cells and on cell-free preparations were made with identical apparatus and illumination techniques.

At present, therefore, there appears to be some controversy about whether isolated chloroplasts show an Emerson effect. Mayne and Brown (*Plant Physiol.*, 37, lxxv, 1962) have also failed to demonstrate enhancement. Gordon (*Plant Physiol.*, 38, 153, 1963) reported an enhancement effect on the photoreduction of TPN by extracts of the red alga *Laurencia obtusa*, but the rates he observed were extremely low. Govindjee, Govindjee, and Hoch (*Biochem. Biophys. Res. Commun.*,

9, 222, 1962) showed a synergistic effect of white light and red light on TPN reduction, and Bishop and Whittingham (*Nature*, 197, 1225, 1963) have observed enhancement of the ferricyanide Hill reaction in flashing light. These positive results have been obtained under rather specialized conditions; their relation to a true Emerson effect may be tenuous and remains to be demonstrated experimentally. No one has yet found an enhancement with cell-free preparations comparable to that observed with intact cells. The only possibly positive evidence we have obtained for the existence of an Emerson effect in chloroplasts is that the action spectra for the rates of TPNH and ATP formation at saturating light intensities show a considerable degree of structure (Black, Fewson, Gibbs, and Gordon, to be published, *J. Biol. Chem.*, 1963). McLeod (*Year Book* 59, p. 342) observed a similar phenomenon for oxygen evolution by intact cells of several algal species. French has suggested that this effect and the Emerson effect may have a common origin.

Probably the most significant results

on cell-free systems could be obtained by examining the enhancement of carbon dioxide fixation by isolated chloroplasts, since this is the system most closely allied to that existing in whole-cell photosynthesis. Unfortunately rates of chloroplast carbon dioxide fixation are so low (about 2 per cent of the rate for intact tissues) and inconsistent that it is doubtful whether such experiments would have much value at present.

ACTION SPECTRA FOR SEPARATED LIGHT REACTIONS IN PHOTOSYNTHESIS

David C. Fork¹

The concept that photosynthesis requires two different light reactions originated largely with Emerson's experiments on the enhancement effect and with Blinks's experiments on chromatic transients. Since then considerable effort has been devoted to determining how different light reactions participate in photosynthesis.

Witt and co-workers have been able to study several of the intermediate reactions of photosynthesis by measuring specific spectral absorption changes caused by illumination. Furthermore, they noted that excitation of *Chlorella* by far-red light ($\sim 710\text{ m}\mu$) resulted in absorption changes corresponding to oxidation of a special chlorophyll *a* and cytochrome (light reaction $h\nu_I$), whereas excitation of light reaction $h\nu_{II}$ with shorter wavelengths ($\sim 670\text{ m}\mu$) resulted in absorption changes corresponding to reduction of compound X, since identified as plastoquinone.

It was possible by appropriate treatment to obtain samples of chloroplast fragments which showed only one or the other of these light reactions at a time.

¹ These experiments, performed in collaboration with Dr. A. Müller and Professor H. T. Witt, and described elsewhere (Müller et al., *Z. Naturforsch.*, 18b, 142, 1963), were made possible through the courtesy of Professors Witt and H. Kuhn of the Physikalisch-Chemisches Institut der Universität, Marburg an der Lahn.

We were then able to measure the action spectrum for each separated light reaction. In the terminology of Witt's laboratory, reaction $h\nu_I$ results from the activation of what we have called the long-wavelength chlorophyll reaction and is evidenced by a decrease in absorption at 433 and 703 $\text{m}\mu$, whereas reaction $h\nu_{II}$ results from activating the accessory pigment system and is evidenced by a decrease in absorption at 475 $\text{m}\mu$ and an increase at 515 $\text{m}\mu$. Since these reactions are interrelated in the chloroplasts, it is necessary to inactivate the one not under investigation to prevent complications caused by simultaneously occurring reactions.

Separation of light reaction $h\nu_I$ and its action spectrum. Vernon, Kamen, and Zaugg demonstrated that aged chloroplasts which can no longer evolve oxygen can, nevertheless, reduce pyridine nucleotide in the light if appropriate reduced compounds are provided. Witt has found that aged chloroplasts with reduced *n*-methylphenazonium methosulfate (PMS) and excess sodium ascorbate exhibit changes of absorption upon illumination which correspond to oxidation of cytochrome and chlorophyll. With increased concentrations of reduced PMS, only the negative absorption changes at 433 and 703 $\text{m}\mu$ are seen, indicating that reduced PMS couples directly to chlorophyll 703. Furthermore, the identical behavior of the 433- and the 703- $\text{m}\mu$ absorption changes with different physical and chemical parameters indicates that they are caused by one and the same phenomenon—oxidation of a particular form of chlorophyll. The discovery of the 703- $\text{m}\mu$ change was made by Kok, whose detailed study of this absorption change also indicates that it is related to oxidation of chlorophyll.

Aged chloroplast fragments that no longer exhibited changes of absorption at 515 $\text{m}\mu$ (discussed later) were therefore used for the determination of the action spectrum for chlorophyll oxidation. In order to use red actinic light we measured

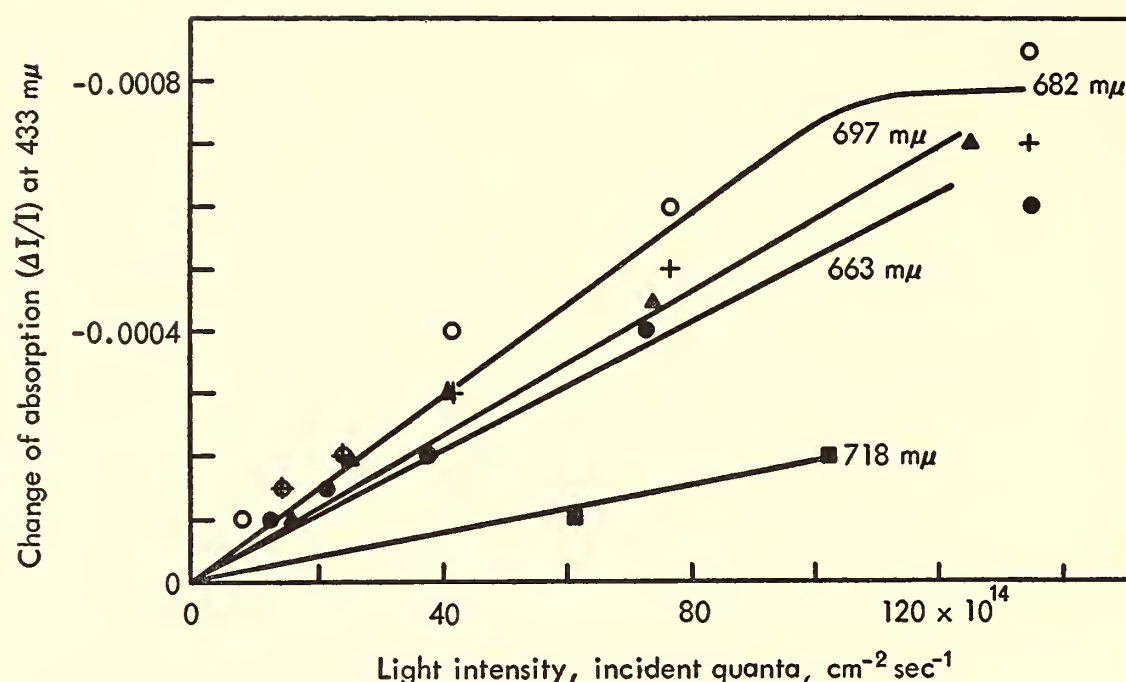


Fig. 5. The 433-m μ absorption change as a function of actinic light intensity for representative wavelengths at 663, 681, 697, and 718 m μ . The solution contained 9.4×10^{-5} PMS, 9.4×10^{-3} M sodium ascorbate, 3.8×10^{-2} M tris buffer (pH 7.2), and spinach chloroplast fragments which gave a final chlorophyll concentration of 0.150 mg/ml. The transmission of this suspension in the 1-mm-path-length cuvette at 674 m μ was 17 per cent; temperature about 21°C. All the saturation curves were obtained from one cuvette of sample. The data from these and other, similar curves were used to plot the action spectrum of figure 7.

the absorption change at 433 m μ instead of at 703 m μ . That PMS, reduced by excess sodium ascorbate, was coupled to chlorophyll directly rather than through cytochrome was seen by the absence of absorption changes characteristic of cytochrome at 401 m μ . At each actinic wavelength used for determining the action spectrum, the 433-m μ absorption change was obtained as a function of light intensity. Figure 5 shows the absorption change at 433 m μ for four wavelengths as a function of the incident light intensity. An intensity (100×10^{14} quanta cm $^{-2}$ sec $^{-1}$) was chosen that fell within the linear region of all the light intensity curves. The resulting absorption changes were then plotted as the action spectrum in figure 7.

Separation of light reaction $h\nu_{II}$ and its action spectrum. Bishop has shown that Hill reaction activity can be restored by recondensing plastoquinone on chloroplasts previously extracted by petroleum ether. A parallel experiment by Müller and by Weikard in Witt's

laboratory has demonstrated that this extraction abolishes the negative change of absorption upon illumination at 475 m μ and the positive change at 515 m μ and that recondensation of plastoquinone restores them. The absorption changes at 475 and 515 m μ are thus found only in the presence of plastoquinone. The reduction of plastoquinone seems to be correlated with oxygen production (Müller et al., *Proc. Royal Soc. London, B*, 157, 313, 1963).

The observation, mentioned earlier, that plastoquinone reduction is more effectively mediated by 670 m μ than by 710 m μ was documented more quantitatively by measuring the action spectrum for the production of the 515-m μ absorption change. For this purpose freshly prepared chloroplast fragments were used. The time course of the absorption change at 515 m μ for fragments suspended only in tris buffer exhibited induction effects. A transient positive spike occurred upon illumination. A steady-state absorption change, lower than the initial spike, was

attained after about 1 second in the light. The height of the 515-m μ absorption change spike was increased by a previous dark period. The oxygen-production spike of chloroplasts was likewise found to be increased by a dark period (*Year Book 61*, p. 336). With these chloroplast fragments the time required for the 515-m μ absorption to decay to half of its original value ($t_{1/2}$) upon darkening was about 100 msec.

A similar preparation of chloroplast fragments in tris buffer but with added potassium ferricyanide and 2,6-dichlorophenol indophenol (DPIP) showed a profound alteration of the 515-m μ absorption change, which no longer showed induction effects, was smaller, and had the $t_{1/2}$ shortened to about 40 msec. These additions apparently rendered the long-wavelength chlorophyll reaction inoperative, since no absorption changes characteristic of this system (at 703 m μ) were detected. Witt has suggested that ferricyanide functions by keeping the long-wavelength chlorophyll oxidized while

DPIP serves as a trap to intercept electrons that normally are passed to long-wavelength chlorophyll *a*.

As was done for the 433-m μ changes, measurements of the 515-m μ absorption change were made as a function of increasing light intensity. Figure 6 shows the absorption change at 515 m μ as a function of light intensity for four wavelengths. A light intensity (25×10^{14} quanta cm $^{-2}$ sec $^{-1}$) was chosen such that, for each light intensity curve, it fell within the region where the 515-m μ change was linear with intensity. The resulting 515-m μ absorption changes were plotted as the action spectrum shown in figure 7. This spectrum has a peak at 674 m μ , a shoulder at 650 m μ , and a far-red limit around 705 m μ . The action spectrum for the 433-m μ absorption change, in comparison with that for the 515-m μ change, remains higher at far-red wavelengths and has a limit around 737 m μ . It shows a small shoulder around 650 m μ , a peak at 682, and another shoulder around 697 m μ .

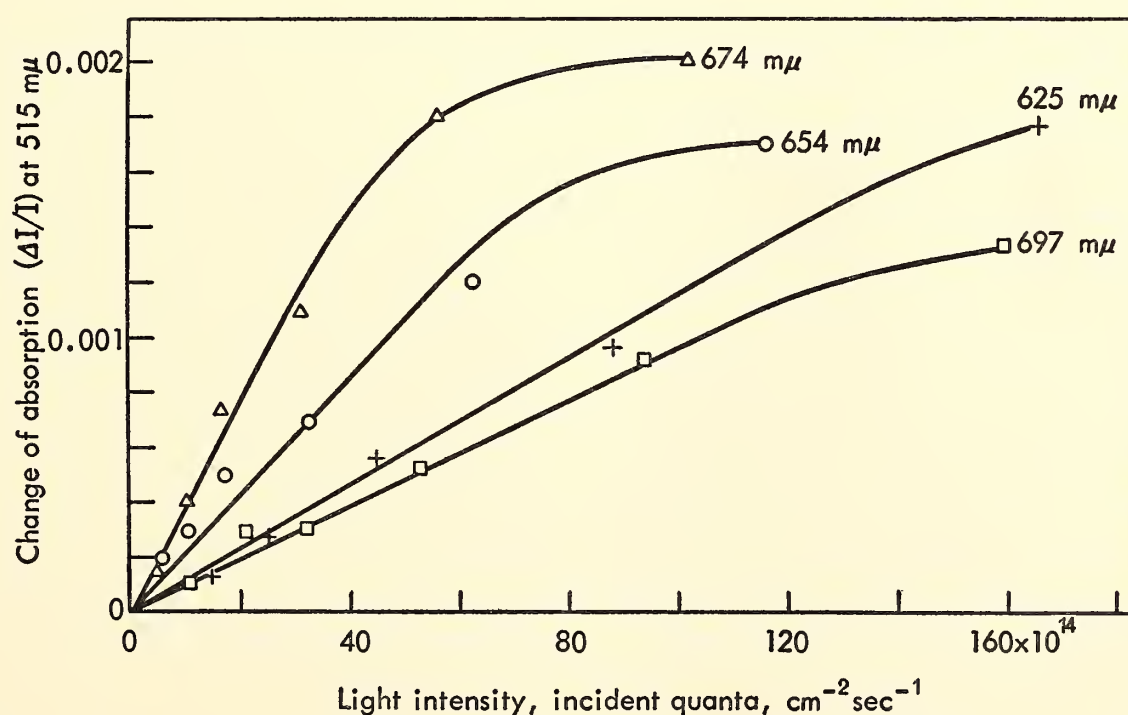


Fig. 6. The 515-m μ absorption change as a function of actinic light intensity for representative wavelengths at 625, 654, 674, and 697 m μ . The solution contained $1.5 \times 10^{-5} M$ DPIP, $1 \times 10^{-2} M$ K $_3$ Fe(CN) $_6$, $5 \times 10^{-2} M$ tris buffer (pH 7.2), and chloroplast fragments which gave a final chlorophyll concentration of 0.115 mg per ml. The transmission of this suspension in the 1-mm-path-length cuvette at 674 m μ was 22 per cent; temperature 21°C. A fresh sample was used for each saturation curve. The data from these curves and other measurements were used to plot the action spectrum of figure 7.

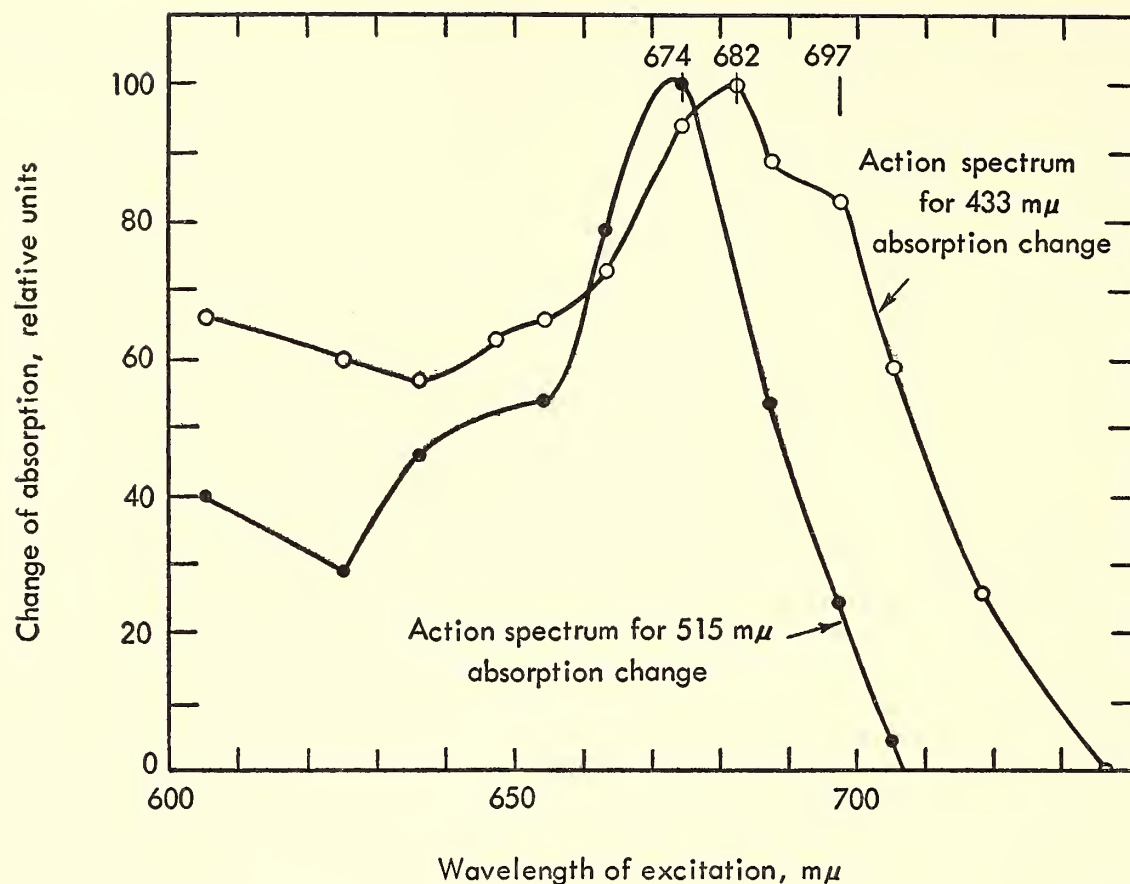


Fig. 7. The action spectrum for the 515-m μ and 433-m μ absorption changes obtained as described in the text. Monochromatic light to excite photosynthesis was obtained from a 1000-watt tungsten-filament lamp by filtering white light through 5 cm of water, 2 mm of a Schott OG-2 glass filter, and appropriate Schott interference filters having half-bandwidths from 11 to 15 m μ .

The resolution of the absorption band of chlorophyll *a* by French and co-workers into three components at 673, 683, and 695 m μ permits an understanding of the peaks and shoulders of these action spectra. It appears that chlorophyll *a* 674 and chlorophyll *a* 695 provide energy to drive light reaction $h\nu_I$.

Oxygen evolution, if intimately involved with the 515-m μ absorption change, would also be expected to continue in a separated system and to be sensitized by light absorbed by chlorophyll *a* 673 and chlorophyll *b*. Oxygen evolution was, in fact, observed by Losada, Whatley, and Arnon in chloroplast fragments treated with DPIP-ferricyanide. Since DPIP-ferricyanide treatment also permitted separation of the light reaction responsible for the 515-m μ absorption change, it may be inferred that Losada's chloroplast fragments and those used here were comparable. Losada found a peak in the

action spectrum for oxygen evolution at 644 m μ for these chloroplast fragments—a result qualitatively similar at least to the action spectrum for the production of the 515-m μ absorption change.

Witt and co-workers have found that the 515-m μ absorption change in *Chlorella* is biphasic in that it starts with a rapid temperature-independent increase, which is followed by a further slow rise that is temperature dependent. As was mentioned earlier, the absorption change at 515-m μ for chloroplast fragments suspended in tris buffer is also biphasic. Upon addition of DPIP and ferricyanide, however, the biphasic behavior disappears and only the rapid rise remains. The slow rise at 515 m μ may be associated with absorption by long-wavelength chlorophyll components, since the action spectrum that we measured for the 515-m μ absorption change in the unseparated system had a longer wavelength limit than it had in the separated system.

NATURE OF THE FORMS
OF CHLOROPHYLL *a**J. S. Brown*

The concept that chlorophyll *a* exists in the plant in different forms is now generally accepted. Most of the evidence is consistent with the existence of two major forms absorbing at about 670 and 683 $m\mu$, and a minor form, variable in amount, at about 695 $m\mu$. Besides differing in absorption maxima, these forms function differently in photosynthesis.

Information about the physical-chemical state of these three forms is practically nil. In fact, we know very little about the chlorophyll lipoprotein complex as it exists in the plant.

By contrast with the situation in mature green plants, the nature of the pigment complex in etiolated plants is well known through the work of Dr. Smith. An active protochlorophyll lipoprotein particle has been isolated. It is a spheroid having a long axis of about 200 Å. When etiolated plants are first illuminated, the protochlorophyll is transformed to chlorophyll *a* with an absorption maximum near 684 $m\mu$. After further illumination more chlorophyll is formed, and the absorption maximum shifts to about 675 $m\mu$, the peak normally observed in mature leaves. However, after chlorophyll has accumulated, it has not been possible to isolate homogeneous suspensions of particles comparable to protochlorophyll holochrome.

Small fragments of spinach chloroplasts obtained by sonication still retain activity for the Hill reaction. Dr. Park at the University of California, Berkeley, has recently taken electron micrographs of these fragments which show them to be made of spheroids resembling the protochlorophyll particles.

Dr. Allen at the Kaiser Laboratory, Richmond, California, has prepared small particles from *Chlorella* by alternate freezing, grinding, sonication at -40°C , and finally a sucrose density gradient

centrifugation. These particles with an absorption maximum at 672 $m\mu$ will perform part of the photoreactions of the whole chloroplast, including a modified Hill reaction, and they give a rapid EPR signal. The function of chlorophyll *a* 672 as a part of the "accessory pigment system" is becoming firmly established, particularly through studies of action spectra for enhancement, which have clearly shown a peak at about 670 $m\mu$.

The nature of the chlorophyll form absorbing at 685 $m\mu$ is less well known. It may be either a discrete particle similar to C_a672 , but with a different lipoprotein composition, or a particular structural arrangement of the chlorophyll lipoprotein complex, or perhaps a dimer of the pigment molecules.

Support for the suggestion that the C_a685 particle is a discrete entity comes from the study of aged *Euglena* chloroplasts. When such chloroplasts were broken into very small pieces and centrifuged at 144,700*g*, two fractions were obtained: one, a sediment having a complex "red" absorption band with a large proportion of the absorption attributable to a pigment, P_a710 , with absorption maximum at 710 $m\mu$; the other fraction, left in the supernatant, which had a simple "red" absorption band with a maximum at 685 $m\mu$, C_a685 . A comparable separation of the two fractions was obtained by centrifugation in a sucrose gradient. Since the fractionation has been done with only aged material, it is possible that the C_a685 particles are artifacts formed during the aging of the cells.

Evidence also supports the thesis that C_a685 is a particular structural arrangement of the chlorophyll lipoprotein complex. Previous reports have described how many deleterious agents such as heat, intense light, acids, and some detergents and fat solvents destroy the absorption at 685 $m\mu$ more than at 670 $m\mu$. Experiments demonstrating selective extraction with ether have been performed in the past year.

When aqueous pigment extracts from *Euglena* were treated with ether, a relative decrease in absorption at about 685 m μ was observed. With Swiss chard chloroplasts, this decrease was present but smaller. Figure 8A illustrates the types of absorption changes obtained by

depends on various factors encourages us to continue these studies on the nature of the chlorophyll lipoprotein complex.

NEW ALGAE FOR PHOTOSYNTHESIS STUDIES

J. S. Brown

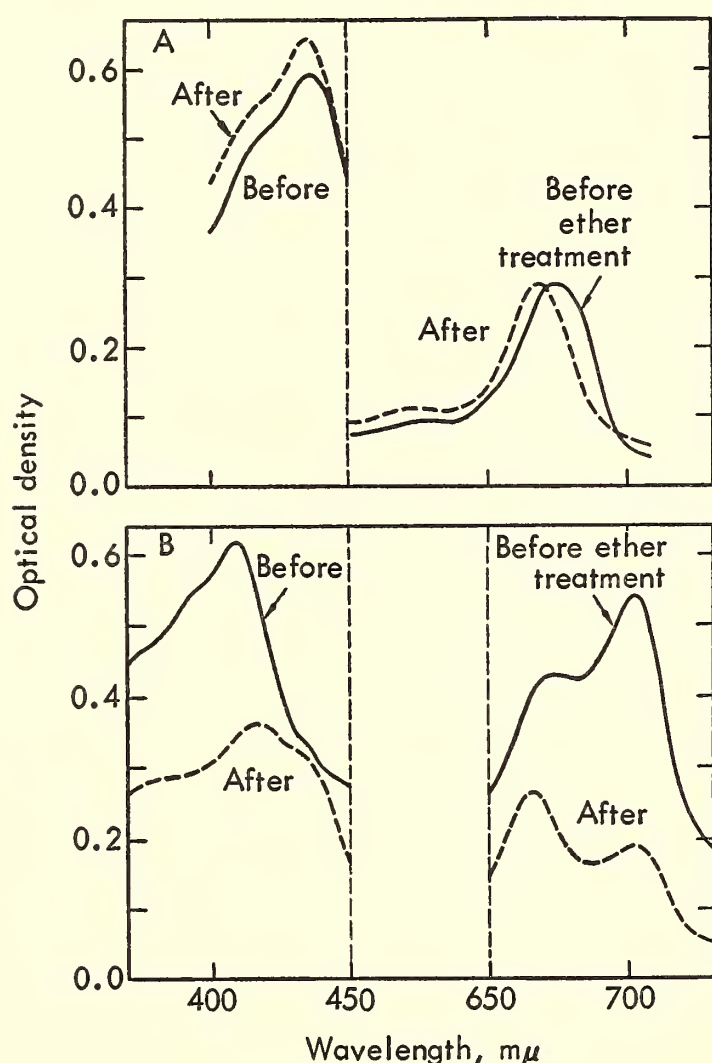


Fig. 8. Absorption changes following treatment of chloroplast fragments with ethyl ether: A. Aqueous suspension of chloroplast fragments from *Euglena* grown in intense light, before and after having been extracted with an equal volume of ethyl ether. B. Cytoplasmic fraction of *Euglena* aged in darkness, before and after having been extracted with ethyl ether. The absorbancies in the red and blue regions of the spectra are not quantitatively comparable.

ether treatment of aqueous suspensions prepared from *Euglena* grown with intense light; figure 8B, from cytoplasmic fractions of *Euglena* aged to form P_a710.

The observation that ethyl ether selectively extracts the longer-wavelength forms of chlorophyll *a* in a way that

Comparative studies of action spectra and of the variation of enhancement effects with wavelength in algae with different pigment systems have provided the basis for the current concept of the need for two separate photochemical steps in photosynthesis. We are beginning a search for plants, particularly algae, with different photosynthetic pigments and with different ratios of the known pigments that may be particularly suitable for studies of the interaction of pigment systems.

An interesting green alga, resembling *Stichococcus* in appearance, has been isolated from a stock solution of 1 M MgSO₄·7H₂O. This organism grows well in a liquid or agar Knop's medium with 0.5 M MgSO₄ using 5 per cent CO₂ in air for the liquid cultures. Previous studies with known *Stichococci* have indicated that this genus can be adapted rather easily to a wide range of salt concentrations. The ratio of chlorophyll *a* to chlorophyll *b* in *Stichococci* growing with high salt concentrations is less than 2 to 1. Most green plants have a ratio of about 3 to 1, and *Euglena* grown with very weak light has a ratio of 7 to 1.

Figure 9 compares derivative absorption spectra of *Stichococcus* and *Dunaliella* whole cells. The short-wavelength, positive, derivative peak is caused by chlorophyll *b* absorption. The maximum chlorophyll *a* absorption at about 680 m μ is where the curve changes from positive to negative. The shoulder on the positive portion of the chlorophyll *a* derivative peak is caused by the overlapping absorption bands of C_a670 and C_a685. The relative height of this shoulder with respect to the zero line indicates the

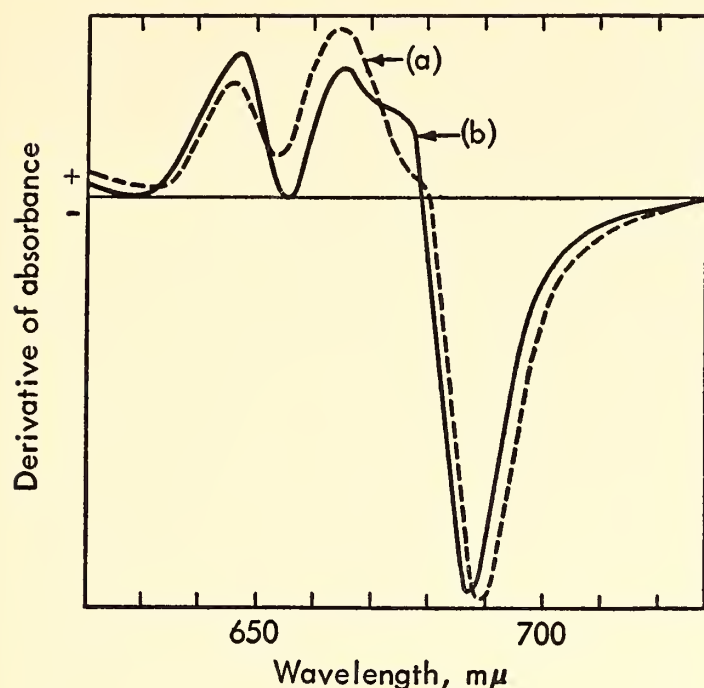


Fig. 9. Derivative absorption spectra of *Dunaliella* and *Stichococcus* cells.

proportions of these two forms of chlorophyll *a*.

The spectrum for *Dunaliella* is typical of most green algae and higher plants. By comparison *Stichococcus* has a higher proportion of chlorophyll *b*, and the proportion of C_{a685} to C_{a670} is also significantly higher. This organism may be valuable for investigation of the nature of the chlorophyll forms and for study of the function and formation of chlorophyll *b*.

PHOTOSYNTHESIS IN *Stichococcus* Govindjee

Measurements of action spectra of photosynthesis and comparisons between action and absorption spectra have been used for a long time in the evaluation of the role of different pigments in photosynthesis. Dr. Jeanette S. Brown has isolated and cultured a particular strain of a green alga, probably a *Stichococcus*, which contains a high proportion of chlorophyll *b* as described in this report.

Rates of photosynthesis of this alga were measured by means of a platinum electrode as described elsewhere (Year Book 60, p. 362). The circulating medium (Knop's solution + 1 M $MgSO_4$) was

gassed with 5 per cent CO_2 in air, and its temperature was 22°C. The action spectrum of oxygen evolution was measured by the automatic action spectrophotometer (Year Book 58, p. 323), using a constant number of incident quanta at different wavelengths.

Figure 10 shows a typical time course of oxygen evolution in *Stichococcus* with 670-mμ light. Upon repeated illumination, the rate of photosynthesis reaches a steady state after about 2 minutes. If the cells were left in the dark for a period of 10 to 12 hours it took 1 to 1½ hours to attain the steady state. In addition, an initial spike was clearly noticeable. The time course of oxygen exchange in darkness (after illumination) shows an immediate sharp drop followed by a slower decline (see arrow in fig. 10).

Gingras, Lemasson, and Fork have observed a clear positive peak in the time course curve of *Chlorella* after white light was turned off. When DCMU was added just before the light was turned off, oxygen evolution in light was strongly inhibited but the positive peak was relatively unaffected, showing that the peak was not due to oxygen evolution. It is therefore believed to be due to a transient decrease of cellular respiration. On the basis of these considerations it may be inferred that the observed kinetics in *Stichococcus* may be simply due to an interaction of two opposing effects of

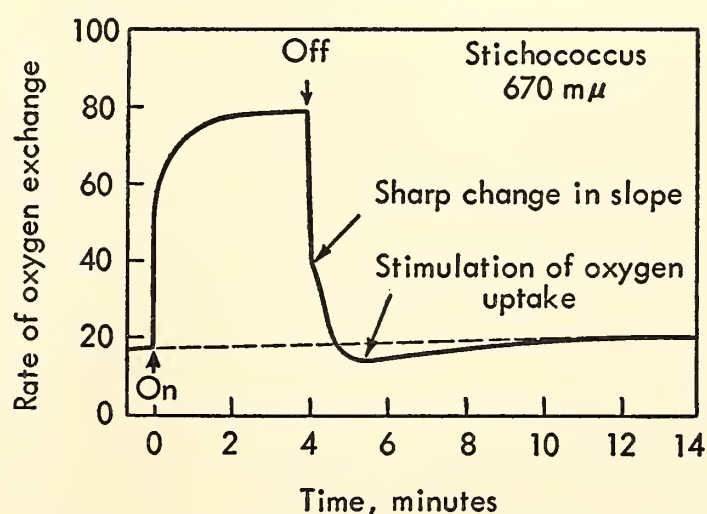


Fig. 10. Time course of oxygen exchange in *Stichococcus*.

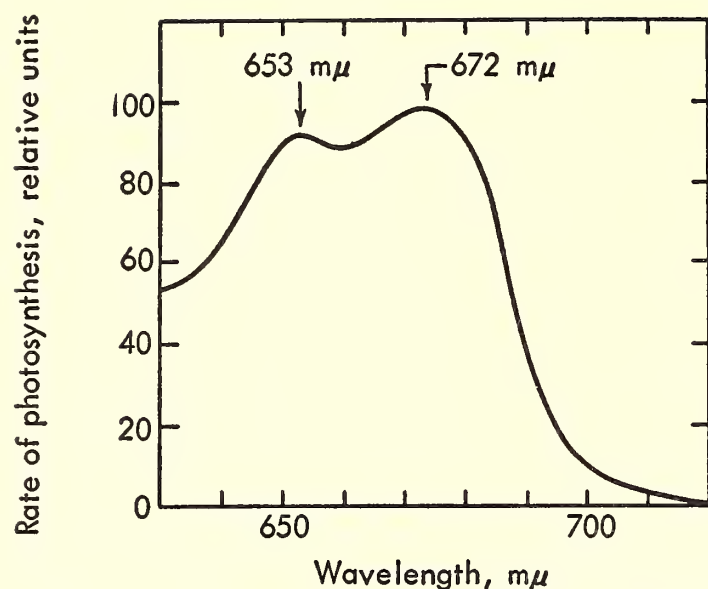


Fig. 11. Action spectrum of photosynthesis in *Stichococcus*.

light on oxygen uptake—an inhibition and a stimulation of oxygen uptake. A clear stimulation in oxygen uptake is noticed as the rate curve dips below the original dark rate. An inhibition effect of light during the illumination period has been observed by Hoch and co-workers in several algae.

Figure 11 shows the action spectrum of photosynthesis made on a thin suspension of *Stichococcus*. There are two peaks—one at 672 mμ due to chlorophyll *a*, and the other at 653 mμ due to chlorophyll *b*. The ratio of the relative height of chlorophyll *b* to chlorophyll *a* peaks, observed in the action spectrum of photosynthesis in this alga, is 0.94—a very high ratio in comparison with that

found in other green algae. This higher activity observed in the chlorophyll *b* region is paralleled by the findings of Brown that *Stichococcus* contains a high proportion of chlorophyll *b*.

The enhancement phenomenon was studied by using 650-mμ and 710-mμ light separately and in combination. As shown in table 4, an enhancement of rate of photosynthesis ranging from 1.2 to 2.3 was obtained between the two wavelengths. The occurrence of enhancement indicates that two photoreactions are also necessary for *Stichococcus* photosynthesis.

The same culture that showed enhancement at one time failed to show it at another time under very similar conditions. A difference in the effect of light on respiration (during illumination) in separate and in combined lights may complicate the observed results. Unless the effects of light on respiration are very variable, however, such different results should not be found in enhancement studies. The factors responsible are under investigation. Why enhancement is not always observed is still an open question. Perhaps the occurrence of enhancement depends on the pool of an unknown compound, and a change in pool size (indirectly affected by respiration) may be the cause of variable results on enhancements.

Govindjee acknowledges the support from the National Science Foundation grant G19437 and a Carnegie Institution of Washington travel grant.

TABLE 4. Enhancement in *Stichococcus*, 22°C, 5 Per Cent Carbon Dioxide in Air
Rate of photosynthesis in arbitrary units

A	B	C	D	E
710 mμ	650 mμ	Sum of 710 and 650 mμ	710 and 650 Combined Lights	Emerson Enhancement*
12.8	22.0	34.8	37.5	1.2
12.8	45.0	57.8	63.0	1.4
18.2	182.0	200.2	224.0	2.3

* The Emerson enhancement is defined here as $E = (D - B)/A$.

SOME OBSERVATIONS ON THE REVERSIBLE
LIGHT-INDUCED INHIBITION OF
RESPIRATION IN NONSULFUR
PURPLE BACTERIA

D. C. Fork² and J. C. Goedheer

Nakamura, in 1937, was the first to report inhibition of respiration by light in a purple bacterium. Since then numerous investigators have confirmed the observation and have studied it in more detail. One interpretation is that substrate hydrogen, which normally reduces oxygen via the respiratory chain, is diverted upon illumination to the reduction of carbon dioxide through the photochemical apparatus. Nakamura, therefore, assumed that it was possible to study bacterial photosynthesis by measuring light-induced changes of respiration. Duysens in his thesis in 1952 (Stelling VI) also suggested that action spectra for photosynthesis in bacteria could be determined by measuring the inhibition of their respiration by light. We have measured the action spectrum for the inhibition of respiration by light, compared it with the spectral absorption by the photosynthetically active pigments, and also have observed the influence of a redox dye and of a poison of oxygen evolution on this light-induced inhibition.

Horio and co-workers (personal communication) have reported (*J. Biol. Chem.*, in press) an action spectrum for light inhibition of respiration in *Rhodospirillum rubrum* in the 410- to 610-m μ region which appears to be similar to those reported here.

The bacteria used in this study were grown anaerobically under incandescent illumination at about 25°C: *Rhodospirillum rubrum* in 1 per cent peptone and 0.5 per cent NaCl, pH 7; *Rhodopseudomonas spheroides* in 0.5 per cent yeast extract, 0.5 per cent MgSO₄, 0.3 per

cent L-malic acid, and 0.2 M phosphate buffer at pH 6.8. Tap water was used for both media. For the action spectra determinations the cells were harvested after 1 day's growth.

The Teflon-covered platinum electrode described in *Year Book 61*, page 343, was used to follow respiratory changes. A drop of a thin suspension of bacteria in fresh medium was placed on the Teflon-covered electrode and held in place with another piece of 6-micron-thick Teflon film. Air was then passed at a constant rate over this suspension. The liquid-circulating system was not needed when the electrode was being used for action spectra determinations but was used when the effects of inhibitors were being studied.

Monochromatic light was obtained from a 500-mm-focal-length Bausch and Lomb monochromator with a 100 by 100 mm grating having 600 grooves per millimeter. Each action spectrum was done in three parts with the slits set to pass a beam having a half-bandwidth of 3.3 m μ : from 940 to 740 m μ , a 600-m μ cutoff filter to remove spectral impurities from second-order wavelengths and a 48 per cent transmission neutral density filter were inserted in the monochromator beam; from 650 to 550 m μ , only the 48 per cent transmission filter was used; and from 550 to 450 m μ , no filters at all. The precision of measurement was lower for 550 to 450 m μ than for the other portions of the action spectrum because the light intensities were low and the resulting responses small. The monochromator wavelength dial was turned manually 1 m μ every 10 seconds, and a continuous recording of respiration was made. This record was then corrected for equal incident quanta and for loss of activity with time (if any) and replotted at 5-m μ intervals.

A time course for the inhibition of respiration by 880-m μ light is shown in figure 12. A deflection of the trace above the dark base line indicates decreased respiration, since more oxygen, diffusing

² It is a pleasure to thank Professor J. B. Thomas, who made all the facilities of the Biophysical Research Group of the State University at Utrecht available.

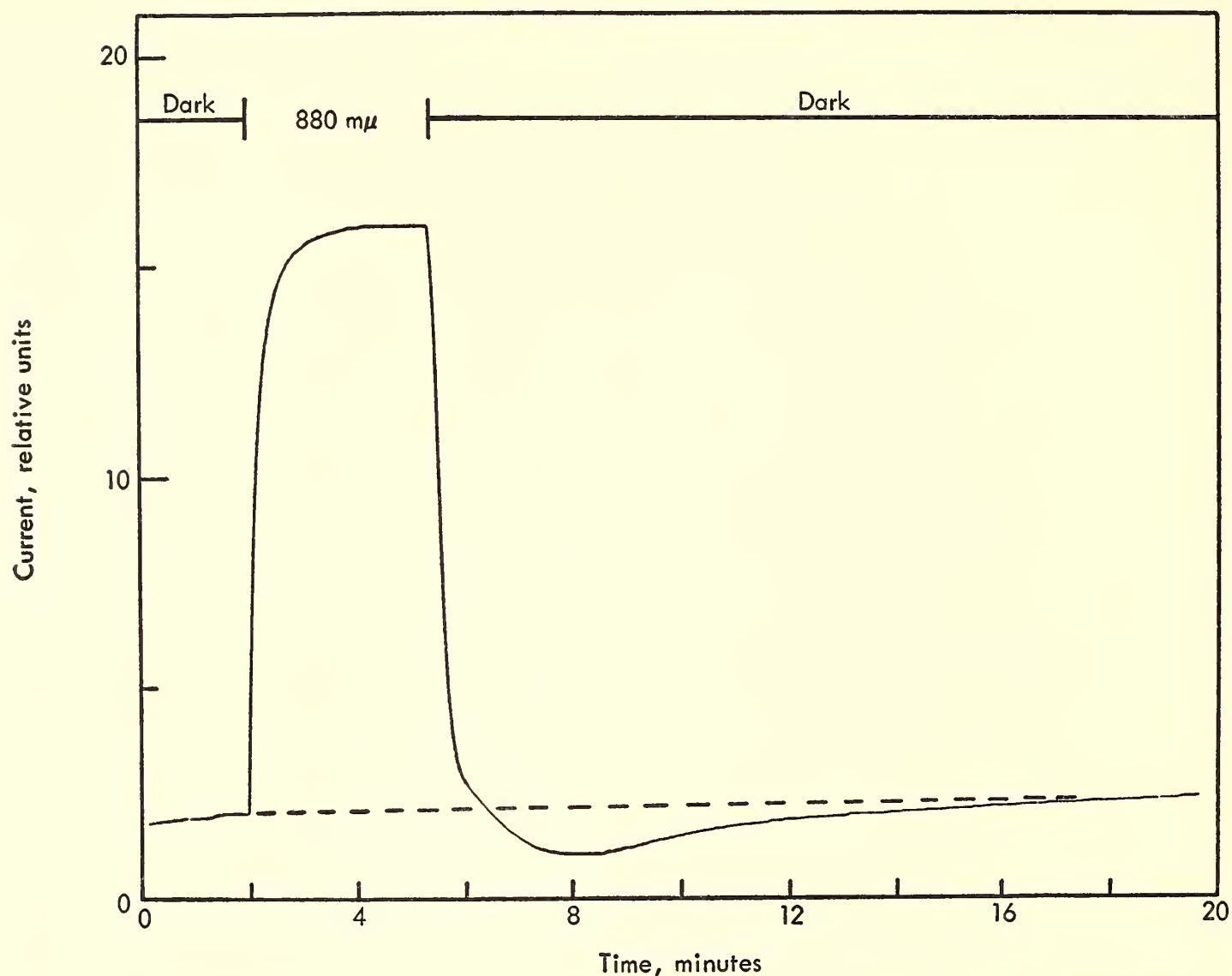


Fig. 12. The time course of inhibition of respiration of *Rhodospirillum rubrum* upon exposure to 880-m μ light (497 ergs cm⁻² sec⁻¹) having a half-bandwidth of 10 m μ . The cells were harvested after 2 days' growth and resuspended in fresh medium. Gas phase, 5 per cent CO₂ in air.

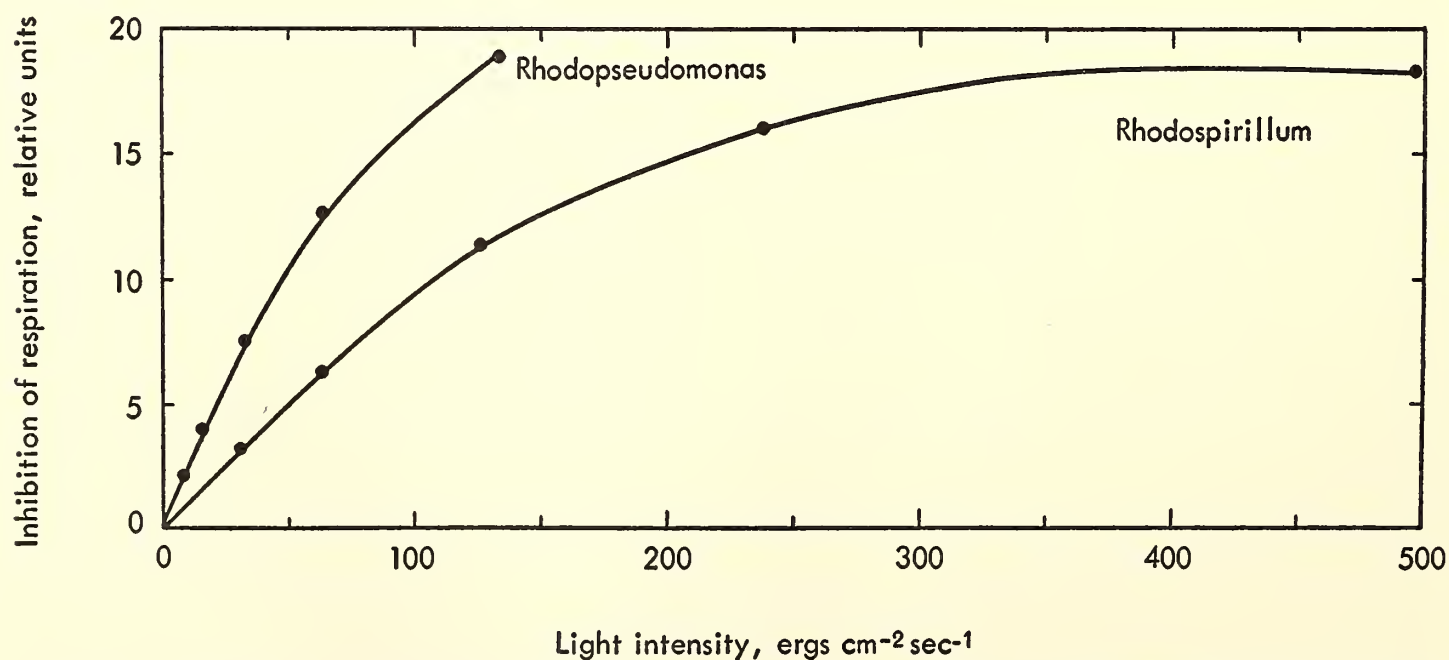


Fig. 13. Inhibition of respiration as a function of light intensity. For *Rhodopseudomonas* the 850-m μ light used had a half-bandwidth of 3.3 m μ . Cells from a 1-day-old culture were suspended in fresh medium and gassed with air. This sample was used for the determination of the action spectrum. For *Rhodospirillum* the 880-m μ light used had a half-bandwidth of 10 m μ . The 2-day-old culture was gassed with 5 per cent CO₂ in air. Another sample was used for the action spectrum in figure 15.

from the circulating medium, can be reduced at the electrode when the respiratory uptake is lowered. Oxygen production will cause a deflection in the same direction. However, Johnston and Brown showed in their study with the O^{18} isotope that the photosynthetic bacteria do not evolve oxygen. When the bacteria on the electrode are made anaerobic (gas phase N_2) the light effect disappears (unlike oxygen evolution in green plants, which may continue under anaerobic conditions). The potent inhibitor of oxygen evolution, DCMU, 3-(3,4-dichlorophenyl)-1,1-dimethylurea, at a concentration of $6.5 \times 10^{-5} M$ did not have an appreciable effect on light-induced inhibition of respiration.

The time course shown in figure 12 indicates that the inhibition becomes constant after about 2 minutes in the light. Darkening the cells causes the recorder tracing to dip below the dark base line established previously. The respiration rate attains its former dark level after about 12 minutes. This temporarily increased respiration after a light exposure is apparently similar to the respiratory stimulation observed after the red alga *Porphyridium cruentum* was exposed to red light (*Year Book 60*, p. 352). Respiratory stimulation after exposure of *Rhodopseudomonas* to 850-m μ light has also been seen frequently, but not invariably.

The inhibition of respiration as a function of incident light intensity is shown in figure 13. Since these curves start to bend at low light intensity, the action spectra were determined with intensities as low as possible. The same *Rhodopseudomonas* sample was used to determine the saturation curve of figure 13 and also the action spectrum. At 850 m μ the intensity of the monochromator beam when used as described above was 64.3 ergs cm $^{-2}$ sec $^{-1}$. At this intensity the effect per unit intensity is 16 per cent less than at the lowest usable intensities. Since the calculations of the action spectrum were made by assuming a linear relationship between inhibition of respiration and light inten-

sity the action spectrum is somewhat flattened where this error occurs.

The action spectrum for light-induced inhibition of respiration in *Rhodopseudomonas* (fig. 14, lower curve) has peaks at 850, 800, 590, 510, and 480 m μ and a shoulder around 880 m μ . The absorption spectrum of chromatophores (upper curve), prepared from a different sample, is shown for comparison. The action spectrum for *Rhodospirillum* (fig. 15, lower curve) has peaks at 880, 810, 595, ~ 520 , and ~ 485 m μ . The absorption spectrum of a chromatophore preparation from a different sample is also shown (upper curve).

The light inhibition of respiration was disrupted by the redox dye *n*-methylphenazonium methosulfate (PMS). Figure 16 shows this effect with *Rhodospirillum*. Exposure to 880 m μ before the addition of PMS resulted in a 75 per cent inhibition of respiration. (The zero respiration line is the electrode dark current after the cells were killed at the end of the experiment by adding formaldehyde solution in a final concentration of about 4 per cent to the circulating solution.) After a 4-minute exposure to 880 m μ the cells were darkened and a temporary stimulation of respiration about 25 per cent greater than the previous dark respiration occurred. PMS was added to the circulating solution while the cells were in the dark (arrow); an 80 per cent increase in the dark uptake of oxygen resulted. Another exposure to 880 m μ after the addition of PMS resulted in only an 18 per cent inhibition of respiration. The time course of inhibition of respiration upon illumination in the presence of PMS shows an induction period followed by a slow increase. The time course of the respiratory recovery in the dark after 880 m μ is complex. No stimulation of respiration followed illumination in the presence of PMS. Repeated exposures to 800 m μ light resulted in a gradual decrease in the amount of light-induced inhibition of respiration as well as a gradual retardation in the time course.

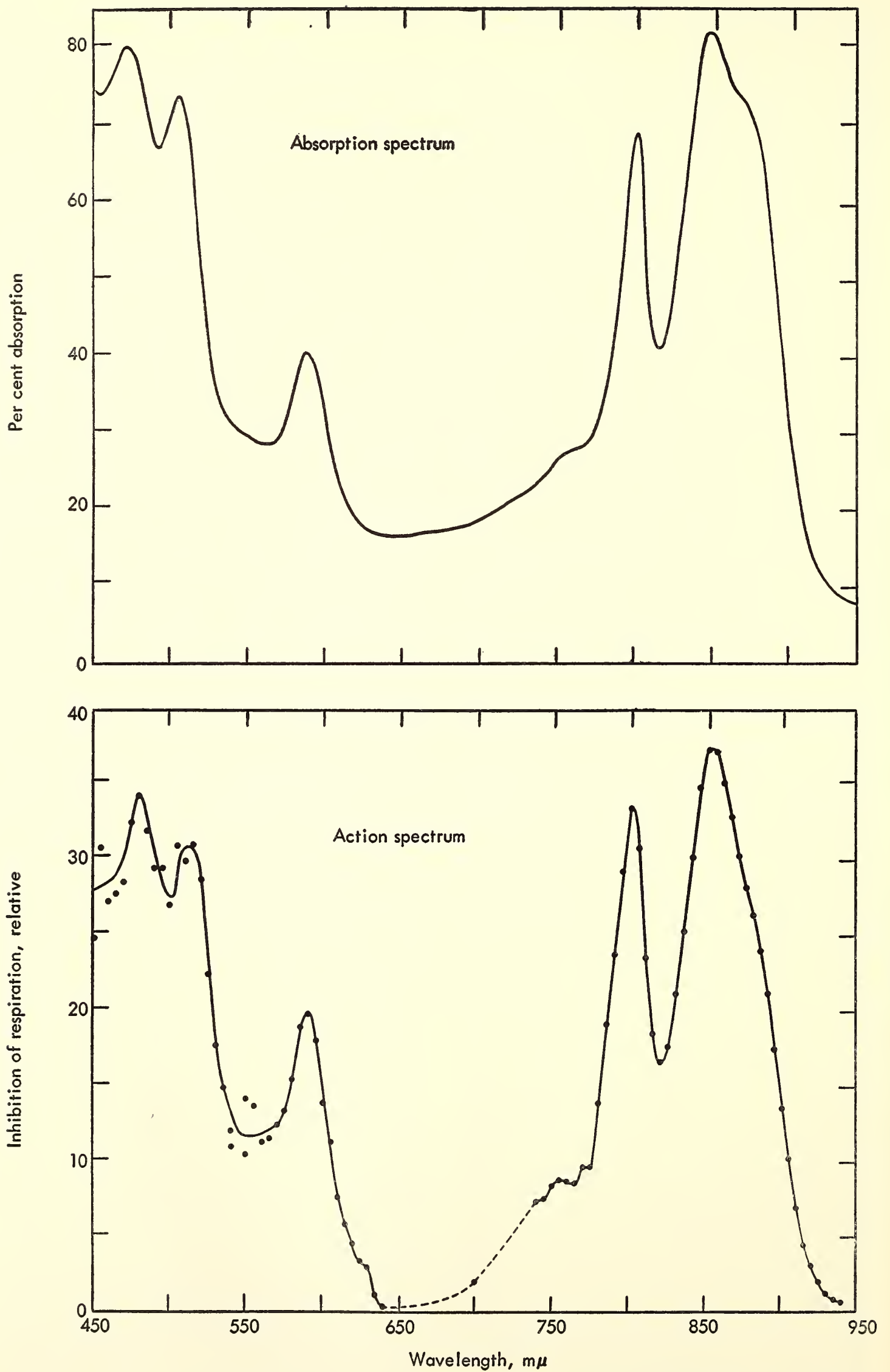


Fig. 14. Lower half: Action spectrum for inhibition of respiration in *Rhodopseudomonas*. Upper half: Absorption spectrum of chromatophores in phosphate buffer.

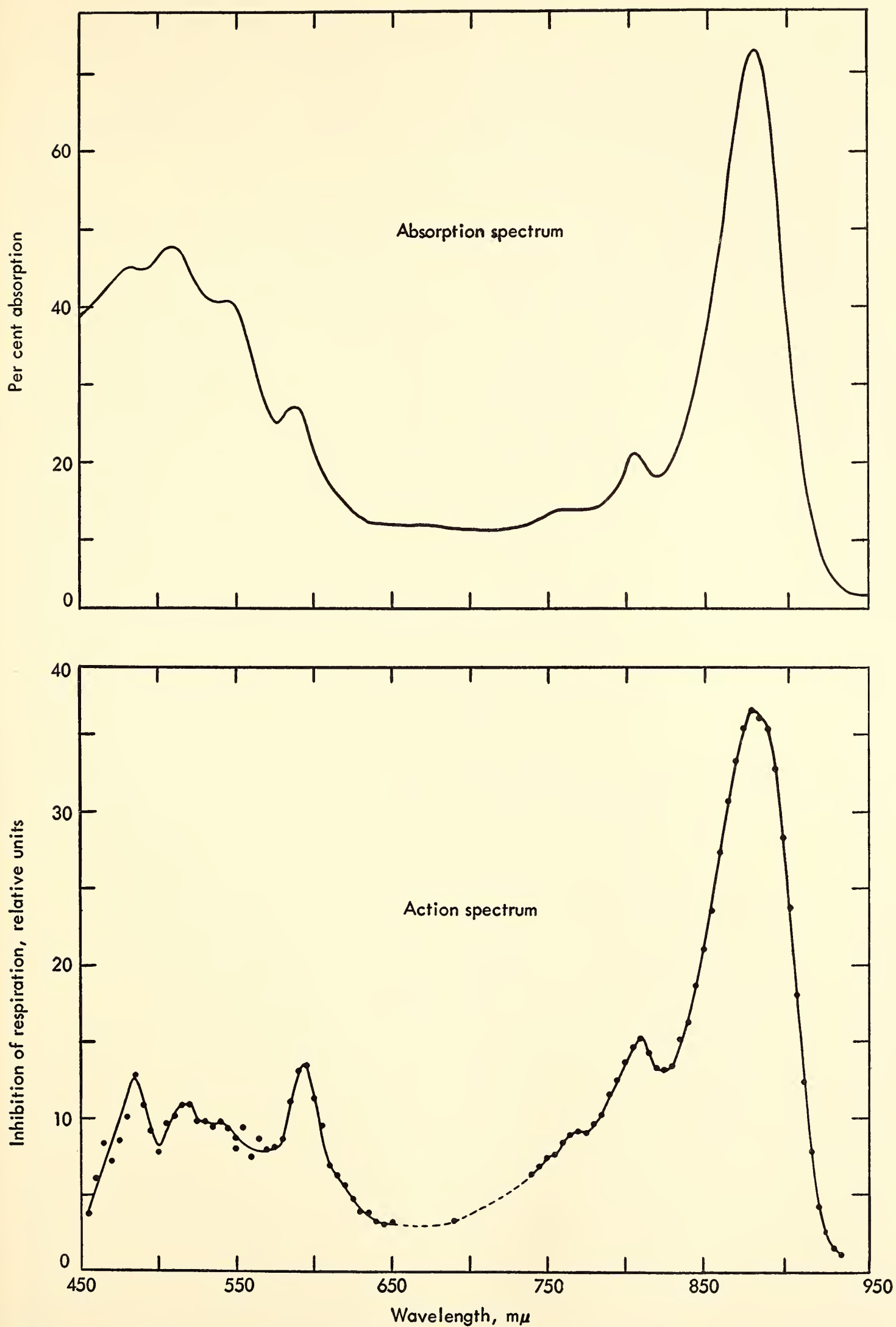


Fig. 15. *Lower half*: Action spectrum for inhibition of respiration by light in *Rhodospirillum rubrum*. One-day-old culture in growth medium; gas phase, air. *Upper half*: Absorption spectrum of chromatophores in phosphate buffer from a different sample from that used for the action spectrum.

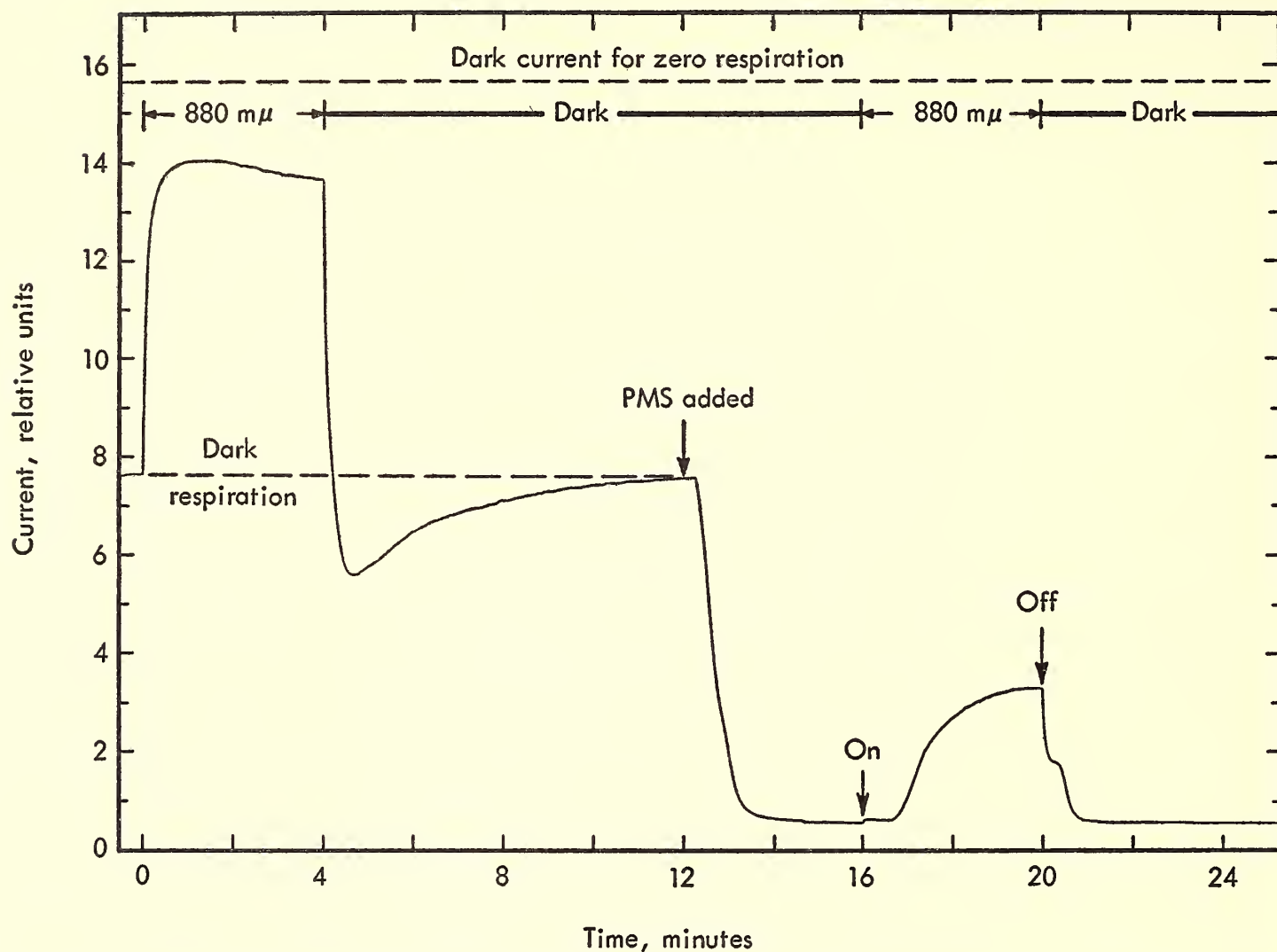


Fig. 16. Effect of PMS on inhibition of respiration by light in *Rhodospirillum*. Cells from a 7-day-old culture in 0.01 *M* sodium butyrate and 0.02 *M* $\text{Na}_2\text{HPO}_4\text{--KH}_2\text{PO}_4$ buffer, pH 7.45; gas phase, air. The 880- $\text{m}\mu$ light (half-bandwidth 10 $\text{m}\mu$) had an intensity of $497 \text{ ergs cm}^{-2} \text{ sec}^{-1}$. The same intensity at 880 $\text{m}\mu$ was used after the addition of PMS to a final concentration of $3.3 \times 10^{-4} \text{ M}$.

The action spectra for light-induced inhibition of respiration follow the absorption of the photosynthetically active pigments and suggest an intimate coupling between photosynthesis and respiration. Horio and Kamen explained light-induced inhibition of respiration on the basis of a competition between the photoactive pigments and an intermediate in the respiratory electron-transport chain. Nishimura and Chance advanced a similar idea, that electron transport for both photosynthesis and respiration passes through a common cytochrome.

An explanation for the inhibition effect based on a competition between photophosphorylation and oxidative phosphorylation for a common phosphate acceptor was ruled out by Katoh, who found added adenosine diphosphate to

be without effect. He also noted that inhibitors of photophosphorylation such as *o*-phenanthroline and 2,6-dichlorophenol indophenol did not affect photo-inhibition.

PMS may act as a by-pass of an intermediate common to both photosynthesis and respiration, mediating a more rapid flow of electrons to oxygen, which would result in an increased dark oxygen uptake and a decreased effect of light on respiration.

The activity of carotenoids in relation to bacteriochlorophyll in sensitizing inhibition of respiration is higher in *Rhodopseudomonas* than in *Rhodospirillum*. Goedheer has also observed a more efficient transfer of energy for carotenoids to bacteriochlorophyll in *Rhodopseudomonas* than in *Rhodospirillum*.

IS THE PHOTOCONVERSION OF PROTOCHLOROPHYLL IMMEDIATE?

Axel Madsen³

Introduction. Since the transformation of protochlorophyll into chlorophyll *a* is dependent on temperature, it has been suggested by Smith and Benitez (*Plant Physiol.*, 29, 135, 1954) and by Boardman (*Biochim. Biophys. Acta*, 64, 205, 1962) that some steps other than pure photochemical reactions are involved. These other reactions, if any, could possibly be slower than the photochemical step. They might be detected as a time delay in the transformation after exposing active protochlorophyll to sufficiently short illumination and then immediately measuring any changes observed in the absorption spectrum. Previous investigations have shown that, in chloroplasts

³ Mr. Madsen's visit to the laboratory was made possible by a grant from the W. K. Kellogg Foundation.

from etiolated barley, the transformation of protochlorophyll is completed in less than 0.04 second after illumination (Madsen, Progress in photobiology, *Proc. III Intern. Congr. Photobiol.*, p. 567, 1960). The aim of the present work was to make faster measurements of the transformation of protochlorophyll in intact leaves and in protochlorophyll-holochrome preparations.

Plant material. Barley was grown in darkness for 6–7 days at 26°C. About 2.5-cm-long pieces were cut 1 cm below the apex and were placed close together between two glass slides. Beans were grown under the same conditions (for 18 days), and the protochlorophyll holochrome was prepared according to Smith (*Year Book 57*, p. 287) and Smith and Coomber (*Year Book 59*, p. 325). All operations were carried out under a weak green light.

Measurements. The transformation was measured by the increase in absorption by chlorophyll of a weak beam at 680 mμ

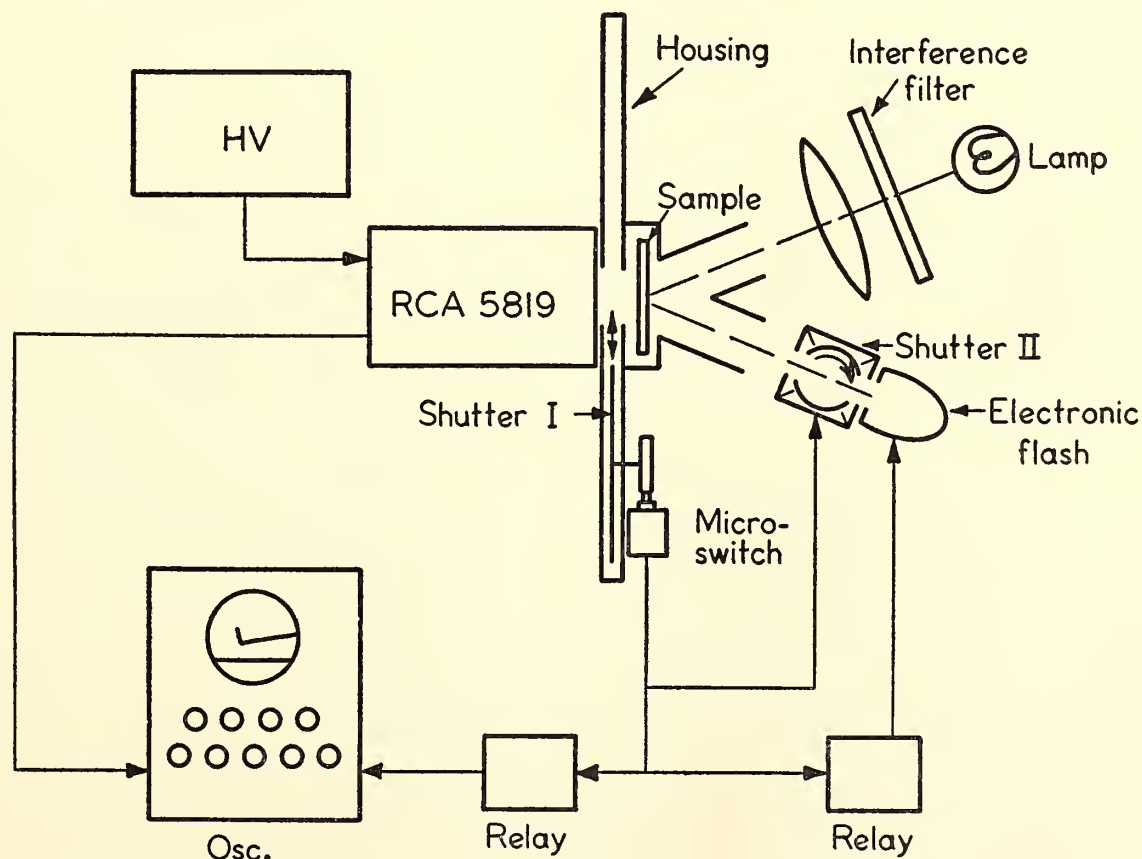


Fig. 17. Arrangement for measuring absorption of light in intact leaves. Shutter I between the sample and the phototube (RCA 5819) is closed during the flash; it opens for the measuring beam when shutter II has cut off the flash beam. The proper sequence, achieved by an adjustable micro-switch and adjustable relays, is: (1) triggering the flash; (2) closing shutter II; (3) triggering the oscilloscope; and (4) opening shutter I.

immediately after a bright flash of light covering most of the visible spectrum.

The setup for measuring changes in absorption in leaves is pictured in figure 17. Light from a 6-volt tungsten lamp was passed through an interference filter (B-1 6800, Baird Atomic, Inc.) and focused on the leaves. Flashes of light were obtained from a photographic flash apparatus (Honeywell Strobunar Futuramic II Electronic Flash). To shorten the duration of illumination a shutter (a tin can with oppositely placed holes) was put between the flash apparatus and the leaves. The shutter was rotated 90° in its housing by means of a spring after being released by an electromagnet; as it moves with increasing speed it produces a very sharp cutoff. The closing time is about 1.5 msec, depending on the spring tension. Another shutter is placed between the leaves and the photomultiplier for protection against the high-intensity flash. In this shutter a spring-loaded disk sector is held by a trigger in a position where it closes the aperture in its housing. When

the shutter is released by hand it actuates a microswitch and opens to the phototube. Its opening time is 1.5 msec. The moment of contact with the microswitch can be adjusted. By means of a battery and suitable wiring the microswitch releases the flash beam shutter and, through adjustable relays, triggers the flashtube and the oscilloscope. With proper adjustment of the microswitch and the relays it is possible to have the setup ready to measure changes in the absorption in the leaves 4 msec after the beginning of illumination.

In the arrangement for measuring transformation in holochrome preparations the flash beam is oriented perpendicular to the measuring beam, figure 18. The sample is held in a cell made of Perspex mounted in a black holder provided with two perpendicular perforations, for the flash beam and the measuring beam, respectively. To get rid of stray light the measuring beam is focused on a narrow aperture 20 cm in front of the phototube. The shutter

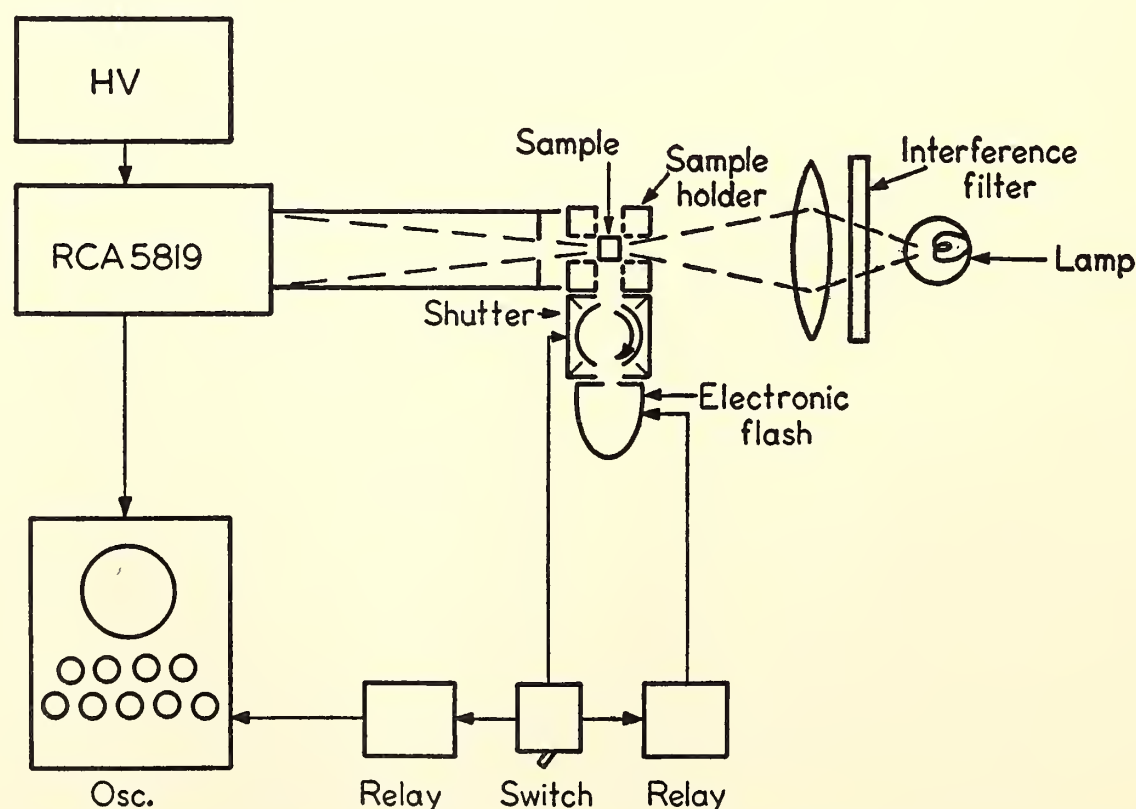


Fig. 18. Arrangement for measuring absorption of light in solutions. The incident flash beam is normal to the sample and perpendicular to the measuring beam. Instead of a shutter, a 20-cm-long nonreflecting tube is mounted in front of the phototube to protect it. A switch triggers the flashtube, the oscilloscope, and the shutter movement. The sequence of events is determined by adjustable relays.

between the flash tube and the sample is the same as in the setup shown in figure 17. The hand-operated switch releases the shutter and, by adjustable relays, triggers the flash tube and the oscilloscope.

Results with intact leaves. With the shutter between the leaves and the phototube in open position the absorption in the etiolated leaves before illumination was marked on the scale of the oscilloscope. The shutter was closed and then released by hand, starting the sequence of flash, shutter, and sweep. After a 1-msec illumination, which caused about 60 per cent transformation of the protochlorophyll, the oscilloscope showed a deflection of approximately 3 cm from the base-line level, which represented the absorption before illumination.

Any delay in the change of absorption after illumination would show up on the screen as a curve starting at the initial level and rising gradually to the level of absorption caused by illumination. This was not the pattern. Three milliseconds after illumination the track was horizontal, showing that in etiolated leaves the change in absorption is completed within 4 msec after the beginning of illumination. These experiments were carried out at room temperature.

If the temperature coefficient of the transformation results from reactions of enzymatic nature a possible delay of the change in absorption would be amplified by low temperature. Experiments with leaves stored in dry ice for 1 hour and measured when frozen showed that the rate of transformation was not affected measurably by low temperature. Only the amount of protochlorophyll transformed per flash was diminished. Measurements of the change in absorption during thawing after illumination showed that no increase in absorption followed the rise in temperature. The absorption was constant until the ice in the leaves disappeared. At this point sap leaked from the leaves and the absorption decreased rapidly.

Results with a purified protochlorophyll-holochrome preparation. When a preparation of protochlorophyll holochrome was used for the measurements, the amount of scattered light from the sample was very low and the setup shown in figure 18 made it possible to measure changes in absorption immediately after 1 msec of illumination.

The lower time limit for measurements in holochrome preparations is determined by the speed and the intensity of the flash. In these experiments 1-msec illumination was necessary to produce about 60 per cent transformation. Experiments carried out at room temperature showed that there is no further change in the absorption in protochlorophyll holochrome after 1-msec illumination. Ultra-short flashes of correspondingly higher intensity could be used for measuring the rate of transformation in holochrome preparations containing enough active protochlorophyll and no light-scattering material.

Summary. The formation of chlorophyll from protochlorophyll in intact etiolated leaves measured as the increase in absorption at 680 m μ is completed within 4 msec after the beginning of 1-msec illumination. Lowering the temperature did not slow the rate measurably. In protochlorophyll-holochrome preparations the change in absorption was completed during 1-msec illumination.

FRACTIONATION OF PROTOCHLOROPHYLL HOLOCHROME BY DENSITY GRADIENT CENTRIFUGATION

Axel Madsen

Preparations of protochlorophyll holochrome often show very strong light absorption at wavelengths shorter than 450 m μ . The sharp absorption maximum of protochlorophyll holochrome at 442 m μ is thus obscured. Furthermore, the preparations often contain light-scattering components that show up in the absorption spectra as an apparent increase in absorption toward shorter wavelengths.

These disturbing factors increase the difficulty of making exact measurements of the transformation of protochlorophyll holochrome to chlorophyll holochrome. An attempt was therefore made to purify the material further by centrifugation in a density gradient. A protochlorophyll-holochrome preparation was made from dark-grown bean leaves according to Smith and Coomber (*Year Book 59*, p. 325).

The absorption spectrum of the preparation measured with a Beckman DK spectrophotometer, using a 1-cm cell, is shown in figure 19. The continuous line represents the absorption before illumination and the dashed line after 3 minutes' illumination with incandescent light. The peaks at 640 and 674 $m\mu$ representing protochlorophyll holochrome and chlorophyll holochrome, respectively, indicate that the preparation contains active protochlorophyll holochrome, but the maximum at 442 $m\mu$ is completely obscured.

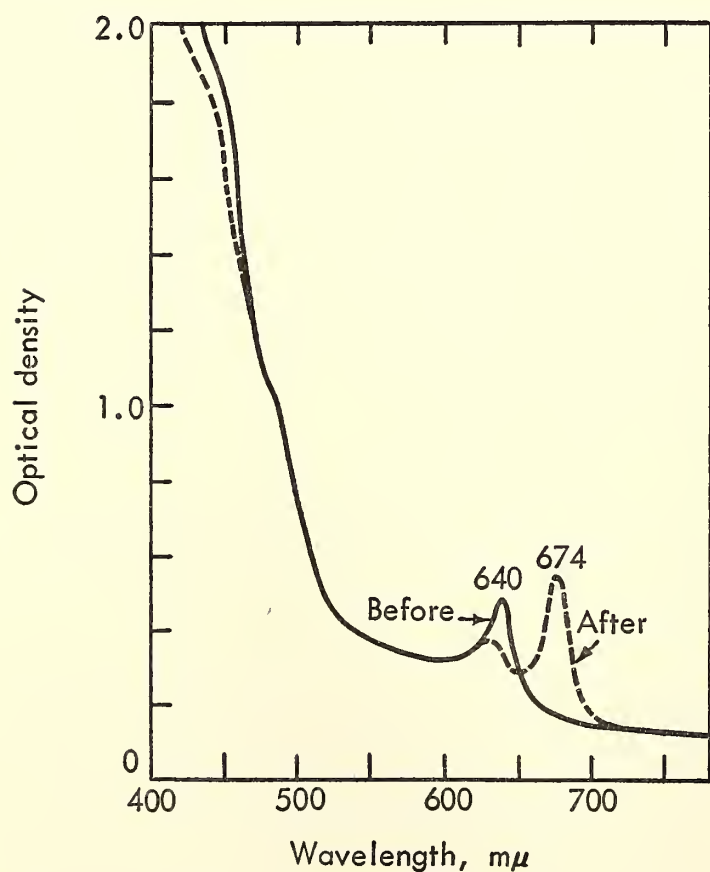


Fig. 19. The absorption spectra of a protochlorophyll-holochrome preparation before density gradient fractionation. The spectra are shown before and after the photochemical conversion to chlorophyll *a*.

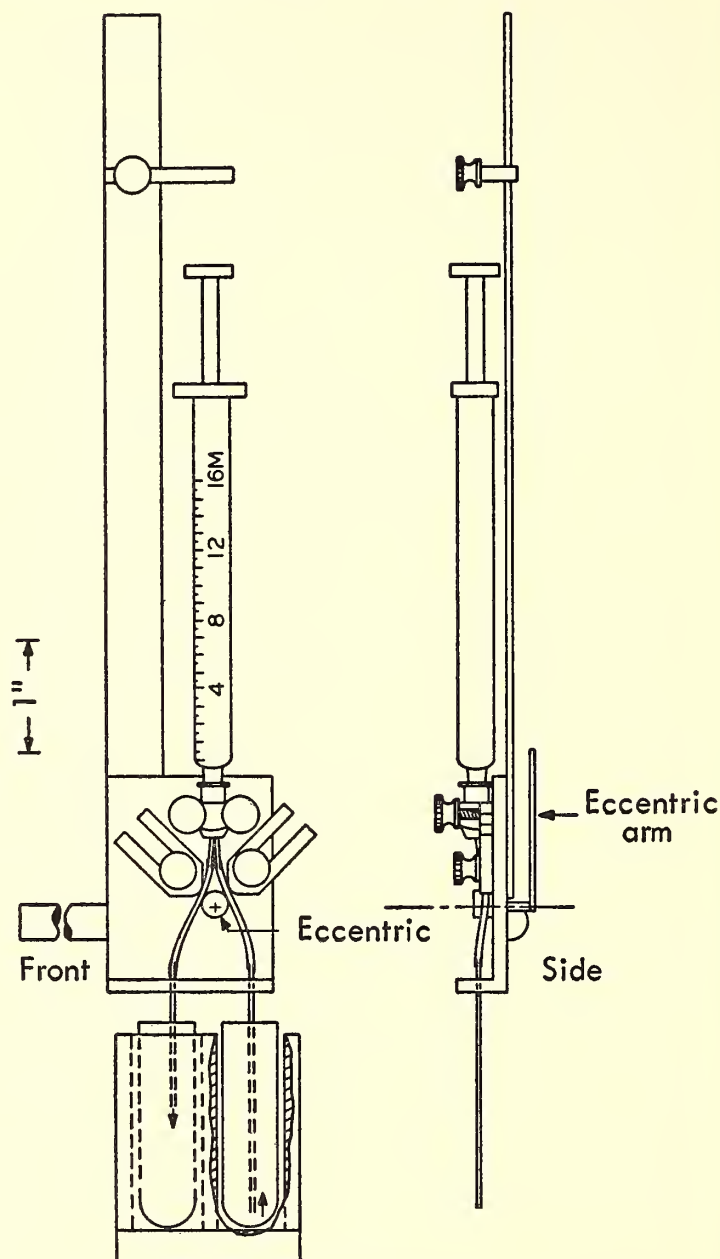


Fig. 20. A syringe attachment for the sharp separation of fractions in a centrifuge tube.

One milliliter of this preparation was placed in a centrifuge tube on top of 4 ml of a density gradient solution made from sucrose in 0.1 *M* NaCl (density 1.07 to 1.20). It was spun at 96,000*g* for 5 hours in a Spinco "model L" ultracentrifuge. After centrifugation the solution was removed in 0.5-ml fractions from the bottom of the tube.

A device was built for the separation of these protochlorophyll-holochrome preparations after density gradient centrifugation, which appears to have general use in biochemical work. It is illustrated in figure 20.

The tube containing the centrifuged material is placed on the right in a frame

along with the tube to receive the desired fraction on the left as shown in the illustration. The frame is supported by a rack and pinion drive not shown in the figure. With the eccentric clamp compressing the micro tubing on the left side, measured samples are drawn up into the syringe. A stop allows fractions of equal volume to be withdrawn. Then with the eccentric clamp in its other position the sample is ejected into the left tube.

Figure 21 shows the absorption spectra of fractions 2 to 6, the numbers corresponding to positions in the tube shown in the insert.

The ratio OD_{674}/OD_{640} gives a measure of the activity of the protochlorophyll

holochrome; the ratio OD_{640}/OD_{442} is the criterion for purity of the preparation.

From top to bottom the fractions show decreasing contamination and increasing activity.

Fraction 1 contained only a trace of protochlorophyll holochrome and no yellow pigments, whereas fractions 7 and 8 absorbed strongly at wavelengths below $450\text{ m}\mu$ and contained a small amount of inactive protochlorophyll holochrome.

OXYGEN EXCHANGE BY *Euglena* CELLS UNDERGOING CHLOROPLAST DEVELOPMENT

Jerome A. Schiff

Dark-grown cells of *Euglena gracilis* var. *bacillaris* contain proplastids that develop into chloroplasts when the cells are exposed to light (Epstein and Schiff, *J. Protozool.*, 8, 427-432, 1961). The entire process of development, which takes 72 hours at the optimal intensity of light (100 foot-candles) can be studied in cells suspended in a resting medium lacking carbon and nitrogen sources so that the cells do not divide. Under these conditions electron microscopy of a thin section of cells shows that the first lamellar disc invaginates from the inner proplastid membrane at about 2 hours of development, and many more discs are produced subsequently. At about 12 hours of development the discs become extensively fused in twos and threes to form lamellae, although the first signs of fusion can be detected as early as 4 to 6 hours. From 12 hours onward the formation of lamellae is linear with time until the chloroplast is completed at 72 to 95 hours.

Previous studies at Brandeis University of the photosynthetic ability of *Euglena* cells while developing chloroplasts have shown that chlorophyll and carotenoid synthesis begins at a slow rate when the cells are exposed to light. The rate increases at about 10 to 12 hours and becomes linear with time (like lamellar

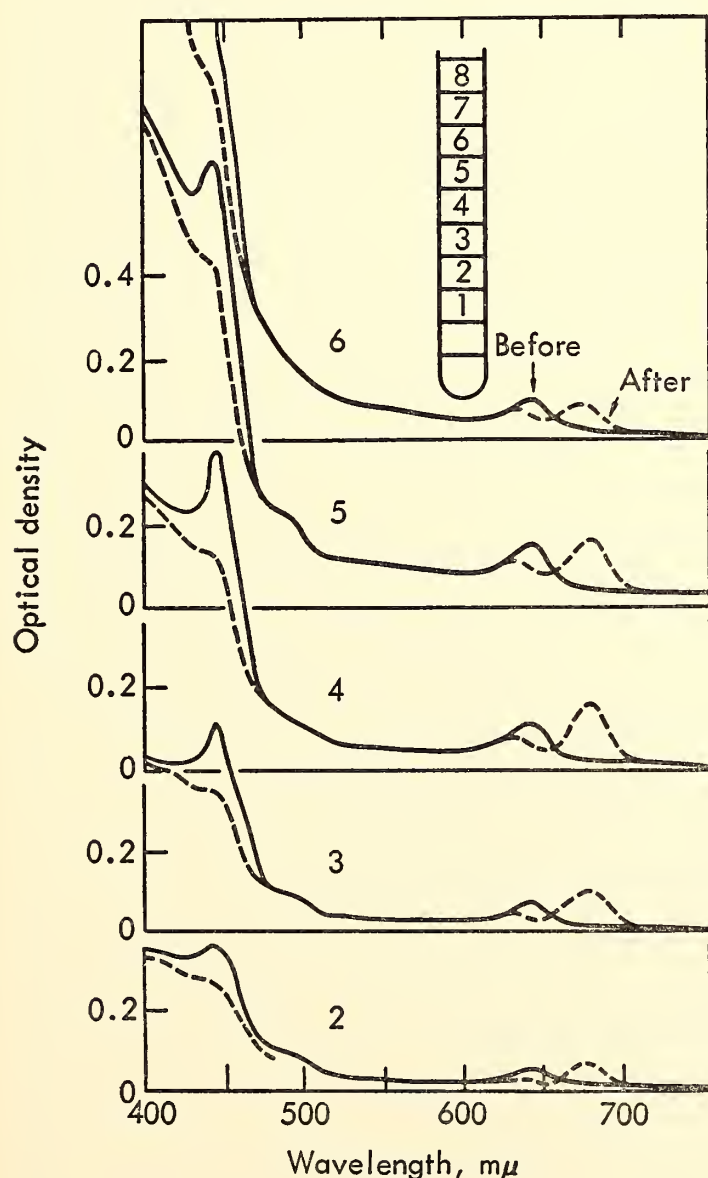


Fig. 21. The absorption spectra before and after transformation of several fractions of protochlorophyll holochrome separated by density gradient centrifugation.

formation) until the chloroplast development is completed. Photosynthetic carbon dioxide fixation begins after about 4 to 5 hours of development and parallels the formation of pigments. Photosynthetic oxygen evolution has been followed as early in development as the precision of Warburg manometry permitted. Oxygen evolution was found to parallel the

kinetics of chlorophyll formation from about 8 hours onward. It was of interest, therefore, to study oxygen evolution with a more sensitive method during the still earlier stages of chloroplast development to find out when photosynthetic oxygen evolution begins.

To do this the modification of the Blinks oxygen electrode devised by Fork

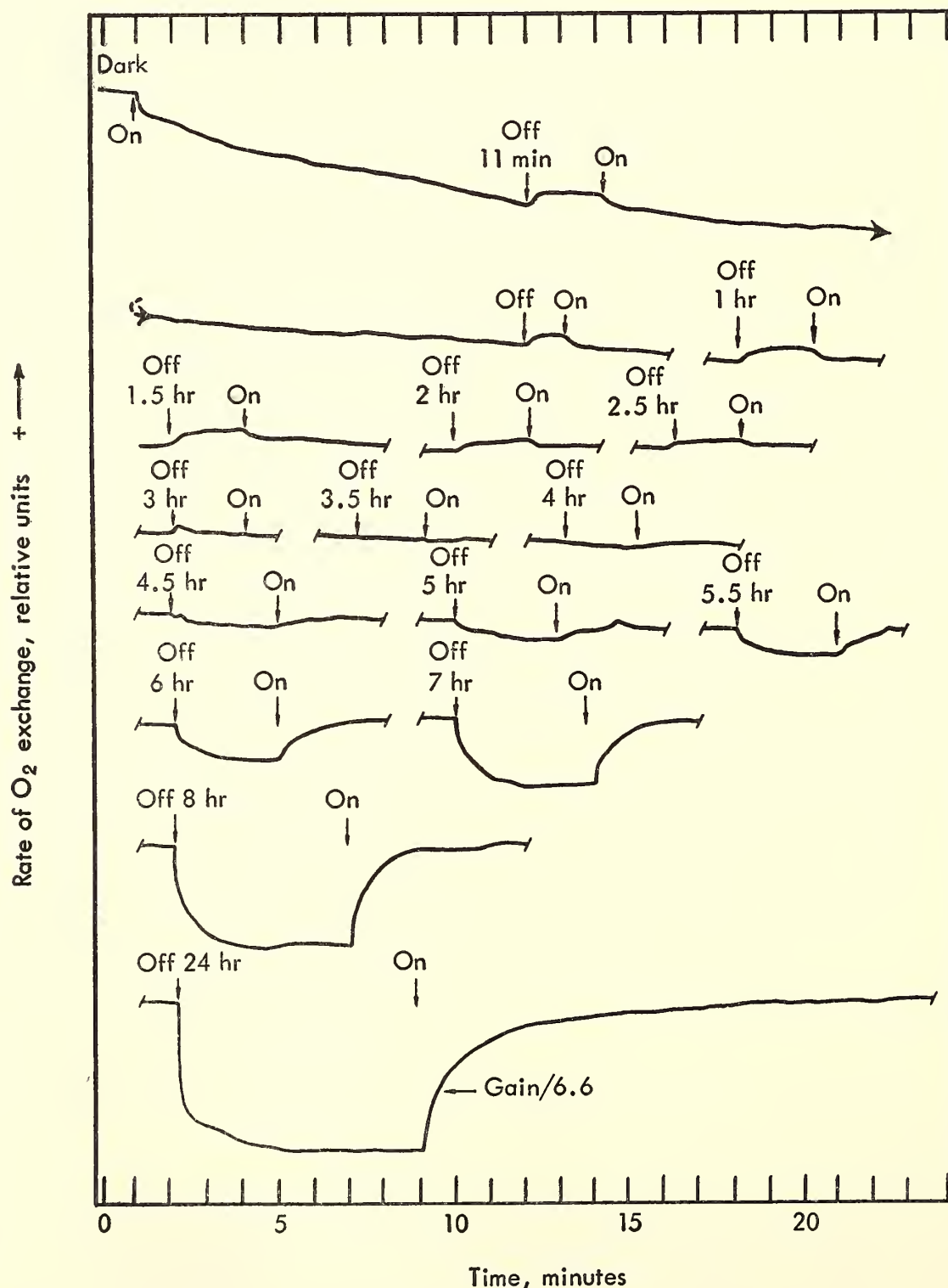


Fig. 22. The oxygen exchange of dark-grown *Euglena* after being placed in 100-fc white light. The light was turned off for short times at various intervals. Each line is the continuation of the one above it. At first the light increases oxygen uptake. After 4 to 5 hours the photosynthetic system has developed, and from then on light produces oxygen. The time in hours marked on the curves is the total since the start of illumination.

(*Year Book 61*, pp. 343–345) was employed. Dark-grown resting cells of *Euglena* were prepared as described previously (Stern, Schiff, and Epstein, *Plant Physiol.*, in press) and centrifuged into a pellet. The packed cells were placed on the Teflon-covered electrode and held in place with a dialysis membrane. Resting medium, as described by Stern, Schiff, and Epstein, bubbled with 5 per cent carbon dioxide in air, was circulated at room temperature over the dialysis membrane. The above operations were performed under a green safelight. After the recorder trace showed that the rate of oxygen exchange had become constant, white light of 100 fc was turned on the cells at a time that was taken as zero on the record. To judge the extent of light-catalyzed changes in the rate of oxygen exchange, the light was turned off at half-hourly intervals for a long enough period to establish a dark base line (1 or 2 minutes, usually) and was then turned on to allow chloroplast development to continue. A negative deflection when the light was turned on indicated the occurrence of light-catalyzed oxygen consumption, whereas a positive deflection showed the rate of light-catalyzed oxygen evolution.

As can be seen in figure 22, illumination of the dark-grown cells results in a large increase in the rate of oxygen consumption, most of which is irreversible, as is shown by the changes recorded when the light was turned off and on 12 minutes after light exposure. A part, however, is reversible and constitutes a photostimulation of oxygen consumption. This photostimulation decreases with time of development until by 3.5 hours it has disappeared completely. At that time there is no change in rate of oxygen exchange when the light is turned off and on. Subsequently (4 hours and beyond) there is a net photostimulation of oxygen evolution the magnitude of which increases steadily with time as the chloroplasts develop.

In some experiments a somewhat differ-

ent pattern was found. In figure 23 there is still the initial large irreversible increase in the rate of oxygen consumption, but it also shows several transients superimposed on the curve. When the light is subsequently turned off and on, complex transients accompany the changes. Each time up to 3.5 hours that the light is turned off the rate of oxygen exchange decreases but does not remain lowered. Instead it rises almost to the light level while still in the dark. Establishment of a true dark base line begins at about 3.5 to 4 hours, showing a true increase in oxygen evolution when the light is turned on. This is consistent with the time of occurrence of net oxygen evolution inferred from the data of figure 22. The conditions governing the differences between the two types of results (figures 22 and 23) are not known. Since the deflections measured in the second experiment are so much larger than the first, it may be that more cells were placed on the electrode and that interactions between cells led to the observed transients.

At any rate, two interesting findings come out of these experiments. First, there is a large irreversible increase in the rate of respiration when the dark-grown cells are initially induced to form chloroplasts by exposure to light. Second, the time for development of net photosynthetic oxygen evolution is about 4 hours for the experiment of figure 22 and about 1 hour for a transient oxygen evolution in figure 23 which becomes stable after about 3.5 hours.

The initial increase in respiration is probably correlated with the activation of synthetic pathways for the synthesis of chloroplast constituents. Chloroplast development in *Euglena* involves the synthesis of unique proteins not present in the dark-grown cells, including chloroplast cytochromes as well as photosynthetic pigments and other compounds. Before the cells become photosynthetically competent, the energy for these syntheses must come from respiration.

The appearance of net photosynthetic

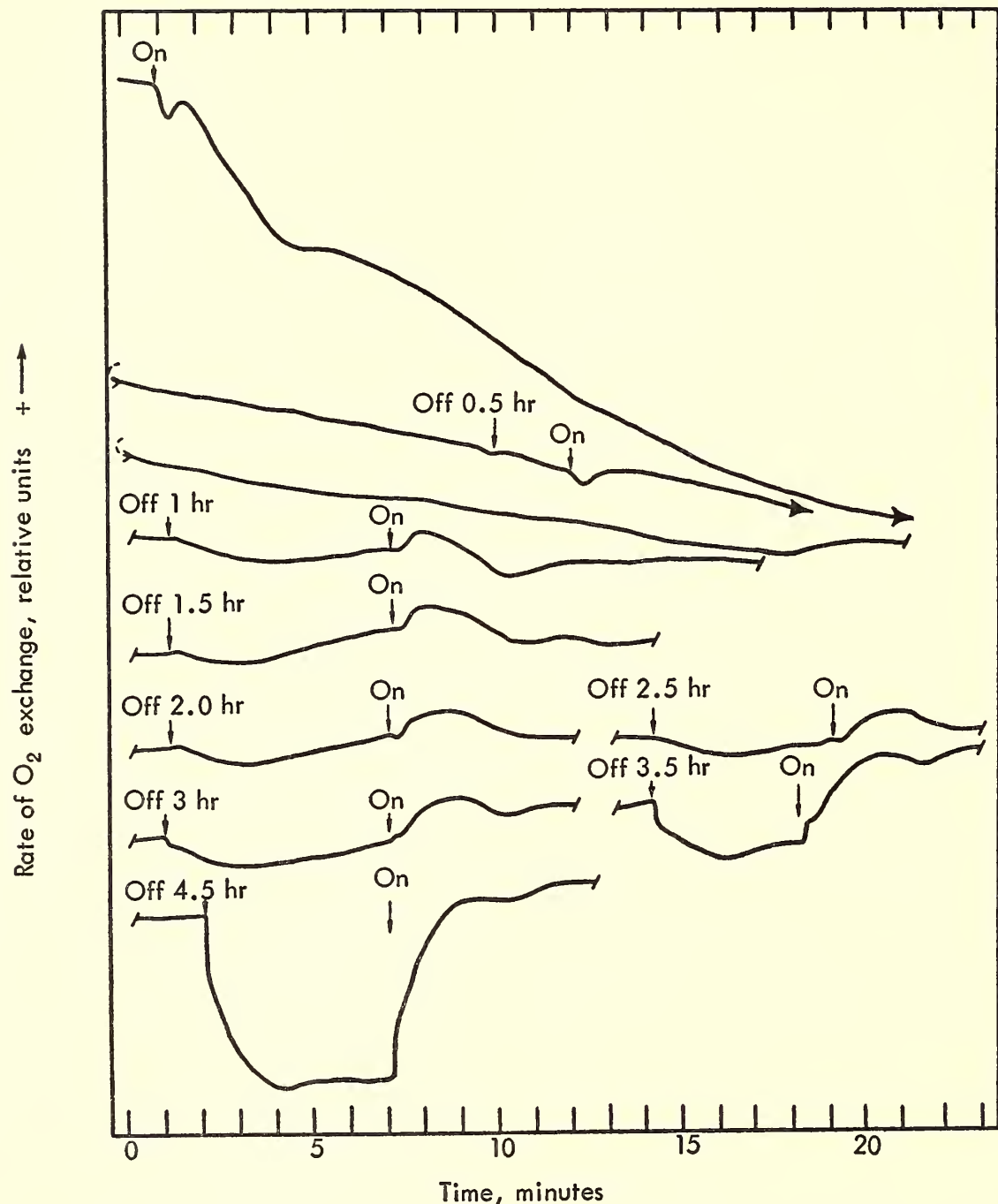


Fig. 23. An experiment similar to that of figure 22 but with an earlier development of photosynthetic capacity, showing first as a short period of oxygen evolution that soon turns into oxygen consumption.

oxygen evolution at about 4 hours of development correlates well with the inception of carbon dioxide fixation (4 to 5 hours of development). It is not known whether oxygen evolution precedes carbon dioxide fixation as reported by Smith (*Plant Physiol.*, 29, 143-148, 1954) for higher plants. The onset of photosynthesis in *Euglena* occurs when only one or two unfused lamellar discs are seen by electron microscopy; in some cases these have fused to form the first lamella. This would suggest that the minimum structure necessary for photosynthesis is either the young lamella (consisting of a fused

disc) or perhaps only a portion of the lamella—a single disc.

Acknowledgments. Some of the materials used in this work were provided by research grant RG-6344 from the National Institutes of Health to H. T. Epstein and J. A. Schiff, Biology Department, Brandeis University. The present project grew out of previous work done in collaboration with Dr. Epstein.

During the course of this work J. A. Schiff profited greatly from many discussions with Dr. James H. C. Smith about the physiology of chloroplast development.

A REVERSIBLE PHOSPHATE ELECTRODE AND ITS POSSIBLE APPLICATION TO PHYSIOLOGICAL PROCESSES

James H. C. Smith

Phosphate metabolism is involved in photosynthesis, and evidence has been provided by Roux and his collaborators (*Compt. rend.*, 251, 1925-1927, 1960) that the oxygen evolved in photosynthesis originates in phosphate. In order to examine the possibility of a correlation between oxygen evolution and phosphate absorption we intend to follow concurrently oxygen production and phosphate uptake under various conditions of temperature, light intensity, and light quality. An electrical procedure for simultaneously determining and continuously recording both oxygen evolution and phosphate uptake would be advantageous for this purpose. An apparatus already exists for tracing the evolution of oxygen under the desired conditions, and we hope that a similar arrangement can be developed for following phosphate uptake.

In Chance's laboratory an electrical method has been developed for estimating phosphate uptake by recording extremely small changes in hydrogen-ion concentration by means of a glass electrode. Since these changes would be difficult to distinguish from changes caused concurrently by gaseous exchange of carbon dioxide in photosynthesis or respiration, a different type of phosphate-ion detector is being sought.

Another type of electrode that responds to phosphate-ion concentration is the metal/metal phosphate/phosphate-ion electrode. Several such electrodes exist, for example: mercury/mercurous phosphate, lead/lead phosphate, zinc/zinc phosphate, and silver/silver phosphate. Of these, the last is the most easily handled, and its properties have been examined.

The silver/silver phosphate electrode has certain advantages over the others

mentioned: (1) It is not fouled by reacting with the oxygen of the air or with water. The surface remains active for long periods of time. (2) Silver phosphate of the empirical formula Ag_3PO_4 is easily precipitated from solutions of a wide range of hydrogen-ion concentrations; it is easily washed free of extraneous ions. (3) The solubility of silver phosphate is relatively low. (4) The solubility equilibrium with phosphate approaches completion quickly.

Silver phosphate has the disadvantage of being rapidly decomposed by daylight, but, by working in relatively weak light from an incandescent lamp, the decomposition can be controlled so as not to pose serious difficulties.

The electromotive force cell used for measuring the phosphate-ion concentration was essentially a silver/silver-ion concentration cell. The reference electrode was a silver rod that dipped into a solution of constant silver-ion concentration provided by a saturated solution of silver phosphate in 0.05 M potassium borate buffer at pH about 8.8. The analytical electrode was a silver rod coated with a dense suspension of silver phosphate in agar gel which dipped into the same buffer solution but in which the silver-ion concentration was varied through variation of the phosphate-ion concentration.

By algebraic combination of the mathematical expressions for the ion-product constant of secondary phosphate ion, the solubility product for silver phosphate, and the Nernst equation for electromotive force, the following equation has been derived for the dependence of electromotive force on secondary phosphate-ion concentration:

$$E = E_0 + 0.0195 \log [\text{HPO}_4^{--}] \quad (1)$$

That this equation holds for the experimental observations is shown in figure 24. The observed values of potential were taken from tracings made with a recording potentiometer. Their conformity with theoretical expectation amply

demonstrates the possibility of recording phosphate changes in a medium by electrical means.

In figure 24 the differences in electromotive force between the analytical silver/silver phosphate electrode and the reference electrode are plotted against the logarithms of the total phosphate

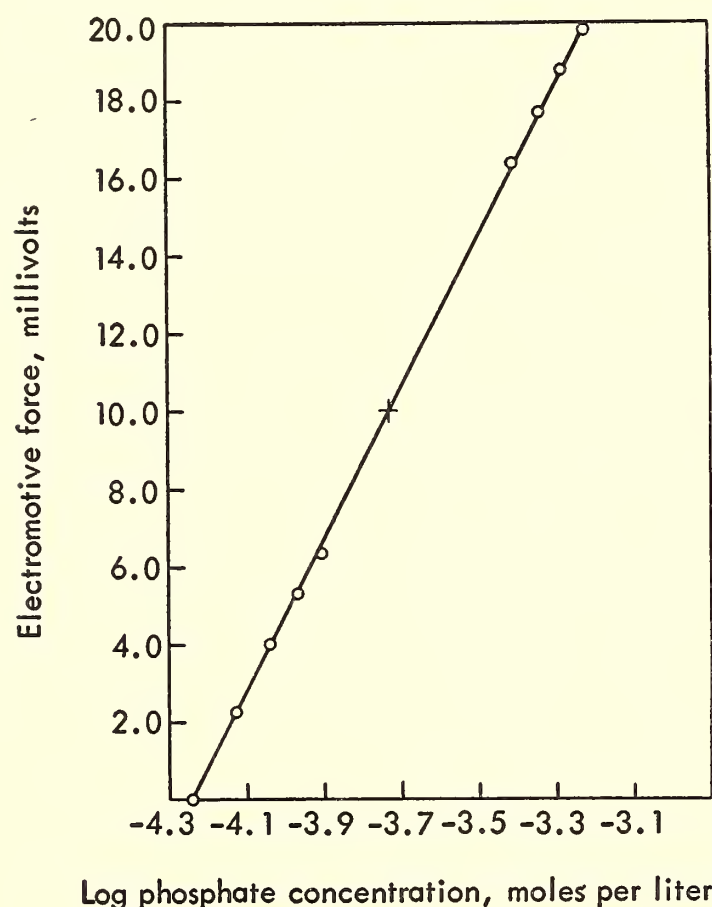


Fig. 24. The dependence of the silver/silver phosphate electrode potential on phosphate concentration. *Ordinate*: electromotive force of cell in millivolts. *Abcissa*: \log_{10} of phosphate-ion concentration in moles per liter. *Circles*: observed potentials at defined phosphate concentrations. *Cross*: average of experimental observations. *Line*: straight line of theoretical slope drawn through average of experimental values.

concentrations in the analytical electrode compartment. The experimental points are marked with circles. The average of these points is designated by a cross through which a line of theoretical slope 19.5 (equation 1) has been drawn. The probable deviation of an experimental point from the theoretical was ± 0.1 millivolt. The maximum deviation ob-

served was -0.22 mv. With the probable deviation of 0.1 mv, the limit of sensitivity of the method is roughly 7×10^{-7} mole per liter. Since 1 ml is ample for a determination, this corresponds to 7×10^{-10} mole of phosphate.

The tracings from which the observed points were taken were produced by a recording potentiometer manufactured by the Nesco Instrument Company, Costa Mesa, California. Full-scale deflection of the potentiometer was 10 mv. For higher voltages, compensation was made by a Leeds and Northrup potentiometer.

The total phosphate concentration always included the phosphate contributed by the saturated silver phosphate. The value used, 0.0000570 M/l, was estimated from the electrical measurements themselves. This solubility is greater than the 0.0000155 M/l given in the literature, probably because of the influence of the salt effect and *pH* of the buffer solution.

The silver phosphate electrode should be useful for phosphate determinations under many circumstances. It was found, however, in collaboration with Dr. D. C. Fork, that this electrode is impractical for certain biological applications, as, for example, in the measurement of phosphate uptake during photophosphorylation by broken chloroplasts. The medium used for this reaction contains chloride ion, ascorbate, and tris buffer, all of which react with silver ion. Interference by these constituents completely invalidates the use of the silver phosphate electrode. If a reaction mixture can be found that will permit action by the chloroplast fragments and yet not react with the silver phosphate, this electrode would have great advantages.

Work is in progress either to discover a medium in which the silver phosphate electrode can be used or to develop another electrode of comparable accuracy and sensitivity for measuring phosphate uptake in a medium suitable for biological systems.

AUTOMATIC CONTROL OF SCANNING SPEED
FOR THE ACTION SPECTROPHOTOMETER*Jerome A. Schiff*

The operation of the action spectrophotometer which continuously records the rate of photosynthetic oxygen evolution as a function of wavelength of the visible spectrum was described in *Year Book 58*, page 323. As the wavelength of light applied to the algal cells changes, the device records the effectiveness of each wavelength in mediating photosynthesis. In one mode of operation the measured rate of photosynthesis is used to control the light intensity so as to keep the photosynthetic rate constant. The reciprocal of the required intensity in quanta per unit of time is continuously plotted against wavelength.

On steep slopes of the action spectrum the light intensity must be changed rapidly or the scanning speed must be lowered to stay within the capacity of the system to adjust itself.

Since the action spectrophotometer is a servo device, there are certain limitations on its time of response which the scanning rate must not exceed. The characteristics of the algal cells themselves form a part of the servo loop controlling the light intensity. The response of the photosynthetic rate to a change of light intensity is not instantaneous. The lag period of photosynthesis is the limiting factor in the speed of response of the system. It is possible to scan at such a speed that the response time of the system is not exceeded during the periods of most rapid change in rate of oxygen evolution. However, a disadvantage is that more time is needed to complete an action spectrum, and the biological system under study may change its properties with time.

To avoid such delay, the rate of scan has been continuously adjusted by the investigator to suit the rate of change of oxygen evolution with wavelength. The constant attention of the investigator is

required over the entire period, and often his reflexes are not fast enough to make the necessary compensation. To eliminate these difficulties, we have incorporated into the action spectrophotometer a circuit that permits the instrument to adjust its own rate of scan for optimal results. Such an arrangement is found in some commercial recording spectrophotometers.

A measure of whether the response time of the system is being exceeded is the degree of imbalance in the servo system. Ideally the servo should be in balance at every instant except for the small error voltage needed to activate it. The rate of scan should be such that at each increment of wavelength change the light intensity is in balance with the rate of photosynthesis before proceeding to the next wavelength increment.

The voltage delivered to the motor that adjusts the light intensity has therefore been used to reduce the wavelength sweep speed whenever it becomes excessive. The motor control voltage is rectified, filtered, and applied to the input of a "Labac" voltage controller, which contains silicon-controlled rectifiers operated by a magnetic amplifier. Its output drives the wavelength sweep. When the servo controlling the light intensity is balanced, its output is zero and no d-c signal appears in the control circuit of the magnetic amplifier. Under these conditions the monochromator motor scans at the maximum speed which has been set by the investigator at the beginning of the run. If, as the wavelength changes, the response time of the system is exceeded, a d-c voltage proportional to the imbalance appears in the control circuit of the magnetic amplifier which reduces the voltage to the monochromator's wavelength sweep motor circuit, thus slowing the rate of scan. If the imbalance is sufficiently great, the monochromator motor stops completely and waits until balance is restored before proceeding. In this way the optimal rate of scan is maintained. The automatic

scanning device requires a stable oxygen electrode and associated servo electronics, and also well behaved cells, since any small disturbances in the servo balance from these sources will slow or halt the scan.

AN AUTOMATIC PLOTTER FOR PLANE TABLE SURVEYING WITH A RANGE FINDER

C. S. French and R. W. Hart

The production of topographic maps from air photographs, though widely practiced, seems unlikely to displace plane table surveying for small areas of a few acres, particularly in heavily wooded regions. We have made an experimental model of an instrument that may facilitate plane table surveying.

Instruments built on the principle described here might be of practical value in topographic surveys for construction work ranging in scale from single houses to highways, for general grading purposes, and for filling in topography and detail on a base map of large scale. Other obvious applications are for archeological and ecological field surveys where an abundance of detail must be plotted. Such an instrument, however, being based on an optical range finder, does not seem applicable to high-precision work or small-scale mapping of large areas. One man could operate it where the objects or ground points to be plotted can be seen from the stations occupied, although a rod man would be essential for locating points on the ground in heavy brush.

The direction of points to be located on a map are easily obtained from an alidade on the plane table station; but the process of determining the horizontal distance to a point by tape or stadia measurements, reducing the data to the horizontal distance, and then scaling the data on the map takes some time for each point.

The machine we have made locates an index marker over the map position of a sighted point. This is done as rapidly as the telescope can be brought to bear on

the point and a range finder adjustment made to bring two images in the telescope into coincidence. Also at this time the elevation of the sighted point appears on a dial reading directly in feet above or below a desired standard elevation. No calculations are needed.

An experimental model, cumbersome but usable, has been constructed; it is being tested to evaluate the practical utility of such a device and to estimate the precision attainable. The design of a production model has not been attempted. The principles, the construction of the experimental model, and some preliminary performance tests are described.

Principle. Our idea was to build a range finder into a telescopic alidade so that the setting crank of the range finder would simultaneously position an index over the map position of the sighted point. To use this principle for other than horizontal work a triangle solver of some sort must be included to convert the slope distance measured by the range finder into the true horizontal distance on the map and to calculate the elevation of the observed point.

This triangle solver receives two inputs: the slope distance, that is, a displacement proportional to the hypotenuse of the right triangle to be resolved; and the elevation angle from the instrument to the sighted object. The two output quantities of the resolver are proportional to the vertical and the horizontal sides of this triangle. The horizontal output is used to position the index marker on the map; the vertical output gives the elevation of the object on a dial.

General arrangement of parts. Figure 25 shows the relation of the instrument to the landscape. The round 32-inch-diameter plane table is mounted on a heavy tripod and arranged so that it can be leveled and rotated about its center point to align the map with the landscape. The table is then locked in position. The tripod and mounting is a war surplus "Instrument, observation, M1," from which the elbow telescope was removed.

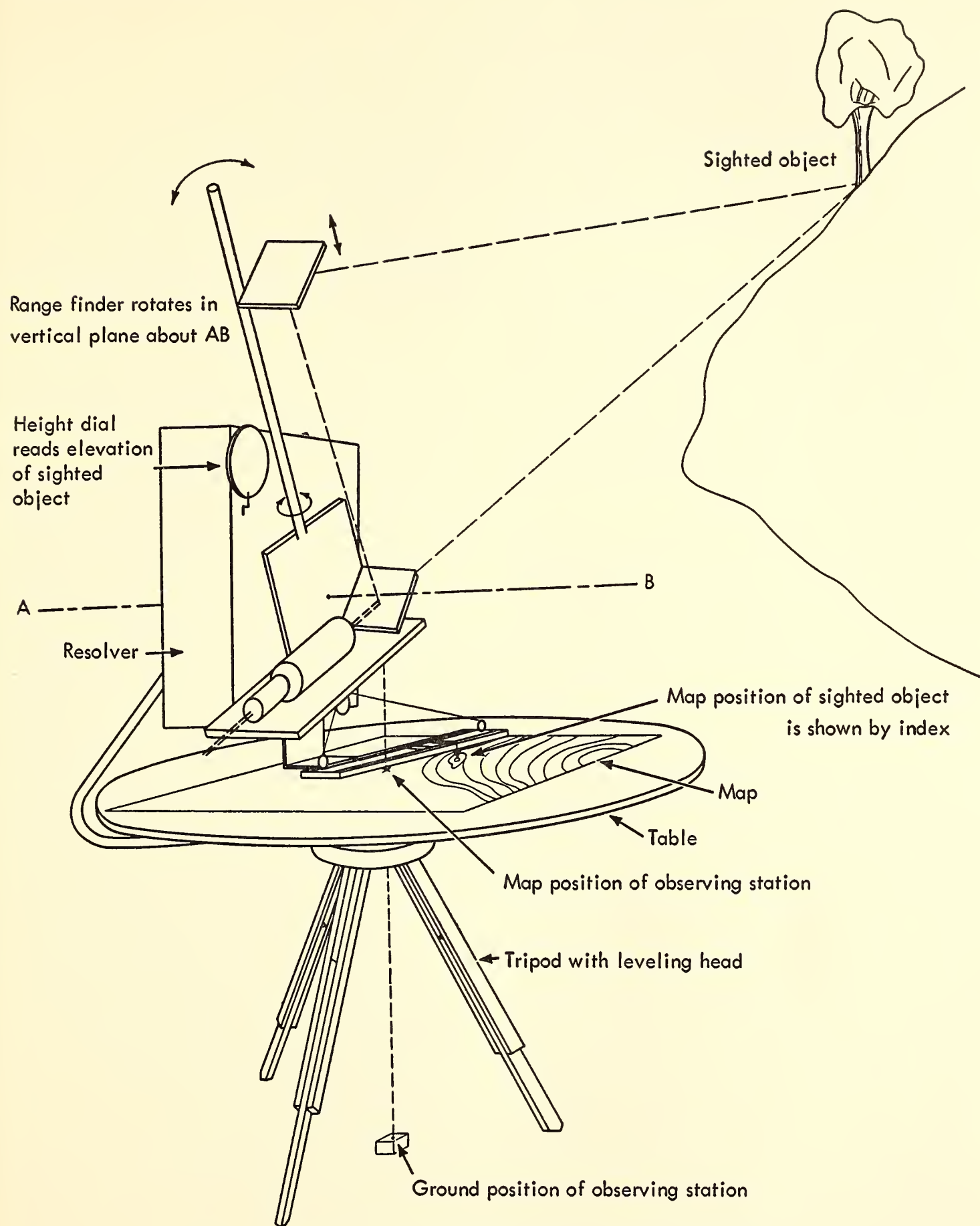


Fig. 25. The plane table plotter in relation to the landscape.

Although the weight of the plane table is supported by a bearing on the rotating part of the original instrument, the table may be locked to a center rod attached directly to the fixed tripod head.

All other parts of the device are supported by the rotatable outer case of the original instrument mounting. This is of massive construction and has an azimuth scale readable to 0.1 mil. The scale is not

an essential part of the instrument but can be used if angular measurements of greater than graphical accuracy are desired. An angle iron frame supports the resolver in its cast aluminum case above the plane table and also carries an aluminum guideway with a slider. The slider positions the index marker over the map.

The telescope with its range finder components is mounted directly on one horizontal input shaft of the resolver. Since the optical axis of the telescope has to rotate about the center point of the plane table the resolver has to be off center. A counterweight under the table on the opposite side of the frame balances the weight of the resolver.

The table and also the entire assembly above it are removable for transporting the device from one observing station to the next. Adjustments are provided to allow crossed levels on the resolver to be made horizontal. A separate level is attached to the telescope.

The range finder. The resolver must receive an input proportional to distance. To allow direct coupling of the range finder and the resolver the range finder must have a linear scale. Standard varieties of range finders have inverse scales which would require a correction cam to link them to the resolver input. We therefore used a very simple range finder principle having a setting directly proportional to distance. It violates most of the accepted principles of good range finder design and requires precise guideways even for moderate performance.

The optical system of the range finder is shown in figure 26. One image of the object, O , is seen on the telescope cross hairs directly through the beam splitter. Another image coming from the mirror M , and reflected from the surface of the beam splitter, is coincident with the direct image for a certain mirror-to-beam-splitter distance MP . If the angle between the mirror and the beam splitter remains constant, the distance MP is proportional to OP , the distance from the instrument

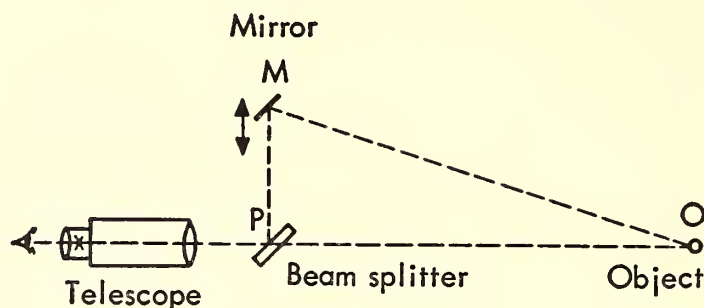


Fig. 26. The range finder works on the principle that the corresponding legs of similar triangles are proportional to each other.

to the object. The mirror is moved on guideways parallel to the line MP by the range setting crank, which is also geared to the resolver's hypotenuse input shaft. The map scale is determined by the angle between the mirror and the face of the beam splitter. The mirror angle is adjustable by three screws. The image seen straight through the dichroic beam splitter is orange; that reflected from its face is blue. At coincidence the image has its normal color.

The entire optical assembly and the guideways for the mirror are attached to the angle input shaft of the resolver as shown in figure 27. This shaft rotates in elevation about point P , the optical center of the instrument. Point P is located over the center of rotation of the plane table. The mirror is held on a carriage which runs on ball bearings between two aluminum guide tubes. A floating nut engages the screw without transmitting wobble of the screw to the carriage. The guide tubes and the drive screw are held in position at the top and bottom by aluminum castings. The limiting factor in the accuracy of the range finder measurement is the precision of the guide tubes.

At the suggestion of Dr. Ira Bowen we have tried out a movable two-mirror system in place of the single mirror. This arrangement, similar to a penta prism, gives a line of sight at nearly 90° which is independent of small errors in the carriageways. The scale is adjustable by setting the angle between these two mirrors. Because this system inverts the

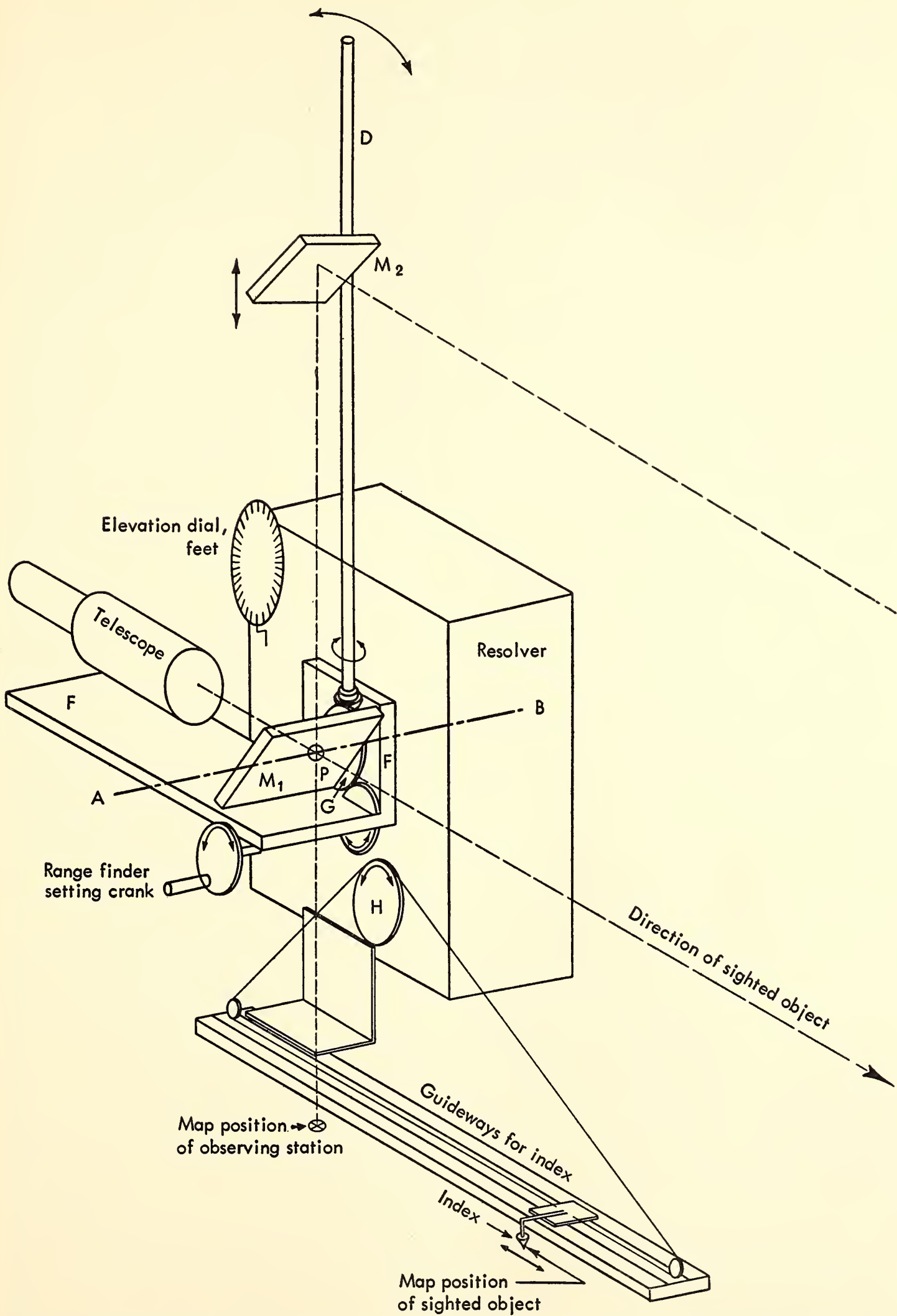


Fig. 27. The range finder is mounted on the resolver's hypotenuse input shaft, which rotates on the axis *AB*. The horizontal output shaft of the resolver drives the index marker to the map position of the sighted object; the vertical output sets an elevation dial.

image a Pechan prism is placed in front of the beam splitter. Preliminary tests with this system show an improvement in repeatability of settings over the single-mirror system.

The resolver. The surplus mechanical resolver used for military fire control purposes is well suited for the present purpose because of its two concentric input shafts. It therefore serves as a stable mounting for the optical system as well as functioning as a computer. Unfortunately it weighs 23 pounds.

The outputs of the resolver are shafts which make about 1.6 revolutions for full scale. An aluminum drum was attached to the horizontal output shaft. A cable around it drives the index marker over the map. The path of the index is kept parallel to the optical axis of the telescope by 16-inch aluminum guideways.

The elevation output shaft carries a coarse dial reading directly in feet for several different map scales; a fine dial geared up 10:1 from the coarse dial facilitates the elevation reading. The zero positions of the dials are adjustable so that the reading can be made to refer to elevations above or below any desired elevation. Only one dial is shown in the figures.

Figure 27 shows how the optical parts are mounted on the resolver. The aluminum block *F* clamps on the angle input shaft of the resolver and supports the telescope, the beam splitter *M*₁, and the assembly carrying movable mirror *M*₂. The mirror drive screw *D* positions the mirror carriage on its guide tubes, which are supported by a casting attached to block *F*. The figure does not show the guide tubes, their supports, or the carriage.

The entire range finder assembly

rotates around the *AB* axis under the control of a worm gear and crank mounted on top of the resolver (omitted from the figure).

The double gear *G* is carried on the resolver's hypotenuse input shaft concentric with the axis *AB*. The inner part of gear *G* is a bevel gear driving the mirror-positioning shaft *D*; its outer part is a spur gear driven by a gear on the setting crank of the range finder.

Map scales. The scale of the map can be set for any usable range by changing the tilt of the mirror. To make the elevation dials read directly in feet without a conversion factor, however, the map scale and the elevation dial scales must agree. The dials have been graduated for the following scales: 1 inch = 10, 20, and 50 feet.

The relation between the elevation dials and the map scale is determined by the diameter of the drum on the horizontal output shaft of the resolver. This diameter, 3.155 inches, was chosen to give 1 revolution of the coarse elevation dial for 100 feet of elevation at a map scale of 1 inch = 10 feet. The fine elevation dial has 100 divisions, and, being $5\frac{3}{8}$ inches in diameter, can be read to 0.1 division. One division corresponds to 0.1-foot elevation at a map scale of 1 inch = 10 feet or to 0.5-foot elevation for a scale of 1 inch = 50 feet.

Performance. A line of test stakes at 20–700 feet is used for checking the accuracy of the distance measurement. At a scale of 1 inch = 10 feet the range of the instrument is 160 feet. Our best set of test data with that scale gave results within 1 foot. Limited tests on the elevation dials show an accuracy within 0.1 foot for small angles. Modifications are still in progress.

EXPERIMENTAL TAXONOMY INVESTIGATIONS

Progress has been made during the year along all the four approaches of our program designed to clarify mechanisms of natural selection and evolution of

higher plants: combined genetic and transplant studies; controlled environment studies; quantitative physiological measurements; and work with tissue

cultures. The principles applied in pursuing these four approaches, all of which are focused on our major objectives, were reviewed last year (*Year Book 61*, pp. 311-312).

Emphasis in the present report is placed on a review of some of the accumulated results stemming from the first of these methods of inquiry. The most prominent feature is new evidence that establishes experimentally the general validity of an important concept—the principle of genetic coherence—as a reality in the evolution of higher plants. This principle is of importance not only for understanding processes of speciation but also for the orientation of the lines of inquiry aimed more specifically at discovering mechanisms underlying natural selection by the other three approaches.

GENETIC COHERENCE IN THREE SPECIES-COMPLEXES

*William M. Hiesey, Malcolm A. Nobs, and
Harold W. Milner*

Genetic coherence is the tendency for characters distinguishing recognizable biological entities to be inherited together as a unit rather than to be distributed to progeny purely at random. Coherence can be studied experimentally by crossing contrasting ecological races of the same or closely related species and analyzing the characters of their first-, second-, and later-generation progeny. The expression of coherence tends to be overshadowed by the spectacular recombinations of characters typically found among F_2 and F_3 progeny of such crosses.

Although the recombinations themselves are of much evolutionary interest, they tend to obscure and render difficult the experimental demonstration of genetic coherence. The study of coherence and of its consequences is greatly aided by observing the expression of characters in cloned F_1 and F_2 progenies grown at the altitudinal transplant stations at Stanford, Mather, and Timberline. A wide range of expression of the parents and of

the progeny can thus be analyzed critically.

Evidence clearly demonstrating the existence of coherence in higher plants was found in the *Potentilla glandulosa* complex and was reported in Carnegie Institution of Washington Publication 615, volume IV of *Experimental Studies on the Nature of Species*, by Clausen and Hiesey. This complex is a highly diverse diploid group with $n = 7$ chromosomes. Distinguishing features marking contrasting ecological races are not transmitted by simple Mendelian inheritance but by systems of multiple genes whose components are carried in more than one chromosome. Combinations of dissimilar characters distinguishing one climatic race from another are thus carried by all the seven chromosomes and are loosely tied together through genetic linkage of the multiple gene systems.

The over-all result is that, when distinct races are crossed, there is a higher frequency among F_2 progeny of plants having characters like one parent or the other than would be expected on the basis of free random recombination. The extent of this tendency can be measured statistically by determining the value of the correlation coefficient r computed from the frequency with which any pair of dissimilar characters is expressed together in individuals of the same F_2 segregating population.

Since the expression of a given character in a particular environment is almost without exception the result of the interaction of multiple genes, it can be rated on an arbitrary scale covering the extremes of its expression. Coded on a scale of 9, the data for each such character for each individual F_2 plant of a population can be transferred to punched cards and then analyzed with the help of computing machines. The existence of genetic coherence in *Potentilla* was established by computing the values of the correlation coefficients between all possible combinations of 12 and 14 pairs of dissimilar characters in two highly seg-

regating F_2 progenies from crosses between contrasting altitudinal races.

Comparable studies have been completed recently in *Achillea*, a genus of the sunflower family, and *Mimulus* of the figwort family. The results from both groups are in conclusive agreement with the earlier data from *Potentilla* of the rose family. The independent evidence from three species-complexes belonging to diverse plant families now establishes firmly the concept of genetic coherence as a principle operating in the evolution of higher plants.

The evidence from *Achillea* comes from a cross between contrasting latitudinal races of *A. borealis*, a dwarf form from Kiska Island at 52°N latitude, and a

giant race from the San Joaquin Valley at 36°N. The F_2 progeny from this cross segregated widely, showing various recombinations of the parental characters (cf. *Year Book 51*, pp. 122-124 and pl. 1). The inheritance of 9 characters distinguishing the parents was studied in 300 F_2 individuals. Of the 36 combinations possible among pairs of these 9 characters, 7 combinations, or 17 per cent, had values of r ranging from zero to 0.11, indicating random distribution. The great majority, 29 combinations, or 83 per cent, had r values above 0.11, indicating a significant degree of correlation at the 1 per cent level or better, and 15 of the 29 combinations had r values ranging between 0.25 and 0.64. Despite

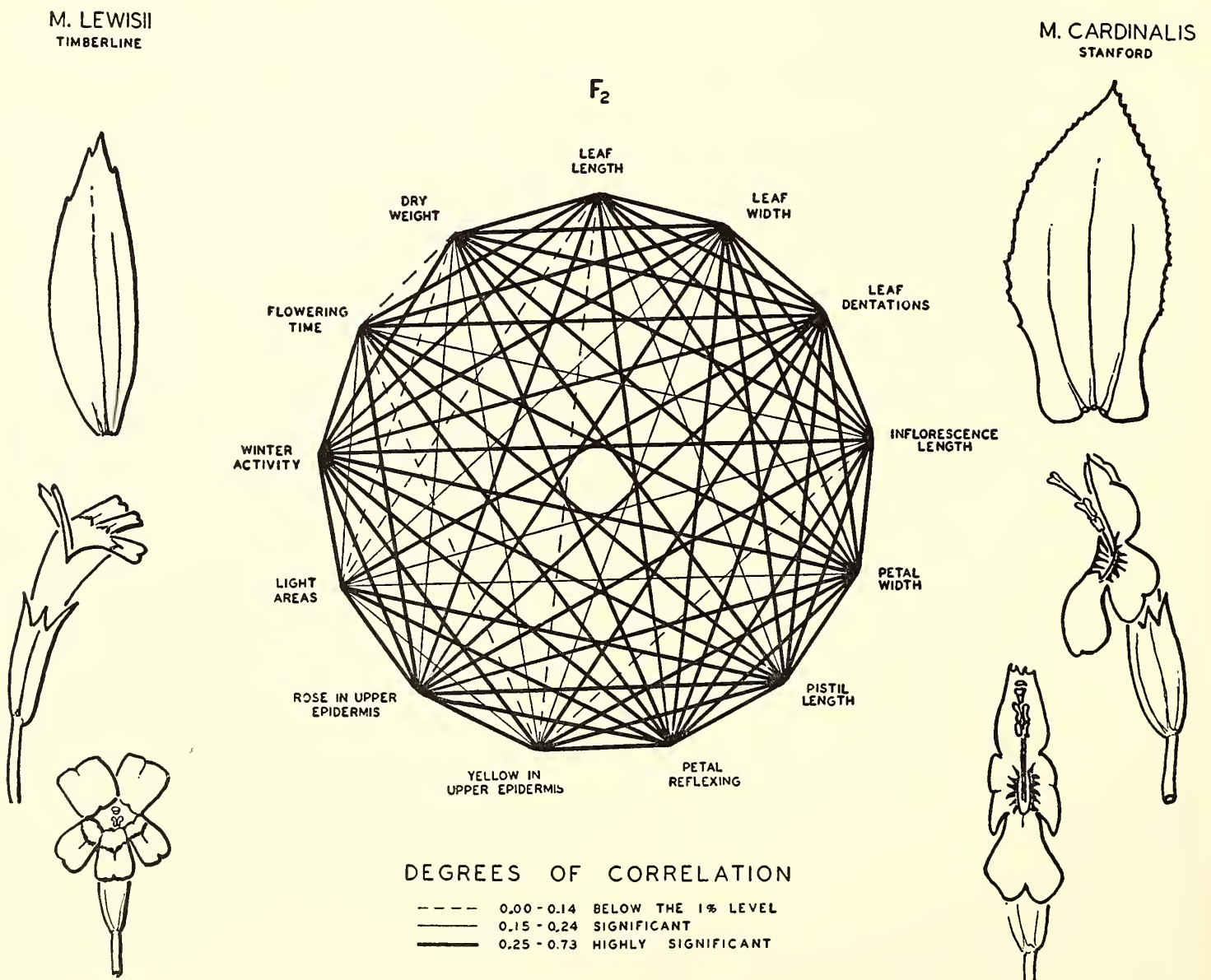


Fig. 28. Genetic coherence in *Mimulus* as expressed by the frequency of individuals within a segregating F_2 population sharing in the expression of pairs of characters. The degree of coherence is indicated by the values of the correlation coefficient r computed from observations on 300 plants. Some of the character differences between the parents are shown by the drawings.

the great range of parental recombinations observed in the F_2 population, there is an unmistakable tendency for F_2 progeny resembling either one parent or the other to occur with higher frequency than would be expected statistically on the basis of free random recombination.

The data from the *Mimulus cardinalis-lewisii* complex provide even more convincing evidence of the reality of genetic coherence. Many of the ecological races of *Mimulus* are distinguished by vegetative and floral characters that serve as excellent markers. A cross between the red-flowered, broad-leaved form of *M. cardinalis* from 45 meters elevation near the California coast and the lavender-flowered narrow-leaved alpine *M. lewisii* from 3300 meters in the Sierra Nevada yields highly segregating F_2 populations that exhibit conspicuous recombinations of the parental characters.

The average expression of 13 dissimilar characters that distinguish the parental races was determined over a 5-year period at the three altitudinal transplant stations. The values of the correlation coefficient r for all possible combinations of paired characters were computed. Results from the Stanford data are shown in simplified form in figure 28. Of the 78 possible paired combinations of the 13 characters scored, 73 combinations, or 94 per cent, are significantly correlated at the 1 per cent level, and only 6 per cent have values of r indicating random distribution. The statistical evidence unquestionably supports the reality of genetic coherence in *Mimulus*.

Genetic coherence appears to be the mechanism by which ecological races, subspecies, and species have become differentiated through natural selection over periods of geologic time. Through coherence, combinations of characters that have attained equilibrium by natural selection tend to be preserved; at the same time the wide range of recombinations that occur after hybridization provide extensive possibilities for selection and the evolution of new coherence

systems that are in equilibrium with new selective pressures.

TRANSPLANT RESPONSES OF *Mimulus* IN RELATION TO GENETIC COHERENCE

Malcolm A. Nobs, William M. Hiesey, and
Harold W. Milner

The tendency for morphological characters of *Mimulus* to be genetically linked with capacity for survival at the Stanford and Timberline transplant stations was noted in *Year Book 60*, pages 381-384. More complete data now available are summarized in figure 29, which presents the most important features relating to the performance of a genetically segregating F_2 population of 300 cloned plants originating from a cross between the form of *M. cardinalis* from Los Trancos near Stanford and an alpine form of *M. lewisii* from near our Timberline station.

In the figure the performance patterns of the F_2 plants are divided into the nonsurvivors at the left and the survivors at the right. This classification is based on 5 years' accumulated data. The nonsurviving individuals were replanted several times at each station in order to distinguish as closely as possible between failure due to accidental causes and failure due to the inability of the plant to cope with the climate.

The entire F_2 population was classified into three groups: those tending to resemble the *M. lewisii* parent (black bars), those tending to resemble the lowland *cardinalis* parent (white bars), and intermediate types tending to resemble the F_1 (crosshatched bars). The grouping of the F_2 plants into these three categories is based on index values assigned to each individual plant on the basis of seven contrasting, essentially nonmodifiable vegetative and floral characters distinguishing the original parents.

For each transplant station, data on the F_2 plants are arranged into classes according to the mean total dry weights of the above-ground parts of the plants at the end of the growing season. These

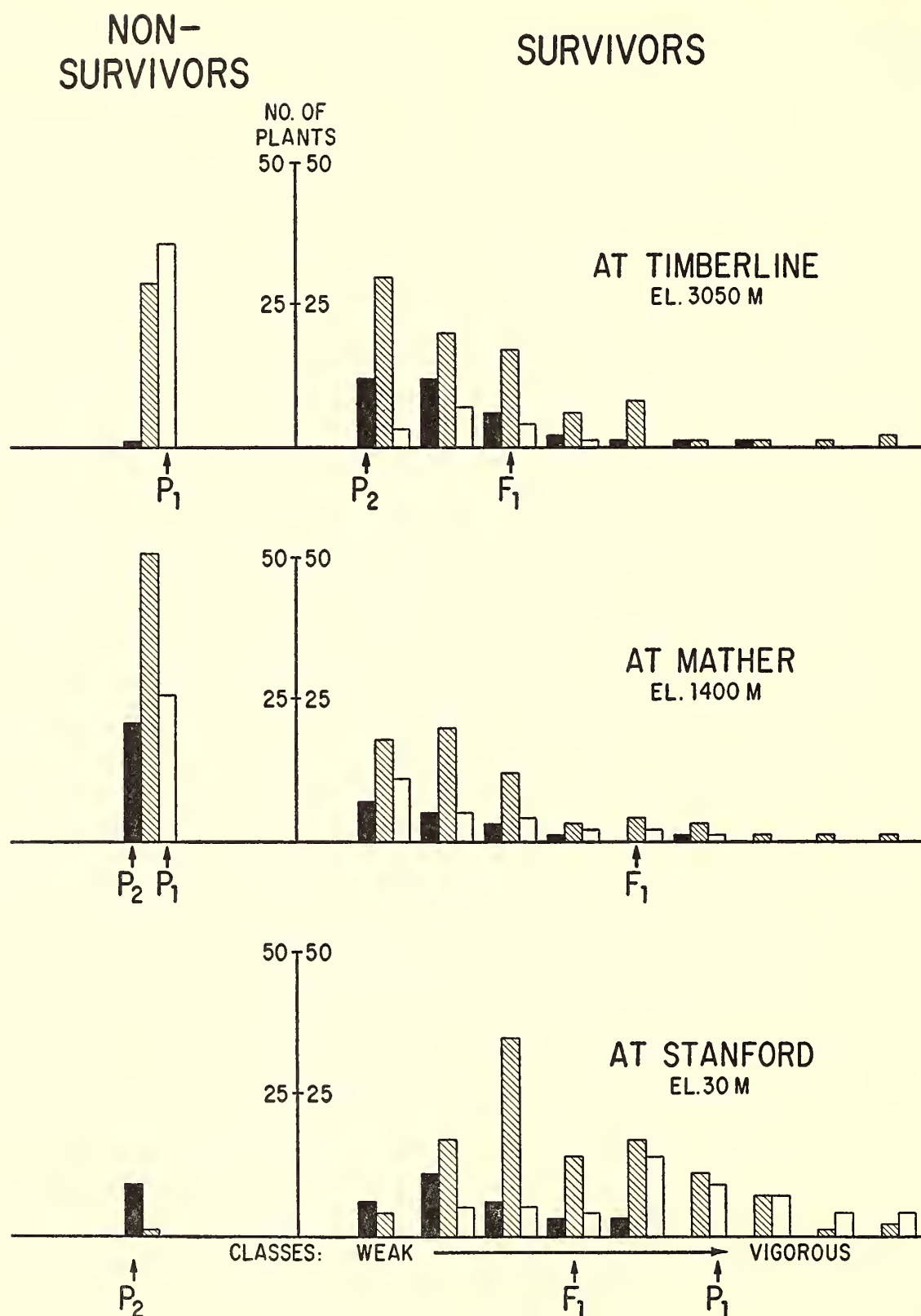


Fig. 29. Responses at the Stanford, Mather, and Timberline transplant stations of 300 cloned individuals of a highly segregating F₂ population from a cross between a coastal form of *Mimulus cardinalis* (P₁) and an alpine form of *M. lewisii* (P₂) from 3300 meters elevation.

weights are taken as a measure of over-all bulk growth, or vigor, at each station. The relative positions of the lowland *M. cardinalis* parent (P₁), the alpine *M. lewisii* parent (P₂), and their F₁ progeny are indicated by the arrows at each station.

At Stanford, where the alpine *M.*

lewisii parent (P₂) is a nonsurvivor and the coastal *M. cardinalis* parent (P₁) a vigorous survivor, the F₁ displays intermediate vigor. Among the F₂'s the percentage of over-all survival is excellent except for a relatively small fraction that morphologically resembles the *M. lewisii* parent. Among the survivors the most

vigorous are those resembling either the *M. cardinalis* parent or the F_1 -like recombinations. The weaker survivors at Stanford consist mostly of F_2 individuals resembling the *M. lewisii* parent or recombinations resembling the F_1 . The fact that there are a few *lewisii*-like F_2 's that have a fairly high degree of vigor and also a few *cardinalis*-like plants with low vigor is also noteworthy. The marked enhancement in vigor of a few F_2 individuals at Stanford as compared with the coastal *M. cardinalis* parent is also of considerable interest, indicating the capacity of the nonsurviving alpine *lewisii* parent to contribute something to the F_2 progeny which in certain recombinations enhances its growth in the Stanford environment.

At Timberline the relative performance of the same cloned F_2 progeny is markedly different. The proportion of nonsurvivors is much higher than at Stanford, the unsuccessful F_2 plants consisting mostly of *cardinalis*-like and intermediate F_1 -like individuals. The lowland *M. cardinalis* parent (P_1) is clearly a nonsurvivor, and even the alpine *M. lewisii* parent is a relatively weak survivor in the transplant garden⁴ whereas the F_1 hybrid is quite vigorous. Among the surviving F_2 progeny in this rigorous environment the most vigorous as well as the weaker classes include F_1 -like recombinations and *lewisii*-like individuals. The weaker classes include the few surviving *cardinalis*-like recombinations.

The situation at Mather is anomalous. A high proportion of the F_2 progeny are nonsurvivors, like both the lowland *M. cardinalis* and the alpine *M. lewisii* parents. The F_1 , on the other hand, is highly vigorous. Among the survivors, the most vigorous are F_1 -like recombinations together with an occasional *cardinalis*-like or *lewisii*-like individual. The

weak classes include individuals of all three recombination types without bias in their relative frequencies. Of particular interest at Mather are, first, the complementary effect of adding the heredities of the nonsurviving lowland and alpine parents to produce an F_1 vigorous in this environment, and, second, the fact that the selective bias is clearly in favor of a very small segment of F_1 -like types which appear to have inherited a certain critical physiological balance needed for survival in that environment. Neither *cardinalis*-like nor *lewisii*-like F_2 's are favored in the Mather environment—another manifestation of genetic coherence.

At Stanford coherence is expressed in the tendency for *cardinalis*-like F_2 progeny to be more vigorous than the *lewisii*-like recombinations, whereas at Timberline *cardinalis*-like individuals are eliminated in higher frequency than the *lewisii*-like progeny. The same coherence in the same cloned F_2 plants is thus expressed in opposite directions in these contrasting environments.

Early observations this year on transplant responses at Stanford and Mather of new plantings made last year of F_1 hybrid combinations between a series of ecologic races of *M. cardinalis* and *M. lewisii* already show some conclusive results. Not only do different F_1 hybrid combinations between various races of either *M. cardinalis* or *M. lewisii* show significant differences in their winter survival and subsequent summer growth at Stanford and Mather but also F_1 hybrids between almost any race of *M. cardinalis* and any of *M. lewisii* show outstanding capacity to survive at both Stanford and Mather. Such complementary enhancement in the F_1 strongly confirms some of the results reviewed above. The differences in performance among the F_1 progenies of various crosses reveal in clearer perspective the relative physiological importance of interracial as compared with interspecific differentiation in the *Mimulus cardinalis-lewisii* complex.

⁴ *M. lewisii* in its natural environment grows on rocky talus slopes above the transplant area at Timberline station, where maximum temperatures during the growing season exceed those in the transplant garden.

PHYSIOLOGY OF CLIMATIC RACES

Harold W. Milner, William M. Hiesey, and
Malcolm A. Nobs

In preceding Year Books we have described the photosynthetic responses of climatic races of *Mimulus cardinalis*. We found that six races, native in six widely differing localities, had different responses of photosynthetic rate to temperature and light intensity, and that under conditions for maximum photosynthesis the rates decreased to different extent with time. Comparable data are needed for climatic races of *M. lewisii* to complete a survey of the *M. cardinalis-lewisii* species-complex. Until recently such data were entirely lacking because of the inability of *M. lewisii* to grow satisfactorily in either the garden or greenhouse at Stanford.

During the past year encouraging progress has been made toward obtaining satisfactory *M. lewisii* plants. Experiments described below with our controlled environment growth cabinets are pointing the way to selection of conditions suitable for the growth of *M. lewisii*. Measurements of photosynthesis have been made on some of the cabinet-grown plants.

The still incomplete data obtained for four clones of the Timberline race of *M. lewisii* indicate that it reaches maximum photosynthesis at a little higher temperature, it requires a higher light intensity to saturate photosynthesis, and its photosynthetic rate declines more during 12 hours than the rates for races of *M. cardinalis*.

The plants used for measurements of photosynthesis were seedlings. Current emphasis is being placed on vegetative propagation of the seedlings as clones in the cabinets. It now appears likely that by means of the cabinets we can establish and maintain clones of a number of climatic races of *M. lewisii* for measurements of their physiological responses.

The growth responses of *Mimulus* in controlled environments emphasize the

high sensitivity of these plants to external variables. Characteristic differences between climatic races of *M. cardinalis* are evident and can now be studied in detail with the present facilities. That similar differences also occur within altitudinal and latitudinal races of *M. lewisii* is becoming apparent from experiments with seedling material. Previously the racial differences within *M. lewisii* were obscured by the inability of any of the races to grow sufficiently well under uncontrolled conditions at Stanford.

Controlled cabinet studies using vegetatively propagated clones of diverse altitudinal races of *M. cardinalis* are being continued along the lines described in *Year Book 61*, pages 317-320. The variables studied include temperature, light intensity, and carbon dioxide concentration. Experiments with clones are now being supplemented with studies on seedling populations of races of *M. cardinalis* and *M. lewisii*.

Two cabinets are being built for operation with natural light in addition to the four cabinets with artificial illumination. The new cabinets will extend the range of combinations possible in experiments in which light intensity and spectral distribution will be important variables.

STUDIES ON TISSUE CULTURES

Frank Nicholson, Kathe Picken, and
William M. Hiesey

The work begun last year on methods of growing tissues of selected clones of *Mimulus* has advanced to the point where comparative growth studies can be started. Beginning in March 1963, Mrs. Picken was able to devote full time to the testing of various modifications of media for growing different kinds of *Mimulus* tissues. Mr. Hart has completed controlled temperature cabinets for growing liquid cultures in roller drums.

Experiments in establishing plant tissues from stem internodes, roots, stem tips, callus tissues, and sterilized seeds have been tried with *M. cardinalis* and to

a lesser extent with *M. lewisii*. In this work the basic medium of Laetsch and Briggs mentioned in *Year Book 61*, pages 323-325, has chiefly been used. More recently another medium described by Murashige and Skoog (*Physiol. Plantarum*, 15, 473-497, 1962), having a considerably higher concentration of inorganic salts and vitamins instead of coconut milk, was tried; it appears to have some special advantage for culturing tissues of *M. lewisii* seedlings.

As was mentioned last year, tissues from a number of races of *M. cardinalis* were established quite readily from peeled stem internodes in the Laetsch and Briggs medium. Subsequent work with various concentrations and combinations of supplements has substantiated these results and has extended our range of experience in handling material of this species. One modification containing 10.0 mg of proteose peptone and 0.5 mg of naphthalene-acetic acid per liter (medium G) produced the greatest abundance of roots; another containing 0.1 mg per liter of indoleacetic acid (medium U) produced steady moderate growth of callus in a high percentage of the cultures; still another modification with 0.6 mg of 2,4-dichlorophenoxyacetic acid per liter (medium T) produced bizarre, rapid growth in a few cultures. Five other combinations of supplements produced less significant results.

In *M. lewisii* the above technique of starting with peeled internodes was much less successful than in *M. cardinalis*. Recent work with seedlings of *M. lewisii* germinated on agar has, however, yielded encouraging results that indicate the feasibility of growing clones of both *M. cardinalis* and *M. lewisii* on a comparative basis.

Seeds of the Timberline *M. lewisii* race (7405) were sterilized in 1 per cent hypochlorite solution, rinsed in sterile distilled water, and germinated on agar medium at room temperature. From these stock cultures either entire seedlings or parts of seedlings were transferred to liquid Laetsch and Briggs medium in roller

drums. The parts transferred included roots, roots and lower portions of the main stem, the entire main stem minus the basal portion, the central portion of the main stem only, and the stem apex with one or two pairs of leaves attached. Both the intact seedlings and the assorted parts with the exception of the roots grew in liquid culture at room temperature in diffuse light. After a month they developed characteristic differences. Seedlings with an intact apex continued to elongate and produced a few side shoots, whereas those with the apex removed developed a great abundance of side shoots so that the cultures became a mass of stems, leaves, and, frequently, adventitious roots. Pieces of such material consisting of a terminal bud and two or three pairs of leaves continued to grow with reasonable vigor when transferred to fresh Laetsch and Briggs medium. Corresponding pieces of the same seedlings grown in the Murashige and Skoog medium produced longer internodes and larger leaves than those grown in Laetsch and Briggs medium.

Seedling cultures of *M. lewisii* in the same medium generally grow faster in liquid than on agar. There are also characteristic differences in color and mode of growth in the two even though the added nutrients are the same. For our purposes, both the solid and the liquid media appear to be useful, the solid for maintaining stock cultures, the liquid for comparative growth studies.

A simple method for rapid feeding of liquid cultures by a Cornwall automatic pipetting syringe was developed. It greatly facilitates maintenance of the relatively large number of cultures needed for comparative growth studies.

We intend to embark on our main program after establishing a stock of healthy, consistent root, callus, and seedling cultures. The objective of the program is to supplement knowledge of growth responses of intact plants that have been grown in controlled growth cabinets. Parts of these same cloned plants will be grown in tissue culture; their responses

will be studied and compared with those of the whole plants. In this way many aspects of the physiological characteristics of the ecologic races can be examined in the light of different sets of relationships. With these findings, and quantitative measurements on photosynthesis, we hopefully anticipate a new comprehension of how and why contrasting ecologic races function as they do in their widely differing natural environments.

In summary, we are well on the way to developing methods and equipment for systematic studies on the comparative growth and development of tissues of the key climatic races of *Mimulus*. We hope to be able to integrate the results with the other three principal approaches of our over-all program as outlined in the introduction of this report.

STUDIES ON THE DISTRIBUTION OF TREE SPECIES

Jens Clausen

During a visit to Brazil in the fall of 1953 (*Year Book 53*, pp. 151, 162-164) the low altitudinal limits of tree growth on the southeast Brazilian mountain massifs were observed. Through the following years this observation led to a search of the botanical literature for information about the location of tree lines in regions around the earth. The search disclosed that the limits of tree growth are determined not only by altitude and latitude and other factors of the environment but to an even greater extent by the nature of the germ plasms of the tree species themselves, which differ greatly in their ranges of tolerance. Each tree species, accordingly, has its own tree line. Furthermore, the general tolerance range is a characteristic not only of the species but also of the genus, family, and taxonomic order.

The most widely distributed tree species belong to species-complexes and genera that circle the earth within characteristic latitudinal limits. Each

species-complex or genus has a common gene pool. The most hardy trees of high latitudes are conifers of the pine family, aspens, willows, birches, alders, and the mountain ashes. They compose a small elite of 12 species-complexes that are limited to the northern hemisphere. Cedars, oaks, chestnuts, beeches, and eucalypts belong to a group of a few thousand species of medium tolerance that compose the forests at medium latitudes of the northern and southern hemispheres.

By far the largest number of tree species on the earth, possibly 50,000 or more, compose the forests within the low latitudes. These species are limited roughly between 25°N and 25°S. They are members of families and orders that are extremely sensitive to frost and through the evolutionary periods have remained within tropical climates.

A fair number of tree genera are intermediate between the three major groups. Also, within each complex of species the genetic variability and recombination enable individual species to adjust to ecologically diverse situations within the latitudinal belt. Most orders and families of trees, however, have not escaped the zones to which their germ plasms generally are adjusted. This observation suggests the existence of evolutionary limitations within many families and orders.

The families and orders are based on morphological criteria. The strong regional limitation of orders and families suggests that deep-seated physiologic-hereditary differences are associated with the morphological ones.

Population studies of trees in the Harvey Monroe Hall Natural Area. During the late summer months of 1960-1962, population studies were conducted on tree species near the tree line in the Slate Creek Valley of the Harvey Monroe Hall Natural Area surrounding the Timberline transplant station. Approximately 150 population samples containing more than 36,000 individual trees were classified as

to species and variation in growth form within species in relation to altitude and slope exposure.

The Harvey Monroe Hall Natural Area is within the Inyo National Forest and adjoins the east side of the Yosemite National Park. It is composed of approximately 7 square miles of rugged terrain at altitudes of 3050 to 3900 meters on the east slopes of White Mountain, Mount Conness, and North Peak (cf. *Year Book* 32, pp. 20–21, 180). Three glaciated valleys run west to east, providing north- and south-facing slopes which have contrasting climates. A varied topography, including rock slopes, talus, screes, alpine pavements, glaciers, cirques, small lakes, streams, waterfalls, bogs, meadows, gravel beds, and a small lava cone, provides a highly diversified array of habitats for plant and animal life. The area has an unusually rich vegetation—about 350 species of flowering plants and ferns—for such a high altitude.

Three conifers, whitebark pine (*Pinus albicaulis* Engelm.), lodgepole pine (*P.*

murrayana Grev. et Balf.), and mountain hemlock (*Tsuga mertensiana* (Bong.) Kerr.), have tree lines within the Hall Area. Each develops large trees up to near the tree line, which are followed by knee-high cushions of elfinwood higher up. In the tree-line zone the growth forms of each of the three species are highly intermixed. The existence of contrasting forms in juxtaposition suggests that the differences are primarily genotypic. The tree line of a species may be defined as the altitude beyond which it no longer exists as a tree. The species may exist at higher elevations in the form of a low cushion, or even as a carpet.

Slate Creek Valley within the Harvey Monroe Hall Natural Area is well adapted for the study of the dynamics of tree lines. As the glaciers of the Pleistocene period retreated toward the cirque in the westernmost part of the valley, they left approximately 11 terminal moraines, which traverse the valley in a south-north direction. The trees follow the moraines across the valley, from the tree line on the north-facing slope to the tree line on

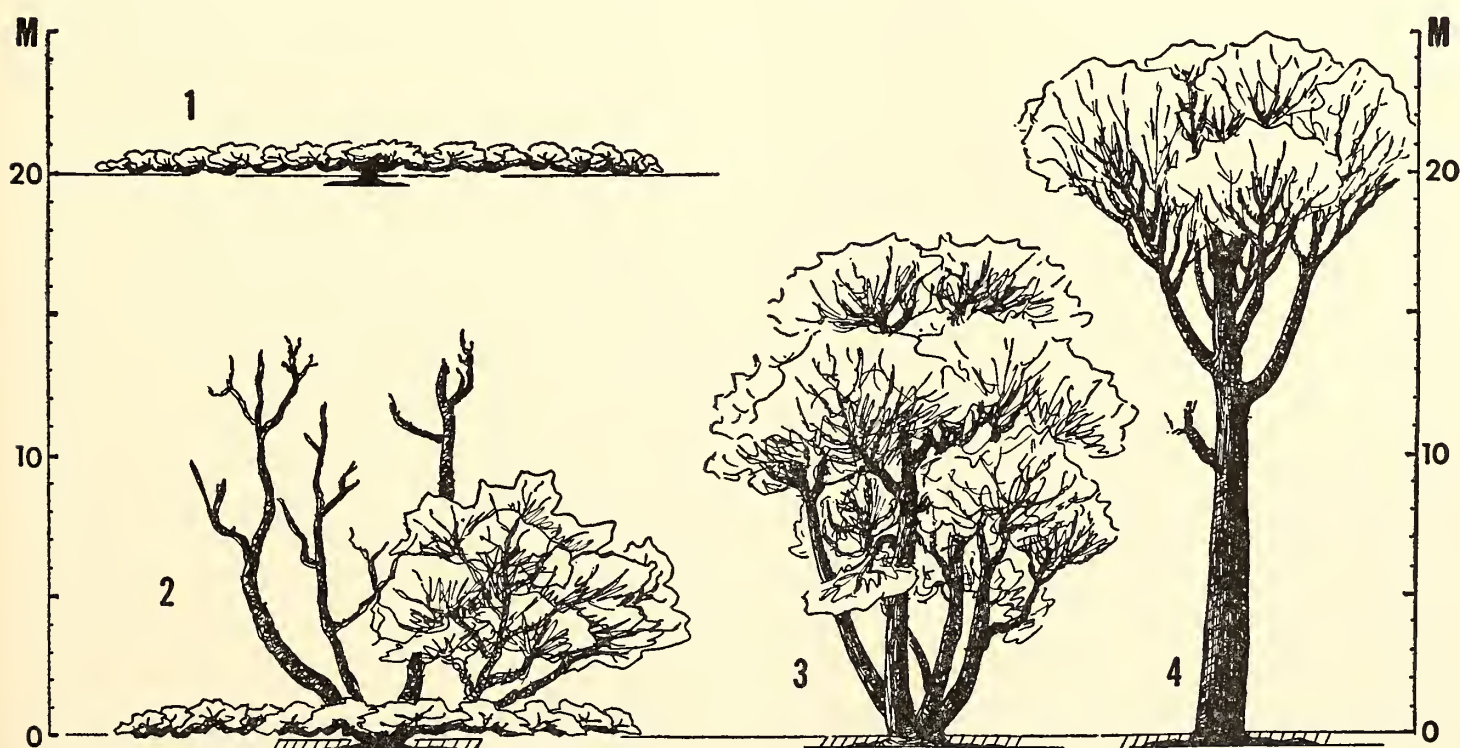


Fig. 30. Examples of growth habits of *Pinus albicaulis* near tree line in the Harvey Monroe Hall Natural Area. 1. Elfinwood. 2. Intermediate form with elfinwood base and dead erect trunks. 3. Erect multitrunk tree (most common form). 4. Single-trunk tree (rare). The scale is in meters. Cf. tables 5 and 6.

the opposite south-facing slope. Abrupt rock escarpments limit individual populations on the moraine.

The 150 population samples taken varied in area between 20,000 and 90,000 square meters, and included from 100 to 1800 trees per sample. In each sampled area all trees, including small seedlings, were counted. Trees having trunks less than 25 cm in diameter seldom have cones and were classed as immature. Among the mature trees a giant class was recognized having trunks more than 75 cm in diameter. All three species have trees up to 150 cm in trunk diameter. The largest tree, a hemlock, had a trunk diameter of 2 meters.

The mature trees were subdivided into groups on the basis of growth form as shown in figure 30. Each species has both single-trunk (fig. 30, 4) and multitrunk

growth forms (fig. 30, 3), differing in frequency among the three species. The occurrence of elfinwood (fig. 30, 1) and of intermediates of many combinations indicates that tree line is approaching. The elfinwoods appear to be genetically distinct forms, although direct experimental evidence for this deduction is lacking. The most interesting intermediates are forms having elfinwood at the base combined with erect trunks (fig. 30, 2). In the vicinity of tree line the erect trunks are often killed, but the elfinwood bases survive and continue to bear cones, evidence of the severe environment for tree growth and also of the survival value of the elfinwood growth form.

Six samples listed in table 5 illustrate the trends found in these population studies, three series from north-facing

Table 5. Composition of Samples of Populations of *Pinus* Species, Slate Creek Valley

A. North-facing slope						
Growth Form*	3065- to 3080-m alt.		3125- to 3140-m alt.		3265-m alt.	
	<i>albicaulis</i> , %	<i>murrayana</i> , %	<i>albicaulis</i> , %	<i>murrayana</i> , %	<i>albicaulis</i> , %	<i>murrayana</i> , %
1. Elfinwood	---	---	44.3	---	73.4	---
2. Intermediate	---	---	25.5	---	12.5	---
3. Multitrunk	28.5	---	16.8	---	---	---
4. Single trunk	4.6	2.8	---	---	---	---
5. Immature	40.5	23.6	10.7	2.7	14.1	---
Total %	73.6	26.4	97.3	2.7	100.0	0
Total trees	209	75	145	4	60	0
B. South-facing slope						
Growth Form*	3065- to 3110-m alt		3140- to 3155-m alt.		3290- 3360-m alt.	
	<i>albicaulis</i> , %	<i>murrayana</i> , %	<i>albicaulis</i> , %	<i>murrayana</i> , %	<i>albicaulis</i> , %	<i>murrayana</i> , %
1. Elfinwood	---	---	---	---	29.2	2.8
2. Intermediate	---	---	---	---	60.1	0.6
3. Multitrunk	2.1	0.9	0.7	0.3	1.1	---
4. Single trunk	---	8.1	0.1	16.3	---	---
5. Immature	6.5	82.4	4.2	78.4	5.6	0.6
Total %	8.6	91.4	5.0	95.0	96.0	4.0
Total trees	83	882	111	2133	171	7

* See figure 30.

Table 6. Composition of Conifer Sample of 3114 Trees from East-Facing Slope at 3080 to 3155 Meters Altitude

Growth Classes	<i>Pinus albicaulis</i> , %	<i>Pinus murrayana</i> , %	<i>Tsuga mertensiana</i> , %
1. Elfinwood	---	---	0.12
2. Intermediate	---	0.4	0.03
3. Multitrunk	4.1	0.3	1.55
4. Single trunk	0.2	9.4	2.50
5. Immature	4.5	75.0	1.90
Total %	8.8	85.1	6.10
Total trees	274	2646	194

slopes and three from south-facing, both series progressing in altitude. The floor of the Slate Creek Valley at 3050 meters is used as a reference point.

Pinus albicaulis dominates on the north-facing slope (table 5), although large trees of *P. murrayana* also occur at altitudes up to 3080 meters. Below this altitude all trees are erect. At the 3125- to 3180-meter altitude only rare immature trees of *P. murrayana* with dead tops remain. Here many elfinwood and intermediate forms of *P. albicaulis* make their appearance in juxtaposition to erect, multitrunk trees 10 meters tall. Extreme elfinwoods are less than a meter high but up to 20 meters wide, as suggested in figure 30, 1. Many forms of vigorous intermediates exist here with or without elfinwood base; some intermediates have as many as 30 slender, erect trunks on a single bush. At 3265 meters altitude on the north-facing slope only elfinwood forms and dwarfish intermediates with elfinwood base are found, and at higher elevations only elfinwoods.

The situation is different on the south-facing slope (table 5, B, 1). In two samples from altitudes at 3065–3110 and 3140–3155 meters only 5 to 8 per cent of the trees are *P. albicaulis*, but here *P. murrayana* is exceedingly vigorous and develops large trees up to the 3200-meter level. At 3290–3360 meters *P. albicaulis* is dominant, consisting predominantly of elfinwood and intermediates having elfinwood bases. *P. murrayana* at this

elevation has also evolved typical elfinwood plants.

The east-facing slopes (table 6) are similar to the south-facing slopes in the ratio of the frequency of *Pinus albicaulis* to *P. murrayana*, but the hemlock, *Tsuga mertensiana*, contributes a moderately conspicuous element. The growth forms of the hemlocks are as varied as those of the whitebark pine, ranging from single- and multitrunk trees through intermediates to low elfinwood types that are draped over the rocks.

A total of 11,626 trees of the *Pinus albicaulis*, 24,201 *P. murrayana*, and 644 *Tsuga mertensiana* were found among 150 population samples enumerated. In addition, *P. jeffreyi* Grev. et Balf. was represented by 5 small and immature although probably very old individuals, *Juniperus communis* L. by numerous specimens all of which were elfinwood, and the chinquapin, *Castanopsis sempervirens* (Kell.) Dudl., by a single elfinwood plant.

Each of the three most frequent species of conifers in the Harvey Monroe Hall Natural Area has its specific tree line, and each differs also in its slope preference. The hemlock, *Tsuga*, is limited primarily to steep, east-facing slopes between 3000 and 3125 meters in altitude, but single individuals were found in most of the samples, and cone-bearing elfinwood specimens occur up to 3375 meters. The lodgepole pine, *Pinus murrayana*, predominates on warm east- and south-facing

slopes, where its tree forms extend to 3200 meters. Its elfinwood form is rare and limited to certain pockets. The white-bark pine, *P. albicaulis*, has its tree limit at 3200 meters on north-facing slopes and 3300 meters on south-facing slopes, but the elfinwood forms ascend to the 3600- to 3700-meter levels.

All three species have an altitudinal transitional zone of approximately 60 meters within which multitudes of recombination types between the erect and elfinwood races intermingle. The situation appears to be a highly dynamic one, in which the lower- and higher-altitude races appear to interbreed and segregate, a tension zone where severe natural selection operates. The existence of intermediate steps between the extremes suggests an expression of the interaction between many genes and environmental modification in the intermediates.

The willows, members of the genus *Salix*, have counterparts of the variants observed among the conifers. *Salix eastwoodiae* Ckll. exists only as a tall bush up to approximately 3400 meters altitude. In contrast, *S. petrophila* Rydb. and *S. nivalis* Hook. are "lawn" types that creep among the grasses and drape themselves over rocks up to high altitudes. Two species, *S. monica* Bebb. and *S. orestera* C. K. Schneid., behave like the conifers. At 3050 meters these species are erect bush types 1 meter tall, but at 3080 meters populations of these species are composed of aggregates of matted lawn types interspersed by erect to divaricate bush types. Classification of a sample of 157 mature plants within an area 300 meters long beside Slate Creek indicated 77 plants of the horizontal lawn type as compared with 80 erect to intermediate plants. Some of the erects were found growing in the middle of lawn-type plants, suggesting genetic distinctness.

Within the Harvey Monroe Hall Natural Area, accordingly, five species have evolved parallel, highly variable populations near the limits for their erect tree and bush forms. Such transitional

forms precede the actual tree line, which is at a slightly higher altitude. The variability in the intermediate populations is high.

CYTOTAXONOMY AND DISTRIBUTIONAL ECOLOGY OF WESTERN NORTH AMERICAN VIOLETS

Jens Clausen

During the years from 1932 to 1943 (*Year Book 36*, pp. 213-214) the chromosome numbers of most of the western North American violets were determined. This investigation was conducted in cooperation with the late Professor Milo S. Baker. Since the results had not previously been organized and published, the task was undertaken this year.

Of the 14 taxonomic sections in the genus *Viola*, 4 occur in western North America. The section *Chamaemelum* has its center of variation in this area. It is a relatively primitive yellow-flowered group having a basic chromosome number of 6. All levels of polyploidy are represented, from the diploid $n = 6$ to the duodecaploid $n = 36$, and at least 7 evolutionally distinct polyploid lines have been established within the section.

Another section is *Plagiostigma*, a group of meadow violets having the chromosome numbers $n = 12, 24$, and 48 in multiples of 12. The eastern stemless blue violets constitute a separate group within the section. They uniformly have $n = 27$ pairs of chromosomes. The stemmed blue violets of the *Rosatellata* section follow a 10 series, having $n = 10, 20$, and 40 chromosomes. The only North American member of the *Melanium* section, the pansies, has $n = 17$ pairs of chromosomes.

The existence of ecologically distinct subspecies that are adapted to different habitats across the west has enabled the violets to occupy nearly a full range of environments within western North America without change in chromosome number. Superimposed on this pattern of diploid distribution are series of polyploid

species and likewise series of sections having different basic numbers. All these species are able to coexist without interbreeding. Distinct sections, accordingly,

have been able to superimpose their polyploids on the diploids of simpler differentiation. The *Viola* genus is one of the most versatile groups of higher plants.

SPEECHES

Brown, J. S., Forms of chlorophyll *a* and photosynthesis, Photosynthesis Colloquium, Centre National de la Recherche Scientifique, Gif-sur-Yvette, France, July 1962.

Brown, J. S., Forms of chlorophyll *a*, Centre de Recherches de Gorse, St. Trond, Belgium, August 1962.

Clausen, Jens, Populations: (1) Geographically separated populations from a single climatic zone; (2) Populations from distinct climates in a uniform garden; (3) Adjustment of populations to contrasting climates; (4) Hereditary control of adjustment to climate; (5) The evolutionary function of climatic races and populations; National Science Foundation Summer Institute for College Teachers in Botany, Vanderbilt University, Nashville, Tennessee, July 1962.

Clausen, Jens, Population studies among trees around tree line in the Harvey Monroe Hall Natural Area, Western Society of Naturalists, San Jose State College, San Jose, California, December 1962.

Clausen, Jens, Tree lines and germ plasms—a study in evolutionary limitations, National Academy of Sciences, Washington, D. C., April 1963.

Clausen, Jens, Significance of the germ plasm in the limitation of tree growth, University of Tennessee, Knoxville, Tennessee, April 1963.

Clausen, Jens, Evolutionary limitations for tree growth, Vanderbilt University, Nashville, Tennessee, April 1963.

Fork, D. C., The influence of a Hill-oxidant on the action spectrum for oxygen production in Swiss chard chloroplasts, Photosynthesis Colloquium, Le Centre National de la Recherche Scientifique, Gif-sur-Yvette, France, July 1962.

Fork, D. C., Studies on endogenous oxygen evolution in Swiss chard chloroplasts, Nederlandse Photosynthese Groepen, N. V. Philips' Gloeilampenfabrieken, Eindhoven, the Netherlands, October 1962.

French, C. S., Comparative studies of kinetic schemes for photosynthesis, American Society of Plant Physiologists, Oregon State University, Corvallis, Oregon, September 1962.

French, C. S., and W. M. Hiesey, Plant growth in atmospheres of controlled CO₂ concentration, Society of General Physiologists, Oregon State University, Corvallis, Oregon, September 1962.

French, C. S., The major and accessory pigments in photosynthesis, Chemistry Department Seminar, California Institute of Technology, Pasadena, California, March 1963.

French, C. S., Light, pigments, and photosynthesis, Graduate Students Plant Physiology Society, University of California, Davis, California, May 1963.

French, C. S., O₂ evolution from algae given double light flashes of two colors, American Society of Plant Physiologists, Western Section, Stanford University, California, June 1963.

Hiesey, W. M., Studies on the genetics and transplant responses of climatic races of the *Mimulus cardinalis-lewisii* complex, Genetics Section of the Division of Plant Industry, CSIRO, Canberra, Australia, September 1962.

Hiesey, W. M., Environmental responses of climatic races of *Mimulus*, Biosystematists, Stanford, California, November 1962.

Hiesey, W. M., Discussion leader at symposium on environmental control of plant growth, Canberra, Australia, August 1962.

Hiesey, W. M., Genetic-physiologic studies on mechanisms underlying natural selection of climatic races (ecology), American Society of Plant Physiologists, Western Section, Stanford University, California, June 1963.

Hiesey, W. M., *see also* French, C. S.

Milner, Harold W., Genetic-physiologic studies on mechanisms underlying natural selection of climatic races (physiology), American Society of Plant Physiologists, Western Section, Stanford University, California, June 1963.

Milner, Harold W., Photosynthesis in climatic races of *Mimulus*, Biosystematists, Stanford, California, November 1962.

Nobs, Malcolm A., Experimental studies on biosystematic relationships in *Ceanothus*, Czechoslovak Botanical Society, 50th year Jubilee, Prague, Czechoslovakia, July 1962.

- Nobs, Malcolm A., Genetics of climatic races of *Mimulus*, Biosystematists, Stanford, California, November 1962.
- Nobs, Malcolm A., Genetic-physiologic studies on mechanisms underlying natural selection of climatic races (genetics), American Society of Plant Physiologists, Western Section, Stanford University, California, June 1963.
- Smith, James H. C., The "Star - Spangled Scotchman," Andrew Carnegie, Fellowship Forum, Palo Alto, California, December 1962.
- Smith, James H. C., The "Star - Spangled Scotchman," Andrew Carnegie, the Sequoias Retirement Home, Portola Valley, California, January 1963.
- Smith, James H. C., Reversible phosphate electrode and its possible application to physiological processes, American Society of Plant Physiologists, Western Section, Stanford University, California, June 1963.

BIBLIOGRAPHY

- Fork, D. C., Action spectra for O₂ evolution by chloroplasts with and without added substrate, for regeneration of O₂ evolving ability by far-red, and for O₂ uptake, *Plant Physiol.*, **38**, 323-332, 1963.
- Fork, D. C., *see also* Gingras, G.; Müller, A.
- French, C. S., Photosynthesis, in *This is Life*, edited by Willis H. Johnson and William C. Steere, Holt, Rinehart and Winston, New York, pp. 3-38, 1962.
- French, C. S., The post-illumination survival of photosynthetic O₂ evolution, in *Studies on Microalgae and Photosynthetic Bacteria*, edited by Japanese Society of Plant Physiologists, University of Tokyo Press, pp. 271-279, 1963.
- French, C. S., and W. M. Hiesey, Plant growth in atmospheres of controlled CO₂ concentration (abstract), *J. Gen. Physiol.*, **46**, 357A-367A, 1962.
- French, C. S., *see also* Smith, James H. C.
- Gingras, G., C. Lemasson, and D. C. Fork, A study of the mode of action of 3-(4-chlorophenyl)-1,1-dimethylurea on photosynthesis, *Biochim. Biophys. Acta*, **69**, 438-440, 1963.
- Hart, Richard W., Electrically isolated transparent liquid pump, *Rev. Sci. Instr.*, **33**, 781-782, 1962.
- Hiesey, W. M., and H. W. Milner, Small cabinets for controlled environments, *Botan. Gaz.*, **124**, 103-118, 1962.
- Hiesey, W. M., *see also* French, C. S.
- Jorgensen, Erik G., Antibiotic substances from cells and culture solutions of unicellular algae with special reference to some chlorophyll derivatives, *Physiol. Plantarum*, **15**, 530-545, 1962.
- Latimer, Paul, Is selective scattering a universal phenomenon? in *Studies on Microalgae and Photosynthetic Bacteria*, edited by Japanese Society of Plant Physiologists, University of Tokyo Press, pp. 213-225, 1963.
- Lemasson, C., *see* Gingras, G.
- List of Publications, *Experimental Taxonomy*, Carnegie Institution of Washington, Department of Plant Biology, 1928-1962, 1963.
- List of Publications, *Biochemical Investigations*, Carnegie Institution of Washington, Department of Plant Biology, 1928-1962, 1963.
- Macdowall, Fergus D. H., Potentiometrically measured reduction of low concentrations of dye by illuminated chloroplasts, *Plant Physiol.*, **37**, 505-508, 1962.
- Madsen, Axel, The time course for the photo-conversion of protochlorophyll by flash illuminations, *Physiol. Plantarum*, **16**, 470-473, 1963.
- Milner, H. W., *see* Hiesey, W. M.
- Müller, A., D. C. Fork, and H. T. Witt, The function of different chlorophylls in photosynthesis and the action spectra of separated light reactions, *Z. Naturforsch.*, **18b**, 142-145, 1963.
- Nobs, Malcolm A., *Experimental Studies on Species Relationships in Ceanothus*, Carnegie Inst. Wash. Publ. 623, v + 94 pages, 119 figures, 1963.
- Smith, James H. C., and C. S. French, The major and accessory pigments in photosynthesis, in *Ann. Rev. Plant Physiol.*, **14**, edited by Leonard Machlis, Annual Reviews, Palo Alto, Calif., pp. 181-224, 1963.
- Weaver, Ellen C., Possible interpretation of the slow-decaying EPR signal in algal suspensions, *Arch. Biochem. Biophys.*, **99**, 193-196, 1962.
- Weaver, Ellen C., and Harry E. Weaver, Electron resonance studies in *Chlamydomonas reinhardi* (abstract), *Plant Physiol.*, **37**, Suppl., iii, 1962.
- Weaver, Harry E., *see* Weaver, Ellen C.
- Witt, H. T., *see* Müller, A.
- Wolf, Frederick T., Growth inhibition of *Chlorella* induced by 3-amino-1,2,4-triazole, and its reversal by purines, *Nature*, **193**, 901-902, 1962.

Department of Embryology

James D. Ebert
Director

Baltimore, Maryland

Carnegie Institution of Washington Year Book 62, 1962-1963

Contents

Introduction 405

Cellular Regulatory Mechanisms. 408

 Development of machinery for protein synthesis 408

 Synthesis of high-molecular-weight RNA 409

 Variables concerned with isolation of undenatured RNA 409

 Synthesis of high-molecular-weight RNA during oogenesis 414

 Regional synthesis of ribosomes in *Rana pipiens* 414

 Isolation and partial characterization of aminoacyl-sRNA synthetases from *Rana pipiens* embryos 415

 Deoxyribonucleic acid in eggs and early embryos of *Rana pipiens* and *Xenopus laevis* 418

 “Cytoplasmic DNA” 419

 A protein fraction from *Rana pipiens* eggs 420

Chemistry and Physiology of the Developing Heart 421

 The inhibitory action of antimycin A in the early chick embryo 421

 The action of antimycin A in an oxygenated environment 422

 Reversal of effects of antimycin A 423

 Methods for obtaining aqueous extracts of mitochondria (AAAF) 424

 Preventive action of AAAF 424

 Effects of antimycin A on enzyme activity in the early embryo 425

 Effects of other inhibitors 426

 Projection 427

Developmental, Kinetic, and Immunological Studies of Enzymes 428

 Hypoxanthine dehydrogenase in the chick 428

 HXDH activity in adult and embryonic liver and kidney 429

 Characterization of HXDH from liver, metanephros, and mesonephros 430

 Kinetic properties. 430

 Heat stability 432

 Electrophoretic properties 432

 Immunochemical properties 432

 Purification 433

 Conclusions 434

 Lactic dehydrogenase in the adult and embryonic chick 434

 Starch gel electrophoresis 435

 LDH in adult chicken tissues 435

 LDH during embryonic development of liver and kidney 437

 Conclusions 437

Clonal Analysis of Myogenesis 437

Inductive Tissue Interactions 443

 Epidermal-dermal interactions in the formation of feathers, scales, spurs, and beak 443

Spatial Organization in Embryogenesis 444

 Media for disaggregating and cultivating *Drosophila* imaginal discs 445

 Preliminary observations on cultured imaginal discs 446

Organ Culture of Embryonic Chick Thyroid 447

 Effects of thyrotropin, thiourea, L-goitrin, and iodide on histogenesis and iodine incorporation 447

The Labile Chorioallantoic Membrane	447
Changes effected by Rous sarcoma virus	447
The infection of the chorioallantoic membrane in vitro with the Rous sarcoma virus	447
Inhibitory effect of media conditioned by growth of membranes previously exposed to virus	448
Changes effected by antigenic stimuli and immunologically competent cells	451
Immunologically Induced Aspermatogenesis	452
Mechanisms of aspermatogenesis	452
The antigenic factor	455
The humoral antibody	458
Antibodies against Sperm	460
Subcutaneous Implants of Homologous Ventral Prostate	460
The Embryo in Relation to Its Environment	461
Mechanisms of implantation of the ovum	461
Anatomy and physiology of the placenta	462
Study of human placental vasculature	465
Differentiation and Morphogenesis in the Human Embryo	465
The collection of human embryos	465
Establishment of the cardiac primordium in human embryos at presomite stages	465
An abnormal heart in a 6.6-mm human embryo	466
Relation to corrected transposition of the great vessels	466
Observations on the "organizer" area of the human embryo at presomite stages	467
Prenatal development of the joints of the clavicle	467
The human fetal thyroid: Its weight in relation to body weight, crown-rump length, foot length, and estimated gestation age	468
Teratogenesis	468
Preliminary studies in the production of malformations with thalidomide	468
Experimental production of cloacal exstrophy	469
Apparatus and Techniques	471
A method for the rapid separation of ribonucleotides	471
Staff Activities	472
Bibliography	474
Personnel	477

INTRODUCTION

How does a field of inquiry develop? What forces shape its dimensions? Specifically, what forces are now operating in molding the field of embryology? The principal theme, coursing through and underlying research in embryology today, is the impact of genetics on development. More than at any time in the past half-century, molecular embryology is clearly the logical extension of molecular genetics. There are occasional rumblings—warnings—of the vast, uncharted areas in the murky realm of morphogenesis that are being neglected in the tidal wave of interest in nucleic acids and cell regulatory mechanisms; but it is that very wave that is sweeping inventive minds and skillful hands into the study of the problems of development. The solutions (or partial solutions) they are already obtaining, coupled with the enormous breadth of developmental biology, the opportunity to explore developmental mechanisms in a wide variety of forms, are fostering, in fact are in large part responsible for, the emergence of developmental biology as one of the focal fields of research of the coming decade. We may confidently expect the problems of embryology to occupy the center of the stage just as those of genetics (and the application of biochemistry to genetics) have dominated the past several decades. But note that I have said that the problems of embryology—not embryologists—will occupy the center of the stage. To be sure, students of embryology will play leading roles, but they will find themselves costarring with chemists and geneticists, immunologists, microbiologists, and neurobiologists. For the key problems in all these fields today are problems of differentiation, growth, and morphogenesis.

We may pause to consider also how much of our crude, general understanding of development springs from studies using

the light microscope. We have scarcely begun to explore the fine structure of cells and cell associations during differentiation and morphogenesis. When we reflect on how much has been learned of, say, the structure of spermatozoa, by successive advances in microscopic technique—light, phase contrast, and electron microscopy—we may glimpse the array of intriguing observations that lie ahead.

Finally, and more important than we sometimes believe, is the impact, on the field, of clinical and practical research. Although we are often told that such forces operate only in the opposite direction, advances in, and pressures from, practical aspects of science have helped to shape the course of basic research. As an example, consider that much of what we know (and a clear idea of what we need to know) about the metabolism of sperm is derived from programs designed to develop techniques for handling and preserving sperm for artificial insemination, in animal husbandry and medical practice.

Two major practical forces are impinging on the field of embryology today. *First*, many problems in obstetrics and pediatrics, e.g., in infection and nutrition, are being resolved, enabling investigators in those fields to concentrate their attention on congenital defects, the errors of development that are among the more important unmet medical problems of childhood. Large funds, both private and public, are now being directed toward their solution. To be sure, embryologists and geneticists have their contribution to make to the study of these problems, but they have much to learn also, and it cannot be denied that the student of normal development will gain immeasurably from such programs. *Second*, and of even greater moment, is the awakening interest in population control, which must inevitably inspire widespread investiga-

tions of reproductive physiology, adding to our understanding of development.

What should be the role of the Department of Embryology in the face of the pressures, both financial and political, that will be brought to bear on these areas of research? The basic problems are not new to the Department; in fact, to a large extent both areas have themselves been influenced profoundly by members of the staff, led by Mall, Corner, and Hartman, up to the present day. The Department can contribute most effectively by holding fast to its policy of taking basic approaches to specific problems in these areas at the discretion of its individual staff members. Beyond this, it can serve as a center of advice and technical competence, providing guidance and leadership, helping to ensure that the large resources that will be available are used productively; individual staff members can, at appropriate intervals, effect syntheses of the basic and applied findings, stressing the intercommunity of the approaches.

It is realized, too, that, as investigators trained in other fields are attracted to the problems of development and reproduction, increasing numbers of them will seek opportunities for specialized training in embryology. This problem must be faced squarely in a number of laboratories. It is already upon us. Of thirty-one applicants for ten places open for visiting investigators in the year under review, and forty-two applicants for twelve places in 1963-1964, seventeen and twenty-four, respectively, had little or no earlier training in embryology. The two "outside" disciplines most frequently represented in these two groups are biochemistry and pediatrics.

Of only two current Fellows, in fact, J. Douglas Caston and Yvon Croisille, could it be said that, by virtue of both training and interest, they would fall readily into the "niche" embryologist. Caston, a Fellow of Carnegie Institution of Washington, continued his studies of protein-synthesizing mechanisms in *Rana*

pipiens embryos, isolating and partially characterizing aminoacyl-sRNA synthetases. On July 1, 1963, he took up a new appointment in the Department of Anatomy at Western Reserve University. Croisille, who is associated with Professor Étienne Wolfe in the Laboratory of Experimental Embryology in Paris, arrived in September 1962 to spend a year as a Fellow of Carnegie Institution of Washington. Already skilled in immunochemical and electrophoretic techniques, he has made important progress in developmental, kinetic, and immunological studies of the enzymes hypoxanthine dehydrogenase and lactic dehydrogenase.

The three biochemically trained visiting investigators in residence during the year had a common origin, all of them having received either predoctoral or postdoctoral training at Massachusetts Institute of Technology. Gerald L. Carlson, Given Foundation-National Research Council Fellow in Academic Medicine, continued his collaborative study with D. W. Bishop of the nature of the testicular antigen in induced aspermatogenesis. In January 1963 he joined the Department of Biochemistry at the University of Alabama School of Medicine. Igor B. Dawid took up a two-year appointment as a Fellow of Carnegie Institution of Washington during November 1962, centering his attention on the cytoplasmic deoxyribonucleic acid of the frog's egg. Minocher Reporter was named an assistant investigator in September 1962 to work in cooperation with James D. Ebert on the chemistry of the developing heart in the early chick embryo.

Thomas H. Shepard of the Department of Pediatrics, University of Washington, spent five months in the Department during 1962, supported by a grant from the United States Public Health Service. During this period he studied the effects of thyrotropin, thiourea, L-goitrin, and iodide on histogenesis and iodine incorporation in the embryonic chick thyroid, using organ culture techniques. Also, he began a descriptive study, continued with

H. J. and H. Andersen at the University of Copenhagen, on the growth of the human fetal thyroid.

Edward C. Muecke, a surgeon and a student of pediatric urology, Dunnington Foundation Fellow and Research Fellow in Surgery, the New York Hospital-Cornell University Medical Center, spent a year in the Department, with the aim of gaining a better understanding of embryogenesis, especially of the genitourinary system. In the course of the program he succeeded in producing exstrophy of the cloaca in the embryonic chick experimentally.

Charles R. Green, senior lecturer in the department of pathology, University of Melbourne, Victoria, Australia, worked in the Department for nine months. His earlier interest in teratogenesis raised questions about mechanisms of maldevelopment and led to his visit to gain experience with experimental techniques.

Ali Mehrizi, instructor in pediatrics at Johns Hopkins University School of Medicine, and Arentje Dekker, of Leiden, Holland, Fellow of the United States Public Health Service, divided their time between the Department and Harriet Lane Home, Cardiac Clinic, Johns Hopkins Hospital, where they worked under the guidance of Helen Taussig. A major goal of this cooperative undertaking was to provide the necessary background on the experimental production of limb defects in rabbits with thalidomide for a comprehensive biochemical analysis to be initiated during the coming year.

Dekker also completed a substantial part of a comprehensive descriptive study of the normal and abnormal development of the human heart in relation to corrected transposition of the great vessels.

Other frequent visitors to the Department whose continuing investigations are reported in these pages included Frank D. Allan, G. W. Corner, Jr., Martin W. Donner, W. Richard Ferguson, and Benjamin C. Moffett, Jr.

But not all visitors were "inbound." One member of the research staff, Robert

L. DeHaan, spent the major part of the year (October 1, 1962, to June 30, 1963) in the Institute of Zoology, University of Zurich, enjoying the hospitality of Professor Ernst Hadorn and his colleagues.

It is singularly appropriate in the year in which the Department celebrated its own fiftieth anniversary, as well as the one hundredth anniversary of the birth of its founder, Franklin P. Mall, that the Collection of Human Embryos was used effectively, and that, from the efforts of a number of competent visiting scientists, several significant contributions to our knowledge of human embryology should emerge. It is right, too, that some emphasis has been placed on problems of teratogenesis, a field in which Mall was a leader. And what could be more fitting than to have the year marked by a major advance in an area in which the Department has pioneered since the days of the Lewises? I refer to Irwin R. Konigsberg's clonal analysis of myogenesis, announced in the pages of *Science* in June 1963. A résumé of the major published evidence plus a preliminary statement of newer findings will be found in the pages to follow.

There were other highlights in a year in which advances were made in most of the Department's continuing programs.

In *Year Book 61*, pages 373-384, the initial stages in an intensive study of ribosomal development were presented. Now, Donald D. Brown has described the general pattern of events in the synthesis of ribosomal ribonucleic acid in the eggs of *Xenopus laevis*. Brown became a member of the scientific staff of the Department on July 1, 1962, having previously been a Fellow, first of the United States Public Health Service and then of Carnegie Institution of Washington.

Reporter, working with Ebert and Green, made substantial progress in a large-scale investigation of the metabolism of the early chick embryo. Of the several approaches being taken, two in which the preliminary findings are un-

commonly promising may be emphasized. Evidence is advanced that when the embryo is cultivated, in vitro, in a highly oxygenated environment, the metabolic pathways are adapted so that the whole embryo becomes sensitive to low concentrations of the antibiotic antimycin A. It will be recalled that ordinarily at critical concentrations only the prospective heart cells of the embryo are sensitive to the inhibitor. In further studies a fraction has been extracted from mitochondria that is capable of preventing the action of antimycin A; efforts to isolate and characterize this factor are continuing, to gain a better understanding of the mechanisms and site of action of the inhibitor.

Croisille's analysis of the development of the enzyme hypoxanthine dehydrogenase is particularly striking. Here is an enzyme, the activity of which appears at three different sites at three very different

periods during development in the chick. It can be detected in the mesonephros as early as the fifth day of incubation, reaching a maximum at 15 days; as the enzyme declines in that organ, it begins to increase rapidly in the metanephros, until hatching. Then, as Morgan and Kato (*Year Book* 60, pp. 397-399) observed earlier, it rises dramatically in the liver.

Croisille has shown the enzymes in these three sites to be very closely related, if not identical.

I spoke earlier of the enormous breadth of developmental biology; in the pages to follow are recorded observations on *Drosophila*; on embryos of the chicken and frog, monkey and man; on tumor viruses and interferon; and on rabbits and thalidomide—using techniques of enzymology, immunology, and X-ray cinematography—all focused on mechanisms of development.

CELLULAR REGULATORY MECHANISMS

DEVELOPMENT OF MACHINERY FOR PROTEIN SYNTHESIS

It was reported in *Year Book* 61 (pp. 372-384) that new cytoplasmic ribosomes do not appear until the tail-bud stage in *Rana pipiens* embryos. Preliminary experiments by D. D. Brown and J. D. Caston suggested that there were few cytoplasmic ribosomes in earlier stages of development; nevertheless, an appreciable amount of protein synthesis could be demonstrated. Is the small number of ribosomes present in early embryos sufficient for protein synthesis? Is the protein formed synthesized by another mechanism during early development? Both possibilities must be considered, but the preponderance of evidence favoring ribosomes as the site of protein synthesis necessarily forces attention first to the ribonucleoprotein particles found in young embryos.

During the year, these investigators have continued their studies along two separate, but interconnected, lines. Brown has extended the study of RNA synthesis to earlier stages of development, his interest in this aspect of the problem having been heightened by the recent discoveries of others that ribosomes of unfertilized sea urchin eggs are inactive in synthesizing protein in vitro. Active ribosomes can be detected very shortly after fertilization, even before the first cleavage. Emphasis has been placed on the chemical and physical characteristics of RNA and ribosomes before the tail-bud stage as a prelude to a detailed study of their biological activity, to be conducted in collaboration with Caston, who initiated a program designed to obtain a defined cell-free protein-synthesizing system from amphibian embryos, to be used ultimately in an assay for ribosomal function.

Synthesis of High-Molecular-Weight RNA

Many of the experiments to be described have been performed on eggs and embryos of *Xenopus laevis*, the South African "clawed toad." The reasons for using this animal are manifold. First, homogenates of *Rana pipiens* eggs and embryos bind ribosomes, RNA, and DNA (see *Year Book 61* for detailed description, as well as page 420 in this report). Brown has not succeeded in reversing this binding. Because of it, only small quantities of ribosomes can be prepared from free-swimming stages of *Rana pipiens*. The eggs of *Rana pipiens* also appear to contain ribonucleases, since high-molecular-weight RNA was frequently found to be degraded after careful isolation. Eggs and embryos of *Xenopus laevis* do not have these disadvantages. There are other, special advantages to using *Xenopus*. Unlike *Rana pipiens*, this amphibian can be reared and fed conveniently in the laboratory. Furthermore, ovulation and mating can be induced artificially at any season by injecting both male and female with commercial pituitary hormones. The same female can be induced to ovulate repeatedly, thus making studies of oogenesis possible.

Initial studies conducted with *Rana pipiens* utilized methylated serum albumin columns for isolation of ribosomal RNA. Developing embryos that had been made radioactive by injection of $P^{32}O_4$ into the gravid female before ovulation were found to synthesize labeled 28S and 18S RNA first at the neurula stage, about 1 to 2 days before radioactivity appeared in the cytoplasmic ribosomes. This finding prompted a study of RNA synthesis before the neurula stage, with emphasis on the rapidly labeled RNA fraction. The methylated serum albumin column has been found by other workers to yield unsatisfactory results in fractionating this RNA. Furthermore, under the conditions of the earlier studies by Brown and Caston, the two pieces of RNA having

characteristic sedimentation constants of ribosomal RNA (28S and 18S) were eluted together from the column. For these reasons, most of the studies reported here have utilized the density gradient zonal centrifugation technique.

Variables Concerned with Isolation of Undenatured RNA

Finding conditions for reproducible extraction and separation of the RNA formed in the early embryo has been a major concern. It became apparent to Brown soon after he began these studies that extreme care had to be taken to avoid bacterial contamination. Eggs were often contaminated with feces, and bacteria from P^{32} -labeled females are highly radioactive; therefore, mating and early development to hatching were carried out in the presence of penicillin and streptomycin. Furthermore, each embryo, before hatching, was dejellied manually. These two precautions have completely eliminated problems of bacterial contamination.

The pH of extraction is also important. In figure 1, results from two batches of neurulae extracted at pH 5.1 and pH 7.3 are compared. The radioactivity sedimenting at an intermediate rate between the two RNA peaks is DNA. The amount of radioactive DNA greatly exceeds radioactive RNA until after hatching. Since some DNA is extracted into the aqueous phase even at pH 5.0, incubation with crystalline DNase has been an important step. This digestion at pH 5.0, although not extensive enough to render the DNA acid-soluble, nevertheless reduces its sedimentation constant sufficiently so that it does not obscure the much smaller quantity of radioactive RNA. However, the need to use DNase introduced another problem: since commercial preparations of DNase are usually contaminated with RNase, it is necessary to add an RNase inhibitor. Extraction and purification have been carried out in the constant presence of polyvinyl sulfate, an

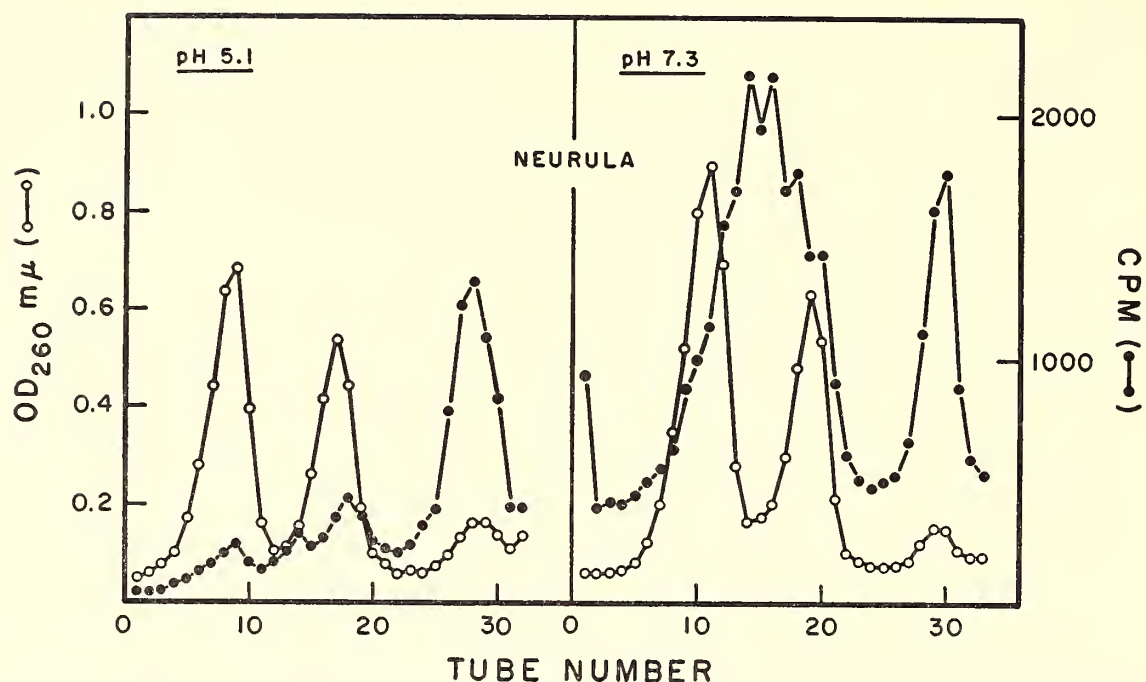


Fig. 1. Comparison of sucrose density gradient patterns of purified nucleic acids isolated from neurulae by extraction at pH 5.1 and 7.3.

inhibitor of basic RNase first described by Fellig and Wiley. This inhibitor is so effective that purified RNA incubated at 37°C, pH 5.0, with 10 μ g/ml pancreatic RNase and 1 μ g/ml polyvinyl sulfate has the same sedimentation pattern as the control. All RNase digestions have been carried out at pH 7.0, where the inhibitor is much less effective (figs. 2, 3, 4).

Brown has also compared the hot and cold phenol extraction methods. Hot

phenol extraction has been used by many investigators for the purification of rapidly labeled and viral RNA. Brown has analyzed all stages of development in *Xenopus* between cleavage and neurula, comparing hot and cold phenol extraction. A sample of the differences revealed by these methods is shown in figure 2. Invariably, hot phenol extraction causes a reversal in the relative amounts of 28S and 18S RNA with more optical density

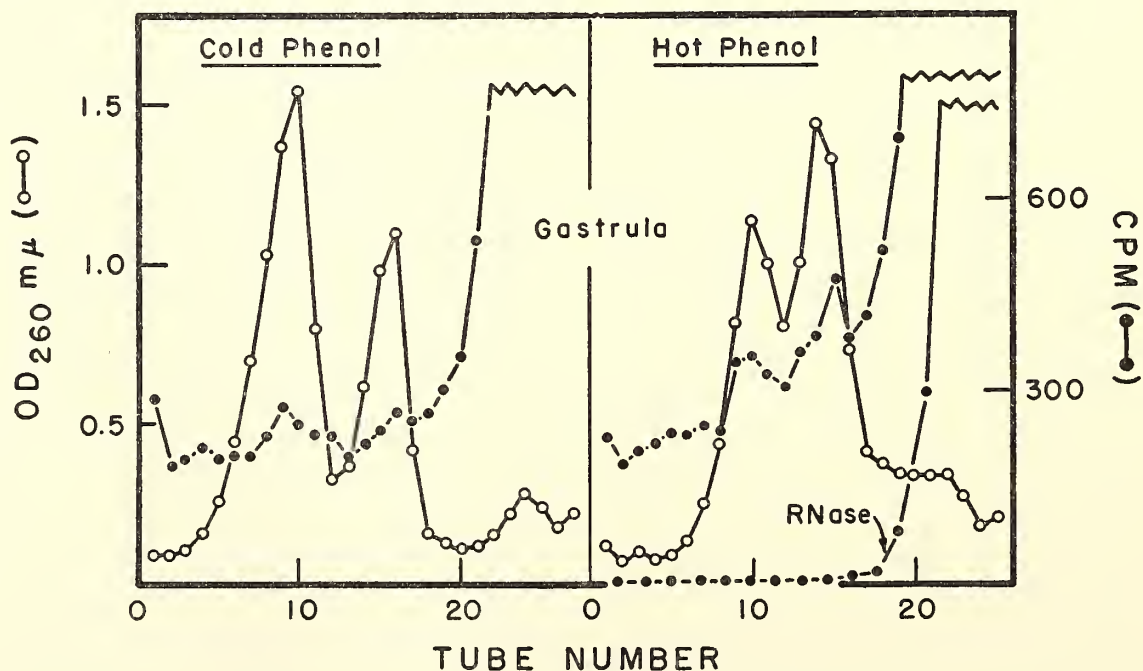


Fig. 2. Sedimentation patterns of gastrula RNA purified by the hot phenol and cold phenol techniques.

in the lower sedimenting region (4S–8S). On the other hand, there is no qualitative difference in the radioactive pattern obtained, implying that extraction with cold phenol does not partition any particular class of RNA into the phenol phase. Extensive degradation of *R. pipiens* RNA occurs when hot phenol extraction is used. This breakdown is not inhibited by polyvinyl sulfate. Another advantage of the cold phenol method is its inability to extract bacterial RNA. Because of this advantage, coupled with the apparent partial degradation caused by hot phenol extraction, the initial homogenization and phenol denaturation steps have been performed at 0°C.

A final important variable is the composition of the sucrose gradient. A quantity of literature is accumulating which implies that different classes of RNA aggregate to a greater or lesser degree according to the ionic strength and divalent cation content of the medium. In Brown's experience, incorporation of sodium chloride and magnesium in the gradient solutions causes RNA to sediment much more diffusely. Addition of

versene to dilute sodium acetate buffer at pH 5.0 gives reproducible centrifugation patterns and sharp banding of RNA.

The final procedure in its entirety is as follows. Mature toads (*Xenopus laevis*) are mated at 18°C in a modified dilute Holtfreter's solution containing magnesium chloride (see *Year Book 61*) and 0.02 mg/ml penicillin and streptomycin. After fertilization, as much debris as possible is removed and the eggs are allowed to develop at 18°C in the same medium, now containing 0.1 mg/ml penicillin and streptomycin. At the appropriate stage, 300 embryos are dejellied manually, rinsed once with cold 0.1 M sodium acetate at pH 5.0 containing 4 µg/ml polyvinyl sulfate, and then frozen at –70°C. This number of frozen embryos is thawed in 15 ml 0.1 M sodium acetate at pH 5.0, with 0.5 per cent sodium lauryl sulfate. An equal volume of fresh, H₂O-saturated phenol is added. The mixture is shaken at 0°C for 10 to 15 minutes. After centrifugation, the nucleic acids are precipitated from the aqueous phase with 0.1 M sodium chloride and 2 volumes of ethanol. After about 2 hours

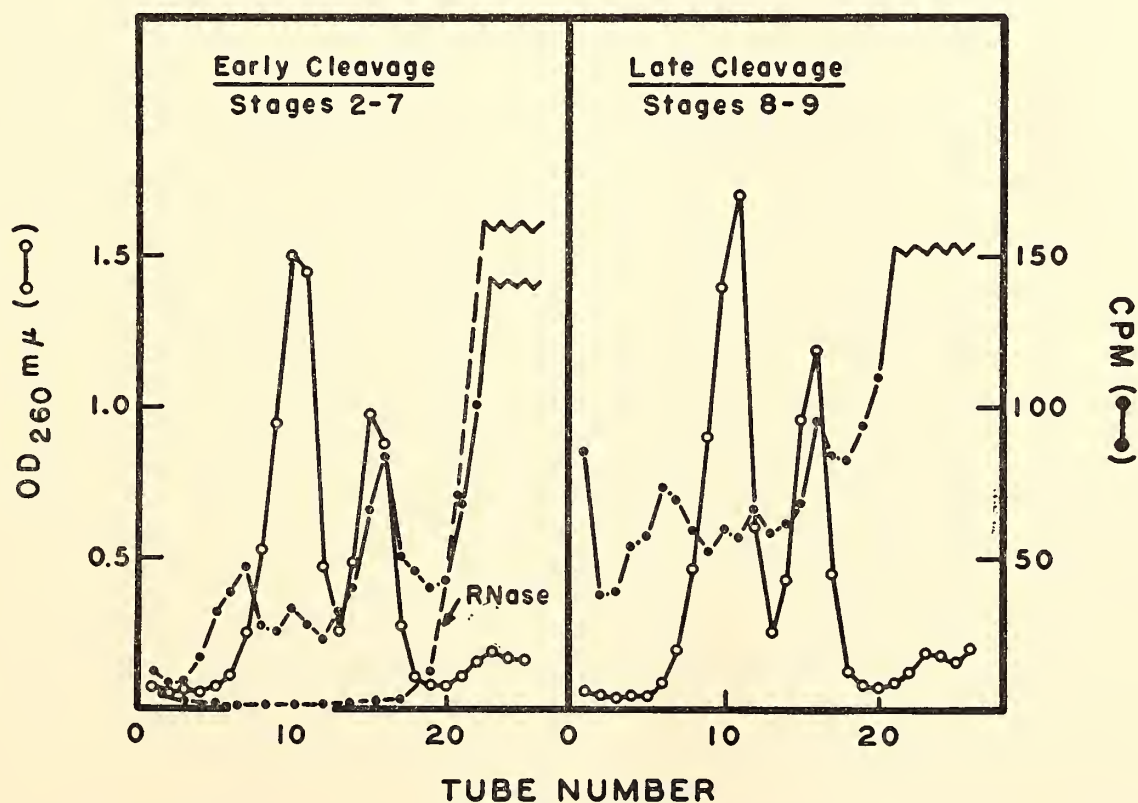


Fig. 3. High-molecular-weight RNA from early and late cleavage stages approximately 2 and 6 hours after fertilization respectively at 18°C.

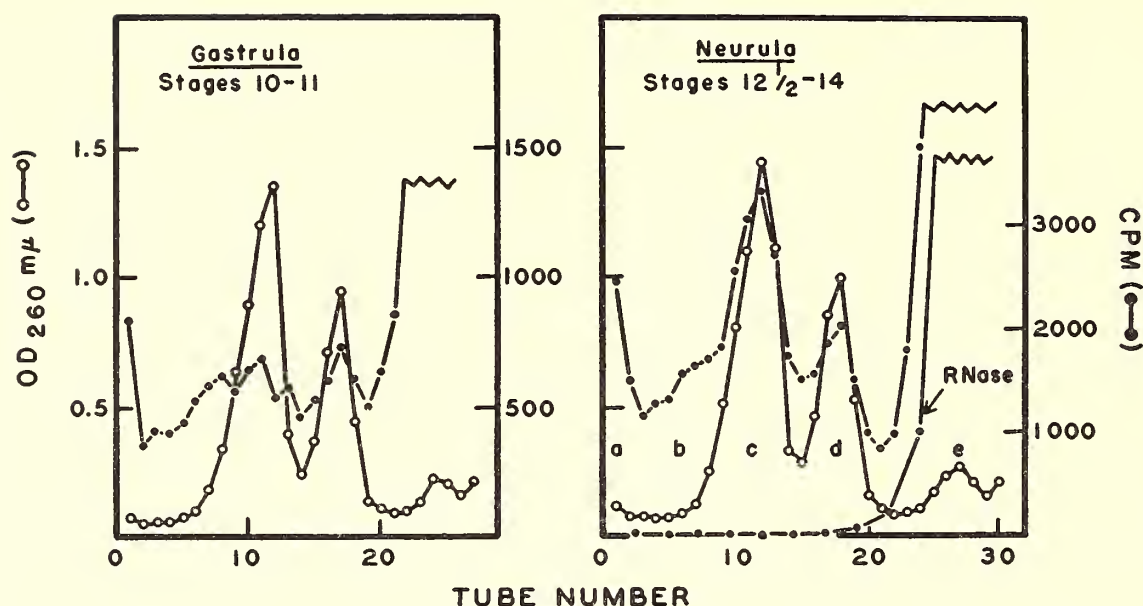


Fig. 4. High-molecular-weight RNA from gastrulae (26 hours) and neurulae (33 hours).

at -20°C the suspension of nucleic acids is centrifuged, and the resulting pellet is resuspended in 0.01 M sodium acetate with $1\text{ }\mu\text{g/ml}$ polyvinyl sulfate. Incubation with $5\text{ }\mu\text{g/ml}$ crystalline DNase I is performed at this time at 20°C for 10 minutes after the addition of 10^{-3} M magnesium chloride. Precipitation with ethanol-sodium chloride is repeated twice. The final pellet is dissolved in the dilute acetate buffer containing polyvinyl sulfate and clarified by centrifugation. The resulting supernatant fluid is layered on the sucrose gradient. The linear gradient varies from 5 to 20 per cent sucrose concentration and contains 0.01 M sodium acetate and 10^{-4} M versene at $\text{pH } 5.0$. Centrifugation is performed in the

SW-25 horizontal rotor of the Spinco model L ultracentrifuge at 0°C for $14\frac{1}{2}$ hours at 24,000 rpm.

For accurate staging, P^{32}O_4 (1 mc) was injected into a female; 4 hours later 1000 units of commercial gonadotrophic hormone was injected. The male was injected with 250 units on the previous day and again at the same time as the female. Ovulation and fertilization occurred about 12 to 16 hours after the pituitary injection.

Figures 3 to 5 record the pattern of synthesis of high-molecular-weight RNA from early cleavage (2- to 32-cell stages) to post hatching stages. RNase-treated controls are included in figures 3 and 4. Radioactivity first appears most promi-

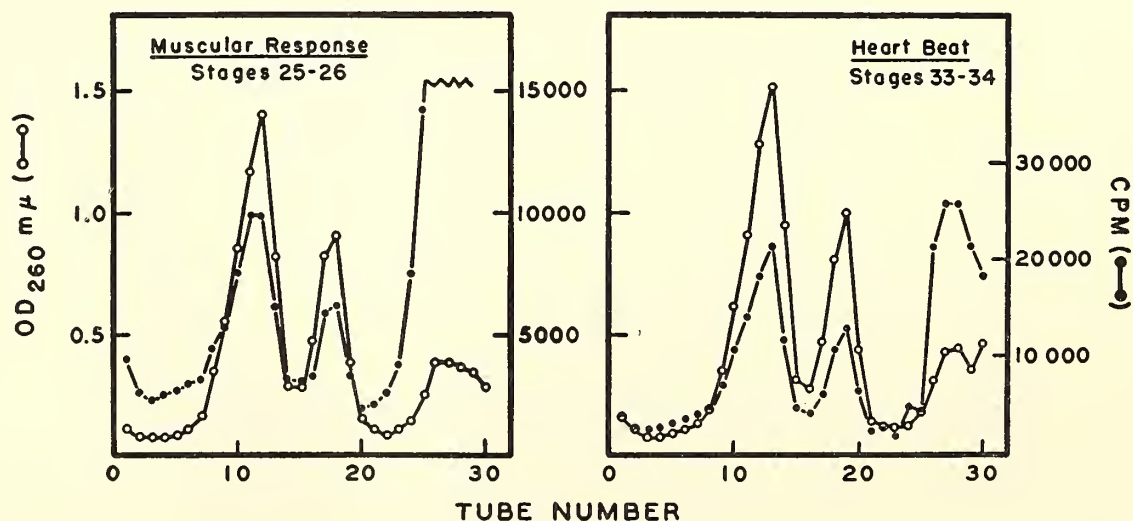


Fig. 5. High-molecular-weight RNA from tail-bud (54 hours) and muscular response (74 hours) stages.

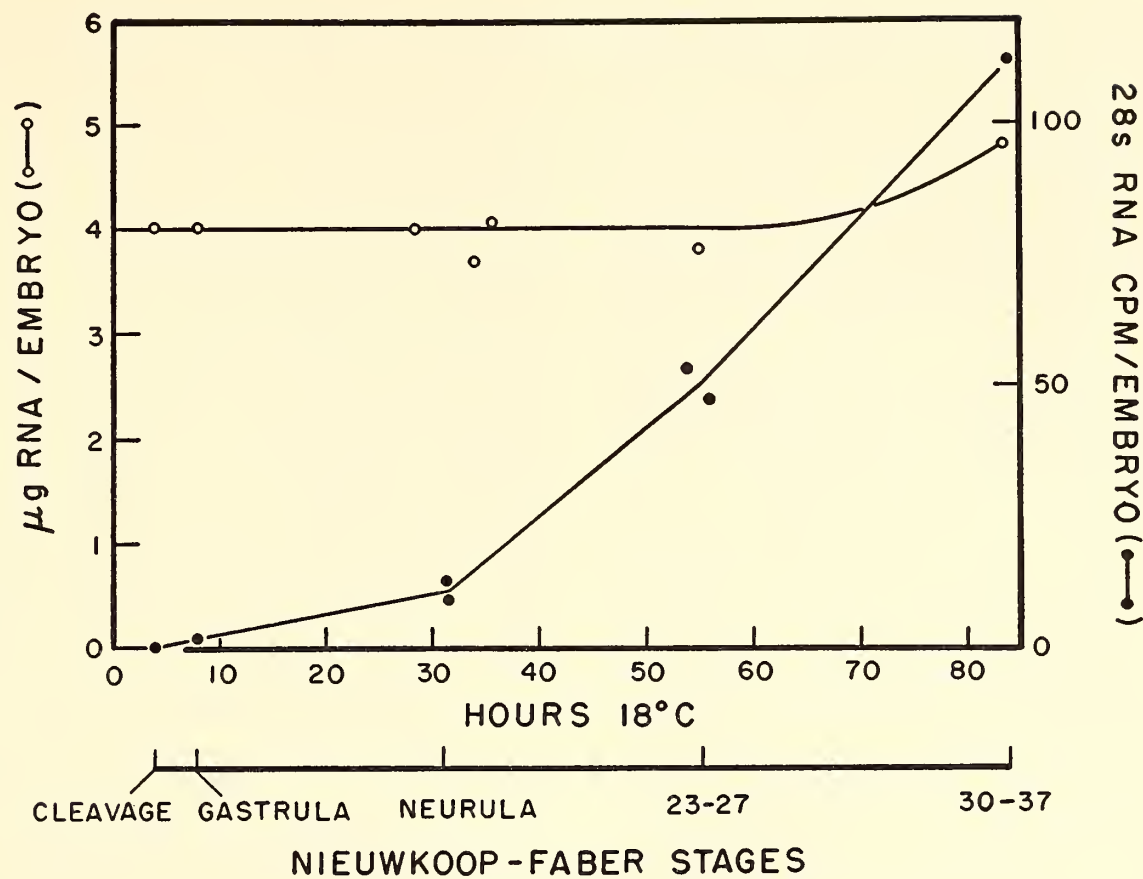


Fig. 6. Appearance of radioactive RNA sedimenting at 28S compared with total RNA at different developmental stages.

nently in two different-sized RNA moieties (fig. 3). One has a sedimentation constant greater than 28S RNA, the second distinct peak being slightly smaller than the 18S component, having a presumed sedimentation constant of about 16S. As development proceeds, radioactivity appears in the 28S and 18S RNA and the relative amount of radioactivity in the heavy RNA decreases. Acid-soluble P³² is still present at stages 33 to 34 (fig. 5), and, until it has been completely utilized (stages 39–40), radio-

active RNA can be demonstrated in the region sedimenting more rapidly than 28S RNA.

The synthesis of 28S RNA is shown in figure 6. Rapid synthesis begins at neurulation. Before that stage the heterogeneity of the newly synthesized RNA makes it difficult to quantitate the actual amount of 28S and 16S RNA.

Base analysis of P³²-labeled RNA was carried out after alkaline hydrolysis and paper chromatography to separate the four 2'(3')-ribonucleotides. Table 1 sum-

TABLE 1. Base Composition of P³²-Labeled RNA of Neurulae Compared with Base Composition of the Bulk of the RNA

	Radioactive Peak					Optical Density Peak*		
	a	b	c	d	e	28S	18S	4S
Approximate S value	>45	35–40	28	16–18	4
AMP	30	25	24	27	20	17	22	20
GMP	23	27	31	28	31	37	31	28
CMP	19	23	27	21	30	30	29	32
UMP	28	25	17	23	19	16	18	20

* Prepared by acid hydrolysis and paper chromatography of purified RNA from unfertilized eggs. Values are for the free purines and the pyrimidine nucleotides.

marizes data obtained from hydrolyzed radioactive RNA isolated from five separate portions of the gradient (areas *a-e*, fig. 4). Approximate sedimentation constants are included as well as base composition of RNA from the major three peaks (28S, 18S, and 4S) measured by optical density readings and calculated from known extinction coefficients. The smallest radioactive component (4S) is identical in base composition to the bulk of the RNA sedimenting in that region and has a high G-C content characteristic of soluble RNA (transfer RNA). Materials sedimenting in the 18S and 35S regions have base compositions intermediate between those of ribosomal RNA and DNA, and the most rapidly sedimenting radioactive RNA (peak *a*) has a DNA-like base composition. Finally, 28S RNA radioactivity and optical density have the typically high G-C content that has been described for ribosomal RNA. Of particular interest is the discrepancy in the 18S region, where the base composition of the bulk of the RNA differs from that of the newly synthesized P^{32} RNA. It is of further interest that radioactive RNA appears in this area (fig. 3) before any substantial amount of radioactive 28S RNA is synthesized. Preliminary results show that, as development proceeds, the radioactive RNA in the 16S-18S region gradually shifts in base composition from a high A-U content to the high G-C content characteristic of the bulk of material with this sedimentation constant. It should be noted that the base composition of the bulk of 18S RNA has a slightly higher A-U content than the 28S RNA (table 1).

Synthesis of High-Molecular-Weight RNA during Oogenesis

It was observed that, if P^{32} was injected more than 2 days before ovulation (20°C), some radioactive 28S and 18S RNA could be detected in the unfertilized eggs. This finding led to

studies of RNA synthesis and metabolism during oogenesis of *Xenopus laevis*. Initial studies have demonstrated that different-sized eggs have distinctly different capabilities of RNA synthesis. Three days after P^{32} injection at 18°C, there is extensive incorporation of label into ribosomal RNA of small and of medium-sized eggs, but little into that of mature eggs. At 5 days after P^{32} injection at 18°C there is substantial radioactivity even in the ribosomal RNA of mature eggs. At 2 days and earlier the specific activity of RNA in ovarian tissue exceeds that in all three classes of eggs. The data indicate that rapid synthesis of ribosomal RNA in ovarian tissue precedes its appearance in eggs. Future experiments will be designed to ascertain the site of synthesis of ribosomal RNA more precisely. Is ribosomal RNA made by the surrounding ovarian tissue and incorporated into oocytes as RNA or even as preformed ribosomes? It would represent an astonishing amount of RNA synthesis for these cells, if this is in fact DNA-dependent RNA synthesis.

Regional Synthesis of Ribosomes in Rana pipiens

In *Year Book 61* (table 4, p. 382), Brown and Caston reported finding a difference in ribosome content between ventral and dorsal regions of *Rana pipiens* embryos at swimming stages. A more careful investigation of this seemingly striking difference has clearly shown it to be an artifact related to the nucleic acid binding phenomenon. The substance responsible for binding of ribosomes appears to be associated with the yolk. The ventral region of the embryo is much richer in yolk than the dorsal region. When the study was repeated using the sensitive isotope dilution method to correct for binding, similar amounts of ribosomes were found in dorsal and ventral regions when expressed as μg ribosomes/ μg DNA. Furthermore, when the P^{32} -labeling technique was used,

TABLE 2. Comparison of Ribosome and Ribosomal RNA Content in Dorsal and Ventral Sections of Radioactive *Rana pipiens*

	Dorsal	Ventral
Stage 19		
DNA	2.54*	0.54
RNA	8.6	4.4
cpm/ μ g RNA	34.6	35.3
Stage 24		
DNA	8.9	2.7
Ribosomes	12.9	2.8
Cpm/ μ g ribosomes	6.48	5.72
μ g ribosomes/ μ g DNA	1.45	1.02

* Values in micrograms per embryo.

radioactive ribosomes and ribosomal RNA were present in comparable amounts in the two embryonic portions at stages 19 and 24 (table 2). It can be said that, at least with respect to these two general halves of the embryo, RNA content per cell is similar, and new RNA and ribosomes are formed at the same rate in each part of the embryo.

Discussion. A general pattern of events can be described for the synthesis of ribosomal RNA in *Xenopus laevis*. During oogenesis, as the oocyte matures, RNA synthesis seems to decrease, but radioactivity does appear in ribosomes and ribosomal RNA of mature eggs fully capable of being ovulated and fertilized.

After fertilization, synthesis of new high-molecular-weight RNA has been detected in early cleavage stages, but the sedimentation constant of this RNA differs from the sedimentation constant of the bulk of the RNA already present in the early embryo. The more rapidly sedimenting RNA is similar to the early labeled nuclear RNA described by Darnell et al. for HeLa cells. However, radioactivity also appears in lower sedimenting fractions. Of primary importance will be careful determinations of the base composition of these peaks at each stage of development. At present no single scheme can be advanced to unify the data and identify each different class of early

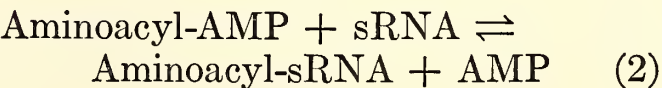
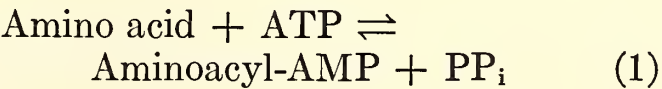
labeled RNA as precursor for a known RNA fraction.

As was described above, the use of *Xenopus* permits investigation of the ribosomes themselves at different stages of development. This study will be the subject of a future report.

Isolation and Partial Characterization of Aminoacyl-sRNA Synthetases from Rana pipiens Embryos

As the characterization of embryonic nucleic acids proceeded, it became apparent that, ultimately, tests of their biological activity would hinge on the availability of an assay system in which protein could be synthesized reproducibly in vitro. Douglas Caston initiated experiments looking toward the development of such a system. In order to obtain critical data, the assay system must be defined not only qualitatively but quantitatively as well; i.e., the operation of each step in the sequence from amino acid activation to peptide formation must be determined. In the event of failure to demonstrate protein synthesis, the defective step, be it aminoacyl-sRNA synthetase, sRNA, transferase, messenger RNA, or ribosome, can more easily be identified in a well defined system than in a crude one.

As a first step Caston undertook the isolation and partial characterization of aminoacyl-sRNA synthetases from *Rana pipiens* embryos at Shumway's stage 25. These enzymes catalyze the following reactions:



Of the several isolation procedures tried, the following has proved most effective in yielding reproducible results. The 105,000-g supernate, obtained from homogenated embryos as previously described, was made 0.1 M with respect to tris HCl, pH 7.5, and 0.005 M ethylenediamine

tetraacetic acid (EDTA). After standing for 30 minutes at 4°C, the solution was filtered through a Sephadex column (G-50 or G-100), and the protein fraction was precipitated with ammonium sulfate at 70 per cent saturation. The precipitate was dissolved in 0.1 *M* tris buffer, and the protein solution was dialyzed against distilled water. The resulting solution, containing 8–12 mg protein per milliliter, was frozen in 3.0-ml aliquots. Just before use, an aliquot was thawed and 0.5 micromole glutathione was added per milligram protein.

of nucleic acids or nucleotides in these preparations.

In table 3 requirements of three synthetase preparations obtained by different treatments are compared. Only after Sephadex filtration could a dependency on ATP, amino acid, and Mg^{++} be demonstrated. The dependency on added cofactors varied from preparation to preparation, but two preparations treated with Sephadex G-50 showed no PP_i exchange without addition of amino acid to the reaction mixture and very little exchange (2 per cent of the complete

TABLE 3. Aminoacyl-AMP Formation by Stage 25 Enzymes
ATP- PP_i exchange reaction

	Dialysis*		Sephadex G-50		Sephadex G-100	
	Before	After	Before	After	Before	After
Complete system†	466‡	480	510	642	518	582
Less enzyme	0	0	0	0	0	0
Less ATP	160	200	210	152	214	92
Less amino acid mixture	400	398	406	54	420	134
Less GSH	446	68	480	10	490	22
Less $MgCl_2$	468	450	530	28	514	36
Less KF	15	20	30	218	22	110
Less tris, +100 μM PO_4^{---}	440	460	480	622	474	594

* 105,000*g* supernate was dialyzed against three changes of 6000 volumes 10^{-2} *M* tris buffer, pH 7.5.

† In $\mu M/ml$: tris HCl, 100; KF, 50; $MgCl_2$, 5; ATP, 5; $P^{32}P_i^{32}$, 5 (about 85,000 cpm); amino acids, 0.1 each of 20 amino acids; 1.0 mg protein. Final pH is 7.4; reaction carried out at 22–23°C for 20 minutes. After 20 minutes' incubation, reaction stopped by addition of 2 volumes cold 5 per cent TCA; the ATP was isolated by the charcoal method and hydrolyzed with hot HCl. Radioactivity was determined with a gas-flow counter; phosphate was measured by the method of Fiske-Subba Row.

‡ Counts per minute.

Enzymes prepared in this manner show properties of synthetases obtained from other sources, as judged by hydroxamate formation and ATP- PP_i exchange. They are activated by thiols, require Mg^{++} , depend on added ATP and amino acids, and show similar temperature and pH optima. After Sephadex treatment, the enzymes are stable for at least 3 months at $-70^\circ C$ but rapidly lose activity upon repeated freezing and thawing. Ultraviolet absorption spectra give no evidence

system) without added ATP. Thus Sephadex appears to be highly effective in removing bound cofactors from the synthetase preparations.

Although Sephadex treatment had no apparent effect on the specific activity of the preparations, it did increase the period of linearity of the amino acid activating reaction from about 20 minutes to at least 60 minutes (fig. 7), possibly by removing cofactors of some other reaction requiring ATP. These preparations

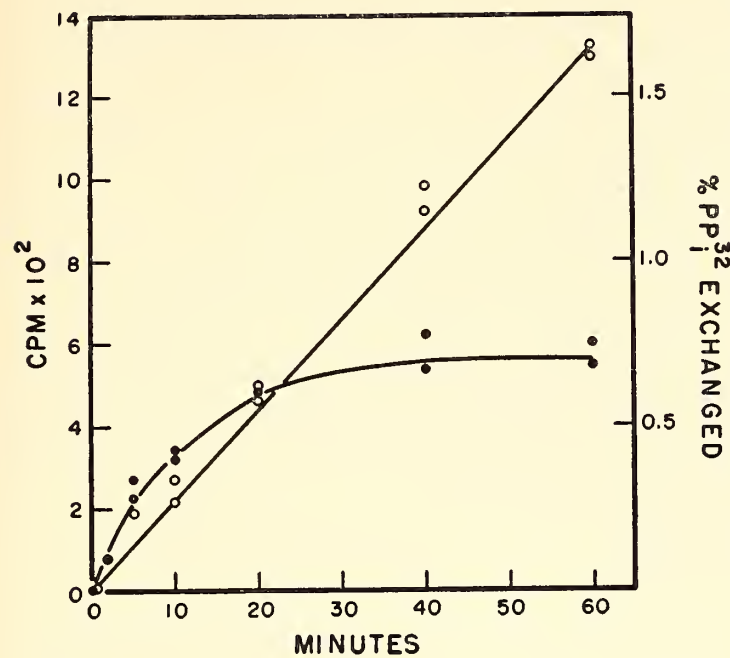


Fig. 7. ATP-PP_i exchange as a function of time before (solid dots) and after (open dots) filtration of aminoacyl-sRNA synthetase preparation through Sephadex G-50. Conditions same as in table 3 except 80,000 cpm PP_i³² were added to reaction mixture.

customarily show a specific activity of about 0.2 micromole amino acid activated per hour per milligram protein (fig. 8).

The response of the synthetases to individual amino acids varied considerably; consistent results have been obtained for only three amino acids (fig. 9).

The response to methionine and valine appears to be similar to the response to phenylalanine, leucine, and isoleucine, but too few determinations have been made to permit a firm conclusion. Tyrosine activation seems to require the addition

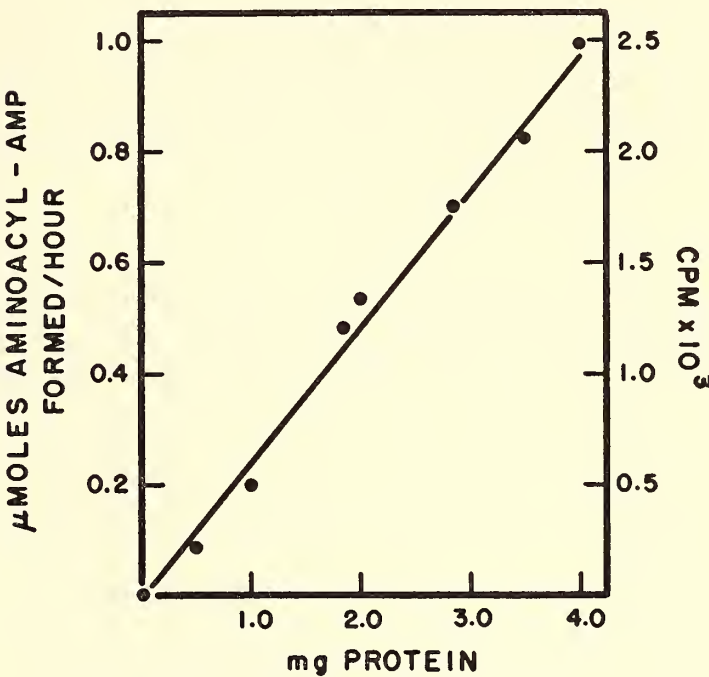


Fig. 8. Aminoacyl-AMP formation as a function of enzyme concentration (enzymes filtered through Sephadex G-50). Conditions same as in table 3 except 100,000 cpm PP_i³² were added to reaction mixture. Reaction stopped after 20 minutes.

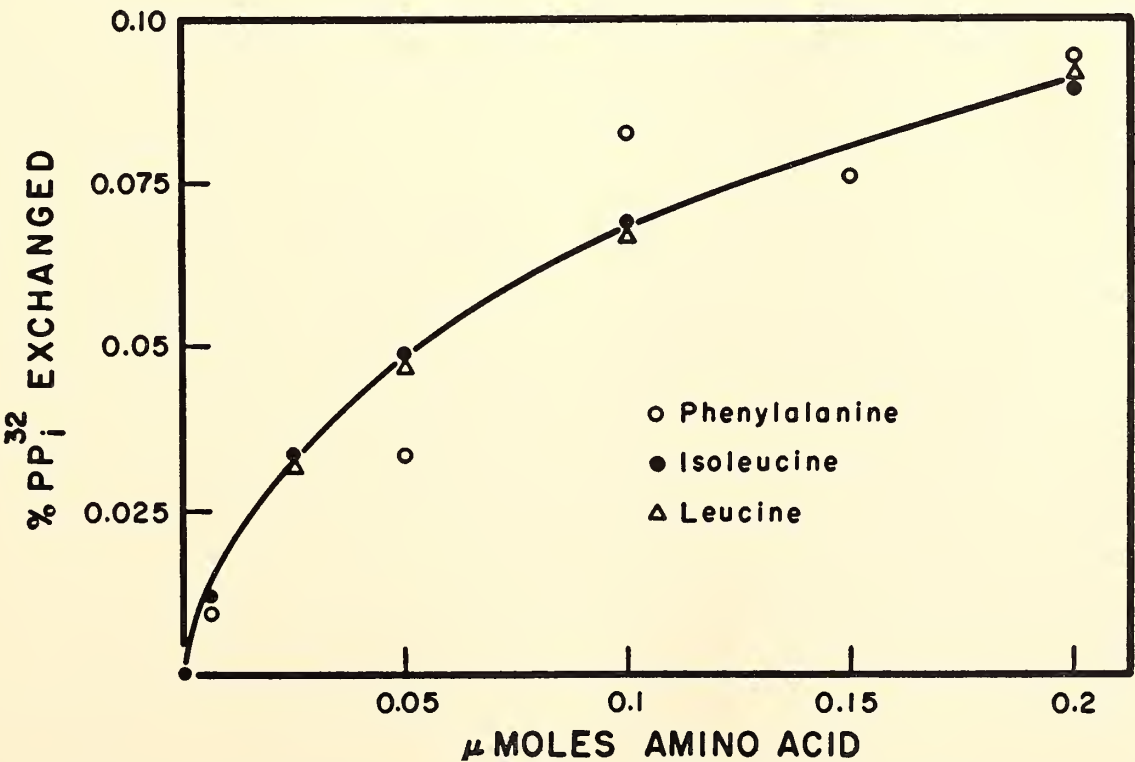


Fig. 9. ATP-PP_i exchange in response to individual amino acids. Conditions same as in table 3 except 168,000 cpm PP_i³² and 2.4 mg protein were added to reaction mixture. Reaction stopped after 20 minutes.

TABLE 4. Incorporation of Amino Acids into "Active" and "Inactive" Stage 25 sRNA

	Active Stage 25 sRNA	Inactive Stage 25 sRNA
Complete system*	1600†	1200
Less ATP	45	150
Less CTP	1590	0
Plus 1.0 mg rabbit muscle enzyme	1200
Less synthetase	0	0

* In $\mu\text{M}/\text{ml}$: tris 100; MgCl_2 5; ATP 10; CPT 1; 100 μg sRNA 2×10^5 cpm C^{14} -algal hydrolysate; 2.0 mg synthetase preparation. Incubated at $22^\circ\text{--}23^\circ\text{C}$ at pH 7.2; after 20 minutes reaction stopped by addition of equal volume cold, water-saturated phenol. sRNA isolated from aqueous phase by ethanol precipitation. Radioactivity determined with a gas-flow counter.

† Counts per minute.

of potassium chloride, but results have been inconsistent and no definite conclusion can be reached at present.

Preliminary experiments have been conducted on the amino acid acceptor activity of soluble RNA (sRNA) purified from several developmental stages of *Rana pipiens*. sRNA was purified from the supernatant fluid after centrifugation at 105,000g by the phenol method, and amino acids were discharged from it by incubation in 0.5 M tris buffer, pH 8.8, at 37°C for 45 minutes.

Pilot experiments on sRNAs have given conflicting results. For example, three preparations of sRNA from stage 25 embryos showed good amino acid acceptor activity, whereas one preparation from stage 25, two from first-year tadpoles, and two from adult frog liver were completely inactive.

Inactivity of at least one of these preparations (stage 25 sRNA) was probably due to the absence of the terminal nucleotide sequence -pCpCpA from this preparation, since this sRNA became active in accepting amino acids when CTP was added to the usual incorporating system (table 4). No increase in amino acid acceptor activity was found if nucleotide-incorporating enzymes from rabbit muscle were added to the system. Thus, it appears that the synthetase preparations also contain nucleotide-incorporating systems. This observation must be tested further.

The inactivity of frog liver and tadpole sRNAs with stage 25 synthetases could be due to a similar loss of terminal nucleotides, or it may reflect a specificity of stage 25 synthetases for embryo sRNAs. Experiments to distinguish between these possibilities are under way.

Figure 10 illustrates the incorporation of amino acids derived from C^{14} -algal hydrolysate into stage 25 sRNA as (a) a function of sRNA concentration and (b) a function of time. Incorporation of leucine and isoleucine into sRNA represents about 2 per cent of the values shown in these graphs. The incorporation of other amino acids is yet to be tested.

DEOXYRIBONUCLEIC ACID IN EGGS AND EARLY EMBRYOS OF *Rana pipiens* AND *Xenopus laevis*

Eggs of *Rana pipiens*, as well as of other amphibian species, contain more DNA than would be expected on the basis of the amount found in sperm. This excess DNA, frequently referred to as "cytoplasmic DNA," has been characterized as material giving chemical and microbiological reactions for deoxyribose, and, in some instances, as being insoluble in cold, and extractable in hot, acid. The quantitative data obtained in different laboratories are considerably at variance. The incorporation of precursors into DNA in embryonic development of *Rana pipiens* was studied by Grant, who found

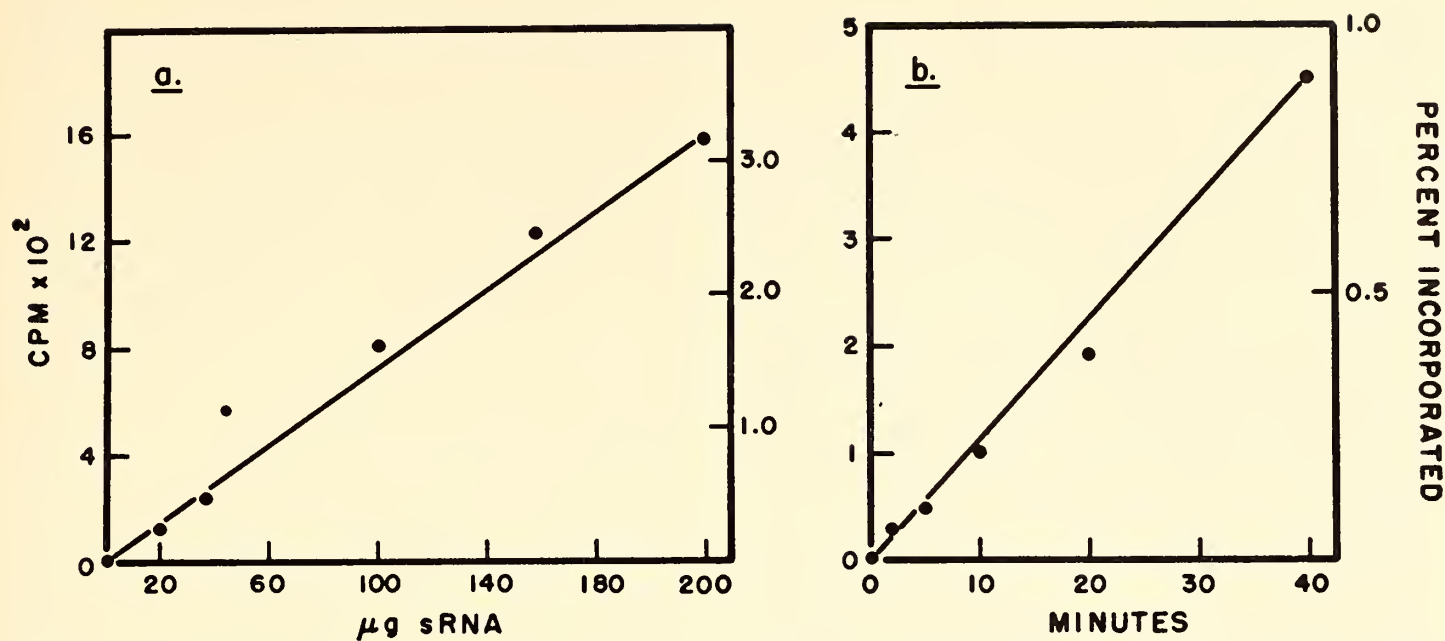


Fig. 10. Incorporation of C¹⁴-amino acids from algal hydrolysate into stage 25 sRNA: (a) as a function of sRNA concentration (conditions same as in table 4); and (b) as a function of time (conditions same as in table 4 except 40 μg sRNA was added to the reaction mixture).

no incorporation of P_i³² up to Shumway's stages 7-8.

There have been speculations about a possible specific role of "cytoplasmic DNA," particularly with respect to the formation of nuclear DNA during cleavage. In the absence of evidence for the incorporation of precursors it might be argued that "cytoplasmic DNA" is in some way channeled into the chromosomes of the newly formed nuclei. Therefore, Igor Dawid undertook a characterization of "cytoplasmic DNA," aiming to study the incorporation of

precursors in early cleavage at a higher level of sensitivity, believing that earlier studies could not have detected the amount of radioactivity expected to be incorporated into nuclear DNA under the conditions used. An additional problem emerged in the course of these experiments.

"Cytoplasmic DNA"

The Burton modification of the diphenylamine reaction was used for the assay of deoxyribose. Table 5 shows

TABLE 5. DNA in Eggs and Sperm

Material	mμg "DNA"* per Egg	
	Average	Range
<i>Rana pipiens</i>		
Material soluble in cold acid	50	40-72
Material insoluble in cold acid and soluble in hot acid	9	8-11
Material extractable with detergent-phenol and insoluble in 66% ethanol and cold acid	6	3-8
<i>Xenopus laevis</i>		
Material extractable with detergent-phenol and insoluble in 66% ethanol and cold acid	3.6	1.7-4.8
<i>Rana pipiens</i> sperm (England and Mayer, 1956)		
		0.0065

* Commercial salmon sperm DNA was used as standard in the Burton modification of the diphenylamine reaction.

values obtained from several samples from different animals and at different times. The values for *Rana pipiens* are of the same order of magnitude as those reported by Grant; there are no reports on the DNA content of *Xenopus laevis* eggs.

Chemical characterization of this material was not feasible with the quantities available. Therefore, Dawid tried to label DNA specifically with tritiated thymidine. *Rana pipiens* females were injected with 0.5 mc thymidine- H^3 , kept 2 to 4 months at 3°C, and ovulated. *Xenopus laevis* females were ovulated, injected with 0.5 mc of thymidine- H^3 , kept 3 months, and ovulated again. The eggs of both species were extracted by a detergent-phenol procedure, and the fraction insoluble in 66 per cent ethanol, stable to RNase and alkali, and digested by DNase, was regarded as DNA. In both species only 2 per cent of the radioactivity of the eggs resided in the DNA fraction (1 cpm/egg). The rest was distributed nonspecifically in other cell constituents. This approach has thus failed.

Incorporation studies. P_i^{32} and tritiated thymidine were used for the study of DNA formation in the development of *Rana pipiens* through stage 7 (32 cells). Owing to technical difficulties, some of which led to the observations recorded below, no definite conclusions have been reached so far.

A Protein Fraction from Rana pipiens Eggs

In the incorporation experiments mentioned above, it was observed that extracts prepared from a mixture of eggs and liver failed to give the expected DNA peak on chromatography on methylated serum albumin on kieselguhr (MAK), according to Mandell and Hershey. The DNA was present in the extract but was

not absorbed to the column. If eggs were extracted alone, and the material obtained in the ethanol precipitate of the aqueous phase was combined with purified frog liver DNA, this DNA was also prevented from being absorbed to MAK. This effect could be abolished by treatment with trypsin: the responsible material is therefore a protein or, more likely, a mixture of proteins.

Since this protein fraction is partitioned into the aqueous phase of a water-phenol system, it can be separated from the bulk of the egg's proteins, which appear in the phenol phase. To separate the protein fraction from the accompanying nucleic acids, the extract was treated with RNase and DNase, again extracted with phenol, and passed through a column of Sephadex G-100. The protein (detected by the Lowry reaction) was completely separated from the nucleic acid derivatives. This experiment also indicated a high molecular weight for the protein fraction, but the possibility of aggregation has not been excluded.

An assay for the binding capacity was devised, in which a suspension of MAK is mixed with radioactive DNA and the protein sample to be tested; the mixture is incubated for 15 minutes and centrifuged. In the absence of the protein fraction all the DNA is bound to the MAK; in its presence DNA appears in the supernatant. If the logarithm of the weight ratio of protein to DNA is plotted against the amount of DNA excluded from the binding to MAK, a curve of the shape of a titration curve is obtained, the inflection point being close to a weight ratio of 1. The effect is not species-specific and could also be observed with commercial salmon sperm DNA. The protein fraction from eggs differs from calf thymus histone in solubility properties and, most probably, in molecular weight.

CHEMISTRY AND PHYSIOLOGY OF THE DEVELOPING HEART

THE INHIBITORY ACTION OF ANTIMYCIN A IN THE EARLY CHICK EMBRYO

Ahmad, Schneider, and Strong demonstrated the effects of antimycin A, an antibiotic isolated from a species of *Streptomyces* by Dunshee, Leben, Keitt, and Strong, on the growth of yeast, on the activities of enzymes in the succinoxidase system, and on rats. Potter and Reif argued that the factor blocked by antimycin A was probably identical with the "Slater factor," and they showed that in certain tissues there is an antimycin A-insensitive pathway for DPN oxidation.

Duffey and Ebert showed that, like sodium fluoride, antimycin A produced marked inhibitory effects in the early chick embryo when applied to the hypoblast; at low concentrations, within a narrow range, embryos developed essentially normally except for the absence of the heart. At the same or slightly higher concentrations, in older embryos, somites formed but did not persist.

In extending the study McKenzie and Ebert demonstrated that the location of abnormalities produced depends on the method of administration as well as on the concentration of the inhibitor. When antimycin A is presented via the epiblast, brain and spinal cord are affected more than the mesodermal derivatives.

Despite the striking nature of the earlier findings on cardiogenesis, confirmed in the course of the present investigation by C. R. Green and M. C. Reporter, the mechanism of action of antimycin A in the early embryo has remained obscure. During the year under review, Reporter, with the cooperation of Green and J. D. Ebert, and the unstinting aid of Jeannie Hubbard and Pauline Stott, has begun to probe more deeply into the metabolism of the early blastoderm.

During the period October through May 1962-1963, 83 experiments were

performed in the course of which some 3900 individual chick embryos were explanted under a number of different environmental conditions. Spratt's technique was used in explanting embryos to an albumen-agar medium (1:1) employing Howard's modification of chick Ringer's solution. Embryos, staged according to Hamburger and Hamilton, were exposed to a number of inhibitors added to the medium for periods ranging from 18 to 24 hours.

Studies with antimycin A have been emphasized. Figures 11 and 12 summarize experiments showing the relations between antimycin A dosage, stage at

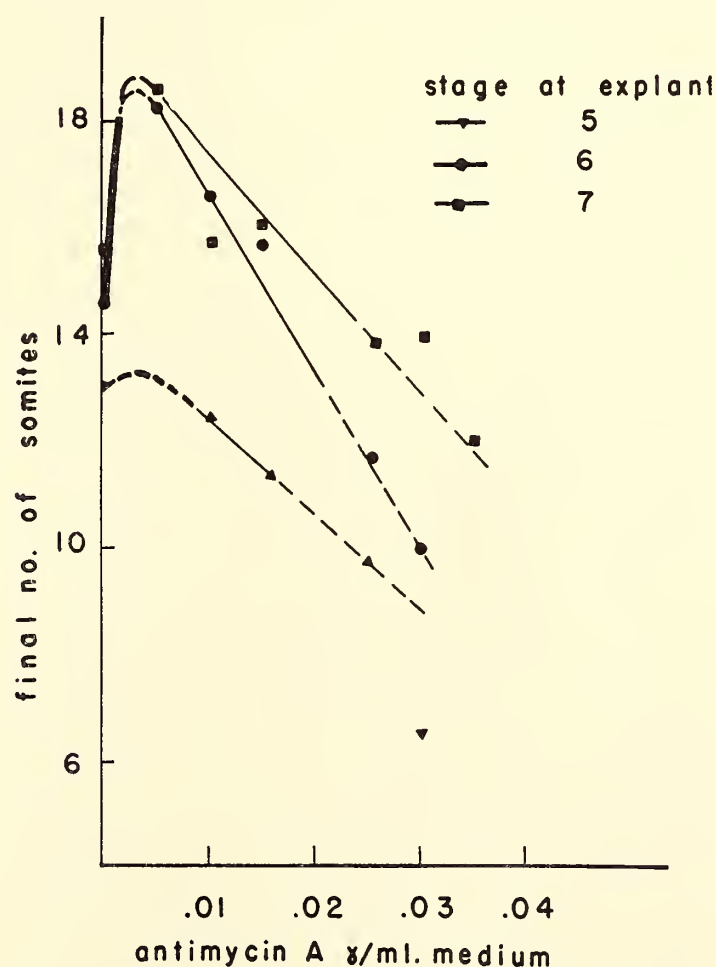


Fig. 11. Plot of the number of pairs of somites formed during cultivation against dosage of antimycin A ($\mu\text{g}/\text{ml}$ medium), for three stages at which embryos commonly were explanted. Effect of antimycin A at concentrations below $0.01 \mu\text{g}/\text{ml}$ medium is extrapolated in the heavy parts of the curve at left. The broken parts of the curve at right indicate absence of the heart. At the highest doses of the antibiotic, embryos with only residual axial structures are recovered.

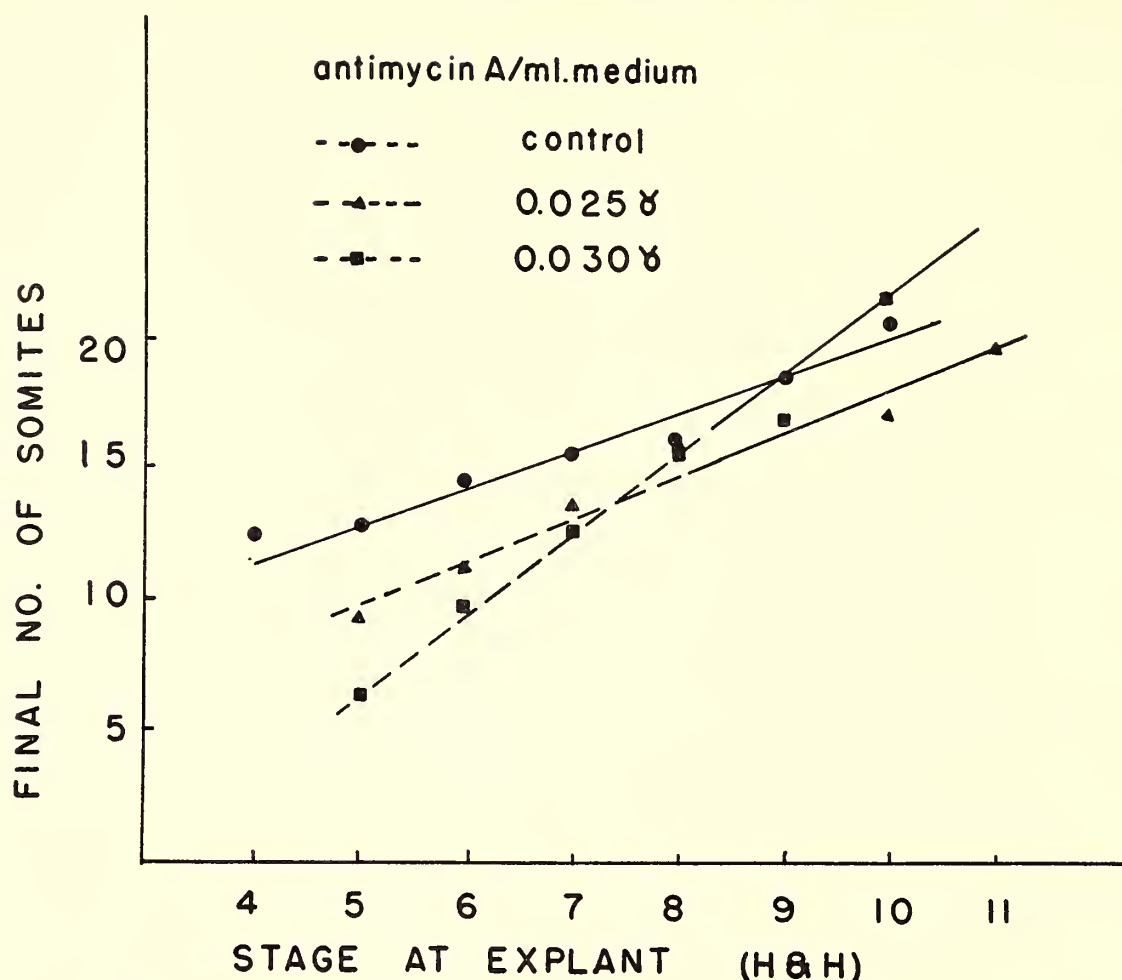


Fig. 12. The stage at which embryos were explanted is plotted against the final number of somites for two concentrations of antimycin A, compared with control explants. Absence of the heart is denoted by broken lines.

explantation, and extent of development at recovery, based on (1) presence or absence of a normal or rudimentary heart and (2) number of pairs of somites present. Hemoglobin is formed in embryos cultivated in the presence of antimycin A.

The data in these figures were obtained from a pool comprising observations on individual embryos recovered in experiments conducted over a period of 4 months, the mean number of pairs of somites being calculated for embryos recorded initially by stage and treatment.

It will be seen that, in addition to the importance of the concentration of the inhibitor and route of administration, the action of antimycin A is shown to be proportional to the initial morphological stage of the explant.

The Action of Antimycin A in an Oxygenated Environment

By chance, Green and Hubbard observed that the antimycin A sensitivity

of embryos cultivated in a highly oxygenated environment was markedly increased. This finding is being explored systematically by Reporter and his associates. At high levels of oxygen, concentrations of antimycin A that usually affect only cardiogenesis have far more pronounced effects on the embryo as a whole, resulting in embryos showing only residual axial structures. Perhaps it is an oversimplification to do so, but it can be argued that the early chick embryo has two pathways of oxidative metabolism, one sensitive and one insensitive to antimycin A. Under the usual conditions of explantation, the heart-forming regions and, to a lesser extent, the somites are operating via an antimycin A-sensitive pathway, the remainder of the embryo via predominantly insensitive pathways. Under high levels of oxygen, however, for reasons as yet unknown the entire embryo adjusts to the predominantly antimycin A-sensitive route. Moreover, the question

is raised whether the explanted embryo may be sensitive to different levels of oxygen as well as to relatively low levels of inhibitors that block electron flow. A case for the existence of aerobic phosphorylation could also be made if the system is shown to be sensitive to uncouplers and inhibitors of mitochondrial phosphorylation.

Figure 13 summarizes the effect of oxygen on control embryos as compared with antimycin A-treated embryos ($0.03 \mu\text{g}$ antimycin A/ml medium). A new set of data is shown in this figure, individual points being averages of the means from six different experiments. Presentation of the rate of somite formation emphasizes the effect of oxygen on the embryo. Different concentrations of oxygen for these experiments were obtained by

mixing streams of N_2 with 99 per cent O_2 + 1 per cent CO_2 under conditions giving 100 per cent relative humidity. Collated data show that the effect of high concentrations of oxygen on the total number of somite pairs developed is proportional to the stage of the embryo at explantation. In contrast, the few control points obtained with total nitrogen show that all embryos explanted at stages 5 through 9 develop only 9 to 10 pairs of somites during some 20 to 22 hours of exposure. Hearts were arrested or completely absent in these embryos.

REVERSAL OF EFFECTS OF ANTIMYCIN A

The inhibition of cardiogenesis by antimycin A could not be prevented by lipid extracts of mitochondria made with

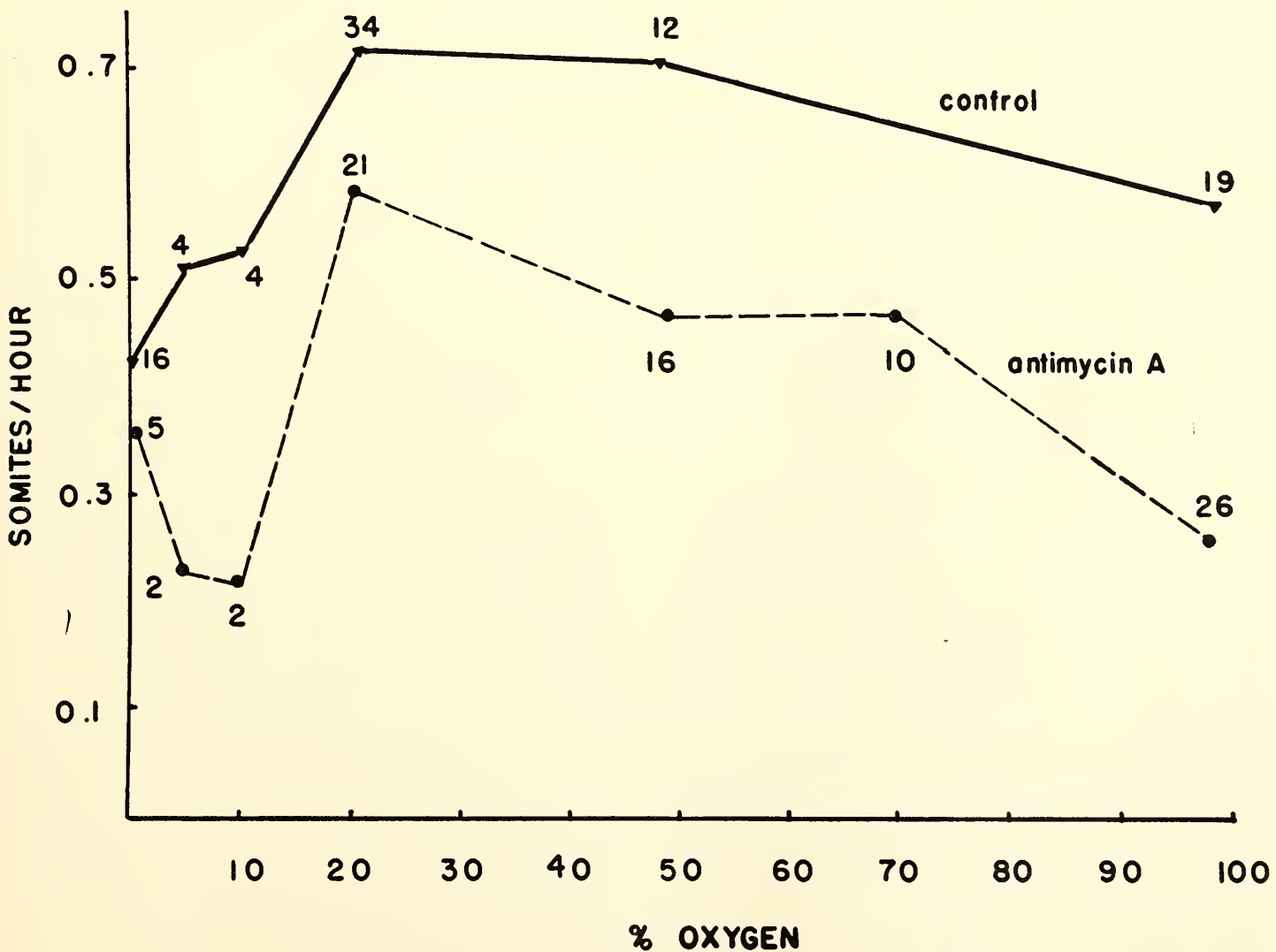


Fig. 13. The effect of varying concentrations of oxygen on the growth rate (number of pairs of somites formed per hour) in control embryos (solid line) and antimycin A-treated ($0.03 \mu\text{g}/\text{ml}$ medium) embryos (broken line). All control embryos grown in oxygen concentrations above 10 per cent developed hearts. None of the embryos in antimycin A-treated groups formed hearts.

mild extractants such as petroleum ether or with the more drastic chloroform-methanol treatment. Preparations of this type were added in ethanol or in aqueous emulsions made with albumen, cytochrome c, or myosin. Commercial coenzyme Q preparations were not effective. The inhibition by antimycin A could not be prevented by bypassing the presumed block of mitochondrial electron flow at the coenzyme Q-cytochrome b level, i.e., by activating the D-T diaphorase system by addition of TPN with vitamin K₃-bisulfite.

Aqueous extracts of chicken liver and heart mitochondria have been used successfully to prevent the inhibitory action of antimycin A.

Methods for Obtaining Aqueous Extracts of Mitochondria (AAAF)

The extracts that prevent the effects of antimycin A on the chick embryos are prepared as follows:

Mitochondria are isolated by standard procedures in 0.25 *M* sucrose buffered in 0.05 *M* tris, pH 7.8, with 10⁻⁴ *M* EDTA. The mitochondrial pellet resulting from centrifugation at 10,000*g* is washed twice in buffered sucrose, and the supernatant fluid is discarded after centrifuging twice at 12,000*g*. The mitochondrial pellet from 20–30 grams of fresh liver is then suspended in 10 ml of distilled water, the pH being controlled by residual sucrose–tris medium. The preparation is frozen for 1 hour at –70°C and then thawed. At this stage, 1 mg of glutathione is added per 5 grams of liver in the original sample. (Glutathione itself does not protect embryos against antimycin A, nor does it affect normal development in concentrations up to 2 mg per milliliter of medium.) The treated pellet is shaken on a Vortex Jr. machine and frozen at –70°C for an additional 90 minutes, after which it is again thawed and shaken for three 30-second periods at 0° to 4°C. Finally, the crude protective factor (AAAF) is isolated as an optically clear, straw-

colored supernatant fluid after centrifugation at 100,000*g*. Further purification has been achieved by Sephadex G-200 filtration, this step removing about 75 per cent of the protein, including a highly fluorescent component. These purification experiments are still in preliminary stages.

Preventive Action of AAAF

These extracts afford protection against antimycin A under conditions that ordinarily yield explants showing, at best, only residual axial structures. The protective action is noted even when embryos are incubated with the antibiotic under 99 per cent oxygen. Under these conditions, embryos without AAAF are severely affected after being in contact with antimycin A for 6 to 8 hours. Furthermore, protection is obtained if the mitochondrial factor is included in the fresh medium to which antimycin A-treated embryos are transferred. Embryos cultivated in media containing 0.03 µg of antimycin A per milliliter for as long as 6 or 8 hours, and then transferred to fresh medium without antimycin A but containing AAAF, recover. Embryos similarly exposed to antimycin A and then transferred to normal medium lacking AAAF do not recover.

There is some evidence also that protection is afforded when embryos are first explanted to medium containing AAAF and then transferred to medium containing antimycin A. The data are not fully convincing, however, for it is difficult to determine to what extent the “protection” is simply the consequence of the fact that the embryos are older at the time of exposure to the inhibitor.

The lowest effective concentrations of the crude, fresh protective factor (AAAF) employed thus far contain 2.5 to 3 µg of protein per milliliter of medium.

On noting that the crude factor is capable of yielding ATP from ADP and P_i in the presence of Mg⁺⁺, additional attempts at preventing inhibition of

antimycin A were made. Phosphagens in the form of creatine phosphate and phosphoenol pyruvate were tried alone and in combination with ADP/ATP. None of these attempts were successful even in combination with creatine and pyruvate kinases. Myokinase, an enzyme detected in liver mitochondria but not in heart mitochondria, also proved unsuccessful when used alone or in conjunction with myosin, with and without ADP/ATP. It may be mentioned that AAAF is isolated from liver more easily than from heart.

EFFECTS OF ANTIMYCIN A ON ENZYME ACTIVITY IN EARLY EMBRYO

Activities of creatine kinase, lactate dehydrogenase, and NADH-cytochrome c reductase, together with protein, have been determined on individual embryos.

Enzyme determinations. Protein content has been determined by the method of Lowry.

Single embryos were exposed to ultrasound for two 10-second periods in 0.1 ml of H₂O at 0°C. (A Branson instrument was used with a microprobe and a circulating water pump for temperature control.)

Cytochrome c reduction was measured at 550 m μ in a Beckman DK-2 recording spectrophotometer. The reaction was carried out with 0.02 ml homogenate, 0.05 ml cytochrome c (15 mg/ml), 0.005 ml KCN (0.01 M), 0.01 ml of NADH (10 mg/ml), and 1 ml of sucrose-tris buffer, pH 7.8 (0.25 M sucrose, 0.05 M tris, 10⁻⁴ EDTA). Reference cuvettes contained all ingredients except cytochrome c, buffer being used to make up the difference. Specific activity was expressed as O.D. min⁻¹ mg⁻¹ protein homogenate.

Lactic dehydrogenase was also measured in the DK-2 spectrophotometer. In these determinations 0.005 ml homogenate, 0.01 ml pyruvate (0.02 M), 0.01 ml NADH (10 mg/ml), and 1 ml tris-sucrose-EDTA buffer were used. Reference cuvettes did not contain NADH. Specific activity was

measured at 340 m μ and expressed as O.D. min⁻¹ mg⁻¹ protein homogenate.

Creatine-kinase determinations were made by following ATP formation from ADP and creatine phosphate by the firefly luciferin-luciferase system. Highly purified luciferin and luciferase were kindly supplied by H. Seliger of McCollum-Pratt Institute. One one-hundredth milliliter of suitably diluted luciferin-luciferase mixture was used together with 0.03 ml embryo homogenate, 0.005 ml MgSO₄ (12 per cent), 0.04 ml creatine phosphate (10⁻³ M), 0.02 ml ADP (10⁻³ M), and arsenate buffer (0.02 M) at pH 7.5 to make 0.5 ml in the cuvette. Standard curves were also made with known amounts of ATP. The resulting light signal was amplified by a 1 P 21 phototube used in conjunction with an Aminco photomultiplier and a Photovolt recorder. Specific activity was expressed as reciprocal of the time, 10³/sec, to make 0.06 μ g of ATP per milligram protein homogenate. Commercial preparations of rabbit muscle creatine kinase were employed for reference.

Initial straight-line slopes for 1 to 2 minutes were used for all enzyme determinations.

Table 6 summarizes results from one experiment in which explants were transferred from an albumen-agar medium containing antimycin A to another that lacked the antibiotic.

Results of three such experiments show increased protein and specific enzyme activities after transfer as compared with normal controls. Although the specific activity for cytochrome c reductase was lowered by growing embryos on a medium containing antimycin A, the activity was not abolished under the conditions employed. Similar observations have been made in one experiment in which chick embryos were grown in albumen-agar medium and the homogenates were subsequently exposed to antimycin A during the assay period in the spectrophotometric cuvettes. The enzyme system in these whole-embryo homogenates is rela-

TABLE 6. Enzymes Assayed in Chick Embryo Explants

Group*	Total No. Somites	Somite Pairs per Hour	Protein, $\mu\text{g}/\text{embryo}$	Creatine Kinase†	Lactic Dehydrogenase	NADH-Cytochrome c Reductase†
A	16.5	0.742	123	288	3.43	0.359
B	13.2	0.619	123	202	2.90	0.320
C	15.0	0.667	171	295	2.60	0.487
D	9.5	0.431	131	220	2.97	0.350

* A: controls—no additions, no transfer.
B: controls with antimycin A, no transfer.
C: controls, no additions—transferred to normal medium after 8 hours.
D: embryos explanted on medium containing antimycin A—transferred to normal medium after 8 hours.
† Specific activities per milligram protein shown.

Note: Four embryos were assayed per group, and the results were averaged. Embryos were explanted at stage 6. Where indicated, antimycin A at a concentration of $0.03\text{ }\mu\text{g}/\text{ml}$ was used ($4.6 \times 10^{-11}\text{ mole}/\text{ml}$). Total time between explants and harvest was 22 to 24 hours. Hearts were absent in embryos grown on medium containing antimycin A.

tively resistant to antimycin A. Succinate-cytochrome c reductase of these embryos was not noticeably affected.

To clarify the possible relations between these enzymes and developing muscle, determinations were made on cells cultured from 11-day-old chick embryo leg muscle. These monolayer cultures were kindly supplied by I. R. Konigsberg.

In these cultures, the specific activity of creatine kinase only was proportional to protein increase, in contrast to the other two enzymes, suggesting that it may be possible to detect a major increase in

myogenic elements of explanted chick embryos (table 7).

EFFECTS OF OTHER INHIBITORS

In order to better evaluate the results with antimycin A, experiments were also performed with other inhibitors, including (1) those that interfere with (a) oxidation or (b) phosphorylation in isolated mitochondria and (2) those that unbalance metabolic controls.

Dicumarol, 2,4-dinitrophenol (2,4-DNP), carbonyl cyanide *m*-chlorophenyl hydrazone (*m*-CCP), and thyroxine were tested in millimicromolar to micromolar

TABLE 7. Enzymes Assayed in Chick Muscle Tissue Culture

Group	Protein, $\mu\text{g}/\text{culture}$	Creatine Kinase*	Lactic* Dehydrogenase	NADH-Cytochrome c Reductase*
4-day controls	374	530	4.77	1.35
4 days with creatine	268	500	3.58	1.85
6-day controls	766	1130	4.84	1.41
6 days with creatine	675	910	5.32	1.42

* Specific activity per milligram protein shown.

Note: Samples were collected at 4 and 6 days of culture. Groups marked creatine were grown in a medium containing creatine hydrate. Four cultures were assayed separately in each group under conditions similar to those used for embryo explants. Average values for these groups at 4 and 6 days are shown.

concentrations as representatives of group 1. Specific effects on the heart were noted with oligomycin and dicumarol, oligomycin inhibiting heart formation in concentrations higher than 0.08 $\mu\text{g}/\text{ml}$ medium and dicumarol causing heart enlargement and general hemorrhage in concentrations higher than 0.05 $\mu\text{g}/\text{ml}$ medium. Amytal, arsenate, and thyroxine distorted the nervous system; *m*-CCP produced anomalies, with relatively small hearts developing. 2,4-DNP was not effective in changing the normal pattern of development, even in millimolar quantities.

Substances in group 2 ranged from higher concentrations of (a) Krebs cycle intermediates; (b) ADP, ATP; (c) H_2O_2 , phenazine methosulfate; (d) catalase, peroxidase, and cytochrome c; (e) *p*-chloro-mercuro benzoate and *n*-ethyl maleimide. These substances were tested alone and in combination with members of group 1. Oligomycin inhibition of heart formation could not be reversed by molecules that enhance mitochondrial ATPases such as 2,4-DNP, or by combinations such as dicumarol with phosphate, or amytal with ADP, that activate mitochondrial respiration. Such agents exhibit antagonism to certain effects of oligomycin in mitochondrial preparations.

PROJECTION

Under the conditions of culture now employed, protein values from hundreds of explanted chick embryos have failed to show consistent proportionality with either the initial stage (5, 6, or 7) at which explants were made or with their morphology at recovery. A consistent increase in protein in the chick embryo is measurable after 2.5 days of incubation. It would appear that the biochemical and morphological elaboration observed *in vitro* before this time occurs from the protein pool already present within the immediate environment extirpated with the embryo.

Mitochondria are one of the highly organized membrane systems being elaborated during formation of the heart. From studies of other workers with the cytochrome system in *E. coli* and with the photosynthetic apparatus of *R. rubrum*, it appears that higher than optimal concentrations of oxygen during growth may suppress structures capable of yielding energy via aerobic pathways. The findings with varying concentrations of oxygen in the present experiments suggest that such a system may operate in the early embryo. Coincident with the organization of the heart in the chick embryo, the NADH pathway of electron transport seems to play a more important role than the succinate pathway because the latter is less sensitive to antimycin A. The electron transport mechanism presumably provides conditions for liberating energy in the right place at the right time at a particular locus within the embryo because exogenous energy sources such as ATP or ATP-generating systems are ineffectual—assuming the uptake of ATP by the embryo. The type of energy source provided seems to be either in the form of ATP or an energy-yielding intermediate closely associated with ATP formation, because oligomycin, which acts by blocking an energy-yielding compound just before ATP formation, is also capable of suppressing formation of the heart. The use of inhibitors, however, can often be misleading, and these assumptions need to be borne out by study of P:O ratios in mitochondria isolated from these early embryos. More definite statements about such mechanisms can also be made when it is possible to demonstrate specific biochemical reactions catalyzed by the factor present in aqueous extracts of chicken liver and heart mitochondria that prevents antimycin A inhibition of cardiogenesis. To strengthen these hypotheses, it is also necessary to demonstrate the presence of this factor in mitochondria isolated from pooled, normal explants of early chick embryos.

DEVELOPMENTAL, KINETIC, AND IMMUNOLOGICAL STUDIES OF ENZYMES

Over the past few years, Yvon Croisille, working in the Laboratory of Experimental Embryology of the Collège de France, Paris, has devoted himself to a study of the formation of proteins during the development of the liver and kidney in the chicken. The use of immunochemical techniques permitted the demonstration of a minimum number of components that have been shown to appear progressively during embryonic life. Some of them can be detected only after hatching. Better characterization of most of these constituents was achieved by the combination of electrophoretic, immunochemical, and histochemical (especially enzymological) techniques.

During the year under review, Croisille, a Fellow of Carnegie Institution of Washington, first attempted to apply these techniques to the developing gonad in the chick embryo, believing that such an approach would provide some information about the effect of steroid hormones on the synthesis of specific proteins during the differentiation of the sex organs. Unfortunately, this aim could not be achieved. Antisera produced in rabbits against adult chicken ovary reacted only with serum and tissue-common components. Antiadult chicken testis sera were found to react specifically with adult testis extract, but no such specific reaction could be detected with extracts of embryonic testis (12 to 20 days of development).

Studies on hypoxanthine dehydrogenase and lactic dehydrogenase during development of liver and kidney were more successful and will be described in detail.

HYPOXANTHINE DEHYDROGENASE
IN THE CHICK

Since the early work of Needham, it has been accepted that, in the chick embryo, the mechanisms of nitrogen excretion are

elaborated in three stages: the embryo first excretes ammonia, then urea, and, finally, uric acid. Thus, urea was thought to be the major excretory product of the mesonephros. According to Fisher and Eakin, however, this scheme cannot be accepted fully, since uric acid appears to be the major product of excretion after the 5th day of development.

Hypoxanthine dehydrogenase (HXDH), a key enzyme in uric acid synthesis, was first reported by Morgan to be absent from embryonic liver and to appear in embryonic kidney at about the 15th day of development. Repeating and extending Morgan's findings, Kato (*Year Book 60*, pp. 379-399) found that a low, but measurable, HXDH activity is present in liver throughout embryonic life; suddenly, after hatching, there is a striking increase in activity of the enzymes in liver until the level characteristic of the adult is reached.

Although it was known that in the adult chicken HXDH activity could be demonstrated mainly in liver and kidney, until the very recent study by Chaube nothing was known of the formation of this enzyme during the early stages of kidney development. Chaube demonstrated that HXDH is present in the mesonephros as early as the 5th day of development, reaching its maximum activity at day 15, then decreasing. Just 2 days before it decreases in the mesonephros, it starts increasing rapidly in the metanephros and continues to increase until hatching.

According to these several observations, then, HXDH activity appears at three different sites at three very different periods during development. It was of interest to investigate whether HXDH activity in the three different tissues could be related to the presence of identical enzyme proteins.

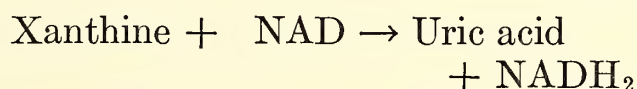
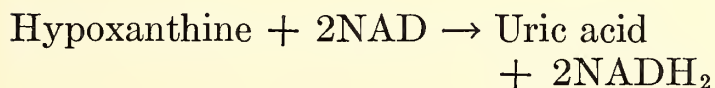
Croisille's aim was first to study the developmental pattern of the enzyme in

liver and kidney and then to try to characterize the enzyme, using as many criteria as possible in order to identify the proteins responsible for HXDH activity in the different tissues.

HXDH Activity in Adult and Embryonic Liver and Kidney

Richert and Westerfeld have shown that, in contrast to the HXDH found in cow's milk and mammalian liver, the avian enzyme is a dehydrogenase rather than an oxidase, since aerobic activity is negligible in comparison with the activity in the presence of methylene blue. Morell found that, in chicken liver, uric acid synthesis is associated with nicotinamide adenine dinucleotide (NAD) reduction. Landon and Carter later extended this finding to chicken kidney HXDH.

HXDH catalyzes the following reactions:



Croisille has determined HXDH activity in extracts of adult and embryonic liver and kidney of White Leghorn chickens. The organs have been homogenized in 0.05 M sodium phosphate buffer, pH 7.4, and centrifuged at 25,000g for 30 minutes, the supernatant fluid being used for enzyme assays. All experiments were performed with freshly prepared extracts.

To measure enzyme activity, 0.01 to 0.05 ml of extract was added to 1.0 ml of sodium phosphate buffer (0.05 M, pH 7.4) containing 0.4 micromole NAD and 0.2 micromole hypoxanthine. The mixture was incubated in silica cuvettes (1 cm light path) at 22°C, and the increment absorption at 290 mμ and 340 mμ was followed in a Beckman DU spectrophotometer for determination of the amount of uric acid and NADH₂ formed during

the reaction. Usually the reaction was read against a blank from which hypoxanthine was omitted (controls from which NAD or extract was omitted yielded the same results) and was followed minute by minute for a period ranging from 10 to 20 minutes. During that period the reaction appeared to be strictly linear with time.

The specific activities (millimicromoles of uric acid formed per minute per milligram protein) are recorded in figure 14. A slight HXDH activity is present in embryonic liver until hatching. This observation was not constant, however; several batches of embryonic liver extract showed no HXDH activity. In the mesonephros, enzyme activity starts slowly at day 5, increases, passes a maximum at day 14, and then decreases. The decrease coincides with the mesonephric involution that takes place from the 14th day on. Just 1 day before the decrease of activity in mesonephros, metanephric HXDH begins to increase until day 18, when a sudden drop in specific activity is noticed. This decrease is related to a striking increase in amount of other soluble proteins between 17 and 18 days of development; the absolute activity of HXDH remains constant. A similar decrease in specific activity of a number of enzymes has been reported by Russo-Caia at about the same period during development of the metanephros.

Despite the use of crude extracts, a good correspondence between uric acid and NADH₂ formation is observed. When hypoxanthine is used as substrate, average values of uric acid and NADH₂, calculated from the data of all experiments, are 3.54 and 7.21 millimicromoles per minute, respectively, indicating that the HXDH reaction was measured without interference from other systems, the production of 1 millimicromole uric acid being accompanied by the production of 2 millimicromoles NADH₂ as expected.

After hatching, the specific activity of HXDH increases dramatically in liver, whereas in kidney it decreases slightly.

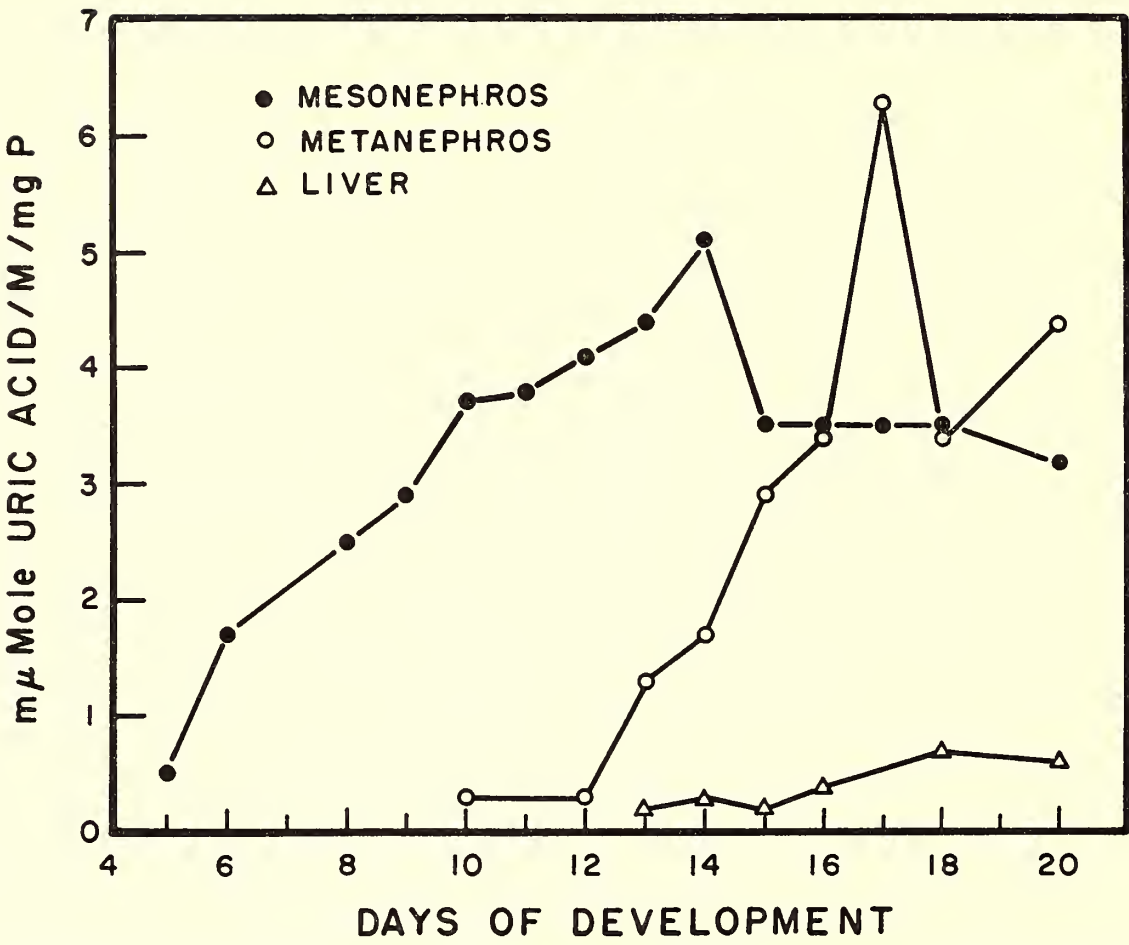


Fig. 14. Specific activity of HXDH in mesonephros, metanephros, and liver during development.

Thus, in the adult chicken, the specific activity of the enzyme is about 2 to 4 times higher in liver than in kidney (varying with the individuals; table 8).

Croisille has completely confirmed Kato's and Chaube's findings, it being clear that HXDH activity can be detected

in at least three different tissues at three different periods during development.

To determine whether this activity is an expression of the same enzyme protein in each of these three organs, a series of experiments was initiated in which kinetic, heat inactivation, electrophoretic, and immunochemical studies have been made on enzyme preparations from adult liver, adult kidney, and embryonic mesonephros.

TABLE 8. HXDH Activity in Liver and Kidney Just before and after Hatching

Stage	mμ Moles Uric Acid/min/mg Protein Formed in Liver Extract	mμ Moles Uric Acid/min/mg Protein Formed in Kidney
Embryo		
18-day	0.6	3.4
20-day	0.6	4.4
Chick		
3 days	9.5	...
6 weeks	6.6	3.0
12 "	4.3	2.4
14 "	2.7	1.3
16 "	4.1	1.8
18 "	4.0	1.0
20 "	4.5	1.6

CHARACTERIZATION OF HXDH FROM LIVER, METANEPHROS, AND MESONEPHROS

Kinetic Properties

Determination of Michaelis constant. As shown in figures 15 and 16, K_m values for hypoxanthine in the presence of 10^{-3} M NAD are identical whether the enzyme comes from adult liver, adult kidney, embryonic mesonephros, or metanephros. In contrast to the findings of Landon

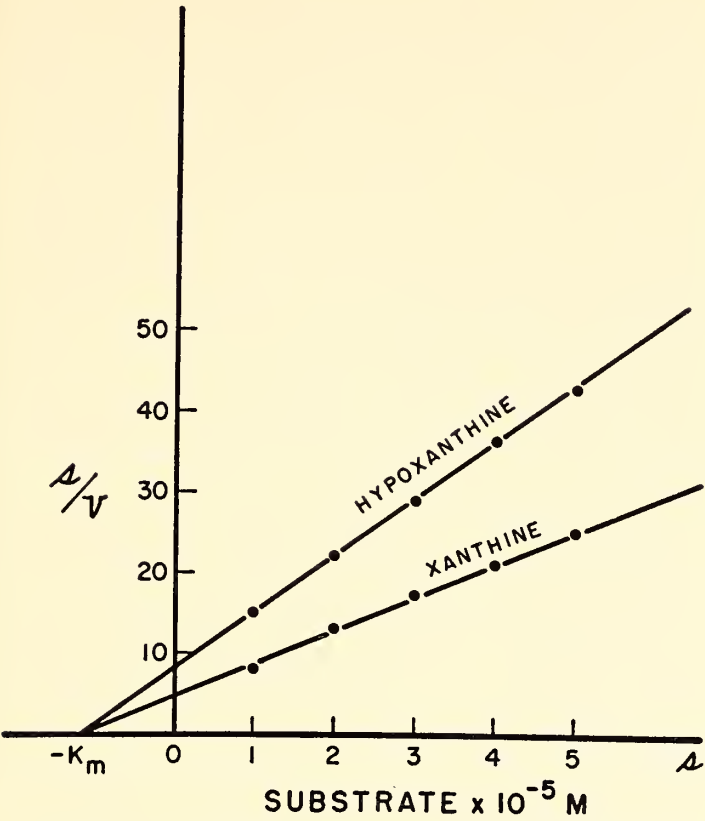


Fig. 15. Determination of K_m for hypoxanthine and xanthine with adult chick liver HXDH. Values found for the two substrates are identical (1.1).

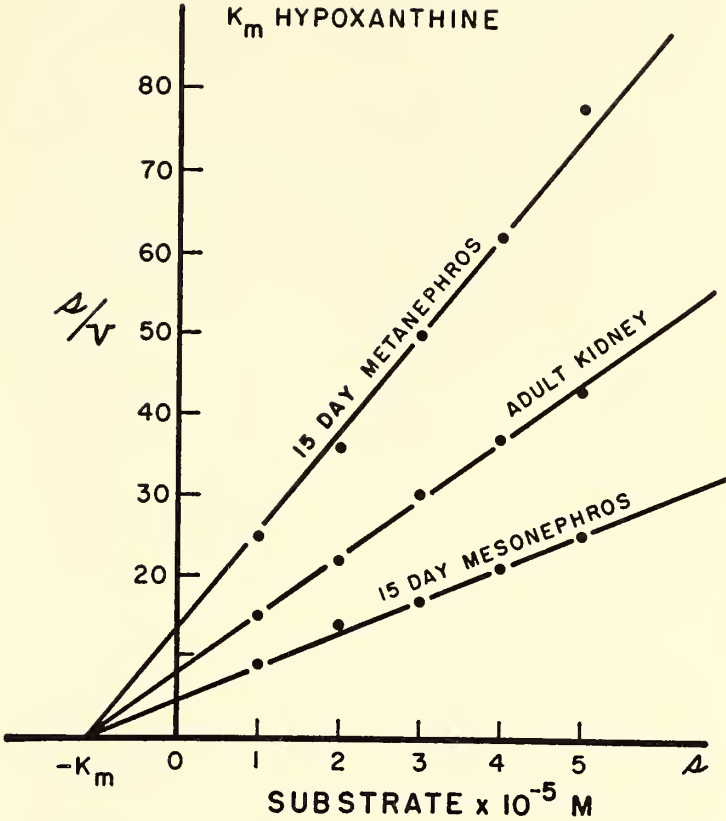


Fig. 16. K_m values for hypoxanthine are identical (1.1) whether HXDH comes from adult kidney, 15-day mesonephros, or 15-day embryonic metanephros.

and Carter, K_m values for hypoxanthine and xanthine in the presence of 10^{-3} M NAD appear to be the same.

Excess substrate inhibition. In the presence of 1 micromole hypoxanthine, the enzyme activity was decreased by 50 per cent in preparations from all three tissues.

Effect of hydroxylamine. It has been suggested that hydroxylamine can function as a hydrogen acceptor for the kidney enzyme, whereas, at the same concentra-

tion, it inhibits the liver enzyme. Croisille could not confirm these findings; from the present experiments it appears that 5×10^{-3} M hydroxylamine inhibits HXDH activity by about 20 per cent as compared with the standard reaction, regardless of the origin of the enzyme. Furthermore, hydroxylamine acts as a hydrogen acceptor for the kidney and liver enzyme as well. The result of the reaction is about 15 per cent as compared with the standard activity in the presence of NAD (table 9).

TABLE 9. Effect of Hydroxylamine on Chick HXDH

Substrates Used	Per Cent HXDH Activity with Respect to Enzyme Source			
	Adult Liver	Adult Kidney	15-Day Mesonephros	15-Day Metanephros
Hypo X + NAD (standard)	100	100	100	100
Hypo X + NAD + 5×10^{-3} M hydroxylamine	81	71	76	86
Hypo X + 5×10^{-3} M hydroxylamine	18	12	10	19
Hypoxanthine	1	1	1	1

TABLE 10. Heat Inactivation of Chick Liver and Kidney HXDH (75°C)

Time, minutes	Per Cent of Enzyme Inactivated		
	Liver	Kidney	Mixture of L and K
1	16	18	12
2	24	30	28
4	41	50	40
6	55	58	58
8	78	82	80
10	80	85	82
14	91	92	90
20	95	98	97

Heat Stability

So far, heat-inactivation experiments have been carried out only on adult liver and kidney enzymes. As shown in table 10, kidney and liver HXDH are affected to the same degree when heated at 75°C, provided that the same amount of enzyme is present at the beginning of the experiment.

Electrophoretic Properties

Unfortunately, hypoxanthine dehydrogenase could not be localized directly by the dehydrogenase technique after starch gel electrophoresis; agar gel electrophoresis, however, was more successful. In sodium barbital buffer (pH 8.2), HXDH of adult liver and kidney, mesonephros, and metanephros migrates as one component (pl. 1, fig. 17) toward the cathode. The enzyme can be localized by incubating the agar plates in the following mixture:

	ml
(a) Sodium phosphate buffer 0.05 M, pH 7.4	10
(b) NAD, 3 mg/ml	5
(c) Nitro BT, 1 mg/ml	15
(d) Xanthine 5×10^{-3} solution	20
(e) Phenazine methosulfate, 4 mg/ml	0.3

Immunochemical Properties

Quantitative precipitation. Antisera produced in rabbits against homogenates of adult chicken liver or kidney were found to inhibit HXDH activity pro-

gressively when increasing amounts of antiserum were added to the same amounts of liver, kidney, or mesonephros extract.

One unit of HXDH being defined as equivalent to the production of 1 millimicromole uric acid per minute under the standardized conditions described, it was found that the same amount of antiserum was required to inhibit completely 1 enzyme unit whether from liver, kidney, or mesonephros.

One enzyme unit was completely inhibited by 0.08 ml antiliver serum and by 0.12 ml antikidney serum (antisera 5 times diluted). The addition of normal rabbit serum, antitestis serum, and anti-egg yolk serum was without effect on HXDH activity.

Antiliver and antikidney sera, absorbed by either liver or kidney extract, no longer inhibited HXDH activity when tested against extracts of these tissues containing the enzyme.

That the antibodies reacting with HXDH are of the precipitating type is demonstrated by the fact that, at the equivalence point of precipitation (i.e., when no more enzyme activity is detectable in the supernatant fluid), nearly all the initial activity can be detected in the precipitate.

This observation leads to the conclusion that the sites of enzymatic and antigenic activity of the HXDH molecule are completely different. Furthermore, previous incubation of the enzyme with hypoxanthine and NAD (which combine with the enzymatic active sites) does not protect HXDH against precipitation by antibodies.

Double diffusion tests in agar gel (Ouchterlony). If antiliver serum is tested against adult chicken liver extract in double diffusion tests, a number of precipitation lines can be observed. As shown in plate 1, figure 18, incubation of double diffusion plates in the same mixture used for electrophoresis plates permits identification of a single precipitation line, corresponding to HXDH. Further-

more, when antiliver serum is used, this technique appears to demonstrate complete immunochemical identity of HXDH whether from adult liver, adult kidney, embryonic mesonephros, or embryonic metanephros.

More recent double diffusion experiments, in which three different antiliver sera and one antimesonephros serum were used, clearly confirmed the previous findings. No differences could be detected in the enzymes from liver, intestine, pancreas, kidney, and mesonephros.

However, when *antikidney serum* was tested against liver, intestine, pancreas, kidney, and mesonephros extracts, or purified kidney HXDH, a very faint spur was noticed at the sites where kidney or mesonephros HXDH was to be compared with liver, intestine, or pancreas enzyme. This observation suggests that antikidney serum contains antibodies reacting with some antigenic determinant present on kidney and mesonephros HXDH, but not present on the liver, intestine, and pancreas enzyme. As expected from these results, antikidney serum absorbed with liver extract no longer reacted with liver, intestine, and pancreas HXDH, but a very faint precipitate was observed with kidney and mesonephros enzyme. (Antiliver sera absorbed with kidney extract no longer reacted with HXDH whatever the source of the enzyme.)

Thus, there may be very subtle differences between the liver and kidney enzymes. Are there at least two closely related enzymes in the chick tissues, one present in mesonephros and kidney, the other in liver, intestine, and pancreas? In the three latter tissues,

HXDH undergoes the same developmental changes (very low concentration just before hatching, and sudden increase after hatching). Are the minor differences meaningful? If kidney and mesonephros extracts or purified kidney HXDH are individually tested against antiliver, anti-kidney, and antimesonephros sera, no spur can be observed. To explain this puzzling situation, and before any decisive conclusion can be reached, more experimental evidence obtained with a variety of antisera has to be produced.

Immunoelectrophoresis. More direct evidence that the precipitation line that appeared to be related to HXDH in double diffusion tests really corresponds to the enzyme is provided by immunoelectrophoresis. After immunoelectrophoresis of extracts of adult liver, kidney, or mesonephros in the presence of antiadult liver serum, only one precipitation line gives a color reaction when the plates are incubated in phosphate buffer containing xanthine, NAD, and Nitro BT (pl. 1, fig. 19). This line is localized exactly in the area where the enzyme could be demonstrated after simple agar gel phoresis. These findings are convincingly supported by the fact that purified liver or kidney enzyme, when tested against antiadult serum, yields only a single precipitin band that corresponds perfectly to the line previously described.

Purification

Although the experimental data strongly indicated that there was no interference from other systems, it was decided to purify at least the adult liver and

TABLE 11. Purification of Chick Liver HXDH

Fraction	Specific Activity	Enzyme Units	Yield, %
Homogenate 25,000 × g sup	5	2400	100
Heat step 56°C	9	2400	100
40–55% ammonium sulfate	23	1600	66
Sephadex G-200	98	1300	54
DEAE	545–660	580	24

kidney enzymes to obtain more convincing evidence.

After the organ extracts were heated at 56°C for 5 minutes, the 40 to 55 per cent ammonium sulfate fraction was prepared and subjected to gel filtration on a Sephadex G-200 column. As shown in table 11, this step permitted a 20-fold purification with a relatively good yield. After Sephadex filtration the enzyme fraction was adsorbed on a DEAE cellulose column and eluted with a linear sodium phosphate gradient (0.005 to 0.25 *M*). This procedure permitted a 100- to 130-fold purification, the final yield being 24 per cent.

All the results obtained with these purified enzyme preparations corroborated previous findings with crude extracts.

Conclusions

So far, all the experimental evidence points to the conclusion that HXDH activity in different tissues of the chick can be attributed to the presence of the same enzyme protein or to two very closely related proteins. The enzyme is synthesized in at least three different tissues at three different periods during development. It might be argued that the absence or low level of HXDH activity in embryonic chick liver is not due to the absence of enzyme protein but rather to the presence of the enzyme in an inactive form. However, dialysis does not increase HXDH activity of embryonic liver extract. Furthermore, the addition of embryonic chick liver extract to another enzyme preparation does not affect the activity of that preparation. Thus, it seems that there is no dissociable inhibitor in embryonic liver. On the other hand, absorption experiments of antiadult liver serum with embryonic liver extract indicate that very little, if any, enzyme protein is present in 9- and 12-day-old embryonic chick liver.

Attempts to interfere with HXDH synthesis by means of injections of

hypoxanthine or uric acid in the 3-day-old embryo have so far failed.

With regard to the distribution of HXDH in other tissues of the chick, it has been found that the enzyme also exists in adult intestine and pancreas, but not in testis, heart, muscle, brain, or serum. So far, experimental evidence suggests that the enzyme is absent from these tissues during the whole developmental period.

During embryonic life, then, HXDH activity is specifically localized in the kidney, whereas, after hatching, it is mainly present in the liver.

Lactic Dehydrogenase in the Adult and Embryonic Chick

Lactic dehydrogenase (LDH) of most vertebrate tissues has been reported to exist in five distinct molecular forms as revealed by starch gel electrophoresis. Two main forms of LDH have been recognized: one predominant in heart, the other predominant in skeletal muscle. These two forms are distinct entities as judged by their physical, kinetic, and immunological properties.

Purified "heart" LDH can be dissociated into four identical subunits (A) by treatment with guanidine HCl and mercaptoethanol. Purified "muscle" LDH also appears to be composed of four identical subunits (B), as shown by Apella and Markert and by Cahn and his associates. The subunits A and B have different electrophoretic mobilities. Peptide patterns from heart LDH (LDH₁) are different from those of muscle LDH (LDH₅). Moreover, amino acid analysis shows that the two main forms of LDH are different in their primary structure. Thus, A and B appear to be very different polypeptides.

These data led Markert and Kaplan to the formulation of the following hypothesis: LDH₁ is a tetramer composed of four identical A subunits; LDH₅ is a tetramer composed of four identical B subunits (the structure of A and B being determined by two different genes). This

hypothesis predicts that, if both genes are active, the combination of subunits A and B in all possible associations of four would yield five distinct molecular forms all having LDH activity ($1 = A_4B_0$; $2 = A_3B_1$; $3 = A_2B_2$; $4 = A_1B_3$; $5 = A_0B_4$).

As was mentioned previously, starch gel electrophoresis of most vertebrate tissues permits the demonstration of five forms of LDH. The most positively migrating corresponds to LDH₁. Forms 2, 3, and 4 appear to be intermediate with respect to their electrophoretic and immunochemical properties.

In the course of a study concerned with protein changes during embryonic development of the chick liver and kidney, Croisille decided to initiate some experiments on the development of LDH. His decision was prompted by the observation by Markert and Ursprung that LDH patterns exhibit tissue and ontogenetic specificity.

The first aim of the present investigation was to study the LDH patterns of different tissues in the adult chicken.

Surprisingly, the LDH patterns of most of the adult chicken tissues studied yielded seven distinct bands after starch gel electrophoresis. Since additional bands had occasionally been described in the literature, but usually discarded as artifacts, it was decided to investigate whether the two additional bands observed by Croisille could be accounted for as artifacts.

In this report, the details of the techniques used as well as the changes in the LDH patterns of liver and kidney during development will be described.

Starch Gel Electrophoresis

For the preparation of starch gels, 13 grams of hydrolyzed starch (Connaught) per 100 ml of 0.0235 *M* boric acid, 0.0094 *M* sodium hydroxide buffer were used. The pH of this buffer is initially 8.9, but during the preparation of the gel it drops to 8.4. The ends of the starch strips were connected to the buffer tanks (0.235 *M*

boric acid, 0.094 *M* sodium hydroxide) by cellulose sponge bridges. This procedure was found to avoid shrinkage and swelling of the starch, which were commonly observed when other connections were used; moreover, it permits a constant voltage at the ends of the starch for periods ranging from 18 to 24 hours. A voltage gradient of 6 v/cm was applied, and the experiments were usually run for 18 hours.

The organ extracts are prepared in the following way: 1 gram of tissue is homogenized in 1 ml of sodium phosphate buffer (0.05 *M*, pH 7.4) and centrifuged at 25,000*g* for 30 minutes; 0.05 to 0.1 ml of extract is adsorbed on two sheets of Whatman 3 MM filter paper. The paper, when sufficiently dry, is inserted into a slit previously cut in the starch.

After electrophoresis the starch is sliced horizontally. The slices are incubated for 1 hour at 37°C in the dark in sodium phosphate buffer 0.05 *M*, pH 7.4, containing Nitro BT, NAD, KCN, lactate, and phenazine methosulfate.

LDH in Adult Chicken Tissues

Under the conditions described, several adult chicken organs (liver, kidney, testis, ovary) yield an LDH pattern of seven bands. As described in the literature, two main forms (LDH₁ and LDH₅) and the three intermediate forms were observed. Besides these five forms, two more positively migrating bands (*a* and *b*) have been found (fig. 20; pl. 1, figs. 21 and 22). Since this seven-band pattern was completely reproducible, the following experiments have been initiated to study the two extra bands:

1. No reaction is observed when the strips are incubated in the previously described mixture from which lactate was omitted.

2. Since it had been suggested that additional bands could be attributed to overloading of the gel and avoided by dilution of the extract, serial dilutions ($\frac{1}{2}$, $\frac{1}{4}$, $\frac{1}{8}$, $\frac{1}{16}$, $\frac{1}{32}$) of the original adult liver

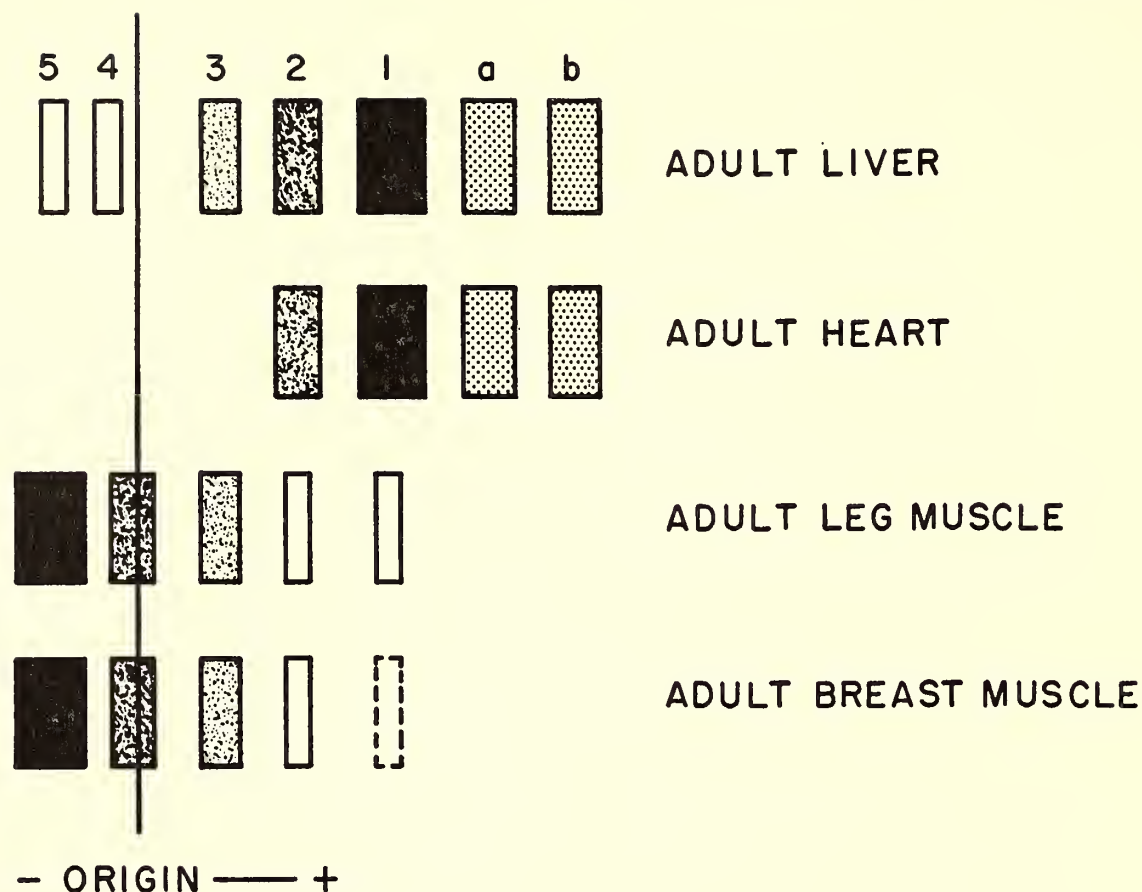


Fig. 20. Schema of the LDH pattern of adult chick liver, heart, and muscle extract.

extract have been made. From these experiments it appeared that, during dilution, bands 5, 4, and 3 fade away and disappear well before the intensity of the additional bands *a* and *b* is affected.

3. It was also thought that the substrate could be involved in the manifestation of additional bands. Different preparations of lactic acid have been used: sodium lactate syrup (Fisher Scientific Company), lactic acid sodium 40 per cent solution (Mann), lactic acid calcium salt (Mann). All these preparations yield the same result.

4. Preliminary experiments having been conducted at 12°C, it was thought that the temperature rise during the 18-hour run could perhaps account for the observation of additional bands, and so experiments have been conducted at 3°C; after 18 hours the temperature checked directly in the gel was 9°C. Whether run at 12°C or 3°C, the same seven-band pattern was obtained. There is, however, a difference in migration: at 12°C, two forms migrate to the cathode and five to

the anode; at 3°C, three to four forms migrate to the cathode.

5. Electrophoresis in phosphate-citrate buffer pH 7.0, instead of borate buffer pH 8.4, also yields a seven-band pattern.

6. If, after a first electrophoresis, the zones corresponding to bands *a*, *b*, 1, and 2 are cut out and subjected to a second 18-hour run, each band migrates to the same place as during the first run. This experiment makes it clear that each of the seven bands corresponds to a component with a different electrophoretic mobility (pl. 1, fig. 23).

7. Different extraction procedures were tested. If the organs are extracted in distilled water pH 6.6, in sodium phosphate buffer pH 7.4, in sodium barbital buffer pH 8.2, or in borate buffer pH 8.9, the same seven-band pattern is observed.

8. Patterns obtained with freshly prepared extracts, extracts stored at -20°C for several weeks, and extracts kept for 24 hours at room temperature are identical.

LDH during Embryonic Development of Liver and Kidney

Embryonic liver extracts, in addition to the seven forms already described, contain two more positively migrating forms, designated E. These two forms are observed only during embryonic life. They are clearly visible in embryonic liver between 6 and 16 days of incubation. From the 16th day on, they tend to fade away, and at hatching they have disappeared (fig. 24; pl. 1, fig. 25).

A similar transitory band is found in mesonephros. It has the same mobility as bands E in embryonic liver and is present from days 8 to 15 of development (pl. 1, fig. 26).

To date, no transitory embryonic bands have been found in heart, brain, metanephros, or intestine.

Conclusions

From these experiments it can be concluded that the seven bands observed in several adult tissues can be related to

the existence of seven electrophoretically distinct components having LDH activity. Moreover, in embryonic chick liver, nine such components are clearly demonstrable.

Evidence for the existence of seven LDH forms in several tissues of the adult rat has been presented recently by Conklin and Dewey.

It might be argued that in the present experiments no attempt has been made to apply equivalent amounts of enzyme for comparative studies. It is a fact that rather high amounts of protein have been applied, but the application of smaller amounts would not have permitted the detection of the transitory forms.

So far, it is not clear whether the additional bands observed are true isozymes or whether they represent incomplete LDH forms such as trimers or dimers. A striking fact is that additional bands *a* and *b* are observed only in tissues where LDH₁ is predominant.

Whatever the explanation, the reproducibility of the results was considered to justify their detailed description.

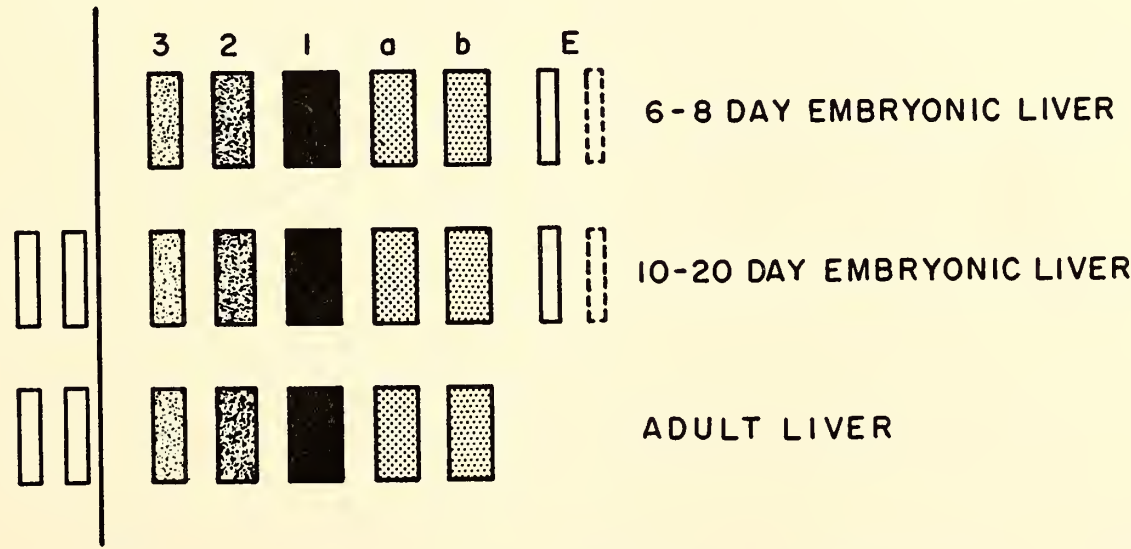


Fig. 24. Schema of the changes in LDH pattern of liver during embryonic development.

CLONAL ANALYSIS OF MYOGENESIS

The differentiation of muscle cells in culture has engaged I. R. Konigsberg's interest for several years. A new approach to the analysis of this problem was

reported in *Year Book 61* (pp. 397-400). The cell plating technique of Puck and his associates was applied to freshly isolated cell suspensions prepared from

embryonic leg muscle. Approximately 1 out of 10 of the discrete colonies that formed during the 2-week incubation period could be identified positively as a colony of muscle cells. The significance of the ratio of muscle to non-muscle colonies was, at the time, of primary interest.

Clarification came, as frequently happens, from a line of investigation designed primarily to answer another question. A parallel investigation of the role of cell density in myotube formation in culture indicated that medium recovered from confluent mass cultures and reutilized promoted precocious differentiation. When such "conditioned" medium was used in single cell plating experiments a puzzling variability was noted. Both the plating efficiency and the rate of increase of colony size were increased in conditioned medium. Myotube formation was, as in monolayer culture, also precocious, but the percentage of muscle colonies, scored at the end of 2 weeks, was extremely variable. However, occasional lots of conditioned medium did yield a proportion of muscle cell colonies 2 to 4 times the ratio observed with unconditioned medium. This observation suggested that the relatively low frequency observed in unconditioned medium might not reflect the competence of the cell population per se but rather the inadequacy of the culture environment (pl. 2, figs. 28, 29).

The variability pointed to a threshold of the effects of conditioned medium; therefore, Konigsberg undertook a systematic appraisal of the various parameters of its preparation. In time, a technique evolved that has yielded more consistent results.

Table 12 summarizes the results of all the tests, using the conditioning protocol finally adopted, conducted between June and December of 1962. It represents a total of 20 individual trials with a pooled sample size of 69 petri plates. The average plating efficiency, it will be seen, is somewhat higher than the estimated 10 per cent attained with unconditioned medium. This value is still well below the range of plating efficiencies reported for long-term cultivated cell strains. There is no reason to assume that it represents an upper limit, however.

Of greater interest from a developmental standpoint is the higher "frequency of differentiation" that results when properly conditioned medium is used. This higher frequency represents approximately a fourfold increase over Konigsberg's earlier results using unconditioned medium.

The distribution of the individual values summarized in table 12 is graphed in figure 27. Both plating efficiency and frequency of differentiation show reasonably good agreement to a normal distribution. The slight skewness in the

TABLE 12. Plating Efficiency and Frequency of Muscle Differentiation in Single Cell Plating Experiments Using Conditioned Medium (June–December 1962)

No. Experi- ments	Total No. Petri Plates	Total All Colonies	Plating Efficiency		Total No. Muscle Colonies	Frequency of Muscle Differentiation	
			$\left(\frac{\text{Colonies}}{\text{Cell plated}} \times 100\right)$			$\left(\frac{\text{Muscle colonies}}{\text{Total colonies}} \times 100\right)$	
			Av. \pm s.d., %	Range, %		Av. \pm s.d., %	Range, %
20	69	3104	17.6 \pm 5.9	5.5–37	1313	41.3 \pm 12.1	14.8–64.6

The averages, standard deviations ($s(x - \bar{x})^2/n$), and ranges are based on the pooled sample of 69 petri plates.
Inoculum sizes (cells/petri plate) were 100 (1 experiment), 200 (11 experiments), and 400 (8 experiments).

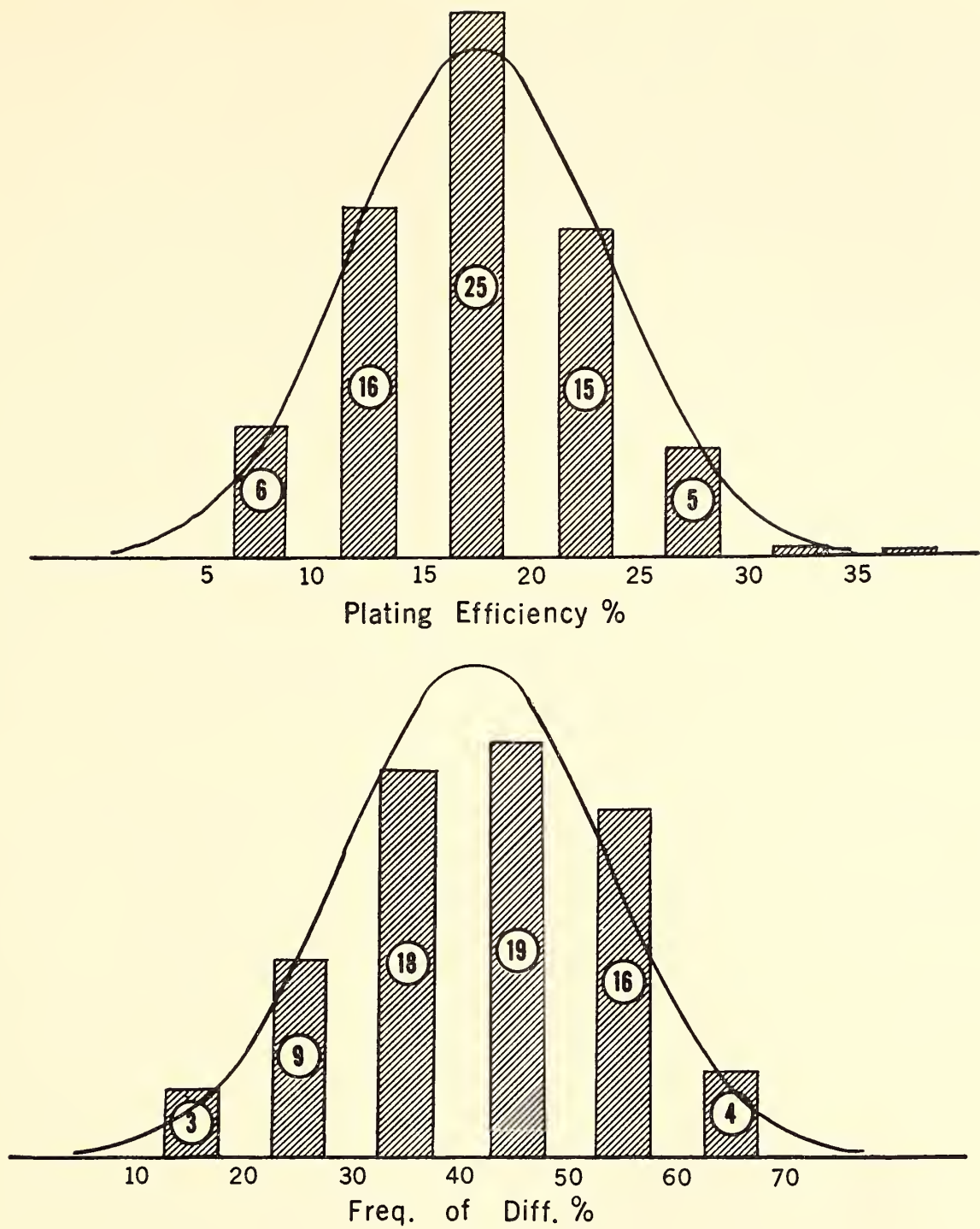


Fig. 27. Distribution of plating efficiency and frequency of differentiation for the sample of 69 petri plates. Bars represent numbers of plates having values falling within the percentages marked on the abscissa. Solid curves are the theoretical normal distributions of samples of 69 items having the same means and standard deviations (see table 12).

distribution of frequency of differentiation might have been anticipated. With larger numbers of muscle colonies per petri dish, the probability that two such colonies might overlap and be scored as one would be greater. Thus, the higher values of the frequency of differentiation are obscured.

This experience with conditioned medium emphasizes the critical role of the medium in the subsequent developmental

behavior of isolated cells. More is involved than merely providing an adequate milieu for survival and growth. Indeed, conditioning schedules alternative to the one finally adopted frequently support much higher plating of luxuriant colonies, the vast majority of which are devoid of any indication of muscle differentiation.

One is reminded of the frequent statements that the component processes of development are experimentally separa-

ble; that survival and growth can occur under conditions that do not favor differentiation. It would seem more prudent, therefore, to avoid, in general, reading into negative data more than that particular culture conditions may be inappropriate for supporting differentiation.

Many alterations of the medium probably occur during the conditioning process, depletions as well as additions. The work of Eagle and his associates indicates that the effectiveness of conditioned medium may, at least in part, be due to the extremely "leaky" nature of the animal cell in culture. Molecular entities lost from cells accumulate in the medium and may, when a sufficiently high concentration is reached, prevent further losses by simple mass action. This

be selected with a high degree of accuracy. As soon as single cells attach and stretch out on the substratum, they can be classified as belonging to one of two major morphological groups (pl. 3, fig. 30). One cell type has a distinctly bipolar shape with a small ruffled membrane, usually restricted to one tip of the cell. Strikingly different in appearance, the other cell type is greatly flattened with a noticeably larger surface area. It has a more extensive ruffled membrane with no discernible localization. Because of its flattened shape, nuclear detail and cyto-organelles are more sharply delineated. It soon became apparent that the muscle colonies were derived from the bipolar cells. Moreover, at all stages of colony formation, muscle cell colonies could be distinguished from colonies of "fibroblast-like" cells by

TABLE 13. Tests of Reliability of Morphological Criteria of Cell Type

Class of Cell	Total No. Cells	Total No. Colonies	Distribution of Colony Types	
			"Fibroblastic"	Muscle
"Fibroblastic"	99	61	52	9
Bipolar	72	53	2	51

leakiness may also help to explain the advantages of organ culture over cell culture in fostering differentiation as well as the numerous demonstrations of the dependency of differentiation upon a minimal mass of cells. The use of conditioned medium has, in Konigsberg's studies, proved an effective means of circumventing such requirements.

With the much higher frequency of differentiation afforded by adequately conditioned medium, more critical examination of clonal development became feasible. Single cells could be followed through the stages of colony formation and differentiation with a greater probability that a reasonable fraction of cells selected would yield muscle colonies. It was soon discovered, however, that the muscle-colony progenitors could, in fact,

virtue of this stable difference in cell shape.

To test the reliability of this criterion of cell type, Konigsberg and his able assistant, F. J. Kupres, scanned several series of cultures, located individual cells, and marked their positions on the petri plate, using colored inks to record their predictions. The results were scored after fixation and stained on the 13th day of culture. They are presented in table 13. Approximately 85 per cent of the viable flattened cells gave rise to fibroblast-like colonies, and 96 per cent of the viable bipolar cells developed into muscle colonies. The smaller number of flattened cells that gave rise to muscle colonies may represent the error in recognizing these differences in cell shape.

This finding illustrates the advantages

of clonal analysis. Although similar differences in cell shape were observed earlier in monolayer cultures, it was not possible to assess their significance. It has been amply demonstrated that cell morphology in culture can be altered drastically by changing the texture of the substratum or the composition of the medium. Under the conditions of these experiments, it is clear that the differences in cell shape reflect intrinsic, stable differences between cells. By immediate spatial separation of the cells of the inoculum, such differences are readily detected and the overgrowth of one cell type by another is prevented; for this reason, in Konigsberg's earlier experiments, before the use of conditioned medium, he was able to detect muscle colonies despite their relatively low frequency.

Selecting muscle cells on the basis of these morphological criteria, the positions of single cells were marked, and photographic records were made, at regular intervals, from the 1st through the 13th day of culture (pl. 4, fig. 31; pl. 5, fig. 32). Analysis of the records may be summarized as follows:

1. Myoblasts divide initially (day 1 to day 4) with a mean generation time (MGT) of the order of 12 to 18 hours. This is considerably faster than the cells of the tissue of origin (MGT = 48 hours) or the same cells in monolayer culture in unconditioned medium (MGT = 24 hours).

2. During this initial period the colony consists of a discrete locus of dispersed cells. (The same is true also for fibroblast-like colonies.) Muscle cells observed to be in contact are generally associated end to end.

3. Sometime between day 4 and day 6, the formation of long multinuclear myotubes is initiated (earlier than previously observed in unconditioned medium, namely, day 6 to day 9). On the basis of previous evidence (Konigsberg's and others'), it is assumed that myotubes form by the fusion of cells.

4. At the time myotubes are first observed, and at all subsequent stages, a variable number of mononucleated cells remain unassociated. Subsequent enlargement of the myotube network most probably occurs by incorporation of such mononucleated cells, which, while free, increase in number by mitotic division. (The best evidence indicates that the myotube nuclei themselves are non-proliferative.) Colonies in which myotube formation involves all the cells remain minute.

5. The network of myotubes enlarges subsequently by increase in length of the individual "fibers" as well as by increase in the number of myotubes. By the 13th day of culture a macroscopic muscle colony has formed which even with the unaided eye can be distinguished from the colonies of fibroblast-like cells. Colonies of fibroblast-like cells have a regular circular outline with no obvious structural detail. Muscle colonies, in contrast, have an irregular periphery, are frequently elongated, and present a "fibrous" appearance.

6. Examination of muscle colonies derived from single cells, using optics, reveals the presence of typically cross-striated myofibrils in the myotubes.

Finally, in order to definitely test the thesis that muscle colonies do, in fact, arise from *single* cells, a number of myoblasts (bipolar cells) were studied in physical isolation. After the positions of such single cells were located and marked, a glass cylinder was cemented in place over the cell with silicone grease. The chamber formed by the cylinder and the floor of the petri plate was filled with medium. A small coverslip was placed on the top of the cylinder to permit examination of the floor of the chamber with phase contrast optics. In this way confirmation was obtained that the chamber contained only the one cell originally observed. Under these conditions the possibility of contamination by a foreign cell is completely ruled out. At the end of approximately 2 weeks of culture, it is observed

that such isolated cells have indeed given rise to colonies of differentiated muscle (pl. 5, fig. 33; pl. 6, fig. 34).

It is clear that single myoblasts can, through cell multiplication, give rise to a colony of differentiated muscle of macroscopic dimensions. The capacity to differentiate is not lost during the many successive cell divisions that ensue. Neither does the observed brevity of the generation time seem to adversely affect the capacity to differentiate.

Of all the parameters investigated so far, the type of medium used has the greatest influence on the frequency with which differentiated colonies are detected. In a problem area like this, which has suffered from "overgeneralization" in the past, it would seem that progress can be best served by parsimonious interpretation of the data. However, it may not be overly rash to suggest that, when a specific type of differentiation *cannot* be achieved in culture, the medium used may be one of the many factors contributing to failure.

It would be of interest to determine when stability is acquired by the prospective myoblast. The possibility cannot yet be excluded that some of the colonies of fibroblast-like cells are derived, in fact, from a prospective myoblast in which stability had not been established. (The morphological evidence indicates that at 12 days the leg musculature consists of a heterogeneous population of cells at various stages of differentiation.) Consistent differences are observed between fibroblast colonies, which would probably not be obvious in mixed populations of these same cells, suggesting that Konigsberg is probably not dealing with a single type of nonmyogenic cell.

An additional source of the fibroblast colonies other than true fibroblasts (or other bona fide cell types) or unstable myoblasts is their possible origin from a recognized cell type by some culture-induced alteration. Since Konigsberg is able to distinguish between muscle cell progenitor and fibroblast-like cell within

the first 24 hours after isolation, such alteration, if it occurs, must occur rapidly. This is not unlikely, however, and there is some evidence in the literature that indicates rapid "dedifferentiation."

Probably the most unexpected finding to date is the recognition that myoblasts and fibroblast-like cells could be discriminated on the basis of gross morphological criteria alone. The distinctive bipolar shape of the myoblast is a stable characteristic perpetuated through the many cell divisions that ultimately produce the macroscopic colony. At all stages, even before myotube formation, colonies of myogenic fate can be recognized by the characteristic shape of the component single cells. Irrespective of the exact nature of the molecular basis of this feature, it quite obviously is a differentiated character and one that does not conform to the dictum that differentiation and cell proliferation are mutually antagonistic processes.

By definition, a myoblast is an embryonic cell which will become a muscle cell or the progeny of which will differentiate into muscle cells. Although it can be determined experimentally whether cells from a particular region will become muscle cells, in practice it is impossible to determine whether or not any particular cell is a myoblast. At best, the observer can only approximate an identification by choosing a characteristic feature of the differentiated cell and determining when he can detect the first indication of this feature. However, is a cell bearing this first indication of a differentiated feature (a myofibril, for example) a myoblast, a muscle cell, or something in between? It seems paradoxical that a technique of such recent vintage as single cell plating should finally permit the concept of myoblast to be defined operationally as well as in theory.

It is equally surprising that the bipolar shape attributed to prospective myoblasts should prove to be so reliable a criterion, a

criterion, moreover, not based on any definitive property of the fully dif-

ferentiated cell but peculiar to the embryonic state.

INDUCTIVE TISSUE INTERACTIONS

EPIDERMAL-DERMAL INTERACTIONS IN THE FORMATION OF FEATHERS, SCALES, SPURS, AND BEAK

The epidermal derivatives of birds are products of the developmental interaction of two tissues of different embryonic origin. Unique to this system is the diversity in form exhibited by the final product in clearly defined regions of the body. The origin of this marked regional specificity presents a number of intriguing problems, which are being explored by Mary E. Rawles.

Her approach, which has furnished interesting and significant information, is a reciprocal exchange of the two reacting tissues. Such exchange involves removal of small areas of skin from different regions of the body of the embryo at varying developmental stages; separating the ectoderm (prospective epidermis) from the mesoderm (prospective dermis); recombining the two in new contact relations; and transplanting the "chimeras" thus formed to the chorioallantoic membrane for further development.

Results of such recombinations have shown that the ectoderm acquires its specific properties through reaction to inductive stimuli arising in the underlying mesoderm. The reaction is a mutual one and dependent on the properties of both tissues. In this reaction many different factors are brought into play, variation in any one of which may have a pronounced effect on the final product. Epidermal-dermal recombinations have shown, for instance, that both the inductive capacity of the dermis and the competence of the epidermis vary with position on the body and with developmental stage. Such differences in the

reacting tissues can be demonstrated in terms of the final product only after exchange is made between the two components.

The inductive capacity of the dermis from different regions, such as the tarsometatarsus, middorsum, spur, and beak, when tested in combination with epidermis from another region, reveals differences that may be compared in terms of their relative strength, i.e., intensity of the dermal stimulus. Dermis from the tarsometatarsus appears to be the "weakest" as well as the latest in ontogeny to acquire demonstrable inductive capacity. It does not reach a degree of intensity sufficiently high to elicit a specific scale-forming response in overlying epidermis until approximately the 13th day of incubation. Dermis from the spur is strongly inductive at 9 days and remains strong throughout the age span tested (9 to 15 days). Similarly, dermis from the beak and middorsum has intense inductive capacity at 5 days—the earliest stage tested—and continues to have a high inductive capacity through the subsequent stages (6 to 8½ days). Thus, there is no loss of, or decrease in, inductive power within this wide age range.

The ability of the middorsal epidermis (5 to 8½ days) to respond to specific inductive stimuli from the dermis of the 13- to 15-day tarsometatarsus changes rapidly within a relatively short period between 7½ and 8½ days. Scales are induced in the earlier 5- to 7½-day epidermis, but the later 8- to 8½-day epidermis continues to develop in a feather direction. Epidermis from the foot (tarsometatarsus) exhibits less change with age than that from the middorsum. Between the ages of 9 and 13 days, the response of the tarsometatarsal epidermis to middorsal dermis is strictly in a

feather-forming direction. Differences in the structural quality of the feathers, however, are notable; those arising from 9- to 11-day epidermis are structurally normal; those from epidermis of the later stages become increasingly aberrant.

The differences noted above in response of epidermis from the middorsum and from the tarsometatarsus, interestingly enough, can be entirely masked (or erased) if each is placed in contact with

dermis from the beak—a stronger inducer. In response to beak dermis (5 to 8½ days) both the 8- to 8½-day middorsal epidermis and the 13-day foot epidermis develop perfect beaks. The ability of the epidermis to alter its course of differentiation at relatively late development stages is, indeed, remarkable.

These examples will serve to illustrate a few of the complexities involved in epidermal-dermal interaction.

SPATIAL ORGANIZATION IN EMBRYOGENESIS

For several years Robert L. DeHaan has been concerned with the large problem of spatial organization in embryogenesis, directing his attention to such questions as: Why do particular cells occupy specific positions in the embryo at any given stage? What causes cells to move about from one location to another? What forces guide such movements? Is there a direct relation between the position of a cell within a primordial region and its later differentiation during organogenesis? He has concentrated, in most of his earlier studies, on the precardiac mesoderm of the early chick embryo, using techniques that have provided information about the position, shape, and movements of cells, and their contact relations with one another. This approach has been, and no doubt will continue to be, instructive.

A second, equally valid, set of questions concerning spatial organization may be derived from the fact that the shape and structure of organs and tissues, and the arrangement of the component cells, are controlled or influenced by genetic factors. Other workers have already gained insights into the genetics of patterned structures, including the concept of pre-patterning in organisms of different genotypes and the effects of the genome on cell division; but how information embodied in the genetic code controls the migratory behavior or position of a cell is a complete mystery. It cannot be said, in

fact, that such control exists at the cell level rather than at the level of statistical probabilities within cell groups. Answers to such questions have awaited the development of culture techniques and of methods of separating and recombining cells and tissue fragments, of known or controllable differentiative fate, taken from an organism in which many relevant genetic mutants are known. Such techniques, which are used routinely on tissues from vertebrate embryos, have so far not been applied successfully to organisms in which ample genetic information is available, such as *Drosophila*.

An initial attack on the problem has been made by Ernst Hadorn and his co-workers at the University of Zurich. They have based their approach on the observation (first made by Ephrussi and Beadle three decades ago) that fragments of the primordial hypodermal thickenings, or "imaginal discs," from *Drosophila* larvae, differentiate and metamorphose as implants within the abdomen of a second host larva, during the pupation and hatching of that host. Thus, a larval host, injected with a fragment of leg, wing, or genital imaginal disc, will carry in its abdomen, as an adult fly after metamorphosis, a well formed part of the leg, wing, or genital apparatus derived from the donor fragment. With this method, these investigators have described fate maps of imaginal discs, have studied processes of regeneration and regulation

in fragmented discs, and have combined fragments of disc tissue containing different genetic markers in order to study the organization of bristle patterns in the resulting mosaic organs.

At the generous invitation of Professor Hadorn, DeHaan spent ten months in Zurich; the visit provided a superb opportunity to attempt to work out techniques and media for culture of such imaginal tissues, in order better to combine the genetic and embryological approaches. DeHaan has devoted the greater part of the past year to the solution of the technical problems involved in the cultivation of these tissues.

MEDIA FOR DISAGGREGATING AND CULTIVATING *Drosophila* IMAGINAL DISCS

Three media have been devised: a balanced isotonic salt solution, a complete culture medium, and a disaggregation medium.

The balanced salt solution (BSS 125), containing amino acids and carbohydrates, is described in table 14. Organs, imaginal discs, or tissue fragments, from second- or third-instar *Drosophila* larvae, survive in this solution for several hours and are apparently healthier than when held in the standard insect Ringer's solution as modified by Ephrussi and Beadle.

A complete culture medium (medium 1432) is shown in table 15. The extracts mentioned are made up in BSS 125, as follows:

Chick embryo extract. By sterile technique, 10 nine-day-old chick embryos are extruded through the tip of a 10-ml syringe, to yield about 20 ml of embryo brei. The brei is mixed with an equal volume of BSS 125 and allowed to stand for 18 hours at 4°C. After centrifugation for 15 minutes at 3000*g*, the supernatant fluid is distributed in 2-ml aliquots to sterile capped centrifuge tubes, and stored frozen. After thawing, the extract should be centrifuged lightly (10 minutes, 500*g*) before using.

TABLE 14. Balanced Salt Solution (BSS 125)

Solution A	
12.5	g NaCl
0.25	g CaCl ₂ ·2H ₂ O
1.0	g MgSO ₄ ·7H ₂ O
100	ml distilled water (Autoclave)
Solution B	
100	mg yeast extract (Difco)
2	g casein hydrolyzate (Fluka enzymatic)
100	ml distilled water (Autoclave)
Solution C	
0.6	g K ₂ HPO ₄
0.3	g KH ₂ PO ₄
0.3	g KCl
0.6	g glucose
0.6	g fructose
0.6	g trehalose
0.05	g sodium acetate
200	ml distilled water
Adjust pH to 6.9 with 1 M KOH. (Filter or boil for 30 minutes; do not autoclave.)	
Balanced Salt Solution 125	
10	ml solution A
10	ml solution B
10	ml solution C
170	ml distilled water

Drosophila extract. About 1 gram of adult flies (or an equal mixture of third-instar larvae and early pupae) is washed for 1 minute in 70 per cent ethanol, weighed, washed briefly in insect Ringer's, and then transferred to 10 volumes of BSS 125. The mixture is warmed quickly by immersion in a 60°C water bath and is held at that temperature for 30 minutes to inactivate tyrosinase. After rapid freezing and thawing, the flies (or larvae) are ground, with a loose-fitting glass homogenizer, to produce a milky homoge-

TABLE 15. Complete Culture Medium 1432

2	ml chick embryo extract
2	ml <i>Drosophila</i> -larval pupal (or adult) extract
1	ml banana extract
5	ml BSS 125
100	units penicillin G
100	μg streptomycin sulfate

nate, which is allowed to stand for 18 hours at 4°C. After centrifugation for 15 minutes at 3000*g*, the supernatant fluid is stored frozen.

Banana extract. By sterile technique, about 10 grams of fresh ripe banana is ground with 2 volumes of BSS 125. After standing overnight at 4°C, the brei is centrifuged at 3000*g* for 15 minutes. The clear, viscous supernatant is diluted 5-fold with BSS 125 and adjusted to pH 7.2 by the addition of a few drops of sterile KOH. This extract should not be frozen, but may be kept for a week or two at 1°–4°C.

Numerous workers have attempted to dissociate the cells of larval insect tissues, but with variable success. M. Martignoni and his collaborators have used an extract of snail hepatopancreas, as a source of hydrolytic enzymes, to disaggregate the integument of the cutworm. Hadorn and co-workers, especially H. Ursprung and R. Nöthiger, have applied similar extracts, and other enzyme preparations, to *Drosophila* imaginal discs, but have

diaminetetraacetic acid (EDTA), dissolved together in a buffered isotonic solution free of calcium or magnesium.

Wing discs from third-instar larvae, after incubation in the disaggregation medium (DM 144) for 30 to 60 minutes at 20°C, swell slightly and become sticky, but remain intact. They can then be passed rapidly through four changes of culture medium 1432, and dissociated into a cell suspension by sucking in and out of a small-bore pipette. In a typical preparation, 40 wing discs, so treated and suspended in 0.2 ml of medium, yielded a suspension of 4.4×10^5 cells per milliliter. Such suspensions consist mostly of single cells, with many groups of 2 and 3 cells and a few larger clusters of 5 to 30 cells.

The fresh disaggregates represent a heterogeneous population of cell types, the main type being a small spherical cell about 4 to 6 microns in diameter, which attaches only slowly to the glass substratum and retains its rounded shape. A second, less numerous, type is a larger spindle-shaped cell, usually 15 to 20 microns long, which attaches much more readily and exhibits marked pseudopodial activity.

TABLE 16. Disaggregation Medium 144

Trypsin (Difco 1 : 200)	1.5%
EDTA disodium salt	0.1%
Snail hepatopancreas lyophilizate	1.0%

Dissolve components together in a solution composed of 10 ml 14 per cent NaCl, 10 ml solution C of BSS 125, and 180 ml distilled water. Adjust pH to 7.5.

obtained only partial dissociation. The resulting suspension consisted mostly of clumps of cells, stuck together in mucoid matrix. Therefore, the effect of mixtures of various disaggregating agents was examined. The mixture that proved successful was modeled after a medium originally devised by M. Steinberg for dissociating refractory vertebrate tissues such as heart. It is described in table 16. It is composed of a crude, lyophilized snail hepatopancreas extract, purified trypsin, and a chelating agent, ethylene

Preliminary Observations on Cultured Imaginal Discs

Preliminary results obtained with such cultures may be summarized as follows: (1) Fragments of wing discs, cultured in sealed microdrops of medium 1432, survive for 2 weeks or longer and produce a halo of outwandering cells which adhere firmly to the glass substratum. (2) Some cells within a cultured fragment die during the first days of cultivation. (3) Fragments of wing discs maintained in culture for 3 days retain their capacity for differentiation, as is demonstrated by injecting such tissues into host larvae. After cultivation for longer than 3 days, disc fragments apparently begin to lose their capacity for differentiation. (4) In cultures of disaggregated cells, the small

spherical cells survive in much greater numbers than the larger cells. In many cultures, after 6 days, only the small spherical cells are to be seen. (5) Whether mitotic activity occurs in these cells in culture cannot yet be stated with

certainty. Distinct metaphase plates have not been observed either in living or in stained preparations. Studies with colchicine, time-lapse microcinematography, and cloning techniques should provide a definitive answer.

ORGAN CULTURE OF EMBRYONIC CHICK THYROID

EFFECTS OF THYROTROPIN, THIOUREA, L-GOITRIN, AND IODIDE ON HISTOGENESIS AND IODINE INCORPORATION

Thomas H. Shepard devoted much of his time to mastering techniques that would be useful in his projected broad attack on the development of the thyroid gland. Of the several studies initiated, one may be singled out for discussion. Shepard has had a long-standing interest in the effects of the thioamides L-goitrin and thiourea on the action of the thyroid. It is generally believed that their effects are mediated through the anterior pituitary. In testing this hypothesis, Shepard analyzed the effects of these drugs, as well as the effects of thyrotropin and

iodide, on the histogenesis of the embryonic chick thyroid in vitro, using an organ culture method. The preliminary findings may be summarized briefly:

Thyrotropin stimulates the production of granules that stain with periodic acid-Schiff reagent in the thyroid of the 11-day chick embryo. The glands were explanted, and treatment was begun at 7½ days; after 4 days, the stimulation was observed. At this time the gland in vitro is similar histologically to the normal 11-day thyroid. Concentrations of the hormone above 0.01 unit/ml caused degenerative changes in the capsular fibroblasts.

Goitrin and thiourea had no effect on the histogenesis of the thyroid, but both decreased the gland's ability to concentrate I¹³¹.

THE LABILE CHORIOALLANTOIC MEMBRANE

CHANGES EFFECTED BY ROUS SARCOMA VIRUS

At a recent symposium held in memory of the late A. M. Schechtman, J. D. Ebert further examined the thesis that animal viruses can be used to detect differences in cell-specific properties and to explore some of the problems of their origin. In an article in the *American Zoologist*, he described some of the properties of an interferon-like inhibitor produced by the chorioallantoic membrane in vitro, relating it to the emergence of immunologic mechanisms in the chick embryo and to the morphologic changes effected in the labile chorioallantois by Rous sarcoma virus and by mixtures of that virus and cardiac microsomes.

The Infection of the Chorioallantoic Membrane in Vitro with the Rous Sarcoma Virus

The experiments to be described owe their origin to the perfection by Chinami Takata (*Year Book 61*, pp. 404-406) of an organ culture technique for cultivating the chorioallantoic membrane in vitro. In further experiments Takata demonstrated that the chorioallantois could be infected with Rous sarcoma virus in vitro, and she described some of the cytopathology of the infected membrane. The stock of virus employed in her experiments was a strain (Mun-II) of the Rous no. 1 chicken sarcoma virus, obtained originally from F. B. Bang and T. Borsos, maintained by Mun by serial passage of crude or

partially purified virus on the chorioallantois in ovo, and stored at -70°C for about a year. All dilutions were made in the same medium as that employed in the subsequent cultivation of the membrane. Three different media were compared: (1) 65 per cent Hanks' solution, 20 per cent horse serum, 15 per cent embryo extract; (2) 80 per cent Hanks' solution, 20 per cent horse serum; (3) 50 per cent Hanks' solution, 10 per cent calf serum, 40 per cent Puck's medium N-16. Fragments of chorioallantois supported on filter paper were rinsed in Hanks' solution and cultured in medium containing a standard dilution of virus (usually 1 ml of a 10^{-7} dilution of strain Mun-II). After exposure for either 24 or 48 hours, they were transferred to fresh culture medium without virus, the medium then being changed every second day. After incubation at saturation humidity for 6 days at 37.5°C , they were fixed in Bouin's fluid and either mounted whole or sectioned at 5 microns, and stained with Weigert's iron hematoxylin. Pocks or lesions were counted microscopically in the whole mounts.

Takata found that all these media permitted some conversion of ectodermal and mesodermal cells of the membrane into cells having the altered morphology characteristic of Rous sarcoma. In the lesions in thickened membranes, round basophilic cells and fibroblast-like fibromyxosarcoma cells were found. In some cultures almost complete necrosis of ectodermal cells was observed. Keratogenic metaplasia was not common. In the initial studies by Takata the frequency of production of pocks or lesions varied widely from 40 to 70 per cent from experiment to experiment, seemingly without any clear relation to the nature of the medium employed.

*Inhibitory Effect of Media Conditioned
by the Growth of Membranes
Previously Exposed to Virus*

In examining Takata's findings Ebert was struck by the consistently low

frequency of infection and morphologic alteration. The embryos employed from the outset of the study had been from a variety of White Leghorn fowls (Elder Farms) in which, in earlier studies, the percentage of nonreactors had been 17.4. It seemed only remotely possible that there had been a substantial increase in resistance in this variety since it was last tested. However, in view of the compelling evidence available for the influence of the genotype of the chick embryo on tumor production by Rous sarcoma virus, a further series of comparisons was made. Membranes from four types of donor were explanted and inoculated: (1) a cross of California Gray \times White Leghorn in which the percentage of nonreactors had earlier been set at 34; (2) White Leghorn (Elder Farms); (3) selected White Leghorns (Elder Farms) in which maternal antibody to Rous sarcoma virus was known to be present; (4) a single-comb White Leghorn variety, obtained from F. B. Bang, in which maternal antibody to the virus was known to be absent. Significant differences in frequency of alteration were not observed (table 17).

Attention was focused next on the composition of the medium. Since the morphological alteration of chick and turkey embryo fibroblasts by virus has been shown to depend on the physiological state of the cells at the time of infection, i.e., morphological response can be regulated by choice of medium and by infection at various times after preconditioning, it seemed essential that the causes of variation be explored. In a more extensive series of membranes cultured in medium 3 (50 per cent Hanks' solution, 10 per cent calf serum, 40 per cent Puck's medium N-16), the over-all frequency of morphologic alteration was 37 per cent. Temin had reported earlier that cells infected with Rous sarcoma virus may display no visible morphologic alteration. As Prince has emphasized, further evidence of infection without morphologic alteration is provided by his finding that only a small fraction of virus-producing

TABLE 17. Tumor Response of Chorioallantoic Membranes Cultured from Chick Embryos from Different Sources

Source of Membrane	No. Explanted	No. Showing Lesions	Mean No. Lesions per Membrane
California Gray × White Leghorn	60	21	27
White Leghorn (Elder Farms)	59	22	59
White Leghorn (Elder Farms), maternal antibody present	49	16	31
White Leghorn, Rous antibody absent	44	15	19

cell clones can be distinguished from uninfected clones, and by Rubin's observation that fetal calf serum can suppress the appearance of foci of morphologically altered cells after infection of monolayers with small amounts of virus but does not change the proportion of infected cells. In the current study, however, infection and morphologic alteration, judging by the appearance of lesions within 6 days (i.e., 4 or 5 days after removal from medium containing virus), appear to be synonymous, for the recovery of crude virus for assay in ovo 3, 4, or 5 days after initial exposure to virus revealed evidence of infection in only 41 per cent of cultures, a figure which does not differ significantly from the 37 per cent with clearly recognizable lesions.

Neither the addition of 10 per cent tryptose broth nor infection of cells after

varying periods of starvation markedly favored the production of morphological alteration except that the post-starvation treatment increased the occurrence of keratogenic metaplasia. Therefore, in an effort to increase the frequency of morphologic alteration, experiments with conditioned media were initiated. Surprisingly, such media had an effect opposite to that expected.

Cultures grown in the presence of virus for 24 hours were removed to fresh medium without virus for an additional 48 hours. At the time the medium was next changed, the old medium, so "conditioned," was saved and used in combination with fresh virus and varying amounts of fresh medium as the primary infecting medium and as the medium for subsequent transfers of new cultures. As summarized in table 18, morphologic

TABLE 18. Production of Inhibitor by Chorioallantoic Membrane in Vitro after Infection with Rous Sarcoma Virus

Source of Membrane	No. Explanted	Medium; Ratio Fresh/Conditioned	No. Showing Lesions	Mean No. Lesions per Membrane
California Gray × White Leghorn	30	0/100	0	0
White Leghorn (Elder Farms)	29	50/50	0	0
White Leghorn (Elder Farms)	60	75/25	0	0
White Leghorn (Elder Farms)	57	90/10	2	3.5
California Gray × White Leghorn	59	95/5	9	11
California Gray × White Leghorn	30	99/1	8	24
White Leghorn (Elder Farms)	30	95/5*	4	19
White Leghorn (Elder Farms)	29	95/5†	11	37

* Heated 56°C 30 minutes.
† Heated 85°C 15 minutes.

alteration instead of being increased was suppressed. These experiments suggested that an inhibitor had been produced. Accordingly, the following preliminary experiments were undertaken, looking toward its characterization.

1. Either 1 ml of heated or 1 ml of active Rous sarcoma virus, stock Mun-II, was added to membranes cultured in medium 3. A total of 134 cultures was incubated for either 72 or 96 hours, after which the culture fluids were tested for inhibitory activity after centrifugation for either 2 or 4 hours at 100,000*g*. One or two milliliters was added to newly explanted fragments of membrane at the time of infection. Fluids from cultures exposed to either active or inactive virus contained the inhibitor.

2. Culture fluids were dialyzed versus 5 changes of 10 volumes of Hanks' solution over a 24-hour period. Changes in *pH* were examined, the following solutions being tested: *pH* 2, *pH* 4, *pH* 6.8, *pH* 10. There was little effect on the activity of the inhibitor.

3. The effects of heating the culture fluids in a water bath were determined. Heating at 56°C for 30 minutes had no effect; at 72°C inhibitory activity was partly destroyed. The effectiveness of the inhibitor was destroyed completely by heating at 85°C for 30 minutes.

4. Trypsin was added at a final concentration of 1.5 mg per liter at *pH* 7.2 for 6 hours (37°C), after which the solution was heated at 50°C for 30 minutes. The inhibitory activity was markedly suppressed.

5. Pepsin, which according to Bader was more effective than trypsin, proved equally effective in two experiments conducted under the conditions described by him (1 mg per liter, *pH* 2, for 4 hours).

6. In agreement with Bader, deoxyribonuclease and ribonuclease did not affect the inhibitor.

7. The inhibitor did not appear to act on the virus directly. Preincubation of inhibitor and virus in varying concentrations from 1 to 3 hours at 20°, 25°, and

37°C did not result in a significant diminution of effectiveness as compared with virus samples diluted with normal medium and incubated for the same periods.

8. Addition of the inhibitor to the medium at the time membranes were transferred from the infecting medium to one without virus, 24 or 48 hours after inoculation, produced no effect.

9. Inhibition was most pronounced when the inhibiting fluid was added shortly before or at the same time as the addition of virus. Bader has studied the addition of interferon to chick embryo fibroblasts at intervals after infection with virus. His evidence shows that the inhibitor loses effectiveness progressively; it must be present early in the developmental cycle of the virus. Ebert's findings are less clear, and, although they point in the same direction, the data are too fragmentary to warrant a conclusion.

It appears likely that the inhibitor produced by the chorioallantois exposed to active or to heat-inactivated Rous sarcoma virus *in vitro* is interferon, described by Isaacs and Lindenmann as a nonviral substance formed by the interaction of inactivated influenza virus and living cells. When transferred to normal cells it renders them resistant to infection with the same and other viruses. Cells chronically infected with virus *in vitro* produce interferon, and the amount of interferon allowed to accumulate in them seems to decide whether the chronic infection is maintained. Bader has recently demonstrated the presence of interferon in chick embryo cells exposed to Rous sarcoma virus *in vitro*.

Experiments in several laboratories point to the conclusion that interferon, which is believed to be a protein having a molecular weight of about 60,000, affects virus multiplication. It does not inactivate virus or viral RNA directly, nor does it prevent the penetration of viruses. Virus multiplication appears to be blocked after penetration and before the formation of precursor RNA and viral

protein. Moreover, the intruding nucleic acid is not degraded; it remains intact, and is not damaged by cellular nucleases.

Like interferon, the inhibitor recovered from culture fluids after infection of the chorioallantois with virus blocks virus reproduction and the formation of lesions. It differs from other inhibitors of Rous sarcoma virus which appear to act directly upon the virus. Its characteristics, from the experiments conducted so far, are compatible with the view that interferon has been produced. There is no evidence in this study that the inhibitor is the resistance-inducing factor (RIF) described by Rubin and since shown to be one of the avian leukosis viruses, possibly lymphomatosis virus. In fact, as Dougherty and Simons have pointed out, there is no evidence that infection of an embryo with RIF induces resistance to infection of the chorioallantois.

Yet the question remains: If the interferon produced by the membrane in vitro is meaningful, i.e., if it has a bearing on the resistance of the membrane to morphologic alteration by virus, why is it not produced, or why is it ineffective, in ovo?

CHANGES EFFECTED BY ANTIGENIC STIMULI AND IMMUNOLOGICALLY COMPETENT CELLS

Although there is no compelling evidence of the production of antibodies or the capacity to mount a homograft reaction in the chick embryo, there is an increasing body of evidence, including that offered by Mun, Tardent, Errico, Ebert, DeLanney, and Argyris in a recent article in the *Biological Bulletin*, that the embryo is capable of mounting a response to antigenic stimuli in the chorioallantoic membrane, a reaction, as Burnet put it, like the foreign-body reaction. Whether such reactions can be demonstrated in vitro remains to be established.

As described in *Year Book 61* (pp. 404-406), one of the objectives in Ebert's continuing analysis of the development of immunologic mechanisms in the chick is

to determine the origin of the focal lesions appearing in the chorioallantoic membrane after grafts of adult spleen or the inoculation of suspensions of spleen cells. Although most investigators now agree that these lesions are largely derived from the host even though they contain cells from both donor and host, the precise origin of the host's contribution is entirely unknown. Do these cells migrate in from the embryo? Are they mobilized in the membrane in situ?

With the development by Takata of a technique for cultivating the membrane, one major technical obstacle has been hurdled. It was necessary next to perfect a method for disaggregating adult tissues containing immunologically competent cells, e.g., spleen, so as to ensure production of inocula containing isolated cells in known concentrations. Moreover, such cells had not only to be viable but also to retain their ability to affect the embryo.

During the year under review, Charles R. Green made substantial progress toward this goal, devising a technique incorporating the following steps: (1) Exposure of finely fragmented adult chicken spleen to 0.1 per cent trypsin in calcium-, magnesium-, and phosphate-free saline, pH 7.4, at 37°C, for 10 minutes. (2) Repeated treatment of the cells with fresh egg albumen (20 per cent in chick Ringer's solution) in the cold. (3) Preparation of cell suspensions by repeated centrifugation, filtration, and resuspension in 20 per cent egg albumen. (4) Assessment of the effectiveness of such cell suspensions by inoculating them on the chorioallantoic membrane at various times from the 8th through the 14th day of incubation.

According to Green, such suspensions contain approximately 90,000 cells per cubic millimeter, of which an estimated 20,000 are erythrocytes, the remainder comprising other cell types. Preliminary findings indicate that adult chicken spleen cells, disaggregated by this technique, retain at least some of the recognized capacity of nondissociated splenic frag-

ments to induce splenomegaly in host embryo recipients. Definite conclusions require greater statistical support.

As DeLanney and Ebert had noted earlier, host splenomegaly was usually, but not invariably, associated with

obvious changes in the chorioallantoic membrane. Moreover, also in keeping with previous observations, macroscopically obvious changes in chorioallantoic membranes were not always accompanied by splenomegaly.

IMMUNOLOGICALLY INDUCED ASPERMATOGENESIS

Further investigations of the nature of, and factors involved in, immunologically induced aspermatogenesis have been conducted by D. W. Bishop in collaboration with G. L. Carlson, E. C. Muecke, and C. B. Kimmel. Renewed emphasis on the problem appeared warranted as a result of several recent developments:

1. Improved methods of extraction and characterization have facilitated the isolation of an aspermatogenic factor of relatively high purity and more precise chemical composition.

2. The circulating antibody that accompanies sensitization against crude testicular antigen has proved to be precipitable, uniform (one band in gel-diffusion plates), and quantitatively related to the onset of germinal epithelial destruction. The relation of humoral antibody to immune responses of the delayed hypersensitivity type, of which induced aspermatogenesis is probably an example, has been stressed in recent immunologic literature, notably by Eisen and Karush.

3. More and more attention is being given to the possible use of immunologic methods in selectively modifying fertility rates. The aspermatogenic syndrome undoubtedly offers one general line of approach to the problem but, at the same time, suggests certain limitations of immunologic procedures in the search. The advantages and restrictions of the exploitation of antigens of reproductive tissues in relation to fertility control have been enumerated in the proceedings of the Conference on Immunoreproduction (La Jolla, California, September 1962), and reviewed by Tyler and Bishop in the

book *Mechanisms Concerned with Conception*, edited by Carl G. Hartman.

Recent findings will be considered here under three headings: the mechanisms of aspermatogenesis, the antigenic factor, and the humoral antibody elicited by testis sensitization.

MECHANISMS OF ASPERMATOGENESIS

Following earlier unsuccessful attempts to suppress the aspermatogenic response by administration of 6-mercaptopurine to guinea pigs sensitized to testis, X irradiation was employed to determine whether the immune response can be inhibited and the reaction of the germinal epithelium prevented or modified by this means. Bishop believed that so little was known about the mechanism of the aspermatogenic reaction that the experiment was worth trying, even though attempts in the past to suppress hypersensitivity reactions of the delayed type by irradiation have not been very rewarding.

An exploratory investigation on guinea pigs sensitized with defined or cellular antigen either combined with irradiation or without irradiation was conducted by C. B. Kimmel (table 19). Preliminary tests established that the approximate LD₅₀ at 60 days for mature guinea pigs was 300 r, and that the effective time of irradiation was 1 to 2 days before sensitization. All irradiation exposures were administered at 250 peak kilovolts and 25 milliamperes, employing 0.5-mm copper and 1.0-mm aluminum filters, and a tube-to-midbody distance of 50 cm; target dosage averaged 97 r/minute. Protection of the testis was accomplished by a 0.5-inch lead shield. Antigens, bovine

TABLE 19. Summary of Procedures and Results after X Irradiation and Sensitization of Guinea Pigs with Bovine Gamma Globulin or Testicular Antigen

Group and Age	No. Ani-mals	Antigen, mg		Irradiation, r*		Blood Counts	Serology		Testicular Cytology
		BGG, I.M.	Testis, I.C.	No Shield	Shield		PCA	Gel-Diffusion	
A. Adult females	8	37.5	75				-5 day +10-15 day	-5-15 day	
B. Young males	6	37.5					-5 day +10-60 day		Normal at 60 days
C. Neonatal males	11			250-650					Complete destruction of germinal epithelium of survivors at 2½ months (600 r)
D. Adult males	6	75		300		Total and diff. w.b.c.	-5 day +10-60 day	-5-15 day	Severe damage to germinal epithelium at 60 days; some tubules with mature germ cells
E. Young adult males	8	37.5		300		Total and diff. w.b.c.	-5 day +10-60 day	-5-15 day	Severe damage throughout at 60 days; some spermatozoa; Sertoli cells present
F. Young adult males	12	37.5			300		-5 day +10-60 day		Of 8 animals surviving 60 days, 5 had normal testes, 3 showed partial damage
G. Adult males	12		250		300	Total and diff. w.b.c.	-5 day +10-60 day		Of 9 animals surviving 60 days, all showed moderate to severe damage to germinal epithelium
H. Adult males	12		250		300		-5 day +10-60 day		Of 9 animals surviving 60 days, 8 showed moderate to severe damage, 1 essentially normal
I. Neonatal males	12		250		250-850				2 survivors at 60 days (850 r) and 75 days (550 r) showed "normal" undifferentiated germinal epithelium

* Groups D and E irradiated 1 day, and groups F to I 2 days, before sensitization.

gamma globulin (BGG) or homogenized testis, were administered with adjuvant, intramuscularly and intracutaneously, respectively. Blood samples were taken by intracardial puncture for leucocyte counts and for serological assay. The levels of irradiation employed were sufficient to depress leucocyte count severely, to about one-eighth or one-ninth normal at 10 days, and to produce serious damage in the unshielded testis (table 19). They were, however, of either too low dosage or too short effect to significantly depress antibody titer against BGG or testicular antigen. Attention is directed in table 19 to the testicular responses in groups F, G, and H, a comparison of which indicates that testicular antigen induces aspermatogenesis in all irradiated, testis-shielded animals, whereas in similarly irradiated BGG-sensitized animals most surviving testes at 60 days are normal. The exceptional animals may have resulted, in part, from incomplete shielding. These preliminary findings suggest that the immunologic system stimulated by testicular antigen is not affected by this amount of X irradiation, but what the effect of fractional doses applied over

a longer period might be is yet to be determined. Such X irradiation is surprisingly well withstood by younger animals (groups C and I).

Aspermatogenesis is readily induced in guinea pigs by injection of testis homogenate incorporated in complete (Freund) adjuvant when administered by the intracutaneous route. Freund himself emphasized that this route of sensitization is essential to facilitate the cellular response. Since earlier work has shown that testis antigen need not be directly incorporated with adjuvant to evoke germinal damage (*Year Book 60*), and since the guinea pig responds well to intramuscular administration of antigen (Glover and Bishop, 1963), the possibility was explored of inducing aspermatogenesis by intramuscular injection of testis combined with adjuvant. The results of a preliminary experiment are summarized in table 20. All injections were administered to the forelegs, 1.0 ml emulsion per animal, each sensitizing dose containing approximately 250 mg testis wet weight. Seven out of twelve guinea pigs displayed severe germinal damage when sacrificed 2 months after sensitiza-

TABLE 20. Induced Aspermatogenesis by Intramuscular Administration of Testis Homogenate and Adjuvant
Adult Hartley strain guinea pigs injected in forelegs with 1.0 ml antigenic emulsion containing approximately 250 mg testis per milliliter.

Animal No.	Testicular Response*		Serological Response†	
	Minimum	Maximum	PCA	Gel-Diffusion
1367	0	1	—	—
1368	3	4	+	+
1369	2	4	+	—
1370	4	4	+	+
1371	4	4	+	+
1372	0	1	±	—
1373	4	4	+	+
1374	0	2	—	—
1375	3	4	+	—
1376	2	4	+	—
1377	0	3	—	—
1378	0	1	+	—

* Index of germinal epithelial response ranges from normal, 0, to complete destruction, 4.
† Sera collected at time of sacrifice, 2 months after sensitization.

tion (pl. 7, fig. 35*a, b*); three others were less seriously impaired. Judgment is reserved whether the same immunologic mechanism is involved when the routes of antigen administration are different, but it may be noted that the circulating antibody usually elicited by intramuscular injection shows the same reactivity as that evoked by intracutaneous injection when the sera are tested either by the passive cutaneous anaphylactic (PCA) reaction or by gel-diffusion methods (pl. 7, fig. 36*a, b*).

Further evidence has been sought to resolve whether induced aspermatogenesis may be regarded as a reversible type of response when induced by testis homogenate and adjuvant. It is evident from earlier work (see *Year Book 60*) that even carefully bred (Hartley) guinea pigs vary one from another in their response to the inducing factor, but in general the two members of a pair of testes tend to respond the same. Evidence has been compiled thus far on a total of more than 50 guinea pigs semicastrated at 1½ to 2 months and sacrificed at 6 months. A comparison of the gonads shows apparent recovery in some animals (pl. 8, fig. 37*a, b*) but a high proportion of recovery lack

in others (pl. 8, fig. 37*c, d*). The testes of some animals appear resistant to the immune sensitization throughout (pl. 8, fig. 37*e, f*). Six months is acknowledged to be a short recovery period, but at the end of this interval there is, in severely affected testes, no sign of restitution of germinal epithelium. Reversible or temporary aspermatogenesis in the guinea pig may become more manageable with purification of the antigenic factor, but Carlson's findings suggest no control of recovery of germinal epithelium after immune destruction induced by graded milligram doses of highly purified testicular antigen.

THE ANTIGENIC FACTOR

Work on the characterization of the testicular antigenic factor has been continued by G. L. Carlson. The polysaccharide that accounts for about 20 per cent of the dry weight of the chloroform-purified material (CPM), acid-extracted from guinea pig testes (*Year Book 61*, pp. 342–343), has proved to consist predominantly, if not exclusively, of galactose, as determined by paper chromatography on 0.25 *N* sulfuric acid-hydrolyzed samples, and quantitatively

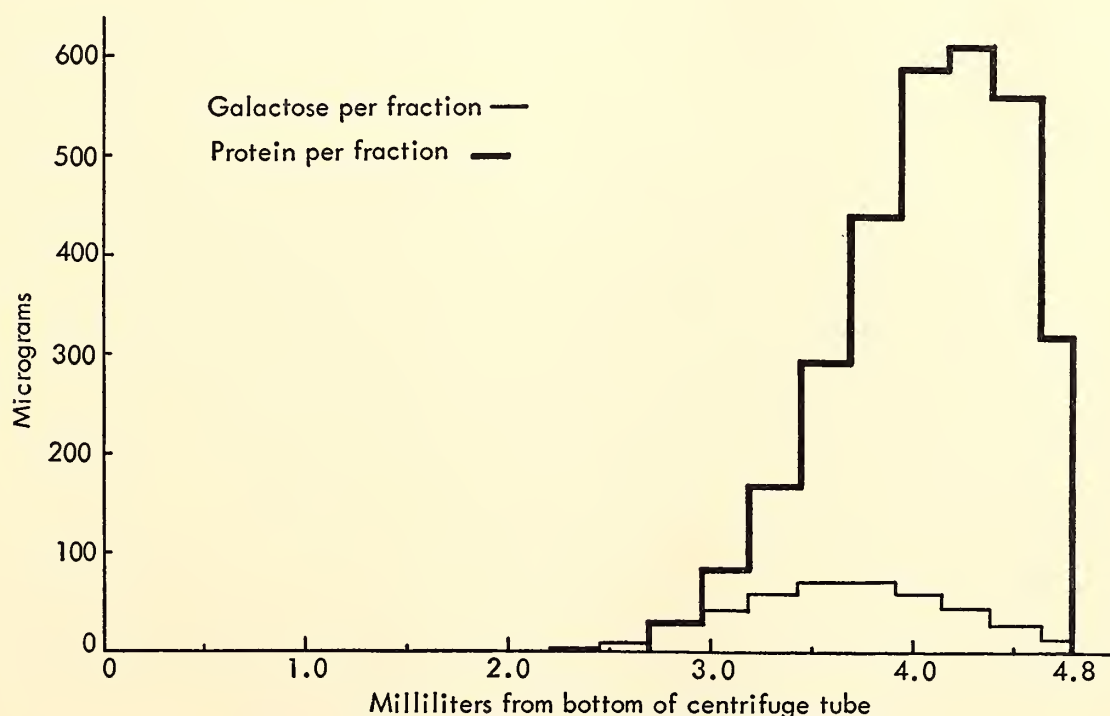


Fig. 38. Distribution of galactose and polypeptide components obtained by sedimentation of CPM fraction layered on a sucrose gradient of from 3 to 20 per cent.

confirmed by assay in the "Galactostat" system employing galactose oxidase of the mold *Polyporus circinatus*. This enzyme reacts with galactose in unhydrolyzed preparations of polysaccharide, thus serving as a useful test of reactivity of samples both enzymatically and aspermatogenically active.

Although the extent of oxidation of galactose in CPM is not yet known, the galactose that is oxidized must be linked at a position other than the number 6 carbon normally oxidized by the enzyme.

Sucrose-gradient methods have been employed in a further analysis of the heterogeneity of CPM derived from testis. The differential sedimentation pattern of the galactose-containing component and polypeptide in CPM is shown in figure 38. These curves were prepared from data obtained by layering CPM on a linear gradient of 3 to 20 per cent sucrose, centrifugation for 11 hours at 38,000 rpm in an SW 39 L swinging bucket, recovery of fractions, and determination of galactose and protein by the galactose oxidase and Lowry or biuret procedures, respectively. There is a pronounced shift in ratios of galactose component to polypeptide, the galactose component having a larger sedimentation constant, which indicates that the two moieties are

probably not firmly bonded, as by covalent linkages.

When aspermatogenicity of the various sucrose-gradient fractions is compared with the chemical data, the antigenic factor is found to sediment more rapidly than the polypeptide component (figs. 39, 40) and to correspond more closely to the distribution of polysaccharide. However, though aspermatogenic, the CPM polysaccharide fails to produce PCA reactions with sera from aspermatogenic guinea pigs, which suggests that it must be bound to polypeptide in order to function both as an aspermatogenic agent in vivo and as a challenging antigen in the PCA procedure or serological tests in vitro.

Sedimentation analysis of a preparation less purified than CPM, namely, the trichloroacetic acid-soluble material (TCASM), yields fractions with a PCA-effective factor, which, however, does not appear to be identical to either the polypeptide or the galactose component and may even be distinct from the aspermatogenic component present in CPM (fig. 41). Further refinements in the methods of extraction and characterization of the antigenic material, and more precise methods of determining cellular responses, should clarify some of these discrepancies.

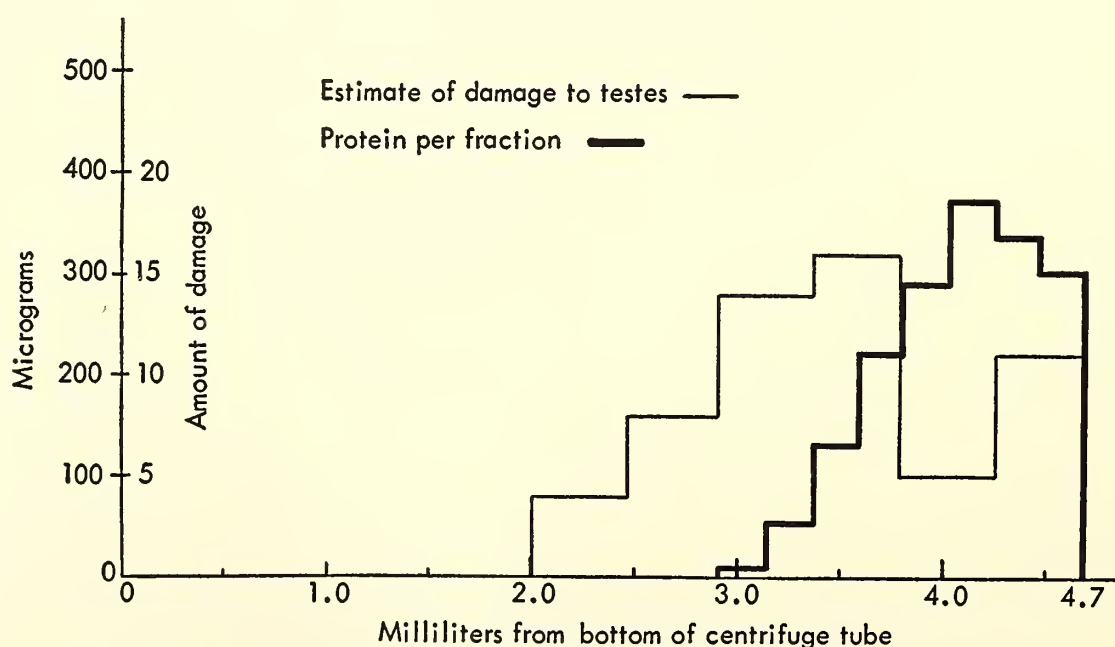


Fig. 39. Distribution of aspermatogenic fraction and polypeptide component of CPM in sucrose gradient.

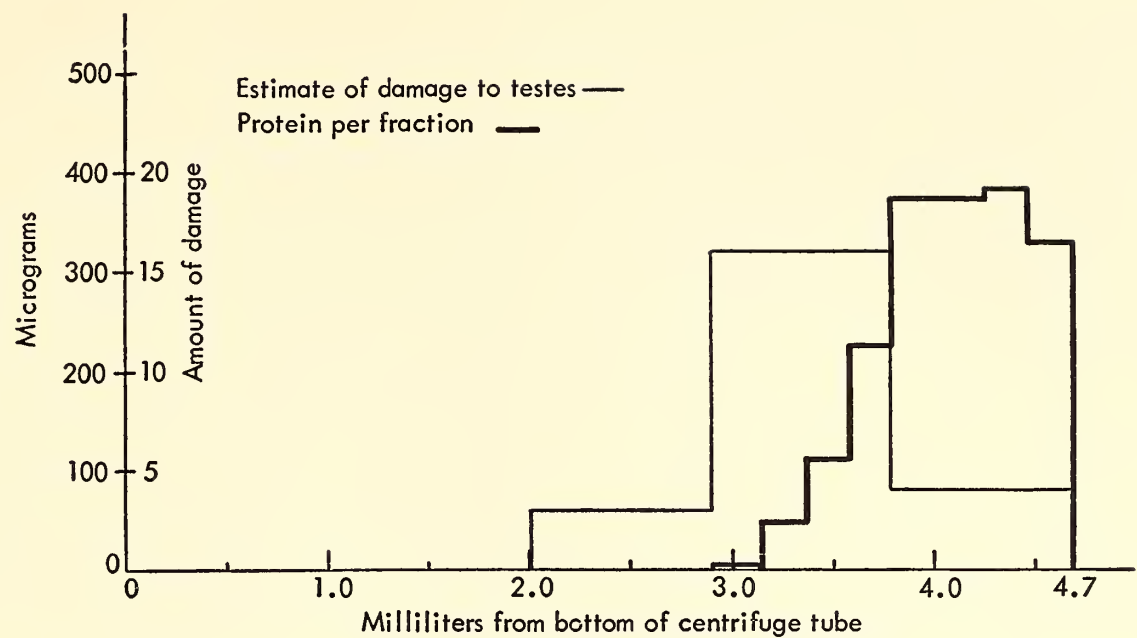


Fig. 40. Same as figure 39, but fewer fractions assayed and at higher resolution.

The amino acid composition of CPM was determined quantitatively by hydrolysis with 6 N HCl followed by chromatography on a Beckman Spinco amino acid analyzer. This analysis was kindly performed through the courtesy of C. L. Markert, Johns Hopkins University. As may be seen in table 21, the polypeptide is characterized by high proline and glutamic acid contents. Also, unusual basic amino compounds previously detected by high-voltage paper electro-

phoresis were resolved into five compounds by the amino acid analyzer. Whether or not these unidentified bases are specific to the aspermatogenic material, and the relationship of these unusual bases to the tissue specificity evident in the induction of aspermatogenesis, are areas remaining to be explored. The acrosome of the mature germ cell appears to be the site of the principal component of the antigenic factor as demonstrated by Schiff reagent (basic

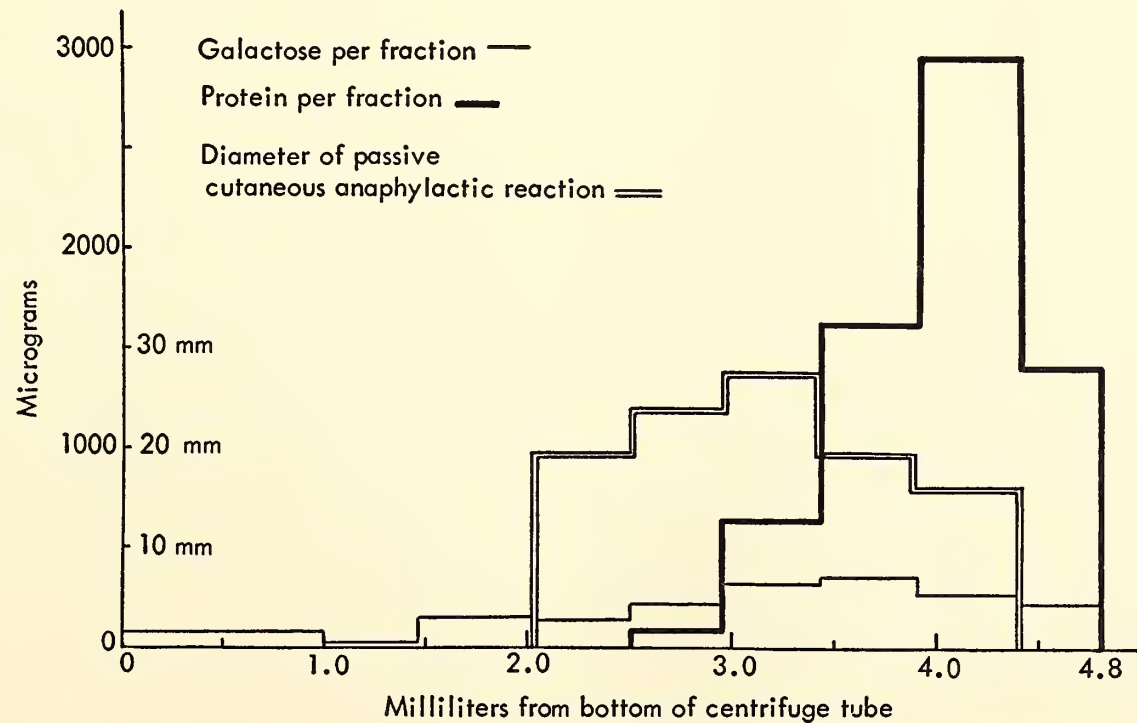


Fig. 41. Fractionation by sedimentation in sucrose gradient of TCASM extracted from guinea pig testes.

TABLE 21. Amino Acid Composition of Chloroform Purified Material

Amino Acid	Mole Per Cent
Lysine	6.95
Histidine	2.70
Ammonia	16.55
Arginine	2.62
Aspartic acid	6.08
Threonine	6.36
Serine	5.54
Glutamic acid	10.8
Proline	10.87
Glycine	6.41
Alanine	7.87
Valine	5.00
Methionine	1.33
Isoleucine	2.50
Leucine	4.95
Tyrosine	0.875
Phenylalanine	2.41

fuchsin) staining of fresh and extracted sperm cell smears. Selective extraction removes or alters the polysaccharidic moiety so that, after acid hydrolysis, reactive aldehyde groups fail to reveal themselves in the acrosome.

Owing to the polysaccharidic nature of the aspermatogenic factor and of the antigen that evokes circulating, precipitable antibodies after testicular sensitization, some attention has been given the possibility of doubly staining, for polysaccharide and protein, the antigen-antibody complex that forms in gel-diffusion plates. A single major band develops, which can be stained prominently with amido black or more weakly with basic fuchsin (pl. 9, fig. 42*a*, *b*). A procedure for concurrent double staining of the same band is under development. More than the technical trick of staining antigen and antibody together is involved here; the test indicates that formation of an antigen-antibody complex does not irreversibly mask the antigenic aldehyde groups necessary for positive Schiff reaction.

Preliminary steps have been taken in a chemical exploration of the basis of the so-called common antigenicity of brain

and testicular tissue. Thirty years ago J. H. Lewis reported, and many others since have noted, the cross reactivity of these two tissues on a basis of complement-fixation tests and the aspermatogenic reaction (see *Year Book 56*). All Lewis's brain preparations showing cross reactions with materials extracted from reproductive tissues were simple alcoholic extracts of the whole or undefined portions of the brain. Nevertheless, since a kind of aspermatogenesis can be induced in guinea pigs by intracutaneous injection of brain homogenate and adjuvant, a brain extract was prepared by the same procedure used to extract the ammonium sulfate-purified material (ASPM) from testis. Brain ASPM evoked little response in the germinal epithelium of most of the treated guinea pigs, but in 2 out of 12 animals severe damage was presumably induced within 2 months (pl. 9, fig. 43*a*, *b*). Should subsequent tests with similar and more highly purified preparations substantiate this finding, it would support the notion that a chemical identity may underlie the demonstrations of common antigenicity of these two tissues.

THE HUMORAL ANTIBODY

The "nonprecipitable" antibody found in sera of practically all testis- or ASPM-sensitized guinea pigs (*Year Book 60*) has now been demonstrated to be an antibody of the precipitating type, detectable by gel-diffusion methods. Demonstration of the formation of an antigen-antibody complex has been facilitated by using semimicro diffusion slides at 4°C. Whether this humoral factor plays a vital role either in the onset of germinal epithelial breakdown or in "mopping-up" operations remains to be clarified, but its association with sensitization leading to aspermatogenesis provoked considerable study. Several points bear mention here:

1. The antibody is produced as a result of sensitization by either testis homogenate or ASPM combined with adjuvant; it constitutes the only gel-diffusion band

when tested with ASPM antigen (pl. 10, fig. 44).

2. The same antibody is produced whether injections are by the intracutaneous or the intramuscular route (pl. 7, fig. 36*a, b*).

3. Absorption of antisera with kidney, liver, or brain does not impair their reactivity in either gel-diffusion or PCA tests (pl. 10, fig. 45*a, b*).

4. The antibody is nonreactive with, and fails to be absorbed by, hyaluronidase derived from bovine testis.

5. Although formed against, and reactive with, polysaccharide, antibody inhibition cannot be brought about by the simple sugar galactose.

6. Antibody titers in sensitized and aspermatogenic guinea pigs rarely exceed levels which permit a 100-fold dilution without loss of detectability by PCA methods (pl. 10, fig. 46).

7. Calculations of circulating antibody concentration in sensitized and aspermatogenic animals give a value of the order of $1-2 \times 10^{-7} M$.

8. Attempts to induce a testicular response in secondary recipients by transfer of serum alone have met with failure. In one experiment each of six recipients received a total of 125 intraperitoneal injections of pooled sera from actively sensitized guinea pigs, representing the equivalent of about 5 times the total serum volume of an adult animal. Injections were made 6 times weekly, and each animal received a total of approximately 2000 μg of circulating antibody. Although highly sensitized, as judged by active cutaneous hypersensitivity tests and anti-ASPM serum titers, these secondary recipients showed no indication of germinal epithelial failure.

To test the effects on aspermatogenesis of removal of the sensitized testis to a nonsensitized guinea pig and, reciprocally, the introduction of normal testis into a presensitized animal, E. C. Muecke has explored the possibility of implanting mature testicular tissue into subcapsular sites in the kidney. Although the results

have proved disappointing with respect to continued differentiation of germinal epithelium, some explanation for the failure seems to be indicated from Muecke's observations based on 35 hosts which received an average of 5 implants each. Autografts and homografts of both Hartley and the closely inbred Strain 13 guinea pigs were prepared.

The results may be summarized as follows: (1) Homografts in Hartley strain animals were uniformly rejected with marked round cell infiltration and connective tissue proliferation. (2) Graft sites of autografts and homografts of Strain 13 guinea pigs, examined less than 1 month after implantation, showed a moderate amount of amorphous material (necrotic graft tissue), capsular edema, and subcapsular hemorrhage. In intact tubules, germinal epithelium appeared hypoplastic and spermatogenesis was not maintained; no mitoses were seen (pl. 11, fig. 47*a, b*). (3) After 1 month, conditions appeared more stabilized, and intact seminiferous tubules were dispersed among the hypertrophic connective tissue elements that made up the thickened renal capsule. The germinal elements were markedly hypoplastic, with Sertoli cells as the dominant cell element. After 3 months the capsule appeared contracted. Apparently the formation of definitive scar tissue caused contracture of capsule and graft. In all animals there was a great difference in the size of the original graft and the area examined at sacrifice. On gross examination the graft site was depressed, with a noticeably thickened whitish capsule overlying it. (4) At 1 month and at 3 months there was essentially no difference between autografts in Hartley or Strain 13 and the homografts in Strain 13 animals (pl. 11, fig. 48*a, b, c*).

Aside from the fact that an autoimmune reaction may have been established in these animals comparable to induced aspermatogenesis by homologous or autologous testis, the cytological findings strongly suggest cryptorchid inhibition, an idea that is being put to further test.

ANTIBODIES AGAINST SPERM

An attempt has been made by M. L. Hartman, working in collaboration with Bishop, to find evidence for immobilization antibodies specific for sperm. A review of the immunological literature by Tyler and Bishop revealed more than two dozen papers published over the past 64 years reporting the presence of so-called sperm-immobilizing antibodies in anti-sperm serum. In no report, however, was a specific immobilizing action, discrete from agglutination or killing of the cells, clearly discerned; nor were any of these studies concerned with the reaction of individual cells as opposed to sperm suspensions. Moreover, the spermatotoxic effects of complement and of thermolabile toxic factors in normal serum have not always been taken into account. Bishop's primary interest in the problem is to ascertain the mode of action of sperm-immobilizing antibodies if, in the literal sense, they exist. Such a specific anti-flagellar antibody, without killing effect, has been prepared against the protozoan *Naegleria* by C. Fulton.

Employing simple microscopic procedures involving glass-slide or capillary-tube observation chambers, no specific paralyzing antibody activity could be observed in absorbed or unabsorbed, heated or unheated antisera of the rabbit or guinea pig prepared against washed sperm of the bull, cock, rabbit, or guinea pig and cross-reacted with fresh sperm of the bull, cock, rabbit, or guinea pig. Precipitable antibodies, detected by gel diffusion, were present in most sera, and agglutinins were common in many; species-specific agglutination was most pronounced in rabbit antibull sperm serum tested against washed bull spermatozoa. Sustained exposure of sperm to agglutinins in high concentration resulted in loss of motility and death of the cells. Guinea pig serum, both normal and immune, heated (56°C, 30 minutes) or unheated, tended to be more toxic than rabbit serum on all species of sperm. Further work on this problem, with more adequate and quantitative procedures, is anticipated.

SUBCUTANEOUS IMPLANTS OF HOMOLOGOUS VENTRAL PROSTATE

Brief mention may be made of a preliminary study of the effect of the immune state of recipient animals on subcutaneous implants of homologous ventral prostatic tissue from outbred rats. Price, Mann, and others have shown that homologous implants of accessory reproductive gland tissue in subcutaneous sites may persist in a functional state for periods up to 3 months or longer; skin homograft rejections, as is well known, occur within a matter of 1 to 3 weeks. Bishop's work was done in association with C. H. McAllister, and the preliminary findings were discussed at the Conference on the Biology of the Prostate, sponsored by the National Cancer Institute. The prostate has since been found

rather less than satisfactory for such a study, and further investigation is planned involving the seminal vesicle, but the early results indicate that immunologic conditions should not be ignored. With useful data from a total of only 23 host animals, the following tentative conclusions may be drawn. (1) The sera of recipient rats, bearing viable implants of rat ventral prostate, fail to show detectable antibody when assayed by the passive cutaneous anaphylactic procedure using saline extract of prostatic tissue as challenging antigen. (2) The successful implantation of several (8 to 10) prostatic implants fails to inhibit a second set of grafts from homologous donors. (3) Rats, presensitized against ventral prostate

(saline extract) administered intramuscularly in adjuvant, rejected homologous prostatic grafts implanted 4 to 5 weeks later. Thus, the implants do not appear to sensitize the host sufficiently to evoke detectable antibody by this test method

(PCA) or to impair the successful implantation of a second set of (homologous) grafts, but the implants are sensitive to, and rejected by, a state of preimmunization of the host.

THE EMBRYO IN RELATION TO ITS ENVIRONMENT

MECHANISMS OF IMPLANTATION OF THE OVUM

Only a year (or perhaps a decade) from now will we be able to judge the success of this year's efforts by Bent G. Böving in studying the mechanisms of implantation of the rabbit blastocyst. Much of the report year was given over to criticism and review (including a healthy portion of self-criticism). In the course of this review, two major syntheses have been prepared, one on implantation mechanisms, to appear in *Mechanisms Concerned with Conception*, edited by Carl G. Hartman, and another on trophoblast penetration of uterine epithelium scheduled for publication in *Klinische Wochenschrift*.

Several interpretations of the data now available on the components and mechanisms involved in trophoblastic invasion of endometrium are possible. Familiar ideas, derived from several species by several different methods, attribute invasion to proteolytic, phagocytic, or amoeboid faculties of the trophoblast or to the decidual reaction of the endometrium. Since 1960 three unfamiliar and contradictory interpretations have arisen from different ways of studying a single species, the rabbit. Larsen's observations, made with the electron microscope, suggest that invasion consists of fusion of syncytial trophoblast with syncytial uterine epithelium. Implantation in vitro is said by Glenister to involve cellular trophoblast and uterine epithelium converted into symplasma at the site of invasion, presumably by a trophoblastic cause. Histological and chemical studies

by Böving suggest that syncytial trophoblast knobs penetrate uterine epithelium while it is still cellular, shortly before it becomes transformed into symplasma. The penetration is attributed to differential dissociability at high pH elicited in epithelial cells overlying capillaries; the cells dissociate, whereas the adjacent trophoblast prevails because it is syncytial and therefore remains undissociated. Separately, each of the studies has contributed something to the ever-improving description and explanation of the events that occur. Together, the three studies, whose contradictory conclusions cannot be attributed to species differences, provide an opportunity to discern pitfalls of method and interpretation.

Clearly, it is not enough to determine that a mechanism is a necessary precursor for a succeeding one; it must also be ascertained whether it is a sufficient cause. Consider Böving's hypothesis that rabbit trophoblast penetrates uterine epithelium over blood vessels because an alkaline reaction is elicited there and the epithelial cells become loosened from each other, whereas the trophoblast at the site prevails by reason of its syncytial structure that is not subject to dissociation. These factors seem to explain the clearing of a path, but in addition there may be some kind of mechanical push that sends the trophoblast along it. Both aspects are currently under study; equipment is being tried and improved. There are serious manipulative difficulties and perhaps even more serious theoretical bars to a refined analysis. The objective of gaining reliable quantitative data from microdissection in vivo has not been

attained, and it may prove judicious to attempt no more than an identification of the general kind of mechanism providing the push of trophoblast through uterine epithelium.

Another conclusion recently brought home is that it is not enough to identify the components of a physiological mechanism and describe the course of events from the stimulus to the result; one can be sure that an explanation is incomplete if he has not also explained how the mechanism is "turned off." Böving has tested the idea that trophoblast invasion is turned off by the uterine epithelium's becoming syncytial, just like the trophoblast, and thereby becoming insusceptible to dissociation. The conversion to symplasma occurs about 8 or 9 days after mating in the antimesometrial part of the uterus where the temporary yolk-sac placenta is formed, and after that there is no further massive penetration in that region. (According to Larsen, electron micrographs show some progression, however.) Yet, at the same time, trophoblast invasion begins for the definitive placenta in the opposite (mesometrial) part of the uterus, whose conversion to symplasma lags. Thus, at 9 days after mating, different structure and different resistance to trophoblast invasion exist in opposite parts of the rabbit uterus. Into the lumen of such a uterus was injected a 0.15 *N* solution of NaCO_3 . After 7 minutes, fixation was performed by injecting enough concentrated formalin to bring the final concentration to 10 per cent. The results, shown in plates 12 and 13, figures 49 to 51, demonstrate that the regional difference in dissociability by the high pH of NaCO_3 parallels the regional differences in susceptibility to invasion. Thus, we may take more seriously the proposed idea that rabbit trophoblast invasion is "turned off," in part, by the epithelial conversion to symplasma. (Decreased HCO_3^- concentration in the blastocyst probably plays a part also.)

That should end the story, but much

of the older literature indicates that the conversion to symplasma is stimulated by the corpus luteum and, more particularly, by progesterone. Recently, various observations by Glenister, by Larsen, and by Böving have indicated that the conversion to symplasma is speeded by or may even be dependent on the presence of a blastocyst. Thus, it is not enough to identify the change in maternal structure that arrests trophoblast invasion. We must recognize a new idea requiring further exploration—that the conceptus helps turn off its own invasion by stimulating the formation of symplasma.

ANATOMY AND PHYSIOLOGY OF THE PLACENTA

At the end of June 1963, George W. Corner, Jr., of the department of gynecology and obstetrics of the Johns Hopkins Hospital, who has collaborated with Elizabeth M. Ramsey since 1956, will leave to assume an appointment in another city. In regretful anticipation of the termination of this valued and fruitful association, an effort has been made during the year under review to tie up as many as possible of the loose ends of the experiments in progress and to round off the current phase of the over-all study. Thus, it seems appropriate to make a retrospective survey of the past 7 years before looking ahead to the problems awaiting study.

In 1956 the anatomical studies that had occupied several previous years had reached the point where it was possible to formulate a hypothesis of circulation in the maternal placenta. This hypothesis envisaged the *vis a tergo* of maternal blood pressure as the propulsive force and rested on the assumption that there is an appreciable pressure gradient between the maternal arteries, the intervillous space, and the maternal veins. The series of physiological experiments begun in 1956 was designed to test this assumption, first by determining the pressure in the

intervillous space and the amniotic cavity. Techniques employed for such determinations in humans were adapted for use in monkeys, which had never before been studied in this way. A by-product of the first year's work was the discovery that myometrial activity in the monkey (as reflected in changes in intrauterine pressure) is markedly different at different stages of pregnancy.

In the *next reproductive season* this line was followed; the pattern and intensity of myometrial activity in each stage of pregnancy was worked out through study of a large group of different animals pregnant for different periods of time and also by repeated studies (up to 5 apiece) in the same animal at intervals throughout a single pregnancy. It became possible to diagnose the stage of pregnancy on the basis of pressure recordings alone, without reference to breeding dates, and to predict onset of labor or abortion.

In the *third year* of the study two additional pressure leads were employed, the femoral artery and the femoral vein, thus establishing values for the other components of the pressure gradient assumed in the circulatory hypothesis. It was recognized that the arterial and venous leads were unsatisfactorily distant from the placental margin, yet their testimony to the assumed gradient was clear. An unexpected finding was the mirroring of myometrial activity in pressure changes within the femoral vein. This phenomenon permitted determinations of myometrial activity before laparotomy. It also emerged from this study that pressure in the amniotic cavity and in the intervillous space is so nearly the same that a lead in either cavity alone is sufficient for determination of effective intrauterine and intraplacental pressure.

Up to the beginning of the *fourth year* all work had been done under conditions as nearly physiological as possible. In the 1959-1960 season, since it was considered that a reliable base line of normality had

been established, experiments were instituted employing progesterone and progesterone-like drugs in an attempt to alter the nature of the myometrial contractions. A slight quieting of activity in early pregnancy was the only demonstrable effect of the drugs. This finding being added to the data already assembled, it became possible to formulate certain generalizations about myometrial behavior. Particular attention was directed to the contour of the contraction wave as an indicator of myometrial coordination. Such coordination is as essential as suitable speed and intensity of contractions for expulsion of the conceptus.

Observations of the effect of the contraction-stimulating drug Syntocin may be cited at this point, although they were actually carried out in a subsequent year. These experiments were undertaken in an attempt to induce labor electively at term so that intrauterine pressure during labor could be studied. Success in this attempt was nil. It became apparent that the calendar duration of pregnancy is as unreliable an indication of readiness for delivery in female monkeys as in women, and oxytocics are effective only when the uterus and cervix have become responsive. In the human, the criterion of readiness is the condition of the cervix, determined by palpation. In the monkey, no study of the cervix and its changes during pregnancy had ever been made. A series of such observations was begun as a part of this study, but several breeding seasons will be required for its completion.

Simultaneously with the above, exploratory investigations were undertaken during the third and fourth years, with the cooperation of Russell Morgan, director of the department of radiology of the Johns Hopkins Hospital, and in collaboration with Martin W. Donner of that department, to establish a radioangiographic technique for direct visualization of circulation in the placenta. As continued on through the *fifth*, the *sixth*, and the present (*seventh*) years, these stud-

ies have provided further and highly objective confirmation of the basic hypothesis of placental circulation. Both rapid serial radiography and cineradiography have been employed, and simultaneous intrauterine pressure recordings have been made, to permit correlation of circulatory pattern with the state of uterine contraction.

By the end of the *sixth year* the pattern and dynamics of the arterial side of the circulation had been demonstrated. It was found that blood (dye) enters the intervillous space from the endometrial spiral arterioles in discrete, funnel-shaped streams identical with the "spurts" observed in anatomical preparations; that inflow is cut off during strong uterine contractions and curtailed during weaker ones; that different arterioles may be patent from one contraction to another. This final point, which suggests independent activity of individual arterioles, is of particular significance, and it will be a major object of study in the coming years. It harks back to a basic tenet of the 15-year-long study, namely, that the spiral arterioles are the "dynamic determinants" of placental function.

Within the past 6 months, rounding out the *seventh year* of the current phase of the program, injection of radiopaque dye directly into the intervillous space has permitted cineradiologic visualization of the pathways of venous drainage from the placenta through orifices of exit in its base and via the venous channels of the uterine wall out into the mother's systemic circulation. Preliminary observations suggest that drainage is slower during myometrial contractions. The finely feathery, fan-shaped accumulation of dye forming in the intervillous space at the tip of the injection needle contrasts sharply with the pattern of the dye-filled uterine venous channels. This difference will be of interest and value to students of placental transfer, who are often uncertain of the location of their needle when they attempt to sample intervillous space blood.

From the foregoing it can be seen that the 7 years of the physiological phase of the study have been characterized by several gratifying examples of serendipity. Each year's work has disclosed unexpected aspects of uterine and placental function and opened unexpected bypaths requiring exploration before further progress could be made along the main road. The road has also contained a number of obstacles in the form of unexpected technical difficulties. Each new approach has required a year or more of painstaking study of the surprisingly unknown and unexplored subject of the research: the female rhesus monkey. Her normal reproductive anatomy and physiology, her behavior as an obstetrical patient, and her gynecology are far less known than is generally appreciated. At no time is it possible to write her off as "just like the human but smaller." Her pelvis is anthropoid (rendering many structures surgically inaccessible); her preconversion myometrial activity is in excess of any yet described in the human; her labor is unannounced by premonitory signs or complaints; she must, for the most part, be handled under anesthesia, which eliminates subjective components but introduces pharmacological ones—the list might be extensively prolonged. Thus, one of the major "by-products" of this study has been the insight gained into the subject of the investigations, but no change has occurred in the initial opinion that the rhesus monkey is similar to the human in all important aspects of reproductive structure and function. The variations between the two species are in minor matters only. These may often introduce tedious complications into the experimenter's program, but they do not justify use of the familiar alibi "species difference" as explanation of variations in data from experiments in the two types of subject. As investigations into primate reproductive physiology gain momentum in many laboratories in the future, the experiences of the past 7 years with the Carnegie Colony of breeding

monkeys may be expected to have wide usefulness.

Monkey Colony. Ten female monkeys and one male were purchased in July 1962. Although fine, healthy animals, they were younger than their weight indicated and apparently not completely mature. As a result, the pregnancy rate was very low just at the time when, in view of Corner's impending departure, adequate experimental material was particularly needed. An appeal to colleagues with breeding colonies brought forth a generous response. Donald E. Pickering of the Oregon Primate Research Center, Beaverton, Portland, Oregon, loaned two of his fine pregnant animals to us, despite our frank statement that the monkeys do not always survive the operative and radiologic procedures employed. Leon H. Schmidt of Christ Hospital Institute of Medical Research, Cincinnati, Ohio, loaned us six of his well known colony. It is a pleasure both to acknowledge the generosity of these colleagues and to record a remarkable example of scientific cooperation of the highest order.

The Colony has remained tuberculin free and in good health throughout the year. As always, this achievement rests upon the skill and fidelity of William Cleary and his staff. His cooperation and that of A. G. Rever are valued components of the research in the monkey.

Study of Human Placental Vasculature

Ramsey's transatlantic collaboration with J. W. S. Harris of the department of anatomy at the London Hospital Medical College has progressed smoothly and productively. Harris has completed three models of placental vasculature at 20 days, 9 weeks, and term, respectively, and Ranice Davis of the department of art as applied to medicine of the Johns Hopkins School of Medicine is preparing illustrations of them. Several further models of important developmental stages will be made in the coming year, after which arrangements will be made for the preparation of a manuscript for publication by Harris and Ramsey.

DIFFERENTIATION AND MORPHOGENESIS IN THE HUMAN EMBRYO

THE COLLECTION OF HUMAN EMBRYOS

In the year covered by this report, Elizabeth M. Ramsey examined 60 specimens sent by twelve physicians and laboratories from five states. Of these specimens, 45 were discarded as of no research value, at the end of 3 months after reporting to the donor and in the absence of instructions to the contrary. Fourteen specimens had sufficient research value to justify preservation. One specimen was returned to the donor.

ESTABLISHMENT OF THE CARDIAC PRIMORDIUM IN HUMAN EMBRYOS AT PRESOMITE STAGES

Previous studies of the development of the heart in human embryos indicated

that, as in lower forms, it forms by the fusion of bilateral primordia. Recently, Orts Llorca suggested that the primordium is represented in the early embryo by an endothelial plexus anterior to the prechordal region of the embryo.

During the year, Frank D. Allan has made use of the Collection to conduct a preliminary survey of 10 human embryos at presomite stages. His studies indicate that the mesoderm bridging the anterior end of the embryonic disc is well established in the presomite period and does, indeed, serve as the source of the cardiac primordium. Allan believes that the bulboventricular part of the heart, rather than being formed by fusion of paired primordia, arises in situ from an elaboration of the mesoderm noted above, i.e., by

formation of an endothelial tube intimately associated with the endoderm and less closely associated with the splanchnic mesoderm which eventually becomes the epimyocardial mantle. The tube is linked to the paired sinoatrial portions of the heart which, although flanking the anterior intestinal portal of early somite embryos, are represented by delicate tubes placed more laterally in the mesoderm of the cardiogenic zone in presomite embryos. Indications of an aortic arch flanking the buccopharyngeal membrane have been noted in some embryos.

AN ABNORMAL HEART IN A 6.6-MM HUMAN EMBRYO

Relation to Corrected Transposition of the Great Vessels

In examining young human embryos of Streeter's age groups x and xi, in particular, embryos having 8 to 14 somites, Arentje Dekker noted that the bending of the heart tube appears to be related to an active cell multiplication in the caudal part of the tube (embryos with 8 to 13 somites), this part then filling out the left half of the pericardial sac. That movement is followed shortly (11 to 14 somites) by the initiation of another center of growth, in the cranial part of the tube (deviating only slightly to the right and, in its truncal part, bent ventrad). This proliferation results in linear growth, resulting in a downward movement to the right, the cranial part then occupying the still available space in the right half of the pericardial sac.

Both Davis, in his classic paper on the early development of the heart in man (*Contributions to Embryology*, 19, pp. 245-284), and, more recently, de Vries and Saunders in their extensive study of the heart (*Contributions to Embryology*, 37, pp. 87-114), present drawings in which the predominance of the caudal end of the tube is recognizable. They appear, however, to have overlooked its significance for the normal development of the ventricular loop.

Dekker's observation acquired additional meaning when, during a further examination of older embryos, an embryo was encountered in horizon xiv in which the heart was abnormal: the supposedly primitive "left" ventricle was found at the right, and the truncus and distal infundibulum were deviated to the left, being at sharp angles to the trabeculated right ventricle. This heart was examined intensively; Dekker's study required modeling of the heart in order to determine the spatial relations of the chambers.

From the appearance of the models (one plaster reconstruction of the outer form of the heart, one plaster reconstruction of the walls and septa of the heart, and one plaster cast of the heart cavity; magnification in all three of them 62.5X), closely compared with the sections, the following conclusions can be drawn.

The heart as a whole is displaced to the right. Truncus and distal infundibulum are situated at the left of the embryo's sagittal midplane, in an almost transverse plane, from dorsal toward ventral. Proximal infundibulum and trabeculated right ventricle are likewise situated in a transverse plane, from the sagittal midline toward the right parallel to the ventral body wall, thus causing a sharp angulation. The ventricle is small, rectangular on cross section, and seems to be compressed between the right atrium and the forebrain. It lies on top of the other, "left," ventricle, which, however, is situated on the right side, reaching even farther toward the right than the trabeculated right ventricle and extending farther dorsally, beneath the right atrium. This "left" ventricle also extends downward. The atrioventricular canal connects this ventricle with the left atrium. Its main direction is from right anterior to left posterior, being adjacent to the lowermost part of the interventricular communication. The lowermost part of the proximal infundibulum and trabeculated right ventricle lies nestled against the interventricular canal. The left atrium lies for some distance beneath the truncus

and the infundibulum, hardly protruding at their left side, but extending down almost as far as the left ventricle.

These findings, combined with her observations on the heart in normal embryos, have led Dekker to the following tentative explanation for the anomaly. An initial abnormal proliferative pattern resulted in the growth of the caudal part of the cardiac tube toward the right. Thus, the right half of the pericardial sac was filled, and the downward movement to the right of the cranial end became impossible. The elongating truncus and infundibulum took refuge to the left, but the trabeculated right ventricle nestled on top of the right-sided primitive "left" ventricle, creating the sharp angulation. However, only toward the left and caudally was space available; and so, as growth continued, the chamber was "pushed" in that direction, possibly in relation to the growth of the right atrium.

Had development continued, the trabeculated right ventricle might have descended on the left side, leading to the anomaly known as corrected transposition of the great vessels: the anatomically right and left ventricle are exchanged; the left-sided right ventricle is interposed between the left atrium and the (likewise left-sided) aorta, the right-sided left ventricle being interposed between right atrium and dextroposteriorly placed pulmonary artery. This situation is hemodynamically normal, but other anomalies often supervene.

But such speculations, however intriguing to the student of cardiogenesis and teratogenesis, are too specialized for further discussion at this point, being reserved for a technical account now in preparation.

OBSERVATIONS ON THE "ORGANIZER" AREA OF THE HUMAN EMBRYO AT PRESOMITE STAGES

In the course of his study of the earliest stages of cardiogenesis, Frank D. Allan observed extracellular granules with the same staining characteristics and size as

nucleoli (nucleoli being abundant in the nuclei of cells comprising these tissues) in a number of human embryos at presomite and early somite stages. In general, these granules occur in regions of the embryonic disc thought to be active in organization of the embryo, i.e., prechordal plate, notochordal process, medullary plate, and primitive streak. They are not believed to be fixation or stain artifacts, nor are they artifacts due to autolytic changes. According to Allan, their staining properties suggest that they may be RNA or ribonucleoprotein. Their significance, if any, remains to be determined.

PRENATAL DEVELOPMENT OF THE JOINTS OF THE CLAVICLE

Benjamin C. Moffett's present investigation is an outgrowth of his earlier study (*Contributions to Embryology*, 36, 19-28) on the development of the temporomandibular joint in man. The findings of the original investigation suggested two hypotheses, which he is now examining: (1) that the synovial joints lacking hyaline articular cartilage have developed from discontinuous blastemata, the intervening mesenchyme becoming the articular tissue; (2) that the articular discs in certain synovial joints represent muscle tendons that were intercepted by the developing joints.

The joints of the clavicle provide a test of the two hypotheses, for they contain articular discs, lack hyaline cartilage, display frequent variations in man, and show marked anatomical differences in various mammals. Furthermore, the details of their prenatal development are not available in the literature.

A study of this problem is now in progress using human embryos in the Carnegie Collection. Human and insectivore fetuses are also being compared, important information being obtained from the Bluntschli Collection.

Examination of the human specimens indicates that: (1) The articular disc of the sternoclavicular joint represents the intercepted tendon of the clavicular part

of the sternocleidomastoid muscle. (2) The occasional presence of an articular disc in the acromioclavicular joint represents a part of the trapezoid ligament which has been incorporated into the joint. (3) The coracoclavicular ligaments appear to have been derived from the tendon of the pectoralis minor muscle. Examination of fetuses from *Centetes ecaudatus*, an insectivore from Madagascar, indicates that in this animal: (4) The sternoclavicular joint is rudimentary and lacks an articular disc as well as a clavicular part of the sternomastoid muscle. (5) The acromioclavicular joint is normally absent. (6) The acromion and the clavicle do not contact each other but are joined by a muscle having a common origin from these two bones. (7) The lateral tip of the clavicle rests against the head of the humerus and is held in position by a ligament which attaches to the coracoid process. (8) At its clavicular attachment, this ligament is impinged between the clavicle and humerus in what appears to be the primitive form of a joint with an articular disc. The significance of these preliminary findings will be clarified by the dissection and histologic study of a newborn *Centetes* in the Bluntschli Collection.

Data from the present study support the proposed hypotheses and represent specific facts not yet published on the embryology of joints.

THE HUMAN FETAL THYROID: ITS WEIGHT IN RELATION TO BODY WEIGHT, CROWN-RUMP LENGTH, FOOT LENGTH, AND ESTIMATED GESTATION AGE

There are few records of the weight of the thyroid gland in man at intervals

during pregnancy, especially during the first half of the gestation period. To provide a basis for further studies, T. H. Shepard, H. J. Andersen, and H. Andersen have determined the weights of 79 human fetal thyroids as compared with crown-rump length, foot length, weight, and estimated gestation age. Of the fetuses examined, 22 were from the Carnegie Collection and 57 from the department of human anatomy at the University of Copenhagen. Lillie's fixative caused a 20 to 30 per cent loss of weight of the gland, whereas formaldehyde fixation was associated with weight gain. The thyroids of fetuses fixed in formalin and subsequently transferred to 70 per cent ethyl alcohol weighed about the same as the unfixed fresh glands.

Thirty per cent of the examined thyroids had a pyramidal lobe.

The ratio of thyroid to body weight was lower in the smaller fetuses and gradually increased until the fetus was 70 to 90 mm in crown-rump length, when the ratio reached a value close to that of the newborn and adult. The period during which this ratio is attaining its peak is roughly correlated with follicle formation and onset of ability to concentrate iodine.

A comparison of the estimated age of fetuses in the Danish material and the formalin-fixed fetuses from the Carnegie Collection suggests that the Danish fetuses under 40 mm in crown-rump length are 4 to 6 days older than the average given by Streeter. Shepard and his associates believe that Streeter's averages may be too low and that the relative ages of the two groups may be comparable.

TERATOGENESIS

PRELIMINARY STUDIES IN THE PRODUCTION OF MALFORMATIONS WITH THALIDOMIDE

In cooperation with Helen Taussig, Arentje Dekker and Ali Mehrizi under-

took to test the effect, on the offspring, of administering thalidomide to pregnant rabbits.

Their initial experiments confirmed Somers's observation that limb abnormalities occurred in litters from New

Zealand white rabbits fed thalidomide in a dose of 150 mg/kg body weight from day 8 to day 16 of gestation.

The next step was to find the most reliable method of administering the drug for the production of the anomalies. Thalidomide was given by tube feeding, mixed with food pellets, made into pellets together with the food, and by medicine dropper in corn oil suspension. The last method proved to be the most satisfactory.

The period of administration was then reduced to 4 days, namely, from day 8 through 11, the period in which the initial, critical stages of limb formation are accomplished. Nine pregnant New Zealand white rabbits, fed a corn oil suspension of thalidomide by medicine dropper for 4 days, starting on day 8, produced malformed fetuses in 100 per cent of the litters; i.e., each of the nine litters had abnormal offspring. Among the total of 51 offspring, 48 were malformed. All these 48 animals had malformed extremities, ranging from mild to marked curving of the limbs to clubfeet, and in one of them the left forelimb was lacking. Moreover, 13 animals among the 48 had additional abnormalities: in 4 of them the tail was absent; in 3 others the tail was very short; 5 had an abnormal nose; 2 had skull defects; and 3 had malformed external genitalia. Clearing of the specimens and staining of the bones with alizarine disclosed that the radius and tibia were particularly affected. Two control rabbits gave birth to 18 fetuses, all of them normal. In a further attempt to pinpoint the time at which thalidomide is effective, a series of experiments was planned in which the drug was administered in different combinations of 2 or 3 days within the aforementioned 4-day period (days 8, 9, and 10; 9, 10, and 11; 8 and 9; 9 and 10); administration was in one dose on day 8 only and on day 9 only; administration was in three doses every 8 hours on day 9 of gestation. These experiments are still in progress. The results obtained thus far indicate that administration during these shorter peri-

ods results, on the whole, in less severe malformations (often "bayonet-wrist"; sometimes exclusively defects of the skull or of the nose), and that the incidence of anomalies is lower.

In a group of 10 pregnant rats, thalidomide, injected intraperitoneally, did not produce any limb malformations.

EXPERIMENTAL PRODUCTION OF CLOACAL EXSTROPHY

In the practice of pediatric urology, the surgeon is confronted by a wide range of genitourinary congenital anomalies, many of which threaten life or are socially unacceptable and thus have to be corrected. Attempts in reconstructive surgery demand a thorough understanding of the pathogenesis of each developmental defect as well as its physiology.

In a comprehensive clinical study of one such anomaly, exstrophy of the bladder, Marshall suggested that the defect underlying all cases of epispadias and exstrophy of the urinary bladder is an overly developed cloacal membrane which does not regress during the first 6 weeks of embryonic life.

In the human embryo at 30 days, the prominent cloacal membrane occupies the central part of the infraumbilical abdominal wall. Mesoderm from the primitive streak passes around the lateral margins of this deltoid-shaped membrane; its proliferation along these margins forms the raised genital folds. The cloacal membrane normally reaches its greatest dimension (0.575 mm) in the 4- to 5-mm embryo; thereafter it regresses in size, thereby allowing the mesoderm to reinforce the essentially bilaminar central part of the infraumbilical abdominal wall. An abnormally large and persisting cloacal membrane during this early embryonic period could act as a mechanical barrier to mesodermal movement and hold apart the developing structures of the lower abdominal wall. The characteristic wedge defect of the musculoskeletal structures in the exstrophy complex would result. The cloacal mem-

brane ruptures normally in 15- to 16-mm embryos, establishing the urogenital opening. Thus, depending on the size and superior extent of the cloacal membrane at the moment of its perforation, variations in exstrophy of the bladder could be achieved. Therefore, the wedge effect of an abnormally large cloacal membrane in the first 6 weeks of embryonic life appears to be the key in the genesis of the exstrophy complex.

The origin of the cloacal membrane has to be considered in experimental approaches to this problem. Originally, it lies adjacent to the primitive streak remnant of the early embryo. With rapid elongation of the embryo and concomitant formation of its tail, this membrane, with the tail, rotates from the dorsal to the ventral position and forms the anterior wall of the primitive cloaca. The same process occurs in the chick embryo. At the 24- to 27-somite stage (52-60 hours of incubation) the tail fold begins to form. With consequent infolding of the posterior splanchnopleure in the formation of the tail fold, the anterior wall of the hindgut and cloaca is formed. Thus, before the formation of the tail fold, the extraembryonic region immediately caudad to the primitive streak remnant is the anlage of the cloacal membrane.

For experimental purposes Edward C. Muecke chose an early embryonic stage in the chick, the dorsally located primordium of the cloacal membrane being surgically altered by the insertion of an inert plastic (Millipore) graft. Theoretically, such a graft, simulating a nonregressing cloacal membrane, would be expected to act as a mechanical barrier to mesodermal movements as this region rotates ventrally to form the infra-umbilical abdominal wall. Experimental results showed that this indeed was the case. Cloacal exstrophy was produced,

supporting Marshall's hypothesis that the basic defect in the exstrophy complex occurs during early embryogenesis in the form of an overly developed, nonregressing cloacal membrane acting as a mechanical barrier to mesodermal flow. The inert plastic graft, surgically placed to simulate an enlarged and persisting cloacal membrane, holds apart developing structures of the lower abdominal wall in the chick embryo, producing results strikingly analogous to those of human exstrophy.

Muecke's is the first experimental production of exstrophy. Spontaneous occurrence of the anomaly has not been reported in the chick. Among mammals, exstrophy is most common in man, occurring once in 50,000 live births. In other mammals the exstrophy complex is exceedingly rare; only two cases have been described in the veterinary literature. A possible explanation for this observed variation in incidence according to species may lie in the varying importance to embryonic survival of structures adjacent to the cloacal membrane, particularly the allantois. In the chick the allantois is important to respiration, and interference with the developing allantoic vasculature is incompatible with fetal viability. This point was demonstrated in the present study by the low survival rate of embryos operated upon once the tail bud had formed (later than 52-60 hours of incubation). In domestic animals also, such as pig, horse, dog, and sheep, the allantois is of vital importance. Therefore, an early defect in the tail-bud allantoic region could well have fatal consequences for the embryo. In man, however, the allantois is a vestigial structure. Abnormalities in the neighboring cloacal area might be better tolerated, and significant incidence of the exstrophy complex in live births could be expected.

APPARATUS AND TECHNIQUES

A METHOD FOR THE RAPID
SEPARATION OF RIBONUCLEOTIDES

An improved simple gradient of formic acid has been devised by G. L. Carlson for use in the rapid separation of small amounts of ribonucleotides on columns of the formate form of Dowex-1-resin. Elution of the ribonucleotides in volumes of liquid in the neighborhood of 100 ml together with reproducible control of the elution pattern results from the use of a steep gradient of ever-increasing slope.

Depending on the resolution intended, columns of Dowex-1-formate resin of 6-mm diameter and lengths of 75 mm or more are prepared. The columns of resin are washed extensively with distilled water, and solutions of nucleotides (300–1000 μg nucleotides) adjusted to pH 7.2–8.0 are applied to the top of the resin.

In forming the gradient, a standard 50-ml Ehrlenmeyer flask serving as a reservoir is bridged by an inverted U tube to a 100-ml beaker serving as a mixing chamber to provide constant equalization of the levels in the vessels. The reservoir is filled initially with 50 ml of 45 per cent

formic acid, and the mixing chamber is then filled with water (70 ml) to a height equal to that of the formic acid. After the two vessels are connected by a water-filled U tube and mechanical stirring of the mixing chamber is begun, a siphon arrangement carries the contents of the mixing chamber to the column of resin. Flow rates through the column of 15–40 ml per hour yielded satisfactory separations. An example of an elution pattern is shown in figure 52.

The slow early increase in formic acid concentration selectively elutes the cytidylic and adenylic acids, which are more positively charged at moderately low pH . The gradient then increases more rapidly, and the lowered pH together with the increasing competition for the resin by the formic acid brings guanylic and uridylic acids off the column in rapid succession.

Intermittent observation of a continuous recording of the absorption at $254\text{ m}\mu$ of the column effluent permitted the collection of four fractions in which the bases were separated for the spectrophotometric analyses shown in figure 53.



Fig. 52. Separation of ribonucleotides on Dowex-1-resin. *Escherichia coli* microsomal RNA hydrolyzed 18 hours at 37° with 0.2 N KOH, adjusted to pH 7.5, and placed on 0.6 by 75 mm column of Dowex-1-formate. Elution conditions as described in the text. Absorption at and near $254\text{ m}\mu$ measured with a Uviscan monitor equipped with a nickel sulfate solution filter and recorded over 3.6 hours with a Varicord 43 potentiometer.

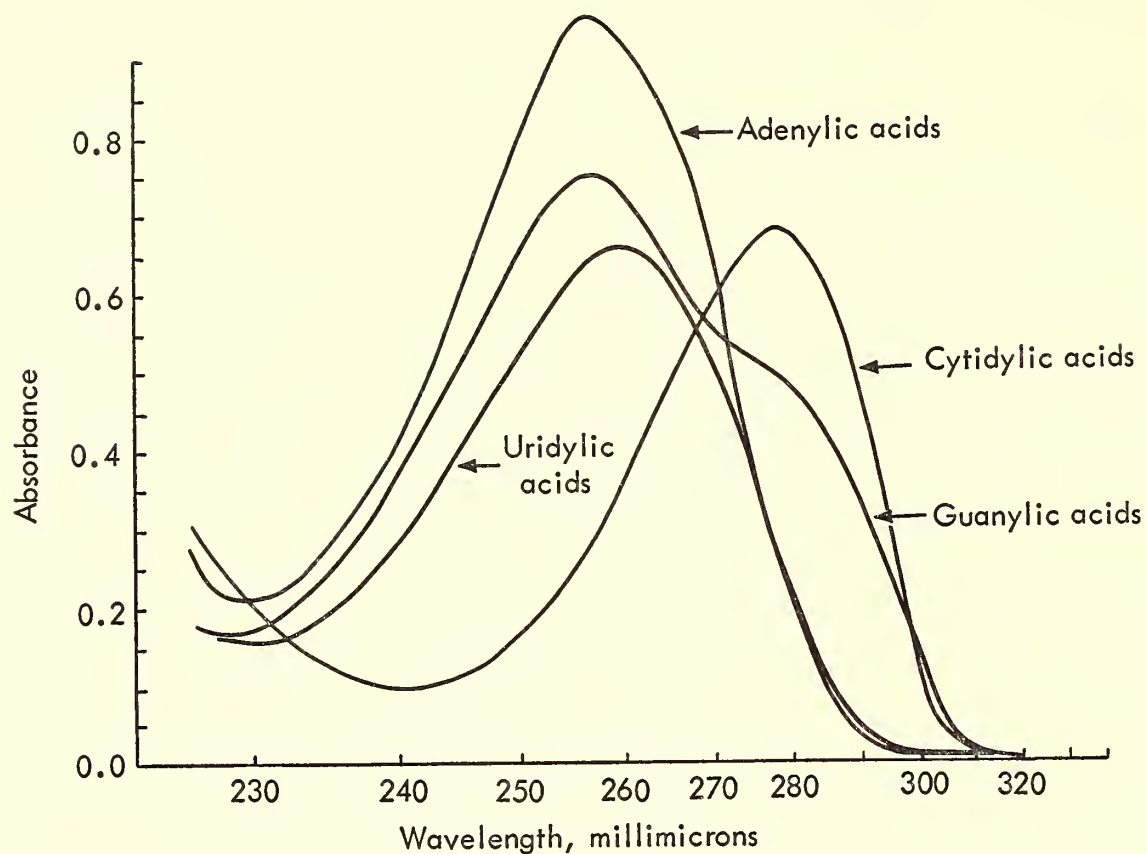


Fig. 53. Spectra of ribonucleotides separated on Dowex-1-resin. Nucleotide fractions separated as described in text, taken to dryness in vacuo, and dissolved in 0.08 *N* HCl. Absorbance recorded versus water in a Beckman DK2 spectrophotometer.

STAFF ACTIVITIES

Mall, Franklin P., Johns Hopkins University, Baltimore, Md. Grant No. 874, allotted Feb. 20, 1913. Embryological research. \$15,000. The grant for embryological research was made available upon March 21, 1913, and steps were taken at once to inaugurate the work.

With these lines, extracted from a two-page report in *Year Book 12*, pages 290–291, began the first report of organized embryological research in Carnegie Institution of Washington, leading, a year later, to the founding of the Department of Embryology. On April 8, 1963, scientists representing many different fields of research, including a number of biologists who were in Washington, D.C., to attend the Diamond Jubilee meeting of the American Association of Anatomists, gathered in the Institution's Elihu Root Hall to celebrate the fiftieth anniversary of the founding of the laboratory and the one hundredth anniversary of the birth of Franklin P. Mall.

Guests at the ceremonies heard George W. Corner, past Director of the Depart-

ment of Embryology and professor of embryology, emeritus, at Johns Hopkins Medical School, discuss the aims and achievements of Mall. A second major address was given by Clement L. Markert, professor of biology, Johns Hopkins University, who took as his theme "Insights and Perspectives in Embryology."

These lectures were among the highlights in a year in which the roster of speakers at the seminars organized by the Department to serve all those working in developmental biology in the area included a number of distinguished names: J. T. Bonner, Princeton University; T. W. Glenister, London; Jerome Gross, Massachusetts General Hospital; Milan Hasek, Prague; Elizabeth Hay, Harvard Medical

School; Martin Nemer, Institute for Cancer Research; Harold Nitowsky, Sinai Hospital, Baltimore; Keen Rafferty, Johns Hopkins University School of Medicine; Roger Robineaux, Paris; J. P. Trinkaus, Yale University; Colette and Roger Vendrely, Paris; Lutz Wiese, Princeton University; C. E. Wilde, Jr., University of Pennsylvania.

Among the principal lectures presented by our own staff members, fellows, and visiting investigators, the following should be mentioned: a series of lectures delivered under the auspices of the Patten Foundation at Indiana University during February and March 1963; and lectures at the following colleges and universities: Brandeis University, the Universities of Connecticut and Delaware, Duke University Medical School, University of Geneva (Switzerland), George Washington University Medical School, Goucher College, Harvard Medical School, University of Iowa, Marquette University, Medical College of Virginia, Universities of Michigan, Milan, and Palermo, Princeton University, Universities of Rome, Toronto, and Virginia, Wabash College, Washington University (St. Louis), Western Reserve University, Yale University, and University of Zurich.

Other research centers at which lectures were given included the Gerontology Branch of the National Heart Institute, RIAS, and Rockefeller Institute.

Staff members and fellows also took part in several international and national meetings, including the Fourth World Congress of Cardiology, held in Mexico City; the International Symposium on Implications of Organic Peroxides in Radiobiology at Argonne, Illinois; the International Physiological Congress at Leiden, Holland; the UNESCO Symposium on Biological Organization at the Cellular and Supercellular Level held at Varenna, Italy; the Conference on Uterine Motility and Physiology of the Placenta, at Charlottesville, Virginia; and a conference on developmental biology at MIT's Endicott House.

Other learned societies at meetings of which members of the group participated were the American Association for the Advancement of Science, American Association of Anatomists, American Institute of Biological Sciences, American Society of Biological Chemists, American Society for Cell Biology, American Society of Zoologists, Biophysical Society, Federation of American Societies for Experimental Biology, Histochemical Society, Society of American Bacteriologists, Society for Experimental Biology and Medicine, Society for the Study of Development and Growth, Society of General Physiologists, Society for Gynecologic Investigation, and Society for Pediatric Research.

Advisory and consultative services included membership on the editorial boards of *American Zoologist*, *Biological Bulletin*, *Journal of Embryology and Experimental Morphology*, the section on Human Developmental Biology of *Excerpta Medica*, and the board of consulting editors of *Developmental Biology*. One member of the staff continued to serve on the Divisional Committee for Biology and Medicine in the National Science Foundation, the Cell Biology Study Section of the National Institutes of Health, the Subcommittee on Congenital Malformations of the U. S. National Committee on Vital and Health Statistics, and the Visiting Committee, Department of Biology, Massachusetts Institute of Technology.

Several members of the staff rendered service by acting in the following capacities: president, AIBS; president, Maryland Section, Society of Experimental Biology and Medicine; chairman, American Organizing Committee for the forthcoming International Conference on Organogenesis (International Institute of Embryology); secretary, Society of General Physiologists; secretary, Section F, AAAS; member, Newcomb Cleveland Prize Award Committee, AAAS; chairman of the Life Sciences Committee (National Science Foundation) for Post-

doctoral Fellowships (through the National Research Council); member of the Executive Committee of the American Association of Anatomists.

One member of the group took part in an effective undergraduate educational program, the Visiting Scientist Program of the American Physiological Society, by giving two series of lectures to undergraduates at Lafayette College and Randolph-Macon Woman's College.

Other activities directed largely toward teaching included the participation of four members of the Department in the Embryology Training Program, Marine Biological Laboratory, Woods Hole, Massachusetts; service on the Commission on Undergraduate Education in the Biological Sciences; and participation in an educational television program produced

by AIBS and the Society of General Physiologists.

As in the past, several members of the group took limited part in formal courses in several departments of the Johns Hopkins University and School of Medicine, including anatomy, biochemistry, and biology, and in a special course in McCoy College.

Special mention should be made of honors accorded two members of the group. Dr. Elizabeth M. Ramsey was elected an honorary member of the Society for Gynecologic Investigation. Edward C. Muecke was awarded first prize in the 1963 Annual Prize Essay Contest sponsored by the New York Section of the American Urologic Association and the Section on Urology of the New York Academy of Medicine.

BIBLIOGRAPHY

- Allan, F. D., Observations on the organizer areas of the human presomite embryo, *Anat. Record*, 145, 199, 1963.
- Allan, F. D., Observations on the establishment of the cardiac primordium in the human presomite embryo, *Anat. Record*, 145, 307, 1963.
- Argyris, B. F., Loss of acquired tolerance to skin homografts in mice, *Transplant. Bull.*, 30, 140-141, 1962.
- Argyris, B. F., Adoptive tolerance; transfer of the tolerant state, *J. Immunol.*, 90, 29-34, 1963.
- Argyris, T. S., see Mun, A. M.
- Bishop, D. W., Oscillating systems of cell motility with particular reference to sperm flagellation, in *Scritti in onore del Professor Giuseppe Tesauero*, edited by V. Danesino, Montanino Editore, Naples, Italy, pp. 151-161, 1962.
- Bishop, D. W., Review of "Mechanisms of Antibody Formation," *Am. Scientist*, 51, 79A-80A, 1963.
- Bishop, D. W., Antitestis antibody concentration in sensitized guinea pigs, *Proc. Biophys. Soc.* (7th Ann. Meeting, February 18-20, 1963), MA1, 1963.
- Bishop, D. W., see also Carlson, G. L., and Glover, T. D.
- Böving, B. G., Conflicting interpretations of trophoblastic invasion, *Anat. Record*, 145, 210, 1963.
- Böving, B. G., Medical research on animals, Letter to the Editor of *The Sun*, Baltimore, Md., June 24, 1963.
- Brown, D. D., and J. D. Caston, Biochemistry of amphibian development, I, Ribosome and protein synthesis in early development of *Rana pipiens*, *Develop. Biol.*, 5, 412-434, 1962.
- Brown, D. D., and J. D. Caston, Biochemistry of amphibian development, II, High molecular weight RNA, *Develop. Biol.*, 5, 435-444, 1962.
- Brown, D. D., and J. D. Caston, Biochemistry of amphibian development, III, Identification of ferritin in the egg and early embryos of *Rana pipiens*, *Develop. Biol.*, 5, 445-451, 1962.
- Carlson, G. L., and D. W. Bishop, Chemical nature of a preparation which induces aspermatogenesis in the guinea pig, *Am. Zoologist*, 2, 511, 1962.
- Caston, J. D., Appearance of catechol amines during development of *Rana pipiens*, *Develop. Biol.*, 5, 468-482, 1962.
- Caston, J. D., see also Brown, D. D.
- Coleman, J. R., Deoxyribonuclease activities in the development of the leopard frog, *Rana pipiens*, *Develop. Biol.*, 5, 232-251, 1962.
- Coleman, J. R., Acid deoxyribonuclease activity in amphibian metamorphosis, *Biochim. Biophys. Acta*, 68, 141-143, 1963.
- Corner, G. W., Jr., The fetal and maternal circulation of the placenta, *Clin. Obstet. Gynecol.*, 6(1), March 1963.

- Corner, G. W., Jr., Elizabeth M. Ramsey, and Herbert M. Stran, Patterns of myometrial activity in the rhesus monkey in pregnancy, *Am. J. Obstet. Gynecol.*, **85**, 179-185, 1963.
- Corner, G. W., Jr., *see also* Ramsey, E. M.
- Davis, R. W. B., *see* Ramsey, E. M.
- DeHaan, R. L., Organization of the cardiogenic plate in the early chick embryo, *Acta Embryol. Morphol. Exptl.*, **6**, 26-38, 1963.
- DeHaan, R. L., Regional organization of pre-pacemaker cells in the cardiac primordia of the early chick embryo, *J. Embryol. Exptl. Morphol.*, **11**, 65-76, 1963.
- DeHaan, R. L., Migration patterns of the precardiac mesoderm in the early chick embryo, *Exptl. Cell Res.*, **29**, 544-560, 1963.
- DeHaan, R. L., Oriented cell movements in embryogenesis, in *Biological Organization at the Cellular and Supercellular Level*, edited by R. J. C. Harris, Academic Press, New York, pp. 147-164, 1963.
- Dekker, A., Anatomical and embryological features of truncus and pseudotruncus arteriosus, *Anat. Record*, **145**, 221, 1963.
- DeLanney, L. E., *see* Mun, A. M.
- Donner, M. W., *see* Ramsey, E. M.
- Ebert, J. D., Review of "Mechanisms of Antibody Formation" by M. Holub and L. Jaroskova, *Quart. Rev. Biol.*, **36**, 302-303, 1961.
- Ebert, J. D., Tissue transplantation, reprinted in *Anales del Desarrollo*, **10**, 91-106, 1962, and *Frontiers of Modern Biology*, edited by Gairdner Moment, Houghton Mifflin Company, Boston, pp. 94-102, 1962.
- Ebert, J. D., Ontogenesis of the immune response, in *Hereditary, Developmental and Immunologic Aspects of Kidney Disease*, edited by Jack Metcalf, Northwestern University Press, Evanston, Illinois, pp. 48-53, 1962.
- Ebert, J. D., Congenital defects, in *Year Book of Science and Technology*, McGraw-Hill Book Company, New York, pp. 205-206, 1963.
- Ebert, J. D., Discussion of "Developmental studies of mouse thymus and spleen" by R. Auerbach, *Natl. Cancer Inst. Monograph* **11**, 32, 1963.
- Ebert, J. D., "Biology on the cuff"—Is AIBS worth saving? *Science*, **139**, 321-322, 1963.
- Ebert, J. D., The labile chorioallantoic membrane: Changes effected by viruses and inhibitors, *Am. Zoologist*, **3**, 235-243, 1963.
- Ebert, J. D., In search of a new focus, *AIBS Bull.*, **13**, 8, 1963.
- Ebert, J. D., *see also* Mun, A. M.
- Errico, J., *see* Mun, A. M.
- Glover, T. D., and D. W. Bishop, Effect of the route of administration of bovine gamma-globulin on antibody formation in the guinea pig, *Nature*, **198**, 901-902, 1963.
- Hendley, D. D., A. S. Mildvan, M. C. Reporter, and B. L. Strehler, The properties of isolated human cardiac age pigment, I, Preparation and physical properties, *J. Gerontol.*, **18**, 144-150, 1963.
- Konigsberg, I. R., The developmental potency of the outgrowth of adult skeletal muscle tissue in vitro, in *Biological Aspects of Aging*, edited by N. W. Shock, Columbia University Press, New York, p. 296, 1962.
- Konigsberg, I. R., Review of "Animal Tissue Techniques," *Science*, **137**, 332, 1962.
- Konigsberg, I. R., Review of "Methods of Tissue Culture," *Science*, **137**, 275, 1962.
- Konigsberg, I. R., Clonal analysis of myogenesis, *Science*, **140**, 1273-1284, 1963.
- Konigsberg, I. R., *see also* Reporter, M. C.
- McKusick, A. B., *see* Scott, P. P.
- McKusick, V. A., *see* Scott, P. P.
- Mehrizi, A., Origin of both great vessels from the right ventricle, *Anat. Record*, **145**, 260, 1963.
- Mildvan, M. C., *see* Hendley, D. D.
- Mun, A. M., P. Tardent, J. Errico, J. D. Ebert, L. E. DeLanney, and T. S. Argyris, An analysis of the initial reaction in the sequence resulting in homologous splenomegaly in the chick embryo, *Biol. Bull.*, **123**, 366-387, 1962.
- O'Rahilly, R., Some features of the histogenesis of the otic vesicle in staged human embryos, *Anat. Record*, **145**, 268, 1963.
- Papaconstantinou, J., R. A. Resnik, and E. Saito, Biochemistry of bovine lens proteins, I, Isolation and characterization of adult α -crystallins, *Biochim. Biophys. Acta*, **60**, 205-216, 1962.
- Ramsey, E. M., Placental circulation, in *Blood and Lymph Vessels*, edited by D. I. Abramson, Academic Press, New York, pp. 465-485, 1962.
- Ramsey, E. M., Circulation in the intervillous space of the primate placenta, *Am. J. Obstet. Gynecol.*, **84**, 1649-1663, 1962.
- Ramsey, E. M., G. W. Corner, Jr., and M. W. Donner, Serial and cineradiographic visualization of maternal circulation in the primate (hemochorial) placenta, *Am. J. Obstet. Gynecol.*, **86**, 213-225, 1963.
- Ramsey, E. M., and R. W. B. Davis, A composite drawing of the placenta to show its structure and circulation, *Anat. Record*, **145**, 366, 1963.
- Ramsey, E. M., *see also* Corner, G. W., Jr.
- Reporter, M. C., I. R. Konigsberg, and B. L. Strehler, Kinetics of accumulation of creatine phosphokinase activity in developing embryonic skeletal muscle in vivo and in monolayer culture, *Exptl. Cell Res.*, **30**, 410-417, 1963.

- Reporter, M. C., and B. L. Strehler, Studies of factors affecting photosynthetic luminescence, in "Studies of Microalgae and Photosynthetic Bacteria," *Plant Cell Physiol. Tokyo* (Tamiya Festschrift Issue), 4, 281-290, 1963.
- Reporter, M. C., *see also* Hendley, D. D.
- Resnik, R. A., *see* Papaconstantinou, J.
- Saito, E., *see* Papaconstantinou, J.
- Scott, P. P., V. A. McKusick, and A. B. McKusick, The nature of osteogenesis imperfecta in cats, *J. Bone Joint Surg.*, 45A, 125-134, 1963.
- Stran, H. M., *see* Corner, G. W., Jr.
- Strehler, B. L., *see* Hendley, D. D., and Reporter, M. C.
- Tardent, P., *see* Mun, A. M.
- Wilson, I. B., A new factor associated with the implantation of the mouse egg, *J. Reprod. Fertility*, 5, 281-282, 1963.

PERSONNEL

Year Ended June 30, 1963

(including those whose services began or ended during the year)

Research Staff

David W. Bishop, General Physiology
 Bent G. Böving, Physiology
 Donald D. Brown, Biochemistry
 Robert L. DeHaan, Experimental Embryology
 James D. Ebert, Director
 Irwin R. Konigsberg, Experimental Embryology
 Elizabeth M. Ramsey, Placentology; Pathology
 Mary E. Rawles, Experimental Embryology

Assistant Investigator

Minocher C. Reporter

Research Associates (Extramural)

Louis B. Flexner, Philadelphia
 Arthur T. Hertig, Boston
 Chester H. Heuser, Augusta, Georgia
 Samuel R. M. Reynolds, Chicago

Fellows

Gerald L. Carlson, Fellow of the Given Foundation-National Research Council
 J. Douglas Caston, Fellow of Carnegie Institution of Washington
 Yvon Croisille, Fellow of Carnegie Institution of Washington
 Igor B. Dawid, Fellow of Carnegie Institution of Washington
 Mark L. Hartman, Predoctoral Fellow of Carnegie Institution of Washington
 Edward C. Muecke, Dunnington Foundation Fellow
 Gretchen Schabtach, Predoctoral Fellow of Carnegie Institution of Washington

Visiting Investigators

Frank D. Allan, Washington, D. C.
 George W. Corner, Jr., Baltimore
 Arentje Dekker, Leiden
 Louis E. DeLanney, Crawfordsville, Indiana
 Martin W. Donner, Baltimore

W. Richard Ferguson, Baltimore
 Charles R. Green, Melbourne
 R. D. Laurenson, Kingston, Ontario
 Ali Mehrizi, Baltimore
 Benjamin C. Moffett, Jr., Detroit
 F. Orts Llorca, Madrid
 E. Carl Sensenig, Birmingham, Alabama
 Thomas H. Shepard, Seattle

Clerical and Technical Staff

Mary N. Barton, Librarian
 Franklin R. Baytops, Custodian
 James Blackwell, Custodian
 George Boettinger, Porter
 Barbara Brown, Dishwasher
 J. W. Chase, Assistant Recorder
 William I. Cleary, Recorder
 Lloyd Crane, Technician
 Lawrence E. Dorsey, Custodian
 William H. Duncan, Senior Technician
 Ernest W. Edwards, Custodian
 Linda Fuson, Technician
 Wilbur F. Garde, Assistant Recorder
 Thomas F. Garnett, Technician
 Norman R. Gortt, Assistant Recorder
 Richard D. Grill, Photographer
 Charles E. Hargett, Assistant to the Director
 Ernest Harper, Chief Custodian
 Virginia Hicks, Laboratory Helper
 Jeannie Hubbard, Technician
 Elaine C. Kerby, Stenographer
 Leo Kormann, Technician
 Frank J. Kupres, Technician
 Edna G. Lichtenstein, Secretary
 Elizabeth Littna, Technician
 Ellen P. Monaghan, Technician
 Arlyne Musselman, Technician
 John Pazdernik, Building Engineer
 Margaret J. Proctor, Secretary
 Arthur G. Rever, Fiscal Officer
 Pauline M. Stott, Technician
 Nancy J. Sype, Technician
 John L. Wiser, Machinist

Special Technical Assistant pro tempore

Joseph P. Drane



PLATES

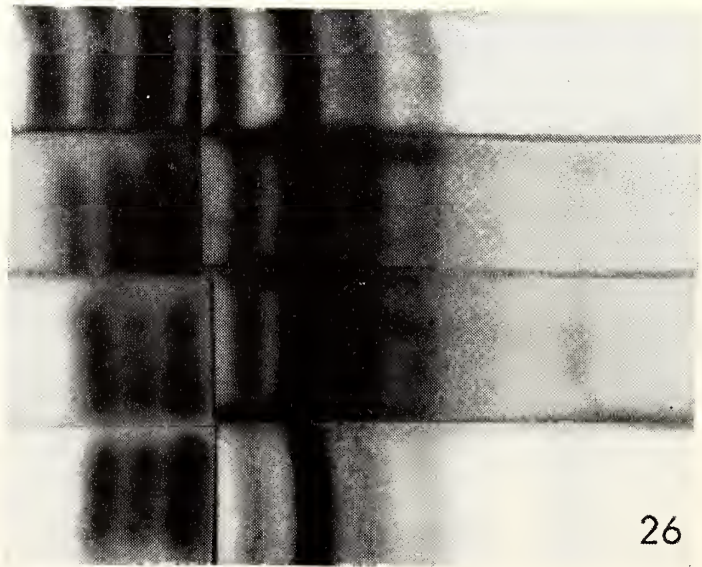
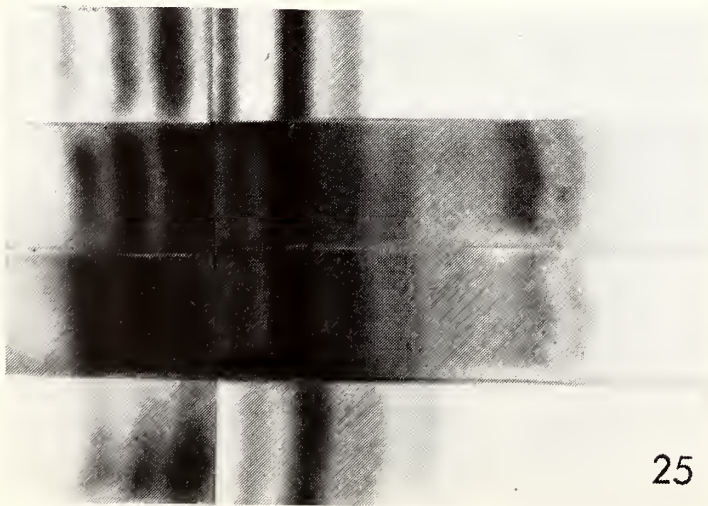
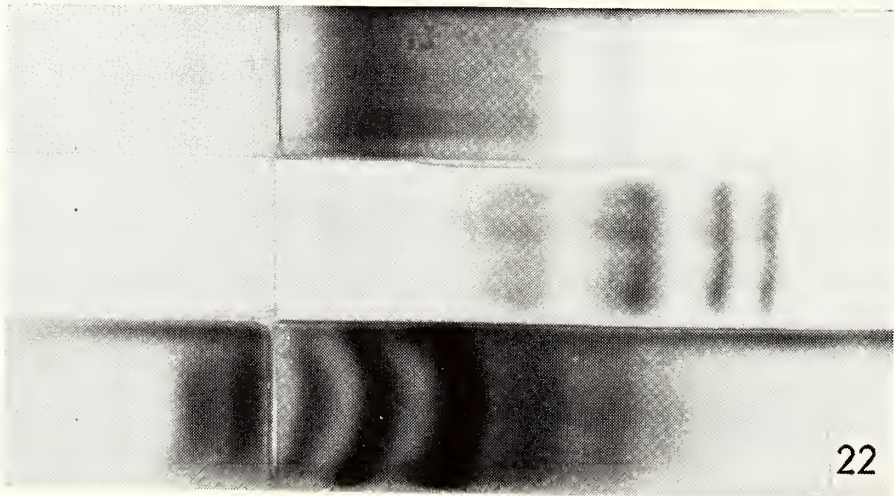
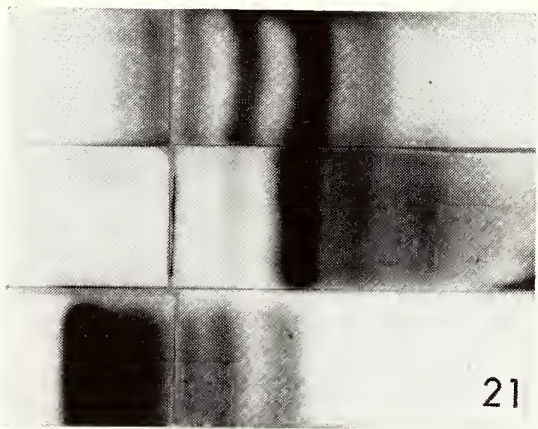
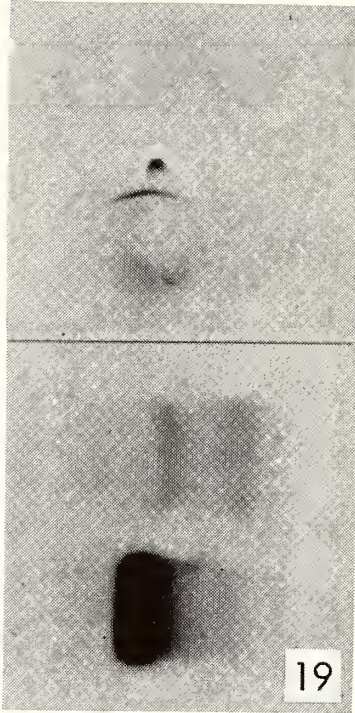
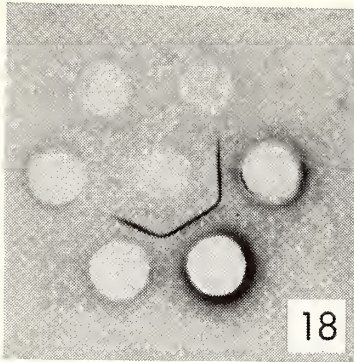


Fig. 17. Agar gel electrophoresis of adult chick liver extract, purified liver HXDH, and adult chick kidney extract. The plate at the top was incubated in the mixture described in the text from which xanthine was omitted. In the presence of substrate (plate at bottom) HXDH can be directly localized; it appears to migrate as one component toward the cathode.

Fig. 18. Double diffusion plate in which different organ extracts are tested against antiadult chick liver serum. Incubation of the plate in phosphate buffer containing xanthine, NAD, and Nitro BT permits the demonstration of HXDH activity on one single precipitate. HXDH of adult kidney, adult liver, and embryonic mesonephros is immunologically identical; the enzyme cannot be detected in adult brain, heart, or muscle extracts.

Fig. 19. Immunelectrophoresis (in the presence of antiliver serum) (top) and agar electrophoresis (bottom) of 10-day embryonic liver and mesonephros extracts. Both experiments show that HXDH can be detected only in mesonephros. No enzyme activity is found in liver at this stage of development.

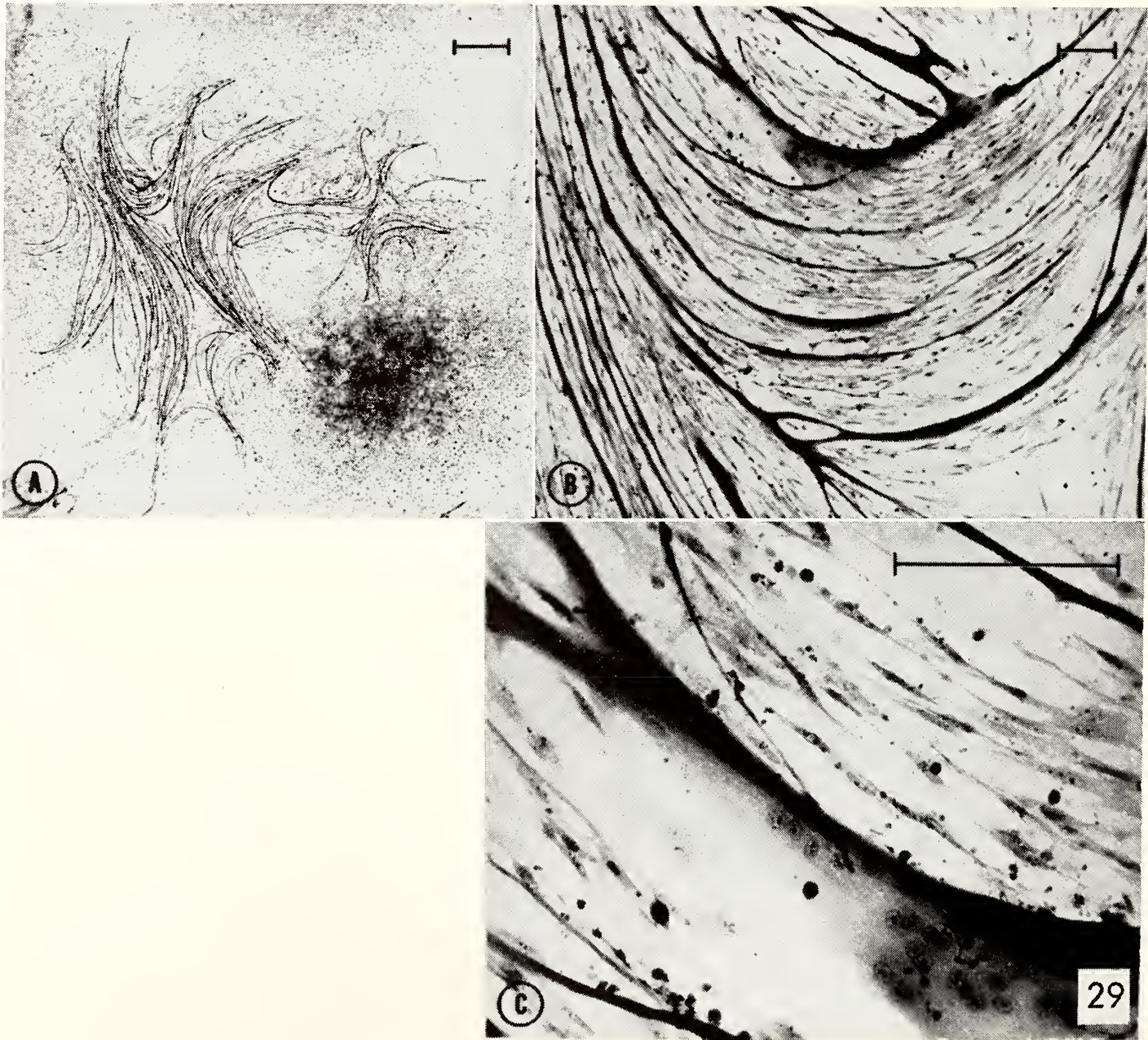
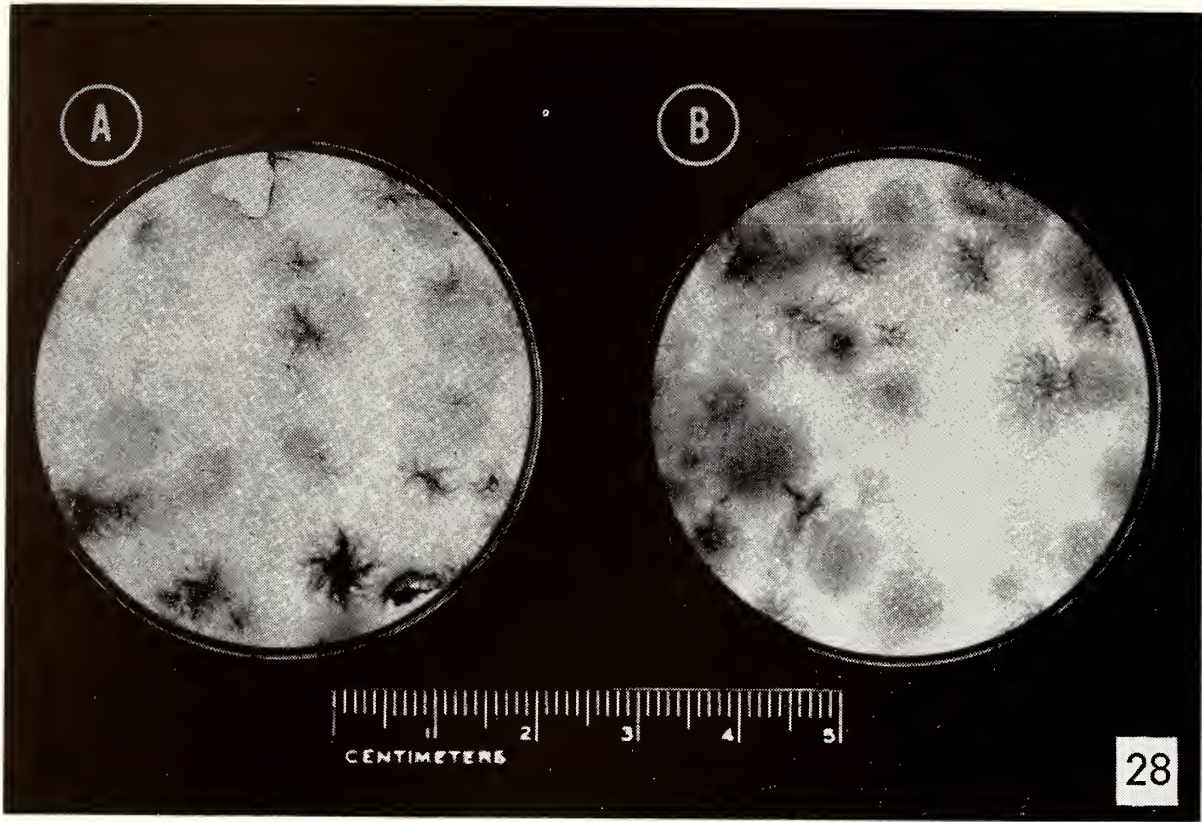
Fig. 21. From top to bottom: LDH pattern of adult liver, heart, and muscle. Additional bands *a* and *b* are most clearly seen in heart.

Fig. 22. Comparison of LDH patterns of mouse liver (top), mouse kidney (middle), and chick liver (bottom). Whereas it takes only 6 hours for the separation of LDH isozymes in mouse tissue extracts, 18 hours are required, under the same conditions, for the separation of LDH in chick organ extracts.

Fig. 23. From top to bottom, bands 2, 1, *a*, and *b* of adult chick liver after the first electrophoresis, and second electrophoresis of bands 2, 1, *a*, *b*. It is clear that components 1, 2, *a*, and *b* are different electrophoretic entities.

Fig. 25. From top to bottom, LDH patterns of adult liver, 10-day embryonic liver, 15-day embryonic liver, 20-day embryonic chick liver.

Fig. 26. LDH pattern of adult kidney, 10-day embryonic mesonephros, 15-day embryonic mesonephros, 18-day embryonic mesonephros.



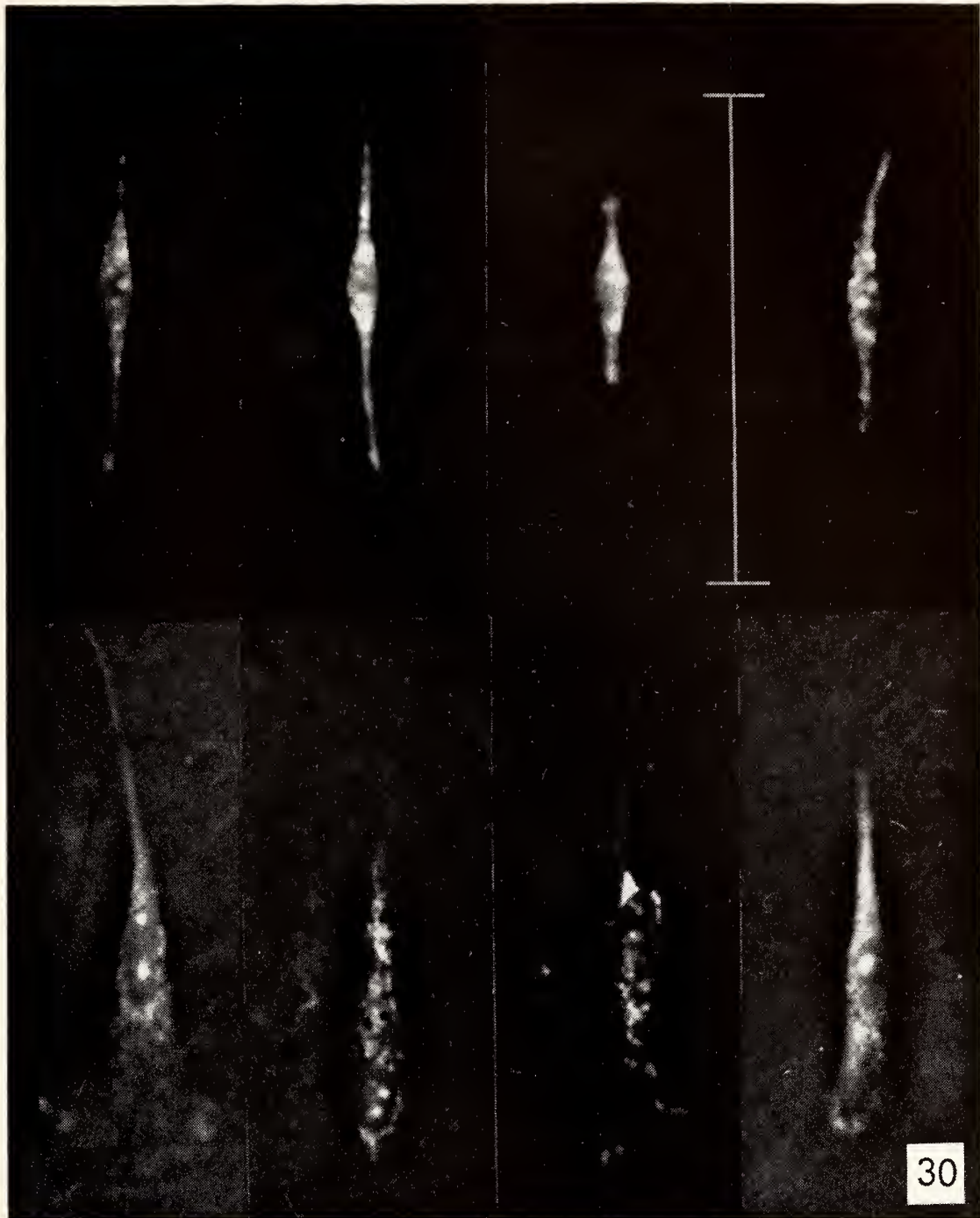


Fig. 30. Photomicrographs of living cells photographed 18 to 24 hours after plating (taken at an initial magnification of $200\times$, using bright medium phase contrast optics). The cells in the upper row produced muscle colonies; those in the row beneath gave rise to colonies of fibroblast-like cells. Scale marker, 0.1 mm.

Legends for plate 2

Fig. 28. Plating cultures established with inocula of 200 cells, freshly isolated from the leg musculature of 12-day chick embryos. Cultures were fixed on the 13th (*A*) and 16th (*B*) day. Ehrlich's hematoxylin, no counterstain.

Fig. 29. *A*. Higher magnification of an area of culture *B* of figure 28. Note the alignment of the dark staining fibers into sworls. Scale marker, 1.0 mm. *B*. Segment of the muscle colony in *A*. Fibers are clearly syncytial ribbonlike myotubes. Scale marker, 0.1 mm. *C*. Branched part of a myotube from the field represented in *B*. The multinuclear nature of the myotube is evident. Scale marker, 0.1 mm.

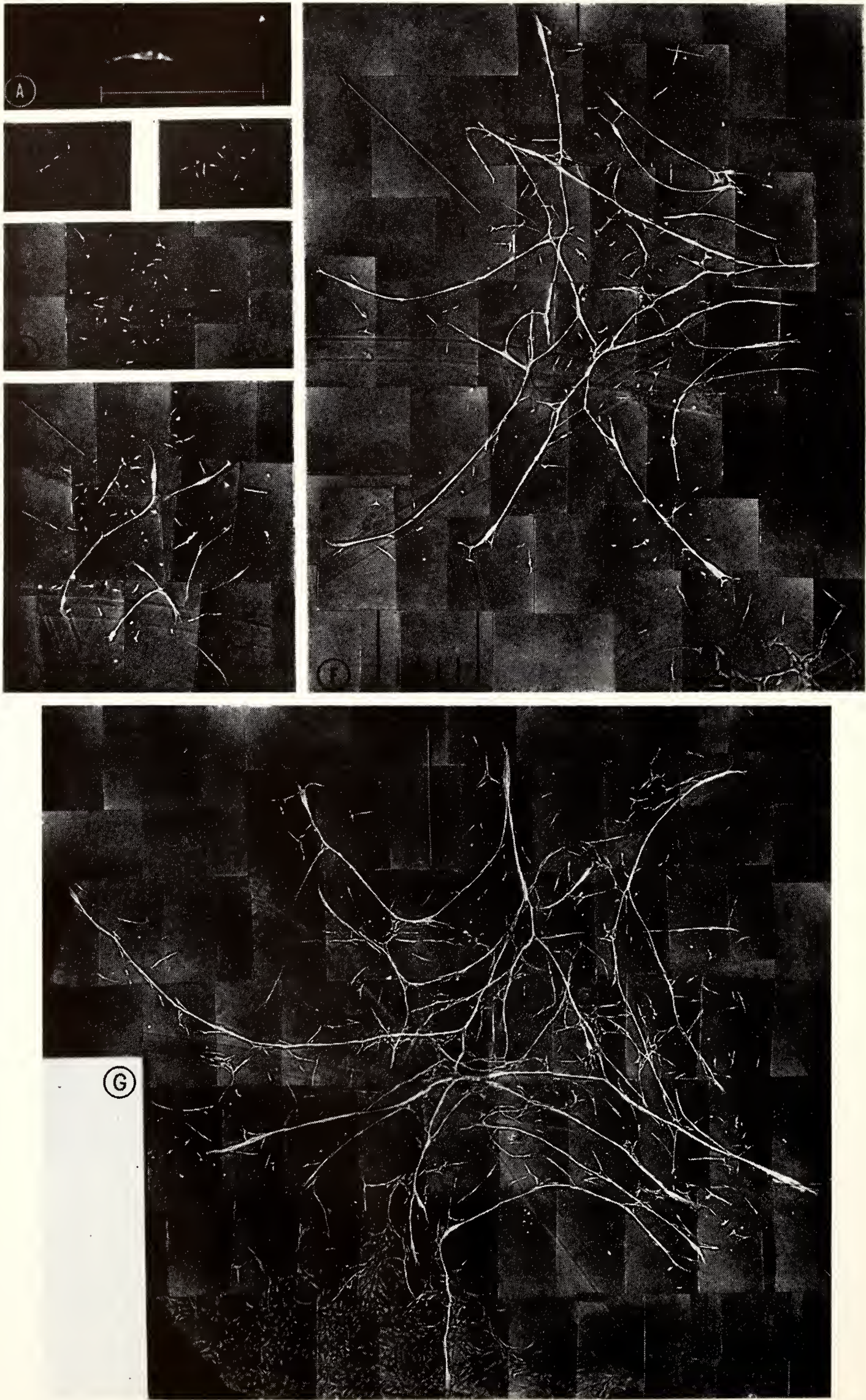


Fig. 31. Photomicrographic record of the development of a muscle colony from a single bipolar cell. The living cells were photographed at an initial magnification of $200\times$ (*A*) or $100\times$ (*B* through *G*), using bright medium phase contrast optics. *D* through *G* are composites of several successive overlapping frames covering the progressively greater expanse of the colony on succeeding days.

A. The single cell photographed some time between 18 and 24 hours (day 1) after plating. Nucleus contains one prominent nucleolus. A cluster of highly refractile granules is present in each juxtannuclear zone. Note ruffled membrane at the tip of the process at the left. Scale marker, 0.1 mm.

B. Colony produced by the cell in *A* during the first 24 hours of recording (day 2). Scale marker in *E* applies to photomicrographs *B* through *E* and equals 0.1 mm.

C. Colony on day 3. Three of the cells in the field are rounded and are presumably in an early stage of division.

D. Colony on day 4.

E. Colony on day 6. Long multinuclear myotubes have formed (first observed 24 hours earlier). Arrows in photomicrographs *E*, *F*, and *G* indicate orientation of colony with respect to the orientation in *G* (which was changed to facilitate photographing). Orientation is confirmed by matching pattern of strain marks in the plastic petri plate.

F. Colony on day 9. Network of myotubes has expanded considerably, but note the presence of single cells among the myotubes. Cells of the leading edge of an invading colony of fibroblast-like cells can be seen in the lower right corner of the photomicrograph. Each division of the scale equals 0.1 mm.

G. Colony on day 13 of culture. Myotubes are both longer and more numerous than in the previous photomicrograph. Single cells are still present. Continued proliferation of these single cells is suggested by the rounded appearance of some of them and associations typical of late anaphase. The invading fibroblast-like cells observed in *F* are now quite obviously the periphery of a contiguous colony. Compare the cells of the impinging colony with the single cells of the muscle colony. Scale as in *F*.

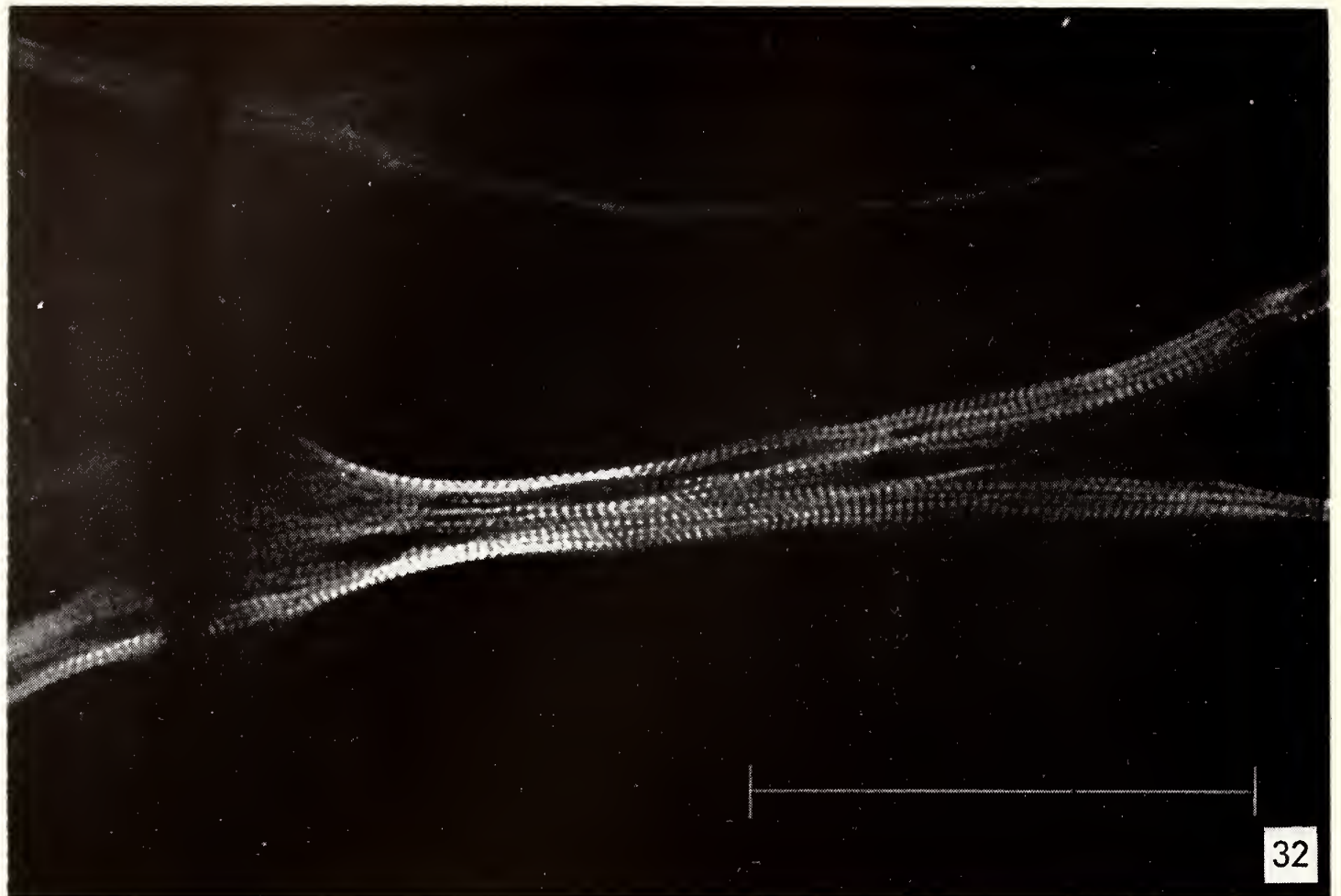


Fig. 32. An area of the colony in figure 31G (roughly, the area at the lower edge of the sixth frame from the right in the fourth row from the bottom). Polarizing optics demonstrate cross-striated myofibrils. Fixation: osmium vapor after storage at -20°C in 50 per cent glycerol. Scale marker, 0.1 mm.



Fig. 33. A colony derived from a single cell isolated by a glass cylinder photographed in situ (dark-field) after fixation. The bright semicircle is a continuous bead of silicone grease extruded by pressing the cylinder into position. Scale marker, 1.0 mm.

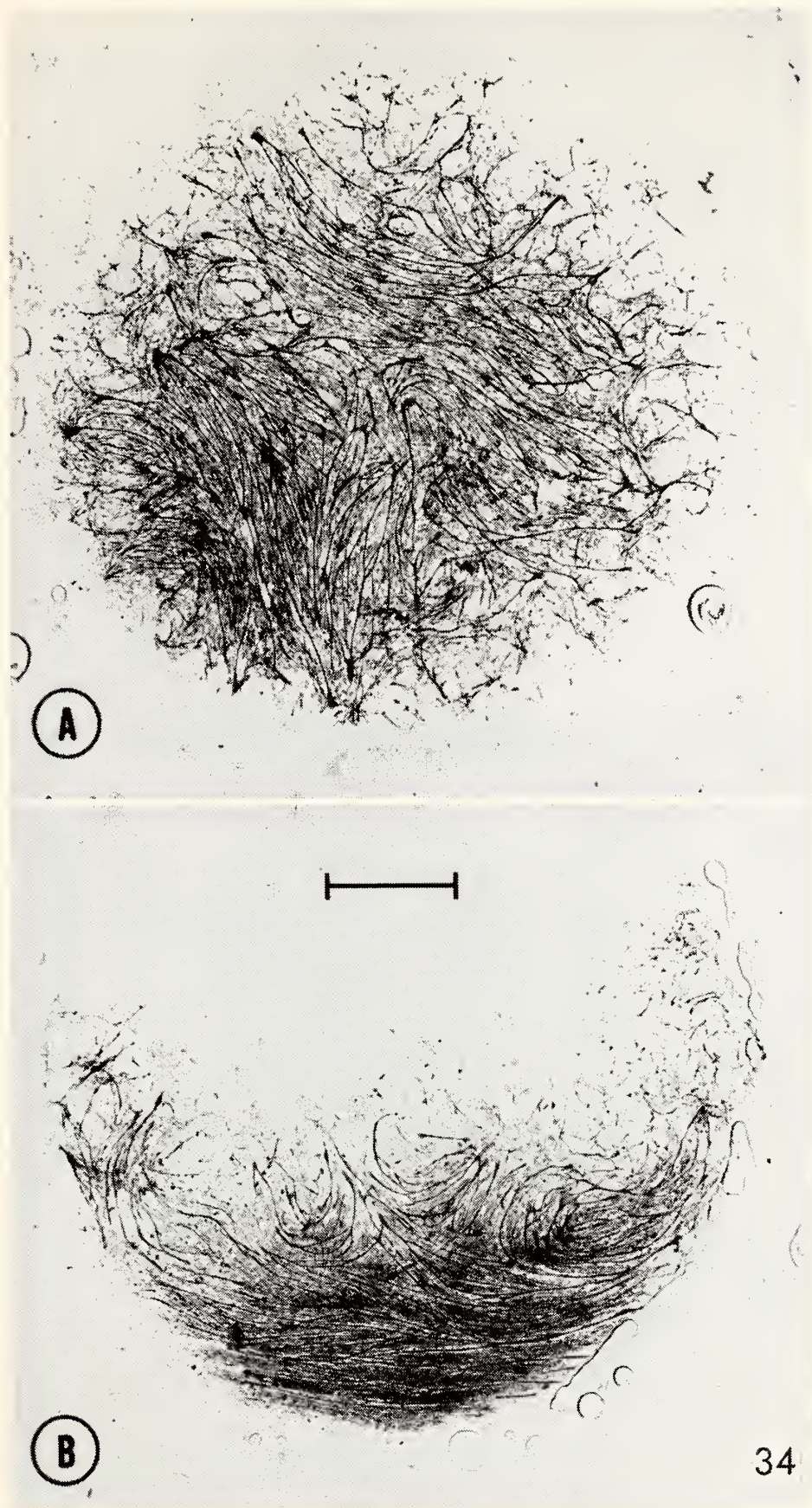


Fig. 34. Two colonies that arose from single cells isolated by glass cylinders. The darkly stained "fibers" are multinucleated myotubes. Fixation in Bouin's was followed by staining in Ehrlich's hematoxylin (no counterstain). Scale marker, 1.0 mm.

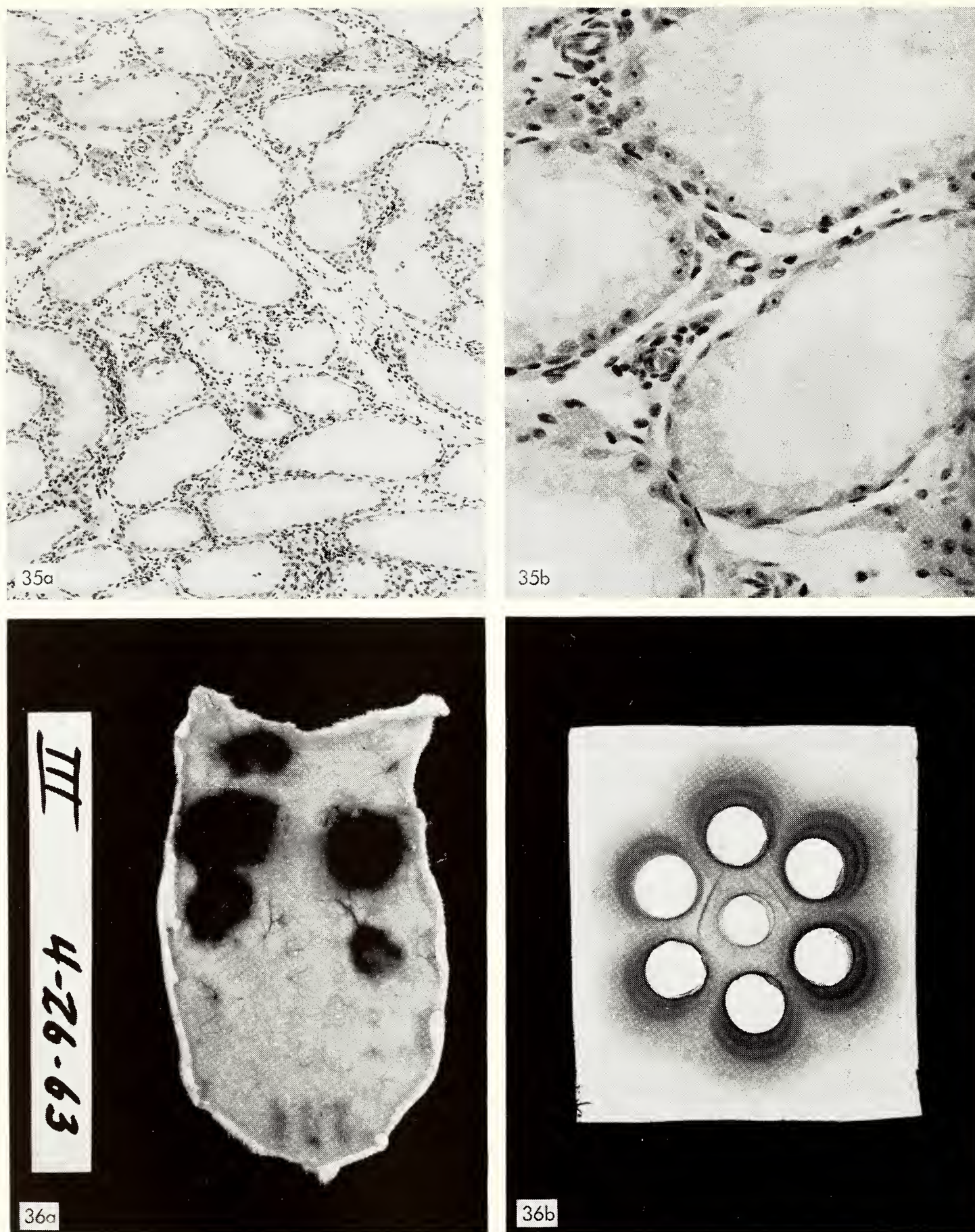


Fig. 35. Induced aspermatogenesis by intramuscular injection of testis homogenate combined with complete (Freund) adjuvant, 2 months after sensitization. *a*, 100 \times ; *b*, 400 \times .

Fig. 36. *a*. PCA test guinea pig skin (seen from inside), showing positive reactions with sera from intramuscularly sensitized animals (two spots upper left and two right), compared with serum from guinea pig injected intracutaneously (lower left spot); negative normal serum reaction at lower left. *b*. Gel-diffusion slide stained with amido black; antisera in outside wells, ASPM antigen in center well; single band given by serum from intramuscularly injected animal at upper right, from intracutaneously injected guinea pig at upper left.

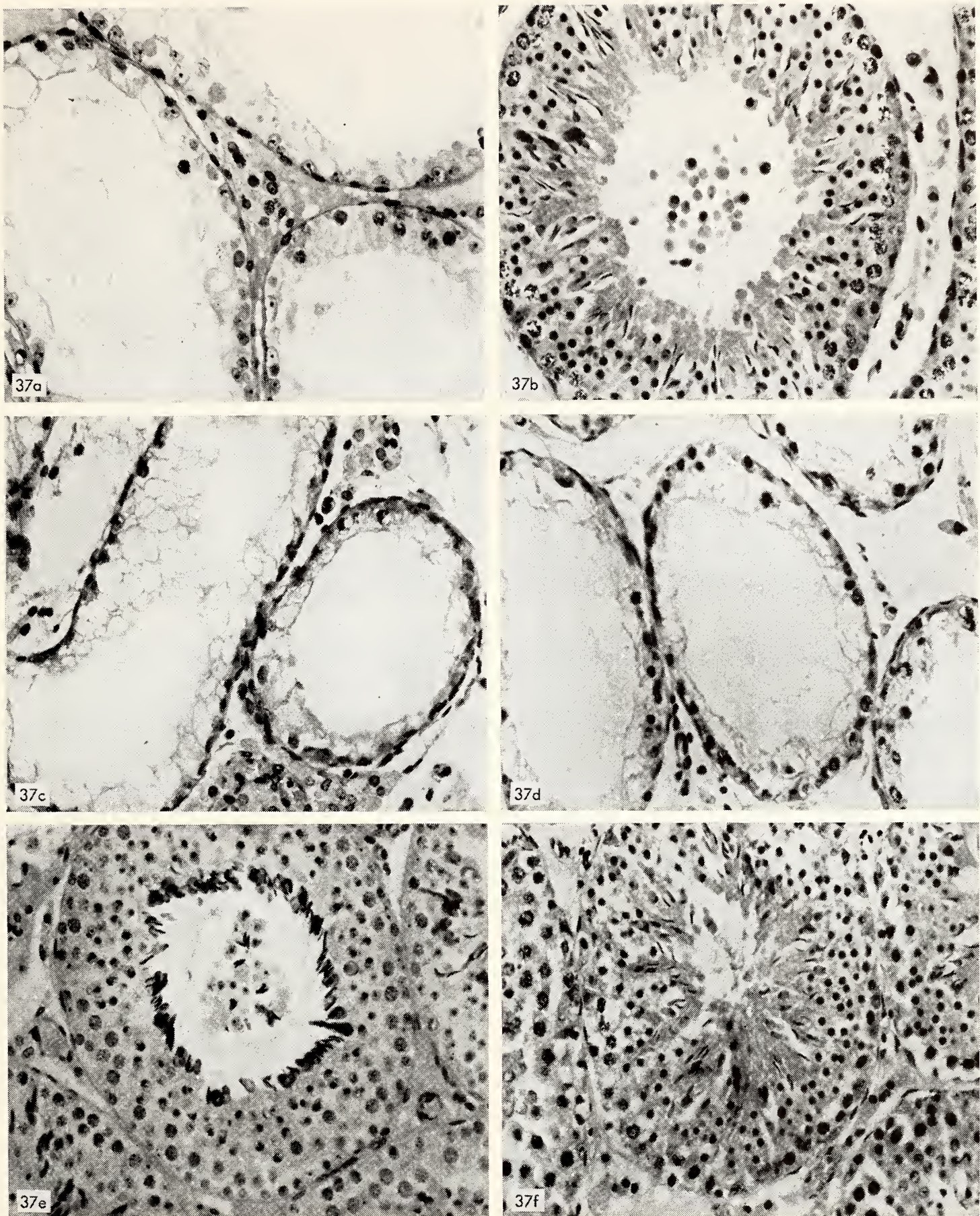


Fig. 37. Variation in apparent "reversibility" of aspermatogenic response after sensitization with testis and adjuvant, 400 \times . *a*, testis removed at 2 months (no. 1344). *b*, contralateral testis removed at 6 months suggesting "recovery." *c*, aspermatogenesis in testis removed at 2 months (no. 1347). *d*, similar condition in opposite testis removed at 6 months. *e*, essentially normal germinal epithelium in sensitized animal at 2 months (no. 1341). *f*, contralateral testis at 6 months.

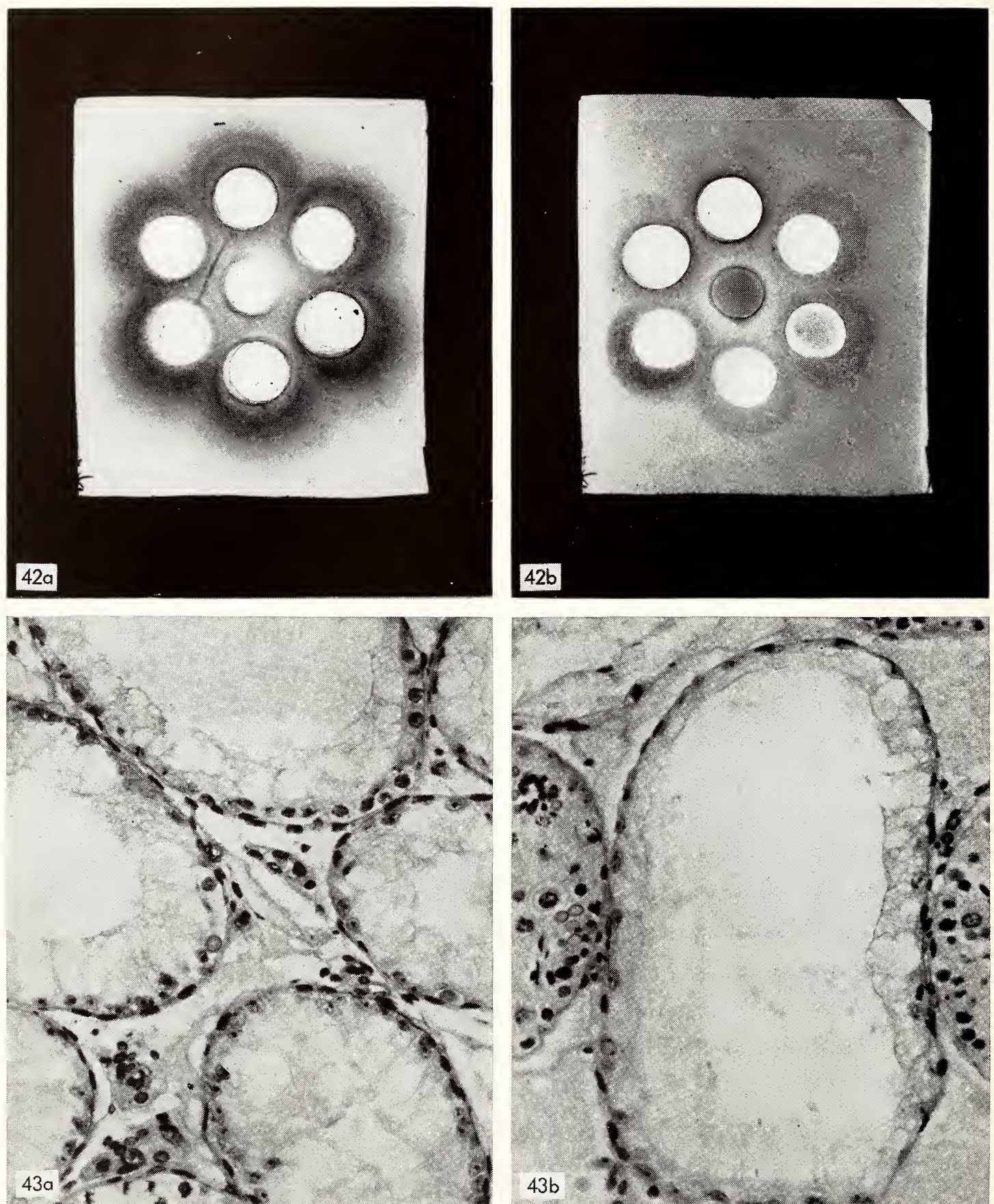


Fig. 42. *a*. Precipitation band in gel-diffusion slide stained for protein with amido black; serum from testis-sensitized guinea pig in outer well, ASPM antigen in center well. *b*. Duplicate to *a*, stained for polysaccharidic aldehyde groups with Schiff reagent.

Fig. 43. Apparent induced aspermatogenesis in guinea pig 2 months after sensitization with brain ASPM, 400X. *a* and *b* from different animals.

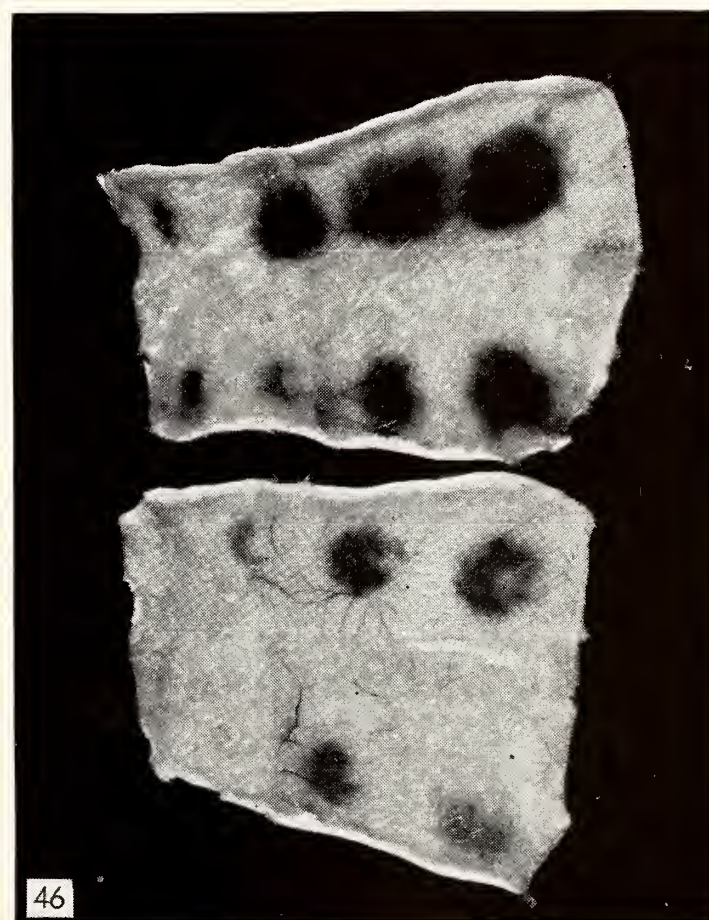
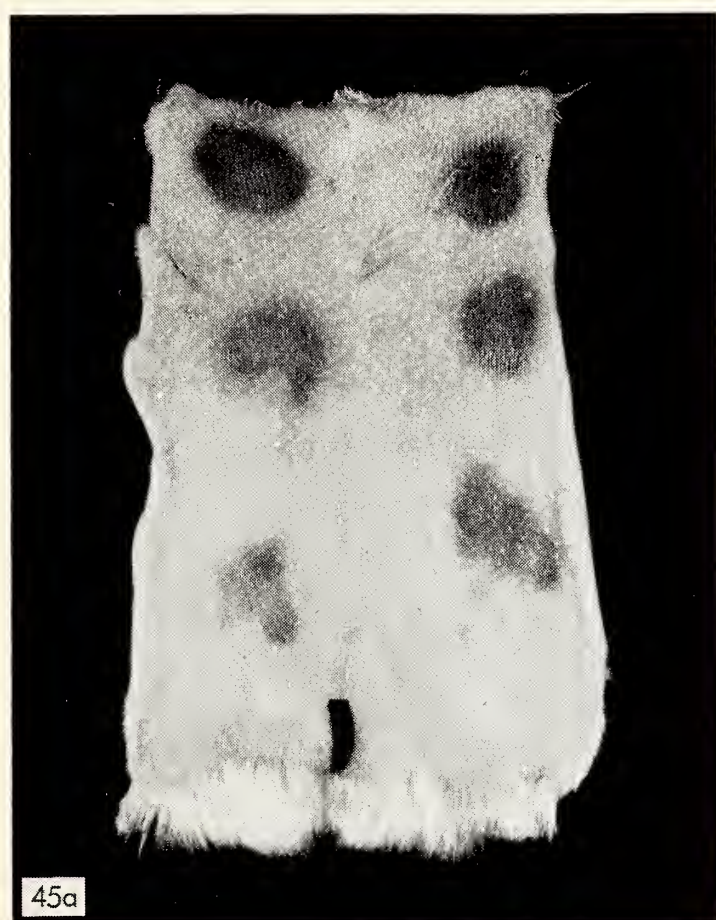
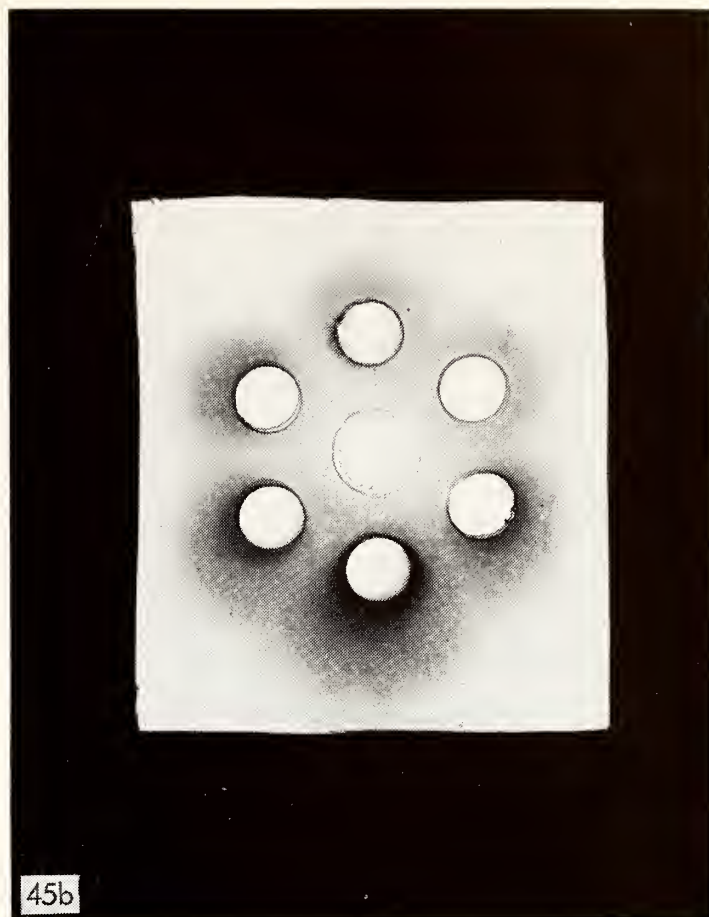
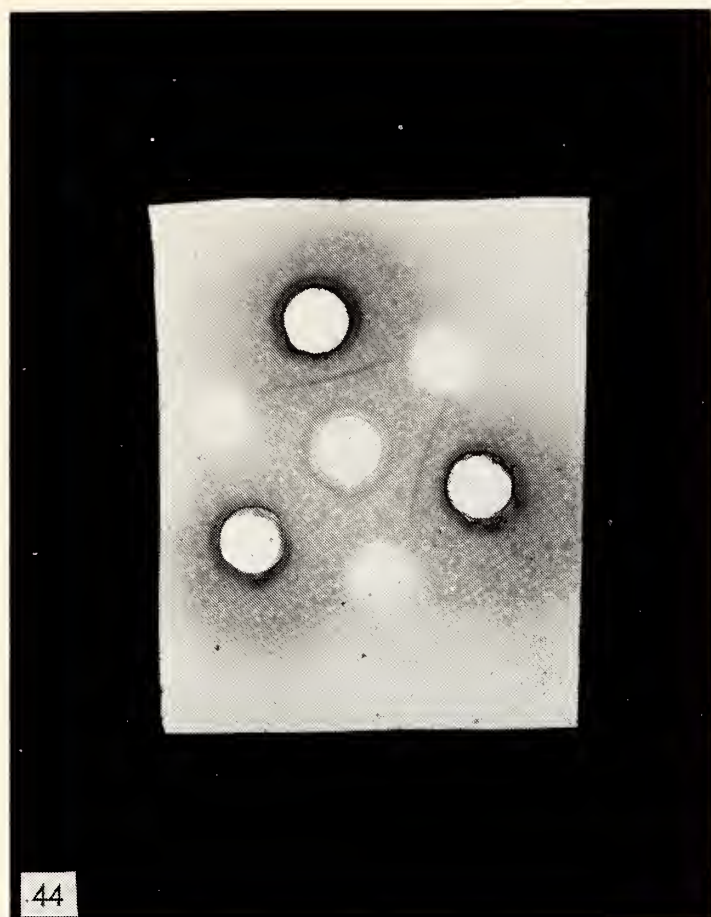


Fig. 44. Single prominent gel-diffusion band formed in reaction between ASPM antigen (center well) and pooled antisera from testis-sensitized guinea pigs (two identical outer wells); third outer well, normal serum.

Fig. 45. *a.* PCA reactions with absorbed (left) and unabsorbed (right) antiserum from testis-sensitized, aspermatogenic guinea pig. Absorption by brain (upper left), liver (middle left), and kidney (lower left) extracts (12 hours, 4°C). *b.* Gel-diffusion reactions with absorbed serum (outer wells); ASPM antigen, 5 mg/ml (center well). From top clockwise, antiserum absorbed by ASPM, unabsorbed, testis, liver, kidney, and brain.

Fig. 46. Dilution series of sera from two sensitized guinea pigs tested by PCA and challenged by ASPM. Undiluted serum at upper right of each skin. Dilution on lower test positive to 1/16; on upper, positive to 1/128.

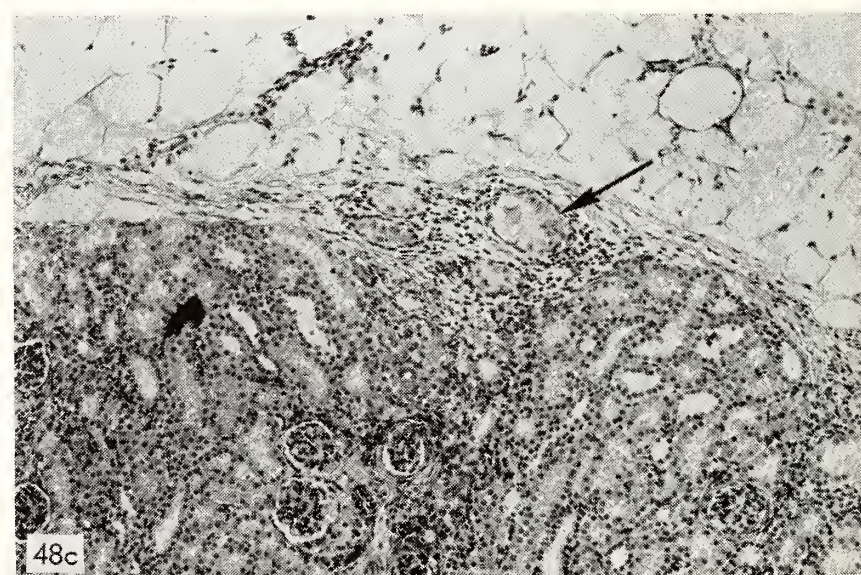
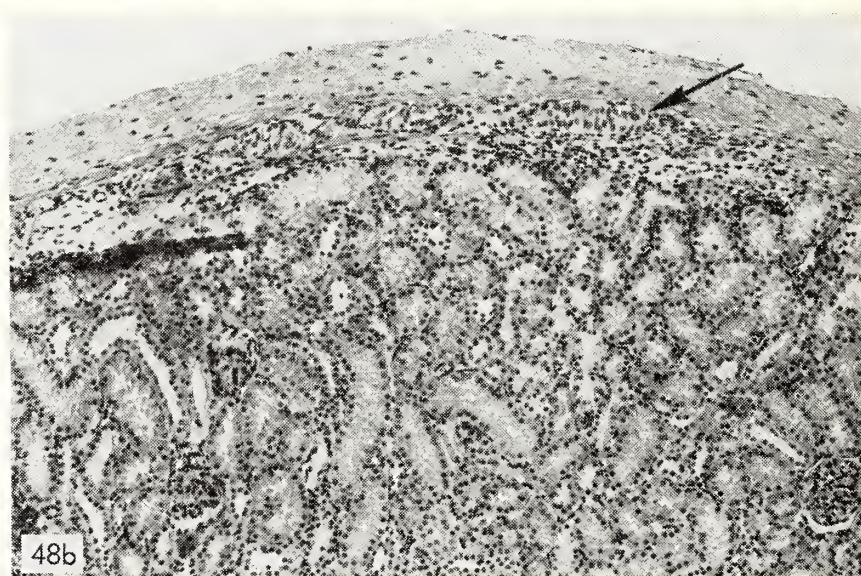
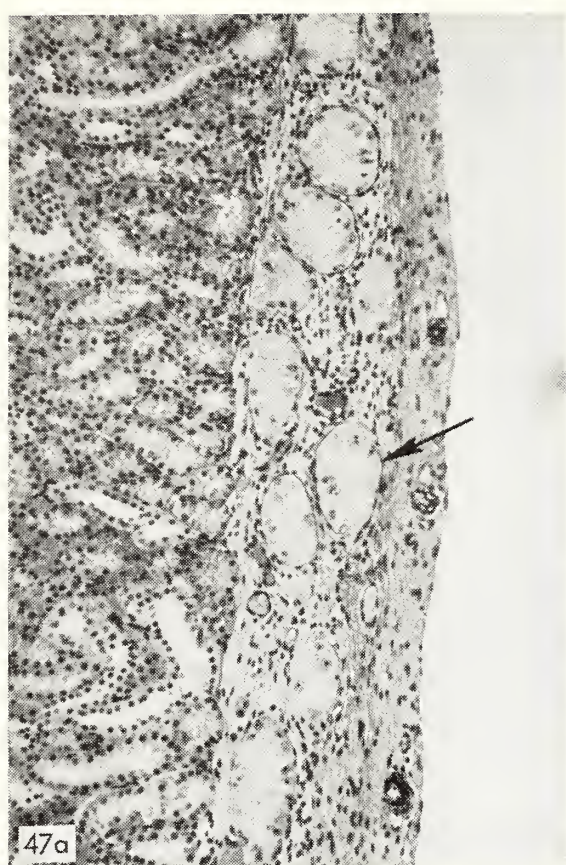


Fig. 47. *a*. Autologous testicular implant into subcapsular site of Strain 13 guinea pig kidney, sacrificed at 1 month; germinal epithelium hypoplastic and dedifferentiated. *b*. Homologous implant similar to *a*.

Fig. 48. *a*. Testicular autograft at 3 months; Hartley strain guinea pig. *b*. Autograft similar to *a*; Strain 13. *c*. Homograft similar to *a*; Strain 13.

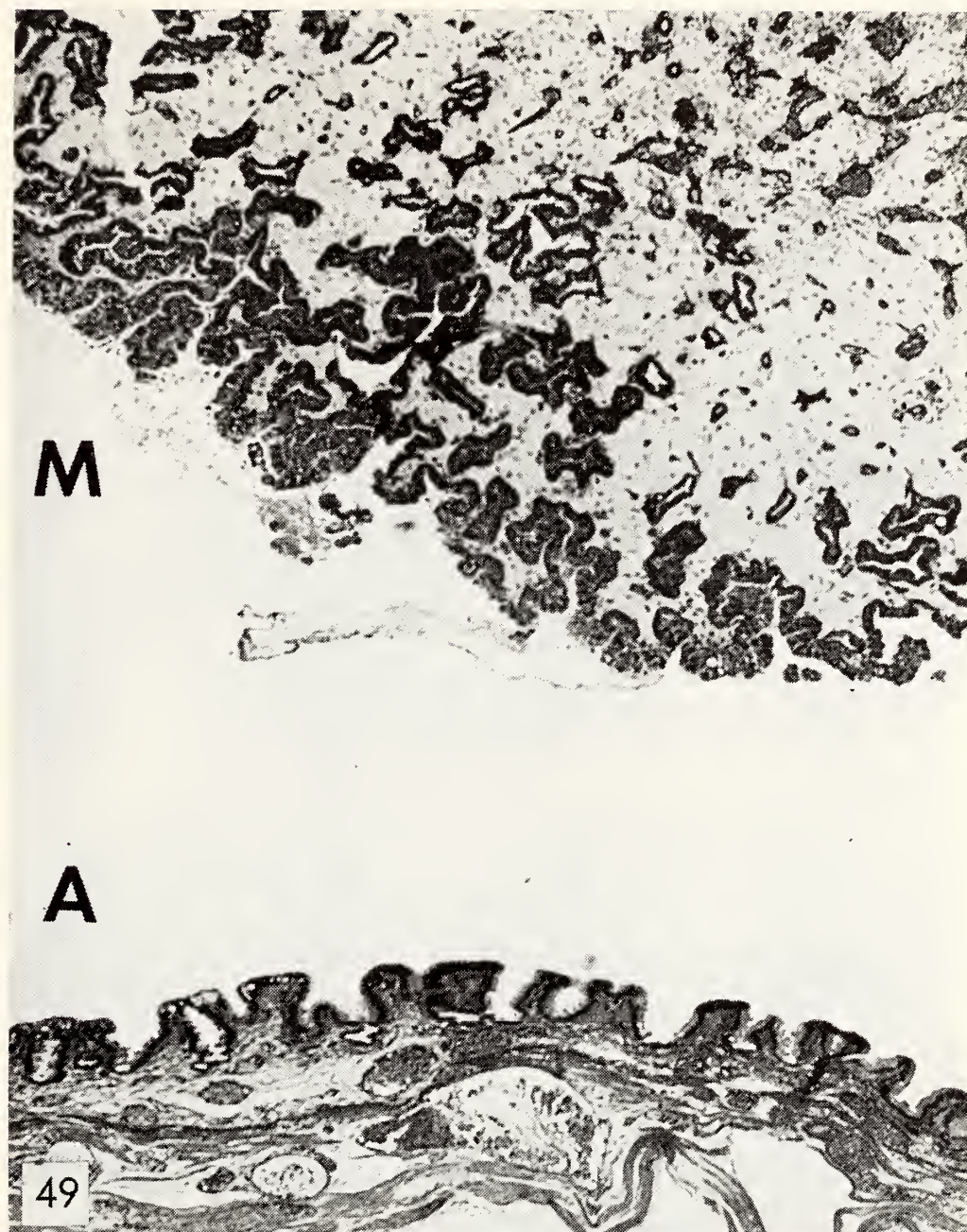


Fig. 49. The lumen of this rabbit uterus was filled with 0.15 N NaCO_3 in vivo for 7 minutes before fixation. On the mesometrial aspect (*M*), the epithelium consists of individual cells and multinucleate giant cells, and it has suffered dissociation at high alkalinity. On the anti-mesometrial aspect (*A*), the epithelium has become a symplasma and has resisted dissociation. (L-455-B/8-13, 45 \times .)

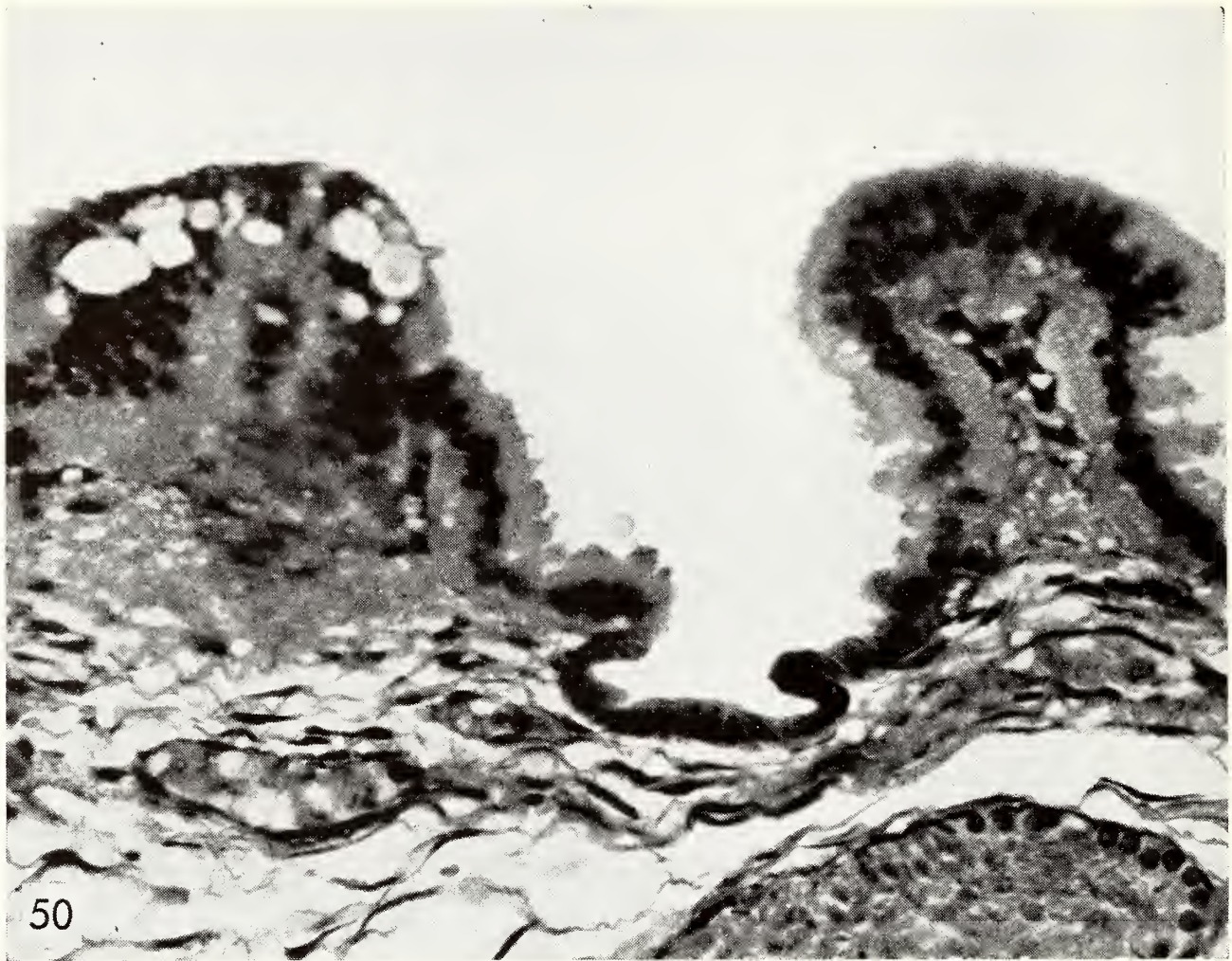


Fig. 50. The undissociated symplasma is shown at higher magnification than in figure 49. (L-455-B/8-17, 350 \times .)

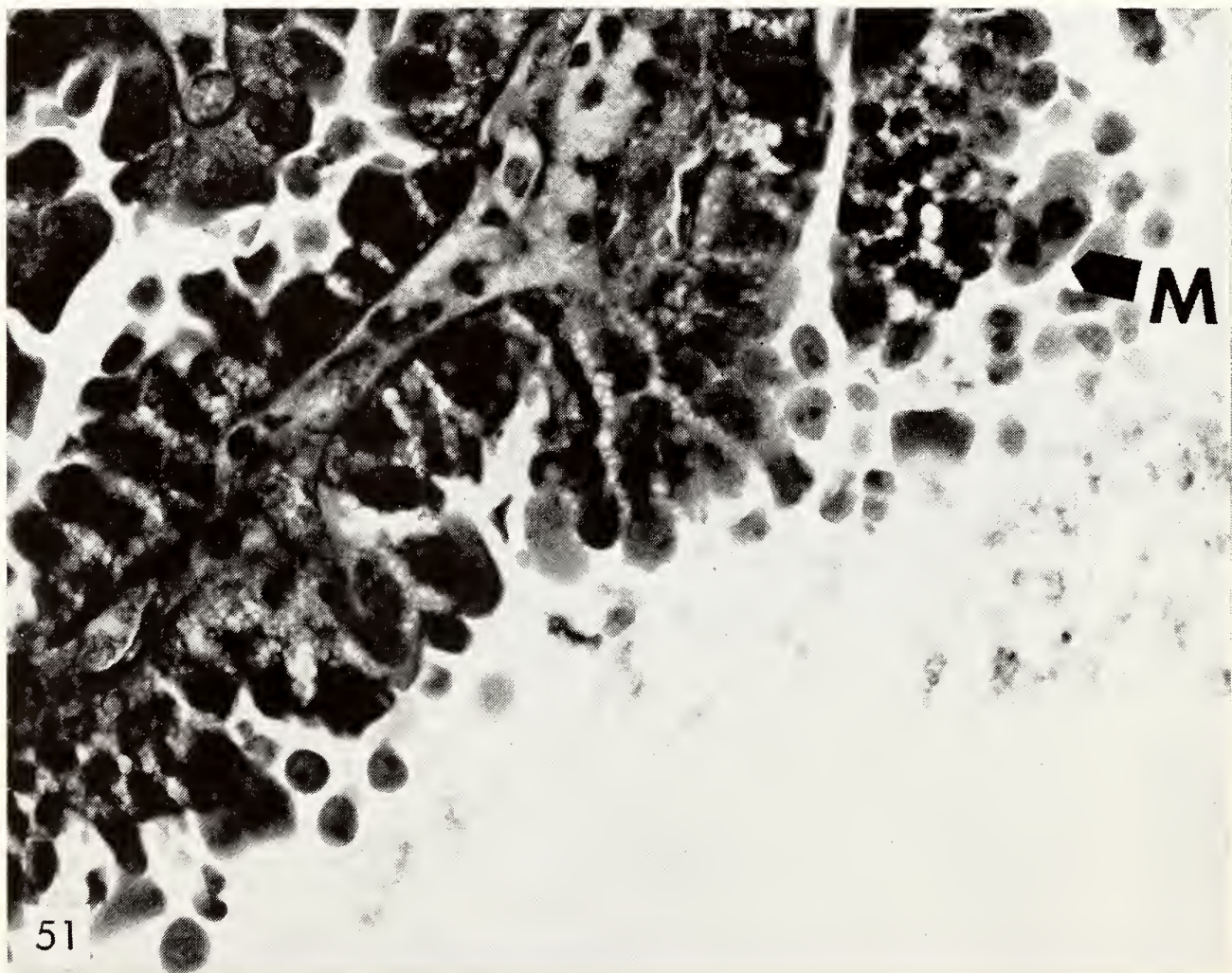


Fig. 51. Cellular dissociation is shown at higher magnification than in figure 49. The epithelium is composed of both uninucleate and multinucleate cells (*M*), and the separation at high alkalinity occurs at the cell boundaries. (L-455-B/8-17, 350 \times .)

Genetics Research Unit

Alfred D. Hershey
Director

Cold Spring Harbor, New York

Contents

Introduction	481
Some Idiosyncrasies of Phage DNA Structure	481
Molecular-weight measurements	482
Genetic deletions in phage lambda	482
Cohesive sites in lambda DNA	482
Intramolecular heterogeneity	483
Variation in T4 phage particles	485
Breakage points in T5 DNA	485
Intrabacterial T2 DNA	486
Further Studies of Gene-Control Systems in Maize	486
Modified states of α_1^{m-2}	488
Extension of <i>Spm</i> control of gene action	491
Further studies of topographical relations of elements of a control system	491
Enzymology	493
Preparation of Z protein from ribonuclease	494
Properties of Z protein	497
Bibliography	500
Personnel	500

INTRODUCTION

IN spite of numerous distractions connected with the reorganization of our own group and the formation of the new Laboratory of Quantitative Biology, we in the Genetics Research Unit have enjoyed a lively year of research. Individual reports will be found in the following pages.

Barbara McClintock, serving as a Trustee of the Laboratory of Quantitative Biology, played an important role in its organization. Through that organization the Genetics Research Unit has gained tangible assets, notably a welcome new colleague in John Cairns, Director of the new laboratory.

The Unit has also suffered a loss. Margaret McDonald, a member of the former Department of Genetics since 1943, is leaving to continue her research at the Waldemar Medical Research Foundation. We shall miss her and wish her well.

As a sequel to her past work in South America, sponsored by the Rockefeller Foundation, Dr. McClintock and Dr. William L. Brown are supervising the research of four Latin American Fellows now studying at North Carolina State College. The general purpose is to encourage research in maize genetics and cytology, research that is equally important in the Americas for botanical, historical, and economic reasons.

The *Drosophila* Educational Project,

under Jennie S. Buchanan, Curator, continues to thrive. During the current year about 3500 requests for cultures, and 950 for copies of the *Drosophila Guide*, have been filled. The cultures go mainly to college and high school teachers, who use them in classroom work.

The Library continued under the capable management of Mrs. G. C. Smith, who makes it possible for our small group to enjoy the near-luxury of a reasonably complete reference source in biology and biochemistry.

All members of the staff benefited through visits to and visitors from other laboratories within and without the Institution. Notable quantitatively was the annual Phage Meeting, which brought to Cold Spring Harbor some dozens of scientists interested in a field of research still neither too wide for intimacy nor too narrow for mutual stimulus among its practitioners. The meeting was organized by Elizabeth Burgi, with advice from George Streisinger and Frank Stahl of the University of Oregon.

Our justification for existence as a Unit, however, resides in the value of our research. We like to think that much of that value is as unstatable and as durable as other human produce that cannot be sold. Some can be put on paper, however. That we offer with the usual human mixture of pride and diffidence.

SOME IDIOSYNCRASIES OF PHAGE DNA STRUCTURE

*A. D. Hershey, Elizabeth Burgi, Fred R. Frankel, Edward Goldberg,
Laura Ingraham, and Gisela Mosig*

Our work for the past five years, though often proceeding by indirection, has been guided by specific questions about the biology of phage. What is the structure corresponding to the single chromosome revealed by genetic experiments? What

aspects of that structure can account for synapsis, heterozygosis, genetic deletions, and other phenomena familiar to geneticists but obscure to structural chemists? Since the phage chromosome is composed of DNA, our questions called for investi-

gation of DNA structure along lines for which, as it turned out, the tools had to be invented.

The first question was given the simplest possible answer by the finding that a particle of phage T2, T5, or lambda contains a single molecule of typical, double-helical DNA, whose length is characteristic of the species (*Year Book 61*). Other questions remain unanswered, but some of the tools are ready, as the following report will suggest.

The work was aided by a grant (CA-02158) from the National Cancer Institute, National Institutes of Health, and by postdoctoral fellowships from the U.S. Public Health Service, for Mosig and Frankel, and from The National Foundation, for Goldberg.

Molecular-Weight Measurements

Burgi and Hershey

A minimum requirement for the study of DNA structure is a means of determining size, shape, and uniformity of the molecules. In the absence of information about either size or shape, the analysis is a formidable task (see *Year Book 60*). Fortunately, most phage DNA's prove to be typical double-helical molecules. For these, length is the principal variable, and is conveniently measured from the rate of sedimentation in a density gradient of sucrose. The general relationship between lengths (L) and distances sedimented (D) of two DNA's proves to be $D_2/D_1 = (L_2/L_1)^{0.35}$. In addition, the pattern formed by the sedimenting bands says a good deal about the homogeneity of the preparation. Several applications of the method are mentioned in this report. Other details are being published in the *Biophysical Journal*.

Genetic Deletions in Phage Lambda

Burgi

Two mutations have been described in phage lambda that were recognized as hereditary changes in the density of the particles, apparently as a result of reduc-

tions in their DNA content (Kellenberger, Zichichi, and Weigle). One, called b_2 , lies in a segment of the DNA molecule that directly interacts with the bacterial chromosome in lysogeny. Another, b_5 , lies in the region controlling the immunity to lytic infection that characterizes bacteria in the lysogenic state.

Burgi has shown that the mutations were accompanied by literal deletions of two different segments of the lambda DNA molecule, measurable because the mutant molecules sediment more slowly, and resist higher rates of shear before breaking, than those of the wild-type phage. (Chromatographic differences support the other measurements.) The double mutant carrying both deletions has lost 20 per cent of the original molecular length. The remaining DNA contains about 48 per cent guanine-plus-cytosine, as compared with 46 per cent in the DNA as a whole. The two deletions therefore occurred in regions containing only 38 per cent of the bases named. Further work along these lines could lead to the assignment of specific phage functions to specific molecular segments.

Cohesive Sites in Lambda DNA

Hershey and Burgi

Analysis of molecular deletions in phage lambda was hampered for a long time by exceptional properties of its DNA. The difficulties were finally traced to the tendency of the DNA to form complexes. The phenomenon proved interesting in its own right, and was studied in some detail.

When freshly prepared by extraction from phage particles at very low concentration (2 $\mu\text{g/ml}$), the DNA consists of linear molecules about 15 microns long (molecular weight 31 million). These molecules are of typical double-helical structure, as shown by the normal relation between sedimentation rate and fragility under shear, as well as by radioautographic measurements of length (Cairns, *Year Book 60*).

The unusual properties of the DNA are best described in terms of the model needed to explain them. Each molecule carries two cohesive sites, one situated near each end, which have the property of adhering to each other but not to other parts of the molecule or to DNA in general.

At DNA concentrations below 5 $\mu\text{g/ml}$, only cohesive sites belonging to the same molecule can join, giving rise to folded molecules (presumably rings or hairpins). These structures are best recognized by the fact that they sediment 1.13 times faster than linear molecules in a centrifugal field. The transition from linear to folded molecules is rapid and complete at 60°C in 0.6 *M* salt solution. It occurs very slowly at low temperature in 0.1 *M* NaCl. At 75°C, the reverse change occurs, and one gets linear molecules by heating the solution briefly at that temperature and cooling it quickly.

At higher DNA concentrations, cohesive sites belonging to two or three molecules can join to form dimers sedimenting 1.25 times faster and trimers sedimenting 1.43 times faster than linear molecules. According to their sedimentation rates, these must be open, more or less end-to-end structures. Side-by-side aggregates do not form in appreciable numbers.

Aggregation and folding occur under identical conditions, except for the dependence on DNA concentration, and are reversed by the same treatments. Moreover, they are mutually exclusive: folded molecules do not aggregate, nor do aggregates fold. Therefore the same cohesive sites can engage in either process, and one site is satisfied by a single partner.

The several forms of lambda DNA behave differently under shear. Trimers are more fragile than dimers. Folded molecules are much more resistant than either, but can be opened up at a shear rate just insufficient to break the skeletal bonds. Thus linear molecules can be prepared by shearing as well as by heating

and, after either treatment, can be converted back to the alternative forms.

The identification of cohesive sites may furnish a clue to some of the ways in which chromosomes function. We shall try next to locate and analyze molecular segments having adhesive properties.

Intramolecular Heterogeneity

Hershey and Burgi

Systematic analysis of bacterial DNA's showed some years ago that their base compositions are species specific and vary among different species from about 25 to 75 per cent in guanine-plus-cytosine content. Fragments derived from any one species, on the other hand, are relatively uniform in composition. The variations can have little to do with the functions of genes, which must be generally similar in many different bacterial species as well as individually distinct in any one species. The conclusion was reached that all DNA's are subject to some constraint (presumably the coding requirement) tending toward a composition of 50 per cent, and that other evolutionary pressures (presumably part of the process of speciation) produce the deviants. According to these results, the base composition of DNA is a clue to its phylogenetic origin, and the internal homogeneity of the DNA in a chromosome is one measure of its "age," that is, of the time during which it has persisted as an isolated structural entity.

The meager information about the DNA's of higher organisms is consistent with these ideas. Those analyzed show about 50 per cent guanine-plus-cytosine but prove to be heterogeneous, perhaps reflecting the likelihood that individual chromosomes are older than their assortment in a given species. (If so, a sample of animal DNA, fractionated to obtain a uniform intermolecular composition, should prove to be intramolecularly homogeneous as well.)

Lambda DNA is exceptional in the

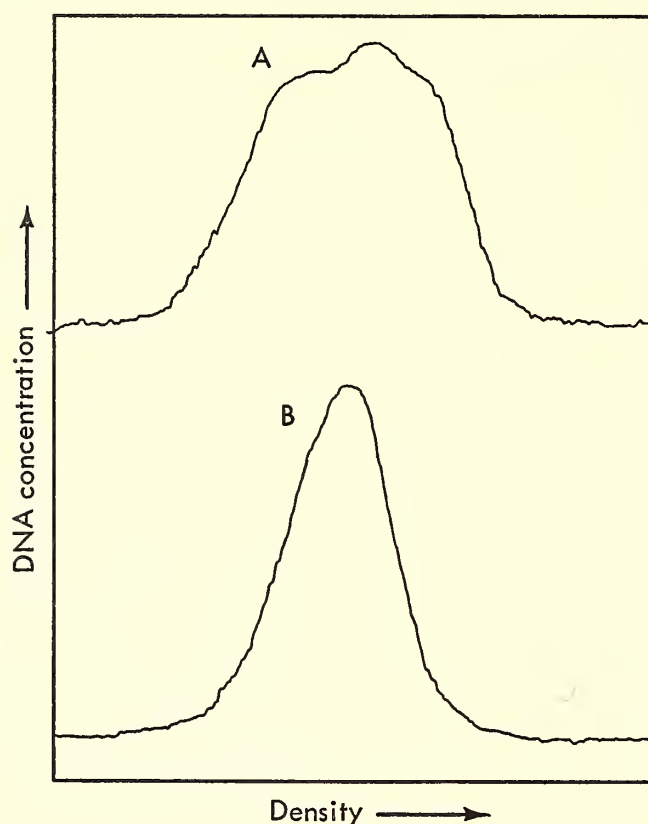


Fig. 1. A. Band formed in CsCl by fragments of lambda DNA, molecular weight 5 million. B. Band formed in CsCl by fragments derived from the DNA of *Escherichia coli*. The two bands are shown at the same magnification.

respects discussed, as shown in several ways.

1. It melts through a broad range of temperatures (*Year Book 61*), suggesting heterogeneity of composition that is not seen in other phage DNA's.

2. After breakage into 4 to 6 pieces, the molecules yield fragments that are readily separable into chromatographic fractions ranging in guanine-plus-cytosine content from 41 to 51 per cent as measured either by nucleotide analysis or in terms of density.

3. The *b2* deletion, already mentioned, occurred in a segment having only 38 per cent guanine-plus-cytosine.

4. The results cannot be explained in terms of a random assortment of small segments varying continuously in base composition, but call for a few (probably three) internally homogeneous segments. This interpretation is supported by the density distribution of fragments of molecular weight 5 million (still large compared with the dimensions of genes), which reveals a few classes of roughly equal size. By contrast, fragments of the

same molecular weight derived from *Escherichia coli* DNA show a density distribution strongly centered about its average (fig. 1).

In view of these results, the similar over-all base compositions of *E. coli* and lambda DNA's, though conforming to a proposed rule for temperate phages and their hosts, appear to be an accident having neither evolutionary nor functional significance. Perhaps lambda phage contains a "young" chromosome of diverse origins. Note that this interpretation by no means excludes the possibility, which we hope to pursue, that the internal heterogeneity of lambda DNA reflects an effective functional differentiation among its segments. A clue pointing in that direction comes from the work of Cowie, which demonstrates for the first time that there are homologous parts in the DNA's of *E. coli* and lambda (see report of the Biophysics Section, Department of Terrestrial Magnetism, this *Year Book*). These like segments in virus and host must have a common origin and related functions, and they deserve study by all available means.

*Variation in T4 Phage Particles**Mosig*

Mosig had found, in Doermann's laboratory, that she could separate T4 phage particles on the basis of buoyant density into classes of different biological properties. Since joining our group, she has begun an analysis of the DNA content of the particles. In so doing she has turned up materials favorable for studying several different questions.

Most of the phage particles are of average density and contain a single DNA molecule of unit length (about 50 microns, molecular weight 130 million).

Another class, which may be quite numerous among phage progeny produced late after infection, consists of particles of lower than average density, which contain a DNA fragment measuring 0.67 of the unit length. This class is homogeneous, and intermediate lengths of DNA are not found. The particles are individually noninfective, but two or more attaching to a single bacterium can infect successfully. Genetic analysis shows that different particles lack different parts of the phage genome. According to an idea familiar in phage genetics, two particles can infect a bacterium when every gene is represented in one or the other of the particles. When the infection succeeds, viable progeny are produced that contain normal DNA, into which atoms from the parent fragments are incorporated. The preliminary results are consistent with the idea that the fragments represent chromosomal segments of fixed length cut at random with respect to positions on the circular genetic map. The ability of two segments of analyzable structure to cooperate in the production of phage particles with complete genomes provides a novel means for studying mechanisms of replication and genetic recombination. For example, the results so far obtained with genetically marked phages afford evidence for replication in one direction only through the marked region of the chromosome.

Other exceptional particles, denser than average, are formed particularly at early times after infection. These particles, when crossed, produce few recombinants. They contain DNA molecules of unit length and two classes of fragments averaging about 0.05 and 0.2 of a unit long, respectively. The dense particles are also potentially heterozygous, as shown by Doermann and Boehner. A simple interpretation would be that the small fragments represent the redundant region of a partially diploid chromosome. This interpretation is not entirely satisfactory, however, and a more attractive alternative is now being investigated.

All these findings raise interesting questions about the mechanism of determination of length of DNA molecules which, in this material, evidently operates at several lengths. The 0.67-unit fragments, for instance, are apparently determined neither by self-reproduction nor by recognition of specified end points, but by a device that cuts to measure.

*Breakage Points in T5 DNA**Hershey and Burgi*

When subjected to critical rates of shear, DNA molecules from T2 and lambda phage break near their centers. T5 DNA, on the other hand, often breaks first into a 40 per cent and a 60 per cent fragment, and the larger of these often breaks in turn into a 40 per cent and a 20 per cent fragment. (The weak points are very slightly weaker than other points, so that the over-all fragility is little affected.) We tried to show that the weak points lie at specific locations in the nucleotide sequence. The initial attempts failed because significant differences in density could not be detected among the resulting fragments. Thus molecules of T5 DNA, in contrast to those of phage lambda, are extremely homogeneous internally. This finding is consistent with the narrow range of temperatures through which T5 DNA melts.

*Intrabacterial T2 DNA**Frankel and Ingraham*

DNA synthesized in the presence of chloramphenicol after infection of bacteria with phage T2 can be recovered by phenol extraction and chromatographic purification in 5 to 25 per cent yield. Such material, when isotopically labeled, is chemically recognizable as phage-specific DNA. No small fragments are found. No DNA molecules of the length (50 microns) found in phage particles are

recovered either, owing to the use of the antibiotic to prevent late stages in phage growth. The properties of the material suggest variable structures about 100 microns long. Apparently, therefore, a mechanism exists for joining ends of DNA molecules, presumably in the specific way required for genetic function. Such a mechanism is likely to be related to the circular form of the genetic map. Comparative experiments with a phage characterized by a two-ended map may illuminate that relation.

FURTHER STUDIES OF GENE-CONTROL SYSTEMS IN MAIZE

Barbara McClintock

Continued study of the *Spm* system of control of gene action in maize has produced additional evidence of the system's versatility. A control system of this type is capable of regulating the action of many genes during development. In view of the large number of genes present in the nuclei of higher organisms, and the need for coordination of their action during development, it is reasonable to assume that evolutionary processes would have initiated superregulatory mechanisms to accomplish that end. The *Spm* system serves as a model of the mode of operation of one type of superregulatory mechanism. Such a system can activate or inactivate particular genes in some cells early in development, and activate or inactivate other genes later in development. It can turn on the action of some genes at the same time that it turns off the action of others. It can adjust the level of activity of a particular gene in different parts of an organism. Some evidence to support these statements has been presented in previous *Year Books* and other publications, and additional evidence will be reported here.

At the time they were first detected, controlling elements were distinguishable from genes because, unlike genes, they could be transposed from one location to another in the chromosome complement. Thus the operator element of a regulatory

system may be inserted at the locus of a gene, whose action is then subject to control by the system to which the operator element belongs. Because the detected controlling elements of a system may reside at different locations in the chromosome complement, they have been likened to episomes in bacteria. This comparison is justified, since it is known that the activity of bacterial genes may be subject to control by episomes. In maize, however, the operator element of either the *Ac* (Activator) or the *Spm* (Suppressor-mutator) system may become integrated into a chromosome in such a way that it no longer undergoes transposition. In its fixed position it continues to respond to signals from the regulator, and its responses are made evident by changes in action of the gene with which the integrated operator element is associated. At present, there is no direct evidence for or against episomal origin of the components of known gene-control systems in maize. It is conceivable, nevertheless, that some superregulatory mechanisms in higher organisms may have originated through incorporation and adaptation of the gene-control components of episomes.

The *Ac* and *Spm* gene-control systems are not considered to play a vital role in coordinating gene action during development of the maize plant, at least as far

as the known states of the component elements are concerned. If they did play such a role, it is doubtful that they could have been analyzed so readily; for then the selected mutants of the regulator elements, which have provided much evidence about the modes of operation of the systems, would have so altered coordination as to affect adversely the growth of plant or kernel. Adverse effects have not been noted. Thus, the controlling elements of the examined systems may represent foreign, nonessential, episome-like components that have been integrated into the maize genome; or, on the other hand, they may be true chromosomal components of present-day maize, whatever their evolutionary origins and histories may have been. Some evidence supporting the second consideration will be reviewed briefly.

My study of gene-control systems in maize was initiated with an experiment conducted some years ago, which utilized the chromosome type of breakage-fusion-bridge cycle. The unexpected results of this experiment, reported at the time, should again be emphasized here. In the self-pollinated progeny of a number of plants that had commenced development with a chromosome pair undergoing the breakage-fusion-bridge cycle, it was startling to observe that many unrelated genes, whose action had previously been normal with respect to expression in plant tissues, were now exhibiting marked differences in activity in different parts of plants. The patterns of change in the somatic tissues, regardless of the cellular function with which a particular modified gene was concerned (that is, plastid development, chlorophyll synthesis, anthocyanin synthesis, or capacity of the cell for growth or division), reflected some mechanism of control of action of these genes during development.

Studies were then begun to examine these gene-control mechanisms. Later, when the components of a control system were recognized, it was possible to reconsider the basic question posed by the results of the initial experiment: Why

were control systems so suddenly revealed and at so many different gene loci? It was concluded that regulatory elements, distinct from the genes, must have been present in the nuclei of the maize plants before the breakage-fusion-bridge-cycle experiment was conducted, and that this cycle, in some yet unknown manner, had induced modifications in the pre-existing elements. The evidence was so compelling that it was later decided to test the conclusion. If it was correct, the breakage-fusion-bridge cycle should be able to induce a known type of regulatory element from some unknown element in a nucleus whose ancestor nuclei, in their past history, through many plant generations, had never given evidence of its presence. The experiment, reported in *Year Book 50*, was successful. There was no doubt that *Dt*-type regulation could be induced, independently, in a number of different nuclei where the cycle was in effect. It was also evident that each induction was the consequence of a single event involving some component in an individual cell. After induction, the regulatory activity of the induced element was registered in the descendent cells.

Additional evidence for considering that the examined types of controlling elements are derived from components normally present in maize chromosomes comes from studies of induction of change in action of a presumed "wild-type" gene by particular alleles of the gene. This induction effect is termed "paramutation" by R. A. Brink in studies of alleles of the *R* gene, located in chromosome 10, and is termed "conversion" by E. H. Coe in studies of alleles of the *B* gene, located in chromosome 2. With regard to either *R* or *B*, the initially recognized allele that induced change in action of a presumed normal allele would have been placed in the "mutable gene" category had its behavior been analyzed in earlier years. Indeed, genes under the control of the *Ac*, *Spm*, and *Dt* systems were at first referred to as mutable genes, since they exhibited phenotypes to which this term had been applied in many early genetic

investigations. It seems most likely that induction of change in gene action of "wild-type" alleles, and the subsequent capacity of some of the changed alleles to induce similar changes, resides in controlling elements normally associated with the genes.

The resemblance between effects brought about by the inducing alleles, described above, and those produced by elements of known control systems is further illustrated in studies conducted by Dr. Brink and his students with the *R* alleles. The initially recognized inducing allele, *Rst*, gives rise to a distinctive pattern of pigmented areas in a nonpigmented background in the aleurone layer of the kernel. The frequency of occurrence of change from inactive to active expression of the *R* gene in the cells of the endosperm during its development may be determined readily by examining the numbers of such pigmented areas in the kernel. There is a dominant modifier that markedly increases the frequency of occurrence of these events without altering the time during development when they take place. Initially, this modifier was placed approximately six crossover units distal to the locus of *Rst*. Its effect resembles in detail that of a dominant modifier element in the *Spm* system, reported in *Year Book 57*, and like that element it undergoes transposition. Thus, accumulating evidence obtained in studies of the *R* and *B* alleles now makes it reasonable to consider that "paramutation" and "conversion" reflect alterations induced by and in components of gene-control systems normally present in maize. It would be instructive to determine, therefore, whether or not the individual components of these systems could be identified through transposition and insertion elsewhere in the chromosome complement.

Modified States of a_1^{m-2}

In *Year Book 61* the mode of control by the *Spm* system of gene action at a_1^{m-2} was reviewed. As was stated there, the

regulator element, *Spm*, resides close to the locus of the *A₁* gene. When this element is in an active phase, the *A₁* gene is active, but during an inactive phase of the element gene action is inhibited unless an active *Spm* element is present elsewhere in the chromosome complement. When an active *Spm* is present, release of gene action from the control of the *Spm* system occurs in some somatic cells, and is accompanied by the production of mutants of the *A₁* locus, the classes of which were described last year. When the *Spm* element associated with the a_1^{m-2} locus is inactive, and no additional active *Spm* is present in the nuclei of plant or kernel, such mutants are not produced.

In this study of a_1^{m-2} , an occasional kernel on a testcross ear exhibited an atypical phenotype with respect to expression of the *A₁* gene. Plants were grown from some of these kernels, and each was subjected to testcrosses in order to explore the cause of the modified gene expression. It could be determined by this means that the atypical phenotypes arose through modification of either the regulator element, *Spm*, or the operator component residing at the *A₁* locus.

*Modified states of *Spm* at the a_1^{m-2} locus.* There are several readily recognized types of modification of the *Spm* element. One type changes its phase of activity; another type alters the time of its transposition during development; a third markedly alters its capacity to effect responses of the operator element that result in release of gene action from the control of the *Spm* system. The third type of modification, discovered initially in studies of a_1^{m-1} and a_2^{m-1} , was designated *Spm^w* and was described in *Year Book 56*. With a_1^{m-1} and the class I states of a_2^{m-1} , the inhibitory effect of *Spm^w* on gene action at either of these loci is pronounced, but its capacity to induce responses of their operator elements that release the genes from *Spm* control is very much weakened. Few mutants of this type are produced.

The type of control of *A₁* gene action

when an *Spm^w* is present at the a_1^{m-2} locus is that expected. The gene is active, since the inhibitory effect of *Spm* on gene action at a_1^{m-2} is the reverse of that on gene action at a_1^{m-1} and a_2^{m-1} . In the kernels, pigment of medium intensity is distributed over the aleurone layer. The weakened capacity of *Spm^w* to induce modification of gene action is expressed in the kernel either by an absence of mutant areas or by the presence of one or several very small areas showing a mutant phenotype. Thus, *Spm^w* differs from standard *Spm* (which in this account will be designated *Spm^s*) in capacity to effect mutation-inducing responses of the operator element of the system.

Two isolates of a_1^{m-2} in which the associated *Spm^s* element had mutated to *Spm^w* were examined this past year. The *Spm^w* mutants differ in frequency of reversion to *Spm^s*, one reverting frequently and the other rarely. Previous studies of *Spm^w* mutants, conducted with plants having either a_1^{m-1} or a_2^{m-1} , had shown that, when *Spm^w* and *Spm^s* are both present in the nuclei of a plant or kernel, *Spm^s* exerts a dominant effect. *Spm^w* is not altered by the association, however, but can be recovered quite unchanged in the progeny of plants having both the *Spm* elements. Each of the isolates of a_1^{m-2} with *Spm^w* located close to it responds in this same manner to *Spm^s* located elsewhere in the chromosome complement, and the response is similar to that seen when *Spm^s* resides at the locus of a_1^{m-2} . Moreover, tests conducted with one of these isolates have indicated that *Spm^w* is recovered unaltered in the progeny of plants in which an independently located *Spm^s* element is also present.

Altered states of the operator element at a_1^{m-2} . Kernels exhibiting atypical phenotypes were selected with the intent of finding among them examples in which the regulator element, *Spm*, but not the operator element had been removed from the locus of a_1^{m-2} . Tests were initiated with plants derived from 7 selected

kernels, and continued with their progeny. It was learned that the modified phenotype in 4 of these kernels could be ascribed neither to an event that had removed *Spm* from the locus of a_1^{m-2} nor to change in *Spm* action. These 4 modified states of a_1^{m-2} differ from the original state mainly in the frequency of occurrence of each of the types of A_1 gene expression that arise in conjunction with release of the gene from control of the *Spm* system. The remaining 3 altered states show no evidence of the presence of *Spm* at the modified a_1^{m-2} locus. Each, however, responds in its own way to an active *Spm* element located elsewhere in the chromosome complement. Two of these states promise to provide new evidence about kinds of control of gene expression during development.

One of them illustrates the manner in which anthocyanin pigment of different intensities may be produced in individual cells of a tissue. Such differences may be due to "cross-feeding" between adjacent cells that, individually, either cannot synthesize pigment or can synthesize very little. The phenomenon is suggested by the distribution of pigmented cells in kernels having one of the two mentioned states of a_1^{m-2} and an active *Spm* element. These kernels have pigmented areas in a colorless or nearly colorless background. Some areas are not solidly pigmented, but are bounded by a band of pigmented cells. The intensity of pigment in the cells composing these ring-shaped bands is not uniform. Many of the bands have an inner row of deeply pigmented cells. The cells on both sides of this inner row exhibit a decreasing gradient of intensity of pigment, fading gradually into colorless or nearly colorless cells. The origin of the ring-shaped bands, in which some cells exhibit pigment intensities approaching that produced by the normal A_1 gene, may be explained by cross-feeding between adjacent cells that differ genotypically. The shapes of the pigmented bands indicate that the cells enclosed by each band are descendants of one in

which the genotype was modified, and the modifications appear to have been controlled by the *Spm* system.

The second of these two modified states of a_1^{m-2} was mentioned in *Year Book 61* during a discussion of a_1^{m-2} that considered potential isolates having an operator element of the *Spm* system but no *Spm* regulator element associated with the locus. This state was detected, initially, in a kernel that exhibited an atypical phenotype characterized by some lightly pigmented areas in a colorless background. The intensity of anthocyanin pigmentation differed among the cells of an area: some were more intensely pigmented than others, and some appeared to have no pigment, but none was deeply pigmented. As was reported last year, there was no evidence of the presence of *Spm* in the plant derived from this kernel.

The results obtained in initial tests conducted with this plant and in more extensive tests of its progeny will be summarized here. It was learned that the phenotype described above appears in kernels in subsequent generations as long as the altered state of a_1^{m-2} has not passed through a plant generation in which an active *Spm* element is also present in the nuclei. When an active *Spm* is introduced by appropriate crosses, the phenotype of the kernels that have received the altered a_1^{m-2} locus from one parent and an active *Spm* from the other parent, and also the phenotype of the plants derived from these kernels, is similar to that produced by the original state of a_1^{m-2} . When test-crosses were conducted, however, with the plants that had received a newly introduced *Spm*, some of the kernels on the resulting ears exhibited a decidedly modified phenotype, which appeared only among kernels that had received the altered state of a_1^{m-2} but no *Spm*. These kernels had mottled areas, within which many of the cells were intensely pigmented. The presence of intense pigmentation in the mottled areas allowed recognition of confluence of these areas in

a manner that gave rise to a clearly defined pattern of pigment distribution over the aleurone layer. Microscopic examination of the kernels showed that the distribution and intensity of pigment in individual cells within an area very much resembled those produced by the kind of cross-feeding between adjacent cells described above.

Among the kernels on these ears that had a_1^{m-2} but no *Spm*, a wide range in expression of maximum pigment intensities was noted, although within an individual kernel all the mottled areas showed the same range of intensity of cell pigmentation. Among the different kernels the maximum intensity ranged from very dark to rather faint. Kernels with strikingly enhanced pigmentation in the mottled areas appeared on ears produced by crosses conducted with each of 11 tested plants that commenced development with a newly introduced *Spm*. They did not appear on ears produced by similar crosses conducted with 26 sister plants that had not received *Spm*. Therefore it is suspected that *Spm* induced, in many cells of the germ line, a particular type of modification of the operator element of the altered state of a_1^{m-2} . This change enhanced the capacity of the A_1 gene to contribute to pigment formation in cells of a mottled area after *Spm* had been removed from the nucleus in the meiotic process. In some respects this phenomenon resembles the paramutagenic effect described earlier.

Study of a_1^{m-2} has added to our appreciation of gene-control mechanisms in that it suggests cooperation between two or more regulatory mechanisms. With the original state, activation and inactivation of the A_1 gene are controlled by *Spm*. Another regulatory mechanism must operate, however, when the gene is active. This fact was revealed early in the study of a_1^{m-2} , by the restricted distribution of anthocyanin in plant tissues described in *Year Book 61*. It is also strikingly revealed by the very distinctive pattern of arrangement of mottled areas

in the kernels just described. It is again manifested by the distribution of pigment in the cob: large areas of deep pigmentation often appear in cobs of plants carrying the original state of a_1^{m-2} and an active *Spm* element. They are not due to a heritable modification of a_1^{m-2} , as is shown by the results of tests and is also indicated by the fact that kernels above these areas have the same phenotype as other kernels on the ear. A heritable change would be reflected both in the cob areas and in the kernels overlying them, since the a_1^{m-2} locus in the cells of all is descended from one that was present in a common ancestor cell.

Extension of Spm Control of Gene Action

These studies, over a period of years, have uncovered a number of examples of gene control by foreign systems that have not yet been reported because of inadequate identification. Whether or not the system controlling a particular gene was *Ac* could be determined rapidly, because precise methods of testing were available. Early methods for testing whether or not a system might be *Spm* were much less direct and, as applied to some genes, were considered too indirect to be efficient. Therefore some of the isolates, after they had been found not to represent *Ac* control, were temporarily dropped from study. When it was determined that wx^{m-8} was under the control of the *Spm* system, it became possible to construct tester stocks that could directly reveal *Spm* control of gene action at other loci. Five suspected examples of control of gene action by this system could now be tested with wx^{m-8} . Two, isolated some years ago, involve the C_1 locus in chromosome 9 and are designated c_1^{m-5} and c_1^{m-6} . Two others, recently isolated, involve the C_2 locus in chromosome 4 and are designated c_2^{m-1} and c_2^{m-2} . The last involves the *Pr* locus in chromosome 5.

This past year, the required combinations of gene markers for such tests were available only in plants having c_1^{m-5} .

Plants that were $c_1^{m-5} Sh_1 wx/c_1 sh_1 wx^{m-8}$ in constitution were crossed with plants that were homozygous for c_1 , sh_1 , and wx and carried no *Spm*. Other plants, $c_1^{m-5} wx/c_1 wx$ in constitution, were crossed with plants that were $c_1 wx^{m-8}/c_1 wx$ and had no *Spm*. Among the kernels on the ears produced by these crosses, response of wx^{m-8} to *Spm* was correlated with the presence of c_1^{m-5} in the kernel. These initial tests placed *Spm* close to the locus of c_1^{m-5} in the examined plants. They also indicated that the origin of some of the stable mutants produced by c_1^{m-5} was associated with transposition of *Spm* to a new location in the chromosome complement.

Further confirmation of *Spm* control of gene action at c_1^{m-5} was obtained from tests conducted with one plant in which *Spm* underwent change from the inactive to the active phase late in development. On the ears of this plant, some kernels that had received both c_1^{m-5} and wx^{m-8} gave no evidence of the presence of *Spm* except in one sector, produced by descendants of the cell in which *Spm* had changed to the active phase. A well defined area in the aleurone layer exhibited the types of pigmented spots that are produced by change in gene action at c_1^{m-5} ; and only in the underlying cells, derived from the common ancestor cell, did the starch in individual cells or clusters of cells display a phenotype produced by mutation at wx^{m-8} .

It may be added here that wx^{m-8} has also been useful in analyses of change in phase of activity of *Spm* at the a_1^{m-2} locus. Responses of the two loci to phase of activity of *Spm* are similarly correlated.

Further Studies of Topographical Relations of Elements of a Control System

In *Year Book 61*, the origin of a two-element system of control of gene action from an apparently single-element control system was outlined with respect to the *Ac* system in its relation to bz^{m-2} and one of its altered states, Bz^w . Initially,

the regulator element, *Ac*, was present at or very close to the locus of the bronze gene, which is involved in the biosynthetic pathway leading to anthocyanin formation in plant and kernel. In studies, with bz^{m-2} , of the relation between transposition of *Ac* away from the bronze locus and initiation of *Bz* gene action, one instance was found in which *Bz* expression appeared in conjunction with transposition of *Ac* to a position in chromosome 9 between the locus of the *Bz* mutant and that of *Wx*, approximately 10 crossover units distal to *Wx*. In one type of testcross, pollen from a plant that was *I Sh Bz(standard) wx Ds/C sh Bz(mutant) Ac Wx* in constitution was placed on the silks of ears of plants that were homozygous for *c, sh, Bz*, and *wx* and had no *Ac*. On one of the resulting ears, a single nonpigmented kernel was present in which changes in *Wx* gene action, from a low level to a high level of gene expression, had occurred in some cells during endosperm development.

In order to examine the system responsible for control of *Wx* gene action in this kernel, a plant was grown from it in the summer of 1961. When pollen collected from this plant was stained with an I-KI solution, half the grains stained a red-brown (*wx*) but, unexpectedly, the other half stained a deep blue as if to indicate the presence of a normal *Wx*

gene. It was then suspected that only the endosperm of the kernel that gave rise to the plant had received the modified *Wx* gene, and that the normal *Wx* gene had been delivered to the zygote. To verify this suspicion, a few testcrosses were conducted with the plant. It was crossed reciprocally with an *Ac*-tester plant, homozygous for *C, Sh, Bz, wx*, and *Ds* (standard location). It was also crossed to plants that were homozygous for *C, sh, bz*, and *wx*, either with or without *Ac* in their nuclei, and to a plant whose constitution was *c Sh bz wx/c sh bz wx*, no *Ac*. The kernels produced by these crosses revealed that the zygote had, in fact, received the modified *Wx* gene and that its action was under the control of the *Ac* system. Moreover, *Ac* was found to be located very close to this modified *Wx* gene, which was then designated wx^{m-9} because it represented the ninth detected change in the Cold Spring Harbor cultures whereby the action of the normal *Wx* gene had become subject to a foreign control system.

Results of these initial tests and of others conducted during the past year show that return to a high level of *Wx* gene action is usually associated with removal of *Ac* from the locus of wx^{m-9} . The results of two types of testcross conducted with plants carrying wx^{m-9} are given in tables 1 and 2. They demonstrate

TABLE 1. Phenotypes of Kernels on Ears Produced by Reciprocal Crosses of Plants Having the Constitution $c_1 wx^{m-9}/c_1 wx$ with *Ac*-Tester Plants That Were Homozygous for *C*, *wx*, and *Ds* (Standard Location) and Had No *Ac*

♀ = heterozygote employed as ear parent; ♂ = heterozygote employed as pollen parent.

Level of Expression of Waxy Gene in Starch of Endosperm	Pigmentation of Aleurone Layer				Totals
	Uniformly Pigmented (No <i>Ac</i>)		Colorless Areas in Pigmented Background (<i>Ac</i>)		
	♀	♂	♀	♂	
High level throughout (germinal mutation)	8	11	12	11	42
Low level with sectors of high level	0	0	1834	986	2820
Low level throughout	5	3	0	0	8
Null level (<i>wx</i> allele)	1818	1003	30	64	2915
Totals	1831	1017	1876	1061	5785

TABLE 2. Phenotypes of Kernels on Ears Produced by Reciprocal Crosses of Plants Having the Constitution $I\ wx^{m-9}/c_1\ wx$ with Ac -Tester Plants That Were Homozygous for C_1 , wx , and Ds (Standard Location) and Had No Ac

The colorless kernels received I , whereas the pigmented kernels received the allele c_1 from the heterozygous parent. ♀ = heterozygote employed as ear parent; ♂ = heterozygote employed as pollen parent.

Level of Expression of Waxy Gene in Starch of Endosperm	Pigmentation of Aleurone Layer						Totals
	Colorless		Uniformly Pigmented (No <i>Ac</i>)		Colorless Areas in Pigmented Background (<i>Ac</i>)		
	♀	♂	♀	♂	♀	♂	
High level throughout (germinal mutation)	17	1	1	2	2	0	23*
Low level with sectors of high level	1212	117	0	0	418	33	1780
Low level throughout	3	0	0	1	1	0	5
Null level (<i>wx</i> allele)	479	51	1214	110	27	0	1881
Totals	1711	169	1215	113	448	33	3689

* Six plants derived from these kernels were examined; 4 had no Ac , and 2 had Ac unlinked to markers in chromosome 9.

the location of Ac before transposition, and the relation of transposition of Ac to release of Wx gene action from control by the Ac system.

Among the total of 9474 kernels recorded in tables 1 and 2, 13 kernels with the wx^{m-9} phenotype showed no evidence of the presence of Ac . Two of them appeared on ears produced by crosses conducted with the original plant carrying wx^{m-9} . During the past year, plants were grown from these two kernels and each plant was tested for the presence of Ac in its nuclei and also for the response of the derivative of wx^{m-9} to introduced Ac . The tests showed that neither plant had Ac , and that the low level of gene expression characteristic of derivatives of wx^{m-9} remained unchanged as long as Ac

was absent. When Ac was introduced, however, each responded to it. Mutations occurred in individual cells, whose descendent cells exhibited a high level of Wx gene action. The time during development when the mutations occurred reflected the dose of Ac present in the nuclei of the kernels: the higher the dose of Ac , the later the time of occurrence of mutations. The genic marker constitution of the chromosome 9 carrying wx^{m-9} in these two plants indicated that the removal of Ac from the immediate vicinity of the original wx^{m-9} locus could not be attributed to crossing over. Thus, wx^{m-9} provides another example of origin of a two-element system of control of gene action from an apparently one-element system.

ENZYMOLGY

Margaret R. McDonald and Anne K. Carhart

By the time this report is published Dr. McDonald will have joined the staff of the Waldemar Medical Research Foundation. During the past year we

have concentrated our efforts on completing problems already initiated, preparatory to the termination of our association with the Genetics Research Unit.

Since our main effort has been to accumulate a supply, and to study the properties, of a heretofore unidentified contaminant present in some samples of crystalline pancreatic RNase, which showed aberrant results in our cytochemical studies with Dr. Berwind P. Kaufmann and Dr. Helen Gay (*Year Books* 49, 54, 60, 61), we shall restrict this report to that aspect of our investigations.

As was mentioned last year, the location of DNA in fixed tissues can be determined cytochemically by means of two color reactions: that produced by the Feulgen test, which is regarded as specific for deoxyribose; and that produced by methyl green, which colors highly polymerized, but not depolymerized, DNA. Treatment of tissue sections with either DNase I or DNase II prevents both Feulgen and methyl green staining of the chromosomes, as would be anticipated from the known specificities of these enzymes. An unexpected result was observed, however, when fixed tissue sections were treated with high concentrations of crystalline RNase free of all measurable traces of DNase. Such treatment rendered the chromatin nonstainable with methyl green without reducing the intensity of the Feulgen reaction (*Year Book* 49). The failure to stain with methyl green did not appear to be due to combination of RNase as a basic protein with the DNA of the chromosomes (although such combination undoubtedly occurred), since other basic proteins, such as lysozyme, cytochrome *c*, and chymotrypsinogen, tested under identical conditions, did not alter methyl green colorability (*Year Books* 54, 60). Furthermore, the reduction in methyl green stainability of fixed sections treated with RNase was dependent on time, temperature, and concentration (*Year Book* 60) and thus definitely suggestive of an enzymatic reaction, although no such reaction was observed when isolated DNA or DNA-histone was treated with RNase.

The results were explicable on the

supposition that chromosomes contain a complex nucleic acid composed of both deoxyribo- and ribonucleotides. If the ribonucleotides occupied intercalary positions, and the number of adjacent deoxyribonucleotides was large, removal of the ribonucleotides by the specific action of RNase would depolymerize the DNA sufficiently to impair its ability to stain with methyl green without impairing its Feulgen stainability. Such an explanation was in fact offered in *Year Book* 49, and subsequent developments in other laboratories regarding RNA-DNA complexes tended to support the hypothesis.

Last year, however, working in conjunction with Dr. Helen Gay and Miss Ann Weingart, we noted that some preparations of crystalline RNase did not efface methyl green stainability of tissue sections. The ability of the samples that did was traced to their content of a foreign protein. We named this contaminant "Z protein" because its mode of action had not been established. Unfortunately, despite intensive efforts on our part, the enzymatic activities of the protein have not yet been definitely ascertained, and the name is being retained.

Preparation of Z Protein from Ribonuclease

Z protein is obtained by chromatographing contaminated RNase on carboxymethyl cellulose ion-exchange columns buffered with tris(hydroxymethyl)-aminomethane-hydrochloric acid at pH 8.0 according to the method of Taborsky, with increasing concentrations of sodium chloride as the eluant. Figure 2 shows the chromatogram obtained with RNase 70 (see *Year Book* 61), one of our most effective RNase samples for the elimination of methyl green stainability of tissue sections. Four distinct fractions are observed. The material in fraction I appears to be deoxyribonucleotide on the basis of analyses of its ultraviolet

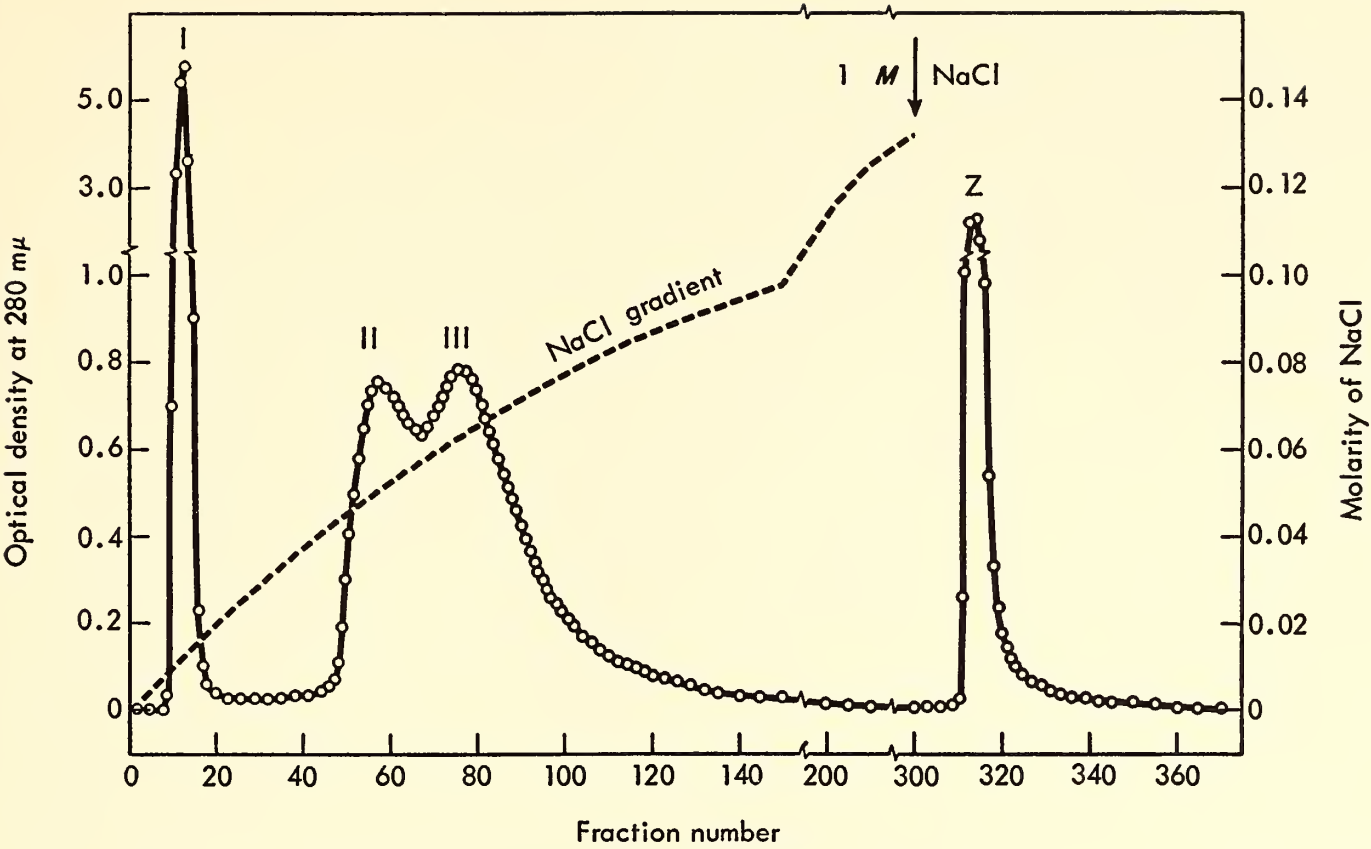


Fig. 2. Chromatography of ribonuclease 70. CM-cellulose, 2.5 × 32 cm column; 0.005 M tris-HCl buffer pH 8.0-NaCl gradient as shown; 2°C; 200 ml per hour; 14-ml fractions; 2000-mg load.

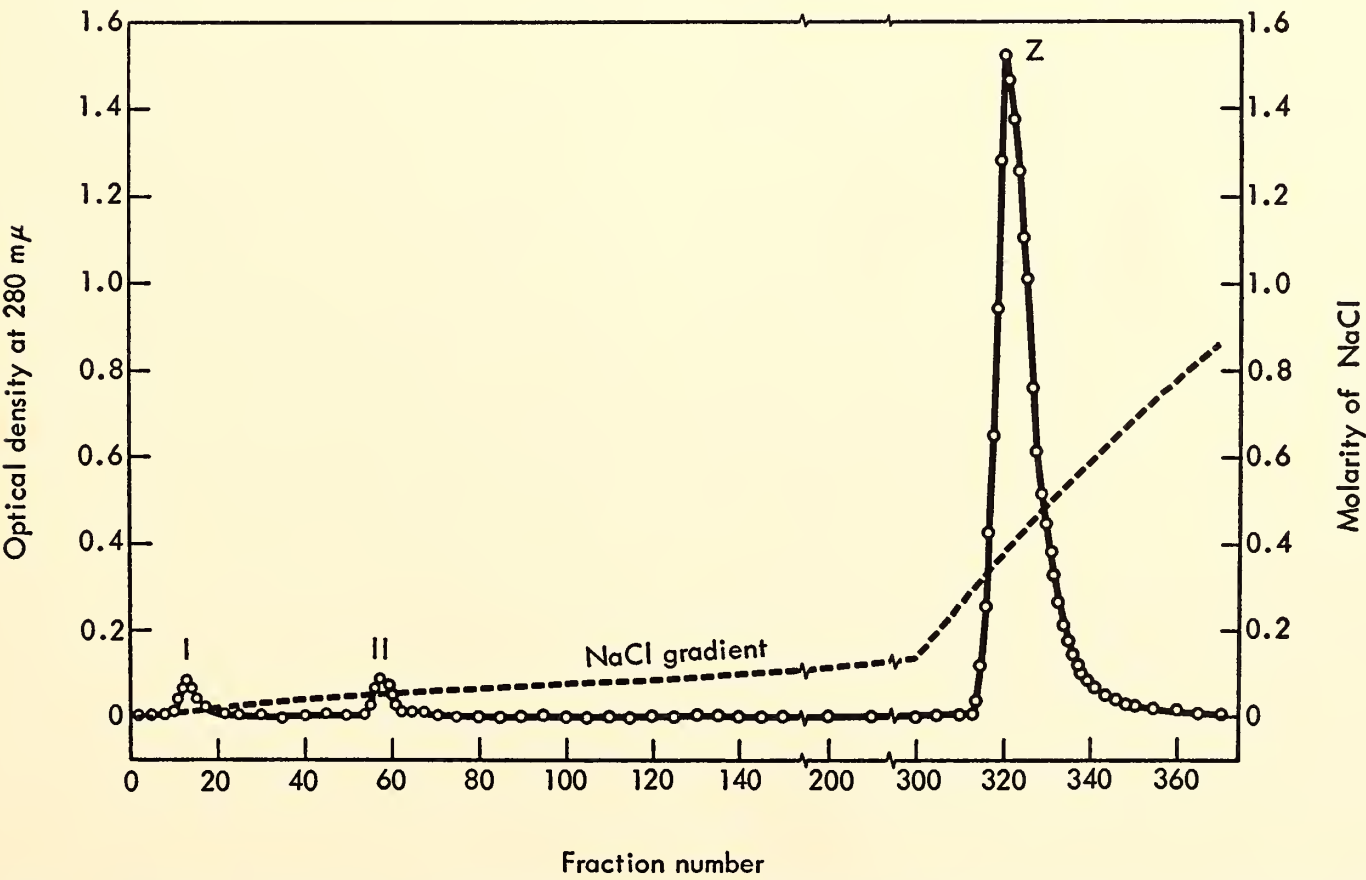


Fig. 3. Rechromatography of dialyzed Z protein prepared as shown in figure 2. CM-cellulose, 2.5 × 32 cm column; 0.005 M tris-HCl buffer pH 8.0-NaCl gradient as shown; 2°C; 200 ml per hour; 14-ml fractions; 500-mg load.

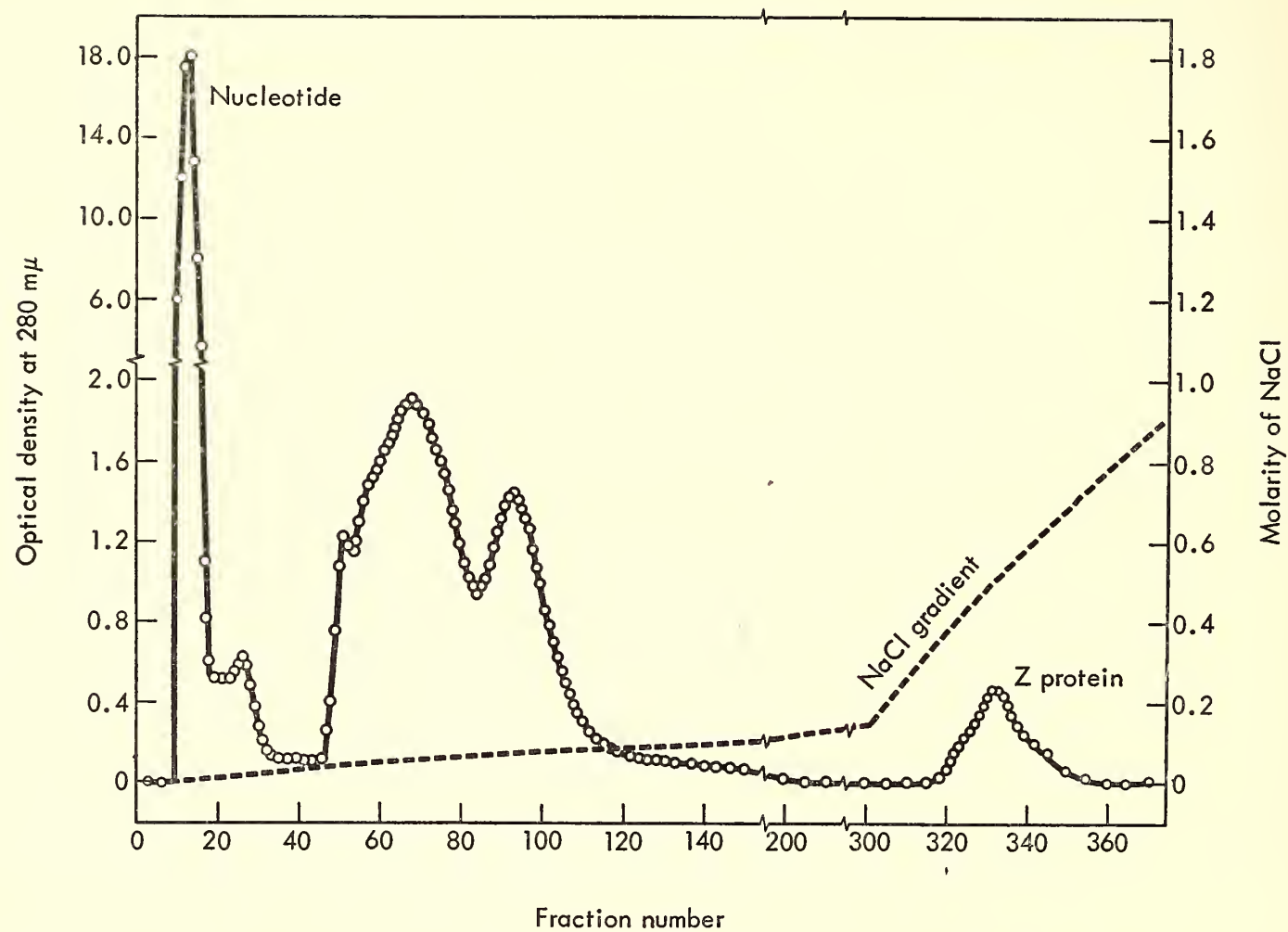


Fig. 4. Chromatography of second mother liquor from ribonuclease 4F (see *Year Book 61*). CM-cellulose, 2.5 × 32 cm column; 0.005 M tris-HCl buffer pH 8.0-NaCl gradient as shown; 2°C; 200 ml per hour; 14-ml fractions; 2500-mg load.

absorption spectrum, phosphorus content, type of sugar, and nondialyzability (*Year Book 61*). Fractions II and III contain essentially all the RNase activity of the original sample (table 3). Fraction Z is protein in nature, and the amount present in any RNase sample is directly correlated with the ability of that sample to impair methyl green stainability in fixed tissue sections. On the other hand, the

materials found in fractions I, II, and III, either alone or in all possible combinations, do not alter the capacity of chromatin to stain with this dye (*Year Book 61*).

As judged from the concentrations of the eluting sodium chloride solutions and the specific activities of the fractions (fig. 2; table 3), fraction III corresponds to Taborsky's fraction D (RNase A of

TABLE 3. Analysis of Chromatographic Fractions of Ribonuclease 70

Fractions	Recovery, %*		Specific Activity†
	OD ₂₈₀	RNase Activity	
I	26		
II	17	27	144
III	34	67	180
Z	15	1	4

* Amount placed on column taken as 100 per cent.

† Specific activity of RNase 70 taken as 100.

Hirs, Moore, and Stein as prepared on Amberlite IRC-50), and our fraction II to his B plus C. Taborsky's fraction E was not found in any of our RNase samples that were analyzed. The RNase fractions are not too well resolved one from another, probably because of overloading of the column and the steep elution gradient. Since they are well separated from fraction Z, however, and our main interest was in collecting large amounts of the Z component, no attempt was made to refractionate them. It should be noted in passing that less of fraction III and more of fraction II were found than was to be expected from Taborsky's results; but RNase 70 had been stored in the dry state for more than 12 years, and it has been observed in other laboratories that such prolonged storage gives rise to materials that move more rapidly than RNase A on IRC-50 columns, with a concomitant loss of RNase A.

Rechromatography of fraction Z (fig. 3), eluting with lower concentrations of sodium chloride, showed small amounts of fractions I and II, most of the material occurring in a single, almost symmetrical band of Z protein. Of the material originally placed on the column, 2 per cent, as measured by optical density readings at $280\text{ m}\mu$, was recovered in fraction I, 3 per cent in fraction II, and more than 90 per cent in fraction Z. No fraction III was observed.

Since the Z protein was detected as a contaminant in RNase, we thought that the mother liquors from which RNase had been crystallized might be a good source for its preparation in large amounts. Investigation of mother liquors still on hand from the original crystallizations of our RNase samples showed, however, that this was not so. Very little Z protein (no sample containing more than 4 per cent) was detected by chromatography (fig. 4), and none of the samples was active in reducing methyl green stainability. As can be seen by the figure, however, they were potent sources of the deoxyribonucleotide fraction.

Properties of Z Protein

Qualitative amino acid analyses of acid hydrolysates of Z protein by descending chromatography on Whatman 1 paper with *n*-propyl alcohol-acetic acid-water solutions (80-10-10) as the solvent showed the presence only of glycine, alanine, valine, leucine (and/or isoleucine, norleucine), serine, threonine, lysine, arginine, histidine, glutamic acid, asparagine, and tyrosine. Hence at least six of the amino acids present in ribonuclease A are not present in Z protein. These are aspartic acid, cystine, glutamine, methionine, phenylalanine, and proline. Tryptophan, which is absent from ribonuclease A, is also absent from Z protein as determined by the Bates modification of the May-Rose test (*Year Book 36*).

All chemical tests to demonstrate enzymatic activity of Z protein on isolated DNA or DNA-histone, with and without added potential activators such as mono- or bivalent ions and reducing agents, have so far yielded negative results. The assays are complicated by the fact that high concentrations of Z protein precipitate DNA (and RNA). With the concentrations that could be tested (less than 0.02 mg/ml), no increase in the ultraviolet absorption of the DNA was observed even after 24 hours of treatment. An increase would be expected if Z protein caused depolymerization of the DNA either by disruption of hydrogen bonding, by rupture of base pairing due to chemical changes (such as deamination) in the bases themselves, or by hydrolysis of the sugar-phosphate linkages. Nor was there any release of dye from DNA that had been combined with methyl green, such as occurs when the combination is treated with either DNase I or DNase II. Similarly, no decrease in methyl green coloration of fixed spots of DNA-histone resulted from their treatment with Z protein, nor was there any decrease in the viscosity of Z protein-treated DNA. The results of these experiments offer no clue to the mechanism by which this protein reduces

TABLE 4. Assays of Z Protein for Ribonuclease Activity

Z Protein, mg/ml*	Duration, min	OD ₂₆₀ †
0	30	0
0.078	20	0.085
0.156	20	0.174
0.313	20	0.342
0.625	20	0.620
0.5	0	0.059
0.5	5	0.197
0.5	10	0.307
0.5	15	0.412
0.5	20	0.462
0.5	25	0.545
0.5	30	0.581

* Increasing precipitation of RNA occurs with increasing concentration of Z protein.

† Read against appropriate blanks of RNA and Z protein incubated separately. Increase in OD₂₆₀ is a measure of increase in acid-soluble split products and hence of RNase activity.

methyl green stainability of fixed tissue sections.

In addition to altering methyl green stainability of fixed tissue sections, Z protein also eradicates pyronin stainability, indicating degradation of RNA. That degradation does occur can be shown chemically. Assays for RNase activity of once-chromatographed Z protein show that the activity per milligram of protein (specific activity) is approximately 4, as compared with 180 for the purest RNase fraction (table 3). Rechromatography reduces it to 3. Although low, the activity appears to be real and not an artifact due to coprecipitation of the protein with the RNA substrate, for the increase in acid-soluble split products that results when RNA is incubated with Z protein is proportional not only to the concentration of the protein but also to the duration of treatment (table 4).

Whether or not the RNase activity is due to an impurity present in the Z protein has not yet been definitely established, and cannot be unless it proves possible to prepare Z protein free of all traces of RNase activity or to inhibit this activity selectively. Standard chemical methods for decision regarding the possible separability of two enzymatic activities cannot be employed, since the cytochemical procedures—our only assay

of the unidentified enzymatic activity of Z protein—are not sufficiently precise. The loss in RNase specific activity when Z protein is rechromatographed is suggestive of extraneous origin. Mean values of 4.26 ± 0.19 and 3.23 ± 0.15 were obtained for once- and twice-chromatographed Z protein. The Diff./S.E. is 4.3 and highly significant. But rechromatography does not appear to be an efficient means of freeing Z protein from RNase. Methods similar to those employed so successfully in freeing pancreatic RNase from protease (*Year Book 46*) and salmon-testes DNase from RNase (*Year Book 60*)—such as selective denaturation by heat or organic chemicals under various conditions of pH and electrolyte concentration—have so far proved ineffective.

The ability of Z protein to reduce pyronin stainability of chromatin, nucleoli, and cytoplasm can be due to its residual RNase content. The only difference noted in pyronin stainability of acetic acid-alcohol-fixed onion root tips after treatment with solutions of crystalline RNase or Z protein of the same RNase activity is in the stainability of the cell walls, which is much more readily reduced by Z protein than by RNase. What this observation means in terms of the chemical composition of the cell walls is not clear; until more is known about

the composition of cell walls in general, speculation about its significance seems futile.

Attempts to inhibit RNase activity of Z protein with enzyme inhibitors such as the ions of heavy metals have not led to conclusive decisions about the nature of the RNase activity. Cupric ions, for example, inhibit pancreatic RNase as judged both chemically and cytochemically. They inhibit the capacity of Z protein to reduce pyronin staining, but they also inhibit its ability to impair methyl green stainability. Since these inhibitors are rather general enzyme

poisons, the results would have been significant only if methyl green staining had not been affected. A much more reliable test would be treatment with specific RNase inhibitors such as that found by Bernheimer in lilac leaves, but time has not permitted their preparation and application.

Unfortunately, the results of all these experiments leave the status and significance of Z protein inadequately defined. They have, however, directed attention to its existence. We hope that future work, whether by ourselves or by others, will eventually clarify the situation.

BIBLIOGRAPHY

- Burgi, E., Changes in molecular weight of DNA accompanying mutations in phage, *Proc. Natl. Acad. Sci. U. S.*, 49, 151-155, 1963.
- Burgi, E., and A. D. Hershey, Sedimentation rate as a measure of molecular weight of DNA, *Biophys. J.*, 3, 309-321, 1963.
- Burgi, E., *see also* Hershey, A. D.
- Dutt, M. K., Changes in pH of Feulgen stain and their effect on the staining of biological material, *J. Histochem. Cytochem.*, 11, 390-394, 1963.
- Frankel, F. R., An unusual DNA extracted from bacteria infected with phage T2, *Proc. Natl. Acad. Sci. U. S.*, 49, 366-372, 1963.
- Goldberg, E., *see* Hershey, A. D.
- Hershey, A. D., E. Burgi, and L. Ingraham, Cohesion of DNA molecules isolated from phage lambda, *Proc. Natl. Acad. Sci. U. S.*, 49, 748-755, 1963.
- Hershey, A. D., E. Goldberg, E. Burgi, and L. Ingraham, Local denaturation of DNA by shearing forces and by heat, *J. Mol. Biol.*, 6, 230-243, 1963.
- Hershey, A. D., *see also* Burgi, E.
- Ingraham, L., *see* Hershey, A. D.
- Mosig, G., Coordinate variation in density and recombination potential in T4 phage particles produced at different times after infection, *Genetics*, 48, 1195-1200, 1963.

PERSONNEL

Year Ended June 30, 1963

- Bocskay, Elizabeth M. (Mrs.), Chief Clerk
 Buchanan, Jennie S. (Mrs.), Curator of
 Drosophila Stocks
 Burgi, Elizabeth, Associate in Microbiology
 Caldarelli, Donald, Maintenance Man
 Carhart, Anne K. (Mrs.), Research Assistant
 Carley, Catherine, Switchboard Operator and
 Computer
 Fisher, Agnes C., Secretary to Director;
 Editor
 Frankel, Fred R., Associate in Research
 Gay, Helen, Cytogeneticist
 Goldberg, Edward, Postdoctoral Fellow, The
 National Foundation
 Hershey, Alfred D., Director
 Jones, Henry H., Photographer
 Klees, Bertha, Dormitory Cook
 Ledinko, Nada, Postdoctoral Fellow, U. S.
 Public Health Service
 McClintock, Barbara, Cytogeneticist
 McDonald, Joseph L., Janitor
 McDonald, Margaret R., Chemist
 McDonald, William T., Janitor
 Maruyama, Keizo, Research Assistant
 Mosig, Gisela, Postdoctoral Fellow, U. S.
 Public Health Service
 Smith, Guinevere C. (Mrs.), Librarian
 Van Houten, William B., Engineer
 Weingart, Eleanor Ann, Research Assistant
 White, Harry S., Superintendent of Buildings
 and Grounds; Chief Mechanic
 Wilson, Carole E. (Mrs.), Technical Assistant
- Temporary and Part-Time*
- Burgess, Donna L., Library Assistant
 Carroll, Ann C., Library Assistant
 Champney, William Scott, Research Assistant
 Gillies, Gloria (Mrs.), Research Assistant
 Ingraham, Laura J. (Mrs.), Research Assistant
 Kurshan, Jane, Research Assistant
 Lutjen, Barbara A., Switchboard Operator;
 Typist
 Lutjen, George P., Jr., Maintenance Man
 Sepe, Domenico, Maintenance Man
 Sparvoli, Elio, Fellow, Italian National Re-
 search Council
 Van Houten, Susan M. (Mrs.), Dormitory
 Housekeeper
 Wyckoff, Marjory (Mrs.), Switchboard
 Operator

Cytogenetics Laboratory of the Carnegie Institution

University of Michigan, Ann Arbor

Helen Gay

Contents

Chromosome Structure and Function

Introduction	503
Analysis of the progress of spermatogenesis in <i>Drosophila</i>	504
Histone transition during <i>Drosophila spermiogenesis</i>	505
H ³ -Thymidine incorporation in bands of the giant chromosomes of the <i>Drosophila</i> salivary gland	507
Continuation of studies of microsporogenesis in <i>Tradescantia paludosa</i>	510

CHROMOSOME STRUCTURE AND FUNCTION

INTRODUCTION

It becomes apparent, as elucidation of genetic systems proceeds at the molecular level, that the functional attributes of a gene reflect its underlying structural organization. That is, a particular molecular configuration or the particular association of a macromolecule with others determines the initiation of a specific metabolic sequence in a cell. Biochemical analyses have shown, in addition, that many complicated interactions of genes and gene products are necessary to produce the phenotype.

Although the cytogeneticist and cytochemist studying chromosome structure and organization in higher organisms cannot yet make use of the precise analytical tools of the molecular biologists and biochemists to obtain results in precise chemical terms, their approach to an understanding of the chromosome must include a consideration of both its structural and its functional aspects. Therefore, the investigations on chromosomes of higher organisms to be undertaken in the future will require probings into the realm of chromosome behavior in a differentiating cell, analysis of the chemical constitution of chromosomes as special functions are performed, and observations on the fine structure of chromosomes during somatic and meiotic mitoses. Superficially, these different types of studies may seem to lead in many directions, but the essential focus of attention remains the chromosome—its structure and function.

There are at present two major hypotheses concerning chromosome structure. The first states that a chromosome is multistranded, being made up of fibrils 100 Å, or thereabouts, in diameter. The observational evidence for this hypothesis comes from light and electron microscopy. It is recognized that the chromatid is the functional unit and that

some integrating mechanism must exist to enable numerous fibrils to act in concert. It is not considered important whether the number of strands is four or sixty-four, since the basic problem of a unifying mechanism must be faced as soon as the number is greater than two. The other major hypothesis, that the chromosome is single-stranded, states that the chromatid contains one linear array of DNA molecules capable of tremendous extension or contraction by folding or unfolding. This interpretation attempts to correlate functional and structural unity of the chromatid. The two divergent points of view, represented in these alternative hypotheses, must be reconciled by the cytogeneticist.

The present report, the first by the author as a sole contributor, follows in many ways the broad general pattern set in the sections of previous annual reports of the Department of Genetics entitled "Organization of the Chromosome," by Berwind P. Kaufmann and co-workers. Some of the work reported below was initiated in 1962 at the Cold Spring Harbor Laboratories in collaboration with members of Dr. Kaufmann's group and has been continued at the Cytogenetics Laboratory of Carnegie Institution of Washington in the zoology department at the University of Michigan, Ann Arbor. The research program has been greatly facilitated and has proceeded with a minimum of interruption as the result of the excellent facilities in the Natural Sciences Building made available to the Institution by Dr. Dugald E. S. Brown, chairman of the department of zoology. Newly furnished and remodeled laboratories, adjacent to the quarters of Dr. Kaufmann and his research group, permit continued close cooperation on problems of mutual interest. Studies of histone transition in *Drosophila* spermatogenesis, an extension of the work reported in *Year Book 61*, were completed this winter

in collaboration with Drs. C. C. Das and B. P. Kaufmann. Part of the work on the progress of spermatogenesis in *Drosophila* to be described below was done in collaboration with Miss Anne Weingart during the summer of 1962 in Cold Spring Harbor while she was employed by Dr. Kaufmann under USPHS grant RG 149. For completing the analysis of the slides of this experiment we are grateful to Dr. C. C. Das.

Mr. Keizo Maruyama, who served as research assistant in the Cytogenetics Laboratory under Carnegie Institution sponsorship during the past year, continued his electron microscope studies of *Tradescantia* microsporogenesis and post-meiotic differentiation, utilizing the new RCA EMU-3 G microscope provided under NSF grant GB-290 to Dr. B. P. Kaufmann. Work on several unfinished problems was terminated when Mr. Maruyama returned to Japan in June 1963 to complete degree requirements at the University of Kyoto. Dr. Elio Sparvoli, who began his Italian National Research Council fellowship work in Cold Spring Harbor in July 1962 under the sponsorship of the Institution, is currently working on problems of electron microscopy of chromosomes. He is supported by Dr. Kaufmann but making his base of operations in the Cytogenetics Laboratory. His interest in studies of the ultrastructure of plant chromosomes will be directed to analysis of the nuclear changes occurring during formation of the gametophyte within the microspore of *Tradescantia*, a key problem in our studies of developmental changes in the closed system afforded by the microspore. Mr. Maruyama, who began the study of *Tradescantia* microsporogenesis, described some of the cytoplasmic changes in *Year Book 61*; others will be reported below. Mrs. Ingeborg Epstein, who became part-time research assistant in June 1963 when Mr. Maruyama returned to Japan, will join in studies of the ultrastructure of the giant dipteran salivary gland chromosomes.

ANALYSIS OF THE PROGRESS OF SPERMATOGENESIS IN *Drosophila*

Many inferences about basic chromosome structure have been drawn from studies of the various types of lesions and breaks produced by ionizing radiations. In recent years much emphasis in this field has centered on efforts to define the stage of mitosis or meiosis at which the chromosomes are most susceptible to irradiation damage. This type of study has been pursued with the thought that some structural component of the chromosome might be responsible for its increased sensitivity. In fact, it had been suggested that in *Drosophila* the chromosomes of the mature spermatozoa are more resistant to radiation than those of the spermatid because they are "protected" by protamine, a basic protein assumed to be combined with DNA at this stage. In preparation for a discussion of radiosensitivity at an international symposium held in Leiden, Holland, last summer, it was decided that cytochemical methods should be employed to demonstrate which types of basic proteins are actually present in *Drosophila* germ cells. Before this problem could be approached, however, it was necessary to determine precisely the most radiation-sensitive stage in the maturation of the sperm.

Available evidence showed that the spermatid in *Drosophila melanogaster* is more sensitive to radiation than most other stages of spermatogenesis. Much of this evidence, however, was based on genetic and cytogenetic experiments using the "brood technique" in which mature sperm are tested at 2-day intervals, and many assumptions are necessary to decide what stage is being treated and how much time is required for a particular type of cell to attain maturity. Since a considerable superstructure of interpretation about susceptibility to radiation rested upon the estimation of time needed for sperm development, it seemed that a more precise time scale might be obtained by labeling certain germ cells with triti-

ated thymidine and making direct cytological radioautographic observations of their progress through spermatogenesis.

Thymidine is built into chromosomes only during the period of synthesis, which as far as spermatogenesis is concerned is limited to the interphase of the gonial division and the spermatocyte. Both larval and adult male *Drosophila melanogaster* were treated with tritiated thymidine for a short period either by feeding for 4 hours or by injecting the isotope into the body cavity. At regular intervals after treatment, usually 24 hours, several males were killed and the testes fixed, sectioned, stained, and then covered with Kodak AR-10 autoradiographic stripping film. The results of the larval treatment, undertaken in collaboration with Miss Weingart, have been published in the symposium volume, *Repair from Genetic Radiation Damage and Differential Radiosensitivity in Germ Cells*.

In general, the results show that the time scale for sperm development previously established by histological studies of larval and pupal testes is essentially correct; i.e., sperm begin to mature $1\frac{1}{2}$ to 2 days before eclosion of the adult, and spermatids first appear in the pupal testis about 4 days before eclosion. However, when an external treatment of 800-roentgen X rays (the maximum dose permissible for survival) was administered to the larva, there appeared to be a 24-hour retardation in the course of spermatogenesis as compared with the unirradiated controls.

Since most radiation studies had been made by treating adult males 3 to 5 days after eclosion, our next question was whether any retardation in the course of spermatogenesis would be effected by irradiation of adult males. We first needed to know whether the course of spermatogenesis in the adult followed the same chronometry as that we had established for the developing testes in the earlier growth stages. Then we needed to determine the effect of administration of an external radiation dose. Our analyses in

which an X-ray dose of 1000 roentgens was used are not based on samples as large as were available in the larval-treatment experiment and, therefore, must be considered preliminary. They suggest, however, that a similar retardation of the course of spermatogenesis is effected by radiation and, more interestingly, that the normal course of spermatogenesis may be somewhat slower in the adult than during development of the larva.

These results, showing a 1-day difference between irradiated and nontreated males in the rate of spermatogenesis in *Drosophila melanogaster*, do not seriously affect the interpretation of results obtained in the analysis of radiosensitivity of relatively long stages. In the pupal testis, for example, the spermatid stage continues for 2 or 3 days. Under these circumstances our observations sustain the conclusion reached by other workers that the spermatid is more sensitive to radiation than the mature sperm. The results of our experiments do raise questions, nevertheless, about the radiosensitivity of stages of shorter duration and about the extent of retardation of spermatogenesis that will be effected by doses of radiation larger than those mentioned above. These parameters are currently being investigated.

HISTONE TRANSITION DURING *Drosophila* SPERMIOGENESIS

Despite the fact that our radioautographic chronometry of *Drosophila* showed some retardation of the process of spermatogenesis due to radiation, we can broadly consider the spermatid the most sensitive stage during sperm maturation. With Drs. C. C. Das and B. P. Kaufmann, we proceeded with a cytochemical analysis of the basic proteins of the maturing male germ cells of *Drosophila melanogaster* to see whether a protein shift occurred at the end of the spermatid stage.

From studies of the development of the spermatozoon in many different types of animals, it is well known that a transition

occurs from a typical somatic lysine-rich histone to an arginine-rich histone at the spermatid stage. This change in the basic nuclear protein is often followed by a further alteration to protamine in the maturing spermatozoon. On the assumption that this kind of change may occur in *Drosophila*, some radiation geneticists have suggested that the nature of the basic protein of the chromosomes of sperm or spermatid might be the factor that modifies radiosensitivity. It was our purpose to describe the pattern of transition of chromosomal proteins in the spermatogenic cycle of *Drosophila melanogaster*, a study that had not been made before.

The testes of larvae, pupae, and adults of the Swedish-b stock of *Drosophila melanogaster* were dissected and fixed in 10 per cent neutral buffered formalin. Spermathecae of adult females, which normally contain functional sperms transmitted by the male during copulation, were also fixed. These tissues were then processed by the usual methods for paraffin embedding and sectioning. The staining procedures for the demonstration of basic proteins consisted mainly of the trichloroacetic acid (TCA)-alkaline-fast-green method of Alfert and Geschwind, which is allegedly specific for histones of the cell nucleus. Bloch and Hew's picric acid-bromophenol blue method, designed to show either singly or collectively TCA-soluble histones or protamines, as well as the basic proteins stained by the Alfert-Geschwind method, was also used. It was attempted to determine the specific nature of the histones by applying deamination or acetylation, which presumably affects primarily the amino groups of lysine, not the guanidine groups of arginine. Thus, failure to stain after deamination or acetylation reveals lysine-rich histones, and persistence of staining after these "blocking" techniques denotes the presence of arginine-rich histones.

When sections of testes of *Drosophila* are treated to block lysine staining, only a small portion of the sperm bundles in the

adult testis (among those showing increased stainability before acetylation or deamination) stain. None of the spermatozoa at earlier stages of spermatogenesis, or nuclei of cells at any other stage of spermatogenesis, reveal comparable stainability. These sperm thus contain a basic protein rich in arginine, in contrast to the lysine-rich histones present in all other types of spermatogenous cells. Spermatozoa in the seminal vesicle of the male and within the spermathecae of the female exhibit a similar staining pattern; that is, they stain intensely with alkaline-fast green, both before and after acetylation or deamination. The picric acid-bromophenol blue procedure revealed a similar staining pattern. This arginine-rich protein present in the nearly mature or mature spermatozoa is a histone rather than a protamine, since it is insoluble in hot trichloroacetic acid. (Alfert and Geschwind state that protamines are leached out of the cell upon hydrolysis in TCA, and our tissues have been so treated.) We can conclude, therefore, that the transition from a lysine-rich to an arginine-rich histone in *Drosophila* spermiogenesis occurs in the final stages of maturation and that no shift to protamine takes place in this organism. We believe that the histone transition accompanies functional maturity, because the sperm are otherwise morphologically indistinguishable from those in slightly earlier stages of development.

The results of our cytochemical studies of basic proteins of chromosomes during spermatogenesis raise serious questions about the validity of the hypothesis that radiosensitivity may be modified by the presence or absence of highly basic proteins. In *Drosophila melanogaster* there appears to be no protamine in the mature sperm. It might be argued that the highly basic arginine-rich histone found in the sperm could function as a radioprotective substance in the same manner as a protamine. However, the transition from lysine-rich to arginine-rich histone does not occur in the spermatid of *Drosophila*,

but takes place only in the final stages of sperm maturation. This does not coincide with the time of shift in radiosensitivity. It would thus appear that modification of the basic protein of the chromosome is not an important factor determining radiosensitivity during spermatogenesis in *Drosophila*.

Our description of the pattern of sequences of chromosomal basic proteins in spermatogenesis in *Drosophila* enables us to consider the significance of these proteins in specifying the nature of the nucleoprotein complexes during cellular differentiation. Recent experimental evidence has brought into sharp focus the extent of involvement of histones in the regulation of cell activity. In some cases, at least, it is the arginine-rich histone or protamine that inhibits DNA from acting as a primer for synthesis of chromosomal RNA. The protein transition during spermiogenesis (whereby arginine-rich histones replace lysine-rich histones) would in these terms be an effective adaptive mechanism for preserving "packaged" genetic information. The release of arginine-rich histones or their replacement by lysine-rich histone, at or somewhat after fertilization, as reported in *Year Book 61*, would be expected to stimulate the release of the messenger RNA's that selectively control the synthetic processes of growth and differentiation of the embryo.

H³-THYMIDINE INCORPORATION IN BANDS OF THE GIANT CHROMOSOMES OF THE *Drosophila* SALIVARY GLAND

A few years ago, with P. Woods and A. Sengün, we published results of experiments in which tritiated thymidine was fed to growing *Drosophila* larvae for various periods of time ranging from 1 hour to several days. These experiments were designed to demonstrate the development of polyteny in the chromosomes. When very young larvae were treated the radioautographs showed only a few silver grains per band across the width of the

fully developed chromosome. If the radioactive precursor was administered to older larvae, the bands were completely covered across the width of the chromosome by silver grains, the amount of label being more or less uniform in all bands.

It has been reported by other workers that in *Drosophila*, as opposed to the sciarids, DNA replicates uniformly along the chromosome and in all bands at once. (In *Rhynchosciara* and *Sciara*, a few bands form DNA "puffs"; i.e., they enlarge and synthesize more DNA than the other bands of the chromosome.) As was reported in *Year Book 59*, our results using the radioactive precursor feeding technique in *Drosophila* agreed with the conclusion that all bands synthesized DNA at the same time. The feeding technique, however, makes it practically impossible to administer radioactive nucleic acid precursors to *Drosophila* larvae for relatively short time intervals by a technique which can be termed "pulse" labeling. Within the past few years several reports have shown that salivary glands excised from third-instar *Drosophila* larvae remain metabolically active in a suitable medium for at least an hour. It should be possible, therefore, to treat excised *Drosophila* salivary glands with a pulse of radioactive label for periods of 1 hour or less in order to determine whether synthesis of DNA occurs in all bands of the giant chromosomes simultaneously and whether synthesis of RNA and protein follows the same pattern as that of DNA.

In the past year our experiments along these lines have involved extirpation from *Drosophila melanogaster* third-instar larvae of salivary glands and their immersion in a modified Ringer's solution buffered at pH 6.8 with phosphate or veronal salts and containing either tritiated nucleosides or amino acids. We have indeed found that these radioactive precursors are incorporated into the chromosomes for periods up to 1 hour. We have allowed the glands to remain in the radioactive solutions for 1, 3, 5, 15, 30,

and 60 minutes. After "hot" treatment, some glands are immediately fixed and squashed to spread the chromosomes; others are transferred to a nonradioactive "cold chase" solution before fixation and squashing. The Feulgen reaction was carried out on the squashes of glands treated with tritiated thymidine, and Kodak AR-10 autoradiographic stripping film was then placed over the preparations. Squashes of glands treated with tritiated arginine and tritiated cytidine were stained, after development of the emulsion, with basic fuchsin and toluidine blue, respectively.

We shall mention only briefly our results from experiments using the RNA precursor, H^3 -cytidine, and the basic protein precursor, H^3 -arginine, since the analyses are preliminary, having been made only on chromosomes from glands subjected to the longer periods of treatment. As would be expected, the cytoplasm, nucleolus, and chromosomes in a cell from a gland incubated for 1 hour in H^3 -cytidine (pl. 1, fig. 1) are labeled, indicating thereby the presence of RNA in these cellular structures. Some bands of the chromosomes are more heavily labeled than others; these regions are RNA puffs or active chromosomal regions. We are currently mapping their location along the chromosome. After 1 hour's treatment with tritiated arginine, the chromosomes become more or less uniformly labeled (pl. 1, fig. 2), although it was expected that this radioactive precursor of histone might be localized heavily in the bands to show the location of DNA-histone. Since the specific activity of the tritiated arginine commercially available is much lower than that of the tritiated thymidine we have used, our interpretation of these results must be held in abeyance pending the completion of other experiments. In addition, following the use of RNA and protein precursors, observations of chromosomal labeling are sometimes complicated by the presence of silver grains in the overlying and adjacent cytoplasm which also incorporated the precursor.

This study will accordingly necessitate a more lengthy microscopic analysis than has been possible to date. It is also apparent, as will be shown in our discussion of the results obtained with tritiated thymidine below, that brief pulse labeling can be achieved in *Drosophila* and that it gives more significant information than longer labeling. Our results thus clearly indicate that the first step in total analysis of the sequence of syntheses of chromosomal nucleic acids and proteins should be the study of the pattern of timing of DNA synthesis.

Our study of radioautographs of chromosomes from glands treated with tritiated thymidine for the longer time intervals, for example, 0.5 or 1 hour, shows that not all cells have incorporated the radioactive precursor. This finding is not unexpected, since we know that the chromosomes of all cells of a salivary gland do not replicate at the same time. In cells in which the chromosomes are labeled, however, they are so heavily covered with silver grains that the underlying chromosome can scarcely be seen. With the short time intervals of administration of the precursor, 3 to 5 minutes followed by "chase," or 10 to 15 minutes without "chase," we found a significant result. Within a single nucleus, not all parts of the chromosomes are uniformly labeled; some groups of bands are heavily labeled, others lightly labeled, and still others are completely devoid of silver grains (pl. 1, fig. 3). Often the chromocenter is heavily labeled. In well spread chromosomes, it can readily be seen that an individual band is labeled but one immediately adjacent to it is not. We were able to note in several chromosomes that, although the two homologues were not synapsed for an appreciable distance, the same bands in both homologues were either labeled or unlabeled (pl. 1, figs. 3 and 3a), indicating that the incorporation is a specific function of the locus and not a random event.

In addition to making certain that unbound radioactive thymidine was eliminated from the cells by the acid hydrolysis

of the Feulgen reaction, before stripping film was applied, we also checked the specificity of incorporation of the precursor into DNA by digesting several sample preparations with deoxyribonuclease. Digestion with this enzyme wiped out all evidence of radioactivity from the chromosomes. We are certain, therefore, that the radioactivity resides in the DNA and is not an artifact of the incubation technique.

Identification of specific chromosome bands in many of our early experiments was complicated by the fact that characteristic regions were often too heavily labeled and the band pattern obscured. Recently, with a carefully timed series of exposures to H^3 -thymidine, we have achieved the proper amount of incorporation to give lightly labeled chromosomes that can be analyzed band for band. In several instances we have been able to analyze the tip of the X chromosome. Among the examples studied to date from several different larvae, no incorporation of H^3 -thymidine was seen in the "bulb" of the X (from 2A to 3A) (see pl. 1, figs. 4-6). In section 1 of the chromosome, in one instance only 1F was labeled (fig. 6); in the others, two or three other bands were also labeled (figs. 4 and 5). On the proximal side of the "bulb," 3C,D was always heavily labeled and 3A often showed a moderate amount of radioactivity. We can cite an example of the type of incorporation observed at the base of the X chromosome (see fig. 6): 20C,D is heavily labeled, but 20A,B and 19F were not; 19D,E was labeled, and 19B,C was not; 19A was labeled, as were 18A-C, 17A, and 16A, but the intervening bands were unlabeled. This preliminary analysis leads us to believe that a much more precise analysis of incorporation of H^3 -thymidine into salivary gland chromosomes must be undertaken. It suggests that not all bands along the chromosome are replicating DNA at the same time. This type of asynchrony has been reported for hetero-

chromatin of somatic and meiotic chromosomes. If the asynchrony of incorporation of H^3 -thymidine we have observed in salivary gland chromosomes is due to late synthesis by heterochromatin, the centers for initiation of replication on these chromosomes are numerous. We obviously cannot determine without double labeling experiments whether we are observing the beginning or end of DNA synthesis; these results, however, do lead to the conclusion that the chromosomal strand is not one continuous DNA molecule.

A recent analysis by Kaufmann has shown a highly suggestive correlation between the regions that have been identified as intercalary heterochromatin (either by high breakage frequency, as described in *Year Books* 38, 43, 44, 45, or by ectopic pairing, also reported in *Year Books* 43, 46, and 47) and those that manifest puffing as described by Becker and independently analyzed in our laboratory. The fact that DNA in the bulb of the X chromosome did not replicate when short pulse labeling was administered suggests the possibility that this "puff" may be involved in some other kind of synthesis (perhaps RNA information transfer). The probable existence of an operational unit is thus suggested in which intercalary heterochromatic materials serve as controlling elements.

Our program for the future will involve a comparison of intercalary heterochromatin and bands showing asynchronous incorporation of H^3 -thymidine. If there is a correspondence, as the preliminary study suggests, we may have found a new criterion for identifying intercalary heterochromatic regions. Since the observed incorporation may be related in some way to the so-called RNA puffing, we shall have to consider possible modification of the pattern due to development of the gland, for earlier experimental evidence has shown that puffs increase or diminish in size from stage to stage during larval growth.

CONTINUATION OF STUDIES OF
MICROSPOROGENESIS IN
Tradescantia paludosa

During the past year the behavior of cell membranes throughout the several successive and different types of cell divisions—premeiotic mitoses, meiotic mitoses, and the microspore mitoses—have been studied by Mr. Maruyama with the electron microscope. It appears that during mitosis the cisternal elements are flattened sacs, whereas during meiosis they disintegrate into small vesicles, some of which swell to form vacuoles. All these elements of the cytoplasmic membrane system appear to take part in the construction of the new nuclear membrane at telophase. Some electron micrographs suggest that the cell wall is also formed by fusion of cisternal elements in which wall substance has accumulated. This last point must be examined further, since other investigators have recently demon-

strated that the vesicles forming the cell plate are released from Golgi bodies.

The electron micrographs have demonstrated that the chromatin material or chromosomes of the vegetative and generative nucleus, as they differentiate, become, respectively, amoeboid, and condensed and crescent shaped. Nevertheless, they fail to demonstrate clear structural subunits of the chromosome because they are so homogeneous. It is expected that the usual osmium fixation, which is excellent for cytoplasmic detail, will have to be modified in order to pursue this aspect of the problem. Cytochemical investigation of the basic protein content of generative and vegetative nuclei by the alkaline-fast-green method of Alfert and Geschwind has been initiated. We hope to trace changes in DNA (as reported last year), RNA, and basic proteins within these two nuclei as they become differentiated and to correlate our findings with changes in fine structure of the chromosomes.

Fig. 1. Incubation for 1 hour in H^3 -cytidine. Heavy label from incorporation of H^3 -cytidine into RNA of the nucleolus at *n*, in the chromosomal "puffs" at arrows, and lighter label in the rest of the chromosomes. In squash preparations the cytoplasm is dispersed, but light label can be seen in the cytoplasmic material at the right of the figure.

Fig. 2. Incubation for 1 hour in H^3 -arginine. Silver grains occur over all parts of the chromosomes.

Fig. 3. Incubation for 10 minutes in H^3 -thymidine. Note the black areas over parts of the chromosomes, caused by a heavy concentration of silver grains in some chromosomal regions, and little or no label in other parts of the chromosomes. At arrow is a region of asynapsis.

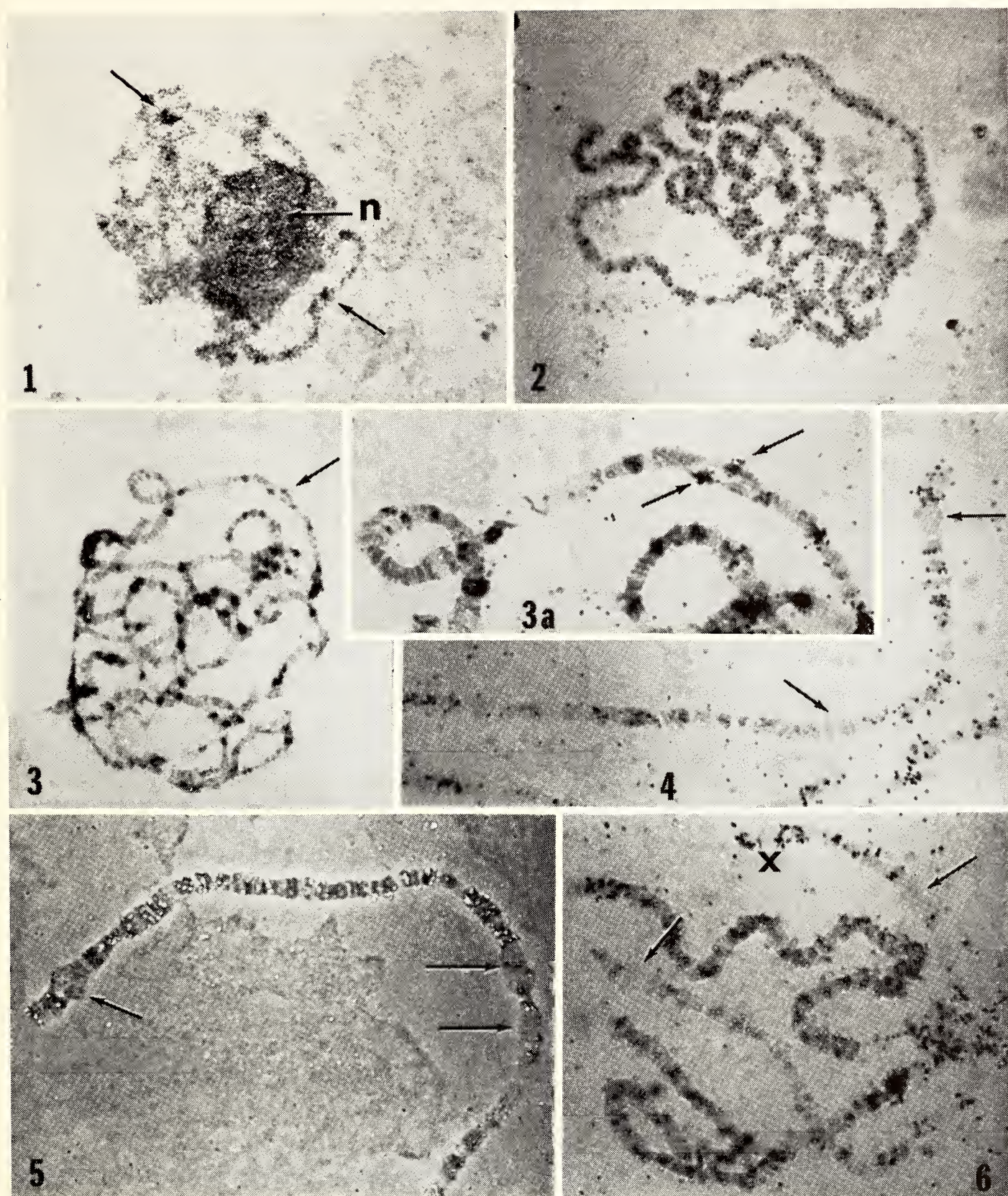
Fig. 3a. Enlargement of upper chromosome of figure 3, showing region of asynapsis. At arrows the same band in both homologues is heavily labeled, whereas adjacent bands are unlabeled.

Fig. 4. Radioautograph of X chromosome

from a gland of a female, incubated for 4 minutes in H^3 -thymidine. The arrow at upper right indicates the bulb of the X (swollen part) devoid of silver grains, whereas band 1F is heavily labeled and a few bands at the extreme tip are lightly labeled.

Fig. 5. Radioautographs of X chromosome from a gland of a female incubated for 4 minutes in H^3 -thymidine. The silver grains appear white in this photograph because they are slightly out of focus in order to focus on the chromosome. The arrow at the left points to the bulb of the X chromosome, which is unlabeled although bands both proximal and distal thereto are labeled. The two arrows at right indicate that the swollen parts on either side of 11A are unlabeled although 11A is labeled.

Fig. 6. Radioautograph of an X chromosome from gland of a male larva, incubated for 3 minutes in H^3 -thymidine. The arrow at left indicates the unlabeled bulb of the X chromosome at the distal end, and X indicates the proximal end. Arrow at right shows unlabeled regions in proximal part of chromosome.



Radioautographs of squashes of cells of third instar *Drosophila melanogaster* salivary glands which were incubated in a modified *Drosophila* Ringer's solution, buffered with phosphate salts at pH 6.8 and containing radioactive nucleosides or amino acids.

Bibliography

July 1, 1962 – June 30, 1963

PUBLICATIONS OF THE INSTITUTION

Year Book 61, 1961–1962. Octavo, xi + 112 + 526 pages, 23 plates, 184 figures. December 10, 1962.

601. Second printing. Ralph Elmer Wilson. *General Catalogue of Stellar Radial Velocities*. Papers of the Mount Wilson Observatory, volume viii. Quarto, x + 344 pages. February 1963.

607. Third printing. Richard B. Roberts, Philip H. Abelson, Dean B. Cowie, Ellis T. Bolton, and Roy J. Britten. *Studies of Biosynthesis in Escherichia coli*. Octavo, xiv + 521 pages, 116 figures. February 1963.

618. Second printing. Allan Sandage. *The Hubble Atlas of Galaxies*. Folio, viii + 32 pages, 50 plates. 1962.

623. Malcolm A. Nobs. *Experimental Studies on Species Relationships in Ceanothus*. Octavo, vii + 94 pages, 119 figures, 15 tables. May 1963.

Drosophila Guide: Introduction to the Genetics and Cytology of Drosophila melanogaster. Seventh edition, second printing. M. Demerec and B. P. Kaufmann, in collaboration with Jennie S. Buchanan (curator), Agnes C. Fisher (editor), and Henry H. Jones (photographer). Octavo, iii + 47 pages, 14 figures. 1962.

Notes from a Ceramic Laboratory

1. *Maya Blue: Alternative Hypotheses*. Anna O. Shepard and Hans B. Gottlieb. Octavo, vi + 18 pages, frontispiece. July 1962.
2. *Beginnings of Ceramic Industrialization: An Example from the Oaxaca Valley*. Anna O. Shepard. Octavo, iv + 24 pages, frontispiece, 2 figures. April 1963.
3. *Imitation Jade Ornaments from Dzibilchaltun, Yucatan*. Anna O. Shepard and E. W. Andrews. Octavo, ii + 13 pages, 2 figures. June 1963.

PUBLICATIONS BY THE PRESIDENT OF THE INSTITUTION

Caryl P. Haskins

Report of the President. *Carnegie Institution of Washington Year Book 61*, pages 1–112. Carnegie Institution of Washington, Washington, D. C. December 10, 1962.

Abstract A4372, *Sociological Abstracts*, volume 11, number 1, pages 57–58, January 1963. (This is an abstract of excerpts from the Report of the President in *Carnegie Institution of Washington Year Book 58*, 1959, reprinted, under the title Society and scientific research, in *Bulletin of the Atomic Scientists*, volume 16, number 5, pages 145–150, May 1960.)

How guard our diversity in science? *Science*, volume 140, number 3563, page 141, April 12, 1963.

(With Richard E. Hewitt, Lovie W. Word, and Edna F. Haskins) Electrophoretic analysis of muscle proteins in several groups of poeciliid fishes especially the genus *Mollienesia*, *Copeia*, number 2, pages 296–303, June 14, 1963.

PUBLICATIONS BY THE EXECUTIVE OFFICER OF THE INSTITUTION

Edward A. Ackerman

Public policy issues for the professional geographer. *Annals of the Association of American Geographers*, volume 52, number 3, pages 292–298. September 1962.

Reasons for research and development on water desalting. *Proceedings of the Conference on Desalination Research organized and convened by the National Academy of Sciences–National Research Council, Woods Hole, Massachusetts, 19 June–14 July, 1961, sponsored by the Office of Saline Water, Department of the Interior, and the National Science Foundation*, pages 5–16. Publication 942, National Academy of Sciences–National Research Council, Washington, D. C., 1963.

Administrative Reports

Report of the Executive Committee

To the Trustees of the Carnegie Institution:

Gentlemen: In accordance with the provisions of the By-Laws, the Executive Committee submits this report to the annual meeting of the Board of Trustees.

During the fiscal year ending June 30, 1963, the Executive Committee held four meetings. Printed accounts of these meetings have been or will be mailed to each Trustee.

The estimate of expenditures for the fiscal year beginning July 1, 1963, has been reviewed by the Executive Committee.

One vacancy exists in the membership of the Board of Trustees, resulting from the death in November 1962 of Henry R. Shepley.

The terms of office of the Chairmen of all Committees of the Board expire on May 10, 1963, as well as the term of office of one member of the Nominating Committee, Richard S. Perkins.

HENRY S. MORGAN, *Chairman*

May 10, 1963

Report of Auditors

LYBRAND, ROSS BROS. & MONTGOMERY

To the Auditing Committee of Carnegie Institution of Washington:

We have examined the statement of assets, liabilities and fund balances of Carnegie Institution of Washington as of June 30, 1963, and the related summary statement of changes in funds for the year then ended and the supporting exhibits and schedules, which have been prepared on the general basis of cash receipts and disbursements and accordingly do not reflect accrued income, accounts payable nor provision for depreciation. Our examination was made in accordance with generally accepted auditing standards, and accordingly included confirmation from the custodian of securities owned at June 30, 1963, and such tests of the accounting records and such other auditing procedures as we considered necessary in the circumstances.

In our opinion, the accompanying financial statements and supporting exhibits and schedules present fairly the assets, liabilities and fund balances of Carnegie Institution of Washington at June 30, 1963, and the changes in funds for the year then ended on a basis consistent with that of the preceding year except for the change, which we approve, in accounting for securities transactions reflected in the Summary of Security Transactions, page 17.

LYBRAND, ROSS BROS. & MONTGOMERY

Washington, D. C.
August 30, 1963

STATEMENT A

ASSETS, LIABILITIES, AND FUND BALANCES

JUNE 30, 1963 AND 1962

	JUNE 30	
	1963	1962
ASSETS		
<u>Operating Funds:</u>		
Cash	\$ 676,027.63	\$ 512,904.28
Advances	17,854.28	17,800.78
Securities - Schedule 2 (See Note)	405,676.04	490,865.29
Prepaid insurance	35,522.66	38,162.66
	<u>\$ 1,135,080.61</u>	<u>\$ 1,059,733.01</u>
<u>Restricted Grants:</u>		
Cash	\$ 205,915.68	\$ 390,903.30
Grants receivable	158,400.00
	<u>\$ 364,315.68</u>	<u>\$ 390,903.30</u>
<u>Endowment, General Reserve, and Special Funds:</u>		
Cash awaiting investment	\$ 22,546.54	\$ 96,925.10
Advances - Building program	5,089.56
<u>Investments:</u>		
Savings account	1,536,031.13	1,477,156.66
Securities - Schedule 2 (See Note)	67,813,365.80	65,973,429.04
	<u>\$69,371,943.47</u>	<u>\$67,552,600.36</u>
<u>Buildings, Land, and Equipment (At Cost)</u>	<u>\$ 6,188,892.69</u>	<u>\$ 6,044,814.64</u>
Total Assets	<u>\$77,060,232.45</u>	<u>\$75,048,051.31</u>

LIABILITIES AND FUNDS		
<u>Operating Funds:</u>		
Income taxes, etc., withheld	\$ 4,959.38	\$ 783.40
Operating Funds Balance - Exhibit 1	1,130,121.23	1,058,949.61
	<u>\$ 1,135,080.61</u>	<u>\$ 1,059,733.01</u>
<u>Restricted Grants - Exhibit 2</u>	364,315.68	390,903.30
<u>Endowment, General Reserve, and Special Funds - Exhibit 3</u>	69,371,943.47	67,552,600.36
<u>Buildings, Land, and Equipment Fund - Exhibit 4</u>	<u>6,188,892.69</u>	<u>6,044,814.64</u>
Total Liabilities and Funds	<u>\$77,060,232.45</u>	<u>\$75,048,051.31</u>

Note: Approximate market value of all securities at June 30, 1963 - \$92,848,794.

STATEMENT B

SUMMARY STATEMENT OF CHANGES IN FUNDS
FOR THE YEAR ENDED JUNE 30, 1963

	Operating Funds (Exhibit 1)	Restricted Grants (Exhibit 2)	Endowment, General Reserve, and Special Funds (Exhibit 3)	Buildings, Land, and Equipment (Exhibit 4)	Total
Balance July 1, 1962	<u>\$1,058,949.61</u>	<u>\$390,903.30</u>	<u>\$67,552,600.36</u>	<u>\$6,044,814.64</u>	<u>\$75,047,267.91</u>
Additions:					
Investment income			\$ 3,427,816.29		\$ 3,427,816.29
Realized capital gain (net) . .	\$ 5,234.62		1,475,015.12		1,480,249.74
Restricted grants		\$361,758.00			361,758.00
Dormitory	5,447.90				5,447.90
Sales of publications	14,536.11				14,536.11
Other income and gifts	1,986.26		23,302.82		25,289.08
Expenditures capitalized:					
Current year				\$ 198,385.02	198,385.02
Prior years				21,880.41	21,880.41
By transfer:					
Budget appropriation -					
July 1, 1962 to					
June 30, 1963	3,116,993.00		(3,116,993.00)		
Harkavy Fund - Income . .	1,000.00		(1,000.00)		
Harry Oscar Wood Fund -					
Income	3,000.00		(3,000.00)		
U. S. Public Health Ser-					
vice FF 280	606.00	(606.00)			
Income credits	(26,866.52)		26,866.52		
	<u>\$3,121,937.37</u>	<u>\$361,152.00</u>	<u>\$ 1,832,007.75</u>	<u>\$ 220,265.43</u>	<u>\$ 5,535,362.55</u>
Deductions:					
Expenditures	\$3,050,765.75	\$387,739.62	\$ 12,664.64		\$ 3,451,170.01
Disposition of equipment . . .				\$ 76,187.38	76,187.38
	<u>\$3,050,765.75</u>	<u>\$387,739.62</u>	<u>\$ 12,664.64</u>	<u>\$ 76,187.38</u>	<u>\$ 3,527,357.39</u>
Net change during the year. . . .	\$ 71,171.62	(\$ 26,587.62)	\$ 1,819,343.11	\$ 144,078.05	\$ 2,008,005.16
Balance June 30, 1963	<u>\$1,130,121.23</u>	<u>\$364,315.68</u>	<u>\$69,371,943.47</u>	<u>\$6,188,892.69</u>	<u>\$77,055,273.07</u>

EXHIBIT 1

CHANGES IN OPERATING FUNDS FOR
THE YEAR ENDED JUNE 30, 1963

Balance July 1, 1962 \$1,058,949.61

Additions - Statement B:

Realized capital gains, net	\$ 5,234.62	
Dormitory	5,447.90	
Sales of publications	14,536.11	
Other income	1,986.26	
Transfers:		
General Reserve Fund - Budget Appropriations July 1, 1962 to June 30, 1963 .	3,116,993.00	
Harkavy Fund - Income	1,000.00	
Harry Oscar Wood Fund - Income	3,000.00	
U. S. Public Health Service FF 280	606.00	
Income Credits	(26,866.52)	3,121,937.37

Total available for expenditure \$4,180,886.98

Expenditures:

Salaries	\$1,632,146.19
Equipment	197,196.37
Laboratory	232,221.64
Buildings - fuel, lights, etc.	136,000.49
Shop	16,096.02
Travel	80,815.96
Dormitory	9,632.89
Operating	89,186.14
Financial Advisory Services	60,446.53
General Publications	57,199.01
Other Publications Expense	29,780.61
Fellowship Program	94,548.54
Awards	7,500.00
Employee Benefits	304,294.75
Insurance, Legal Services, Taxes	85,865.81
Consulting Services	17,834.80

Total expenditures 3,050,765.75

Balance June 30, 1963 \$1,130,121.23

	Balance July 1, 1962	Grants	Expenditures		Transfers	Balance June 30, 1963
			Salary	Other		
<u>Departmental Research Operations:</u>						
<u>Geophysical Laboratory:</u>						
American Geophysical Union	\$ 6,000.00	\$ 6,000.00
Arthur L. Day Library - Gift	\$ 2,427.77	3,015.00	\$ 1,965.27	\$ 3,477.50
National Science Foundation G 42101	200.00	200.00
<u>Department of Terrestrial Magnetism:</u>						
Geological Survey of Finland	17,502.91	12,736.17	4,766.74
National Science Foundation G 5410	1,977.04	1,977.04
National Science Foundation Y/23.1/321	45,494.58	7,605.50	37,889.08
National Science Foundation G 9770	58,130.87	55,830.76	2,300.11
National Science Foundation G 13396	354.59	354.59
National Science Foundation G 14593	960.96	960.96
National Science Foundation G 19568	53,833.70	30,122.02	23,711.68
National Science Foundation G 22227	40,000.00	80,000.00	48,039.31	71,960.69
National Science Foundation G 23929	12,500.00	6,000.00	6,500.00
National Science Foundation GP 285	120,000.00	42,626.43	77,373.57
National Science Foundation GP 1006	58,400.00	22,839.82	35,560.18
<u>Department of Embryology:</u>						
U. S. Public Health Service FF 280	2,501.83	1,895.83	\$606.00
National Science Foundation GB 304	4,800.00	492.64	4,307.36
<u>Mount Wilson Observatory:</u>						
Anonymous	12,000.00	2,500.00	14,500.00
<u>Research Projects, Fellowships, etc.:</u>						
<u>Genetics Research Unit:</u>						
The National Foundation	164.58	1,250.00	863.55	551.03
U. S. Public Health Service RG 149	3,354.39	3,093.00	3,175.00	3,272.39
U. S. Public Health Service C 2158	3,470.02	20,000.00	8,133.33	12,251.71	3,084.98
U. S. Public Health Service GPD 12095.	5.00	5.00
<u>Carnegie Corporation of New York:</u>						
Natural Science Fellowships C 83	133,725.06	107,796.60	25,928.46
Natural Science Fellowships C 85	50,000.00	10,498.20	39,501.80
National Physical Laboratory	15,000.00	2,097.50	12,902.50
Total	\$390,903.30	\$361,758.00	\$17,308.33	\$370,431.29	\$606.00	\$364,315.68

EXHIBIT 3

CHANGES IN ENDOWMENT, GENERAL RESERVE, AND SPECIAL FUNDS
FOR THE YEAR ENDED JUNE 30, 1963

	Balance July 1, 1962	Investment Income	Realized Capital Gain, net	Other Income and Gifts	Appropriations	Transfers	Expenditures	Balance June 30, 1963
<u>Endowment Funds:</u>								
Endowment Fund	\$56,317,514.51	\$1,244,966.64	\$57,562,481.15
Capital Reserve Fund	5,276,301.63	116,670.72	5,392,972.35
<u>General Reserve Fund:</u>								
Unappropriated	1,940,272.04	\$3,427,816.29	97,240.73	\$23,302.82	(\$3,338,378.00)	2,150,253.88
<u>Appropriated:</u>								
Budget (1962-1963)	3,116,993.00	(3,116,993.00)
Budget (1963-1964)	3,338,378.00	3,338,378.00
Building Program	28,883.31	\$12,564.64	16,318.67
<u>Special Funds:</u>								
Bickel Fund	22,859.56	449.97	\$ 1,040.67	24,350.20
Colburn Fund	178,621.43	3,961.58	182,583.01
George E. Hale Relief Fund	8,525.64	157.94	490.31	9,173.89
Harkavy Fund	7,279.95	142.49	7,422.44
Harkavy Fund - Income	1,923.17	21.86	(619.92)	1,325.11
Harriet H. Mayor Relief Fund	10,550.35	219.34	100.00	10,669.69
Special Purpose Funds	93,233.73	1,824.15	4,218.88	99,276.76
Teeple Fund	15,820.24	350.49	16,170.73
van Gelder Fund	2,027.24	42.69	2,069.93
Woloff Fund	38,927.40	765.94	1,771.43	41,464.77
Harry Oscar Wood Fund - Bequest	477,138.80	7,838.54	3,865.44	488,842.78
Harry Oscar Wood Fund - Income	15,728.36	362.04	12,099.71	28,190.11
Total	\$67,552,600.36	\$3,427,816.29	\$1,475,015.12	\$23,302.82	(\$3,116,993.00)	\$22,866.52	\$12,664.64	\$69,371,943.47

CHANGES IN BUILDINGS, LAND, AND EQUIPMENT FUND
FOR THE YEAR ENDED JUNE 30, 1963

	Balance July 1, 1962	Expenditures (Note)	Deductions	Balance June 30, 1963	Classification of June 30, 1963 Balance		
					Buildings and Land	Library	Equipment
Departments of Research:							
Department of Plant Biology							
Stanford, California	\$ 186,229.83	\$ 13,608.66	\$ 199,838.49	\$ 75,519.58	\$ 33,530.19	\$ 90,788.72
Geophysical Laboratory							
Washington, D. C.	610,508.13	64,584.62	\$ 3,015.00	672,077.75	170,383.79	86,295.79	415,398.17
Mount Wilson Observatory							
Pasadena, California	1,737,998.51	32,400.06	419.34	1,769,979.23	314,064.44	95,980.24	1,359,934.55
Department of Terrestrial Magnetism							
Washington, D. C.	1,118,843.73	21,800.45	2,922.44	1,137,721.74	401,081.29	54,000.66	682,639.79
Department of Embryology							
Baltimore, Maryland	183,152.96	31,678.35	91.05	214,740.26	16,218.80	198,521.46
Total Departments of Research . .	\$ 3,836,733.16	\$ 164,072.14	\$ 6,447.83	\$ 3,994,357.47	\$ 961,049.10	\$ 286,025.68	\$ 2,747,282.69
Genetics Research Units							
Long Island, New York and							
Ann Arbor, Michigan	1,281,995.58	35,243.18	65,406.65	1,251,832.11	996,391.01	96,923.00	158,518.10
Office of Administration							
Washington, D. C.	926,085.90	20,950.11	4,332.90	942,703.11	846,029.54	96,673.57
Total	\$ 6,044,814.64	\$ 220,265.43	\$ 76,187.38	\$ 6,188,892.69	\$ 2,803,469.65	\$ 382,948.68	\$ 3,002,474.36
Note: Current Expenditures for Equipment:							
Restricted Grants	\$ 10,182.37						
Operating Funds	188,202.65						
Expenditures Capitalized:							
Prior Years	4,732.11						
Current Year	17,148.30						
Total	\$ 220,265.43						

SCHEDULE 1

BUDGET SUMMARY OF OPERATING FUNDS FOR THE YEAR ENDED JUNE 30, 1963

	Disposition of Total Appropriations							
	Unexpended Appropriations July 1, 1962	Budget Appropriation for the fiscal year ended June 30, 1963	Continuing Appropriations	Allotments	Total Appropriations	Total Expenditures	Unexpended Appropriations	
							Transferred to Unallocated Appropriations Fund	Reserved for Liabilities and Commitments and Unallocated Appropriations Fund
Departmental Research Operations:								
Department of Plant Biology . . .	\$ 7,203.89	\$ 137,100.00	\$ 8,845.91	\$ 153,149.80	\$ 138,135.15	\$ 8,112.26	\$ 6,902.39
Geophysical Laboratory	32,851.87	387,900.00	105,527.14	526,279.01	472,811.40	-12,660.12	40,807.49
Mount Wilson Observatory	14,898.71	409,350.00	\$ 1,639.35	5,000.00	430,888.06	406,454.69	14,167.15	10,266.22
Department of Terrestrial Magnetism	57,230.35	519,300.00	30,669.73	607,200.08	526,782.74	30,002.60	50,414.74
Department of Embryology	11,193.77	348,150.00	19,975.00	379,318.77	338,577.32	20,157.42	20,584.03
Total Departmental Research Operations	\$ 123,378.59	\$ 1,801,800.00	\$ 1,639.35	\$ 170,017.78	\$ 2,096,835.72	\$ 1,882,761.30	\$ 85,099.55	\$ 128,974.87
Non-departmental Research Operations:								
Genetics Research Units	\$ 12,714.34	\$ 135,159.00	\$ 5,447.90	\$ 113,484.97	\$ 266,806.21	\$ 204,273.52	\$ 5,964.33	\$ 56,568.36
Fellowship Program	41,800.04	102,500.00	101,200.00	245,500.04	94,548.54	150,951.50
Research Projects, etc.	53,493.46	38,400.00	952.91	11,893.36	104,739.73	49,307.62	9,987.64	45,444.47
Total Non-departmental Research Operations	\$ 108,007.84	\$ 276,059.00	\$ 6,400.81	\$ 226,578.33	\$ 617,045.98	\$ 348,129.68	\$ 15,951.97	\$ 252,964.33
Administration	11,999.71	266,184.00	33,712.12	311,895.83	310,739.58	1,156.25
Contingent Operating Fund	147,438.58	252,950.00	(345,242.99)	55,145.59	55,145.59
Employee Benefits	219,803.17	311,500.00	5,234.62	12,154.62	548,692.41	304,294.75	22,224.66	222,173.00
Financial Advisory Services	72,000.00	2,073.42	74,073.42	60,446.53	13,626.89
General Publications	40,730.06	30,000.00	14,536.11	85,266.17	58,528.10	26,738.07
Income Credit to Special Funds	35,000.00	(35,000.00)
Insurance, Legal Services, Taxes . .	145.55	71,500.00	17,840.20	89,485.75	85,865.81	3,619.94
Total	\$ 651,503.50	\$ 3,116,993.00	\$ 27,810.89	\$ 82,133.48	\$ 3,878,440.87	\$ 3,050,765.75	\$ 123,276.18	\$ 704,398.94
Unallocated Appropriations Fund . .	407,446.11	(105,000.00)	302,446.11	(123,276.18)	425,722.29
Total	\$ 1,058,949.61	\$ 3,116,993.00	\$ 27,810.89	(\$ 22,866.52)	\$ 4,180,886.98	\$ 3,050,765.75	\$ 1,130,121.23

SCHEDULE 2

SECURITIES, JUNE 30, 1963
AND INCOME RECEIVED DURING THE YEAR

			Per Cent of Total Investments		
		Approximate Market Value	Book Value	Approximate Market Value	Income Received
	<u>Book Value</u>				
Bonds:					
Federal Agencies and United States Government	\$ 4,081,924.57	\$ 4,164,619	5.98	4.49	\$ 221,861.76
Foreign and International Bank .	4,019,687.93	4,044,733	5.89	4.36	120,441.32
Public Utility	8,937,810.15	8,642,345	13.10	9.31	405,722.70
Communication	3,753,573.35	3,512,375	5.51	3.78	146,253.94
Railroad	368,162.39	318,690	.54	.34	16,088.97
Railroad Equipment Trust	1,481.25
Industrial and Miscellaneous . .	<u>16,590,250.94</u>	<u>16,777,938</u>	<u>24.32</u>	<u>18.07</u>	<u>678,499.16</u>
Total Bonds	<u>\$37,751,409.33</u>	<u>\$37,460,700</u>	<u>55.34</u>	<u>40.35</u>	<u>\$1,590,349.10 (a)</u>
Stocks:					
Preferred	\$ 1,539,877.30	\$ 1,541,800	2.26	1.66	\$ 70,900.00
Common	<u>28,927,755.21</u>	<u>53,846,294</u>	<u>42.40</u>	<u>57.99</u>	<u>1,529,236.06</u>
Total Stocks	<u>\$30,467,632.51</u>	<u>\$55,388,094</u>	<u>44.66</u>	<u>59.65</u>	<u>\$1,600,136.06</u>
Total	<u><u>\$68,219,041.84</u></u>	<u><u>\$92,848,794</u></u>	<u><u>100.00</u></u>	<u><u>100.00</u></u>	<u><u>\$3,190,485.16</u></u>

(a) After deducting bond premium amortization of \$14,120.63

SCHEDULE OF SECURITIES

Principal Amount	Description	Maturity	Book Value	Approximate Market Value
Federal Agencies and United States Government Bonds				
\$ 400,000	Federal Farm Loan Consolidated, 4 $\frac{3}{8}$ s	1969	\$ 394,000.00	\$ 406,000
285,000	Federal Farm Loan Consolidated, 4 $\frac{1}{2}$ s	1970	284,330.96	289,275
1,025,000	Federal National Mortgage Association, 4 $\frac{1}{8}$ s	1970	1,015,070.31	1,025,000
465,000	Federal National Mortgage Association, 4 $\frac{1}{8}$ s	1971	465,898.30	465,000
400,000	Federal National Mortgage Association, 4 $\frac{5}{8}$ s	1970	394,500.00	412,000
500,000	Federal National Mortgage Association, 5 $\frac{1}{8}$ s	1972	498,125.00	532,500
780,000	United States of America, Treasury Notes 3 $\frac{3}{8}$ s	1967	780,000.00	780,000
250,000	United States of America, Treasury Notes 5s	1964	250,000.00	254,844
<u>\$4,105,000</u>	Total Federal Agencies and United States Government . . .		<u>\$4,081,924.57</u>	<u>\$4,164,619</u>
Foreign and International Bank Bonds				
\$ 489,000	Aluminum Co. of Canada, Ltd., S.F. Deb. 4 $\frac{1}{2}$ s	1980	\$ 497,021.56	\$ 492,668
150,000	Australia (Commonwealth of) 4 $\frac{1}{2}$ s	1971	147,750.00	151,500
131,000	Australia (Commonwealth of) 5s	1972	131,000.00	134,439
500,000	Australia (Commonwealth of) 5 $\frac{1}{2}$ s	1982	503,012.10	523,125
750,000	Bell Telephone Company of Canada, 1st Mtg. Series "X" 4 $\frac{7}{8}$ s . .	1988	747,300.00	753,750
250,000	British Columbia Power Commission, S.F. Deb. Series "L" 4 $\frac{3}{8}$ s	1987	245,000.00	245,000
125,000	Intl. Bank for Reconstruction & Development, 3s	1976	125,000.00	111,875
125,000	Intl. Bank for Reconstruction & Development, 3 $\frac{3}{8}$ s	1975	123,125.00	116,875
250,000	Intl. Bank for Reconstruction & Development, 4 $\frac{1}{2}$ s	1977	250,000.00	255,625
150,000	Noranda Mines Ltd., S.F. Deb. 4 $\frac{3}{4}$ s	1968	151,049.27	136,313
405,000	Quebec Hydro-Electric Commission, S.F. Deb. 5s	1988	397,912.50	410,063
200,000	Shawinigan Water & Power Co., 1st Mtg. & Collat. Tr. S.F. Series "M" 3s	1971	202,880.00	181,000
500,000	Toronto (Municipality of Metropolitan), S.F. Deb. 5s	1979	498,637.50	532,500
<u>\$4,025,000</u>	Total Foreign and International Bank		<u>\$4,019,687.93</u>	<u>\$4,044,733</u>
Public Utility Bonds				
\$ 125,000	Columbia Gas System, Inc., Series "B" 3s	1975	\$ 126,605.81	\$ 110,625
250,000	Columbia Gas System, Inc., Series "F" 3 $\frac{7}{8}$ s	1981	245,937.50	235,000
237,000	Columbus & Southern Ohio Electric Co., 1st Mtg. 3 $\frac{1}{4}$ s	1970	241,689.93	225,150
300,000	Commonwealth Edison Co., 1st Mtg. Series "R" 3 $\frac{1}{2}$ s	1986	300,605.44	265,500
300,000	Consolidated Edison Co. of N.Y., 1st & Ref. Mtg. Series "L" 3 $\frac{5}{8}$ s	1986	303,069.43	270,750
300,000	Consolidated Edison Co. of N.Y., 1st & Ref. Mtg. Series "N" 5s	1987	301,888.80	320,625
150,000	Consumers Power Co., 1st Mtg. 4s	1986	151,138.86	142,500
143,000	Consumers Power Co., 1st Mtg. 4 $\frac{3}{4}$ s	1987	143,737.01	148,720
300,000	Florida Power Corporation, 1st Mtg. 3 $\frac{7}{8}$ s	1986	301,713.31	279,000
500,000	Illinois Power Co., 1st Mtg. 3 $\frac{3}{4}$ s	1986	497,937.50	461,250
200,000	Minnesota Power & Light Co., 1st Mtg. 3 $\frac{1}{8}$ s	1975	201,956.73	178,000
250,000	Niagara Mohawk Power Corp., Gen. Mtg. 3 $\frac{5}{8}$ s	1986	252,581.50	225,000
400,000	Niagara Mohawk Power Corp., Gen. Mtg. 4 $\frac{7}{8}$ s	1987	402,818.43	424,500
100,000	Ohio Power Co., 1st Mtg. 3 $\frac{1}{4}$ s	1968	101,500.00	96,500
200,000	Pacific Gas & Electric Co., 1st & Ref. Mtg. Series "X" 3 $\frac{1}{8}$ s . .	1984	201,224.94	169,000
300,000	Pacific Gas & Electric Co., 1st & Ref. Mtg. Series "Y" 3 $\frac{3}{8}$ s . .	1987	305,356.89	247,500
250,000	Pacific Gas & Electric Co., 1st & Ref. Mtg. Series "BB" 5s . .	1989	251,591.10	265,000
250,000	Pacific Power & Light Co., 1st Mtg. 4 $\frac{3}{8}$ s	1986	252,513.31	245,000
500,000	Philadelphia Electric Co., 1st & Ref. Mtg. 4 $\frac{5}{8}$ s	1987	500,000.00	517,500
245,000	Potomac Electric Power Co., Deb. 4 $\frac{5}{8}$ s	1982	249,814.44	251,125
200,000	Public Service Co. of Indiana, 1st Mtg. Series "F" 3 $\frac{1}{8}$ s	1975	202,055.75	178,000
400,000	Public Service Co. of Indiana, 1st Mtg. Series "L" 4 $\frac{7}{8}$ s	1987	400,000.00	416,000
500,000	Public Service Electric & Gas Co., 1st & Ref. Mtg. 4 $\frac{7}{8}$ s	1987	503,825.73	520,000
250,000	Southern California Edison Co., 1st & Ref. Mtg. Series "G" 3 $\frac{5}{8}$ s	1981	247,765.00	228,750
250,000	Southern California Edison Co., 1st & Ref. Mtg. Series "H" 4 $\frac{1}{4}$ s	1982	251,406.28	249,375

SCHEDULE OF SECURITIES—Continued

<u>Principal Amount</u>	<u>Description</u>	<u>Maturity</u>	<u>Book Value</u>	<u>Approximate Market Value</u>
Public Utility Bonds—Concluded				
\$ 200,000	Southern California Edison Co., 1st & Ref. Mtg. Series "J" 4 $\frac{7}{8}$ s	1982	\$ 201,672.69	\$ 208,000
500,000	Tennessee Gas Transmission Co., 5s	1982	504,750.00	500,000
254,000	Tennessee Gas Transmission Co., 1st Mtg. Pipe Line 5 $\frac{1}{4}$ s	1977	254,000.00	260,350
500,000	Union Electric Co., 1st Mtg. 3 $\frac{3}{4}$ s	1986	500,085.55	462,500
235,000	Virginia Electric & Power Co., 1st & Ref. Mtg. Series "M" 4 $\frac{1}{8}$ s	1986	238,568.22	229,125
300,000	Washington Water Power Co., 1st Mtg. 4 $\frac{7}{8}$ s	1987	300,000.00	312,000
<u>\$8,889,000</u>	Total Public Utility		<u>\$8,937,810.15</u>	<u>\$8,642,345</u>
Communication Bonds				
\$ 350,000	American Telephone & Telegraph Company, 3 $\frac{1}{4}$ s	1984	\$ 358,453.20	\$ 300,125
800,000	American Telephone & Telegraph Company, Deb. 3 $\frac{7}{8}$ s	1990	817,068.84	752,000
500,000	American Telephone & Telegraph Company, Deb. 4 $\frac{3}{8}$ s	1985	504,552.24	510,625
400,000	Illinois Bell Telephone Co., 1st Mtg. Series "E" 4 $\frac{1}{4}$ s	1988	404,258.72	396,000
200,000	Mountain States Telephone & Telegraph Co., Deb. 3 $\frac{1}{8}$ s	1978	200,700.00	174,500
100,000	New York Telephone Co., Ref. Mtg. Series "E" 3 $\frac{1}{8}$ s	1978	100,690.27	87,500
200,000	Pacific Telephone & Telegraph Co., Deb. 3 $\frac{1}{4}$ s	1978	202,207.30	178,000
300,000	Pacific Telephone & Telegraph Co., Deb. 4 $\frac{3}{8}$ s	1988	305,692.26	303,375
250,000	Southern Bell Telephone & Telegraph Co., Deb. 4s	1983	250,980.94	238,750
300,000	Southern Bell Telephone & Telegraph Co., Deb. 5s	1986	305,219.58	318,000
300,000	Southwestern Bell Telephone Co., Deb. 3 $\frac{1}{8}$ s	1983	303,750.00	253,500
<u>\$3,700,000</u>	Total Communication		<u>\$3,753,573.35</u>	<u>\$3,512,375</u>
Railroad Bonds				
\$ 100,000	Chesapeake & Ohio Railway Co., Gen. Mtg. 4 $\frac{1}{2}$ s	1992	\$ 99,500.00	\$ 99,750
267,000	Fort Worth & Denver Railway Company, 1st Mtg. 4 $\frac{3}{8}$ s Guar.	1982	268,662.39	218,940
<u>\$ 367,000</u>	Total Railroad		<u>\$ 368,162.39</u>	<u>\$ 318,690</u>
Industrial and Miscellaneous Bonds				
\$ 250,000	Aluminum Co. of America, S.F. Deb. 4 $\frac{1}{4}$ s	1982	\$ 250,000.00	\$ 250,938
234,000	Bristol-Myers Co., Deb. 3s	1968	234,248.54	228,150
550,000	C. I. T. Financial Corp., Deb. 4 $\frac{3}{4}$ s	1970	536,937.50	569,250
750,000	Colonial Pipeline Co., Sec. Note 4 $\frac{3}{4}$ s	1990	750,000.00	759,375
400,000	Commercial Credit Co., Notes 3 $\frac{5}{8}$ s	1976	406,074.44	371,000
105,000	Corn Products Co., Sub. Deb. 4 $\frac{5}{8}$ s	1983	109,334.83	110,250
475,000	Crown Zellerbach Corp., Prom. Note 4 $\frac{1}{8}$ s	1981	475,000.00	467,875
675,000	Erie Mining Company, 1st Mtg. Series "B" 4 $\frac{1}{2}$ s	1983	655,344.00	664,875
500,000	Food Machinery & Chemical Corp., S.F. Deb. 3.80s	1981	500,000.00	471,250
311,000	Four Corners Pipe Line Company, Sec. Note 5s	1982	311,000.00	332,770
500,000	General Electric Credit Corp. (N.Y.) 4 $\frac{3}{4}$ s	1987	500,000.00	503,750
500,000	General Electric Credit Corp. (N.Y.) Prom. Note 5s	1975	500,000.00	522,500
200,000	General Motors Acceptance Corp., Deb. 3 $\frac{1}{2}$ s	1972	202,045.54	189,000
480,000	General Motors Acceptance Corp., Deb. 4s	1979	435,037.50	469,800
200,000	General Motors Acceptance Corp., Deb. 5s	1977	195,000.00	212,500
200,000	General Motors Acceptance Corp., Deb. 5s	1981	199,000.00	213,000
150,000	General Portland Cement Co., Conv. Sub. Deb. 5s	1977	154,500.00	164,250
275,000	Goodrich (B.F.) Company, 1st Mtg. 2 $\frac{3}{4}$ s	1965	275,072.49	268,813
750,000	Industrial Acceptance Corp. Ltd., Sec. Note Series "Z" 5 $\frac{1}{4}$ s	1982	750,000.00	750,000

SCHEDULE OF SECURITIES—Continued

Principal Amount	Description	Maturity	Book Value	Approximate Market Value
Industrial and Miscellaneous Bonds—Concluded				
\$ 642,180.22	Instlcorp, Inc., Collat. Tr. Note Series A-16	1991	\$ 620,729.20	\$ 655,024
527,020.80	Instlcorp, Inc., Collat. Tr. Note Series A-19	1991	509,582.57	534,925
281,125.60	Instlcorp, Inc., Collat. Tr. Note Series A-21	1991	271,286.23	286,748
343,791.51	Instlcorp, Inc., Collat. Tr. Note Series A-23	1991	338,222.25	349,807
1,047,972.22	Instlcorp, Inc., Collat. Tr. Note Series A-36	1992	1,005,172.58	1,029,632
400,000	Intl. Harvester Credit Corp., Deb. 4 $\frac{5}{8}$ s	1979	398,000.00	410,000
290,000	Kaiser Aluminum & Chemical Corp., 1st Mtg. 5 $\frac{1}{2}$ s	1987	290,000.00	305,225
236,000	Lorillard (P.) Company, Deb. 3s	1963	236,000.00	235,410
200,000	Montgomery Ward Credit Corp., Deb. 4 $\frac{7}{8}$ s	1980	199,000.00	208,500
95,000	National Dairy Products Corp., Deb. 2 $\frac{3}{4}$ s	1970	95,098.86	86,688
488,000	Phillips Petroleum Company, S.F. Deb. 2 $\frac{3}{4}$ s	1964	488,000.00	483,120
150,000	Quaker Oats Co., Deb. 2 $\frac{5}{8}$ s	1964	148,895.29	148,125
242,000	Scovill Mfg. Co., Deb. 4 $\frac{3}{4}$ s	1982	238,370.00	242,000
525,000	Sears Roebuck Acceptance Corp., Sub. Deb. 4 $\frac{5}{8}$ s	1977	511,505.00	538,125
300,000	Sinclair Oil Corporation, Conv. Sub. Deb. 4 $\frac{3}{8}$ s	1986	315,644.74	309,000
300,000	Superior Oil Company, The (California), Deb. 3 $\frac{3}{4}$ s	1981	300,000.00	284,250
215,000	Talcott (James), Inc., Senior Note 5 $\frac{1}{2}$ s	1966-80	212,850.00	225,750
300,000	Texas Corporation, Deb. 3s	1965	301,088.51	295,500
250,000	Tidewater Oil Company, S.F. Deb. 3 $\frac{1}{2}$ s	1986	250,000.00	217,500
841,217.01	Trailer Train Company, 4 $\frac{7}{8}$ s	1976	841,217.01	855,938
430,000	Tremarco Corporation, 1st Mtg. Series "E" 5s	1983	430,000.00	452,575
400,000	Westinghouse Electric Corp., Deb. 2 $\frac{5}{8}$ s	1971	400,993.86	356,000
250,000	Whirlpool Corporation, S.F. Deb. 3 $\frac{1}{2}$ s	1980	250,000.00	225,000
500,000	Woolworth (F.W.) Co., Prom. Note 5s	1982	500,000.00	523,750
<u>\$16,759,307.36</u>	Total Industrial and Miscellaneous		<u>\$16,590,250.94</u>	<u>\$16,777,938</u>
<u>\$37,845,307.36</u>	Bonds — Funds Invested		<u>\$37,751,409.33</u>	<u>\$37,460,700</u>

Number
of
Shares

Preferred Stocks

1,500	Appalachian Power Co., 4 $\frac{1}{2}$ % Cum. Pref.	\$ 159,000.00	\$ 148,125
1,500	Bethlehem Steel Corporation, 7% Cum. Pref.	183,637.50	234,750
3,800	Carrier Corporation, 4 $\frac{1}{2}$ % Cum. Pref.	197,931.28	188,100
1,900	Consolidated Edison Co. of N.Y., \$5.00 Cum. Pref.	202,815.00	205,200
2,000	Niagara Mohawk Power Corp., 3.60% Cum. Pref.	207,990.00	159,000
1,300	Ohio Power Co., 4 $\frac{1}{2}$ % Cum. Pref.	144,630.02	130,000
3,100	United States Steel Corporation, 7% Cum. Pref.	443,873.50	476,625
<u>15,100</u>	Total Preferred Stocks	<u>\$ 1,539,877.30</u>	<u>\$ 1,541,800</u>

Common Stocks

28,100	Aluminium Ltd.	\$ 825,815.21	\$ 737,625
28,700	American Electric Power Co., Inc.	183,144.44	1,029,613
19,673	American Telephone & Telegraph Company	999,024.37	2,373,056
11,500	Arizona Public Service Co.	432,901.08	345,000
7,000	Armco Steel Corporation	290,041.87	393,750
14,100	Armstrong Cork Company	231,109.31	1,128,000

SCHEDULE OF SECURITIES—Concluded

<u>Number of Shares</u>	<u>Description</u>	<u>Book Value</u>	<u>Approximate Market Value</u>
<u>Common Stocks—Concluded</u>			
10,000	Atchison, Topeka & Santa Fe Railway Co.	\$ 166,235.85	\$ 297,500
11,000	Burlington Industries, Inc.	307,367.34	380,875
6,000	Campbell Soup Company	362,612.33	570,000
12,000	Caterpillar Tractor Co.	97,534.09	517,500
4,800	Christiana Securities Co.	356,143.00	1,065,600
9,800	Coca Cola Company (The)	628,984.09	918,750
18,000	Continental Oil Company, (Del.)	146,960.65	1,102,500
2,500	Corning Glass Works	59,631.83	427,188
10,000	Crown Zellerbach Corp.	545,941.58	501,250
1,500	E. I. du Pont de Nemours & Co.	66,276.95	367,500
11,294	Eastman Kodak Company	127,544.00	1,236,693
9,500	Falconbridge Nickel Mines, Ltd.	550,837.50	528,789
11,474	Farbenfabriken Bayer AG-ADR Par 50 Deutschemark	655,244.34	742,942
12,000	Federated Department Stores, Inc.	582,805.81	594,000
7,403	First National City Bank	348,175.60	757,882
12,000	Florida Power & Light Co.	148,863.69	846,000
29,400	Ford Motor Company	849,086.16	1,532,475
32,000	General Electric Company	735,439.99	2,528,000
33,950	General Motors Corporation	1,257,546.25	2,384,988
2,700	General Reinsurance Corp.	220,697.46	596,700
16,500	Gillette Company	401,418.90	569,250
21,712	Goodyear Tire & Rubber Company	488,401.64	751,778
20,006	Gulf Oil Corporation	154,333.51	897,769
14,000	Household Finance Corp.	659,231.85	782,250
25,000	Ideal Cement Company	568,533.87	615,625
22,000	Illinois Power Co.	589,126.02	838,750
7,100	International Business Machines Corp.	120,760.13	3,097,375
13,800	International Nickel Co. of Canada, Ltd.	379,279.52	848,700
8,500	Kellogg Company	332,482.68	605,625
8,000	Kennecott Copper Corporation	543,784.98	582,000
2,601	Litton Industries, Inc.	156,163.03	193,775
13,000	Mead Corporation	614,427.23	578,500
5,000	Merck & Co.	107,286.55	450,625
5,800	National Cash Register Co.	530,904.80	408,900
20,000	Niagara Mohawk Power Corp.	863,803.67	997,500
2,100	Norfolk & Western Railway Company	217,512.31	252,000
8,600	North American Aviation, Inc.	559,647.34	500,950
9,000	Northwest Bancorporation	231,895.01	430,875
17,000	Ohio Edison Co.	587,855.31	799,000
8,000	Panhandle Eastern Pipe Line Co.	431,553.54	611,000
5,000	Philip Morris Incorporated	493,240.88	396,250
28,350	Philips N.V., Par 25 Guilders	784,874.65	1,279,294
10,300	Pittsburgh Plate Glass Co.	713,847.40	551,051
14,100	Revere Copper & Brass, Inc.	665,214.01	648,600
37,000	Royal Dutch Petroleum Co.	1,354,850.22	1,752,875
12,000	Scott Paper Company	57,173.73	397,500
2,300	Sears, Roebuck and Co.	207,078.03	205,275
3,100	Socony Mobil Oil Company, Inc.	208,828.91	212,738
22,000	Standard Oil Co. (New Jersey)	555,503.23	1,504,250
25,000	Stevens (J.P.) & Co.	707,606.34	837,500
29,704	Texaco, Inc.	276,921.98	2,094,132
7,600	Texas Utilities Co.	104,621.78	399,000
6,000	Travelers Insurance Co.	452,662.70	1,182,000
30,750	Unilever N.V., Par 20 Florin	1,162,805.47	1,426,031
14,000	United Gas Corp.	516,981.45	549,500
14,200	U. S. Plywood Corp.	697,928.16	798,750
21,000	Virginia Electric & Power Co.	253,249.59	895,125
<u>886,517</u>	Total Common Stocks	<u>\$28,927,755.21</u>	<u>\$53,846,294</u>
	Common and Preferred Stocks - Funds Invested	<u>\$30,467,632.51</u>	<u>\$55,388,094</u>
	Aggregate Investments (Bonds and Stocks)	<u>\$68,219,041.84</u>	<u>\$92,848,794</u>

SUMMARY OF SECURITY TRANSACTIONS JULY 1, 1962 TO JUNE 30, 1963

Cash awaiting investment - July 1, 1962 \$ 96,925.10

Sales and Redemptions

	Investment Income	Capital		Book Value
		Gain	Loss	
Bonds	\$ 19,728.75		\$ 166,948.09	\$8,310,028.01
Preferred Stocks			7,847.14	80,000.00
Common Stocks		\$1,864,394.38		1,442,078.77
	\$ 19,728.75	\$1,864,394.38	\$ 174,795.23	\$9,832,106.78
Change in reporting sales from average cost to actual cost basis and to reclassify capital gains .	\$158,727.91		209,349.41	50,621.50
	\$178,456.66	\$1,864,394.38	\$ 384,144.64	\$9,882,728.28
Net Capital Gain - Statement B			1,480,249.74	1,480,249.74
Investment Income	(\$178,456.66)			178,456.66
		\$1,864,394.38	\$1,864,394.38	
Total Sales and Redemptions				11,541,434.68
Income applied to amortization of bond premium				14,120.63
Market value of stock dividend				11,731.54
Cash transferred for investment				9,931.01
Total				\$11,674,142.96

Acquisitions

Bonds	\$7,098,418.70
Common Stocks	4,553,177.72
Total Acquisitions	11,651,596.42
Cash awaiting investment - June 30, 1963	\$ 22,546.54

Abstract of Minutes

of the Sixty-Fifth Meeting of the Board of Trustees

The annual meeting of the Board of Trustees was held in the Board Room of the Administration Building on Friday, May 10, 1963. Mr. Henry, Chairman of the Board, presided.

The following Trustees were in attendance: Amory H. Bradford, Omar N. Bradley, Vannevar Bush, Walter S. Gifford, Carl J. Gilbert, Caryl P. Haskins, Barklie McKee Henry, Alfred L. Loomis, Keith S. McHugh, Margaret Carnegie Miller, Henry S. Morgan, Seeley G. Mudd, William I. Myers, Richard S. Perkins (Secretary pro tem), Elihu Root, Jr., Charles P. Taft, James N. White, and Robert E. Wilson.

The minutes of the Sixty-Fourth Meeting were approved.

The Chairman notified the Trustees of the death of Henry R. Shepley. Mr. Root spoke of the Trustees' high esteem for Mr. Shepley, and of his service to the Institution. Mr. Root proposed the following resolution, which the Trustees adopted unanimously:

Be It Resolved, That the Trustees of the Carnegie Institution of Washington desire to record their deep sense of loss at the death of their distinguished fellow member, Henry R. Shepley.

And Be It Further Resolved, That this resolution be entered on the minutes of the Institution and a copy be sent to Mrs. Shepley.

The annual report of the President was accepted.

The reports of the Executive Committee, the Finance Committee, the Auditor, the Auditing Committee, and the Retirement Committee were accepted.

Article V, Section 4, of the By-Laws of the Institution was amended, to read as follows:

ARTICLE V

Executive Committee

4. The Executive Committee shall consist of the Chairman, Vice-Chairman, and Secretary of the Board of Trustees, the President of the Institution *ex officio*, and, in addition, not less than five or more than eight trustees to be elected by the Board by ballot for a term of three years, who shall be eligible for re-election. Any member elected to fill a vacancy shall serve for the remainder of his predecessor's term.

Frank Stanton was elected a member of the Board of Trustees.

Vacancies in standing committees were filled as follows: Carl J. Gilbert and Crawford H. Greenewalt were elected members of the Executive Committee for three-year terms. Keith S. McHugh was elected to the Nominating Committee for a three-year term. The following were reelected for one-year terms: Henry S. Morgan as Chairman of the Executive Committee, James N. White as Chairman of the Finance Committee, Keith S. McHugh as Chairman of the Auditing Committee, Amory H. Bradford as Chairman of the Nominating Committee, and Omar N. Bradley as Chairman of the Retirement Committee.

To provide for operation of the Institution for the fiscal year beginning July 1, 1963, and upon recommendation of the Executive Committee, the sum of \$3,338,378 was appropriated from the General Reserve Fund.

Articles of Incorporation

Public No. 260. An Act to incorporate the Carnegie Institution of Washington

Be it enacted by the Senate and House of Representatives of the United States of America in Congress assembled, That the persons following, being persons who are now trustees of the Carnegie Institution, namely, Alexander Agassiz, John S. Billings, John L. Cadwalader, Cleveland H. Dodge, William N. Frew, Lyman J. Gage, Daniel C. Gilman, John Hay, Henry L. Higginson, William Wirt Howe, Charles L. Hutchinson, Samuel P. Langley, William Lindsay, Seth Low, Wayne MacVeagh, Darius O. Mills, S. Weir Mitchell, William W. Morrow, Ethan A. Hitchcock, Elihu Root, John C. Spooner, Andrew D. White, Charles D. Walcott, Carroll D. Wright, their associates and successors, duly chosen, are hereby incorporated and declared to be a body corporate by the name of the Carnegie Institution of Washington and by that name shall be known and have perpetual succession, with the powers, limitations, and restrictions herein contained.

Sec. 2. That the objects of the corporation shall be to encourage, in the broadest and most liberal manner, investigation, research, and discovery, and the application of knowledge to the improvement of mankind; and in particular—

(a) To conduct, endow, and assist investigation in any department of science, literature, or art, and to this end to cooperate with governments, universities, colleges, technical schools, learned societies, and individuals.

(b) To appoint committees of experts to direct special lines of research.

(c) To publish and distribute documents.

(d) To conduct lectures, hold meetings, and acquire and maintain a library.

(e) To purchase such property, real or personal, and construct such building or buildings as may be necessary to carry on the work of the corporation.

(f) In general, to do and perform all things necessary to promote the objects of the institution, with full power, however, to the trustees hereinafter appointed and their successors from time to time to modify the conditions and regulations under which the work shall be carried on, so as to secure the application of the funds in the manner best adapted to the conditions of the time, provided that the objects of the corporation shall at all times be among the foregoing or kindred thereto.

Sec. 3. That the direction and management of the affairs of the corporation and the control and disposal of its property and funds shall be vested in a board of trustees, twenty-two in number, to be composed of the following individuals: Alexander Agassiz, John S. Billings, John L. Cadwalader, Cleveland H. Dodge, William N. Frew, Lyman J. Gage, Daniel C. Gilman, John Hay, Henry L. Higginson, William Wirt Howe, Charles L. Hutchinson, *Samuel P. Langley*, William Lindsay, Seth Low, Wayne MacVeagh, Darius O. Mills, S. Weir Mitchell, William W. Morrow, *Ethan A. Hitchcock*, Elihu Root, John C. Spooner,

Andrew D. White, Charles D. Walcott, Carroll D. Wright, who shall constitute the first board of trustees. The board of trustees shall have power from time to time to increase its membership to not more than twenty-seven members. Vacancies occasioned by death, resignation, or otherwise shall be filled by the remaining trustees in such manner as the by-laws shall prescribe; and the persons so elected shall thereupon become trustees and also members of the said corporation. The principal place of business of the said corporation shall be the city of Washington, in the District of Columbia.

Sec. 4. That such board of trustees shall be entitled to take, hold, and administer the securities, funds, and property so transferred by said Andrew Carnegie to the trustees of the Carnegie Institution and such other funds or property as may at any time be given, devised, or bequeathed to them, or to such corporation, for the purposes of the trust; and with full power from time to time to adopt a common seal, to appoint such officers, members of the board of trustees or otherwise, and such employees as may be deemed necessary in carrying on the business of the corporation, at such salaries or with such remuneration as they may deem proper; and with full power to adopt by-laws from time to time and such rules or regulations as may be necessary to secure the safe and convenient transaction of the business of the corporation; and with full power and discretion to deal with and expend the income of the corporation in such manner as in their judgment will best promote the objects herein set forth and in general to have and use all powers and authority necessary to promote such objects and carry out the purposes of the donor. The said trustees shall have further power from time to time to hold as investments the securities hereinabove referred to so transferred by Andrew Carnegie, and any property which has been or may be transferred to them or such corporation by Andrew Carnegie or by any other person, persons, or corporation, and to invest any sums or amounts from time to time in such securities and such form and manner as are permitted to trustees or to charitable or literary corporations for investment, according to the laws of the States of New York, Pennsylvania, or Massachusetts, or in such securities as are authorized for investment by the said deed of trust so executed by Andrew Carnegie, or by any deed of gift or last will and testament to be hereafter made or executed.

Sec. 5. That the said corporation may take and hold any additional donations, grants, devises, or bequests which may be made in further support of the purposes of the said corporation, and may include in the expenses thereof the personal expenses which the trustees may incur in attending meetings or otherwise in carrying out the business of the trust, but the services of the trustees as such shall be gratuitous.

Sec. 6. That as soon as may be possible after the passage of this Act a meeting of the trustees hereinbefore named shall be called by Daniel C. Gilman, John S. Billings, Charles D. Walcott, S. Weir Mitchell, John Hay, Elihu Root, and Carroll D. Wright, or any four of them, at the city of Washington, in the District of Columbia, by notice served in person or by mail addressed to each trustee at his place of residence; and the said trustees, or a majority thereof, being assembled, shall organize and proceed to adopt by-laws, to elect officers and appoint committees, and generally to organize the said corporation; and said trustees herein named, on behalf of the corporation hereby incorporated, shall thereupon receive, take over, and enter into possession, custody, and management of all property, real or personal, of the corporation heretofore known as the Carnegie Institution, incorporated, as hereinbefore set forth under "An Act to establish a Code of Law for the District of Columbia, January fourth, nineteen hundred and two," and to all its rights, contracts, claims, and property of any kind or nature; and the several officers of such corporation, or any other person having charge of any of the securities, funds, real or personal, books, or property thereof, shall, on demand, deliver the same to the said trustees appointed by this Act or to the persons appointed by them to receive the same; and the trustees of the existing corporation and the trustees herein named shall and may take such other steps as shall be necessary to carry out the purposes of this Act.

Sec. 7. That the rights of the creditors of the said existing corporation known as the

Carnegie Institution shall not in any manner be impaired by the passage of this Act, or the transfer of the property hereinbefore mentioned, nor shall any liability or obligation for the payment of any sums due or to become due, or any claim or demand, in any manner or for any cause existing against the said existing corporation, be released or impaired; but such corporation hereby incorporated is declared to succeed to the obligations and liabilities and to be held liable to pay and discharge all of the debts, liabilities, and contracts of the said corporation so existing to the same effect as if such new corporation had itself incurred the obligation or liability to pay such debt or damages, and no such action or proceeding before any court or tribunal shall be deemed to have abated or been discontinued by reason of the passage of this Act.

Sec. 8. That Congress may from time to time alter, repeal, or modify this Act of incorporation, but no contract or individual right made or acquired shall thereby be divested or impaired.

Sec. 9. That this Act shall take effect immediately.

Approved, April 28, 1904

By-Laws of the Institution

Adopted December 13, 1904. Amended December 13, 1910, December 13, 1912, December 10, 1937, December 15, 1939, December 13, 1940, December 18, 1942, December 12, 1947, December 10, 1954, October 24, 1957, May 8, 1959, May 13, 1960, and May 10, 1963.

ARTICLE I

The Trustees

1. The Board of Trustees shall consist of twenty-four members with power to increase its membership to not more than twenty-seven members. The Trustees shall hold office continuously and not for a stated term.
2. In case any Trustee shall fail to attend three successive annual meetings of the Board he shall thereupon cease to be a Trustee.
3. No Trustee shall receive any compensation for his services as such.
4. All vacancies in the Board of Trustees shall be filled by the Trustees by ballot at an annual meeting, but no person shall be declared elected unless he receives the votes of two-thirds of the Trustees present.

ARTICLE II

Officers of the Board

1. The officers of the Board shall be a Chairman of the Board, a Vice-Chairman, and a Secretary, who shall be elected by the Trustees, from the members of the Board, by ballot to serve for a term of three years. All vacancies shall be filled by the Board for the unexpired term; provided, however, that the Executive Committee shall have power to fill a vacancy in the office of Secretary to serve until the next meeting of the Board of Trustees.
2. The Chairman shall preside at all meetings and shall have the usual powers of a presiding officer.
3. The Vice-Chairman, in the absence or disability of the Chairman, shall perform the duties of the Chairman.
4. The Secretary shall issue notices of meetings of the Board, record its transactions, and conduct that part of the correspondence relating to the Board and to his duties.

ARTICLE III

Executive Administration

The President

1. There shall be a President who shall be elected by ballot by, and hold office during the pleasure of, the Board, who shall be the chief executive officer of the Institution. The President, subject to the control of the Board and the Executive Committee, shall have general charge of all matters of administration and supervision of all arrangements for research and

other work undertaken by the Institution or with its funds. He shall prepare and submit to the Board of Trustees and to the Executive Committee plans and suggestions for the work of the Institution, shall conduct its general correspondence and the correspondence with applicants for grants and with the special advisers of the Committee, and shall present his recommendations in each case to the Executive Committee for decision. All proposals and requests for grants shall be referred to the President for consideration and report. He shall have power to remove, appoint, and, within the scope of funds made available by the Trustees, provide for compensation of subordinate employees and to fix the compensation of such employees within the limits of a maximum rate of compensation to be established from time to time by the Executive Committee. He shall be *ex officio* a member of the Executive Committee.

2. He shall be the legal custodian of the seal and of all property of the Institution whose custody is not otherwise provided for. He shall sign and execute on behalf of the corporation all contracts and instruments necessary in authorized administrative and research matters and affix the corporate seal thereto when necessary, and may delegate the performance of such acts and other administrative duties in his absence to the Executive Officer. He may execute all other contracts, deeds, and instruments on behalf of the corporation and affix the seal thereto when expressly authorized by the Board of Trustees or Executive Committee. He may, within the limits of his own authorization, delegate to the Executive Officer authority to act as custodian of and affix the corporate seal. He shall be responsible for the expenditure and disbursement of all funds of the Institution in accordance with the directions of the Board and of the Executive Committee, and shall keep accurate accounts of all receipts and disbursements. Following approval by the Executive Committee he shall transmit to the Board of Trustees before its annual meeting a written report of the operations and business of the Institution for the preceding fiscal year with his recommendations for work and appropriations for the succeeding fiscal year.

3. He shall attend all meetings of the Board of Trustees.

4. There shall be an officer designated Executive Officer who shall be appointed by and hold office at the pleasure of the President, subject to the approval of the Executive Committee. His duties shall be to assist and act for the President as the latter may duly authorize and direct.

5. The President shall retire from office at the end of the fiscal year in which he becomes sixty-five years of age.

ARTICLE IV

Meetings

1. The annual meeting of the Board of Trustees shall be held in the City of Washington, in the District of Columbia, in May of each year on a date set by order of the Executive Committee, unless the date and place of meeting are otherwise set by order of the Executive Committee.

2. Special meetings of the Board may be called by the Executive Committee by notice served personally upon, or mailed to the usual address of, each Trustee twenty days prior to the meeting.

3. Special meetings shall, moreover, be called in the same manner by the Chairman upon the written request of seven members of the Board.

ARTICLE V

Committees

1. There shall be the following standing Committees, *viz.* an Executive Committee, a Finance Committee, an Auditing Committee, a Nominating Committee, and a Retirement Committee.

2. All vacancies occurring in the Executive Committee, the Finance Committee, the Auditing Committee, the Nominating Committee, and the Retirement Committee shall be

filled by the Trustees at the next regular meeting. In case of vacancy in the Finance Committee, the Auditing Committee, the Nominating Committee, or the Retirement Committee, upon request of the remaining members of such committee, the Executive Committee may fill such vacancy by appointment until the next meeting of the Board of Trustees.

3. The terms of all officers and of all members of committees, as provided for herein, shall continue until their successors are elected or appointed.

Executive Committee

4. The Executive Committee shall consist of the Chairman, Vice-Chairman, and Secretary of the Board of Trustees, the President of the Institution *ex officio*, and, in addition, not less than five or more than eight trustees to be elected by the Board by ballot for a term of three years, who shall be eligible for re-election. Any member elected to fill a vacancy shall serve for the remainder of his predecessor's term.

5. The Executive Committee shall, when the Board is not in session and has not given specific directions, have general control of the administration of the affairs of the corporation and general supervision of all arrangements for administration, research, and other matters undertaken or promoted by the Institution. It shall also submit to the Board of Trustees a printed or typewritten report of each of its meetings, and at the annual meeting shall submit to the Board a report for publication.

6. The Executive Committee shall have power to authorize the purchase, sale, exchange, or transfer of real estate.

Finance Committee

7. The Finance Committee shall consist of not less than five and not more than six members to be elected by the Board of Trustees by ballot for a term of three years, who shall be eligible for re-election.

8. The Finance Committee shall have custody of the securities of the corporation and general charge of its investments and invested funds, including its investments and invested funds as trustee of any retirement plan for the Institution's staff members and employees, and shall care for and dispose of the same subject to the directions of the Board of Trustees. It shall have power to authorize the purchase, sale, exchange, or transfer of securities and to delegate this power. It shall consider and recommend to the Board from time to time such measures as in its opinion will promote the financial interests of the Institution and of the trust fund under any retirement plan for the Institution's staff members and employees, and shall make a report at each meeting of the Board.

Auditing Committee

9. The Auditing Committee shall consist of three members to be elected by the Board of Trustees by ballot for a term of three years.

10. Before each annual meeting of the Board of Trustees, the Auditing Committee shall cause the accounts of the Institution for the preceding fiscal year to be audited by public accountants. The accountants shall report to the Committee, and the Committee shall present said report at the ensuing annual meeting of the Board with such recommendations as the Committee may deem appropriate.

Nominating Committee

11. The Nominating Committee shall consist of the Chairman of the Board of Trustees *ex officio* and, in addition, three trustees to be elected by the Board by ballot for a term of three years, who shall not be eligible for re-election until after the lapse of one year. Any member elected to fill a vacancy shall serve for the remainder of his predecessor's term, provided that of the Nominating Committee first elected after adoption of this By-Law one member shall serve for one year, one member shall serve for two years, and one member shall serve for three years, the Committee to determine the respective terms by lot.

12. Sixty days prior to an annual meeting of the Board the Nominating Committee shall notify the Trustees by mail of the vacancies to be filled in membership of the Board. Each Trustee may submit nominations for such vacancies. Nominations so submitted shall be considered by the Nominating Committee, and ten days prior to the annual meeting the Nominating Committee shall submit to members of the Board by mail a list of the persons so nominated, with its recommendations for filling existing vacancies on the Board and its Standing Committees. No other nominations shall be received by the Board at the annual meeting except with the unanimous consent of the Trustees present.

Retirement Committee

13. The Retirement Committee shall consist of three members to be elected by the Board of Trustees by ballot for a term of three years, who shall be eligible for re-election, and the Chairman of the Finance Committee *ex officio*. Any member elected to fill a vacancy shall serve for the remainder of his predecessor's term.

14. The Retirement Committee shall, subject to the directions of the Board of Trustees, be responsible for the maintenance of a retirement plan for staff members and employees of the Institution and act for the Institution in its capacity as trustee under any such plan, except that any matter relating to investments under any such plan shall be the responsibility of the Finance Committee subject to the directions of the Board of Trustees. The Committee shall submit a report to the Board at the annual meeting of the Board.

ARTICLE VI

Financial Administration

1. No expenditure shall be authorized or made except in pursuance of a previous appropriation by the Board of Trustees, or as provided in Article V, paragraph 8, hereof.

2. The fiscal year of the Institution shall commence on the first day of July in each year.

3. The Executive Committee shall submit to the annual meeting of the Board a full statement of the finances and work of the Institution for the preceding fiscal year and a detailed estimate of the expenditures of the succeeding fiscal year.

4. The Board of Trustees, at the annual meeting in each year, shall make general appropriations for the ensuing fiscal year; but nothing contained herein shall prevent the Board of Trustees from making special appropriations at any meeting.

5. The Executive Committee shall have general charge and control of all appropriations made by the Board. Following the annual meeting, the Executive Committee may allocate these appropriations for the succeeding fiscal year. The Committee shall have full authority to reallocate available funds, as needed, and to transfer balances.

6. The securities of the Institution and evidences of property, and funds invested and to be invested, shall be deposited in such safe depository or in the custody of such trust company and under such safeguards as the Finance Committee shall designate, subject to directions of the Board of Trustees. Income of the Institution available for expenditure shall be deposited in such banks or depositories as may from time to time be designated by the Executive Committee.

7. Any trust company entrusted with the custody of securities by the Finance Committee may, by resolution of the Board of Trustees, be made Fiscal Agent of the Institution, upon an agreed compensation, for the transaction of the business coming within the authority of the Finance Committee.

ARTICLE VII

Amendment of By-Laws

1. These by-laws may be amended at any annual or special meeting of the Board of Trustees by a two-thirds vote of the members present, provided written notice of the proposed amendment shall have been served personally upon, or mailed to the usual address of, each member of the Board twenty days prior to the meeting.

Index of Names

Numbers in italic type refer to pages in the Report of the President.

- Abell, George O., studies, 39–40, 44
 Abelson, Philip H., viii, *54*, 60, 234, 239, 240, 241, 258
 publications, 246, 327, 511
 report of Director of Geophysical Laboratory, 51–258
 studies, *35*, 56, 229–234
 Abt, Helmut, 13
 Ackerman, Edward A., x
 publications, 511
 Adams, Walter S., 10
 Agassiz, Alexander, vii, 533
 Agrell, S. O., 158, 159
 Aitken, Yvonne, 347, 348
 Albers, W., 197, 198
 Aldrich, L. Thomas, viii, *34*, 328
 studies, 218–229, 264–280, 280–289
 Allan, Frank D., 407, 477
 publications, 474
 studies, 465–466, 467
 Allen, Eugene T., 95, 97
 Allen, Gordon, 258
 studies, *36*, 60, 236–238
 Aller, Lawrence H., publication, 46, 49
 studies, 40
 Alvarez, Hector, 298, 329
 Aly, M. K., 44
 Ames, L. L., 146, 147
 Anderko, K., 209, 210
 Anders, E., 216
 Andersen, H., 407, 468
 Andersen, H. J., 407, 468
 Andersen, Olaf, 121
 Anderson, Carl D., 3
 Andrade, Victor, *54*
 Anker, H. S., 236
 Aparicio, Pablo, 329
 Appleman, D. E., 166, 173
 Aramaki, S., 158
 Argyris, Bertie F., publications, 474
 Argyris, Thomas S., 451
 publication, 474, 475
 Arnold, Ralph G., 197, 210, 212, 213
 publication, 245, 250
 Arp, Halton C., viii, 21, 27, 45
 publications, 31, 46
 studies, *27*, 14–15, 28–29, 31
 Arpigny, Christine, 45
 Arpigny, Claude, 10
 Asada, Toshi, publication, 326, 327
 Asklund, B., 92
 Atlas, L., 90, 97
 Auer, Lawrence, 13
 Baade, Walter A., 28, 30, 44, 292
 publication, 46
 Baadsgaard, H., *34*, 258, 271, 329
 studies, 264–280
 Babcock, Harold D., 45
 Babcock, Horace W., viii, 3, 6, 45
 publications, 6, 47
 studies, 23, 38–39
 Bailey, D. Kenneth, 241, 258
 studies, 57, 124–133
 Baker, Milo S., 398
 Baldwin, George J., vii
 Bang, F. B., 447, 448
 Banno, S., 123
 Bappu, M. K. Vainu, 23
 Barbour, Thomas, vii
 Barnes, H. L., 241
 Barth, T. F. W., 87, 90, 92, 93, 94, 155, 239
 Baschek, Bodo, 45
 studies, 12, 21, 25
 Bauer, Ailene J., x
 Baum, William A., viii, 45, 331, 333, 335, 337
 publications, 47, 50, 326, 327
 studies, 27–28, 29, 30–31, 39
 Beach, Liselotte, 329
 Beadle, George W., 444, 445

- Beger, P. J., 156
 Bell, James F., vii
 Berger, Jacques, 45
 studies, 17-18, 20
 Berger, Jeanne, 18, 45
 Berkebile, Wilma J., 46
 Berman, Harry, 201
 Bethke, P. M., 197
 Billings, John S., vii, 533, 534
 Binns, R. A., 84
 Birch, F., 136
 Bishop, David W., ix, 406, 477
 publications, 474, 475
 studies, 452-455, 460-461
 Bishop, Norman, 356, 358
 Blaauw, A., 25
 Black, C. C., 355, 356
 Blinks, Lawrence R., 357, 376
 Bliss, Robert Woods, vii
 Bluntschli Collection, 467, 468
 Bocskay, Elizabeth M., 500
 Boise, James W., x
 Bolton, Ellis T., viii, 328
 publications, 326, 327, 511
 studies, 38-40, 303-326
 Bolton, John G., 5
 Bonner, J. T., 472
 Borsos, T., 447
 Bovenkerk, H. P., 106
 Böving, Bent G., ix, 477
 publications, 474
 studies, 461-462
 Bowen, Ira S., viii, 3, 45, 384
 publications, 47
 report of Director of Mount Wilson and
 Palomar Observatories, 3-50
 Bowen, Norman L., 53, 60, 85, 87, 89, 90, 91, 92,
 95, 97, 99, 101, 121, 124, 126, 127, 134, 145,
 146
 Bowin, C., 280
 Bown, M. G., 88
 Boyd, Francis R., Jr., viii, 70, 71, 72, 74, 85, 90,
 92, 94, 95, 97, 98, 99, 103, 104, 105, 106,
 111, 120, 143, 144, 241, 258
 publication, 245, 250
 studies, 57, 58, 118-119, 121-124, 134-137
 Bradford, Amory H., v, vi, 531
 Bradford, Lindsay, vii
 Bradley, Omar N., v, vi, 531
 Bragg, W. L., 173
 Brett, P. Robin, 59, 240, 258
 studies, 193-197
 Briggs, Winslow R., 393
 Brindley, G. W., 139, 140
 Brink, R. A., 487, 488
 Britten, Roy J., viii, 328
 publications, 326, 327, 511
 studies, 38-40, 303-326
 Brookings, Robert S., vii
 Brown, Donald D., ix, 407, 477
 publications, 474
 studies, 408-415
 Brown, Dugald E. S., 503
 Brown, G. M., 82, 88, 90, 148, 239
 Brown, Jeanette S., ix, 345, 346, 348, 353, 363,
 364, 399
 studies, 361-363
 Brown, Louis, 328
 publications, 326, 327
 studies, 302-303
 Brown, M. L., 168
 Brown, William L., 481
 Brueckel, Frank J., 45
 publications, 46, 47
 studies, 15
 Buchanan, Jennie S., 481, 500
 publication, 511
 Buchwald, Manuel, 330
 publication, 326
 Buddington, A. F., 279
 Buerger, M. J., 166
 Bundy, F. P., 106
 Burbidge, E. Margaret, 35
 Burbidge, Geoffrey R., 35
 Burd, Sylvia, 45
 Burgess, Donna L., 500
 Burgi, Elizabeth, ix, 481, 500
 publications, 500
 studies, 37, 38, 481-484, 484-485
 Burke, Bernard F., viii, 54, 328
 publications, 326, 327
 studies, 28, 289-299
 Burlew, J. S., 241
 Burnham, Charles W., 166, 240, 241, 258
 publication, 249, 250
 studies, 59, 158-165, 173-174
 Burri, C., 153
 Buseck, Peter R., 258
 studies, 59, 200-213
 Bush, Vannevar, v, vii, 531
 Byers, T. J., 328
 studies, 38-40, 303-326
 Byström, A., 213
 Cabre, R., S.J., 329
 Cadwalader, John L., vii, 533
 Cairns, Hugh John, 314, 318, 481, 482
 California Institute of Technology, 13, 30, 51, 3,
 5, 38, 41, 42, 45
 Callaghan, E., 141
 Calvert, L. D., 201, 203, 207
 Campbell, William W., vii
 Capriotti, Eugene, 45
 studies, 36
 Carhart, Anne K., 500
 studies, 493-499
 Carley, Catherine, 500
 Carlson, Gerald L., 406, 452, 477
 publication, 474
 studies, 455-456, 471
 Carnegie, Andrew, 534
 Carnegie Collection of Embryos, 407, 465, 467,
 468
 Carroll, Ann C., 500

- Carty, John J., vii
Caston, J. Douglas, 406, 477
 publications, 474
 studies, 408-418
Cayrel, Giusa, publication, 47
Cayrel, Roger, publication, 47
Champney, William Scott, 500
Chandra, Subhash, 46
Chase, J. W., 477
Chayes, Felix, viii, 240, 241, 258
 publications, 242, 246, 247, 250
 studies, 33, 55, 58-59, 149-157
Chevalier, R., 64
Chinner, G. A., 109, 111, 112, 113, 114, 115, 142
 publication, 243, 250
Choy, Jai H., 45
Ciancaglini, Humberto R., 298
Clair, Robert A., 348
Clark, L. A., 177, 178, 181, 207, 241
 publication, 243, 250
Clark, Sydney P., Jr., 122, 135, 178, 179, 241
Clausen, Jens S., 348, 349, 387, 399
 studies, 40, 347, 394-399
Clayton, R. N., 238
Cleary, William I., 465, 477
Code, Arthur D., 19
Coe, E. H., 487
Coffeen, Mary F., 45
Cole, Whitefoord R., vii
Coleman, John R., publications, 474
Coleman, R. G., 173
 publication, 245, 250
Coomber, Janice E. B., 371, 374
Corner, George W., 406, 472
Corner, George W., Jr., 407, 465, 477
 publications, 474, 475
 studies, 462-464
Cowie, Dean B., viii, 328, 484
 publications, 326, 327, 511
 studies, 38-40, 303-326
Cox, E. G., 171
Cragg, Thomas A., 8, 45
 studies, 6, 7
Crick, F. H. C., 12, 14
Croisille, Yvon, 406, 408, 477
 studies, 48, 428-437
Crowley, M. S., 140, 142
Cuffey, James B., publication, 46, 47
Czaplicki, Helen S., 46
Czyzak, Stanley J., 26, 40
- Davis, Ranice, 465
 publication, 475
Dawid, Igor B., 406, 477
 studies, 419-420
Day, Arthur L., 54
Deer, W. A., 78, 91, 166, 167, 168
DeHaan, Robert L., ix, 407, 477
 publications, 475
 studies, 444-447
Dekker, Arentje, 407, 477
 publication, 475
 studies, 466-467, 468-469
De La Haba, G., publication, 326
DeLanney, Louis E., 451, 452, 477
 publication, 475
Delano, Frederic A., vii
Delisle, M., 221, 277
Demerec, Miloslav, publication, 511
de Neufville, John, 108, 114, 115, 258
Dessy, Landi, 15
Deutsch, Armin J., viii, 45
 publications, 47, 48
 studies, 9, 13, 23, 29-30
Deutsch, S., 277
De Vore, G., 84, 91
de Vries, Pieter A., 466
De Vries, R. C., 114
Dittrich, M., 168
Dixon, B. E., 95
Doak, J. B., 329
Dobzhansky, Theodosius, 348
Dodd, R. T., Jr., publication, 326, 327
Dodge, Cleveland H., vii, 533
Dodge, William E., vii
Doe, Bruce R., 241, 258
 publications, 243, 249, 250, 326
 studies, 210-213
Doelter, C., 168
Doermann, A. H., 485
Donnay, Gabrielle, viii, 240, 258
 studies, 59, 166-173
Donnay, J. D. H., 258
 studies, 59, 169-173
Donnelly, Thomas W., 241
Donner, Martin W., 407, 463, 477
 publication, 475
Dove, William N., 329
Du Fresne, E. R., 216
Dunham, Theodore, Jr., 10
Duranton, J., 348
Durovic, S., 158, 161
Dutt, M. K., publication, 500
Duysens, L. N. M., 344, 365
- Eaton, J. P., 84
Ebert, James D., ix, 406, 407, 420, 447, 452, 477
 publications, 475
 report of Director of Department of Embryol-
 ogy, 401-477
 studies, 47-49, 421-427, 448-451
Ecklund, Everett T., 290, 329
 publication, 326
- Daly, R., 156
Das, C. C., 504, 505
Davis, Brian T. C., 116, 240, 258
 studies, 34, 56, 58, 103-107, 119-121
Davis, Carl L., 466
Davis, Gordon L., viii, 34, 258, 277
 publications, 242, 244, 250
 studies, 59, 218-229, 264-280
Davis, R. S., 135

- Edelen, D. G., 44
 Edmunds, L. N., Jr., 329
 Eggen, Olin J., viii, 43, 45
 publications, 16, 17, 47, 50
 studies, 13-14, 15, 16-17
 Emerson, Robert, 343, 352, 356, 357
 Emery, K. O., 229
 England, Joseph L., viii, 70, 71, 72, 74, 94, 103,
 104, 105, 116, 143, 144, 258
 publication, 245, 250
 studies, 58, 118-124, 134-137
 Ephrussi, Boris, 444, 445
 Epprecht, W., 166, 168
 Epstein, H. T., 375, 377
 Epstein, Ingeborg, 504
 Epstein, S., 234
 Ernst, W. Gary, 132, 133, 147, 241
 Errico, James, 451
 publication, 475
 Eugster, H. P., 61, 62, 65, 148, 149
 publication, 242, 250, 251
- Fawcett, J. Jeffrey, 258
 studies, 56, 139-147
 Fenner, C. N., 84
 Fenner, Charles P., vii
 Ferguson, Homer L., vii
 Ferguson, W. Richard, 407, 477
 Fewson, Charles A., 348
 studies, 343, 352-357
 Firor, John W., studies, 7
 Fischer, K., 161, 162
 Fisher, Agnes C., 500
 publication, 511
 Flexner, J. B., publication, 326
 Flexner, Louis B., xi, 477
 publication, 326
 Flexner, Simon, vii
 Forbes, W. Cameron, vii
 Forbush, Scott E., viii, 328
 publication, 326
 studies, 31, 299-302
 Ford, W. Kent, Jr., viii, 263, 326, 328, 334, 335,
 339
 publications, 47, 327
 Fork, David C., ix, 348, 353, 355, 363, 376, 380,
 399
 publications, 400
 studies, 345, 346, 357-360, 365-370
 Forrestal, James, vii
 Forsman, J. P., 229
 Foster, W. R., 98
 Fowler, William A., 34
 Frankel, Fred R., 37, 500
 publication, 500
 studies, 486
 Fredrick, Lawrence W., 330, 335, 336, 339
 publication, 47, 326
 French, C. Stacy, ix, 54, 348, 353, 356, 360, 399
 publications, 400
 report of Director of Department of Plant
 Biology, 341-400
 studies, 45-46, 349-352, 382-386
 Frenzel, G., 214, 215
 Frew, William N., vii, 533
 Frondel, Clifford, 201
 Frye, J. K., 225, 265
 Fryklund, V. C., publication, 245, 250
 Fulk, Harriet M., 348
 Fulton, C., 460
 Fuyat, R. K., 196
- Gage, Lyman J., vii, 533
 Gast, Paul W., xi, 258, 279
 Gastil, R. G., 221, 277
 Gay, Helen, 494, 500
 report of the Cytogenetics Laboratory, 501-
 510
 Gay, P., 88
 von Gehlen, Kurt, 240, 241, 258
 studies, 59, 213-214
 Gehrels, T., 36
 Gerken, J., 329
 Gibbs, Josiah Willard, 4
 Gibbs, Martin, 348
 studies, 343, 352-357
 Gifford, Walter S., v, vi, 531
 Gilbert, Carl J., v, vi, 531
 Gilbert, Cass, vii
 Gillett, Frederick H., vii
 Gillies, Gloria, 500
 Gilman, Daniel Coit, vii, 533, 534
 Gingras, G., 363
 publication, 400
 Giver, L. P., publication, 47, 49
 Glenister, T. W., 461, 462, 472
 Glover, Timothy D., 454
 publication, 475
 Godfrey, J. D., 271
 Goedheer, Joop C., 348
 studies, 346, 365-370
 Goldberg, Edward, 37, 481, 482, 500
 publication, 500
 Goldfarb, L. J. B., 303
 Goldich, S. S., 225, 265
 Gordon, S. A., 355, 356
 Gottlieb, Hans B., publication, 511
 Govindjee, 346, 348, 352, 356
 studies, 363-364
 Govindjee, Rajni, 348, 352, 356
 Green, Charles R., 407, 477
 studies, 47-48, 421-427, 451
 Green, Louis C., 13
 Green, Ronald, 281
 publications, 327
 Greenewalt, Crawford H., v, vi, 531
 Greenstein, Jesse L., viii, 3, 5, 45
 publications, 47, 48, 49
 studies, 26, 10, 11-12, 17, 18, 33-34, 41
 Greenwood, Hugh J., viii, 143, 145, 146, 241, 258
 studies, 58, 137-139
 Griffith, R. F., studies, 40
 Grill, Richard D., 477

- Grønvold, F., 210, 213
 Gross, Jerome, 472
 Gruenenfelder, M., 227, 253, 274
 Gunn, James E., 46
 publication, 48
 studies, 12, 38

 Haas, C., 197
 Hadorn, Ernst, 407, 444, 445, 446
 Hahn, W. C., Jr., 61, 65
 Hall, John S., 35, 331
 publications, 47, 48, 326, 327
 Hall, Richard C., 328
 Hallimand, A. F., 84, 90
 Hansen, E. C., 258
 Hansen, M., 209, 210
 Haraldsen, H., 210, 213
 Hardie, L. A., 170
 Hargett, Charles E., 477
 Harker, R. I., 137
 Haro, Guillermo, 18, 20
 Harris, John W. S., 465
 Hart, Richard W., 258, 348, 392
 publication, 400
 studies, 382-386
 Hart, Stanley R., viii, 34, 241, 273, 328
 publications, 249, 250, 326, 327
 studies, 218-229, 264-280
 Hartman, Carl G., 406, 452, 461
 Hartman, Mark L., 477
 studies, 460
 Hartmann, Olaf, 300
 Harvey, John W., 7, 8
 Harwit, Martin, publication, 48
 Harwood, H. F., 70
 Hasek, Milan, 472
 Haskins, Caryl P., v, vi, x, 531
 publications, 511
 Report of the President, 1-54
 Haskins, Edna F., publication, 511
 Hawley, J. E., 186
 Hay, Elizabeth, 472
 Hay, John, vii, 533, 534
 Hedge, C. F., 279
 Helfer, H. Lawrence, publication, 48, 49
 Hemley, J. J., 147
 Henard, Kenneth R., x
 Henderson, E. P., 84, 90
 Hendley, D. D., publication, 475
 Henry, Barklie McKee, v, vi, 531
 Henry, N. F. M., 95
 Herrick, Myron T., vii
 Hershey, Alfred D., ix, 316, 318, 420, 500
 publications, 500
 report of Director of Genetics Research Unit,
 479-500
 studies, 37, 38, 481-484, 484-485
 Hertig, Arthur T., 477
 Herzog, Emil, 31, 45
 Hess, H. H., 78, 81, 82, 84, 88, 89, 90, 93, 279
 Heuser, Chester H., 477
 Hewitt, Abram S., vii

 Hewitt, Richard E., publication, 511
 Heydenburg, Norman P., viii, 328
 publications, 326, 327
 Heyding, R. D., 201, 203, 207
 Hiesey, William M., ix, 348, 349, 399
 publications, 400
 studies, 40, 387-394
 Higginson, Henry L., vii, 533
 Hill, Robert, 344, 355, 356, 358, 361
 Hiltner, W. A., 36
 Hitchcock, Ethan A., vii, 533
 Hitchcock, Henry, vii
 Hodge, Paul W., studies, 40
 Hoering, Thomas C., viii, 240, 241, 258
 studies, 35, 56, 60, 229-234, 236, 238-239
 Hoglund, B., 297
 Holmes, A., 70, 71, 150, 151
 Holmes, R. J., 201
 Holser, W. T., 138
 Hoover, Herbert, vii
 Hopson, Clifford A., 241, 277
 Hornblower, Marshall, x
 Howard, Robert F., viii, 6, 45
 publications, 6, 48
 studies, 28-29, 6, 7, 8, 37
 Howe, William Wirt, vii, 533
 Howells, E. R., 159
 Hower, J., 242
 Howie, R. A., 84, 166, 167, 168
 Hoyer, Bill, 38, 329
 publications, 327
 studies, 38-40, 303-326
 Hoyle, Fred, 16, 34
 publication, 48
 Hubbard, Jeannie, 421, 422, 477
 Hubble, Edwin P., 30, 511
 Humason, Milton L., 20, 28, 32, 44
 Hunt, J. M., 229
 Hutchinson, Charles L., vii, 533
 Hytönen, Kai, 108, 109, 111, 112, 113, 114

 Imlay, Marjorie E., 239, 258
 Ingamells, C. O., 79
 Ingraham, Laura J., 37, 500
 publication, 500
 studies, 486

 Jäger, E., 228, 229, 275
 Jagger, T. A., 84
 Jakob, J., 168
 Jaschek, Carlos O., 298
 Jayaraman, A., 105
 Jessup, Walter A., vii
 Jewett, Frank B., vii
 Johanssen, A., 156
 Johnson, Harold L., 15
 Johnson, P. A., 329
 publication, 326, 327
 Johnson, P. C., 135
 Jones, D. H. P., 45
 studies, 19

- Jones, Henry H., 500
 publication, 511
 Jorgensen, Erik G., publication, 400
Journal of Geophysical Research, 239
Journal of Petrology, 239
 Joy, Alfred H., 45
 Jugaku, Jun, 45
 publications, 48, 49
 Justice, Wesley B., 348

 Kaplan, Lewis D., 10
 publication, 48, 49
 studies, 30
 Katem, Basil N., 45
 Kato, Yoshihiro, 48, 408, 428, 430
 Katsura, T., 84
 Kaufmann, Berwind P., 494, 503, 504, 505, 509
 publication, 511
 Keenan, J. J., 138
 Keenan, Philip C., publication, 48
 studies, 13, 40-41
 Keith, M. L., 143
 Kempter, C. P., 120
 Kendrew, J. C., 12
 Kennard, Olga, 171
 Kennedy, G. C., 60, 105, 135, 138
 Kennedy, W. Q., 55, 95
 Kerr, P. F., 141
 Keyes, F. G., 138
 Kidder, Alfred Vincent, 50, 51, 54
 Kimmel, Charles B., studies, 452-454
 King, Ivan R., studies, 41
 King, Murray Vernon, 171
 Kingman, P., 169
 Kippenhahn, Rudolph, 45
 Kissell, K. E., 328
 Kleber, W., 170
 Knight, W. L., 138
 Knight, Wiley, Jr., 348
 Knopf, A., 156
 Koch, Robert, studies, 41
 Kok, Bessel, 357
 Konigsberg, Irwin R., ix, 407, 426, 477
 publications, 475
 studies, 47, 437-443
 Koski, W., 169
 Kouvo, Olavi, 34, 213, 328
 studies, 218-229, 264-280
 Kowal, Charles T., 40, 45
 studies, 27, 10, 15-16
 Kraft, Robert P., viii, 23, 45
 publications, 48
 studies, 13, 20-22
 Kron, G. E., 19, 31
 Kuhn, H., 348, 357
 Kullerud, Gunnar, viii, 193, 194, 214, 240, 241, 258
 publications, 247, 248, 250
 studies, 41-43, 55, 59, 175-192, 196-197, 210-213, 215-218
 Kuno, H., 78, 79, 84, 88, 89, 90, 92, 93, 94, 120, 121
 Kupres, Frank J., 440, 477

 Kurshan, Jane, 500
 Kushiro, Ikuo, 87, 110, 111, 120, 121, 123, 145, 147, 258
 studies, 57, 95-103

 Laboratory of Molecular Biology, Cambridge, 12, 13
 Laboratory of Quantitative Biology, 481
 Lacroix, A., 91
 Laetsch, W. M., 393
 LaMori, P. N., 135
 Langley, Samuel P., vii, 533
 Larsen, E. S., 95
 Larsen, Victor R., 461, 462
 Latimer, Paul, publication, 400
 Laurenson, R. D., 477
 Lawrence, Ernest O., vii
 Lawson, Andrew C., 225, 265
 Le Bas, M. J., 110
 Ledinko, Nada, 500
 Leighton, Robert B., 3, 8, 41
 Lemasson, C., 363
 publication, 400
 Lenz, Andrew N., 348
 Leone, J., 168
 Lewis, J. H., 458
 Lewis, Margaret R., 407
 Lewis, Warren H., 407
 Liller, W., 10
 Lindbergh, Charles A., vii
 Lindsay, William, vii, 533
 Lindsley, Donald H., viii, 241, 258
 studies, 55, 60-66
 Lion, David N., 348
 Little, C. A., Jr., 329
 Lodge, Henry Cabot, vii
 Lomnitz, Cinna, 328
 studies, 280-289
 Loomis, Alfred L., v, vi, 531
 Lourens, J. v. B., 15
 publication, 46, 48
 Lovett, Robert A., v, vi
 Low, Seth, vii, 533
 Lowell Observatory, 15, 17, 43, 326, 337, 339
 Lowen, A. Louise, 45
 Lungershausen, W. T., Jr., 46
 studies, 12, 37
 Lutjen, Barbara A., 500
 Luyten, W. J., 18
 studies, 42
 Lynden-Bell, Donald, publications, 47, 48, 49
 Lynds, C. R., 5, 38
 publication, 48
 studies, 26, 34-35

 McAllister, C. H., 460
 McCamy, K., publication, 327
 McClintock, Barbara, ix, 481, 500
 studies, 46-47, 486-493
 McCarthy, Brian J., viii, 328
 publications, 326, 327
 studies, 38-40, 303-326
 McClure, Frank T., publications, 326, 327

- McConnell, Anne, 46
 McDonald, Margaret R., ix, 481, 500
 studies, 493–499
 McDougall, I., 84
 McGee, J. D., xi, 333, 336, 337, 338
 publications, 47
 McHugh, Keith S., v, vi, 531
 McKenzie, John, 421
 McKie, D., 140
 McKinsty, H. E., 195
 McKusick, A. B., publication, 475, 476
 McKusick, V. A., publication, 475, 476
 McLeod, G. C., 356
 McMahon, D., 347
 McNamara, D. H., studies, 42
 McQuillen, Kenneth R., 328
 studies, 38–40, 303–326
 MacVeagh, Wayne, vii, 533
 McVittie, G. C., publication, 48, 49

 Macdonald, G. A., 84
 Macdowall, Fergus D. H., publication, 400
 Madsen, Axel, 348
 publication, 400
 studies, 346, 371–375
 Mall, Franklin P., 406, 407, 472
 Mandell, Joseph D., 420
 Markert, Clement L., 434, 435, 457, 472
 Martignoni, M., 446
 Marton, L. L., 331
 publication, 326, 327
 Maruyama, Keizo, 500, 504
 studies, 510
 Mason, Brian, 166, 167, 168, 216
 Mathews, F. W., 173
 Mathews, Jon, publication, 48
 Mathieu, S., 64
 Matsui, Y., 123
 Matthews, R. E. F., publications, 327
 Matthews, Thomas A., 5, 32
 publications, 48
 Mawson, D., 95
 Mayall, N. U., 20
 Mayeda, T. K., 238
 Mehrizi, Ali, 407, 477
 publication, 475
 studies, 468–469
 Mellon, Andrew W., vii, 50
 Mendez, Manuel E., 24, 25, 26, 46
 Mercy, E. L. P., 66, 67, 68, 69, 71, 74, 75, 76, 84,
 116, 123
 Merriam, John Campbell, vii
 Merrill, Paul W., 13, 24
 publications, 48
 Merwin, Herbert E., 50, 52–53, 84, 132
 Métais, Danielle, 258
 studies, 58, 149–150, 152–155, 156–157
 Meyer, R. P., 280
 publication, 327
 Michels, A., 138
 Michelson, Albert A., 4
 Midgley, John E., 328
 publications, 327

 Mihalas, Dimitri M., 37, 46
 Mikkola, T., 267
 Mildvan, M. C., publication, 475
 Miles, Mary Jane, 239
 Miller, Margaret Carnegie, v, vi, 531
 Miller, Roswell, vii
 Miller, William C., 46
 publication, 48
 Mills, Darius O., vii, 533
 Milner, Harold W., ix, 348, 399
 publication, 400
 studies, 40, 387–392
 Minkowski, Rudolph L., publications, 48
 Mitchell, S. Weir, vii, 533, 534
 Mitchell, Walter E., Jr., 42
 Moffett, Benjamin C., Jr., 407, 477
 studies, 467–468
 Moh, Günter, 258
 studies, 59, 189–192, 197–200, 214–215
 Montague, Andrew J., vii
 Morey, George W., 142, 241
 publication, 246, 250
 Morgan, Henry S., v, vi, 515, 531
 Morgan, Russell, 463
 Morimoto, Nobuo, 193, 194, 241, 258
 publication, 247, 250
 studies, 169–170
 Morrow, William W., vii, 533
 Mosburg, S., 197
 Mosig, Gisela, 482, 500
 publication, 500
 studies, 37, 485
 Mrose, Mary, 172
 Muan, A., 61, 65
 Mudd, Seeley G., v, vi, 531
 Muecke, Edward C., 407, 474, 477
 studies, 452, 459, 470
 Muir, I. D., 84, 93, 147
 Müller, A., 348, 357, 358
 publication, 400
 studies, 345
 Mun, Alton M., 447, 451
 publication, 475
 Münch, Guido, viii, 5, 28, 45
 publications, 48, 49
 studies, 30, 9, 10, 23, 24
 Munoz, J. L., 170
 Murray, Bruce C., studies, 30, 42–43
 Myers, William I., v, vi, 531

 Nadler, M. R., 120
 Nalwalk, A., 280
 National Bureau of Standards, 172, 233
 National Geographic Society–Palomar Observa-
 tory Sky Survey, 42
 Nelson, B. W., 140, 142
 Nemer, Martin, 473
 Newton, R. C., 105
 Nichols, Richard F. F., x
 Nicholson, Frank, 348
 studies, 392–394

- Nicholson, Seth B., 50, 52, 54, 45
 publications, 48, 49
 Nishida, Minoru, 45
 Nitowsky, Harold, 473
 Nobs, Malcolm A., ix, 348, 349, 399
 publication, 400, 511
 studies, 40, 387-392
 Nockolds, S. R., 239
 Noll, F., 168
 Norton, Garrison, v, vi
 Norton, Robert H., publication, 49
 Nöthiger, R., 446
 Nowacki, W., 171
 Noyes, Robert W., 41
- Ochoa, Daniel, 329
 Ocola, Leonidas, 329
 O'Dell, Charles R., 24, 45
 publication, 49, 50
 studies, 24, 25, 26, 27
 O'Hara, M. J., 84, 123, 241, 258
 studies, 56, 57, 66-77, 107-118
 Oke, J. Beverley, viii, 5, 13, 45
 publications, 49
 studies, 26, 12, 18-19, 29, 33, 37-38
 Olson, Edward C., studies, 41
 Ondik, Helen, 172
 O'Rahilly, Ronan, publication, 475
 Orts, Llorca, F., 465, 477
 Orville, Philip M., 241
 publication, 246, 250
 Osborn, E. F., 60, 87, 114, 115
 Osborn, William Church, vii
 Osterbrock, Donald E., 26, 36
 Ottemann, J., 197, 199, 200
 Owen, E. A., 209
- Palache, Charles, 201
 Papaconstantinou, John, publication, 475
 Park, R., 234
 Parker, Patrick L., viii, 240, 241, 258
 studies, 36, 60, 234-236
 Parker, Robert, publication, 49
 Parmelee, James, vii
 Parsons, Wm. Barclay, vii
 Partridge, J. H., 159
 Paton, Stewart, vii
 Patton, Donald J., x
 Peacock, M. A., 133
 Peacor, D. R., 166
 Pearson, W. B., 209
 Peoples, James A., 239
 Peoples, Rowena, 239
 Pepper, George W., vii
 Perfect, D. David, 348
 Perkins, Richard S., v, vi, 515, 531
 Pershing, John J., vii
 Perutz, M., 12
 Peterman, Z. E., 225, 265
 Pettijohn, F. J., 147
 Pettit, Edison, 50, 51-52
 Phillips, D. C., 159
- Phillips, R., 65
 Phinney, W. C., 241
 Picken, Kathe A., 348
 studies, 392-394
 Pickering, Donald E., 465
 Pilling, D., 172
 Pirsson, L. V., 156
 Pizzella, G., publication, 326, 327
 Pleass, C. M., 201
 Pohn, Howard A., 43
 Poldervaart, A., 88
 Pollock, Harry E. D., xi
 Popper, Daniel M., studies, 43
 Posnjak, Eugene, 85, 87, 91, 92
 Prentis, Henning W., Jr., vii
 Presnall, Dean, 258
 Prewitt, Charles T., studies, 173-174
 Price, A. T., 300
 Prince, A. T., 114, 115
 Pritchett, Henry S., vii
 Proskouriakoff, Tatiana, x, 54
- Radoslovich, E. W., 59, 149, 240, 258
 studies, 165-166
 Rafferty, Keen, 473
 Ramberg, Hans, 84, 91
 Ramdohr, Paul, 188, 197, 207, 213, 214, 242-243
 publication, 248, 250
 Ramsey, Elizabeth M., ix, 465, 474, 477
 publications, 475
 studies, 462-464
 Rawles, Mary E., ix, 477
 studies, 443-444
 Reddy, Devender C., 348
 Reed, G. W., publication, 247, 250
 Reichen, L. E., 210, 213
 Rentschler, Gordon S., vii
 Reporter, Minocher C., 406, 407, 477
 publications, 475, 476
 studies, 47-48, 421-427
 Resnik, Robert A., publication, 475, 476
 Rever, Arthur G., 465, 477
 Reynolds, Samuel R. M., 477
 Richards, R. G., 65
 Richter, D. H., 84
 Righini, G., 9
 Ringwood, A. E., 121
 Roberts, Richard B., viii, 328
 publications, 326, 327, 511
 studies, 38-40, 303-326
 Roberts, Stuart L., 37, 39, 46
 Robineaux, Roger, 473
 Rockefeller, David, vii
 Rodríguez B., A., 328
 publication, 327
 studies, 280-289
 Roedder, Edwin W., 85
 Rogers, D., 159
 Rook, J. R., 303
 Rooksby, H. P., 159
 Root, Elihu, vii, 533, 534
 Root, Elihu, Jr., v, vi, 531

- Roseboom, E. H., 193, 201, 204
 Rosenwald, Julius, vii
 Ross, D. R., 197
 Roy, D. M., 140, 143
 Roy, R., 140, 142, 143, 158
 Rubey, William W., v
 Rudin, Hermann, 328
 publications, 326, 327
 studies, 302–303
 Rudnicki, Konrad, 20, 45
 publication, 49, 50
 studies, 31–32
 Rule, Bruce, 46
 Russell, Helen E., 329
 Ryerson, Martin A., vii
- Saa, G., S.J., 329
 Sabels, Bruno E., 258
 studies, 60, 238–239
 Sacks, I. Selwyn, 328
 studies, 280–289
 Sadanaga, R., 158, 159, 161
 Saha, P., 145, 146
 Sahade, Jorge, 298
 Sahama, Th. G., 97
 Saito, E., publication, 475, 476
 Sakata, Y., 108
 Sakko, M., 329
 Salgueiro P., D. R., 328
 Sand, L. B., 146, 147
 Sandage, Allan R., viii, 54, 3, 5, 10, 20, 30, 32, 44, 45
 publications, 47, 48, 49, 50, 511
 studies, 26, 27, 15–16, 34–36
 Sanford, Roscoe F., 20
 Sargent, Wallace L. W., 45
 publications, 49
 Saunders, John B. de C. M., 466
 Schabtach, Gretchen, 477
 Schairer, J. Frank, viii, 104, 105, 106, 120, 121, 143
 publication, 243, 250
 studies, 44, 56, 57, 77–103, 107–115, 124–131
 Schechtman, A. M., 447
 Schiff, Jerome A., 348
 studies, 345–346, 375–378, 381–382
 Schmidt, Leon H., 465
 Schmidt, Maarten, viii, 5, 45
 publications, 48, 49
 studies, 26, 28, 27, 32, 33–34
 Schmitt, M., 207
 Schmucker, Ulrich, xi, 300, 328
 Schneiderhöhn, H., 213
 Schol, K., 197
 Schreyer, Werner F., 109, 111, 122, 144, 241, 258
 publications, 242, 244, 250
 Schulman, Marvin D., 348
 studies, 343, 352–357
 Schwarzschild, Martin, 54
 Scoon, J. H., 79, 84, 147, 245
 Scott, Patricia P., publication, 476
 Scott, Walter E., 329
- Searle, Leonard T., 45
 publications, 49
 studies, 12
 Sears, Robert E., 46
 Segnit, E. R., 108
 Seliger, H., 425
 Sengün, Atif, 507
 Sensenig, E. Carl, 477
 Severny, A. B., 6
 publication, 48, 49
 Shane, C. D., 31
 Sheeley, Joyce E., 45
 Shepard, Anna O., x
 publications, 511
 Shepard, Thomas H., 406, 477
 studies, 447, 468
 Shepley, Henry R., v, vii, 50–51, 515, 531
 Silver, L. T., 277
 Silverman, S. R., 233
 Simon, George W., 41
 Simoni, D., 329
 Singer, A. David, 239, 258
 Sinton, William M., studies, 43
 Smith, Guinevere C., 481, 500
 Smith, James H. C., 346, 348, 361, 371, 374, 378
 publication, 400
 studies, 345, 379–380
 Smith, Joseph Victor, 158, 159
 publication, 244, 250
 Smith, Lewis L., 19
 publications, 49
 Smith, T. Jefferson, viii, 328
 publication, 327
 studies, 280–289
 Smith, Theobald, vii
 Sosman, Robert B., 92
 Sparvoli, Elio, 500, 504
 Spinrad, Hyron, 9, 10, 29
 publication, 49
 studies, 30
 Spitzer, Lyman, Jr., xi, 22, 45
 Spooner, John C., vii, 533
 Stahl, Frank, 481
 Stanton, Frank, v, 53–54, 531
 Steiger, Rudolf H., 34, 258, 275
 studies, 59, 218–229, 264–280
 Stein, B. A., 135
 Steinberg, Malcolm S., 446
 Steiner, William F., 330
 Steinhart, John S., viii, 281, 328
 publications, 327
 studies, 280–289
 Stellar, E., publication, 326, 327
 Stemple, I. S., 139, 140
 Storey, William Benson, vii
 Stott, Pauline, 421, 477
 Straka, W. C., publication, 49
 Stran, Herbert M., publication, 475, 476
 Streeter, George L., 466, 468
 Strehler, B. L., publications, 475, 476
 Streibel, H. R., 328
 Streisinger, George, 481

- Strong, H. M., 106, 135, 136
 Strong, Richard P., vii
 Strunz, H., 166
 Struve, Otto, viii, 50, 51, 45
 publication, 49
 Stryker, Lucile B., x, 239
 Subramaniam, A. P., 84
 Sullivan, James F., x, 53
 Sully, A. H., 209
 Sumner, Roger, 328
 studies, 280-289
 Suzuki, Yoshio, 241, 258
 studies, 155-156
 Suzuki, Ziro, 328
 studies, 280-289
 Swanson, H. E., 196
 Swope, Henrietta H., 21, 30, 45
 Sype, Nancy, 477
 Sztrokay, K. I., 188
- Taft, Charles P., v, vi, 531
 Taft, William H., vii
 Takata, Chinami, 451
 studies, 447-448
 Takeda, H., studies, 169-170
 Takeuchi, Y., 158, 159, 161
 Tammann, Gustav A., 30, 45
 Tardent, Pierre, 451
 publication, 475, 476
 Taussig, Helen, 407, 468
 Taylor, W. H., 158, 159
 Temmer, Georges M., viii, 328
 Thayer, William S., vii
 Thomas, D. M., 258
 Thomas, J. B., 346, 348, 365
 Thompson, H. R., publication, 327
 Thorne, Kip S., publication, 49
 Tift, William Grant, publication, 49
 Tilley, C. E., xi, 66, 67, 68, 69, 74, 75, 76, 109,
 126, 147, 239, 258
 publication, 244, 250, 251
 studies, 44, 56, 77-95
 Tilton, George R., viii, 34, 258, 272, 277
 publications, 244, 247, 249, 250, 327
 studies, 59-60, 218-229, 264-280
 Tokonami, M., 158, 159, 161
 Tomita, T., 91
 Toulmin, P., 197
 Tozer, D. C., 107
 Trafton, Laurence M., 46
 studies, 9, 36
 Trinkaus, J. P., 473
 Trippe, Juan T., v, vi
 Tröften, Per-Fredrick, studies, 210-213
 Tsuboi, S., 89, 90, 92
 Tudge, A. P., 238
 Turner, John F., 355
 Turner, Kenneth C., 328
 publications, 326, 327
 studies, 28, 289-299
 Turnock, Allan C., 65, 85
 publication, 242, 251
- Tuttle, O. F., 137, 145, 146
 Tuve, Merle A., viii, 54, 264, 328, 331
 publications, 326, 327
 report of Director of Department of Terres-
 trial Magnetism, 259-330
 studies, 28, 280-289, 289-299
 Tyler, David B., 452, 460
- Ursprung, H., 435, 446
 Utter, Merwyn G., 6, 8, 45
 publication, 49
- van Woerden, Hugo, 24-25, 45
 Varsavsky, Carlos M., 298, 328
 Velde, Bruce, 241, 242, 258
 studies, 57-58, 147-149
 Vendrely, Colette, 473
 Vendrely, Roger, 473
 Venkatesan, D., publication, 326, 327
 Verhoogen, J., 107
 Vincent, E. A., 64, 65
 Vink, H. J., 197
 Vinogradov, A. P., 229
 Volkmer, Kent, 42
 Volponi, F., 329
 Vuorelainen, Y., 213
- Wade, C., 297
 Wadsworth, James W., vii
 Wager, L. R., 78, 79, 81, 82, 84, 91, 239
 Walburn, Marjorie H., x
 Walcott, Charles D., vii, 533, 534
 Walcott, Frederic C., vii
 Walcott, Henry P., vii
 Walker, Merle F., 20
 Wallerstein, George, 12
 publication, 49
 studies, 11, 44
 Wallis, William Fisher, 50, 53
 Walter, L. S., 137
 Walthall, F. G., 279
 Warren, B. E., 173
 Washington, H. S., 84, 132
 Wasscher, J. D., 197
 Waters, Aaron C., 241
 Watson, J. D., 12, 14
 Weaver, Ellen C., publications, 400
 Weaver, Harry E., publication, 400
 Weed, Lewis H., vii
 Weidemann, Volker, 45
 publication, 49
 Weiner, Ruth, 168
 Weingart, Eleanor Ann, 494, 500, 504, 505
 Welch, William H., vii
 Wells, Harry W., viii, 328
 Wentorf, R. H., Jr., 106
 Wentworth, C. K., 78
 Westerhout, G., 296
 Westphal, J. A., studies, 30, 42
 Wetherill, George W., 277
 publication, 244, 250, 251

- Weymann, Ray, publications, 49
studies, 44
- White, Andrew D., vii, 533, 534
- White, Edward D., vii
- White, Henry, vii
- White, J., 65
- White, James N., v, vi, 531
- White, W. P., 95
- Whiteoak, John B., 45
studies, 19, 36
- Whiteoak, Mary B., 45
- Wickersham, George W., vii
- Wiese, Lutz, 473
- Wiik, H. B., 167
- Wilcock, W. L., publication, 50
- Wilcox, John M., 8
- Wilde, C. E., Jr., 473
- Wildey, Robert L., publication, 50
studies, 30, 42-43
- Willems, H. W. V., 126, 127
- Williams, A. F., 69, 74, 77
- Wilshire, H. G., 147
- Wilson, Albert G., studies, 44
- Wilson, Carole E., 500
- Wilson, Ian B., publication, 476
- Wilson, Olin C., viii, 19, 45, 335
publications, 48, 50
studies, 29, 22-23, 24, 25, 44
- Wilson, Ralph Elmer, publication, 511
- Wilson, Robert E., v, vi, 531
- Winchell, H., 78
- Witt, H. T., 344, 348, 357, 358, 359, 360
publication, 400
studies, 345
- Wolf, Frederick T., publication, 400
- Wolfe, Étienne, 406
- Wones, David R., 61, 62, 65, 169, 242
publication, 249, 251
- Woods, Philip S., 507
- Woodward, Robert Simpson, vii
- Woolley, R. v. d. R., publication, 50
- Word, Lovie W., publication, 511
- Worrell, Gordon, 45
- Wright, Carroll D., vii, 533, 534
- Wright, F. E., 95
- Wright, J. B., 64, 65
- Wright, Tom Ll., 241
- Wulf, Oliver R., publication, 49, 50
- Wurm, K., 24
- Wyckoff, Marjory, 500
- Wyckoff, R. W. G., 84
- Wyllie, P. J., 137
- Yagi, Kenzo, 124, 125
studies, 57, 133-134
- Yardley, D. H., 225, 265
- Yčas, M., 236
- Yoder, Hatten S., Jr., viii, 54, 74, 75, 76, 97, 101,
109, 122, 131, 139, 140, 141, 142, 148, 149,
174, 196, 239, 241, 258
publication, 244, 251
studies, 41-44, 55, 56, 57, 66-71, 77-95,
143-147, 215-218
- Yoss, Kenneth M., studies, 41
- Young, J. A., 329
- Younkin, Robert, 9
- Yund, Richard A., 178, 183, 184, 188, 189, 195,
203, 204, 206, 215
publications, 244, 251
- Zies, Emanuel G., 258
studies, 59
- Zirin, Harold, studies, 7
- Zussman, J., 166, 167, 168
- Zwicky, Fritz, viii, 21, 45
publications, 50
studies, 18, 20, 31, 32

